colloques et séminaires

# GÉODYNAMIQUE ANDINE
## *ANDEAN GEODYNAMICS*
## *GEODINÁMICA ANDINA*

**Résumés étendus**
***Extended abstracts***
***Resúmenes ampliados***

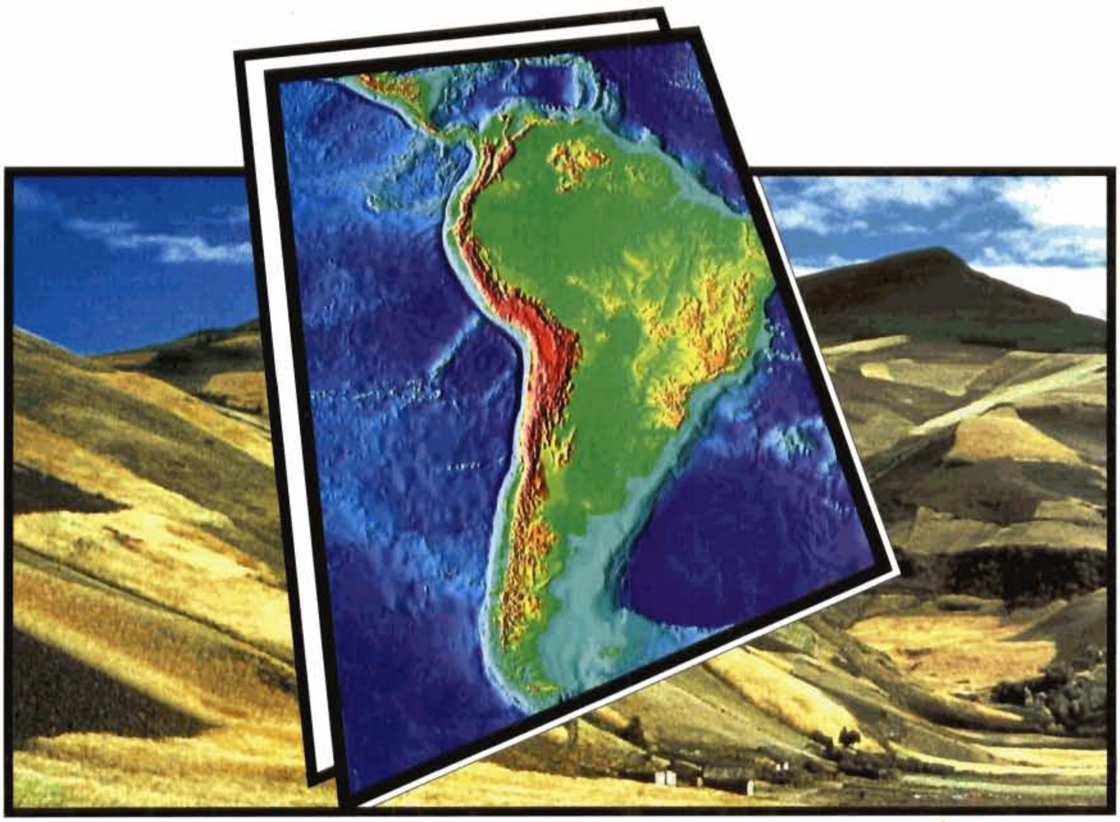

Troisième symposium international
sur la Géodynamique andine.
ORSTOM /Géosciences Rennes
Saint-Malo (France),
du 17 au 19 septembre 1996

ORSTOM éditions

Troisième symposium international sur la Géodynamique andine.
ORSTOM /Géosciences Rennes
Saint-Malo (France), du 17 au 19 septembre 1996

# ISAG 96

# GÉODYNAMIQUE ANDINE
# *ANDEAN GEODYNAMICS*
# *GEODINÁMICA ANDINA*

**Résumés étendus**
***Extended abstracts***
***Resúmenes ampliados***

**Organisateurs / *Organizers / Organizadores***

ORSTOM
L'Institut Français de Recherche Scientifique
pour le Développement en Coopération
Paris, France

GÉOSCIENCES RENNES
CNRS / Université de Rennes I
France

**ORSTOM éditions**
INSTITUT FRANÇAIS DE RECHERCHE SCIENTIFIQUE POUR LE DÉVELOPPEMENT EN COOPÉRATION
Collection **COLLOQUES et SÉMINAIRES**
PARIS 1996

## COMITÉ D'ORGANISATION /
## *ORGANIZING COMMITTEE / COMITÉ ORGANIZADOR*


Peter R. COBBOLD (Géosciences Rennes, CNRS, université de Rennes 1)
Luis FONTBOTE (Université de Genève)
Denis GAPAIS (Géosciences Rennes, CNRS, université de Rennes 1)
Étienne JAILLARD (ORSTOM)
René MAROCCO (ORSTOM)
Georges POUPINET (IRIGM, université de Grenoble)
Pierrick ROPERCH (ORSTOM)
Gehrard WÖRNER (Université de Göttingen)



Le comité d'organisation tient à remercier particulièrement Mmes Arlette FALAISE et Monique LE MOIGNE (Géosciences Rennes) pour leur rôle primordial dans la préparation du Symposium, ainsi que MM. Marc DIRAISON et Marc de URREIZTIETA (Géosciences Rennes) pour leur participation à l'édition de ce volume.


## APPUI FINANCIER /
## *FUNDINGS / APOYO FINANCIERO*


L'organisation de l'ISAG 96 et les aides aux voyages pour un certain nombre de collègues latino-américains ont été rendues possibles grâce au soutien financier de l'ORSTOM (direction de l'Information scientifique et technique, département Terre-Océan-Atmosphère, commission scientifique de Géologie-Géophysique), du CNRS (département Sciences de l'Univers), de l'université de Rennes 1, de la commission des Communautés européennes (DG XII B4, Coopération scientifique internationale), du ministère des Affaires étrangères (direction de la Coopération scientifique et technique, Paris, et ambassade de France au Chili), du conseil régional de Bretagne, et du PICG 345 « Lithospheric Evolution of the Andes » (UNESCO).





ISSN : 0767-2896
ISBN : 2-7099-1332-1

## COMITE D'ORGANISATION
## ORGANIZING COMMITTEE
## COMITE ORGANIZADOR

Peter R. COBBOLD (Géosciences Rennes, CNRS, Université de Rennes 1)
Luis FONTBOTE (Université de Genève)
Denis GAPAIS (Géosciences Rennes, CNRS, Université de Rennes 1)
Etienne JAILLARD (ORSTOM)
René MAROCCO (ORSTOM)
Georges POUPINET (IRIGM, Université de Grenoble)
Pierrick ROPERCH (ORSTOM)
Gehrard WÖRNER (Université de Mayence)

Le comité d'organisation tient à remercier particulièrement Mmes Arlette FALAISE et Monique LE MOIGNE (Géosciences Rennes) pour leur rôle primordial dans la préparation du Symposium, ainsi que Mrs Marc DIRAISON et Marc de URREIZTIETA (Géosciences Rennes) pour leur participation à l'édition de ce volume.

## APPUI FINANCIER
## FUNDINGS
## APOYO FINANCIERO

L'organisation de l'ISAG 96 et les aides aux voyages pour un certain nombre de collègues latino-américains ont été rendues possibles grâce au soutien financier de l'ORSTOM (Direction de l'Information Scientifique et Technique, Département Terre-Océan-Athmosphère, Commission Scientifique de Géologie-Géophysique), du CNRS (Département Sciences de l'Univers), de l'Université de Rennes 1, de la Commission des Communautés Européennes (DG XII B4, Coopération Scientifique Internationale), du Ministère des Affaires Etrangères (Direction de la Coopération Scientifique et Technique, Paris, et Ambassade de France au Chili), du Conseil Régional de Bretagne, et du PICG 345 "Lithospheric Evolution of the Andes (UNESCO).

# SOMMAIRE / SUMMARY / SUMARIO

## LITHOSPHERE ANDINE
## ANDEAN LITHOSPHERE
## LITOSFERA ANDINA

## SISMOTECTONIQUE / NEOTECTONIQUE / RISQUES VOLCANIQUES
## SEISMOTECTONICS / NEOTECTONICS / VOLCANIC HAZARDS
## SEISMOTECTONICA / NEOTECTONICA / RIESGOS VOLCANICOS

## TECTONIQUE / BASSINS SEDIMENTAIRES
## TECTONICS / SEDIMENTARY BASINS
## TECTONICA / CUENCAS SEDIMENTARIAS

## MAGMATISME, PETROLOGIE
## MAGMATISM, PETROLOGY
## MAGMATISMO, PETROLOGIA

## HYDROTHERMALISME / MINERALISATIONS
## HYDROTHERMALISM / MINERALIZATIONS
## HIDROTERMALISMO / MINERALISACIONES

## PROCESSUS DE SURFACE / GEOMORPHOLOGIE
## SURFACE PROCESSES / GEOMORPHOLOGY
## PROCESOS DE SUPERFICIE / GEOMORFOLOGIA

## GEODYNAMIQUE PRE-ANDINE
## PRE-ANDEAN GEODYNAMICS
## GEODINAMICA PRE-ANDINA

# LITHOSPHERE ANDINE
# ANDEAN LITHOSPHERE
# LITOSFERA ANDINA

# THE LIQUIÑE-OFQUI FAULT, GEOPHYSICS RESULTS IN THE PUYUHUAPI REGION

Manuel ARANEDA[1] and María Soledad AVENDAÑO[1]

[1] Depto. de geofísica, U. de Chile, Casilla 2777, Santiago, Chile

**KEY WORDS:** Gravity tectonic, Liquiñe-Ofqui zone.

## INTRODUCTION

The Liquiñe-Ofqui fault zone (LOFZ) is defined as an structural weakening that reaches the upper mantle and its extension is more than 1000 kms in the Southern Andes.
It is studied in the Puyuhuapi zone with three gravimetric profiies that perpendicular cut fault structure. They have been defined as Risopatrón, Puyuhuapi and Peninsula.
Watching the Bouguer anomaly results of the two profiles firstly named, it can be concluded that there is no negative anomaly associated to the fault zone as it was expected (rocks less density). Consequently, in the Risopatrón profile it is proposed that the fault zone is composed by rocks with similar densities to the granitic rocks on the edges of the valley; or, this zone is so thin that it wasn't detected because of the gravimetric stations distribution (c/100m).
Some thing similar occurs in the Puyuhuapi profile, but it is less trustful because it begins at granitic rocks and ends at volcanic rocks. The Peninsula profile has similar characteristics as the ones mentioned before, but the west side begins at old vulcanic rocks composed by basalts with insertions of pyroclast and slag. In this profile, an anomaly of higher amplitude is seem that can be ever bigger. In the present state the residual anomaly is of 6 miligals, that considering a density contrast 0.4 gr/cm$^3$ produces an aproximate depth of 360 meters. The anomaly zone has a lenght of 2400 m.

## THE LIQUIÑE-OFQUI FAULT

The Liquiñe- Ofqui fault zone is a structure with N-S direction, which is affected by different geological process that mainly occur due to the subduction action in Southern Andes.
This structure has been recognized for more than 1000 km, extended from nearby the Ofqui isthmus at the south up to Los Lagos region at the north, limit which is not well defined in Figure 1. Its origin has been related to as oblique subduction under the continental edge (Herve 1976, Beck 1988 , Garcia et al. 1988) or to the subduction effect of the oceanic crust under the continent (Forsythe and Nelson 1985). Muir Wood (1989) shwon details its activity and proved that near the last zone, South-east LOFZ has been active during the cuaternary, he also thinks that there was a vertical relative lifting of the east block of 1200 m. In this way, the LOFZ has been active, at least, since the recent oligocene in its northern side. Since the miocene its location has been controlled by intrusive plutonics, that still control the magma access to the surface in the present chain, Herve (1994).

## GEOPHYSICAL RESULTS AND RECORDS

Considering gravimetric records reported by Araneda and Avendaño (1985), see Figure 2, where obtained negative residual anomalie of even -7 mgales in an approximated length of 2 km, 3 gravimetric profiles where proyected with stations every 100 meters in the Puyuhuapi zone (see Figure 3). This zone would correspond to the main fault zone, which geomorphological characteristics, volcanic lineament and geological structure are similar to the ones seen in the Cayatue- Ralún zone.
The result that were found in the Risopatrón profile, Figure 3a, both extremes binded to granitic rocks show that doesn't exist a zone composed by low density or if this zone exist, its lenght reducess to less than 50 meters. Similar results are seen in the Puyuhuapi profile (Figure 3b), but at the west extreme was not bended to granitic rocks. Anyway, there was no anomaly observed that could be related to the mega structure.
Finally, Peninsula profile (Figura 3c) shows a big anomaly of great amplitude that is open to the west due to granitic rocks were not found.

## ACKNOWLEDGEMENTS

Part of this investigation was financed by proyect FONDEF MI 15 (Geológico Minero Aisén of the professor Alfredo Lashen).

## REFERENCES

Araneda M. y Avendaño M.S. 1985. Estudio gravimétrico de la falla Liquiñe-Ofqui, en los sectores seno Cayatue, Bahía Ralún y Cochanó Punta Pocoihuen. Actas 4[to] Congreso Geológico Chileno Antofagasta, 1(2):1-16.

Beck M. 1988. Analysis of late Jurassic-Recent paleomagnetic data from active plate margins of South America. J S Am Earth Sci 1:39-52.

Forsythe R., Nelson E. 1985. Geological manifestations of ridge collision: Evidence from the Golfo de Penas-Taitao Basin, Southern Chile. Tectonics 4:447-495.

García A., Beck M., Burmester R., Munizaga F., Hervé F. 1988. Paleomagnetic reconnaissance of the Región de Los Lagos, southern Chile and its tectonic implications. Rev Geol Chile 15:13-30.

Hervé M. 1976. Estudio geológico de la falla Liquiñe-Reloncaví en el área de Liquiñe: Antecedentes de un movimiento transcurrente. Actas 1[er] Congr. Geol. Chileno, Santiago, I(b): 39-56.

Hervé F. 1994. The Southern Andes Between 39° and 44° Latitude: The Geological Signature of a Transpressive Tectonic Regime Related to a Magmatic Arc in: Reuther K-J., Scheuber E., Wigger P. (eds.). Tectonics of the Southern Central Andes. Springer, Berlin Heidelberg New York pp 243-248.

Muir Wood R. 1989. Recent normal fautting at the Laguna de San Rafael, Aisen province, southern Chile. Comunicaciones 40: 57-68.

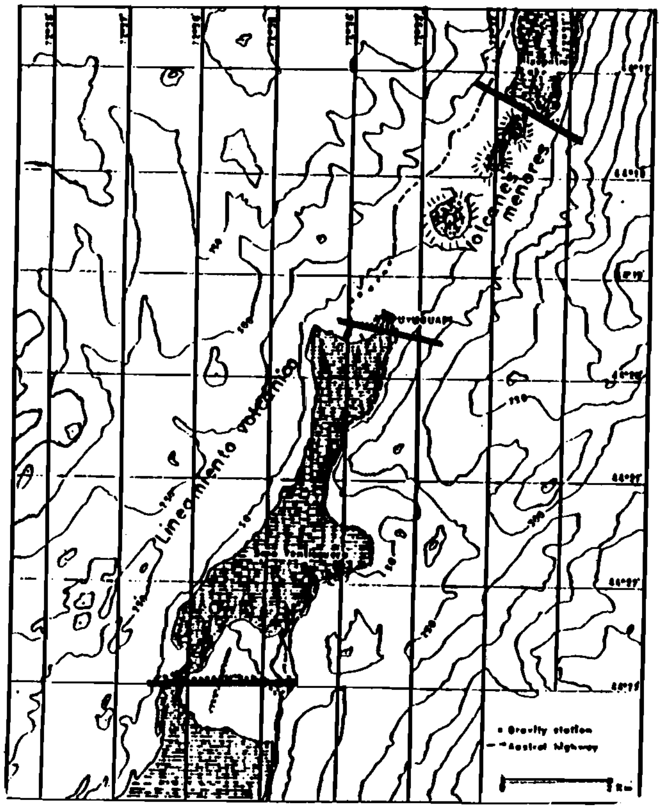


Figura 1

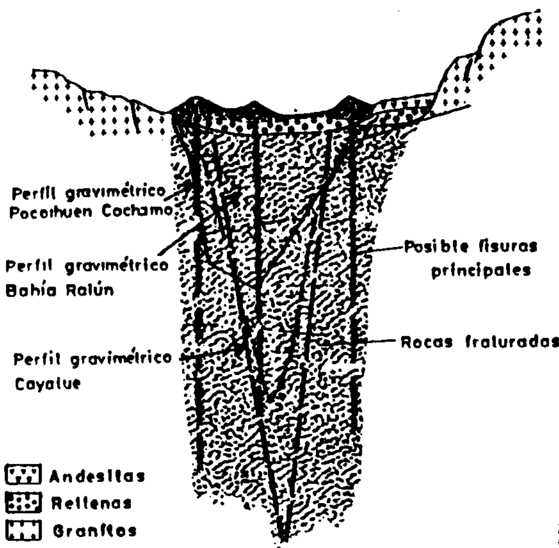


Figura 2

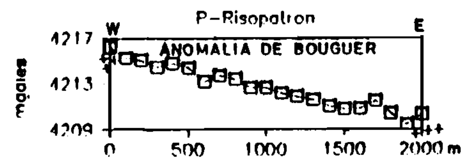


Figura 3a

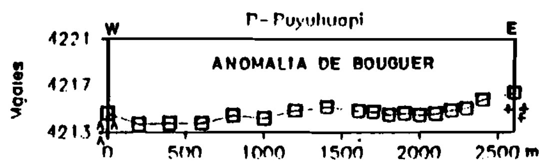


Figura 3b

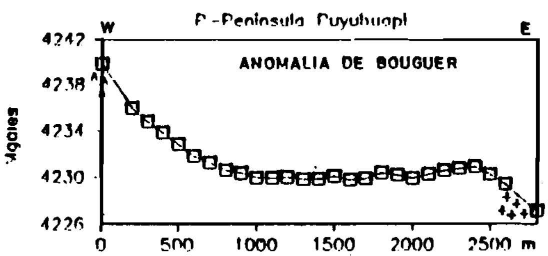


Figura 3c

# GRAVITY IN THE SOUTHERN CENTRAL ANDES, 38°-40° S

Manuel ARANEDA [(1)], María Soledad AVENDAÑO [(1)], Sabine SCHMIDT [(2)], Michael SCHMITZ [(2)], and Hans-Jürgen GÖTZE [(2)]

[(1)] Depto. de Geofísica, U. de Chile, Casilla 2777, Santiago, Chile.
[(2)] Institut für Geologie, Geophysik und Geoinformatik, FU Berlin, Malteserstraβe 74-100, D-12249 Berlin, Germany

**KEY WORDS:** Gravity field, tectonics, Southern Central Andes.

## INTRODUCTION

We present the recent data base of Bouguer Anomaly together with a preliminary interpretation of the local gravity anomalies in the regions of Traiguen-Victoria, Loncoche and Valdivia.
The gravity information was obtained during December 1995 and January 1996 introducing more than 1.000 new data points, which have been normalized and merged with the southern Chilean data base. Additionally, for the elaboration of the Bouguer anomaly map, we collaborated with the National Oil Company (ENAP) who facilitated their data base to us. The gravity map of the region, which extends from 38° to 42°S contains more than 3000 gravity stations.
The gravity survey of this study corresponds to the investigatios entitled "Integrated geophysical study of the seismic risk zone of the Southern Central Andes (38°-42°S). The area under investigation belongs to one of the most active segments of the continental margin. This is manifested in a long series of devastating earthquakes (e.g. 1960, Valdivia earthquake). The investigation also considers the active volcanoes e. g. Lonquimay, Llaima, Villarrica and others, and structures related to the formation of mountain ranges, fault systems. Distribution of gravity is essentially related to all of these. The information of gravity available before this study is contained in a continental map of Bouguer anomaly between lat. 38°-42°S based on a few gravity stations and was obtained by Dragicevic (1971) long time ago. Further there exists information from ENAP which is mainly destributed in the Central Valley.

## FIELD WORK

The spacing of stations is about 3 km along all passable roads. A higher station density e.g. a spacing of 0.2 km, 1 km to 2 km was used in a local area along the Liquiñe-Ofqui fault, volcanoe zones and geological structural zones respectively, see figure 1. All measurement were tied to the IGNS 71 gravity datum via the newly estblished National Chilean Gravity Net. Araneda and Avendaño (1993) with base stations in Temuco, Loncoche and Osorno.
Tidal corrections were computed. The drift control was done every day on a established point located at the Tolten river bridge. The drift of the LaCoste&Romberg instruments (model G 411) rarely exceede 0.5 mgal/day.
The geographic coordinates determination of the stations was possible by using a GPS portable receiver. For the elevation determination at gravity stations, altimeters were used and a special procedure to improve

the quality of the barometric measurement: time-dependent drift corrections were calculated as it is usually done for gravity measurements, using as many benchmarks and repeated measurements as possible. Error estimations showed an accuracy better than 5 m. This gives an error in the Bouguer anomaly of about 1.0 mgal.

## FIRST RESULTS

We present a map of the Bouguer anomaly with contour intervals of 20 mgal. Generally the gravity field decreases to a regional minimun of less than -100 mgal in the area of the western cordillera (recent volcanic arc) related to crustal thickening due to isostatic compensation. Local anomalies can be seen in the Traiguen-Victoria, Loncoche and Valdivia areas. There are also same weaker anomalies, as shown on the preliminary map. All positive residual anomalias are located in Central Valley.
The gravity data presented in this paper correspond to preliminary results of an on going research. The aim of this work beeing on attempt to calculate a mass balance based on Gauss's Theorem.

## ACKNOWLEDGEMENTS

We are thankful to all who gave valuble support during the field work in the Southern Andes, and to the generous financial support of the VW- Stiftung, Germany.

## REFERENCES

Avendaño M.S., Araneda M. 1993. Estado actual de la Red Gravimétrica en Chile. Taller Panamericano sobre redes geodésicas y geofísicas, Costa Rica pp 7.

Dragicevic M. 1971. Carta Gravimétrica de los Andes Meridionales e Interpretación de las Anomalías de Gravedad de Chile Central. Departamento de Geofísica Universidad de Chile .Publicación 93.

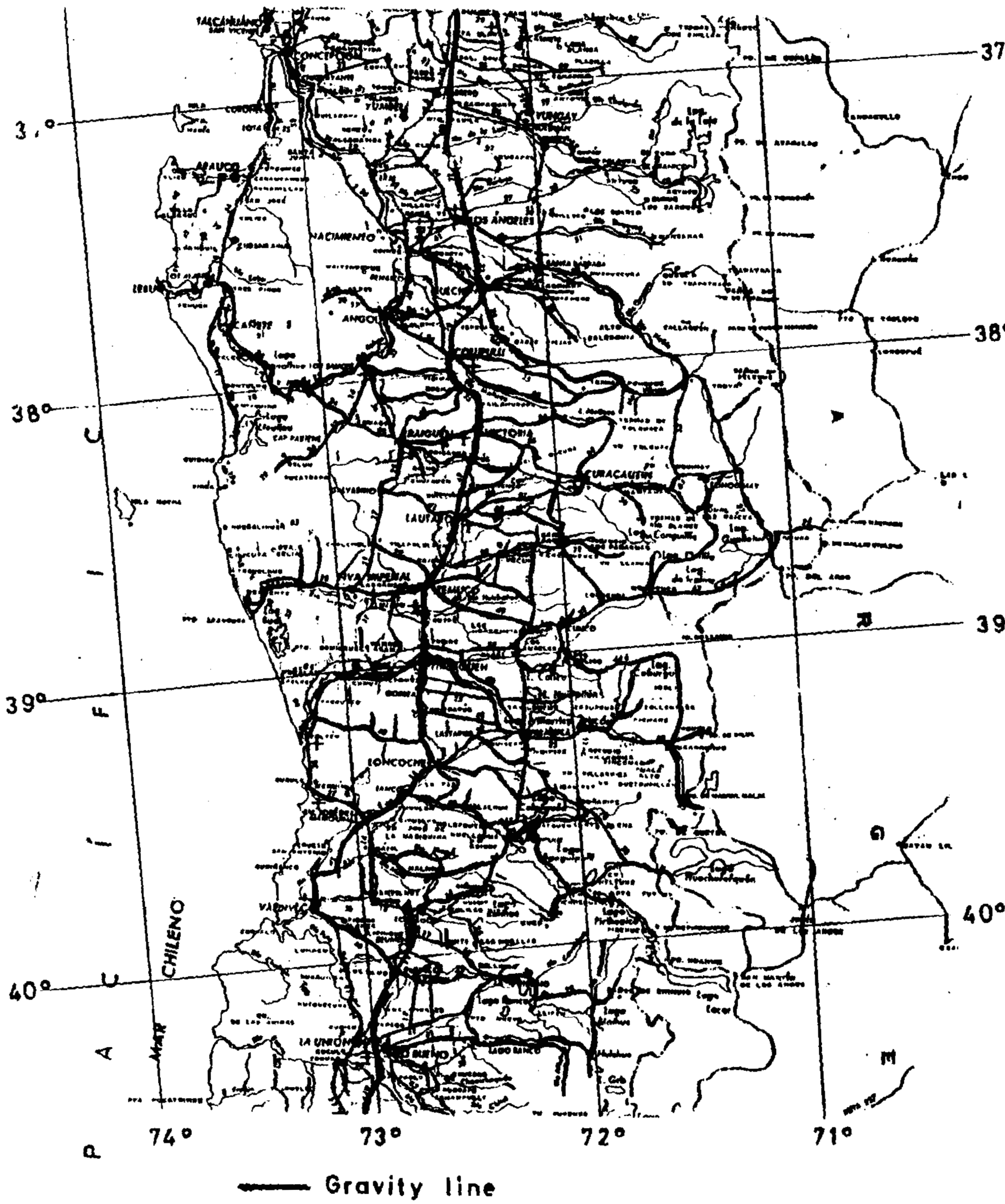
37°
38°
39°
40°
74°
73°
72°
71°
CONCEPCION
LOS ANGELES
ANGOL
VICTORIA
CURACAUTIN
LAUTARO
LONCOCHE
VALDIVIA
LA UNION
MAR CHILENO
Gravity line

FIGURE 1

# STUDY OF THE LATERAL AMPLITUDE VARIATIONS OF REGIONAL PHASES ACROSS THE ANDEAN CHAIN, AT 20°S.

David BAUMONT[1], Anne PAUL[1]

(1) LGIT-IRIGM BP 53 38041 GRENOBLE CEDEX 9 -FRANCE

In 1994, an earthquake survey organised by ORSTOM and INSU-CNRS, was carried out in Northern Chile and Bolivia (Dorbath et al., 1996), (Dorbath et al., this volume). Across an East-West section of the Andes at the latitude of 20°S along 700 km, 56 short period seismic stations of the Lithoscope network were installed during 6 months between June and November. The temporary network ran across the main structural features of the Andes: the coastal range, the Western cordillera, the Altiplano, the Eastern cordillera and the subandean zone. It was composed of 41 one component seismometers ($T_o$=1sec) and of 15 three component ones ($T_o$=5sec). The three component seismometers were installed at every third site.

To infer characteristics of the structure of the crust and of the upper mantle, we study the lateral variations of the amplitudes of the P and S waves along our almost linear network. We focus on regional phases such as Lg waves (Campillo, 1990), which are very sensitive to the variations of the structure of the crust (Chazalon, 1993), thus, very valuable for our studies. In order to study the regional phases, we have selected 17 regional or local events which occured at depth lower than 60 km and for which the hypocentral location is well constrained (Masson et al., this volume). The azimutal repartition of these crustal earthquakes should allow us to point out if the anomaly of propagation of Lg waves along paths perpendicular to the trend of the Andes (Chinn, 1980), really exists. A detailed examination of the seismograms shows strong variations of the amplitudes of the waves. Using simulations, we build synthetic seismograms to better understand interactions of these waves with possible models of crustal structures.

Using deeper local or regional events, we purpose to study the propagation of the direct wave through the upper mantle, for instance beneath the Altiplano.

## REFERENCES

CAMPILLO M.,1990, Propagation and attenuation characteristics of the crustal phase Lg, Pure appl. Geophys., **132**, 1-19.

CHAZALON A., CAMPILLO M., GIBSON R. and CARRENO E., 1993, Crustal wave propagation anomaly across the Pyrenean Range. Comparison between observations and numerical simulations, Geophys. J. Int., **115**, 829-838.

CHINN D.S., ISACKS B.L. and BARAZANGI M., 1980, High-frequency seismic wave propagation in western South America along the continental margin, in the Nazca plate and across the Altiplano, Geophys. J. R. astr. Soc., **60**, 209-244.

DORBATH C., PAUL A. and the Lithoscope Andean group, 1996, A tomography of the Andean crust and mantle at 20°S: First results of the Lithoscope experiment, PEPI in press.

# ANOMALOUS CRUST IN THE CENTRAL ANDES

Susan Beck[1], George Zandt[1], Stephen Myers[1], Terry Wallace[1], Paul Silver[2], Lawrence Drake[3], Estela Minaya[3]

[1]SASO and Dept. of Geosciences, University of Arizona, Tucson, AZ, U.S.A., [2]Carnegie Institution of Washington, DTM, Washington, D.C., U.S.A., [3]San Calixto Observatorio, La Paz, Bolivia

**KEY WORDS**: Altiplano, Crustal Structure, Poisson's ratio, Crustal thickness, Central Andes

## INTRODUCTION

The central Andes, in western Bolivia and northern Chile are the highest and widest mountains associated with regions of ocean-continent convergence. The Andes attain their greatest width in central South America where the Altiplano is bordered on the west by the Cordillera Real (an active volcanic arc) and on the east by the Cordillera Oriental (high mountain range dominated by folding and thrusting) and the Sub-Andean zone (a thin-skin fold and thrust belt). In 1994 and 1995 we deployed two broadband three-component seismic arrays in the central Andean Cordillera of Bolivia and northern Chile with a total of 24 stations (Fig. 1). Our seismic experiment consisted of an east-west transect called the BANJO (Broadband ANdean JOint) experiment and a north-south transect called the SEDA (Seismic Exploration of the Deep Altiplano) experiment. The BANJO experiment consisted of 16 broadband seismic stations along an east-west transect at 19°S to 20°S and extended for nearly 1000 km from near the coast of northern Chile to the Chaco Plain. The SEDA experiment consisted of 7 stations that were deployed in a 350 km north-south transect along the eastern boundary of the Altiplano, between La Paz and Uyuni, Bolivia. We estimated crustal parameters along an east-west transect across the Andes at latitude 20°S and along a north-south transect along the eastern edge of the Altiplano from data recorded on these two arrays.

## CONCLUSIONS

Our passive deployment recorded numerous intermediate-depth earthquakes at near-regional distances. Capitalizing on this source-receiver geometry, we have identified and analyzed shear-coupled P waves trapped within the crustal waveguide. We refer to these phases collectively as "sPnl" due to their similarity to the often observed Pnl wavetrain generated by crustal earthquakes. We modeled several

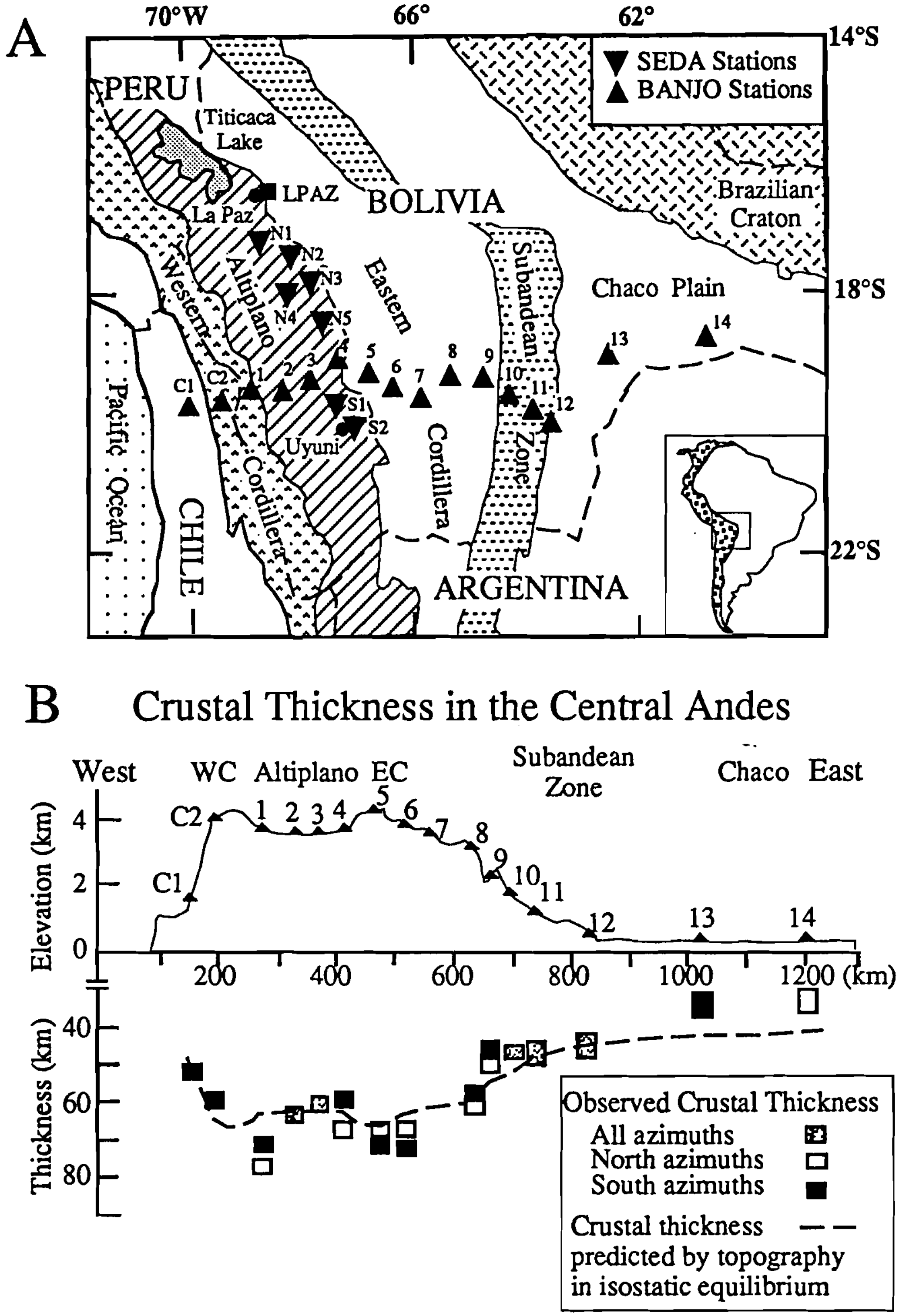


Figure 1: (A) Map showing the station locations in the central Andes. (B) East-west cross-section near 20°S showing topography and estimates of crustal thickness beneath each station.

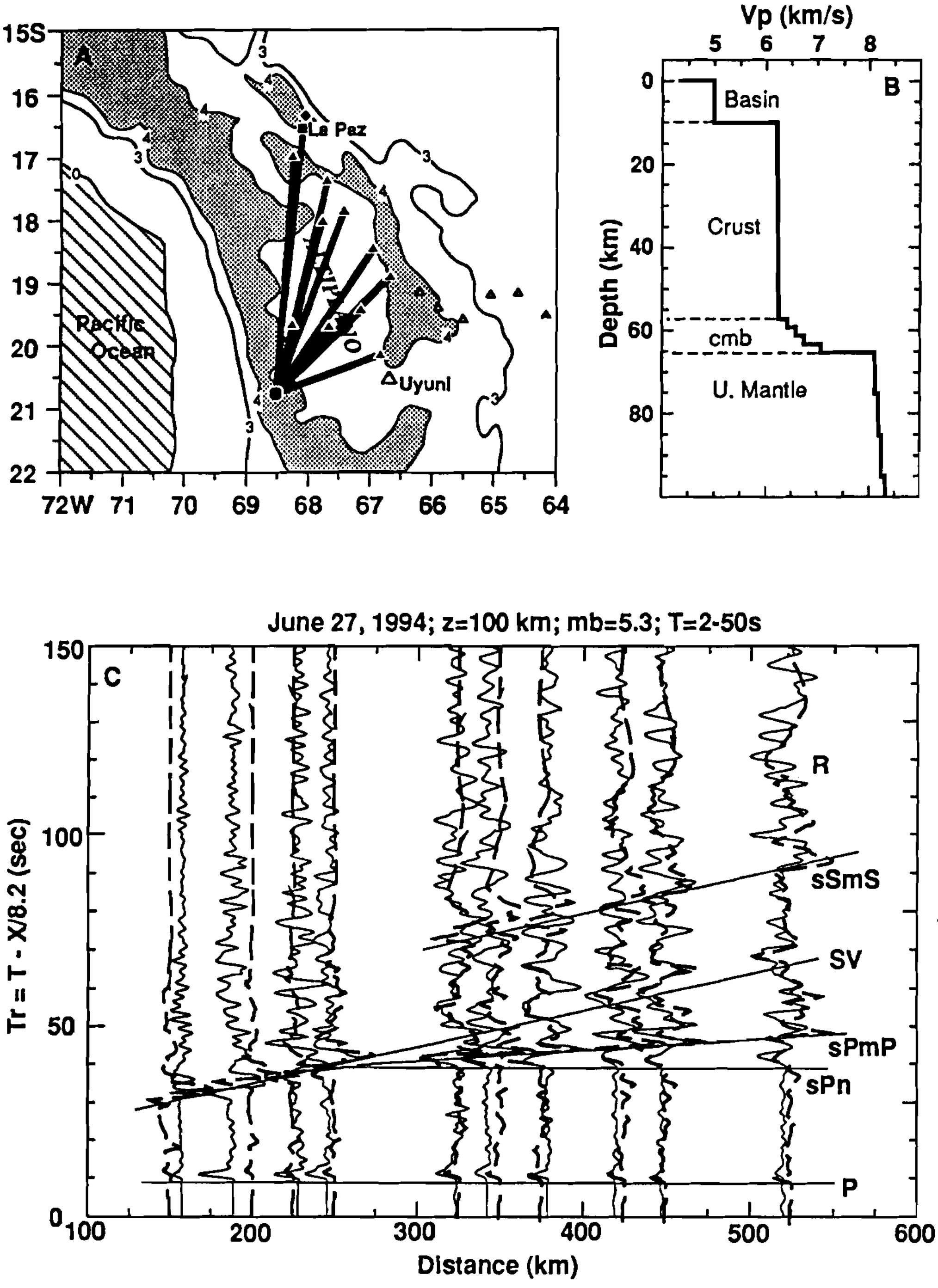


Figure 2: (A) Map showing the location of the stations and the earthquake on June 27, 1994. (B) Best crustal P-wave velocity model determined from the regional waveform modeling. (C) Reduced travel time plot showing the vertical component regional data (thin solid lines) and synthetics (thick dashed lines) for the crustal model shown in B. Major regional phases are shown on the right.

regional distance events to determine average crustal parameters for the Altiplano. The Altiplano crust is characterized by an anomalouly low mean velocity of 6.0km/sec, a Poisson's ratio of 0.25 and a crustal thickness of 65 km (Fig. 2). The combination of low P wave velocities and low Poisson's ratio suggest a thick silicic bulk composition for the crust.

Waveforms of deep regional events in the down-going Nazca slab and teleseismic earthquakes were processed to isolate the P-to-S converted phases from the Moho in order to estimate the crustal thickness. We found crustal thickness variations of nearly 40 km across the Andes, with maximum crustal thicknesses of 70-74 km under the Cordilleras and 32-38 km thick crust 200 km east of the Andes in the Chaco Plain (Fig. 1). The crust also appears to thicken from north (16°S, 55-60 km) to south (20°S, 70-74 km) along the Cordillera Oriental. The Sub-Andean zone crust has intermediate thicknesses of 43 to 47 km. Crustal thickness predictions for the Andes based on Airy-type isostatic behavior show remarkable overall correlation with observed crustal thickness in the regions of high elevation (Fig. 1). In contrast, at the boundary between the Cordillera Oriental and the Sub-Andean zone and in the Chaco Plain, the crust is thinner than predicted, suggesting the crust in these regions is supported in part by the flexural rigidity of a strong lithosphere. The observation of Airy-type isostasy is consistent with thickening associated with compressional shortening of a weak lithosphere squeezed between the stronger lithosphere of the subducting Nazca plate and the cratonic lithosphere of the Brazilian shield.

# ELECTRICAL CONDUCTIVITY STRUCTURES IN NORTHERN CHILE

Heinrich BRASSE [(1)], Fritz ECHTERNACHT [(1)], Markus EISEL[(2)] and Sebastian TAUBER [(1)]

(1) Freie Universität Berlin, Fachrichtung Geophysik, Malteserstr. 74-100, D-12249 Berlin, Germany
(2) GeoForschungsZentrum Potsdam, Telegraphenberg, D-14473 Potsdam, Germany

**KEY WORDS:** Central Andes, electrical conductivity, magnetotellurics, partial melts

## INTRODUCTION

During the last ten years, electromagnetic investigations have been carried out in the Central Andes to study the conductivity structure of the active subduction zone at the South American western margin (Schwarz et al. 1994). They are part of an integrated geological and geophysical project, which also comprises seismic refraction, reflection and gravity studies. The working area is located north and south of the tropic of Capricorn, between the Chilean town of Antofagasta to the Andean foreland in Bolivia and Argentina (Fig. 1).

While natural variations of the horizontal geomagnetic and geoelectric (telluric) field are measured in the magnetotelluric (MT) method, geomagnetic deep sounding (GDS) additionally utilizes the vertical component of the magnetic field. Both methods allow an estimation of conductivity distribution of the subsoil, with depth of penetration depending on period length. The results of data analysis and conductivity (resistivity) modelling for the magmatic arc and forearc regions will be presented in this contribution.

## CONDUCTIVITY DISTRIBUTION IN THE ARC AND FOREARC

The earlier magnetotelluric measurements - carried out along two transects across the Andes (Schwarz et al. 1994, Schwarz & Krüger 1996) - revealed a prominent high conductivity zone (HCZ) beneath the Western Cordillera, which constitutes the present magmatic arc. Two-dimensional models were calculated for data on profiles A and B (Fig. 2, cf. Krüger 1994 and Massow 1994). Commencing at a depth of approx. 20 km, the depth extent of this anomaly is still remaining uncertain but is likely to execeed 60 km. Extremely long period measurements ($T > 1$ day) are necessary to penetrate through this conductor, since resistivity values - derived from 2-D modeling - are remarkably low (0.5 - 2 $\Omega$m).

Recent developments led to completely new magnetotelluric instruments, which enable a broadband recording of electromagnetic variations in the period range from approx. 0.0001 s to more than 1 day and thus yield a resolution of very shallow as well a deep structures. Two field campaigns were carried out in 1993 and 1995 in the north of the previous measuring areas, covering two transversal profiles in Northern Chile, one through the Quebrada de Guatacondo, the other in the area of the town of Pica (profile C in Fig. 1). Again a distinct HCZ was detected, but instead of being located below the magmatic arc, it is surprisingly shifted to the west below the Precordillera. In this region - the so-called Pica gap - no recent volcanism has occured. The electromagnetic data thus hint at a N-S segmentation of the magmatic arc in accordance with geochemical results (Wörner 1994).

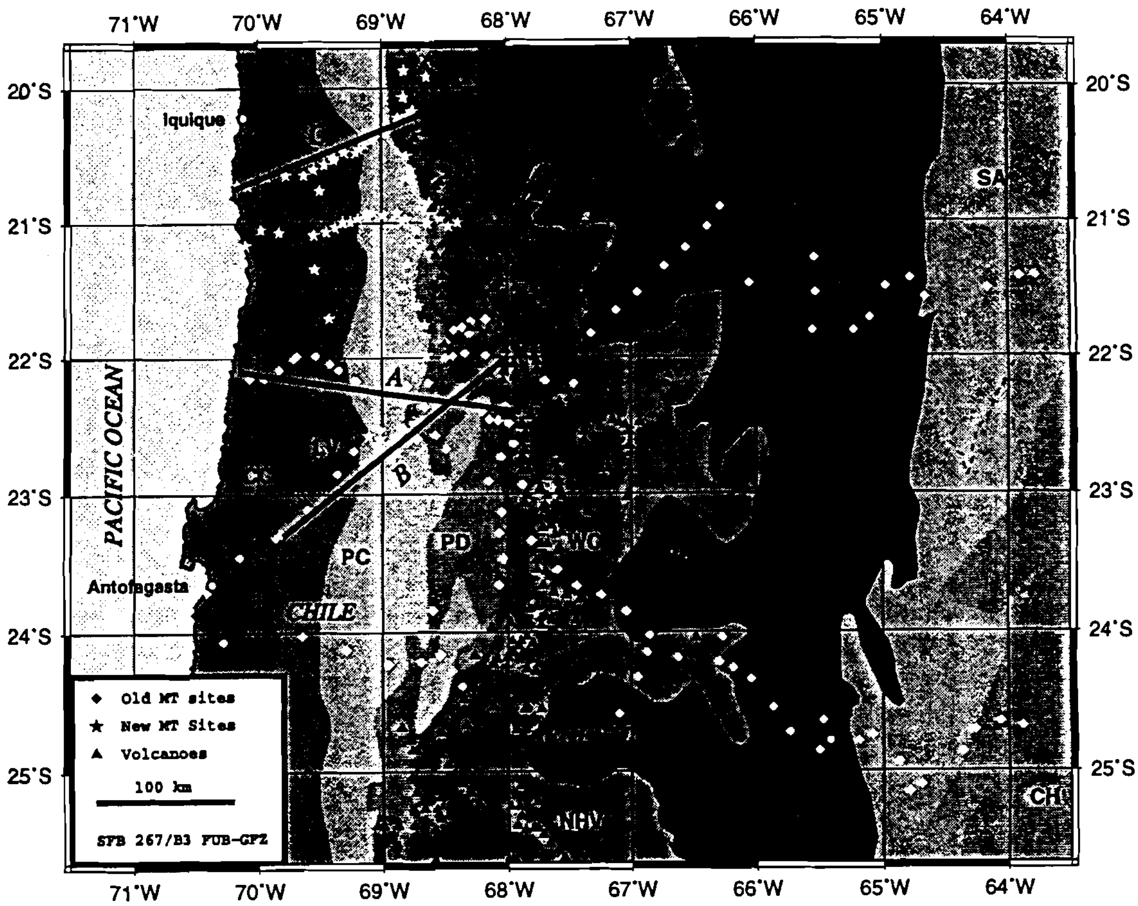


Fig. 1: Location of electromagnetic sites in the Central Andes. Two-dimensional models were calculated for profiles A-C (see Fig. 2).

Three fossil magmatic arcs constitute the area west of the Western Cordillera, which have evolved since the Jurassic. As the oldest of these arcs the Coastal Cordillera, with its occurence of vast batholites, is characterized by high resistivities, but also by anisotropic structures (modelled as dikes in Fig. 2A), which may be due to the influence of the large Atacama fault system, originating from oblique convergence of the former Farallon plate.

The actual slab of the subducted Nazca plate does not appear as a good conductor in model A, which may be explained by the complicated three-dimensional conductivity distribution in the forearc. Despite the highly resistive batholites near the coast, large parts of the forearc crust exhibit suprisingly low resistivities, which is unusual for a consolidated crust and may indicate a generally high amount of fluids, released from the subducted oceanic plate.

In the northern cross section C a diffuse conductive feature is modelled in the middle crust below the Coastal Cordillera. It is not yet clear, if this anomaly is due to released fluids from the slab or/and if there exists a connection to the possibly deep reaching Atacama fault system.

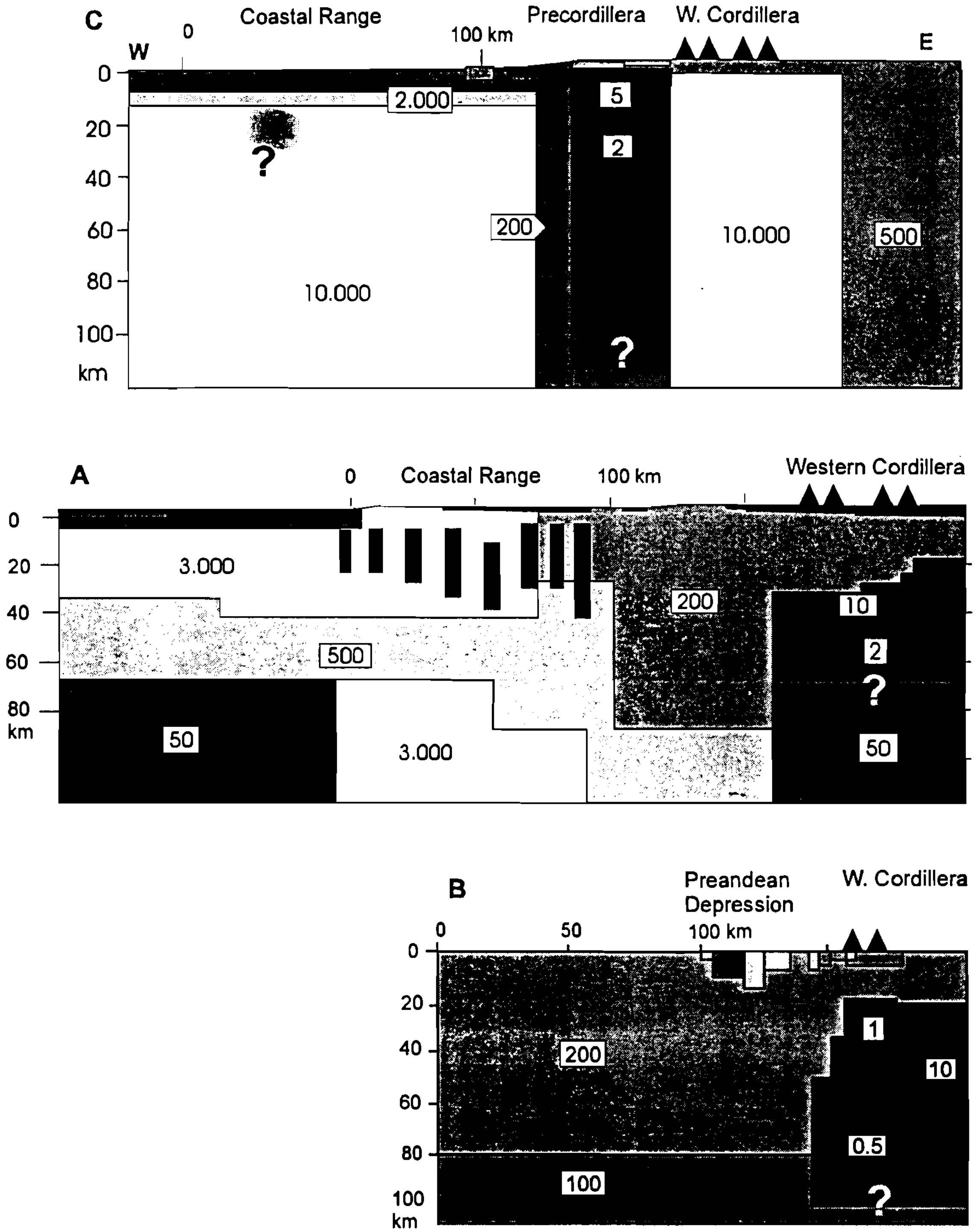


Fig. 2: 2-D models of electrical resistivity derived from electromagnetic measurements along profiles A-C in Northern Chile. Resistivity values in Ωm. Further explanation see text.

## PARTIAL MELTS AS AN EXPLANATION OF THE HIGH CONDUCTIVITIES?

To understand the nature of the petrophysical processes leading to the dominant anomalies below the magmatic arc, the results of other geophysical investigations have to be taken into account. The subduction of the Nazca plate is relatively steep with an angle of 30°. Gravity and seismic investigations indicate a crustal thickness of about 70 km. Several low velocity zones were detected below the magmatic arc. In addition, a zone of high attenuation of seismic waves was deduced from measurements of a recent seismological network, coinciding with the region of high conductivity. There is a distinct correlation between a low of the residual gravity field (approx. -40 mGal) and the strike of the volcanic chain.

Although graphite and large amounts of saline fluids are often responsible for conductivity anomalies, the most likely explanation of the high conductivity values below the volcanic arc is the assumption of vast amounts of partial melts, originating in the release of water from the subducted oceanic plate at about 100 km depth. Laboratory measurements demand a temperature of at least 640 °C and a partial melting rate of at least 20% of silicic magmas to account for conductivities in the range of 1 Siemens/m. Although the actual thermal flow is not well known in this part of the Andes, this constrain should not constitute a major obstacle below a volcanic arc at a depth of >20 km. The existence of other fluid phases may not be excluded, however, and they may even play a substantial role in the explanation of the HCZ. It will be virtually impossible to distinguish between these two sources unless detailed temperature and heatflow data are available.

The large anomaly below the Precordillera in profile C does not necessarily oppose the assumption of this model, if the recent steepening of subduction is taken into account: the low resistivities would thus indicate a region of newly formed partial melts. On the other hand, the assumed prolongation of the Falla Oeste may also have to be taken into account.

## CONLUSIONS

Electromagnetic investigations in the arc and forearc regions of Northern Chile revealed extensive highly conducting zones in a depth of approx. 20-60 km beneath the volcanic chain of the Western Cordillera. Partial melts are discussed as the most likely explanation of the anomalies, especially with regard to gravity and seismic results. The conductive zone is obviously correlated with recent vocanic activity, and is shifted towards the forearc in the so called Pica gap. Future work will concentrate on investigations on a profile in the forearc and Altiplano, where a seismic reflexion programme will also be carried out.

These investigations were conducted within the framework of the Special Research Project "Deformation processes in the Central Andes" at the Free University of Berlin and the Geoforschungszentrum Potsdam in close cooperation with geoscientific institutions in Santiago, Antofagasta and Salta.

## REFERENCES

Echternacht, F., Tauber, S., Eisel, M., Brasse, H., Schwarz, G. & Haak, V. (1996): New broadband electromagnetic measurements to study the active continental margin in Northern Chile, submitted to Phys. Earth. Planet. Int.

Krüger, D. (1994): Modellierungen zur Struktur elektrisch leitfähiger Zonen in den südlichen zentralen Anden, Berliner geowiss. Abh. (B), 21, Selbstverlag Fachbereich Geowiss., Free Univ. of Berlin.

Massow, W. (1994): Magnetotellurik in der Westkordillere Nordchiles, unpublished Diploma thesis, Fachrichtung Geophysik, Free Univ. of Berlin.

Schwarz, G., Chong D.G., Krüger, D., Martinez, M., Massow, W., Rath, V. & Viramonte, J. (1994): Crustal high conductivity zones in the southern Central Andes, in: Reutter, K., Scheuber, E., Wigger, P. (eds.): Tectonics of the Southern Central Andes, Springer, Berlin.

Schwarz, G. & Krüger, D. (1996): Resistivity cross section through the Southern Central Andean Crust as inferred from 2-D modelling of magntotelluric and geomagnetic deep sounding measurements, submitted to J. Geophys. Res.

Wörner, G., Moorbath, S., Horn, S., Entenmann, J, Marmon, R.S., Davidson, J.P. & Lopez-Escobar, L. (1994): Large- and Fine-Scale Geochemical Variations along the Andean Arc of Northern Chile (17.5° - 22° S), in: Reutter, K., Scheuber, E., Wigger, P. (eds.): Tectonics of the Southern Central Andes, Springer, Berlin.

# CENOZOIC DEFORMATION ACROSS SOUTH AMERICA: CONTINENT-WIDE DATA AND ANALOGUE MODELS

Peter R. COBBOLD(1), Peter SZATMARI(2), Claudio LIMA (1,2) and Eduardo A. ROSSELLO(3)

(1) Géosciences-Rennes (UPR 4661 du CNRS), 35042 RENNES Cédex, France
(2) CENPES Petrobrás, Cidade Universitária, 21910 Rio de Janeiro, Brasil
(3) CONICET y Departamento de Geología, Universidad Nacional, 1428 Buenos Aires, Argentina

**KEY WORDS**: South America, Cenozoic, continent-wide deformation, data, analogue models

## INTRODUCTION

According to current seismicity, stresses and plate tectonics, South America is in a state of approximately east-west compression. This is basically attributable to ridge push from the Atlantic and East Pacific rises, modulated by slab pull at the Andean margin. In detail, horizontal compressive stresses vary in trend, especially towards the corners of the continent, where additional forces are associated with strike-slip motions of the Caribbean and Scotia plates, counterclockwise rotation of the Caribbean plate, ongoing collision of Central America with South America and mechanical contrasts between continental and oceanic lithospheres.

The plate tectonic setting of South America has not changed fundamentally since the opening of the Atlantic in the Early Cretaceous. Crustal thickening has accumulated all along the Andes. Thickening appears to have started in the Albian and to have gone through paroxisms in the Early Tertiary and Miocene, all periods of relatively rapid convergence at the Andean margin. Complications can be attributed to collision of Central America in the Miocene, splitting of the Farallon plate into the Nazca and Cocos plates, collision and northwards migration of the East Chile rise, and other events.

Outside the Andes, there is evidence for Cenozoic faulting and deformation at many localities, including the Atlantic margin and central regions of South America. In this paper, we attempt a synthesis of such data at continental scale, paying particulat attention to the reactivation of Mesozoic, Paleozoic and Precambrian faults by Cenozoic stresses. We then compare the data with analogue models of South American plate tectonics.

## DATABASE

Current seismicity is concentrated in the subducting oceanic slabs and in the Andes. We also consider intraplate seismicity and stresses deduced from borehole breakouts. Compressive stresses act across the entire continent. Although their average trend is east-west, there are significant deviations. Stresses tend to act parallel or perpendicular to the eastern margins of Brazil.

Digital topographic maps show how (1) large areas of South America have average altitudes of 1000 m or more, whereas other large areas are near sea level; and (2) ridges or scarps with sharp relief cross-cut the continent. To satisfy estimated rates of erosion, such topographic features must have been maintained by ongoing Tertiary vertical motions.

We have also used geological data obtained at outcrop, subsurface data from the petroleum industry, satellite imagery, and paleomagnetic, geochronological and fission-track data.

## EVIDENCE FOR CENOZOIC DEFORMATION ACROSS SOUTH AMERICA

1. Serra do Mar

The Serra do Mar forms a prominent escarpment up to 2800 m high on the Atlantic coast of Brazil. Outcropping Precambrian gnesisses and granitoids have been shaped by recent erosion into an inselberg topography. Recent studies of apatite fission tracks show that exhumation has been active during the Tertiary. The eroded material has been deposited offshore in the Campos and Santos basins, where the Tertriary succession is several km thick. Exhumation has been attributed to isostatic rebound of an eroded rift shoulder, formed during the Early Cretaceous. However, this process requires an unusually thick elastic lithosphere and an unusually small initial rift shoulder. We prefer to invoke Tertiary compression. Evidence for this is provided, not only by the current stress state, but also by geological data. A Proterozoic shear zone, running from Sao Paulo to near Rio de Janeiro, has been reactivated during the Tertiary, to form the Taubaté basin. Tertiary sediments are offset by synkinematic and postkinematic faults. Strike-slip motions dominated throughout the Tertiary, becaming transpressive in the Neogene. In the Itaboraí Basin near Rio de Janeiro, strike-slip faults are ubiquitous within Paleogene fresh-water limestones. Topographic bulges mark both the NE and SW ends of the Precambrian shear zone, which was reactivated right-laterally.

2. Central Brazilian Highlands

The Central Brazilian Highlands are mostly over 800 m high and they occupy an area over 1000 km wide. The area is wider than any single rift shoulder associated with Atlantic rifting. Moreover, according to gravity data, topography is compensated at depth over most of the area, probably by a Moho up to 50 km deep. Precambrian crystalline basement crops out over most high parts, whereas valleys and basins contain Tertiary, Mesozoic or Paleozoic sediments. Intraplate seismicity is associated with basement highs. Prominent ridges bound the Tertiary basins. Some of these ridges we identify as active faults, of reverse or strike-slip senses.

3. Northeastern Brazil

The Potiguar Basin, which formed as a rift in the Early Cretaceous, shows positive inversion from the Albian onwards. In the Araripe Basin, marine sediments are currently perched at altitudes over 500 m.

4. Paraná Basin and Pantanal

The Paraná Basin conatins a thick sequence of marine Paleozoic sediments, capped by Early Cretaceous basalts, and a thin sequence of Late Cretaceous to Tertiary continental sediments. The edges of the basin have been uplifted, tilted inwards and bevelled by ersoion. Some of this inversion occurred in the Triassic, after a Variscan phase of folding and thrusting; but most of it post-dates the basalts and is attributable to Andean compression.

The Pantanal Basin contains a sequence of Tertiary sediments, several km thick. At the edges of the basin, the base of the Tertiary is offset across reverse faults. Within the basin, folds and reverse faults are visible at outcrop and on seismic lines. To the west, the Chiquitos hills form a linear scarp up to 1400 m high, where the Precambrian basement has been reactivated as a left-lateral wrench zone and overlying Cretaceous and Tertiary sediments show folds and thrusts.

5. Eastern Patagonia

Eastern Patagonia is a plateau up to 1000 m high. Outcropping Late Cretaceous marine sediments prove Tertiary uplift. Seismic and well data reveal a phase of Early Cretaceous extension, followed by a history of basin inversion, fault reactivation, folding and thrusting, which started in the Albian and has continued until the present day.

6. Central and Northern Argentina

The Sierras Australes of Buenos Aires province form a prominent ridge about 1000 m high, where Paleozoic sediments crop out. Rocks underwent low-grade metamorphism, folding and thrusting during the Cape Orogeny (Permo-Triassic). Mesozoic rifts are visible on seismic lines across adjacent basins. However, the current topography is due to Tertiary reactivation of Paleozoic thrusts.

The Sierras Pampeanas of Northwestern Argentina are ranges up to 5000 m high, separated by basins, some with internal drainage. The ranges consist of Precambrian metamorphic basement with mylonitic thrust zones, attributable to the Ocloyic or Taconic orogeny (Silurian). Later Mesozoic rifts became inverted during the Tertiary. Basement blocks became tilted by reactivation of Precambrian and Paleozoic thrusts. The vergences of Tertiary thrusts are inherited from those of the basement.

7. Southern Andes and Magellan Basin

The Southern Andes form an arc, concave to the NE. Altitudes are mostly below 2000 m. Rifting in the Jurassic and back-arc extension during the Early Cretaceous were followed by Andean compression, from the Albian onwards. During the Tertiary, the regional shortening direction was NE. Transpressional conditions predominated, left-lateral in Tierra del Fuego, right-lateral in the Southern Andes. Slow convergence, thrusting and rapid glacial erosion exposed Late Cretaceous amphibolites in Cordillera Darwin. The foreland Magellan basin filled with up to 7 km of Tertiary sediments. Fold-and-thrust belts developed along the Andean foothills. A system of Tertiary rift valleys, trending along the Straits of Magellan, separated the island of Tierra del Fuego from the mainland.

8. Central Andes

From northwestern Argentina to southern Peru, the Altiplano is a major topographic and structural feature, some 4000 to 5000 m high. In Bolivia, the Altiplano is underlain by 10 km of Tertiary sediments. These were trapped between thrusts of opposite vergences, bounding the Cordillera Real to the west and the Cordillera Oriental to the east. In the Cordillera Oriental, Cretaceous rifts, some with marine sediments, became inverted during the Early Tertiary. However, the main crustal structure is a thin-skinned tectonic prism, formed by reactivation of Paleozoic thrusts and inversion of a deep Paleozoic basin. Beyond the mountains to the east is a Tertiary foreland basin.

In NW Argentina, the Puna plateau is a crustal prism, where Tertiary forethrusts and backthrusts separate ridges of Paleozoic and Precambrian basement from basins with internal drainage, underlain by several km of Tertiary sediments. Almost all thrust vergences were inherited from Paleozoic (Ocloyic) and Precambrian equivalents. Tertiary vulcanism is associated with Andean compression. Some volcanoes are aligned along left-lateral, SE-trending wrench zones, which are the reactivated edges of Paleozoic basins.

Rotations about vertical axes, demonstrated by paleomagnetic studies, are clockwise in the south, counterclockwise in the north. They have played a fundamental role in the building of the Central Andes, allowing the central part to advance eastwards more than its southern or northern margins.

In Peru, the main Tertiary thrusts of the Eastern Cordillera are reactivated Early Paleozoic thrusts. Associated Late Paleozoic and Mesozoic basins became inverted, forming the current Andean foothills. The Brazilian crystalline basement became downwarped under the Ucayali and Marañón foreland basins.

9. Northern Andes

In Ecuador and Colombia, crustal thickening was accompanied by right-lateral wrenching in the Paleogene. The shortening direction veered towards the SE during the Neogene, reflecting collision with Central America. The Western Cordillera of Colombia is an uplifted magmatic and volcanic arc, separated from the Cordillera Oriental by the Magdalena ramp basin with its several km of Tertiary sediments. In the

Cordillera Oriental, an Early Cretaceous rift has been inverted. Marine sediments, exhumed at altitudes of up to 4000 m, show low-grade metamorphism. To the east, the Llanos foreland basin is filled with several km of Tertiary sediments. However, the main Tertiary thrusts of the Cordillera Oriental are reactivated basement structures. Episodes of thrusting and associated metamorphism occurred in the Precambrian, Early Paleozoic and Late Paleozoic. The intense Late Paleozoic episode (due to collision of North and South America) differentiates the Northern Andes from the Central Andes.

Towards the Caribbean plate boundary, the Andes of Northern Colombia and Venezuela show increasing components of right-lateral wrenching parallel to the Caribbean plate boundary. The antithetic left-lateral Bucaramanga Fault is a reactivated basement feature and has helped spread the deformation well into the continent.

## ANALOGUE MODELS

We have investigated the plate tectonics of South America and the possibility of continent-wide deformation, using analogue models at fully lithospheric scale. Brittle upper crust was modelled with dry sand; ductile lower continental crust and lithosperic mantle, with silicone putties of appropriate viscosities and densities. For oceanic lithosphere, the ductile lower crust was omitted. Continental South America was given an appropriate triangular shape. The model lithosphere floated on a less viscous asthenosphere. Horizontal forces and velocities were applied at eastern and western boundaries, to simulate spreading at Atlantic and Pacific mid-oceanic ridges. Subduction initiated spontaneously at the Pacific margin of South America. Either crustal thinning or crustal thickening occurred at the Pacific margine, depending on the ratio between the weight of the subducting oceanic slab and the applied rate of convergence. By changing this ratio during the course of an experiment, it was possible to induce tectonic inversions.

For high rates of convergence, deformation tended to occur also at the eastern margin of continental South America, or even in central areas. Because of the triangular shape of the continent, strike-slip motions occurred at boundaries oblique to the convergence direction. At the Pacific margin, partitioning was observed, between dip-slip motions of the subducting slab and strike-slip motions next to it. Strike-slip motions also occurred at the sides of the continent, right-lateral in the north and left-lateral in the south. These motions caused local modifications in the directions of shortening.

In some experiments, we introduced initial weaknesses, by reducing the thickness of the brittle upper crust. In such weak areas, deformation became concentrated, leading to changes in the shape of the continent. A weak area in the central part of the Pacific margin led to indentation of that margin. This may explain the formation of the Arica elbow and the concentration of deformation in the Central Andes.

## CONCLUSIONS

Tertiary compression and crustal thickening are widespread across South America. Crustal thickening is concentrated in the Andes, but significant in other areas, including the Atlantic margin of Brazil. Across South America, Tertiary reverse and strike-slip faults are mostly due to reactivation of similar structures formed during Paleozoic or Precambrian orogenies. Andean compression and crustal thickening are widely documented from the Albian onwards, but appear to have increased in intensity in the Neogene. Wrenching is ubiquitous at the ends of South America, right-lateral against the Caribbean plate and left-lateral against the Scotia plate. In analogue models, forces and velocities applied to the oceanic lithosphere resulted in subduction at the Pacific margin. Deformation was either extensional or compressional, depending on the ratio between the weight of the subducting slab and the rate of convergence at the Andean margin.

# THREE DIMENSIONAL *P*-WAVE TOMOGRAPHY AROUND ANTOFAGASTA, NORTHERN CHILE: STRESS DISTRIBUTION ALONG THE DEEPER PART OF THE SUBDUCTING NAZCA PLATE

Diana COMTE(1) and Mario PARDO(1)
Tony MONFRET(1,2)
Günter ASCH(3), Frank GRAEBER(3) and Alexander RUDLOFF(3)

(1) Depto. de Geofísica, Universidad de Chile, Casilla 2777, Santiago, Chile
(2) Mission ORSTOM, Chile, Román Díaz 264, Santiago, Chile
(3) GeoForschungsZentrum, Potsdam, Dept. 2.4, "Seismology&Tomography", Telegrafenberg A17, D-14473, Potsdam, Germany

KEY WORDS: Seismicity, Northern Chile, 3D Tomography, Stress Distribution

## INTRODUCTION

Northern Chile is located in one of the most active seismic zones of the Circum-Pacific belt, where the subduction is characterised by a young and fast oceanic Nazca plate, which is underthrusting the South American plate. This process, therefore, is associated with a strongly coupled seismogenic interplate contact, which is capable to nucleate large earthquakes. The last great earthquake in northern Chile occurred on May 10, 1877 (Mw~8.7); using the available historical reports, this event seems to be the largest one that took place there. The 1877 rupture area suggests that it ranges from the south of Arica (19°S) to the north of Antofagasta (23°S) reaching approximately 450 km of rupture along the coastline. Using the 1877 earthquake as reference and considering that during this century, has not occurred any thrust event with comparable size, this area has been defined as the Northern Chile seismic gap.

There have been many investigations oriented to better understand the tectonic framework of this gap, some of them using teleseismic data and others, locally recorded microearthquakes. The main behaviours observed with teleseismic data are in agreement with that obtained using local data, however, local data have permitted to obtain a more detailed behaviour of the subducting slab, with the advantage that locally recorded microearthquakes were obtained with only few weeks of observations in comparison with the available teleseismic data obtained along ~30 years. One of the most interesting behaviour observed in the seismicity of intermediate depths using local networks in northern Chile, is the inverted double seismic zone located at about 100 km in depth, that exhibits both normal and reverse faulting microearthquakes in a close spatial relationship, where downdip tensional events are, in general, shallower than the compressional ones [1]. Local data had been also used to obtain a 2D *P*-wave velocity model evidencing a thin layer of oceanic crust attached to the top of the subducting Nazca plate that reaches ~60 km in depth with a *P* wave velocity of 7.3 km/s [2]. Considering that the 2D body wave velocity models consisted of big structures and the focal mechanisms of the double seismic zone have nodal planes not well resolved because the networks used were located mainly near the coast, we added in this work new data recorded by a temporary network, with a complete coverage from the coast to the Andes Cordillera (Figure 1), in order to simultaneously localize the hypocenters and determine 3D lateral heterogeneous seismic velocity structure. We also performed a formal inversion of the best fitting stress tensor based on the first motion polarities of the *P* waves.

## DATA ACQUISITION AND METHOD

Three different sets of *P* and *S* arrival times locally recorded are used in this study. One set corresponds to 336 microearthquakes recorded during the overlapping period of the PISCO and CALAMA networks (5 weeks). The CALAMA network consisted of 11 portable short period vertical analog and digital stations (Figure 1) of the University of Chile through a joint project with ORSTOM. The CALAMA network improved the western coverage of the PISCO network of the Collaborative Reseacrh Center 267 "Deformation processes in the Andes" formed by the Free University of Berlin, the GeoForschungsZentrum at Potsdam, and the Technical University of Berlin, and the eastern coverage of the permanent telemetric seismic network of Antofagasta, installed with the collaboration of the University of Chile, ORSTOM and the IPG, Strasbourg, France. The PISCO network consisted of 32 digital seismic stations, where the majority of them were installed to the east of the Salar de Atacama, near the Chilean and Argentina political boundary. The permanent telemetric network of Antofagasta, installed in June 1990 near the coastline, corresponds to 8 short period vertical stations and one three-component central station. The second set of data used in this study corresponds to 575 microearthquakes recorded by the permanent network of Antofagasta during 1993. The third dataset consisted in 186 events recorded during 8 weeks (1988) by 29 portable stations installed within a 150 km radius of the city of Antofagasta; this data were previously used in the determination of the 2D *P* wave velocity model for the region of Antofagasta.

The arrival times of *P* and *S* waves recorded by the local seismic networks were used to simultaneously determine the hypocenters and seismic velocity structure. The main technique is similar to that used by [4]. The area of study was parameterized as a set of constant velocity blocks of arbitrary dimension. Body wave velocities were specified and determined as independent parameters within each block. The inversion was iterated until changes in velocities became small (<0.05 km/s) and the variance reduction became insignificant (<2-3 %); generally two or three iterations were sufficient. The area of inversion was choosed considering the distribution of seismic stations of the local networks and the microearthquakes recorded. Considering the distribution of the seismicity with depth, we decided to keep the depth range of 0 to 170 km. The first 11 layers had a thickness of 10 km and the three deeper layers were 20 km thick. The strategy of the inversion was to start with megablocks with large dimension (about 120x240x10 $km^3$) and diminish systematically the size of the blocks depending of the ability of the data to resolve them. The smaller block obtained corresponds to a volume of 30x60x10 $km^3$.

## RESULTS OF THE P-WAVE VELOCITY INVERSION

*P*-wave velocity is parameterized initially by a 1-D horizontally layered model, where the velocity gradually increase with depth. This initial velocity model is an average of the 2D model obtained by Comte et al. [1994]. As a first step, we divided the area of study in three NS megablocks with an EW extension of 120 km, those blocks are named as Western, Central, and Eastern, and for each one it was determined a 1D *P*-wave velocity model. It can be observed that, in general, all of the three models exhibit significant variations from the initial model, mainly along the first 60-70 km in depth. In the Western and Central models, the *P* wave velocity in the layer located at a depth of 30-40 km is smaller than in the embedded layers, suggesting a low-velocity with an average velocity of about 6.7 km/s. This tendency vanishes in the Eastern model. In the second step, the 1D velocity model obtained by the inversion is the initial starting model of the 3D laterally heterogeneous *P*-wave velocity model. A serie of inversions with different size of blocks were run to find the smaller block able to be resolved by the inversion. The obtained model has blocks with variable sizes, which depend on the distribution of the ray paths between hypocenters and seismic stations. The resulting 3D velocity model was composed by 680 blocks for the *P* and *S* velocities, using ~27.000 *P* and ~21.000 *S* arrival times. The minimum number of rays crossing each block was constrained to 20; with this condition, only 571 blocks were conserved for the inversion. The distribution of the *P* and *S* residual errors is less scattered in the 3D heterogeneous model than in the 1D model, as it was expected.

The lowest values of *P*-wave velocity are located in the first shallower layer of 10 km depth, mainly beneath the Quaternary volcanoes, at distances of about 300 to 400 km from the trench, with an average velocity of 5.7 km/s. It can be observed that, in general, the velocity increases with depth, except into the range depth of 30 to 40 km, that presents a lower value of ~6.7 km/s, and extends from the coast up to a distance of about 400 km from the trench, that is, beneath the active volcanic arc. The strongest changes in velocity with depth, can be found at a depth of 40 km near the coast, where the velocity increases of ~6.7 km/s to 7.5 km/s. In the obtained 3D velocity model, it is difficult to identify the geometry of an inclined structure associated with the upper part of the subducting slab, however, it can be observed that, between the coastline and distances of about 200 km from the trench, the average *P* wave velocities reaches ~7.5 km/s, up to depths of ~70 km . Moreover, at depths greater than ~80-90 km, velocities higher than ~8.0-8.1 km/s start to be observed, suggesting the presence of the lower part of the descending slab. The highest velocities of the obtained model (8.2-8.5 km/s) observed at depths between 90 to 170 km, and at distances of about 230 to 400 km from the trench, suggest the presence of an upper-mantle wedge. The blocks located above this upper-mantle wedge exhibit lower velocities, ranging from 7.0 to 7.9 km/s, and may be interpreted as the root of the Andes Cordillera in this region.

The reliable hypocenters determined with the obtained 3D model are shown in Figure 2, where it can be observed that the seismicity recorded during July-August, 1988; January-December, 1993; and March-April, 1994 exhibits the same distribution pattern. There is no reliable shallow seismic activity that could be associated with the Atacama Fault System. The shallowest events observed in the profile are blasts of the copper mines existing in the region. There is a southward flattening of the slab observed mainly from distances of about 200-300 km from the trench. This flattening is in agreement with the void in seismicity mentioned before, and could be interpreted as an inflection point of the changes in the dip angle of the downdip the slab.

## FOCAL MECHANISMS OF THE 1994 CALAMA AND PISCO EXPERIMENT

The focal mechanism solutions of 77 microearthquakes recorded by the CALAMA and PISCO field experiment were selected because they exhibit an adequate azimuthal distribution of the polarities. The majority of these events (70) are located beneath the CALAMA AND PISCO stations, that is, at depths >70 km; however, the cluster of seismicity of depths of ~200 km have a lower definition of the auxiliary nodal plane, due to the network is located to the west of them. The cluster of microseismicity with depths between 90 and 140 km, exhibited normal reverse faulting events, therefore, the earthquakes of this cluster were divided in two groups (tensional and compressional), and for each group we did a joint focal mechanism and stress tensor inversion from the first motion polarities using the Rivera and Cisternas [3] algorithm. It was found that there are 42 normal faulting and 11 reverse faulting events, the average depth of the tensional events is 102±2 km, which is smaller than the average depth of the compressional events (110±3 km). This observation is in agreement with that obtained previously by Comte and Suárez [1]. The main component of the obtained stress tensor ($\sigma_3$ for the tensional and $\sigma_1$ for the compressional events) is approximately horizontal and the lower component of the stress tensor ($\sigma_1$ for the tensional and $\sigma_3$ for the compressional) is roughly vertical. The second cluster located at depths of ~200 km, exhibits also normal (7) and reverse (10) faulting events, where the average depth of the tensional events is 201±6 km, while the average depth of the compressional events is deeper, reaching 229±7 km. This is an interesting behaviour of the deeper part of the slab in northern Chile, because this is the first time that there is evidence of compressional events occurring together with tensional seismic activity.

## ACKNOWLEDGMENTS

We thank to Emilio Vera for his invaluable help during the CALAMA experiment. This work was partially supported by FONDECYT project N° 1940491 and ORSTOM. The PISCO measurements are part of the Collaborative Research Group 267, supported by the DFG and the GeoForschungZentrum, Potsdam.

## REFERENCES

[1]Comte, D. and Suárez, G., 1994. An inverted double seismic zone in Chile: evidence of phase transformation in the subducted slab. Science, 263, 212-215.

[2]Comte, D., Roecker, S. W., and Suárez, G., 1994. Velocity structure in northern Chile: evidence of subducted oceanic crust in the Nazca plate. Geophys. J. Int., 117, 625-639.

[3]Rivera, L. and Cisternas, A., 1990. Stress tensor and fault plane solutions for a population of earthquakes. Bull. Seismol. Soc. Am., 80, 600-614.

[4]Roecker , S. W., Yeh, Y. H., and Tsai, Y. B., Three dimensional P and S wave velocity structures beneath Taiwan: Deep structure beneath an arc-continent collision. J. Geophys. Res., 87. 945-959.

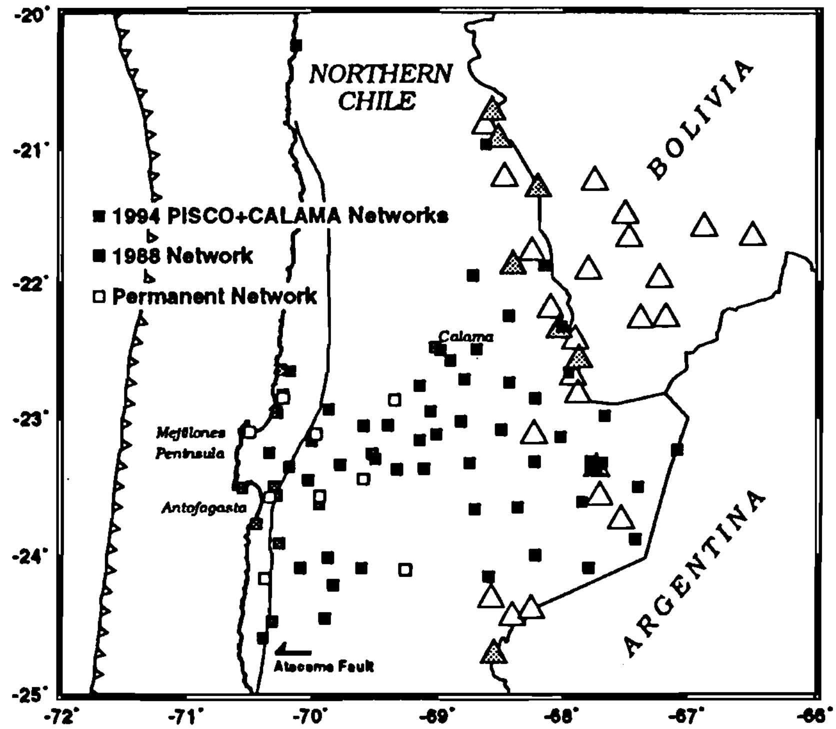


Figure 1.- Distribution of the seismological stations of the networks used in this work. Quaternary and active volcanoes are shown by open and grey triangles, respectively.

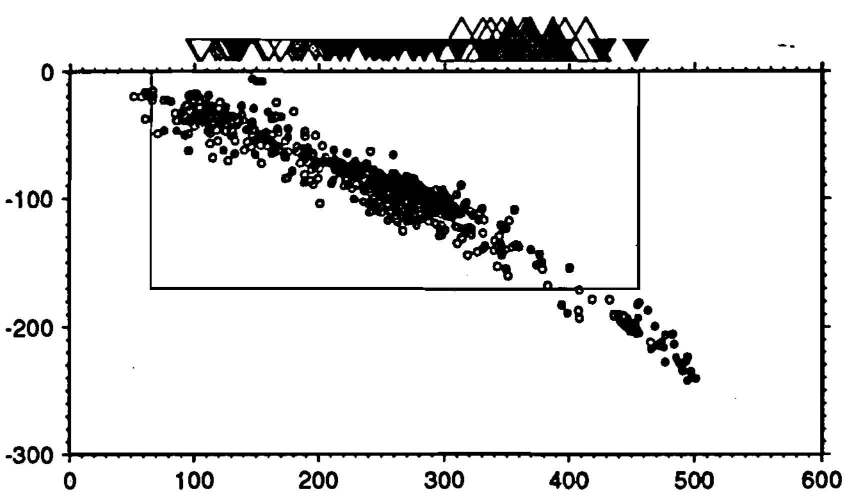


Figure 2.- Depth distribution of the seismicity recorded by the networks used. Dark, grey and open circles corresponds to the events recorded by the 1994 PISCO+CALAMA, 1988, and 1993 permanent networks, respectively. The origin of the profile is the trench, The projection of the seismic station and the quaternay and active volcanoes are also shown. The rectangle corresponds to the area of the 3D inversion.

# A TEMPERATURE AND GRAVITY MODEL OF SPREADING CENTRE SUBDUCTION.

A.J. Daniel[1], P. Styles[1], N.J. Kusznir[1] and R.E. Murdie[2].
1. Department of Earth Sciences, University of Liverpool.
2. Department of Earth Sciences, University of Keele.

The Chile Rise spreading centre is currently subducting south of the ridge-trench-trench Chile Triple Junction, between the Antarctic, Nazca and South American plates (figure 1). The Nazca and Antarctic oceanic plates are approaching South America at relative speeds of 80 mmyr$^{-1}$ and 20 mmyr$^{-1}$ respectively, and the Chile Rise spreading centre itself is approaching the trench at 50 mmyr$^{-1}$. South of the Chile Triple Junction, the geometries of the subducted plates, and the kinematics of the subducted spreading centre, are poorly known.

Our objective was to investigate the geometry and kinematics of ridge-subduction. The model predicts the temperature history of a subduction zone, as a ridge subducts, and is constrained using gravity data. Two hypotheses were tested for Southern Chile:

1) the plates continue to separate after subduction, with no change in kinematics;
2) the plates cease to separate when the ridge segment collides with the trench, and both subducting plates adopt the Antarctic plate velocity.

We used a kinematic thermal conduction-advection model, solved using a finite difference scheme, to predict the temperature cross-section during subduction of a spreading centre, for a variety of slab dips and velocities of the subducting plates. Density deviations were computed from the temperatures, and also included density deviations due to the 400 km olivine-spinel phase change and the 700 km spinel-oxides phase change. Bouguer and Free Air anomalies were calculated from the density deviation fields, and from bathymetry and Moho topography. No independent data exist to constrain the Moho beneath Southern Chile, and the continental crust was assumed to be in perfect Airy isostasy with the southwest Atlantic ocean crust. The modelled gravity anomalies were compared with observed gravity data, comprising land Bouguer anomaly data, collected by University of Liverpool teams, and marine Geosat Free Air data.

*Pre-Ridge Subduction:*

The slab dip north of the Chile Triple Junction, where segments of the Chile Rise have not yet collided with the trench, was investigated by comparing modelled gravity with observed gravity along the profile denoted "-3 Ma" on figure 1, for a Nazca plate velocity of 80 mmyr$^{-1}$ and an Antarctic plate velocity of 20 mmyr$^{-1}$. The upper plot of figure 2 shows the comparison between modelled and observed gravity for this profile, for slab dips of 20° (dashed line), 25° (solid line) and 30° (dotted line). Observed gravity is shown by the grey band; the width of the band corresponds to the error in the observed data. The lower plot of figure 2 shows the modelled temperature field for the pre-ridge subduction profile.

There are short wavelength misfits in the south-east Pacific (0 - 1250 km) and in the south-west Atlantic (2500 - 3000 km), of approximately 20mgal in amplitude. These are probably caused by sedimentary basins in the south-west Atlantic, and variations in crustal thickness in the south-east Pacific, which are not included in our model. The very short wavelength, high amplitude error at 500 km is related to a seamount. A similar error at the trench (1150 km) exists because the components of modelled gravity are varying rapidly at the trench, and a slight horizontal misalignment between the components generates a large but very localised error. Our modelled gravity generally fits observed gravity beneath South America (1250 - 2300 km) very well. Over the active margin (1250 - 1400 km), modelled gravity fits observed gravity best for a slab dip of between 20° and 25°. Beneath the Argentinean continental shelf (1800 - 2300 km), the best fit was obtained for a slab dip between 25° and 30°.

*Post-Ridge Subduction:*

We compared modelled and observed gravity for three post-ridge subduction profiles:

1) a profile through the triple junction itself ("0 Ma" on figure 1);
2) a profile south of the Chile Triple Junction, through a subducted ridge segment which collided with the trench 3 Ma ago ("+3 Ma" on figure 1);
3) the southern-most profile, corresponding to a subducted ridge-segment which collided with the trench 6 Ma ago ("+6 Ma" on figure 1).

Modelled gravity was computed for two kinematic cases:

i) the subducting plates continue to separate after subduction;
ii) the subducting plates cease to separate immediately when the spreading centre segment collides with the trench.

Modelled gravity generally fits observed gravity for the post-ridge subduction profiles best for a 30° slab dip. For the +3 Ma post-ridge subduction profile, a better fit is obtained above the subducted ridge segment if the subducting plates continue to separate, than if they cease to separate. The difference in modelled gravity predicted between continuing and ceasing separation of the subducting plates is, however, only marginally larger than the probable error in the model, and therefore the conclusion that the subducting plates continue to separate after subduction of the ridge segment is tentative. For the +6 Ma post-ridge subduction profile, the gravity difference predicted between continuing and ceasing separation of the subducting plates is certainly less than the error in the model, so we cannot predict the kinematics of old subducted ridge segments.

*Long-Wavelength Misfits Between Modelled and Observed Gravity:*

There are no long-wavelength misfits between modelled and observed gravity for the pre-ridge subduction profile (figure 2). For the post-ridge subduction profiles, two long-wavelength misfits exist:

1) observed gravity is up to 40 mgal lower than modelled gravity in Southern Chile (200 -300 km east of the trench) on the 0 Ma and +3 Ma profiles, but not on the pre-ridge subduction and +6 Ma profiles;
2) observed gravity is up to 30 mgal higher than modelled gravity in Argentina (400 - 700 km east of the trench) on all three of the post-ridge subduction profiles.

These long-wavelength misfits are all east of the subducted ridge segments, and above the subducted Nazca plate.

The locations of the misfits do not correlate with surface geology, and they are sufficiently long wavelength to suggest a deep source, at Moho or slab depths. We speculate that the misfits reflect either deviations of the Moho from Airy isostasy, or thermal anomalies in the upper mantle.

*Acknowledgements.* This project was funded by the Natural Environment Research Council (grant GT/4/93/189/G to A. Daniel). Raleigh International provided logistic support for the field work.

*Figure 1. Regional tectonic map of southern Chile, centred on the Chile Triple Junction. The horizontal and vertical axes are longitude and latitude respectively. The observed gravity anomaly map (Bouguer anomaly on land; Free Air anomaly at sea) is shown by the continuous grey-scale shading. The locations of the modelled profiles are shown.*

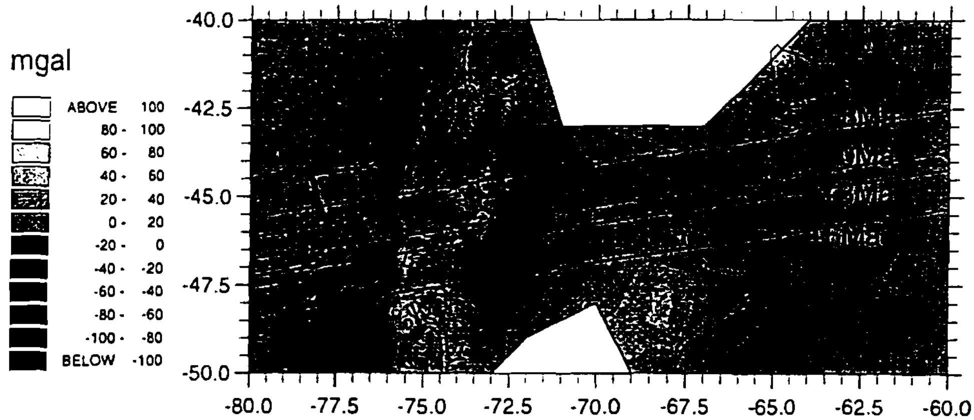


*Figure 2. Comparison for modelled and observed gravity for the pre-ridge subduction (-3 Ma) profile. The lower plot shows the temperature field, contoured at a 200°C interval. In the upper plot, the grey band shows observed gravity, and the black lines show modelled gravity for 20° (dotted line), 25° (solid line) and 30° (dashed line) slab dips.*

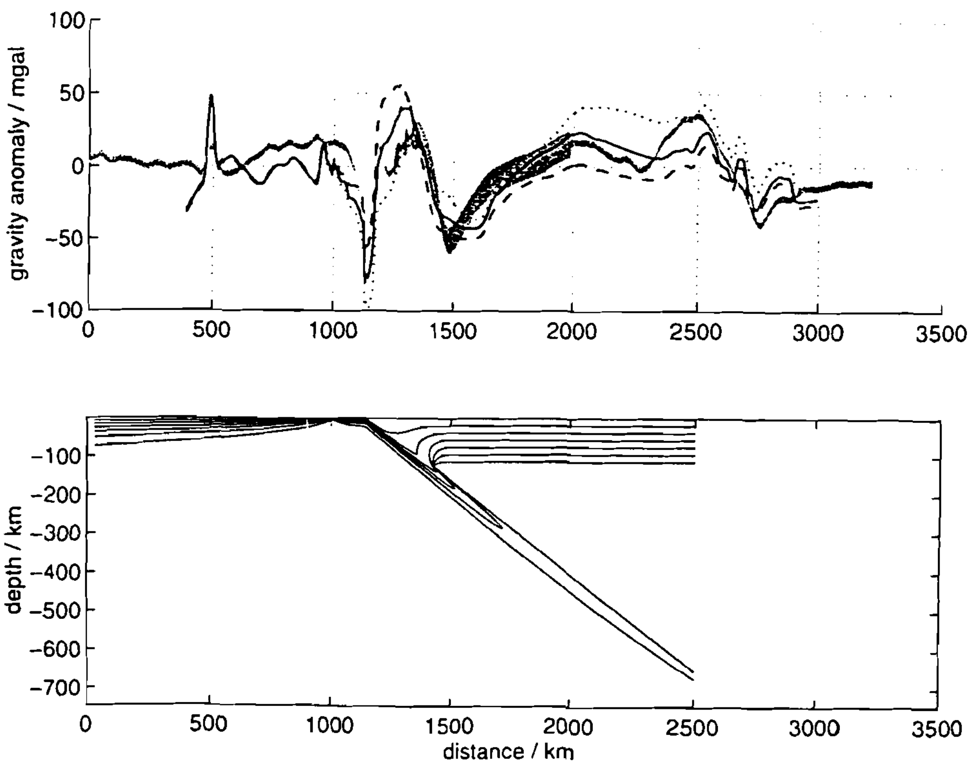

# MAPPING THE CONTINUITY OF THE NAZCA PLATE THROUGH ITS ASEISMIC PART IN THE ARICA ELBOW BY TELESEISMIC TOMOGRAPHY

Catherine DORBATH[1] and the Lithoscope Andean Group

(1) ORSTOM and EOPG, URA CNRS 1358, 5 rue René Descartes, 67084 Strasbourg Cedex, France.

**KEY WORDS:** Teleseismic Tomography - Subduction - Structure of the lithosphere and upper mantle.

## INTRODUCTION

The western part of South America is one of the major plate boundaries on the Earth. It is the largest region in which ocean-continent convergence is happening today. The Andes are the result of the subduction of the Nazca Plate beneath the South American Plate along the Peru-Chile trench since the Cretaceous. This continental margin orogenic belt, continuous for more than 7,000 km, presents distinct broad scale tectonic segments, which remarkably correlate with the variations in the geometry of the subducted Nazca Plate (Barazangi and Isacks, 1976, Jordan et al., 1983). The most noticeable of these segments is certainly the Central Andes (15°S to 27°S): the range is at its widest part (Bolivian Orocline) including the Altiplano-Puna high plateau and the general strike of the structures changes from N320°W to nearly NS (Arica Elbow) (Figure 1).

Along the Peru-Chile trench, the subduction of the Nazca Plate under South America is well underlined by the Wadati Benioff zone. In the Central Andes, the seismicity defines a moderately deeping slab down to about 325 km. The occurence of a scarce seismicity in the 550-650 km depth range, after a complete seismic quiescence, arises the question of the continuity of the slab. To answer this question we performed a 3-D teleseismic tomography of the mantle at 20° S.

## DATA PROCESSING

From June to Novembre 1994, 41 vertical short period stations from the french Lithoscope network were operated along a 700 km long profile crossing the Andean chain in its entirety. Therefore, this profile was placed above the subducted plate from the coast, where its upper part is at a 50 km depth, to its eastern limit as it is defined by the Wadati Benioff zone; the profile ended at the subandean front of deformation, above the very deep seismicity. The profile was designed to be as perpendicular as possible to the structures. The spacing between the stations was about 20 km (Figure 1).

Among the 250 teleseismic events recorded during the 6 months experiment, we selected 120 events which provided clear P-wave arrivals at more than 10 stations. They were evenly distributed in distance and azimuth relatively to the seismic network. Absolute travel-times were calculated using hypocentral data from the USGS's Preliminary Determination of Epicenter's bulletin and Herrin's tables (1968). Next we calculated residuals at every station for every selected event, and then we computed the value of these residuals relatively to the same reference station situated in the Altiplano.

A study of the variation along the profile of these relative residuals shows the strong azimuthal variations of P relative residuals and particularly the difference between the north-eastern quadrant and the other azimuths. For the azimuths between 0 and 40°E, the more we go west, the more the relative residuals are negative, therefore the more rays cross high velocity structures. The decrease from east to west along profile is more gradual for northern than for north-eastern azimuth, but on both profiles the variation reaches 4 s, twice what is observed in others azimuths. Such large scale differences emphasize at the same time that the anomalous structures are deep and that the region sampled by the rays is far from the axial symmetry. This assertion has to be sustained by the tomography.

The travel time residuals are inverted using a version of the "ACH" inversion technic (Aki et al., 1977), extensively described in published litterature. The initial velocity model included 12 layers of blocks of incrasing size with depth. In order to obtain a satisfactory explaination of our data, it is a large reduction in the data variance, we were led to build a 3-D thick initial model. In effect, the reduction of the variance is less than 50% for a 2-D 420 km thick model; it goes up to 73% for a 3-D model of the same thickness, and reaches 82% when we use a 3-D 660 km thick model. Therefore, our initial model includes the complete upper mantel and the transition region down to the 650 km discontinuity.

## TOMOGRAPHIC IMAGES

A vertical EW cross-section at 19.5°S through the smoothed velocity perturbation model is presented in Figure 2, together with the historical seismicity reported by the National Earthquake Information Service for the time period 1974-1994

### *The crust*

Within the continental crust, the results of the tomography can be compared to the results of seismic refraction profiles recorded at 21°S by the Freie Universität Berlin (Wigger et al., 1993; Schmitz, 1993 and 1994). Because the teleseismic inversion has a poor resolution in the vertical direction, we restrict the comparison to the global structure of the crust i.e. its thickness and average velocity.

The teleseismic tomography gives a smoothed image of the lateral velocity variations within the crust that matches the structure determined from refraction surveys. The highest velocities are observed beneath the western end of the profile, below the Coastal Cordillera of Chile. Further east, the positive velocity anomaly decreases rapidly when entering the Axial Valley. The active volcanic arc (Western Cordillera) is characterized by a negative velocity anomaly. A weak (negative) anomaly is observed under the Altiplano, then the eastern part of the Eastern Cordillera is characterized by a positive velocity anomaly. Finally, at the eastern end of the profile, a weak negative anomaly is observed in the Sub-Andean Zone.

### *The continental upper mantle*

Figure 2 shows that the upper mantle between 60 and 140 km has lateral variations in P-wave velocity that are smaller than $\pm 1.5\%$, which is of the order of the standard deviation. The only correlation with the velocity structure in the crust is the extension of the high velocity zone under the western part of the Eastern Cordillera down to a depth of 120 km. Under the Western Cordillera, the Altiplano and the eastern part of the Eastern Cordillera, the lack of correlation between the velocity anomalies in the mantle and the crust shows that the mantle and crust probably are decoupled. We do not find any evidence for a wedge of over-heated mantle material under the thickened crust of the Altiplano and Western Cordillera which could strengthen the hypothesis of lithospheric delamination (e.g. Isacks, 1988).

Since this is the second tomographic experiment conducted in the Central Andes, it is possible to study the along strike variations in the deep structure of the chain. The previous experiment was carried out in northern Bolivia across a narrower part of the chain which included only the Altiplano and the Eastern Cordillera (Figure 1) (Dorbath et al., 1993). The two velocity models are significantly different as velocities in the shallowest layers have weaker and smoother lateral variations along the southern than along the northern transect. However, the most characteristic features are observed on both profiles: the Altiplano is characterized by low velocities down to the Moho depth, and the axial zone of the Eastern Cordillera by high velocities down to the upper mantle. The differences observed between the two models is related to along strike variations in the geometry of the underthrusting of the eastern margin of the Andes under the Brazilian craton, which occurs along steeply dipping faults in the northern narrow segment, whereas it occurs along low angle ramps in the southern wide segment.

### *The subducted Nazca Plate*

A striking feature revealed by our tomography (Figure 2) is the eastward-dipping positive anomaly which crosses the entire profile from the coastal zone to the sub-Andean zone. This 100 km thick structure is characterized by a +2% average velocity contrast with respect to the surrounding mantle,. It is associated with the slab because it coincides with the Wadati-Benioff zone in its seismic part (Figure 2). The continuity of the high velocity anomaly down to 660 km indicates that the slab is continuous across its aseismic part. The strengthening of the velocity perturbation at 400-450 km depth and the general shape of the anomaly indicate that the dip of the descending slab increases below 400 km depth. In a recent paper, Engdahl et al. (1995) used inversion of travel time residuals of teleseismically recorded events of South America to compute tomographic images of the subducted Nazca plate. Their main result is the observation of 2.5% high velocity anomalies spatially correlated to the Wadati-Benioff zone which can be traced down to the base of the upper mantle.but do not exhibit a strong continuity.

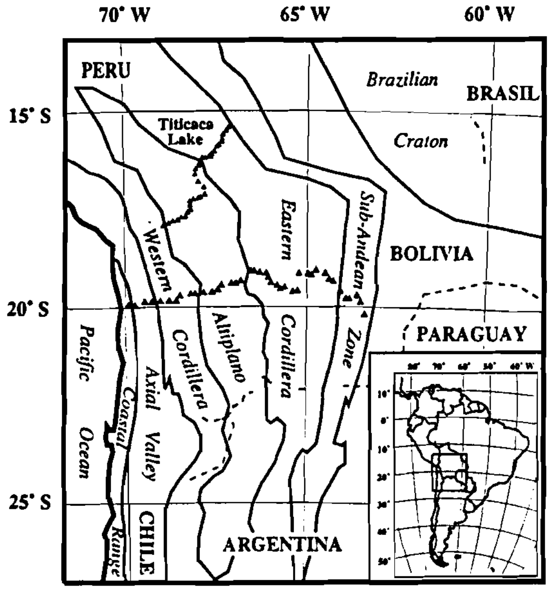


Figure 1

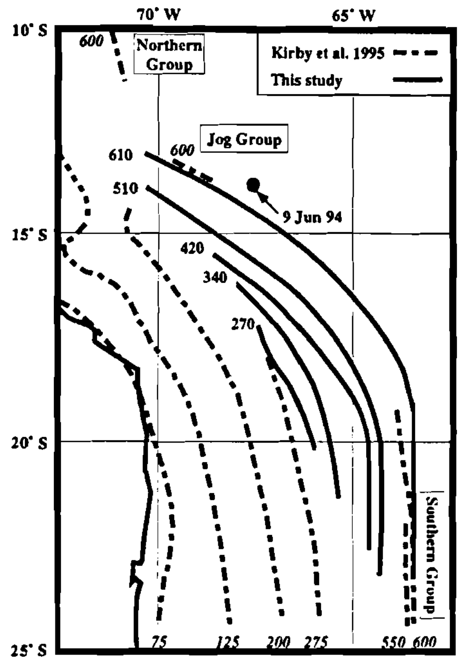


Figure 3

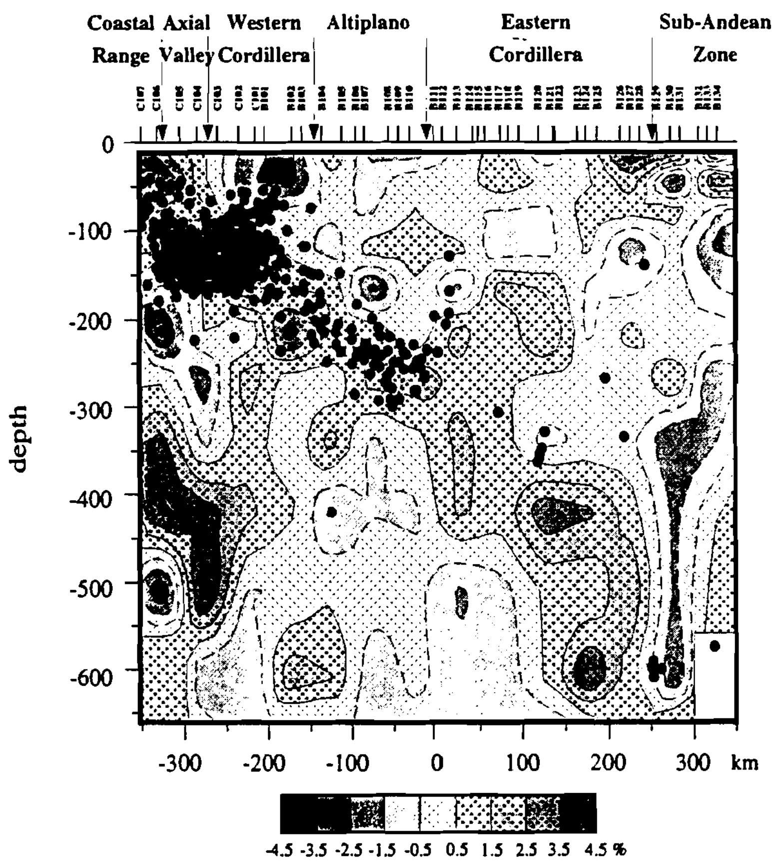


Figure 2

The images obtained by the teleseismic tomography provide a strong supportive evidence for the continuity of the slab over regions with gaps in seismicity. From the surface to 660 km depth, the slab is evidenced on the 3-D images by a laterally continuous high-velocity structure, clearly displaying a pronounced bend on the deepest layers of our final model. A complementary contribution which can only be provided by the tomography is the possibility to follow the slab deeping throughout the seismically quiescent zone. We present on the Figure 3 a schematization of the slab geometry deduced from the 3-D image. For every layer in which the slab is clearly identified by higher velocities, we have drawn a contour passing through the maximum of the positive anomaly. Doing so, we approximate the position of the slab at the mean depth of the layer. On the same figure, we have reported the seismicity of the NEIS for the past 20 years and the iso-depth contours obtained by Kirby et al. (1995). Our network layout allows us to sample only a roof-shaped zone aligned on the seismic profile and consequently the north-south extension of the layers depends on their depth. Therefore our 270 km contour is very short and does not fit well with the 275 km contour, the deepest of the Wadati Benioff zone. On the other hand, our 610 km contour is in good spatial agreement with the 600 km depth events. When drawig a cross-sections of the slab in the Arica Elbow, we observe that the dip of the slab changes with depth. From the trench to a depth of 275 km, the seismicity defines an about 30° dipping slab; then the dip, inferred from the tomography, increases to more than 50° in the aseismic part of the slab. Finally, the dip decreases to about 40° where the deep seismicity is present, suggesting a deflection of the slab at the bottom of the upper mantle.

Finally, the geometry of the deep slab in the transition zone of southern Peru is still an open question. If it is relatively easy to connect our 610 km contour with the Northern Group through a reverse bend, the closing up of the 200 and the 510 km contours at about 15°S involves a steepening of the slab. Therefore, the transition, from the 50° dip of the aseismic part of the slab deduced from the tomography, to the 70° dip inferred by James and Snoke (1990) study beneath Peru, seems to occur in this region of the Arica Elbow, and implies a very complicated geometry of the slab between 13°S and 18°S.

## REFERENCES

Aki, K., Christoffersson, A. and Husebye, E.S., 1977. Determination of the three-dimensional seismic structure of the lithosphere. J. Geophys. Res., 82, 277-296.

Barazangi, M. and Isacks, B.L., 1976. Spatial distribution of earthquakes and subductio of the Nazca Plate beneath South America. Geology, 4, 686-692.

Dorbath, C., Granet, M., Poupinet, G. and Martinez, C., 1993. A teleseismic study of the Altiplano and the Eastern Cordillera in Northern Bolivia: New constraints on a lithospheric model. J. Geophys. Res., 98, 9825-9844.

Engdahl, E.R., Van der Hilst, R.D. and Berrocal, J., 1995. Imaging of subducted lithosphere beneath South America. Geophys. Res. Lett., 22, 2317-2320.

Herrin, E., 1968. Seismological tables for P phases. Bull. Seismol. Soc. Am., 58, 1193-1242.

Isacks, B., 1988. Uplift of the Central Andean Plateau and bending of the Bolivian Orocline. J. Geophys. Res., 93, 3211-3231.

James, D.E. and Snoke, J.A., 1990. Seismic evidence for Continuity of the Deep Slab Beneath Central and Eastern Peru. J. Geophys. Res., 95, 4989-5001.

Jordan, T.E., Isacks, B.L., Allmendinger, R.W., Brewer, J.A., Ramos, V.A. and Ando, C.J., 1983. Andean tectonics related to geometry of subducted Nazca plate. Geol. Soc. Am. Bull., 94, 341-361.

Kirby, S.H., Okal, E.A. and Engdahl, E.R., 1995. The June 9, 1994, Bolivian deep earthquake: An exceptional event in an extraordinary subduction zone. Geophys. Res. Lett., 22, 2233-2236.

Schmitz, M, 1993. Kollisionsstrukturen in den Zentralen Anden: Ergebnisse refraktionsseismisher Messungen und Modellierung krustaler Deformationen. Berliner Geowissenschaftliche Abhandlungen, B, 20, Berlin, 127 pp.

Wigger, P., Schmitz, M., Araneda, M., Asch, G., Baldzuhn, S., Giese, P., Heinsohn, W-D., Martinez, E., Ricaldi, E., Rower, P. and Viramonte, J., 1993. Variation in the crustal structure of the southern Central Andes deduced from seismic refraction investigations, in Tectonics of the Southern Central Andes. K-J. Reutter et al. (eds), 23-48, Springer-Verlag, New York,

# THE INTERDISCIPLINARY GEOSCIENTIFIC RESEARCH PROJECT "DEFORMATION PROCESSES IN THE ANDES"

Peter GIESE

Geophysical Department, Freie Universität Berlin
Malteserstr. 74-100, D 12249 Berlin, Germany

:

KEY WORDS: Central Andean interdisciplinary research project

An interdisciplinary geoscientific research project "Deformations Processes in the Central Andes" has been established at the Freie Universität Berlin, the Technische Universität Berlin, the GeoForschungsZentrum Potsdam and the University Potsdam. This project, started 1993, is funded by these institutions and by the German Research Society (DFG) as a "Sonderforschungsbereich 267" (collaborative research programme 267).

The Central Andean segment between 20° and 25°S has been chosen because along this section the orogenic deformation processes are very well developed.

The main and outstanding features along this geotraverse can be described as follows:

- a high convergence rate of about 10 cm/y and high strain rates,
- a vertical uplift rate of about 1 mm/year
- an extreme crustal thickness up to 60-70 km, caused by magmatic underplating and tectonic stacking,
- zones with extremely high electrical conductivity in various tectonic zones and depths ranges,
- high seismicity in shallow, intermediate and large depth ranges,
- recent and subrecent volcanic activity and high heat flow density,
- a well developed forearc, magmatic arc and back-arc,
- four magmatic arcs which have been evolved succesively by eastwards migrating from Jurassic to recent time,
- variations of the stress regime during the Andean period causing extensional and compressional deformations.

Geophysical, geodetic, geological und petrological studies will be carried along the Central Andean traverse aiming to tackle the following key problems:

- the structure of the lithosphere and its rheological state and behaviour,
- the interaction between upper and lower plate,
- the distribution of the stress field and strain in time and space,
- the tectonic and petrological evolution of the upper plate under varying conditions of convergence,
- the geothermal field and heat transfer,
- the evolution of intramontanous basins and isostasy,
- energy consumption during the orogenic processes.

A number of field projects has been carried out since 1993. In order to investigate the crustal structure of the magmatic arc and the adjacent zones a network of seismic refraction profiles was realized in the Western Cordillera and the Precordillera. In addition 25 mobile seismological stations were set up in this region operating for about 3 - 4 month aiming to record and investigate shallow and intermediate-deep earthquakes (PISCO 94).

In order to study the lithosphere of the eastern Nazca-plate and the transition to the continental lithosphere was investigated by a joint sea-land project applying airgun seismic reflection and refraction survey, gravimetric, magnetic and heat flow measurements. This project CINCA 95 is planned by the Federal Institute for Geosciences and Natural Resources, Hanover,GEOMAR, Kiel and the SFB 267. Magnetotelluric deep sounding measurements will contribute additional information. Detailed gravimetric measurements will be carried out aiming to study the deeper structure of intramontanous basins.

A GPS-profile transversing the Central Andes records recent crustal movements. This study will be remarkably extended by the GeForschungsZentrum Potsdam within an international co-operation with a profile running along the Pacific coast in N-S direction.

Special geological and petrological investigations are carried out in the magmatic arcs aiming to reveal the complicated tectonic development of a magmatic arc system. Neotectonic studies are designed aiming to investigate the recent stress and strain field. Geological investigations will take place in the Eastern Cordillera aiming to reconstruct the Andean shortening of the Paleozoic sediments.

Detailed geochemical studies should reveal the nature of the young volcanism.

Petrophysical studies on rock probes under high temperature and pressure conditions should help to interprete the geophysical field data.

Such a project can be only realised by close cooperations with geoscientific institutions in Argentina, Bolivia and Chile.

The research project is structured as followed:

- Deformation and stress field:
  Neotectonic studies, recent kinematics by GPS measurements, modelling of the recent stress and strain field.
- Rheological stratification at a convergent plate boundary:
  Rock behaviour under high temperature and pressure condition derived from lab and field measurements, temperature field, heat transfer mechanism, rheology and fracturing of the Andean crust. Application of GIS.
- Crustal evolution controlled by varying convergence boundary conditions:
  Structure of magmatic arcs by geological and geophysical studies, magmagenesis and crustal evolution, crustal shortening in the back-arc region.
- Evolution of sedimentary basins and isostasy:
  Evolution of basins in various crustal environments,
  Balancing studies of erosional and sedimentary processes, isostatic studies.

# THE NATURE OF INTERMEDIATE-DEPTH SEISMICITY IN THE CENTRAL ANDES

Peter GIESE[(1)] and Günther ASCH[(2)]

(1) Geophysical Department, Freie Universität Berlin, Malteserstr. 74-100, D 12249 Berlin, Germany
(2) GeoForschungsZentrum Potsdam, Telegrafenberg, D 14473 Potsdam, Germany

KEY WORDS: Central Andes, intermediate-depth seismicity, phase transformations

## INTRODUCTION

Intermediate-depth seismicity is a very typical feature along subduction zones. The detailed shape of this seismic zone may differ from region to region, but there exists some common characteristics. In this contribution the nature of the intermediate depth seismicity is discussed comparing the situation along the converging zones of the Andean belt and in the Japan and the Kuril-Kamchatka arc system. In both regions the intermediate-depth seismicity is localised in the oceanic crust and in the uppermost mantle as well. Therefore the seismicity must be related to two different metastable phase transformations that are associated with the emission of seismic energy. The different shape of the seismic active zone is mainly dictated by the different converging rates, about 1 cm/a along the Japan and the Kuril-Kamchatka arc system and 10 cm/a for the Andean arc.

## THERMAL STRUCTURE OF THE DOWNGOING SLAB

For the study of the metastable phase transformations that are going on in the descending slab, the knowledge of the temperature field in the downgoing slab is of importance. The main parameters controlling the temperature distribution are: the rate of subduction; the age, thickness and dip of the descending slab, frictional heating along the shear plane between the upper and lower plate, the conduction of heat into the slab from the deeper lithosphere and asthenosphere, and the heating of the top of the slab caused by the induced convecting corner flow in the upper plate.

A simple method for an approximate steady-state temperature calculation has been proposed by MOLNAR and ENGLAND (1990) and PEACOCK (1993).Here the method proposed by PEACOCK (1993) has been applied and extended for a depth depending shear stress and variable dip angle. In addition heating of the top of the slab by the induced corner flow has been taken into consideration.

For the following considerations two temperature gradient zones are of importance. In the upper zone, mainly situated in the oceanic crust immediately beneath the shear plane between the upper and lower plate, the temperature decreases with depth. The lower gradient zone in the uppermost oceanic mantle shows a positive temperature gradient. The width of the resulting temperature inversion is strongly controlled by the convergence rate. A low convergence rate of about 1-2 cm/a is associated with an inversion zone of some ten kilometre width, as it is observed in the Japan and the Kuril-Kamchatka arc. A high convergence rate of about 10 cm/a causes an inversion zone of only few tens kilometres thickness, as it is the case along the Central Andean subduction zone.

## METASSTABLE PROCESSES IN THE DOWNGOING SLAB

The upper 8-10 km of the downgoing slab is composed of basaltic and gabbroic rocks forming the oceanic crust. The underlying oceanic mantle is made up by peridotitic rocks with olivine and pyroxene as main components. Therefore two different metastable processes must be considered for the explanation of intermediate-depth seismicity.

The metamorphic evolution of the subducted oceanic crust can be described by calculated P-T-paths and a model of metabasalt phase transformation (PEACOCK 1993). Fig. 1 presents the corresponding phase diagram. In steady-state subduction zones with moderate to low rates of frictional heating and a dip of 20°-30° most of the subducted oceanic crust moves along the low-T and high-P path from the blueschist into eclogite field in the depth interval 70-120 km.. This path is associated with the release of a relative large amount of fluids (up 5.9 wt %), which cause hydraulic fracturing of the overlying rocks. The association between the injection fluids and hydraulic fracturing of rocks and the emission of seismic energy is evidenced experimentally. In contradiction in flat subduction the cooling of the downgoing slab is only moderate and the transformation runs along the high-T and low-P path which enters the eclogite field through the epidote-blueschist and amphibolite facies fields with small release of fluids.

An other process must be considered for the generation of seismicity in the uppermost mantle. KAO and LIU (1995) have studied the double seismic zone along the Japan and Kuril-Kamchatka arc. Here the upper and lower seismic zone are separated more than 30 km. Thus the lower zone is situated in the uppermost mantle and a process must exist, which refers to mantle composition. They propose as the most likely candidate for such a process decomposing of Al-rich enstatite to Al-poor enstatite plus garnet. Like the transformation process olivine to spinel that is associated with the emission of seismic energy, the same is assumed for the enstatite process. Fig. 2 shows the corresponding phase diagram, derived by KAO and LIU (1995) from petrologic, geothermal and seismological data. It should be noted, that the critical phase boundary is situated along a low-P and high-T path below 80-100 km depth in the temperature range 400°-500°C. This is just the same temperature interval of the upper gradient zone in the downgoing slab (Fig.1).

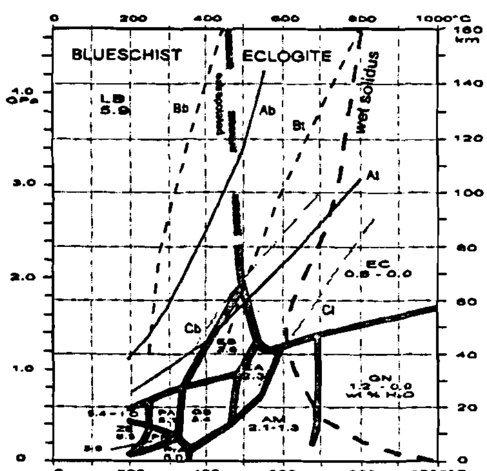


Fig. 1: P-T–diagram of metamorphic facies based on experimental and theoretical phase diagrams compiled by PEACOCK (1993).
At, Bt, Ct :P-T–path of the top of the oceanic crust, model A, B, C
Ab, Bb, Cb :P-T–path of the base of the oceanic crust, model A, B, C

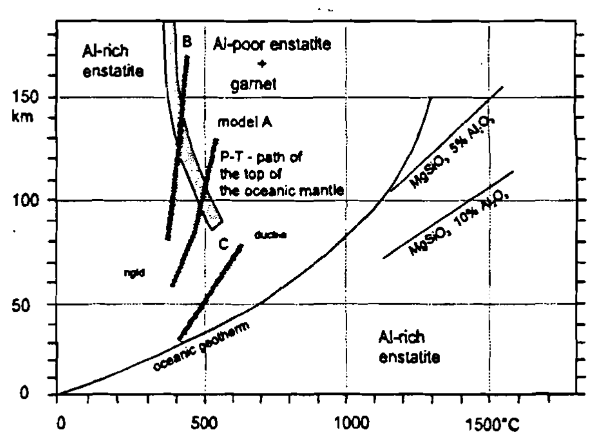


Fig. 2: P-T–diagram of the emstatite system (based on KAO and LIU 1995). The grey zone as seismically active phase is derived from the seismological and geothermal situation along the Japan and Kuril-Kamchatka arc system. It is assumed that this diagram can be applied to other subducting systems as well.

PISCO 94

Aiming to study the detailed structure of the intermediate-depth seismicity a network of about 25 mobile seismic stations were installed in the Precordillera and the Western Cordillera of the Central Andes operating between February and May 1994. The network operated in a continuous mode within an area of 200 km (W-E) x 250 km (N-S). About 50-100 events per day could be recorded in the magnitude range -0.5 to 4 (local magnitude scale). The accuracy of localising is ±2 km. Most of the events could be located in the depth range 75 to 120 km. Fig. 2A, B shows two sections derived from the high resolution PISCO 94 experiment, showing different pattern of seismicity.

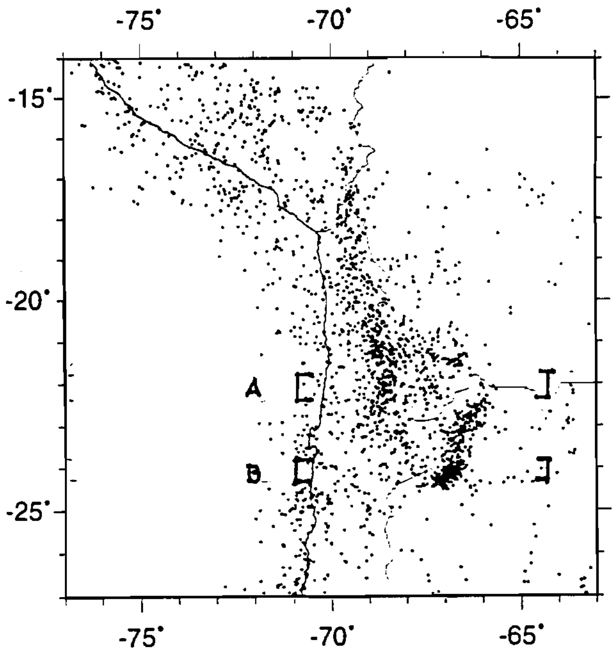


Fig. 3: Seismicity pattern in the Central Andes, based on the PDE catalogue.

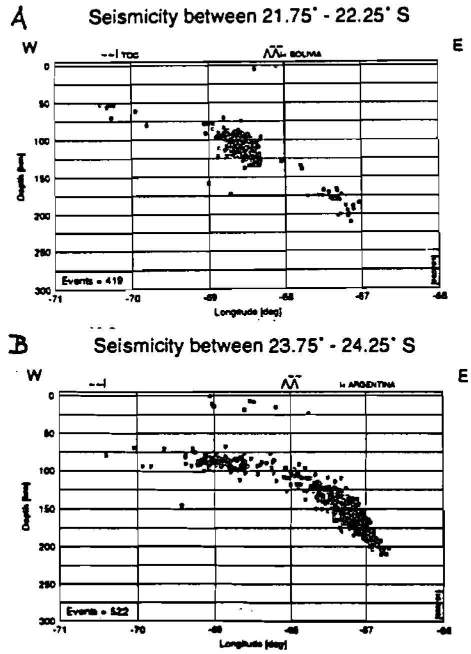


Fig. 4A,B: Two sections through the Central Andes showing the varying shape of the intermediate-depth seismicity

P-T PATHS AND SEISMICITY IN THE CENTRAL ANDEAN CONVERGING SYSTEM.

Aiming to match the observed seismicity with the metastable phase diagrams described above three thermal models with varying subduction parameters were calculated. Following parameters were used:

Table 1

| | model A | model B | model C | |
|---|---|---|---|---|
| convergence rate | 10 | 10 | 10 | cm/a |
| dip of the subduction plane | 17° | 20°/40°/60 km | 15°/8°/40 km | |
| thermal cond. crust/mantle | 2.5./2.0 | 2.5./2.0 | 2.5./2.0 | W/m·K |
| diffusity | 1 | 1 | 1 | $10^{-6}$ $m^{-2}$ |
| mantle heat flux | 0.050 | 0.050 | 0.080 | W/m² |
| frictional heating (1) | 60 / 50 | 40 / 50 | 40 / 50 | km / MPa |
| corner flow heating (2) | 400°/70-200 | 400°/70-200 | 0 | °C/km |

(1) frictional heating increases linearly with depth, given max. depth (km)and max. stress (MPa)

(2) heating of the top of the slab by the induced corner flow, given the temperature increase(°C) and in the corresponding depth interval (km).

The transitional phase boundaries depicted from the phase diagrams are plotted in Fig. 5A, B, C. These transitional zones may have a width of at least 50°-100° C and 0.1-0.2 MPa (3-6 km). In addition the subducted slab may show deviations from the plane structure thus an actual thickness for the transitional phase zones of at least 10 km may result.

Fig 5A should be compared with Fig 4A. The seismicity is concentrated in the depth interval between 80 and 120 km. In Fig 4B, lower section, the seismicity is strechted between 80 and 200 km depth.
The corresponding model in Fig. 5B shows that the transitional phase boundaries are situated between 80 and 160 km. In the third case (Fig. 5C), the flat subduction, there a strongly reduced or even no seismicity in the intermediate-depth level because in both phase diagrams the descending slab moves along the high-T–low-P path associated with only small release of fluids.

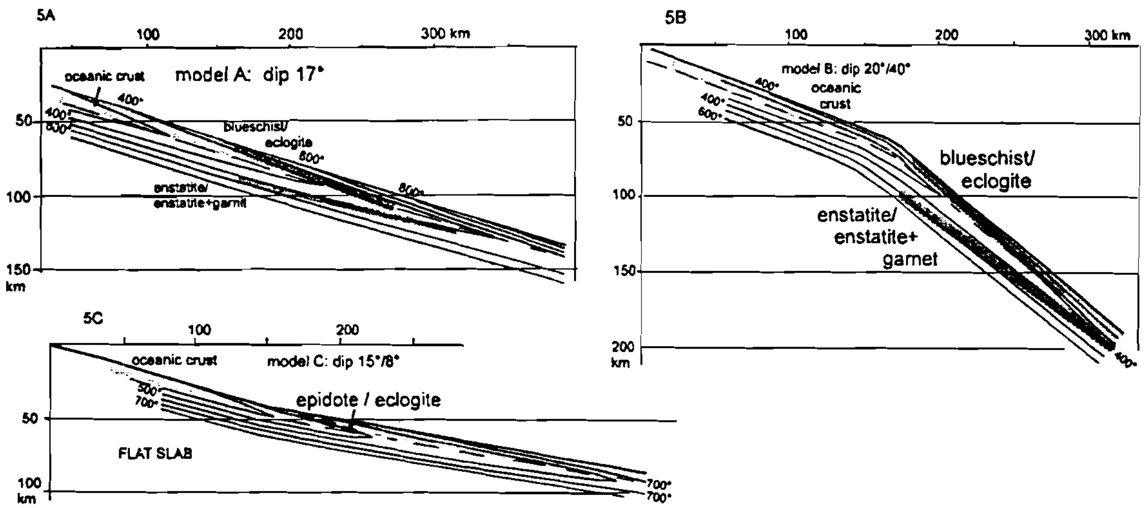


Fig. 5A,B,C The geothermal structure in the downgoing slab (parameters see table 1)
model A: dip 17°; model B: dip 20°/40°; model C: dip: 15°/8°

## CONCLUSIONS

The nature of intermediate-depth seismicity is caused by metamorphic processes going on in the upper and lower temperature gradient zone in the downgoing slab. Considering seismological data, geothermal calculations, and petrologic considerations the intermediate-depth seismicity in the Central Andes is explained by two different metastable phase transformations, which occur in the oceanic crust resp. in the uppermost mantle. Both processes are associated with the emission of seismic energy. The different shape of the seismically active zone in the Central Andes can be modelled by variations of the parameters controlling the temperature field in the downgoing slab. The same processes take place along the Japan and Kuril-Kamtchatka arc system. A clearly recognisable separation of both zones depends on the thermal structure in the downgoing slab, which is dictated by the converging rate.
This project is funded by the Collaborative Research Programme "Deformation processes in the Central Andes"

## REFERENCES

Kao, H. and L. Liu (1995): A hypothesis for the seismogenesis of a double seismic zone Geophys. J. Int., 123, 71-84.

Peacock, S. M. (1993): The importance of hlueschist → eclogite dehydration reactions in subducting oceanic crust. Geological Society of America Bulletin, 105,184--194.

Molnar, P. and P. C. England (1991): Temperature, heat flux, and frictional stress near major thrust faults, J.of Geoph. Res., 95,433-4

# LATE MIOCENE VOLCANIC ARC THICKENING IN THE CHILEAN CENTRAL ANDES :Seismic and gravity constraints

Estanislao Godoy(1), Gonzalo Yañez(1,2) and Emilio Vera(3)

(1) Servicio Nacional de Geología y Mineria. Casilla 10465. Santiago. Chile.
(2) now at Geodatos. Román Diaz 773. Providencia.
(3) Departamento de Geofísica. U. de Chile. Casilla 2777. Santiago.

**KEY WORDS** : arc tectonics, out-of-sequence thrusting, triangular zones.

## INTRODUCTION

Two main unconformities have been advanced for the thick Meso-Cenozoic rocks of the central Chilean Andes : an upper Cretaceous and a Lower Tertiary (Klohn, 1960; Charrier 1981).

The former, however, has either not been recognized east of Santiago (Thiele, 1980) or has been reinterpreted as an out-of-sequence thrust SE of that city (Godoy, 1990). Only recently has the latter, according to Sempere et al (1993) closely related to development of Late Oligocene-Early Miocene foreland basins from Colombia to Central Chile, been subject to a major revision south of 33°45'. Godoy and Lara (1994) report that, south of that latitude and along its eastern margin, the Miocene arc (over 3,000 m thick Middle to Upper Miocene andesites and ignimbrites of the Farellones Formation) lies either conformable or is thrust eastward on top of its lower Cretaceous to lower Miocene (Flynn et al, 1995) pyroclastic basement. Godoy et al (1996), on the other hand, show that most of the miocene arc western margin is underthrusted by that basement.

In this paper we present preliminar seismic and gravimetric data of the arc western margin across 34° S.lat. They support the structural relations of Godoy et al. (1996) and help constrain the Late Miocene to Early Pliocene contribution to upper crustal thickening.

## MIOCENE ARC GEOLOGIC SETTING

Contrary to Thomas (1953) and Godoy (1993), who describe interfingering of the Farellones andesites with its underlying pyroclastics, most authors stress an unconformable contact (Aguirre, 1960; Rivano et al, 1990). Thiele et al (1991), on the other hand, while favoring deposition of the Farellones Formation inside "caldera-grabens", state that "no generalizations can be made about the contact relations between the two formations". Lastly, Crystallini et al (1994), recognize -along its easternmost outcrops- that deformation started before, but outlasted deposition of the lavas.

As recently pointed out (Godoy et al, 1996), three segments characterize the present-day western margin of the Miocene arc. North of 33°35' Farellones is slightly detached westward, mainly along its basal ignimbrite. The detachment is interpreted as the upper limit of a triangular zone whose enclosed volcaniclastics (Abanico formation) become tightly folded southwards. South of 33° 10' the older unit (here known as Coya-Machalí Formation) is tuffaceous siltstone-bearing and tightly folded against the triangular zone. Sub-vertical fault-propagation folds, some of them broken, characterize the intermediate segment of the arc western margin .

In addition to the controversial basal contact relation, age of uplift and erosion rates of the miocene arc in the chilean central Andes have also been debated. 2,000 to 2,350 m of post-Miocene uplift has been calculated using paleobotanic and fluid inclusion data (Pons and Vicente, 1985; Skewes and Holmgren, 1993). Erosion rates of 260 to 150 m/Ma are advanced by the latter authors, while 800 m/Ma for the last 8.4 Ma and 700 m/Ma for the Pleistocene are proposed by Kay and Kurtz (1995) and Godoy (1993).

The isotopic signature of the Coya-Machalí rocks points to magma generation under a thinned crust (Nystrom et al., 1993). The crust was slightly thickened during the mid-Miocene to a 10 km thickness, rapidly increasing to reach a maximum (35 km?) near the Miocene-Pliocene boundary (Kurtz et al., 1995). Thickening controls the dramatic increase of La/Yb ratios (20 to 61) recorded in the El Teniente porphyries (Kay and Kurtz, 1995) and cannot be accounted solely by the upper crustal shortening discussed in this paper. According to the last authors, rapid crustal thickening in the Miocene arc should coincide with failure of the ductile lower crust.

## GEOPHYSICAL FRAMEWORK: A JOINT SEISMIC AND GRAVIMETRIC MODELING

Gravimetric stations were measured every 500 m along the main roads of El Teniente Copper Mine, using differential GPS for the horizontal and vertical positioning. The strong terrain correction has been thoroughly computed using a digital terrain model from 1:50,000 topographic charts and an analytical near-field correction in very rough topography sections. As a whole, the residual gravity signal has an envelope of error below 3 mgals. Additionally a seismic refraction line was acquired using experiment El Teniente Copper Mine induced events (rockbursts) and mining blasts as seismic source. Arrivals from these sources were recorded during a period of several days by portable seismic stations in a total of 14 points located along an approximately E-W profile to distances of about 40 km westward from the mine. A station located inside the mine was used to measure the origin time of the rockburst or blasting events.

The profile in Figure 1 was constructed from the 2-4 per day events, strong enough (magnitude=0.8-1.5) to be detected unambiguously in the different stations. The seismic interpretation was carried out by travel time forward modeling of first arrivals using laterally homogeneous velocity models. Our final model and the predicted travel time curves are also shown in Figure 1. The seismic data indicate a superficial 4.5 km/sec, 2.3-km-thick low-velocity layer overlying a 6.2 km/sec half space. The boundary between the upper low-velocity layer and the high-velocity half space is interpreted as the decoupling plane between a deformed uplifted core of the Coya-Machalí Formation and its more competent lower section. Further east, this detachment plane crops out as a northward shallowing out-of-sequence thrust (Figure 2).

The more continuous and detailed gravimetric experiment uses the seismic modeling constraint expressed in terms of a density contrast between an upper low-density layer at the deformed Coya-Machalí core and relatively high-density layer underneath the detachment. We adopted a standard two-layer density section of 2.67 gr/cm$^3$ in the upper 2.5 km, over a pseudo half space of 2.7-2.75 gr/cm$^3$. Density estimates from seismic velocities are consistent with a pseudo-half space of 2.7 gr/cm$^3$ and a low density zone of 2.45-2.5 gr/cm$^3$ in the upper section (a density contrast of -0.12 gr/cm$^3$ w/r to the standard section). 2-D gravimetric modeling (Figure 3) using the seismic and geological constraints, agrees well with a decoupling plane at ~ 2.5 km, and a deformed core of the Coya-Machalí Formation bounded by two antithetic structures that accommodate deformation and thickening in the western flank of the area.

## CONCLUSIONS

Uplift of the Miocene arc at 34$^o$ S.lat. is related to an asymmetric compressional horst with a 2.5 km deep detachment level. Decoupling is interpreted from seismic and gravimetric profiles in its western flank, where a low velocity/density upper layer of 2.3-2.5 km rests on top of a more competent basement. The geometry of the 2-D gravimetric modeling is also consistent with a compressional regime in the western margin of the arc, a triangular zone linked to a narrow belt of tightly folded underlying volcaniclastics.

Both boundary faults of the horst are younger and thus "out-of- sequence" when compared to the main Neuquén Basin fold-and-thrust belt, close to the Argentinian border. They are however "in-sequence" in relation to the Pleistocene to Holocene basement faults uplifting the Frontal Cordillera.

This Late Miocene to Early Pliocene upper crustal shortening matches the progressively southward shallowing of the Nazca plate recorded by geochemical signatures. Its contribution to crustal thickening, however, is minor (15%) compared to the overall increase. A deeper crustal contribution to thickening is therefore expected.

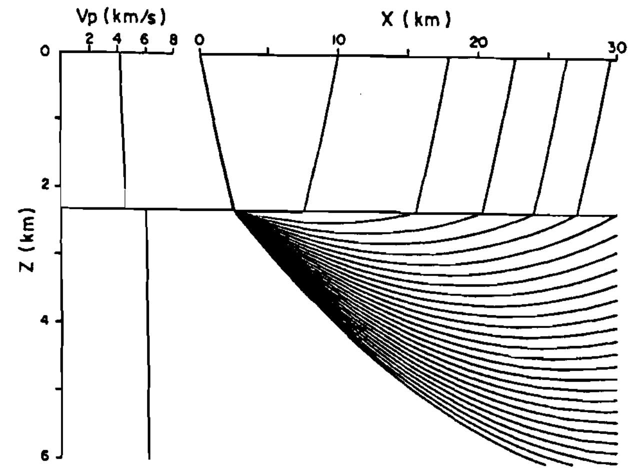


Figure 1: Seismic refraction profile velocity model and predicted travel time curves.

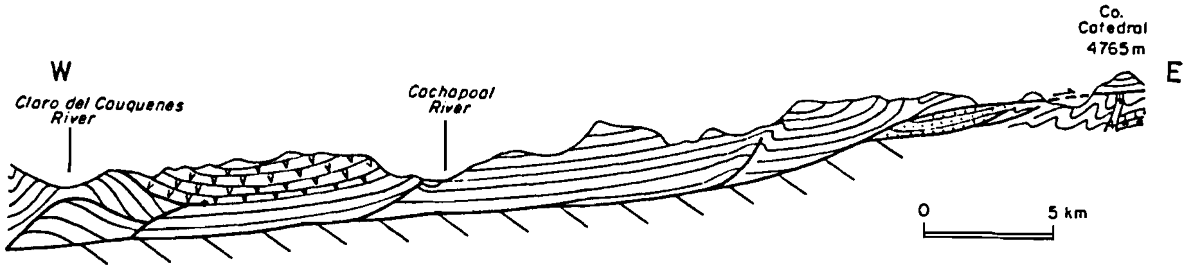


Figure 2: Geological section south of Cachapoal River. Detachment level assumed at the same depth as further north, where geophysical control is available. vv = Farellones Formation overlying Coya-Machalí volcani-clastics. Folded Mesozoic rocks under the C° Catedral klippe.

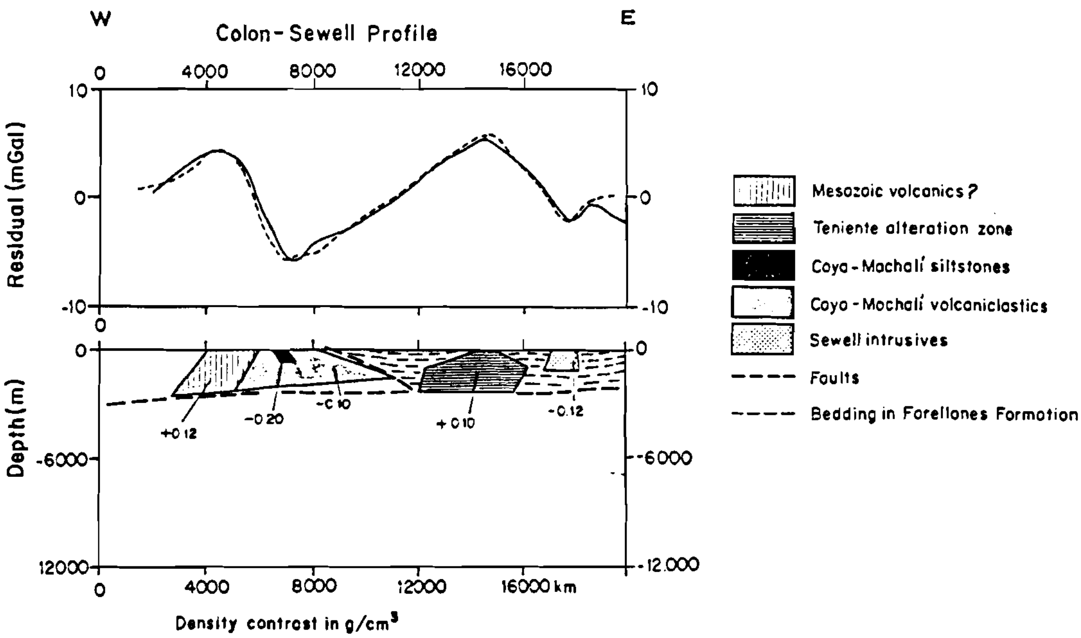


Figure 3: 2-D gravimetric model. Solid line: gravimetric data; dashed lines: predicted model.

**Aknowledgments** : This paper is a contribution to IGCP project 345 Andean Lithospheric Evolution. Research was funded by proyecto **Fondecyt 1940196**. We thank Codelco (Divisi6n El Teniente) for collaboration inside their mine. J. Cañuta, J.M. Capo, H. Zuñiga and M. Navarro helped obtaining the geophysical data.

## References

Aguirre, L. 1960. Geología de los Andes de Chile Central. Instituto de Investigaciones Geol6gicas. Bol. n° 9. Santiago.

Charrier, R. 1981. Geologie der chilenischen Hauptkordillere zwischen 34° und 34° 30' südlicher Breite und ihre tektonische, magmatische und paleogeographische Entwicklung. Berliner Geowissenschaftliche Abhand-lungen A (36) 270 pp. Berlin.

Cristallini, E., Mosquera, A. y Ramos, V. 1994. Estructura de la alta cordillera de San Juan. Asociaci6n Geol6gica Argentina. Revista 49 (1-2), 165-183.

Flynn, J., Wyss, A., Charrier, R. and Swisher, C. 1995. An Early Miocene anthropoid skull from the Chilean Andes. Nature, 373, 603-607.

Godoy, E. 1993. Geología del área entre los rios Claro del Maipo y Cachapoal. Convenio Codelco-Sernageomin. 68 pp. Unpublished.

Godoy, E. y Lara, L. 1994. Segmentaci6n estructural andina a los 33°-34° : nuevos datos en la Cordillera Principal. Actas 7° Congreso Geol6gico Chileno. 2, 1344-1348.

Godoy, E., Navarro, M. y Rivera, O. 1996. Zonas triangulares en el borde occidental de la Cordillera Principal (32°30'-34°30'), Chile: una soluci6n a la paradoja Abanico-Farellones. Actas 13° Cong. Geol. Argentino. Buenos Aires (in press).

Kay, S. and Kurtz, A. 1995. Magmatic and tectonic characterization of the El Teniente region. Convenio Codelco-U. de Cornell. 180 pp. Unpubl.

Klohn, C. 1960. Geología de la Cordillera de los Andes de Chile Central. Instituto de Investigaciones Geol6gicas. Bol. 8. Santiago. 95 pp.

Kurtz, A., Kay, S., Tittler, A., Mpodozis, C. and Godoy, E. 1995. Neogene magmatism in the andean cordillera (26° S to 34° S): evidence for spatial and temporal changes in crustal thickness. EOS. v76, 17, S272.

Nystrom, J., Parada, M. and Vergara, M. 1993. Sr-Nd isotope compositions of Cretaceous to Miocene volcanic rocks in Central Chile : a trend towards a MORB signature and a reversal with time. Second ISAG, Oxford (UK) : 21-23.

Pons, D. et Vicente, J-C. 1985. Découverte d'un bois fossile de fagaceae dans la formacion Farellones (Miocène) des Andes d'Aconcagua (Chili) : importance paléobotanique et signification paléo-orographique. 110 Cong. nat. Soc. sav., Montpellier. fasc. V: 187-207.

Sempere, T., Marshall, L., Rivano, S. and Godoy, E. 1993. Late Oligocene-Early Miocene compressional tectosedimentary episode and associated land-mammal faunas in the Andes of central Chile and adjacent Argentina (32-37o S). Tectonophysics, 229, 251-264.

Skewes, A. y Holmgren, C. 1993. Solevantamiento andino, erosi6n y emplazamiento de brechas mineralizadas en el dep6sito de cobre porfídico Los Bronces, Chile central(33°) : aplicaci6n de geotermometría de inclusiones fluidas. Revista Geol6gica de Chile. 20, 1, 71-84.

Thiele, R. 1980. Hoja Santiago. Instituto de Investigaciones Gel6gicas. Carta Geol6gica de Chile n°39. Santiago.51 pp.

Thiele, R, Beccar, I., Levi, B., Nystrom, J. and Vergara, M. 1991. Tertiary andean volcanism in a caldera-graben setting. Geologische Rundschau, 80/1, 179-186.

Thomas, H. 1953. Informe de la comisi6n geol6gica Thomas-Junge sobre la alta cordillera entre el rio Aconcagua y el rio Colorado. Instituto de Investigaciones Geol6gicas, 75 pp. Unpublished.

# GRAVITY FIELD AND GEOID AT THE SOUTH AMERICAN ACTIVE MARGIN (20° to 29° S)

Hans-Jürgen GÖTZE[1], Sabine SCHMIDT[1], Andreas KIRCHNER[1], Michael KÖSTERS[1], Manuel ARANEDA C.[2] and N.G. LOPEZ[3]

(1) Institut für Geologie, Geophysik und Geoinformatik, FU Berlin, Haus N, Malteserstraße 74-100, D-12249 Berlin, Germany
(2) Departamento de Geofísica, Universidad de Chile, Blanco Encalada 2085, Santiago, Chile
(3) Instituto de Geodésia y Topografía, Universidad Nacional de Tucumán, Av. Independéncia 1800, 4000 Tucumán, Argentina

**KEY WORDS:** Gravity field, geoid, tectonics, 3D modelling, offshore gravity, Central Andes.

## INTRODUCTION

From 1993 to 1996 the international MIGRA group with participants from Chile, Argentina and Germany has surveyed some 3.000 new gravity observations in an Andean geotraverse covering N-Chile and NW-Argentina between 64°- 71° W and 20° - 29° S. MIGRA is a Spanish acronym for "Mediciones Internacionales de GRavedad en los Andes" (Götze and Schmidt, 1993). Including reprocessed older data of Freie Universität Berlin, south American universities, oil and mining industry, there is now a data base of about 15.000 gravity values available, which can be used together with other geophysical and geological information for an interdisciplinary interpretation of the structure and evolution of the Central Andes (Götze et al. 1995, 1996).

In summer 1995 MIGRA took part in the "CINCA" offshore experiment of the german research vessel "Sonne" between the latitudes 20° S to 24° S. The offshore gravity data are connected with the on land survey to draw a complete gravity/geoid picture of this ocean-continent transition. Gravity data at sea were collected along continous survey lines (some 8.000 km). The average density of observational sites amounts to of about 15 observations per km. Gravity survey of cruise SO - 104 was tied to the Chilean National Gravity network of the "Departamento Geofísico, Universidad de Chile, Santiago" at reference stations in Valparaiso, Antofagasta and Iquique. The drift of the KSS31/32 onboard gravity sensor was very low and amounts to -0.048 mGal/day or - 1.44 mGal/month, respectively. The overall drift of the gravity meter was determined to be 0.47 mGal per 92 days.

For all gravity data we calculated gravity reductions within a radius of 200 km. Therefore anomalies calculated are "complete Bouguer anomalies". The data base which includes point data and 10 km * 10 km data grids of free-air-, different types of Bouguer- and isostatic-residual anomalies, are presented here in maps of isostatic residual fields along with a rough interpretation.

## FIELD WORK AND REDUCTIONS

The investigated region covers a 900 km x 1.000 km area in the central part of the Andean orogenic system.

The young Andean orogen between 20° - 29° S comprises different structures which have evolved on a Precambrian-Paleozoic basement (e.g. Reutter et al., 1994). This belt of ancient rocks was also described as the border of the "Faja Eruptiva Occidental". Two of our gravity surveys obtained structural information with new stations covering the northern and southern edges of this belt, near Calama (Chile) and in the Southern Argentinean Puna respectively. The investigated area is characterized by its enormous topography and remoteness, by its aridity, low population density and limited infrastructure. Other difficulties limiting our field work were the lack of topographic maps and geodetic networks in some regions. The spacing of stations amounts to approximately 5 km along all passable tracks aside from some local areas with a higher station density . To complete this data base we included gravity observations from different sources. With the exception of some inaccessible regions in the "Eastern" and "Western Cordillera", the gravity coverage for the region is fairly uniform. All measurements are tied to the IGSN71 gravity datum at base stations in Oran/Argentina, Iquique/Chile and Tucumán/Argentina (Götze et al. 1994).

The large size of the area and the severe logistical problems did not always allow us to determine the drift of the gravity meters by repeating the measurements at each station. However, even when we used bad tracks, the drift of the LaCoste & Romberg instruments (model G) rarely exceeded 0.1 mGal per day. Only about 35% of the gravity sites could be tied directly to benchmarks, such as levelling lines or trigonometric heights, so we used altimeters for height determinations. To improve the quality of our barometric measurements, we calculated time-dependent drift corrections as it is usually done for gravity measurements, using as many benchmarks and repeated measurements as possible. Moreover, the profiles of several days were tied together in order to eliminate systematic errors. The scales of the barometers have been calibrated on levelling lines with an altitude difference of about 2.000 m. Error estimations showed that even in the worst case the accuracy was better than 20 m, giving an error in the Bouguer anomaly of about 4 mGal, which is less than 1% of the overall magnitude of more than 450 mGal.

For the terrain correction (up to 167 km around all stations), a method including calculations of the earth's curvature developed for gravity investigations in the Alps was used, after adapting it to the special situation in the Central Andes. Reduction density was 2.67 g/cm$^3$ and the digital terrain model by Isacks (1988) was used to calculate a true 3D terrain correction..

## GRAVITY ANOMALIES

Onshore the Bouguer anomaly drops down to a regional minimum of about - 450 mGal in the area of the recent volcanic arc, related to crustal thickening by isostatic compensation. The effect of isostatic compensation of topography was calculated assuming the model of Vening-Meinesz with the following parameters: density contrast of the earth's mantle and crust dRHO = 0.35 g/cm$^3$, normal crustal thickness: 35 km and a flexural rigidity of $10^{23}$ Nm. The gravity effect of the isostatic compensation root was eliminated from the Bouguer gravity and the resulting anomaly serves as a residual field (Fig. 1). The most interesting features of this field are: (1) Positive values in the area of the forearc with isolated complexes parallel to the coastline. They are regionally caused by the presence of the dense subducting plate (gravity effect of about 50 mGal; density contrast: 0.05 g/cm$^3$) and locally by uplifted jurassic batholiths intruded into the "Formación La Negra". (2) The NNW-SSE striking positive anomaly from Calama (CAL) by the Salar de Atacama to southern Puna. We explain this gravity maximum by a highly metamorphic and high-density Paleozoic/Precambrian structure, the "Faja Eruptiva Occidental", which is oblique to the N-S orientation of the recent volcanic belt. (3) Local minima along the recent volcanic arc point to reservoirs of partly molten material at depths of 15 - 20 km. (4) Minima following a line from Ollagüe (OLL) to Calama (CAL) along 69° W, are caused by the Eocene volcanic arc with low-density volcanic material in the upper crust. (5) Alternating gravity highs and lows in the backarc region east of 67° W are observed in wide areas of the Argentine Puna and the Eastern Cordillera with a general NE-SW trend. The minima point to the position of mesozoic basins which are located in the Argentine Puna and extend northward to the territory of Bolivia. Gravity highs correlate with outcrops of Precambrian/Paleozoic basement in the Puna and Eastern Cordillera. 3D forward modelling of both gravity and gravity potential (geoid) can explain that most of the observed

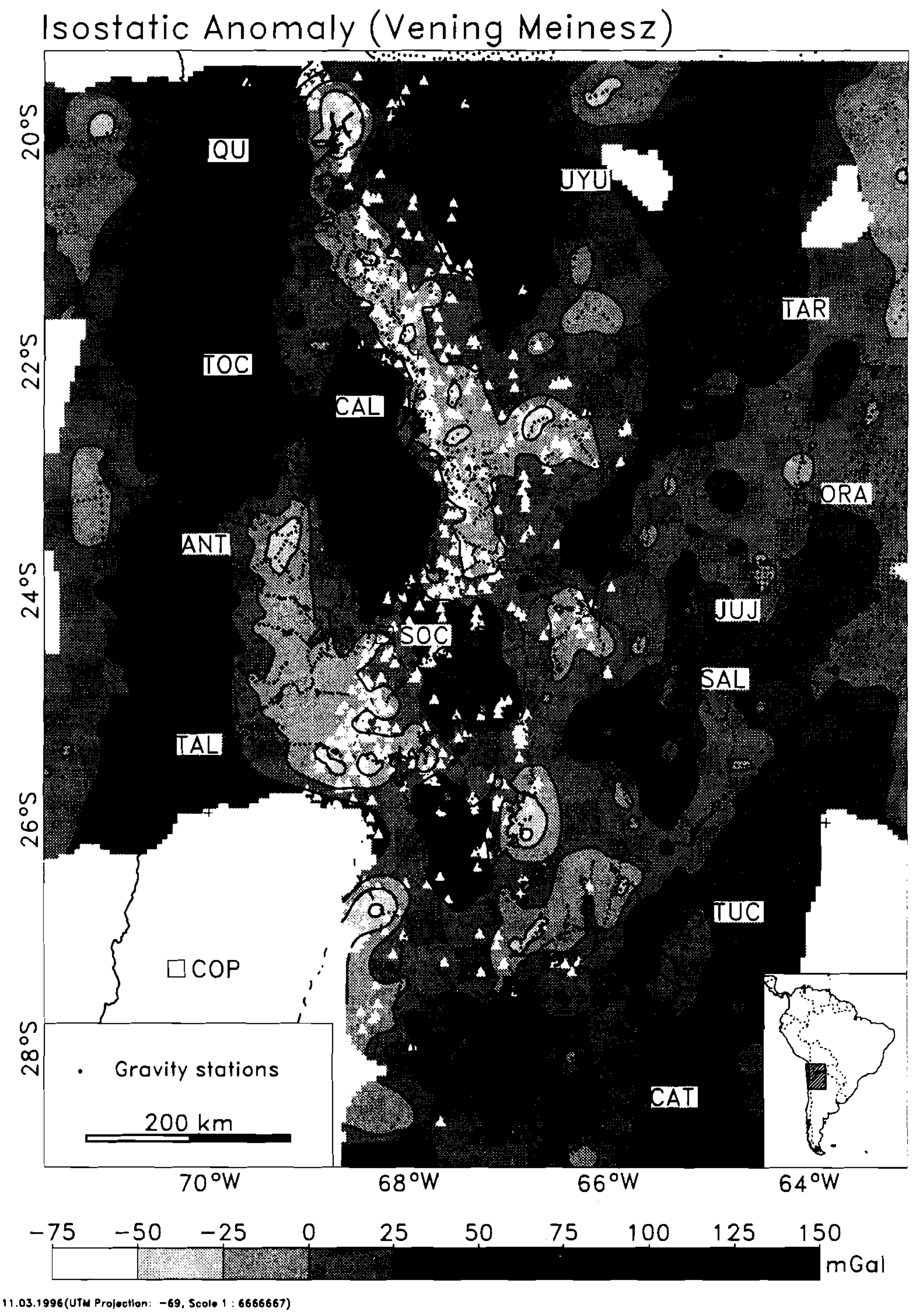


Figure 1: Residual gravity field of the Central Andes. Contour lines 10 mGal. Database is shown together with volcanos and other geographical features.

geoid anomaly (undulation) of 50 - 60 m is caused by Andean topography and isostatic roots. However, also density inhomogeneities in the downgoing slab and in the asthenospheric wedge contribute to undulations of the Earth's geoid in the Central Andes. All 3D density modelling has been proven by the results of refraction seismics (e.g. Wigger et al., 1994). Please, refer also to poster Kirchner, Götze, Lessel and Schmitz (this issu).

## CONCLUSIONS

The updated gravity data base will play an important role in both local investigations of applied geophysics and regional interdisciplinary interpretations of pure geophysics. Andean gravity field seems to be a sensitive indicator which is linked to many processes contributing to the tectonic framework of the Nazca plate subduction zone.

MIGRA data sets are available via FTP for non commercial applications of universities and governmental agencies. You may contact H.-J. Götze at Freie Universität Berlin (Germany) under "hajo@zedat.fu-berlin.de" or refer to the "Gravity Research Group´s" Home page on the WWW for further information: - http://fub46.zedat.fu-berlin.de:8080/~wwwgravi.

## ACKNOWLEDGEMENT

The support with maps and geodetic information by the following institutions is gratefully acknowledged: Institutos Geográficos Militares in Santiago, Buenos Aires and La Paz, Yacimientos Petrolíferos Fiscales of Argentina and Bolivia, Empresa Nacional de Petróleo, and CODELCO both from Chile. This paper presents results of the gravity research group D3 of the SFB 267 which is funded by the Deutsche Forschungsgemeinschaft (DFG) and Freie Universität Berlin and contributes to IGCP 345.

## REFERENCES

Götze, H.-J. und S. Schmidt, 1993. El que conocio el desierto no lo olvida - jamas. In: VERTIENTE, Revista de la Facultad de Ingenieria y Ciencias Geologicas, Universidad Catolica del Norte, Antofagasta, Chile, 9, No. 9, ISSN 0716-1964, pp. 6 - 10.

Götze, H.-J., Lahmeyer, B., Schmidt, S. and Strunk, S., 1994. The Lithospheric Structure of the Central Andes (20°-26°S) as inferred from Quantitative Interpretation of Regional Gravity. In: Tectonics of the Southern Central Andes (Eds.: Reutter, Scheuber, Wigger), pp. 7-21, Springer Verlag Heidelberg.

Götze, H.-J., M. Schmitz, P. Giese, S. Schmidt, P. Wigger, G. Schwarz, M. Araneda, G. Chong D. and J. Viramonte, 1995. Las estructuras litosféricas de los Andes Cantrales australes basados en interpretaciones geofísicas. IGCP Special Volume, Revista Geológica de Chile, Vol 22, No. 2, 179-192.

Götze, H.-J., 1996. Group updates the gravity data base in the Central Andes (20° - 29° S). EOS Transactions, American Geophysical Union, in print.

Isacks, B.L., 1988. Uplift of the Central Andean Plateau and Bending of the Bolivian Orocline. *Journ. Geophys. Res.*, Vol. 93, No. B4, 3211 - 3231.

Reutter, K.-J., E. Scheuber and P. Wigger (Editors), 1994. *Tectonics of the Southern Central Andes*, Springer Verlag, Heidelberg, pp. 333.

Wigger, P.J., M. Schmitz, M. Araneda, M., G. Asch, S. Baldzuhn, P. Giese, W.-D. Heinsohn, E. Martinez, E. Ricaldi, P. Röwer and J. Viramonte, 1994. Variation of the crustal structure of the Southern Central Andes deduced from seismic refraction investigations. In: Tectonics of the Southern Central Andes (Eds.: Reutter, Scheuber, Wigger), Springer Verlag Heidelberg, pp. 23-48 .

# A THREE-DIMENSIONAL MODEL OF SEISMIC VELOCITIES BENEATH NORTHERN CHILE FROM LOCAL EARTHQUAKE TOMOGRAPHY

Frank M. GRAEBER[1], Günter ASCH[1]

(1) GeoForschungsZentrum Potsdam, Dept. 2.4 "Seismology & Tomography", Telegrafenberg A17, D-14473 Potsdam, Germany; e-mail: graeber@gfz-potsdam.de

**KEY WORDS**: Travel-time tomography, 3-D velocity structure, subduction, volcanic arcs, N. Chile

## INTRODUCTION

In the last two decades, structural information about the deep interior of the earth in local, regional and global scale has been drawn extensively from travel-time tomography experiments. Depending on the kind of station network used, two- or three-dimensional (2- or 3-D) models of the p- and s-wave velocity structure are obtained. Tomographic models are in most cases calcutated as deviations to an a priori one-dimensional (1-D) reference model. Thus the method is particularly useful for imaging extended lateral inhomogeneties. Velocity anomalies are mainly caused by differences in density and aggregate state of rocks, both influenced by temperature and pressure. The Cental Andes are, due to the plate collision, characterized by various geophyical anomalies. One of them is the huge amount of seismic activity on and within the subducting plate, making it possible and attractive to apply local earthquake tomography.

## METHOD

In geophysical investigations the physical properties of a targeted volume are often not directly measurable. One has to observe the effects at the surface and calculate back or invert for these properties, in order to get a model of their distribution in space beginning with simple approximations. In travel-time tomography the differences in arival times of earthquake-generated seismic waves at seismometer stations form the set of observed data. Deviations of seismic velocities at discrete points in space with respect to a starting model are the model parameters to invert for. In case of local earthquake tomography the hypocentral coordinates depend on the velocity structure and thus belong to the unknown (model-) parameters too. The linearized hypocenter-velocity-inverse problem is generally ill-posed (or mixed-determined) and according to Levenberg-Marquardt solved iteratively using the damped least squares (DLSQ) technique. The linearization by a Taylor series expandation requires a proper a priori model. Kissling et al. (1994) demonstrated, that the so called minimum 1-D model, which is itself a DLSQ solution of a simultaneous 1-D inversion, is well suited for routine earthquake locations in comparison to estimated 1-D models and gives much more accurate results when used as starting model in the 3-D inversion. The 3-D inversion procedure is performed by the routine SIMULPS12 (Evans, Eberhart-Phillips & Thurber, 1994). The parametrization of the 3-D model is given by nodal planes in x-, y- and z-direction. Velocities are interpolated between the points of intersection. Distances between these planes depend on the station network characteristcs, on the amount and spatial distribution of events and on the dimensions of structural features wished to be resolved. Toomey and Foulger (1989) pointed out the importance of properly considering both model resolution and model fidelity to avoid poorly resolved model parameters as well as spatial aliasing caused by a sparse parametrization. Tests with artificial data, various subsets of data and various model parametrizations are carried out to refine the final 3-D velocity model and to unmask possible artifacts.

## TARGETS OF THE TOMOGRAPHIC INVESTIGATION

The Chilan part of the Central Andes offers very good conditions for a temporary seismological experiment, including local earthquake tomography, with respect to the quantity and quality of data and the existence of targets of special interest. Like other regions of plate collision and subduction, it shows a characteristic distribution of seismic activity. A large number of earthquakes occur at the contact zone of the Nazca plate and the continental plate as well as within the subducting Nazca plate down to more than 600 km depth. Due to fast (> 9cm/a) and moderatly steep subduction, the subducted oceanic plate remains colder as the surrounding material. This thermal anomaly should be expressed in a positive velocity anomaly close to the Wadati-Benioff zone, as similar studies in other subduction zones found out. Related to the subduction is the existence of the volcanic arcs. The recent volcanic arc (Western Cordillera) is characterised by an increased heat flow density, a volume of high electric conductivity, a short wavelength gravity minimum (Götze et al., 1994) and a zone of anomalous high attenuation. These anomalies evaluated together are an indication for a volume of partial melted rocks, which is usualy outlined by lower seismic velocities. The crustal seismic activity is much smaller and could not be mapped previously due to the lack of strong earthquakes.

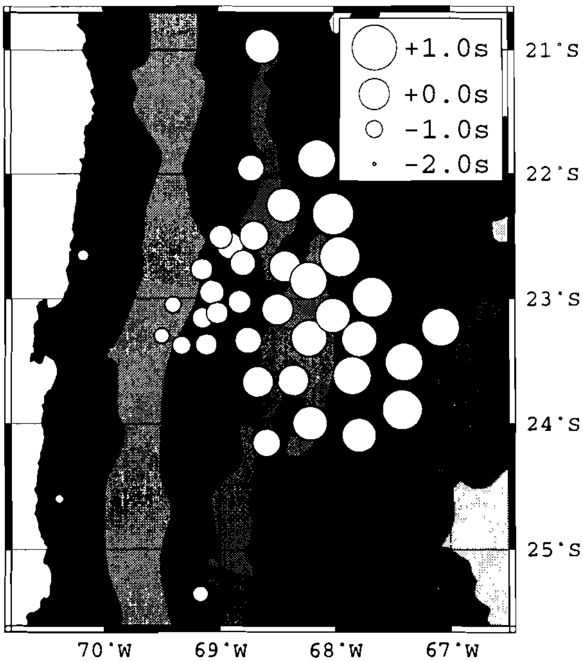


Fig. 1
The PISCO'94 and CALAMA'94 network stations drawn with circle sizes according to their average travel-time residuals from 1-D inversion

## DATA FROM THE PISCO'94 EXPERIMENT

This study takes advantage of the dense and sensible seismological network of the PISCO'94 (Projecto de Investigacion Sismologica de la Cordillera Occidental) experiment, which was operated from January to May in 1994 as part of the Collaborative Research Center 267 "Deformation processes in the Andes" between 21°S to 25°S and 67°W to 70°W (Fig. 1). It combines active and passive seismological measurements. Continuous digital registration of the network stations with 100 samples per second guaranteed a high level of data quality and quantity. The arid climate, caused by the cold Humbold current, and the very low population density promote low noise registrations. Thus a few hundred crustal events of lower magnitudes, including natural earthquakes, mining blasts and shots, and about 5000 earthquakes within the subducting plate could be observed in a 100 days period. Additional data from the temporary seismological network CALAMA, which was operated in April 1994 by the Universidad de Chile, Santiago, is available thanks to a data exchange. Two subsets of high quality data were selected for the inversion procedures: 450 events with more than 10000 p- and s-wave readings for the 1-D inversion and 930 events with more than 20000 p- and s-wave readings for the 3-D inversion.

## RESULTS OF THE 1-D AND 3-D INVERSIONS

The obtained minumum 1-D model with average station residual reflects the extremely thickened crust in the Central Andes. Typical subcrustal velocities of nearly 8 km/s are reached only beneath 70 km depth. Normal upper crust and middle crust velocities can be seen down to 40 km depth and rather high lower crust velocities between 40 km and 70 km depth. The station residual pattern shows a strong trend to higher velocities from the Western Cordillera towards the trench, which might be caused by the thinning of the crust in this direction and/or fast waves, that are propagating along the cold subducting plate. The station residuals are consistent within the morphostructural units.

The Volume of acceptable model resolution in 3-D is described by the resolution matrix and several tests and is, as expected, limited to the crust and mantle beneath the denser part of the network and above the Wadati-Benioff zone. The minimum horizontal and vertical seperation of nodes is 25 km and 10 km, respectively. Horizontal and vertical sections through the actual 3-D model outline four prominent anomalies:

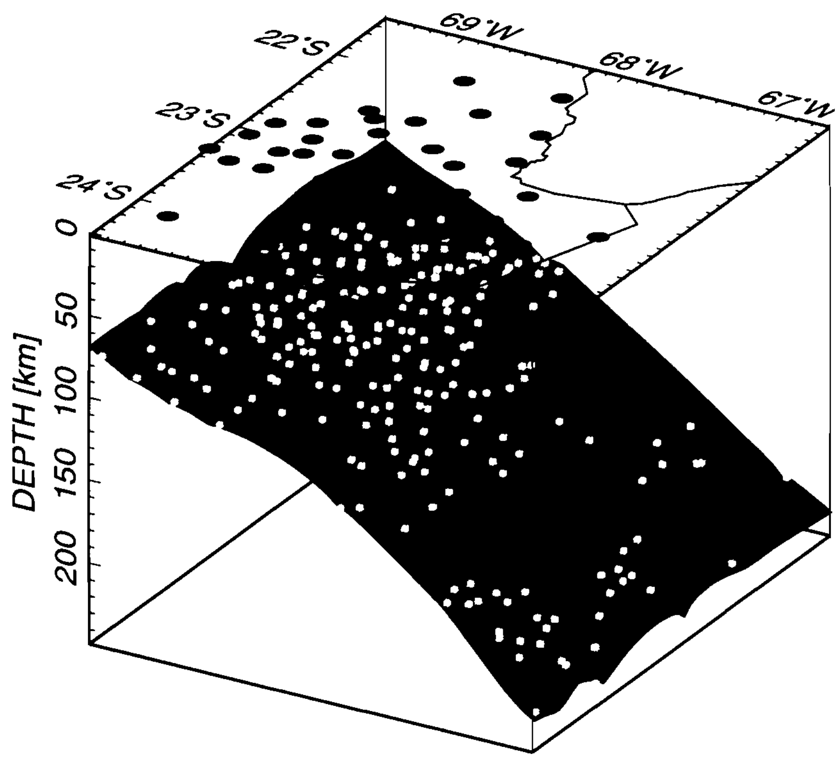


Fig. 2
The top surface of the Wadati-Benioff zone as given by interpolation through the uppermost slab earthquakes of a subset of high quality data

- -1- A narrow zone of lower velocities following the western edge of the recent magmatic arc down to about 65 km, considering previous studies interpreted as partial melts
- -2- A layer with moderately lower velocities beneath the Precordillera, eventually a remnant of the last period of volcanic activities
- -3- High velocities related to the Wadati-Benioff zone, interpreted as cold oceanic lithosphere
- -4- A body of high velocities beneath the Salar de Atacama next to a local short wavelength gravity maximum

Less prominent anomalies have to be discussed in detail. A comparison with 2-D models from the controlled source measurements of the PISCO'94 experiment might support some of them.

The high quality slab earthquakes relocated in the 3-D inversion procedure contract the top of the seismic activity to a clearly shaped plane. Fig. 2 shows an interpolated plane through the uppermost slab earthquakes in each 1/8° sector. At about 68°W the Wadati-Benioff zone becomes slightly steeper towards the east.

## CONCLUSIONS

Especially when the complexity of the true crustal structure limits the interpretation of one- and two-dimensional methods, the obtained tomographic images, though they have to be interpretated very carfully as artifacts might remain undiscovered, offer important 3-D structural information in crustal scale. On the other hand, tomographic results can hardly be evaluated without additional information from other studies. The coordinated studies of different geoscientific disciplines within the Collaborative Research Center 267 "Deformation processes in the Andes" offer the possibility of a compilation of all the different kind of geophysical, geological and petrological data available and will lead to a refined model of the anomalous crust and upper mantle in the area of investigation.

## REFERENCES

Evans J.R., Eberhart-Phillips D. and Thurber C.H. 1994. Users manual for SIMULPS12 for imaging Vp and Vp/Vs: A derivative of the "Thurber" tomographic inversion SIMUL3 for local earthquakes and explosions. *USGS open file report*, 94-431.

Götze H.-J., Lahmeyer B., Schmidt S. and Strunk S. 1994. The Lithospheric Structure of the Central Andes (20-26°S) as inferred from Quantitative Interpretation of Regional Gravity. *Tectonics of the Southern Central Andes (Eds.: Reutter, Scheuber, Wigger), Springer Verlag Heidelberg*, 7-21.

Kissling E., Ellsworth W.L., Eberhart-Phillips D., Kradolfer U. 1994. Initial reference models in seismic tomography. *Journal of Geophysical Research*, 99, B10, 19635-19646.

Toomey D.R. and Foulger G.R. 1989. Tomographic Inversion of Local Earthquake Data From the Hengill-Grensdalur Central Volcano Complex, Iceland. *Journal of Geophysical Research*, 94, B12, 17497-17510.

# LITHOSCOPE EXPERIMENT IN NORTHERN ECUADOR : PRELIMINARY RESULTS

Bertrand GUILLIER[1,2], Jean Luc CHATELAIN[1,2], Alexandra ALVARADO[2], Hugo YEPES[2], Georges POUPINET[3], Jean François FELS[1,2]

[1] ORSTOM, Apartado 17 11 6596, Quito, Ecuador.
[2] Instituto Geofisico, Escuela Politécnica Nacional, Apartado 17 01 2759, Quito, Ecuador.
[3] LGIT, Université J. Fourier, BP 53, 38041 Grenoble, France.

KEY WORDS : sismotectonic, neotectonic, Andes, Ecuador.

## INTRODUCTION

From December 1994 to May 1995, 54 short period seismic stations from the French Lithoscope network, (19 stations 3C, 35 stations 1C) have been operating in the Northern part of the Ecuadorian Andes (0° to 1°30S , 77°20W to 79°20W), along five profiles : 3 North-South profiles at 77°40W, 78°30W, 79°20W and 2 East-West profiles at 0°15S and 1°15S. Data of the national network (27 1C stations) of the Instituto Geofisico of the Escuela Politecnica Nacional of Quito have been incorporated to the Lithoscope data.

## DATA PROCESSING

The hypocenters have been located using HYPOINVERSE (Klein, 1978) with a crustal velocity structure represented by flat homogeneous layers based on an inversion model from local data (Prévot et al., 1996). Travel time is corrected for the elevation of the stations. From December 1994 to March 1995, 1011 local and regional events with more than 6 arrival times have been detected, which represent a total set of 21166 arrivals times (12394 P-waves arrivals and 8772 S-waves arrivals). From the initial set of 1011 local events, a final set of 552 events (figure 1) were selected with the following criteria : a root mean square residual (RMS) less than 1.0 s and a condition number less than 100. Out of these 552 events, 146 are recorded in 20 stations or more. The location have been performed using a Vp/Vs ratio of 1.737 obtained with a (S-S) versus (P-P) diagram (Chatelain, 1978).

## PRELIMINARY RESULTS

At the moment, only the first step of the data analysis has been completed : all arrival times have been read, the events located and selected, and the preliminary spatial distribution analysis of the earthquakes performed.

1.- About 50% of the earthquakes are shallow events concentrated in the Pisayambo nest centered on 1°20S, 78°30W (Figure 1) ;

2.- Under the cordillera only shallow events (0 -30 km) are present (Figure 1), i.e. no earthquakes occur on the subducting Nazca plate beneath the Andes cordillera. This can be clearly seen on the cross-section (Figure 2) where it appears that the seismic nest of Pisayambo in the upper plate is right above the gap of intermediate seismicity in the downgoing plate ;

3.- The shallower intermediate-depth earthquakes (60 to 100 km) are located to the west of the Cordillera, while the deeper events (100 to 200 km) are present to the East of the Cordillera South of 1°S only (Figure 1)

4.- A lack of shallow seismicity (0 - 20 km) is clearly marked South of 0° between the coast and the western Cordillera (between 100 and 200 km on the horizontal scale on figure 2). This absence of seismicity is not an artifact of the location, as stations were installed above this zone.

## CONCLUSION

Preliminary results of the Lithoscope Ecuador experiment have allowed us to precise the spatial distribution of the seismicity beneath Ecuador, revealing at least four interesting features. More detailed study, including about 50 focal mechanisms, currently undergoing in order to relate these features with the tectonics of the area will also be presented.

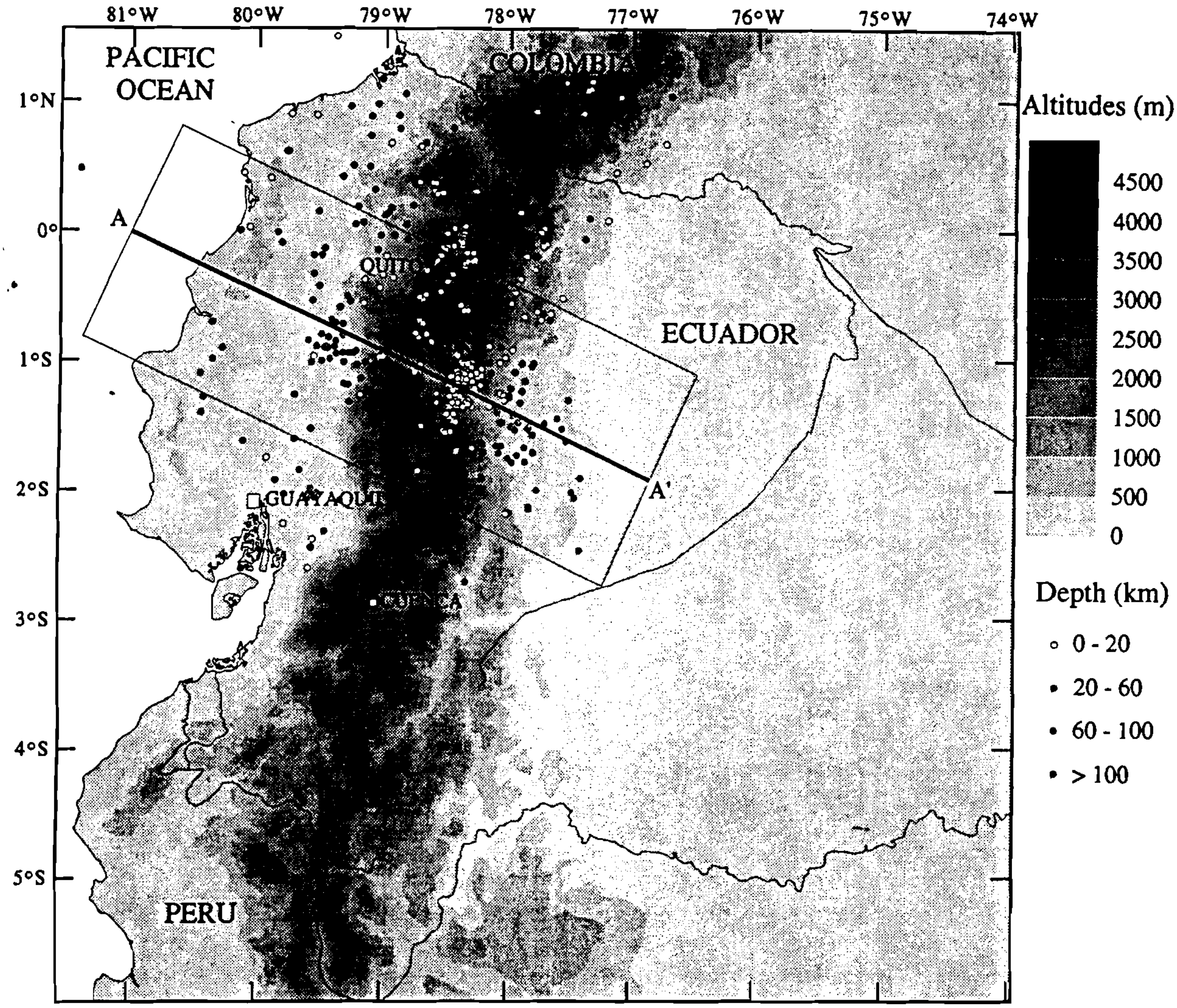


Figure 1 : Location of the selected earthquakes recorded from december 1994 to march 1995, during the Lithoscope experiment. The black line represents the location of the cross-section shown in figure 2. PN : Pisayambo nest.

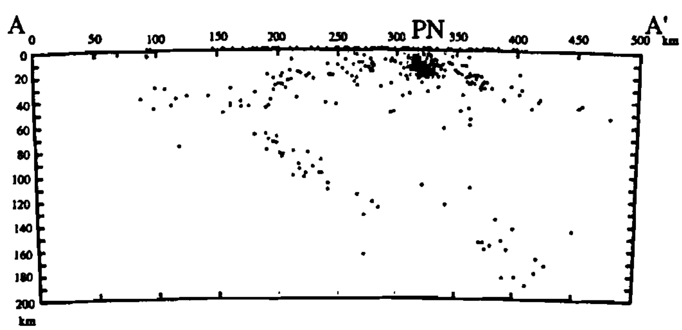


Figure 2 : Depth distribution of the selected earthquakes (open circles) recorded from december 1994 to march 1995, during the Lithoscope experiment, along a NW-SE cross-section. The filled triangles represent the location of the stations. Note the location of the shallow seismicity nest in the upper plate above the seismicity gap in the down-going plate. PN : Pisayambo nest.

REFERENCES

Chatelain, J.-L., 1978. Etude fine de la sismicité en zone de collision continentale au moyen d'un réseau de stations portables : la région Hindu-Kush Pamir, Univ. Scient. Medic. de Grenoble, 219 p..

Prévot R., Chatelain J.-L., Guillier B., Yepes H., 1996. Mapping of the P-wave velocity structure beneath the ecuadorian Andes, this volume.

Klein, F.W., 1978. Hypocenter location program HYPOINVERSE, U. S. Geol. Surv., Open File Rep., 78-694.

# CINCA '95: PASSIVE SEISMOLOGY ON- AND OFFSHORE IN NORTHERN CHILE

S.HUSEN(1), G. ASCH(2), M. BAUMBACH(2), Chr. HABERLAND(3), A. RIETBROOK(4), A. RUDLOFF(2), K. WYLEGALLA(2)

(1) GEOMAR, Wischhofstr. 1-3, 24148 Kiel, Germany
(2) GFZ-Potsdam, Telegrafenberg A17, 14473 Potsdam, Germany
(3) FU-Berlin, FR Geophysik, Malteser Str. 74-100, 12249 Berlin, Germnay
(4) LMU-Munich, Germany

**KEY WORDS**: Northern Chile, passive seismology, seismic tomography

## INTRODUCTION

During the months August to October 1995 within the CINCA[1]-Project the natural seismicity in an area north of Antofagasta was observed. The network is a continuation of the PISCO '94 experiment towards the Coastal Cordillera. PISCO '94 was a combined active and passive seismological campaign in the area of the Pre- and Western Cordillera at the same latitude. It was carried out by the SFB[2] 267 in spring 1994. The aim of both projects is a detailed investigation of the velocity structure of the crust and upper mantle in this region. The results of the passive seismology during the CINCA-Project will be supported and supplemented by off-shore reflection profiles and on- and off-shore refraction profiles in the same area as additional parts of the CINCA-Project.

## FIELD OPERATION

In the beginning the network was designed with 22 PDAS-seismometers onshore and 9 OBH[3] offshore located between the trench and the coast. The situation changed by the 30th of July when an earthquake of magnitude $m_W$=8.1 (HRV) occurred north of Antafogasta. Fortunately no big damage was reported and only a few people were killed. An earthquake in this order causes a huge amount of aftershocks and due to this new situation the network was redesigned. Additional 13 REFTEK-seismometers were installed by the *German Task Force for Earthquakes*, increasing the total number of onshore stations to 35. The final network design is shown in figure 1.
All onshore recording sites were equipped with 3-component Seismometers (Mark L4-3D 1Hz) and each channel was recorded at 100 Hz samplerate. Because there is no way to check the coincidence of the signal against neighbouring stations, it is rather difficult and often impossible to detect events by a single station. Due to this problematic nature all stations were run in continous mode. The raw data were collected on hard disk and for the land stations archived an CDROM. The OBH data were collected and

[1] Crustal Investigation on- and off-shore Nazca Plate and Central Andes
[2] Collaborative Research Group 267, FUB - TUB - GFZ, Deformation processes in the Andes
[3] Ocean Bottom Hydrophon

archieved on DAT tapes. The land stations were checked every six days by two groups, collecting hard disk and changing batteries. The OBH were deployed by the research vessel SONNE in two parts. Each consisted of 12 days and the maximum depth of the OBH was 5500 m.

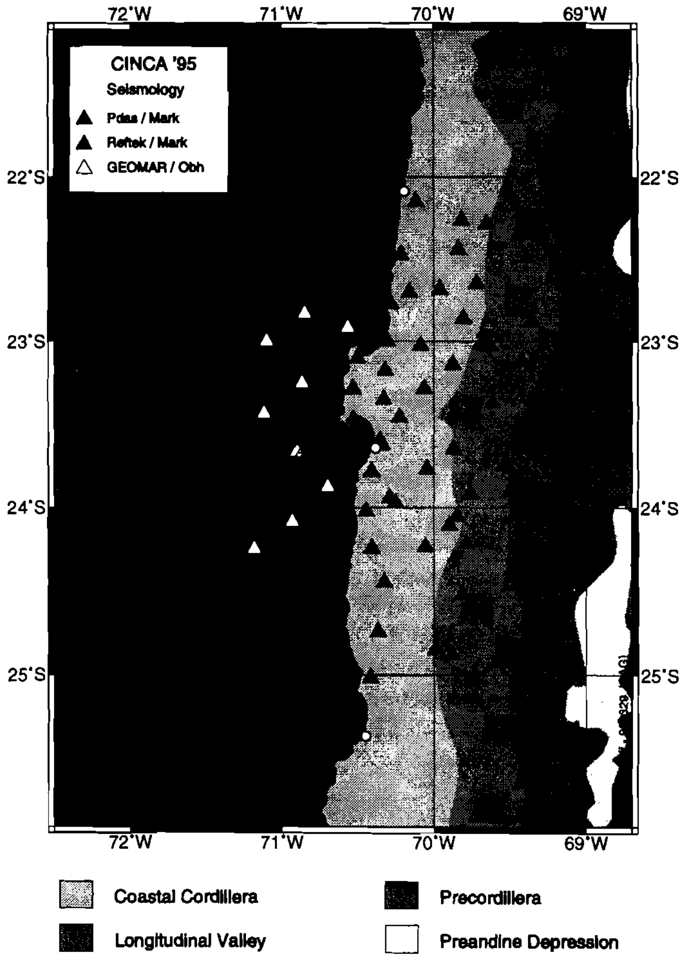


**Figure 1:** network design of the CINCA array

Once the data were achieved on CDROM in the field a triggerlist was created for each day. A criterium for an event was defined by a LTA[4] to STA ratio of 8 and a coincidence of 5 stations. In general about 200 events per day (figure 2) were observed. This unusual high seismicity is caused by the aftershock activity of the Antofagasta earthquake. In contrast to other aftershock studies we do not observe a significant decrease in the number of events per day over the whole observation period.

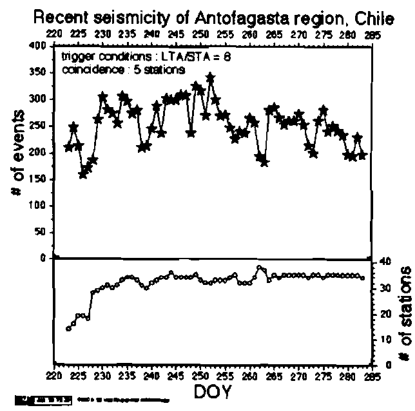


**Figure 2:** regional seismicity during the field campaign

[4] LTA=Long Time Average, STA=Short Time Average

## DATA EVALUATION AND PRELIMINARY RESULTS

After the field campaign all available data (PDAS, Reftek and OBH) were merged together. Based on the triggerlist, which has been recalculated with LTA to STA ratio of 8 and a coincidence of 15 Stations, records of 130s length based on the earliest arrival were cut out of the continous data streams for all three channels. These timepieces have been sorted for each event and stored on CDROMs. In total we produced a catalog consisting of 4500 Events stored on 22 CDROMs, which leads to a data capacity of 13 GByte. All Events have to be localized with the PITSA based package GIANT[5]. Parallel to the localisation procedure a 1D minimum $V_P$-model is calculated through a 1D inversion with the VELEST[6]-Software. For a significant subset of 500 Events the epicenters, a longitudinal section in east-west and north-south direction and the used 1D $V_P$ model is shown in figure 3.

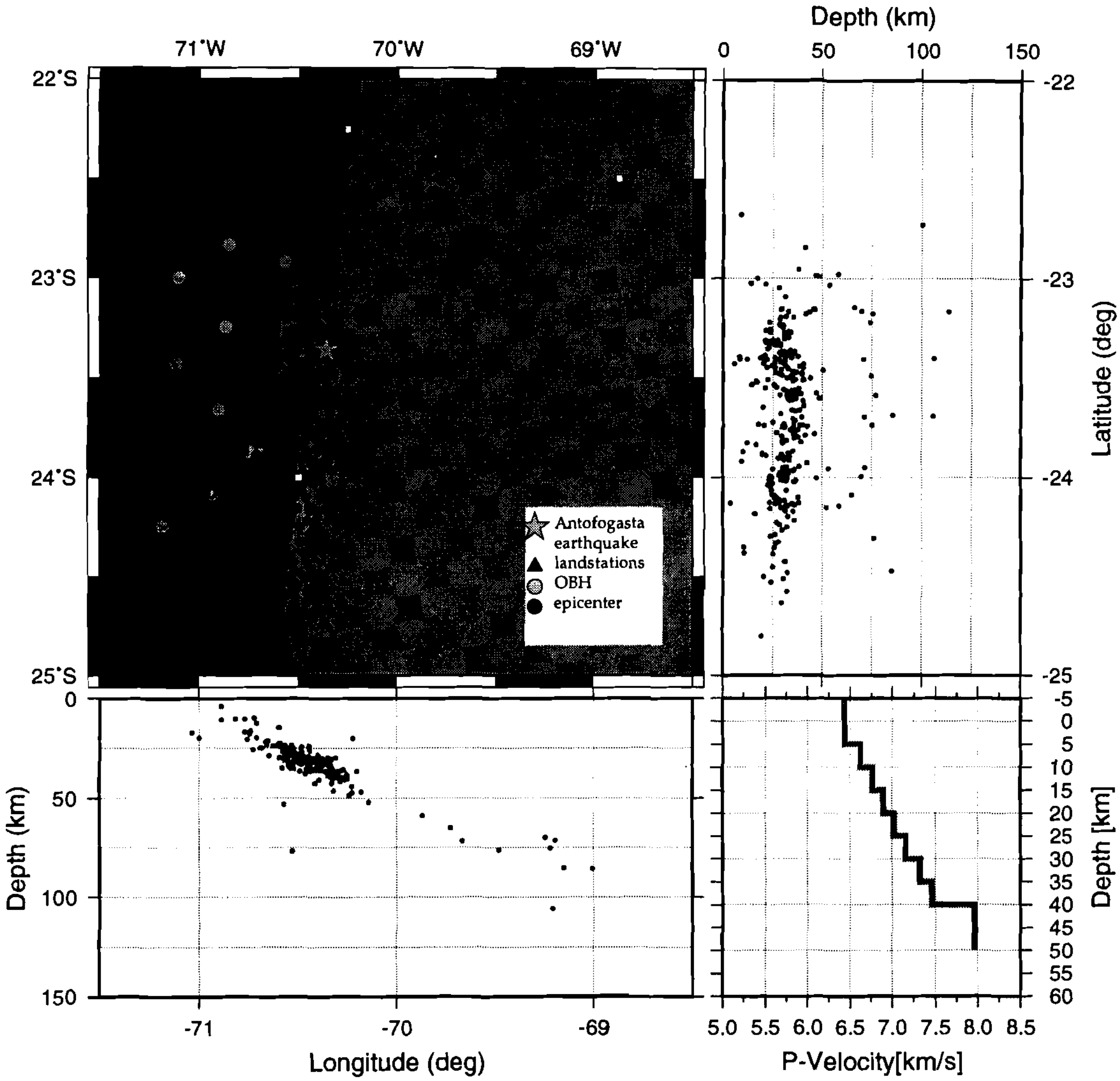


**Figure 3:** Epicenter distribution, longitudinal section in east-west and north-south direction and the used velocity model for hypocenter estimation

[5] A.Rietbrook, LMU-Munich

[6] E. Kissling, ETH Zurich

The epicenter distribution shows a region of high event density in a area south of the Antofagasta earthquake. These events concentrate in a depth at 30km as indicated by the longitudinal section in figure 3. This improves the assumption that the observed unusual high seismicity has been triggered by the main shock.
Most of the events concentrate in a stretch along the coast. This area lies in the border region of the land network and will give uncertanties in the localisation of these events because of the bad coverage of the azimuth. Using the OBH data improves the localisation because of the better azimuth coverage. A good precision in the epicenter estimation is essential for a detailed study of this area.
A longitudinal section in east-west direction (figure 3) gives a good image of the subducting slab. Just a few events occur beside the main trend, which can be caused by uncertanties in estimating the depth. The dip of the subducting slab can be estimated with 12-13$^0$, which is in close agreement to the results of the refraction profiles (Patzwahl et al., this issue).
In the near future we will use this excellent data set for a detailed 3D tomogaphy study. Based on this results an interpretaion of the geodymanic situation will be done.

# THE ARGENTINA-CHILE ANDES. CRUSTAL THICKNESSES, ISOSTASY, SHORTENING AND ANOMALY PREDICTION FROM GRAVITY STUDIES

Antonio Introcaso(1), María Cristina Pacino(1) and Fernando Guspí(1)

(1) IFIR (INSTITUTO DE FISICA ROSARIO) - (CONICET - U.N.R.)
FACULTAD DE CIENCIAS EXACTAS, INGENIERIA Y AGRIMENSURA (U.N.R.)
Av. Pellegrini 250 - 2000 - Rosario - ARGENTINA

KEY WORDS: Andes, Gravity, Isostasy, Shortening, Prediction

## INTRODUCTION, RESULTS AND CONCLUSIONS

We present the results of a comprehensive study made over 14 E-W sections of the Andes across Argentina and Chile, starting at the Pacific Ocean and reaching most the Atlantic Ocean. Isostatic gravity anomalies, crustal models and shortening estimates were analyzed at all them. Particularly at 22°, 25° and 32° S latitude, seismo-gravity models performed indicate that the equilibrium of these Andean sections behaves "grosso modo" as an Airy isostatic system. In all the studied sections, a good correlation is observed between the Andean masses and the regional Bouguer anomalies, and Andean roots calculated by inverting those anomalies also strongly resemble the isostatic roots. Elastic or visco-elastic models under vertical loads, even with complicated hypotheses (e.g. Burov and Diament, 1995), always yield shallower and smoother roots, and therefore they seem not to be adequate for the present situation. Some narrow gravity peaks observed on certain sections, however, may suggest a flexo-compressional deformation; this investigation could be the subject of future work.

Crustal models are better determined on those sections at which deep seismic data are available. Thus, at both 22° and 25° S latitudes, where the Nazca plate subducts with "normal" angle, seismic models render a crust about 60 km deep. (Schmidt et al., 1993; Schmidt, 1994). Our gravity models are consistent with the former as long as one assumes a lithospheric mantle heating of the area, as proposed by Isacks (1988). No significant influence of the plate on the determination of the crustal thicknesses is observed. At 32° S, the seismo-gravity model yields approximately an Airy system (Introcaso et al., 1992). The plate subducts horizontally here, with probable influence of positive sign over the gravity anomalies. From seismic analyses, Regnier et al. (1994) report crustal depths beneath Precordillera and Sierras Pampeanas of San Juan exceding significantly those calculated by gravity inversion without seismic support. This fact seems to suggest that a gravity balance could be developed between the positive effect of the Nazca plate and the negative effect of the deeper roots.

Summarizing, both "normal" and "flat" subduction would produce heterogeneity in the upper mantle, and they would play a role in the determination of the Andean crustal thicknesses.

Table 1 and Fig. 1 report maximum Bouguer anomaly and derived maximum crustal thickness and shortening at each section. Shortening, which indicates a decreasing from N to S in the degree of compression of the Cordillera axis, is undoubtely the main mechanism of the Andean uplift.

Our institute developed last year complete Argentine Bouguer and free-air gravity anomaly charts with a separation of 5' x 5' between grid points (Guspí et al., 1995). They include Chilean anomalies from a SERNAGEOMIN data base. We also prepared charts which represent: (1) Free-air anomalies, (2) Bouguer anomalies, (3) Isostatic corrections, (4) Thermal correction for the central Andes (Pratt), (5) Moho depths (Fig. 2). The observed coherence between (2), (3), (5) and a digital terrain model, and furthermore between (5) for latitudes greater than 22° S and the chart of James (1971) for latitudes less than 22° shows undoubtely isostatic compensation in a wide regional scale, and it comfirms the results obtained for each section. (5), along with the seismo-gravity models at 22°, 25° and 32° S illustrates that gravity models without seismic constraints are also able to define reasonably the crustal thicknesses.

Finally, from all these available sources, four predictive equations were derived. B is mean Bouguer anomaly in mGal and H is mean altitude in km (Fig. 3).

Complete Argentina and Chile: B = 14 - 71.2 H
Northern area (22 - 30° S): B = 25 - 76 H
Central area (30 - 39° S): B = 10 - 66 H
Southern area (> 39° S): B = 2.6 - 69 H

| LOCATION | MAXIMUM BOUGUER ANOMALY mGal | MAXIMUM CRUSTAL THICKNESS Km | SHORTENING Km |
|---|---|---|---|
| 22°S | -410 | 66 | >300 to 220 |
| 25°S | -400 | 60-65 | |
| 27°S | -370 | 68 | |
| 30°S | -340 | 66-70 | 150 |
| 32°-33°S | -300 | 65 | 130 |
| 35°S | -225 | 57 | 90,70 and 23 |
| 36°S | -164 | 48 | |
| 37°S | -120 | 44 | |
| 39°S | -110 | 43 | |
| 41°S | - 90 | 42 | |
| 44°S | - 82 | 41 | |
| 46°S | - 70 | 42 | |
| 50°S | - 78 | 45-47 | |

Table 1.- Location, maximum Bouguer anomaly, maximum crustal thickness and shortening of the Chile-Argentina sections studied in this work, Outcropping Andean masses keep the expected concordance with the compensating subterranean masses (roots).

## REFERENCES

Burov, E.B. and Diament, M., 1995. The effective elastic thickness of continental litosphere. What does it really mean?.Journal of Geophysical Research, 100, 3905-3927.

Guspí, F., Introcaso, A. and Pacino, M.C., 1995. Carta gravimétrica argentina 1995. Su construcción. I Congreso Argentino de Geociencias y Geotécnicas. Actas 88-93

Introcaso, A., Pacino, M.C. and Fraga, H., 1992. Gravity, isostasy and Andean crustal shortening between latitudes 30 and 32° S. Tectonophysics, 205, 31-48.

Isacks, B., 1988. Uplift of the Central Andean Plateau and Bending of the Bolivian Orocline. J. Geophys. Res., 93 (B4): 3211-3231.

James, D.E., 1971. Andean crustal and upper mantle structure.Journal of Geophysical Research, 76,

3246-3271.
Regnier, M., Chiu, J.M., Smalley, R., Isacks, B. and Araujo, M., 1994. Crustal thicknesses variations in the Andean foreland Argentina from converted waves. Bulletin of the Seismological Society of America, 84, 1097-1126.
Schmidt, M., Wigger, P., Araneda, M.,Giese, P., Heisohn, W.D., Rower, P. and Viramonte, J, 1993. The Andean crust at 24° South latitude. XII Congreso Geológico Argentino, Actas, 103-108.
Schmidt, M., 1994. A balanced model of the Southern Central Andes. Tectonics, 13, 484-492.

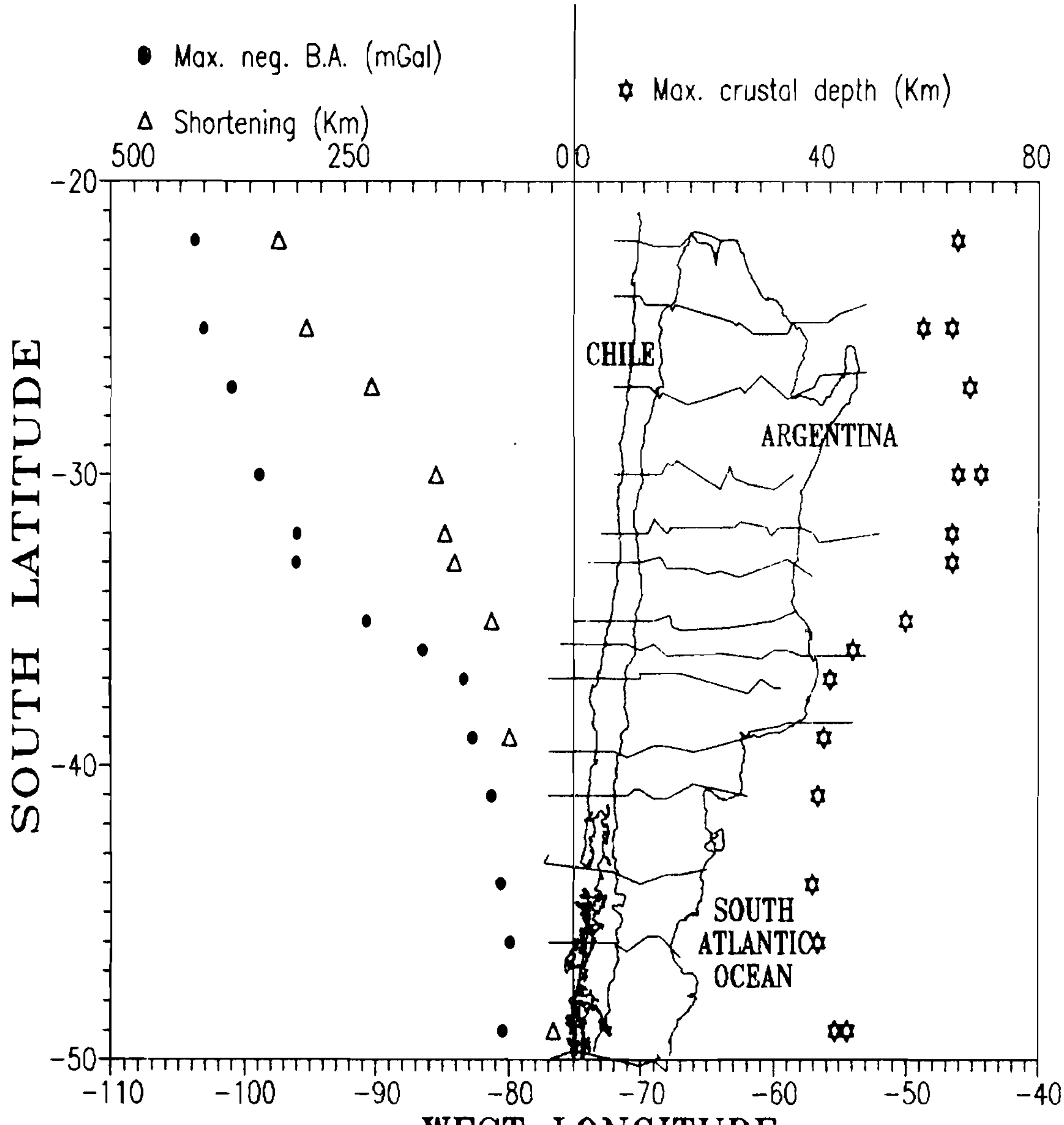


Fig.1: Maxima Bouguer Anomaly (●); Shortening (Δ) and maxima crutal thickness (✡) on 14 E-W Andean gravity sections on Argentina-Chile.

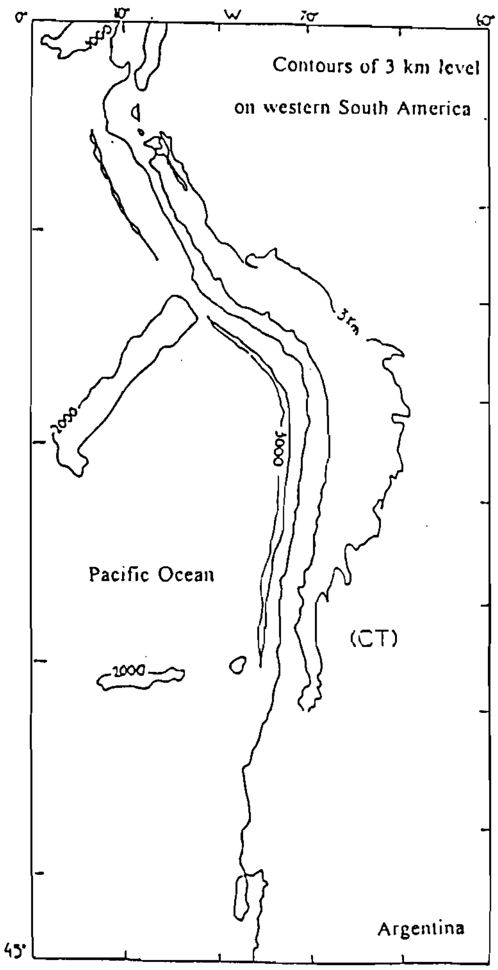


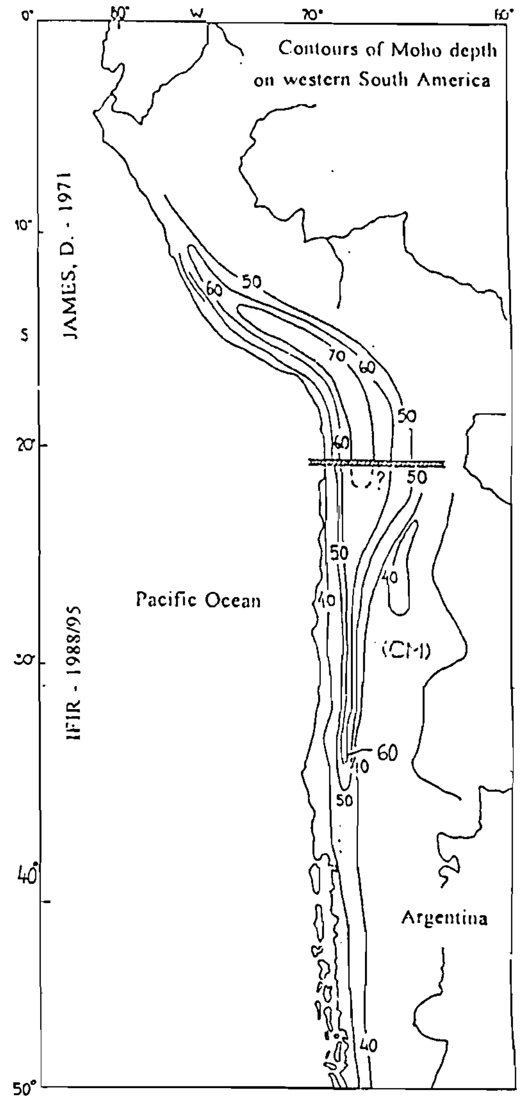


**Fig.2:Left:3000m altitude contour (Cordillera Andina) Right: Moho depth contour over 22°S latitude from seismic results(James, 1971) and at 22°-50° S latitudes from gravity data (this work).**

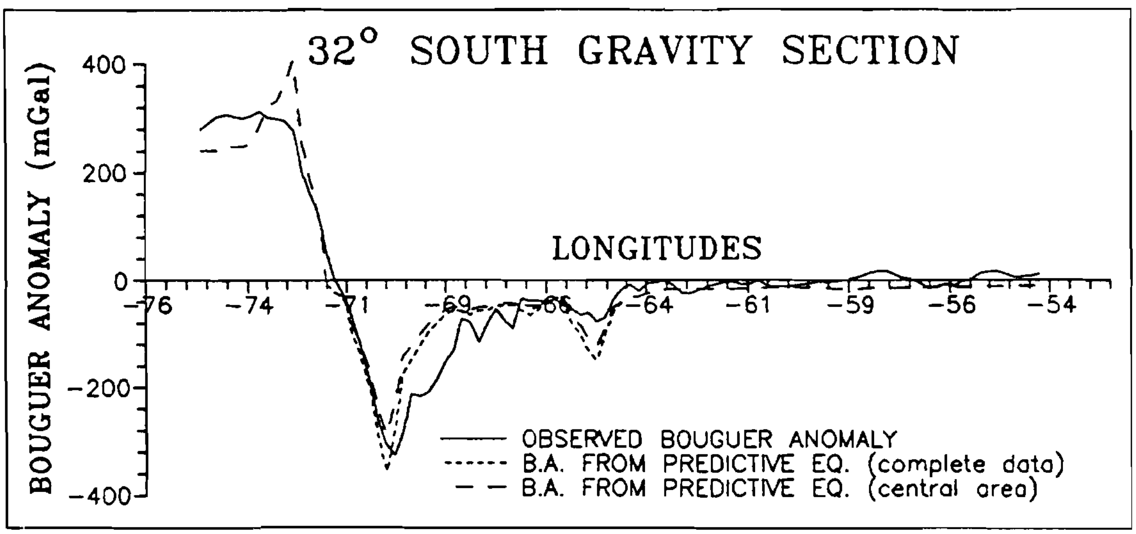


**Fig.3: Relations between predicted Bouguer anomalies at 32°S latitude (by means of altitudes H) and observed Bouguer anomalies.**

# A 3-D MODEL FOR THE CENTRAL ANDES BASED ON JOINT INTERPRETATION OF SEISMICS AND GRAVITY

Andreas KIRCHNER[1], Hans-Jürgen GÖTZE [1], Kerrin LESSEL[1] and Michael SCHMITZ[1]

(1) Institut für Geologie, Geophysik und Geoinformatik, FU Berlin, Malteserstraße 74-100, D-12249 Berlin, Germany

**KEY WORDS:** Seismic refraction, Bouguer gravity, lithosphere, 3D modelling, Central Andes

## INTRODUCTION

Here we present the results of intensive wide angle seismic refraction and gravity research in the southern Central Andes (20°- 28° S) during the 80's and early 90's. The gross crustal structures could be determined covering the principal morphostructural units of the Andes between 21° and 25° S (e.g. Wigger et al., 1994). In 1994 (PISCO 94 - Proyecto de Investigación Sismológica de la Cordillera Occidental) and 1995 (CINCA 95 - Crustal Investigations Off- and On-shore Nazca Central Andes) seismic investigations focussed on the arc and forearc structures in order to provide more detailed insight in the crustal structure of this region (see also posters Lessel, Schmitz and Giese and Patzwahl et al., this issue). The structural and velocity informations obtained by the seismic refraction is available along N-S and W-E trending profiles covering the the central region of the 3D-gravity model.

From 1993 to 1996 the MIGRA group with participants from Chile, Argentina and Germany has surveyed some 3.000 new gravity observations in an Andean Geotraverse covering N-Chile and NW-Argentina between 64°-71° W and 20° - 29° S. MIGRA is a Spanish acronym for "Mediciones Internacionales de GRavedad en los Andes". Including reprocessed older data of Freie Universität Berlin, South American universities, oil and mining industry, there is now a data base of about 15.000 gravity values available, which can be used together with other geophysical and geological information for an interdisciplinary interpretation of the structure and evolution of the Central Andes (Götze et al., 1994). The data base which includes point data and data grids of free-air-, and "complete Bouguer anomalies", isostatic-residual anomalies, were frequently described by Götze et al. (1995) and Götze (1996).

## FOREARC CRUSTAL STRUCTURES FROM SEISMIC REFRACTION DATA

In the Coastal Cordillera between 21° and 24° S, upper crustal P-wave velocities vary between 6.0 and 6.7 km/s. The top of the lower crust is located between 7 and 12 km depth, reaching down to 20 - 22 km, proven by prograde phases with velocities up to 7.2 km/s. The prominent discontinuity at 40 km depth (Vp = 8.2 km/s) is interpreted as Moho of the subducted Nazca Plate with an average velocity of 6.6 - 6.7 km/s (Wigger et al., 1994). Upper crustal as well as lower crustal structures can be followed into the Precordillera with the upper crust increasing to 20 km thickness and the lower crust extending down to about 40 - 45 km depth. Three distinct discontinuities with velocities from 7.3 - 8.0 km/s, separated by low velocity layers, are located between 50 and 70 km depth. $P_n$ observations from the Isla Santa Maria shot point can be correlated to the deepermost discontinuity. The average velocity down to 65-70 km depth decreases to 6.3 km/s. The upper crust as well as deeper crustal units can be followed into the Western Cordillera; however, the average crustal velocity decreases to 5.9 - 6.0 km/s. The most striking feature in the record sections of the Western Cordillera, a discontinuity at 20 km depth (Vp = 6.4 km/s) beneath Ollagüe, is interpreted from structural point of view as the top of the lower crust, although the crustal units below are characterised by partly reduced velocities. Locally limited high-velocity discontinuities in this crustal unit are observed down to approximately 45 - 50 km depth. Assuming this depth range as the base of the lower crust, a 25-30 km thick lower crust results with low average velocities of only 6.0 - 6.2 km/s. Fan observations between the Precordillera and the Western Cordillera give indications for a deep reflector (Vp = 8.2 km/s) which is interpreted as the eclogitized top of the subducted Nazca Plate.

## GRAVITY ANOMALIES

Onshore the Bouguer anomaly drops down to a regional minimum of about - 450 mGal in the area of the recent volcanic arc, related to crustal thickening by isostatic compensation (For more details refer to abstract: Götze, Schmidt, Kirchner, Kösters, Araneda and Lopez, this issue). The gravity effect of the isostatic compensation root was eliminated from the Bouguer gravity and the resulting anomaly serves as a residual field. The most interesting features of this field are: (1) Positive values in the area of the Jurassic forearc with isolated complexes parallel to the coastline. They are regionally caused by the presence of the dense subducting plate (gravity effect of more than 50 mGal; density contrast: 0.05 $g/cm^3$) and locally by uplifted jurassic batholiths intruded into the volcanic "La Negra" formation. (2) The NNW-SSE striking positive anomaly from Calama (CAL) by the Salar de Atacama to southern Puna which can be explained by a highly metamorphic and high-density Paleozoic/Precambrian structure, which is oblique to the N-S orientation of the recent volcanic belt. (3) Local minima along the recent volcanic arc point to partly molten material at depths of 15 - 20 km. (4) Minima following a line from Ollagüe (OLL) to Calama (CAL) along 69° W, are caused by the Eocene volcanic arc with low-density volcanic material in the upper crust.

## 3D MODELLING

A large scaled 3D density model was constructed to investigate the regional structure and density composition of the Andean lithosphere (Figure 1a). The model comprises the new results of seismic refraction and summarizes discussions with colleagues from geology and petrology. Based on various 2D raytracing models seismic cross sections extending from the trench to the magmatic arc were used to design major elements of the Andean crust and mantle transition between 21° through 24° S. Further parts of the density model are the downgoing Nazca plate according to results of Cahill and Isacks (1992) and continental lithosphere together with the Brasilian shield in the east, which is not shown here. As a preliminary study the velocities of seismic models were directly converted into densities by using e.g. the Nafe & Drake relationship or similar density/velocity relations by Wollard. Initial model geometry was slightly modified by the application of interactive computer graphics to verify regional trends implied by the Bouguer gravity field. Although we used various non-linear inversion algorithms to optimize the model density we also tried to follow well established density/velocity relations from laboratory and literature. Due to unknown conditions of high temperature/pressure and the presence of fluids at the crust-mantle interface of the Central Andes we learned from modelling that we have to distinguish a 'gravity' Moho which is characterized by a density contrast of less or equal 0.3 g/ccm from the "seismic" Moho which is not very clear.

In order to interprete long wavelengths of the gravity field we also calculated the potential (geoid) of the 3D density model by forward modelling and compared it with the observed geoid (OSU01A). Andean topography and ist corresponding Airy root (including effects of compensated topography of the entire earth) contribute approx. 18 m to the geoid of the area. Instead of Airy or Vening-Meinesz isostasy we used the 3D model to calculate the gravity and/or geoid contribution of the Andean lithosphere respectively, because usual isostatically equilibrated state is not necessarily representative at an active continental margin. Density inhomogeneities from deeper parts of the mantle also contribute to the observed geoid undulations. Even undulations caused by the core-mantle boundary result in potential signals that dominate the geoid in the Central Andes.

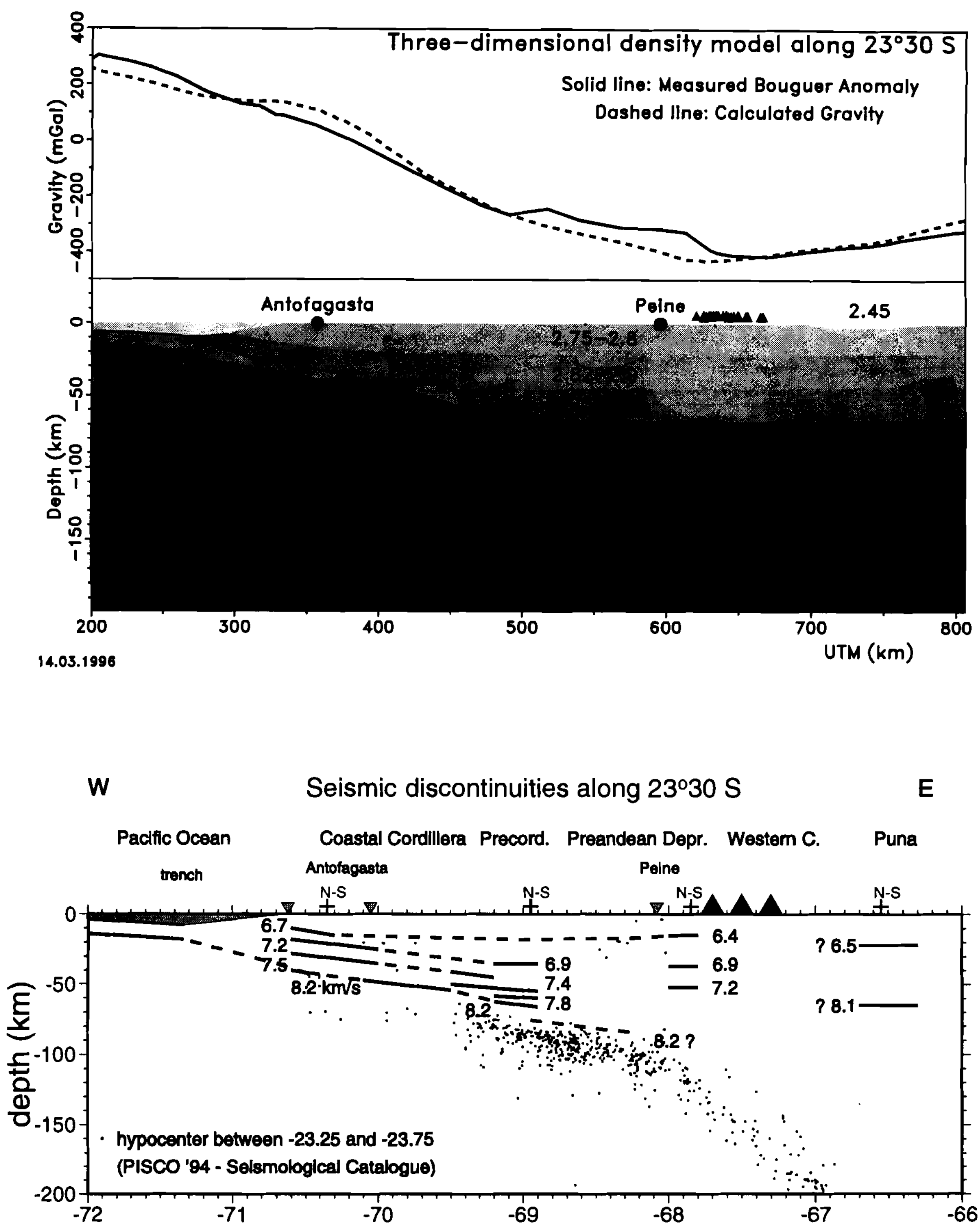


Figure 1: Cross sections with the density structure and modelled / measured gravity fields (a) and seismic discontinuities in northern Chile at lat. 23° 30' S. Crustal structures can be traced from the Coastal Cordillera with increasing thickness towards the Western Cordillera. The shape of the subducted Nazca plate can be inferred from Moho observations in the Coastal Cordillera and from locations of the earthquake hypocenters derived from the PISCO 94 - seismological catalogue (Asch, Rudloff and Graeber, pers. comm., 1995). Crosses indicate the position of corresponding N-S profiles; black triangles give the position of magmatic arc.

## CONCLUSIONS

In the magmatic arc and Puna region of western Argentina the Bouguer anomaly and density modelling (-450 mGal) indicate a crustal thickness in the order of 70 km. There are no Moho observations in this region; the seismic waves are strongly attenuated with a reduction of the seismic velocities. Beneath the magmatic arc the electric resistivities decrease to values of 0.5 - 1 Ohmm at 20 km depth (Schwarz et al. 1994) indicating a zone of partial melting. The continental crust of the forearc has a thickness of 25 - 45 km without indications for a clear Moho. Between the subducting Nazca plate and the continental crust there is a wedge of material with low seismic velocities and with low densities, typical values for crustal material, which are interpreted as a mixture of hydrated upper mantle relicts and material eroded from the continental margin. Our 3D gravity model which is based on structural information of seismic refraction data in its central part unables us to extend these information even to regions where no seismics exists. The gravity field images structural anomalies which require further inverstigations.

This interdisciplinary modelling of results from both seismic refraction and gravity observations plays an important role in regional geodynamics of the Andean lithosphere and interdisciplinary interpretations. Seismic velocities and density distribution in the area of the Central Andes seem to be sensitive indicators which are linked to many processes contributing to the tectonic framework of the Nazca subduction zone.

## ACKNOWLEDGEMENT

The support with maps and geodetic information by the following institutions is gratefully acknowledged: Institutos Geográficos Militares in Santiago, Buenos Aires and La Paz, Yacimientos Petrolíferos Fiscales of Argentina and Bolivia, Empresa Nacional de Petróleo, and CODELCO both from Chile. This paper presents results of the seismic and gravity research groups C4 and D3 respectively of the SFB 267 which is funded by the Deutsche Forschungsgemeinschaft (DFG) and Freie Universität Berlin.

## REFERENCES

Cahill, T. and B.L. Isacks, 1992. Seismicity and shape of the subducted Nazca plate. Journal of Geophysical Research, 97, 17503 - 17529.

Götze, H.-J., Lahmeyer, B., Schmidt, S. and Strunk, S., 1994. The Lithospheric Structure of the Central Andes (20° -26° S) as inferred from Quantitative Interpretation of Regional Gravity. In: Tectonics of the Southern Central Andes (Eds.: Reutter, Scheuber, Wigger), pp. 7-21, Springer Verlag Heidelberg.

Götze, H.-J., M. Schmitz, P. Giese, S. Schmidt, P. Wigger, G. Schwarz, M. Araneda, G. Chong D. and J. Viramonte, 1995. Las estructuras litosféricas de los Andes Cantrales australes basados en interpretaciones geofísicas. Revista Geológica de Chile, Vol 22, No. 2, 179-192.

Götze, H.-J. as reporter of the MIGRA - group, 1996. Group updates the gravity data base in the Central Andes (20° - 29° S). EOS Transactions, American Geophysical Union, in print.

Schwarz, G., G. Chong D., D. Krüger, E. Martinez, W. Massow, V. Rath and J. Viramonte, 1994. Crustal high conductivity zones in the Southern Andes. In: Tectonics of the Southern Central Andes (Eds.: Reutter, Scheuber, Wigger), Springer Verlag Heidelberg, pp. 49-67 .

Wigger, P., M. Schmitz, M. Araneda, G. Asch, S. Baldzuhn, P. Giese, W.-D. Heinsohn, E. Martinez, E. Ricaldi, P. Röwer, and J. Viramonte, 1994. Variation of the crustal structure of the southern Central Andes deduced from seismic refraction investigations, in Tectonics of the Southern Central Andes, edited by K.-J. Reutter et al., pp. 23-48, Springer-Verlag, New York.

# THE GRAVITY FIELD OF THE CONTINENT-OCEAN TRANSITION AT THE WESTERN CONTINENTAL MARGIN OF SOUTH AMERICA

Michael KÖSTERS(1), Jürgen FRITSCH(2), Sabine SCHMIDT (1), Hans-Jürgen GÖTZE (1), and Manuel ARANEDA C.(3)

(1) Institut für Geologie, Geophysik und Geoinformatik, FU Berlin, Haus N, Malteserstraße 74-100, D-12249 Berlin, Germany
(2) Bundesanstalt für Geowissenschaften und Rohstoffe, Postfach 510153, D-30631 Hannover, Germany
(3) Departamento de Geofísica, Universidad de Chile, Blanco Encalada 2085, Santiago, Chile

**KEY WORDS:** Offshore gravity, Free-air and Bouguer anomalies, subduction zone, Chile trench

## INTRODUCTION

Under the framework of the interdisciplinary research project CINCA (Crustal Investigations Off- and Onshore Nazca/Central Andes) gravity surveys of the international MIGRA group with participants from Chile, Argentina and Germany has been extended to the Pacific ocean. In summer 1995 MIGRA took part in the "CINCA" offshore experiment SO - 104 of the german research vessel "Sonne" between the latitudes 20° S to 24° S. The offshore gravity data are connected with the onland survey to draw a complete gravity picture of this ocean-continent transition. Some 6.000 new gravity observations onland in an Andean Geotraverse covering N-Chile, SW Bolivia and NW-Argentina between 64°- 71° W and 20° - 29° S has been put to the data base which already existed when MIGRA started in 1982 (Götze et al., 1994 and Götze et al. 1995). MIGRA is a Spanish acronym for "Mediciones Internacionales de GRavedad en los Andes".

## MEASUREMENTS AND DATA ACCURACY

Gravity data at sea were collected along continous survey lines (some 8.000 km). The average density of observational sites amounts of about 15 observations per km. The gravity survey of cruise SO - 104 was tied to the Chilean National Gravity network of the "Departamento Geofísico, Universidad de Chile, Santiago" at reference stations in Valparaiso, Antofagasta and Iquique. The drift of the KSS31/32 onboard gravity sensor was very low and amounts to -0.048 mGal/day or - 1.44 mGal/month, respectively. The overall drift of the gravity meter was determined to be 0.47 mGal per 92 days.

Further information about the accuracy of the offshore survey provide so called "misties". Misties are crossover errors if the gravity readings of two crossing lines are compared. Assuming this accuracy depends mainly on the gravity sensor several methods have been invented to minimize crossover errors (e.g. Prince and Forsyth, 1984). It has also been argued that misties are frequently caused by bad positioning (Fritsch and Roeser, 1986). Anyway, statistical treatments of misties at intersections of survey lines reveals the precision of the offshore gravity measurements including auxiliary physical quantities. On the 1st leg of cruise S0-104 about 44 intersections have been obtained. Some 80 % of gravity misties were less than 1 mGal and about 80 % of the water depth misties were less than 9 m. These data show the high precision of both gravity and waterdepth measurements on cruise So 104/1. The 2nd leg of the survey was characterized by a more complicated topology of crossing profiles due to the wide angle reflection experiments which required gravity measurements at the same line for three times. Therefore, a more sophisticated algorithm has been used to estimate crossover errors.

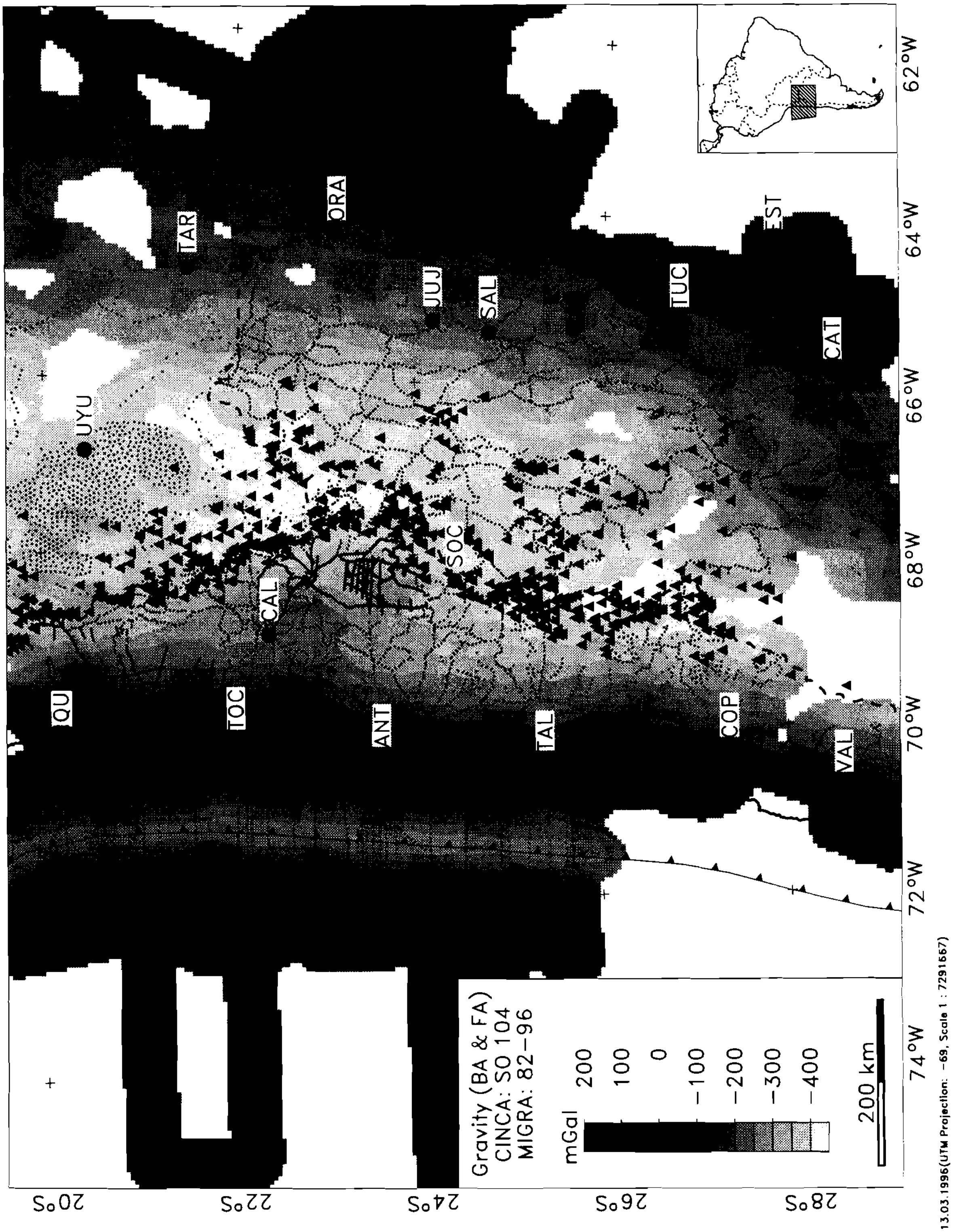


Figure 1: The gravity field of the Central Andes and offshore South America between 20° - 29° S. In the Pacific offshore area Free-air anomalies replace onland Bouguer anomalies Shading intervals: 50 mGal. Gravity database is shown together with volcanoes and other geographical features.

In total, the accuracy of the gravity survey is truly better than 1 mGal, and accuracy of water depth determinations are better than 10 m.

At the continent the investigated region covers a 900 km x 1.000 km area in the central part of the Andean orogenic system. It is an arid/semiarid zone, where elevations vary from sea level up to heights greater than 6.000 m at the Andean volcano summits. The young Andean orogen between 20° - 29° S comprises different structures which have evolved on a Precambrian-Paleozoic basement.The investigated area is characterized by its enormous topography and remoteness, by its aridity, low population density and limited infrastructure. Other difficulties limiting our field work were the lack of topographic maps and geodetic networks in some regions. The spacing of stations amounts to approximately 5 km along all passable tracks aside from some local areas with a higher station density . To complete this data base we included gravity observations from different sources. With the exception of some inaccessible regions in the "Eastern" and "Western Cordillera", the gravity coverage for the region is fairly uniform. All measurements are tied to the IGSN71 gravity datum at base stations in Oran/Argentina, Iquique/Chile and Tucumán/Argentina.

The large size of the area and the severe logistical problems did not always allow us to determine the drift of the gravity meters by repeating the measurements at each station. However, even when we used bad tracks, the drift of the LaCoste & Romberg instruments (model G) rarely exceeded 0.1 mGal per day. Only about 35% of the gravity sites could be tied directly to benchmarks, such as levelling lines or trigonometric heights, so we used altimeters for height determinations. To improve the quality of our barometric measurements, we calculated time-dependent drift corrections as it is usually done for gravity measurements, using as many benchmarks and repeated measurements as possible. Moreover, the profiles of several days were tied together in order to eliminate systematic errors. The scales of the barometers have been calibrated on levelling lines with an altitude difference of about 2000 m. Error estimations showed that even in the worst case the accuracy was better than 20 m, giving an error in the Bouguer anomaly of about 4 mGal, which is less than 1% of the overall magnitude of more than 450 mGal. For the terrain correction (up to 167 km around all stations), a method including calculations of the earth´s curvature developed for gravity investigations in the Alps was used, after adapting it to the special situation in the Central Andes. Reduction density was 2.67 $g/cm^3$. For different morphological units we obtained the following typical values of topographic reduction: Longitudinal valley and Chaco region: 0.5 - 1 mGal, Coastal, Pre- and Western Cordillera, Altiplano/Puna and Subandean Belt: 1 - 10 mGal and steep coast

## GRAVITY ANOMALIES

Both on- and new offshore gravity data base were put together to shed new light on the gravity field at the continent - ocean transition zone at the western continental margin (Figure 1). In the western part of the investigated offshore area the oceanic basement of the downgoing Nazca plate causes positive Free-air anomalies with an average of about 20 mGal; water depth is about 4.500 m. The Peruvian-Chilean trench is characterized by strong negative gravity values which extend to a minimum of less than -250 mGal. In continuation towards the Chilean coast there is a broad zone of alternating positive and negative Free air gravity which vary in size and magnitude. It appears to be difficult to interpret these anomalies without any modelling which will be performed in the next months. However, the character of the gravity field over the continental slope appears to be complicated. It shows several domains with gravity highs and lows which may be interpreted in terms of morphology of the continental slope and density structures which could belong to already eroded parts of the Jurassic Forearc.

Onshore the Bouguer anomaly drops down to a regional minimum of about - 450 mGal in the area of the recent volcanic arc, related to crustal thickening by isostatic compensation. The effect of isostatic compensation of topography was calculated assuming the model of Vening-Meinesz with the following parameters: density contrast of the earth´s mantle and crust dRHO = 0.35 $g/cm^3$, normal crustal thickness: 35 km and a flexural rigidity of $10^{23}$ Nm. The gravity effect of the isostatic compensation root was eliminated from the Bouguer gravity and the resulting anomaly serves as a residual field. The most interesting features of this field are in the forearc region of the Central Andes: (1) Positive values in the area of the forearc with isolated complexes parallel to the coastline. They are regionally caused by the presence of the dense subducting plate (gravity effect of about 50 mGal; density contrast: 0.05 $g/cm^3$) and locally by uplifted jurassic batholiths intruded into the "Formaci6n La Negra" and (2) the minima following a line from Ollagüe (OLL) to Calama (CAL) along 69° W, are caused by the Eocene volcanic arc with low-density volcanic material in the upper crust.

## CONCLUSIONS

Both on- and offshore gravity data will play an important role in local investigations of applied geophysics and regional interdisciplinary interpretations.The Andean gravity field seems to be a sensitive indicator which is linked to many processes contributing to the tectonic framework of the Nazca subduction zone. In close cooperation with the Geological Survey of Chile (Santiago) we are going to complete the survey in the south-west and south part of the traverse (Fig.1) in early 1996 and fill the gaps that still exist due to extreme logistical problems. In 1997 we are planning to join an international seismic reflection program with participants from both Americas and Germany in the Altiplano of Bolivia.

## ACKNOWLEDGEMENT

This paper presents results of the 1995 "CINCA" offshore experiment SO - 104 of the german research vessel "Sonne".Processing and interpretation of gravity data are part of a joint project of the gravity research group at Bundesanstalt für Geowissenschaften und Rohstoffe (Hannover) and the gravity research project D3 of the SFB 267 which is funded by the Deutsche Forschungsgemeinschaft (DFG) and Freie Universität Berlin. This paper contributes also to the IGCP 345.

## REFERENCES

Fritsch, J. And H.A. Roeser 1988. On the accuracy of gravity measurements at sea. Geologisches Jahrbuch, E 42, 195 - 208.

Götze, H.-J., Lahmeyer, B., Schmidt, S. and Strunk, S. 1994. The Lithospheric Structure of the Central Andes (20°- 26° S) as inferred from Quantitative Interpretation of Regional Gravity. In: Tectonics of the Southern Central Andes (Eds.: Reutter, Scheuber, Wigger), pp. 7-21, Springer Verlag Heidelberg.

Götze, H.-J., M. Schmitz, P. Giese, S. Schmidt, P. Wigger, G. Schwarz, M. Araneda, G. Chong D. and J. Viramonte 1995. Las estructuras litosféricas de los Andes Cantrales australes basados en interpretaciones geofísicas. Revista Geol6gica de Chile, Vol. 22 No. 2, p. 179-192.

Prince, R.A. and Forsyth, D.W. 1984. A simple objective method for minimizing crossover errors in marine gravity data. Geophysics, 49 (7), 1070-1083.

# ANOMALOUS DEEPER CRUST BENEATH THE CENTRAL ANDEAN FOREARC AND ARC REGIONS (21°-23°S)

Kerrin Lessel*, Michael Schmitz* and Peter Giese*

*FR Geophysik, Freie Universität Berlin, Malteserstr.74-100, 12249 Berlin; e-mail: seis@zedat.fu-berlin.de

**Key words:** Central Andes, seismic refraction, lower crust, Moho, forearc, magmatic arc

## INTRODUCTION

The central segment of the Andean mountain chain is characterised by active volcanism in the magmatic arc, the Western Cordillera, located on the western margin of a the 2.000 km long and 300 km broad Altiplano plateau with an average height of 3.700 m, uplifted during late Cainozoic (e.g. Isacks, 1988). During the last 200 Ma. the magmatic arc of the central Andes has been displaced eastwards from the Coastal Cordillera to the actual position in the Western Cordillera (Coira et al., 1982; Scheuber et al., 1994), affecting considerably the crustal structure and evolution of the forearc region. Together with the magmatic arc the related forearc and backarc features shifted eastwards into their actual position.

In continuation of previous projects, within the SFB 267 seismic refraction investigations as well as seismological studies (Asch et al., 1994; Schmitz et al., 1994) have been realised in the forearc and arc region (PISCO 94 - Proyecto de Investigación Sismológica de la Cordillera Occidental) in order to improve the results of earlier seismic refraction studies in the area (e.g. Wigger et al., 1994). Whereas the genesis of the thickened backarc crust can be explained by crustal stacking, the evolution of the thick forearc crust is still under discussion. Information about the velocity structure including observations from the crustal base should help to clarify the nature of the deeper crust.

## GROSS CRUSTAL STRUCTURES OF THE FOREARC AND ARC REGIONS

The field work was realised in northern Chile by scientists from the Freie Universität Berlin and the GeoForschungsZentrum Potsdam in co-operation with the Universidad de Chile, Santiago and the Universidad Católica del Norte, Antofagasta. The main seismic refraction profile was located along the western border of the Western Cordillera, the recent magmatic arc (Fig. 1). In addition, in the Precordillera and the Western Cordillera, fan observations were realised. In 1995, complementive profile observations during the CINCA 95 experiment (Crustal Investigations Off- and On-shore Nazca Central Andes) were realised to obtain additional information on the deep stucture of the forearc.

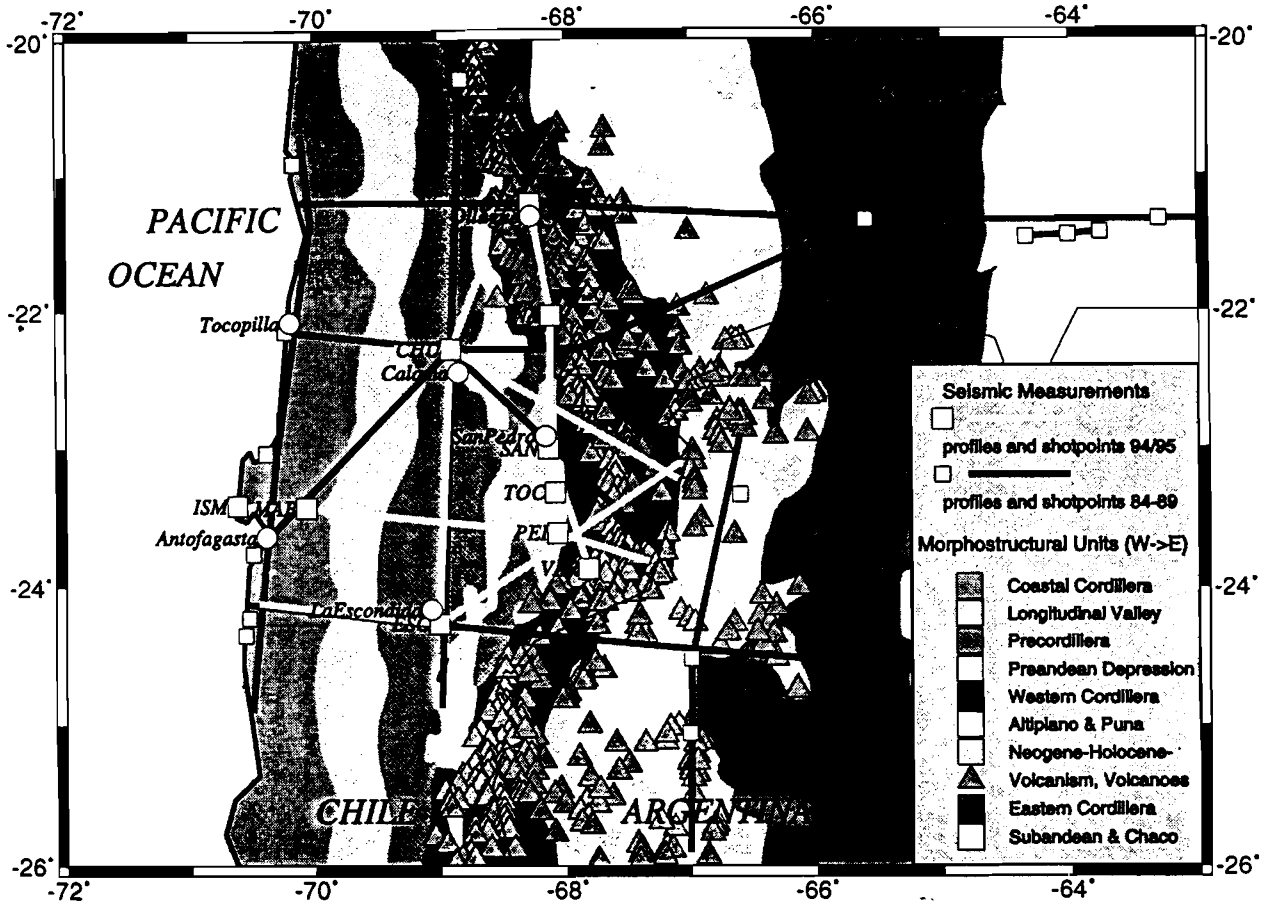


**Figure 1.** Location of the seismic refraction profiles and the main morphostructural units in the central Andes. The N-S profile on the western margin of the Western Cordillera penetrates the zone of active volcanism (grey triangles indicate volcanoes) in the northern part, while it descends to the Preandean Depression in the southern part. Here, the magmatic arc shows a significant retreat towards the east. Shotpoin locations are: ISM = Isla Santa Maria; MAB = Mantos Blancos; CHU = Chuquicamata; ESC = La Escondida; OLL = Ollagüe; INA = Inacaliri; SAN = San Pedro; TOC = Toconao; PEI = Peine; VAR = Pampa Varela.

Lower crustal material is exposed in the Coastal Cordillera south of Antofagasta (e.g. Lucassen and Franz, 1994). From seismic refraction data between 21° and 24°S, the top of the lower crust is located between 7 and 12 km depth, reaching down to 20-22 km, proven by prograde phases. The most prominent discontinuity at 40 km depth is interpreted as Moho of the subducted Nazca Plate. The average crustal velocity of the Coastal Cordillera is 6.6 km/s, increasing towards the south (Wigger et al., 1994). In the Precordillera, the upper crust increases to 20 km thickness and the lower crust extends down to approximately 40-45 km. The depth range 50 and 70 km is composed of high (6.9 - 8.0 km/s) and low (6.4 - 7.0 km/s) velocity layers. The 70 km-discontinuity may be associated with mantle material or the top of the downgoing oceanic crust (eclogite ?). The upper crustal units can be followed into the Western Cordillera; however, the crustal velocity decreases to 5.9-6.0 km/s. The most striking feature in the record sections of the Western Cordillera, a discontinuity at 20 km depth beneath Ollagüe, is interpreted from structural point of view as the top of the lower crust, although the crustal units below are characterised by partly reduced velocities. Locally limited high-velocity discontinuities in this crustal unit are observed down to approximately 45-50 km depth. Assuming this depth range as the base of the lower crust, a 25-30 km thick lower crust results with low average velocities of 6.0-6.2 km/s. No clear signals from depth levels beneath 50 km could be recorded in the Western Cordillera.

## WHAT IS THE NATURE OF THE DEEP CRUST?

There are numerous geophysical indications for a thick crust in the forearc and arc regions (e.g. James, 1971; Götze et al., 1994; Wigger et al., 1994; Zandt et al., 1994), e.g. material with physical properties characterizing crustal material (low density, low seismic velocity), to about 70 km depth beneath the magmatic arc and the Precordillera. In contradiction, from tectonic point of view, no considerable thickening must be assumed for the forearc and arc regions, as Cainozoic crustal shortening is restricted mainly to the backarc (e.g. Kley, 1996). Therefore, with the actual state of knowledge, the origin of the material in deeper levels is under discussion and several solutions have been proposed.

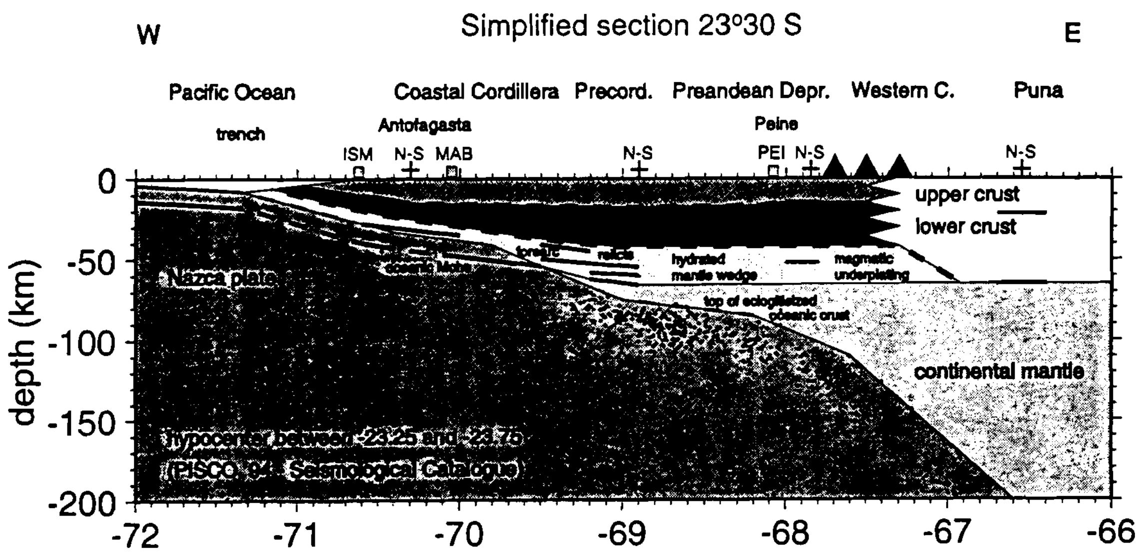


**Figure 2.** Simplified section across the central Andes in northern Chile (23°30' S). Crustal structrures can be traced from the Coastal Cordillera towards the Western Cordillera with increasing thickness of upper and lower crust. The shape of the subducted Nazca plate can be inferred from profile- and fan observations in the forearc, and from locations of the earthquake hypocenters derived from the PISCO 94 - seismological catalogue (Asch, Rudloff and Graeber, pers. comm., 1995). The deepermost crust is very inhomogeneous and may be composed of underplated crustal components (eroded from the continental margin) as well as of mantle material, strongly hydrated by fluids from the descending slab or differentiated by magmatic processes. Squares = shot point locations; crosses = position of N-S crolling profiles; black triangles = position of the magmatic arc.

The question arises, if the depth range 20 to 45 km is interpreted as continental lower crust, what are the consequences for the deeper horizons? Beneath the Precordillera, the top of the downgoing Nazca plate is given by deep reflections and the earthquake hypocenters. For the depth range between the slab and the base of the lower crust alternating high and low velocities are displayed. The seismic nature of the deeper crust and the transition to the mantle is still unclear due to ambiguous data for this depth range. One explanation for the low velocity material in the deeper forearc crust could be hydrated material of the peridotitic mantle wedge showing reduced seismic velocities (Fig. 2). Eroded material from the edge of the continent that has been emplaced in the deeper forearc crust within the subduction process, may contribute to thicken the crust in this depth range as well. Towards the Western Cordillera, partly molten rocks may be responsible for the strongly reduced seismic velocities and the observed high attenuation of the seismic waves.

*Acknowledgements* The project is part of the Collaborative Research Center „Deformation Processes in the Andes" (SFB 267). We want to thank all the field participants who contributed to the data base under the extreme conditions of the cental Andes mountain region. This is a contribution to IGCP Prcject 345.

## REFERENCES

Asch, G., Wyllegalla, K., Graeber, F., Haberland, Ch., Rudloff, A., Giese, P. u. Wigger, P., 1994. PISCO 94: Proyecto de Investigación Sismológica de la Cordillera Occidental - parte I: Registros de sísmos naturales. 7° Congreso Geológico Chileno, Concepción, Actas Vol. 2, 1293-1295.

Coira, B., Davidson, J., Mpodozis, C. and Ramos, V.A., 1982. Tectonic and magmatic evolution of the Andes of northern Argentina and Chile. *Earth Sci Rev,* **18,** 303-332.

Götze, H.-J., Lahmeyer, B., Schmidt, S. and Strunk, S., 1994. The lithospheric structure of the Central Andes (20-25°S) as inferred from quantitative interpretation of regional gravity, in *Tectonics of the Southern Central Andes*, edited by K.-J. Reutter et al., pp. 23-48, Springer-Verlag, New York.

Isacks, B.L., 1988. Uplift of the central Andean plateau and bending of the Bolivian orocline, *J. Geophys. Res.,* **93**, 3211-3231.

James, D.E., 1971. Plate tectonic model for the evolution of the Central Andes, *Geol. Soc. Am.Bull.*, **82**, pp. 3325-3346

Kley, J., 1996 (in press). Transition from basement-involved to thin-skinned thrusting in the Cordillera Oriental, of southern Bolivia. *Tectonics*.

Lucassen F. and Franz, G., 1994. Arc related igneous and metaigneous rocks in the Coastal Cordillera of northern Chile/Region Antofagasta. *Lithos* **32**, 273-298

Scheuber, E., T. Bogdanic, A. Jensen, and K.-J. Reutter, 1994. Tectonic development of the north Chilean Andes in relation to plate convergence and magmatism since the Jurassic, in *Tectonics of the Southern Central Andes*, edited by K.-J. Reutter et al., pp. 121-140, Springer-Verlag, New York.

Schmitz, M., Araneda, Asch, G., Giese, P., Lessel, K. Röwer, P., Ryberg, T., Schulze, A. & Wigger, P. 1994. PISCO 94: Proyecto de Investigación Sismológica de la Cordillera Occidental - Parte II: Sísmica de refracción. 7° Congreso Geológico Chileno, Concepción, p. 1447-1450.

Wigger, P., M. Schmitz, M. Araneda, G. Asch, S. Baldzuhn, P. Giese, W.-D. Heinsohn, E. Martinez, E. Ricaldi, P. Röwer, and J. Viramonte, 1994. Variation of the crustal structure of the southern Central Andes deduced from seismic refraction investigations, in *Tectonics of the Southern Central Andes*, edited by K.-J. Reutter et al., pp. 23-48, Springer-Verlag, New York.

Zandt, G., Velasco, A.A. and Beck, S., 1994. Composition and thickness of the southern Altiplano crust, Bolivia. *Geology*, **22**, 1003-1006.

# ANALYSIS, INVERSION AND MODELLING OF MAGNETOTELLURIC OBSERVATIONS BETWEEN THE CORDILLERA ORIENTAL AND EL CHACO (NW ARGENTINA)

Pamela LEZAETA and Miguel MUÑOZ

Dpto. de Geofísica, Universidad de Chile, Santiago, Chile.

**KEY WORDS:** Magnetotellurics, Distortion Effects, Occam's and RRI Inversions, Forward Modelling, Structure of the Crust and Upper Mantle.

## INTRODUCTION

During the past years several magnetotelluric (MT) studies have been carried out in the Central Andes (Argentina, Bolivia and Chile) - e.g., Muñoz et al., 1992; Schwarz et al., 1994. Some of these studies have revealed high electrical conductivity anomalies beneath the volcanic arc and surrounding areas. The determination of the electrical resistivity of structures in the Andean foreland is greatly endeavoured for understanding the tectonic processes affecting the region. Preliminary results of MT soundings carried out between the Cordillera Oriental and El Chaco were presented by Krüger (1994). In this abstract we present a new electrical model for the region based on a rigorous analysis of the former MT soundings and using a variety of inversion algorithms and forward modelling codes.

## MT SOUNDING PROFILE

The MT measurements examined in this study were carried out by the Research Group of Magnetotellurics of the Free Universty of Berlin. The MT soundings were undertaken in the Andean foreland at 24.5 - 25.5°S and 63 - 65.5°W (NW Argentina) along roughly an E-W profile of 220 km long. Distance between soundings ranges from about 6 to 20 km. The profile traverses the Cordillera Oriental (CO) and the system of Sta. Bárbara (SB), reaching the western area of El Chaco province (C). The MT fields were recorded in the period range 50 - 15,000s. The depths of investigation lie from about 5 - 10 km to 130 - 260 km. The location of the sounding sites along the profile (Col...Vin) is shown in Fig.1 (see the last page of this abstract).

## DATA ANALYSIS AND DISTORTION EFFECTS

The main objects of the analysis are to determine the departure of the sounding data from two-dimensionality (2D) and to individuate the distortion effects of three-dimensional (3D) anomalies. A full account of the analysis of the MT soundings is presented in the work of Lezaeta (1995) and only some few remarks will be presented here.

According to the classification of distortion types carried out by Bahr (1991) only Pal sounding site could be regarded as belonging to class 1 (regional 2D structure with the impedance tensor Z free from distortion effects). Most of the sounding data belong to class 5 (local 3D anomaly within a 2D regional space; strong telluric distortion) for periods generally larger than 500 - 1000 s, and to class 7 (regional 3D anomaly) for lower periods. Particularly, data for periods <1100 s from sites in the eastern area of the profile between SB and C were seen to correspond to a 3D structure.

The regional strike angle was determined by means of the decomposition of the impedance tensor Z as proposed by Groom and Bailey (1989). Chi-square errors resulting of assuming a superimposition model (shallow local 3D anomalies within a 2D regional space) in the decomposition of Z, twist and shear parameters were encountered for each sounding site throughout the data spectrum. It was found that the strike of the 2D structure may be considered to lie in the North-South direction. Subsequently it was observed that the correction for the effects of telluric distortion did not change the original impedance tensor significantly.

Static distortion due to shallow heterogeneities was examined in the data corrected for telluric distortion. A regional apparent resistivity was firstly obtained and the static shift for each TE apparent resistivity curve was achieved thereupon. The same static shift is relevant for the TM curves. The apparent iso-resistivities and iso-phases (corrected and not corrected for static shift) were graphically represented (e.g., Jones and Dumas, 1993) and it was observed that the static correction decreases vertical trends in the iso-values: this ensures the correctness of the former procedure.

## INVERSION AND FORWARD MODELLING

Several 2D models were obtained and their responses compared with apparent resistivities and phases of the impedance tensor corrected for distortion. The modelling was undertaken following two-dimensional synthesis of 1D inversions carried out using the method of Vozoff and Jupp (1975), 1D Occam's inversions (Constable et al., 1987), RRI-rapid relaxation inversions (Smith and Booker, 1991) adopting two-dimensional forward algorithms, and 2D Occam's inversions (deGroot-Hedlin and Constable, 1990). The complete results are presented in Lezaeta (1995).

The models obtained using 1D inversions are similar but dependent on the initial parametrization. 2D inversion is subject to instabilities making difficult the attainment of convergence; this may be partly due to data that show departure from responses expected for 2D structures. Fitness between data and model responses is higher for soundings carried out between the Cordillera Oriental (CO) and the Sta. Bárbara system (SB), where they classify as corresponding to a 2D structure. The rapid relaxation inversions (RRI) were observed to be very sensitive to frozen resistivity vertical sections imposed on the inversion process.

The most reliable former modelling results were adopted to obtain a final model (Fig.1) by using the finite-element forward modelling code of Wannamaker et al.(1987). The best fitness between the corrected data and model responses was obtained for the TE polarization mode. A model based on the representation of multilayered of multilayered structures by analytical functions (Osella and Martinelli, 1993) was attained also. The major features of resistivity distribution are similar in both these models.

## DISCUSSION AND CONCLUSIONS

The final MT model of resistivity distribution (Fig.1) shows that the middle crust has low resistivity (35-100Ωm) in the western area of the profile between Cordillera Oriental and the Sta. Bárbara system. The lower crust is generally conductive all along the profile -this result is in agreement with the observation of Hyndman et al. (1993) about the conductive character of the lower crust in almost any area. A zone of very low resistivity (≤10Ωm) is encountered beneath the western border of the MT profile at 80 km depth; the conductive layer is at about 180 km depth beneath the areas between the Sta. Bárbara system and El Chaco. The whole conductive layer is referred as constituing the electrical asthenosphere. According to empirical relationships between heat flow and depth to the conductive layer in the mantle (e.g., Kaufman and Keller, 1981; Levi and Lysak, 1986) and considering the heat flow distribution in the area (Muñoz and Hamza, 1996) and the electrical properties of mantle rocks (e.g., Shankland and Waff,1977; Hjelt and Korja, 1993) the temperature of this layer may be of about 1200°C.

Examination of the vertical geothermal gradients along the MT profile on the basis of the former results -and taking into account the electrical properties of crustal rocks (e.g., Shankland and Ander, 1983; Hyndman and Shearer, 1989; Glover and Vine, 1994)- has led to some insights on the rheological regime of the crust and upper mantle in this region. The lower crust is ductile all along the western part of the

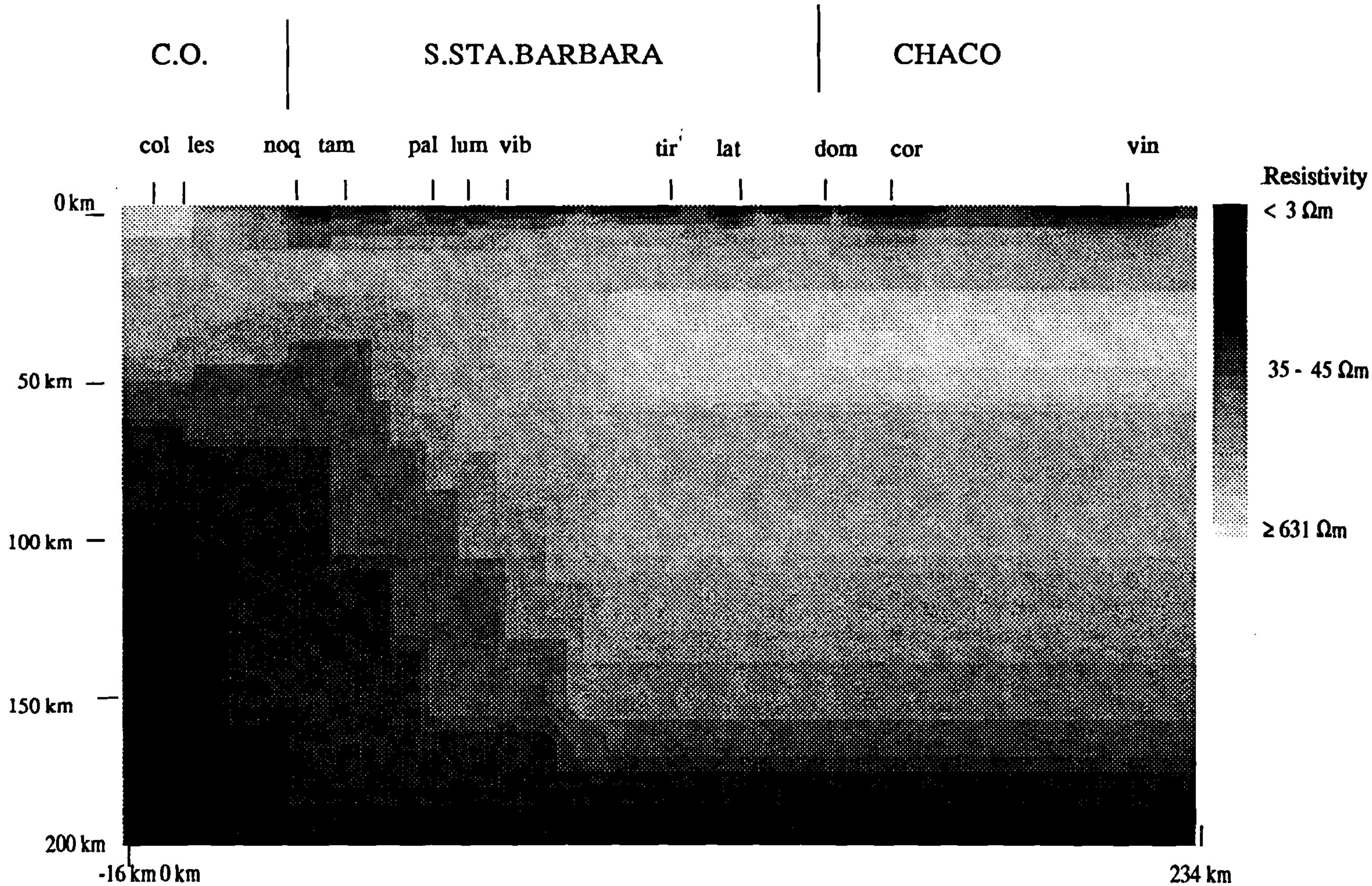
C.O.
S.STA.BARBARA
CHACO
col les noq tam pal lum vib tir lat dom cor vin
0 km
50 km
100 km
150 km
200 km
-16 km 0 km
234 km
Resistivity
< 3 Ωm
35 - 45 Ωm
≥ 631 Ωm

profile while it is in a brittle-ductile transition regime between the Sta. Bárbara system and El Chaco. The critical isotherm (600± 50°C) for the rheologic transition in the mantle (e.g., Chen and Molnar, 1983; Anderson, 1995) is largely surpassed in the western area where the Moho is at about 50 km depth; beneath the eastern areas where the Moho is at about 35-40 km depth the uppermost mantle is in a transition regime that converts into a ductile rheology at about 70-90 km depth. The foregoing insights indicate that the hybrid form of models of seismic attenuation as proposed by Whitman et al. (1992) is a suitable one for the region of the MT traverse (sections at 24.5°S in Whitman et al., 1992). The low resistivity zone -in ductile regime- uprising in the western side of the magnetotelluric model seems to be related to the neighbouring active volcanic arc in direction to the Puna.

## ACKNOWLEDGEMENTS

For the MT data and programs used in this study, computational facilities and support we wish to thank H. Brasse, A.M. Osella, P. Martinelli, A. Favetto, S.C. Constable, M. Eisel, R. Fernández, G. Pérez and D. Mills.

## REFERENCES

Anderson D.L., 1995. Rev. Geophys., **33**, 125-149.
Bahr K., 1991. Phys. Earth Planet. Inter., **66**, 24-38.
Chen W.P. and Molnar P., 1983. J. Geophys. Res., **88**, 4183-42
Constable S.C., Parker R.L. and Constable C.G., 1987. Geophysics, **52**, 289-300.
deGroot-Hedlin C. and Constable S.C., 1990. Geophysics, **55**, 1613-1624.
Glover P.W.J. and Vine F.J., 1994. Elec. Geophys. Res. Lett., **21**, 2357-2360.
Groom R.W. and Bailey R.C., 1989. J. Geophys. Res., **94**, 1913-1925.
Hjelt S.E. and Korja T., 1993. Phys. Earth Planet. Inter., **79**, 137-177.
Hyndman R.D. and Shearer P.M., 1989. Geophys. J. Inter., **98**, 343-365.
Hyndman R.D., Vanyan L.L., Marquis L. and Law L.K., 1993. Phys. Earth Planet. Inter., **81**, 325-344.
Jones A.G., and Dumas I., 1993. Phys. Earth Planet. Inter., **81**, 289-314.
Kaufman A. and Keller G., 1981. The Magnetotelluric Method. Elsevier, Amsterdam, 595 pp.
Krüger D. 1994. Modellierungen zur Struktur elektrisch leitfähiger Zonen in den südlichen zentralen Andean. Berliner geowiss. Abh., Reihe B, Band 21, 91 pp.
Levi K.G. and Lysak S.V., 1986. J. Geodynam., **5**, 113-132.
Lezaeta P., 1995. Inversión y Modelo Bidimensional de Observaciones Magnetotelúricas en el Chaco Argentino. Tesis Magister, Depto. de Geofísica, Universidad de Chile, Santiago, 182 pp.
Muñoz M. and Hamza V.M., 1996. Maps of terrestrial heat flow density distribution in South America. Third Int. Symp. on Andean Geodynamics, St. Malo, (this Volume).
Muñoz M.A., Fournier H.G., Mamaní M. and Borzotta E., 1992. In: Electromagnetic Results in Active Orogenic Zones (Ed.: A. Adám). Special issue Acta Geod. Geoph. Mont. Hung., Budapest, **27**, 65-86.
Osella A.M. and Martinelli P., 1993. Geophys. J. Int., **115**, 819-828.
Schwarz G., Chong Díaz G., Krüger D., Martínez E., Massow V., Rath W. and Viramonte J., 1994. In: Tectonics of the Southern Central Andes (Eds.: K. J. Reuter, E. Scheuber and P. Wigger), Springer, Berlin, 49-67.
Shankland T. J. and Waff H. S., 1977. J. Geophys. Res., **82**, 5409-5417.
Shankland T. J. and Ander M. E., 1983. J. Geophys. Res., **88**, 9475-9488.
Smith J. T. and Booker J. R., 1991. J. Geophys. Res., **96**, 3905-3922.
Vozoff, K. and Jupp D. L. B., 1975. Geophys. J. R. Astr. Soc., **42**, 977-991.
Wannamaker Ph., Stodt J. and Rijo L., 1987. PW2D-Finite element program for solution of magnetotelluric responses of two-dimensional earth resistivity structure. Earth Science Laboratory, University of Utah Research Institute, Publ. ESL-158, 40 pp.
Whitman D., Isacks B. L., Chatelain J. L., Chiu J. M. and Perez A., 1992. J. Geophys. Res.,**97**, 19929-19947.

# MODELLING THE EFFECTS OF CRUSTAL STRUCTURE DURING CONVERGENCE

R.A. Mason and A. Ord
Australian Geodynamics Cooperative Research Centre
CSIRO Exploration and Mining, PO Box 437 Nedlands, WA 6009.

**KEY WORDS :** mechanical modelling, crustal structure, oblique convergence

Kinematic models of oblique convergence by Tikoff and Teyssier (1994) and Teyssier et al. (1995) describe relationships between convergence direction and the orientation of instantaneous strain axes for models with various degrees of strike-slip partitioning on a margin parallel fault. Mechanical modelling by McKinnon (in prep.) of obliquely convergent margins has demonstrated that the major horizontal principal stress is always at a higher angle to the margin than the convergence vector despite reasonable variations in material properties. McKinnon has also shown that, where the margin is characterised by a margin-parallel fault of reasonable strength, thrust deformation will dominate either side of the pre-existing fault regardless of the convergence angle. The results of these two approaches to the problem are compatible and have implications for the interpretation of fault kinematics at plate boundaries which are, or have been, obliquely convergent in the past and which have margin or boundary parallel faults.

Segmentation of the Chilean and Argentine Andes is a function of rate and direction of convergence between the South American and Nazca plates, with the possible influence of long-lived lithospheric scale structures (Jordan et al., 1983). The history of deformation along such large scale structures in the over-riding plate is likely to have been complex given that the Cenozoic convergence history for the Nazca and South American plates has involved a progressive clockwise change in orientation (Pardo-Casas and Molnar 1987). Late Cretacceous motion of the Nazca plate was divergent with the South American plate at a very low angle, it then changed to more northeasterly directed convergent motion through the early Tertiary and became steadly oriented convergence at at high angle to the margin since the Eocene orientation (Pardo-Casas and Molnar 1987). Similarly, deformation along variably oriented crustal structures in Papua New Guinea during oblique convergence in the Tertiary is likely to be complex. A number of proposed crustal structures are considered related to mineral deposits in Papua New Guinea. These range in orientation but form two main groups, they are those which are approximately margin perpendicular and those which are approximately margin parallel (Corbett 1994). Because mineral deposits are often spatially related to crustal structures (e.g. Boric et al. 1990) modelling may be used to investigate conditions of deformation which may have contributed to the locations of mineral deposits at convergent margins (ie. the Andes and Papua New Guinea).

Mechanical modelling is investigated here as a tool for exploring the consequences of various convergence histories on the crustal structure of the Andean and Papua New Guinean margins. It has been carried out using the finite difference computer code FLAC (Fast Lagrangian Analysis of Continua, Cundall & Board 1988, Itasca 1992) on much simplified models of continental margin structure. The code has been successsfully applied to other studies of problems of stress distribution at a continental margin (e.g. Zhang et al. *in* press). Here we explore the possibilities for creating zones of dilation suitable for emplacing mineral deposits or mineral deposit-related intrusions located on or near continental margin, crustal scale structures. We describe the results of modelling some of these structures which may be related to mineral deposits.

The models presented form part of a series of models which progressively incorporate more complexity. The series of models are:

- the Falla Oeste as a planar, margin parallel fault with a variation in plate convergence angles representing strongly contrasting plate motions since the late Cretaceous;
- the Falla Oeste with a more complex yet generally margin parallel, non-planar geometry with the same variations in convergence angles;
- an approximately margin perpendicular structure from Papua New Guinea with convergence angle of approximately 55°.
- an approximately margin perpendicular structure together with a margin parallel structure from Papua New Guinea with convergence angle of approximately 55°.
- the Falla Oeste with a more complex yet generally margin parallel, non-planar geometry with the same variations in convergence angles and including the presence of an out-board margin parallel, planar fault representing the Atacama fault system.

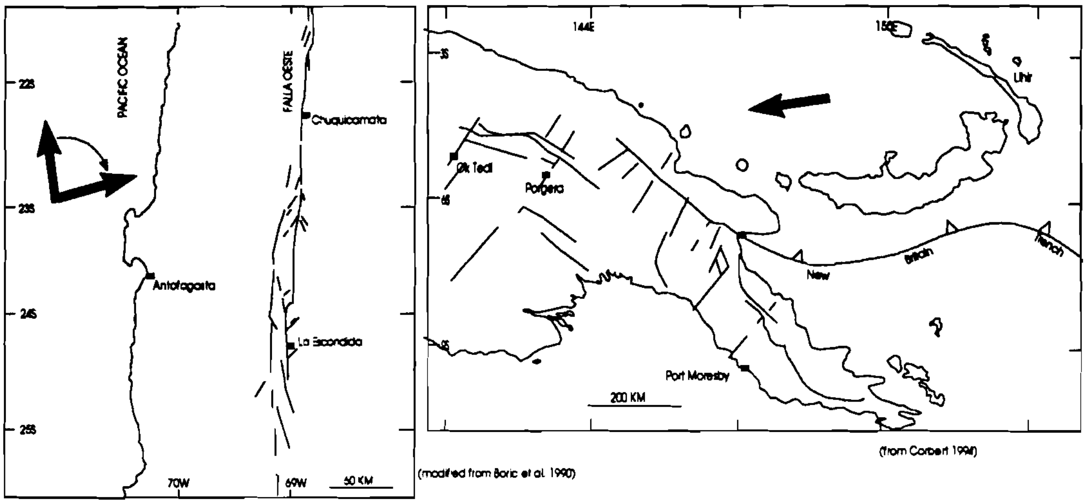


Figure 1. a) The Falla Oeste in the Chilean Andes and range of approximate Nazca plate convergence directions with respect to the South American plate since the late Cretaceous. b) Interpreted crustal scale structures in Papua New Guinea and current convergence direction of the Pacific plate with respect to the Austalian plate.

## REFERENCES

Boric, R., Diaz, F., & Maksaev, V. 1990. Geologia y yacimientos metaliferos de la region de Antofagasta. *Servicio Nacional de Geologia y Mineria - Chile, Boletin no. 40.*

Corbett, G.J., 1994. Regional structural control of selected Cu/Au occurrences in Papua New Guinea. Proceedings of the PNG Geology, Exploration and Mining Conference 1994, Lae. Rogerson, R. (Ed.).

Jordan, T.E., Isacks, B.L., Allmendinger, R.W., Brewer, J.A., Ramos, V.A., & Ando, C.J., 1983. Andean tectonics related to geometry of subducted Nazca plate. *Geol. Soc. Am. Bull.* **94**, 341-361.

Pardo-Casas, F., & Molnar, P. 1987. Relative motion of the Nazca (Farallon) and South American plates since Late Cretaceous time. *Tectonics* **6**(3), 233-248.

Tikoff, B., & Teyssier, C. 1994. Strain modeling of displacement-field partitioning in transpressional orogens. *J. Struct. Geol.* **16**(11) 1575-1588.

Teyssier, C., Tikoff, B., & Markley, M. 1995. Oblique plate motion and continental tectonics. *Geology* **23**(5) 447-450.

Zhang, Y., Scheibner, E. Ord, A., &. Hobbs, B.E. 1996 Numerical modelling of the eastern Australian passive margin.. *In press Australian Journal of Earth Sciences.*

# LOCAL EARTHQUAKE TOMOGRAPHY OF THE ANDEAN CHAIN AT 20°S.

F. Masson[1] and C. Dorbath[1,2]

[1] EOPG, 5 rue Descartes F67084 Strasbourg, URA 1358 CNRS
[2] ORSTOM, 213 rue La Fayette F75410 Paris

**KEY WORDS** : Local Earthquake Tomography - Bolivia and Northern Chile

**ABSTRACT :**

A temporary network of 41 Lithoscope seismic stations was operated for 6 months in Northern Chile and Bolivia, crossing the entire Andean belt at 20°S.
The first step was to study the crust and upper mantle performing a teleseismic tomography. This study allows to image the velocity perturbations associated with the oceanic Nazca plate subducting beneath continental South America.
In our presentation we will focus on the second step devoted to a simultaneous inversion of arrival-time data from local earthquakes located within the Wadati-Benioff zone. This inversion for velocity and hypocentral parameters in a strongly heterogeneous region was carried out in order to test and strengthen the results obtained for the Andean continental lithosphere by classical teleseismic tomography.
Within the crust, the local tomography gives a smoothed image of the lateral velocity variations that matches the structures determined by refraction profiling. A comparison of our results with those obtained previously along other segments of the Andean belt is presented.

# MAPS OF TERRESTRIAL HEAT FLOW DENSITY DISTRIBUTION IN SOUTH AMERICA

Miguel MUÑOZ[(1)] and Valiya M. HAMZA[(2)]

(1) Dpto. de Geoffsica, Universidad de Chile, Santiago, Chile.
(2) Observatório Nacional-CNPQ, Rio de Janeiro, Brasil.

**KEY WORDS:** Heat Flow, Geothermal Data Base, Automatic and Manual Contour Maps.

## INTRODUCTION

Considerable amount of geothermal work has been carried out in South America over the last few decades, but lack of efforts for evaluating the significance of such observations on a continental scale has been an obstacle in understanding the nature of tectonic processes affecting the continent. Attempts to prepare a heat flow map were initiated as early as 1982; during the period 1985-1987 further improvements in the data base for Brazil led to the preparation of a set of geothermal maps for the Brazilian territory (Hamza et al., 1987). The preliminary heat flow map of South America presented here is based on improvements made on these earlier maps. In the present work the available geothermal data have been put together in a form suitable for the evaluation of regional geothermal characteristics. We also report the progress obtained in preparing mosaics of regional heat flow variations in the South American continent.

## DATA BASE AND QUALITY LEVELS

The data compiled in this work are based on both published as well as unpublished reports of geothermal investigations in South America. Because of the large amount of related bibliographical material the sources of geothermal data will not be referenced here. The compilation includes 655 heat flow determinations; thus the overall data density is $37/10^6$ km$^2$, a value comparable to data densities in several regions of eastern Europe at the time of preparation of the preliminary heat flow map of Europe (Cermak and Hurtig, 1979). Different methods have been used for determining heat flow in the South American continent. In order to make use of such data, having a wide spectrum of quality levels, a priority scheme was adopted that takes into account not only the reliability of the technique used but also the nature of primary geothermal data. The distribution of available data within such a priority scheme is shown in Table 1.

**TABLE 1.** Priority of the Geothermal Data

| Priority Level | Geothermal Methods | Percentage of Data |
|---|---|---|
| High | Conventional Logging (CVL)<br>Bottom-Hole Temperature (BHT)<br>Underground Mine Measurements (MGT) | 60 |
| Intermediate | Conventional Bottom Temperature (CBT)<br>Aquifer Temperature (AQT)<br>Oceanic-type Probing (OHF) | 6 |
| Low | Geochemical Estimates (GCL)<br>Thermal Fluid Discharge (TFD) | 34 |

The spatial distribution of data is non-uniform and relatively reasonable data densities are available only for certain specific regions in Chile, Brazil, Venezuela, Bolivia, Argentina and Perú. In spite of such difficulties the available data set has allowed not only the determination of reliable mean heat flow values for a large number of major geological structures but also the preparation of mosaics of regional heat flow variations.

## AUTOMATIC AND MANUAL CONTOURING

In map preparation efforts a variety of contouring schemes were tested using commercially available software packages such as the GMT (Wessel and Smith, 1992) and the SURFER (Golden Software Inc., 1994). The data interpolation methods employed in automatic contour map generation include adjustable tension continuous curvature gridding algorithm as well as kriging. The area selected for automatic contouring lies between latitudes 0°S and 40°S where the data quality is relatively better and its distribution rather uniform. Due to space limitations the automatic contouring maps are not shown in this abstract.

For manual contouring the procedure employed uses information on tectonic setting to control the interpolation scheme, a procedure which has been employed with success by Cermak and Hurtig (1979). The main advantage of this technique is the ease with which geologically meaningful restrictions can be imposed on the aereal extent of anomalies that are of questionable character. The map prepared by manual contouring is presented in Fig.1 (see the last page of this abstract) where an upper limit of 100 $mW/m^2$ has been imposed for the contouring range and 20 $mW/m^2$ was selected for the contouring interval. Contouring has been extended to regions above the Equator using inferred values of heat flow based on the heat flow-age relationship (Polyak and Smirnov, 1968; Hamza and Verma, 1969), employing essentially the same procedure as that adopted by Chapman and Pollack (1975). In the southeastern part of the Patagonian Platform contouring has been based on the geothermal gradient maps of Robles (1987; 1988).

The prominent features in the maps generated by automatic contouring are also encountered in the map produced by manual contouring. There are however some differences in the shapes and sizes of the thermal anomalies, arising mainly as a result of taking into consideration the tectonic background in the interpolation scheme.

## DISCUSSION AND CONCLUSIONS

The preparation of the heat flow maps has led to the identification of some geothermal features that may be related to tectonic processes affecting the South American continent. Prominent among these are east-west trending belts of low heat flow in northern Perú and in central Chile (extending into Sierra Pampeanas in Argentina) as well as the belts of high heat flow in northern Chile (extending into the Altiplano and Bolivia) and southern Chile (extending into western Argentina). The low heat flow belts are found to coincide approximately with the flattening of the Wadati-Benioff zone. Some of these features are found to correlate well with results of studies on anelastic attenuation (e.g., Whitman et al., 1992), electrical resistivity distribution (Muñoz et al., 1992; Schwarz et al., 1994) and some patterns of global seismic tomography (e.g., Zhang and Tanimoto, 1991). These features are not seen in the recent spherical harmonic analysis of heat flow (Pollack et al., 1993), which suggests that use of empirical predictors based on the heat flow-age relationship in divising global heat flow maps should be restricted to tectonically stable areas. Low heat flow values in Panamá and northwestern Colombia could arise as a result of underthrusting of cold oceanic crust eastward of the trench line (Sass et al., 1974).

In the eastern part of the continent heat flow is low to normal (mean values <75 $mW/m^2$) but there are indications that heat flow in the Patagonian Platform is high compared to that in the Brazilian Platform. High heat flow anomalies are observed in the northeastern region and in the Mato Grosso (south-central region) of Brazil. It is worth noting that the anomaly in the northeastern region is contiguous with the westward extension, onto the continent, of the Fernando de Noronha oceanic lineament, known for its recent volcanic and magmatic activities (Almeida, 1958). Recent results of surface wave propagation indicate higher than normal slowness factor for this region (Souza, 1994). In the region of Mato Grosso heat flow is high along a narrow belt extending from the eastern part of Bolivia to the western border of the Sao Francisco craton. This is also an area characterized by the occurrence of a large number of thermal springs. Recent subcrustal magma emplacement could explain the high heat flow anomaly in this region but evidence for associated uplift is lacking.

**REFERENCES**

Almeida F.F.M, 1958. Geologia e Petrologia do Arquipelago de Noronha. Depto. Nac. Prod. Min., Div. Geol. Miner., Rio de Janeiro, Monografía 13, 181 pp.

Cermak and Hurtig E., 1979. Heat flow map of Europe. In: Terrestrial Heat Flow in Europe (Eds.: V. Cermak and L. Rybach), Springer Verlag, Berlin.

Chapman S.S. and Pollack H.N., 1975. Global heat flow: A new look. Earth Planet. Sci. Lett., **28,** 23-32.

Golden Sofware Inc., 1994. SURFER version 5.01. Surface Mapping System, Golden, Colorado.

Hamza V.M. and Verma R.K., 1969. The relationship of heat flow with the age of basement rocks. Bull. Volcan., **23,** 123-152.

Hamza V.M., Frangipani A. and Becker E.A., 1987. Mapas geotermais do Brasil. Internal Report No. 25305, Instituto de Pesquisas Tecnológicas, Sao Paulo.

Muñoz M., Fournier H.G., Mamaní M. and Borzotta E., 1992. A critical review of magnetotelluric studies in diverse tectonic areas in Argentina, Chile and Antarctica. In: Electromagnetic Results in Active Orogenic Zones (Ed.: A. Adám), Special Issue Acta Geod. Geoph. Mont. Hung., Budapest, **27,** 65-86.

Pollack H.N., Hurter S.J. and Johnson J.R., 1993. Heat flow from the Earth Interior: Analysis of the global data set. Rev. Geophys., **31,** 267-280.

Polyak B.G. and Smirnov Y.A., 1968. Relationship between terrestrial heat flow and tectonics of continents. Geotectonics (Eng. Transl.), **4,** 205-213.

Robles D.E., 1987. El gradiente geotérmico actual en Argentina y zonas aledañas de países vecinos. In: Actas 10° Congr. Geol. Arg., San Miguel de Tucumán, Actas III, pp. 313-316.

Robles D.E., 1988. El gradiente geotérmico en la República Argentina y regiones fronterizas. Boletín de Informaciones Petroleras, pp. 88-95.

Sass J.H., Munroe, R.J. and Moses Jr., T.H., 1974. Heat flow from Eastern Panama and Northeastern Colombia. Earth Planet. Sci Lett., **21,** 134-142.

Schwarz G., Chong Díaz G., Kruger D., Martínez E., Massow W., Rath V. and Viramonte J., 1994. Crustal high conductivity zones in the southern central Andes. In: Tectonic of the Central Andes (Eds.: K.J. Reutter, E. Scheuber and P. Wigger), Springer Verlag, Berlin, pp. 49-67.

Souza J.L., 1994. Shear wave velocity beneath eastern part of Brazil. In: Regional Seismological Assembly in South America, Brasilia, Book of Abstracts, p. 65.

Wessel P. and Smith V.H.F., 1992. The GMT - System version 2.1, Technical Reference and Cook-book. School of Ocean and Earth Science and Technology, University of Hawaii, Hawaii.

Whitman D., Isacks B.L., Chatelain J.L., Chiu J.M. and Pérez A., 1992. Attenuation of high-frequency seismic waves beneath the central Andean plateau. J. Geophys. Res., **97,** 19929-19947.

Zhang Y.S. and Tanimoto T., 1991. Global Love wave phase velocity variation and its significance to plate tectonics. Phys. Earth Planet Int., **66,** 160-202.

**Fig.1. Heat flow map of South America produced by manual contouring (see next page).**
Data types are given in Table 1.

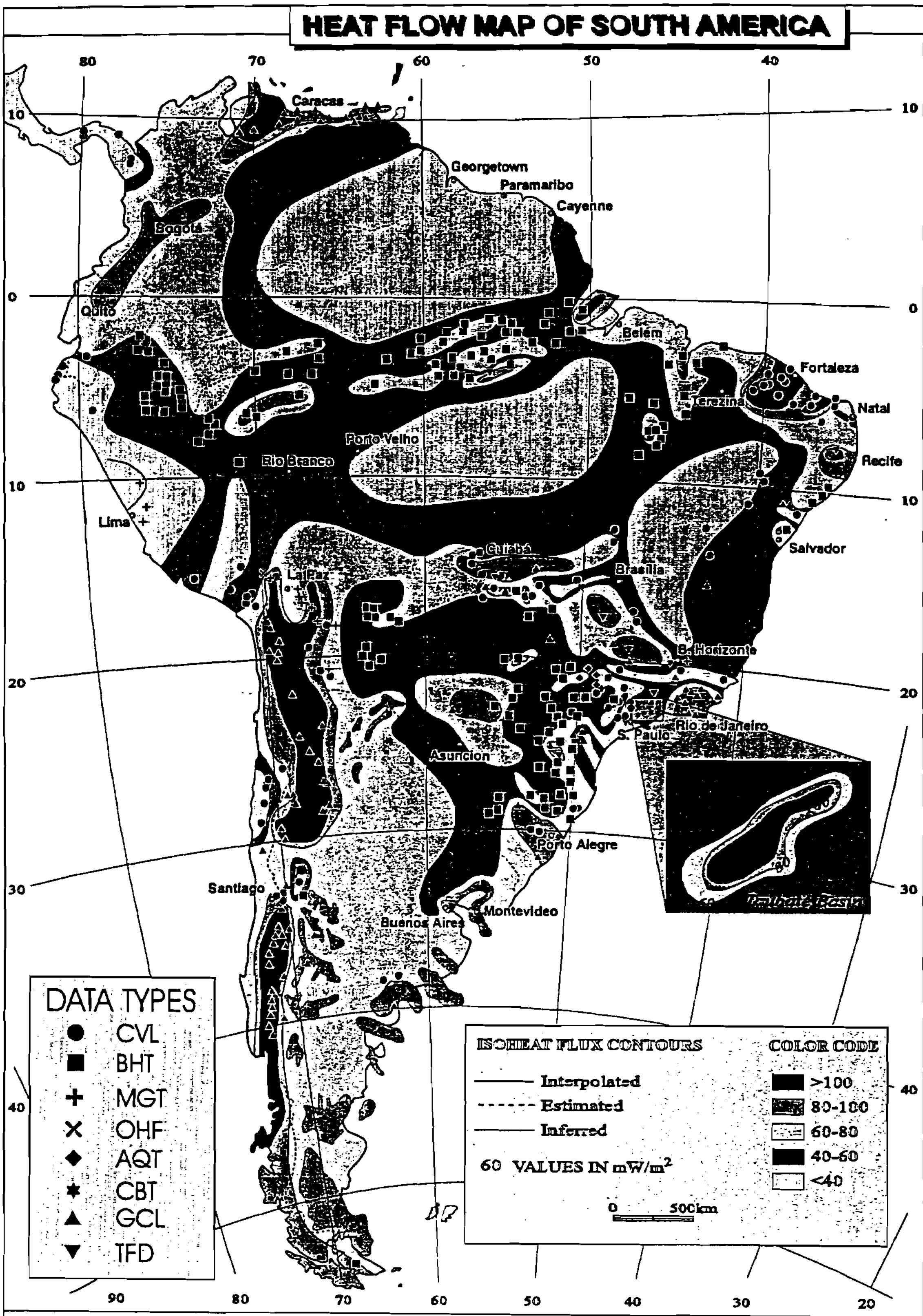
HEAT FLOW MAP OF SOUTH AMERICA
Caracas
Georgetown
Paramaribo
Cayenne
Bogotá
Quito
Belém
Fortaleza
Terezina
Natal
Recife
Porto Velho
Rio Branco
Lima
Salvador
Cuiabá
Brasília
La Paz
B. Horizonte
Rio de Janeiro
S. Paulo
Asuncion
Porto Alegre
Santiago
Buenos Aires
Montevideo
Taubaté Basin
DATA TYPES
CVL
BHT
MGT
OHF
AQT
CBT
GCL
TFD
ISOHEAT FLUX CONTOURS
Interpolated
Estimated
Inferred
60 VALUES IN mW/m²
COLOR CODE
>100
80-100
60-80
40-60
<40
0 500km
g0457

# WIDE-ANGLE SEISMIC MEASUREMENTS DURING THE CINCA95 PROJECT, ON- AND OFF-SHORE CHILE

Regina Patzwahl[1], Albrecht Schulze[2], Peter Giese[1] and James Mechie[2]

[1]Institute of Geophysics, Free University, Malteserstr. 74-100, 12249 Berlin, Germany
[2]GeoForschungsZentrum Potsdam (GFZ), Department 2, Telegrafenberg A17, 14473 Potsdam, Germany

KEY WORDS: Seismic refraction, Chile, South America

## EXPERIMENT DESCRIPTION

In the period from 31st July to 22nd August 1995, during the first phase of the CINCA95 (Crustal Investigations off- and on-shore Nazca/Central Andes) experiment the airgun pulses fired from the RV SONNE (cruise no. 104 of the RV SONNE) along the marine seismic lines (SO104-05 - SO104-29, Fig. 1) were recorded by a mobile land array (Wander Array) of 12 seismic stations at Pos1-Pos5 (Fig. 1) along the Chilean coast. The land array consisted of 12 Geotech PDAS 100 recorders deployed about 1.85 km (1' of latitude) apart. The average spacing of the airgun pulses was 50 m in distance (18 s in time) and thus a total of several tens of thousands of pulses were observed by the Wander Array. The first deployment at Pos1 followed immediately after the large Antofagasta earthquake on 30th July and the aftershock data recorded by the array will be of use in the study of the earthquake activity in the region. Unfortunately, however, the strong aftershocks completely masked the airgun signals and thus no useful data from the airgun pulses were obtained during this deployment. However, useful data from the airgun pulses were obtained from the other four deployments at Pos2 to Pos5. Good quality data were often obtained out to about 100-150 km distance.

During the second period of the CINCA95 campaign from August 28th to September 10th 1995, parts of the shot program from the first period (lines SO104-7, 9 and 13, see Fig. 1) were repeated for recordings on OBHs (Ocean Bottom Hydrophones) and wide-angle stations on-shore. The southernmost line was shifted northwards from SO104-5 to SO104-13. This was a prompt reaction to the Antofagasta earthquake of July 30th 1995, which provided the unique occasion for crossing the aftershock area of a recent earthquake with a seismic profile. The short perpendicular lines (203, 303, 403 and 404) were fired additionally. While OBHs were placed along the marine seismic lines, 22 digital (PDAS-100) and 7 analogue (MARS66) recorders were deployed on-shore with an average spacing ranging from 3-6 km along the eastward prolongation of the marine seismic lines (see Fig. 1, lines SO104-7, 9 and 13). In addition to the airgun pulses chemical explosions were used as seismic sources at the eastern- and

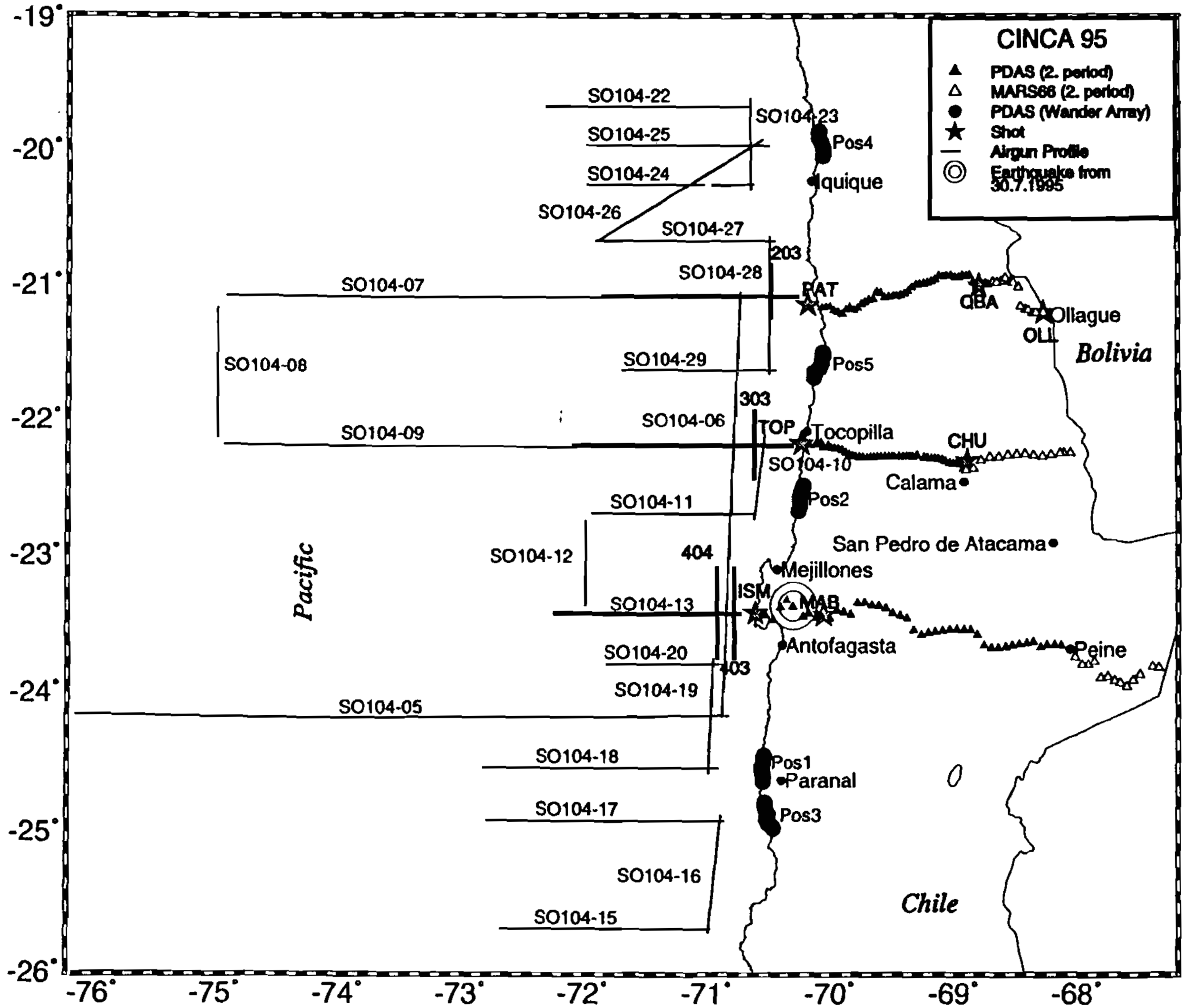


Fig. 1: Location map for CINCA95 on-shore wide-angle seismic experiment. The marine seismic lines SO104-05 - SO104-28 and 203, 303, 403 and 404 are shown together with the positions of the recorders deployed on-shore and the chemical shots and quarry blasts recorded.

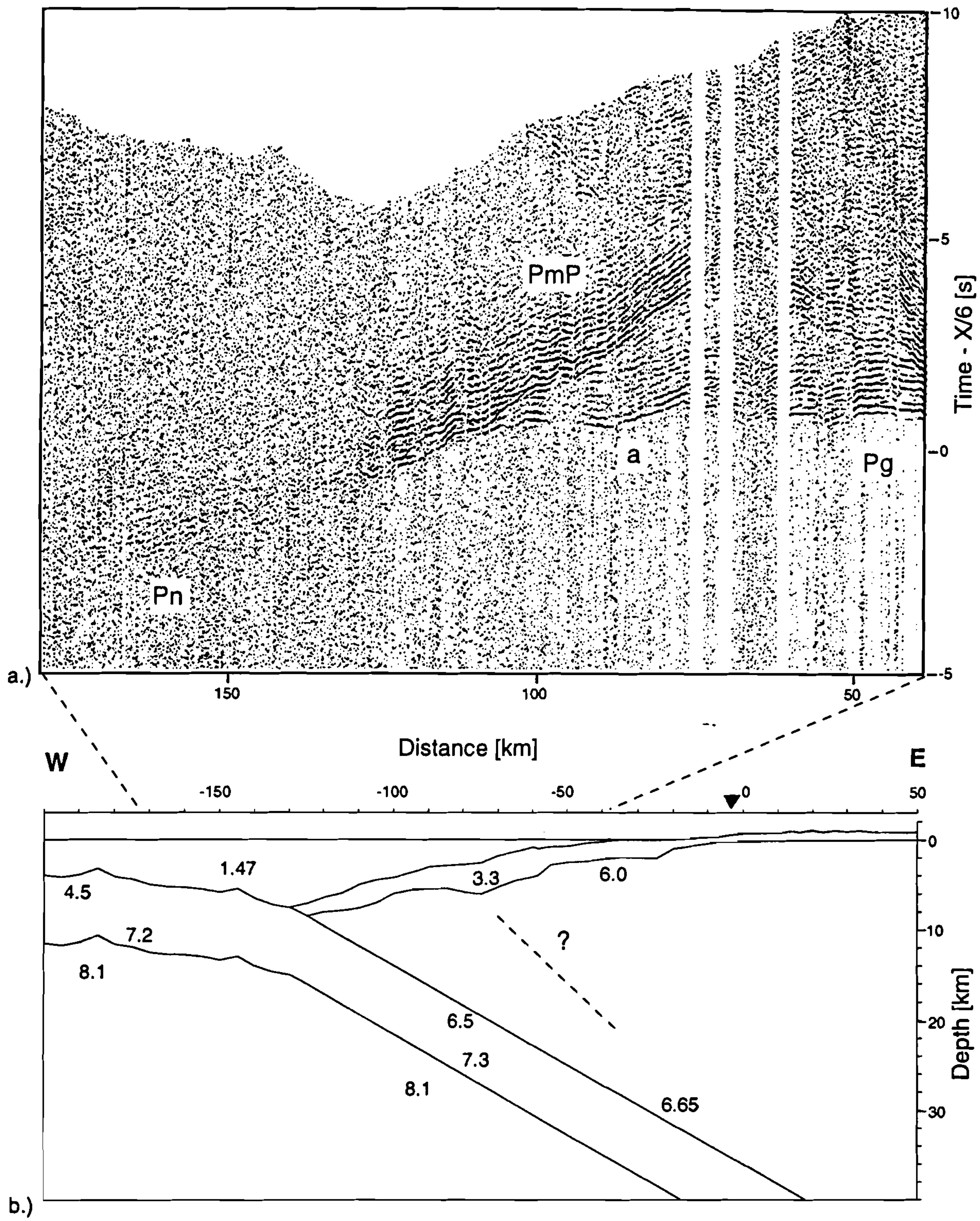


Fig. 2. a) Receiver Gather for receiver no. 2 (nearest to the coast) on seismic line SO104-07. The data have been corrected for water depth and are plotted in the form of a reduced time - distance record section. The 900 traces have been normalized individually and band-pass filtered (3-12 Hz). Reduction velocity = 6 km/s. Key: Pg - refracted phase from the upper crust; PmP - reflected phase from crust-mantle boundary of the Nazca Plate; Pn - refracted phase from the upper-mantle; a - supposed reflection.

b) Two-dimensional velocity cross-section derived from receivers on the land extension of line SO104-07 at 21°S. All velocities are given in km/s.

westernmost ends of the digitally registered lines, providing refraction seismic record sections which give further information on the structure and velocity distribution at the western edge of the south American continent. The average spacing of the airgun pulses was 160 m in distance and the average length of the marine lines was 160 km. The quality of the data in general is good and arrivals can be seen up to a distance of 260 km.

## RESULTS

The data example chosen (Fig. 2a) represents a receiver gather of high quality from profile SO104-7. Up to a distance of 68 km the first arrivals are correlated with the refracted phase through the upper crystalline crust (Pg). Its apparent velocity is 6.0 km/s after correction for water depth. From a distance of 68 km up to a distance of 105 km arrivals with large amplitudes can be recognized in the section. They are interpreted as the reflection from the crust-mantle boundary (Moho) of the subducted Nazca plate (PmP). Beyond a distance of 100 km the first arrivals form a refracted phase (Pn) travelling in the uppermost mantle with an apparent velocity averaging 9.5 km/s after water-depth reduction. This high apparent velocity results from the seismic phase travelling up-dip in the subducted Nazca plate. The first arrivals seen between 70 km and 98 km are at this stage of interpretation modelled as Pg arrivals. However, this phase can clearly be interpreted as a reflection from an intra-crustal reflector on some record sections. The correct identification of this phase will require intense examination and modelling of the data.

The resulting velocity model shows the Nazca plate being subducted at an angle of 12° with the Moho reaching a depth of 40 km underneath the coast. Both the dip-angle and depth are in good accordance with the earthquke locations from the CINCA95 seismological experiment and the Moho depth also agrees with the model of Wigger et al. (1994). The uppermost continental crust off-shore is covered by a layer of low velocity material, which thins towards the east near the land, where the sediment layer thickness does not exceed 1 km. The reflections seen in some of the record sections give rise to a steep reflector forming a wedge with the downgoing plate. This reflector could be interpreted as a shear zone separating the wedge from the rest of the crust.

The complete interpretation of all wide-angle data obtained during the CINCA95 project will give a picture of the trench area between 20° and 25° S and help to understand the character of the processes occurring in connection with the subduction of the Nazca plate.

## REFERENCE

Wigger, P., Schmitz, M., Araneda, M., Asch, G., Baldzuhn, S., Giese, P., Heinsohn, W.-D., Martinez, E., Ricaldi, E., Röwer, P. and Viramonte, J., 1994. Variation in the crustal structure of the Southern Central Andes deduced from seismic refraction investigations. In: K.-J. Reutter, E. Scheuber and P. Wigger (Editors), Tectonics of the Southern Central Andes. Springer, Berlin, Heidelberg, New York, pp. 23-48.

# TOMOGRAPHY OF THE ECUADORIAN ANDES FROM LOCAL EARTHQUAKE DATA OF THE 1995 LITHOSCOPE EXPERIMENT

Anne PAUL [1], Rosa BERNAL [1,2], Bertrand GUILLIER [2], Jean-Luc CHATELAIN [2], Alexandra ALVARADO [3], Hugo YEPES [3], Georges POUPINET [1], and Jean-Francois FELS [1].

[1] Laboratoire de Géophysique Interne et Tectonophysique, CNRS & Université Joseph Fourier, BP 53 X, 38041 Grenoble Cedex, France
[2] ORSTOM, Casilla 17-11-6596, Quito, Ecuador
[3] Instituto Geofisico, Escuela Politécnica Nacional, Quito, Ecuador

KEY WORDS : Ecuador, Andes, crustal structure, tomographic inversion, local earthquakes

A temporary network of 54 Lithoscope stations was operated in Central Ecuador from December 1994 to May 1995. It included 19 3-component stations with 5 s sensors and 35 vertical short-period stations. To allow precise location of hypocenters and 3D tomography of the lithosphere, stations were installed on 2 sub-parallel E-W lines 250 km long intersected by 3 N-S lines 100 km long. The network crossed the whole Andean chain on a width of 100 km between Quito and Riobamba.

One of the main objectives of the experiment was to investigate the lithospheric structure of the Ecuadorian Andes from tomographic inversion of teleseismic traveltime residuals. This goal was impossible to achieve due to the surprisingly small number of teleseismic events that were recorded. We suspect that this lack is due to the presence of a strongly attenuating layer in the mantle and/or the crust beneath the network. We hope that further investigations of local earthquake data will help in understanding the origin of this unexpected observation.

For the seismotectonic study, more than 1000 local events have been located using arrival times from the Lithoscope and the permanent stations of the Instituto Geofisico of Quito (Guillier et al., this volume). The subset of the best events will be used to invert simultaneously for hypocentral parameters and 3D velocity structure following the procedure described by Kissling et al. (1994) and using the iterative inversion method of Thurber (1983). We expect that, thanks to a better distribution of stations, the inversion of this dataset will significantly improve the tomographic image computed by Prévot et al. (this volume) using arrival times at permanent stations.

REFERENCES

Guillier, B., J-L. Chatelain, A. Alvarado, H. Yepes, G. Poupinet and J-F. Fels, 1996, Lithoscope experiment in Northern Ecuador: Preliminary results, ISAG 96, St Malo.

Prévot, R., J-L. Chatelain, B. Guillier, and H. Yepes, 1996, Mapping of the P wave velocity structure beneath the Ecuadorian Andes, ISAG 96, St Malo.

Kissling, E., W.L. Ellsworth, D. Eberhart-Phillips, and U. Kradolfer, 1994, Initial reference models in local earthquake tomography, J. Geophys. Res., 99, 19635-19646.

Thurber, C.H., 1983, Earthquake locations and three-dimensional crustal structure in the Coyote Lake area, central California, J. Geophys. Res., 88, 8226-8236.

# Shear Wave Anisotropy Beneath the Central Andes from the BANJO, SEDA and PISCO Experiments

Jascha Polet (1,2), Paul Silver(2) ; G. Zandt(3); S. Ruppert(4) ; R. Kind(5); G. Bock(5); G. Asch(5) ; S. Beck(3): T. Wallace(3)

(1)Seismo Lab 252-21, Caltech, Pasadena, CA 91125; ph. 818-395-6974; E-mail: polet@seismo.gps.caltech.edu
(2) Carnegie Institution of Washington, DTM, Washington DC, 20015; ph. 202-686-4370; E-mail: silver@dtm.ciw.edu)
(3)SASO, University of Arizona, Tucson, AZ 85721
(4) IGPP, LLNL, Livermore, CA)
(5)GeoForschungsZentrum, Telegrafenberg A6, 14473 Potsdam, Germany)

Key Words: Anisotropy, shear-wave splitting, Central Andes

We analyze broadband data from portable stations of the BANJO, SEDA and PISCO experiments to determine shear wave splitting parameters (fast polarization direction $\phi$, delay time $\delta t$) beneath the arrays. The BANJO array constitutes an 800 km-long east-west transect at a latitude of $20^{\circ}$ south. It extends from the west coast of South America (near Iquique) to the Chaco Plain, east of the Andes. The SEDA array is located between $16^{\circ}$ and $21^{\circ}$ south in a line roughly parallel to and 500km east of the coast. The PISCO array is situated in a roughly equidimensional array between 21 and $26^{\circ}$ south. Results for the BANJO array, using teleseismic SKS, SKKS and PKS as well as ScS from deep-focus events, which take near-vertical paths through the upper mantle, reveal the following pattern. Delay times vary from 0.5 s to 1.3 s. All but one stations show $\phi$ almost EW. This direction is approximately orthogonal to the trench and the slab contours. However, the value of $\phi$ for one station follows the contour of the slab ($-30^{\circ}$). In addition, we have measured splitting in S waves from local deep-focus events from the north (related to the Bolivian earthquake of 1994) and the south (Argentina). These ray paths sample the above-slab region is nearly the same place, but sample the below slab region about 200km north and south of the BANJO line. The resulting values of $\phi$ for the western BANJO stations are more northerly than the teleseismic results for the same station and suggest rapid variations in anisotropic properties north and south of the BANJO line from below the slab. The SEDA stations reveal values of $\phi$ that are locally parallel to the contours of the Nazca slab, with $\phi$ rotating from $60^{\circ}$ in the north to $10^{\circ}$ in the south, and with $\delta t$ around 1s. These are more or less consistent with the values of $\phi$ for the BANJO direct-S measurements that sample the subslab region in the same locale. The PISCO stations further to the south reveal a less clear-cut pattern. There is a mixture of NS and EW values of $\phi$ with a predominance of EW values. Taken together, these results reveal an intriguing pattern: a thin coherent east-west band of EW-fast values of $\phi$, with predominantly trench-parallel values of both north and south of this zone. They furthermore suggest that this pattern originates from below the slab. There is no morphologic feature in the slab itself that could cause the observed pattern. Based on knowledge of how olivine deforms, the observed subslab pattern suggests a complex three-dimensional flow field beneath the Nazca slab, consisting of both trench-normal and trench parallel components. The trench-parallel component may be the result of the trenchward motion of the South American plate in a hot spot reference frame. It has been argued previously that this component provides the large-scale structural control of the Andes (Russo and Silver, 1994; 1996)

In order to isolate the mantle-wedge component above the slab, we have performed splitting analysis on local intermediate-focus events. While the values of $\phi$ are difficult to constrain, the delay times are found to be about 0.3-0.4s. This is larger than the values usually obtained for crustal splitting (global average is about 0.2s, even regions with a large crustal thickness, such as Tibet, see McNamara et al, 1994), suggesting that there is some mantle-wedge component, although it is small compared to the values usually obtained for stable continental regions (Silver, 1996). The remaining signal is due to the subslab region. For the eastern BANJO stations, the top of the slab is deeper than 300 km, so that the subslab zone is below the olivine stability field. Therefore, the subcontinental mantle probably provides the dominant contribution. In this region, the EW direction, subparallel to the relative plate motion of the Nazca plate, could be explained by slab-induced delamination of the subcontinental mantle. Alternatively it could be due to 'fossil' anisotropy associated with the Brazilian Craton. Spltting values obtained from the BLSP experiment further to the east in Brazil (James and Assumpcao, 1996), which show a close correspondence to cratonic geology, suggest the latter interpretation.

James, D. E. Assumpcao, M. 1995. Tectonic implications of S-wave anisotropy beneath SE Brazil. *Geophys. J. Int*, in press.

McNamara, D.E., Owens, T.J., Silver, P.G., Wu, F.T. 1994. Shear wave anisotropy beneath the Tibetan Plateau, *J. Geophys. Res.* 99, 13,655--65

Russo, R., Silver, P.G. 1994. Trench-Parallel flow beneath the Nazca Plate from seismic anisotropy. *Science*, 263, 1105-11

Russo, R., Silver, P. G. 1996. Cordillera formation, mantle dynamics and the Wilson Cycle. *Geology*, in press.

Silver, P. G, 1996. Seismic anisotropy beneath the continents: Probing the depths of geology. *Annu. Rev. Earth Planet. Sci.*, 24, 385-432.

# A VELOCITY - DEPENDENT FORCE BOUNDARY CONDITION APPROACH FOR NUMERICAL MODELS OF PLATEAU EVOLUTION - APPLICATION TO ANDEAN DEFORMATION

Robert PORTH

GFZ Potsdam, Telegrafenberg C3, 14473 Potsdam, Germany, porth@gfz-potsdam.de

KEY WORDS: numerical modelling, plateau evolution, Central Andes, velocity-dependent force boundary condition.

## INTRODUCTION

Andean plateau evolution is controlled by plate driving forces and plateau induced volume forces increasing with plateau elevation. Neotectonic data and the recent stress field indicate that at present both forces are of comparable magnitude (Mercier et al., 1992; Assumpção and M. Araujo, 1993). This is supported by results of two-dimensional analytical (Froidevaux and Isacks, 1984) and elastic numerical(Richardson and Coblentz, 1994) modellings to calculate the state of stress in the Andean plateau and adjacent areas. Wdowinski and Bock (1994a and b) used a temperature dependent viscoplastic flow model to study the evolution of deformation and topography of the Andean plateau. Their model predicts many important large scale features of Andean plateau evolution such as the present day topography and migration of surface deformation from the central part of the Altiplano/Puna to the Subandean range. But, it cannot predict the decrease of indenting velocity with increasing plateau topography as suggested by Wdowinski and O'Connel (1990), because of the used velocity boundary condition (b.c.).

## THE MODEL

In order to investigate the effect of growing plateau forces a velocity-dependent force b.c. was applied to geometrical simple two-dimensional lithosphere models at different stages of plateau evolution. Because of the non-linear and strongly temperature dependent viscosity (power law creep) of the lithosphere a constant force b.c. can lead to very unstable models with unrealistic high strains rates. Thus, in this study a mixed (force, velocity) b.c. was applied following Christensen (1992), who used this type of b.c. in numerical models of lithospheric extension. The force acting at the model boundary is

$$F(v) = F_0 - (F_0/v_0)\,v$$

where $F_0$ is the tectonic force at zero velocity and $v_0$ the maximum possible indenting velocity, the velocity of the right model boundary, caused by $F_0$. The values of $F_0$ chosen in this study are 3, 4.5 and 6 $\times 10^{12}$ Newton per meter lithosphere perpendicular to the two dimensional model. This is equal to an average horizontal tectonic stress acting at the 125 thick lithosphere model of 24, 36 and 48 MPa, respectively. For $v_0$ a value of 3 cm/a was chosen. Considering the model as a part of a larger system the physical idea behind this type of b.c. is that the finite viscosity of the "outside world" limits the indenting velocity even when the model itself is very weak.

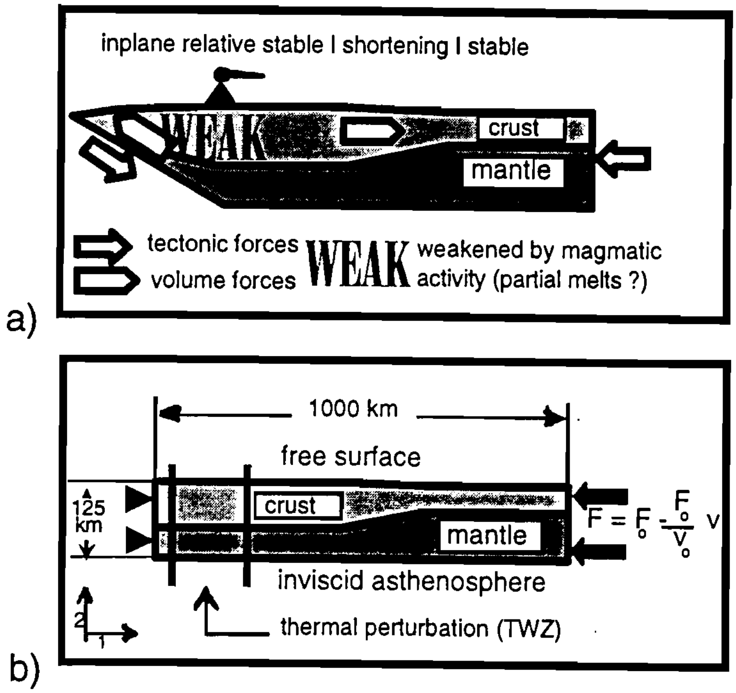


**Figure 1** a) Schematic cross section showing the upper plate of the Central Andean subduction zone (vertical exaggerated). b) Geometry and boundary conditions of the numerical model. The (inplane) relative stable forearc region is not part of the model.

In order to keep it simple the inplane relative stable forearc region is not part of the studied numerical model (Fig. 1). Since the weakened lithosphere in the area of the magmatic arc is not capable to transmit tectonic stress this simplification should have no effect on the deformation in or east of the magmatic arc, where the largest part of crustal shortening is accommodated (e.g. Schmitz, 1994). This model also assumes that mantle drag forces at the base of the lithosphere (within the modelled area) are negligible. The finite element (FE) code used in this study is an adopted version of the code written by Shimon Wdowinski, used and described by Wdowinski and Bock (1994a and b).

## RESULTS

Fig. 2 shows the velocity field and the effective strain rate (the second invariant of the strain rate tensor) of the model with $F_0 = 6 \times 10^{12} Nm^{-1}$ at two different stages of plateau evolution (two and four km elevation). Similar to the models of Wdowinski and Bock (1994a and b) deformation is concentrated in a thermally weakened zone (TWZ) up to about two km plateau elevation and migrates to the non-elevated parts of models with higher plateau elevation (see also Fig. 3a). But in contrast to their models the indenting velocity strongly depends on temperature deflection in the TWZ (not shown here) and decreases with increasing plateau elevation (Fig. 3b) because of the force b.c used here. The tectonic force $F_0$ necessary to drive a plateau evolution of 4 km is at least 4.5 $Nm^{-1}$. This value which coincides with results of static models (Froidvaux an Isacks, 1984; Richardson and Coblentz, 1994) exceeds the value of the ridge push force (e.g. Bott, 1993). This supports the assumption of additional mantle drag forces acting to drive the South America Plate in western direction (Meijer and Wortel, 1992) and therefore contributing to Andean plateau evolution. The force F applied at the models increases with plateau topography and decreasing indenting velocity (Fig. 3c). In contrast to the indenting velocity the force F is remarkably independent of $F_0$ except for elevations between 2.5 and 3.5 km, where the transition from symmetrical pure shear compression in the TWZ (Fig. 2a) to asymmetric plateau forces controlled deformation (Fig. 2b) occurs.

## CONCLUSION

The indenting velocity, the velocity of the right model boundary, decreases significantly with increasing plateau elevation. Because of the non-linear stress-strain relation of dislocation creep controlled rheology this affects not only the velocity but also the style of deformation within the model. This emphasises the importance of a force boundary condition for numerical models of plateau evolution. A comparison between the recent shortening rate and the average value over the last 26 Ma (about 1 cm/a) can be used to constrain the dynamic parameter controlling Andean deformation. The velocity of the model surface can be compared with GPS data of the SAGA 95 profile running from the coast to the undeformed Brazilian shield (at about $23°S$), provided that the data between the magmatic arc and the Brazilian shield reflect the long term deformation.

## REFERENCES

Assumpção, M. and M. Araujo 1993. Effect of the Altiplano- Puna plateau, South America, on the regional intraplate stresses. Tectonophys., 221, 475-96.

Bott, M.H.P. 1993. Modelling the plate-driving mechanism. J. Geol. Soc., 150, 941-51.

Christensen U.R. 1992. An Eularian technique for thermomechanical modeling of lithospheric extension. J. Geophys. Res., 97, 2015-36.

Froidevaux, C. and B.I. Isacks 1984. The mechanical state of the lithosphere in the Altiplano-Puna segment of the Andes. Earth and Planet. Sci. Lett., 71, 305-314.

Mercier, J.L, M. Serbrier, A. Lavenu,, J. Cabrera, O. Bellier, J.-F. Dumont and J. Machare 1992. Changes in the tectonic regime above a subduction zone of Andean Type: The Andes of Peru and Bolivia during the pliocene-pleistocene. J. Geophys. Res., 97, 11,945-82.

Richardson, M.R. and D.D.Coblentz 1994. Stress modeling in the Andes: Contraints on the A-merican intraplate stress magnitudes, J. Geophys. Res., 99, 22,015-55.

Schmitz, M. 1994. A balanced model of the southern Central Andes. Tectonics, 13, 484-92.

Wdowinski, S., R.J. O'Connel 1990. On the choise of boundary conditions in continuum models of continental deformation. Geophysic. Res. Lett., 17, 2413-16.

Wdowinski, S. und Y. Bock 1994a. The evolution of deformation and topography of high elevated plateaus. 1. Model, numerical analysis and general results. J. Geophys. Res. 99, 7103-19.

Wdowinski, S. und Y. Bock 1994b. The evolution of deformation and topography of high elevated plateaus. 2 Application to the Central Andes. J. Geophys. Res. 99, 7121-30.

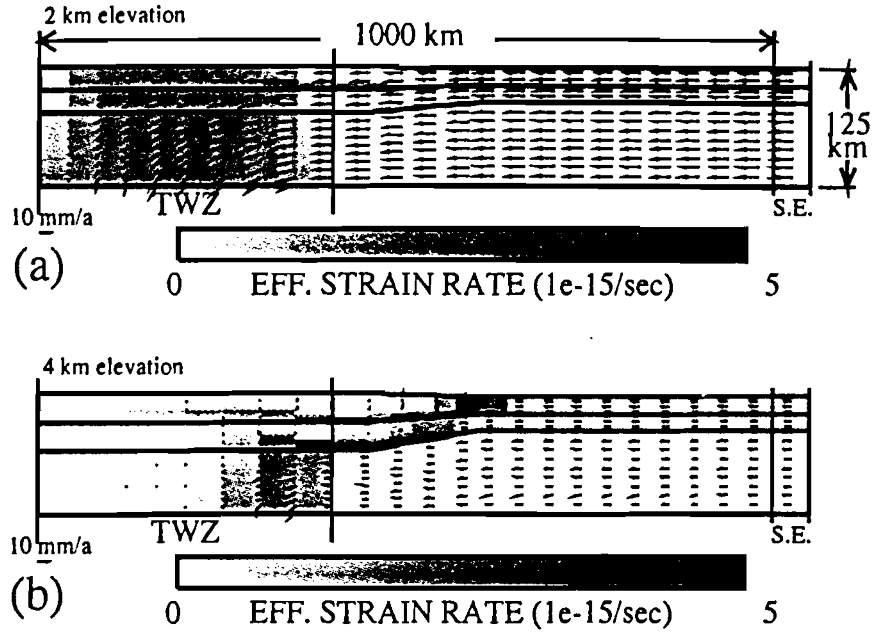


**Figure 2** Effective strain rate and the velocity field of the model with two and four km elevation of the left hand side. The parameter for the mixed b.c. are: $F_0$ : $6 \times 10^{12} Nm^{-1}, v_0$ : 3 cm/year (see text). S.E: elements with a high viscosity to achieve a no-tilt boundaty, not considered to be part of the lithosphere model.

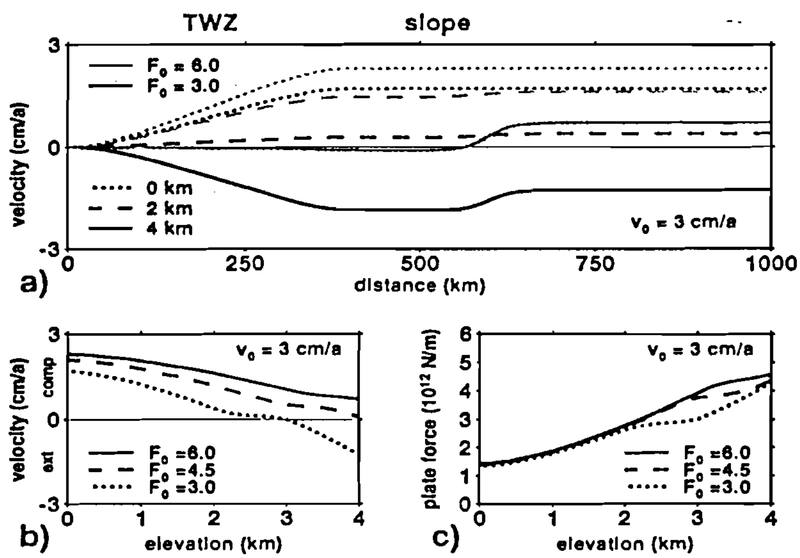


**Figure 3** a) Horizontal velocity (positive to the left) at the surface of the model with the indicated parameters describing the mixed b.c. . The left model boundary is fixed. TWZ: area of a thermal deflection, slope: area of the slope. b) The velocity (positive to the left for compression of the model) of the right model boundary as a function of plateau elevation. ext: extension, comp: compression of the model. $F_0$ in $10^{12} Nm^{-1}$. c) The force F applied at the right model boundary as a function of plateau elevation.

# MAPPING OF THE P WAVE VELOCITY STRUCTURE BENEATH THE ECUADORIAN ANDES

Richard PREVOT(†,1,2), Jean Luc CHATELAIN(1,3), Bertrand GUILLIER(1,3), Hugo YEPES(3)

† Richard Prévot died on December 31, 1994 ;
1 ORSTOM, Quito, Ecuador.
2 LGIT, Université J. Fourier, Grenoble, France.
3 Instituto Geofisico, Escuela Politecnica Nacional, Quito, Ecuador.

KEY WORDS : tomography, crust, moho, lithosphere, Andes, Ecuador

## Introduction

The Andean chain forms an elongated structure about 7500 km-long located along the Western South American margin, with considerable latitudinal variations in width. Our zone of interest, located in Ecuador at the northern termination of the Central Andes segment [Jordan et al., 1983], is a downsized 220 km-wide structure of the 800 km-wide broad structure in Central Bolivia. The main morphological expressions of this reduction are : (1) between the Western and Eastern Cordilleras, the disappearance of the Bolivian Altiplano (220 km wide), replaced by the Ecuadorian Interandean depression (20 km wide), (2) the reducted width of the Cordillera with a great change from 400 km at 20°S (Bolivia) to 140 km at 1°S (Ecuador), and (3) the contraction of the Subandean zone from a 180 km width in Bolivia to 60 km in Ecuador. These variations, described by Winter [1990], are the consequence of the complex process of mountain building in the Central Andes. A better knowledge of the velocity structure will help to constrain and understand this process. Dorbath et al. [1993] performed a tomographic inversion of seismic data for the Bolivian Central Andes and mapped lateral variations of velocity. They found a clear relation between surface structures and the lithospheric velocity structure: lower velocity beneath the Altiplano Plateau, and higher velocity beneath the eastern flank of the Eastern Cordillera. Farther South, at 24.5°S latitude, in the same Central Andes domain, Whitman [1994] mapped variations of the Moho depth beneath the eastern margin of the Andes and found a decrease of its depth from the plateau to the eastern flank. A similar result is also found by Dorbath et al. [1993] in Bolivia.
The aim of this study is to map the velocity structure and the depth of the Moho of a segment of the Andes and to complete the above mentioned previous studies by producing a velocity model at the Northern termination of the Central Andes in Ecuador. In this study, travel time residuals of P-waves recorded by a local network in Ecuador, are inverted to obtain a velocity structure beneath the station array. Teleseismic data have been added to the inversion, to stabilize the velocity at depth. Finally, the velocity structure is associated with surface geomorphological units. We find that there is an apparent continuity in the velocity structure along the Central Andes : in Ecuador, the Cordillera margins have higher velocity than the Interandean depression, and the Moho depth increases beneath them, as observed farther South from previous studies.

## Data and Method

Data used in this study are arrival time of P and S waves of earthquakes at local and teleseismic distances. Local data come from events recorded between 1990 and 1993 by an array of a total of 43 seismic stations from the National Seismic Network run by the Instituto Geofisico of the EPN. From the initial set of 2432 local events located using HYPO78, a final set of 1294 events was used for inversion. These selected events have at least 3S arrival times, and after relocation the root mean square residual (RMS) is less than 1.0 s and the condition number less than 100. P arrival times from 273 regional events, reported by the ISC bulletin between 1971 and 1987, was also used for inversion. Located in Ecuador, these events are recorded by WWSSN seismic stations in South America. All the selected teleseismic events have RMS than less 1.0 s after relocation. Finally a total set of 14684 P arrival times and 7472 S arrival times were used for inversion, where P and S wave velocities and hypocenters are determined simultaneously [Aki and Lee, 1976 ; Roecker, 1982 ; Roecker et al., 1987 ; Abers and Roecker, 1991]. In using this technique, we tried to explain as much residual as possible by first relocating events and calculating station corrections, and then by perturbing the velocity structure. Because of the paucity of published geophysical data in this region ( e.g., S wave attenuation, apparent velocity) to corroborate our results, we consider as reliable results those which are associated with large geomorphological structures of the region.

**Results**

*One-Dimensional structures*

The starting velocity model has been adapted from Ocola et al. (1977), Flüh et al. (1981) and Leeds (1977). Because of the important contrast of velocity at the Moho transition, it is important to set the Moho depth. The previous authors found its depth varying from 43 to 66 km. Dorbath et al. [1993] found a depth of 50 km beneath the Eastern Cordillera in Central Andes. From all these data, we assumed a Moho depth of 50 km.

Results from the one dimensional inversion show both P and S wave velocity monotonically increasing with depth, without obvious low velocity zone (LVZ). However, an important velocity decrease is observed in layer 5, where the initial 6.40 km/s velocity is down to 6.21 km/s. The same pattern, although much more pronounced, is observed in Vanuatu [Prévot et al., 1991] where a clear LVZ appears on the one dimensional profile. By analogy with the Vanuatu study, we suspect the presence of a low velocity body in layer 5 of the three-dimensional structures.

*The Three-Dimensional Structures*

The Ecuadorian Andes topography shows a very contrasted figure which probably reflects complex subsurface tectonics, with a complex associated velocity structure. This region is poorly known, so we are searching only for major velocity structures that can be related to the surface topography. To address this problem, a relatively coarse block model is used in the inversion process. Each layer is divided in 60x60 km blocks. The best azimuthal orientation for the grid is N30E, parallel to the Andes north of 1°S. In this direction, the reduction in variance is maximum, and thus a correlation exists between the geometry of surface structures and the underneath velocity structure. As we are searching for large structures, we are limiting our investigation to the first iteration of the inversion process. We assume that if any major structure exists, it must come up immediately in the inverse study and details will be absorbed into the averaging of the block velocity. As a consequence of this coarse study, the reduction in variance is a low 16% .

**Discussion**

*Shallow structure* (0-10 km ; Figures 1a and 1b)

The only well resolved blocks (resolution > 75%) are those just beneath the seismic array of stations. A common pattern for these first two layers is observed : blocks located beneath the eastern margin of the Cordillera have higher velocity than those located right below the Interandean depression. The lack of resolution beneath the western margin Cordillera prevents us from comparing velocities beneath these two margins. On the other hand, smaller blocks in our model could provide a better picture of the velocity structure but numerous details will appear at the same time and other geophysical data (e.g., refraction data, gravity) are needed to constrain the interpretation of these features, which do not exist.

*Lower crust structure* (10-50 km ; Figures 1c, 1d, and 1e)

As we investigate deeper into the crust, the three layers between 10 and 50 km depth show more blocks with resolution greater than 75%. Layer 3 (10-20 km) shows very little lateral velocity variation and is considered as an homogenous layer (Figure 1c).

In layers 4 and 5 remarkable high velocity blocks are bordering the western flank of the Cordillera, in a direction parallel to the Andes (Figures 1d and 1e). Beneath the Andes, velocity is everywhere

lower. Unfortunately, a lack of resolution prevents us to determine the velocity structure beneath the eastern flank of the Cordillera.
As mentioned above, the one-dimensional velocity profile shows a sensible decrease of velocity in layer 5. In the three-dimensional solution, a particularly low velocity block (6.05 km/s) is found in layer 5.
*Upper Mantle* (50-75 km ; Figure 1f)
Most of the local data are located above 50 km depth and in using only local data, we are unable to have a resolution >75% at this depth. So, teleseismic ISC data have been added to the local data to improve the resolution of the layer beneath 50 km depth. The initial poorly resolved velocity structure is still preserved but resolution is now largely improved. In other words, the addition of ISC data is just improving the velocity image deduced from the local data.
Except for a relatively low velocity zone located along strike the Andes, most of blocks have velocity greater than 8 km/s indicating a transition from the lower crust to the upper mantle and the hypothesis of an average 50 km Moho depth is consistent with these results. A simple explanation to account for the low velocities found in layer 6, is to consider a down dip Moho wiggle, occurring beneath the Cordillera. Unfortunately velocities in layer 7 (75-150 km, figure 1g) are very instable because only the teleseismic events account for determining this structure and it is impossible to determine how deep is the bottom of the Moho wiggle.

## Conclusion

The aim of this study was to investigate if major velocity structures were apparent beneath the Ecuador Andes. Because of the paucity of geophysical studies in this region, we restrain our study to the big structures, which can be related to the surface topography. Generally the crustal velocity beneath the Andes is lower than the velocity found on the margins of the Cordillera (Figure 1g). The volcanic activity along strike the chain inducing a thermal anomaly, could be a factor to explain this relative low crustal velocity. In the lower crust, a permanent nest of seismicity is occurring inside a particularly low velocity zone (6 km/s) at crustal basement (Figure 1e). The most interesting features found in this study are (1) the probable down dip wiggle of the Moho along strike the Ecuadorian Andes, and (2) remarkable high velocity blocks bordering the western flank of the Cordillera, in a direction parallel to the Andes (Figures 1d and 1e), while velocity is lower beneath the Cordillera, as observed farther South from previous studies. We thus find that there is an apparent continuity in the velocity structure along the Central Andes.

## REFERENCES

Abers, G.A., and S.W. Roecker, Deep structure of an arc-continent collision: Relocation of earthquakes and inversion for upper mantle P and S waves velocities beneath Papua New Guinea, *J. Geophys. Res.*, 96,6379-6402, 1991.
Aki, K., and W.H.K. Lee, Determination of three-dimensional velocity anomalies under a seismic array using first P arrival times from local earthquakes, 1. A homogeneous model, *J. Geophys. Res.*, 81, 4281-4339, 1976.
Dorbath, C., M. Granet, G. Poupinet, and C. Martinez, A teleseismic study of the Altiplano and the eastern Cordillera in northern Bolivia: New constraints on a lithospheric model, *J. Geophys. Res.*, 98, 9825-9844, 1993.
Flüh, E. R., B. Milkereit, R. Meissner, R. P. Meyer, J. E. Ramírez, J. del C. Quintero y A. Udías, Observaciones de refraccion sismica en el Noroeste colombiano en la latitud 5.5°N, 83-95, in Investigaciones Geofísicas sobre las Estructuras Océano-Continentales del Occidente Colombiano, Bogotá, Colombia, 1981.
Jordan, T.E., B.L. Isacks, R.W. Allmendinger, J.A. Brewer, V.A. Ramos, and C.J. Ando, Andean tectonics related to geometry of subducted Nazca plate, *Geol. Soc. Am. Bull.*, 94, 341-361, 1983.
Leeds A. R., Mantle velocities in the Colombia-Ecuador region, 237-239, in La transición océano-continente en el suroeste de Colombia, Bogotá, Colombia, 1977.
Ocola L. C., L.T. Aldrich, J. F. Gettrust, R. P. Meyer and J. E. Ramírez, Project Nariño I : crustal structure under southern colombian-northern Ecuador Andes from seismic refraction data, 47-57, in La transición océano-continente en el suroeste de Colombia, Bogotá, Colombia, 1977.
Prévot R., S.W Roecker, B.L. Isacks, and J.-L. Chatelain, Mapping of low P wave velocity structure in the subducting plate of the central New Hebrides, Southwest Pacific, *J. Geophys. Res.*, 96, 19825-19842, 1991.
Roecker, S.W., Velocity structure of the Pamir-Hindu Kush region: Possible evidence of subducted crust, *J. Geophys. Res.*, 87, 945-959, 1982.
Roecker, S.W., Y.H. Yeh, and Y.B. Tsai, Three-dimensional P and S wave velocity structures beneath Taiwan: Deep structure of an arc-continent collision, *J. Geophys. Res.*, 92, 10547-10570, 1987.
Winter, T., Mécanismes des Déformations Récentes dans les Andes Equatoriennes, *Thèse, Université d'Orsay*, 1990.
Whitman, D., Moho geometry beneath the eastern margin of the Andes, northwest Argentina, and its implications to the effective elastic thickness of the Andean foreland, *J. Geophys. Res.*, 99, 15277-15289,1994.

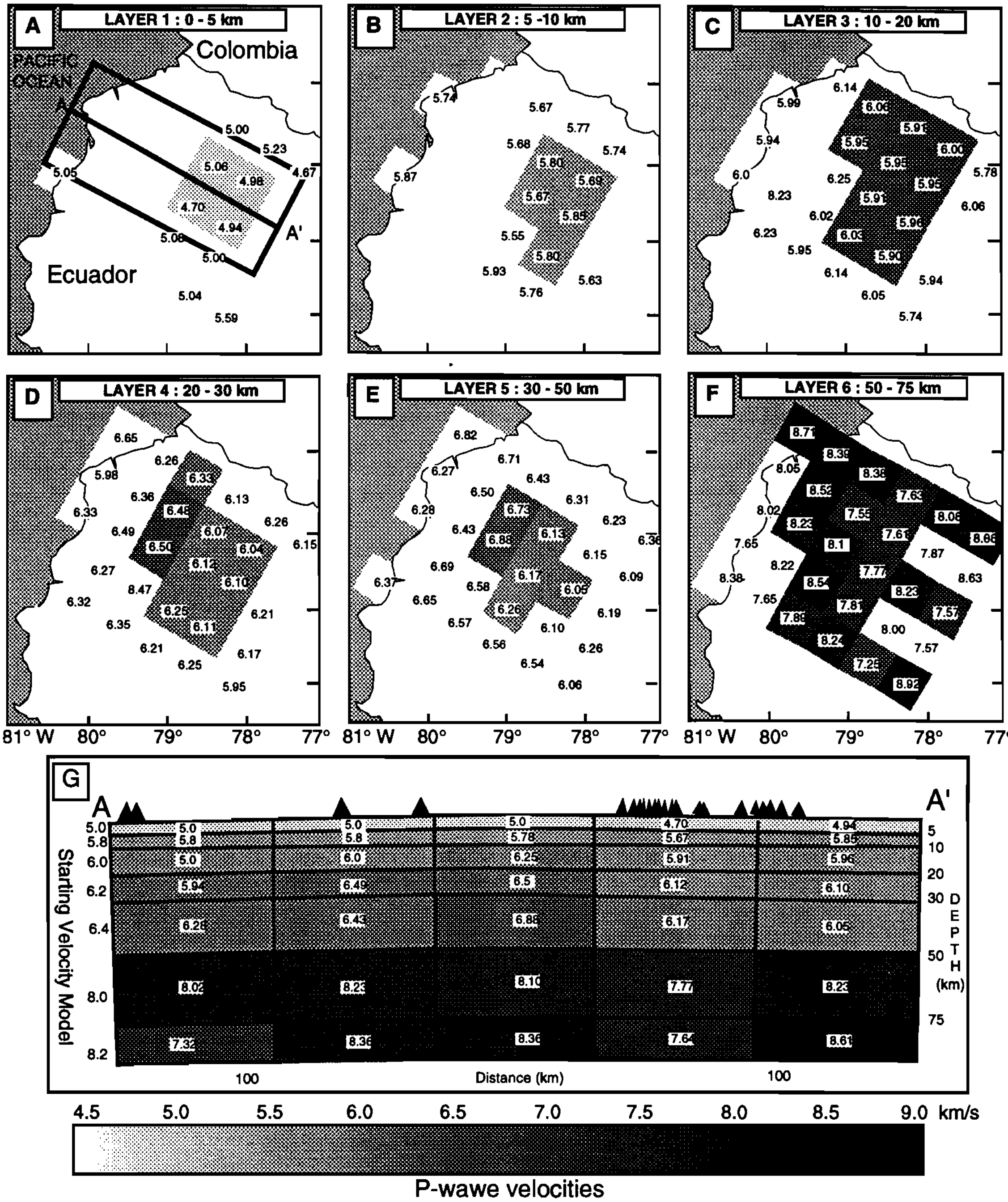


Fig. 1: (A-F) Maps of the block velocity solutions for 6 layers, down to 75 km depth. The uniform colored areas represent solutions with resolution higher than 75%. The dashed colored areas represent solutions with resolution higher than 75%. Numbers inside blocks indicate the mean velocity of each block. Blocks without colors were rejected from inversion. (G) Color codes as for figures 1a-f. Solid triangles represent the stations of the local array. A large number of these stations are located along the Andes Cordillera, therefore the packed stations at the top of the cross section is a good means to locate the Cordillera on the figure. The color velocity scale at the bottom of the figure applies for all maps and the cross section.

# INITIAL RESULTS OF COMBINED GEOSCIENTIFIC INVESTIGATIONS OFF- AND ONSHORE THE ACTIVE NORTH-CHILEAN CONTINENTAL MARGIN

CINCA study group (reporter: Christian REICHERT)

Bundesanstalt für Geowissenschaften und Rohstoffe, P.O.Box 510153, D-30631 Hannover, Germany

KEY WORDS: MC seismic reflection, DSS, Peru-Chile trench, tectonic erosion

## INTRODUCTION

In the summer 1995 a joint geoscientific project was realized incorporating the four German research institutions BGR, GFZ, FUB and GEOMAR in collaboration with Chilean and Spanish institutes: Crustal Investigation Off- and On-shore Nazca Plate/Central Andes (CINCA). Between 18° und 26° South off North-Chile 4,500 km MCS reflection recordings, 1,300 km seismic wide-angle/refraction data using Ocean Bottom Hydrophones and more than 10,000 km gravity, magnetic and bathymetric swathmapping data were collected as well as geological samples and heat flow data during the R/V SONNE cruise SO-104.

Parallel to the offshore seismic measurements onshore seismic observations were made using the signals of the marine seismic airgun array. In opposite direction explosive blasts were recorded by Ocean Bottom Hydrophones.

The aim was a comprehensive study of the geological-tectonical structure of the active North-Chilean continental margin with special focus on the trench, slope and convergence zone proper and to unravel the processes involved.

## INITIAL RESULTS

- Almost none or extremely thin sedimentary cover on top of the oceanic basement.

- The oceanic plate approaching the Peru-Chile Trench reveals strong block and normal fault structures with horst and graben features. A zone of crustal bending is recognized extending over some 50 km in front of the trench.

- Particular blocks of oceanic crust are separated with steep flanks of more than 1,000 m offset in the area of the trench and along the outer trench slope.

- Beneath the inner trench slope the seismic reflection signature of the decollement plane can be traced within certain limits.

- Relatively high seismic velocities and a sub-parallel reflection pattern below the sedimentary cover along the inner trench slope characterize large blocks of obviously continental origin sliding into the more than 7,000 m deep Peru-Chile Trench.

- A deep-seated mass of irregular reflection pattern is observed at the front of the continental wedge underlying the downfaulted and tilted continental blocks. This is interpreted as a melange of tectonically eroded and underplated continental crust and oceanic layer 2 material. Obviously it forms the frontal contact and transition between the downgoing oceanic plate and the continental wedge where the major part of tectonic erosion takes place.

- Geological sampling along ridges paralleling the inner trench slope yielded gneiss, amphibolite schists, phyllites, ignimbrites and other magmatic rocks of continental origin. Asymmetric slope basins between the ridges reach thicknesses of up to 2,000 m and are filled with Quaternary and late Tertiary sediments. At the top of one horst approaching the trench from the west pillow basalt and fine crystalline peridodite were dredged.

- Heat flow data indicate relatively high values of 40 - 60 $mW/m^2$ which probably can be explained by the generation of frictional heat due to the subduction process.

- The magnetic lineations confirm the Eocene age of the subducting oceanic crust at the trench as suggested by Cande & Haxby (1991).

REFERENCES

Cande, S.C., Haxby, W.F. 1991. Eocene Propagating Rifts in the Southwest Pacific and Their Conjugate Features on the Nazca Plate. J.Geophys.Res., 96, B12, 19,609 -19,622.

Hinz, K., von Huene, R., Ranero, C.R. and PACOMAR working group 1996. Tectonic structure of the convergent Pacific margin offshore Costa Rica from multichannel seismic reflection data. Tectonics, 15, no. 1, 54-66.

Huene, R.von, Scholl, D.W. 1991. Observations at convergent margins concerning sediment subduction, subduction erosion, and the growth of continental crust. Reviews of Geophysics, 29, 279-316.

Reutter, K.-J., Scheuber, E., Wigger, P.J. (ed.) 1994. Tectonics of the Southern Central Andes - Structure and Evolution of an Active Continental Margin. Springer-Verlag, Berlin, pp. 333, 3 maps, ISBN 3-540-55232-4.

Scheuber, E., Reutter, K.-J. 1992. Magmatic arc tectonics in the Central Andes between 21° and 25° S. In: Oliver, R.A., Vatin-Pérignon, N., Laubacher, G. (eds.). Andean Geodynamics. Tectonophysics, 205, 127-140.

ACKNOWLEDGEMENT

This project is funded by the German Federal Ministry of Education, Science, Research and Technology.

# Flow-Coupled Plate Interaction or How the Alps Helped to Make the Andes

P.G. Silver (1) R. M. Russo(2)

(1) Carnegie Inst. of Washington, DTM, Washington D.C. 20015;
(2)Lab. Tectonophysique, University of Montpellier II, Montpellier, 34060, France

Key words: Plate motion, Andes, Alps

Recent evidence suggests that some continental plates, especially those of the Atlantic Basin are coupled to and driven by general mantle circulation. Limited candidate driving forces render South America (SA) the most straightforward example of this. Large E-W compressional stresses required to form and maintain the Andes (Russo and Silver, 1996), the absence of an asthenospheric decoupling zone beneath SA as delineated by seismic anisotropy (Silver, 1996; James and Assumpcao, 1996), and tomographic evidence for the coherent translation of the SA plate and upper mantle over the last 100 my (Vandecar et al, 1996), appear to require coupling to the mantle below. We infer that, through coupling, changes in mantle circulation perturb plate velocity; but also, changes in plate motion induce changes in mantle circulation patterns. Thus, we postulate a new type of plate interaction, which we term 'flow-coupled' plate interaction. The mantle flow field, perturbed by the motion and shape of one plate, can in turn alter the motion of neighboring plates. The motions of the SA and African (Af) plates provide evidence for flow-coupled plate interaction. Relative to the Tristan hotspot, the motion of both plates changed abruptly about 30 ma (O'Connor and Duncan, 1990; O'Connor and Le Reux, 1992). Africa's eastward motion decelerated, yet SA-Af divergence velocity appeared to be roughly constant, requiring a westward acceleration of SA. A change in plate motion indicates a redistribution in the force-balance. The collision of Africa with a nearly stationary Eurasia (beginning at 38 ma), is the most plausible explanation for Africa's deceleration. The constant divergence velocity can be explained if both plates (or Atlantic opening in general) are driven by a constant mass flux entering the Atlantic basin mantle. The constant mass flux, combined with Africa's deceleration then produces SA's simultaneous acceleration. This flow-coupled plate interaction not only links plate velocities but also establishes a causal connection between the deformation of these two plates, in this case between the Alpine and Andean orogenies. We have argued previously that Andean deformation is due to SA's westward motion and resistance to that motion by the Nazca slab and subslab mantle. An increase in SA's westward velocity should result in increased Andean compressional deformation. The most important change in SA velocity relative to the deep mantle was during the breakup of Gondwanaland, leading to Andean formation shortly thereafter. The increase in westward velocity at 30 my is synchronous with the Quechua phase of Andean orogeny, which gave rise to the Andean Altiplano and the Bolivian orocline. Thus, through a flow-coupled plate interaction, the Quechua phase of Andean deformation may be ultimately caused by the collision that produced the Alps.

James, D. E. Assumpcao, M. 1995. Tectonic implications of S-wave anisotropy beneath SE Brazil. *Geophys. J. Int*, in press.

O'Connor, J. , Duncan, R. A. , 1990. Evolution of the Walvis ridge-Rio Grade Rise hot spot system: implications for African and South American plate motions over plumes, *J. Geophys. Res*, 95, 17,475-17,502

O'Connor-John-M; le-Roex-Anton-P, 1992, South Atlantic hot spot-plume systems; 1, Distribution of volcanism in time and space, *Earth Planet. Sci. Lett.* 113; 343-364.

Russo, R., Silver, P.G. 1994. Trench-Parallel flow beneath the Nazca Plate from seismic anisotropy. *Science*, 263, 1105-11

Russo, R., Silver, P. G. 1996. Cordillera formation, mantle dynamics and the Wilson Cycle. *Geology*, in press.

Silver, P. G, 1996. Seismic anisotropy beneath the continents: Probing the depths of geology. *Annu. Rev. Earth Planet. Sci.*, 24, 385-432.

Vandecar, J. C., James, D. E., Assumpcao, M. 1995. Seismic evidence of a fossil plume beneath South America: Implications for plate driving forces, *Nature*, 378, 25-31

# HEAT-FLOW DENSITY PATTERN AND IMPLICATIONS FOR THE THERMAL STRUCTURE OF THE CENTRAL ANDEAN CRUST

Michael SPRINGER

GeoForschungsZentrum Potsdam, Telegrafenberg A6, 14473 Potsdam, Germany
springer@gfz-potsdam.de

**KEY WORDS:** Central Andes, heat-flow density, thermal modelling

## INTRODUCTION

The thermal structure of subduction zones is not well defined. In order to understand the tectonic and magmatic processes related to active subduction it is necessary to investigate to what extent different models apply to scenarios constrained by surface geophysical data. For this purpose, the geothermal field and heat-transfer conditions were investigated in the area of the Central Andes between 60-75°W and 15-30°S .

The study was focused on the addition and compilation of new geothermal data for the Bolivian part of the area and for northern Chile to contribute to the heat-flow density pattern. In a second step, different scenarios of thermal conductivity distribution, radiogenic heat production, frictional heat generation, the occurance of heat sources, and the variation of subduction velocity were modelled to investigate the impact of parameter changes on the surface heat-flow density.

## HEAT-FLOW DENSITY

Temperature measurements in northern Chile and a large Bottom-Hole Temperature (BHT) data set for the Bolivian foreland (Chaco) were implemented in heat-flow determinations that were added to the heat-flow database available for the Central Andes (Henry and Pollack, 1988, Pollack et al., 1991). Temperature profiles at 5 localities were measured in the Chilean mining districts located in the forearc region and the magmatic arc. The large BHT data set, available from the Bolivian oil company (YPFB), contains about 1500 values. The BHTs were corrected to undisturbed formation temperatures by a generalized Horner-type method. Heat-flow density was determined on the basis of composite BHT-depth plots for different Bolivian oil fields using thermal-conductivity data from Henry (1981). Estimates of heat-flow density on the basis of thermal logs were made using thermal-conductivity data measured on rock samples collected from nearby outcorps. A total of 68 thermal-conductivity determinations were made under laboratory conditions. Thermal conductivity of sedimentary rocks was corrected according to logged or bottom hole temperatures respectively and porosity-depth relationships (Coudert et al., 1995). On the hole 29 heat-flow density values were determined or revised (Henry and Pollack, 1988). On the basis of these data the Central Andean subduction zone shows the following heat-flow density pattern (Fig. 1): (1) low values within the oceanic Nazca plate with minimum values of about 10 $mW/m^2$ in the region of the Peru-Chile trench, which can be related to the subduction of the cold oceanic lithosphere plate; (2) a gentle increase of values in the forearc region (20—60 $mW/m^2$); (3) a sharp increase of heat-flow density to about 120 $mW/m^2$ in the area of the magmatic arc which indicates the occurence of heat sources in the upper crust; (4) high values in the backarc region (80 $mW/m^2$), and (5) a decrease of heat-flow density to about 40 $mW/m^2$ in the Andean foreland.

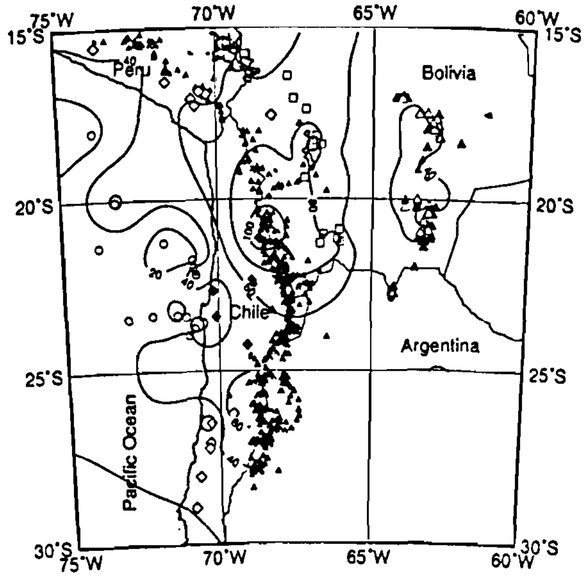


Figure 1: Map of the Central Andes showing localities of geothermal data and magmatic arc (shaded triangles). White symbols: heat-flow density determinations prior to this study, black symbols: new heat-flow density data. Heat-flow pattern with 20 $mW/m^2$ contour intervals.

## NUMERICAL MODELLING

Heat-flow density projected to a 2D W-E cross section is used to constrain different scenarios of thermal modelling at a geotraverse covering an area from the trench in the west to the Altiplano area in the east. A simplified model including the subducting Nazca plate and the overriding South American plate was taken from Schmitz (1994). The thermal structure of the geotraverse is calculated using a finite element (FE) code. The models consider different radiogenic heat production distributions ($A(z) = const., A(z) = A_0 e^{-z/10}$), temperature dependent thermal conductivities ($\lambda(T) = const., \lambda(T) = \frac{\lambda_0}{1+cT}$), different amounts of frictional heat generation ($\sigma$V), a subduction velocity of 10 cm/a and heat sources (Fig. 2).
The models show that the temperatures at the plate contact and within the overriding plate are influenced mainly by the subduction of cold material and the amount of frictional heating considered. Generally, temperatures in the forearc region are very low. Melting temperatures in the area of the magmatic arc can only be accomodated by high frictional heat generation rates ($\sigma \approx$90 MPa). In the situation of moderate frictional heat generation ($\sigma$ up to 40 MPa), temperatures in the lower crust and mantle are not sufficient to produce melting (Fig. 2). To reach higher temperatures in the subsurface of the magmatic arc a flow within the mantle wedge has to be considered. Therefore the effect of the asthenospheric mantle wedge was modelled as a temperature boundary condition and the extent of the asthenospheric mantle wedge into the forearc region was investigated.

## RESULTS

All modells do not show significant differences with regard to calculated surface heat-flow density in comparison to measured one. Modelled heat flow is within the scatter of measured heat-flow density. Consequently, the boundary of the asthenospheric wedge can not be inferred from surface heat flow.
Variation of radiogenic heat production in the overriding plate affects the surface heat flow considerably but has only a small impact on the lithospheric thermal structure.
Frictional heating and the extent of the asthenospheric mantle wedge into the forearc region have

a large impact on the temperatures in the subducting and overlying crust, but contribute only to a small extent to the surface heat flow.

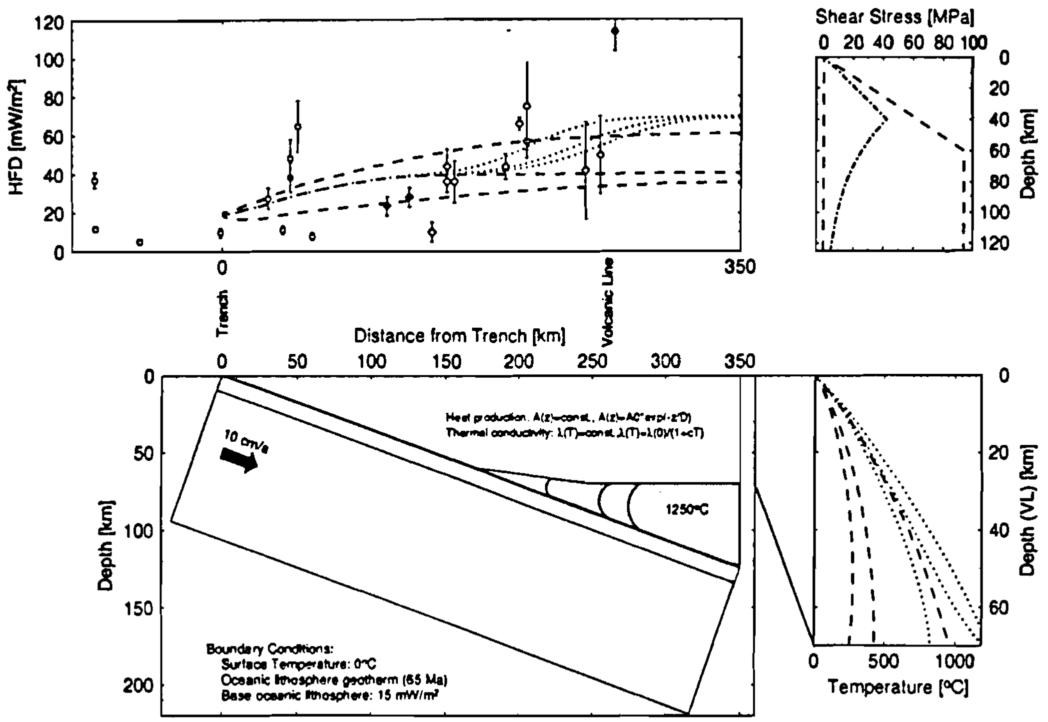


Figure 2: Simplified geometry and boundary conditions for thermal modelling of the Central Andean subduction zone. Assumed shear stress along the plate contact for frictional heat generation rates. Modelled surface heat-flow density along the cross section and subsurface temperatures at the magmatic arc. Results are for different frictional heat generation rates (- - -) and for different extent of the asthenospheric mantle wedge into the forearc region (· · ·).

## ACKNOWLEDGEMENTS

This work was funded by the Collaborative Research Center SFB267, Deformation Processes in the Andes, which is an institution of the German science foundation (DFG).

## REFERENCES

Coudert, L., Frappa, M., Viguier, C., Arias, R. 1995. Tectonic subsidence and crustal flexure in the Neogene Chaco basin of Bolivia. Tectonophysics, 243, 277-292.

Henry, S.G. 1981. Terrestrial heat flow overlying the Andean subduction zone. Ph. D. thesis, Univ. of Michigan.

Henry, S.G. and Pollack, H.N. 1988. Terrestrial Heat Flow Above the Andean Subduction Zone in Bolivia and Peru. Journal of Geophysical Research, 93(B12), 15153-15162.

Pollack, H.N., Hurter, S. and Johnson, J.R. 1991. The new global heat flow compilation. Univ. of Michigan, Ann. Arbor, data file.

Schmitz, M. 1994. A balanced model of the southern Central Andes. Tectonics, 13(2), 484-492.

# THERMOMECHANIC SEGMENTATION OF THE ANDES (15°-50°S): A FLEXURAL ANALYSIS APPROACH.

Andrés TASSARA & Gonzalo YAÑEZ#.

Both at SERNAGEOMIN, Avda. Santa María 0104, Providencia, Santiago, Chile.
sernageo@huelen.reuna.cl.
# Present Address: GEODATOS, Roman Diaz 773, Providencia, Santiago, Chile

**KEY WORDS**: Andean Segmentation, Elastic Thickness, Yield Strength Envelope, Thermomechanic State.

## INTRODUCTION

The Andes is the classical example of an active non-collisional orogen. Its most prominent characteristic is the along-strike segmentation in its tectonic regime [e.g. Jordan *et al.*, 1983; Cahill & Isacks, 1992], that resembles the long-term segments of the Andean geological evolution (Middle Mesozoic to present) [Mpodozis & Ramos, 1990]. The continental topography and Bouguer anomaly (long-term Moho morphology) are related one each other by the elastic thickness *Te*, a flexural parameter that conditions the degree of compensation of the orogen, allowing an indirect characterization of its segmentation. This study have evaluated the spatial *Te* variations of The Andes between 15° and 50°S latitude applying a flexural analysis to the continental margin. Then, the observed along-strike *Te* systematics are interpreted in terms of the compositional and thermomechanic state of the lithosphere. The link between this state and the tectonic segmentation of the margin, allow us to infer some controlling factors in the construction and evolution of The Andes.

## FLEXURAL ANALYSIS METHODOLOGY AND ELASTIC THICKNESS INTERPRETATION

The flexural analysis assumes the lithosphere is a 2D elastic plate, downward deflected by topographic loads [e.g. Turcotte & Shubert, 1982]. The degree of deflection is controlled by the elastic thickness *Te*: minimum (no compesation) for infinite *Te*, and maximum (Airy compensation) for zero *Te*. The Bouguer anomaly is used as a signal of the lithospheric deflection, reproduced through a forward modelling of the elastic lithospheric thickness, assuming topographic loads. Analyssing 15 topo-gravimetric sections, homogeneously distributed on the continental margin (see Figure 1), we obtained a 3D characterization of *Te* and the associated crustal thickness between 15° to 50°S latitude (Figure 1).

These results were semi-quantitatively studied using the Yield Strength Envelope (*YSE*) concept [e.g. Burov & Diament, 1995]. The *YSE* gives, at a particular depth z, the maximum stress absorbed elastically by a compositionally given lithosphere (quartzitic or non-quartzitic crust with an olivinic mantle) before the elastic yield stress, for a given crustal thickness, heat flow and strain rate. The underlined parameters are the free ones that define the thermomechanic lithospheric state. When a stress gradient is applied to this lithosphere by loading, the depth range where this stress is lower than the yield stress will define the elastic thickness *Te*. According to this brittle-elasto-ductile rheology, *Te* is proportional to the strain rate, and inversely proportional to the crustal thickness, quartzitic content of the crust and heat flow. With this relation it is possible to evaluate the thermomechanic state of the margin from the flexural analysis observations. The along-strike variations of this state is finally linked with the tectonic segmentation of The Andes.

## THE ANDES: FLEXURAL ANALYSIS AND TECTONIC SEGMENTATION

Between 15° and 50°S, The Andes can be divided in two main segments, subdivided in five sub-segments. Following the Figure 2, the 34°S is the border line between the Central Andes to the north and the Austral Andes to the south. The former is characterized by elevations over 4000 m (maximum of 6500 m) with a width of 400 km at the Northern Segment (15°-23°S) that narrows southward to ~150 km at the Central Segment (28°-34°S). This topography shows very good correlation with a Bouguer anomaly lower than -350 mGal (minimum of -450 mGal), that is an expression of a 55-60 km crustal thickness (maximum of ~70 km, see Figure 1). Consequently, the predicted *Te* shows values lower than 10 km at the main axis of the orogen. The main tectonic features of the Central Andes are (Figure 3): a) along-strike changes in the deep angle of subduction from ~30° at the Northern Segment to subhorizontal at the Central Segment [e.g. Cahill & Isacks, 1992], b) 200 km wide, acidic high-potassium calcalkaline to shoshonitic volcanic arc (Central Volcanic Zone, CVZ) from 13° to 28°S, c) volcanic gap from 28° to 34°S, and d) along-strike variations in the foreland deformation styles, from the Subandean foldthrust belt (Northern Segment), through the basement involved Santa Barbara thrust belt (Northern Transitional Segment, 24°-28°S), to the coupled Frontal Cordillera, thin-skinned Precordillera and thick-skinned Sierras Pampeanas system (Central Segment) [e.g. Jordan *et al.*, 1983].

The Austral Andes elevation decrease along the Southern Transitional Segment (34°-38°S) from 3000 m to 1500 m over a ~250 km wide range. At the Southern Segment (39°-50°S) the range shows a constant elevation of 1500 m with a wider wavelength (~500 km). The Bouguer anomaly lose correlation with the topography and gradually decrease the amplitude of its minimum from -200 mGal to -100 mGal, reflecting a southward crustal thinning from 45 km to 35 km. *Te* increases from 20 km to 40 km at 38°-39 °S, value that is kept constant towards the south. The tectonic elements of the Austral Andes are: a) constant ~30° deep slab angle, b) volcanic arc (Southern Volcanic Zone, SVZ) with a progressively less crustal geochemical signature [e.g. Hildreth & Moobarth, 1988] toward the characteristic intermediate to basic calcalkaline to tholeitic Southern Segment volcanism, spaltial and genetically linked with c) the Liquiñe-Ofqui Fault Zone (LOFZ), a dextral strike-slip lithospheric structure [e.g.Hervé, 1994].

## LONGITUDINAL VARIATIONS ON THE THERMOMECHANIC STATE OF THE ANDES

Following the previous section, the two main segments of The Andes represent two different lithospheres. The high elevation, thick crust and low elastic thickness of the Central Andes, contrasts with the lower elevation, thinner crust and higher elastic thickness of the Austral Andes. From the *YSE*, this is mainly associated with a first order compositional difference, regardless of any particular along-strike variation on heat flow and strain rate. Accordingly, the very low *Te* values of the Central Andes reflects a very weak, quartz-rich crust. On the other hand, the comparatively rigid Southern Segment lithosphere, reflects a non-quartzitic, feldspar-rich crust. The Southern Transitional Segment probably represents some compositional mixture between both end members. This main configuration is in agreement with the complex pre-Andean (mostly pre-Mesozoic) collisional history of the margin.

Given the along-strike compositional structure of The Andes, the *Te* systematic of each segment should reflect the variations of the heat flow and strain rate along the margin. The assumed quartz-rich and thick crust of the Central Andes are necessary, but not sufficient conditions, to reproduce its low *Te*. In addition, there must be a favorable combination of high heat flow and/or low strain rate. Heat flow measurements on the Northern Segment [Henry & Pollack, 1988] indicates anomalously high values (~100 $mW/m^2$), probably associated with a very active asthenospheric wedge almost in contact with a partially molten crust. This high heat flow by itself can reproduce the *Te* range, keeping a fixed strain rate (mean geological number of $10^{-15}$ $s^{-1}$ in our *YSE* computations). The near zero *Te* observed over the Northern Transitional Segment can be explained by an unreported higher heat flow, probably produced by the proposed 4-2 Ma lithospheric delamination [e.g. Kay & Kay, 1993]. However, the deformational difference between both segments could reflect a lower strain rate, that in part may explain the lower *Te*. This argument can be applied to the Central Segment, where the subhorizontal subduction preclude the high heat flow shown by the segments where an active asthenospheric wedge is present. If this is true, to reproduce the low *Te* of the Central Segment, it is necessary to assume a lower strain rate than the adopted to the Northern Segment. The particular deformation style of the Central Segment could be intrinsically linked with this probably lower strain rate. In fact, Jordan & Allmendinger [1986] report a

$\sim 10^{-17}$ $s^{-1}$ average deformation rate (=strain rate?) for the last 10 My Sierras Pampeanas uplift, a lower limit in geological strain rates. Alternatively, the low *Te* -- low heat flow combination of the Central Segment could represent a weaker crustal composition than the previously assumed, compositional difference that is only partially supported by others independents observations.

On the other hand, the observed *Te* southward increment along the Southern Transitional Segment, to the characteristic 40-50 km of the Southern Segment, is the effect of the observed crustal thinning coupled with a probably southward decrease in the quartzitic crustal component and in the heat flow (lesser crustal participation in the SVZ magmagenesis). The high *Te* shown by the Southern Segment, expression of a hard composition and thin crust, reflects a non-vertically decoupling crust-mantle lithosphere, that keeps an elastic behavior over its entire thickness. This behavior probably is perturbed at the LOFZ axis, where there is localized a high heat magmatic advection and dextral simple shear deformation, that does not have an expression on the long wavelength flexural analysis.

## CONCLUSIONS.

The first order compositional configuration of the continental margin is the dominant factor not only in its present thermomechanic state, derived from its Late Cenozoic evolution, but probably through all of its Meso-Cenozoic history [Yáñez, 1995]. In this context, the present tectonic segmentation of The Andes, is the geodynamic reply of the convergence system to the thermomechanic evolution of an anisotropically configured continental lithosphere.

## AKNOWNLEDGEMENTS.

This project was supported by FONDECYT grant NO 1930164, and is a contribution of IGCP No 345, "Andean Lithospheric Evolution".

## REFERENCES.

Burov E.B. & Diament M. 1995. The Effective Elastic Thickness (*Te*) of Continental Lithosphere: What Does it really Mean? *Jour. Geophys. Res.*, V100, NO B3, 3905-3927.

Cahill T. & Isacks B. 1992. Seismicity and Shape of the Subducted Nazca Plate. *Jour. Geophys. Res.*, V97, NO B12, 17503-17529.

Henry S.G. & Pollack H.N. 1988. Terrestial Heat Flow above the Andean Subduction Zone in Bolivia and Perú. *Jour. Geophys. Res.*, V93, NO B12, 15153-15162.

Hervé F. 1994. The Southern Andes between 39° and 44°S Latitud: Geological Signature of a Transpressive Tectonic Regime related to a Magmatic Arc. *Tectonics of the Southern Central Andes: Structure and Evolution of an Active Continental Margin*, R. Omarini & H-J. Götze Eds., Springer-Verlag, 243-248.

Hildreth W. & Moorbath S. 1988. Crustal Contributions to Arc Magmatism In The Andes of Central Chile. *Contrib. Mineral. Petrol.*, 98, 455-489.

Jordan T. & Allmendinger R. 1986. The Sierras Pampeanas of Argentina: A Modern Analogue of Rocky Mountain Foreland Deformation. *American Journal of Science*, V286, 737-764.

Jordan T., Isacks B., Allmendinger R., Brewer R., Ramos V. & Ando C. 1983. Andean Tectonics related to Geometry of Subducted Nazca Plate. *Gelogical Study of America Bulletin*, V94, 341-361.

Kay R. & Kay S. 1993. Delamination and Delamination Magmatism. *Tectonophysics*, V219, 677-720.

Mpodozis C. & Ramos V. 1990. The Andes of Chile and Argentina. *Geology of the Andes and its relation to Hidrocarbon and Mineral Resources*, G. Ericksen, M. Cañas-Pinochet & J. Reinemund Eds., Circum-Pacific Council for Energy and Mineral Resources Earth Sciences Series, V11, 59-90.

Turcotte D. & Shubert G. 1982. *Geodynamics: Applications of Continuum Physics to Geological Problems*.Jonh Wiley & Sons Eds.

Yáñez G. 1995. Some Aspects of the Long Term Lithospheric Evolution: Remanent Magnetization of the Ocean Basins and Deformation at Convergent Margins. *Ph. D. Thesis*, Graduate School of Art and Science, Columbia University.

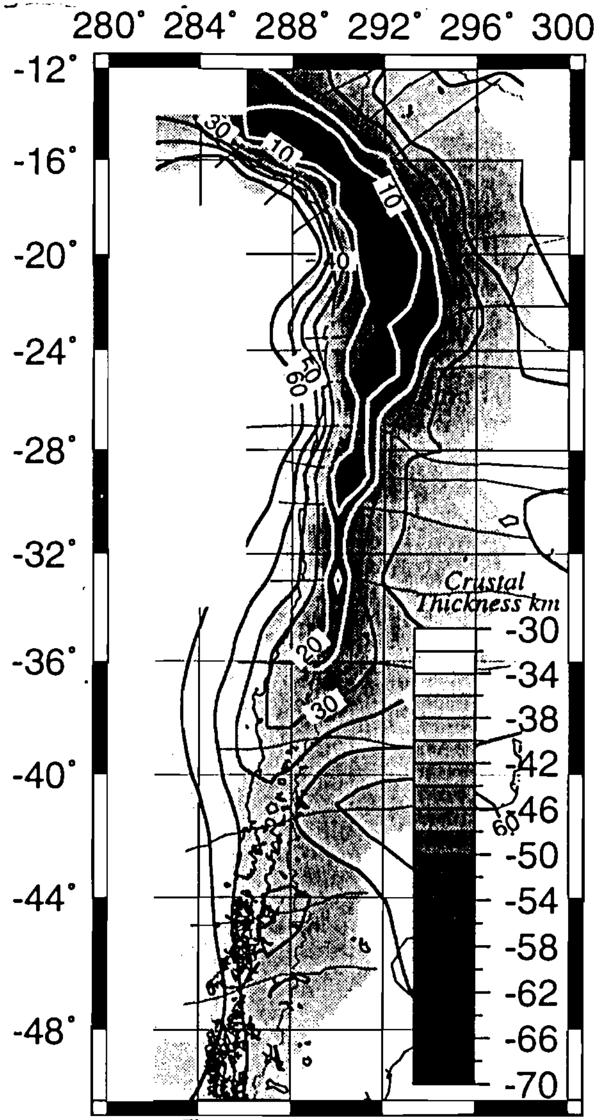


Figure 1. Elastic Thickness (contour) and Crustal Thickness (shade-grey)

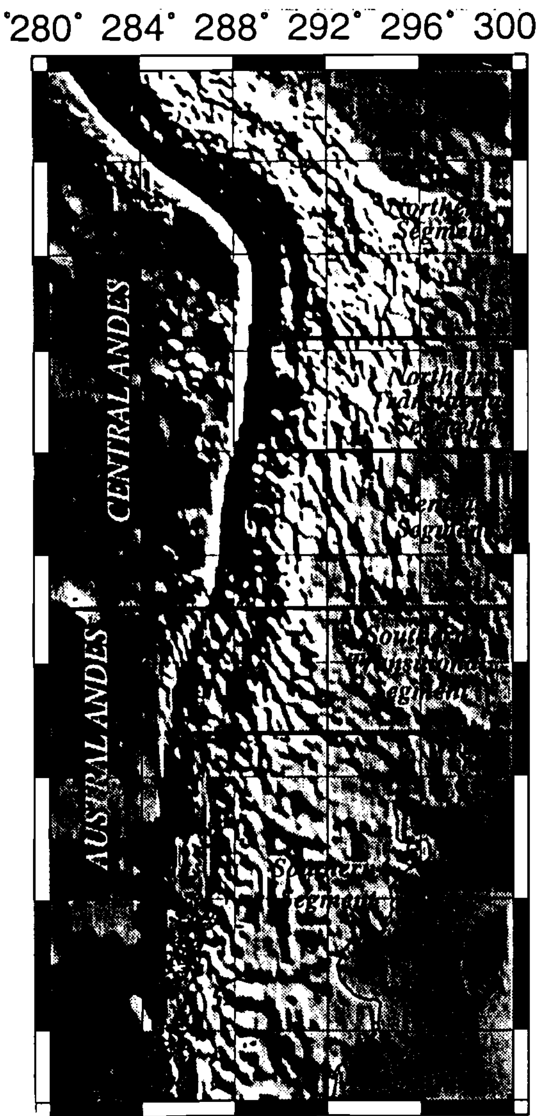


Figure 2. Andean Segmentation on First-Order Topography.

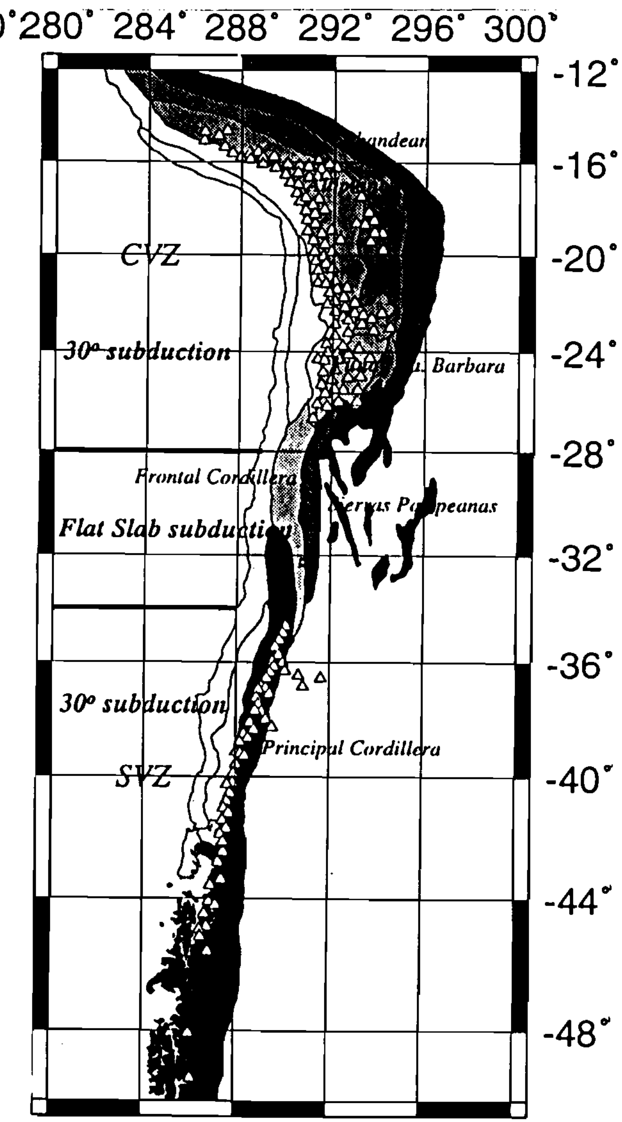


Figure 3. Morphotectonic Units of The Andes

# COMPARISON OF THICK CRUST IN THE ANDES AND TIBET STUDIED BY PASSIVE BROADBAND SEISMIC DEPLOYMENTS

George Zandt[1], Susan L. Beck[1], and Thomas J. Owens[2]

[1]SASO and Dept. of Geosciences, University of Arizona, Tucson, U.S.A.
[2]Department of Geological Sciences, University of South Carolina, Columbia, U.S. A.

**KEY WORDS:** Andes, Altiplano, Tibet, Seismology, Crust

## INTRODUCTION

The great thickness of the high plateau crust of the central Andes and Tibet has been established for more than two decades, but the bulk composition and thickening processes are still actively debated. Two recent deployments of PASSCAL broadband seismic stations in the central Andes of Bolivia (1994-1995) and along a north-south traverse across the central Tibetan plateau (1991-1992) provide excellent pure-path crustal sampling of these highlands.

In the Andes, intermediate-depth earthquakes in the subducting Nazca Plate generate near-regional seismic waves that interact with the overlying Andean crust. Large amplitude, S-to-P converted, post-critical Moho reflections (SPmP) are modeled for average crustal properties of the Altiplano crust. Deep earthquakes and teleseisms are sources for a receiver function study of crustal variations across the entire Andean orogen.

For Tibet, our study was motivated, in part, by the observation of an impulsive, high signal-to-noise ratio S-wave of a 450-km-deep teleseismic earthquake recorded by the 1991-92 Tibet PASSCAL experiment (Owens et al., 1993). Especially energetic S-to-P converted phases and associated multiples (Zandt and Randall, 1985) from the Tibetan crust-mantle boundary are clearly visible prior to and following the S-wave arrival. These shear-coupled P-waves can be analysed to estimate bulk crustal properties beneath each seismic station.

## OBSERVATIONS

The Andean Altiplano crust is characterized by relatively uniform bulk properties: an anomalously low mean velocity of 6.0 km/s, a Poisson's ratio (PR) of 0.25, and a thickness of 65 km. The crust thickens under both the western and eastern Cordillera and thins abruptly beneath the sub-Andean zone and Chaco Plain. The combination of the low mean P–velocity and relatively low PR of the Altiplano crust can be best explained by a predominantly silicic bulk composition. The velocity structure is consistent with tectonic models of thickening due to compressional shortening concentrated within a weak felsic layer. Some of the details of this work are described in a companion abstract by Beck et al. (1996).

In Tibet, we observed a P-wave arrival ~10 s before the S-wave that is the conversion from the Moho, Sp. A large up-swing ~12 s after the S-wave is a P-wave reflection after conversion at the free-surface, SsPmp. Comparing the displacement S-waveforms across the N-S network of PASSCAL stations (FIG. 1) reveals some striking similarities and consistent variations. All sites have an Sp arrival ~10s prior to S, although the Sp pulse is double-peaked at the southern stations (LHSA, XIGA, GANZ, SANG) and a simple pulse at the northern stations (AMDO, WNDO, USHU, BUDO, ERDO). From N to S there is a systematic moveout of the SsPmp phase from ~10 s at the northernmost stations (BUDO, ERDO) to ~15 s at the southernmost stations (LHSA, XIGA).

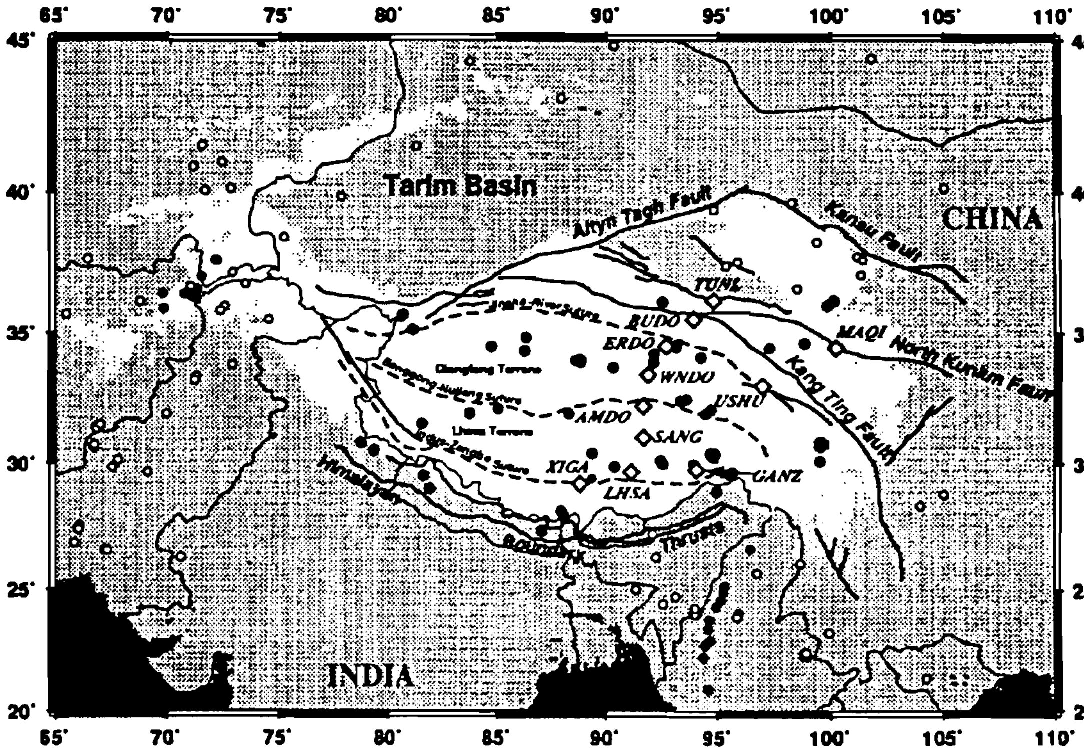


The relative timing of these phases with respect to the S-wave are dependent on three crustal properties: mean crustal P-velocity, Vp; mean crustal S-velocity, Vs; and crustal thickness, H. The consistent changes observed are direct evidence of a systematic N-S variation in crustal properties across Tibet. By measuring the differential traveltimes (SsPmp - S) and (S - Sp), we constructed a suite of H–Vp and PR–Vp tradeoff curves at all the stations (FIG. 2). We calculated both the H–Vp and PR–Vp tradeoff curves for all the PASSCAL stations. These curves represent the range of crustal thickness consistent with the (SsPmp - S) times and the range of crustal PR consistent with the (S - Sp) times. Two end-member models are possible. In one, the crustal thickness is constant, say at 70 km with a constant PR of 0.27, and the mean crustal Vp ranges from 6.0 km/s in the south (LHSA) to 6.8 km/s in the north (BUDO). In the other end-member, the crustal Vp is constant, say at 6.3 km/s, then the crustal thickness must vary from 78 km in the south to 52 km in the north, and PR varies from 0.22 in the south to 0.35 in the north. To choose between the end-member models, or any in between, other data or constraints are required.

In our final model, crustal thickness decreases and PR increases from south to north across the Tibetan plateau. In southern Tibet, the crust is 70-75 km thick, with low-to-normal PR, and a high-velocity lower crustal layer. In the middle latitudes, the crust is ~70 km thick with a higher PR of ~0.27-0.28, and the lower crustal layer terminates near the latitude of the Bangong suture. Further north, the crust thins to < 55 km and is characterised by unusually high PR > 0.3. More detailed studies in this region by the French Lithoprobe team indicates the thinning occurs abruptly near the Jinsha suture (Herquel et al., 1995). The relatively thin, high PR crust overlaps the northern half of the zone of Sn blockage and low Pn velocity in northern Tibet indicative of high mantle temperatures (McNamara et al., 1995).

## CONCLUSIONS

Comparison of the crustal structures estimated from PASSCAL experiments across the Andean and Tibetan orogens reveals some similarities but also some significant differences. The narrower Andean orogen is characterized by relatively uniform bulk properties that are consistent with formation by compressional shortening of a weak lithosphere between two stronger lithospheres. The highlands appear to be in isostatic balance at the Moho. The Tibetan crust exhibits a systematic N-S variation in crustal thickness and PR not reflected in its relatively uniform elevation. The high PR of northern Tibet is probably due to pervasive partial melting of the crust that reduces the S–wave velocity more than the P–wave velocity. Isostatic forces in the upper mantle or nonisostatic forces must be acting to maintain the uniform elevation of the plateau.

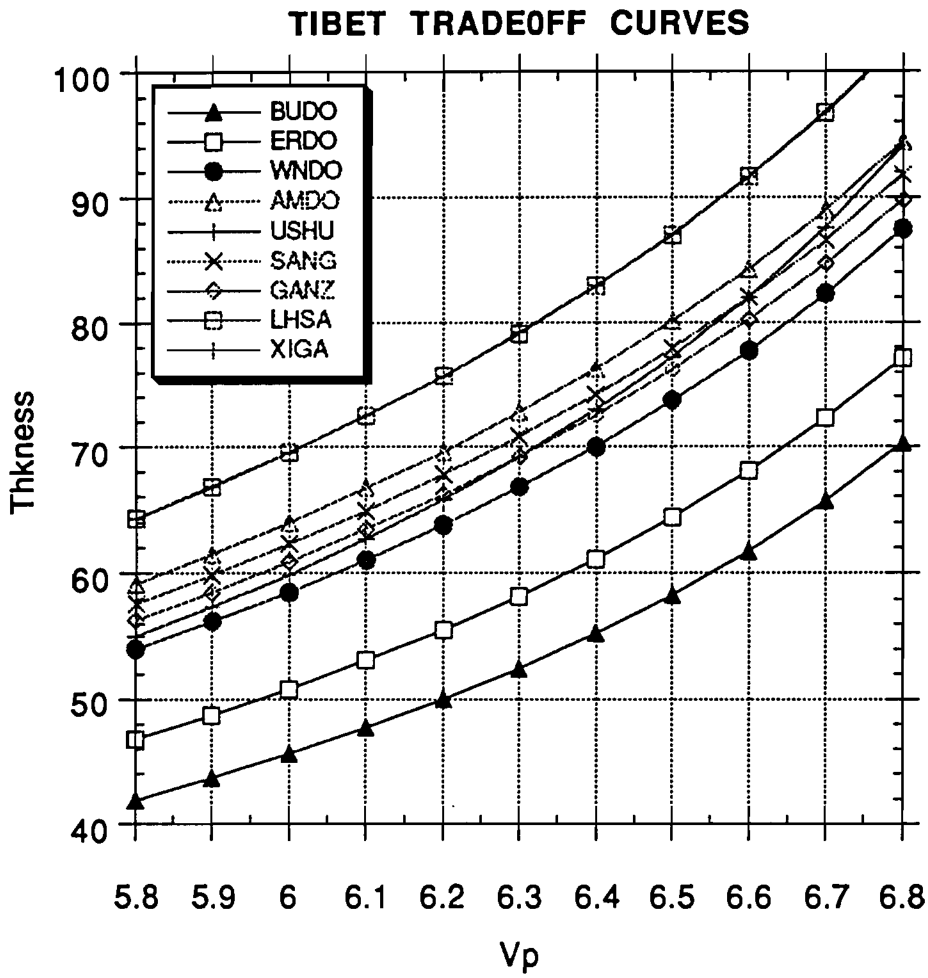


## REFERENCES

Beck, S. , G. Zandt, S. Myers, T. Wallace, P. Silver, L Drake, E. Minaya, 1996, Anomalous crust in the central Andes, *Third International Symposium on Andean Geodynamics*, St Malo, France (abstract).

Herquel G., G. Wittlinger, J. Guilbert, 1995, Anisotropy and crustal thickness of Northern-Tibet, new constraints for tectonic modelling, *Geophys. Res. Lett.*, *22*, 1925-1928.

McNamara D., T. J. Owens, W. W. Walter, 1995, Observations of regional phase propagation across the Tibetan plateau, *J. Geophys. Res.*, *100*, 22,212-22,229.

Owens T. J., G. E. Randall, F. T. Wu, R. S. Zeng, PASSCAL instrument performance during the Tibetan Plateau passive seismic experiment, 1993, *Bull. Seism. Soc. Am.*, *83*, 1959-1970.

Zandt G., and G. E. Randall, 1985, Observations of shear-coupled P waves, *Geophys. Res. Lett.*, *12*, 565-568.

# SISMOTECTONIQUE / NEOTECTONIQUE / RISQUES VOLCANIQUES
# SEISMOTECTONICS / NEOTECTONICS / VOLCANIC HAZARDS
# SEISMOTECTONICA / NEOTECTONICA / RIESGOS VOLCANICOS

# THE PISAYAMBO, ECUADOR, SEISMICITY NEST : TOWARDS THE BIRTH OF A VOLCANO ?

Jorge AGUILAR(1), Jean Luc CHATELAIN(1,2), Bertrand GUILLIER(1,2), Hugo YEPES(1)

1 Instituto Geofisico, Escuela Politécnica Nacional, Apartado 17 01 2759, Quito, Ecuador.
2ORSTOM, Apartado 17 11 6596, Quito, Ecuador.

KEY WORDS : seismicity nest, Poisson process, b-value, birth of a volcano, Ecuador

## INTRODUCTION

The center of the Pisayambo seismicity nest is located at about 1.1°S 78.3°E. This nest is very active : about 40 % of the activity detected by the permanent Ecuadorian network comes from this nest at the 3.1 magnitude detection level of the network. This nest produces very few events big enough to be detected by the worldwide network (45 events with magnitude ≥ 4.2 from 1963 to 1991). The only other nest of activity observed in Ecuador is located about 75 km to the SE, known as the Puyo nest, shows opposite characteristics, i.e. it is only constituted of magnitude > 4.2 events (126 events from 1963 to 1991) located by the worldwide network, while the permanent local network does not detect small magnitude events. It also shows a much more sporadic activity.

The very steady and important small magnitude events activity of the Pisayambo nest is concentrated in a small 20 by 20 km. zone, located in-between and a little bit East of the Tungurahua and Cotopaxi volcanoes (Figure 1). Above the nest is located a hydroelectric dam with a reservoir of about 0.1 $km^3$, as well as several smaller lagoons. Very little geological information of the zone is available. Only Yepes et al. [1979] and Bonilla et al. [1992] describe a network of SW-NE trending faults above the nest.

## DATA

Data used for this study come from two sources : the earthquakes recorded by the Ecuadorian permanent network from 1989 to 1995, and data obtained with the Lithoscope experiment from December 1994 to May 1995. A station of the Lithoscope experiment was installed above the nest. A station of the permanent network is working above the nest only since July 1995. The permanent network has been extended from 7 stations in 1988 up to 33 stations in 1995

The earthquakes were localized using the HYPOINVERSE [Klein, 1978] and HYPOCENTER programs, with a one dimension flat layered velocity model taken from the results of the inversion by Prévot et al. [1996], a Vp/Vs ratio of 1.737 obtained with a (S-S) versus (P-P) diagram [Chatelain, 1978]. From the initial set of 2297 events, a final set of 737 events were selected with the following criteria : a root mean square residual (RMS) less than 1.0 sec and a condition number less than 1.0. Out of these 737 events, 51 are recorded in 15 stations or more.

The earthquakes were then used (1) to show their spatial distribution, (2) to evaluate the Gutemberg Richter b-value, and (3) to test the dependency in time of the occurrence of the events in order to find an explanation to the presence of the only nest of persistent seismic activity in Ecuador.

## SPATIAL DISTRIBUTION OF THE EARTHQUAKES

The distribution in map view of the best located events shows that the activity of the nest is confined to a small 20 by 20 km zone where 50 % of the events occur, located East of the line defined by the Tungurahua and Cotopaxi volcanoes and in-between them, centered on 1.1°S - 77.3° E (Figure 1).

In depth the nest is clearly composed of two clusters ; the first between 0 and 10 km , the second between 17 and 20 km. (Figure 2). Both clusters appear in both data sets obtained with the two programs used for the location, and appear also clearly on the Lithoscope data set for witch a station was located above the nest. We therefore assume that this gap is real and not an artifact of the localization process.

The Pisayambo nest is a 20x20x20 km column divided in depth in two clusters separated by about 7 km

## GUTEMBERG-RICHTER b-VALUE

While for all Ecuador b-value is 1.13, estimation of this parameter for the nest taken as a whole leads to a 1.71 value. This value becomes 1.51 for the shallowest cluster, and 1.86 for the deepest cluster when considered separately. These values are quite high, and quite different between the two clusters. B-value of the shallowest cluster is in the rank of observation of values linked to highly fractured zones [e.g. Scholz, 1968], while b-value of the deepest cluster is in the rank of values observed for volcanic related events [e.g. Talandier and Okal, 1984].

## APPLICATION OF THE POISSON PROCESS

The temporal distribution of the earthquakes in a 10 km radius circle centered on 1.1°S - 78.3 ° W does not fit a simple Poisson process, i.e. the events are time dependent. The events in the upper cluster fit a generalized process when taken by groups in 13 hours windows (Figure 3) and the lower cluster events when taken by groups in 25 hours windows (Figure 4), with a confidence level of 90%. Therefore the events are time dependent within 13 or 25 hours in groups which are time independent. The E parameter is found to be 2.1 and 2.5 for the upper and deeper clusters respectively. Values of $E \geq 2.5$ have been associated to tectonics events, while values $\leq 2.0$ have been associated with volcanic events [Savage, 1972 ; Udias and Ruffle, 1975 ; Bottari and Neri, 1983 ; De Natalle and Zollo, 1986]. We therefore find a second characteristic, after the differences observed for b-value, that tends to differentiate the origin of the two clusters between tectonics and volcanic.

Analysis of the groups within the two time scales used for the generalized Poisson process also show distinctive patterns. In the groups of the upper cluster the event with the highest magnitude tends to be in the center of the sequence, while it is not the case for the groups of the lower cluster (Figure 5). Mogi [1985] interpreted the occurrence of the main event in the middle of earthquake sequences as related to highly heterogeneous zones, with a concentration of efforts in the volume where the sequences occur.

## DISCUSSION AND CONCLUSION

The Pisayambo nest occupies a 20x20x20 km volume. This nest is divided into two clusters, separated by about 7 km, occurring on top of each other. The upper cluster presents characteristics

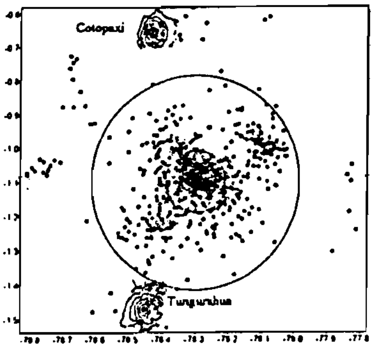


Figure 1. Disribution of the selected events of Pisayambo nest recorded from 1989 to 1995. The two 10 km and 35 km radius circles used for the study of the Poisson process are also shown.

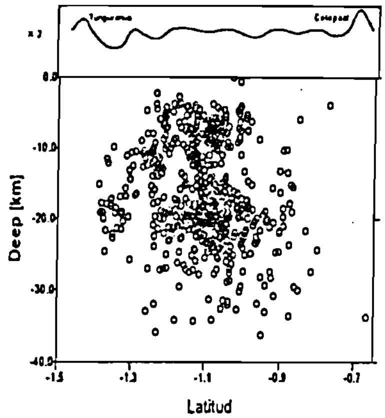


Figure 2. Depth distribution of the selected events in the zone of the Pisayambo nest, along a South-North cross section. Note the two swarms separated by about 7 kilometers.

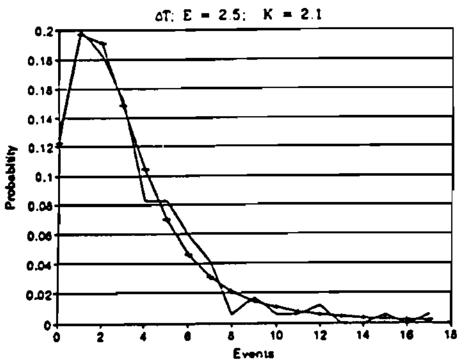


Figure 3. Generalized Poisson process applied to the shallowest swarm of the Pisayambo nest for the events included in the 10 km radius circle shown in figure 1.

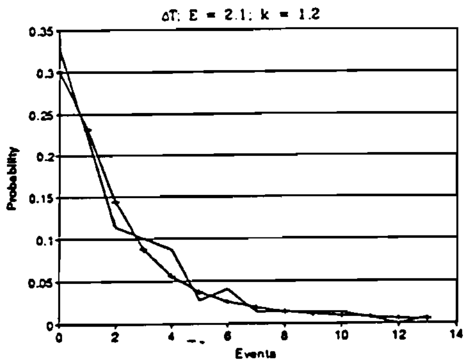


Figure 4. Generalized Poisson process applied to the deepest swarm of the Pisayambo nest for the events included in the 10 km radius circle shown in figure 1.

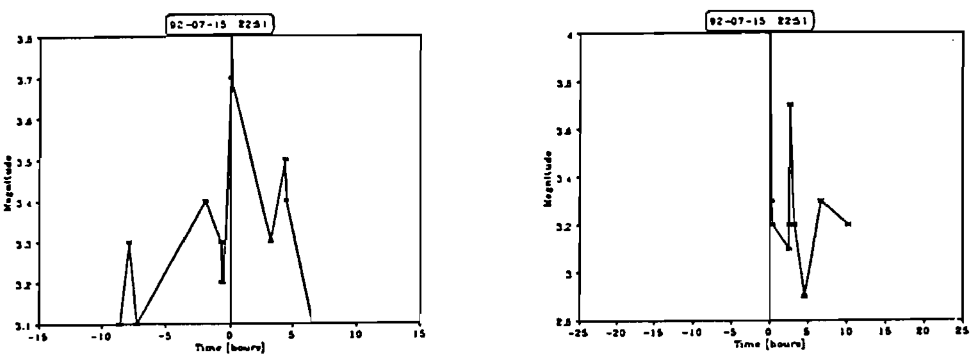


Figure 5. Magnitude versus temporal distribution 13 hours before and after the main event of a sequence of dependent events in the shalowest swarm (left) ; 25 hours before and after the main event of dependent events in the deepest swarm (right).

of tectonics events occurring in a highly fractured area, while the lower cluster presents characteristics of volcanic events. Behavior of other parameters, such as slight P-wave velocity and Vp/Vs decrease with depth in the upper cluster can be linked a saturated, i.e. highly fractured zone. Finally, the Pisayambo nest is located in the upper plate right above a seismicity gap in the subducting plate (see figure 2 of Guillier et al., this volume).

All things considered a plausible explanation for the presence of the Pisayambo nest could be the following :

- the gap in the descending plate can be interpreted as due to a detachment of the bottom part of the plate ;
- hot mantelic material is uprising where the subducting plate is absent towards the surface ;
- uprising of the hot material produces bulging of the upper crust, fracturing and weakening it, which could conduct to its rupture giving birth to a volcano, in the best of the cases, or a caldera.

Focal mechanisms and aerial photo analysis, other geophysics and field studies will be carried out to see if their results fit into this hypothesis.

REFERENCES

Bonilla F. and M. Ruiz, (1992), Evaluacíon del Peligro Sismico en le Ecuador, Tesis de Grado, Escuela Politecnica Nacional, Quito, Ecuador.

Bottari A and G. Neri, (1983), Some Statistical Properties of a Sequence of Historical Calabro Peloritan Earthquakes, *J. Geophys. Res.*, 88, 1209-1212.

Chatelàin, J.-L., 1978. Etude fine de la sismicité en zone de collision continentale au moyen d'un réseau de stations portables : la région Hindu-Kush Pamir, Univ. Scient. Medic. de Grenoble, 219 p..

Klein, F.W., 1978. Hypocenter location program HYPOINVERSE, U. S. Geol. Surv.,Open File Rep., 78-694.

Mogi K., (1985), Earthquake Prediction, Academic Press.

Natalle de G. and A. Zollo, (1986), Statistical Analysis and Clustering at Phlegraen Fields, Bull. Seism. Soc.Am, 799-814.

Pennington, W.D., (1981), Subduction of the Eastern Panama Basin and Sismotectonics of Northwestern South America, *J. Geophys. Res.*, 86, 10753-10770.

Prévot R., Chatelain J.-L., Guillier B., Yepes H., 1996. Mapping of the P-wave velocity structure beneat the ecuadorian Andes, in this volume.

Scholz C. H., (1968), The Frequency-Magnitude Relation of Microfracturing in Rock and its Relation to Earthquakes, *Bull. Seism. Soc. Am.*, 58, 399 - 415.

Shlien, S. and M.N. Toksöz (1970), A Clustering Model for Earthquake Ocurrence, *Bull. Seism. Soc.Am*, 60, 1765-1787.

Talandier J., E.A. Okal, (1984), The Volcanoseismic Swarms of 1981-1983 in the Tahiti-Mehetia Area, French Polynesia, *J. Geophys. Res.*, 89, 11216 - 11234.

# THE Mw 6.8 MACAS EARTHQUAKE IN THE SUBANDEAN ZONE OF ECUADOR, OCTOBER 3, 1995.

Alexandra ALVARADO[1], Monica SEGOVIA[1], Hugo YEPES[1], Bertrand GUILLIER[1,2], Jean Luc CHATELAIN[1,2], Jose EGRED[1], Darwin VILLAGOMEZ[1], Mario RUIZ[1], Pablo SAMANIEGO[1], Roberto SANTACRUZ[1]

(1) Instituto Geofisico, Escuela Politécnica Nacional, Apartado 17 01 2759, Quito, Ecuador.

(2) ORSTOM, Apartado 17 11 6596, Quito, Ecuador.

KEY WORDS : sismotectonics, neotectonics, seismic hazard, Andes, subandean zone, Ecuador.

## INTRODUCTION

At 01:51 on 3 October 1995 (UT) a Mw 6.8 earthquake (Figure 1) occurred on the south-eastern flank of Cutucu cordillera, a NNE-SSW Jurassic-Cretacic anticline (Figure 1), located on the western edge of the subandean zone, overthrusting the lower part of the subandean zone along several reverse N-S faults.

No foreshocks were detected before the main shock at the detection level (Ml = 3.0) of the permanent network run by the Instituto Geofisico of the Escuela Politecnica Nacional of Quito. Four large aftershocks (magnitude ≥ 5.1) were observed within the first 4 days after the main event, including a magnitude (mb) 5.6 six minutes later, and the main aftershock (Mw = 6.4) eleven hours later. Three other aftershocks with magnitude (mb) 5.1 occurred in the period 21 - 29 October. About 750 aftershocks (Ml ≥ 3.0) were detected by the permanent network one week after the main shock, amounting to more than 2100 until December 31 ; 350 of them had a magnitude 4 or larger, of which over 100 were felt in the epicentral zone. Three portable MEQ-800 stations were installed during 48 hours (2 from 5 to 6 October, and 1 from 11 to 13 October ; Figure 1). The latest recorded 1140 aftershocks, while the permanent network detected only 126, showing that the level of activity following the main event was much higher than observed with the permanent network because of its station distribution with respect to the seismic activity.

The epicenter of the main shock is located about 60 km SSE of the city of Macas (population 12,000). It has been widely felt in the entire country, including in the capital city of Quito (I = IV) and in the major cities (Guayaquil, I = IV ; Cuenca, I = V). It has also been felt in the neighboring countries of Colombia (as far as Bogota) and Peru (as far as Tarapoto). Fortunately this event occurred in a very low density populated area in the upper-amazonian jungle. Nevertheless at least 2 people were reported killed in Puyo (140 km North of the epicenter) and in Baños (170 km NNW of the epicenter) and several injured in the epicentral area. A complete survey of casualties and destructions in the zone was impossible to conduct due to the difficult logistic conditions (dense virgin rain forest covers most of the macroseismic zone). No surface ruptures have been observed. In the epicentral area decametric-size landslides and avalanches occurred on steep slopes. The bridge over the Upano river (60 km North of the epicenter) collapsed, interrupting the transit on the main road from the North to the eastern provinces ; cracks were observed on the roads, as well as power supply cuts and breaks of water supply pipes in several cities and villages up to Macas. Minor damages to buildings occurred in localities located along the Upano river, although some non-earthquake resistant buildings suffered slight to light damage in Puyo, Tena, Shell Mera, Cosanga, and as far as Gayaquil. Direct economic losses were estimated at $US 5 millions. Fortunately the earthquake occurred during a period of severe draught, otherwise the consequences could have been much more dramatic, as those following the 1987 Mw 6.8 earthquake that occurred in the northern part of the subandean zone (300 km North of the 3 October 1995 event) during a heavy rainy period, which killed over 1000 people and had much more economic consequences, most of them due to large landslides and mudflows related to the earthquake.

Preliminary location of 930 of the aftershocks during the 3 October - 31 December period shows a distribution of activity with a NW-SE trend (Figure 2), between 0 and 25 km depth, which does not correspond to any known fault. The Harvard University centroid-moment tensor solution for the main event shows reverse faulting with a nodal plan oriented N30E (Figure 2), sub-parallel to the sub-andean structures, with reverse thrust motion, compatible with an E-W compression.

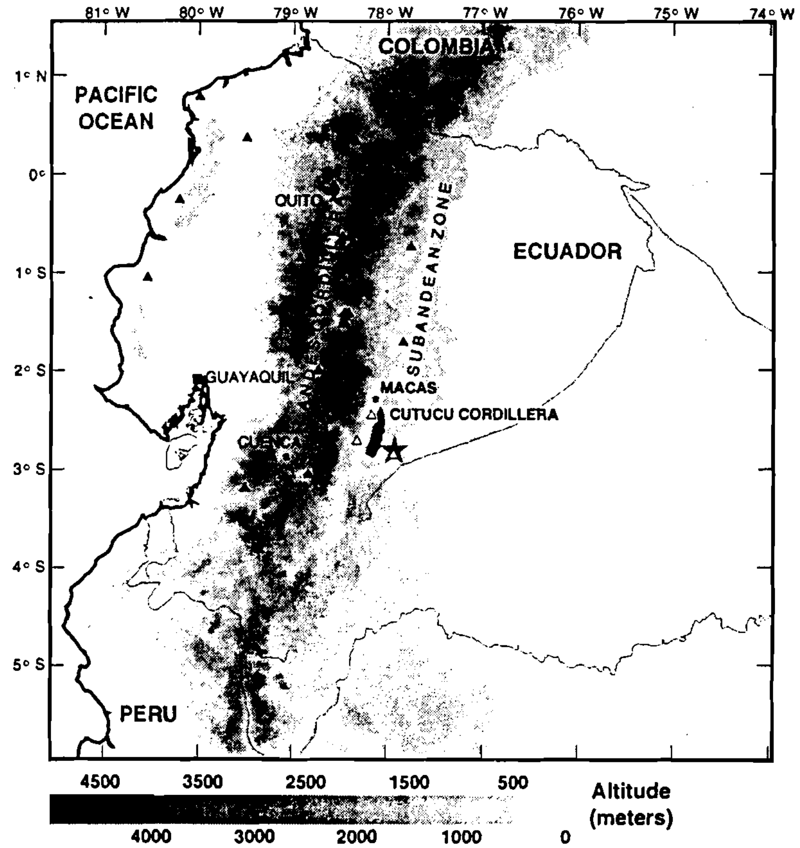


Figure 1. Map of Ecuador. The star is the epicenter of the 1995 Macas earthquake. Filled triangles are permanent stations of the ecuadorian seismic network. Open triangles are the temporary stations installed after the earthquake. The dark zone represents the Cutucu Cordillera.

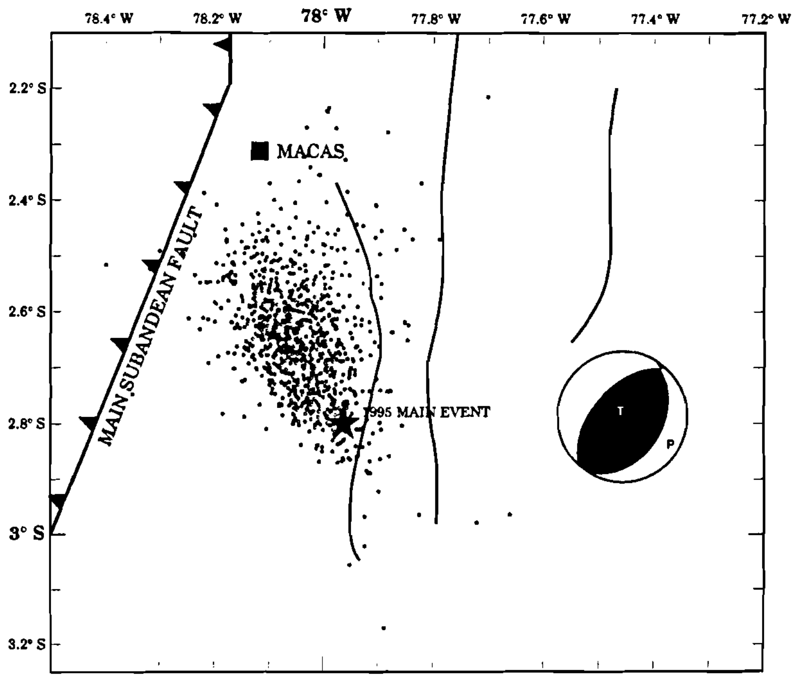


Figure 2. Epicenters of 940 selected aftershocks (RMS< 1.0. condition number > 100) during the period 3 October - 31 December 1995. Centroid-moment tensor solution for the main event from the Harvard University.

This earthquake is the largest shallow event to have occurred in this zone since at least 1952. A magnitude (Mw) 6.8 occured on May 10, 1963 about 90 kilometers NE of the 1995 event at a depth of 25 kilometers, and a magnitude (Mw) 7.5 earthquake on July 27, 1971, about 100 kilometers SE of the 1995 event at a depth of 90 kilometers. No data is available prior to 1952. There are no detailed reports describing the consequences of the 1971 and 1963 events in the epicentral areas. However, these two earthquakes produced similar consequences in the country as the 1995 event, and were also felt in the neighboring countries of Colombia and Peru.

The seismic hazard in the Andean-Sub-andean zone of Ecuador should be of major concern for the ecuadorian authorities as, for example, all the magnitude ≥ 6.5 ecuadorian events since 1985 occurred in the sub-andean zone, and a magnitude MS 5.7 hit the Latagunga region on 28 March 1996 provoking several tenths of casualties and major damage in the epicentral zone.

# TECTONIC STRESSES IN THE NORTH-WEST OF ARGENTINA AND THEIR RELATIONSHIP WITH MAIN SHALLOW EARTHQUAKES

**Mario A. ARAUJO[1,2] and Juan C. CASTANO[1,2]**

(1) Instituto Nacional de Prevención Sísmica - INPRES - Roger Balet 47 Norte - 5400 - San Juan - ARGENTINA
(2) Universidad Nacional de San Juan - Av. José Ignacio de la Roza 350 Este - 5400 - San Juan - ARGENTINA

## ABSTRACT

The principal Seismogenic Sources in the north-west of Argentina have been studied. Due to these sources this region is the second in the country as regards seismic hazard.
Main shallow earthquakes in this zone have produced many casualties and building damages delimited into one zone with direction SSW-NNE. In this area, the orientation of the maximum horizontal stress, produced by the collision of the Nazca Plate and the South American Plate, has been modified due to local stresses.
One of the reasons of this modification might be that the high Andes are in a distensional process transmited to the east in the South American Plate.

**KEY WORDS:** Seismogenic Sources, tectonic stresses, main earthquakes.

## INTRODUCTION

At this time more than 2,000,000 people live in the north-west region of Argentina (NWA). In this area buildings have been constructed, in general, without earthquake resistant provisions.
The NWA main industries are: mining, sugar-cane, tobacco, petroleum, etc. The points mentioned above show the importance to carry out seismogenic sources studies to base future urban planning of the main cities on their results.
This zone classified as the second most hazardous seismic zone in the country has particular tectonic characteristics compare with other zones subjected to tectonic processes.
Generally, in this area the Nazca Plate subduction is similar to that of the southern part of Bolivia (so-called normal subduction) from latitude 21.5° to 23.5° South. To the South of this zone, between 23.5° and 27.5° S, the subducted plate makes a contortion without changes until 28.5° S where it becomes horizontal. In the NWA region most of the events are intermediate earthquakes and some deep and shallow ones.
The occurrence of shallow earthquakes is not as frequent as the intermediate ones, however, many of them have caused several casualties and injuries and severe damage to buildings.

**Main Earthquakes in the region**

| Event | Year | Province and Locality | Intensity MM |
|---|---|---|---|
| 1 | 1692 | Salta (Talavera de Esteco) | VIII |
| 2 | 1826 | Tucumán (Trancas) | VIII |
| 3 | 1844 | Salta (Palomitas) | VIII |
| 4 | 1863 | Jujuy (San Salvador de Jujuy) | VII |
| 5 | 1871 | Salta (Orán) | VII |
| 6 | 1874 | Salta (Orán) | VIII |
| 7 | 1892 | Catamarca (Pomán) | VIII |
| 8 | 1899 | Yacuiba (Límite Argentino - Boliviano) | VII |
| 9 | 1906 | Tucumán (Tafí del Valle) | VII |
| 10 | 1930 | Salta (La Poma) | VIII |
| 11 | 1931 | Tucumán (El Naranjo) | VII |
| 12 | 1948 | Salta (Palomitas) | IX |
| 13 | 1959 | Salta (San Andrés) | VIII |
| 14 | 1966 | Catamarca (Belén) | VII |
| 15 | 1973 | Salta (Santa Clara) | VII |
| 16 | 1974 | Salta (Santa Victoria) | VII |
| 17 | 1974 | Salta (Orán) | VII |

## THE SEISMOTECTONIC SETTING

The region under study is located in a tectonic setting resulting from the ongoing subduction of the Nazca Plate eastward beneath the South American Plate. This process has created major structural features as complex faulting, the Puna Plateau and to the east, the Subandean Rangers.
Considering the existing megastructures in the region, it has been observed that these structures constitute barriers limiting shallows from intermediate earthquakes.

## SEISMOGENIC SOURCES

The seismotectonic process is quite complex towards east, especially after the 3,000 m contour. Taking the megastructures into account besides the 3,000 m contour, it is observed that the main earthquakes direction will be SSW to NNE, starting from Catamarca to Yacuiba ( at the Argentina-Bolivia border). In this zone the most dangerous earthquakes have occurred.

## LOCAL TECTONIC STRESSES

The W-E direction of the maximum horizontal tectonic stresses, which are caused by the collision between both plates, are altered by the local horizontal stresses. Therefore, the final orientation results almost perpendicular to the 3,000 m of the Puna contour.
Some of the focal mechanisms for this zone have been very well determined in previous studies and their representations confirms the above statements. Besides, it is possible to assert that the high Andes are under a tensional process that is transmitted to the puna step by step (e.g. the normal faults near to the 3,000 contour). East of the 3,000 m contour the maximum horizontal tectonic stress caused by the collision between both plates is predominant and therefore the principal stress direction suffers no changes.

## CONCLUSIONS

Main shallow earthquakes in this region have occurred close to the 3,000 m contour, which indicates that

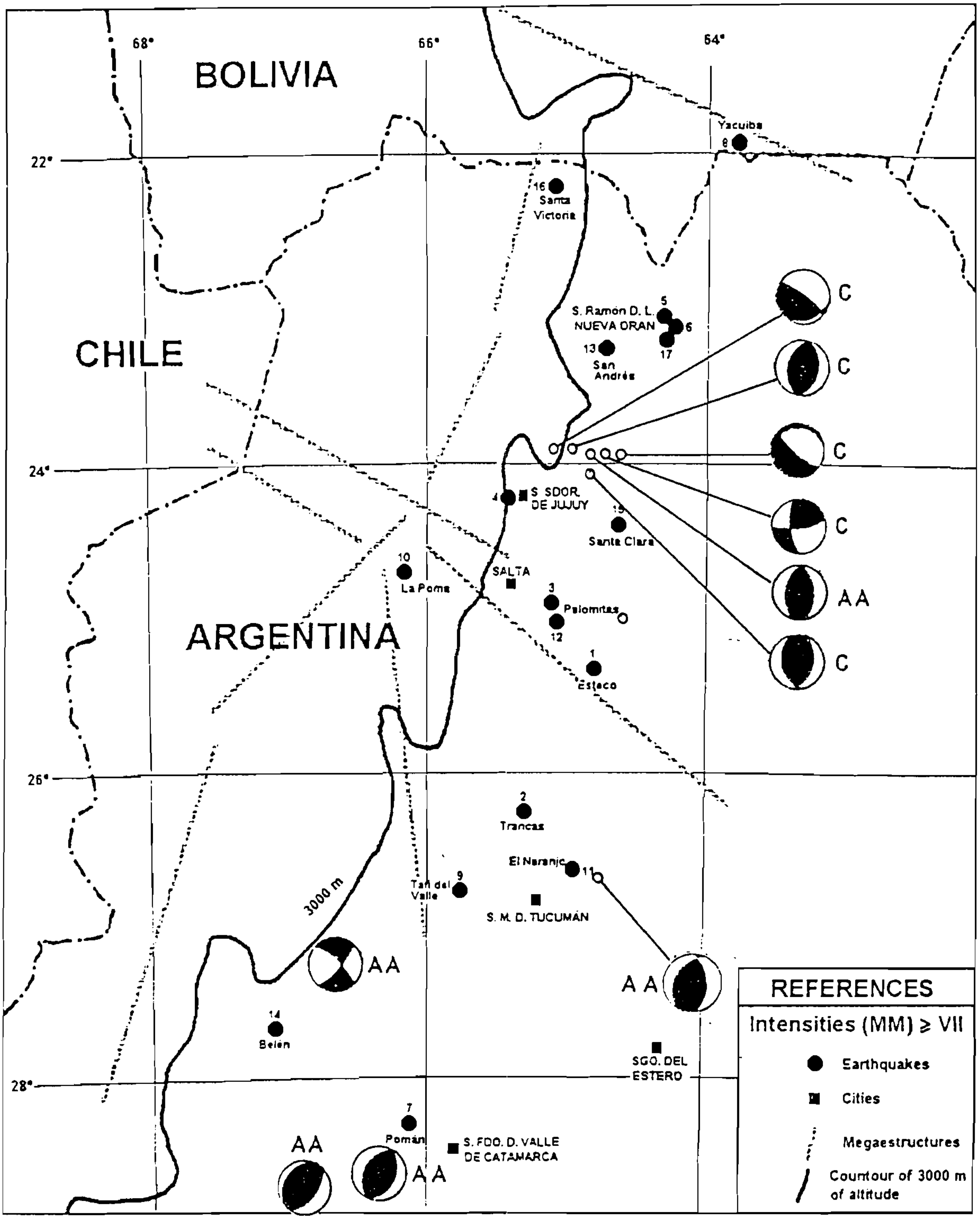


MAXIMUM REPORTED INTENSITIES

studies must be focused on the tectonic process close to the 3,000 m Puna contour. On this area very few active fault recognitions have been made mainly due to the weather erosion or to the vegetation which covers the potential surface evidences of faults.

**REFERENCES**


- Allmendiger R. W., 1986. Tectonic development, southeastern border of Puna plateau, northwestern Argentine. Geol. Soc. Am. Bull., 97 : 1070 - 1082.
- Allmendiger R. W., Strecker M., Eremchu K., J. E. And Francis P., 1989. Neotectonic deformation of the southern Puna plateau, NW Argentina. I. S. Earth Sci., 2 : 111 - 130.
- Araujo M. And Suarez G., 1994. Geometry and State of Stress of the Subducted Nazca Plate, Beneath Central Chile an Argentine: Evidence from Teleseismic Data. Geophysical Journal International, vol. 116, pages 283 - 305.
- Araujo M. and Assumpçao M., 1992. Esfuerzos Tectónicos en una zona del Nor-Oeste Argentino. XVII Reunión de la Asociación Argentina de Geofísicos y Geodestas. Resúmenes de la reunión, Ma MB3 CC.
- Araujo M., Castano J., Figueroa M. y Navarro C., 1994. Actividad Sísmica superficial detectada en San Francisco (Departamento Valle Grande - Provincia de Jujuy) desde diciembre de 1993 hasta marzo de 1994. XVIII Reunión Científica de la Asociación Argentina de Geofísicos y Geodestas. Resúmenes de la reunión, 1TA3 página 28.
- Assumpçao M., 1992. The regional intraplate stress field in South America. J. Geophys. Res., 98 : 11,889 - 11,903.
- Assumpçao M. and Suárez. G., 1988. Source mechanism of moderate - size earthquakes and stress orientation in midplate South America. Geophys. J., 92 : 253 - 267.
- Assumpçao M. and Araujo M. 1993. Effect of the Altiplano - Puna plateau, South America on the regional intraplate stresses. Tectonophysics, 221 : 475 - 496.
- Cahil T., Isacks B. L., Whitman D., Chatelain J. L., Perez A. And Chin J. M., 1992. Seismicity and tectonics in Jujuy province, NW Argentina. Tectonics, 11 : 944 - 959.
- Castano J. C., 1977. Zonificación Sísmica de la República Argentina - Publicación Técnica N° 5, 42 páginas.
- Castano, J. C. and Araujo M., 1993. Seismogenic Sources and Regional Tectonic Stresses In the Subandean Zone of Major Seismic Hazard of Argentina. ISAG 92. Oxford England, pages 63 - 66.
- Fleitout L. and Froidevaux C., 1983. Tectonic stresses in the Litosphere. Tectonic, 2 : 315 - 324.
- Froidevaux C. And Isacks B. L., 1984. The mecenical state of the Litosphere in the Altiplano-Puna segment of the Andes. Earth Planet. Sci. Lett., 71 : 305 - 314.
- Jordan T. E., Isacks, B. L., Almendiger, R. W., Brewer, J. A., Ramos V. A. and Ando C. F., 1983. Andean Tectonics related to geometria of subducted Nazca Plate. Geol. Soc. Am. Bull. 94 : 341 - 361.
- Lyon-Caen H. and Molnar P., 1988. Some simple physical aspect of the support, structure, and evolution of mountain belts. Geol. Soc. Am. Spec. Pap., 218 : 179 - 207.
- Mercier J. L., 1981. Extensional - Compressional tectonics asociated with the Aegean Arc : Comparison with the Andean cordillera of south Perú and north Bolivia. Philos. Trans - R. Soc. London sev. A., 300 : 337 - 355.
- Mercier J. L., Sebrier M., Levenu A., Cabrera J., Bellier O., Dumont, J: F. and Marcharé J., 1992.
- Wdowinski S. and O'Connell R. J., 1991. Deformation of the central andes (15° - 27° S) derived from a flow model of subduction zones. J. Geophysical Res. 96 : 12,245 - 12,255.
- Zoback M. L., 1992a. First and second orden pattern of stress in the litosphere : the world Step Map proyect. J. Geophy. Res., 97 : 11,703 - 11,728.
- Zoback M. L., 1992b. Stress field constrain on intraplate seismicite in eastern North America. J. Geophy. Res., 11,761 - 11,782.

# QUATERNARY TECTONIC ACTIVITY OF THE LLANOS FOOTHILLS THRUST SYSTEM, EASTERN CORDILLERA OF COLOMBIA: GEOMORPHOLOGICAL AND GEOLOGICAL EVIDENCES FROM LA FLORIDA ANTICLINE, BETWEEN THE UPÍA AND CUSIANA RIVERS.

Franck A. AUDEMARD M.[1] and Kim ROBERTSON [2]

(1) Funvisis, Apartado Postal 76880, Caracas 1070-A, Venezuela. Fax:+(58-2)2579977. e-mail:faudem@funvisis.internet.ve
(2) IGAC, Subdirección de Geografía, Apartado Aéreo 6721, Bogotá, Colombia. Fax:+(57-1)3680946.

KEY WORDS: Fold-and-thrust belt, Active folding, La Florida anticline, Eastern Cordillera, Colombia.

## INTRODUCTION

It is well known that oil exploration started at the end of the 19th century by drilling domes and anticlines as its main targets. However, large oil fields in fold-and-thrust belts are still uneasily discovered nowadays worldwide, such as the Cusiana anticline (name given in the oil industry literature; Cazier *et al.*, 1995 and Cooper *et al.*, 1995), located in the Llanos foothills of the Colombian Eastern Cordillera. However, for that particular case, that would seem astonishing since: (a) that fold had already been mapped, though it used to be known as the La Florida anticline (Ulloa and Rodriguez, 1981); (b) Robertson (1989) reported several geomorphic evidences of its Quaternary tectonic activity; and (c) that structure involves rocks as young as Pleistocene in age. Besides, several authors also indicate that the tectonic inversion and/or foreland overthrusting of the Eastern Cordillera is a recent process (Ulloa and Rodriguez, 1981; Hebrard, 1985; Page, 1986; Robertson, 1989; Cazier *et al.*, 1995; Cooper *et al.*, 1995). Therefore, all these facts put together clearly indicate the recent character of this deformation and also suggest undirectly its high oil prospectivity. In this paper, we present additional geomorphological and surface geological data that confirm the recent activity of a short segment of the Llanos fold-and-thrust belt of the Eastern Cordillera roughly east of Bogotá, and particularly of the La Florida (Cusiana) anticline.

## REGIONAL FRAMEWORK

Colombia is a country of sharp contrast: the Andes mountains in the west and the Llanos plains in the east. The studied area corresponds to a short segment of the frontier between these two huge geographical and geological units, known as the Eastern Cordillera Llanos foothills (Fig. 1). This topographical unit geologically corresponds to the east-vergent frontal fold-and-thrust belt of the Eastern Cordillera. La Florida (Cusiana) anticline belongs to this belt and is between the Upía and Cusiana rivers. This fold affects the entire Mesozoic-Cainozoic sedimentary sequence of the Llanos basin (Cazier *et al.*, 1995; Cooper *et al.*, 1995) and its eroded core exposes the Mio-Pliocene Caja Formation (Ulloa and Rodriguez, 1981). These authors report that this fold is symmetrical and no brittle deformation is associated to it. However, it can be observed that this anticline is in perfect prolongation to the south of the El Yopal fault -name given in the oil industry- (also Known as the San Miguel fault -name given in the geological maps of Colombia-) that dies out near the northern banks of the Cusiana river (Fig. 1), thus allowing to infer that the La Florida anticline south of this river is a Yopal fault-propagation fold with a southern periclinal clousure. However, as we are going to demonstrate next, this fold is also gentetically related to a more basinward reverse fault than the El Yopal (San Miguel) fault - non identified in Colombian surface geology maps-, thus being a fault-bend fold located in the hangingwall block of the Cusiana fault which has been recentlly identified by seismic profiling by Cazier *et al.* (1995) and Cooper *et al.* (1995).

## GEOMORPHOLOGICAL AND GEOLOGICAL OBSERVATIONS

Besides the various geomorphic features of Quaternary tectonic activity of La Florida anticline already reported by Robertson (1989)*, this author also indicates the existence of a ≈50 m high SE-looking fault scarp flanking the fold on the southeastern edge of la Mesa de Sisigua and northeast of it, between the Chita and Cusiana rivers, that he named the San Pedro-Sisigua fault. Nevertheless, this geomorphic feature should be regarded as a flexural scarp instead of a conventional fault scarp, between the Catuya and Chita rivers as observed in an abandoned cobble pit (Fig. 2a). At this locality (Fig. 2a), cobble beds correlable to La Corneta Formation (or younger Quaternary alluvial units), are warped around the clayey-silty beds of the Mio-Pliocene Caja Formation. The presence of this scarp on its own does not prove the existence of brittle deformation (major fault) at surface or in the near subsurface and neither do the other evidences mentioned by Robertson (1989), though it does definitely prove the occurrence of Quaternary folding in the Llanos foothills of the Eastern Cordillera. Nevertheless, we can provide further geological and geomorphological facts that prove that the La Florida anticline is partly an active fault-bend fold with respect to the Cusiana fault (the most basinward fault), besides being a fault-propagation fold: (a) a NW-SE landscape profile across the La Mesa de San Pedro, that corresponds to elevated Quaternary alluvial terrace deposits, shows an asymmetric, long-radius bend with a gently dipping rangeward backlimb and a shorter, steeper basinward forelimb; (b) the same configuration is also observed farther north, east of Monterrey and across La Loma de Buena Vista, but the core of the anticline is excavated and exposes the Caja Formation (Fig. 1), indicating a more evolved geomorphological stage due to the occurrence of topographic inversion. The previously mentioned flexural scarp (Fig. 2a) corresponds to the steeper forelimb of the fold. It is impossible in the field to differentiate the two coarse alluvial sequences that cap the Caja Formation on both flanks, though they are mapped as different units by Ulloa and Rodriguez (1981); (c) the presence of a tectonic "gutter" along the foot of the eastern scarp of La Mesa de San Pedro (Fig. 1), implying tectonic loading due to foreland-vergent thrusting; (d) recent road cuts of the main Llanos road under construction during early 1994, between the Catuya and Chita rivers, across the steeper southeastern anticline flank, have exposed brittle deformation (Pleistocene-or-younger, southeast-vergent, low-angle reverse faults; Fig. 2b and c). At depth, the presence of the reverse fault has been confirmed by recent seismic profiling (the Cusiana fault of Cazier *et al.*, 1995 and Cooper *et al.*, 1995). These authors also consider this fault as active.

## CONCLUSIONS

The La Florida anticline and the Cusiana fault are tectonically active structures within the fold-and-thrust belt of the Eastern Cordillera Llanos foothills; confirming thus the activity of this belt. The Cusiana fault is a SE-vergent, low-angle reverse fault. The Florida anticline is an asymmetric fold with a northwest gently dipping backlimb and a steeply dipping forelimb. It can be genetically explained by two different but simultaneous mechanisms: a) fault-bend folding on the hangingwall block of the Cusiana fault and b) fault-propagation folding associated to the southern end of the El Yopal (San Miguel) fault.

Besides, it seems clear from this experience that comprehension of the Neotectonics framework is playing an important roll in identifying new oil prospects in areas as complexly deformed as fold-and-thrust belts -the new fashionable target of today's oil exploration-.

---

* (1) radial drainage of La Mesa de San Pedro, indicating the southern periclinal clousure of the anticline at surface and allowing to prolong the original Ulloa and Rodriguez's fold axis farther southwest for some extra 15 Km; (2) over-a-100-m high and densely dissected SE-looking scarp of La Mesa de San Pedro; (3) westward tilt of Quaternary alluvial units at La Loma de Buena Vista (east of Monterrey) on the northwestern flank of the fold and respective river pattern inversion (flow from the basin towards the range); (4) SW diversion of the Cusiana and Tua rivers, suggesting dyachronic and differential fold growth (older and stronger deformation to the north); and (5) several small fault scarps affecting Quaternary alluvial terraces on the Llanos flank of the fold, between the Chita and Cusiana rivers.

## REFERENCES

Cazier, E.; Hayward, A.; Espinosa, G.; Velandia, J.; Mugniot J-F. and Leel, W. jr. 1995. Petroleum Geology of the Cusiana Field, Llanos Basin Foothills, Colombia. *AAPG Bull.*, 79(10):1444-63.

Cooper, M.; Addison, F.; Alvarez, R.; Coral, M.; Graham, R.; Hayward, A.; Howe, S.; Martinez, J., Naar, J.; Peñas, R.; Pulham, A. and Taborda, A. 1995. Basin Development and Tectonic History of the Llanos Basin, Eastern Cordillera, and Middle Magdalena Valley, Colombia. *AAPG Bull.*, 79(10):1421-43.

Hebrard, F. 1985. Les Foot-hills de la Cordillère Orientale de Colombie entre les rios Casanare et Cusiana. Evolution Géodynamique depuis l'Eo-Crétacé. Thèse Doctorat 3ème cycle Univ. Paris VI. 162 p.

Page, W. 1986. Seismic Geology and Seismicity of Northwestern Colombia. *Woodward-Clyde Consultants' Unpubl. Rpt. for ISA Interconexión Eléctrica S.A.*

Robertson, K. 1989. Actividad neotectónica del piedemonte de la Cordillera Oriental. Sector Villavicencio-Tauramena, Colombia. *V Congreso Colombiano de Geología*, Bucaramanga, 170-192.

Ulloa, C. and Rodriguez, E. 1981. Geología del Cuadrángulo K-13, Tauramena. *Bol. Geol. Ingeominas*, 24(2):3-30 + annex.

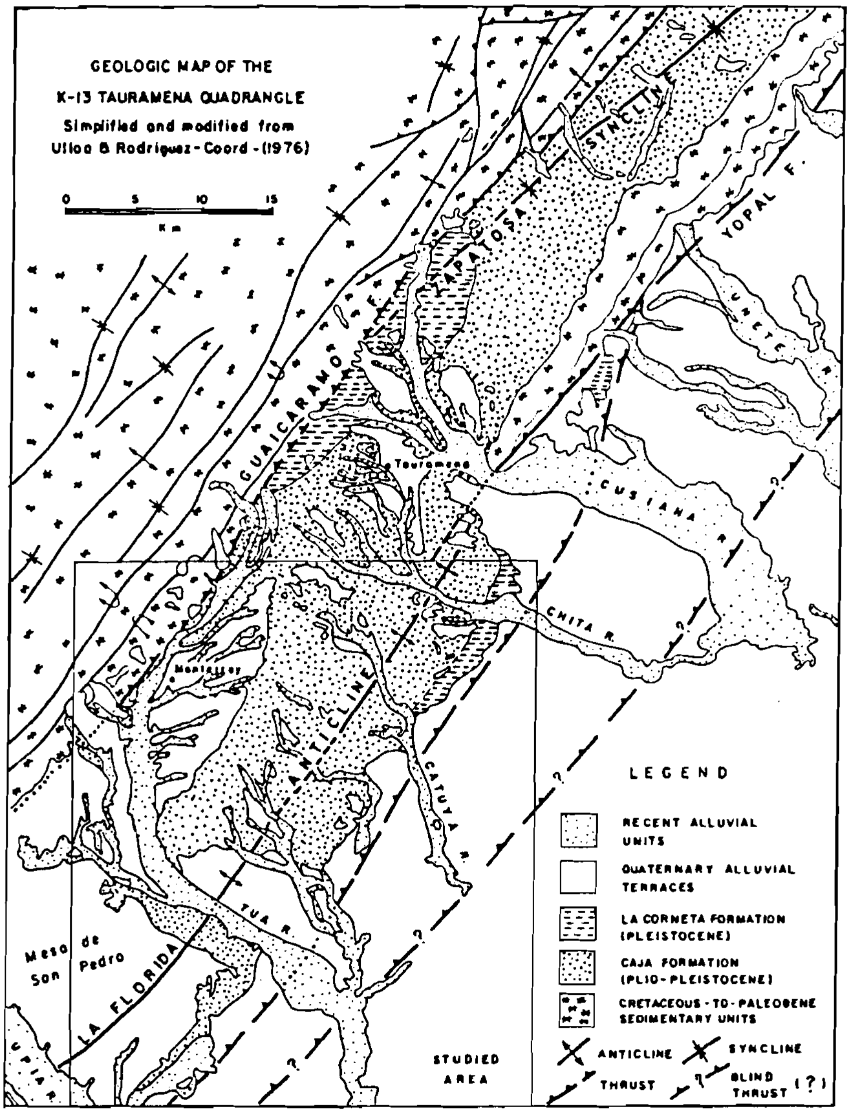


Figure 1.- Geologic map of a short segment of the Llanos fold-and-thrust-belt of the Colombian Eastern Cordillera, roughly east of Bogotá.

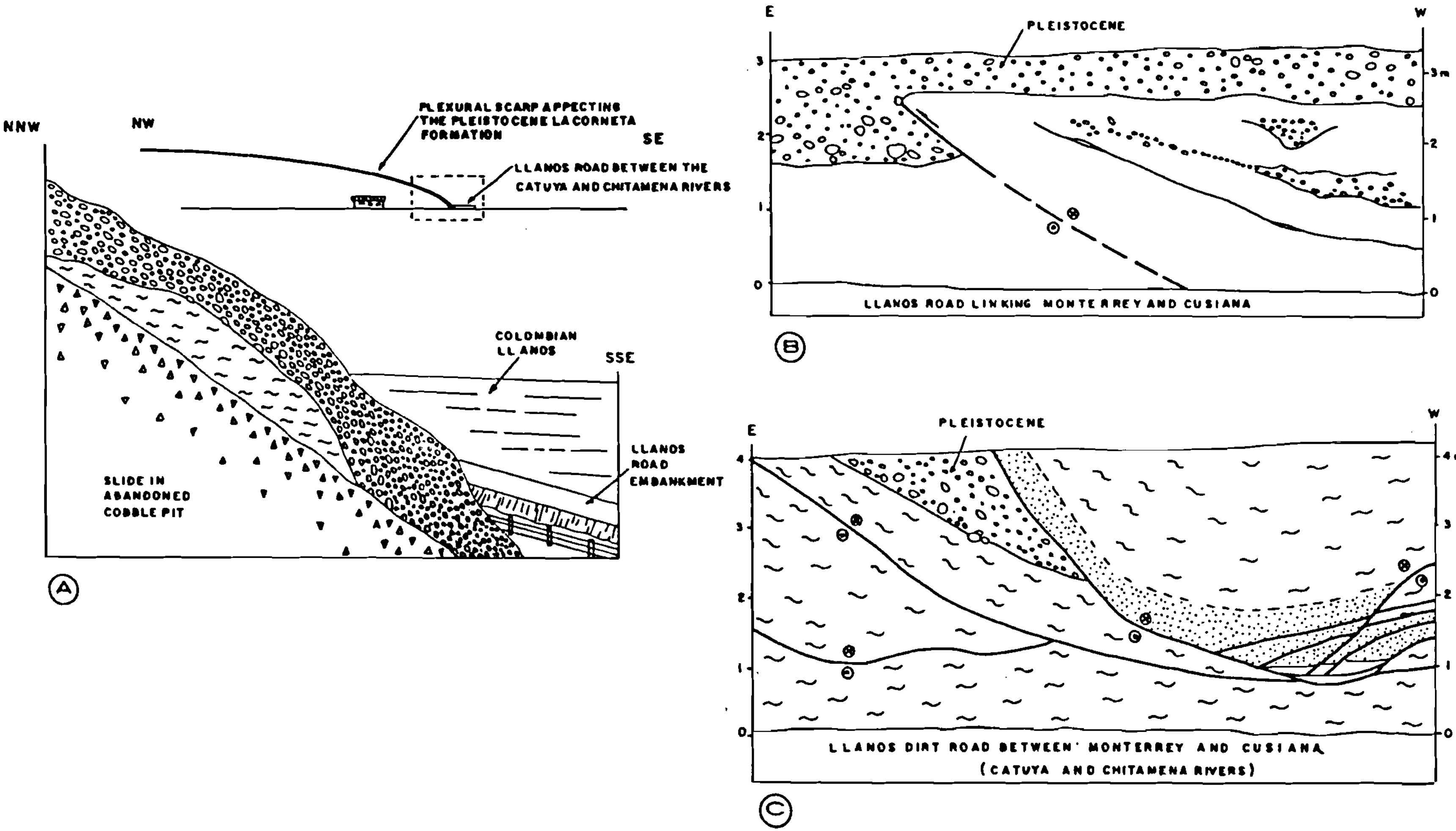


Figure 2.- (a) Flexural scarp on the southeast forelimb of the asymmetric La Florida (Cusiana) anticline, between the Catuya and Chita rivers, affecting the Pleistocene La Corneta Formation cobbles (or younger alluvial units?). (b) and (c) Pleistocene-to-Holocene, southeast-vergent, low-angle reverse faulting on the forelimb of the La Florida anticline, in recently-dug road cuts of the Monterrey-Cusiana road, slightly north of the Catuya river.

# SEISMICITY AND STATE OF STRESS IN THE CENTRAL ANDES: BOLIVIAN OROCLINE REGION

R. Ayala[1,2] and G. Wittlinger[1]

[1] EOPG, 5 rue Descartes, Strasbourg, FRANCE
[2] OBSERVATORIO SAN CALIXTO, C.P. 12656, La Paz, BOLIVIA

## ABSTRACT

The central Andean seismicity recorded from July 1988 to November 1994 by the Bolivian network and some other neighbours stations was located using a 3-D velocity model. The highest concentration of crustal events is located near the bending of the Bolivian orocline. A cluster of intermediate events is also located beneath the Peru-Bolivia border region. The stress orientations for shallow intraplate events is characterised by a principal ENE horizontal compression in the forearc region and Subandean Ranges. This direction is parallel to the direction of the Nazca-South American plate convergence. The western High Andes are caracterized by a principal N-S horizontal tensional stress. The Nazca plate is dominated by a tensional stress oriented parallel to the down dip direction of the slab.

**KEY WORDS**: 3-D velocity model, earthquake location, seismicity, stress regime

## INTRODUCTION

The Central Andes region presents a very important shallow seismicity related to compressional tectonic induced by the convergence of the Nazca and South America plates along the forearc, and in the both sides of the Andes Cordillera, and a extensional tectonic in the High Andes (Assumpçao, 1992; Mercier *et al.*, 1992).

The Central Andes subduction zone has two different geometries: a subhorizontal segment beneath Central Peru and a subducted slab dipping approximately 30°E beneath southern Peru-Bolivia-northern Chile region related to extensional stresses (Cahill & Isacks, 1992). The upper-part of the slab present a interplate coupling zone defined by a change of compresional to tensional stress field.

The two main objectives of this study are first the location of the seismicity recorded by the Bolivian network and not reported by the regional and international bulletins and second the determination of the state of stress in the Central Andes region as deduced from focal mechanism solutions.

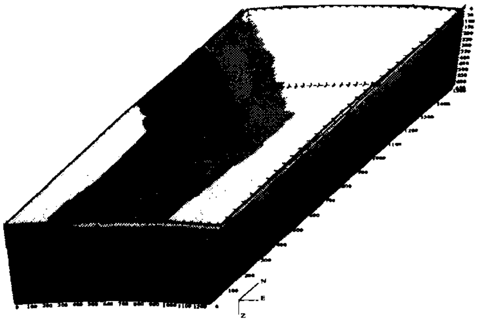

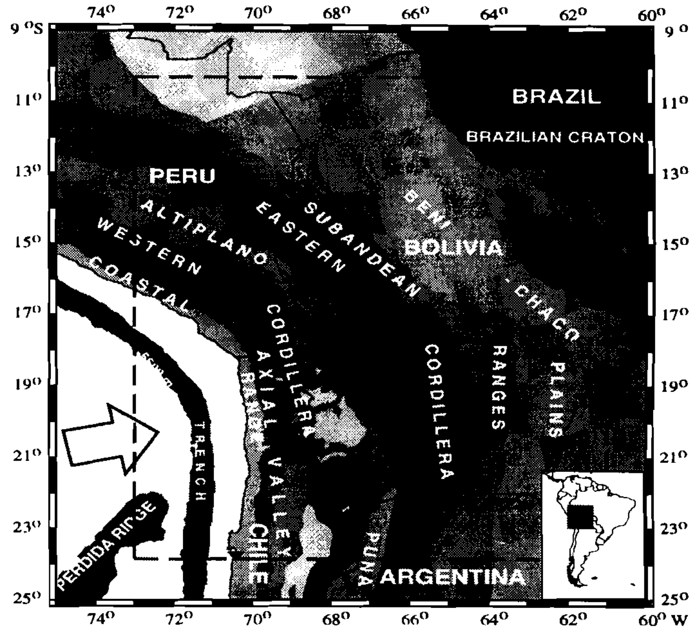


Fig. 1. Map showing the studied area and the limits of the main morphostructural units in Central Andes region. Triangles show the seismological stations used for earthquake location; large arrow indicates the direction of the Nazca-South American plate convergence (DeMetz *et al.*, 1990). The 3-D velocity model used to earthquake location is a cubic volume of 1500 km in north-south direction by 1280 km in east-west direction and down to 650 km depth.

## SEISMICITY PATTERNS

Seismic data recorded from July 1988 to November 1994 by the seismic network of Bolivia and some neighbours seismological stations were used (fig. 1). Earthquakes were located using finite differences computations for traveltimes and a fully non linear approach for the inversion (Wittlinger *et al.*, 1993). A preliminary 3-D velocity model for this region was gathered using published geological data, velocity models deduced from seismic refraction (Schmitz, 1993) and from local seismic tomography (Dorbath & Granet, 1996). The shape of the Nazca plate was modelised like a continuous slab (Cahill & Isacks, 1992) with a velocity 2.0% faster that the surrounding mantle velocity (Dorbath *et al.*, 1995).

The recorded crustal earthquakes (fig. 2) are located in the northern part of the Bolivian foreland region, in the Altiplano near La Paz, and in the southern Peru-western Bolivia region. A more sparse crustal seismicity is also observed in south-western Bolivia. The highest concentration of crustal seismicity is located in the Western Cordillera and in the Subanden Ranges near the bending of the Bolivian orocline. The deeper earthquakes (fig. 3) related to the subducted slab show a continuous distribution, and indicate a deep slab beneath northern Bolivia (region of the great earthquake from June 9, 1994). A cluster of seismicity is located beneath Peru-Bolivia border region from 70 to 150 km depth.

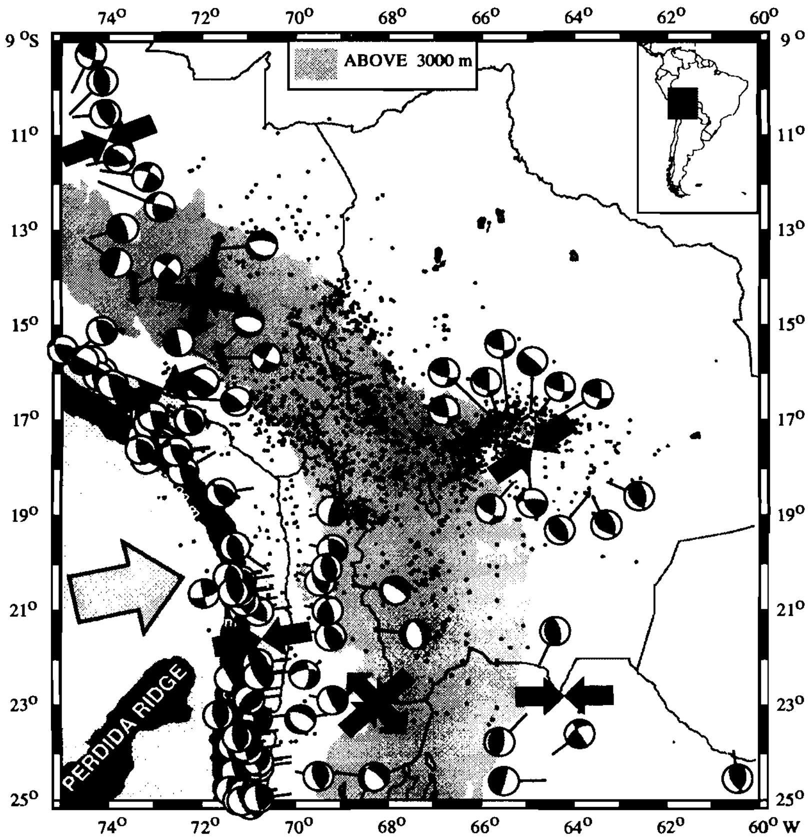


Fig. 2. Map showing the located shallow seismicity (less than 70 km depth). Balloons stand for lower-hemispheric projection of focal mechanism solutions. Convergence arrows stand for principal compressive horizontal stress direction ($\sigma_1$); big divergence arrows for principal tensional horizontal stress direction ($\sigma_3$) obtained from the inversion of focal mechanism solutions. The T-axes direction of tensional events for the High Andes is given by small divergence arrows.

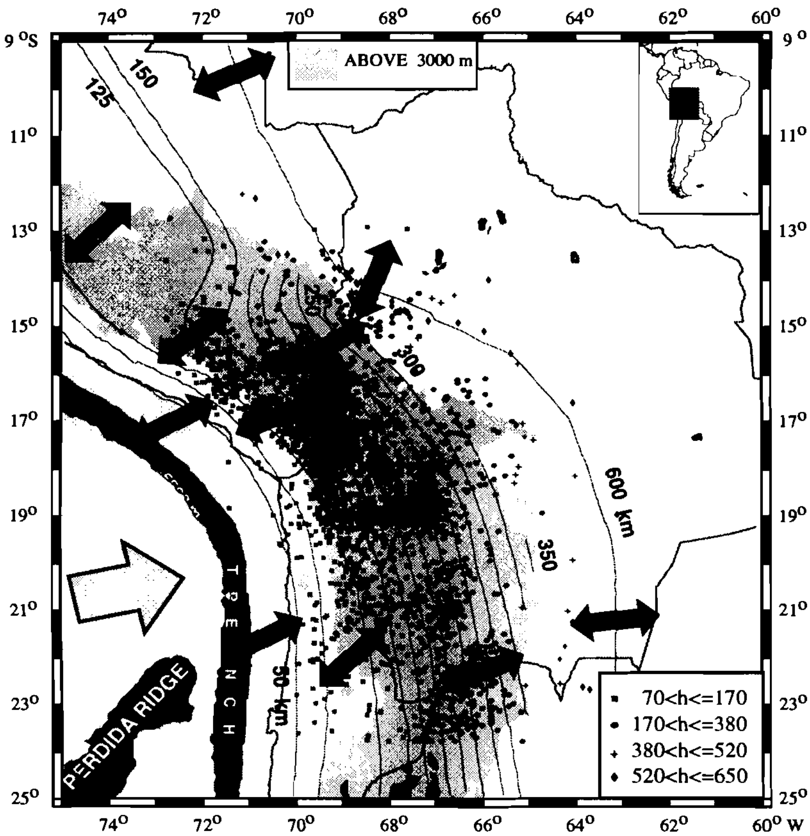


Fig. 3. Map showing the located intermediate and deep seismicity (from 70 to 640 km depth); depth contours of the Wadati-Benioff zone are from Cahill & Isacks (1992). Divergence arrows indicate principal tensional stress direction ($\sigma_3$) obtained from the inversion of focal mechanism solutions.

## STATE OF STRESS

The focal mechanism solutions for 111 shallow intraplate events and 294 subduction zone events were compilated from the literature. Other 18 focal mechanisms for shallow earthquakes include also our data. The focal mechanisms were grouped by geographic region and depth range and inverted for the orientation and relative magnitude of the stress using the method developed by Rivera & Cisternas (1990).

In the forearc region and in the Subandean Ranges the stress pattern is characterised by a ENE horizontal compressional stress ($\sigma_1$) and a vertical $\sigma_3$ (fig. 2). A horizontal tensional stress ($\sigma_3$) oriented N-S (in the north-west) and NW-SE (in the south-west) and a horizontal $\sigma_1$ characterise the western High Andes.

The stress pattern for the tensional events of the subduction zone (fig. 3) is characterised by a principal ENE tensional stress ($\sigma_3$) in the down dip direction of the Nazca plate and a vertical $\sigma_1$.

## CONCLUSIONS

There is an evidence of a correlation of the crustal seismicity with the direction of the main morphostructural units. The crustal seismicity near to the "bending of Santa Cruz" is related with the compressive forces induced by the Nazca-South American plate convergence. The Subanden Ranges and forearc region are under a triaxial compressional stress regime. Southward of the Subandean Ranges from 20°S, the principal compressional stress direction change of NE-SW to E-W following the trend of the Cordillera The western side of Andean Cordillera is under a shearing stress regime. The stress orientations calculated agreement with the stress orientations deduced from a field study of fault kinematics (Mercier *et al.*, 1992) and with the regional stress field (Assumpçao, 1992). The seismogenic interplate contact zone is about 60 km depth. The slab is dominated by a triaxial extension stress regime with a principal extensional stress direction parallel to downdip direction of the Nazca plate.

## REFERENCES

Assumpçao, M., 1992. The Regional Intraplate Stress Field in South America, *J. Geophys. Res.*, **97**, 11889-11903.

Cahill, T. & B. L. Isacks, 1992. Seismicity and Shape of the subduction of the Nazca Plate, *J. Geophys. Res.*, **97**, 17503-17529.

DeMetz, C., R. G. Argus, & S. Stein, 1990. Current plate motion, *Geophys. J. Int.*, **101**, 425-478.

Dorbath C. & Granet, M., 1996. Local earthquake tomography of the Altiplano and the Eastern Cordillera of northern Bolivia, *Tectonophys* (accepted).

Dorbath C., Paul, A. and Lithoscophe Andean Group, Tomography of the Andean Lithosphere at 20°S: Preliminary results of the Lithoscophe experiment (soumitted to EPI Letters section, 1995).

Mercier, J. L., M. Sébrier, A. Lavenu, J. Cabrera, O. Bellier, J-F., Dumont and J. Macharé, 1992. Changes in the tectonic regime above a subduction zone of Andean type: The Andes of Peru and Bolivia during the Pliocene-Pleistocene, *J. Geophys. Res.*, **97**, 11945-11982.

Rivera, L. & Cisternas, A., 1990, Stress Tensor and Fault plane solutions for a population of earthquakes, *Bull. Seismol. Soc. Am.*, **80**, 600-614.

Schmitz, M., 1993. Kollision strukturen in den zentralen Andean: Ergebnisse refraktion seismischer Messungen und Modellierung Krustaler Deformationen, 1993, Inaugural - Dissertelion zur Erlangung des Doktorgrades am Fach bereich Geowissenschaften der Frein Universital Berlin.

Wittlinger, G., Herquel, G. & Nakache, T., 1993. Earthquake location in strongly heterogeneous media, *Geophys. J. Int.*, **115**, 759-777.

# ON PREDICTING COASTAL UPLIFT AND SUBSIDENCE DUE TO LARGE EARTHQUAKES IN CHILE

Sergio E. BARRIENTOS

Depto. de Geoffsica, Universidad de Chile, Casilla 2777, Santiago, Chile

**KEY WORDS:** Crustal movements, seismogenic zone, coastal uplift

## SUMMARY

Vertical elevation changes, observed for three large earthquakes in Chile (1960, 1985 and 1995 events), are used to determine the downdip extent of the seismogenic region. Interpolation of the axis of the observed null elevation change for these three large earthquakes, as a function of their distance to the trench, to other zones of the country allow future estimations of coast uplift or subsidence.

## INTRODUCTION

In subduction zones like the Chilean convergent margin, the size of a large earthquake is determined by the length, width (updip and downdip extension) of the rupture region as well as the amount of displacement on it. The location of the downdip extension of rupture determines the position of greater subsidence -and the null elevation change axis- at the surface and concurrently, the location of greater subsidence and null coseismic change give a very good estimation of the location of the downdip end of faulting. This place is almost independent of the updip extension location. The amount of slip on the fault only acts as a scaling factor, it does not produce any change in the shape of the elevation change as a function of distance from the trench.

The most common way to estimate the downdip extension of the rupture zone is to locate the transition zone between reverse and tensional faulting along the dip of the subducted region, as revealed by earthquake focal mechanisms. In this work, we use crustal deformation observations of three large earthquakes in Chile as well as an estimation of the downward curved Wadati-Benioff zone to estimate no only the downdip extension of the seismogenetic region but the implication that its location has along the coast of Chile, i. e., expected uplift or subsidence along the coast.

## DATA and ANALYSIS

Crustal deformation has been well documented for three large earthquakes in Chile: The May 22, 1960 $M_W$=9.5, the March 3,1985 $M_W$=8.0 and the July 30, 1995 $M_W$=8.1 events, we briefly describe the related information on each event.

The 1960 earthquake has been the largest event recorded in this century (Kanamori, 1977). Remarkable changes in land levels were observed in a region 1000 km long and 200 km wide. Extreme coseismic changes ranged from 5.7 m of uplift at Guamblin Island to 2.7 m of subsidence in Valdivia. Plafker and Savage (1970) analyzed the static deformation data and presented teleseismic surface wave evidence to support their preferred uniform slip dislocation model that involved between 20 and 40 m of slip on a rupture 1000 km long by 60 km wide. Later, Plafker (1972), Linde and Silver (1989) and Barrientos and Ward (1990) revisited the deformation field concluding that the main portion of slip took place on a roughly 900-km long fault by 120-150 km wide. Fig. 1 (C and D) shows the elevation changes on three profiles according to Plafker and Savage (1970).

The $M_W$=8.0, 1985, Central Chile earthquake has been the largest event in this region since 1906. Aftershock surveys, body-wave modeling, surface wave analysis, gravimetric observations and geodetic estimates revealed a rupture length of approximately 160 km in a north-south orientation with maximum slip of about 3.5 m (Christensen and Ruff, 1986, Comte et al, 1986, Barrientos, 1988; Choy and Dewey, 1988). A first-order leveling lines, repeatedly surveyed in 1981 and four months after the earthquake, evidenced 0.5 m of uplift at the coast nearby the city of San Antonio and a 10-cm subsidence about 60 km inland. The projected elevation changes on a profile perpendicular to the coast is shown in Fig. 1(B).

The deformation field produced by the 1995, $M_W$=8.1, Antofagasta earthquake has been the first ever detected by a GPS array in Chile. This is one of the largest events during this century in the region and took place just south of the estimated rupture region of the 1877 $M_W$=8.7 earthquake. GPS observations (Ruegg et al, 1996) were made in 1992 and two weeks after the great event. Comparisons between these two groups of observations indicate relative horizontal displacement, to the east-southeast, of 0.7 m of the coastal bench marks. Those points located inland subsided several centimeters and the one located in Mejillones Peninsula was uplifted more than 15 cm (Fig. 1A).

In this work, the null axis of the elevation change profiles is the input to establish the depth of the downdip extension of the coupling region. An additional ingredient to estimate this parameter is the shape of the Wadati-Benioff zone. For the Chilean convergent margin, the shape of the Wadati-Benioff region is roughly the same down to depths of the order of 60 km (Kadinsky-Cade, 1985; Pardo et al., 1996).

As a first step, we plot the observed null elevation change points as a function of distance from the trench. Fig. 1 (left) shows a plot of distance trench-coast as a function of latitude in which are superimposed the places where null coseismic observations were made: Antofagasta, Central Chile and two for the 1960 event, labeled A, B, C and D. Those regions in which the distance coast-trench is less than the expected null elevation change (dashed line) the coast is expected to be uplifted with each large event. This is the case for the region between 26¤S and 35¤S, and the Mejillones and Arauco Peninsulas. Conversely, those regions in which the distance trench-coast is greater than the expected null elevation change will subside. This is expected for northern Chile (north of Mejillones Peninsula, 23S) and the Valdivia region.

To establish the relation between depth extent of the seismogenic zone and elevation changes, instead of using rectangular fault planes embedded in an elastic halfspace, we describe the surface changes as a product of the superposition of line sources, infinite along strike located along the seismogenic zone as described by Pardo et al. (1996). We will be presenting these results.

**Acknowledgments.** This work has been partially funded by Fondo Nacional de Ciencia y Tecnología (FONDECYT) grant 1950623.

## REFERENCES

Barrientos, S. and S. Ward, The 1960 Chile earthquake: coseismic slip from surface deformation, *Geophys. J. Int., 103*, 589-598, 1990.

Barrientos, S., Slip distribution of the 1985 Central Chile earthquake, *Tectonophysics, 145*, 225-241, 1988.

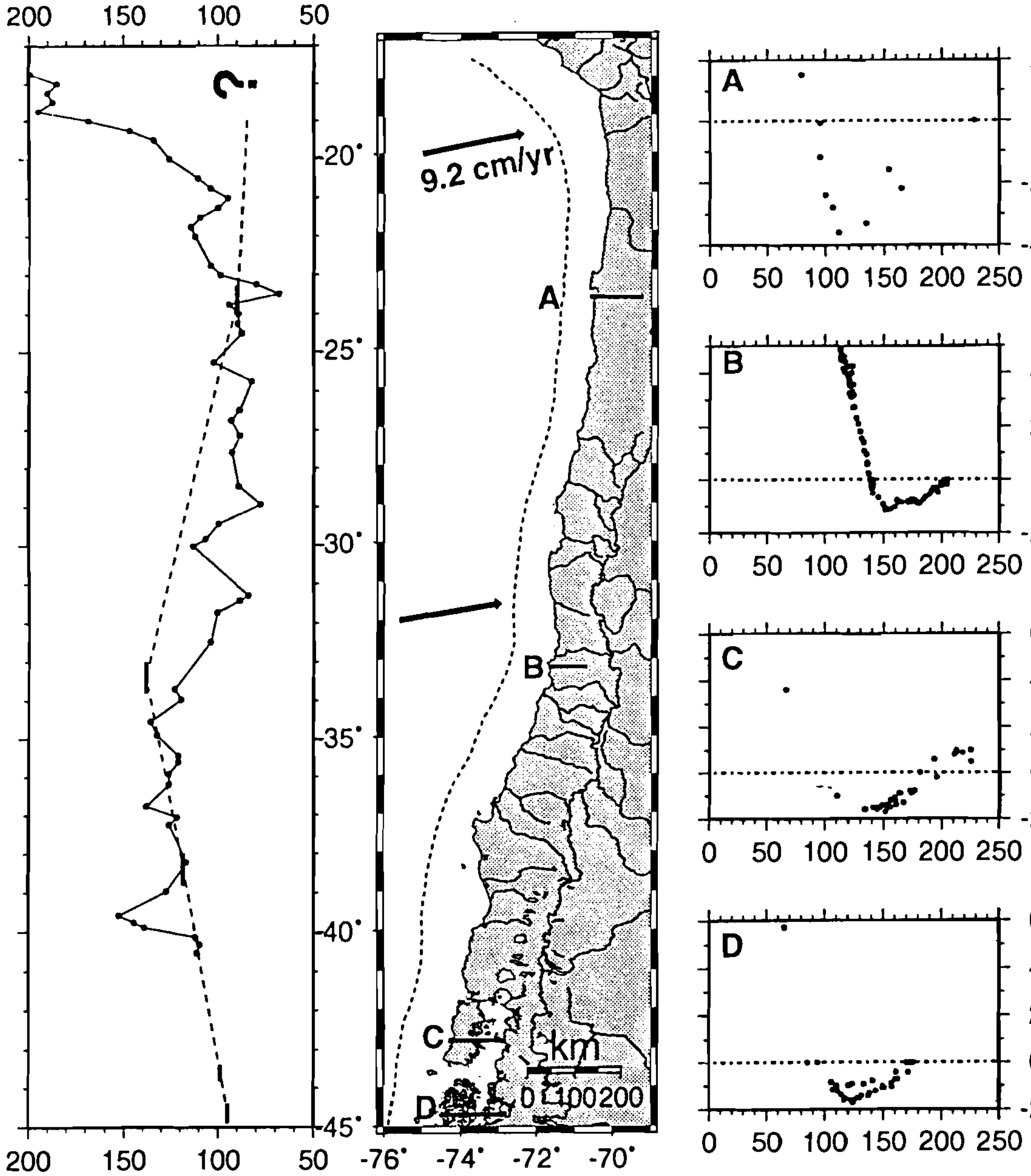


Fig. 1. Location of the trench in relation to the coast (middle) and the distance between the coast and the trench (left, solid line). The dashed line (left) is the interpolated curve of null coseismic elevation change determined from the four profiles A,B,C and D (right). If the solid line is to the right of the dashed line (25-34¤S), it means that the coast will be subjected to uplift because the trench-coast distance is less than the corresponding to the null coseismic axis. Conversely, the other regions will be subjected to subsidence.

Kadinsky-Cade, K., Seismotectonics of the Chile margin, Ph. D. Thesis, 153 pp, Cornell University, Ithaca, New York, 1985.

Kanamori, H., The energy release in great earthquakes, *J. Geophys. Res. 82*, 2981-2987, 1977.

Choy, G. and J. Dewey, Rupture process of an extended sequence: Teleseismic analysis of the Chilean earthquake of March 3, 1985, J. Geophys. Res., 93, 1103-1118, 1988.

Christensen, D. G. and L. J. Ruff, Rupture process of the March 3, 1985 Chilean earthquake, *Geophys. Res. Lett., 13*, 721-724, 1986.

Comte, D., A. Eisenberg, E. Lorca, M. Pardo, L. Ponce, R. Saragoni, S. K. Sing and G. Suárez, The great 1985 Central Chile earthquake: A repeat of previous great earthquakes in the region?, *Science, 233*, 449-453, 1986.

Linde, A. T. and P. Silver, Elevation changes and the great 1960 earthquake: support for aseismic slip, *Geophys. Res. Lett, 16*, 1305-1308, 1989.

Plafker, G. and J. Savage, Mechanism of the Chilean earthquake of May 21 and 22, 1960, *Geol. Soc. Am. Bull., 81*, 1001-1030, 1970.

Pardo, M., D. Comte, T. Monfret, E. Vera and N. González, Central Chile seismotectonics and stress distribution along the subducted Nazca plate (25-40S), ISAG, 1996, this issue.

Plafker, G., Alaskan earthquake of 1964 and Chilean earthquake of 1960: Implications for arc tectonics, *J. Geophys. Res., 77*, 901-925, 1972.

Ruegg, J. C. J. Campos, R. Armijo, S. Barrientos, P. Briole, R. Thiele, M. Arancibia, J. Cañuta, T. Duquesnoy, M. Chang, D. Lazo, H. Lyon-Caen, L. Ortlieb, J. C. Rossignol and L. Serrurier, The Mw=8.1 Antofagasta (Northern Chile) Earthquake of July 30, 1995: First results from teleseismic and geodetic data, *Geophys. Res. Lett.*, in press.

Tichelaar, B. and L. Ruff, Variability in depth of seismic coupling along the Chilean subduction zone, J. *Geophys. Res., 96*, 11997-12022, 1991.

# INTRAPLATE SEISMICITY IN CENTRAL CHILE

Sergio BARRIENTOS[(1)], Emilio VERA[(1)]
and Tony MONFRET[(1,2)]

(1) Depto. de Geofísica, Universidad de Chile, Casilla 2777, Santiago, Chile
(2) Mission ORSTOM, Chile, Román Díaz 264, Santiago, Chile

**KEY WORDS:** Seismicity, Central Chile, Intraplate seismicity

## SUMMARY

Shallow intraplate seismic activity in Chile is poorly understood. This is mainly the result of lack in association of seismic activity with recognizable fault features at the surface. This work is an attempt to understand the tectonic environment which gives rise to earthquake activity in the occidental flank of the Andes of central Chile. This region, located less that 100 km away from Santiago, has been subjected in the past to earthquakes with magnitudes up to 6.9, and several smaller shocks have taken place in the last few years. Because most of the events lie outside, to the east, of the Central Chile Seismic Network, it is essential to have an adequate knowledge of the velocity structure in the Andean region to produce highest quality epicentral locations. A north-south refraction line using mining blasts of Disputada de Las Condes open pit mine has been acquired. These blasts have been detected as far as 250 km to the south; preliminary interpretation of the travel times indicates a model consisting of 3 layers, 1.5, 5.35 and 8.6 km thick, overlying a halfspace; their associated P wave velocities are 5.2, 5.95, 6.35 and 7.0 km/s respectively.

Hypocentral relocation of earthquakes occurring in the last 10 years, using the newly developed velocity model, reveals several regions of concentration of seismicity. One of them clearly delineates the fault zone, and its extensions, of the strike-slip earthquake that took place in September, 1987. Other pockets of activity are the regions near San José volcano and the birth of the Maipo river. A temporary array of seismographs, installed in the high Maipo region, allowed us to establish the hypocentral location of events with errors less than 1 km. Focal mechanisms of these events were determined using waveform modeling of the records produced by a recently deployed broad-band seismograph at 20 km distance. Focal mechanisms indicate that the region is currently subjected to E-W compression.

## INTRODUCTION

In general, seismogenic zones in Chile are basically well established: large shallow (0-50 km) thrust earthquakes along the coast, large deeper (70-100 km) tensional events within the subducting plate, and in few places, like Magellan Strait and the cordilleran region of central Chile, where very shallow seismicity (0-20 km) occurs.

The large thrust earthquakes are located along the coast from Arica (18°S) to Taitao Peninsula (46°S). With magnitudes that can reach values over 8, these events are usually accompanied by tsunamis; their rupture extent is limited to the coupled region between the Nazca and South American plates (Tichelaar and Ruff, 1991). Their spatial and time distributions have been studied (Barrientos, 1981; Martin, 1991), so the seismic hazard due to these large events has been assessed.

More recently, the hazard produced by large, deep tensional earthquakes has been recognized. These events are caused by faulting within the subducting Nazca plate at depths between 80 and 100 km with apparently high stress drops (Kausel, 1991). A clear example of these type of events is the 1950 Calama earthquake (Kausel and Campos, 1992) and possibly the 1939 Chillán event (Beck et al, 1993).

Another seismogenic region, which has not been fully studied and quantified in the past, is the one located at shallow depths in the Andean cordillera in the central part of Chile. Two relatively large, shallow (less than 10 km depth), earthquakes have taken place in this region: September 4, 1958 (M=6.9, Lomnitz, 1961; Piderit, 1961) and September 13, 1987 (M=5.9, Barrientos and Eisenberg, 1988), the former producing a maximum Mercalli intensity of X. Only recently, with the permanent operation of the Central Chile Seismic Network (CCSN), we have recognized this region as highly active with its corresponding seismic potential (Fig. 1). After 10 years of operation of the CCSN we are now able to adequately locate the seismogenic zones as well as define their geometric characteristics and rates of activity.

The understanding of the seismotectonic phenomena in this area is crucial for the assessment of the seismic hazard in central Chile. In fact, three large mines (El Teniente, Disputada, and Andina) as well as water supply for the city of Santiago are located in this seismic area; five medium size hydroelectric plants and several smaller ones are less than 50 km away from the area of interest.

## DATA and RESULTS

To produce highest quality epicentral locations in the area we needed to establish an adequate velocity model in the Andean region and a set of station corrections, particularly because most of the events lie outside, to the east, of the CCSN.

The velocity model stems out from a north-south refraction line (Fig. 2a) using several mining blasts of Disputada de Las Condes open pit mine (70.27°W, 33.15°S) as seismic source. These blasts were recorded in some of the permanente stations of the CCSN as well as portable seismographs deployed in several complementary locations (Fig. 1) when a sufficiently large blast took place. We used the closest permanent station at Farellones as a reference for the zero- time after recording simultaneously three monitored explosions in the mine; the P-waves travel time from the mine to Farellones is 3.5 s. These blasts have been detected as far as San Fernando, 180 km to the south of the Disputada mine (Fig. 2a). preliminary interpretation of the travel times indicates a model consisting of 3 layers, 1.5, 5.35 and 8.6 km thick, overlying a halfspace; their associated P wave velocities are 5.2, 5.95, 6.35 and 7.0 km/s respectively (Fig. 2b).

Analysis of ten years (1986-1995) of shallow seismicity in the Andean region of central Chile clearly delineates the pattern of activity (Fig. 1). The most important feature is the concentration of events south of Pangal river and east of Cipreses river centered about 34.4°S and 70.2°W. This region was the site of an Ms=5.9 earthquake in 1987; the focal mechanism and aftershock distribution reveals strike-slip faulting on a NE-SW trending feature. This is mainly the result of an east-west compression. Other sites of activity are the Maipo valley, about 20 km south of Las Melosas (epicenter of the Ms=6.9, 1958 earthquake) where most of the activity began in November, 1994. Concentrated activity is also evident near Disputada de Las Condes and El Teniente, both are product of induced seismicity; blasting at Disputada and blasting and rockburtsts at El Teniente. Minor seismicity nearby San José volcano is thought to be of volcanic origin; 50% of this activity took place in the first 4 months of 1990. During this period, events with magnitudes between 3.6 and 5.0 are well represented by $\log N = 7.14 - 1.55M$ ($N$ is the annual cumulative number), but this relationship underestimates the frequency of occurrence of events with magnitudes $M > 5.5$.

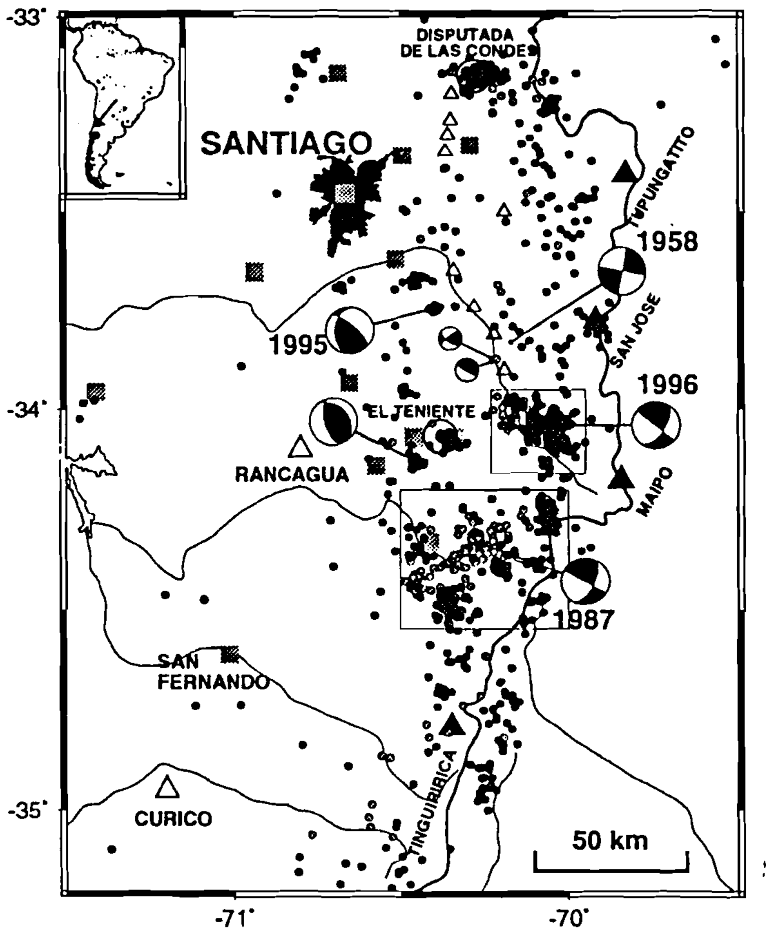


Fig. 1. Epicenters of shallow (< 20 km depth) earthquakes in the Central Chilean Andes during the period 1986-1995 as determined by the Central Chile Seismic Network (squares) of the Dept. of Geophysics of the University of Chile. The two highlighted regions are zones of recent high activity. Portable seismographs deployed for the acquisition of the refraction line (Fig.2) are represented by open triangles.

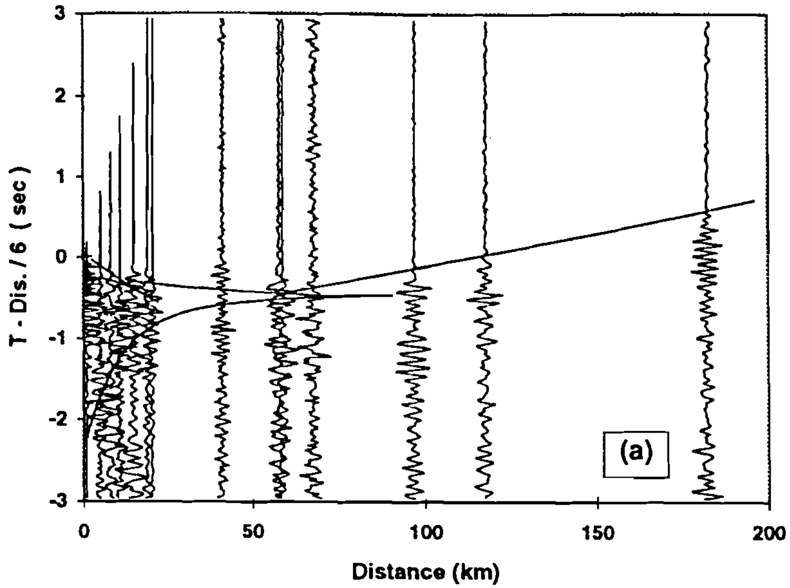


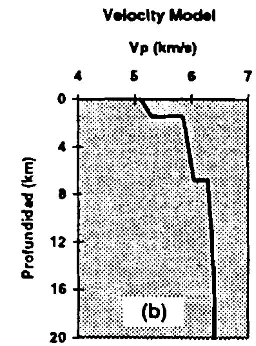


Fig. 2. Refraction profile acquired using the Disputada de Las Condes mining blasts (a). Travel time curves for the P-wave velocity model shown in (b) are superimposed on the traces. The time scale has been reduced using a velocity of 6 km/s. First arrivals are matched within few tenths of a second.

A portable network, consisting of 8 L4C Mark Products and EDA digital recorders operated for a period of one and a half month (January-March, 1996) in the region between Maipo and Volcán rivers, one the sites of highest activity in the past few years. During this period, more than 20 shallow earthquakes were recorded at 4 or more stations. We are currently analyzing the characteristics of this seismicity in addition to developing moment tensor inversion at local distances.

**Acknowledgments.** We would like to thank Patricia Alvarado for help in the fieldwork and Luis Alvear for relocating more than 10 years of earthquakes. This work has been partially funded by FONDECYT grant number 1950623 and FONDEF MI-20.

## REFERENCES

Acevedo, P. 1985. Estructura cortical y estudio sismotectónico de Chile central entre las latitudes 32.0°S y 34.5°S, M. Sc.Thesis, Facultad de Ciencias Físicas y Matemáticas, Universidad de Chile 172 pp.

Barrientos S. and E. Kausel, 1993. Características de la sismicidad andina superficial en la zona central de Chile, *VI Jornadas Chilenas de Sismología e Ingeniería Antisísmica*, Santiago.

Barrientos, S. and A. Eisenberg, 1988. Secuencia sísmica en la zona cordillerana al interior de Rancagua, *V Congreso Geológico Chileno*, Santiago, F121-F132

Barrientos, S. 1981. Regionalización sísmica de Chile, M. Sc.Thesis, Facultad de Ciencias Físicas y Matemáticas, Universidad de Chile.

Beck, S. L., T. Wallace, M. Reyes, E. Kausel and S. Barrientos, The 1928 and 1939 subduction zone earthquakes along the coast of southern Chile, *Seism. Res. Lett.*, *64*, 13, 1993.

Kausel, E. and J. Campos, 1992. The M=8.0 tensional earthquake of December 9, 1950 of northern Chile and its relation to the seismic potential of the region, *Phys. Earth Planet. Int.*, *72*, 220-235, 1992.

Kausel, E., 1991. The influence of large thrust an normal earthquakes in teh assessment of the seismic hazard, Workshop: New Horizons in Strong Ground Motion: Seismic Studies and Engeneering Practice, Santiago, Chile.

Lomnitz, C., 1961. Los terremotos del 4 de Septiembre de 1958 en el Cajón del Maipo, *Anales de la Facultad de Ciencias Físicas y Matemáticas*, *18*, 279-306, Publicación N 3, Depto. de Geofísica.

Martin, A., 1991. Hacia una nueva regionalización sísmica de Chile, Memoria para optar al título de Ingeniero Civil, Facultad de Ciencias Físicas y Matemáticas, Universidad de Chile.

Piderit, E., 1961. Estudio de los sismos del Cajón del Maipo el año 1958, Memoria para optar al título de Ingeniero Civil, Facultad de Ciencias Físicas y Matemáticas, Universidad de Chile, 125 pp.

Tichelaar, and L. Ruff, 1991. Seismic coupling along the Chilean subduction zone, *J. Geophys. Res.*, *96*, 11997-12022.

# THE EL PILAR FAULT ACTIVE TRACE (NORTHEASTERN VENEZUELA): NEOTECTONIC EVIDENCES AND PALEOSEISMIC DATA.

Carlos BELTRAN*, André SINGER* y José A. RODRIGUEZ*

*Fundación Venezolana de Investigaciones Sismológicas ( FUNVISIS )
Apartado Postal 76.880, Caracas 1070-A, Venezuela. Fax: (58-2) 257 99 77
dptoct@funvisis.internet.ve

KEY WORDS: El Pilar fault, neotectonic, active trace, geomorphologic evidences, paleoseismic events, Venezuela.

## INTRODUCTION

The El Pilar Fault, considered by many authors as the southern boundary between the Caribbean and Southamerican Plates, has generated a big controversy, even recently, because differents workers haven't agreed yet about its kinematics and its cartographic trace.

Even though this fault is the most important tectonic element in northern Venezuela (350 Km long.), only 80 Km can be followed on- shore, between Muelle de Cariaco (west) and Caño Ajies (east). Both extremities can be followed off-shore and are connected to the San Sebastian (west) and Los Bajos-El Soldado faults system (east).

## RESULTS

Neotectonics evaluation of the on-shore section (including trenching and trial pits) allowed to confirm the right lateral movement. Four segments can be differentiated along the El Pilar Fault active trace:

A.- An off-shore segment located western of Cumana), where this fault is connected to the San Sebastian fault, and generating thus two pull-apart basins (Cariaco through). This connection occurs, south of the La Tortuga Island, along two "en échelon" segments, producing a transtension zone of 30 Km long and 160 Km wide, where two deep depressions ("graben-like") can be easily identified. The pull-apart here defined is narrower than the one mentioned by SCHUBERT (1982).

B.-An 80 Km long segment, located even on shore and off-shore (Cariaco Golf), between Cumana and Casanay. A sinistral "échelon" step, produce a transpressive zone, where the Caigüire hills, have been elevated since the Pleistocene. Boths flanks of these hills, present evidences of right lateral displacement, with an important reverse component ( conic folds, knee folds and high angle reverse faults), which have been mentioned by ASCANIO (1972 ) and MACSOTAY & VIVAS (1988).

Also, shutter ridges, obturated drainages, fault trench and a offsetted creek along a secundary fault, have been identified.

A surface rupture generated during the1929-17-01 earthquake (PAIGE, 1930), indicates a right lateral displacement (Caigüire hills). Toward the east, between Cariaco and Casanay towns (Fig.1), off-seted creeks, sag ponds, shutter ridges and a Holocene scarplet, suggest also a right lateral movement.

C.- Between Casanay and El Pilar (30 Km long), numerous geomorphologic evidences of recent right lateral activity have been mapped (Fig.2). This segment shows a complex anastomosed geometry, and it's located between the Cariaco and Paria gulfs.

Between Casanay and Rio Casanay towns, the main active trace offset a middle Pleistocene colluvion deposit, and the Tunapuy limestone unit; 375 m of dextral offset can be measured along a middle Pleistocene shutter ridge, generated in the fault zone. A trench excavated in 1994, allowed to expose a 20m gouge zone associated to a flower structure geometry, with fault planes oriented E-W and containing horizontal slickensides (less than 10° pitch). Using $C^{14}$ method, we have interpreted four paleoseismic events : 7.080 ± 1.460; 5.985 ± 735 ; 5.595 ± 275 and 4.805 ± 1.050 years BP.

Along the most southern active branch, sag ponds, an Holocene scarplet ( 50 cm high), a Pleistocene scarp ( 6 m ), as well as an extruded serpentinite body mentioned by METZ (1968), have been mapped.

Between Rio Casanay and El Pilar towns, two active traces can be recognized, following a E-W direction; along these two segments, numerous evidences of recent activity ( sag-ponds, scarps, shutter-ridges ), as well as, an intense hydrothermal activity have been reported. A 10 m high scarp affects a Pleistocene detritic ramp, near Nueva Colombia, between Casanay and El Pilar.

D). several "en échelon" steps can be followed along this most eastern segment (Fig.2) ; some controlled drainages,and also, a horst-graben geometry feature can be mapped along the Holocene marsh deposits. Toward the east , in the gulf of Paria, the El Pilar fault is connected to the Los Bajos-El Soldado system, instead of continuing to the Northern Range of Trinidad (SOULAS, 1986; BELTRAN & GIRALDO, 1989 y BELTRAN, 1993 and 1994).

## CONCLUSIONS

Diagnostic evidences of active faulting along the EL Pilar fault system on-shore segments indicate a predominantly right-lateral displacement during the Quaternary. These evidences have been confirmed, by studying the coseismic structures well exposed on a trench excavated , as well as , on trial- pits, along the active trace of this fault.

## REFERENCES

ASCANIO, G. (1972 ) "Geologia de los cerros de Caigüire, Cumaná, estado Sucre". *Mem. IV Cong. Geol. Venez., Bol. Geol., Pub. Esp. 5,* 2:1279-1288.

BELTRAN, C.(1993) "Mapa neotectónico de Venezuela", esc. 1:2.000.000 *FUNVISIS, Dpto. Ciencias de la Tierra.*

BELTRAN, C. (1994) "Trazas activas y síntesis neotectónica de Venezuela a escala 1:2.000.000. *Mem. VII Cong. Venez. Geofís., Caracas, sept. 1994, Soc. Venez. Ing. Geofís.* 541-547.

BELTRAN, C. & GIRALDO, C. (1989) "Aspectos neotectónicos de la región nororiental de Venezuela" *Mem. VI Cong. Geol. Venez., Barquisimeto, 1989,* Tomo III, p. 999-1.021.

MACSOTAY, O. & VIVAS, V. (1988) "Estación 3, quebrada María de la Cruz" *In: "Excursión al Frente de Montañas, Venezuela Oriental", II Simp. Bolivariano Expl. Petrolera Cuencas Subandinas,* marzo 1988, *Soc. Venez. Geol.* 51 p.

METZ, H. (1968) "Stratigraphic and geologic history of extreme northeastern Serrania del Interior, state of Sucre, Venezuela". *Mem. IV Caribbean Geol. Conf., Trinidad,* 275-292.

PAIGE, S. (1930) "The earthquake at Cumana, Venezuela. January 17, 1929". *Bull. Seism. Soc. Am.,* 20(1):1-10

SCHUBERT, C. (1982) "Origin of Cariaco basin, southern Caribbean Sea". *Marine Geology,* 47:345-360.

SOULAS, J. P. (1986) "Neotectónica y tectónica activa en Venezuela y regiones vecinas". *Mem. VI Cong. Geol. Venez., Soc. Venezolana Geol.,* Caracas, 1985, 10:6639-6656.

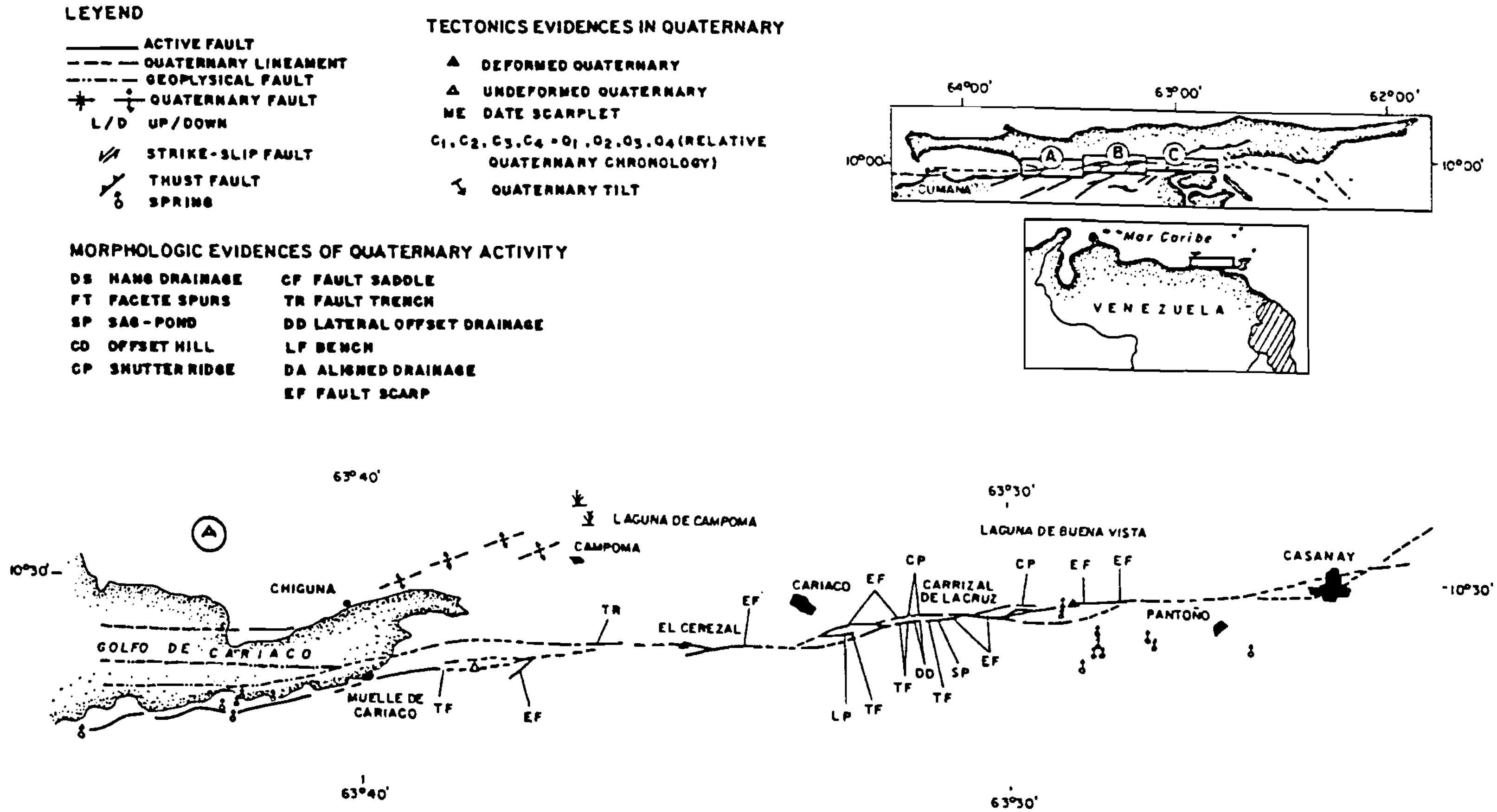


Fig.1 Geomorphic evidences of recent tectonic activity along the El Pilar active fault trace.

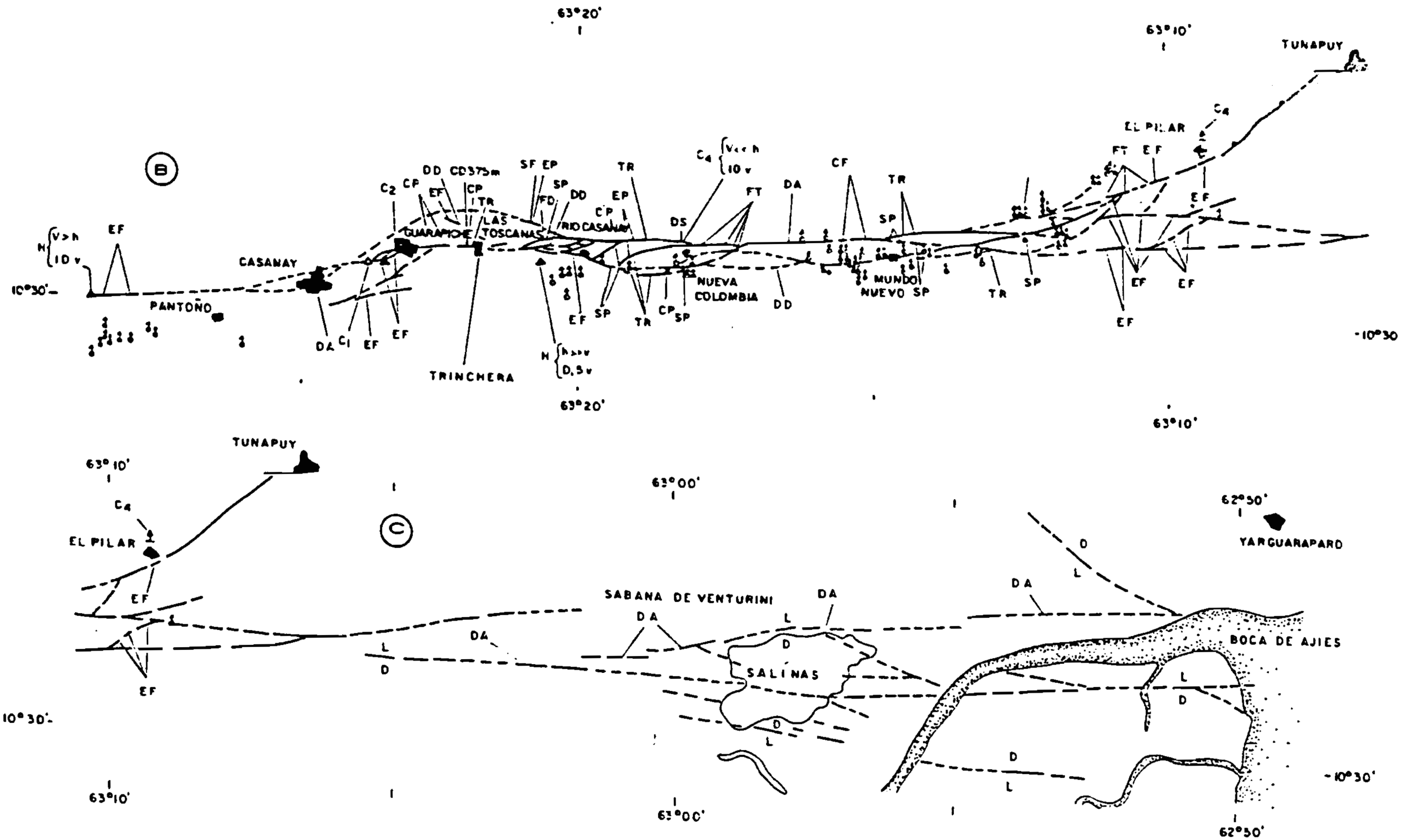


Fig.2 Geomorphic evidences of recent tectonic activity along the El Pilar active fault trace ( Continuation).

# SEISMOTECTONIC FEATURES OF THE WADATI-BENIOFF ZONE IN THE ANDEAN REGION

Jesus BERROCAL and Celia FERNANDES

Instituto Astronômico e Geofísico/Universidade de São Paulo
Caixa Postal 9638, CEP 01065-970/São Paulo, SP - Brasil
e-mail: berrocal@geofisica.iag.usp.br

**KEY WORDS:** Andean region seismotectonics, W-B zone, deep earthquakes

## INTRODUCTION

The interaction among the South American and Nazca plates forms one of the most typical Wadati-Benioff (W-B) zones existent on Earth. However, a detailed examination of that zone shows some peculiarities that cause controversies in the interpretation of its own structure, both in depth and laterally, and in the satisfactory explanation of some related phenomena, such as the origin and the mechanism responsible for the deep earthquakes in South America, among others. Some seismotectonic features of the W-B zone in the Andean region, based on the spatial distribution of hypocentres of selected earthquakes and the space-time distribution of the deep earthquakes, are presented with the purpose of contributing in the solution of some of the controversies mentioned above.

The data used in this work have been selected from the International Seismological Centre (ISC) Bulletin Data Base (BDB) CD-ROM, for the time interval January 1964 - August 1987, and from the Global Hypocenter Data Base (GHDB) CD-ROM, for the periods earlier than 1964 and after August 1987 up to December 1988. This data was complemented with hypocentre data contained in magnetic tapes furnished by the National Earthquake Information Center (NEIC/USGS), of earthquakes occurred up to June 1990. The selected earthquakes for the present work were past through a selection procedure using as reference the method of Barazangi & Isacks (1979). From a total of 9132 earthquakes with $m_b \geq 4.0$ compiled from those catalogues, only 2236 (24%) were selected as hypocentral determinations of good quality to be used in this work.

## RESULTS

The spatial distribution of the selected hypocentres is made through epicentral maps and profiles corresponding to portions of the Andean region with the seismic foci projected into vertical sections that follow the assumed direction of the Nazca plate subduction. These projections clearly show several known seismotectonic features of this W-B zone, as for instance the flat portions of W-B zone located at around 30°S in Central Chile/NW Argentina and in Central/Northern Peru and the absence of seismic activity among 300 and 500 km of depth, as discussed in Barazangi & Isacks (1976, 1979), James (1978), Hasegawa & Sacks (1981), Boyd et al. (1984), Smalley & Isacks (1987), among others.

The seismic sections also show some evidences of a twisted W-B zone, specially beneath the Peru-Chile-Bolivia-Argentina borders region, as shown by Schneider & Sacks (1987), and the existence of some probable lateral discontinuities between portions of the W-B zone, that have different behaviour.

This can be seen in the sections for the portion 25°S-32.5°S where the flat slab in Central Chile does not seem to correlate with the deep earthquakes of NW Argentina. The continuity of the slab in depth is more evident in the sections corresponding to the portion 20°S-25°S. The last sections suggest the presence of two kinds of slab with different characteristics: 1) a 25 km thick slab dipping from the trench with an angle of near 20° down to a depth of no more than 150 km, as a continuation of the slab portion near the trench in Central Chile, and 2) a 40 km thick slab dipping with an angle that increases from 30°, near the trench, to almost 45° at 300 km of depth, that apparently continues dipping through the aseismic gap, up to meet the deep focus earthquakes. These features suggest the existence of a lateral discontinuity that begins near the Arica elbow and passes through the southern extreme of the deep earthquakes epicentral area in NW Argentina as proposed by Berrocal (1974). The transverse sections in the other portions of the Andean region do not show conspicuous profiles of the W-B zone, specially in the northern latitudes.

The longitudinal S-N section shown in Fig. 1, permits to correlate the deep earthquakes with features of the slab suggested by the spatial distribution of shallower seismicity, mainly in the central portion of the Andean region, suggesting the continuity of the W-B zone, both in depth and laterally. The depth of the W-B zone gradually increases from around 50 km in its southern extreme (45°S) up to depths of the order of 200 km at 27.5°S. Then comes a gap of intermediate depth activity in 27.5-26°S, followed by a decrease on the depth of the slab to around 100 km up to 25°S. The characteristics of the W-B zone following to the north, clearly change between 25°S and 24°S. Here the seismic activity gets deeper, going rapidly from 150 km to almost 300 km of depth at 23°S. This block of the W-B zone, located beneath northern Chile and southern Peru, is extended up to latitude 14.5°S and seems to correlate well with the almost S-N oriented Southern Segment of deep earthquakes located in northern Argentina and southern Bolivia, as shown in Fig. 1. That interpretation suggests that the Nazca plate subducting between 23°S and 14.5°S, is being twisted relatively to the South, in such an amount that the deep extremes of this portion of the slab are beneath latitudes 29°S and 17°S, respectively. This interpretation may explain the suggested existence of two different slabs in Northern Chile.

After 14.5°S the seismic activity gets shallower from 250 km to around 100 km of depth and increases a little up to around 150 km just to the North of 10°S. This forms a block of the W-B zone beneath Central Peru that seems to correlate with the Central Segment of the deep portion of the slab with scarce seismicity, where occurred the $M_w$ 8.3 deep event of June 1994 under the Peru-Bolivia border region. The surface projection of the Central Segment of deep earthquakes follows the SE-NW direction, suggesting that the slab is still twisted to the South, in a smaller amount than the southern portion, but bent to the NW. Then come a small gap of intermediate depth activity followed by a sudden increase of activity among 150 and 200 km of depth beneath 9°S that keeps constant until around 1°S, where it ends abruptly, with the slab bent northwards. That forms another block of sallower activity that can be correlated with the Northern Segment of deep earthquakes located between latitudes 11°S and 1.5 °S, beneath the Peru-Brazil border region and southern Colombia. The Northern Segment of deep earthquakes is fairly active only in its southern portion, between 11°S and 6.5°S, then follows a large inactive portion up to its northern extreme where have occurred the $M_w$ 8.2 deep earthquake of July 1970 and other two large deep events, in 1911 and 1922. This portion of the W-B zone related to the Northern Segment of deep events is less twisted to the South than the portions related to the Southern and Central segments of deep earthquakes, specially its northern extreme.

The space-time distribution of deep South American earthquakes (h>500 km), using all data existent in the catalogues mentioned above covering the interval from 1911 to present, shows that consistent data for this type of events exists only since the 1960's. The three segment of deep earthquakes are evident in the latitude/time distribution, showing the following peculiarities: 1) the activity in terms of the number of events, is higher in the Southern Segment and very low in the Central one; 2) the southern portions of the Southern and Northern segments of deep earthquakes are the most active within each segment; 3) the activity in the portion between 27°S and 29°S is continuous along the last 35 years, whereas the other portions of deep earthquakes present large periods of inactivity, some of them of several years; 4) the activity in the northern portion (18°S-22°S) of the Southern Segment has increased from six events in the interval 1960-1980, to ten events in the last 15 years; and 5) the scarce activity in the Central Segment increased from three earthquakes occurred in 1958 (2 events) and 1969 (1 event) to three important earthquakes occurred in the last two years, including the $M_W$ 8.3 deep event of June 1994 and its aftershocks.

Time correlation between reliable hypocentral determinations for deep South American earthquakes is possible for events occurred since 1964. There is a clear correspondence among events in the Southern Segment with the earthquakes of the Northern Segment suggesting an interchange of energy from south to north, that during the 1964-1968 period use to occur with an interval of a few days to a few weeks. During the second half of 1968 that interchange suddenly stopped, the deep activity in the Northern Segment also stopped, a few months later occurred in the Central Segment of deep earthquakes an unusual event at around 13°S in the Peru-Bolivia border region, and the suggested flux of energy apparently inverted its direction, modifying completely the seismicity behaviour in the Southern and Northern segments, in relation to that observed in the 1964-1968 period. After this inversion, that lasted up to the end of 1969 or beginning, the $M_W$ 8.2 deep earthquake of July 1970 occurred in southern Colombia. It was a milestone event in South American seismotectonic activity, because its occurrence was preceded and followed by clear changes in the seismic behaviour of the entire deep portion of the W-B zone beneath the Andean region, but specially in the Northern Segment, that presented very low rates of activity up to the end of 1982.

During the last five years, deep activity in South America has been very high, reaching very unusual rates, including the Central Segment. This, together with the changes occurred before and after the July 1970 deep event in the northern extreme of the Northern Segment, and the probable time correlation between the events of the Southern and Northern segments of deep earthquakes in South America, suggests the lateral continuity of the slab under the central portion of the Andean region.

## CONCLUSIONS

The space-time correlation of deep South American earthquakes, and its apparent correlation with shallower seismic activity in the W-B zone, beneath the central portion of the Andean region, suggests the continuity of the slab, both in depth and laterally, in the central portion of that region. They also suggest the slab being twisted to the South, with more intensity in its southern deep extreme and almost nothing in the northern extreme, with its central portion bent to the West. This new model of the W-B zone under the Andean region may help to solve some of the existent controversies.

## REFERENCES

Barazangi M. and Isacks B.L. 1976. Spatial distribution of earthquakes and subduction of the Nazca plate beneath South America. Geology, 4, 696-692.

Barazangi M. and Isacks B.L. 1979. Subduction of the Nazca plate beneath Peru: evidences from spatial distributions of earthquakes. Geophys. J.R. astron. Soc., 57, 537-555.

Berrocal J. 1974. South American seismotectonics from SAAS data. Ph.D. theses, Edinburgh University, Scotland - UK, 240 pg.

Boyd T., Snoke A.,Sacks I.S. and Rodriguez A. 1984. High resolution determination of the Benioff zone geometry beneath southern Peru. Bull. Seismol. Soc. Am., 74, 557-566.

Giardini D. 1986. Terremoti profondi. PhD. thesis, University of Bolonha, Italy, 188 pg.

Hasegawa A. and Sacks I.S. 1981. Subduction of the Nazca plate beneath Peru as determined from seismic informations. J. Geophys. Res., 4971-4980.

James D. 1978. Subduction of the Nazca plate beneath Central Peru. Geology, 6, 174-178.

Schneider J.F. and Sacks I.S. 1987. Stress in the contorted Nazca plate beneath Southern Peru from local earthquakes. J. Geophys. Res., 92, 13887-13902.

Smalley R.F. and Isacks B.L. 1987. A high-resolution local network of the Nazca plate Wadati-Benioff zone under Western Argentina.

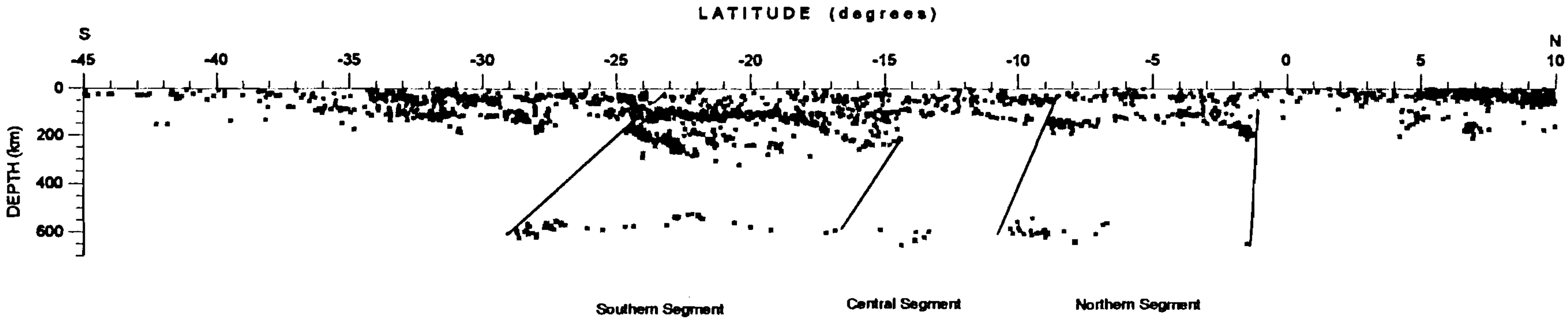


Figure 1.- South-North longitudinal section of Andean seismicity, showing only selected hypocentres in the time interval 1964 - 1990, except for the Central Segment where are included the deep earthquakes occurred after 1994.

# SOCIAL SEISMOLOGY : THE EARTHQUAKE RISK MANAGEMENT PROJECT IN QUITO, ECUADOR

J.-L. Chatelain[1,2], B. Guillier[1,2], H. Yepes[2], J. Fernandez[2], J. Valverde[2], B. Tucker[3], M. Souris[1,4], G. Hoefer[3], F. Kaneko[5], T. Yamada[5], G. Bustamante[4], C. Villacis[5].

1 ORSTOM, Quito, Ecuador.
2 Escuela Politecnica Nacional, Quito, Ecuador.
3 GeoHazards International, Stanford, USA.
4 Ilustre Municipio de Quito, Ecuador.
5 Oyo Corporation, Saitama, Japan.

KEY WORDS : seismic scenario, risk mitigation, social seismology, hazard, Ecuador, Quito

**Introduction**

The worldwide threat from earthquakes is growing : in 1900, one of every three large earthquakes killed humans, while today nearly two out of three are fatal. Earthquakes are not more frequent nor more powerful, rather, the number and size of vulnerable cities is growing. The world's urban population is dramatically increasing : from about 30% of the world's population in 1950 it is expected to reach roughly 50% by 2000. This growth is absorbed by cities becoming larger and more vulnerable : in 1950, only 25% of the world's 50 largest cities were located within 200 kilometers of an historical magnitude 7 earthquake compared to about 50% in the year 2000.

As countries become more developed, earthquakes cause fewer deaths and greater economic losses : the 1987 Loma Prieta earthquake (USA) caused 62 deaths and $4.7 billion of economic losses in and around San Fransisco, while a similar sized earthquake in Spitak (Armenia) killed over 20000 people and $570 million of economic losses. The economic loss in Spitak represented 95% of Armenia's GNP, while the loss from the Loma Prieta Earthquake represented only 0.2% of the United States GNP.

The Quito earthquake risk management project is a pilot project in social seismology launched in a developing country. Its purpose was to provide direction to government officials, business leaders, and the public in general, to reduce damage and injury in the next major earthquake. The scientific work involved institutions from Ecuador, Canada, France, Japan and the United States, in the fields of seismology, geology, soil mechanics, structural engineering, and city planning.

The project was divided into three phases. In the first, damaging earthquakes and their effects on Quito were analyzed. In the second, the impact on life in Quito during the month following one of these earthquakes was described in vivid, non technical terms. Finally, based on the first two phases of the project, recommendations for managing Quito's earthquake risk were formulated by a group of Ecuadorian and international specialists.

To provide objectivity, a group of international experts in the various fields involved in the project was formed. Its task was to check and endorse the work done. A group of potential users of the data was also formed in order to insure that the results of the project could be used. This group included representants of the local authorities, the main economical elements (e.g., banks, insurance, industry, and commerce) and the agencies responsible for the city services (e.g., water, electricity, sewage, and streets system).

**Why an earthquake risk management project in Quito ?**

Out of the 23 events felt in Quito with an intensity of VI or bigger since 1541, 8 produced intensities of VII or bigger in 1587, 1627, 1698, 1755, 1797, 1859, 1868, and 1923.

The past damaging earthquakes occurred while Quito was quite different from the modern Quito. The city has changed significantly in the last 40 years. In that period, the population increased from 420 000 to 1.2 million, with a considerable expansion of the city. This has resulted in increased urban densities, which, linked to expanding poverty, have resulted in an increase in poorly-constructed buildings and development in hazardous areas such as steep mountain slopes. In addition, high-rise buildings that did not exist in the 1950's have spread in the northern lower lands as a result of a more dynamic economy. Furthermore, the outcome of this dramatic growth is uncontrolled development and construction practices. Apart from the city's large modern structures, most dwellings in Quito were constructed without engineering guidelines. The Quito of today and tomorrow will respond to repetitions of the large historical earthquakes in very different ways than the Quito of the past.

It is expected that because of Quito's growth and earthquake history, the city's vulnerability will increase in the future unless concerted action is taken. While in 1990 the city began drafting a detailed development plan, in which earthquake hazards were taken into account, the inadequacy of available data hampered efforts to enhance the city's earthquake preparedness through planning guidance.

In order for the residents of Quito - including government officials, business leaders and the general public - to prepare for the next major earthquake, they must first understand the earthquake threat and the effects that a destructive earthquake will have on Quito. Only then can Quito begin a risk reduction program to reduce damage and loss of life in the next major earthquake.

**Description of the project**

First phase : future earthquakes and their effects on Quito.

The objective of this phase was to determine the effects of several possible damaging earthquakes on the city. Five steps were taken to reach that objective :

1.- Selection of several possible earthquake sources (location, magnitude) that could threaten the city. From an analysis of the historical seismicity and the distribution of seismogenic structures of the country, ten possible earthquakes with destructive potential for the city of Quito were identified. Three representative earthquakes were selected for detailed analysis :

a.- An inland earthquake of magnitude 7.3 and epicentral distance of 80 km from Quito, selected as a representative earthquake in the subandean region, in the zone of the 1987 earthquake.

b.- A coastal earthquake of magnitude 8.4 and epicentral distance of 200 km, selected because studies indicate a 60% probability of occurrence before the year 2000.

c.- A local earthquake of magnitude 6.5 and epicentral distance of 25 km. The 1990 Pomasqui earthquake indicated that the Catequilla fault is active, and the geometry of the fault

indicates that it has the potential for generating a larger magnitude earthquake. This earthquake is also modeling the 1587 earthquake located, possibly, on an active North-South trending fault.
At the same time, twenty-three earthquakes that produced intensities of VI or greater during Ecuador's 460 years of written history, which includes 1104 seismic intensity observations, were used to establish attenuation relations for the country, which were then corrected for application to the city of Quito.

2.- Division of the city into seismic zones : soil characteristics were obtained from over 2,000 drillings from various sources (e.g., private consultants, municipality files, and EPN studies). Based on topography, soil characteristics, and surface geology the city has been divided into 20 zones. For each of these zones a representative soil column was established down to a depth of 20 meters, usually not reaching the base rock, whose depth is unknown.

3.- Evaluation of the intensity distribution in the city based on these zone to prepare seismic intensity distribution (SID) maps for each of the three chosen earthquakes. Intensities in the 20 zones were computed using soil models and seismic responses, peak accelerations and soil amplifications, for the 3 hypothetical earthquakes, leading to the following results intensity ranges : subduction earthquake : 5.6 - 6.1 ; inland earthquake : 6.1 - 6.9 ; local earthquake : 6.3 - 8.0
These results were checked by comparing the computed intensity with observed intensities for the 1987 event.

4.- Evaluation of the location and distribution of different structural types (buildings, houses) throughout the city. Fifteen main types of structures were identified in Quito. Among those, each of the 9 most common types of buildings were subdivided in three categories, according to building heights. Then, each city block has been classified according to its predominant structural system, i.e. the structural type that covered the greatest area of the block.
In order to estimate the structural vulnerability of the structures, some buildings that we considered as representative of each type of structures were evaluated individually. Special structures such as hospitals, schools, industrial facilities, as well as the sewage system, water reservoir tanks, transmission towers, gas and oil stations near the city, and the airport were inspected individually with more scrutiny.

5.- Evaluation of the consequences of the intensity distribution on the buildings and city services. Physical damage caused by ground shaking was estimated using a relationship between the damage factor versus Modified Mercalli Intensity scale. In the method used, the damage factor is defined as the ratio of the estimated cost due to earthquake damages divided by the facility replacement value. We considered 7 states of damages : none, slight, light, moderate, heavy, major, destroyed. Finally, the time of recovery for lifelines was estimated. The method has been tested by comparing computed damages to observed damages for the 1987 earthquake.

Second Phase : a month in Quito following a future earthquake.

The scientific analysis of this project, while providing detailed estimates of damage from potential earthquakes, does not communicate the impact of such disasters. The purpose of the second phase of the project was to describe life in Quito during the month following the local earthquake, in order to help government officials, emergency service planners, business leaders and the general public to visualize the consequences of a future major earthquake, and provide the motivation and understanding required to act. The scenario is based on the scientific analysis of the local earthquake and a vulnerability study of Quito's city services, public buildings, and infrastructure.
The vulnerability study was performed by interviewing officials from 17 different city organizations, including sewer, water, power and transportation departments, Civil Defense, and fire and police departments. In a multi-stage process, the interviews were written up and returned to the interviewees

for review. The revisions then underwent further scrutiny at a meeting grouping all participants to the interviews. From this process, a detailed understanding of public services and the functioning of the city was gained and then used to estimate the earthquake's consequences.
The seismic hazard and damage assessments as well as the interviews were combined into a vivid description of possible consequences of the local earthquake. The scenario described the consequences of the earthquake in 6 parts : when the earthquake strikes, one hour later, the first 24 hours, and then at 2 days, 1 week, and one month.

Third phase : Proposition of recommendations to minimize the consequences of the next major earthquake on the city.
After the scientific analyses were reviewed by the international advisory committee, international and Ecuadorian specialists from the fields of business and industry, city government, city planning, emergency services and lifelines met for a two-day workshop in Quito. After estimating the effects on such factors as production capacity, employment, sales and services, the participants developed lists of specific recommendations within their field of expertise for reducing earthquake risks in Quito. For each recommendation, the participants described the steps necessary and the sources of funding, the responsible agencies, and expected start and completion dates. The primary recommendation was the establishment of a Seismic Safety Advisory Board, whose responsibility would be to review, revise and then administer a Seismic Hazard Reduction Program. Other high priority recommendations include projects concerning existing facilities, new facilities, earthquake planning, earthquake recovery and further research needed to improve the findings of this projects.

**Conclusion**

Because of this project, different scientific groups worked together towards a common goal, which would not have happened otherwise. It was an opportunity to gather and evaluate all earthquake related data for the country. It integrated existing research data and results that were previously scattered in different institutions, and presented them to international experts in each field, seeking their critique. Also, through this project we were able for the first time to convince the Mayor and the other civic leaders that the city was threatened by earthquakes.

This project is only a beginning at defining Quito's seismic hazard. The results represent the state of knowledge presently available in Ecuador for evaluating the seismic risk in the Capital city. In addition, it is a diagnosis of the research needed for making more reliable seismic damage assessments, as well as for improving the awareness of seismic hazard in the city, among the local government, utility managers, emergency services, private sector and the people living in the city.

These results are noteworthy because they reflect decades of work in the fields of seismology, soil engineering and structural engineering. They also represent five years of effort made by the Planing Service of the municipality to map the city on a computer with ORSTOM's GIS Savane©. Without all this previous information, it would have been impossible to accomplish our job in only one and a half years.

Finally, one of the main goals of the experiment was to raise awareness about the seismic threat in Quito. The project has been widely published by Ecuadorian newspapers and presented on TVs and radios as well as in professional journals and presented in various meetings. An overview of the project has been published and distributed to the politic and economic leaders. As consequences of this project, a seismic safety commission has been set up by the Municipality, a seismic code is under way and a project to retrofit several of Quito schools has been launched.

# NEOTECTONIC MAP OF THE ATACAMA FAULT ZONE (CHILE) FROM SAR ERS-1 IMAGES

Jean CHOROWICZ, Jean-Claude VICENTE, Pierre CHOTIN and Catherine MERING

Département de Géotectonique, URA CNRS 1759, Case 129, Université Paris 6, 4 place Jussieu, 75252 Paris cedex 05, France

KEY WORDS : ATACAMA, CHILE, FAULTS, NEOTECTONICS, RADAR, REMOTE SENSING

## INTRODUCTION

The Atacama Fault Zone (AFZ) runs for more than 1,100 km long and 30 to 50 km large in northern Chile. Mapping of the neotectonic fault pattern is needed in the frame of fault activity analysis. For analysis of large regions, satellite imagery has already proved to be an efficient tool allowing estimate of finite displacements along faults (Mercier et al., 1992; Chorowicz et al., 1995). Radar imagery is particularly convenient because it accentuates topographic features, specially scarps and thalwegs which mainly express neotectonic structures. The aim of our work is to map the neotectonic faulting from radar imagery.

## THE ATACAMA FAULT ZONE

The Northern Chilean Coastal Cordillera (Fig.1) has suffered several tectonic events since the beginning of the Andean cycle in late Triassic time (Scheuber and Reutter, 1992; Scheuber et al., 1994). In the early Jurassic, the Andean back-arc basin was separated from the Pacific Ocean by a volcanic arc. A first tectonic event in the late Jurassic-early Cretaceous prompted intra-arc ductile deformation, including 1 km wide mylonitic shear zones along the N-striking Atacama fault zone (Scheuber and Andriessen, 1990; Scheuber, 1994). In the early Cretaceous a belt was formed in the west, probably in a compressive (or transpressive ?) regime (Turner et al., 1984). In mid-Cretaceous time (Peruvian event), the Andean basin suffered compression. From Oligocene to Miocene, extensional regime occurred. Since the late Miocene, the AFZ has suffered major brittle reactivations, continuing until Present. All these events have produced fault activity and our aim is to map the neotectonic active faults only.

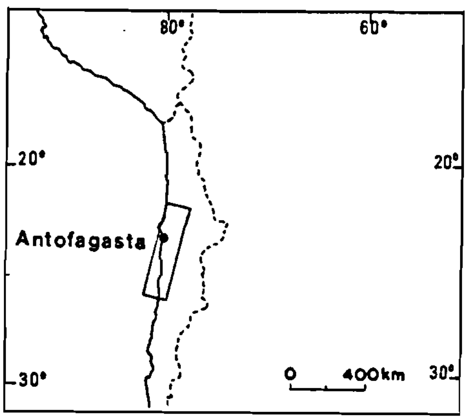


Figure 1. Location of the studied area and example of SAR ERS image.

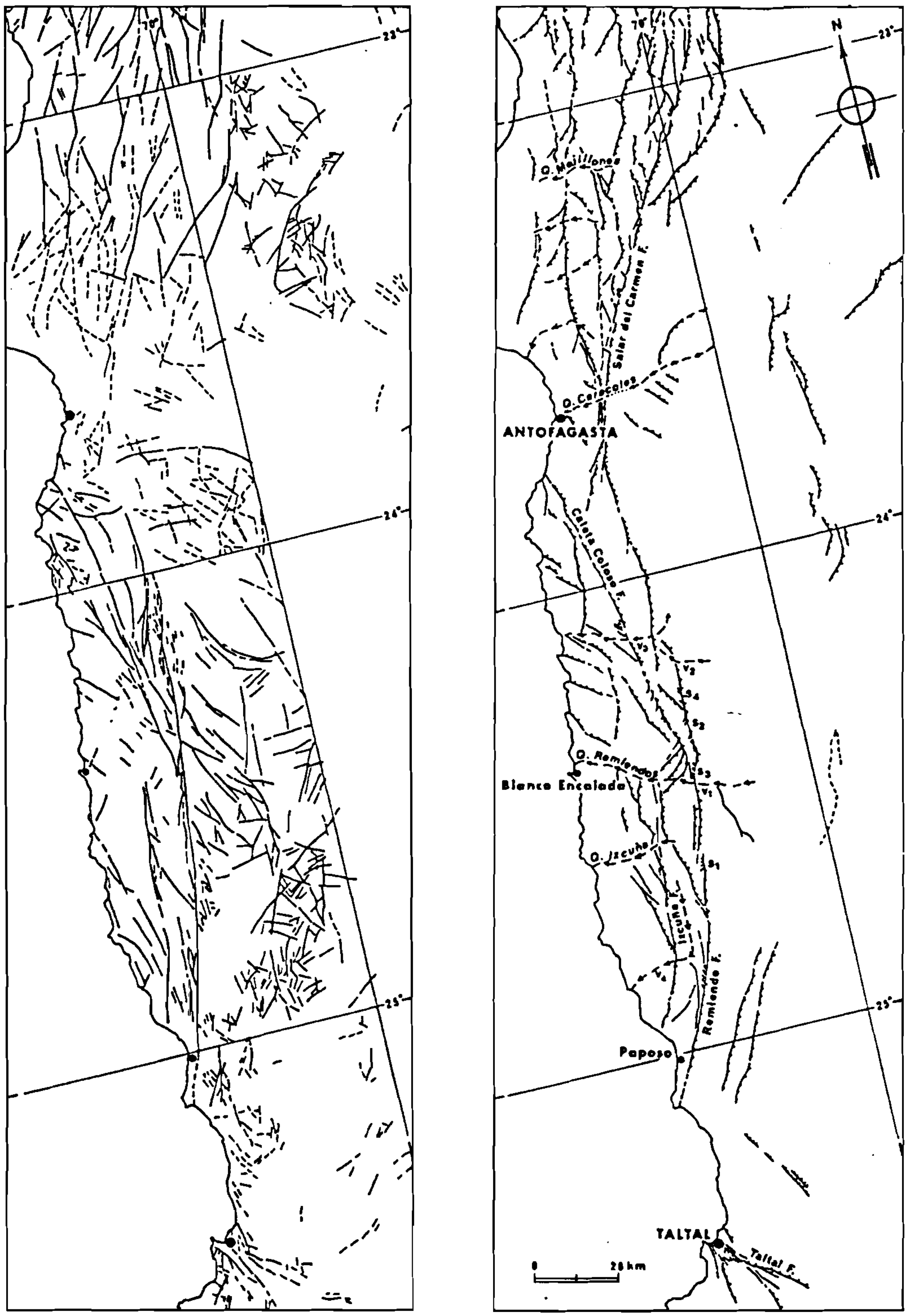


Figure 2. Comparative maps of the AFZ fault pattern. Left: faults previously mapped; right: neotectonic faults drawn from radar image analysis.

*-We have analysed a set of Synthetic Aperture Radar (SAR) scenes of the first European Remote Sensing (ERS-1) satellite. ERS-1 was launched on July 1991. This satellite views the earth surface using a SAR operating in band C (5.3 GHz). Each scene covers an area 100 x 100 km. From the original records with 12.5 m ground pixel size, we have generated images yielding 25 m ground resolution. Images were produced at 1/250,000 scale, in negative prints (Fig.1). This type of presentation of the image has the advantage to display saturated slopes facing the radar in dark, giving the impression of shadows, and is more convenient for geological analysis. These slopes are anyway poor in information because of shortening and layover. Slopes backing the radar are then clear and give the impression to be illuminated. They are rich in information because stretched.

In the study area, active faults can be identified from continuous scarps. Some have been first described by Okada (1971), and afterwards by other workers who sometimes changed the names. When possible, we below preferably use the original terminology from Okada (1971). Active faults are characterised by scarps changing in height along the strike. Most of fault scarps in the studied area look east, nearly at right angle to the radar beam illuminating the scene from ESE. The fault scarps are more or less straight in the whole, but in the detail they present acute changes in direction.

## RESULTS

Many of the faults we have observed on the radar images had been previously partly mapped (Fig.2). However, radar imagery has significantly enhanced the mapping of the neotectonic fault system. There is also a number of ancient (lower Cretaceous to early Cenozoic) faults previously mapped, which are not portrayed on the images. Some faults are underlined by distinct scarps but they also are partly overlain by recent deposits. We classify these faults as 'recent but inactive'. The radar system principally displays changes in the relief due to recent (post-Miocene) deformation. The radar images also show regular back-slopes of large dimensions (10 km in the east-west direction.) which all dip westwards. The back-slopes are principally regular planes of tilted blocks, typical of an extensional regime, and we consequently consider that the faults are normal. Reverse faults would have been associated with topographic domes corresponding to anticlines. Most of the Neogene basins located along the footwall are half-grabens. The major faults have already been described as normal and not reverse (Ferraris and Di Biase, 1978; Gonzales et al., in press) dipping 60° to the east.

In the northern Region, the N30°-striking Salar del Carmen major fault divides the region into two domains : (i) to the east, a few inactive but recent (distinct scarp) faults are overlain by late Quaternary deposits; (ii) to the west, the Coastal Cordillera is cut by several active faults. Most of the largest faults strike N160 to N170°. A few smaller faults strike N00 to N20°, and connect southward with the Salar del Carmen fault. The Ordonez fault strikes N170 to N190°.

In the central Region, the faulted part of the Coastal Range is easterly bounded by the N-striking Remiendo fault, facing east (Okada, 1971, referred as the Paposo fault by Hervé, 1987). In the east of the region, the fault scarps are ancient because they are eroded and partly burried under recent deposits.

In the southern region, the Coastal Range is easterly bordered by the Remiendo fault. More to the south, the Atacama fault system reappears on land but the pattern is very different. The coastal range is bounded by the El Salado fault, trending north, quite the same direction as the Remiendo fault. Another N-striking fault is noticed inside the range. These faults are cut to the north by the Taltal N130° striking faults, lying at high angle to the Atacama system.

## CONCLUSIONS

SAR ERS imagery has permitted a pertinent discrimination between neotectonic and more ancient faults. The overall fault zone geometry is that of normal faulting bounding west-dipping tilted blocks.

ACKNOWLEDGEMENTS

We thank the European Space Agency for providing ERS SAR data in the frame of research project AO.F7.

REFERENCES

Chorowicz J., Luxey P., Yürür T., Rudant J. P., Gündogdu N. and Lyberis N. 1995. Slip motion estimation along the Ovacik fault near Ercinzan (Turkey) using ERS1 radar image. *Rem. Sens. Environment*, 52, 66-70.

Ferraris F. and Di Biase F. 1978. Hoja Antofagasta. Inst. Inv. Geol. Chile. Carta Geologica Chile 1:250.000, n°30, 48 pp.

Gonzales L.G., Niemeyer R.H. and Martinez D.L.R. in press. Evolucion tectonica cenozoica del borde continental el las inmediaciones de Antofagasra : su relacion con la sedimentacion y la morgologia. Revista Geol. Chile.

Hervé, A. 1987. Movimiento normal de la falla Paposo, Zone de Falla Atacama, en el Mioceno. Chile. *Rev. Geol. Chile*, 31, 31-36.

Mercier J.L., Sébrier M., Lavenu A., Cabrera J., Bellier O., Dumont J.F. and Marchare J. 1992. Change in the tectonique regime above a subduction zone of Andean type: the Andes of Peru and Bolivia during the Plio-Pleistocene. *J. Geophys. Res.*, B.8, 11,945-11,982.

Okada A. 1971. On the neotectonics of thee Atacama region. Preliminary notes on late Cenozoic faulting and geomorphic development of the Coast range of Northern Chile. *Bull. Dept. Geography Univ. Tokyo*, 3, 47-65.

Scheuber E. and Andriessen P.A.M. 1990. The kinematic and geodynamic significance of the Atacama fault zone, norhtern Chile. *J. Struct. Geol.*, 12(2), 243-257.

Scheuber E. and Reutter K.J. 1992. Relation between tectonics and magmatism in the Andes of Northern Chile and adjacent areas between 21° and 25°S. *Tectonophysics*, 205, 127-140.

Scheuber E., Bogdanic T., Jensen A. and Reutter K.J. 1994. Tectonic development of the North Chilean Andes in relation to plate convergence and magmatism since the Jurassic. In: *Reutter K.J., E. Scheuber & P. Wiggereds*, Tectonics of the Southern Central Andes, Springer, 121-139.

Scheuber E. 1994. Tektonische enwicklung des nordchilenischen aktiven kontinentalandes : der einflub von plattenkonvergenz und rheologie. *Geotektonische Forschungen*, 81, E. Schweizerbart'sche Verlaysbuch, Stuttgart, 131p.

# EXTENSIONAL STRESS REGIME IN THE ANTOFAGASTA COASTAL AREA (NORTHERN CHILE)

B. DELOUIS[1], H.PHILIP[2], L. DORBATH[1,3]

1. Institut de Physique du Globe, 5 rue R. Descartes, 67084 Strasbourg-Cedex, France
2. Lab. de Géophysique et de Tectonique, Univ. Sci. Tech. Languedoc, Pl. E. Bataillon, 34060 Montpellier-Cedex, France
3. ORSTOM, 213 rue La Fayette, 75480 Paris-Cedex 10, France

**KEY WORDS** : neotectonic, Atacama Fault System, stress regime

Recent works in the area have demonstrated that the Atacama Fault System has undergone left-lateral displacement contemporaneous with the development of the Jurassic - early Cretaceous magmatic arc in the present coastal cordillera (Naranjo et al., 1984; Herve, 1987a; Thiele and Pincheira, 1987; Scheuber and Andriesen, 1990). It has been indicated that part of the Atacama Fault System has been reactivated since late Tertiary with a dominant vertical componant of displacement (Arabasz, 1971; Okada, 1971; Herve, 1987b; Naranjo, 1987). Armijo and Thiele (1990) showed that many faults are presently active in the region. Acording to Armijo and Thiele (1990)' s work normal faults would characterize only the westernmost part of the coastal area, in particular the Mejillones Peninsula and the coastal scarp, though left-lateral displacement would be predominent along the Atacama Fault System near Antofagasta. However, an extensive study of aerial photographs covering the Antofagasta region lead us to think that normal faulting is indeed dominant in the whole coastal region, including the Atacama Fault System in the coastal cordillera. A neotectonic Field work has been designed to acquire an overview of the fault kinematics in the area, concentrating in places where faults cut into alluvial formations.

Field observations confirm that normal faulting prevails, although horizontal components of relative displacement, both left-lateral and right-lateral, are observed at some places. The orientation of pure normal faults ranges between N350° and N20°. Tensile cracks are often observed parallel to the main scarp of those faults. The lateral component is observed to vary with the azimuth of the faults. Faults oriented more towards the NW-SE have a right-lateral component while those oriented more to the NE-SW have a left-lateral component. Therefore, the component of relative displacement varies quite coherently with the strike of the faults and is indicative of EW extension. To quantify the stress regime we applied to the field observations an algorithm of inversion of the stress tensor orientations and shape factor. Results clearly indicate an extensional stress regime with the $\sigma_3$ (minimum stress compression) horizontal, striking in the EW direction, and $\sigma_1$ (maximum stress compression) vertical . Figure 1 shows the main studied faults. Sites where relative displacement could be accounted for without ambiguity and which where included in the stress tensor inversion are indicated by the small circles.

Normal faulting is attested too by the widespread 'half-graben' structure observed at the decakilometric scale. Footwall scarps commonly reach a height of several hundreds of meters. A modelization of the topography has been carried out over an area where several 'half-graben' interacts, forming a sequence of westward tilted blocks, using a simple model consisting of faults embedded in an homogeneous elastic medium. The angle of the slip vector on the faults is given by the stress tensor found above. On the other hand, the amount of slip ìn each fault segment has been determined by a trials and errors procedure so has to obtain a good fit between the observed topography and the calculated surface deformation. Though many aspects of the tectonic processes are neglected in this simple model, such as isostasy, erosion, sediment filling and viscous relaxation of stresses at depth, the actual topography could be reasonably well fitted if we add to the topographic effect of the faults a regional topographic trend. Our simple model does not pretend to unicity but shows how the characteristic short wavelentgh (10-20 km long) features of topography in the area can be controled by the known big faults, under EW extention.

## THE EXTENSIONAL STRESS REGIME IN THE ANTOFAGASTA COASTAL AREA

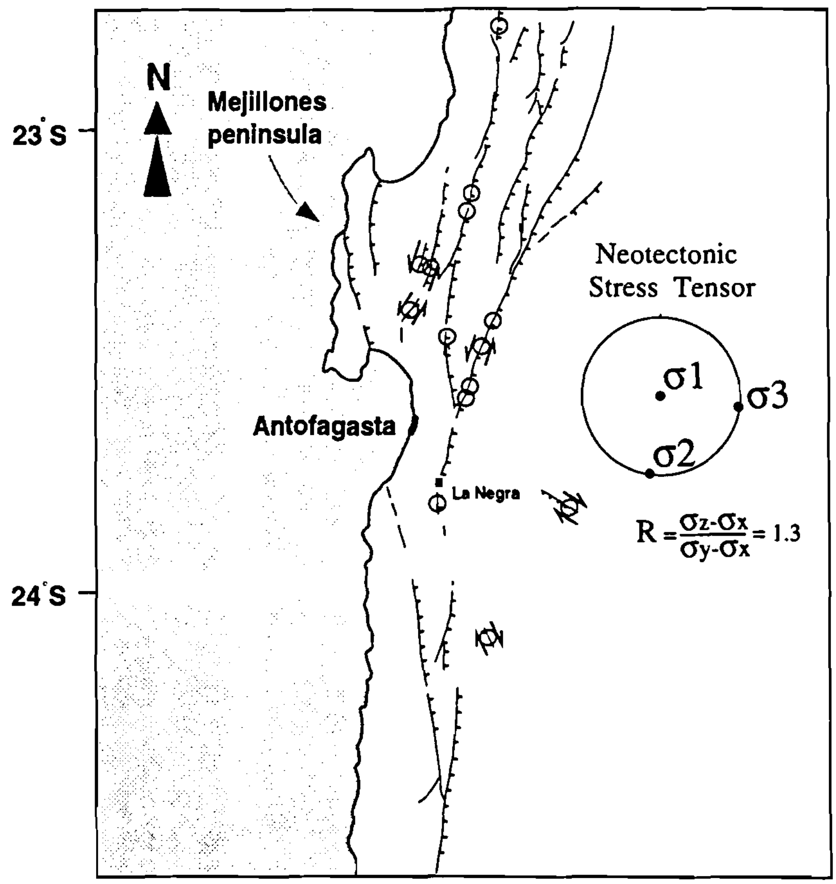


O : place of neotectonic data for stress inversion

Figure 1 : main studied faults in the Antofagasta coastal area. Ticks indicate the downthrow direction of normal faulting. Double arrows indicate the horizontal component of displacement at places where it has been locally observed.

The forearc region near Antofagasta seems to have been under an extensional tectonic regime for a long time (since Miocene ?). The erosional rate in this desertic region is particularly slow and allows an exceptional preservation of the tectonic structures. However, some scarps much fresher than others attest of repeated ruptures under EW extension in the very recent (historical ?) time. Field observations show the compatibility of faulting in the whole coastal area, up to 40-50 km East of the coast, with the EW extension. The existence of an extensional stress regime at a convergent plate boundary may seem contradictory. However, extension may occur as a local modification of the general compressional state caused either by some crustal bending effect or by a transient disturbance of the stress field following the occurrence of very strong subduction earthquakes.

**REFERENCES**

Arabasz, W.J., 1971. Geological and geophysical studies of the Atacama Fault Zone in Northern Chile. Ph.D. Thesis, California Institute of Technology, 264 p. Pasadena, U.S.A.

Armijo, R. and Thiele, R., 1990. Active faulting in northern Chile: ramp stacking and lateral decoupling along a subduction plate boundary ? Earth and Planetary Science Letters, 98 : 40-61.

Hervé, M., 1987a. Movimiento sinistral en el Cretacico inferior de la zona de falla Atacama al Norte de Paposo (24°S), Chile. Revta geol. Chile, 31: 37-42.

Hervé, M., 1987b. Movimiento normal de la falla Paposo, zona de falla Atacama, en el Mioceno, Chile. Revta geol. Chile, 31: 31-36.

Naranjo, J. A., 1987. Interpretation de la actividad Cenozoica superior a lo largo de la zona de falla de Atacama, Norte de Chile. Revista geol. Chile 31, 43-55.

Naranjo, J. A., Hervé F., Prieto, X., Munizaga, F., 1984. Actividad Cretacica de la falla Atacama al Este de Chanaral: milonitizacion y plutonismo. Comucicaciones Univ. de Chile, Santiago.

Okada, A., 1971. On the neotectonics of the Atacama fault zone region - Preliminary notes on Late Cenozoic faulting and geomorphic development of the Coast Range of Northern Chile . Bull. Dep. Geogr., Univ. of Tokyo, 3: 47-65.

Scheuber, E., and Andriessen, P., 1990. The kinematic and geodynamic significance of the Atacama fault zone, northern Chile. Journal of Structural Geology, 12: 243-257.

Thiele, R., and Pincheira, M., 1987. Tectonica transpresiva y movimiento de desgarre en el segmento Sur de la zona de falla Atacama, Chile. Revta geol. Chile, 31: 77-94.

# FORCASTING THE END OF A GAP : THE LARGE ANTOFAGASTA (NORTHERN CHILE) EARTHQUAKE OF JULY 30, 1995

B. Delouis [1], T. Monfret[2,3], L. Dorbath [1,2], M. Pardo[3], L. Rivera[1], D. Comte[3], H. Haessler[1], J. P. Caminade[2,3], L. Ponce[3], E. Kausel[3], A. Cisternas[1]

1) Institut de Physique du Globe. 5 rue R. Descartes. 67084 Strasbourg Cedex. France.
2) ORSTOM. 213 rue Lafayette. 75480 Paris Cedex 10. France.
3) Departamento de Geofísica. Universidad de Chile. Casilla 2777. Santiago. Chile.

**KEY WORDS** : subduction, seismic gap, foreshocks and aftershocks, body wave modeling

The July 30, 1995 Antofagasta earthquake ($M_w = 8$), and its aftershock sequence, were precisely monitored by a local network previously installed in the region in order to study the seismic evolution of the large 1877 gap in Northern Chile. One strong foreshock ($M_w = 6.2$) six months before the main event, and several smaller ones are described. The main rupture started under the Antofagasta airport region and propagated southwards with a velocity of 2.8 km/sec, in a N200° direction, over an area of 185*80 km$^2$, the total seismic moment being $1.2 * 10^{28}$ dyne-cm. Very little destruction resulted from this earthquake in spite of its size. Waveform modelling of body waves gives insight on some details of the rupture process, in particular its start as a double event, and its end near the trench in normal faulting. Accelerations in Antofagasta reached 30% of gravity. The Atacama fault showed coseismic centimetric surface ruptures next to Sierra Remiendos, among other places. A tsunami wave, 2 m high, was observed along the coast from Mejillones to Taltal. The aftershock distribution delineates a very well defined rupture surface along the subduction interface. The epicenters during the first 24 hours of activity are limited by a sharp northern boundary across the Mejillones peninsula. Aftershocks during the following two weeks indicate growth of the initial rupture zone both north and south. The mechanisms of the strongest aftershocks are consistent with the thrust along the subduction interface. The Mejillones peninsula acts like a barrier for the propagation of the rupture to the north into the region of the 1877 gap. Nevertheless, compressional stresses under the northern half of the peninsula increased after the main shock along a direction tranverse to the trench. Thus, the chances for the activation of the 1877 gap are greater now.

## REFERENCES

Comte D. and Pardo M., 1991. Reappraisal of great historical earthquakes in the northern Chile and southern Peru seismic gaps. Natural Hazards, 4: 23-44.

Comte D., Pardo M., Dorbath L., Dorbath C., Haessler H., Rivera L., Cisternas A., Ponce L., 1994. Determination of seismogenic interplate contact zone and crustal seismicity around Antofagasta, northern Chile,using local data. Geophys. J. Int. 116: 553-561.

Delouis B., Cisternas A., Dorbath L., Rivera L., Kausel E., 1996. The Andean subduction zone between 22°S and 24°S (northern Chile): precise geometry and state of stress. Tectonophysics, in press.

Departamento de Geofísica. Descripci6n y evaluaci6n del terremoto de Antofagasta del 30 de Julio 1 995. Informe para el Ministerio de Obras Públicas. Universidad de Chile. December 1995.

Kelleher J., 1972. Rupture zones of largeSouth American earthquakes and some predictions. J. Geophys. Res., 77: 2087-2103.
Kausel E., 1986. Los Terremotos de Agosto de 1868 y Mayo de 1877 que Afectaron el Sur del Peru y Norte de Chile. Boletin de la Academia Chilena de Ciencias, 3: 8-12.
Kausel E. and Campos J. 1992. The Ms=8 tensional earthquake of 9 December 1950 of Northern Chile and its relation to the seismic potential of the region. Phys. Earth. Planet. Inter., 72: 220-235.
Lomnitz C., 1970. Major earthquakes and tsunamis in Chile during the period 1535 to 1955. Geolog. Rundsch., 59:938-960.
Milne A., 1880. The Peruvian Earthquake of 9th May, 1877. Trans. Seismol. Soc. Jpn., II: 50-97.
Nishenko S.P., 1985. Seismic potential for large and great interplate earthquakes along the Chilean and Southern Peruvian margins of South America: a quantitative reappraisal. J. Geophys. Res, 90: 3589-3615.

# THE 1995 ANTOFAGASTA EARTHQUAKE AND ITS CONNEXION TO THE 1877 SEISMIC GAP

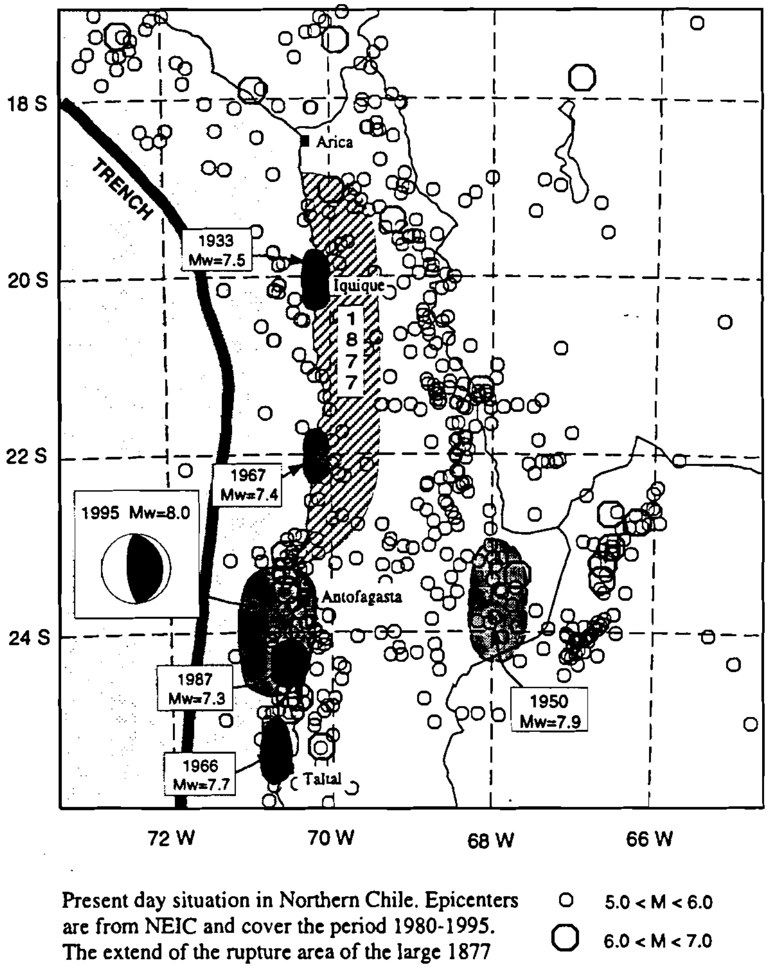


Present day situation in Northern Chile. Epicenters are from NEIC and cover the period 1980-1995. The extend of the rupture area of the large 1877 earthquake is inferred from the isoseismal VIII and is indicated by the long stripped zone. Rupture zones associated with known strong events this century are represented by the gray shaded zones. Seismicity forms a doughnut shape around the likely next rupture of the 1877 sesmic gap.

# NEOTECTONICS OF THE COASTAL REGION OF ECUADOR : A NEW PLURIDISCIPLINARY RESEARCH PROJECT

Jean François DUMONT(1), Stalin BENITEZ(2), Luc ORTLIEB(3), Alain LAVENU(4), Bertrand GUILLIER(5), Alexandra ALVARADO(6), Claude MARTINEZ(7), Christian JOUANNIC(1), Guillermo TOALA (2) , Jorge VIVANCO (2) and Jean Thomas POLI(8)

(1) ORSTOM, UMR Geoscience Azur (EP 125), BP 48, 06230 Villefranche-sur-Mer, France.
(2) PetroProduccion, km 6½Via a Salinas, P.O. Box 10829, Guayaquil, Ecuador
(3)ORSTOM, Casilla 1190, Antofagasta, Chile
(4) Mission ORSTOM, Casilla Postal 53390, Correo Central, Santiago 1, Chile.
(5) Mission ORSTOM, Apartado 17.11.6596, Quito, Ecuador, and EPN, Quito.
(6) Instituto Geofisico, Escuela Politecnica Nacional, Apartado 2759. Quito, Ecuador
(7) ORSTOM, Laboratoire de Géologie des Bassins, Case 58, USTL Montpellier II, 34095 Montpellier cedex 05, France
(8) L.G.G.S.T., UPMC, 4 Place Jussieu, 75230 Paris, France.

KEY WORDS : Ecuador, Plio-Quaternary, Neotectonics, Marine terraces, Geomorphology,

## INTRODUCTION

The coastal margin of Ecuador, 150 to 200 km wide onshore, comprises oceanic terranes accreted onto the Andes during the Paleocene and emerging after the Late Eocene (Benitez 1995, Jaillard et al. 1995). Presently, this area is in the position of a fore-arc ridge and basin, mostly emerged, in relation to the subduction of the Nazca plate beneath the South American plate (Lonsdale 1978), that proceeds with a N80ºE convergence and at a rate of 8 cm/year (Daly 1989, DeMets et al. 1990).

The main features of the geodynamic pattern are (fig.1) : i) an oblique subduction (15º to 25º), that favors transcurrent movements, evidenced for instance by the dextral Dolores-Guayaquil Megashear (Winter and Lavenu 1989) ; ii) the opening of the Gulf of Guayaquil, related to the motion along the Dolores-Guayaquil Megashear ; iii) the subduction of the Carnegie Ridge between 0º and 2ºS, that causes the trench to lift up by about 1500m.

At the scale of the whole South American continent, the margin of the South American plate is broadly convex near the Peru-Ecuador boundary, and the geometry of the slab changes from a nearly flat subduction south of 3ºS to a more normally dipping one to the north.

Regarding the seismic activity, few strong historical earthquakes are reported in the southern part of the coastal block, but several major earthquakes shook the northwestern Ecuador and southwestern Colombia since the beginning of the century. Nishenko (1989) considers the Esmeraldas area in northwestern Ecuador as an area of high seismic risk.

In order to understand the relations between the subduction system and the present tectonic evolution of the Ecuadorian coastal block, we started a neotectonic study focused on the various manifestations of recent deformations (uplift, subsidence and strike-slip). A pluridisciplinary approach including detailed stratigraphy of marine terraces, fault kinematics, and geomorphologic studies of drainage anomalies, will be used.

## MARINE TERRACES

An important feature of the coastal region of northern Peru and Ecuador is the occurrence of emerged Quaternary marine terraces, called "Tablazos" (De Vries 1988, Macharé and Ortlieb 1994). In Ecuador, such terraces are observed up to an elevation of 320 m in the Manta area, and up to 90 m in the Santa Elena area. Several intermediate levels are observed. The lowermost well preserved and extensive terrace, observed at up to +20 m in the Manta and Chanduy areas, was likely formed during the last major high stand of sea level, i.e. stage 5e of the last interglacial period, about 125 ka BP. Assuming that this high sea level was +6 m above present sea level, an uplift of the terrace by some 14 m is calculated and a mean uplift rate of about 110 mm/ky is evaluated.

Lower, younger terraces are observed west and east of Manta, between 3 to 10 m above present mean sea level : they may correspond to later episodes of the last interglacial period (stages 5c and 5a, respectively 105 and 80 ka) and to the Holocene period. Higher and older terraces of Middle and Early (?) Pleistocene age are preserved at various elevations, up to +300 m.

The Tablazo Formation overlays Eocene and Pliocene deposits in the Manta area (San Mateo and Canoa Formations respectively), and the Eocene Ancón Formation in the Santa Elena area. The Pliocene Canoa Formation is deposited in shallow environment. In the Esmeraldas area, erosion surfaces overlay the Pliocene Onzole Formation, deposited in a lower middle bathyal deposition environment (Bianucci et al. 1993). The different depositional environment of Pliocene formations suggest that the Quaternary terraces take place after a relatively complex Pliocene history.

Controversial hypotheses have been made in the past regarding the tectonic significance of the terrace sequences in the region (Marchant 1961). A flight of three or more terraces exists, but local or regional faults make the feature more or less complicated. For instance, a lineament observed on radar image in the Santa Elena neighborhood suggests the fault duplication of a terrace, with an upthrow of up to 40 m. Moreover, near this place, a fault plane gives evidence of an extensional displacement contemporaneous with the deposition of the basal conglomerate of a Santa Elena equivalent terrace.

## FAULT ANALYSIS

The preliminary results of fault analysis from random sites along the coastal area are consistent with a NS extension. Such deformations are observed in fan conglomerates of the Western Cordillera piedmont, as well as in terraces in the Santa Elena and Esmeraldas areas. An extensional tectonic event probably represents the most recent stage of deformation, and just pre-dates or is contemporaneous of the deposits of terraces estimated to be of Late Pleistocene age. The Pliocene beds display more complex fault systems, especially in the Esmeraldas area. The important uplift of the Pliocene of Onzole Formation at Esmeraldas (Bianucci et al. 1993) cannot be explained by the moderately developed normal faulting resulting from the extensional event. More complex fault motions are to be expected in the coastal area, close to the upper part of the internal wall of the trench.

## GEOMORPHOLOGIC MARKERS

Because of the coastal range relief, the drainage issued from the Andes in Ecuador reaches the Pacific Ocean in only two points, the Gulf of Guayaquil through the Daule-Babahoyo Basin to the south, and the Esmeraldas area to the north, the former being the most important. The Daule and the Babahoyo Rivers follow respectively the western and eastern margins of the Daule-Babahoyo Basin. In the SE part of the basin, the Babahoyo River flood plain morphology suggests that it is an area of active subsidence superimposed over the northern branch of the Dolores-Guayaquil Megashear.

Some observations made on topographic and radar SAR images show that the NE-SW trend of the rivers inside the basin is related to recent fault motion. The fault movement deduced from morphological evidences is partly normal, with ria lakes or swampy lands sharply separated from dry lands, and drainage deflected along this morphological separation line. This suggests a transtensional tectonic system, but the close relation between plate motions and the Dolores-Guayaquil Megashear remains speculative.

## CONCLUSIONS AND PROJECT OUTLOOK

The neotectonic evolution of the coastal area of Ecuador includes several types of deformations, such as uplift and accretionary tectonics on the coast side, or subsidence of wide flood plains involving probably normal as well as strike slip faults on the Andean side. Therefore, the understanding of the geodynamic evolution during the Quaternary up to present time can only be obtained by a pluridisciplinary approach involving specific study methods according to the style of deformation and the morphology. As far as the relation with active deformation is concerned, local seismic studies are planned to constrain the seismotectonic activity, specially in the Esmeraldas and Manta areas.

A comprehensive approach will be applied first to the different areas using remote sensing approach (by means of Spot and ERS1 images principally). At a further stage of analysis, correlation between the various neotectonic data will be made combining thematic documents with satellite images and digitized topography.

## REFERENCES


Benitez, S. 1995. Evolution géodynamique de la province côtière sud-équatorienne au Crétacé supérieur-Tertiaire. Thèse, Labo. Chaines Alpines, Grenoble, 221pp.

Bianucci, G., Cantalamessa, G., Landini, W., Ragaini, L. and Valleri, G. 1993. Fossil assemblages from the Pliocene of Onzole Formation (Esmeraldas, NW Ecuador) and their implications in the panimic bioprovince evolution. Docum. Lab. Géol. Lyon, n°125:43-58.

Daly, M.C. 1989. Correlations between Nazca/Farallon plate kinematics and forearc basin evolution in Ecuador. Tectonics, vol.8, n°4:769-790.

DeMets C., Gordon R.G., Argus D.F., Stein S. 1990. Current plate motion. Geophysical Journal International, 101, 425-478.

De Vries, T. 1988. The geology of late Cenozoic marine terraces (tablazos) in northwestern Peru. Journal of South American Earth Sciences, 1,2:121-136.

Jaillard, E., Ordoñez, M., Benitez, S., Berrones, G., Jiménez, N., Montenegro, G., and Zambrano I. 1995. Basin Development in an accretionary, Oceanic-floored fore-ars setting: southern coastal Ecuador during Late Cretaceous-Late Eocene time. AAPG memoir 62:615-631.

Lonsdale, P. 1978. Ecuadorian Subduction System. AAPG Bulletin, v.62, n°12:2454-2477.

Macharé, J. and Ortlieb, L. 1994. Morfoestratigrafia de los tablazos del noroeste peruano: neotectonica y fluctuaciones del nivel del mar. VII Congreso Peruano de Geologia, Resumenes extendidos, pp. 238-241.

Marchant, J. 1961. A photogeological analysis of the structure of the westerm Guayas province, Ecuador: with discussion of the stratigraphy and Tablazo Formation, derived from surface mapping. Q. J. Geol. Soc. London. vol.117:215-232.

Nishenko, S. P. 1989. Circum Pacific seismic potential 1989-1999. USGS Open File Reports, 85-89.

Winter, T., and Lavenu, A., 1989. Morphological and microtectonic evidence for a major active right-lateral strike-slip fault across central Ecuador (South America). Annales Tectonicae, vol.3, n.2:123-139.

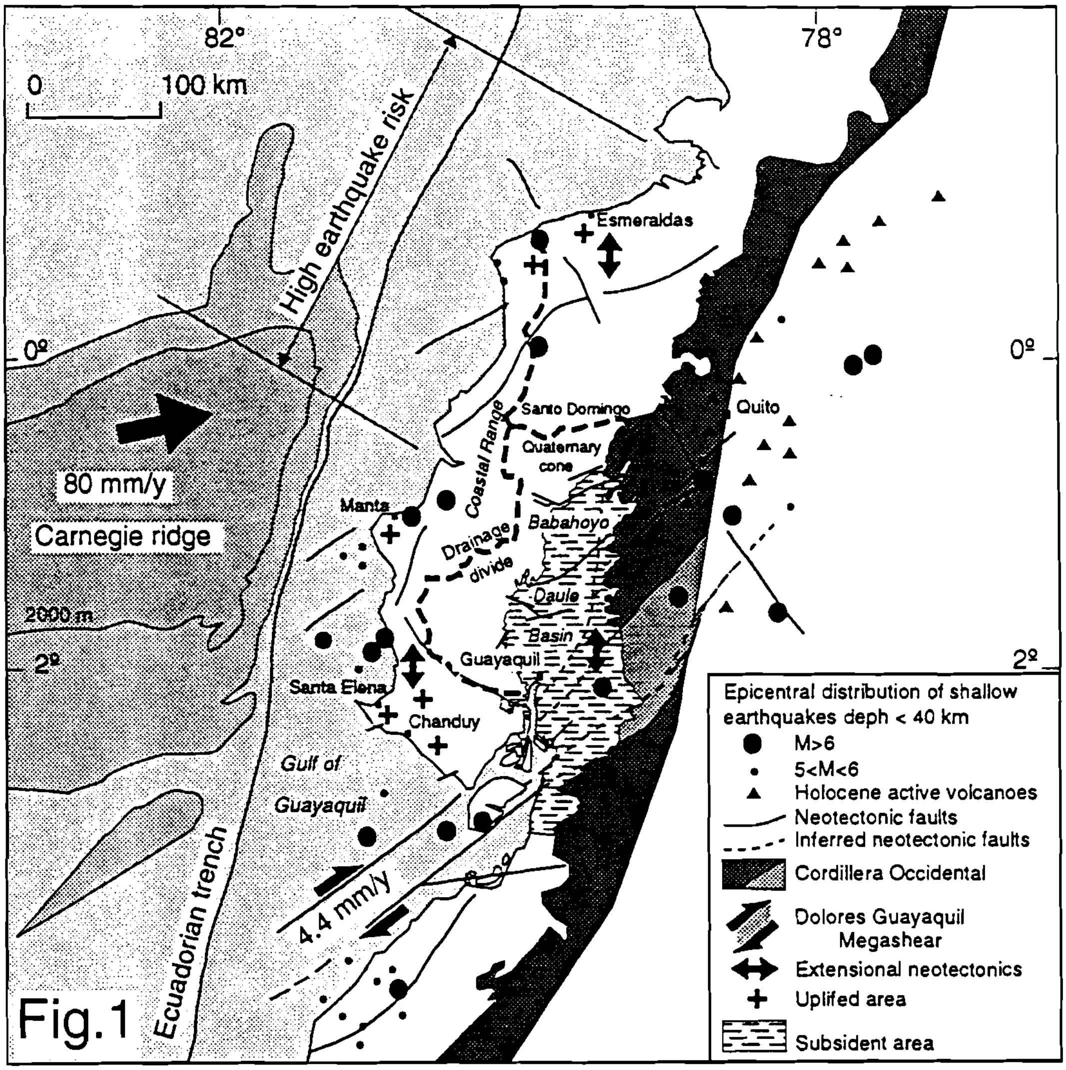


Neotectonic scheme of the coastal block of Ecuador.

# PRELIMINARY PALEOMAGNETIC RESULTS FROM THE PLEISTOCENE VILLARICA VOLCANO AND MIOCENE FARELLONES FORMATION

A. GOGUITCHAICHVILI[1,2], A. CHAUVIN[2], P. ROPERCH[2,3], M. VERGARA[4] AND H. MORENO[5]

(1) Univ. Montpellier, Montpellier, France.
(2) Géosciences Rennes, Campus de Beaulieu, 35042 Rennes, France
(3) ORSTOM and Dep. Geologia, Univ. Chile, Santiago, Chile
(4) Dep. Geologia, Univ. Chile, Santiago, Chile
(5) SERNAGEOMIN, Santiago, Chile

KEY WORDS: Paleomagnetism, Geomagnetism, Tectonic rotations, Secular variation

## INTRODUCTION

The Geomagnetic field can be described mainly as the field developed by a geocentric axial dipole and this property is at the core of successful applications of paleomagnetism to tectonics. The study of the spatial and temporal characteristics of the secular variation of the geomagnetic field is important to understand its origin. The uneven geographic distribution of paleomagnetic results with few available data in the southern hemisphere, however, impedes an accurate analysis of the fine-scale changes in the statistical characteristics of paleosecular variations [See Jacobs, 1994] .

The behavior of the earth magnetic field during polarity reversal has also been recently the subject of large debate on a possible confining of transitional field paths over specific longitudinal bands and it is interpreted as evidence for core-mantle interaction [Gubbins, 1994].

Although many paleomagnetic studies have been devoted to tectonics in Chile, they are few results directly available to describe secular variations and transitional behavior [Brown et al., 1994]. In december 1995, we started a project of paleomagnetic secular variations which includes the sampling of 21 sites in Pleistocene-Holocene lavas from the Villarica volcano and two sections (31 sites) of the Miocene Farellonnes volcanic formation. Such paleomagnetic studies are not only relevant to the geomagnetic field but they may also provide additional information on the timing of volcanic eruption or tectonic rotations.

### The VILLARICA volcano

The Villarica is a Quaternary and active volcano at the latitude of 39°S. There is no available cross-section of the volcanic sequence. However, based on characteristic pyroclastic flows with radiocarbon ages, it is possible to assign a relative age to several of the lava flows that outcrop as small valley filling (Moreno in preparation). We have sampled 21 sites mostly in the post-glacial lavas. The secular variation appears relatively low and many sites record similar directions. Absolute paleointensities by the Thellier and Thellier method will bring additional information on secular variations. In the end we also hope that between-site correlation of paleomagnetic results might help constrain the timing of the volcanic activity.

### The Miocene FARELLONES formation.

The Farellones formation is a middle Miocene volcanic formation with available K-Ar radiometric ages in the range 16-19 Ma (Beccar et al., 1986). Farellones volcanics outcrop along the road going to the ski resorts east of Santiago. We drilled 7 flows in a 150m section below the village of Farellones. The other sequence ( 24 sites) is a 450m thick section below the ski resort of Valle Nevado located about 10

Km east of the Farellones section. In our study area, the Farellones volcanic formation does not show evidence for a tectonic tilt or folding. The Farellones section is at a lower elevation than the Valle Nevado section and it is thus assumed to be older than the Valle Nevado section (Fig. 1).

The magnetic susceptibility is high for almost all sites except two (average 2.8 $10^{-2}$ SI) in agreement with the andesitic nature of this volcanism (Beccar et al., 1986). After removal by thermal cleaning of a secondary overprint in the present-day field, characteristic directions were easily determined for most sites.

The Farellones section is only of normal polarity and two reversals are observed in the Valle Nevado section suggesting that the Farellonnes volcanism did not last more than 2 Ma. One precise $Ar^{39-40}$ radiometric age is however needed before to attempt a correlation with the reference geomagnetic reversal time-scale.

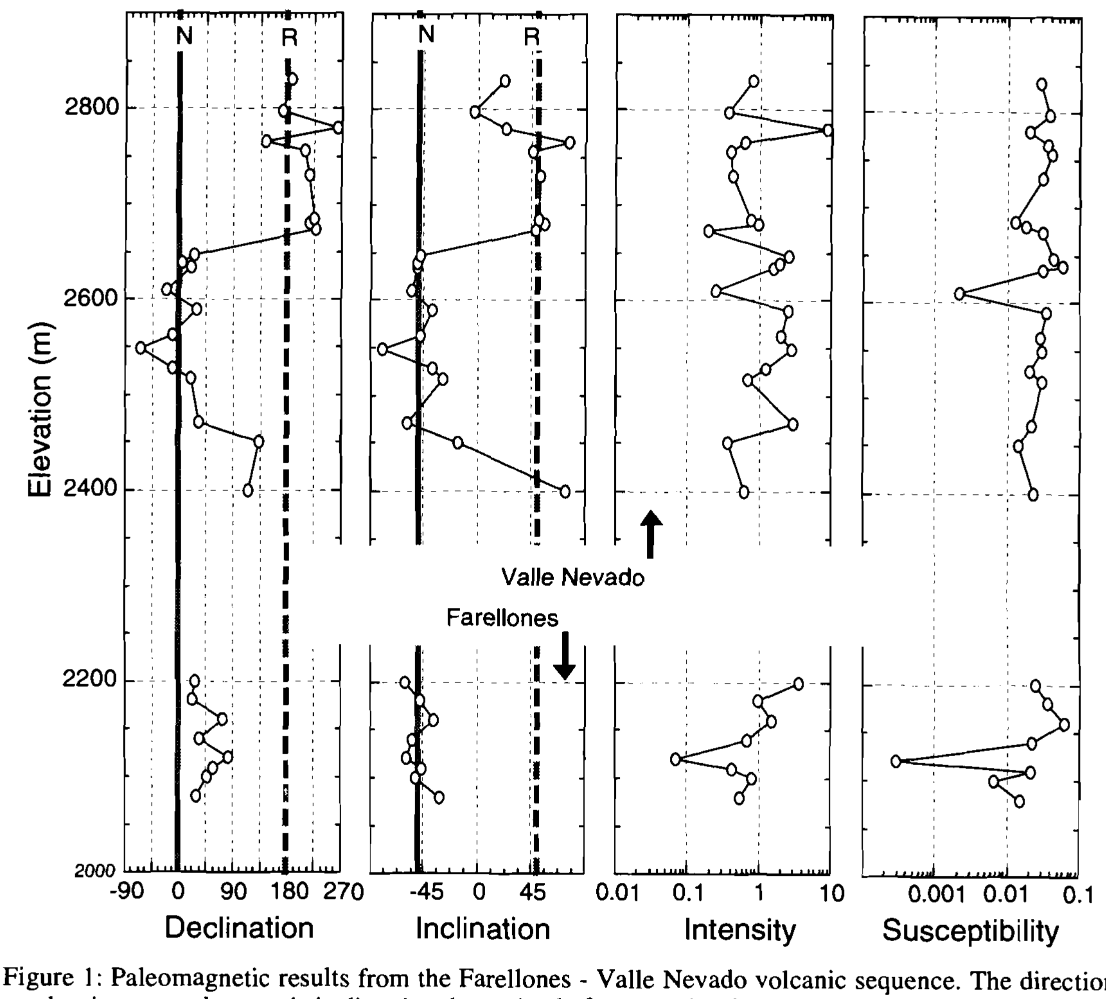


Figure 1: Paleomagnetic results from the Farellones - Valle Nevado volcanic sequence. The direction is the site-mean characteristic direction determined after stepwise thermal cleaning. Geometric site-mean values of the intensity of the natural remanent magnetization in $Am^{-1}$. Geometric site-mean values of the magnetic susceptibility in SI.

An other interesting observation is that the mean direction (Declination: 28° Inclination: -53.7°) is significantly different from the expected middle Miocene direction (357°, -57°). This preliminary result suggests that the Farellones-Valle Nevado area rotated clockwise since about 17 Ma. Clockwise rotations have also been reported by Beck et al. [1986, 1990] in areas located about 100 km north and south of Santiago. Further work is still needed to confirm this rotation and better understand the late Tertiary tectonics of the area.

REFERENCES

Beck, M.E. Jr, R.F. Burmester, A. Garcia and S. Rivano, 1990, Paleomagnetic results from Cretaceous rocks in the Llaillay - San Felipe -Putaendo region: Implications for block rotations in the Andean forearc, Rev. Geol. Chile, 117, 115-130.

Beck, M.E. Jr, R.E. Drake, R.F. Butler, 1986. Paleomagnetism of Cretaceous volcanick rocks from central Chile and implications for the Tectonics of the Andes. Geology, 14, 132-136.

Beccar, I., M. Vergara and F. Munizaga, 1986. Edades K-Ar de la formacion Farellones, en el codon del Cerro La Parva, Cordillera de los Andes de Santiago, Chile, Rev. Geol. de Chile, 28-29, 109-113.

Brown, L., J. Pickens, and B. Singer, 1994. Matuyama-Brunhes transition recorded in lava flows of the Chilean Andes: Evidence for dipolar fields during reversals, Geology, 22, 299-302.

Gubbins, D., 1994. Geomagnetic polarity reversals: A connection with secular variation and core-mantle interaction? Rev. Geophys., 32, 61-83.

Jacobs, J.A., 1994. Reversals of the earth's magnetic field, 346 pp. Cambridge, New York.

# MICROZONING AND SEISMIC RISK IN QUITO, ECUADOR: PRELIMINARY RESULTS

Philippe GUEGUEN[1,2], Jean-Luc CHATELAIN[1,2], Bertrand GUILLIER [1,2], Hugo YEPES [2] and Jorge VALVERDE [2]

(1) ORSTOM-Ecuador, apartado 17.11.06596, Quito, Ecuador
(2) Escuela Politecnica Nacional, apartado 2759, Quito, Ecuador

**KEY WORDS:** Nakamura's technique, microzoning, seismic risk, Quito, Ecuador

## INTRODUCTION

Out of the 23 events felt in Quito with an intensity bigger than V since 1541, 5 produced intensities of VII or bigger in 1587, 1755, 1797, 1859, and 1868. The past damaging earthquakes occurred while Quito was quite different from the modern Quito. The city has changed significantly in the last 40 years. In that period, the population increased from 420 000 to 1.2 million, with a considerable expansion of the city. This has resulted in increased urban densities, which, linked to expanding poverty, have resulted in an increase in poorly-constructed buildings and development of hazardous areas such as steep mountain slopes. In addition, high-rise buildings that did not exist in the 1950's have spread in the northern city as a result of a more dynamic economy. The Quito Earthquake Risk Management Project [Chatelain et al, 1995, Escuela Politecnica Nacional et al, 1994, 1996], a pilot project in social seismology, has been conducted to provide direction to government officials, business leaders, and the public in general, to reduce damage and injury in the next major earthquake. One of the recommendations of this project was to undertake more precise zoning of the city, and that parameters more directly usable than seismic intensities by civil engineers should be estimated. The study presented in this paper is therefore one of the direct consequences of the above mentioned social seismology project. Its goal is the evaluation of site effects in the city of Quito during an earthquake, due to the various geological settings throughout the city. This evaluation is currently under way using three different techniques to measure the fundamental period as well as the relative and absolute amplification of soils, in order to produce isoperiod and isoamplitud maps of the city. In this paper we present the first results obtained by recording microtremors throughout the city.

## TECHNIQUES USED

1.- The main technique used is the recording of microtremors (ambient vibration of the ground), moving a single station at about 400 points throughout the city, in order to calculate the spectral ratio between horizontal and vertical signals to obtain the transfer function at each site, using Nakamura's technique [1989] to remove source effects from the records. Good results have been obtained with Nakamura's technique in Mexico City, Oaxaca and Acapulco [Lermo and Chavez-Garcia, 1993], in San Fransisco [Ohmachi et al., 1991], and in France [Duval, 1995], while Lachet and Bard [1995] have shown the theoretical limitations of the technique. We used a station developed by LEAS (France) in collaboration with J. Frechet from the Laboratoire de Géophysique Interne et Tectonophysique of Grenoble, recording the signal from a three component L-4-3D Mark Products seismometer. The sites of recording were chosen to cover all the main geological zones described in the Quito Earthquake Risk Management Project, and to help precise their boundaries. At each site, the signal from the three components is recorded during 2 minutes, at a 50 Hz rate, from which five 10 seconds samples are selected. For each 10 seconds sample, a FFT of each component is calculated, smoothed with a triangular window, and used to get the NS/Z and EW/Z ratios. This method will allow us to obtain information about the resonance frequency of the soil column at each site, as well as the relative potential amplitude between each site.

2.- A second technique is used to get the absolute amplification ratios. One reference station is installed on hard rock, and four stations are installed at fixed sites within the city, are recording weak motion of natural seismicity, mainly from small magnitude earthquakes. The absolute amplification ratio at each of the four sites is obtained by dividing the FFT of the NS and EW signals recorded at the site by those recorded at the reference station. Then the absolute amplification ratio at each site used with the first technique is obtained by comparing their relative amplification to the absolute amplifications calculated at the fixed sites.

3.- The third technique is to apply a similar technique that the first but using the natural seismic signals recorded at the fixed stations.

## PRELIMINARY RESULTS

Based on topography, soil characteristics, and surface geology the city has been divided into 3 main zones (Figure 1) : the flanks of Pichincha volcano to the west (F) , the central lowlands mainly filled with recent fluvio-lacustrine deposits (L), and a zone of hills to the East mainly formed of Cangahua and ash deposits (Q). These zones were then divided into 20 sub-zones (figure 1 ) according to variations of local geological conditions and mechanical characteristics.

As an example, results obtained using the first technique along an E-W profile crossing zones q2n, l3, and f4 (Figure 1) show that the fundamental frequency appears clearly at each site, varying according to the local geological conditions (Figure 2), whose boundaries can be corrected (for instance the boundary between zones l3 and q2 should be moved slightly to the East, as the amplification as well as the fundamental frequency observed at stations 031305 and 031303 are very similar). Variations also show up within the zones themselves, as for instance in zone l3 (stations 022708, 031306, and 031307).

We will present isoamplitude and isoperiod maps of the city and compare them with the spectral content of earthquakes recorded in Quito in order to precise the earthquake hazard in the city. The earthquake risk will be then assessed by crossing these data with the building distribution available in the municipality data base using the Savane SIG [Chatelain et al, 1995].

## REFERENCES


Chatelain J.-L., H. Yepes, B. Guillier, J. Fernandez, J. Valverde, F. Kaneko, M.Souris, E. Duperier, G. Hoefer, T. Yamada, G. Bustamante, B. Tucker and C. Villacis. 1994. Les Scenarios Sismiques comme Outils d'Aide à la Décision pour la Réduction des Risques : Projet Pilote à Quito, Equateur. *Rev. Geogr Alp.*, Tome LXXXII, n°4, 131-150.

Chatelain J.-L., B. Guillier, M. Souris, E. Duperier and H. Yepes. 1995. SIG et Evaluation des Risques Naturels : Application aux Risques Sismiques de Quito. *Mappemonde.*, 3, 17-22.

Chavez-Garcia F., Pedotti G., Hatzfeld D. and Bard P.Y. 1990. An experimental study of site effects near Thessaloniki (Northern Greece). *Bull. Seism. Soc. Am.*, 80, 784-806.

Duval A.M. 1995. Détermination de la réponse d'un site aux séismes à l'aide du bruit de fond: Evaluation expérimentale. *Thèse de doctorat de l'Université P. et M. Curie*, Paris VI, 265 pages.

Escuela Politecnica Nacional, GeoHazards International, Ilustre Municipio de Quito, ORSTOM, OYO Corp. 1994. The Quito, Ecuador, Earthquake Risk Management Project: An Overview. *GeoHazards International Publication*, San Fransisco, USA.

Escuela Politecnica Nacional, GeoHazards International, Ilustre Municipio de Quito, ORSTOM, OYO Corp. 1996. Proyecto para el Manejo del Riesgo Sismico de Quito : Sintesis. *ORSTOM - IMQ Publicacion*, Quito, Ecuador.

Lachet C. and Bard P.Y. 1994. Numerical and theoretical investigations on the possibilities and limitations of the Nakamura's technique. *Journal of Physics of the earth*, 42-4, 377-397.

Lermo J. and Chavez-Garcia F.J. 1993. Site effect evaluation using spectral ratios with only one station. *Bull. Seism. Soc. Am.*, 83, 1574-1594.

Nakamura Y. 1989. A method for dynamic characteristics estimations of subsurface using microtremors on the ground surface. *QR of RTRI*, 30, 25-33.

Ohmachi T., Nakamura Y. and Toshinawa T. 1991. Ground motion characteristics of San Franscisco Bay area detected by microtremor measurements. *Proc. of Second Int. Conf. on recent advances in geotechnical earthquake engineering and soil dynamics*, Missouri, paper LP08, 1643-1648.

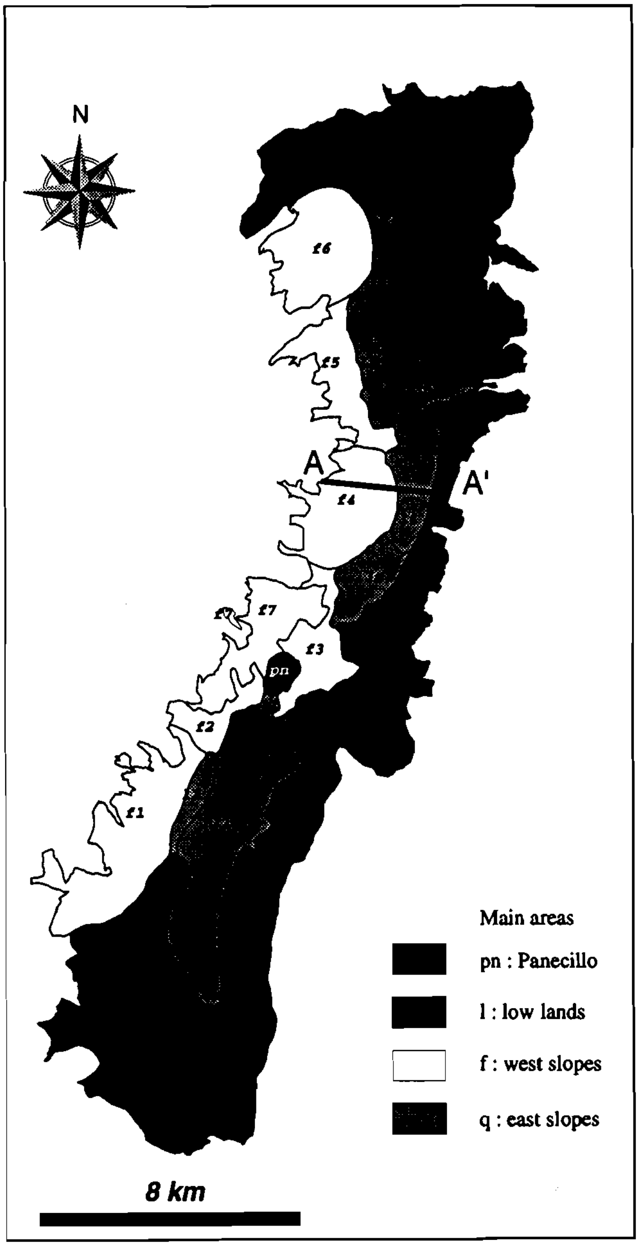


Figure 1 : zoning of Quito city used in the Earthquake Risk Management Project and location of the profile shown in figure 2.

stations 031310 031309 031307 031306 022708 031305 031303 031302

A____x____x________x____x____x____x________x____x____A'

zones f4 l3n q2n

<-------------------><-------------------------------------------------------><--------------->

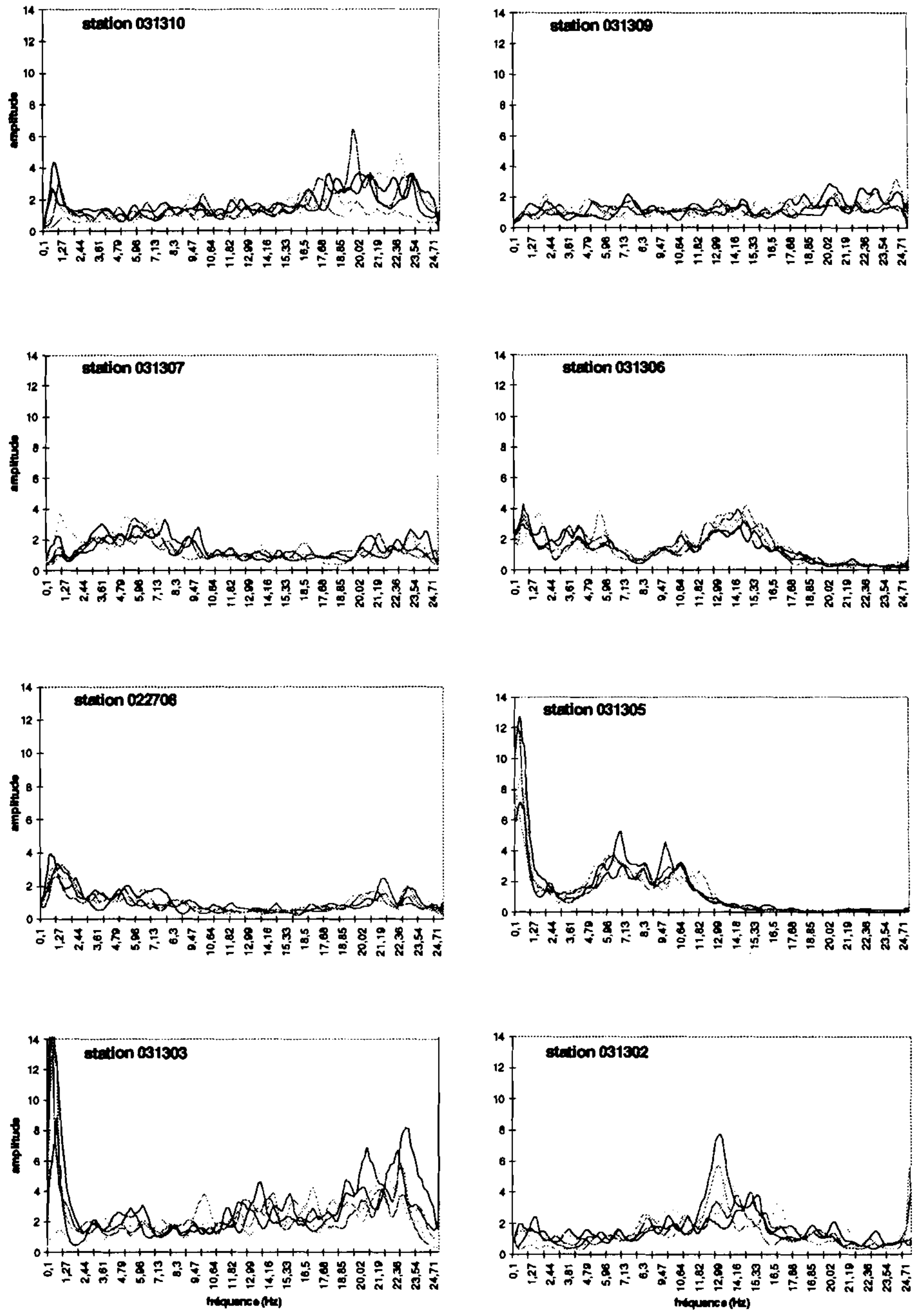


figure 2: spectral ratios between NS and Z components. For each station, along the AA' cross section (see figure 1), 5 windows of 10 s recording are represented from 2 min total recording.

# SEISMICALLY ACTIVE FRACTURE ZONES IN THE CONTINENTAL WEDGE OF THE CENTRAL PART OF ANDEAN SOUTH AMERICA

Václav HANUŠ, Jiří VANĚK and Aleš ŠPIČÁK

Laboratory of Global Tectonics and Metallogeny, c/o Geophysical Institute, Academy of Sciences of the Czech Republic, Boční II 1401, 14131 Prague 4, Czech Republic

**KEY WORDS:** seismotectonics, continental wedge, Andean South America

Detailed studies of the geometry of distribution of earthquake foci revealed that the process of subduction is generally accompanied by a relatively high seismicity in the overlying continental wedge (Hanuš and Vaněk 1977-78, 1979, 1983, 1984a,b, 1987, 1992; Hanuš et al. 1987; Vaněk and Hanuš 1988). In the regions where the oceanic lithosphere is underthrusted below the continental plate about one third of earthquakes is located in the continental wedge. It appears that practically all these earthquakes are not distributed randomly showing a clear tendency to accumulate in well-separated linear zones. These zones can be interpreted as a system of deep seismically active fractures induced or activated in the overlying plate by the process of subduction.

The aim of the present work is to differentiate the earthquake foci situated in the continental wedge from those localized in the Wadati-Benioff zone, to attribute the individual earthquake foci to pertinent seismically active fracture zones and to delineate the seismotectonic pattern of the western margin of the South America plate between the parallels 22-35°S.

For the delineation of seismically active fracture zones the International Seismological Centre (ISC) data for the period 1964-92 were used. All hypocentral determinations with lower accuracy, characterized by errors greater than 0.2° in epicentral coordinates, and determinations based entirely on observations of local stations ($\Delta<20°$) were rejected. The orientation of several fracture zones was confirmed by fault plane solutions from the list of Harvard centroid moment tensor solutions.

In the rectangle limited by parallels 22-35°S and meridians 63-72°W thirteen seismically active fracture zones were delineated. Their pattern is given in Fig. 1. On the basis of their orientation in relation to the Peru-Chile trench they can be divided into the following three groups:

1/ Fracture zones rougly parallel to the trench [a] inclined in the same direction as the subduction zone (Z2, Z6), [b] inclined against the subduction zone (Z3), or [c] vertical or very steeply inclined fractures (Z1, Z4a,b, Z10a,b, Z11). The steeply inclined zones seem to represent the activated older pre-subduction tectonic features.

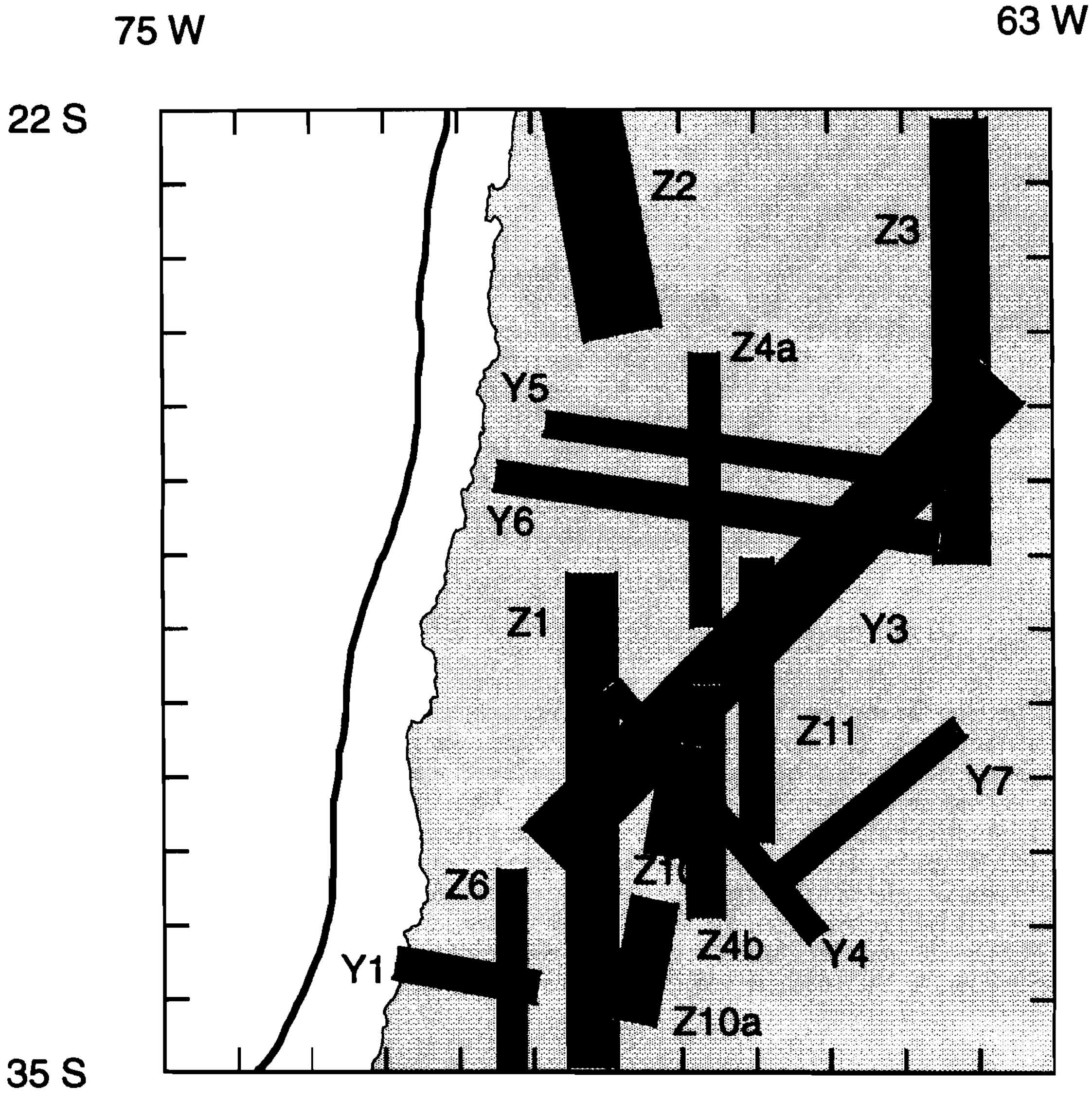


**Fig. 1** Pattern of seismically active fracture zones in the continental wedge. The axis of the Peru-Chile trench is denoted by a heavy line.

2/ Fracture zones roughly perpendicular to the Peru-Chile trench (Y1, Y5, Y6). They represent the continuation of transform faults in the subducted oceanic plate into the overlying continental wedge. These fracture zones are vertical or steeply inclined and portray the boundaries of individual segments of the subduction zone. They are independent on the internal structure of the continental wedge.

3/ Fracture zones oblique to the Peru-Chile trench (Y3, Y4, Y7), which are oriented under an angle of about 45° in relation to the direction of the recent Andean subduction.

The individual seismically active fracture zones can be geometrically well documented and found in vertical sections perpendicular to the trench axis, as shown by selected examples in Fig. 2.

## REFERENCES

Hanuš V. and Vaněk J. 1977-78. Subduction of the Cocos plate and deep active fracture zones of Mexico. *Geofisica Internacional*, 17, 14-53.

Hanuš V. and Vaněk J. 1979. Morphology of the Wadati-Benioff zone, andesitic volcanism, and active fracture zones in Central America. *Studia Geoph. Geod.*, 23, 218-234.

Hanuš V. and Vaněk J. 1984a. Earthquake distribution and volcanism in Kamchatka, Kurile Islands, and Hokkaido. *Studia Geoph. Geod.*, 28, 36-55, 129-148, 248-271.

Hanuš V. and Vaněk J. 1984b. Subduction induced fracture zones and distribution of hydrothermal activity in Mexico. *Tectonophysics*, 103, 297-305.

Hanuš V. and Vaněk J. 1987. Deep seismically active fracture zones in Ecuador and northern Peru. *Studia Geoph. Geod.*, 31, 8-25, 156-175.

Hanuš V. and Vaněk J. 1992. Seismotectonics of continental wedges overlying circum-Pacific subduction zones. *Časopis Miner. Geol. (Prague)*, 37, 277-287.

Hanuš V. , Vaněk J. and Sandoval G. 1987. Seismically active fracture zones and distribution of hydrothermal springs in Ecuador. *Studia Geoph. Geod..*, 31, 258-265.

Vaněk J. and Hanuš V. 1988. Historical disastrous earthquakes and deep fracture zones in Ecuador. In: W. H. K. Lee, H. Meyers, K. Shimazaki, eds., Historical seismograms and earthquakes of the world, Academic Press, San Diego, 362-369.

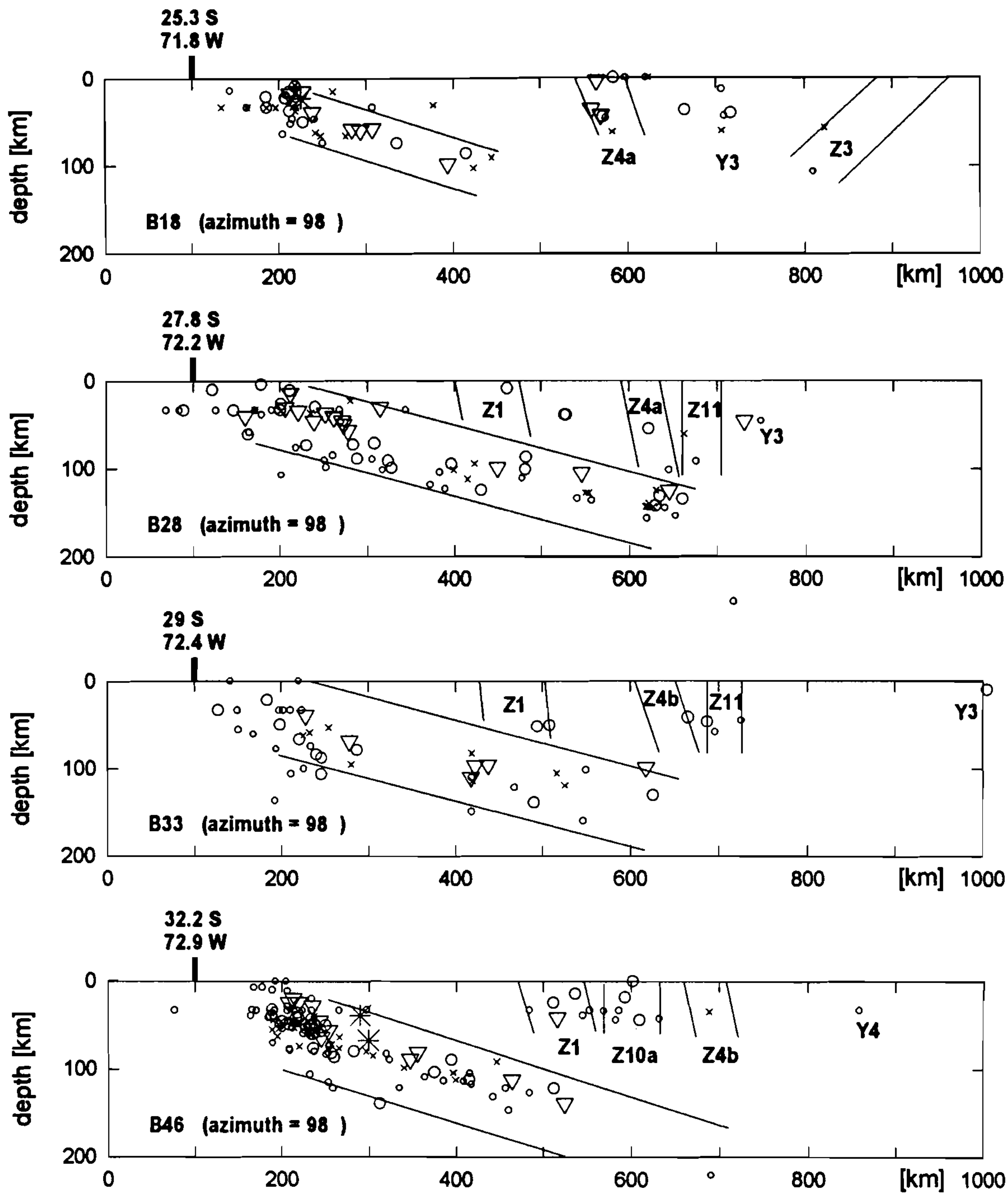


**Fig. 2** Vertical sections perpendicular to the trench giving the depth distribution of earthquake foci; width of sections 25 km, ISC foci are denoted with different symbols according to ISC magnitude, Wadati-Benioff zone by heavy parallel lines, individual fracture zones are labelled as in Fig. 1.

# HOLOCENE SEISMICITY AND TECTONIC ACTIVITY OF THE QUITO FAULT (ECUADOR): A PALEOSEISMIC HISTORY RECORDED IN LACUSTRINE SEDIMENTS

Christian HIBSCH(1), Alexandra ALVARADO(2), Hugo YEPES(2), Michel SÉBRIER(3)
Victor Hugo PÉREZ✝(2)

(1) Institut Français d'Etudes Andines, Ecuador, (*write to:* 45 Av. de Nonneville, 93600 Aulnay-sous-bois, France. Fax: (33-1) 48.66.25.46; E-mail: hibsch@world-net.sct.fr)
(2) Instituto Geofisico, Escuela Politécnica Nacional, Quito, Ecuador. Fax: 593-2 567-847, E-mail: hyepes@instgeof.ecx.ec
(3) URA-CNRS (1369) Géophysique et Géodynamique interne, Bât 509, Université de Paris-Sud, F-91 405 Orsay, France. Fax: 33-1 60-19-14-46, E-mail: sebrier@geol.u-psud.fr

---

**KEY WORDS:** paleoseismicity, neotectonics, paleoliquefaction, Holocene, Ecuador

## INTRODUCTION

Over the 460 years of Ecuadorian written history, several seismic events were registered, some of them reaching intensity IX (MSK) in Quito (CERESIS, 1985; Del Pino and Yepes, 1990). From the various seismogenic sources able to produce damage in the city, the Quito Fault is thought to be able to produce higher intensities in case of a rupture of the fault along its entire length (45 Km), making this structure the potentially more dangerous seismogenic source for the city. In the historical record, such activity of this fault was only registered once in 1755, were part of this fault could have ruptured producing an intensity VIII-IX (MSK) in Quito (Del Pino and Yepes, 1990). In order to assess the recurrence of major events, clearly overpassing the historical time span, it has been necessary to study the geological record. The paleoseismicity was evidenced by mean of the analysis of earthquake-induced paleoliquefaction horizons produced in a lacustrine environment. Evidences of the regional and local seismic activity were observed during the analysis of the Holocene sediments of Quito, as well as evidences of the Quito fault activity such as synsedimentary faults and seismotectonic deformation.

The Quito reverse fault system is active at least since the Late Pleistocene. The fault dip to the west below the city. Its Quaternary activity has created a series of tectonic ridges bordered to the east by a scarp of about 500m high due to compressive folding at the upper termination of the fault (Winter, 1990; Soulas *et al.*, 1991; Ego, 1995). Normal faulting occurred at the back of the overriding block and created a kind of piggy back basin filled by fluvial-lacustrine deposits until the 17$^{th}$ century. The sedimentological analysis of these deposits allowed us to precise the paleoseismic history of Quito for the rest of AD. times (pre-Hispanic history). A relatively complete paleoseismic record was observed in the northern basin, where a particular exposure in the "Calle Pinzón" shows the succession of at least 20 earthquake-induced contorted bedding horizons (Fig. 1). These paleoseismic features occurred at the bottom of lakes, at the water - sediments interface, as shown by erosional disconformities (Fig. 1). From the comparizon between published examples (Sims, 1975), relation between horizontal ground acceleration and intensity such as log

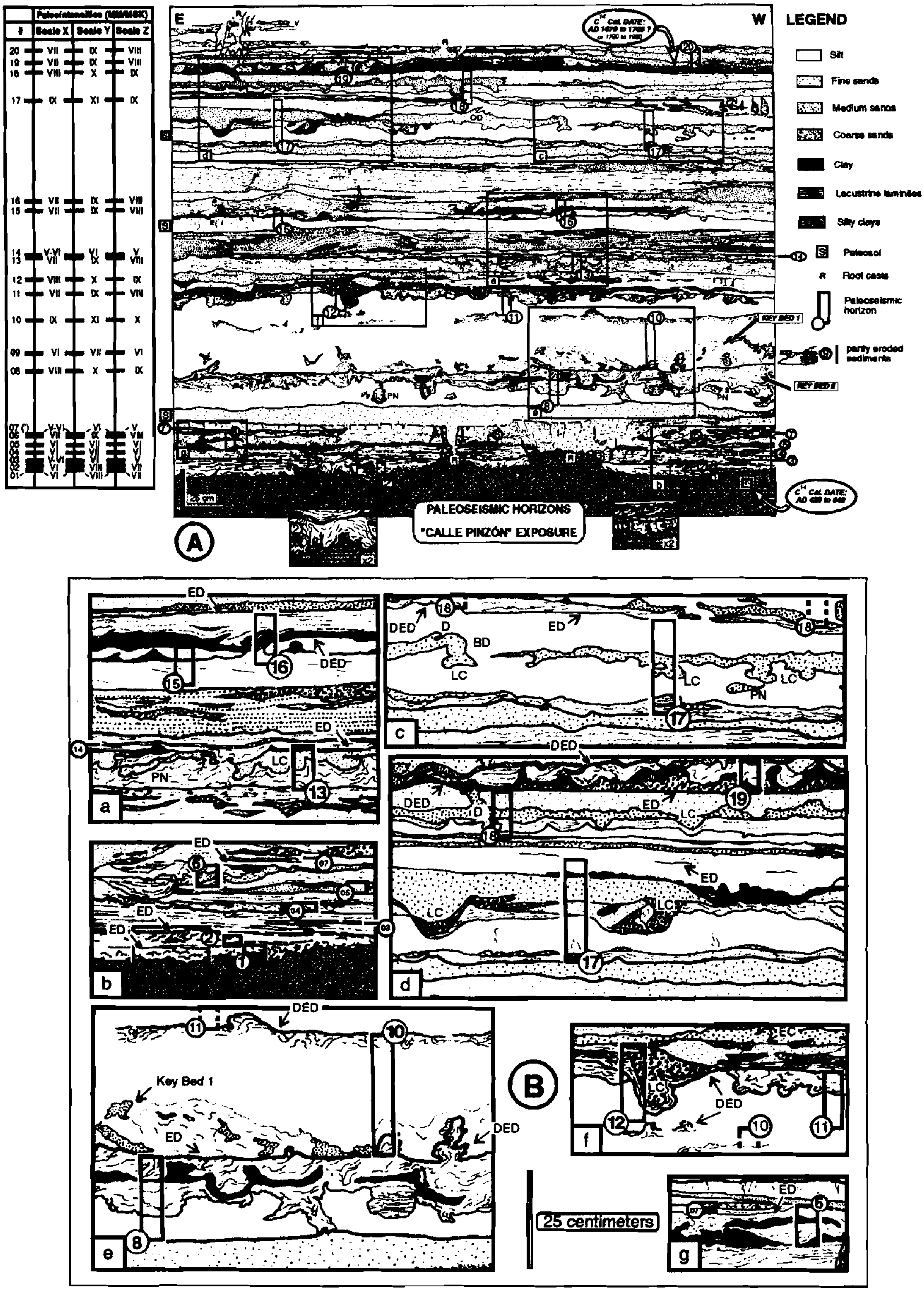
E
W
LEGEND
Silt
Fine sands
Medium sands
Coarse sands
Clay
Lacustrine laminites
Silty clays
Paleosol
Root casts
Paleoseismic horizon
partly eroded sediments
KEY BED 1
KEY BED 2
PALEOSEISMIC HORIZONS
"CALLE PINZÓN" EXPOSURE
A
B
Key Bed 1
25 centimeters
ED
DED
LC
PN
BD
EC

$a_H = 0.014 + 0.30 \ln_{MM}$ (Trifunac and Brady, 1975) and intensity distribution inferred from the historical seismicity (Del Pino and Yepes, 1991), we propose to define a scale of seismic paleointensity according to the thickness of earthquake-induced contorted bedding horizons :

In <=> $x^{(n-n_0)} \cdot h_0$ [± 1/3 In] (cm.), where n => intensity value (MM or MSK; n is an integer value), $n_0$ => intensity threshold able to produce contorted bedding, $h_0$ => thickness of the contorted bedding horizon produced by an intensity $n_0$ and $x$ => multiplier factor obtained with the relation between acceleration and intensity $a_{Hn+1} = x \,.\, a_{Hn}$ thus giving $x$=1.995 (Trifunac and Brady, 1975); $n_0$ and $h_0$ should vary according to the sediment type. In Quito lacustrine sediments, beeing clay, silts and silty sands alternations, we chose $n_0$ = V and $h_0$ = 1.25 cm. The obtained intensity distribution for intensities I≥VII (MM/MSK) shows a good coherence with the intensity distribution inferred from the historical seismicity (Fig. 2). The geological record covers an average 1500 years period which complete the Hispanic historical record.

## CONCLUSIONS

Both the historical seismicity and geological paleoseismicity indicate an average recurrence of 115 yr. for major events with intensities I≥VIII. We must notice that the last seismic event corresponding to this intensity range occurred in 1868, more than 125 years ago, but also that, within the 460 years of historical seismicity, this recurrence varied from 168 to just 9 years (Del Pino and Yepes, 1990). The use of the above mentioned scale also permit to evidence the probable occurrence of a major event of intensity IX-X (MM/MSK) between the 10$^{th}$ and the 16$^{th}$ century. Several paleoseismic horizons were successfully correlated with this event thanks to the presence of a volcanic key bed deformed by this paleoseismic shaking. These horizons were also correlated with seismotectonic deformation in the basin, making the Quito fault the most probable seismic source able to explain this major intensity overpassing the historical maximum intensity by almost one degree.

## REFERENCES

CERESIS, 1985. - *Catálogo de terremotos para América del Sur. Vol. 5-6, Ecuador, Lima.*

DEL PINO, I. & YEPES, H., 1990. - Apuntes para una historia sísmica de Quito. *in: Centro Histórico de Quito. Problematica y perspectivas. Dirección de Planificación. I. Municipio de Quito, Ecuador.*

EGO, F. (1995).- Accomodation de la convergence oblique dans une chaîne de type cordilléraine: les Andes d'Equateur. *Thèse Univ. Paris XI, 256 p.*

SIMS, J. D., 1975. - Determining earthquake recurrence intervals from deformational structures in young lacustrine sediments. *Tectonophysics, 29: 141-152.*

SOULAS, J.P., EGÜEZ, A., YEPES, H. & PÉREZ, V.H., 1991. - Tectónica activa y riesgo sísmico en los Andes Ecuatorianos y el extremo Sur de Colombia. *Boletín Geológico Ecuatoriano, 2, N° 1: 3-11.*

TRIFUNAC, M.D., & BRADY, A.G., 1975. - On the correlation of seismic intensity scales with the peaks of recorded strong ground motion. *Bulletin Seismological Society of America, 65, N° 1: 139-162.*

WINTER, T., 1990. - Mécanismes des déformations récentes dans les Andes équatoriennes. *Thèse Univ. Paris-Sud, Orsay, 205p.*

**Figure 1:** Drawing of the paleoseismic horizons from the "Calle Pinzón" exposure (#C2).

**A:** General view; position of dated samples; Zooms a & b are showing different soil response to the same paleo-earthquake due to the presence of a thick underlying silty argillaceous deposits; a to f refer to zooming in B; the intensities attributed to the paleoseismic horizons refer to different paleoseismic scales X, Y and Z (scale Z for Figure 2); PN: Pseudo-Nodules, OD: Oriented Dikes.

**B:** Detail view of a to f areas from A; LC: Load Casts, PN: Pseudo-Nodules, D: Dikes, BD: Bed Disruptions, ED: Erosional Disconformity, DED: Deformed Erosional Disconformity (due to the effect of the following paleoseismic event).

------>

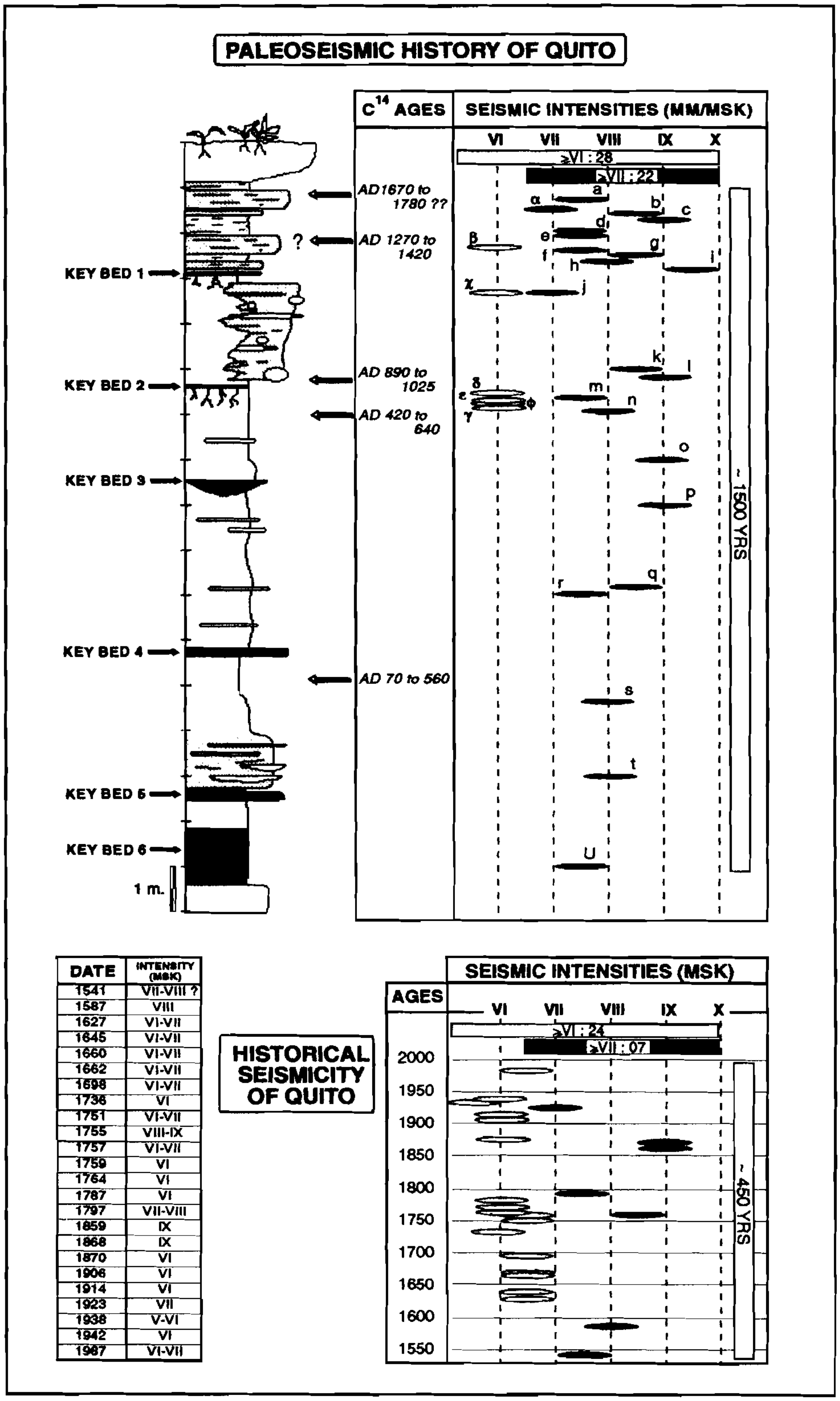


| DATE | INTENSITY (MSK) |
|---|---|
| 1541 | VII-VIII ? |
| 1587 | VIII |
| 1627 | VI-VII |
| 1645 | VI-VII |
| 1660 | VI-VII |
| 1662 | VI-VII |
| 1698 | VI-VII |
| 1736 | VI |
| 1751 | VI-VII |
| 1755 | VIII-IX |
| 1757 | VI-VII |
| 1759 | VI |
| 1764 | VI |
| 1787 | VI |
| 1797 | VII-VIII |
| 1859 | IX |
| 1868 | IX |
| 1870 | VI |
| 1906 | VI |
| 1914 | VI |
| 1923 | VII |
| 1938 | V-VI |
| 1942 | VI |
| 1987 | VI-VII |

**Figure 2:** Historical seismicity of Quito and complementary paleoseismic history obtained with geological analysis. To notice the few amount of low intensity events detected by the method of paleoliquefaction analysis, the relatively good coherence between historical intensity distribution and paleoseismic intensity distribution for the number of events with I > VII (considering about three times the duration of the geological record with respect to the historical record), and the show off of a possible paleo-earthquake of intensity IX-X between the 10th. and the 16th. century.

# NEOGENE TO QUATERNARY STATE OF STRESS IN THE CENTRAL DEPRESSION AND ALONG THE LIQUIÑE-OFQUI FAULT ZONE (CENTRAL AND SOUTHERN CHILE)

Alain LAVENU [1,2], José CEMBRANO [2], Francisco HERVÉ [2],
Gloria ARANCIBIA [2], Gabriel VARGAS [2], Ivan GARRIDO [3], Sergio BARRIENTOS [4],
Tony MONFRET [1,4]

1, ORSTOM, casilla 53 390, Correo central, Santiago 1, CHILE. email: alavenu@dgf.uchile.cl
2, Departamento de Geología, Universidad de Chile, casilla 13 518, Correo 21, Santiago, CHILE
3, Phelps Dodge Chile, Santiago, CHILE
4, Departamento de Geofísica, Universidad de Chile, casilla 2 777, Santiago, CHILE

KEY WORDS: Neotectonics, State of Stress, Neogene, Quaternary, Andes, Chile

## INTRODUCTION

Great earthquakes have affected central and southern Chile during the last 400 years (Nishenko 1985; Barrientos 1988; Barrientos *et al.* 1992).

Multidisciplinary research programs have been set up by the Geology and Geophysics Departments of the University of Chile and ORSTOM with the goal of determining the Cenozoic long-term and short-term kinematics of this part of the Chilean Andes. The main objectives are:

1 - To assess the neotectonics of the 1500 km-long Central Depression, the development of its basins and the geometry and kinematics of regional-scale boundary faults;

2 - To determine the kinematics and displacement rate of the Liquine-Ofqui fault zone which constitutes the eastern boundary of the southern Andes forearc.

To address these problems we have started analyzing the brittle deformation and characterizing the stress field in the sedimentary rocks, recent volcanic deposits and intrusive rocks of the Central Depression, the Coastal Cordillera, and the Main Range (*cf.* Structural map; ~ 40 analyzed microtectonic sites). Seismologic and seismotectonic studies are currently being undertaken in the northern part of the region. We have also analized the Neogene-Recent stress field along the Liquiñe-Ofqui fault zone; a seismic survey started in 1995 to address the present-day seismicity of the fault.

## CENTRAL DEPRESSION

First results of the microtectonic analysis of the Miocene, Pliocene and Quaternary faults have allowed to determine the stress field in the northern and central portions of the study area, using Carey's inversion algoritm (Carey and Brunier 1974; Carey 1979).

During the Late Miocene-Pliocene (9.8-2.7 Ma) the region from 33° to 38° S underwent brittle deformation compatible with a $\sigma_{Hmax}$ ($\sigma_1$) trending E to NE. During the Pleistocene (post 2.7 Ma) $\sigma_1$ trended NNE (Central Depression and Main Range) and E in the Coastal Cordillera (*cf.* Table).

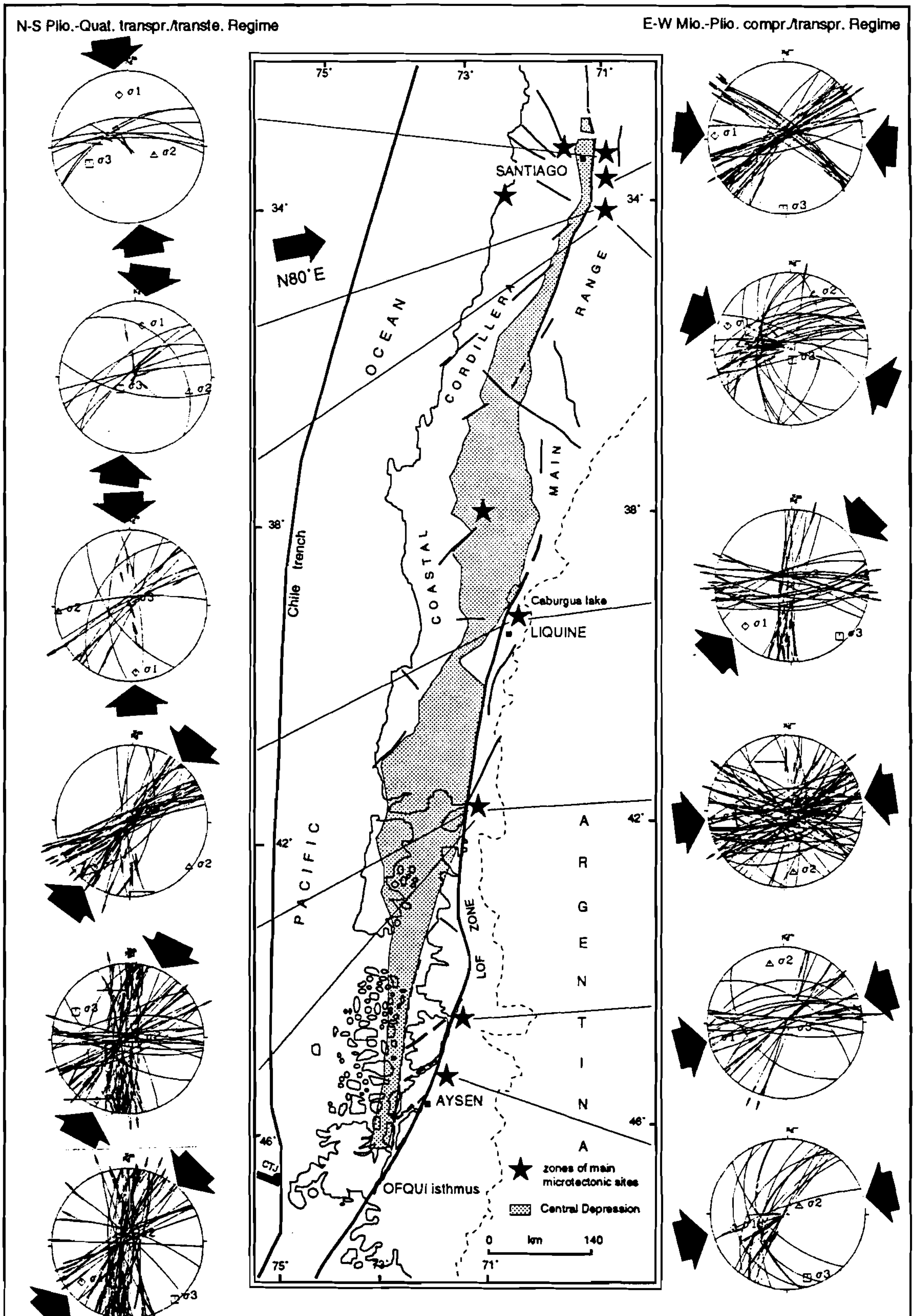


SIMPLIFIED STRUCTURAL MAP OF CENTRAL-SOUTHERN CHILE

## LIQUIÑE-OFQUI FAULT ZONE

According to Cembrano *et al.* (1996a), the NNE-trending 1000 km long Liquiñe-Ofqui fault zone (LOFZ), is a Cenozoic dextral strike-slip duplex (*cf.* Map). Marked contrasts in the nature and timing of deformation recorded along the LOFZ suggest a more complicated history than previously recognized (Schermer *et al.*, 1995).

From Lago Caburgua (north) to Aysen (south) it was possible to identify two main brittle tectonic events, a compressive-transpressive one of Miocene-Pliocene age and a dextral strike-slip event of Plio-Quaternary age (*cf.* Table). An extensional event, with $\sigma_3$ trending NW, may be compatible with the emplacement of Holocene minor eruptive centers (Lopez-Escobar *et al.*, 1995).

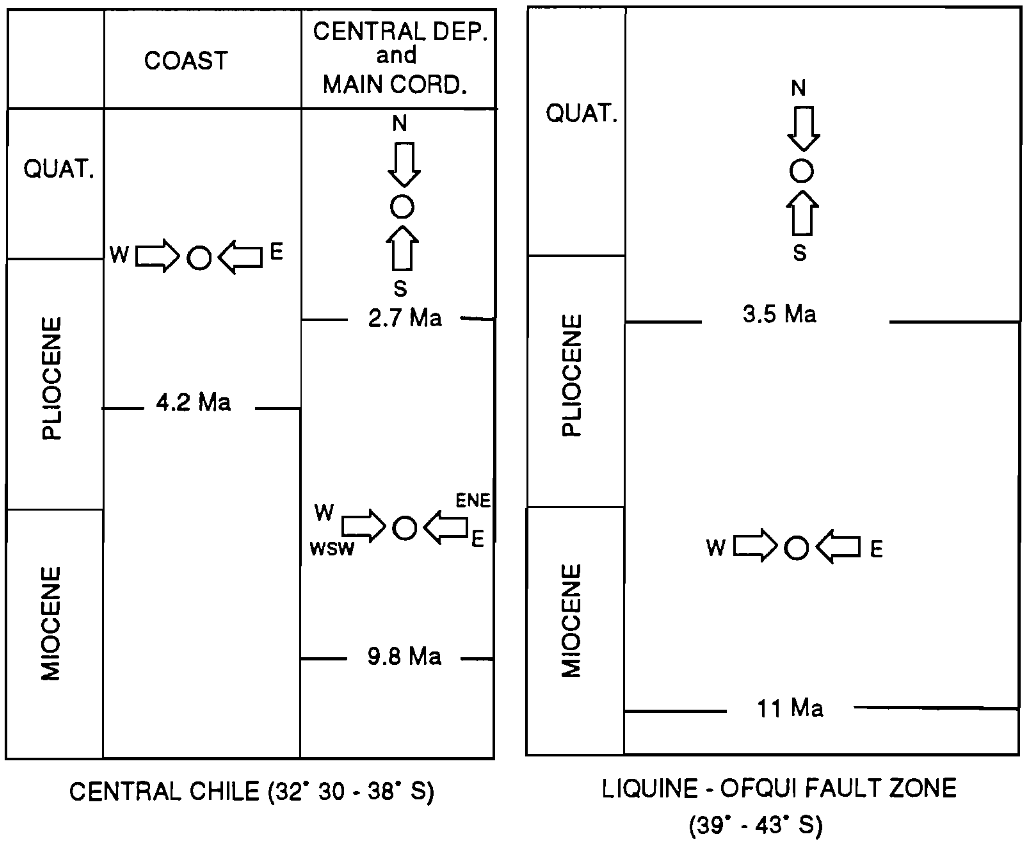


TABLE . Chronology and orientation of the different tectonic regimes

## CONCLUSIONS

From this first systematic brittle kinematic analysis carried out in Neogene-Quaternary rocks over an area of several hundred square kms in central and southern Chile it is possible to identify a compressive to dextral strike slip event acting from the Late Miocene in the Central Depression and the Liquiñe-Ofqui fault zone.

From 10 Ma to 3 Ma the direction of $\sigma_{Hmax}$ is roughly parallel to the Nazca-South America convergence direction (DeMets et al. 1990). This period may correspond to a high degree of coupling resulting from high convergence rates (David Engebretson, written communication). A compressive to transpressive tectonic regime would then prevail in the overriding plate.

From 3Ma, the direction of $\sigma_{Hmax}$ is NNE to NS and may be related to a period of low degree of coupling related to slower rates of convergence producing a transpressional to transtensional tectonic regime (Zoback, 1991).

Different driving mechanisms have been proposed for intra-arc strike-slip faults, namely oblique subduction (Fitch 1972; Beck 1983; Jarrard 1986) or indenters (Tapponier and Molnar 1976; Woodcock 1986; Nelson et al. 1994). Considering the large scale of the forearc sliver outboard the LOFZ oblique subduction seems to be the more likely driving mechanism for intra-arc shear in southern Chile, ridge subduction may apply to a more local scale in the vicinities of the triple junction (CTJ), separating the Antartica, Nazca and South American plates.

**Acknowledgements:** This work was funded by the Institut Français de Recherche Scientifique pour le Développement en Coopération (ORSTOM), FONDECYT 1950497 and 1950623, CODELCO-El Teniente, Killam fellowship (Dalhousie University) to J.C.

## REFERENCES

Barrientos S. 1988. Slip distribution of the 1985 Central Chile earthquake. *Tectonophysics*, 145, 225-241.

Barrientos S., Acevedo-Aranguiz P. 1992. Seismological aspects of the 1988-1989 Lonquimay (Chile) volcanic eruption. *Journal of Volcanology and Geothermal Research*, 53, 73-87.

Barrientos S., Plafker G., Lorca E. 1992. Postseismic coastal uplift in Southern Chile. *Geophysical Research Letters*, 19, 7, 701-704.

Beck Jr. M.E. 1983. On the mechanism of tectonic transport in zones of oblique subduction. *Tectonophysics*, 93, 1-11.

Carey E. 1979. Recherche des directions principales de contraintes associées au jeu d'une population de failles. *Revue de Géographie physique et Géologie dynamique*, 21, 57-66.

Carey E., Brunier B. 1974. Analyse théorique et numérique d'un modèle élémentaire appliqué à l'étude d'une population de faille. *Comptes Rendus de l'Académie des Sciences, Paris, D,* 279, 891-894.

Cembrano J., Hervé F., Lavenu A. 1996. The Liquiñe-Ofqui fault zone: a long-lived intra-arc fault system in southern Chile. *Tectonophysics*, (in press).

Cembrano J., Schermer E., Lavenu A., Sanhuesa A. 1996. Contrasting nature of deformation along an intra-arc shear zone, the Liquiñe-Ofqui fault zone, southern Chilean Andes. *Geological Society of America Bulletin*, (in press).

DeMets D., Gordon R.G., Argus D.F., Stein S. 1990. Current plate motions. *Geophysical Journal International*, 101, 425-478.

Fitch T.J. 1972. Plate convergence, transcurrent faults, and internal deformation adjacent to southeast Asia and the western Pacific. *Journal of Geophysical Research*, 77, 4432-4461.

Jarrard R.D. 1986. Terrane motion by strike-slip faulting of fore-arc slivers. *Geology*, 14, 780-783.

López-Escobar L., Cembrano J., Moreno H. 1995. Geochemistry and tectonics of the Chilean southern Andes basaltic Quaternary volcanism (37-46°S). *Revista geologica de Chile*, 22, 2, 219-234.

Nelson E., Forsythe R., Arit I. 1994. Ridge collision tectonics in terrane development. *Journal of South American Earth Sciences*, 7, 3/4, 271-278.

Nishenko S. 1985. Seismic potential for large and great interplate earthquakes along the Chilean and southern Peruvian margins of South America: a quantitative reappraisal. *Journal of Geophysical Research*, 90, 3589-3615.

Schermer E.R., Cembrano J., Sanhueza A.1995. Along-strike variation in intra-arc deformation, S. Chile. Geological Society of America, Annual Meeting, Abstracts , 27, 6, A-409.

Tapponier P. and Molnar P. 1976. Slip-line theory and large-scale continental tectonics. *Nature*, 264, 319-324.

Woodcock N.H. 1986. Strike-slip fault systems at plate boundaries. *Philosophical Transactions, Royal Society of London*, A, 317, 13-29.

Zoback M.D.1991. State of stress and crustal deformation along weak transform faults. *Philosophical Transactions, Royal Society of London*, A, 337, 141-150.

# DETECTION OF RECENT FAULTING AND EVALUATION OF THE VERTICAL OFFSETS FROM NUMERICAL ANALYSIS OF SAR-ERS-1 IMAGES. THE EXAMPLE OF THE ATACAMA FAULT ZONE IN NORTHERN CHILE.

Catherine MERING[1][2] Jean CHOROWICZ[2][3], Jean Claude VICENTE[3] and Cherif CHALAH[3]

[1] ORSTOM, 213 rue Lafayette 75010 Paris. France.

(2) URA 1759 CNRS, UPMC, Case 129-T26E1. 4 Place Jussieu

F 75252 Paris Cedex 05, e-mail: mering@ulysse.lgs.jussieu.fr

(3) Département de Géotectonique, UPMC, 4 Place Jussieu, F 75252 Paris Cedex 05

**KEYWORDS**: CHILE, IMAGE ANALYSIS, RADAR IMAGERY, TECTONICS

## TOPOGRAPHIC EFFECT OF RECENT FAULT SCARPS ON RADAR SAR IMAGES

Its is already well known that the relationship between the antenna depression angle of the incident beam and the surface slope of macro-scale features is very significant in the interpretation of radar images.

The foreslopes of topographic features (slopes facing the antenna) are responsible for strong echoes with the greatest amount of reflection occuring when the local slope is perpendicular to the radar beam (Ulaby et al., 1982), which corresponds to a 67°C angle in the case of SAR ERS-1 images. This condition, known as normal incidence, produces a very bright area on the image. Abrupt scarps such as those of recent faults (see Fig. 1) which face radar illumination can be then considered as creating conditions for such a foreslope brightening .

Besides, the presence of topographic relief in a scene can introduce distorsions known as *foreshortening* and *layover*. We will see whether the specific conditions of the viewing on fault scarps are affected by these distorsions.

With radar imaging, all foreslopes are shortened relatively to their true lengths (Fig. 1). The degree of shortening is a function of the illumination geometry and the foreslope angle acording to the equation (1):

$$A'B = AB\cos\alpha^{+}\left(1 - \tan\alpha^{+}/\tan\theta\right)\sin\theta \quad (1)$$

where $\alpha^+$ is the foreslope angle and $\theta$ is the look angle.

The greater the foreshortening, the more energy per unit area is displayed on the image until so much is avalaible that it saturates the reciever.

Besides, *layover* is an extreme case of foreshortening that occurs whenever the look angle is smaller than the fore slope angle. In this situation, the echo from the foreslope summit will be recieved first because the slant range is shorter to the top of the feature than it is to the base.. In this case a topographic feature will appear to be laid over on its side towards the near range. (Fig.1). The layover occurs mainly when steep slopes are encountered in the near range (Franceschetti et al., 1994).

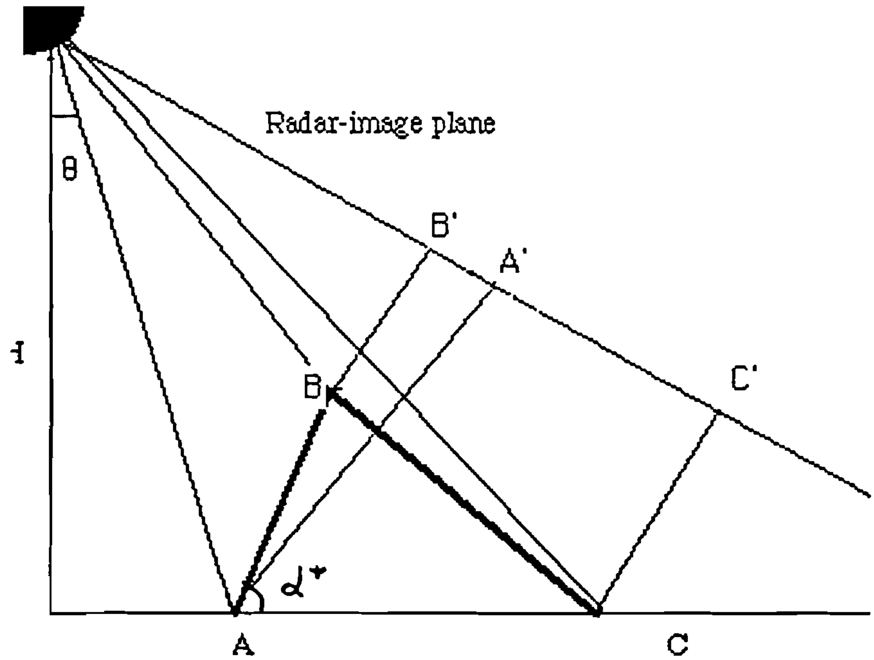


Figure 1

We suppose here that the slope AB on Figure 1 corresponds to the part of the fault plane where the slope angle is constant. The foreshortening effect will then be constant for the corresponding range A'B' on the image. The lower and the upper parts of the versant are affected by erosion so that their slope angles are smaller and their radiometry will be lower than that of the middle part AB.

## ANALYSIS OF THE RADAR SCENE OF THE ATACAMA FAULT ZONE

The training zone is situated here on segments of the Atacama fault in Northern Chile. In late Miocene, the Atacama Fault Zone (AFZ) has suffered major neotectonic reactivation and deformation continues until Present (Armijo and Thiele, 1991).

The SAR ERS-1 scenes were acquired on 02 June 1992, from an orbit 785 km in altitude, using an antenna inclined 23° off nadir operating in the C-band (5.3 Ghz). The observed earth surface is 100 by 100 km and ground resolution is 12,5 m .We show on figure 2 a segment of the fault from a subscene of a Radar SAR ERS-1 image.

Most of the segments of the AFZ are oriented NW-SE (Okada, 1972) and are consequently sub orthogonal to the radar beam. Within such a context, it is obvious that radar SAR ERS-1 images significantly enhances the mapping of this fault system. Recent faults corresponds thence to white lineaments on the image.

This type of fault is characterized by changes in the scarp height along the strike which corresponds on the image to variations of the thickness of the fault line (see Fig 2). In this case, we suppose that the fault dip is constant and that only the scarp height varies. The foreshortening effect must consequently be constant along the scarp and the fault line appears as a light line, the width of which beeing proportional to the slope length and therefore to the scarp height.

It is then possible to estimate relative fault throws along the same fault line, by calculating the width of the line on the radar image.

The features to extract correspond to sharp white lines on the radar image (Chorowicz et. al., 1993). The extraction is achieved by an image filtering reducing speckle noise called the connected center filter $\beta_c$ (Mering and Parrot, 1994) followed by a high tresholding. The white components still remaining on the image.being thinner than the object to exctract are eliminated by a *Geodesic Reconstruction* (Serra, 1988), while thicker ones are eliminated after a labelling (Fig.3).

## EVALUATION OF VERTICAL OFFSETS

The thickness of the line corresponding to the fault scarp is calculated by an image transformation called the *distance function* (Daniellson, 1980) which provides for each pixel of any connected component, a grey tone value which corresponds to a numeric distance between the pixel and the edge of the component . Such a *distance function* is used here to evaluate the thickness of irregular shapes on binary images. The *Maximal Thickness* of a connected component is then obtained by propagation of the highest value of the *distance function* inside each component. It provides an image on which each pixel has the numering value of the Maximal Thickness inside the connected component. (Fig. 4).

The result of computation of the *distance function* on the binary image (Fig. 3) gives 12 pixels as the value for the *Maximal Thickness*. From computation of the thickness of the lines which correspond to the A'B' in equation (1), we can deduce an estimation of the vertical fault throw h, knowing that:

$$h = AB\sin\alpha^{+}$$

The vertical fault throw h along the fault line. was calculated from a value of 12,5 meters for the pixel of the ERS-1 scene, and from a A'B' displacement value on the image of 8 pixels, which corresponds to one component on the example shown on Figure 4.

According to recent measurements on the ground, the slope along the scarp on this fault segment is about 77° (Gonzales et al, 1996). We conclude therefore that, taking into account both the *layover* and the *foreshortening*, effects on ERS-1 image, the fault throw at this place of the fault, can be estimated in this case as 120 meters high, from image analysis.

## REFERENCES


Armijo R. and Thiele H., 1990. Active faulting in Northern Chile: Ramp stacking and Lateral Decoupling along a Subduction Plate Boundary. *Earth Planet. Sci. Lett.*, vol 98, 1990, pp40-61

Chorowicz J., Deffontaines B., Huaman-Rodrigo H., Luxey P., Pubellier and J.P. Rudant, 1993 Geomorphic objects detected by ERS1-SAR images in different geodynamic contexts. *Proceedings of Second ERS-1 Symposum Space at the Service of our Environment*, Hamburg, Germany, 11-14 October 1993, pp923-929.

Daniellson P.E., 1980, Euclidian Distance Mapping, *Computer Graphics and Image Processing*, vol14, pp227-248.

Dewey J.F. and Lamb S.H. , 1992. Active tectonics of the Andes, *Tectonophysics, vol 205*, pp 79-95.

Franceschetti G,.Marino R., Migliaccio M. and Riccio D. On SAR simulation on three-dimensional scenes. SPIE, Vol 2316, *SAR Data Processing for Remote Sensing*, 1994, pp192-198.

Gonzales L.G., Niemeyer H., Martinez E., 1996. Evolucion Tectonica Cenozoica del bordo continental en las immediaciones de Antofagasta: su relacion con la sedimentacion y la morfologia. Revista Geol. de Chile (in press).

Mering C. and Parrot J.F., 1994. Radar image analysis using morphological filters. *Mathematical Morphology and its Applications to Signal Processing*, eds J. Serra and P. Soille, Kluwer Academic Publisher, pp353-360.

Okada A. , 1972. On the neotectonics of the Atacama region. Preliminary notes on Late Cenozoic Faulting and geomorphic development of the Coast range of Northern Chile. *Bull. Dept Geography, Univ. Tokyo*, v3, pp47-65.

Serra J., 1988. Image Analysis and Mathematical Morphology. Vol. 2, Theoritical Advances, Academic Press, London, 411 p.

Ulaby F.T., Moore R.K and Fung A.K., 1982. Microwave Remote Sensing, vol 2, *Archtech House Inc.*

Figure 2: ERS-1 subscene of the Atacama Fault Zone

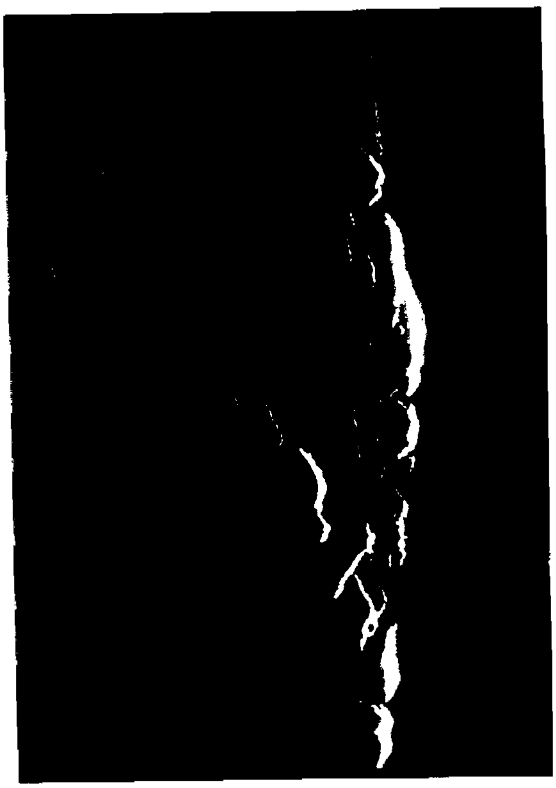

Figure 3: Extraction of fault scarps

Figure 4: Maximal Thickness image

# SEISMOLOGICAL INTERPRETATION OF THE HISTORICAL DATA RELATED TO THE 1929 CUMANA EARTHQUAKE, VENEZUELA

Antoine MOCQUET(1), Carlos BELTRAN(2), Miguel LUGO(2), José A. RODRIGUEZ(2) and André SINGER(2)

(1) Laboratoire de Géophysique et Planétologie, U.F.R. des Sciences et Techniques, 2 rue de la Houssinière, 44072 Nantes Cedex 03, France. E-mail: mocquet@chimie.univ-nantes.fr
(2) FUNVISIS, Fundacion venezolana de investigaciones sismologicas, Departamento de Ciencias de la Tierra, Prolongacion calle Mara, Urbanizacion El Llanito, Petare, Departamento Sucre, Apartado postal 76880, Caracas 1070-A, Venezuela.

**KEY WORDS** : Venezuela, historical seismicity, seismic hazard, barrier

## INTRODUCTION

The January 17, 1929 Cumana earthquake, northeastern Venezuela, was associated with the activity of the El Pilar Fault Zone, along which the dextral motion between the Caribbean and South-American plates is presently taking place. Nowadays, seismic activity concentrates towards the easternmost tip of the Fault Zone, close to its junction with the Lesser Antilles subduction zone. This seismic activity can be divided into three main types (e. g. Russo et al., 1993): shallow earthquakes displaying right-lateral strike-slip motions when located along east-west trending quasi-vertical faults, deep earthquakes (focal depth h greater than 60 km) associated with the descending slab of the Lesser Antilles subduction zone, and intermediate depth earthquakes (20 km < h < 60 km) which are representative of the complex strain release taking place at the junction between the El Pilar Fault Zone and the subduction zone, in the vicinity of Trinidad island. The area close to Cumana city contrasts with these later regions by its low level of seismic activity. Three different hypothesis can be proposed to explain this observation: (1) creep phenomena contribute mainly to the motion in this area, (2) seismic motion has already been accomodated during historical large events, (3) tectonic stresses are presently accumulating in this area. In this context, a detailed study of the 1929 event is important because it is the latest major event which occured in the area prior to 1962, when the Worl-Wide Standard Seismograph Network became operational. In particular, were the reported widespread damages due mainly to local site effects, or was this event a major one ?

## INTERPETATION OF HISTORICAL DATA

Cumana city is settled on a compressional fault jog of the El Pilar Fault Zone. The total width of the fault jog reaches 5 km in a north-south direction, and Cumana city is located on the northern edge of the jog, on the western side of the so-called Cerros de Caiguïre (Figure 1). These 2 km wide hills consist of folded pliocene sediments. These folds accomodate stress changes due to the termination of the northernmost branch of the El Pilar Fault Zone. This kind of geological structure is now widely recognized as an impediment to the propagation of seismic rupture (King, 1986; Sibson, 1986). Indeed, Paige (1930) reported that during the 1929 event, two linear surface ruptures emerged south of Punta Delgada, propagated westward, and stopped their propagation soon after affecting the Cerros de Caiguïre (Figure 1). There is no strong evidence for a further westward propagation of the rupture. A 3 m high sea-wave invaded the harbour in the place named El Salado. In this area, the slope of the coast is very steep, up to 45°, and overlain with loosy water-saturated sediments. Seaward lateral spreading of the headland bar was documented during the earthquake (Beltran and Rodriguez, 1995). Therefore, slumping can explain the occurence of this wave. The presence of a shattered zone within the area where rupture ends has been documented for californian earthquakes by Scholz (1990). Such phenomenon can explain the strong ground motions reported in Cumana City. Shaking was also amplified by local site effects. Indeed, the town was built on loosy sediments. Detailed geomorphological mapping (Beltran and Rodriguez, 1995) showed that most of severe damages occured within sites where buildings were constructed either on lagunal areas or upon deserted meanders of the Manzanares river (Figure 1).

First-hand historical documents, photographs, reports, and testimonies related to damages inside and outside Cumana city have been carefully compiled by Rodriguez and Chacin (1993). These descriptions include the damages and destructions which affected public buildings and houses, ground fractures, liquefaction phenomena, water and sand blows, induced landslides, collapse spreadings, and ground noise. The most destructive effects were concentrated along a 30 km long narrow band fringing the southern coast of the Gulf of Cariaco. These macroseismic data enable us to draw the isoseismal map shown in Figure 2. The instrumental epicenter relocated by Russo et al. (1992) is also shown. The error ellipse of the relocated epicenter is rather large because instrumental data were sparse. However, this location is concordant with the MKS VIII intensity area derived form macroseismic data. The white dots in Figure 2 represent the locations where aftershocks were most strongly felt up to one week after the main shock. In our view, these data indicate that the ruptured fault length should not have been longer than 25 to 30 km.

One of the most important macroseismic data was the widespread testimony that people in Cumana city felt shaking during 5 to 15 sec (Paige, 1930). While we make the hypothesis that this duration was not overestimated by frightened people, its value must be regarded as a maximum value, because it involves the total source duration $\tau$, the different arrivals of near-field seismic waves, and the response of soil and buildings. Since the total seismic moment $M_0$ of an earthquake scales with $\tau^3$ (e. g. Furumoto and Nakanishi, 1983), these maximum values correspond to $10^{17}$ Nm $\leq M_{0max} \leq 10^{19}$ Nm, or equivalently, $5.3 \leq M_{Wmax} \leq 6.7$, where $M_W$ is the energy magnitude defined by Kanamori (1977). Unfortunately, no scaling relations are available yet for venezuelan earthquakes. By analogy with californian earthquakes, these values correspond to maximum fault lengths comprised between 5 and 30 km. This latest value is in good agreement with the maximum fault length inferred from macroseismic data.

## CONCLUSIONS

The 6.9 magnitud derived by Gutenberg and Richter (1954) from the instrumental record of Pasadena (California) should be regarded as an extreme possible value, because it would involve fault length and source duration values greater than 40 km, and 20 sec, respectively. Macroseismic data indicate that the total fault length must have been smaller than 30 km. Most destructions are explained by local site effects. This interpretation means that (1) the 1929 Cumana earthquake did not release a significant amount of tectonic stress along the southern Caribbean plate boundary, and that stresses are going on accumulating in this area, (2) local soil conditions in Cumana city and surrouding regions are very poor in the sense that they amplify greatly the destructive effects of moderately sized earthquakes.

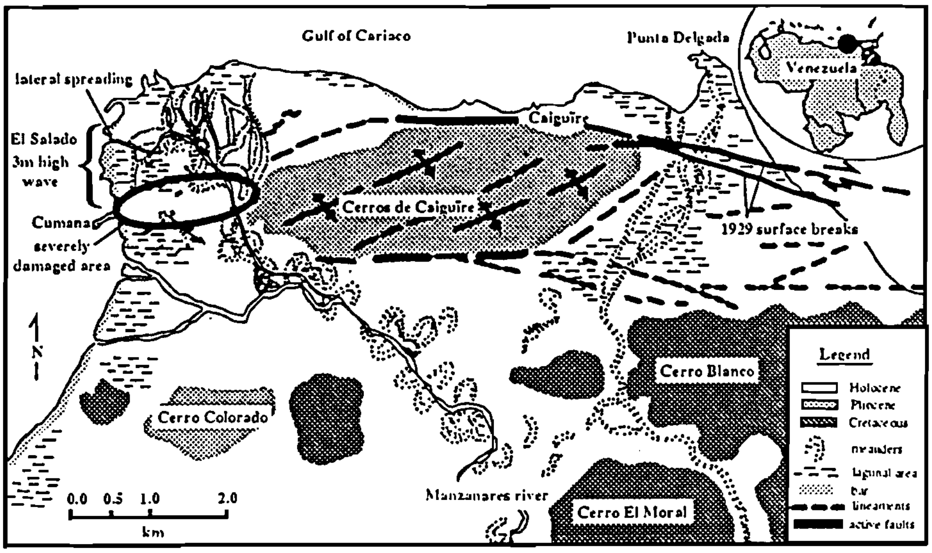


Fig. 1. Tectonic map of Cumana city and surrounding area, after Beltran and Rodriguez (1995).

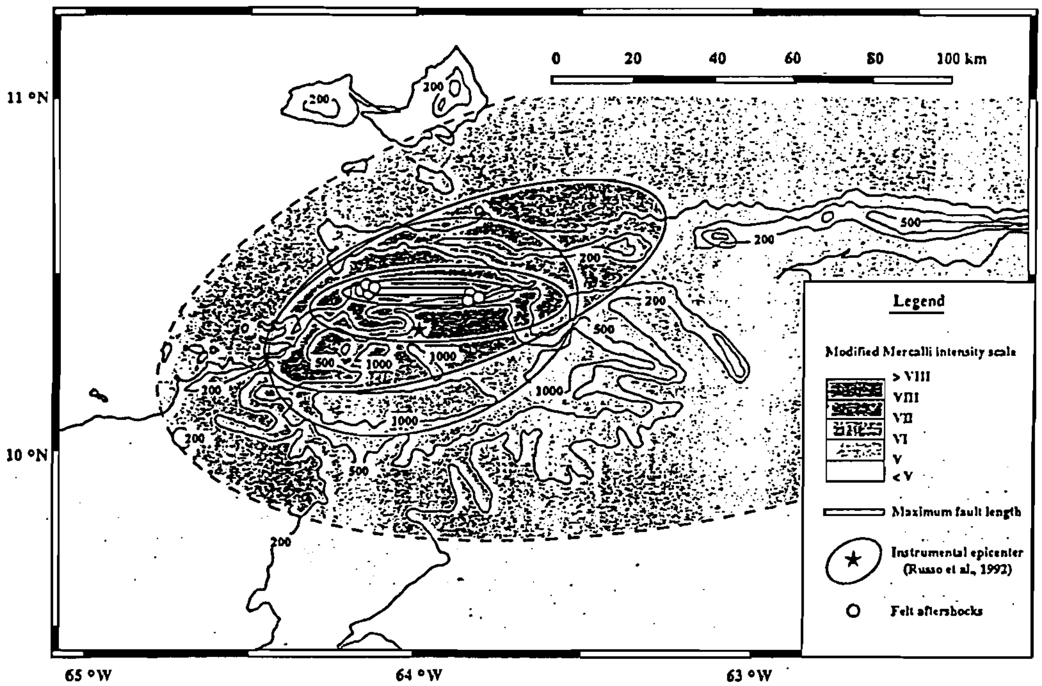


Fig. 2. Isoseismal curves of the January 17, 1929 Cumana earthquake, Venezuela. Topography is indicated in meters.

**REFERENCES**


Beltran, C., and J. A. Rodriguez 1995. Ambientes de sedimentacion fluvio-deltaica y su influencia en la magnification de daños por sismos en la ciudad de Cumana, Venezuela, *Mem. 2ndo. Coll. Micr. Sism.*, Cumana, Venezuela, 11-14 Junio 1995, in press.

Furumoto, M., and I. Nakanishi 1983. Source times and scaling relations of large earthquakes, *J. Geophys. Res.*, 88, 2191-2198.

Gutenberg, B., and C. Richter 1954. *Seismicity of the Earth and associated phenomena*, Princeton Univ. Press, New-York, U.S.A., 310 p.

Kanamori, H. 1977. The energy release in great earthquakes, *J. Geophys. Res.*, 82, 2981-2987.

King, G. C. P. 1986. Speculations on the geometry of the initiation and termination processes of earthquake rupture and its relation to morphology and geological structure, *Pageoph*, 124, 567-585.

Paige, S. 1930. The earthquake at Cumana, Venezuela, January 17, 1929, *Bull. Seism. Soc. Am.*, 20, 1-10.

Rodriguez, J. A., and C. A. Chacin 1993. Relacion documentada del sismo de Cumana del año 1929, *II Jorn. Cient. Escuela Geologia, Minas y Geofisica*, Univ. Central Venezuela, Caracas, Venezuela, 7 p.

Russo, R. M., E. M. Okal, and K. C. Rowley 1992. Historical seismicity of the south-eastern Caribbean and tectonic implications, *Pageoph*, 139, 87-120.

Russo, R. M., R. C. Speed, E. A. Okal, J. B. Sheperd, and K. C. Rowley 1993. Seismicity and tectonics of the southeastern Caribbean, *J. Geophys. Res.*, 98, 14,299-14,319.

Scholz, C. H. 1990. *The mechanics of earthquakes and faulting*, Cambridge Univ. Press, Cambridge, U. K., 439 p.

Sibson, R. H. 1986. Rupture interaction with fault jogs, in *Earthquake source mechanics*, Das, S., J. Boatwright, and C. H. Scholz eds., pp. 157-168, Maurice Ewing Series 6, A. G. U. monograph 37, Washington, D. C.

# CODA WAVE ATTENUATION BEFORE AND AFTER THE ANTOFAGASTA MAJOR EVENT OF JULY 30, 1995

Tony MONFRET

Mission ORSTOM, Chile, Román Díaz 264, Santiago, Chile.
Departamento de Geofísica, Universidad de Chile, casilla 2777, Santiago, Chile.

**KEY WORDS:** intrinsic attenuation, scattering attenuation, precursor.

## INTRODUCTION

Most of the methods used to find a precursor signal to big earthquakes in seismic gaps have generally failed, mainly because they are not reproducible in space and time. From a seismological point of view, the usual parameters which are looking for as a medium or short term event precursors, are the local seismicity pattern versus time, temporal variations of seismic velocities and coda wave attenuation [1].

At the beginning, coda wave was mainly focused on a simple way to study the seismic source and later the attenuation between the source and the receiver. Complex processes as interferences of S-waves with heterogeneities into the propagation medium is considered to be one of the cause of coda wave generation. Furthermore, coda wave is also involved in defining site effect, magnitude and seismic moment.

Single scattering theories were developed in order to explain, for an isotropic medium, the observed coda wave decay with time as a function of the attenuation, where it is not necessary to take out the instrumental response from the signal and to know precisely the source mechanism, but only the absolute S-arrival time [2,3]. In a first approximation, coda wave attenuation $Q^{-1}$ is the sum of the intrinsic attenuation $Q_i^{-1}$ or absorption, which dissipates seismic energy into heat and the scattering attenuation $Q_s^{-1}$ as the result of heterogeneities into the propagation medium which redistributes seismic energy into a certain volume. However, these theories assume that only one body can scatter the seismic ray between the hypocenter and the sensor.

Our study is involved mainly with the behavior of coda wave attenuation prior and after the Antofagasta July 30, 1995 earthquake, the biggest one which occured in the Antofagasta region, by using a multiple scattering attenuation method to analyze the time evolution of the intrinsic and scattering attenuation at different seimic stations of the Antofagasta local seismic network, whose the closest station (CEN) to the epicenter of the main event was at distance of about 20 km [4].

## METHOD AND DATA PROCESSING

Nowadays, several isotropic multiple scattering methods are available and consider a more realistic travel path between the source and the station to better fit the coda amplitude decay. Therefore, for our purpose, we used the isotropic multiple scattering algorithm developed by Zeng [5] for the acoustic approximation, to calculate $Q_i^{-1}$ and $Q_s^{-1}$ and applied it to a set of local earthquakes recorded at the Antofagasta seismic network between January 1993 and the first months of 1996. As we are interested in following the variations of attenuation versus time, we consider every attenuation measurement as the result of an independent physical process and do not make any average to smooth the results. Otherwise, we chose the mean free frequency $\partial$ ($\partial=\omega Q^{-1}$) as a better parameter to represent the attenuation process and which can be determined without filter the coda at different frequencies. We focused mainly our observations on the attenuation behavior prior and after the Antofagasta seismic event of July 30, 1995 of magnitude $M_w$ 8.1.

During June, 1990, The Institut de Physique du Globe of Strasbourg (France), ORSTOM (France) and the University of Chile (Chile) installed a telemetric seismic network of nine short period (1s) stations around the city of Antofagasta, in order to monitor the local microseismicity of magnitude more than 2. This network is situated on the southern edge of the rupture zone of the 1877's Northern Chile earthquake of magnitude $M_W$ 8.8. In spite of some lacks of data because of some power cuts and acquisition failures, the dataset of more than five years of local seismicity is almost complete previous, during and after the Antofagasta big earthquake of last July 30, 1995. With the threshold used in the Antofagasta telemetric local network, between five to ten earthquakes were commonly daily recorded prior to the Antofagasta earthquake. The majority of this microseismicity is localized along the Benioff zone from depths of about 25 km till depths of about 250-300 km.

In this study, we were mainly interested in earthquakes with an arbitrary epicentral distance of less than 30 km from the seismic stations considered, because the higher the epicentral distance, the bigger the volume involves in generating coda wave and the more difficult to interpret one attenuation measurement from another. Obviously, if the distance between the station and the epicenter is to short , the number of data will not be enough to follow the attenuation behavior versus time. Keeping in mind these conditions, we select from the nine stations of the Antofagasta seismic network, only 5 (MEJ,CEN, GOR, PAS and APB) where the attenuation time sequence is almost continuos from 1993 to march 1996. The station CEN is localized upon the modeled fault plane of the Antofagasta earthquake, at 20 km away from the epicenter, and MEJ at about 45 km far of the northern edge of the rupture zone [6]. Once a seismogram is chosen at a station, it must be not saturated (in general, the magnitude $M_L$ of the seismic event must be less than 3.5), the coda wave must reach the noise level (in fact, twice the amplitude of the noise prior to the first P-arrival) and no glitches have to be included into the coda portion. The number of events selected varies from one station to another mainly because the seismicity in that region is not uniform in both space and time.

## DISCUSSION AND CONCLUSIONS

The mean free frequencies $\partial_i$ and $\partial_s$ for the time period 1993 to 1996 are still in process at CEN, APB, GOR and PAS and could not be part of the following discussion, but will be incorporate later. They were, however, performed at MEJ but with a dataset not complete in time as it was expected. Thus, although our discussions and conclusions will be partial and concerned only the region around MEJ, we can nevertheless make some remarks.

The propagation medium between the interface of the Nazca subducting plate and the South American plate around MEJ is mainly homogeneous in space and time because intrinsic attenuation always exceeds scattering attenuation and thus control the attenuation process (figure 1). Furthermore, the intrinsic attenuation in this study is in fact the total attenuation calculated by the single scattering attenuation theory of Sato [3] as it was already observed for intrinsic scattering as a function of frequency [7].

Although each local attenuation measurement in time can be very different to the others (day 1096 on figure 1), probably because they are generated by different scattering volumes, the general temporal behavior of intrinsic attenuation is uniform and does not show any evidences of variation prior and after the Antofagasta earthquake of July 30, 1995 (figure 1). On the other hand, the scattering attenuation is in general higher in 1995 prior to the big event than in 1993 and the beginning of 1996 (figure 1). However, more attenuation measurements should be performed at MEJ, specially for the year 1994, to improve the temporal coverage of scattering attenuation, in order to localize in time, with a better precision, this variation.

We used our program to calculate intrinsic and scattering attenuation from synthetic coda waves which had crossed different propagation mediums. Each medium has a different number of scatters, randomly distributed in an equal volume. Though, they were generated for the single isotropic scattering case [8], we found that when the number of scatters increases of a factor of 2 for a same volume, the intrinsic and total attenuation decrease of a factor of about 2, whereas scattering attenuation increases of a factor closed to 4.5. So, if the scattering attenuation increases before and decreases after a major earthquake as it seems to be the case for the Antofagasta earthquake, therefore, the number of scatters increased prior to the main event and diminished after. These observations could be explained by a dynamical system of earthquake occurrence where shear stress an pore pressure control both the spatial and temporal pattern of the distribution of heterogeneities or scatters [9].

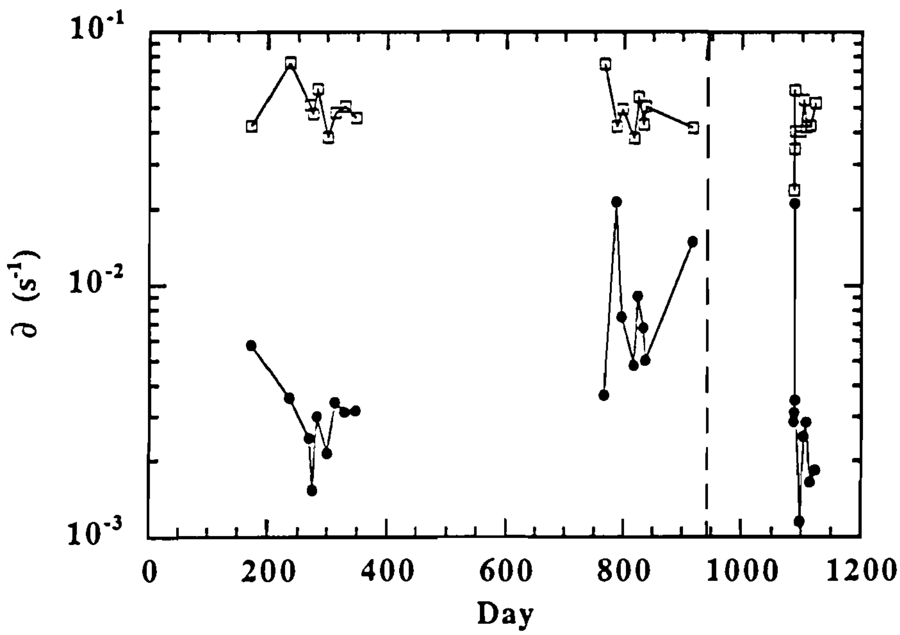


**Figure 1:** Intrinsic (open squares) and scattering (black dots) mean free frequency versus time calculated at MEJ. Each symbol is an independent measure. Segments link the different symbols according to their time occurrence. The day 0 is January 1st, 1993. The vertical dashed line represents July 30, 1995 when occurred the big Antofagasta earthquake of magnitude $M_W = 8.1$.

## ACKNOWLEDGMENTS

I am grateful to Juan Thomas, Jean-Philippe Caminade and Helmut schatte for having localized the seismicity recorded at the Antofagasta network from 1993 to 1996.

## REFERENCES

[1] Sato H, 1988. Temporal change in scattering and attenuation associated with the earthquake occurrence - A review of recent studies on coda waves, Pure Appl. Geophys., 126, 465-497.
[2] Aki K. and B. Chouet, 1975. Origin of coda waves: source, attenuation and scattering effects, *J. Geophys. Res.*, 80, 3322-3342.
[3] Sato H., 1977. Energy propagation including scattering effects, single isotropic scattering approximation, *J. Phys. Earth*, 25, 27-41.
[4] Monfret T., L. Dorbath, J.P. Caminade, M. Pardo, D. Comte, L. Ponce, A. Cisternas, B. Delouis and L. Rivera, 1995. The July 30, 1995 Antofagasta earthquake: an "hypocritical" seismic event, *EOS Trans. AGU*, 76, 46, S51-25.
[5] Zeng Y., 1991. Compact solutions for multiple scatterd wave energy in time domain, *Bull. Seism. Soc. Am.*, 81, 1022-1029.
[6] Ruegg J.C., J. Campos, R. Armijo, S. Barrientos, P. Briole, R. Thiele, M. Arancibia, J. Cañuta, T. Duquesnoy, M. Chang, D. Lazo, H. Lyon-Caen, L. Ortlieb, J.C. Rossignol and L. Serrurier, 1996. The $M_W$=8.1 Antofagasta (North Chile) earthquake of July 30, 1995: first results from teleseismic and geodetic data, *Geophys. Res. Lett.*, in press.
[7] Monfret T., 1994. Coda S-wave attenuation calculated by single, double and multiple isotropic scattering theories, *EOS Trans. AGU*, 75, 44, S31C-04.
[8] Korneev V. A. and L. R. Johnson, 1993. Scattering of elastic waves by a spherical inclusion - 1. Theory and numerical results, *Geophys. Journ. Int.*, 115, 230-250.
[9] Miller S. A., A. Nur and D. L. Olgaard, 1996. Earthquake as a coupled shear stress - high pore pressure dynamical system, *Geophys. Res. Lett.*, 23, 197-200.

# QUATERNARY MORPHOSTRATIGRAPHY AND VERTICAL DEFORMATION IN MEJILLONES PENINSULA, NORTHERN CHILE

**Luc ORTLIEB[1, 2, 3], José Luis GOY[4], Cari ZAZO[5], Claude HILLAIRE-MARCEL[6], Bassam GHALEB[6], Nury GUZMAN[2] & Ricardo THIELE[3]**

[1] ORSTOM (UR 14, Programme DESIRS), Casilla 1190, Antofagasta, Chile
[2] Facultad de Recursos del Mar, Universidad de Antofagasta, Casilla 170, Antofagasta, Chile
[3] Departamento de Geología, Universidad de Chile, Plaza Ercilla, Santiago, Chile
[4] Depart. de Geología, Facultad de Ciencias, Universidad de Salamanca, 37008 Salamanca, Spain
[5] Depart. de Geol., Museo Nac.de CC.Nat., C.S.I.C., J.Gutierrez Abascal 2, 28006 Madrid, Spain.
[6] GEOTOP, Université du Québec à Montréal, Case 8888 (Centre ville), Montréal, H3C3P8, Canada.

KEY WORDS: Neotectonics, Marine terraces, Uplift, Quaternary, Chile

## NORTHERN CHILE SUBDUCTION PLATE-BOUNDARY AND QUATERNARY UPLIFT MOTIONS

At subduction plate boundaries, it is commonly expected that relatively strong vertical motions occur. The coast of northern Chile, like that of southern Peru (Goy et al., 1992; Macharé & Ortlieb, 1992; Ortlieb et al, 1995a; 1996) did register such positive vertical deformation that is linked to the subduction of the Nazca plate below the South-American plate (Barazangi and Isacks, 1976). Emerged marine terraces are preserved along long stretches of the northern Chile coast (Radtke, 1989). Recent studies focused on the identification, age determination and morphostratigraphy of the remnants of Pleistocene shorelines, to decipher the neotectonic behaviour of the 1000 km-long coastal segment located south of the Peruvian border. The methodology points to a quantification of the vertical deformation, at a $10^5$y scale, and to the detection of variations in local/regional uplift rates during the late and middle Quaternary. The study also deals with the determination of differential vertical movements between structural blocks, and the obtention of a chronostratigraphical framework for the reconstitution of Quaternary faulting activity in the coastal area..

At the present stage of the co-operative project, we completed a general reconnaissance of the Quaternary marine terraces in the whole study area, and realised detailed studies in the sector between Antofagasta and Hornitos (Ortlieb et al., 1995b, 1997). Geological, paleontological and geomorphological surveys in the Antofagasta-Hornitos region now provide a morphostratigraphical interpretation of the various types of coastal remnants: wave-cut terraces, beach ridges, marine deposits. Geochronological and geochemical analyses involving U-series dating, amino-acid stratigraphy and stable isotope measurements assess the chronostratigraphical framework currently being established (Hillaire-Marcel et al., 1995).

In the coastal sector between Antofagasta (23°30'S) and Iquique (20°S), the oldest Pleistocene marine remnants and Late Pliocene sediments are usually found at the foot of the Coastal Escarpment, at elevations of the order of +100 to +200 m (Ortlieb et al., 1995b). In this coastal region, Middle and Late Pleistocene marine terraces are often set in staircase disposition, with the oldest terraces covered by alluvial fans. The most recent and best preserved terrace was formed during the last interglacial stage (isotopic stage 5, ca. 120 ka). The elevation of its inner edge varies from a few metres above present MSL (e.g. at Coloso, S of Antofagasta) to more than +40 m (asl) (Hornitos).

At Antofagasta, the vertical motions were relatively slow during Quaternary time (ca. 50 mm. $10^{-3}$ y) on the long range. North of Mejillones Peninsula the mean net uplift rate, for the whole Quaternary, is about 100 mm.$10^{-3}$ y (Ortlieb et al., 1995b). However, looking in more detail, distinct tendencies were inferred. At Coloso (Antofagasta), the uplift rate appears to have diminished through time (no uplift in the last 125,000 y), while it increased at Hornitos and more to the north. Geochronological measurements on marine shells and morphostratigraphical considerations led to interpret that the Hornitos area was uplifted at a rate of 240 mm.$10^{-3}$ y in the course of the last 330 ky (Ortlieb et al., 1997). It can be inferred that, in the Hornitos area and in a large sector of the northern Chile coast, between 20° and 23°S, vertical deformation was slow in Early Pleistocene/early Middle Pleistocene, and that it accelerated in late Middle Pleistocene/Late Pleistocene times.

## MARINE TERRACES AND BEACH RIDGES IN MEJILLONES PENINSULA

Between Antofagasta and Hornitos, the peninsula of Mejillones registered strong Quaternary deformations. Large fracture zones that trend N-S and NW-SE, delineate a series of structural blocks which were vertically displaced by amounts reaching hundreds of metres, in the course of the last few million years. Some of these deformations are still active. The flat tops of several mesas, like Cerro Bandurria (+400 m), that clearly result from wave erosion, were classically interpreted as formed during the Quaternary (Okada, 1971; Armijo & Thiele, 1990). Actually, the sediments that cover these high-lying wave-cut surfaces include a typical nearshore Pliocene fauna (with *Chlamys vidali, Chlamys simpsoni, Ostrea ferrarisi, Fusinus remondi).* We interpret that some of the highest wave-cut terraces that surround Morro Mejillones, generally devoid of sedimentary and faunal remains, are also of Pliocene age.

The highest-lying Pleistocene marine deposit identified (on paleontological grounds) in the peninsula is located 2 km ESE from Morro Mejillones, at an elevation of +440 m (Ortlieb et al., 1995b) and close to the N-S trending Mejillones Fault. The strong deformation evidenced along Mejillones Fault (apparent vertical offset of the order of 500 m) most probably reflect altogether an extensional normal component related to the semi-graben structure of the northern peninsula and a net positive uplift motion.

In the central and eastern parts of the peninsula, the latest Pliocene and earliest Pleistocene marine deposits are commonly lying at elevations of the order of +200 to +220 m, thus suggesting that the amount of Quaternary uplift of the whole isthmus and eastern peninsula was not greater than about 220 m (Ortlieb, 1993).

Three large sequences of regressive beach ridges are preserved in the northern (Pampa Mejillones), northwestern (Caleta Herradura de Mejillones) and southern (Pampa del Aeropuerto) parts of the peninsula (Fig. 1). These series of exceptionally well-preserved coastal features cover wide, gently seaward sloping, surfaces that reach maximum elevations of ca. +220 m. Several discrepant chronostratigraphic interpretations were proposed for these beach-ridges (Herm, 1969; Okada, 1971; Ferraris & Biase, 1978; Armijo & Thiele, 1990; Ortlieb, 1993). For several geochemical and methodological reasons, it has been difficult up to now to establish the age of the ridges. Only recently, we obtained chronostratigraphic elements that suggest an (early) Middle Pleistocene age for some of the oldest sets of beach-ridges (Ortlieb et al., 1995b). The lateral correlation between the northern and southern beach-ridge series was based on the occurrence of a anomalous warm-water assemblage of mollusk shells (including: *Cerithium stercusmuscarum, Olivella* sp., *Prunum curtum, Turbo* cf. *T. fluctuosus, Bulla punctulata, Anomia peruviana, Arcopsis solida, Mactra velata, Ostrea megodon, Donax peruvianus* and *Trachycardium* cf. *T. procerum).* Geochronological data combined with geometric considerations led to propose that the « thermally anomalous molluscan assemblage » be

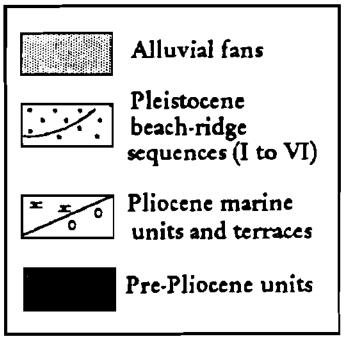


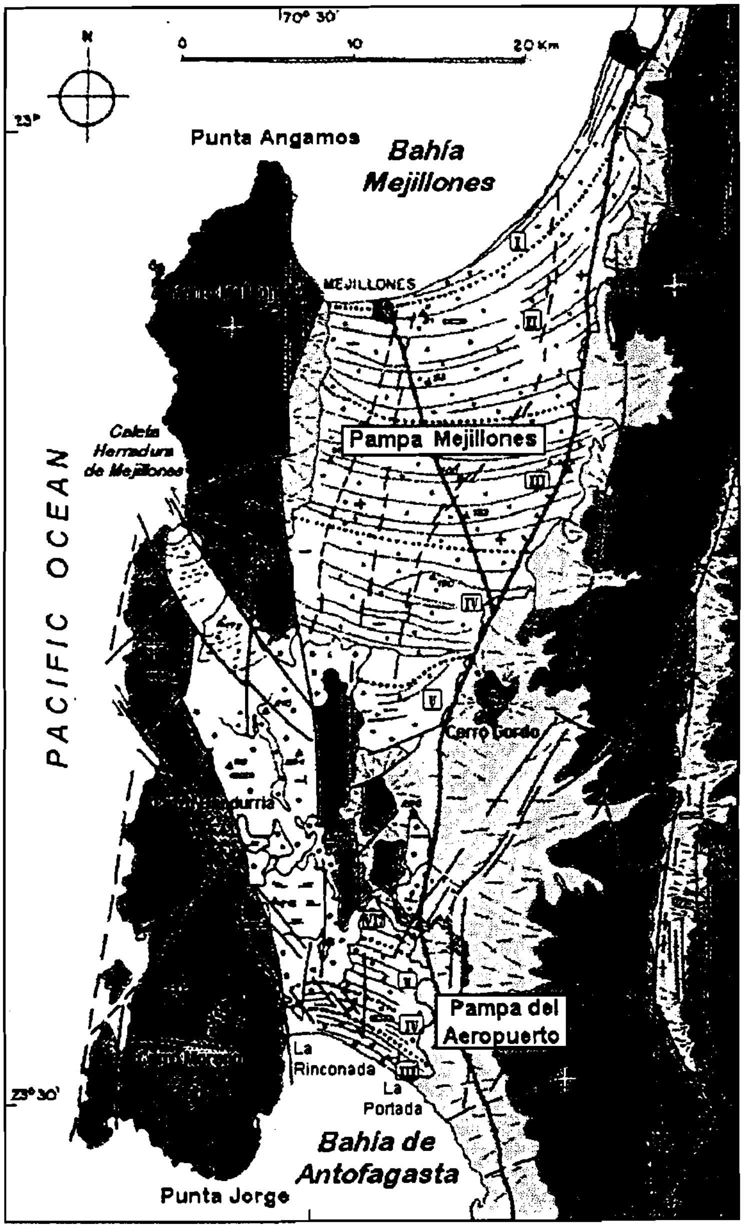


**Figure 1.** Tectonic sketch map of Mejillones Peninsula showing the large sequences of Pleistocene beach ridges (in white) which document relatively slow uplift motions of the Mejillones graben (200 - 100 mm. $10^{-3}$ y). Wave-cut marine terraces on the western part of the peninsula are not shown here.

assigned to the isotopic stage 11 high seastand (400 ka) (Ortlieb et al., 1995b). This chronostratigraphic interpretation suggests a higher uplift rate than previously proposed (Ortlieb, 1993) during the last half-million years, and much slower motions during the period late Pliocene- early Middle Pleistocene.

## CONCLUSIONS

The peninsula of Mejillones is a composite crustal block that was uplifted by a mean net amount of the order of 200 m within the last 2 My or so. This motion was not significantly stronger than those registered in the coastal region north of Hornitos. Previous interpretations that implied more rapid uplift motions of the peninsula were based upon unverified chronostratigraphic assumptions. The uplift of some faulted compartments of the western peninsula, which amounts to a maximum value of 240 m, seems to result from compressional deformation.

***Acknowledgements.*** *Co-operative scientific agreements between ORSTOM and Univ. de Chile, ORSTOM and Univ. de Antofagasta, CSIC (Madrid) and Univ. de Chile. Awards from the Fonds FCAR (Québec) and Natural Science & Engineering Research Council of Canada (CHM). Contribution to IGCP Project 367, and to both Neotectonics and Quaternary Shorelines Commissions of INQUA.*

REFERENCES

Armijo R. & Thiele R., 1990. Active faulting in northern Chile: ramp stacking and lateral decoupling along a subduction plate boundary? *Earth Planet. Sci. Lett.*, 98: 40-61.

Barazangi M. & Isacks B.L., 1976. Spatial distribution of earthquakes and subduction of the Nazca plate beneath South America. *Geology*, 4:.686-692.

Ferraris F. & Biase F., 1978. Hoja Antofagasta, región de Antofagasta. *Carta Geol. Chile* n°30, Inst. Invest. Geol. Chile. 48 p., 1 mapa 1:250.000.

Goy J.L., Macharé J., Ortlieb L. & Zazo C. 1992.- Quaternary shorelines and neotectonics in southern Peru: The Chala embayment. *Quaternary International*, 15-16: 99-112.

Herm D., 1969. Marines Pliozän und Pleistozän in Nord und Mittel-Chile unter besonderer Berücksichtigung der Enwicklung der Mollusken-Faunen. *Zitteliana* (München), n°2, 159 p.

Hillaire-Marcel Cl., Ghaleb B., Cournoyer L. & Ortlieb L. 1995. Allo/isoleucine (A/I) and Th/U measurements in mollusk shells from Michilla and Mejillones Bay, northern Chile. Intern. Geol. Correl. Progr. Proj. 367, II annual meeting (Antofagasta, Nov. 1995), ORSTOM-Antogfagasta, Abstr. vol., p. 47.

Macharé J. & Ortlieb L. 1992. Plio-Quaternary vertical motions and the subduction of the Nazca Ridge, central coast of Peru. *Tectonophysics*, 205 (1-3): 97-108.

Okada A., 1971. On the neotectonics of the Atacama fault zone region. Preliminary notes on late Cenozoic faulting and geomorphic development of the Coast Range of northern Chile. *Bull. Depto. Geogr. Kyoto*, 3: 47-65.

Ortlieb, L.. 1993. Vertical motions inferred from Pleistocene shoreline elevations in Mejillones Peninsula, northern Chile: Some reassessments. II International Symposium on Andean Geodynamics (Oxford, 1993), ext. abstr. vol., 125-128.

Ortlieb L., Ghaleb B., Hillaire-Marcel Cl., Goy J.L., Macharé J., Zazo C. & Thiele R. 1995a. Quaternary verrtical deformation along the southern Peru-northern Chile coast: Marine terrace data. XIV INQUA Congr. (Berlin, 1995), Abstr. vol., *Terra Nostra*, 2/95, p. 205.

Ortlieb, L., in coll. with J.L. Goy, C. Zazo, Cl. Hillaire-Marcel and G. Vargas 1995b.- *Late Quaternary coastal changes in northern Chile*. Guidebook for a fieldtrip, II annual meeting of the International Geological Correlation Program, Project 367 (Antofagasta, 19-28 Nov. 1995), ORSTOM, Antofagasta, Chile. 175 pp.

Ortlieb, L., Zazo, C., Goy, J., Dabrio, C. and Macharé, J. 1996. Pampa del Palo: An anomalous composite marine terrace in the uprising coast of southern Peru. *Jour. South-Amer. Earth Sci.*, 9, (in press).

Ortlieb L., Zazo C., Goy J.L., Hillaire-Marcel C., Ghaleb B. & Cournoyer L. 1997. Coastal deformation and sea level changes in northern Chile subduction area (23°S) during the last 330 ky. Submitted to *Quatern. Sci. Rev.*

Radtke U., 1989. Marine Terrassen und Korallenriffe. Das Probleem der Quartären Meeresspiegel-schwankungen erläntert an Fallstudien aus Chile, Argentinien und Barbados. *Düsseldorfer geographische Schriften*, Heft 27, 245 p.

# CENTRAL CHILE SEISMOTECTONICS AND STRESS DISTRIBUTION ALONG THE SUBDUCTED NAZCA PLATE (25°-40°S)

Mario PARDO(1), Diana COMTE(1), Tony MONFRET(1,2), Emilio VERA(1) and Nelson GONZALEZ(1)

(1)Departamento de Geofísica, Universidad de Chile. Casilla 2777, Santiago, Chile.
(2)Mission ORSTOM, Román Díaz 264, Santiago, Chile.

**KEY WORDS:** Nazca Plate, Subduction, Seismotectonics, Stress Distribution, Central Chile.

## INTRODUCTION

The seismicity and tectonic of central Chile is mainly characterized by the subduction of the oceanic Nazca plate beneath the continental South American lithosphere. The rate of convergence between these two plates is relatively constant within the studied region due to the distant location of their rotation pole. This convergence rate is about 8.4 cm/yr in the N78°E direction [1].

Several studies have shown that the shape of the oceanic downgoing slab in the region, exhibits lateral variations in the dip [2,3,4]. Major changes in dip had been interpreted as segmentation of the downgoing slab bounded by tears or by continuous flexure of the slab. Based on teleseismic locations, the boundaries between these segments have been interpreted as tears in the oceanic slab [2,5]. In Chile-western Argentina, a continuous contortion of the slab around 33°S has been proposed [4,6,7]. Beneath the latitudes 28°-33°S, the subducted Nazca plate extends eastward in an almost subhorizontal trajectory for hundreds of kilometers at a depth of ~100 km before reassuming its downward descent [4,7]. These investigations are mainly focused around the principal changes in dip and there are no detailed studies south of 34° S, where the seismicity level is lower than in other regions of Nazca plate.

In this study, we improve the local and teleseismic hypocenter locations and determine new focal mechanisms, which along with those reported within the region permit a better analysis of the seismotectonic characteristics of central Chile relative to the shape of the subducted Nazca plate, the associated stress field and the geometry of the interplate coupled zone.

## LOCAL AND TELESEISMIC DATA

The data used in this study are accurately determined hypocenters obtained from local data recorded by seismological stations at the zone and from events recorded at teleseismic distances by the world wide seismological network, which were relocated using the method of Joint Hypocenter Determination (JHD) [8]. Focal mechanisms of 18 events that occurred between 1980 and 1987, were determined using body wave inversion [9] of the long-period P, SH and SV wave forms recorded at teleseismic distances ($25° \geq \Delta \geq 90°$) by the Global Digital Seismograph Network. Focal mechanisms reported by other authors were also used.

Accurate hypocenters of local earthquakes were determined using data from the permanent telemetric network of the University of Chile since 1980 (32.7°-34.6°S) and from temporary networks deployed in the zone in 1985 (32.9°-34.5°S), 1986 (32.4°-33.7°S) and 1995 (34.0°-35.5°S).

Earthquakes with magnitude mb≥4.8 recorded at teleseismic distances, were relocated in central Chile with the JHD method [8], using the phase readings reported by the International Seismological Centre (ISC) between 1964 and 1994. The calibration events used in this relocation correspond to 15 earthquakes locally recorded and focal depths constrained by the body-wave inversion. The reason to relocate hypocenters from teleseismic data is the observed mislocation between the hypocenters reported by the international agencies (ISC, NEIC) and the ones determined with local data. On average, this mislocation results to be of ~10 km in the N67°E direction, but in many cases this mislocation can exceed 20 km.

## DISCUSSION

The epicentral distribution of the accurately located local and teleseismic events is presented on Figure 1. To analyze the geometry and state of stress of the subducted slab, eight cross-sections of the seismicity, including focal mechanisms, were drawn (Figure 2). The cross-sections are oriented in the direction of convergence between the Nazca and South American plates [1], and their origins coincide with the trench axis.

The shallow part of the subduction zone indicates a constant interplate geometry, under a compressional stress regime, that initially dips ~10°E and gradually increases to ~25°E at a depth of ~60 km (Figure 2). This geometry is observed throughout the subduction zone in central Chile, and appears to be independent of the age and relative convergence rate of the interacting plates. No lateral changes of the interplate geometry are observed at places where major bathymetric features are subducted, as the Juan Fernandez Ridge (JFR) around 33°S (Figure 1).

The depth extent of the seismogenic interplate contact can be estimated from the maximum depth of the shallow thrust earthquakes and the depth of transition between compressional to tensional events [10]. This depth is ~60 km throughout the studied zone of central Chile, in agreement with previous results on selected places along the chilean subduction zone [10,11,12]. This result yields a maximum seismogenic width of 145 km, assuming an average dip of the subducted slab of 20° and considering that the slab is aseismic at the first 10 km from the trench.

The subducted Nazca plate shows lateral variations in the dip angle at depths greater than 60 km, where the stress regime is tensional (Figure 2). The seismicity pattern at these depths defines two regions within the downgoing slab bounded by the inland projection of the JFR, which is parallel to the convergence direction (Figure 1):

(1) A northern region, where the seismicity defines a Wadati-Benioff zone with variable dip, from ~30°E (Figure 2A) to a gradually shallower dip to the south, where the slab becomes almost subhorizontal underplating the continental crust between latitudes 28° S and 33°S at depths of ~100 km (Figures 2C, 2D). The seismicity is well observed down to depths of 200 km, from where a void in seismicity is present until depths between 550 and 600 km, where the plate is again seismic active (Figures 2A, 2B, 2C). If no detachment of the Nazca plate is assumed, the slab is sharply bended around depths of 200 km and then it sinks into the mantle with an almost constant dip of ~45°, with seismicity that reaches to maximum depths of 600 km.

(2) A southern region, where the seismicity is more scarse and defines a Wadati-Benioff zone that reaches maximum depths < 200 km, at closer distances from the trench than in the northern region (Figures 2E, 2F, 2G, 2H). The deep seismicity observed at depths between 550 and 600 km in the northern region, disappears in this region.

Back-arc crustal shallow seismicity occurs mainly in the zone of subhorizontal geometry of the downgoing Nazca plate. This geometry permits to transfer compressional stress to the overriding plate and inhibits the presence of a mantle wedge, so there are no active volcanoes over this zone (Figures 2C, 2D). Outside this zone, the active Quaternary volcanoes are well developed and they are located over the zone where the Nazca plate reaches depths of ~100 km.

A sharp flexure in the slab occurs around 33° S, with strike parallel to the convergence direction between the interacting plates. The intersection of the JFR with the trench near latitude 33° S, which is

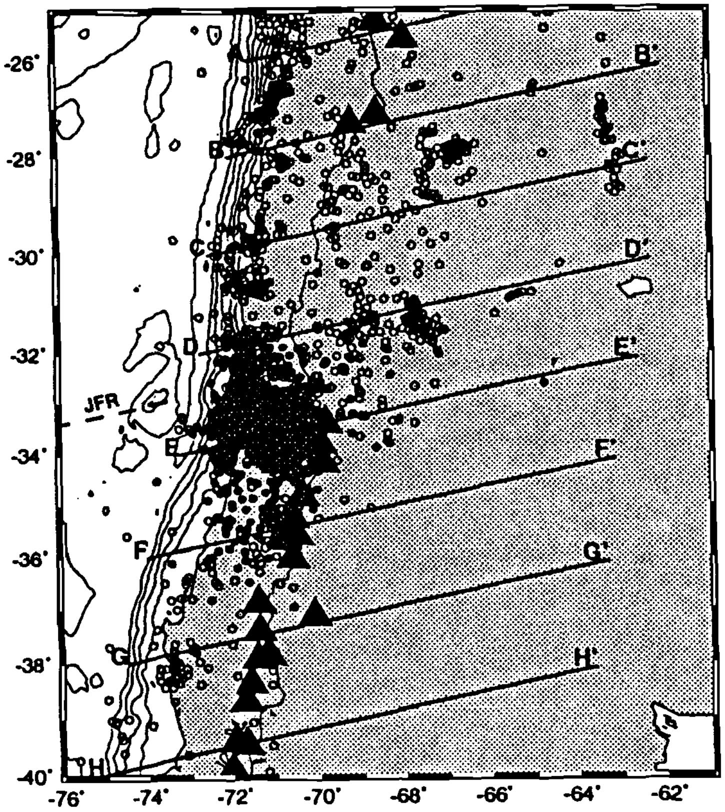


**Figure 1.-** Epicenters of the earthquake dataset used in this study from local data (solid circles) and from teleseismic data (open circles). The locations of the cross-sections of Figure 2, the Quaternary volcanoes in the zone (solid triangles) and the projection of the JFR (dashed line) are also shown.

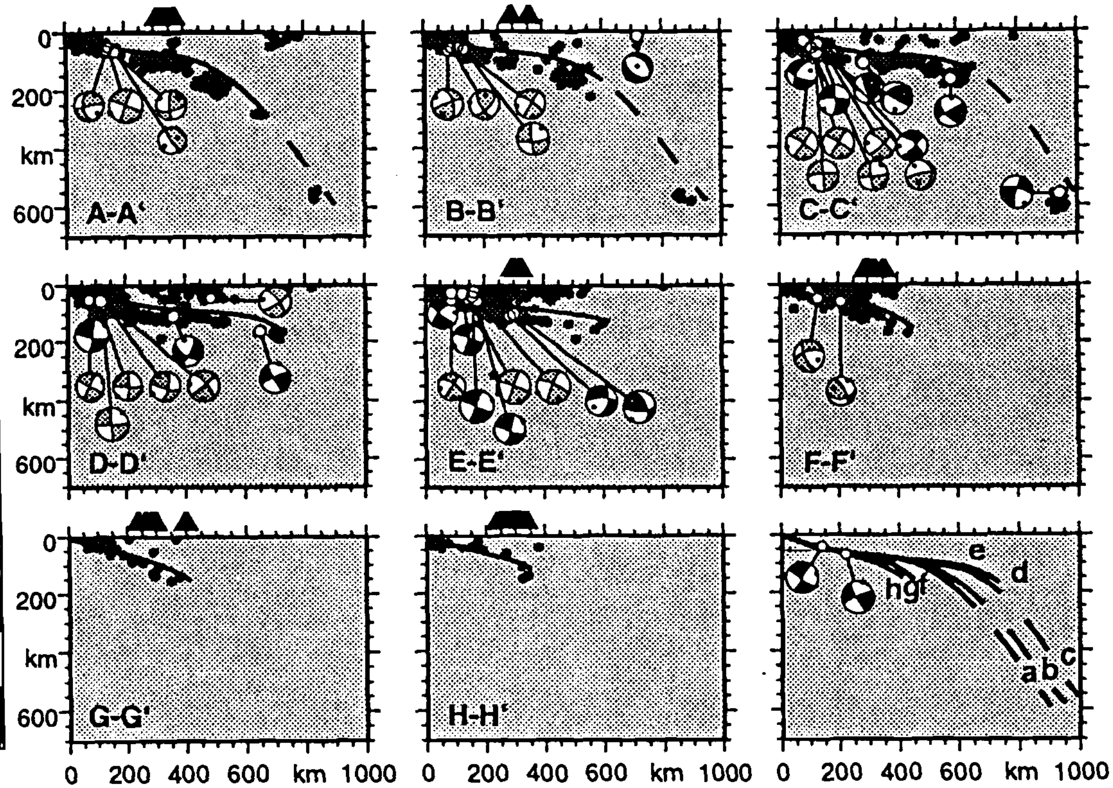


**Figure 2.-** Cross-sections of the relocated seismicity of Figure 1. The origin is at the trench and oriented in the convergence direction (N78°E). Focal mechanisms determined in this study (black) and reported from wave inversion (grey) are presented on a side-looking, lower hemispheric projection. The top of the downgoing oceanic Nazca plate is shown on each cross-section with a solid line; a dashed line is shown where it is interpolated. The location of Quaternary volcanoes (black triangles) are also projected at the top of each cross-section. At the right bottom, a summary of the Wadati-Benioff zone observed in each cross-section is presented.

located at the northern edge of the Challenger Fracture Zone, implies that lithospheric plates of different ages are subducted, being younger to the south of this boundary

## CONCLUSIONS

These observations suggest an older segment of the Nazca plate to the north of the projection of the JFR at 33°S, which sinks into the mantle down to depths of 600 km and bends probably due to gravitational forces. Between latitudes 28°S and 33°S however, at intermediate depths (60-100 km) the slab flattens and moves upwards probably related to the subduction of buoyant lithosphere associated to the the JFR. To the south of 33°S, a younger and shorter Nazca plate is suggested.

The observed stress pattern shows compression at shallow depths (<60 km) related to the coupled plate interface between the oceanic and the continental overriding plates. Downdip, at depths greater than 60 km, the downgoing plate is under tensional stress regime with T-axes oriented, in general, along the direction of the subducted oceanic plate.

The subhorizontal geometry of the subducted Nazca plate between 28°S and 33°S, at depths less than100 km and distances from the trench between 200 and 500 km, may be responsible of the absence of Quaternary volcanism, the crustal shortening of the Andes and the associated back-arc crustal seismicity in Argentina, among other tectonic anomalies that occurs in this region of central Chile.

**ACKNOWLEDGMENTS.** This work was partially funded by projects FONDECYT-1950578, FONDEF-MI20 and ORSTOM.

## REFERENCES

[1] DeMets, C., R. G. Gordon, D. F. Argus and S. Stein, Current plate motions, *Geophys. J. Int.*, **101**, 425-478, 1990.

[2] Barazangi, M. B. and B. Isacks, Spatial distribution of earthquakes and subduction of the Nazca plate beneath South America, *Geology*, **4**, 686-692, 1976.

[3] Bevis, M. and B. Isacks, Hypocentral trend surface analysis: Proving the geometry of Benioff zones, *J. Geophys. Res.*, **89**, 6153-6170, 1984

[4] Cahill, T. and B. Isacks, Seismicity and shape of the subducted Nazca plate, *J. Geophys. Res.*, **97**, 17503-17529, 1992.

[5] Swift, S. and M. Carr, The segmented nature of the chilean seismic zone, *Phys. Earth Planet. Inter.*, *9*, 183-191, 1974.

[6] Fuenzalida, A., M. Pardo, A. Cisternas, L. Dorbath, C. Dorbath, D. Comte and E. Kausel, On the geometry of the Nazca plate subducted under central Chile (32°-34.5°S) as inferred from microseismic data, *Tectonophys.*, **205**, 1-11, 1992.

[7] Araujo, M. and G. Suárez, Geometry and state of stress of the subducted Nazca plate beneath central Chile and Argentina: evidence from teleseismic data, *Geophys. J. Int.*, 116, 283-303, 1994.

[8] Dewey, J. W., Seismicity studies with the method of Joint Hipocenter Determination, *Ph.D. Thesis, U. of California, Berkeley*, 1971.

[9] Nábelek, J., Determination of earthquake source parameters from inversion of body waves, *Ph.D. Thesis, Mass. Inst. Technol., Cambridge*, 1984.

[10] Suárez, G. and D. Comte, Comment on 'Seismic coupling along the chilean subduction zone' by B. W Tichelaar and L. R. Ruff, *J. Geophys. Res.*, **98**, 15825-15828, 1993.

[11] Pacheco, J. F., L. R. Sykes and C. H. Scholz, Nature of seismic coupling along simple plate boundaries of the subduction type, *J. Geophys. Res.*, **98**, 14133-14169, 1993.

[12] Tichelaar, B. W. and L. R. Ruff, Seismic coupling along the chilean subduction zone, *J. Geophys. Res.*, ***96***, 11997-12022, 1991.

# FOREARC DYNAMICS AND NEOTECTONIC ARC DEFORMATION CENTRAL ANDES, NORTHERN CHILE

Claus-Dieter REUTHER and Jürgen ADAM

Geologisch-Paläontologisches Institut und Museum, Universität Hamburg, Bundesstraße 55
D-20146 Hamburg GERMANY; E-Mail: REUTHER@geomat.math.uni-hamburg.de

**KEY WORDS:** Forearc prism, subduction erosion, brittle crustal deformation, dynamic wedge models

## INTRODUCTION

The upper brittle crust of the wedge shaped forearc lithosphere between the Chile trench and the Western Cordillera of the Andean System can be subdivided into distinct crustal sub-wedges characterising an outer forearc domain with submarine toe erosion and active extensional deformations onshore, and an inner forearc domain with recent compressional deformation which also affects the western margin of the active magmatic arc. Dynamic wedge models, developed by Dahlen et al. (1984), are applied to explain the neotectonic processes of the north Chilean trench-arc system between 22° S and 24° S.

## RECENT NORTH CHILEAN TRENCH - ARC SYSTEM

The forearc prism is bounded by (a) the recent slope between the trench and the active magmatic arc, (b) the subduction zone, and (c) a intracrustal detachment in the overriding continental plate. The forearc region is segmented by large N-S trending strike-slip fault zones (fig. 1a) and the Atacama fault separates the onshore outer extensional forearc from the inner compressional forearc region (Buddin et al. 1993). The forearc prism consists of several sub-wedges and we distinguish between tectonic wedges within the brittle upper crust and deeper crustal/mantle wedge structures (fig. 1b)

The outer forearc region extends 120 km from the trench axis to the Atacama fault zone and is devided into two wedges: The toe-wedge with a trench slope dipping 6° and the outer forearc wedge with a trench slope of 3,5° continuing onshore into the western slope of the coastal range (bathymetry data from Schweller et. al 1981). The bottom of the toe- and outer wedge dips 10° and parallels the subducting Nazca plate. The toe and the upper part of the outer forearc wedge consist predominantly of magmatic, volcanic and sedimentary rocks of an old Jurassic-Early Cretaceous arc system, Palaeozoic basement rocks and an incomplete succession of Cretaceous to Recent deposits. The lower part of the outer forearc wedge has been interpreted as partly serpentinized Jurassic-Cretaceous mantle rocks (Wigger et al. 1994).

The inner forearc wedge extends over a distance of 210 km and is situated between the Atacama Fault and the western margin of the active magmatic arc. The topographic slope of the wedge is approximated with 1°. We define the base of this internal forearc wedge with an intracrustal discontinuity dipping 7° to the east, represented by a low velocity zone in interpreted seismic sections between Tocopilla and Chuquicamata/Calama (Schmitz 1993; Wigger et al. 1994). The inner forearc wedge hosts Mid Cretaceous to Upper Cretaceous arc rocks and uplifted Precambrian to Lower Palaeozoic metamorphic rocks, Carboniferous-Permotriassic magmatic and sedimentary rocks, and a Cretaceous to recent marine / continental sediment succession with intercalated evaporitic layers. The western rim of the active magmatic arc is dominated by Upper Miocene to Pleistocene ignimbrites and Neogene to recent andesites and dacites.

Neotectonic surface structures between the Chile trench and the Western Cordillera are caused by active extension in the outer forearc domain, affecting Pliocene and Pleistocene deposits between the Mejillones Peninsula and the Atacama fault. The inner forearc domain and the western margin of the active magmatic arc are characterised by recent compression. Here Quaternary lacustrine sediments and Upper Miocene to Pleistocene ignimbrites are faulted by trenchward verging thrusts north of San Pedro de Atacama in the Rio Salado and Vilama areas and arcward verging thrusts, with the eastern most, the Talabre thrust, beneath the Tumisa and active Lascar volcanoes bounded in the east by a more than 100 km N-S trending lineament, the Miscanti fault, where post-Pliocene transpressive deformation can be observed (fig. 1).

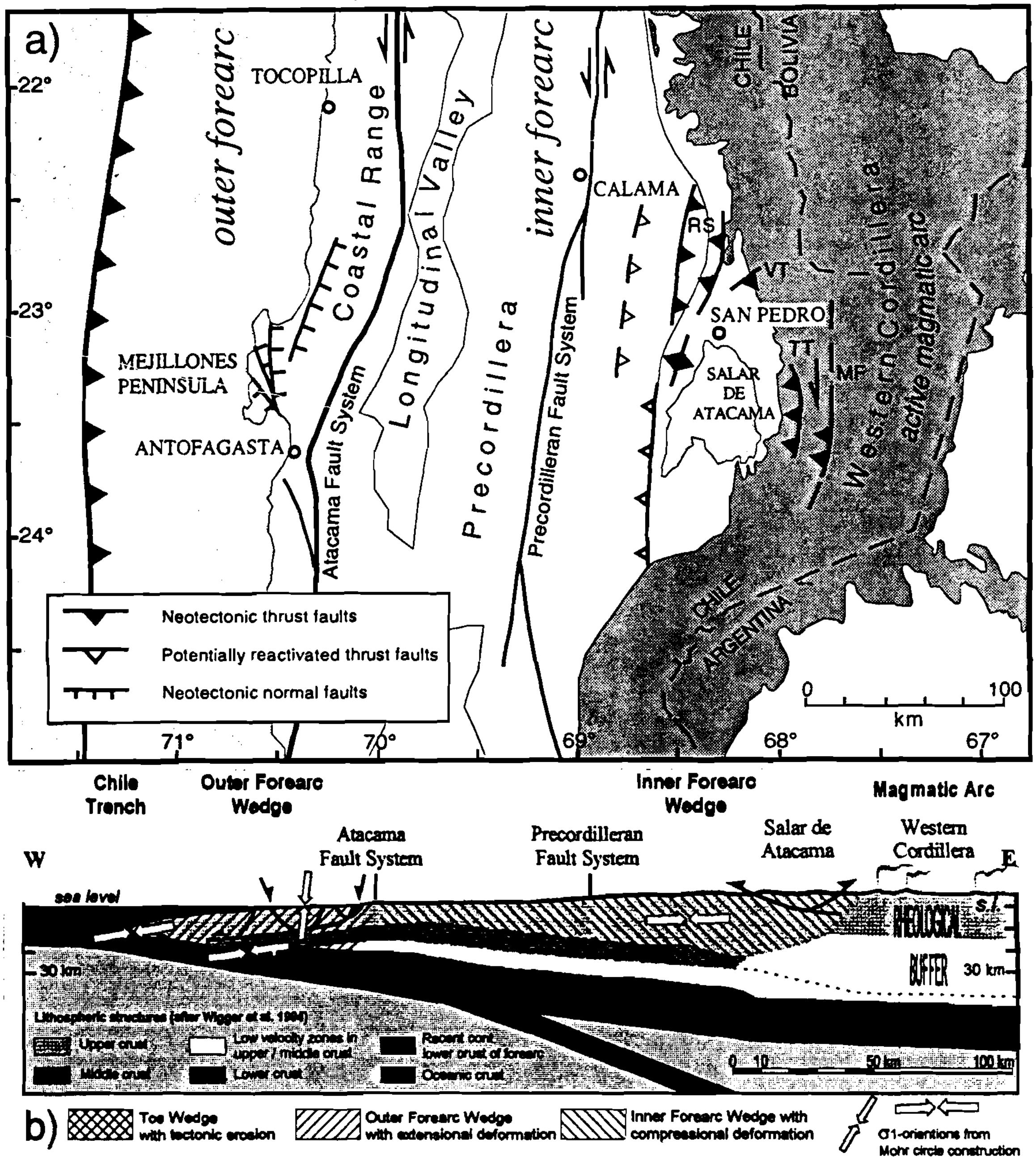


**Fig. 1: a. Main structural features and neotectonics of the North-Chilean trench-arc system.**
(RS Rio Salado Area, VT Vilama thrusts, TT Talabre Thrust, MF Miscanti Fault; Atacama- and Precordilleran fault kinematics after Armijo & Thiele 1990; Yáñez et al. 1994).
**b. Schematic dynamic cross section of the trench-arc system of Northern Chile.**

## WEDGE MECHANICS AND DYNAMICS

Active lithospheric stresses are transmitted from the subducting Nazca Plate onto the overriding South-America Plate due to high frictional resistance between the plates. For Northern Chile, between 18° S and 24° S, Tichelaar & Ruff (1991) estimated a plate coupling extending to depths of 45 - 48 km. The North-Chilean convergent plate margin is a non-accreting margin characterised by subduction erosion with removal and transport of rock material from the upper plate to greater depths (Huene & Scholl, 1991). In our dynamic model the rigid wedges of the forearc lithosphere are backstopped by the rheological buffer of the thermally weakened active magmatic arc (fig. 1 b).

Wedge mechanics illustrated by Mohr stress circles (fig. 2) demonstrate the limit stress conditions and required geometric relationships between the topographic slopes, subduction fault, crustal detachments, internal toe detachments, normal- and thrust faults, and stress field orientation of the rigid forearc wedges.

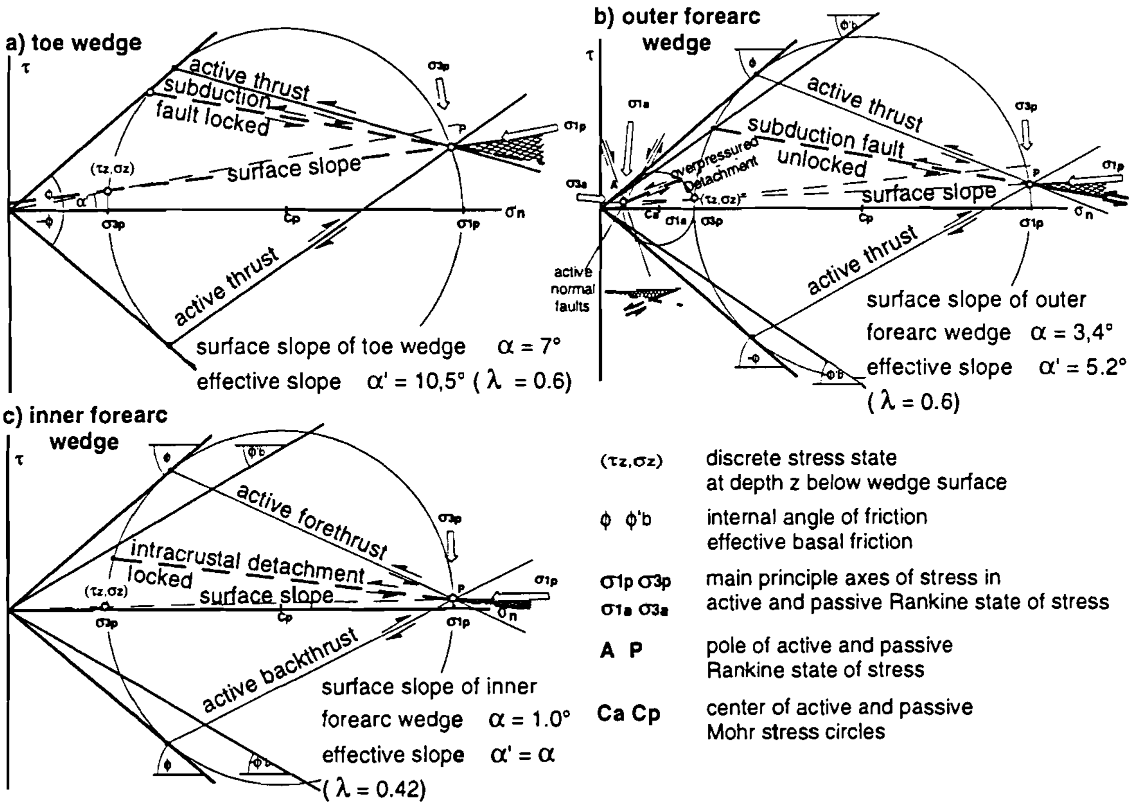


**Fig. 2: Limiting stress conditions and fault mechanics in the North Chilean forearc system (a) toe wedge (b) outer forearc wedge (c) inner forearc wedge.**

The compressional stress regime and similar rheological properties in the toe-wedge and along its base prohibit a discrete wedge base and a stable wedge geometry. Internal deformation favours west verging detachments with off-scraping of the basal part of the toe-wedge carried away with the subducting Nasca plate, stress conditions are shown in fig. 2a. Increasing pore fluid pressure and/or decreasing basal friction along the descending subduction fault lead to underplating of these crustal slices and thickens the outer forearc wedge. The basal accretion rises basement rocks into upper crustal levels (Platt 1986). This mechanism influences the uplift of the basement rocks of the Coastal Range in the north Chilean onshore outer forearc. Thrust faulting indicated by focal mechanisms of shallow earthquakes (depth $\leq$ 30 km, Comte et al. 1992) support this dynamic model. In contrast to this compressive basal accretion mechanism, neotectonic and active surface structures in the outer forearc show trench parallel extension. These normal faults are dynamically interpreted as a result of the extensional collapse of a supercritical wedge build up by continuous thickening during basal accretion. The simultaneous critical extensional and compressional stress conditions and the geometric relation of fault mechanics in the outer forearc wedge are modelled in the Mohr stress circles in figure 2 b.

The inner forearc wedge is characterised by neotectonic west-verging forethrusts and east-verging backthrusts, represented by out-of-the-sequence thrusts, favoured by numerous evaporitic layers within the rock succession and by older upper crustal discontinuities of former tectonic stages. This wedge is under active compression and in a subcritical stage (fig. 2 c).

## CONCLUSIONS

Based on observations of surface structures in the Chilean trench-arc system frictional plastic wedge models have been developed which help to understand the dynamics of the rigid crust in the forearc region. Mohr circle constructions illustrate the varying rheological conditions in defined subwedges of the forearc system and explain the relationships between neotectonic deformation processes and the active state of stress. The uplifted basement rocks of the Coastal Range and neotectonic to active N-S trending normal faults in the onshore region of the outer forearc are governed by toe erosion and underplating processes and by contemporaneous internal extensional adjustment of wedge geometry. Synchronous post Pliocene/Pleistocene west verging forethrusts, East-verging backthrusts and folds in the inner forearc and along the western rim of the recent Andean magmatic arc reflect compressional internal deformation within a subcritical crustal wedge backstopped by the rheological buffer of the active magmatic arc.

## REFERENCES


Armijo, R. & Thiele, R. (1990): Active faulting in northern Chile: ramp stacking and lateral decoupling along a subduction plate boundary? Earth and Planetary Sc. Lett., 98: 40-61.

Buddin, T.S., Stimpson, I.G. & Williams, G.D. (1993): North Chilean forearc tectonics and Cenozoic plate kinematics.- Tectonophysics, 220: 193-203.

Comte, D., Pardo, M., Dorbath, I., Dorbath, C., Haessler, H., Rivera, L., Cisternas, A. & Ponce, L. (1992): Crustal seismicity and subduction morphology around Antofagasta, Chile: Preliminary results from a microearthquake survey.- Tectonophysics, 205: 13-22.

Dahlen, F.A., Suppe, J. & Davis D. (1994): Mechanics of fold-and-thrust belts and accretionary wedges: Cohesive Coulomb Theory.- J. Geophys. Res., 89(B12): 10.087-10.101.

Huene, R. v. & Scholl, D.W. (1991): Observations at convergent margins concerning sediment subduction, subduction erosion, and the growth of continental crust.- Rew. Geophys., 29: 279-316.

Platt, J.P. (1986): Dynamics of orogenic wedges and the uplift of high-pressure metamorphic rocks.- Geol. Soc. Am. Bull, 97: 1037-1053.

Schmitz, M. (1993) Kollisionsstrukturen in den Zentralen Anden: Ergebnisse refraktionsseismischer Messungen und Modellierung krustaler Deformationen.- Berl. Geowiss. Abh. 20(B): 1-127.

Schweller, W.J., Kulm, L.D. & Prince, R.A. (1981) Tectonics, structure, and sedimentary framework of the Peru-Chile Trench.- Mem. Geol. Soc. Am., 154: 323-349.

Tichelaar, B.W. & Ruff, L.J. (1991): Seismic coupling along the Chilean subduction zones.- J. Geophys. Res., 96, B7: 11.997-212.022.

Wigger, P.J., Schmitz, M., Araneda, M., Asch, G., Baldzuhn, S., Giese, P., Heinsohn, W.-D., Martinez, E., Ricaldi, E., Röwer, P. & Viramonte, J. (1994): Variation in the crustal structure of the southern central Andes deduced from seismic refraction investigations.- in: Reutter, K.-J., Scheuber, E. & Wigger, P.J. (Eds): Tectonics of The Southern Central Andes, pp 23-48. Springer.

Yáñez, G., Mpodozis, C. & Tomlinson, A.J. (1994) Eocene dextral oblique convergence and sinistral shear along the Domeyko fault system: A thin viscous sheet approach with asthenospheric drag at the base of the crust.- 7° Congreso Geol. Chileno 1994, Actas Volumen II: 1478-1482.

# SEISMICITY AND FOCAL PARAMETERS IN NORTHERN CHILE AS OBSERVERD BY TEMPORARY LOCAL NETWORKS

Alexander F. RUDLOFF & Günter ASCH

GeoForschungsZentrum Potsdam, Dept. 2.4 "Seismology & Tomography",
Telegrafenberg A17, D-14473 Potsdam, Germany; email: rudloff@gfz-potsdam.de

**KEY WORDS**: Seismology, Seismicity, Stress regime, Focal Parameters, Northern Chile

## INTRODUCTION

This paper will report about two local networks which have been operating in northern Chile in the years 1994 and 1995. The regional geodynamic setting is dominated by the fast subduction (more than 9 cm/a) of the oceanic Nazca plate beneath the South American continent. This process is accompanied by recent volcanic and seismological activity.

The first network, PISCO '94 (*Proyecto de Investigación Sismológica de la Cordillera Occidental*) was part of the studies of the Collaborative Research Center 267 "Deformation processes in the Andes" from Berlin and Potsdam/Germany. A temporary network was installed covering an area between 21° and 25° S and 67° and 70° W. It was situated a little further east than the Chilean network of 1988, described by Comte et al. [1994]. For a period of 100 days, more than 30 digital seismological stations were recording continously (see Figure 1, black triangles). The preliminary catalogue contains more than 5.000 events, mostly of local origin. Its distribution is concentrated in two parts: one, uniformly distributed over a large area at an average depth of about 100 km; and a second, smaller but dense cluster at about 200 km depth. The magnitude distribution ranges from - 0.2 to 6.0 ($M_{PISCO}$), with a threshold magnitude of about 2.0 and a maximum number of events between 0.7 and 2.5. From broadband seismograms data of teleseismic events are used to get information about anisotropy and upper mantle discontinuities. Results from a subset of the data will be also presented by Comte et al. [1996] (this issue).

The second project was deployed in the middle of 1995. On July 30 a $M_W = 8.1$ (HRV) earthquake struck Antofagasta and the whole north of Chile. At this time the active part of the project CINCA '95 (*Crustal Investigations and on- and off-shore Nazca Plate/Central Andes*) was at full operation. It was a combined land and sea program with a participation of several German groups, working with different geophysical methods. The seismological network on land was operating between August and October 1995, covering an area of 250 km north-south and 100 km east-west. More than 30 digital stations plus 6 strong motion recorder were used. From the end of September on, the network was extended towards the trench by nine Ocean Bottom Hydrophones (see Figure 1, white squares). The analyses of the data from this project is in its beginning (Husen et al. [1996], this issue).

Further more two projects are planned in the near future (see Figure 1, dashed lines). The ANCORP '96 network will be an extension of the PISCO '94 network towards the north. It will be placed both on Chilean and Bolivian territory. The network will also support the ANCORP seismic traverse which will go along the 21° S latitude, from the coast to the high mountain ranges. The PUNA '97 network is planned to extend the PISCO '94 network towards the east, on the Argentinian side.

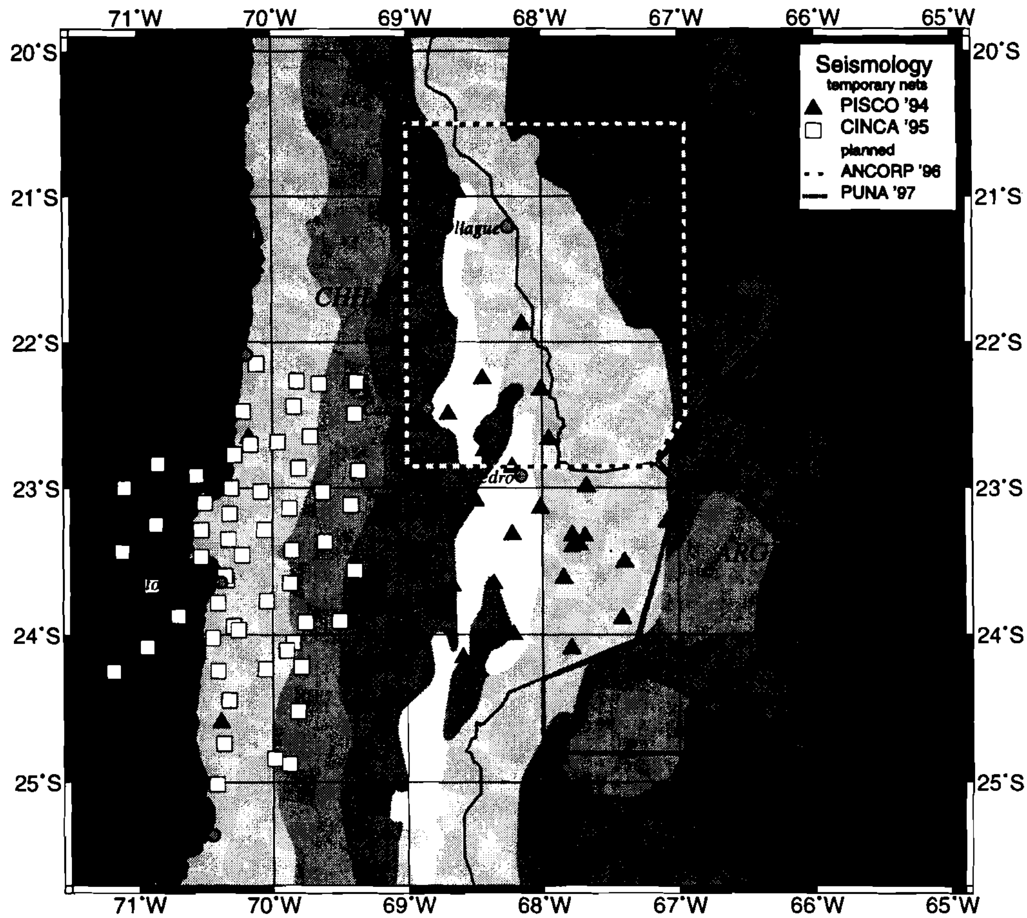


**Figure 1:** Map of temporary local networks in northern Chile (past & future)

## RESULTS

About 40% (~ 2100) of the events from the PISCO '94 network are quite well located and lay within the borders of the network or at least close to it. We use events with medium size magnitudes and stronger to calculate fault plain solutions (by now 41). All these events lie along the subducting plate, between 50 and 150 km. To a depth of 70 km fault plain solutions describe a compressional regime. Within the region of the strongest activity, between 80 and 120 km, nearly all events are extensional, with their t-axis pointing in the direction of subduction. Plunge values vary between 0° and 40°, with azimuths of 50-120°. The stress regime for this depth region seems to be mainly of extensional type. The tomographic studies are presented by Graeber [1996] within this issue. From Figure 2 one gets a good impression what temporary seismological nets can be good for. Two sections are shown, each half-a-degree wide, projected on a east-west-profile. The seismicity presented is taken from a period of less than 4 month. The Wadati-Benioff-Zone can be seen very clearly, as a sharp line

One of the most interesting results of the CINCA '95 project is the high activity following the main shock, even after 60 days later. There is no descrease during the whole period. More than 200 events were triggered each day, which is twice the amount detected by the PISCO '94 project.

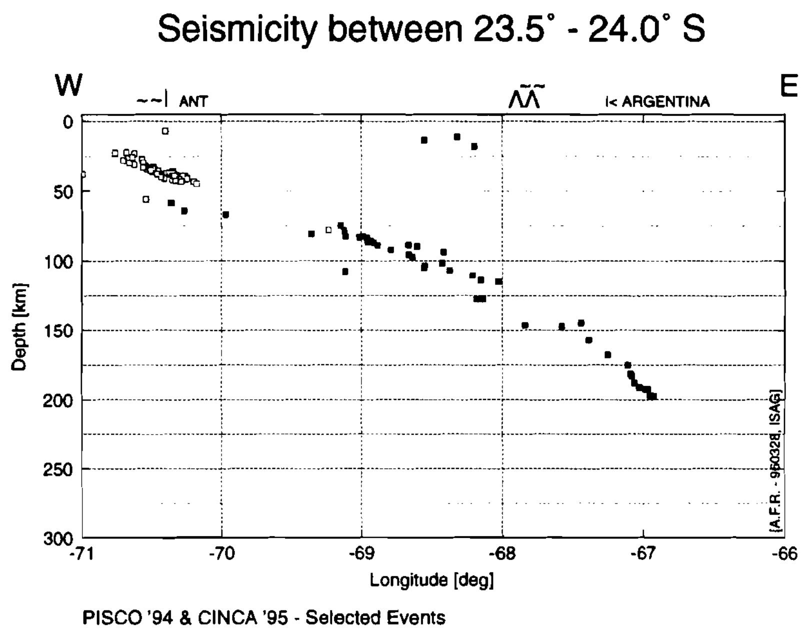


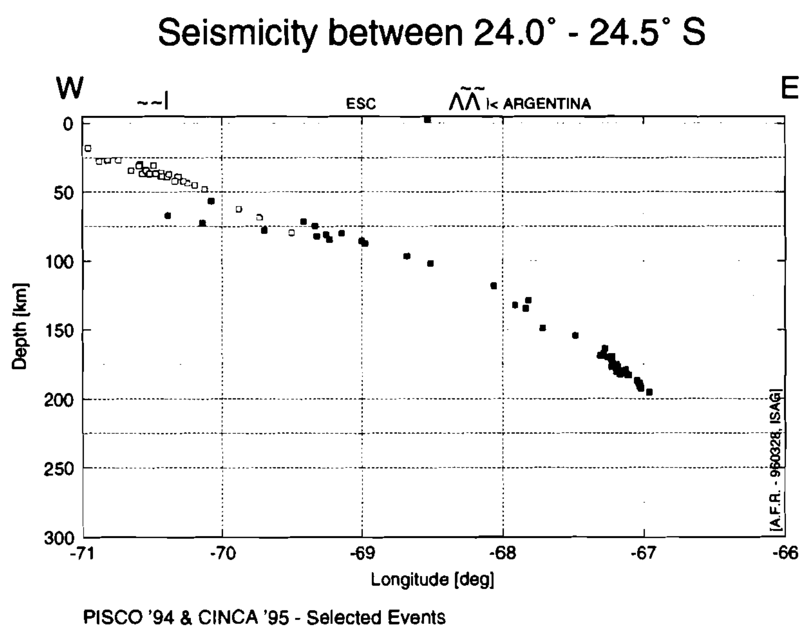


**Figure 2:** Vertical sections of the merged data set (PISCO: black, CINCA: white)

## CONCLUSION

Up to now a double seismic zone could not be identified as clear as by Comte & Suaréz [1994]. This is mainly caused by the fact, that we found only two compressional events at a depth of about 100 km. Comte & Suaréz estimated a double seismic zone, derived from the results of a local network and the existance of two different zones of stress.

With data from all projects as marked in Figure 1 a unique set of information will be formed for a large area. For local seismological studies a period of 3 months seems to be the minimum, if a broad scale analyses is planned (especially for tomography). Studies with teleseismic methods make poor sense for shorter than a year.

## REFERENCES

Comte D. & Suaréz G. 1994. An Inverted Double Seismic Zone in Chile: Evidence of Phase Transformation in the Subducted Slab. *Science*, Vol. 263, 212-215.

Comte D., Pardo M., Dorbath L., Dorbath C., Haessler H., Rivera L., Cisternas A. & Ponce L. 1994. Determination of seismogenic interplate contact zone and crustal seismicity around Antofagasta, northern Chile using local data. *Geophys. J. Int.*, Vol. 116, No. 3, 553-561.

Comte D., Pardo M., Monfret T., Asch G., Graeber F., & Rudloff A. 1996. Three dimensional P-wave tomography around Antofagasta, northern Chile: Stress distribution along the deeper part of the subducting Nazca plate. *this issue*

Graeber F.M. & Asch G. 1996. A three-dimensional model of seismic velocities beneath northern Chile from local earthquake tomography. *this issue*

Husen S., Asch G., Baumbach M., Haberland Chr., Rietbrook A., Rudloff A., & Wylegalla K. 1996. CINCA '95: Passive seismology on- and off-shore in northern Chile. *this issue*

# The $M_W$=8.1 Antofagasta (North Chile) Earthquake of July 30, 1995: First results from teleseismic and geodetic data.

J.C. RUEGG[1], R. ARMIJO[1], J. CAMPOS[2], S. BARRIENTOS[2]
and french-chilean team for the study of the seismic cycle(*) :

(1) Institut de Physique du Globe, 4 place Jussieu , 75252 Paris cedex 05 Paris, France
(2) Universidad de Chile, Santiago, Chile

KEY WORDS: seismic cycle, North Chile, GPS, deformation models

A strong earthquake Mw = 8.1 occurred on July 30, 1995 in Antofagasta (Northern Chile). This is one of the largest events during this century in the region, where the historical record contains a sequence of two great subduction earthquakes (M = 8.5 - 9) in 1868 (Southern Perú) and 1877 (Northern Chile). The 1995 earthquake ruptured the southernmost portion of a seismic gap in Northern Chile, between 18°S and 25°S, a region that we had already selected as a target for a study of the seismic cycle and a search for seismic precursors. The project included a GPS network with about 50 bench marks covering a region nearly 500 km long (N-S) and 200 km wide (E-W). Fourteen of these marks were re-surveyed with GPS after the 1995 earthquake during a ten day period (August 12 to 22) to characterize the deformation. Comparison with 1992 positions indicate relative horizontal displacement of the coastal bench marks towards the trench of the order of 0.7 m. Bench marks located inland subsided several tens of cm. The bench mark located in Mejillones Peninsula was uplifted by more than 15 cm. Teleseismic body wave modelling of VBB records gives a focal mechanism with N8°E strike, 19° dip, and 110° rake. The source time function shows three distinct episodes of moment release. There is southward directivity with average rupture velocity of 3.3 km $s^{-1}$. Modelling the displacement field using a dislocation with uniform slip in elastic half-space suggests a rupture zone extending to a depth no greater than 50 km with N-S length of ~180 km and an average slip of ~5 m.; in close agreement with the body-wave model and with the interplate thrust geometry. The observed component of right-slip does not require slip partitioning at the plate boundary. Normal faulting along the Coastal Scarp is likely to accommodate interseismic deformation. That the well-constrained northern end of the 1995 rupture zone is under the southern part of the Mejillones Peninsula increases the probability for a next rupture in the gap north of it.

(*) French-chilean team for the study of the seismic cycle : R. Armijo, P. Briole, H. Lyon-Caen, J.C. Rossignol, J.C. Ruegg, *Institut de Physique du Globe, Paris, France*; T. Duquesnoy, *IGN, St Mandé, France;* L. Ortlieb, *ORSTOM, Paris, France & Antofagasta, Chile,* S. Barrientos, J. Campos, R. Thiele: *Universidad de Chile, Santiago, Chile*; M. Arancibia, J. Cañuta, *SERNAGEOMIN, Santiago, Chile*; D. Lazo , L. Serrurier: *Universidad Arturo Prat, Iquique, Chile*; M. Chang, *IGP, Lima, Peru.*

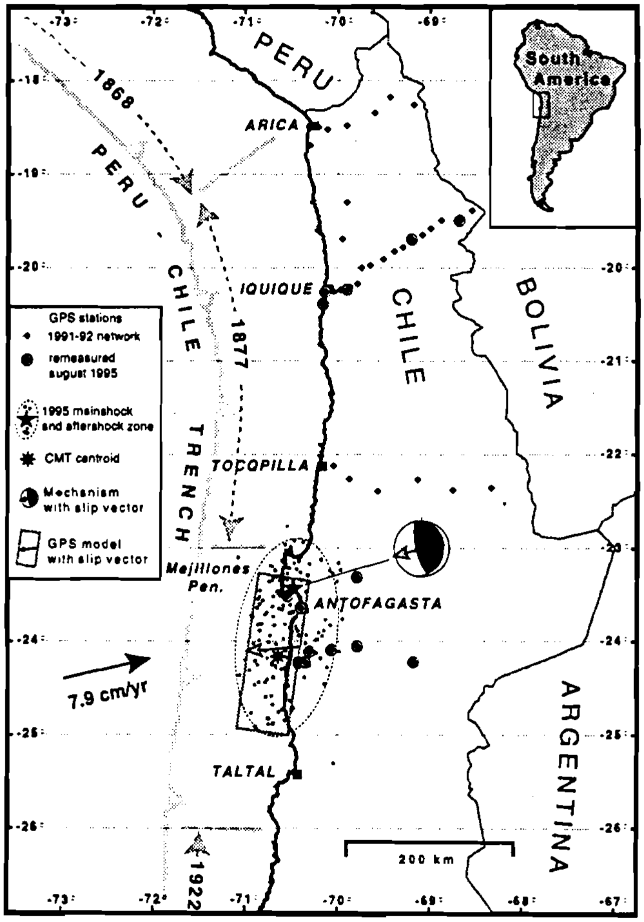


**Figure 1** : Subduction segments and seismic gap in Northern Chile, GPS network,, aftershocks and models for the 1995 Antofagasta earthquake. Plate convergence (7.9 cm/yr) from De Mets et al.(1990).

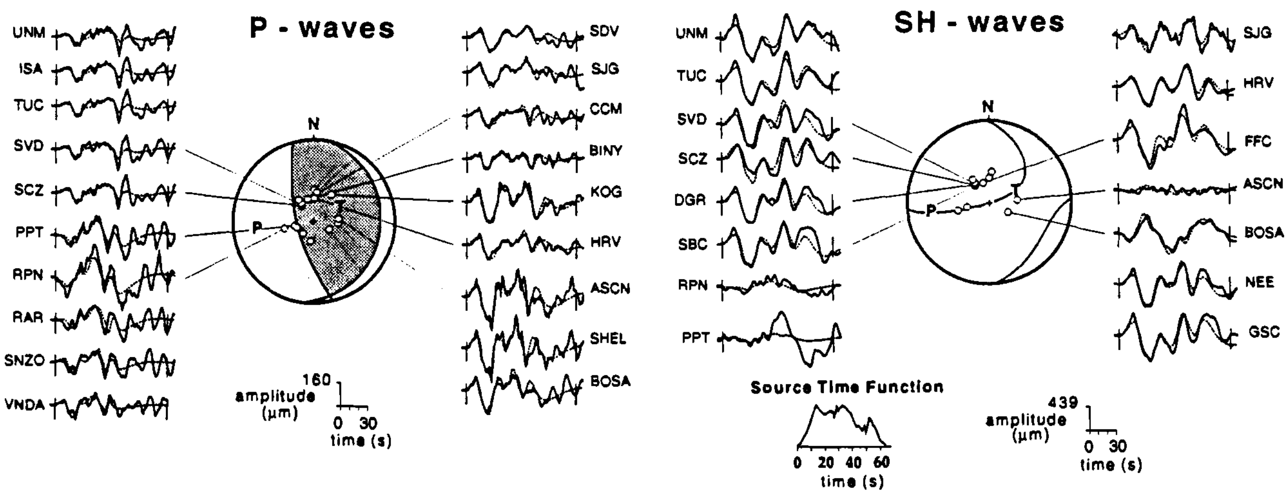


**Figure 2 :** Average fault plane solution corresponding with the 3 point sources model used in the inversion and corresponding observed and synthetic body wave band pass filtered displacements.

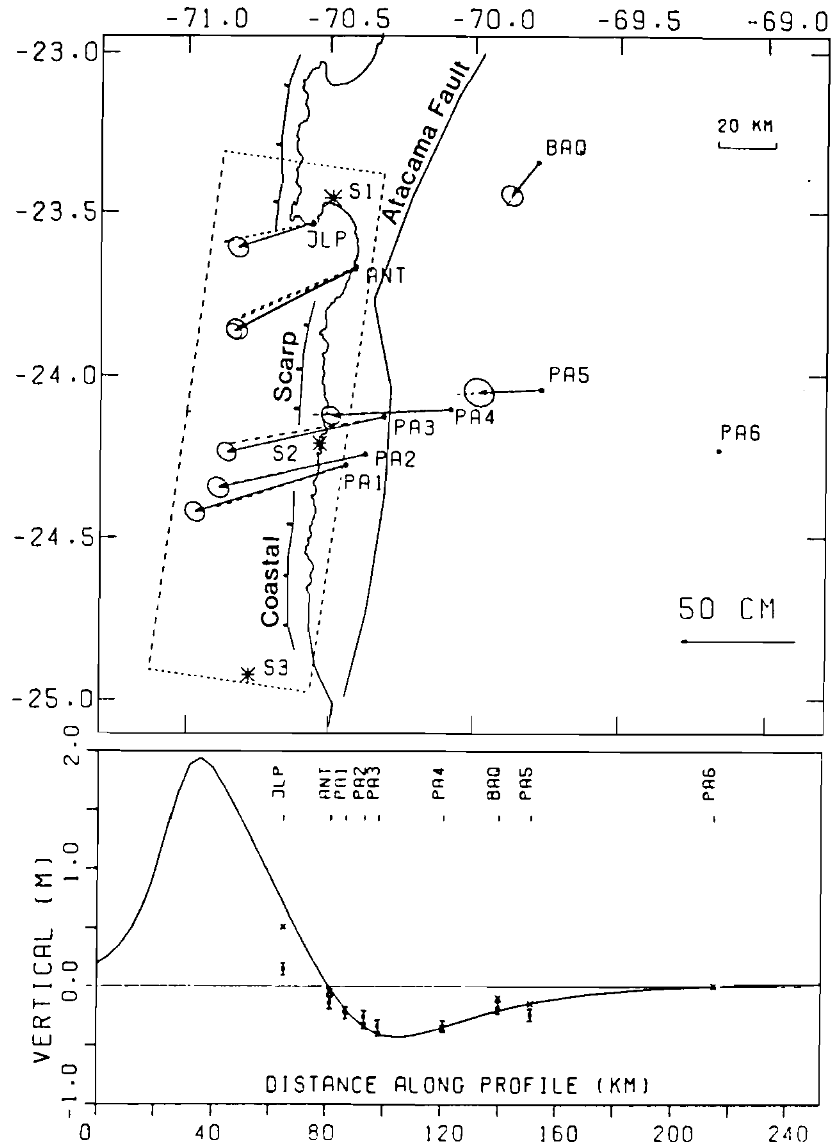


**Figure 3** : Uniform slip model based on GPS measurements. Observed and modelled values : (a) Fit to horizontal displacements with 19° dip (solid arrows with 95% confidence ellipses: observed; dashed : modelled) . S1, S2, S3 are the three point sources from body waves modelling. Fit to vertical displacements with 24°dip (squares with error bars, observed; crosses, modelled; curve, modelled across AB section).

## REFERENCES


Armijo R. and R. Thiele, Active faulting in Northern Chile: ramp stacking and lateral decoupling along a subduction plate boundary, *Earth Planet Sci. Lett., 98*, 40-61, 1990.

Comte, D. and M. Pardo, Reappraisal of great historical earthquakes in the Northern Chile and souther Peru seismic gaps, *Natural Hazards, 4*, 23-44, 1991.

DeMets, C., R.G. Gordon, D.F. Argus and S. Stein, Current plate motions, *Geophys. J. Int., 101*, 425-478, 1990.

Monfret T., L. Dorbath, J.P. Caminade, M. Pardo, D. Comte, J. Thomas, A. Cisternas, B. Dellouis and L. Rivera, The July 30, 1995 Antofagasta earthquake: an "hypocritical" seismic event, *EOS Trans. AGU 76 (46)*, 375, 1995.

Ortlieb, L., S. Barrientos, A. Lavenu and T. Montfret, Coseismic uplift motion near Antofagasta, N Chile, related to the July 30, 1995, Ms=7.3 event: first field evidence from the intertidal area, *EOS Trans. AGU 76 (46)*,427, 1995.

Ruegg, J.C., J. Campos, R. Armijo, S. Barrientos et al., The $M_W$=8.1 Antofagasta (North Chile) Earthquake of July 30, 1995: First results from teleseismic and geodetic data, Geophys. Res. Letters (in press), 1996.


-----------------------

# NON-CLUSTERED ACTIVITY OF "LONG PERIOD" EVENTS IN COTOPAXI VOLCANO, ECUADOR

Mario RUIZ(1), Jean Luc CHATELAIN(1,2), Bertrand GUILLIER(1,2) and Monica SEGOVIA(1)

[1] Instituto Geofísico, Escuela Politécnica Nacional, Apartado 17 01 2759, Quito, Ecuador.
[2] ORSTOM, Apartado 17 11 6596, Quito, Ecuador.

KEY WORDS: Long Period Events, cluster, volcano, seismology, Ecuador.

## INTRODUCTION

The Cotopaxi Volcano is one of the most important volcanoes of the Ecuadorian Andes due to its very active history during the last 5.000 years, the variety of volcanic hazards linked to its activity, and the highly populated area located in the probable affected zone.
Its seismic behavior shows many interesting features, including high rates of the so-called "long period" events, which are studied in this paper.

## SEISMICITY OF COTOPAXI VOLCANO

The Cotopaxi volcano is continuously monitored, since 1986, by an 1Hz vertical seismic station located at 5.8 km of the crater. Three additional stations were installed in 1990 at distances of 7.0, 9.2 and 10.4 km from the sommital crater. Using this network, 3868 local seismic events have been recorded from January 1991 to December 1995. We classified them as High Frequency A Type (HFA), High Frequency B Type (HFB) and "Long Period" (LP) events, following the criteria of Minakami (1974) and Chouet (1994). The (LP) events are the most observed (77 % of the recorded events ; figure 1).

## THE L.P. EVENTS

The Cotopaxi LP events have fundamental frequencies in the range of 0.8 to 2 Hz. The power spectra densities of 26 LP events recorded by the station closest to the crater from October 1993 to December 1994 show peaks in the same frequency range (figure 2). The Cotopaxi LP events have the same characteristics pointed out by Chouet (1994) : 1) an abrupt onset with a burst of high frequency energy evident at small epicentral distances, 2) an extended monochromatic coda (figure 3), 3) sharply peaked velocity spectra , and 4) stability of the spectra peaks across multiple stations (figure 2).
Since 1991, two stages of activity have been recognized in the monthly number of LP events. The minor one runs from January 1991 to December 1992, and the more active one from January 1993 to December 1995 with averages of 21.5 and 66.3 events/month respectively. However, during the period 1991-1995 a stable behavior of the distribution of fundamental frequencies, magnitude ranges and monthly energy release is observed. No peaks of activity nor total calm periods have been observed in the LP activity of the Cotopaxi volcano.

We were able to reliably locate only 42 LP events (RMS ≤ 0.5 sec. and condition number <90) using HYPOINVERSE (Klein, 1978). The top of the velocity model used for the location has been set at 6 km above sea level, i.e., the elevation of the Cotopaxi volcano.
These 42 events are widely distributed in and around the volcanic cone, with a cluster (20 events) located beneath the flanks of the cone (figure 4). They are distributed between the summit of the volcano and 17 km depth ; 15 % only are shallower than 4 km, while 66 % fall in a range between 8 to 18km, confirmaing the intermediate depth characteristic of the LP Cotopaxi events.

## DISCUSSION AND CONCLUSION

Prior to the Redoubt volcano eruption, events with frequency characteristic lying in a range of 1.3 to 1.9 Hz and 1.9 to 2.3 Hz occurred (Stephens et al, 1994), as well as before the 1993 eruptions of Galeras volcano (Fisher et al., 1994) . As pointed out by Chouet et al. (1994), swarms of LP events preceded the 1958 and 1983 eruptions of Asama Volcano, the 1987 eruption of Meaken-dake volcano, the 1981 eruptions of St. Helens, the 1982 eruption of El Chichon and the 1991 paroxysmal eruption of Pinatubo, and less intense activity of LP preceded the 1988-1989 eruptions of Tokachi-dake, the 1985 eruption of Nevado del Ruiz. These observations were strongly in favour of using LP events activity as an important clue to volcanic eruption prediction (Chouet, 1994), leading to the elaboration of several pre and co-eruptions models in order to explain the LP activity origin.
Long period events are indicators of pressure transients or transport of fluids involving both liquid and gas phases in cracks or conduits beneath the volcano (Chouet, 1994). Julian (1994) proposed that LP events were provoked by oscillations caused by disturbances of a steady flow such as earthquakes near the fluid-carrying channel or sudden changes in the channel network, without great impedance contrast between the fluid and the channel walls. Fisher et al. (1994) relate LP events to degasing in open vents. Nishimura et al. (1990) found that LP events have a shallower origin than explosion event. Hamaguchi et al. (1992) mentioned vertical forces associated to collapses or landslides as LP generators Shallow LP events are interpreted by Gil-Cruz et al. (1987) and Martinelli (1990) as produced by thermal interaction between magmatic heat and a separated ground water system. Finally, Weaver and Malone (1976) associated LP events recorded in St. Helens to glacier movements.

In the Cotopaxi case, the spatial distributions of epicenters and focal depths discard an origin of LP events inside the ice-snow cap as Weaver and Malone (1976) found in St. Helens. The sign, fundamental frequencies, spectra and long coda of the Cotopaxi LP events suggest an volcanic-related origin. There is no evidence of collapses or landslides to support a source controlled by the action of a vertical force in the generation of these events as found by Hamaguchi et al. (1992). There are minor fumaroles in the sommital crater and on the upper flanks of the volcano, but it is thought not to be enough to produce these events, and at the time present there is not any evidence of a relationship between those and the LP events. Despite small and constant fumarolic activity, there is no signal of important unrest of the volcano which could be linked to the LP activity. The stability of many parameters such as the temporal distribution of the frequency content, magnitude and energy release, since the LP seimicity started being monitored in 1991, suggest that the LP activity is a normal pattern of the Cotopaxi volcano, possibly produced by transient of fluid at intermediate depth beneath the volcano.

## REFERENCES

Chouet, B., in press 1994. Volcano seismology as an approach to eruption forecasting, Nature.
Chouet, B., Page, R., Stephens, C., Lahr, J., Power, J., 1994. Precursory swarms of long-period events al Redoubt Volcano ( 1989-1990), Alaska: Their origin and use as forecasting tool. J. Volcanol. Geotherm. Res., 62, p. 95-135.
Bonilla, A., 1995. Identificación de Eventos Sísmico-Volcanicos en base a un Sistema Neuronal Artificial, Tesis Previa a la obtención de Mestría en Informítica del Programa Escuela Politécnica Nacional-Universidad Andina Simón Bolívar, Ecuador, 97 p.

Fisher, T., Morrissey, M., Calvache, M.L., Gómez, D., Torres, R., Stix, J., Williams, S., 1994. Correlations between SO2 flux and long-period seismicity at Galeras volcano, Nature,Vol. 368, p-135-137.

Gil Cruz F., Meyer H. J., Chouet B. and Harlow D., 1987. Observation of long period events and tremors at Nevado del Ruiz volcano, 1985-1986, Abstr. Hawaii Symp. How Volcanoes Work, 19-25, Jan. 1987, Hilo, Hawaii, p90.

Hamaguchi, H., Nishimura, T., and Zana, N., 1992. Process of the 1977 Nyiragongo Eruption Inferred from the Analysis of Long-Period Earthquakes and Volcanic Tremors, in Geophysical Study on the Hotspot Volcanoes in the Africa Continent, Faculty of Science, Tohuko University, Japan, p. 33-54.

Julian B. R., 1994. Volcanic tremor : nonlinear excitation by fluid flow, Journ. Geoph. Research, 99, B6, 11859-11877.

Klein, F.W., 1978. Hypocenter location program HYPOINVERSE, U. S. Geol. Surv.,Open File Rep., 78-694.

Martinelli, B., 1990. Analysis of seismic patterns observed at Nevado del Ruiz, Colombia during August-September 1985, J. Volc. Geoth. Res., 41, 297-314.

Minakami, T., 1974. Seismology of volcanoes in Japan. In: Civetta, L., Gasparini, P., Luongo, G., and Rapolla, A. (Eds.), Solid Earth Geophysics, Physical Seismology. Ed. Elsevier, p. 1-27.

Nishimura, Y., Miyamachi, H., Ueki, S., Nishimura, T., Shimizu ,H., Ohmi, S., and Okada, H., 1990. Joint Seismometrical Observations by the National University Team during the 1988-1989 Eruptive Activity of Mt. Tokachi, Hokkaido. Bull. Volcanol. Soc. Japan, Ser. 2, Vol. 35, No. 2, p. 163-173.

Stephens, C., Chouet, B., Page, R., Lahr, J., Power, J., 1994. Seismological aspects of the 1989-1990 eruptions of Redoubt Volcano, Alaska: the SSAM perspective. . Volcanol. Geotherm. Res., 62, p. 153-182.

Weaver, C., and Malone, S., 1976. Mt. Saint Helens seismic events: volcanic earthquakes or glaciar noise?. Geophys. Res. Letters, V. 3, No. 3, p. 197-200.

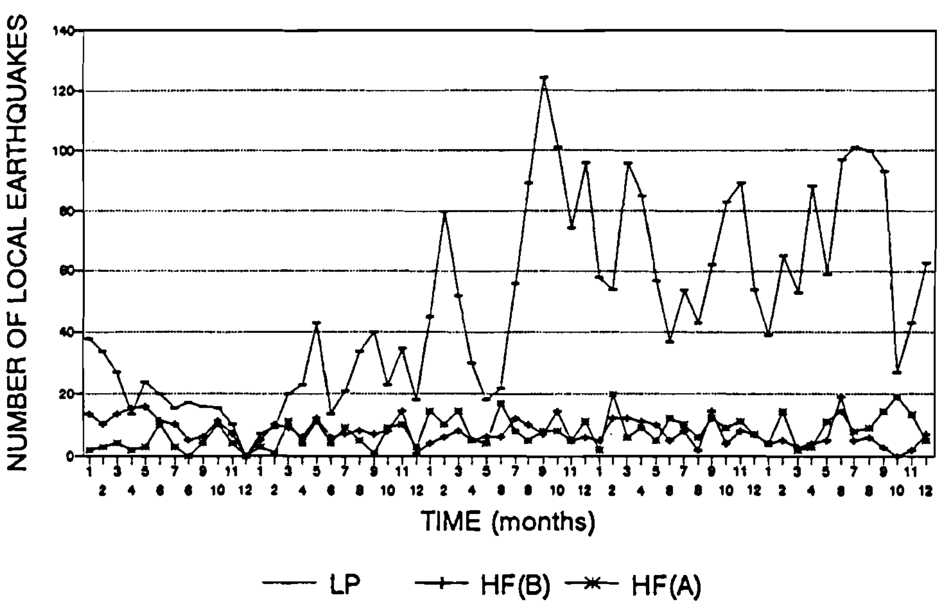


Figure 1 : Monthly distribution of LP, HF(A) and HF (B) earthquakes of the Cotopaxi volcano from 1991 to 1995, recorded at the closest (5km) station from the crater.

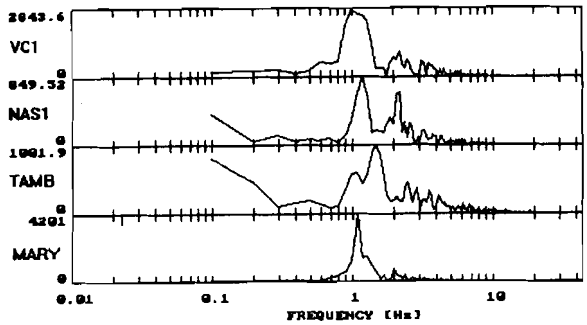


Figure 2 : Example of spectra obtained at the four Cotopaxi seismic stations for a LP event, signal of this event is shown in figure 3.

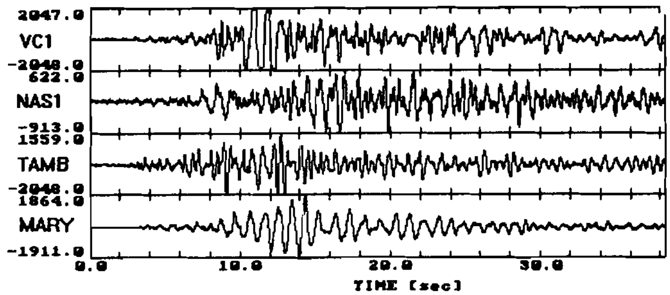


Figure 3 : Example of a LP event signals recorded at the four Cotopaxi seismic stations.

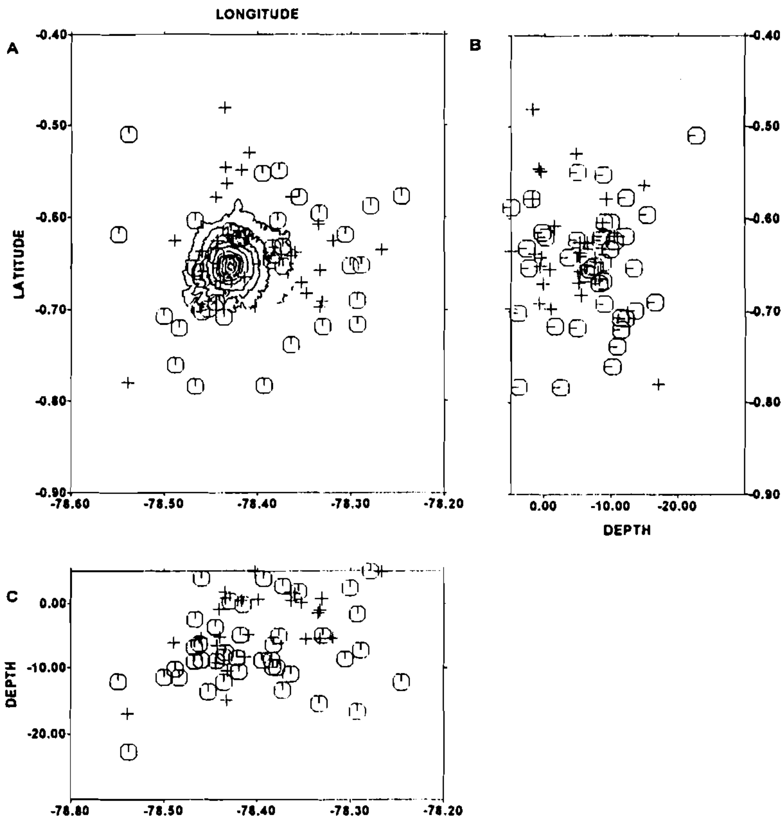


Figure 4 : Spatial distribution of the best located earthquakes in the Cotopaxi area. A : map view ; B N-S cross-section ; C : E-W cross-section.

# TEPHROCHRONOLOGY OF THE LAST 5000 YEARS AT CAYAMBE VOLCANO (ECUADOR)

Pablo SAMANIEGO (1), Michel MONZIER (2) and Claude ROBIN (2)

(1) Instituto Geofísico -Escuela Politécnica Nacional, Apartado Postal 17-01-2759, Quito, Ecuador (email: psamanie@ig134.epn.edu.ec)
(2) ORSTOM, Apartado Postal 17-11-6596, Quito, Ecuador (e-mail: monzier@orstom.ecx.ec)

**KEY WORDS:** volcanology, tephrocronology, pyroclastic flow, Holocene, Cayambe volcano, Ecuador

## INTRODUCTION

In their work about the Holocene tephrostratigraphy of volcanoes of Ecuador, Hall and Mothes (1994) succintly presented the recent activity of Cayambe volcano. Since 1995, this volcano has been studied by the Geophysical Institute of the National Polytechnical School of Quito and ORSTOM (French Scientific Research Institute for the Development in Cooperation). To date, a detailed tephrochronology of the last 5000 years of Cayambe's activity and a preliminary geochemical study showing unusual chemical characteristics of its rocks are available and presented here.

## CAYAMBE VOLCANO: GENERAL STRUCTURE

Cayambe volcano is constructed on the northern Cordillera Real of Ecuador, which is composed by immense glacial capped stratocones sitting astride a basement which pertains to the easternmost metamorphic chain of the ecuadorian Andes (Fig. 1). The central part of this metamorphic belt mainly consists of triassic semi-pelitic schists and paragneises of continental origin (Loja Division; Litherland et al., 1994). A N35°E and N125°E fault system probably controls the location of the volcano, the La Sofia - Rio Chingual fault being the most important (Soulas et al, 1990; Tibaldi and Ferrari, 1992; Ego et al, 1995) which ends in the NE quadront of the volcano.

Cayambe is a large composite volcano, which has a rectangular base at about 2800 m elevation. Its summit reaches 5790 m and is covered by a huge glacial cap, more than 100 m-thick. Glaciers reach down to 4200 m on the eastern flank and only to 4600 m on the western side. As a whole, the volcano is formed by (Fig. 2) : 1/ A western mostly lavic edifice, the Old Cayambe, which shows strong evidences of glacial erosion. Barberi et al. (1988) report an age of 0.25 ± 0.05 Ma for a dacite sample from this edifice; 2/ The Nevado Cayambe, less voluminous, which was built over the remnants of the Old Cayambe probably after a caldera collapse event. Nevado Cayambe consists of basal lava flows topped by an active summit dome complex which is the source of several recent pyroclastic flows; 3/ a small eastern edifice, called "Cono de La Virgen" from which several thick lavas flowed toward the eastern slopes of the Cordillera (Planada de la Virgen lava flows).

## UPPER HOLOCENE PYROCLASTIC ACTIVITY

On the NE flank of Nevado Cayambe, four pyroclastics flow deposits are observed. The older three (PF1 to PF3, Fig. 2) are large dome collapse block and ash flow deposits, whereas the youngest (PF4) is represented by a minor sequence of surges. Within these deposits, dacitic blocks are usually dense, but a few pumitic ones are also encountered. Mineralogical heterogeneity and banding show evidence of magma mixing in the juvenile blocks of three deposits (PF2, PF3 and PF4). The oldest flow deposit (PF1) is massive, 20-30 m-thick, and originated in a dome collapse near the eastern summit (5487 m). PF2, a 100 m-thick multi-layered flow deposit with 15-20 layers has its origin at the small "Tarugo

**Fig. 1**

Location of Cayambe volcano in Ecuador

1. COTACACHI
2. CUICOCHA
3. IMBABURA
4. CUBILCHE
5. MOJANDA
6. CUSIN
7. **CAYAMBE**
8. REVENTADOR
9. PULULAGUA
10. CASITAGUA
11. PAMBA MARCA
12. IZAMBI
13. PUNTAS
14. RUCU PICHINCHA
15. GUAGUA PICHINCHA
16. ILALO
17. PAN DE AZUCAR
18 ATACAZO
19. PASOCHOA

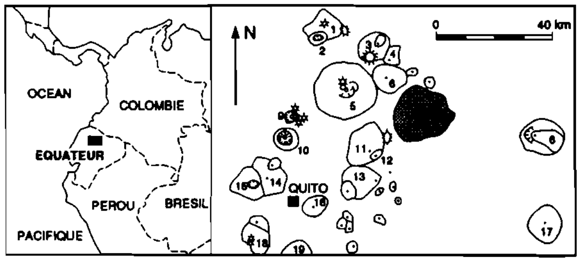


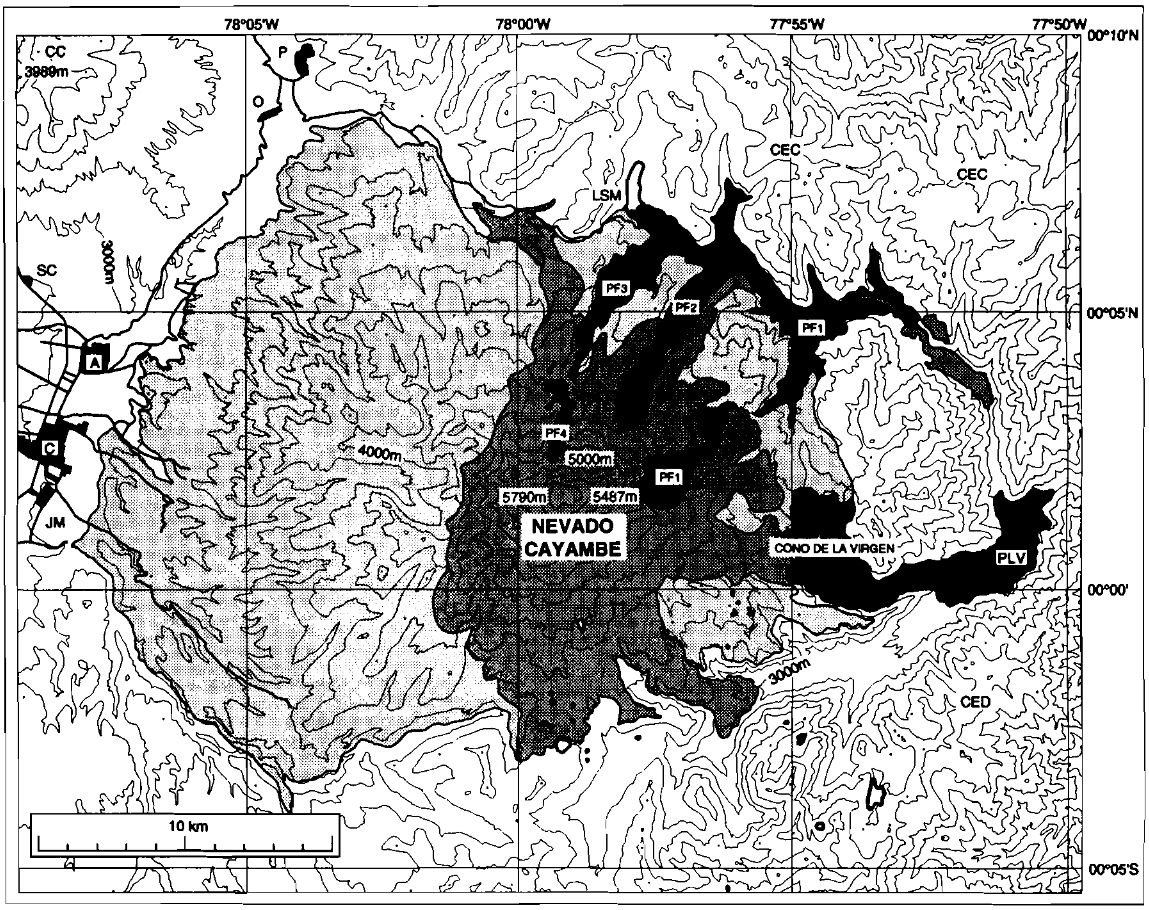


**Fig. 2** Cayambe volcano (Ecuador). C= Cayambe town, JM= Juan Montalvo, A= Ayora, SC= Santa Clara, O= Olmedo, P= Pesillo, CC= Cerro Cusin, LSM= Laguna San Marcos, CEC= Cordillera Espinal Chupa, PLV= Planada de la Virgen, CED= Cordillera El Diviso

Cono de la Virgen (active) and Planada de la Virgen lava flows

Nevado Cayambe (active). PF1 to PF4: recent pyroclastic flows

Old Cayambe

Corral" dome (4553 m) , located on the high north slope of the eastern summit. PF3 is massive, also 100 m-thick, and corresponds to the collapse of a dome extruded near the main 5790 m summit ; it dammed the Azuela river, forming San Marcos Lake. Lastly, PF4 corresponds to a sequence of surge deposits which have a total thickness > 10 m. A C14 date obtained from carbonized plants within the soil layer beneath PF4 gives an age of 360 ± 70 y BP.

On the SW flank of Nevado Cayambe, at ≈4000 m elevation, a small glacial valley is presently occupied by an active peatbog. Here, a detailed 4 m-thick section has been studied (Fig. 3), giving us a fairly good record of the last 5.000 years of ashfall and/or pyroclastic flows events of the Nevado Cayambe.

Two eruptive periods which include numerous events, separated by quiescence, form the recent activity of the volcano. Three C14 dates on peat samples from the lower part of the section were obtained. They show a long period of eruptive activity from 3900 to 1800 y BP. A second long period has been observed, up to present time. The results of three additional datings will constrain the duration of this second period which has probably not concluded. As evidence, Ascazubi (1802) in a letter to A. von Humboldt describes an small eruptive event of Cayambe in 1785, i. e. ≈165 y BP, which could be considered the last eruption. At present, mountainers frequently report a strong sulphur smell in the summit area of the Nevado.

## GEOCHEMISTRY

55 samples from Old Cayambe, Nevado Cayambe and Cono de La Virgen have been analyzed for major and trace elements. All SiO2 contents range from 59 to 67% (LOI free and total recalculated to 100%). The rocks are medium-K andesites and dacites, except for samples from Cono de La Virgen which are high-K andesites. All the rocks from Nevado Cayambe are depleted in Y and Yb and have high La/Yb and Sr/Y ratios. The origin of these rocks (adakites) is discussed by Monzier et al. (this volume). On the contrary, the few rocks analized from the Old Cayambe are normal calc-alkaline series.

## CONCLUSIONS

Nevado Cayambe volcano has been very active during the last 5000 y BP, this activity being mainly characterized by lava dome extrusions, dome collapses and pyroclastic flows. The geochemical characteristics of the resulting products argue for a dominant melting process leading to a large adakitic suite in which crystal fractionation only plays a minor role. Magma mixing is also present, especially in the recent phases of the volcano.

## REFERENCES

-Ascasubi, J. J., 1802. Letter to Baron von Humboldt in "von Humboldt, A., Briefe aus Amerika, 1799-1804", Herausgegeben von Ulrike Moheit, Akademic Verlag, Berlin, 1993, ---p.

-Barberi, F., Coltelli, M., Ferrara, G., Innocenti, F., Navarro, J.M. and Santacroce, R., 1988. Plio-Quaternary volcanism in Ecuador. *Geol. Mag.* 125, 1, 1-14.

-Ego, F., Sebrier, M., Lavenu, A., Yepes, H. and Eguez, A., 1993. Quaternary state of stress in the northern Andes and the restraining bend model for the ecuadorian Andes. Second ISAG, Oxford (UK), 21-23/9/1993, extended abstracts, Editions de l'ORSTOM, Paris 1993, p. 89-92.

-Hall, M. L. and Mothes, P., 1994. Tefroestratigrafia holocenica de los volcanes principales del Valle Interandino, Ecuador. *Estudios de Geografia*, Vol. 6, 47-67, Quito.

-Litherland, M, Aspden, J. A., and Jemeilita, R. A., 1994. The metamorphics belts of Ecuador. *Overseas Memoirs of the Brithish Geological Survey*, No. 11, Keyworth, Nottingham.

-Soulas, J., Egüez, A., Yepes H., and Pèrez H., 1991. Tectonica activa y riesgo sismico en los Andes ecuatorianos y el extremo sur de Colombia. *Bol. Geol. Ecuat.* Vol. 1, n° 1., 3-9.

-Tibaldi, A. and Ferrari, L. 1992. Lastest pleistocene-holocene tectonics of the ecuadorian Andes. *Tectonophysics*. 205, 109-125.

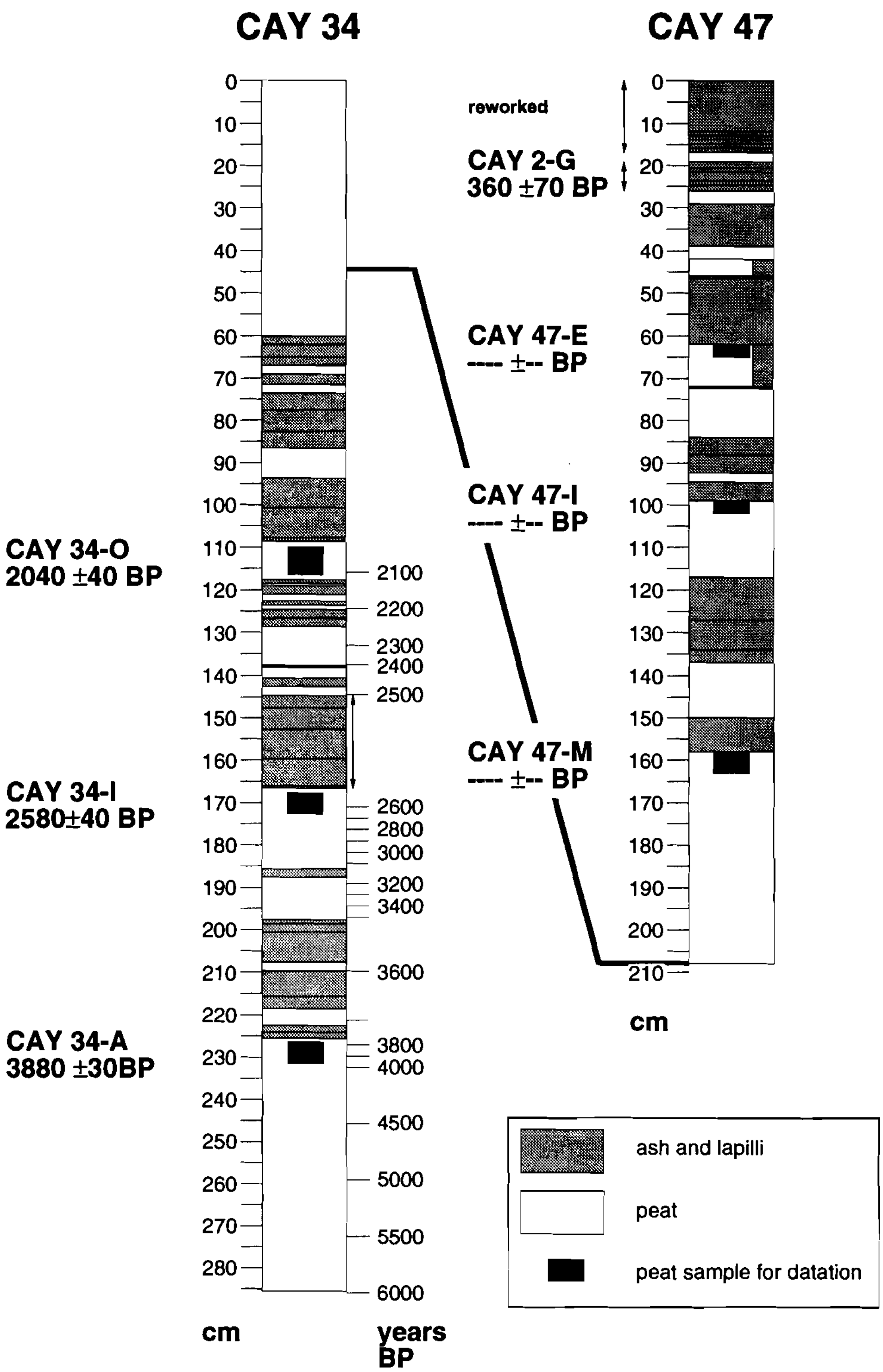


**Fig. 3** Nevado Cayambe bog. Cross-section through the ash and lapilli and peat layers; C14 dated samples are shown (results of the last three datations are soon expected). Ages on the right side of the columns are calculated assuming the layers of tephra were deposited instantaneously.

# SEGMENTATION AND HORIZONTAL SLIP-RATE ESTIMATION OF THE EL TIGRE FAULT ZONE, SAN JUAN PROVINCE (ARGENTINA) FROM SPOT IMAGES ANALYSIS.

Lionel SIAME [1], Michel SEBRIER [1], Olivier BELLIER [1] Didier BOURLES [2], Juan Carlos CASTANO[3], Mario AUROJO[3], Françoise YIOU[2] and Grant M. RAISBECK[2].

[1] URA-CNRS - Géophysique et Géodynamique Interne, Bât 509, Université Paris-Sud, 91405 Orsay Cedex, FRANCE.
[2] Centre de Spectrométrie Nucléaire et de Spectrométrie de Masse, $IN_2P_3$-CNRS, Bât 108, Université Paris-Sud, 91405 Orsay Cedex, FRANCE.
[3] Instituto Nacional de Prevencion sismica (INPRES), Roger Ballet 47 Norte, 5400 San Juan, Republica Argentina.

KEY WORDS : El Tigre Fault, segmentation, slip rate and cosmonucleids.

## INTRODUCTION

In the subduction areas associated with oblique convergence, relative plate motion should be partitionned between displacements along the subduction plane and parallel-to-the margin strike-slip deformation within the overriding plate. The Nazca/South American N76°convergence off Chile is strictly oblique and has to be mechanically accommodated by strike-slip (shear) deformation (Fitch, 1972; Jarrard, 1986; Sébrier and Bellier, 1993; Bellier and Sébrier, 1995; Ego et al., 1995) which could be localised, at about 30°-31°, along the El Tigre Fault (Bastias and Uliarte, 1988; Bastias et al., 1990). This N10°E-trending dextral fault is located on the eastern side of the intra-Andean Calingasta-Iglesia Valley (Armijo and Sébrier, 1991) (Fig.1). Geomorphologic analysis on SPOT images allow us to precisely characterize the fault geometry and to quantify the active deformation along the El Tigre Fault Zone.

**Segmentation and Geometry of the El Tigre Fault Zone**

The 120-km-long El Tigre Fault Zone, is subdivided, from South to North, into 26, 48 and 46 km-long main segments (Fig.1). Both Quaternary to recent geomorphologic features and stream channel offsets outstandingly agree with the apparent Present-day fault activity. According to previous studies (Bastias, 1990) this fault should have a 800 km long rupture length. Nevertheless, no evidence has been observed from the SPOT images analysis to justify such a rupture length. Indeed, the southern tip of the southernmost segment (#1 Fig.1) is characterized by a merging within the Precordilleran Paleozoic strata and, because of its very distributed surface deformation, the northernmost segment (#3 Fig.1) is interpreted as the northern termination of the El Tigre Fault Zone.

**Late Quaternary horizontal displacement along the El Tigre Fault Zone**

The high resolution (10 m a pixel) panchromatic SPOT images provide evidences of recent tectonic activity such as stream channel offsets within Quaternary fan deposits along the central segment (#2 Fig.1). These alluvial fans are composed by imbricated detritic fans which can be related to locally or regionaly significant climatic pulses. The measured offsets range between 60 and 180 m. The larger offsets inside the fans are assumed to be the older because they are probably not as much rejuvenate by erosion than the smaller on the borders. Thus, as a mean value we assume 170 ± 10 m to be the maximum Late Quaternary right-lateral strike-slip displacement on the El Tigre Fault Zone.

**Seismic Hazard of the El Tigre Fault Zone**

The geometric parameters (surface rupture lengths and horizontal displacements) inferred from the SPOT images analysis allow us to improve the seismic hazard evaluation along the El Tigre Fault Zone using statistical empirical laws (Wells and Coppersmith, 1994). Estimates of the moment magnitude (Mw) for the maximum expected earthquake, i.e. earthquake reactivating the total segment length, are of about 7 ± 0.5.

**Horizontal slip-rate estimation using in-situ produced $^{10}$Be**

In order to constrain the El Tigre Fault Zone horizontal slip-rate we decided to date the along-strike displaced morphological features as it has been performed in Mongolia (Ritz et al., 1995). We thus sampled alluvial fan surfaces to determine their cosmic ray exposure dates using in situ-produced $^{10}$Be (Lal, 1991; Cerling and Craig, 1994). Preliminary results, obtained at the Tandetron AMS facility (Gif-sur-Yvette, France), seem to indicate that each detritic pulse that led to the deposition of the alluvial fans is related to known interglacial stages. These data, combined with the measured-offsets of stream channels allow us to estimate an horizontal slip-rate roughly of the order of 1 mm/year.

## CONCLUSIONS

Considering the linkage between the Precordilleran mountain ranges geometry and the segmentation of the fault, a crustal signification is given to the El Tigre Fault Zone. Parallel to the mountain belts motion on the faults depends on the mountain belts trending with respect to the plate convergence (N76°E), thus reverse motion should occur on N-S to NNW-SSE trending structures, whereas transpressive motion should occurs on NNE to SSW trending structures. The Calingasta-Iglesia Valley, and the Precordillera at 30°-31°S, can be seen as a transpressive zone of crustal scale : deformation being partitioned between right-lateral strike-slip motion along the El Tigre Fault Zone and reverse motion on the Precordilleran thrust faults.

## REFERENCES


- Armijo R. et M. Sébrier (1991), Découplage et bifurcation parallèles à la chaîne des Andes : Analyse des failles d'Atacama et de El Tigre avec SPOT, Journée Scientifique du 24 Octobre 1991 : Tectoscope - Positionnement, CNRS - INSU.
- Bastias H.E. (1990), Discontinuidades tectonicas a la latitud de 32° Sur y su importancia en la hipotesis de evolucion de Precordillera, Decimo Congresso Geologico Argentino, San Juan, Actas II, p. 407-411.
- Bastias H.E., E. Uliarte, J. de Dios Paredes, A. Sanchez, J.A. Bastias, L. Ruzycki y P. Perucca (1990), Neotectonica de la Provincia de San Juan, Primer Congreso Geologico Argentino, San Juan.
- Bastias H.E. and E. Uliarte (1988), Neotectonic of the "El Tigre" fault system, Quaternary activity and geologic hazard relationship, XXXV Congresso Brasileiro de Geologia.
- Bellier O. and M. Sébrier (1995) Is the slip-rate variation on the Great Sumatran Fault accommodated by fore-arc stretching?, Geophys. Res. Lett. (22), 15, p. 1969-1972.
- Cerling T.E. and H. Craig (1994), Geomorphology and in-situ cosmogenic isotopes, Annu. Rev. Earth Planet. Sci., 22, p. 273-317.
- Ego F., M. Sébrier and H. Yupes (1995), Is the Cauca-Patia and Romeral fault system left or right-lateral?, Geophys. Res. Lett. (22), 1, p. 33-36.
- Fitch T.J. (1972), Plate convergence, transcurrent faults, and internal deformation adjacent to Southeast Asia and Western Pacifique, J. Geophys. Res., 77, p.4432-4460.
- Jarrard R.D. (1986), Relations among subduction parameters, Rev. Geophys., 24, 2, p. 217-284.

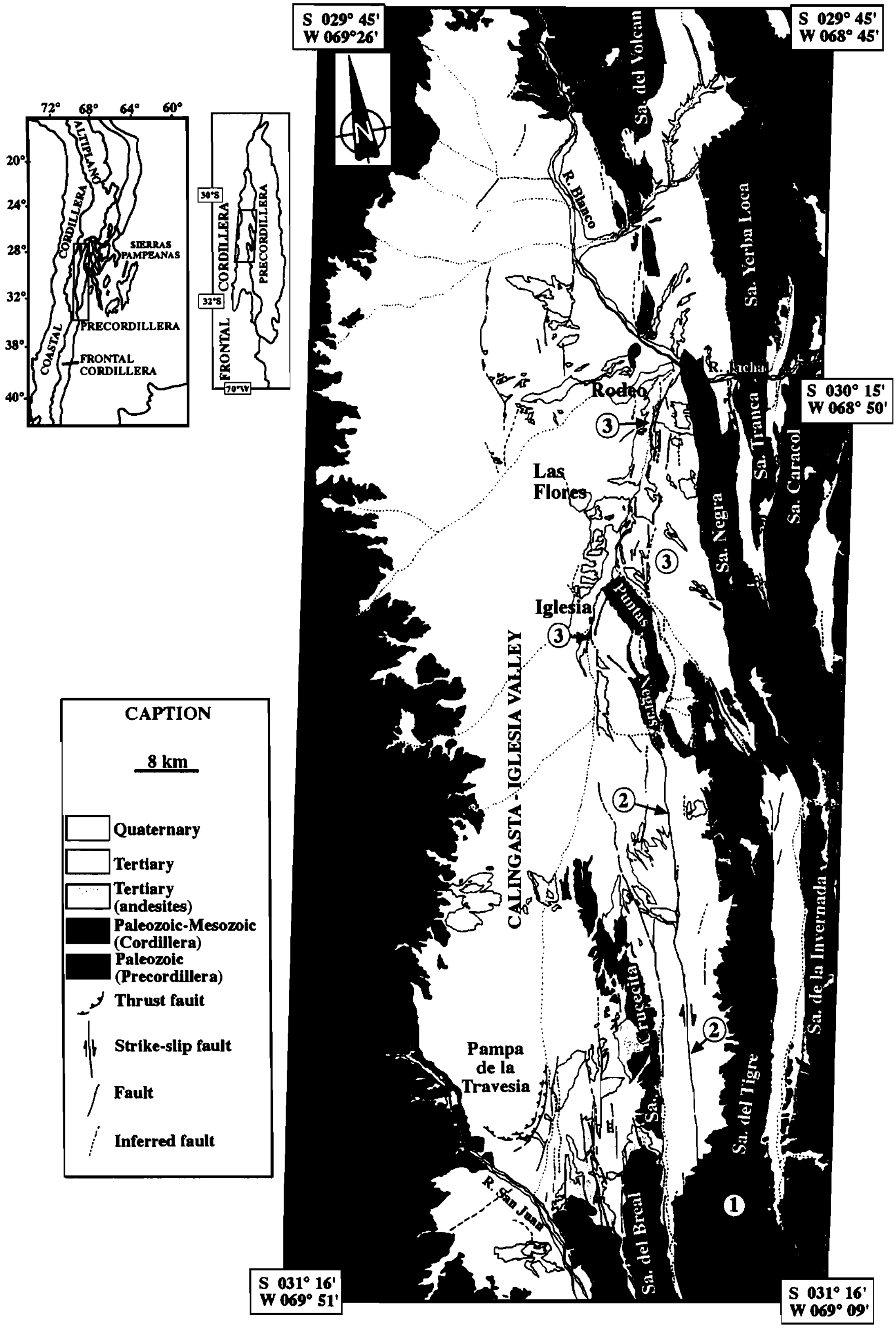
S 029° 45'
W 069°26'
S 029° 45'
W 068° 45'
S 030° 15'
W 068° 50'
S 031° 16'
W 069° 51'
S 031° 16'
W 069° 09'
72°
68°
64°
60°
20°
24°
28°
32°
38°
40°
CORDILLERA
ALTIPLANO
SIERRAS PAMPEANAS
PRECORDILLERA
COASTAL
FRONTAL CORDILLERA
30°S
32°S
70°W
FRONTAL
CORDILLERA
PRECORDILLERA
Sa. del Volcan
R. Blanco
Sa. Yerba Loca
R. Jachal
Rodeo
Sa. Tranca
Sa. Caracol
Las Flores
Sa. Negra
Iglesia
CALINGASTA - IGLESIA VALLEY
Pampa de la Travesia
Sa. del Tigre
Sa. de la Invernada
Sa. del Breal
R. San Juan
CAPTION
8 km
Quaternary
Tertiary
Tertiary (andesites)
Paleozoic-Mesozoic (Cordillera)
Paleozoic (Precordillera)
Thrust fault
Strike-slip fault
Fault
Inferred fault

- Ritz J.F., E.T. Brown, D.L. Bourlès, H. Philip, A. Schlupp, G.M. Raisbeck, F. Yiou and Enkhtuvshin (1995), Slip-rates along active faults estimated with cosmic-ray exposure dates : Application to the Bogd Fault, Gobi-Altaï, Mongolia, Geology, V.23, N°11, p. 1019-1022.
- Lal D. (1991), Cosmic ray labeling of erosion surfaces : in-situ nuclide production rates and erosion models, Earth and Plan. Sci Lett., 104, p. 424-439.
- Sébrier M. and O. Bellier (1993), How is accommodated the parallel-to-the-trench slip component in oblique convergent subduction : the Andean case, Second ISAG, Oxford (UK), 21-23/9/1993, p. 139-141.
- Wells D.L. and K.J. Coppersmith (1994), Updated empirical relationships among magnitude, rupture length, rupture area and surface displacement, Bull. Seism. Soc. Am., 84(4), p.974-1002.

# ACTIVE FAULTING IN THE SOUTHERN VENEZUELAN ANDES AND COLOMBIAN BORDERLAND

André SINGER and Carlos BELTRAN

Venezuelan Foundation for Seismological Research (FUNVISIS), E-Mail: dptoct@funvisis.internet.ve.

Key words: Venezuelan Andes, South Boconó active fault, slip rate, damping, barriers, seismic sources.

## INTRODUCTION

Along the Southern Venezuelan Andes, the Boconó fault shows a progressive displacement to the West of his NE-SW trending active trace with respect to its axial position exhibited North of Mérida (Fig. 1). Such a shifting of the Boconó active trace is produced by the introduction of a sigmoidal releasing bend connection between several NE-SW segments of the fault, which are characterized by a right steppover geometry. This kind of double deflection pattern occurs close to several highly complicated structural sites located along the fault trace, which constitute significant potential barriers to fault rupture propagation, as may be the case for the following neotectonic features: La González-Estanques pull apart, South of Mérida; Bailadores steppover; La Grita double bend; Los Mirtos-Zumbador composite pull apart and Capacho restraining bend, West of San Cristóbal; La Mulera and Cerro Rangel transpressive push-up ridges in the venezuelan margin of the Rio Táchira, and La Huchena right steppover on the colombian side of this river (Fig. 2). At several of these potential barrier sites, the Boconó active fault displays a system of secondary active traces characterized by a dense branching pattern on the east side of the master fault, and by a progressive damping to the South against the NW-SE sinistral reverse Bramón fault system.

Between Mérida and San Cristóbal, we have surveyed the following secondary branch faults (Fig. 2): San José de Bolivar, Queniquea and La Colorada-La Maravilla right lateral faults, and the San Cristóbal right lateral reverse fault. Between the Capacho restraining bend and the Táchira river, the Boconó main active trace displays a left lateral active branch on each side: to the South, the Caña Brava faults cutting across the Rubio basin (MEIER *et al.*, 1987) and to the North, the Llano Grande Fault. Close to the Colombia borderland, the Boconó active trace gets a conspicuous anastomosed pattern along the transpressive push-up structures of the La Mulera and Cerro Rangel ridges.

Such an occurrence of branching and transpressive faulting features, observed along the southern end of the Boconó active fault and the associated Sierra de Cazadero thrusting structures (MEIER, 1984), take place as a consequence of the convergent movement produced by the Boconó and Bramón fault systems into a squeezing zone defined by the geometry of these faults. In the same way, these kinematic conditions explain the occurrence of a significant damping of the strike-slip motion of the Boconó fault and the accommodation of the corresponding decreasing activity through compressional deformations.

As an attempt to estimate the importance of the Boconó fault damping along its southwestern end, we have got evidences of a markedly decrease of its slip-rate activity using a paleomagnetic age controlled Pleistocene offset drainage, located transversally to the Peribeca pull apart (North-South Catarnica-Velandría canyon drainage) and other drainage offsets data obtained near the Dantera canyon cross-site, close to the Colombian border. In this way, the slip-rate of the Boconó fault at the first site is less than 1 mm/yr and at the second site, probably as low or less than 0.5 mm/yr (SINGER *et al.*, 1991).

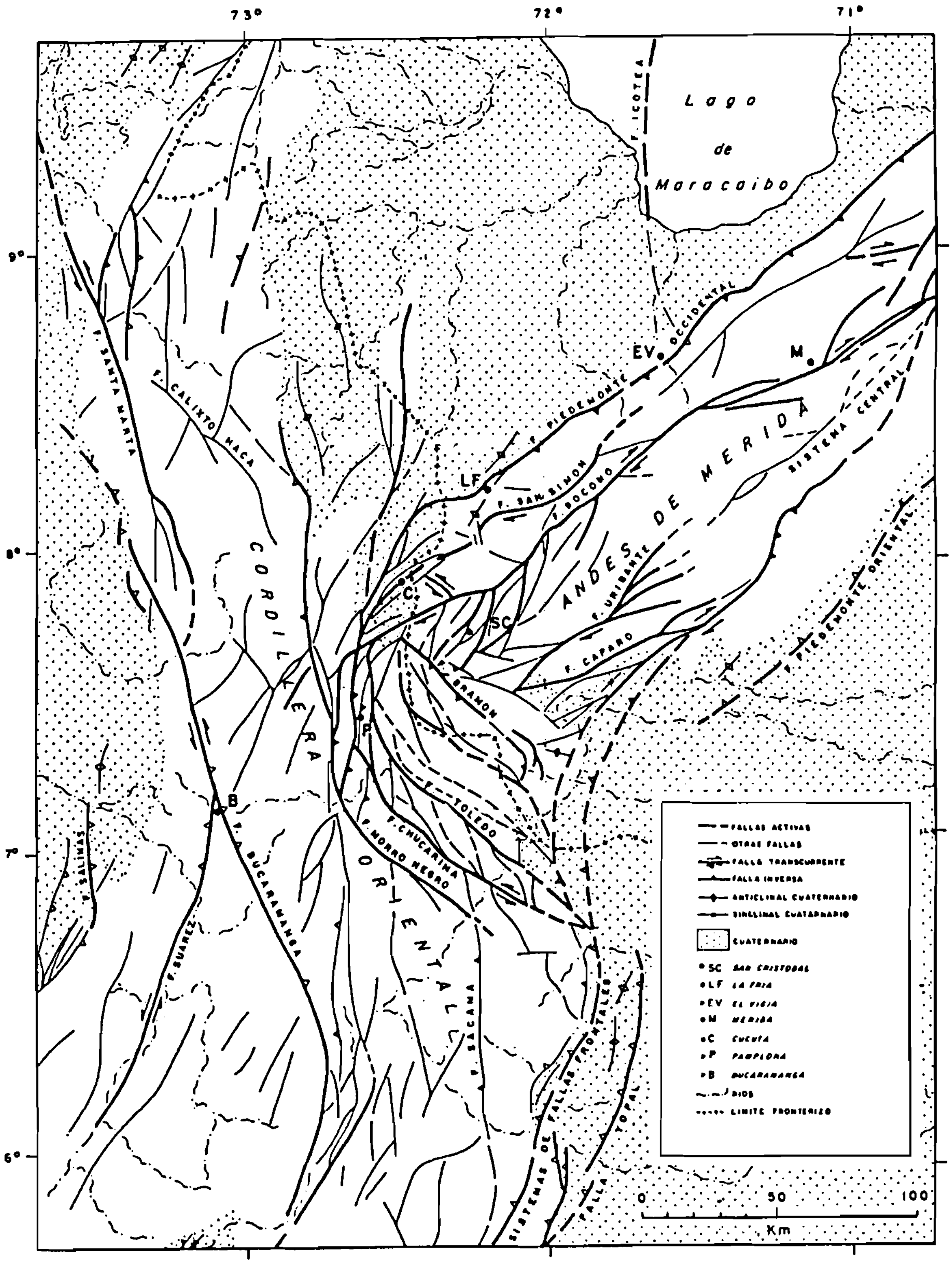


Fig. 1 General tectonic setting of the Southwestern Venezuelan Andes and Colombian borderland.

According to the above slip-rate estimate, it appears that a rate right lateral rate displacement as high as 5 to 7 mm/yr obtained by SCHUBERT *et al.* (1983) South of Mérida along the Plio-Pleistocene La González-Estanques pull apart and 5 to 6 mm/yr obtained by AUDEMARD & SOULAS (1995) from paleoseismic trenching assessment at La Grita, cannot be extrapolated to the southern venezuelan segment of the Boconó fault and also along its prolongation beyond the Colombian frontier through the Palo Colorado fault (BOINET, 1985). Additionally, the above mentioned evidences of a decreasing activity of the slip rate along the southern end of the Boconó fault, is consistent with the apparent existence of a kinematic discontinuity introduced by the connection pattern between this right lateral strike-slip fault and the Chinácota and Chucarima left lateral reverse faults, that define part of the geometry of the "Pamplona indenter" in the colombian borderland (BOINET, 1985).

Moreover, the progressive deactivation of the main lateral motion of the Boconó master fault seems to be accommodated by subparallel right lateral active fault system identified on both sides of the main fault (Fig. 2). On the west side, the active traces of the three SW-NE branches of the San Pedro-Aguas Calientes fault cross the Táchira and Pamplonita alluvial valleys through the Cúcuta and Villa de Rosario urban areas, respectively along the Cerro Bogotá (or Libertad) hill and the Lomitas-Hacienda San Javier fault scarps. A good correlation can be observed between these active fault traces and the epicentral area of the 1875 earthquake, which destroyed both cities. However, this earthquake was previously attributed to the Boconó seismogenic source. In fact, it appears that the contribution of the southern end of the Boconó fault as a seismic source, loses importance with respect to the northern segment located between La Grita and Mérida where the 1610 and 1894 earthquake occurred, and also when compared to the faults that define the "Pamplona indenter", probable source for several destructive earthquakes.

## CONCLUSIONS

A significant decrease of the right-lateral motion of the Boconó fault, considered as plate boundary between the Caribbean and South America plates, may occur in the Venezuelan Southern Andes as a result of a conspicuous branching and damping of the fault activity against the transversal Bramón fault system. Additionally, the progressive deactivation of the main movement of the Boconó fault is consistent with the kinematic connection pattern between this fault and the left lateral reverse faults of the Pamplona indenter, and is also explained by the occurrence of subparallel active faulting on each side of the main fault, which contribute to absorb another significant amount of the relative Caribbean and South America plates displacement occurring along the Venezuelan Andes range. Therefore, the seismogenic sources scenario of the Venezuela-Colombia borderland is much more complex than previously considered.

## REFERENCES

AUDEMARD, F. & SOULAS, J.P. (1995). Trench confirmation of historical earthquakes on the Boconó fault systems, southern Venezuelan Andes; Terra Nostra, 2/95;16 (Abstract XIV INQUA Intern. Congr.).

BOINET, T., BOURGOIS, J., MENDOZA, H. y VARGAS, R. (1985). Le poinçon de Pamplona (Colombie): un jalon de la frontière méridionale de la plaque caraïbe; Bull. Soc. Geol., France. T.I. (3):403-413.

MEIER, B., SCHWANDER, M. & LAUBSCHER, H.P. (1987). The tectonics of Táchira: a sample of North Andean Tectonics; in: The Anatomy of Mountain Ranges, Schaer & Rodgers Ed., 229-237.

SCHUBERT, C., SINGER, A. & SOULAS, J.P. (1983). The Boconó fault between Mérida and San Cristóbal; Trip Field, Int. Symp. on Neotectonics, Seismicity and Geologic Hazards in Venezuela and the Caribbean, Caracas, Unpubl. 62 p.

SINGER, A., BELTRAN, C. & LUGO, M. (1991). Características neotectónicas y parámetros sismogénicos de las fallas activas cuaternarias, y efectos geológicos de la actividad sísmica en la región del Proyecto SUMANDES II; Unpubl. Report Co. MARAVEN-FUNVISIS, Caracas, 2 Vol. 239 p.

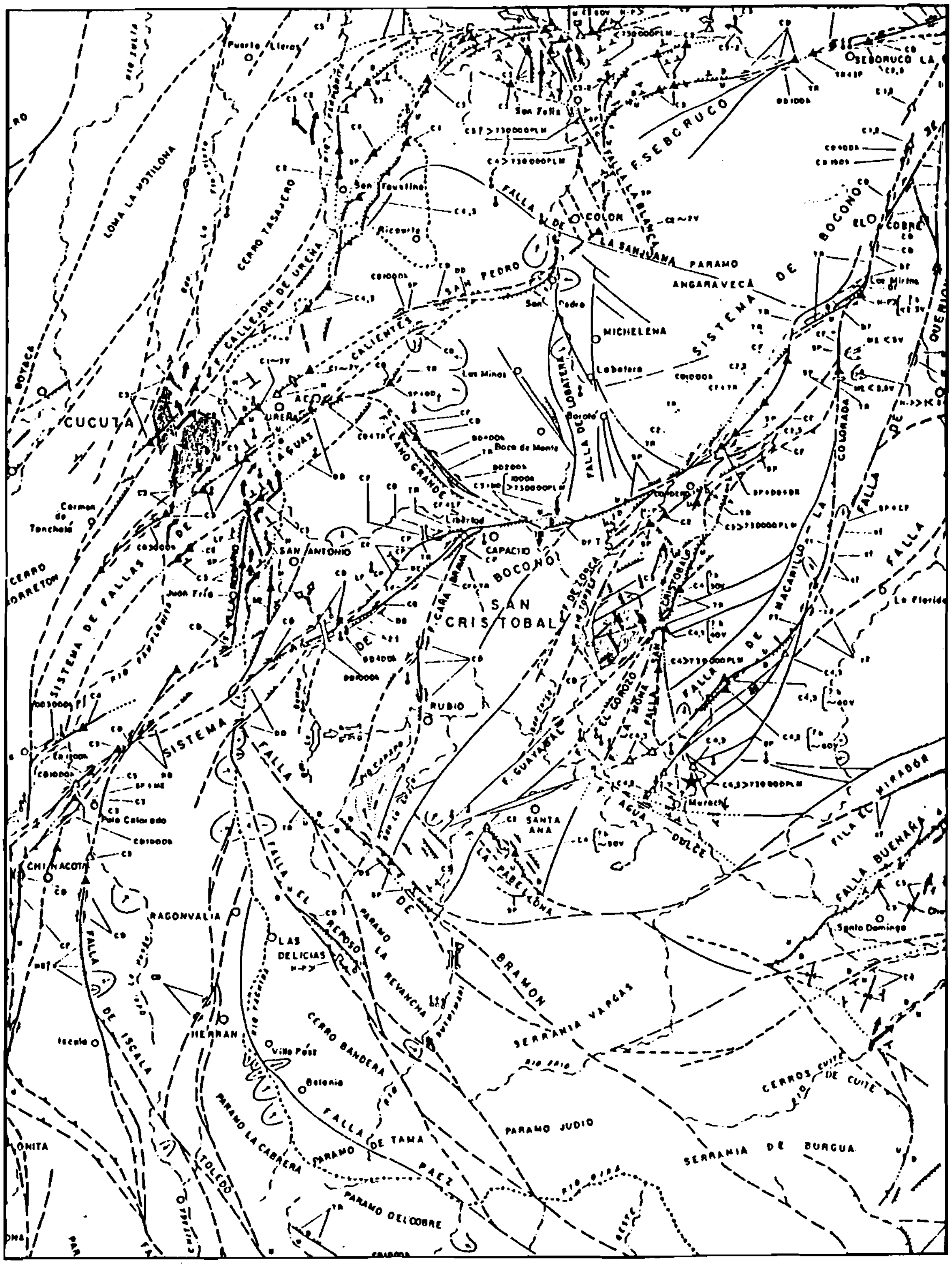


Fig. 2 The Bocono active fault system and other minor active faults in the Venezuelan and Colombian borderland.

# HUAYNAPUTINA VOLCANO, SOUTH PERU: SITE OF THE MAJOR EXPLOSIVE ERUPTION IN HISTORICAL TIMES IN THE CENTRAL ANDES

Jean-Claude THOURET[1,2], Alain GOURGAUD[2], and Jean-Luc LE PENNEC[2,3]

(1) ORSTOM (UR 14)-Instituto Geofisico del Peru, La Molina, Lima 100, Peru - Fax 51 14 368 437 14 379 923 e-mail jct @ geo.igp.gob.pe
(2) CRVet URA10-OPGC, Université Blaise Pascal, 5 rue Kessler, 63000 Clermont-Ferrand, France; (3) now at Centre Orstom, Brest, France.

**KEY WORDS :** Huaynaputina volcano, South Peru, Plinian eruption

The major explosive eruption in historical times in the Central Andes took place at Huaynaputina, a small volcanic center (16°37'S, 70°51'W) located in the northern part of the Central Volcanic Zone (South Peru, Figs. 1 & 2). Huaynaputina does not display a typical volcano morphology but relatively uncommon volcanic structures (de Silva & Francis, 1991): three nested funnel-like vents and ash cones located on the floor (4,200m) of a 2.5x1.5 km horseshoe-shaped caldera which reamed out the eastern edge of a volcanic plateau. The summit (4,800 m) is breached towards the East, forming an amphitheater open to the deep canyon of Rio Tambo, 6 km horizontally and 2.7 km vertically from the crater rim. Most of the caldera has been formed prior to the 1600 eruption, resembling other horseshoe-shaped scars which eat away the volcanic plateau ≥ 4,200 m in elevation (Fig. 1). Lava flows, ignimbrites, and pyroclastic deposits of no more than 500 m thick built up this high-plateau which includes one early extrusive lava dome to the south edge, and overlies the deeply dissected sedimentary bedrock of Mesozoïc age.

According to chronicles, the A.D. 1600 eruption began on February 19 after at least 4 days of intense seismic activity, while the Plinian stage lasted until February 21. Repeated ash fallout and earthquakes unil March 2 devastated 7 indian villages as far as 15 km away from vent and damaged Arequipa city 75 km away (Barriga, 1951). The bulk volume of the eruptive deposits is estimated at about 10 $km^3$ (Gonzales-Ferran, 1990). The deposits include: (1) a very widespread plinian fallout (Fig. 2); (2) large-volume pumice-flow deposits, including proximal lag brecciae and channelized ≥ 30 km in the Tambo valley (Fig. 3); (3) pyroclastic-surge deposits, observed on the caldera slopes and as far as 13 km in the Quebrada del Volcan (Fig. 4), and; (4) late ashfall and debris flows. An additional minor explosive event in 1667 may have contributed to the last ashfall. The plinian-fall deposits are distributed in two lobes, the most voluminous extending several hundreds of km to the West and WNW (≥ 10 cm thick in Arequipa, ≥ 3 cm at the Pacific coast 150 km due WSW), and the second several tens of km towards the North. In addition, fine white ash observed along the NW-trending Pacific coast as far as 900 km from source, was carried away by SE high-altitude winds.

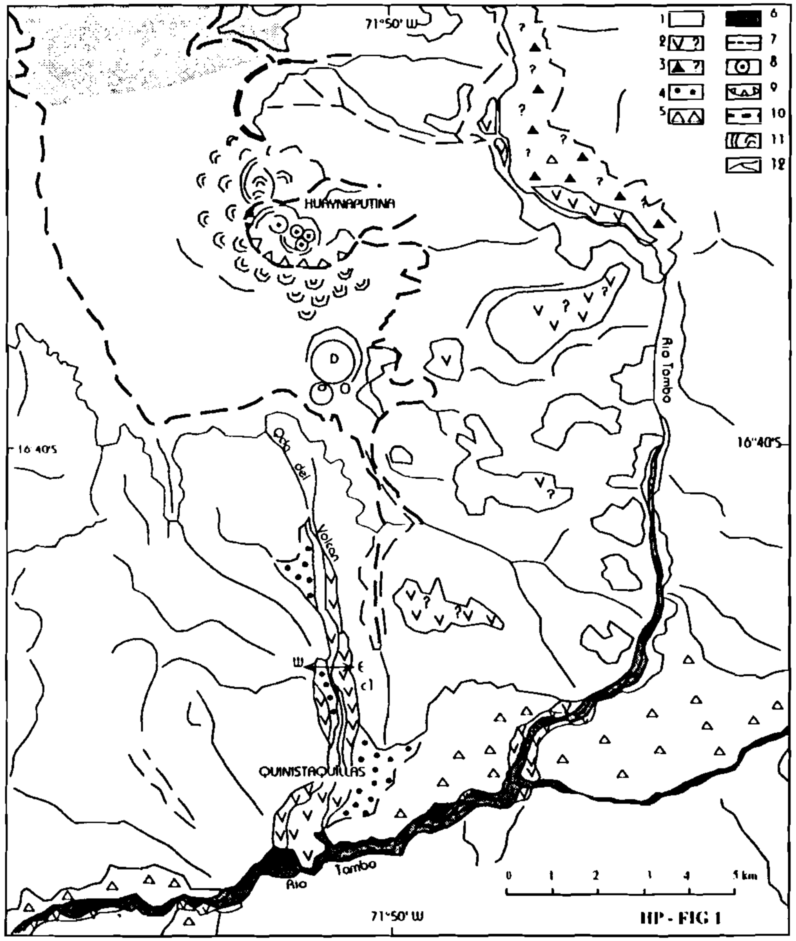


Figure 1. Schematic map of the area of Huaynaputina volcano and related volcanic deposits and features (based on one SPOT satellite image and air-photos).
1. Plinian fallout deposit: ≥ 2m thick (a) < 2m (b). 2. Ignimbrite=pumice-flow deposit, mostly channelized (? where inferred). 3. Probable debris-avalanche deposit (dashed where inferred, upper Rio Tambo). 4. Block-and-ash flow deposit prior to the A.D. 1600 event. 5. Large-scale debris-avalanche deposit from the Ticsani stratovolcano, to the East. 6. Floodplain and alluvial terraces. 7. Limit of the volcanic high-plateau (dashed where inferred). 8. Pre-1600 dome ; A.D. 1600 vents. 9. Scar of the pre-1600 caldera. 10. Fresh scar of debris avalanche ; subdued scar of landslide. 11. Ring fractures and collapse features. 12. Ridge in sedimentary bedrock. Arrow W-E in Qda del Volcan indicates location of cross-section in Fig. 4.

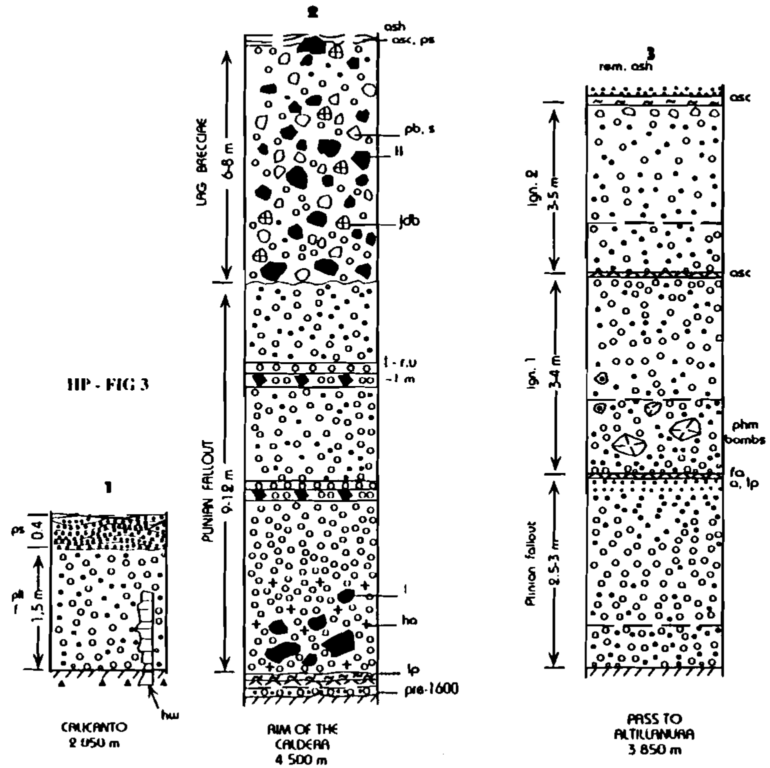


Figure 3. Measured stratigraphic section of the A.D. eruptive deposits at Huaynaputina
1. Calicanto, 2050 m, 13 km from vent: ps pyroclastic surge deposit, wall of the buried houses and tilled terraces. 2. Rim of the caldera, 4500 m, 1 km from vent (from top to base): asc, ps ash-cloud surge, pyroclastic-surge deposit; pb, s pumice blocks, scoriae; l l large lithics (accidental and accessory, including sediments); jdb juvenile dacite blocks. l-r.u. lithic-rich units. l lithics, ha hydrothermally altered lithics, lp leaves of *puna* vegetation, pre-1600 soil, removed ash and pumice lapilli. 3. Pass to altillanura, 3850 m, 5 km from vent: rem. removed ash, asc ash-cloud surge deposit, phm phreatomagmatic bombs, Ign 1, 2 ignimbrite = pumice-flow deposits.

According to preliminary field data, we infer that the pre-1600 edifice and early domes were blown away during the eruption, leading to the formation of the complex crater, the failure of the north rim of the caldera, and finally to the nested vents and low cones of silicic tephra (Fig. 1). In addition, pumice-rich pyroclastic flows and probable debris avalanches choked the upper Rio Tambo (Fig. 1). The canyon reportedly was dammed at least 28 hours, leading to two temporary lakes and subsequent catastrophic release of large-scale debris flows.

The proximal sections (Fig. 3) show the thick Plinian, massive tephra-fall deposit, overlain by lag-breccia deposit which form high and large crescent-shaped dunes protruding from the ash apron that surround the caldera rim (Fig. 1). Interestingly, the base of the tephra-fall includes a large amount of sedimentary blocks and hydrothermally altered lithic lapilli. Recurrent 1-m-thick lithic-rich units are interspered in the middle and upper part of the otherwise massive pumice-fall deposit. The medial sections (Fig. 4) show a complex pyroclastic sequence. The pre-1600 units encompass: (1) block-and-ash flow and dome collapse deposits; (2) a pyroclastic sequence including a Plinian tephra-fall deposit similar in composition to the 1600's. The A.D. 1600 sequence entails: (1) a Plinian pumice-fall deposit; (2) two to three nonwelded pumice-flow deposits, the earliest carrying phreatomagmatic bombs; (3) a pyroclastic-surge deposit showing cross-stratified bedding and dune-like features, and; (4) a late ashfall layer.
The mineral assemblage of the erupted dacite encompasses plagioclase, biotite, amphibole, magentite, and ilmenite. However, the evolution from deposit 1 to deposit 4 is correlated with significant chemical and mineralogical changes : (1) decrease of $SiO_2$ (65.5 to 62.8 %) and $K_20$ (2.9 to 2.6 %) contents, while MgO (1.7 to 2.15 %), CaO (4 to 4.5 %), $Fe_20_3$ (4.2 to 4.5 %) and Sr (696 to 754 ppm) increase; (2) increase of Mg/Mg+Fe of biotite (58 to 70) and amphibole (56 to 71) and of An % content of plagioclase ($An_{25-52}$ to $_{34-59}$). These preliminary results are consistent with emptying of a zoned dacitic magma chamber.

Our preliminary data preclude to indicate what caused such a catastrophic explosive eruption (VEI 6). However, we suggest two triggering processes: (1) a small amount of basaltic component exists in the tephra-fall; (2) a significant amount of hydrothermally altered lithics at the base and lithic-rich units throughout the Plinian fallout, as well as phreatomagmatic bombs in the lower ignimbrite, witness to hydromagmatic interaction. The deposits including lag brecciae and volcanic features such as funnel-like vents and landsliding of part of the caldera point to eruptive processes involved in maar-like craters and small explosive calderas. Such a large-scale explosive silicic eruption did not involve caldera collpase; however, ring-fractures and collapse features surround the vents and the northern caldera rim (Fig. 1).

**References**

Barriga V.M. 1951. Los terremotos en Arequipa (1582-1868). La Colmena, 426 p.
de Silva S. and Francis P.W. 1991. Volcanoes of the Central Andes. Springer, 216 p.
Gonzales-Ferran O. 1990. Huaynaputina volcano: the biggest historical dacitic eruption in the Central Andes of South America, on February 19, 1600. *IAVCEI Volcanological Congress, Mainz, 1990 (Abstract).*
Gourgaud A., Thouret J.-C., Salas G. 1995. The A.D. 1600 Plinian eruption of Huaynaputina (Peru). Preliminary stratigraphy and petrology of the eruptive products. *EUG8, 1995 (Abstract), Terra Abstracts, vol. 7, p.134.*

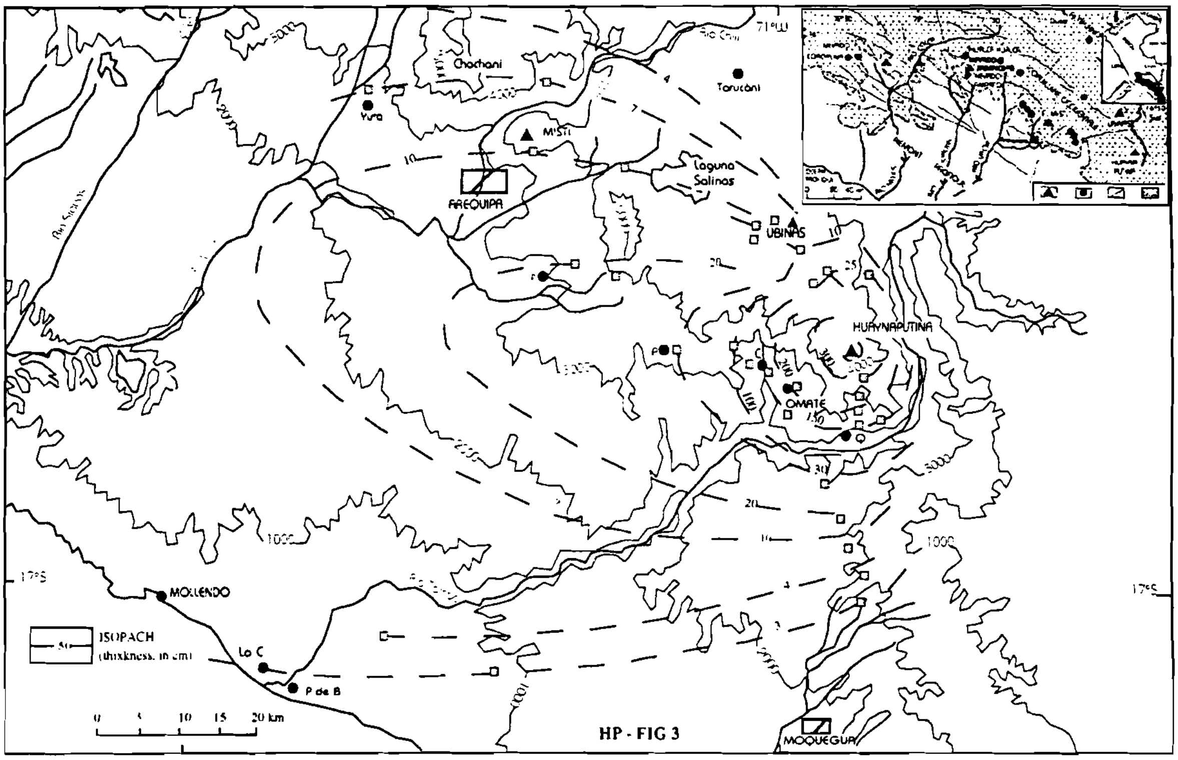


Figure 2. Schematic map showing the approximate extent of the A.D. 1600 Plinian fallout from Huaynaputina.
tephra-fall isopach, thickness in cm; x are measured sections (preliminary data, 1995).

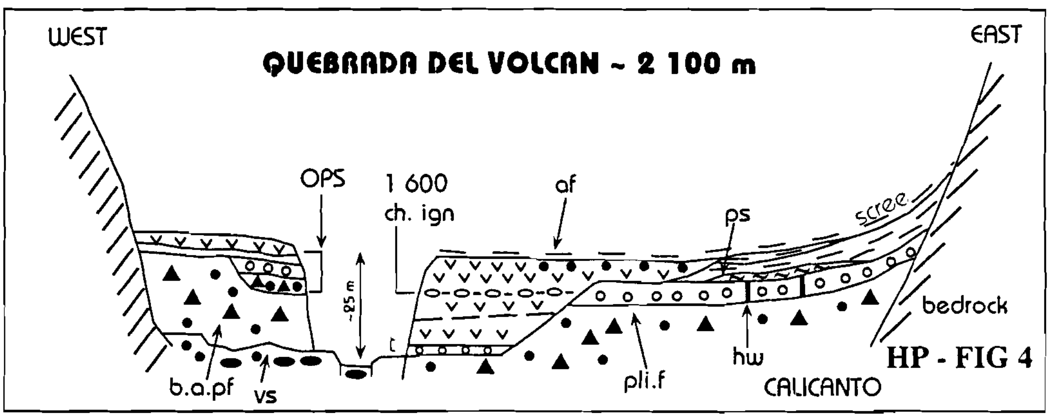


Figure 4. Cross-section of Quebrada del Volcan, 12 km South from vent (arrow in Fig. 1). 1. Pre-1600 deposits: vs volcaniclastic sediments; b-a.pf block-and-ash pyroclastic flows; OPS old pyroclastic sequence (probably lower Holocene in age). 2. A.D. 1600 deposits: Pli.f Plinian-fall deposit; ch. ign. channelized pumice-flow deposits; ps pyroclastic-surge deposit; af ashfall deposit. hw house wall of the buried Calicanto village. scree, debris talus from bedrock and removed ash.

# EL MISTI STRATOVOLCANO, SOUTH PERU : ERUPTIVE HISTORY AND IMPLICATIONS FOR HAZARD ASSESSMENT

Jean-Claude THOURET[(1)], François LEGROS[(2)], Alain GOURGAUD[(2)], Maria-Luisa MACEDO[(3)]

[(1)] ORSTOM (UR 14)-I.G.P., Calle Calatrava 216, Urb. Camino Real, La Molina, Lima 100, Peru - Tel-Fax 51 14 368437-14 379 923 e-mail jct @ geo.igp.gob.pe
[(2)] CRV-OPGC, Université Blaise Pascal, 5 rue Kessler, Clermont-Ferrand, France.
[(3)] I.G.P., Instituto Geofisico del Peru, Cayma, Oficina regional de Arequipa, Peru.

KEY WORDS : El Misti, Peru, stratigraphy, eruptive history, volcanic hazards.

About 900,000 people live at risk in Arequipa area 17 km away from the vent of the active El Misti stratovolcano (16°17'45"S, 71°24'30"W), in the northern part of the Central Volcanic Zone (Figs. 1 and 2). El Misti has been built on 200 to 300-m-thick ignimbrites (upper Tertiary) overlain by 200-m-thick volcaniclastic sediments (mostly debris flows and interbedded ignimbrites). El Misti encompasses two edifices: a 'modern' stratocone, to the East and SE, has been built up side by side and has overlapped in part an 'older' stratovolcano, to the West and NW.

The older stratovolcano (lower to middle ?) Pleistocene in age consists of 400-m-thick and long andesite lava flows, overlain by debris-avalanche deposits at least 100 m thick towards the West and SW. These deposits burying a piedmont in excess of 50 km$^2$ in area record the probable destabilization of the 'older' stratovolcano, which occurred sometime before late Pleistocene (see the scar of the probable flank failure in Figs. 1 & 2). To the SE, they intertwine with similar deposits from the extinct Pichu-Pichu stratovolcano (Fig. 1).
The bulk of the ca. 70 km$^3$ and 5,825 m high stratocone consists of stubby lava flows and pyroclastic debris piling up to 1.8-2.4 km in thickness. On top of the cone-shaped summit, the historical crater 500 m across and 200 m deep including an andesitic plug nests in another crater 900 m wide, whose horsheshoe-shaped walls parallel NS- and WNW-ESE-trending fractures. Both vents are located within a summit explosive caldera 1.5 km across, whose rim partly buried to the West may correspond to the scar of the probable flank failure (Figs. 1 and 2).
Based on fieldwork and interpretation of air-photos and SPOT satellite image, five units of deposits record the late Pleistocene eruptive history, as follows (Fig. 3).

(I) Lava flows, block-lava flows, and buried domes form the lower stratocone (above 3,000 m) towards the South, SW and NE. This is overlain by an old pyroclastic sequence (block-and-ash flows) and stubby lava flows which have built up the cone-shaped summit, above 4,000 m (see composition of lavas in Fig. 4).

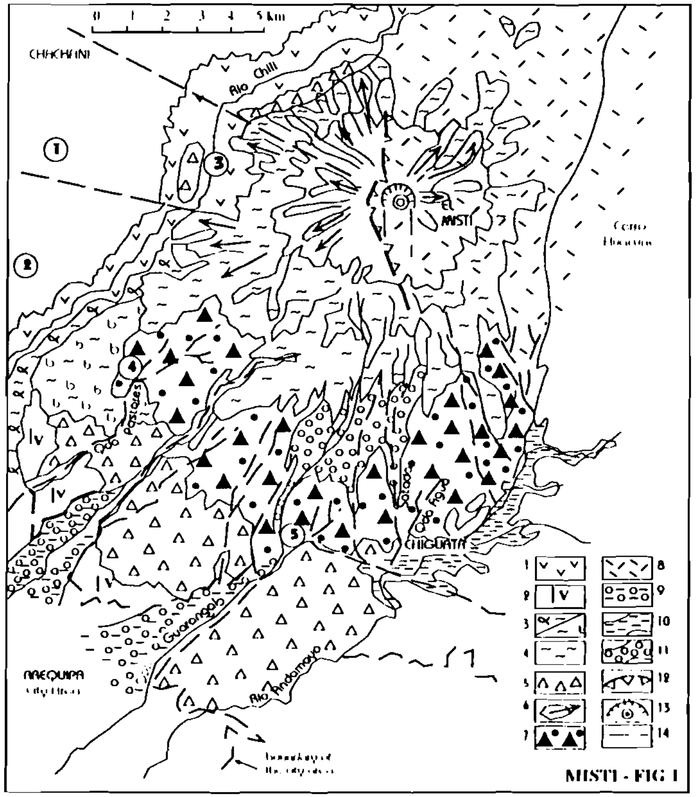


FIGURE 1. Sketch map of volcanic deposits on El Misti and in Arequipa area

1. Ignimbrites of upper Tertiary overlain by volcaniclastic sediments of Plio-Quaternary age. 2. Old lava flows (pre-Misti ?). 3. 'Older' stratovolcano (lower to middle ?) Pleistocene in age: a) andesite lava flows; b) block-lava flows. 4. Lava flows of the lower 'modern' stratocone (middle to late ?) Pleistocene in age. 5. Debris-avalanche deposits (end of middle Pleistocene ?). 6. Summit stratocone of late Pleistocene to Holocene. 7. Piedmonts built up of pyroclastic deposits (units II to V, Fig. 3). 8. Area mantled by black scoriae and ash deposits (related to the summit caldera-forming eruption ?). 9. Fans of volcaniclastic deposits in the lower radial valleys. 10. Lacustrine deposits of the (Last Glacial ?) Chiguata basin. 11. Pumice-flow deposit 1920 ± 200 yr B.P. old. 12. Scar of the probable flank failure. 13. Nested craters and plug. 14. Main fracture.

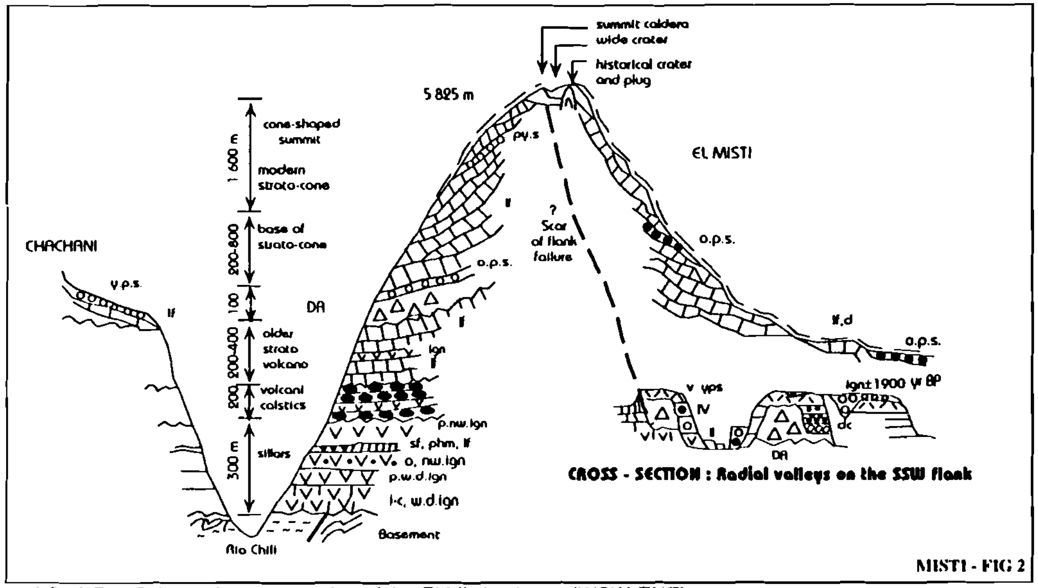


FIGURE 2. Schematic cross-section of the El Misti volcano (WSW-ENE)

Basement (Precambrian gneiss and Jurassic sediments). Sillars=ignimbrites, l-c=light-colored, p=pink, o=orange, pu=purple, w=welded, d=devitrified. sf.phm = scoria-flow and phreatomagmatic deposit. lf=lava flow. d= dome. ign=ignimbrite. DA=debris-avalanche deposit. o.p.s. / y.p.s. = old / young pyroclastic sequence.

(Right-hand corner) Schematic cross-section of the radial valleys, SSW flank. DA=debris-avalanche deposit. dc= deposit of dome collapse. III-V y.p.s.=units of the young pyroclastic sequence (Fig. 3). ign 1900 yr B.P.=radiocarbon dated pumice-flow deposit.

(II) A pyroclastic sequence (mostly scoria flows and fall) mantles the flanks of the extinct Chachani stratovolcano to the West and the North and NE Misti's flanks. Based on interspersed deposits of glacial source, this sequence can be placed close to the last glacial period.
(III) A pile of pumice or ash-flow and tephra-fall deposits, rhyolitic in composition, may reflect an explosive episode which lead to the formation of the summit caldera. Organic material on top of a brown soil within the upper part of these deposits yielded a radiocarbon age of 33,870 ± 1800/1460 yr B.P. (GrN 21574).
(IV) Block-and-ash pyroclastic-flow deposits up to 50 m thick on the south and SW flanks include interbedded pumice and lithic-rich flow deposits. They record alternated dome growth and destruction.
(V) A ≤10-m-thick pile of pumice and ashfall deposit, postglacial in age, show that El Misti has erupted explosively at least 20 times over the last ca.14,000 years. The Plinian-subplinian activity has decreased or come to rest for short periods only, as shown by poorly developped soils in ash. One pumice-rich flow deposit has formed a pyroclastic fan ≥10 $km^2$ in area and was channelized 12 km from vent in gorges that cut deeply the south flank (Fig. 1). Its basal pumice-fall deposit yielded a radiocarbon age of 1920 ± 200 yr B.P. (i.e., calibrated 200 yr BC-AD 200). On the surface, a ≥10-cm-thick ashfall layer witnesses to some explosive activity at A.D. 1440-1480, as refered to in historical accounts. El Misti has been reportedly active at the end of the 1700's and 1800's, while fumarolic activity at the crater plug resumed in 1949 and 1984-1985.

Stratigraphy and sedimentology point to alternating, large-scale plinian activity and dome growth for at least the last 40,000 years. Thus, the most severe volcanic hazards for the 900,000 people of Arequipa are as follows (Fig. 4).

(1) Low Plinian columns (<5 km) may cause ash fallout in the city, as shown by the approximate extent of the mid-1500's ashfall (Fig. 4). For higher columns (20-25 km) based on mapping of the 3cm and 5cm isopleth of the ca. 1900 yr B.P. plinian tephra-fall deposit carried towards Arequipa by prevailing NE winds, the thickness of the relevant layer could amount 50 cm in the city.
(2) The expected extent of the pyroclastic flows is towards the south, SW, and SSE, owing to the crater wall geometry (Fig. 4). The destruction of the summit dome can yield block-and-ash flows which are expected to travel 8 to 12 km downstream when valley-confined; thus, they might hit the NE suburbs of Arequipa. More mobile pumice flows are expected to travel another 4-8 km further downstream, as well as towards the populated Chiguata area. The pumice-flow tuff ca.1900 yr B.P. old was channelized in the radial valleys as far as the present suburbs of Arequipa, while subsequent small-volume lahars spread out further downvalley.
(3) Finally, flank failures can occur along fractures on the steep-sided West and SSE flanks of the volcano. Subsequent debris avalanches may choke the Chili valley and spread out on the southern piedmont.

References

Thouret J.-C., Legros F., Gourgaud A., Salas G., Juvigné E., Gilot E., Uribe M., Rodriguez A. 1995. Un exemple de prévision des risques volcaniques au Pérou méridional (région d'Arequipa), fondé sur l'étude de l'activité éruptive récente du strato-volcan El Misti. *C.R. Acad. Sci.*, t.320, sér. IIa, 923-929.

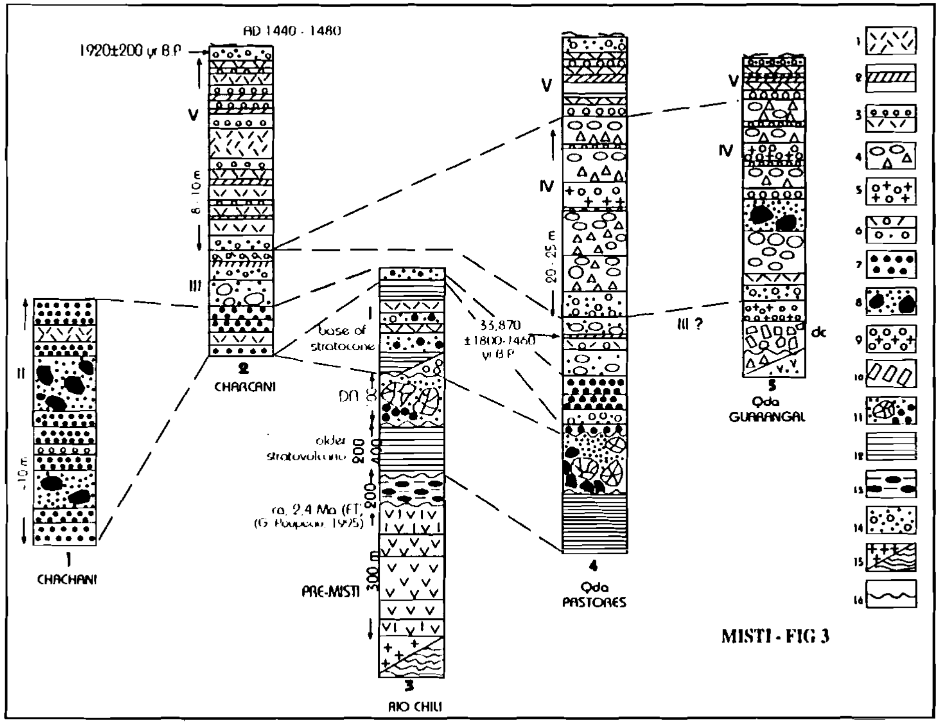


FIGURE 3. The stratigraphy of El Misti stratovolcano (measured sections in Fig. 1). Basement (15) same as Fig. 2. Pre-Misti: ignimbrites (14) and volcaniclastic sediments (13). 'Older' stratovolcano: lava flows (12) and debris-avalanche deposits (11). Lower 'modern' stratocone = Unit I, andesite or block-lava flows and old pyroclastic sequence. Summit stratocone: lava flows and young pyroclastic sequence (Units II-V). Unit II = 10: deposit of dome collapse 9:lithic-rich pyroclastic-flow deposit, 8:scoria-flow deposit, 7: scoria-fall deposit. Unit III = 6: pumice-flow and fall deposit, rhyolitic in composition. Unit IV = 5. pumice and lithic-rich pyroclastic-flow deposits, 4: block-and-ash flow deposits. Unit V = 3. Plinian pumice-flow and pumice-fall deposit, 2: poorly developed soil in ash, 1:ashfall layer AD 1540-1580. 16: stratigraphic unconformity.

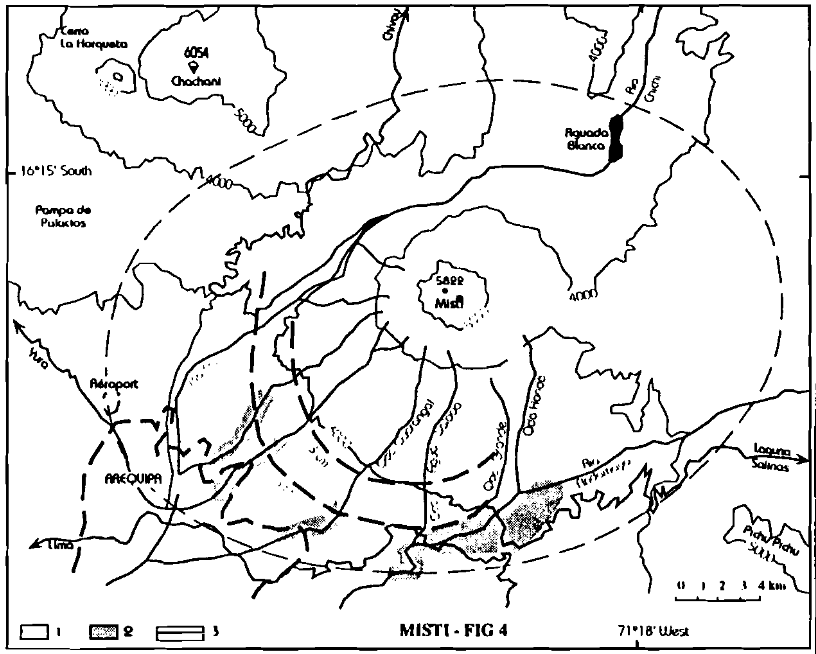


FIGURE 5. Expected extent of future pyroclastic flows and tephra-fall at Misti Circle areas (1) represent block-and-ash flows with H/L = 0.25 and an energy line of < 16° as typical values at Misti. Dashed areas (2) represent more mobile pumice flows with H/L = 0.20 and an energy line of < 13° as typical values at Misti. The elliptical shape (3) outlines the area likely to be covered by a 10-cm-thick ashfall deposit in case of a moderately explosive event alike the mid-1500's eruption. The 5-cm and 3-cm isopleths of the ca.1900 yr B.P. old Plinian eruption are also shown.

# EVIDENCE OF SUCCESSIVE IMPACTS OF THE NAZCA RIDGE UPON THE CONTINENTAL MARGIN OF CENTRAL-SOUTHERN PERU AS SUGGESTED BY SAR ERS-1 IMAGERY

Jean-Claude VICENTE, Catherine MERING , David HUAMAN & Marc CERNICCHIARO

Département de Géotectonique, Université Pierre et Marie Curie
4, Place Jussieu, T26-E1, Case 129, F-75252 PARIS Cedex 05

KEY WORDS: Central Andes, Southern Peru, Neotectonics, Radar imagery, Subducting Aseismic Ridge, Oblique indentation.

## INTRODUCTION

Since the discovery of the Nazca Ridge offshore of Central-Southern Peru by 16°S latitude (SCHWEIGGER 1947), many are the authors which have been interested on the possible tectonic effects on the overriding forearc of the shallow subduction of that major oceanic high.

RUEGG (1952) was the first to notice the existence of an abnormaly elevated sector in the Coast Range, culminating near 1800 m at Cerro Huaricangana, just facing that aseismic ridge.and to suggest a possible relation between them. While it falls to TEVES (1975) to have drawn attention on the magnitude of the coastal uplift near San Juan de Marcona as testified by the exceptionnaly high number of marine terraces developped there (BROGGI 1947; LEGAULT 1963), and on the striking deflexion of the hydro graphic system about Ica and Nazca sectors.

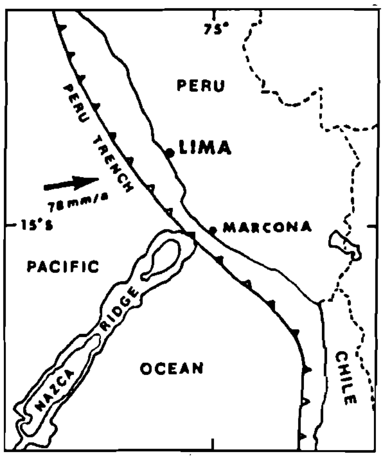

Fig. 1. Location of Marcona studied area and its geodynamic context.

Since then, detailed studies about marine terraces height variations and stratigraphy along the coast between Paracas (13.5°S) and Lomas (15.6°S) (MACHARÉ 1987; MACHARÉ & ORTLIEB 1992; HSU 1988, 1992) have revealed a striking quaternary longitudinal deformation of the coastal area. The pattern of deformation displays indeed an asymmetrical curviplanar dome-shaped curve, very similar to the bathymetric cross-section of the Nazca Ridge but with a maximum altitude of around +900 m for the highest terrace (upper Pliocene) which apex is clearly displaced southeastward above the southern flank of the ridge as a predictable consequence of oblique ridge subduction. In the present geodynamic context (Fig. 1) i.e. a plate convergence direction about N080° at a rate of 78 mm/a (DE METS *et al.* 1990) and a trench axis trending approximately N315°, the orientation of the long axis of the ridge about N040° implies that during the last million years the ridge in the course of its oblique consumption has been scanning the continental margin southeastward at the rate of about 50 km/Ma (MACHARÉ 1987). Founded on old rates of convergence and a simplified trigonometric calculus an overestimated scanning of 71 km/Ma has been set up by HSU (1992), but revised with the more recent estimates of plate motions (DE METS *et al.*1990,1994) it shows to be very nearest to the previous value.

Attemps of modelling the coastal uplift as induced by the geometry and kinematics of the subducting Nazca Ridge have been proposed (MORETTI 1982; HSU 1988, 1992), but concerned exclusively by the vertical effects. In a word, any of the proposed models have considered the possible horizontal compressive effect the system may produce. That derives from the fact that according to SÉBRIER *et al.*. 1985) the onshore geology along the Pacific coast opposite the Nazca Ridge reveals a preferential quaternary and recent extensional regime manifested by a normal faulting with metric throws. Whence the emphasis put by HSU (1992) on the lack of compressional tectonics and by MACHARÉ & ORTLIEB (1992) on the idea the ridge does note collide with the South American Margin.

## EVIDENCE OF COMPRESSIONAL NEOTECTONICS

However, consequential evidences of early Quaternary compressional deformations affecting the Pliocene marine beds between Pisco and Nazca have been reported by MACHARÉ (1987). The structures are specially obvious at the boundary between the Coast Range and the Piedmont Depression of Ica-Nazca and result in impressive flexures with kilometric throws apparently induced by reverse faulting with NE vergence.in the basement.

From that point of view, one of the most privileged site of observation of that kind of structures is decidedly the Huaricangana periphery from Río Grande to Lomas. Furthermore it focused the main MACHARÉ's observations evidencing particularly the Rio Nazca Flexure which accounts for the northwestward deflexion of the stream and the significant folding of the Pliocene. Noteworthy too is the size of the area involved by compressional deformations since it seems to extend as far north as 30 km from the front of the massif. As regards the punctual measurements of microstructures, they give variable directions of shortening from NNW-SSE to NE-SW (MACHARÉ 1987) which fit the very shape of the massif.

However, the standart mapping (CALDAS 1978) having evidenced a major NW-SE trending fault bounding the northeastern edge of the Huaricangana (Tunga Fault), the Rio Nazca Flexure is interpreted as its extension. Beyong, an eventual connexion with the western fault of Ica is also considered (MONTOYA, GARCIA & CALDAS 1993).

## RADAR IMAGERY AND NEOTECTONIC PATTERN

With the aim to specify the accurate neotectonic pattern of the area we turned to a SAR ERS-1 image. Radar imagery has proved to be particularly convenient for neotectonic studies because it enhances topographic features, specialy scarps and thalwegs, more than optical imagery and permits extensive observations at regional scale (CHOROWICZ *et al.* 1995). We used a scene centred upon Marcona, active illumination is from the ENE on descending orbits. The image covers an area 100x100 km, it was produced at 1/250 000 scale and inversed (Fig. 2). This type of presentation of the image has the advantage to display in dark the bright slope facing the radar and affected by shortening and layover effects,

Fig. 2. Reverse print of ERS-1 SAR Marcona scene.

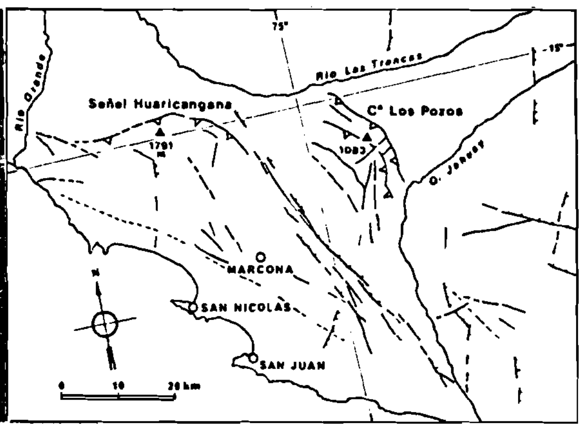


Fig. 3. Structural interpretation of the Marcona scene.

giving the impression of shadow. Slopes backing the radar are then clear and give the impression to be illuminated. They are rich in information because generally stretched. More-over, the image was pre-processed with the *Connected Center Filter* $\beta_C$ ( MERING & PARROT 1994) to reduce the speckle while preserving the connectivity of the lineaments. On the filtered image, light continuous lines are interpreted as recent faults and therefore extracted by mean of an upper thresholding of the grey tones.

Fig. 4. Extraction of the Huaricangana fault line by mean of an upper thresholding of the SAR image.

Visual analysis of the SAR scene shows immediatly the striking symmetry in the deflexion of the hydrographic system seeing that the Rio Las Trancas swerves to the NW and the Q. Jahuay to the SSE. The other outstanding stroke is the clear scarp facing northeastward girdling the C° Huaricangana from the mouth of the Rio Grande to Lomas. By its continuity and convexity we interpret this feature as product of a major reverse fault involving a global thrust of the massif to the NNW. (Fig. 3). The extraction of the fault line merely confirms the continuity and sweep of the fault and therefore the geometry suggested (Fig. 4). The third feature to mention deals with the structures revealed by the small massif of C° Los Pozos isolated at the mouth of the funnel-shaped interstream between Las Trancas and Jahuay rivers. It appears to be cut indeed by a set of faults slightly curved with convexity and scarps facing to the ENE we interpret, there again, as reverse faults.

## CONCLUSIONS

This remarkable neotectonic pattern with its rather astonishing symmetry proves indisputably the area has undergone horizontal compressional forces oriented mainly towards the NE which appears consistent with the direction of convergence and so can be considered as tectonic effects of the subducting Nazca Ridge. However, since the symmetry is not perfect (the axis of curvature of the Huaricangana Fault doesn't fall in the one of C° Los Pozos), the relation seems more complex and may imply some rotations during the time in consequence of the oblique subduction. In short, much would be to learnt from a modelisation at lithospheric scale seeing that we are confronted with a complicated case of oblique indentation by a trapezoidal-shaped wedge, apparently not yet investigated by the literature.

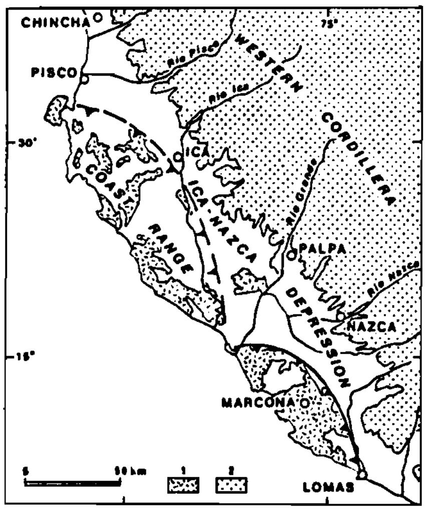


Fig. 5. Tectonic interpretation of the Coast Range of Central-Southern Peru as the result of two successive impacts of the Nazca Ridge upon the continental margin. *Pre-Cenozoic bedrocks of the Coast Range (1) and the Western Cordillera.(2)*

At last, considering the tectonic signification of the hydrographic deflexions just discussed and the striking analogy between the pattern observed at Marcona and the one shown at Ica with the Rio Pisco turned to the W and the Rio Ica to the SSE, this leads to believe the subducting Nazca Ridge has produced two major successive impacts upon the continental margin of central-southern Peru (Fig. 5). This militates for a morphology of the ridge axialy rather irregular and discontinuous for the recently subducted part e.i.. fairly comparable with the one developped offward (MAMMERICKX & SMITH 1978). This irregular morphology could explain the apparent contradiction between the compressive neotectonics preserved onshore and the actual offshore evidences for a very minor compressional deformation in the lower forearc (HAGEN & MOBERLY 1994). In short, the "big bone" should have passed. This recalls, at a greater, scale the general model of subduction of a seamount proposed by VON HUENE & LALLEMAND (1990). So, the dynamic morphotectonic reply of the forearc to subduction of asperities should be quicker than usually accepted.

Finally, one should not be surprised by such an inland extent of horizontal convergent structures, Costa Rica neotec-tonics in consequence of the Cocos Ridge subduction provides an other example but in a normal convergent context (KOLARSKY *et al.* 1995).

REFERENCES

BROGGI J.A. 1946. Las terrazas marinas de la bahia de San Juan de Ica. Bol. Soc. Geol. Perú, 19, 21-33.

CALDAS J. 1978. Geología de los Cuadrángulos de San Juan, Acarí y Yauca. *Bol. Inst. Geol. Miner. Perú*, 30. 78 pp.

CHOROWICZ J., CHALAH C., CHOTIN P., MERING C., RUDANT J.-P., VICENTE J-C., ARKIN Y., ICHOKU C. & KARNIELI A. 1995. A new approach to map active faults related to seismic hazards: Examples of the Atacama (Chile) and Dead Sea (Middle East) Fault Zones. *Proc. II ERS Appl. Worksp. Lond.*, 6 pp.

DE METS C., GORDON R.G., ARGUS D.F. & STEIN S. 1990. Current plate motions. *Geophys. J. Int.* 101, 425-478.

DE METS C., GORDON R.G., ARGUS D.F. & STEIN S. 1994. Effect of recent revisions to the geomagnetic reversal time scale on estimates of current plate motions. *Geophys. Res. Let.* 21, 2191-2194.

HAGEN R.A. & MOBERLY R. 1994. Tectonic Effects of a Subducting Aseismic Ridge: The Subduction of the Nazca Ridge at the Peru Trench. *Marine Geophys. Res.*, 16. 145-161.

HSU J.T. 1988. Emerged Quaternary marine terraces of southern Peru: Sea level changes and continental margin tectonics over the subducting Nazca ridge. *Ph.D. Thesis Cornell Univ.*, 310 pp.

HSU J.T. 1992. Quaternary uplift of the peruvian coast related to the subduction of the Nazca ridge: 13.5 to 15.6 degrees south latitude. *Quatern. Int.*, 15/16. 87-97.

KOLARSKY R.A., MANN P. & MONTERO W. 1995. Island arc reponse to shallow subduction of the Cocos Ridge, Costa Rica. In: MANN P. ed., Geologic and tectonic development of the Caribbean Plate Boundary in Southern Central America. *Geol. Soc. Amer.*, Spec..Pap. 295, 235-262.

LEGAULT R. 1960. Preliminary study of marine terraces in the Marcona-San Juan area of Southern Peru. *Unpubl. Spec. Pap. Univ. Michigan.* 23 pp.

MACHARÉ J. 1987. La marge continentale du Pérou: Régimes tectoniques et sédimentaires cénozoiques de l'avant-arc des Andes centrales. *Thesis Univ. Paris XI*, 391 pp.

MACHARÉ J. & ORTLIEB L. 1992. Plio-quaternary vertical motions and the subduction of the Nazca Ridge, central coast of Peru. *Tectonophysics*, 205. 97-108.

MAMMERICKX J. & SMITH S.M. 1978. Bathymetry of the southeast Pacific. *Geol. Soc. Amer.*, Map and Chart Ser. MC-26.

MERING C. & PARROT J.F. 1994. Radar image analysis using morphological filters. In: SERRA J. & SOILLE P. eds., Mathematical Morphology and its Application to Signal Processing. *Kluwer Acad. Publ.* 353-360.

MONTOYA M., GARCIA W. & CALDAS J. 1994. Geología de los Cuadrangulos de Lomitas, Palpa, Nasca y Puquio. *Bol. Inst. Geol. Miner. Perú*, 53. 100 pp.

RUEGG W. 1962. Rasgos morfológicos-geológicos intramarinos y sus contrapartes en el suelo continental peruano. *Bol. Soc. Geol. Perú*, 38. 97-142.

SÉBRIER M., MERCIER J.L., MÉGARD F., LAUBACHER G. & CAREY-GAILHARDIS E. 1985. Quaternary normal and reverse faulting and the state of stress in the central Andes of South Peru. *Tectonics*. 4. 739-780.

TEVES N. 1975. Aspectos sedimentarios y estructurales del sector costanero Peruano frente a la Dorsal de Nazca. *Bol. Soc. Geol. Perú*, 50. 87-98.

VON HUENE R. & LALLEMAND S. 1990. Tectonic erosion along the Japan and Peru convergent margins. *Geol. Soc. Amer. Bull.* 102, 704-720.

# TECTONIQUE / BASSINS SEDIMENTAIRES
# TECTONICS / SEDIMENTARY BASINS
# TECTONICA / CUENCAS SEDIMENTARIAS

# STRATIGRAPHY, SEDIMENTOLOGY AND TECTONIC EVOLUTION OF THE RIO CAÑETE BASIN : CENTRAL COASTAL RANGES OF PERU

**Antenor M. Aleman**
**Amoco Production Co**
**Houston, Texas 77293**

KEY WORDS: Lima stratigraphy, frontal arc, arc extension, Central Coastal Ranges evolution.

## ABSTRACT

The Rio Cañete Basin in the Central Coastal Ranges of Peru (C.C.R.P.) represents a fault-bounded frontal-arc Late Jurasic (Tithonian) to Albian sequence formed by aborted intra-arc spreading process during the early evolution of the Andes (Fig.1). The sequence, exposed in the Lima area, consists of more than 6000 meters of volcaniclastic sedimentary rocks, lava flows, lime mudstones, shales, quartz rich sandstones and subordinated fossiliferous limestones and evaporites. The stratigraphy records several episodes of volcanism and extension along and across the basin and provides new insight in the evolution and crustal growth of the Central Andes.

## INTRODUCTION

Four widespread groups and one areally restricted formation mark important stages in the stratigraphic, sedimentologic and tectonic evolution of the Rio Cañete Basin. The Puente Piedra Group consists of volcaniclastic debris, basaltic to andesitic lava flows, shales and subordinate limestones that document the presence of a Jurassic volcanic arc (Fig.2). The overlying quartz rich sandstones and shales of the Morro Solar Group (fig.3) records an abrupt change in sedimentation and tectonic style. Ensialic extension accompanied by subsidence of the volcanic arc and concomitant uplift of the Paleozoic to Precambrian "Coastal Cordillera" (Paracas Block) explains the change of source and provenance. The areally restricted Pucusana Formation (Fig.4), made up of alkaline lavas, volcanic breccias and lapillistones, is interpreted to represent a localized volcanic center perhaps related to subduction of oceanic fractures. Above the Morro Solar is the Lima Group (fig.5) consisting mainly of lime mudstone, shale, gypsum and bioclastic limestone that represent the maximum pulse of the Neocomian transgression. Spatial and temporal volcanism took place along and across the basin coeval with this shale-limestone sequence, reflecting early pulses of volcanic activity related to the emplacement of the Coastal Batholith of Peru. The widespread nature of the volcanic activity is recorded in the overlying Chillon Group (Casma Group) which represents volcanism (Fig.6) coeval with the early emplacement of Albian gabbros and diorites of the Coastal Batholith. Extension was coeval with volcanism as documented by the presence of quartz rich sandstones in this group.

## BASIN EVOLUTION

The Rio Cañete Basin was formed at least as early as the Late Jurassic with the deposition of the arc-derived Puente Piedra Group. Ensialic extension concurrent with arc volcanism played a paramount role in the evolution of the Andes at least since Late Triassic when an arc trench setting was established (James, 1971; Cobbing, 1978; Atherton et al, 1983, 1985). Narrow, elongated, fault-bounded basins were perhaps formed in response to embryonic ensialic back arc spreading in similar way to the mechanism described by Levi and Aguirre (1981) and Veragara et al (1995) in central Chile and Petford and Atherton (1995) in central Peru. Integration of stratigraphic and sedimentologic information in the Rio Cañete Basin have allowed the recognition of several stages during its evolution.

**STAGE I.-** The early stage in the evolution of the Rio Cañete Basin was initiated with the formation of the Jurassic volcanic arc and deposition of the Puente Piedra Group derived largely from arc activity. Deposition took place in a narrow elongate basin, as documented by Cobbing (1978), formed by extensional processes related to embryonic back-arc spreading. Both effusive and explosive volcanism alternated throughout deposition of this group with several periods of volcanic quiescence as it is recorded in several shale sequences (Fig.2). These shale/volcaniclastic sequences are interpreted to represent relative small transgressive-regressive cycles within an overall global sea level rise.

**STAGE II.-** During the Late Berriasian, a new period of ensialic extension (Atherton, 1983, 1985) took place along the Western Peruvian Trough as documented by the abrupt change in source terrane from an arc derived to a continental block suite. This new episode of extension was probably related to changes in the rate of plate motion in the south American plate and changes in the angle of subduction as it is documented by cessation in volcanism. Extension was probably episodic and contemporaneous with sedimentation and perhaps accounts for the uplift of Paleozoic or Precambrian rocks. Partial subsidence of the Jurassic arc and its roots was concomitant with deposition of quartz rich sandstones of the Salto del Fraile Group. The positive nature of these older rocks is documented in the west and northwest by the continuation offshore of the Coastal Cordillera which makes up he Paracas Block (Myers, 1975), also known as the Outer Shelf High.

**STAGE III .-** In this stage, the uplifted Paleozoic or Precambrian terranes were submerged during a global rise of sea level. This was accompanied by a change in deposition from a quartz-rich sandstone facies to a limestone-shale facies with significant to moderate volcanic contributions along and across the basin (Lima Group). Some of the submerged Paleozoic highs may have played a very important role in restricting the circulation and communication of the basin with the open ocean, therefore, increasing the likelihood of evaporite precipitation within the basin. Deposition of a shale-limestone sequence alternating with perverse arc volcanism varied in space and time along and across the basin and may have been associated to third order global sea level changes and early phases of cauldron subsidence and gabro intrusions of the Coastal Batholith. Furthermore, variation in volcanic activity in these formations along the basin might also be related to segmentation of the Coastal Batholith which accounts for temporal and spatial variations in plutonic activity in time and space (Cobbing et al, 1977). Subduction of deep crustal fractures, in the same way as envisioned by De Long et al (1975), might account for the localized and odd nature of the volcaniclastic, alkaline lava flows of the Pucusana Formation.

**STAGE IV.-** Embryonic back-arc extension persisted throughout the Middle Albian with deposition of the volcanic derived Chillon Group. This group represents the maximum paroxysm of volcanic activity associated with the early emplacement of the Coastal Batholith (Cobbing, 1978). Renewed pulses of extension, contemporaneous with the Chillon Group, might have exposed the sandstones of the Morro Solar Group as it is documented in some of the quartz-rich beds found in the lower part of the Chillon Group in the Perico Hill. Widespread subaqueous volcanic activity in the Chillon Group is correlated with the gabbro to gabbrodiorite plutonic intrusions (Patap Super-unit) and cauldron subsidence of the Coastal Batholith of Peru (Pitcher and Cobbing, 1985).

**STAGE V.-** Extension was interrupted at the end of the Middle Albian by a short-lived compressional event related to the initial stages of the Andean Orogeny (Mochica Phase). North of Lima, in the Huarmey Basin, where this phase is relatively well expressed, the Casma Group (equivalent to the Chillon Group) has been folded following a NW-SE trend subparallel to parallel to the Coastal Batholith (Webb, 1976; Child, 1976). The folds are open, upright and parallel, rarely showing a slight SW vergence (Guevara, 1980). This orogenic phase is expressed with variable intensity in the Western Peruvian Trough and may be linked to different rates of subduction along the arc-trench system.

**STAGE VI.-** Soon after the Mochica Phase of the Andean Orogeny, the frontal-arc basin rocks were uplifted due to pervasive underplating along the roots of a long-lived arc. Indeed, deep seated plutonic rocks of the Coastal Batholith were emplaced along the Rio Cañete Basin and provided the roots for isostatic uplift.

| Sy | St. | Grp | Formation | Paleontological Zones |
|---|---|---|---|---|
| Cretaceous | Al. | Chillon | Temblor | Venezoliceras sp. |
| Cretaceous | Ap. | Chillon | S. Augustin | Parahoplites nicholsoni (?) |
| Cretaceous | Bar | Chillon | Cañas | Toucasia carinata |
| Cretaceous | Bar | Lima | Atocongo | Astieridiscus cf. morleti |
| Cretaceous | Ha. | Lima | Pamplona | Acanthodiscus radiatus |
| Cretaceous | Valangin. | Lima | Lurin / Pucusana | Olcostephanus cf. asterianus |
| Cretaceous | Valangin. | Morro Solar | Marcavilca | Raimondiceras raimondii |
| Cretaceous | Berria. | Morro Solar | Herradura | Raimondiceras raimondii |
| Cretaceous | Berria. | Morro Solar | S. del Fraile | |
| Cretaceous | Berria. | Puente Piedra | Ventanilla | |
| Jur. | Titho | Puente Piedra | Puente Inga | Substeueroceras steuri |
| Jur. | Titho | Puente Piedra | Tambo Inga | |

Fig.1

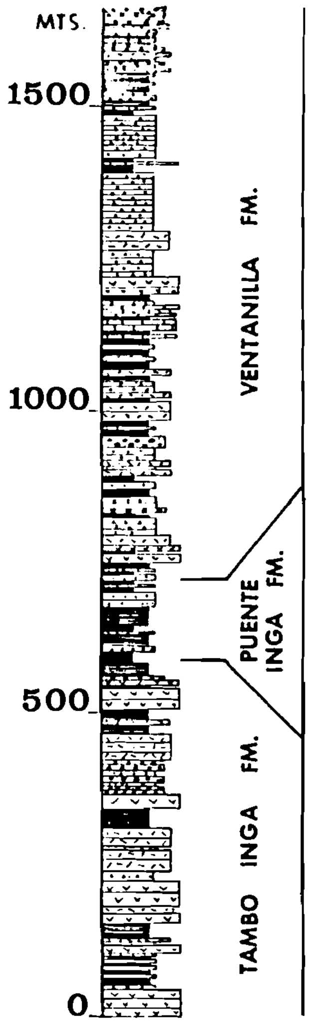

Fig.2

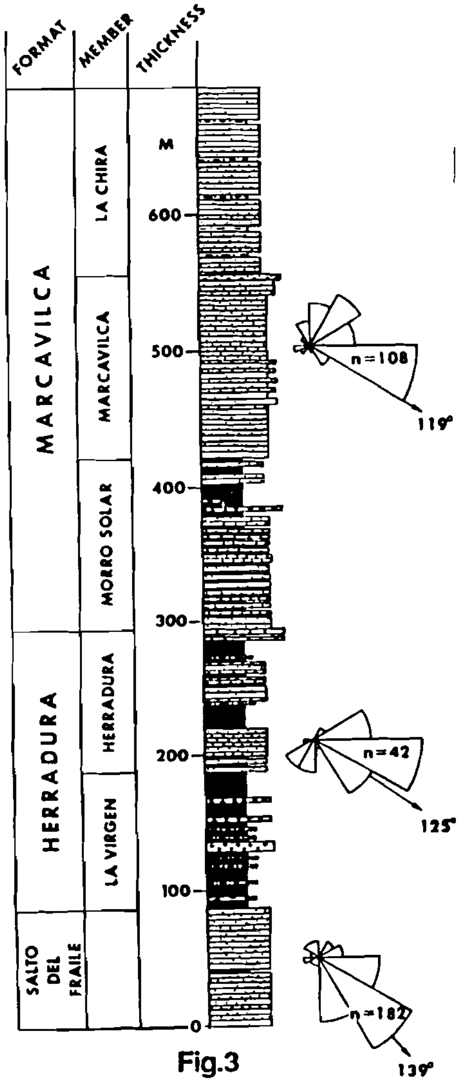

Fig.3

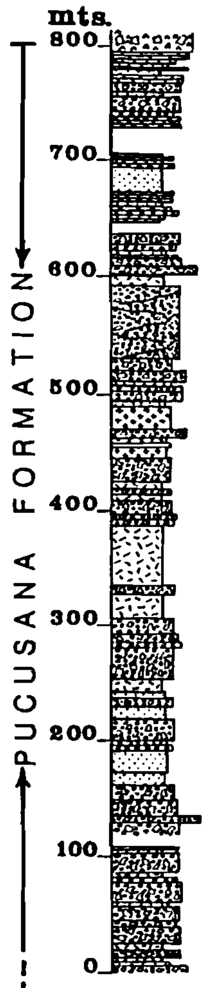

Fig.4

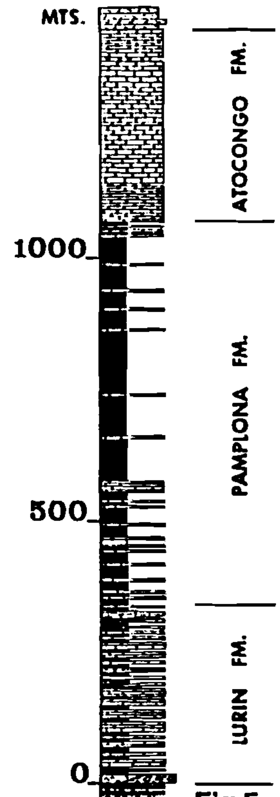

Fig.5

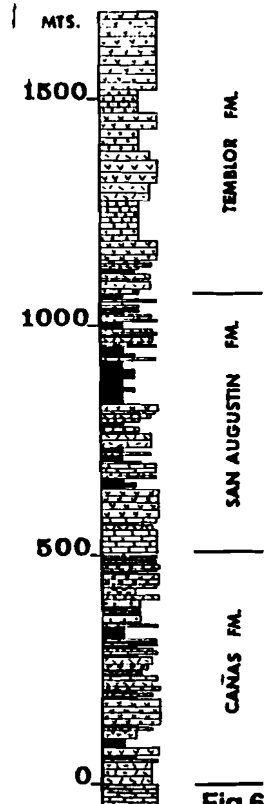

Fig.6

Third ISAG, St Malo (France), 17-19/9/1996

## REFERENCES

Alleman Vera, 1985, Virgotrigonia : Genero nuevo de Trigoniidae Lamarck, 1819 (Mollusca : vivalvia) : Soc. Geol. del Peru , no. 75, p. 1-11.

Atherton, M. P., Pitcher, W. S., and Warden, V.,1983, The Mesozoic marginal basin of central Peru: Nature, 305, p. 303-306.

Bosc, E., 1963, Geología de la región comprendida entre la Quebrada de Parca (Chilca) y el Valle de Mala: Umpub. Thes. Univ. Nac. Mayor de San Marcos, Lima, Peru, 84 pp.

Child, R., 1976, The Coastal Batholith and its envelope in the Casma region of Ancash, Peru : Umpubl. Ph. D. Thesis, Univ. of Liverpool.

Cobbing, E. J., 1985, The tectonic setting of the Peruvian Andes: in Pitcher, W. S., Atherton, M. P., Cobbing, E. J., and Beckinsale, R. D., (eds.): "Magamtism at a Plate Edge", p. 3-18, John Wiley and Sons.

De Long, S. E., Hodges, F. N., and Arculus, R. J., 1975, Ultramafic and mafic inclusions, Kanaga Island, Alaska and the ocurrence of alkaline rocks in island arc: Jour. Geol., v. 83, p. 721-782.

Fernandez, J., 1966, Geología de la Region Marquez y Ventanillas (Lima): Univ. Nac. Mayor de San Marcos, Bach. Thesis.

Fernandez-Concha J., 1958, Geología del Morro Solar, Lima: Soc. Geol. del Peru, no. 33, p.3-50.

Guevara, C., 1980, El Grupo Casma del Peru Central entre Trujillo y Mala: Soc. Geol. del Perú, no. 67, p. 73-83.

Levi, B., and Aguirre, L.,1981, Ensialic spreading-subsidence in the Mesozoic and Paleocene Andes of central Chile: Jour. Geol. Soc. London, v.138, p.75-81.

____, 1907, Geología de Lima y sus alrededores, Imprenta Gil, Lima.

Myers, J. S., 1974, Cretaceous stratigraphy and structure, Western Andes of Peru between latitudes 10° - 10 30 °: Bull. Amer. Ass. Pet. Geol.,v. 58, pp. 474-487.

Pitcher, W. S. , and Cobbing, E. J., 1985, Phanerozoic plutonism in the Peruvian Andes: in Pitcher, W. S., Atherton, M. P., Cobbing, E. J., and Beckinsale, R. D. (eds.), "Magmatism at a Plate Edge", p. 19-25.

Rivera, R.,1951, La fauna de los Estratos Puente Inga : Soc. Geol. del Peru, v.22, p. 5-53.

____, G. Petersen, and M. Rivera, 1975, Estratigrafía de la Costa de Lima: Soc. Geol. del Perú, no. 65, p.159-186.

Rosenzweig, A. , 1953, Geología de la Isla San Lorenzo: Bol. Inst. Nac. Invest. y Fomento Minero, no. 7, 30 pp.

Scott, R. and A. Alemán, 1984, A Lower Cretaceous Biostrome, Peru, Jour. of Paleontology, v., p. 1136-1142.

Vergara, M., Levi, B., Nystrom, I.O., and Cancino, A.; 1995; Jurassic and early Cretaceous island arc volcanism ,extension and subsidence in the Coast range of central Chile: Geol. Soc. Ame.,v.107,p. 1427-1440.

Webb, S. E. , 1976, The volcanic envelope of the Coastal Batholith in Lima and Ancash, Peru : Umpubl. Ph. D. Thesis, Univ. of Liverpool.

# THE ANDEAN STRUCTURE OF THE CORDILLERA ORIENTAL FROM REPROCESSED YPF SEISMIC REFLECTION DATA

Richard W. ALLMENDINGER[(1)] and Tomás R. ZAPATA[(1, 2)]

(1) Department of Geological Sciences and Institute for the Study of the Continents, Snee Hall, Cornell University, Ithaca, New York 14853-1504, USA
(2) now at: YPF S.A.

**KEY WORDS:** Cordillera Oriental, Subandean belt, decollement

## INTRODUCTION

The processes by which topography is developed and maintained in active mountain belts have captivated geoscientists for the last decade or more. The greatest uplift on Earth, the Tibetan-Himalayan system seems intuitively straight forward in the context of a continent-continent collision, even though the details of the lithospheric architecture and mechanics remain controversial. More enigmatic is the Altiplano-Puna of the central Andes. This second highest continental plateau — more than half a million square kilometers at an average elevation of almost 4 km — has developed in the absence of significant continental collision or terrane accretion. Nearly all workers in the Central Andes agree that crustal thickening by structural shortening is responsible for the topographic uplift, with lesser contributions from magmatic addition and lithospheric thinning (e.g. Isacks 1988). Although shortening is deemed important, virtually nothing is known of the geometry of major faults or the distribution of shortening at depth.

The location and geometry of the Subandean decollement beneath the Cordillera Oriental is a first order problem with substantial importance for estimates of Late Cenozoic shortening and its relation to topographic uplift of the Central Andes. Seismic reflection data have the potential to image that decollement beneath the Cordillera Oriental, but general lack of known economic targets and the rugged terrain have discouraged exploration. The seismic reflection surveys carried out during the mid-1980's by Yacimientos Petrolíferos Fiscales (now, YPF S.A.) just south of the international border in the vicinity La Quiaca, Argentina constitute virtually the only seismic reflection data collected in the entire Cordillera Oriental of the Central Andes. We have reprocessed four crossing lines from that YPF S.A. data set, using the technique of VIBROSEIS extended correlation, to obtain data lengths of 15 s (about 45 km). Our reprocessing shows a remarkable suite of deep reflections which we interpret to be a ramp in the Subandean belt decollement and possible duplexing of the lower crust farther west.

## GEOLOGIC SETTING AND PREVIOUS WORK

The region of study lies within the southern part of the Cordillera Oriental, west of the Subandean fold and thrust belt. These two tectonic provinces are separated from each other by two major fault zones, the Cabalgamiento Frontal Principal (CFP) and the Cabalgamiento Andino Principal (CANP). To the east of the CFP, the decollement of the Subandean fold and thrust belt is within Silurian rocks and, at the surface, isolated ridges of Paleozoic units are surrounded by extensive outcrops of Tertiary strata (Baby et al. 1992, Dunn et al. 1995, Kley 1993, Mingramm et al. 1979). Although interpretations of internal fold and thrust geometry within the Subandean belt vary widely, the depth to the decollement is similar in most interpretations: it lies between 13 and 15 km below the surface outcrop of the CFP (about 12-14 km below sea level). Shortening within the Subandean belt increases progressively northward from less than 60 km in northern Argentina at 22°30'S latitude (Allmendinger et al. 1983, Mingramm et al. 1979) to 100 or more km in southern Bolivia at 21°S (Baby et al. 1992, Dunn et al. 1995, Kley 1993, Kley & Reinhardt 1994). The Subandean belt dies out between 23° and 24°S, due to southward erosion of the Paleozoic stratigraphic wedge beneath the Upper Cretaceous Salta basin, cutting out the decollement horizon (Allmendinger & Gubbels 1996, Allmendinger et al. 1983, Mingramm et al. 1979). This important lateral change occurs 1-2 degrees of latitude farther south than the seismic lines described here.

West of the CANP, extensive outcrops of Ordovician strata, covered by minor Cretaceous and Tertiary units, characterize the Cordillera Oriental. One of the highest amplitude folds in the Cordillera Oriental is the Camargo syncline, a structure that can be traced for nearly 200 km along strike and is imaged on the seismic lines shown here. The seismic data which we have reprocessed was first interpreted by Bianucci et al. (1987), who described the well-displayed shallow thrust structures, including the Yavi thrust which bounds the west side of the Camargo syncline.

The San Juan de Oro surface truncates virtually all of the major structures in this part of the Cordillera Oriental. Deposits above the surface are flat-lying or gently dipping and have been dated at about 10 to less than 2 Ma (Cladouhos et al. 1994, Gubbels et al. 1993). The youngest deformed rocks, which may be either syn- or pre-deformation in age, are 13 to 18 Ma (Cladouhos et al. 1994, Gubbels et al. 1993). The surface deposits are cut locally by young strike-slip and normal faults which have, in general, displacements of less than 10 m (Cladouhos et al. 1994). The timing of deformation in the Subandean belt is much less certain, owing to the primitive state of knowledge of the upper Cenozoic strata over much of the area. Gubbels et al. (1993) proposed that the deformation was younger than about 10 Ma based on the perceived age of the Yecua Formation. However, Reynolds et al. (1994) have recently shown that the Anta formation of northwest Argentina (25–26°S), which is considered to be the lateral equivalent of the Yecua, is about 14 Ma. They suggest that uplift in the Puna began by 15 Ma and in the Cordillera Oriental by about 13 Ma.

## THE SEISMIC REFLECTION DATA

We have reprocessed four seismic reflection lines located just east and southeast of La Quiaca, Argentina, which were acquired during the middle 1980's by YPF S. A. as a part of the exploratory work carried out in the Puna. We have extended these data to 15 seconds using a "self-truncating" extended correlation (Okaya & Jarchow 1989). The reprocessed lines form an intersecting network, providing excellent 3-D control and confirming that the major features described below are in the plane of section and not side-swipe. Preliminary constant velocity migrations have been carried out to get first order control on the location and dip of the major dipping features on the lines. The datum for the reprocessed lines is 4 km above sea level, all depths are given with respect to sea level, and all times sited below are two-way travel times.

## INTERPRETATION

Because of the east-northeast strike of surface structures, the NW-SE trending Line 4219 provides an approximate true dip section. However, all features described below can be tied with crossing lines.

The main features visible on the original correlated 5 s data and described by Bianucci et al. (1987) can also been seen on our reprocessed lines, although our processing was optimized for deeper parts of the section. The Camargo syncline is clearly visible on all of the lines beneath the Miocene unconformity. The high amplitude reflectors at the base of the syncline were interpreted by Bianucci et al.

(1987) to be from the Cretaceous Salta Group; where they flatten out on the west limb a about 2.5 s, they are about 0 to 2 km below sea level. The syncline is bounded on its western side by the Yavi thrust, which is somewhat listric and dips about 25-30°. Like the syncline, the thrust is exposed in southern Bolivia north of the continuous part of the San Juan de Oro surface. To the east of the Camargo syncline, subtle thrust structures can be discerned on large scale copies of the lines.

One of the most striking features of all the seismic lines is a band of strong mid-crustal reflections which occur between 4.5 and, locally, 6 s (about –9 to –13 km; all depths are given with respect to sea level and the datum of the reprocessed lines is +4 km). The top of this band was imaged on the original fully correlated data but it's true extent only became apparent upon extended correlation. The internal structure of the band of events is quite complicated and is distorted by velocity pull-down beneath the Camargo syncline. At least locally, thrust imbrications appear to splay from the band, suggesting that it may be a shallow zone of decollement. However, the band would appear to be 5 to 10 km too shallow for the Subandean belt decollement and does not clearly correlate with any mapped feature farther east; it is, conceivably, related to the down-dip projection of the CANP. Alternatively, it may be related to the shallow zone of high conductivity described by Schwarz (1994), or both.

At about 7-8 s (–16-20 km) on the east end of line 4219, a band of reflections dips steeply west at about 35° (migrated). Cross line control shows that this event dips to the northwest and strikes parallel to Andean folds and faults. Beneath this dipping reflection, scattered horizontal reflections are present to about 12 s (–32 km). Reflections to the west above the dipping event have geometries similar to hanging wall anticlines and appear to be truncated against the event. This dipping event underlies the east limb of the Camargo syncline and correlates closely with the westward projection of the Subandean decollement. In fact, Mingramm's (1979) section showed the beginning of the footwall ramp in the decollement almost exactly where the dipping reflector is located. The crossing lines suggest more complicated structure to the west of the Camargo syncline, with reflections to 15 s (–41 km), displaying a series of truncations and horizontal and dipping segments which we tentatively interpret as ramps and flats and multiple decollement levels. It is unlikely that any of these lines have sufficient penetration to image Moho, which is reported to lie at about 50-55 km on the Berlin refraction data to the north Wigger (1994).

## DISCUSSION

We tentatively propose that the Camargo syncline coincides with the position of the footwall ramp in the Subandean decollement. If correct, this interpretation allows us to determine a minimum displacement of 50-60 km on the Cabagalmiento Andino Principal and the Subandean belt farther east at this latitude; shortening farther west within the Eastern Cordillera has not been determined. The ramp apparently extends to near the base of the crust and, thus, would also mark the western limit of under-thrusting of undeformed craton beneath the orogen. It is possible that the location of the ramp was controlled by Late Precambrian and/or early Paleozoic tectonic features. Shortening should increase farther north as suggested by previous authors and as can be observed by the northward divergence of the Camargo syncline and the major thrusts in southern Bolivia. Indeed, in southern Bolivia at 21°S, Dunn et al. (1995) interpret about 100 km of shortening in the Subandean belt and the distance between the CFP and the Camargo syncline is 105 km.

Although the ramp appears to correlate spatially with the Camargo syncline, the kinematic and temporal relations between the syncline and thrusting on the ramp remain enigmatic. If most of the shortening in the Subandean belt is younger than 10 Ma, then the location of the syncline above the ramp must be totally coincidental because folding of the syncline was completely finished by 9 Ma. Alternatively, if substantial shortening in the Subandean belt is older than suspected (e.g. younger than 14 Ma) then there may be a kinematic relationship between the Camargo "hanging wall" syncline and the footwall ramp of the Subandean belt decollement. Finally, it may be that the CFP, the ramp and the syncline are kinematically and temporally related but that subsequent shortening in the Subandean belt was accommodated along a deeper decollement. However, there is no evidence of such a ramp on the existing seismic.

The steepness of the ramp is striking. This area is located reasonably close to the southern limit of flexural compensation and it is possible that the steepness is related to that transition. If so, we might expect that the ramp dips at a considerably shallower angle to the north. The northward termination of the Camargo syncline is consistent with this hypothesis. A northward shallowing of the dip of the ramp would be clearly consistent with the observation that deeper structural and stratigraphic levels are exposed in the Argentine Cordillera Oriental than along strike to the north in Bolivia.

We have proposed a regional deep seismic reflection line to test these hypotheses.

## REFERENCES


Allmendinger, R. W. & Gubbels, T. 1996. Pure and simple shear plateau uplift, Altiplano-Puna, Argentina and Bolivia. *Tectonophysics* in press.

Allmendinger, R. W., Ramos, V. A., Jordan, T. E., Palma, M. & Isacks, B. L. 1983. Paleogeography and Andean structural geometry, northwest Argentina. *Tectonics* **2**, 1-16.

Baby, P., Herail, G., Salinas, R. & Sempere, T. 1992. Geometry and kinematic evolution of passive roof duplexes deduced from cross section balancing: Example from the foreland thrust system of the southern Bolivian Subandean Zone. *Tectonics* **11**, 523-536.

Bianucci, H. A., Fernández Garrasino, C. A. & Sánchez, E. G. 1987. Corrimientos de bajo angulo entre La Quiaca y Abra Pampa (Provincia de Jujuy, Argentina). *X Congreso Geológico Argentino* **1**, 165-168.

Cladouhos, T. T., Allmendinger, R. W., Coira, B. & Farrar, E. 1994. Late Cenozoic deformation in the Central Andes: Fault kinematics from the northern Puna, northwest Argentina and southwest Bolivia. *Journal of South American Earth Sciences* **7**, 209-228.

Dunn, J. F., Hartshorn, K. G. & Hartshorn, P. W. 1995. Structural styles and hydrocarbon potential of the Sub-Andean thrust belt of southern Bolivia. In: *Petroleum basins of South America* (edited by Tankard, A. J., Suárez S., R. & Welsink, H. J.). *Memoir* **62**. American Association of Petroleum Geologists, Tulsa, Oklahoma, 523-543.

Gubbels, T., Isacks, B. & Farrar, E. 1993. High-level surfaces, plateau uplift, and foreland development, Bolivian central Andes. *Geology* **21**, 695-698.

Isacks, B. L. 1988. Uplift of the central Andean plateau and bending of the Bolivian orocline. *Journal of Geophysical Research* **93**, 3211-3231.

Kley, J. 1993. Der übergang vom Subandin zur Ostkordillere in Südbolivien (21°15 - 22° S): Geologische, struktur und kinematik [Ph.D. dissertation], Freie Universität, Berlin.

Mingramm, A., Russo, A., Pozzo, A. & Casau, L. 1979. Sierras subandinas. In: *Segundo simposio de geología regional argentina*. Academía Nacional de Ciencias, Córdoba, 95-138.

Okaya, D. A. & Jarchow, C. M. 1989. Extraction of deep crustal reflections from shallow Vibroseis data using extended correlation. *Geophysics* **54**, 555-562.

Reynolds, J. H., Idleman, B. D., Hernández, R. M. & W., N. C. 1994. Preliminary chronostratigraphic constraints on Neogene tectonic activity in the Eastern Cordillera and Santa Bárbara System, Salta Province, NW Argentina. *Geological Society of America Abstracts with Programs*.

Schwarz, G., Chong D., G., Krüger, D., Martinez, E., Massow, W., Rath, V. & Viramonte, J. 1994. Crustal high conductivity zones in the southern Central Andes. In: *Tectonics of the southern central Andes: Structure and evolution of an active continental margin* (edited by Reutter, K.-J., Scheuber, E. & Wigger, P. J.). Springer-Verlag, Berlin, 49-67.

Wigger, P., Schmitz, M., Araneda, M., Asch, G., Baldzuhn, S., Giese, P., Heinsohn, W.-D., Martínez, E., Ricaldi, E., Röwer, P. & Viramonte, J. 1994. Variation in the crustal structure of the southern Central Andes deduced from seismic refraction investigations. In: *Tectonics of the southern central Andes: Structure and evolution of an active continental margin* (edited by Reutter, K.-J., Scheuber, E. & Wigger, P. J.). Springer-Verlag, Berlin, 23-48.

# SEQUENCE STRATIGRAPHY OF THE MESOZOIC DOMEYKO BASIN, NORTHERN CHILE

John ARDILL(1), Stephen FLINT(2), Ian STANISTREET(2) and Guillermo CHONG(3)

(1) Esso Exploration & Production UK Ltd, Leatherhead, Surrey, KT22 8UY, U.K.
(2) STRAT Group, University of Liverpool, Liverpool, L69 3BX, U.K.
(3) Departamento de Geociencias, Universidad del Norte, Antofagasta, Chile

**KEY WORDS** sequence stratigraphy, Jurassic sea-level, Gondwana break-up

## INTRODUCTION

The Domeyko basin in northern Chile (Fig. 1) originated as one of a series of Upper Permian to Triassic transtensional rift basins along the western margin of Gondwana. Initial syn-rift continental clastics are overlain by Norian (Upper Triassic) marine limestones in the area of the Precordillera between 23°30'-26°30'S (Fig. 1). Subsequent Jurassic-Early Cretaceous post-rift thermal subsidence is recorded by a 2000 m thick mixed carbonate and siliciclastic marine succession. The depositional system is interpreted as a mixed carbonate and siliciclastic ramp environment, characterised by the deposition of siliciclastic-dominated successions at times of low accommodation space (lowstand and late highstand systems tracts) and carbonate-dominated successions during periods of high accommodation space (transgressive and early highstand systems tracts). The end of the Jurassic is marked by a regional marine regression and followed by continental red-bed deposition of Early Cretaceous age.

## SEQUENCE STRATIGRAPHY

Sequence stratigraphic analysis has identified five Exxon-type unconformity bounded sequences which provide a time framework for the understanding of chronostratigraphic development of the Domeyko basin (Fig. 2). Relative sea-level fall in the upper Lower Sinemurian, earliest Pliensbachian, earliest Aalenian, Lower Callovian, earliest Valanginian, and rises in the earliest Hettangian, earliest and Late Toarcian, Lower and Late Bajocian, Late Bathonian and earliest Oxfordian of the Domeyko basin appear time-equivalent to similar events in other southern and northern hemisphere basins and thus are interpreted to be products of eustatically driven, global sea-level cycles (Fig. 3). Relative sea-level falls in the earliest Bathonian, latest Oxfordian, earliest Valanginian and rises in the Late Kimmeridgian are interpreted to be tectonically-driven, continental-scale changes in accommodation space (Fig. 3). Although the earliest Valanginian relative sea-level fall has been documented in northern hemisphere basins, the sequence boundary is interpreted to be tectonically-enhanced through regional uplift in Chile and Argentina.

## AN EXAMPLE OF A TECTONICALLY-DRIVEN SEQUENCE BOUNDARY & LOWSTAND SYSTEMS TRACT

The latest Oxfordian (Late Jurassic) of the Domeyko basin is characterised by a 10-200 m thick, sharp-based succession of basinal evaporite facies interpreted as lowstand deposits, directly overlying offshore marine siltstone facies of the previous highstand (Fig. 2). The evaporite facies record an abrupt shallowing and basinward shift in facies seen throughout much of the basin, indicating sequence boundary formation. This interpretation is supported by the biostratigraphic data which shows the evaporites to have a synchronous duration of five ammonite Zones, Bimammatum-Acanthicum (Gygi & Hillebrandt 1991), lasting approximately 7.5 Ma. The latest Oxfordian-Late Kimmeridgian evaporites are predominately subaqueous basinal evaporite facies with limited marginal sabkha evaporite facies seen in the north (22°S).

The Neuquén Basin records similar aged latest Oxfordian-Upper Kimmeridgian evaporite facies (Auquilco Formation) directly overlying marine carbonates (La Manga Formation) interpreted to have resulted from restricted marine connection associated with barring of the basin (Legarreta & Uliana, 1991). The large spatial distribution of lowstand evaporites traceable for over 2000 km along the back-arc basins of Chile and Argentina, with a marked Late Oxfordian unconformity in southern Peru (Jaillard *et al.*, 1990) are interpreted to record a continental-scale tectonic event affecting all the back-arc basins of western Gondwana (Fig. 3). In the Neuquén basin there is abundant evidence for structural inversion in the Late Oxfordian (Vergani *et al.*, 1995). Uplift of the basin floor and volcanic arc caused the barring and relative

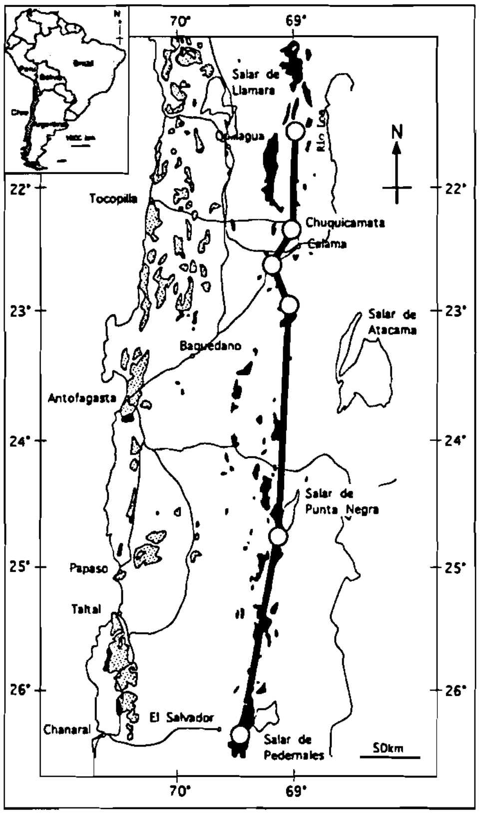


**Figure 1** Map of northern Chile showing the Jurassic volcanic arc (La Negra Formation) in stipple outcropping along the Coastal Cordillera and the Jurassic marine rocks in black outcropping predominately along the Chilean Precordillera, (modified from Prinz et. al., 1994).

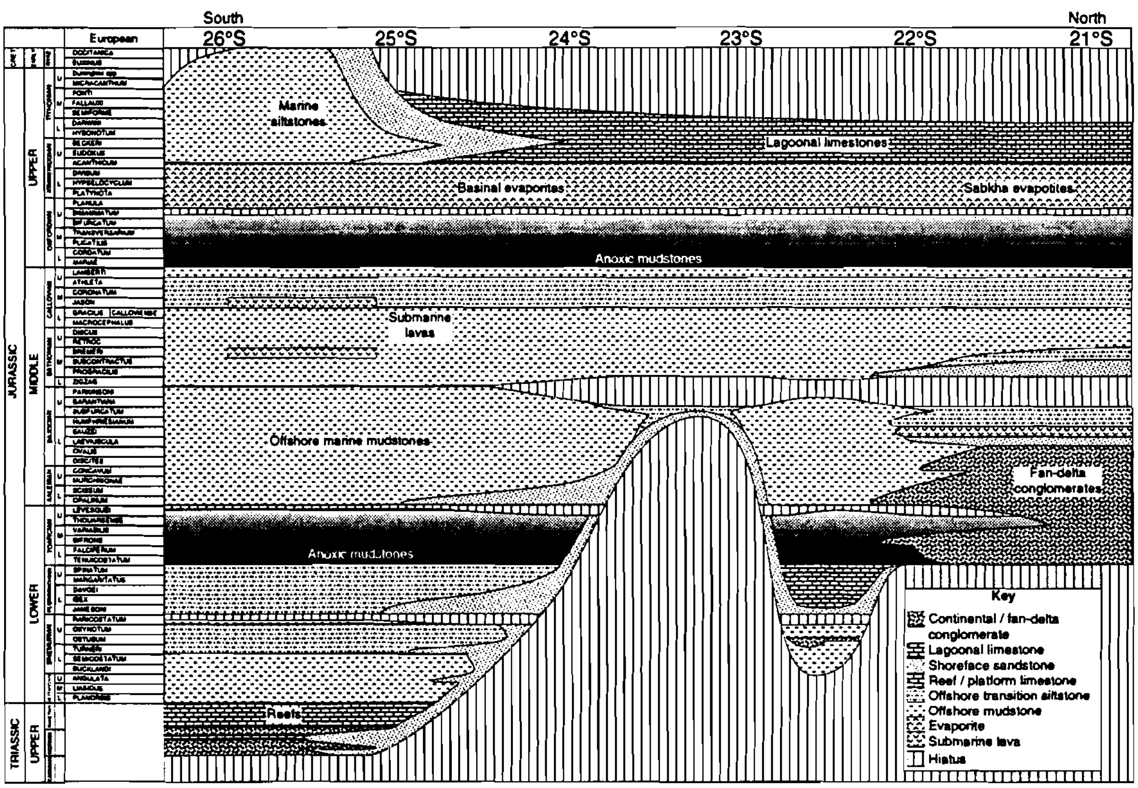


**Figure 2** Chronostratigraphy of the Domeyko basin from Late Triassic-Early Cretaceous.

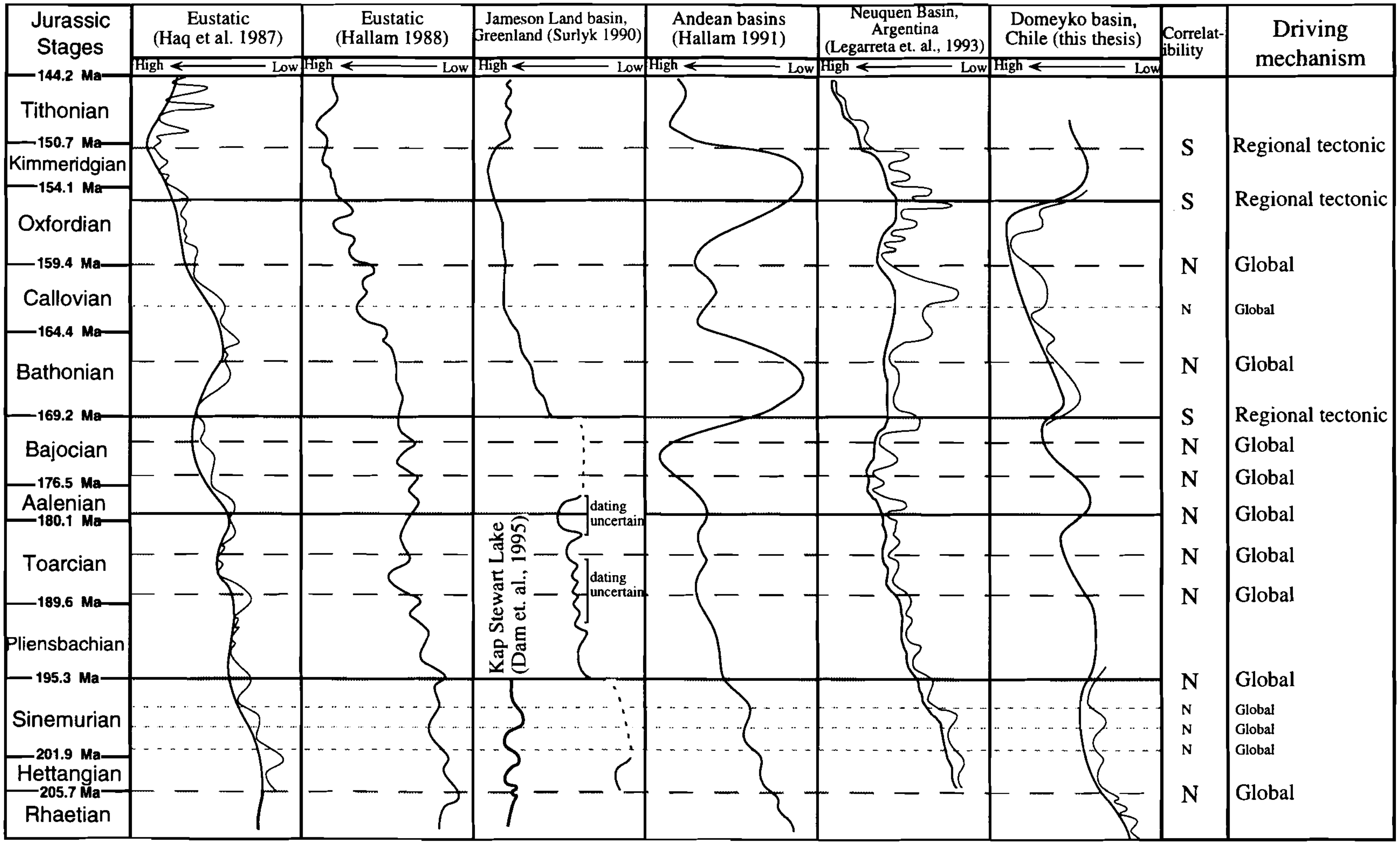


**Figure 3** Comparison of Jurassic relative sea-level changes in northern Chile with global (Haq et al. 1987; Hallam 1988) and relative sea-level changes in the Jameson Land basin, Greenland (Surlyk 1990), Andean basins (Hallam 1991) and Neuquen Basin (Legarreta et. al., 1993). Absolute ages of stage boundaries are taken from Gradstein et. al., (1994). The F' and R' inflection points mark sequence boundaries (Solid lines) and flooding surfaces (Dashed lines) respectively with prominent third-order surfaces (Dotted lines) indicated. Correlatability of events is based on whether the event is seen throughout the South American basins (S) or if it can be traced into the northern hemisphere basins (N). The subsequent interpretation of principle driving mechanism is explained in the text and indicated as either regional tectonic or global.

sea-level fall within the basins (Legarreta & Uliana, 1996), despite a pronounced Late Jurassic global eustatic sea-level rise (Haq *et al.*, 1988) (Fig. 3).
The first episode of oceanic spreading within Gondwana took place with its bisection along the Somali, Mozambique and Weddell Sea Basins. Upper Jurassic sea-floor has been recognised along the length of this ocean strait (Simpson *et al.* 1979). Oceanic onset is well constrained particularly midway along the strait in the Mozambique Basin, where the Jurassic Magnetic Quiet Zone has been detected adjacent to the continental margin (Simpson *et al.* 1979) and the onset unconformity on the Mozambique shelf is dated at 157 Ma (Salman & Abdula 1995). The effect of Gondwana bisection on the southern Andes was to introduce northward transgression from the newly formed ocean in the south. Previously all marine transgressions entered the basins from the north, through Peru and northern Chile (Jaillard *et al.* 1990). We suggest that it was this intra-Gondwana spreading event that caused regional contraction, resulting in barring of the Andean back-arc basins and triggering regional evaporite precipitation. The scale of the evaporite deposits is similar to that of the Messinian evaporites of the Mediterranean and such an ocean-spill model has provided an analogue (Legarreta & Uliana 1996). This continental-scale relative sea-level fall was effected during rising global eustatic sea-level.

## IMPORTANCE OF SUPERCONTINENTAL FRAGMENTATION EPISODES

Previously the origin of contractional tectonic events affecting the South American margin have been difficult to explain (Vergani *et al.* 1995). Almost exclusively changes in subduction activity associated with oceanic spreading and ocean plate splitting in the Pacific area have been proposed as their principal cause (Vaughan 1995). This is despite the fact that there are no particular signatures in terms of the variation in spreading rates (Larson 1991) that stand out to explain each of the compressional episodes that we document. We believe that thermally induced Gondwanan fragmentation episodes provide a more immediately viable explanation, in that they provide a mechanism for plate re-organisations driving changes along the circum-supercontinental subduction zone. Increased subduction coupling is considered to result in uplift recorded in the marginal basins as tectonically-driven sequence boundaries. Specific basin responses include: (a) Type-1 and -2 sequence boundaries in fully marine successions; (b) basin barring and regionally extensive evaporite formation by spill replenishment; (c) incremental and overall changeover from marine to continental deposition systems; and (d) stepwise eastward migration of the volcanic arc. Plate tectonic theory emphasises the dynamic interaction between adjacent plates, whereby relative rates of motion can be fixed to either the underiding or overriding plate as a reference frame. With reference to the circum-Gondwana subduction zone, we believe that in the past an overemphasis has been placed on the motions of plates in the Pacific region, while our conclusions point to the importance of thermally induced spreading effecting relative motions of plates *within* Gondwana as the principal driving agent promoting subductional coupling. Thus, careful sequence stratigraphic analysis of active margin sedimentary basins provides a high resolution record, presently under-utilised in detecting, identifying and analysing global tectonic events in time.

## CONCLUSIONS

The Domeyko basin succession thus appears to be dominantly controlled by global sea-level fluctuations during the Early-Middle Jurassic and by continental-scale (but not global) fluctuations during the Middle Jurassic to Mid-Cretaceous. The global sea-level fluctuations are interpreted to have been driven by glacio-eustasy, while the continental-scale tectonic events are interpreted to have been driven by the break-up of Pangea and subsequent fragmentation of Gondwana.

## REFERENCES

Gygi, R.A. & Hillebrandt, A.v. 1991. Ammonites (mainly Gregoryceras) of the Oxfordian (late Jurassic) in northern Chile and time-correlation with Europe. *Memoires Suisses de Paleontologie*, **113**, 136-167.

Jaillard, E., Soler, P., Carlier, G. & Mourier, T. 1990. Geodynamic evolution of the northern & central Andes during early to middle Mesozoic times: a Tethyan model. *J. Geol. Soc. Lon.*, **147**, 1009-1022.

Larson, R.L. 1991. Latest pulse of Earth-Evidence for a mid-Cretaceous superplume. *Geology*, **19**, 547-550.

Legarreta, L. & Uliana, M.A. *in press*. The Jurassic succession in west-central Argentina: stratal patterns, sequences and palaeogeographic evolution. *Palaeogeog., palaeoclimat. and palaeoecology*.

Salman, G. & Abdula, I. 1995. Development of the Mozambique and Ruvuma sedimentary basins, offshore Mozambique. *Sedimentary Geology*, **96**, 7-41.

Simpson, E.S.W., Sclater, J.G., Parsons, B., Norton, I. & Meinke, L. 1979. Mesozoic magnetic lineations in the Mozambique basin. *Earth and Planetary Science Letters*, **43**, 260-264.

Vaughan, A.P.M. 1995. Circum-Pacific mid-Cretaceous deformation and uplift: A superplume-related event? *Geology*, **23**, 491-494.

Vergani, G.D., Tankard, A.J., Belotti, H.J. & Welsink, H.J. 1995. Tectonic evolution and palaeogeography of the Neuquen basin, Argentina. *In:* Tankard, A.J., Saurez-Soruco, R. & Welsink, H.J. (eds.), *Petroleum basins of South America*. **Memoir 62,** A.A.P.G., 383-402.

# JURASSIC TO LOWER EOCENE TRANSTENSIONAL TECTONICS IN THE ARC AND BACK-ARC OF THE ATACAMA REGION, CHILE.

Carlos AREVALO and John GROCOTT

School of Geological Sciences, University of Kingston, Kingston-upon-Thames, KT1 2EE, UK.

**KEY WORDS**: Magmatic arc, back-arc, transtension, northern Chile.

## INTRODUCTION

Studies of the kinematic and chronologic history of the Jurassic-Lower Cretaceous Andean arc between 25° and 27° S, in combination with the recognition that magmatism and deformation were coeval (Brown et al., 1993; Grocott et al., 1994; Dallmeyer et al., 1996), have confirmated that the magmatic arc developed in a wide transtensional setting which involved a change from a ductile dip-slip dominant to ductile strike-slip dominant displacements in the Early Cretaceous (c.130 Ma).

Recently published results on younger rocks farther to the east document the existence of two other events in the Lower Cretaceous back-arc and in the Upper Cretaceous-Lower Eocene arc which were also dominated by dip-slip and by strike slip (Arevalo, 1994; Arevalo, et al., 1994; Arevalo, 1995). These suggest that the extension and/or transtension perhaps intermittently continued within the arc and back-arc until the Lower Eocene. The way that dip-slip and strike-slip were partitioned is matter of current research.

## REGIONAL SETTING

The Copiapó area is located on the west side of the Andes in the central part of the Atacama Region between 27° and 28°S.The area is distinguished by three morpho-geologic elements. From west to east: (1) a coastal range formed by an eastward migrating **Plutonic Arc** of Jurassic-Cretaceous age which intrudes a basement formed by Upper Palaeozoic metasedimentary rocks and Permian intrusions; (2) a central zone with a very thick sequence of Cretaceous volcanic and volcaniclastic rocks and limestones interpreted to have developed in a **Back-Arc Basin** (Coira et., al, 1982) and (3) unconformably covering the back-arc association, an eastern zone of Upper Cretaceous-Lower Eocene sedimentary rocks, lava flows and ignimbrites which infilled a system of **Rifts and Calderas** (Arevalo et al., 1994), bounded to the east by the Domeyko-La Ternera Fault System.

## THE JURASSIC-CRETACEOUS ARC: A SYNPLUTONIC EXTENSIONAL/TRANSTENSIONAL FAULT SYSTEM

In the plutonic arc many workers (Brown et al., 1993; Grocott et al. 1994 and Dallmeyer et al., 1996) have shown that the emplacement of Lower Jurassic to Lower Cretaceous plutonic complexes was associated with a progressively east-stepping extensional fault system that culminated in the initiation of the Atacama Fault Zone as a mainly strike-slip structure in the Early Cretaceous (c.130 Ma). The construction of the plutonic arc was closely associated with the displacements on syn-plutonic mylonite belts defined by hornblende and biotite schists (Grocott et al., 1994; Dallmeyer et al.,1996) that trend parallel to the north-south elongate pluton margins.

## THE LOWER CRETACEOUS BACK-ARC: A STACK OF EXTENSIONAL ALLOCHTONS

The back-arc is associated with a thick sequence of calcareous and volcanic rocks of Early to Mid-Cretaceous age (Valanginian to Santonian). The basal rocks have been subdivided into five formations: Punta del Cobre, Abundancia, Nantoco, Totoralillo, and Pabellón (Chañarcillo Group; Sergerstrom and Parker, 1959) which interfingers with the Bandurrias Formation to the north and south. Both Chañarcillo and Bandurrias units are overlain by the Cerrillos Formation.

The Bandurrias Formation and the Chañarcillo Group constitute tectonic units detached from the Punta del Cobre Formation (parauthocton ) by the Punta del Cobre detachment which shows a variety of structures indicative of extension: low angle "young over old" faults and large blocks disposed in extensional domino geometries.

In Sierra de Fraga Region, detachments of unequivocal extensional origin have been described (Mpodozis and Allmendinger, 1993). These have affected the Permian to mid-Cretaceous (Aptian) strata in a broad domain east and southeast of Copiapó, probably during the Late Cretaceous (post Aptian, pre-Campanian), are similar in style to those of the Basin and Range province in the Western United States (Critenden et al., 1980), and have been related to the opening of an aborted marginal basin in Central Chile (Levi and Aguirre, 1981). Deposition of Mid-Cretaceous sedimentary and volcanic sequences (Cerrillos Formation) in the Cerrillos basin immediately inboard (east) of the Lower Cretaceous back-arc basin could reflect subsidence associated with these detachments.The closing of the Cerrillos Basin is asociated with an important compressive deformative phase during the Upper Cretaceous indicated by the Cerrillos Thrust and by the Chañarcillo and Lautaro fold and thrust belts, of similar formation age.

## THE UPPER CRETACEOUS-EOCENE ARC: A SYSTEM OF EXTENSIONAL RIFTS AND CALDERAS

The rocks of these periods are mainly related to the evolution of the Hornitos Basin (Arevalo et al., 1994). The basin started as a volcanotectonic depression limited to the west by a system of normal-slip growth faults with a right lateral component of movement where rhyolitic dome complexes were synchronously emplaced. Talus breccias were deposited along the borders of the basin while alluvial conglomerates and lacustrine sandstones and siltstones were deposited toward the centre of the basin. A thick and widespread sequence of high potassium basalts and trachybasalt lava flows infilled the basin. The evolution of the basin finished with a phase of explosive volcanism and lava flows which preserve extraordinarily well most of the primary volcanic superstructure (megacalderas, nested caldera complexes, stratovolcanous).

Synsedimentary structures and geometric features recognized in the basin are compatible with deposition in a dilatational transfer zone between the system of normal growth faults and the southern termination of the Domeyko-La Ternera Fault System. Both these characteristics, and the bimodal and tholeitic geochemical behaviour interpreted for volcanic rocks of the same suites in the Salvador region (Cornejo, et al., 1993), imply a regional extensional setting for the Upper Cretaceous-Eocene arc.

## REFERENCES

Arévalo, C. 1994. Mapa Geológico del cuadrángulo Los Loros. Servicio Nacional de Geología y Minería, Documentos de Trabajo No 6.

Arévalo, C.; Rivera, O.; Iriarte, S.; Mpodozis, C. 1994. Cuencas Extensionales y Campos de Calderas del Cretácico Superior Terciario Inferior en la Precordillera de Copiapó (27°-28° S), Chile. Congreso Geológico Chileno No 7, Actas, 2, 1288-1292.

Arévalo, C.1995. Mapa Geológico de la Hoja Copiapó (1:100.000): Región de Atacama. Servicio Nacional de Geología y Minería, Documentos de Trabajo No 8.

Brown, M.; Díaz, F.; Grocott, J. 1993. Displacement History of the Atacama Fault System, 25°00'S 27°00'S, Northern Chile: Geological Society of America Bulletin., 105, 1165-1174.

Crittenden, M.D. Jr.; Coney, P.J.; Davis, G.H. 1980. Cordilleran Metamorphic Core Complexes. Geological Society of America Memoir, 153, 490 p.

Cornejo, P.; Mpodozis, C.; Kay S.M.; Tomlinson., A.; Ramirez, C. F. 1993. Upper Cretaceous-Lower Eocene Potassic Volcanism in an Extensional in the Precordillera of Copiapo, Chile: Proceedings of Second International Symposium on Andean Geodinamics, 347-350, Oxford, U.K.

Coira, B.; Davidson, J.; Mpodozis, C.; Ramos V. 1982. Tectonic and magmatic evolution of Northern Argentina and Chile. Earth and Science Review, 18, 303-332.

Dallmeyer, D.; Brown, M.; Grocott, J.; Taylor, G.K.; Treloar, P. 1996. Mesozoic Magmatic and Tectonic Events Within the Andean Plate Boundary Zone, 26°-27°30', North Chile: Constraints from $^{40}Ar/^{39}Ar$ Mineral Ages. Journal of Geology, 104, 19-40.

Grocott, J.; Brown, M.; Dallmeyer, G.; Taylor, G.; Treloar, P. 1994. Mechanism of continental grow in extensionals arcs: an example from the Andean Plate Boundary Zone. Geology, 22, 391-394.

Levi, B.; Aguirre, 1981. Ensialic spreading-subsidence in the Mesozoic and Paleogene of Central Chile. Journal of the Geological Society of London, 138, 75-81.

Mpodozis, C.; Allmendinger, R. 1993. Extensional Tectonics, Cretaceous Andes, Northern Chile (27°S). The Geological Society of America Bulletin, 105, 1462-1477.

Segerstrom, K.; Parker, R.L. 1959. Cuadrángulo Cerrillos, Provincia de Atacama, Instituto de Investigaciones Geológicas, Carta Geológica de Chile, 1, 33 p.

# THE GUADALUPE-CHUCHURE THRUST FAULT SYSTEM, FALCÓN BASIN, NORTHWESTERN VENEZUELA: NATURAL EXAMPLE AND ANALOG MODELLING OF A TRANSFER ZONE.

Franck A. AUDEMARD M. (1) and Sylvain CALASSOU (2)

(1) Venezuelan Foundation for Seismological Research (Funvisis), Apdo Postal 76880, Caracas 1070-A, Venezuela. Fax: +(58-2) 257 99 77. e-mail: faudem @ funvisis.internet.ve
(2) Institut des Sciences de la Terre, de L'Eau et de l'Espace de Montpellier, Université de Montpellier II, case 060, Place Eugene Bataillon, 34095 Montpellier, Cedex 5, France. Fax: + (33) 67 14 47 85.

KEY WORDS: thrust system, transfer zones, analog modelling, sand box, Facón basin, Venezuela.

## INTRODUCTION

Analog modelling has become a relatively common practice in Structural Geology from the beginning of the last century. This technique aims to make models the closest possible to the geometry and/or mechanical behaviour of their natural equivalents. Nevertheless, experimental models generally simplify natural problems due to an unsufficient knowledge of the geological setting to be reproduced (precise geometry of rock masses and mechanical behaviour of rocks under stress) or to technical reasons (physical difficulties in reproducing mechanical parametres of rocks or their geometry). Consequently, diverse heterogeneities of nature are not taken into account. Therefore, if models are simplified versions of natural problems, the arisen conclusions should also reflect this fact. However, experimental modelling allows to study large-scale deformation in an original manner and to establish the relations between initial conditions imposed to a model and the geometry of generated structures, as well as their evolution during deformation.

The main objective during this study has been to reproduce the geometry of a segment of the Guadalupe-Mina de Coro-Chuchure thrust fault system that juxtaposes the today-inverted Oligo-Miocene Falcón basin and the Paraguaná high, in northwestern Venezuela. The comprehension of the geometry and origin of thrust faults associated with sedimentary wedges has deeply progressed due to analog modelling results but the compressive structures reproduced during most of those experiments did not try to comprehend the oblique deformations that very frequently perturb the lateral continuity of such structures in nature, such as: strike-slip faults, "en échelon" folds, thrusts or imbricated lateral connectors. These oblique zones to fold-and-thrust belts are classically described as tear fault zones (Harris, 1970; Harding, 1985), implying certain amount of strike-slip motion along certain faults. Several of such oblique structures have been identified along the Guadalupe-Chuchure thrust fault (Fig.1). Calassou *et al.* (1993) have been able to model analogically those complexly deformed zones by imposing, during modelling, several geometrical and mechanical initial conditions: variable thickness of sedimentary cover, offset thrust front, different friction law at thrust sole and variable angle between the maximum horizontal stress and the basin axis. Recently, Baby *et al.* (1993) have also modelled the last condition in order to explain transfer zones in the foreland basin at the foothills of the Bolivian Eastern Cordillera.

## GEOLOGICAL SETTING

The north-vergent Guadalupe-Mina de Coro-Chuchure thrust system extends westward for some sixty kilometers in northwestern Venezuela from the town of Puerto Cumarebo to the village of Las Piedras

(Audemard, 1993), located south of Sabaneta (Fig.1). Its easternmost segment corresponds to the north-vergent arcuated Guadalupe thrust, located offshore along the northern coast of La Vela anticline. The associated La Vela brachy-anticline is bounded on the west by the Carrizal fault, that strikes N010°-N015°, and on the east by the NW-SE trending fault system that controls the eastern coast of the Falcón State (Fig.1). The thrust system front is disrupted twice by short left-lateral (tear) faults or complex zones that can offset it southward of few to about ten kilometers, such as east of Coro. There, the front jumps south, between the villages of Caujarao and La Vela, from the southern Carrizal fault tip to a north steeply-dipping monocline affecting the fanglomerates of the Late Pliocene-Early Pleistocene Coro formation (Fig.1). In between, the thrust plane does not outcrop, but its presence is underlined by a set of NE-SW trending "en échelon" folds that connects both segments (Audemard, 1993) (Fig.1). This geometry and the associated structures suggest the existence of a transfer zone. Further west, the second front disruption happens at the western end of the segment extending between Caujarao-El Isiro and San Antonio, SW of the city of Coro. (Fig.1). The San Antonio or Hatillo fault offsets it 2.5 km left-laterally, but the post-Pliocene slip is less than 1 km. Even further west, between San Antonio and Sabaneta, the thrust fault is located south of la fila Capote within the mudstones of the Middle Miocene Querales formation and along the valley of the small village of Chuchure (Fig.1).

## ANALOG MODELLING

An experimental modelling approach was followed to reproduce those oblique stuctures observed across the main east-west trend of the Guadalupe-Mina de Coro-Chuchure thrust system. We only modelled its segment located east of Coro, though it corresponds to the most complex portion, comprising strike-slip faults and "en échelon" folds. Large sandbox experiments have been performed because they allow a 3-D analysis of structures after deformation (along-strike structural variations).

Many investigations, either theoretical or experimental, have proven that dry sand is an excellent analog of sedimentary sequences, because it is a brittle material that follows the Mohr-Coulomb rupture criteria (Hubbert, 1951; Byerlee, 1978; Dahlen, 1984; Krantz, 1991; Lallemand *et al.*, 1994). The sand used for building the models is made of well-rounded quartz grains of eolian origin. This dry non-cohesive sand is characterized by a 30° friction angle and presents a Navier-Coulomb rheology. Its density is about 1.6 $gr/cm^3$ and its granulometric sorting, smaller than 50 $\mu m$, is obtained after sieving. Thin horizontal markers have been intercalated within the sand fill and a coloured 10 cm x 10 cm reference grid was drawn on top of it in order to observe deformation.

The designed experimental apparatus tries to reproduce the basement geometry, whereas the sand fill represents the Oligo-Miocene sedimentary sequence of the Falcón graben before tectonic inversion, taking into account collected field geological data as well as previously published and interpreted seismic profiles. Then, the apparatus comprises three undeformable wooden blocks, sliding freely on a waxed P.V.C. table (Fig.2). The table is 1.20 m in width, thus allowing to study the along-strike structural variations away from free-face perturbated table edges. The wooden blocks were cut respecting the 60º dip of normal faults limiting the graben, and blocks have been placed on the table reproducing the geometric problem. The imposed analogies are: (1) NW compartment → Paraguaná high with rather thin sedimentary cover; (2) NE compartment → La Vela bay basin; (3) central compartment → deepest part of the Falcón graben; and (4) south compartment → southern margin of the Falcón basin.

## MODELLING RESULTS

From the very beginning of the experiment, a wedge started to form normal to motion of the south block. This wedge comprised in-sequence imbricated structures. When approaching the differentiated geometry of the northern compartments, an important virgation developed. The thrust front prograded to a more northern position on the NE compartment (analog to basin of La Vela bay), where the basement is deeper (Fig.3a). The virgation formed right above the basement step, thus corresponding to a transfer zone.

During this experiment, common facts have been observed with Calassou *et al.* (1993)'s experiments: virgation develops right above basement jump (Fig.3a); thrust front progrades to a more external position where basement is deeper; for each thrust formed in the thick-sequence compartment (Fig.3c), two smaller thrusts form in the thin-sequence compartment (Fig.3b); complex structures affect the sedimentary fill above the basement step as observed in normal-to-wedge cross sections.

The experiment allows us to make the following analogies with the Guadalupe-Mina de Coro-Chuchure thrust system: (a) on surface, virgation is comparable to the one offsetting the thrust system front, southeast of Coro (Fig. 1 and 3a). Therefore, Los Médanos fault is responsible for such virgation because it vertically displaces the basement between the Paraguaná block (NW compartment) and the basin of La Vela bay (NE compartment); (b) the transfer zone of the Guadalupe-Chuchure thrust comprises a left lateral fault (Carrizal fault) and a set of "en échelon" folds located at the southern tip of this fault. The "en échelon" folds correspond to the folded structures observed in the parallel-to-wedge cross sections. Then, the Carrizal fault should be considered as a lateral ramp; (c) Comparing a NE compartment cross-section (Fig.3c) to a seismic profile across La Vela anticline interpreted by Cabrera (1985) (Fig.4), a close resemblance is observed. Let us recall that a large portion of the upper part of the La Vela anticline is already eroded. We also observe the fault plane where it dips about 30ºS, very similar to the dip of the modelled fault plane at depth. Model's backthrusts are equivalent to those of the natural example.

## CONCLUSIONS

From the close similarities between the performed analog modelling and the natural example, we can conclude that the virgation of the Guadalupe-Mina de Coro-Chuchure thrust fault system, located southeast of Coro, is closely linked to the difference of Neogene sediment thicknesses between the Paraguaná high and the contiguous basin of La Vela bay, producing a typical transfer zone right above a basement step, in turn, generated by the Los Médanos fault (down-to-the-east normal fault). The transfer zone of this thrust system comprises a short lateral ramp (the left-lateral Carrizal fault) and a set of NE-SW trending "en échelon" folds, responsible for transport of the La Vela anticline to the north, in a more external position.

## REFERENCES


Audemard, Fr. 1993. Néotectonique, Sismotectonique et Aléa Sismique du Nord-ouest du Vénézuéla (système de failles d'Oca-Ancón). *Thèse Doctorat Université Montpellier II.* 369 p.

Baby, P.; Spetch, M.; Mendez, E.; Guillier, B.; Colletta, B. and Letouzey, J. 1993. Development of transfer zones and location of oil and gas field in frontal part of Bolivian Andean fold-and-thrust belt. *AAPG/SVG Int. Cong. & Exh., Caracas;* 36. *(Abstract).*

Byerlee, J. 1978. Friction of rock. *Pure Appl. Geophys.*; 116: 615-626.

Cabrera de Molina, E. 1985. Evolución estructural de Falcón Central. *Tésis M.Sc., Esc. Geol. Min. y Geof., Univ. Central de Venezuela.* 59 p.

Calassou, S.; Larroque, C. and Malavieille, J. 1993. Transfer zones of deformation in thrust wedges: an experimental study. *Tectonophysics;* 221(3/4):325-344.

Dahlen, F. 1984. Non-cohesive critical Coulomb wedges: An exact solution. *J. Geophys. Res.*; 89:10125-10133.

Harding, T. 1985. Structural styles, plate tectonic setting, and hydrocarbon traps of divergent (transtensional) wrench faults. In K.T. Biddle and N. Christie-Blick (Editors), *Strike slip deformation, basin formation, and sedimentation.* Doc. Eco. Paleont. Min., Sp. Publ.Nº 37, 386 pp.

Harris, L. 1970. Details of thin-skinned tectonics in parts of valley and ridge and Cumberland plateau provinces of southern Appalachians. In G.W. Fischer, F.J. Petitjohn, J.C. Reed and K.N. Weaver (Editors). *Studies in Appalachian geology: Central and Southern.* Interscience, New York; 161-173.

Hubbert, M. 1951. Mechanical basis for certain familiar geologic structures. *Geol. Soc. Am. Bull.;* 62:335-372.

Krantz, R.W. 1991. Mesurements of friction coefficients and cohesion for faulting and fault reactivation in laboratory models, using sand and sand mixtures. *Tectonophysics*; 188:203-207.

Lallemand, S.; Schmürle, P. and Malavieille, J. 1994. Coulomb theory applied to accretionary and nonaccretionary wedges: Possible causes for tectonic erosion and/or frontal accretion. *J. Geophys. Res.*; 99(B6):12033-12055.

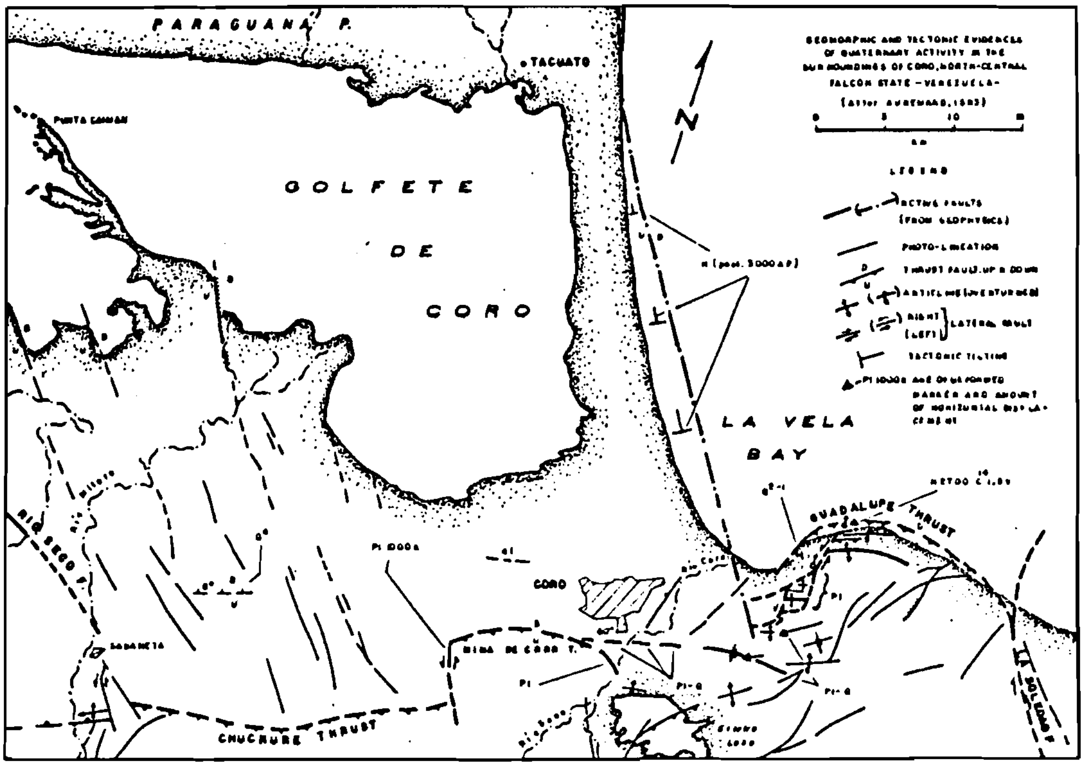


**Fig.1** Neotectonic setting of northern Falcón State, near Coro, showing the Guadalupe-Mina de Coro-Chuchure thrust system and its virgations (after Audemard, 1993).

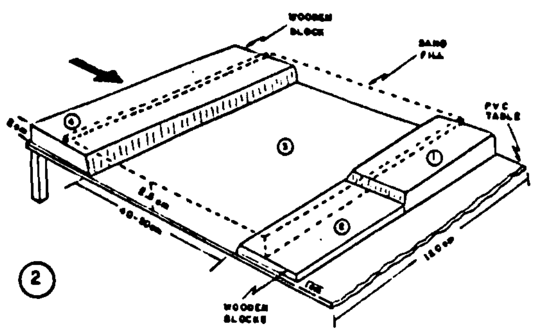

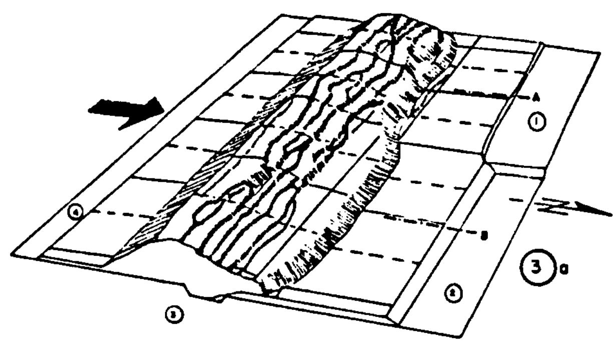

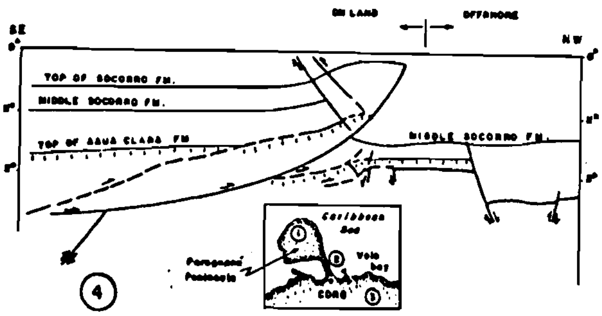

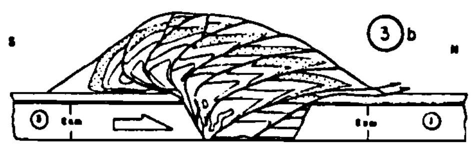

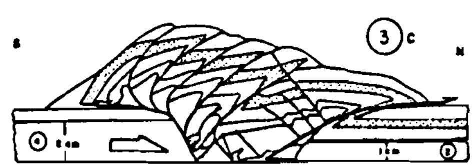

**Fig.2** Apparatus used during analog modelling of transfer zone and graben inversion. **Fig.3** Final condition after deformation: a) bird-eye view of model showing transfer zone formation above basement step. Large arrow indicates kinematics imposed; b) NW compartment cross-section; c) NE compartment cross-section. **Fig.4** Interpreted seismic profile across the La Vela anticline (after Cabrera, 1985).

# NEOGENE THRUST GEOMETRY AND CRUSTAL BALANCING IN THE NORTHERN AND SOUTHERN BRANCHES OF THE BOLIVIAN OROCLINE (CENTRAL ANDES)

Patrice BABY (1), Philippe ROCHAT(2), Gérard HÉRAIL(3) Georges MASCLE(2) and Anne PAUL(4)

(1) ORSTOM, Apartado 17.11.6596, Quito, ECUADOR. e-mail: baby@orstom.ec
(2) LGCA, Institut Dolomieu, 15 rue Maurice Gignoux, 38031 Grenoble, Cedex, FRANCE
(3) ORSTOM, Casilla 53390, Correo Central, Santiago 1, CHILE
(4) LGIT, IRIGM, BP 53X F-38041, Grenoble cedex, FRANCE

**KEYWORDS** : Andes, Bolivia, thrust tectonics, crustal balanced cross-sections, crustal thickening, Neogene.

## INTRODUCTION

The Central Andes, between 10 and 28°S, are characterised by the elbow shape of the mountain range (The Bolivian orocline), a thick crust (55-75 km), high relief (several summits over 6000 m) and an enigmatic high plateau (the Altiplano) with an average altitude of 3650 m.a.s.l.. Recent works have shown the importance of crustal shortening for the development of the structural pattern of the Central Andes [Allmendinger et al., 1983; Isacks, 1988; Roeder, 1988; Roeder and Chamberlain, 1995; Sheffels, 1990; Baby et al., 1989, 1992a, 1992b, 1995; Gubbels et al., 1993; Schmitz, 1994; Kley et al., 1995].

The purpose of this paper is to present two crustal balanced cross-sections across the northern and southern branches of the Bolivian orocline, which show the Neogene thrusts geometry of the back arc system and the Neogene shortening contribution to crustal thickening.

## TECTONIC SETTING

In Bolivia, the Andean thrust tectonics started in Late Oligocene [Sempere et al., 1990] and is still developing. The sediments involved in thrusting consists of an pre-orogenic series from Cambrian to Oligocene and an Oligo-Miocene to recent continental syn-orogenic infill.

The back arc system of the Bolivian orocline is divided from east to west into five morphotectonic units (cf. Fig.). The Chaco and Beni plains correspond to a poor deformed Neogene foreland basin underlain by the Brazilian shield. It is overthrusted by the Subandean Zone, a complex thin-skin fold and thrust belt characterised in its central part (Santa Cruz elbow) by important transfer zones, and which developed since 10 My [Gubbels et al., 1993]. The pre-orogenic sedimentary series presents (Ordovician to Cretaceous) lateral variations of facies and thicknesses which play an important role in controlling the structural geometry. The Interandean zone and the Cordillera Oriental correspond to thick-skin fold and thrust belts. The Interandean zone is only built of Devonian and Silurian sediments. In the Cordillera Oriental - built mainly of Ordovician anchimetamorphic sediments - the Neogene thrust system is superimposed on a deeply eroded pre-Cretaceous fold belt. The Altiplano is a complex intermontane basin overthrusted by the Cordillera Oriental, and characterised by a thick Cenozoic sedimentary infill deformed by a Neogene thrust and tectonic inversions. Maximum crustal thicknesses of 70-74 km under the Altiplano and Cordillera Oriental thin to 32-38 km 200 km east of the Andes in the foreland basin [Beck et al., 1995].

## SURFACE AND SUB-SURFACE THRUST STRUCTURES

**Subandean zone**

The northern branch of the Subandean Zone is characterised by important thrust sheets (10-20 km) and broad synclines filled by Neogene sediments - piggy back basins with 6,000 m of syn-tectonic sediments [Baby et al., 1995]. Surface mapping, reflection seismic data, and drilling information provided by the Bolivian State Oil Company (YPFB) show that the main detachments are located in the Ordovician shales, in the Silurian shales, in the Devonian shales and in the Permian shales. The foredeep has a bottom that slopes at 4°. In our cross-section (cf. Fig.), the amount of shortening taken from tectonic balancing is 74 km, i.e. 50%.

In the southern branch, an important east verging thrust (Mandiyuti Thrust) divides the southern Bolivian Subandean Zone into two fold and thrust belts that differ according to their thrust system geometry. The western belt is characterised mainly by fault propagation folds and fault bend folds, whereas the eastern belt is characterised by fault propagation folds and passive roof duplexes [Baby et al., 1992a]. The main detachments are located in the Silurian dark shales, in the early Devonian shales, and in the base and top of the Middle to Late Devonian dark shales. The Silurian-Devonian succession is covered by more than 2000 m of late Paleozoic and Mesozoic sandstones with no potential detachments; in some places it is also covered by several thousan l meters of syn-orogenic Neogene sedimentary rocks. The foredeep has a bottom that slopes at 2°. Total shortening decreases from 20° S (140 km, i. e. 50%) toward the south (70 km, i. e. 35%, at 22° S).

**Interandean zone and Cordillera Oriental**

They are deformed by involved basement east-vergent thrusts and associated back-thrusts. Near the surface, shortening is concentrated in the west-vergent thrust system at the western part of the Cordillera Oriental and - in the southern branch - in the Interandean zone (cf. Fig.). The Cordillera Oriental is characterised by presence of small Neogene piggyback basins which have recorded the deformation history [Hérail et al., 1996]. Surface data allowed to construct some balanced cross-sections. An amount of shortening between 80 and 100 km is estimated.

**Altiplano**

The combined study of field and seismic reflection data shows that the Altiplano is structured by Oligocene extensional basin partially inverted during the Neogene, and by the west-vergent thrust system of the Cordillera Oriental [Rochat et al., 1996].

The northern Altiplano (cf. Fig.) is characterised by a very thick series of Cenozoic continental sediments (more than 10 000 m) which come from the Oligocene extensional tectonics and from the Neogene uplift of the Cordillera Oriental. The southern Altiplano shows the maximum amount of shortening. It is deformed by an important east-vergent thrust system [Baby et al., 1992b]. Construction of balanced cross sections has been made possible due to surface mapping, reflection seismic data, and drilling information provided by the Bolivian State Oil Company (YPFB).

## DEEP DATA AND CRUSTAL BALANCING

From surface and geophysical data obtained in the last decade, we have constructed two crustal balanced cross-sections (Fig.).

In the northern branch of the orocline, some results of the French Lithoscope experiment - a teleseismic field experiment [Dorbath et al., 1993] - have been used to construct the deep structures. The Moho shape was established from PKP residuals. In the southern branch, the results of the Berlin Group - seismic refraction data [Wigger et al., 1994] - give a Moho shape and show that high velocity zones under the Cordillera Oriental can be interpreted as high positions of lower crustal material.

In the two crustal balanced cross-sections, the total amount of shortening in the Paleozoic, Mesozoic and Cenozoic cover, calculated from our regional studies, is accommodated by the development of a duplex of middle and lower crust. This duplex can explain the crustal thickening under the Cordillera Oriental, but not under the Altiplano. These results are in accordance with the balanced model of Schmitz (1994) in the southern Central Andes.

## CONCLUSIONS

From north to south, our balanced cross-sections show that, in the back arc system of the Bolivian orocline, the total amount of shortening varies from 191 km to 231 km. These values are in

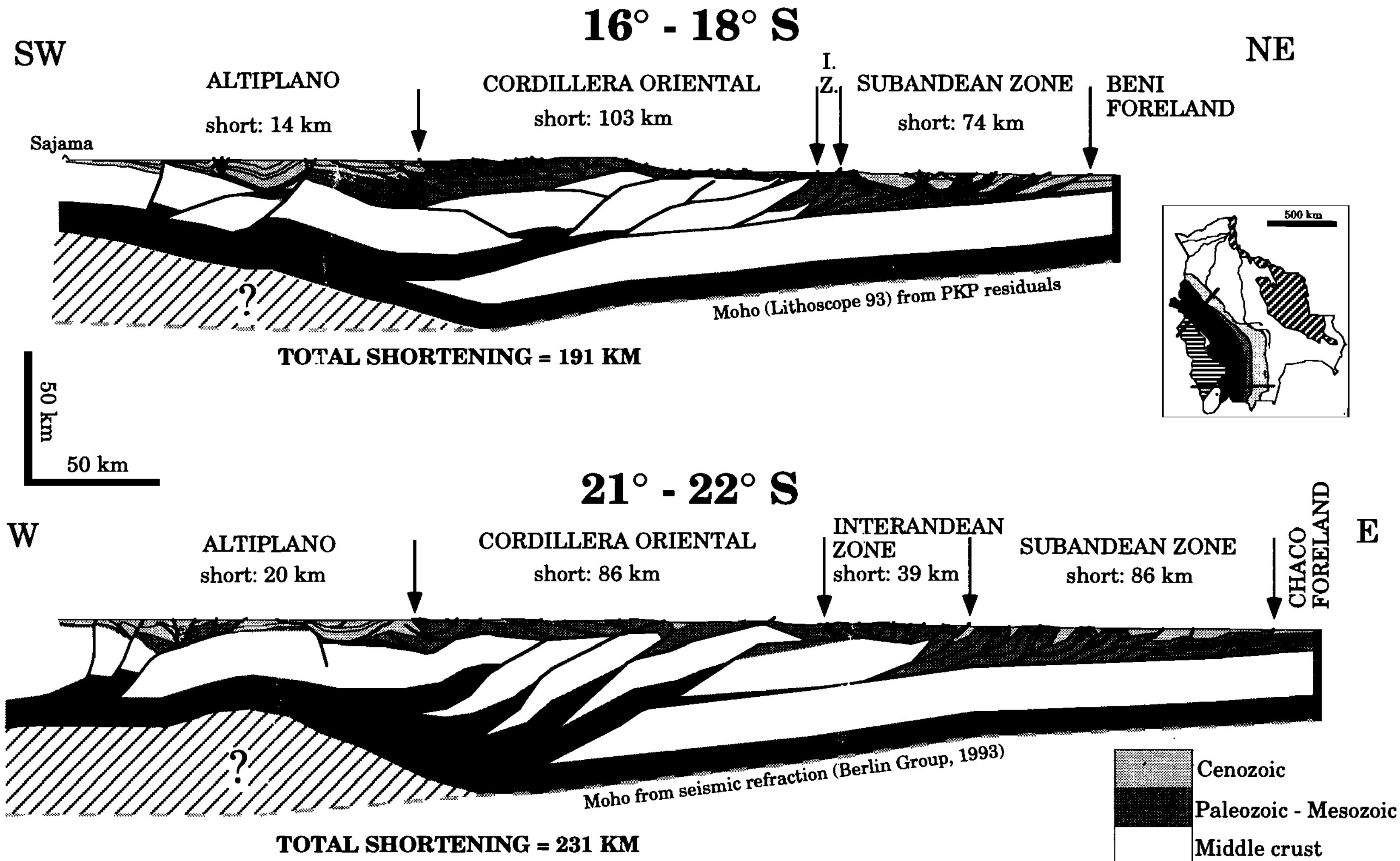


Crustal balanced cross-sections
in the northern and southern branches of the Bolivian Orocline

accordance with the amount of shortening (210 km) calculated by Sheffels (1990) in the central part of the Bolivian orocline. This increase of shortening from north to south coincide with an increase in the crustal thickness [Beck et al., 1995] and an increase in the width of the chain - the chain is wider in the south where the Interandean and the Subandean zones are more developed.

In the north as in the south, the Neogene shortening is insufficient to produce the crustal thickening evidenced by geophysical data under the Altiplano. This crustal thickening can be explained by a pre-Neogene shortening, but we have not evidence of other important shortening later than the pre-Cretaceous erosion. Other processes of crustal thickening must been suggested.

## REFERENCES

Allmendinger R. W., Ramos V. A., Jordan T. E., Palma M. and Isacks B. L. 1983. Paleogeography and Andean structural geometry, Northwest Argentina. *Tectonics*, 2, 1, 1-16.

Baby P., Hérail G., López M., López O., Oller J., Pareja J., Sempere T. and Tufiño D. 1989. Structure de la zone subandine de Bolivie : influence de la géométrie des séries sédimentaires antéorogéniques sur la propagation des chevauchements. *C. R. Acad. Sci. Paris*, 309, II, 1717-1722.

Baby P., Hérail G., Salinas R. and Sempere T. 1992a. Geometry and kinematic evolution of passive roof duplexes: examples from the foreland thrust system of the Subandean belt of Bolivia. *Tectonics*, 11, 3, 523-536.

Baby P., Sempere T., Oller J. and Hérail G. 1992b. Evidence for major shortening on the eastern edge of the Bolivian Altiplano: the Calazaya nappe. *Tectonophysics*, 205, 1-3, 155-169.

Baby G., Coletta B. and Zubieta D. 1995. Etude géométrique et expérimentale d'un bassin transporté: exemple du bassin subandin de l'Alto Beni (Andes centrales). *Bull. Soc. Géol. de France*, 166, 6, 797-811.

Beck S., Zandt G., Myers S. C., Wallace T. C., Silver P. et Drake L. 1995. Crustal Thickness Variations in the Central Andes. *Geology*, Submitted.

Dorbath C., Granet M., Poupinet G. and Martinez C. 1993. Teleseismic study of the Altiplano and the Eastern Cordillera in northern Bolivia: new constraints on a lithospheric model. *J. Geophys. Res.*, 98, B6, 9825-9844.

Gubbels T. L., Isacks B. L. and Farrar E. 1993. High-level surfaces, plateau uplift, and foreland development, Bolivian central Andes. *Geology*, 21, 695-698.

Hérail G., Oller J., Baby P., Blanco J., Bonhomme M. G. and Soler P. 1996. The Tupiza, Nazareno and Estarca basins (Bolivia): Strike-slip faulting and related basins in the Cenozoic evolution of the southern branch of the Bolivian Orocline. *Tectonophysics*, in press.

Isacks B. L. 1988. Uplift of the Central Andean Plateau and Bending of the Bolivian Orocline. *J. Geophys. Res.*, 93, 3211-3231.

Kley J. 1993. Der Übergang vom Subandin zur Ostkordillere in Südbolivien (21°15'-22°): geologische Struktur und Kinematic. *Berliner geowissenschaftliche Abhandlungen*, 156, (A), 1-88.

Rochat et al. 1996. Geometry and kinematics of the northern Bolivian Altiplano within the Central Andes, *ISAG 96*, this volume.

Roeder D. 1988. Andean-age structure of Eastern Cordillera (Provine of La Paz, Bolivia). *Tectonics*, 7(1), 23-39.

Roeder D. and Chamberlain R. L. 1995. Petroleum System of the northern and central bolivian Sub-Andean Zone. *in* : Tankard A.J., Suárez S. R. et Welsink H.J., éd., Petroleum Basins of South America, AAPG Memoir 62, 459-479.

Schmitz M. 1994. A balanced model of the southern Central Andes. *Tectonics*, 13, 2, 484-492.

Sempere T., Hérail G., Oller J. and Bonhomme M. 1990. Late Oligocene-early Miocene major tectonic crisis and related basins in Bolivia. *Geology*, 18, 946-949.

Sheffels B. 1990. Lower bound on the amount of crustal shortening in the central Bolivian Andes. *Geology*, 18, 812-815.

Wigger P. J., Schmitz M., Araneda M., Asch G., Baldzuhn S., Giese P., Heinsohn W.-D., Martinez E., Ricaldi E., Röwer P. and Viramontes J. 1994. Variation in the crustal structure of the Southern Central Andes Deduced from Seismic Refraction Investigations. *in* : K.-J. Reutter E. Scheuber P.J. Wigger, éd., Tectonics of the Southern Central Andes, Springer-Verlag, Berlin, 23-48.

# NEOGENE STRIKE-SLIP BASINS AND THE WEAK FAULT CONCEPT FOR THE COLLISIONAL SUTURES OF ECUADOR AND COLOMBIA

Roger BAUDINO

Laboratoire de Géodynamique et Modélisation des Bassins Sédimentaires. IPRA. Université de Pau. 64000 PAU. FRANCE

KEY WORDS : Neogene, Northwestern Andes, strike-slip basins, collisional sutures, weak faults

## INTRODUCTION

The accretion of exotic terranes to the south American margin during Mesozoic and Cenozoic time characterizes Northern Andes. In Ecuador and Colombia several allochtonous terranes (or blocks) limited by collisional sutures have been identified (Fig. 1; Mc Court *et al.*, 1984; Mégard, 1989; Duque-Caro, 1990; Van Thournout *et al.*, 1992; Aspden & Litherland, 1992, and references therein). In northwestern Colombia the Chocó block is bounded to the east by the *Cordillera occidental* and to the south by the Istmina fault zone (IFZ). The coastal plain with the *Cordillera occidental* of Colombia and Ecuador form the oceanic Coastal Terrane. The Calacalí-Pallatanga Suture (CPF) and the Cauca Fault (CF) limit the latter from the Chaucha-Amaime Terrane which accreted along the Peltetec (PF) and Romeral (RS) Sutures. In northern Peru, the Amotape-Tahuin Block (ATB) is bounded to the north by the Raspas Fault (RF) and to the east by the Las Aradas Fault (LAF). Strike-slip motion, related to increased subduction rate, occured along the sutures triggering basins formation during the Neogene (Baudino, 1995). The study of two Neogene strike-slip basins of Ecuador, structurally linked to the CPF and PF sutures, revealed that their evolution is however incompatible with classical pull-apart models.

## BASINS ANALYSIS

The Chota basin, in the northern ecuadorian Andes is located between the CPF and the PF (Fig. 1). Unconformable non-marine deposits of Miocene age, with a minimum thickness of 2400 m, overlie a Mesozoic metamorphic basement and are discordantly topped by Plio-Quaternary volcanics. The sedimentary fill is bounded by NE and N striking faults.

Sedimentologic analysis shows that the sedimentary fill can be divided into two main sequences (Baudino, 1995; Barragan *et al.*, 1996). Fining upward fluvial and lacustrine deposits form the lower main sequence, whereas the upper one is made of coarsening upward lacustrine and alluvial fan deposits. Local unconformities separate the two main sequences which correspond to different stages of the basin's evolution : opening during lower to middle Miocene and closing during upper Miocene.

Structural analysis revealed near horizontal slickensides, the migration through time of the deposition center towards the most active zones and flower structures, which are arguments for strike-slip basin related to dextral motion of the bounding faults. In addition, synsedimentary tensional faults, resulting of N120°E extension, indicate simultaneous fault-normal extension during lower to middle Miocene. Folding and faulting, resulting of N120°E (along NE striking bounding faults) and E-W (along N striking faults) compression indicate simultaneous fault-normal compression during upper Miocene.

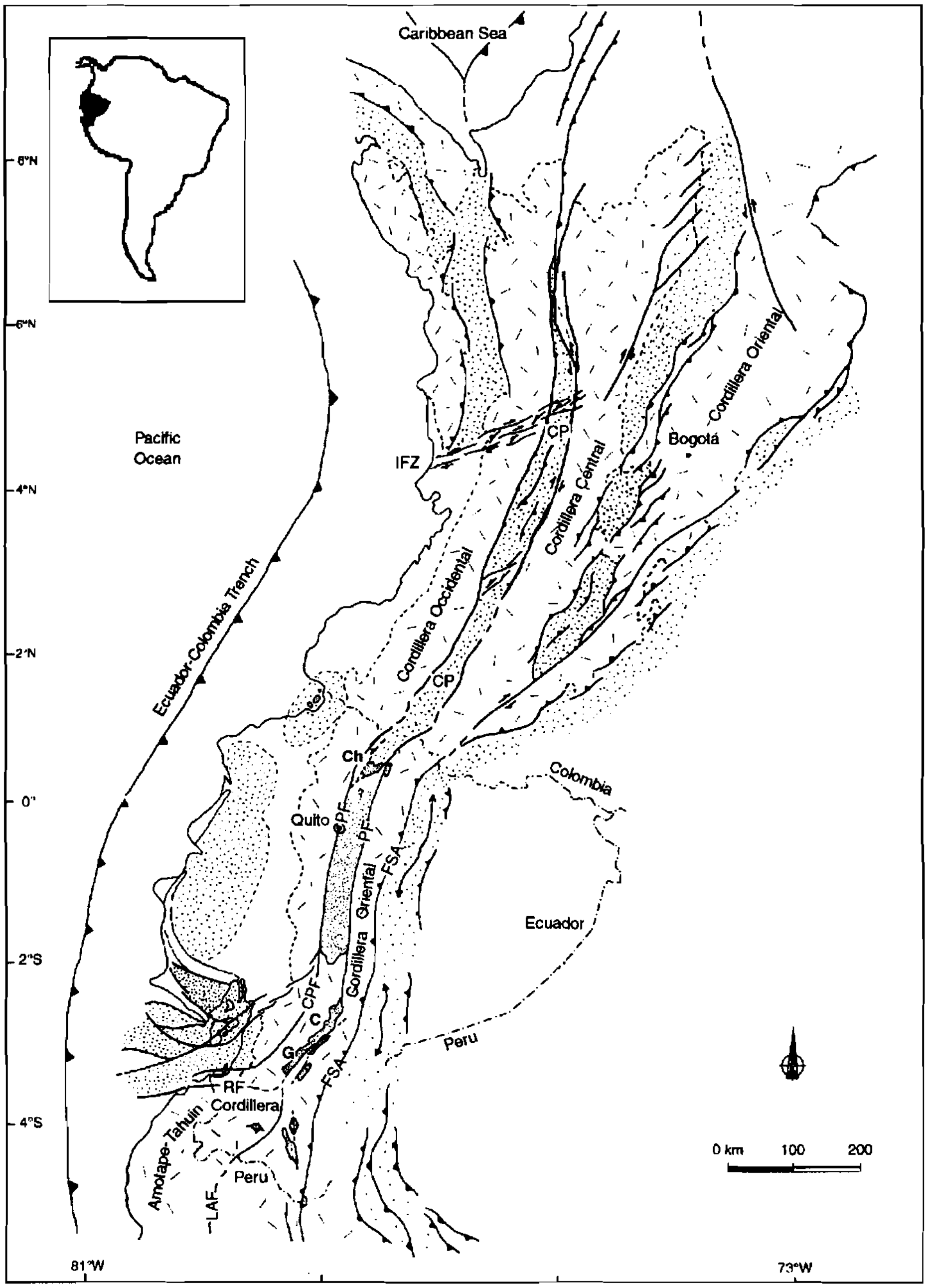


Figure 1: Morpho-tectonic map of Northwestern Andes showing ranges (hached) and Neogene sedimentary basins (dotted); Ch. Chota basin; C-G. Cuenca-Girón basin; CP. Cauca-Patía Depression; IFZ. Istmina Fault Zone; CPF. Calacalí-Pallatanga-Palenque Suture; PF. Peltetec Suture; RF. Raspas Fault; LAF. Las Aradas Fault; FSA. Ecuadorian Subandean Tectonic Front.

The Cuenca-Girón basin, in the southern ecuadorian Andes is an episutural basin situated upon the PF (Fig. 1). More than 5000 m of Miocene continental deposits unconformably overlie a late Oligocene and Mesozoic basement, and are discordantly topped by Plio-Quaternary volcanics. The Cuenca and Girón basins were formerly considered separately, but recent studies have shown that it is a unique asymetric basin with a thicker sedimentary fill near the eastern bounding fault (Baudino, 1995). This bounding fault is NE striking in the Girón and southern Cuenca basins (the active Girón Fault) and N striking in the northern Cuenca basin.

The sedimentary evolution is characterized by two main sequences (Noblet *et al.*, 1988; Mediavilla, 1991; Baudino, 1995) : a lower fining upward main sequence (made of fluvial and lacustrine deposits), and an upper coarsening upward main sequence (made of lacustrine and coarse alluvial fan deposits). These two sequences correspond to different stages of the basin's evolution : opening during lower to middle Miocene and closing during middle to upper Miocene.

In the light of detailed structural analysis, the Cuenca basin was defined a strike-slip basin related to dextral motion of regional faults by Noblet *et al.* (1988). These authors and Lavenu *et al.* (1995) proposed that a compressive stress field affected the basin with NNE-SSW to NE-SW shortening (and normal NW and WNW-ESE related extension) during the opening stage, rotating to an E-W and WNW-ESE shortening during the closing stage. However, the same authors described a synsedimentary extension normal to the bounding faults which counters the compressive stress field hypothesis during the opening stage. The NNE-SSW to NE-SW shortening was deduced from conical synsedimentary folds. These folds are however located near and have axis normal to the bounding faults, and appear then to be better explained by strike-slip motion of the faults rather than being characteristic of a regional compressive stress field. I think, thus, that transtension (simultaneous strike-slip motion and fault-normal extension) should be better used to characterize the tectonic regime affecting the Cuenca basin during the opening stage. Compression was coeval with strike-slip motion during the closing stage (Noblet *et al.*, 1988; Lavenu *et al.*, 1995). Moreover, a carefull examination of synsedimentary folds location show that compression is normal to the bounding faults, giving rise to N-S elongated folds in the northern part of the Cuenca basin and NE-SW elongated folds in the southern part. Transpression, thus, can be better used to characterize the tectonic regime affecting the basin during the closing stage.

In the Girón basin, transtension (with Girón Fault-normal extension) during the opening stage, and transpression (with fault-normal compression) during the closing are well documented (Baudino, 1995).

## DISCUSSION

Stress fields associated with right-lateral strike-slip motion on the N and NE trending bounding faults of the Chota and Cuenca-Girón basins, and nearly parallel folding and faulting (normal or reverse) are incompatible with classical faulting theory. In the latter, the direction of maximum horizontal compression is expected to be 30°-45° for a vertical strike-slip fault plane (Anderson, 1951). One could invoke rotations affecting pull-apart basins and triggering tectonic inversion on a same fault in a stable compressional stress field (e.g. Richard *et al.*, 1995). In the present dextral strike-slip setting, however, this should be a clockwise rotation of the basins and not the anti-clockwise rotation suggested by Noblet *et al.* (1988) and Lavenu *et al.* (1995) for the Cuenca-Girón basin. Neither the Chota nor the Cuenca-Girón basins can thus be interpreted as pull-apart basins. An alternative to pull-apart basins has been proposed by Ben-Avraham & Zoback (1992) : relatively large-scale extensional or compressional features can develop parallel to transform faults that are best explained by the strong crust - weak transform conceptual model developped by Zoback *et al.* (1987) for the San Andreas fault system. In such cases, the horizontal principal stresses have to rotate to orientations approximately parallel and perpendicular to the weak transform fault so as to minimize shear stress on the fault. This reorientation resulted in fault-normal extension during lower to middle Miocene and fault normal compression during upper Miocene in the ecuadorian strike-slip basins genetically linked to collisional sutures. The Neogene basins of the Cauca-Patía Depression of Colombia, are related to strike-slip motion along the Cauca and Romeral Sutures (Fig. 1). Transtension during lower to middle Miocene and transpression during upper Miocene is also well documented in these basins (discussion in Baudino, 1995).

## CONCLUSIONS

In the light of the previuous considerations it appears that the collisional sutures of the Andes of Ecuador and Colombia, which are deep crustal faults comparable to transform, acted as weak faults during the Neogene. Northward motion of the allochtonous terranes triggered transtension along the sutures. Strongest coupling between the subducting and overriding plates with buttressing effect provided by the Chocó block accretion and underthrusting of the Caribbean plate are probably responsible for the occurence of transpression during the upper Miocene (Baudino, 1995).

## REFERENCES

**Anderson E. M.** 1951. The dynamics of faulting and dyke formation with applications to Britain (second edition). Edinburgh, Oliver and Boyd, 83 p.

**Aspden J.A. & Litherland M.** 1992. The geology and Mesozoic collisional history of the Cordillera Real, Ecuador. Tectonophysics, 205, 187-204.

**Barragan R.** ***et al.*.** 1996. Geodynamic evolution of the Neogene Intermontane Chota Basin, Northern Andes of Ecuador. J. of South Am. Earth Sci., 9, (in press).

**Baudino R.** 1995. Evolution des Andes d'Equateur au Néogène: les enseignements de l'étude des bassins intramontagneux. Ph. D. Thesis, Université de Pau, France, 431 p.

**Ben-Avraham Z. & Zoback M.D.** 1992. Transform-normal extension and asymetric basins: An alternative to pull-apart models. Geology, 20, 423-426.

**Duque-Caro H.** 1990. The Chocó Block in the northwestern corner of South America: Structural, tectonostratigraphic and paleogeographic implications. Journal of South American Earth Sciences, 3 (1), 71-84.

**Lavenu A.** ***et al.*.** 1995. Neogene ongoing tectonics in the Southern Ecuadorian Andes. Analysis of the evolution of the stress field. Journal of Structural Geology, 17 (1), 47-58.

**Mc Court W.J.** ***et al.*.** 1984. New geological and geochronological data from Colombian Andes: continental growth by multiple accretion. Journal of the Geological Society of London, 141, 831-841.

**Mediavilla J.** 1991. Evolución geodinámica de la Cuenca terciaria de Girón - Santa Isabel, Sur del Ecuador. Master Thesis, Escuela Politécnica Nacional, Quito, 206 p.

**Mégard F.** 1989. The evolution of the Pacific ocean margin in South America north of Arica elbow (18°S), *In* : The evolution of the Pacific ocean margin. Oxford monographs on Geology and Geophysics, v. 8, Oxford University Press, 208-230.

**Noblet C.** ***et al.*.** 1988. Etude géodynamique d'un bassin intramontagneux tertiaire sur décrochements dans les Andes du Sud de l'Equateur: l'exemple du bassin de Cuenca. Géodynamique, 3, 117-138.

**Van Thournout F.** ***et al.*.** 1992. Allochtonous terranes in northwestern Ecuador. Tectonophysics, 205, 205-221.

**Zoback M.D.** ***et al.*.** 1987. New evidence on the state of stress of the San Andreas fault system. Science, 238, 1105-1111.

ACKNOLEDGEMENTS: This work is part of a cooperation project for the study of the Neogene Ecuadorian Andes by Institut Français de Recherche Scientifique pour le Développement en Coopération (ORSTOM), Institut Français d'Etudes Andines (IFEA) and Escuela Politecnica Nacional de Quito (EPN). I thank J. Delfaud, A. Lavenu, R. Marocco and M. Sébrier for fruitful discussions.

# THE EVOLUTION OF THE AYSEN BASIN, AN EARLY CRETACEOUS EPICONTINENTAL INTERIOR SEAWAY IN SOUTHERNMOST SOUTH AMERICA

C. Michael Bell*, Rita De la Cruz+, Manuel Suarez+ and Marisia J. Townsend*

*Department of Geography and Geology
Cheltenham and Gloucester College of Higher Education
Francis Close Hall
Swindon Road
Cheltenham GL50 4AZ
United Kingdom

+Servicio Nacional de Geología y Minería
Avenida Santa María 0104
Santiago
Chile

KEY WORDS: Aysen, Cretaceous, Sedimentary Basin, Southern Andes, Tectonics,

## INTRODUCTION

The Aysen Basin is a north-south elongated basin (Fig. 1) in which over 1200 m of shallow marine sediments accumulated in a narrow, epicontinental sea parallel to the continental margin in the southern Andes during early Cretaceous times (Suárez and De la Cruz, 1994). The basin formed in a back-arc setting as a thermal sag during a period of volcanic and tectonic quiescence. It was linked to the Magallanes Basin to the south. The sediments were derived from the continental San Jorge Basin in the east.

## TECTONIC SETTING

Extensive marine and continental sedimentary basins developed on the continental crust of southernmost South America during the Mesozoic and Cainozoic. The early Cretaceous evolution of these basins (Fig. 1) was controlled by two major tectonic events, one on either side of the continent. In the west, subduction of an oceanic plate produced a magmatic arc parallel to the continental margin. At the same time, in the east, the split-up of the Gondwana supercontinent and the opening of the South Atlantic Ocean resulted in the development of an extensive passive margin. The basins are of great economic significance as they enclose the petroleum provinces of Chile and Argentina.

Early stages of basin development during mid-Jurassic to earliest Cretaceous times were associated with extensional rifting of the continental crust. Subsequently, during the Lower Cretaceous, the dominant tectonic style over most of the area was a slow, gentle and broad subsidence, probably related to thermal sagging. There is little evidence in the sedimentary record for syndepositional tectonic or magmatic activity related either to the subduction in the west or the extension in the east. A foreland basin, associated with a western fold and thrust belt, only started to develop in the Magallanes Basin in the southern part of the region in the uppermost Cretaceous.

The sedimentary basins are floored with metasedimentary continental basement rocks, some of which were probably the product of terrane accretion. These are unconformably overlain by a widespread succession of late Jurassic subaerial volcanic rocks. By early Cretaceous (Berriasian) times broad subsidence and downwarping had resulted in the development of two major NW-SE trending sedimentary basins (Fig. 1). In the north-east between 45°and 47°S was the east-west elongated San Jorge Basin. This was separated by the uplands of the Deseado Massif from the larger Magallanes Basin to the south (Riccardi, 1988). The San Jorge Basin was filled with predominantly lacustrine and fluvial continental sediments and the Magallanes Basin with pelitic marine sediments. The evidence from prograding sequences identified by seismic stratigraphy (Biddle et al., 1986; Fitzgerald et al., 1990) indicates that most of the sedimentary infill of both the San Jorge and the Magallanes basins was derived from the north and north-east. The Somuncurá Massif was the source of sediments in the San Jorge Basin and the Deseado Massif provided clastic debris to the Magallanes Basin.

## AYSEN BASIN

Linking the San Jorge and Magallanes Basins in the west, and probably cut off by an inactive segment of a magmatic arc from the Pacific Ocean farther to the west, was the north-south elongated Aysen Basin (Suárez and De la Cruz, 1994). Although most of the clastic debris which fills this basin was derived from the erosion of volcanic rocks, there is little direct evidence for contemporaneous volcanic activity in the form of interbedded pyroclastic deposits or lava flows. A lack of soft-sediment deformation structures, mass flow deposits and turbidites suggests that the area was tectonically stable during the accumulation of the sediments.

Marine sedimentary rocks of the Coyhaique Group (Table 1) infilled the Aysen Basin. Limestones, sandstones and pyroclastic rocks of the Toqui Formation form the base of the succession. They were deposited as reefs and beaches during a marine transgression across the rocky shores of active silicic volcanoes. Deepening of the seas to form a large, sheltered marine embayment, resulted in the deposition of a thick succession of carbonaceous black shales of the Katterfeld Formation. Fossil fauna assemblages indicate that the Aysen basin was linked to the Magallanes Basin to the south. The fossils also suggest that the basin was isolated from basins to the north. The black shales are overlain, with a sharp and probably regionally significant contact, by rippled sandstones and shales of the Apeleg Formation. Sandstone lithologies and paleocurrents in the Apeleg Formation indicates that the sediments were derived from rivers flowing westward from the continental San Jorge Basin (Fig. 2).

The thick successions of well-sorted, fine-grained sandstones and mudstones, together with abundant plant debris, indicate that the sediments of the Coyhaique Group were derived from densely-vegetated areas of low relief with a warm, humid climate. The Katterfeld Formation was deposited in a large restricted marine embayment produced by flooding of the continental shelf from the south. Subsequent opening up of this embayment to the influence of tidal currents sweeping through the narrow seaway, produced the Apeleg Formation, characterised by the deposition of large, low-relief offshore tidal sandbars in a shallow shelf sea. The sea level rises which produced the initial flooding and subsequent opening of the embayment may have been related to global sea level rises of Valanginian and Hauterivian times (Vail et al., 1977),

The Aysen Basin developed in a back-arc position between an active continental margin and an undeformed continental platform (Fig. 1). Despite this setting it does not display the sedimentary characteristics of a foreland basin (Allen and Homewood, 1986). The area was apparently tectonically stable and the sediments show no evidence of eastwards thinning or fining successions. The paleocurrents indicate derivation from the continental landmass to the east rather than from a magmatic arc or a fold and thrust belt in the west.

Marine sedimentation in the Aysen Basin ended with a minor and localised episode of deformation, uplift and erosion in Barremian to Aptian times. These events were followed by extensive Aptian-Albian calc-alkaline subaerial volcanic activity which produced the unconformably overlying sedimentary and silicic volcanic rocks of the Divisadero Formation. This late Cretaceous volcanic activity was associated with a major phase of plutonic activity in the Patagonian batholith (Fig. 1).

## CONCLUSIONS

The epicontinental Aysen Basin of southern Chile and Argentina formed during early Cretaceous times as an interior seaway between an volcanically and tectonically quiescent segment of a subduction-related active continental margin in the west and a passive margin in the east.

Sedimentary basins in southernmost South America record a variety of distinctive tectonic histories. Cretaceous thermal subsidence in the Aysen and San Jorge Basins was followed by Tertiary uplift and erosion (Fitzgerald et al., 1990). By contrast the northern part of the Magallanes Basin evolved from an early Cretaceous continental thermal sag, with sediment derived from the northeast, into a late Cretaceous and Cainozoic foreland basin, with sediment derived from a fold and thrust belt in the west (Biddle et al., 1986; Ramos, 1989). Farther south, in the south of the Magallanes Basin, the Rocas Verdes back-arc basin, which opened as a narrow ophiolite-floored sea in the late Jurassic or earliest Cretaceous, became filled with deep marine sediments during the early Cretaceous. This basin was uplifted and deformed in the late Cretaceous (Dalziel, 1981). The distinct magmatic, structural and sedimentary evolution of each of these adjacent areas reflects the segmentation resulting from variations in the geometry of sections of the downgoing oceanic slab.

## REFERENCES


Allen, P.A. and Homewood, P. (eds) 1986 Foreland basins. Special Publication No. 8 of the International Association of Sedimentologists. Blackwell Scientific Publications.

Biddle, K.T., Uliana, M.A. Mitchum, R.M., Fitzgerald, M.G. and Wright, R.C. 1986 The stratigraphic and structural evolution of the central and eastern Magallanes Basin, southern South America. In: Foreland basins. Allen, P.A. and Homewood, P. (eds). Special Publication No. 8 of the International Association of Sedimentologists, 41-61. Blackwell Scientific Publications.

Dalziel, I.W.D. 1981 Back-arc extension in the southern Andes: a review and critical appraisal. Philosophical Transactions of the Royal Society of London, **A 300**, 319-335.

Fitzgerald, M.G., Mitchum, R.M., Uliana, M.A. and Biddle, K.T. 1990 Evolution of the San Jorge Basin, Argentina. American Association of Petroleum Geologists Bulletin, 74, 879-920.

Ramos, V.A. 1989 Andean foothills structures in northern Magallanes basin, Argentina. American Association of Petroleum Geologists Bulletin, 73, 887-903.

Riccardi, A.C. 1988 The Cretaceous System of southern South America. Geological Society of America Memoir 168.

Suárez, M. and De la Cruz, R. 1994 Estratigrafia del Jurasico-Cretacico Inferior de la Cordillera Patagonica Oriental (45° - 46° Latitud Sur). Chile: facies. paleogeografia. Unpublished report, Servicio Nacional de Geologia y Mineria.

Vail, P.R., Mitchum, R.M. and Thompson, S. 1977 Seismic stratigraphy and global changes of sea level, Part 4: Global cycles of relative changes of sea level. In: Payton, C.E. (ed.) Seismic stratigraphy - applications to hydrocarbon exploration. American Association Petroleum Geologists Memoir 26.


| | | Age | Succession or event | Interpretation |
|---|---|---|---|---|
| Divisadero Formation | | Aptian-Albian | Subaerial calc-alkaline volcanism | Magmatic activity in western arc |
| | | Barremian-Aptian | Local unconformity. Deformation and uplift | Minor folding and thrusting |
| Coyhaique Group | Apeleg Formation | Hauterivian-Aptian | Rippled sandstones and shales | Tidal sandbars in narrow seaway |
| | Katterfeld Formation | Valanginian-Hauterivian | Fossiliferous black shales | Embayment with restricted circulation |
| | Toqui Formation | Berriasian | Limestones, sandstones and pyroclastics | Marine transgression across active volcanoes |
| Ibañez Formation | | Mid to Upper Jurassic | Subaerial silicic volcanism | Magmatic arc in west, crustal extension in east |
| | | Early Mesozoic | Regional unconformity | Uplift and erosion |
| Metasedimentary basement | | Late Proterozoic to Palaeozoic | Continental basement rocks | Possible Paleozoic terrane accretion |

Table 1. Stratigraphy of the Aysen Basin

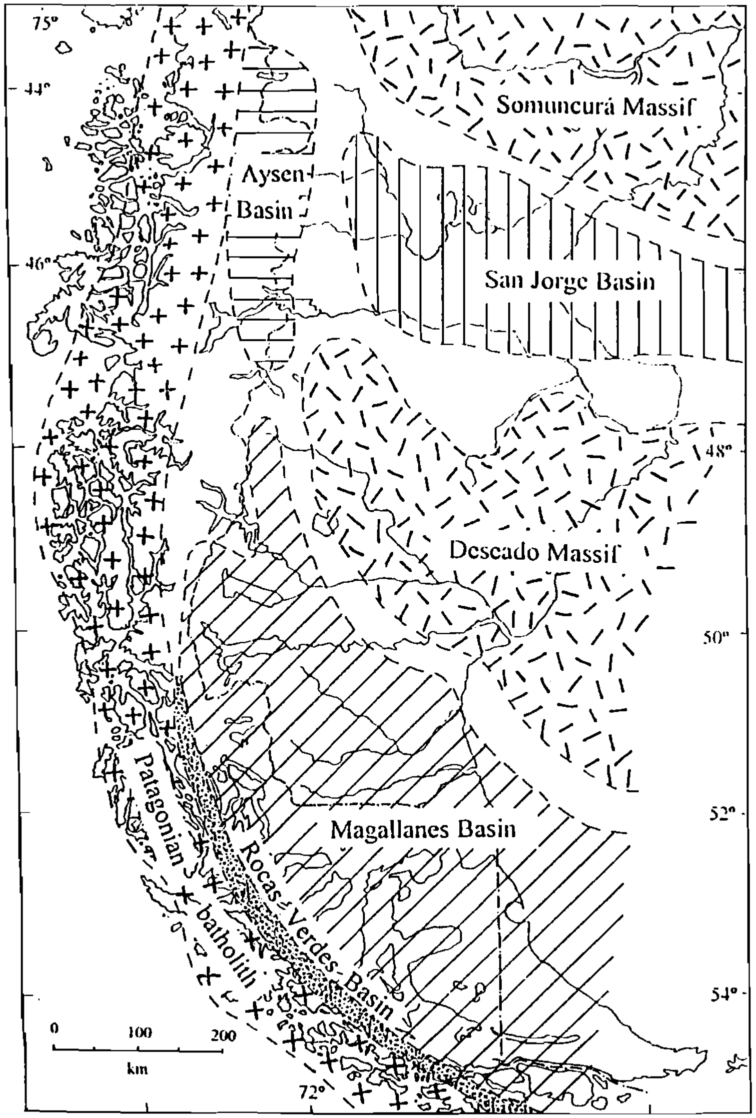


Fig. 1. Distribution of early Cretaceous sedimentary basins in southernmost South America.

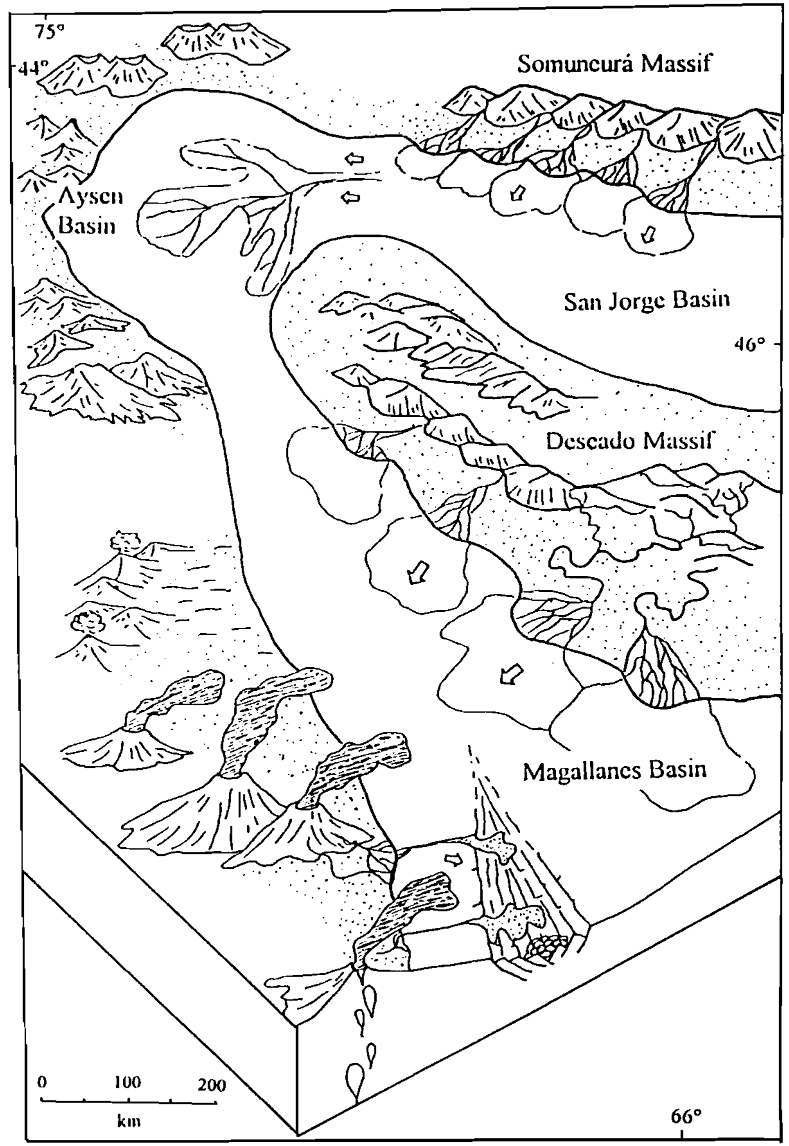


Fig. 2. Paleogeography of southern South America during the early Cretaceous.

# FORE-ARC GEODYNAMIC EVOLUTION OF THE ECUADORIAN SUBDUCTION SYSTEM

Stalin BENÍTEZ

Petroproduccion, Casilla 10829, Guayaquil, Ecuador

**KEY WORDS:** Cretaceous, Paleogene, Andean Margin, Oceanic Terranes, Accretion, Ecuador

## REGIONAL GEOLOGY

The Ecuadorian country has a physiography and a geology deeply related to the subduction system affectin uninterruptedly the West South American margin from Colombia to Chile. Consequently, there are recognized in Ecuador three main morphotectonic regions: the Coast or Forearc Region, the Sierra (Highlands) or Volcanic arc (two chains: Western and Eastern or Real) and the Oriente or backarc region which joins to the Amazonian foreland.

The Ecuadorian subduction system is characterized by the oceanic origin cretaceous basement of the forearc region and Cordillera Occidental. The same situation has been postulated for the equivalent colombian regions. Both, the colombian and ecuadorian Andes, compose the so called Northern Andes. The oceanic terranes accretion has been performed during the Palegene provoking a very deep paleographic change.

## FOREARC STRATIGRAPHY

Two main paleographic zones has ben distinguished in the forearc region. At present they are separated by the Colonche Fault. To the North of this fault in the Chongon-Colonche Hills outcrops the early cretaceous oceanic origin basement (the Piñon Formation), covered by a thick volcanoclastic sequence (the Cayo Formation) dated as upper Cretaceous. At the top of this sequence it is found a finer marine sequence (the Guayaquil Formation) with sparse intercalations of tuffaceous material dated Maastrichtien in the more cherty base and Paleocene in the slighty more calcareous resto of the formation. The top of the Cayo Formation and the Guayaquil Formation have been laterally replaced in the Manta zone by volcanic series of island arc origin called San Lorenzo Formation (Lebrat, 1985). Over the oceanic-volcanic related series and after a diastrophic event in the Paleocene-Eocene boundary there are turbiditic limestones (San Eduardo Formation) of Early to Middle Eocene age followed by hemipelagic siliceous mudstones (Las Masas and Cerro Formations). The sands and conglomerates (San Mateo Formation) deposited at the end of the Middle Eocene clearly indicates the beginning of the continental feeding just at the time of the collision between the oceanic terrain against the continental southamerican landmass. From the late Eocene until the Oligocene there are found only argilaceous neritic to upper bathyal deposits, Resting unconformably on the previous series we found the mainly Miocene to Quaternay sequences corresponding to the filling of the forarc basins formed after the collision stage.

To the South of the Colonche Fault in the Santa Elena Peninsula oilfield district cretaceous and paleogene rocks also outcrop but much more deformed tha those of the Chongon-Colonche Hills. The basement presumably of the same oceanic origin doesn't crop out, but only tectonized fragments of it are found intercalated with contorted radiolarian shales similar to those of the Guayaquil Formation. They are dated Campanian to Paleocene. After unconformity of middle Paleocene age the Azucar turbidic sands and conglomerates dated late Paleocene are found. This formation is mainly composed of quartz and matamorphics detrital elements which indicates a contienental basement provenance, corroborated by NNE trend of the paleocurrents; the area souce is certainly the Amotape NW peruvien province. After a new diastrophic event they are deposited in the Early?-Middle Eocene the turbidites and argilaceous beds of the Ancon Group in a paleoenvironment of neritic to bathyal depth. An unconformably neogene filling is found in the subsiding zones of Progreso and Jambeli forearc basins.

## VOLCANIC ARC STRATIGRAPHY

In the Cordillera Occidental a similar to the Northern Coast Cretaceous to Paleogene stratigraphic sequence is found, though more deformed and less known at present. Tectonic scales of an oceanic basement, and of late cretaceous volcano-clastic series have been mapped. There are also found arc-island origin series named Macuchi unconformably covered by turbiditic Eocene limestones (Unacota Limestone), followed by the Apagua Formation sandstones and conglomerates (Eguez, 1986; Santos and Ramirez, 1986). The first calcalkaline volcanic arc rocks are the Alausi adn Lower Saraguro Formations recently dated Late Eocene by radiometric methods by Lavenu et al (1982).

In the Cordillera Oriental or Real, buitl-up of metamorphic and igneous rocks of jurasic age reseted in the Late Cretaceous (Aspden, 1992), it is not found a younger sedimentary or volcano-clastic cover but some datings in igneous intrusions seems to indicate a volcanic arc activity during the Paleocene-Eocene, contermporaneously with the Macuchi island arc.

## GEODYNAMICS

Three main evolutionary stages are distinguished in the forearc region and Cordillera Occidental. During the first stage (late Aptian-Early Campanian, 108-08 Ma) or pre-collision stage, this region underwent an oceanic type evolution. The early cretaceous oceanic crust (Piñon Formation) was unusually thickened due to the influence of a hot spot. Over this crust it developed an dipping East island-arc system which emerged locally (Cayo Arc). The arc products originated thic grawackes deposits (Cayo Fm.) in the barck-arc marginal basin located between the arc and the Southamerican continent.

The second stage or collision stage does not occur simultaneously in the whole forearc region. The collision is essentially oblique, beginning in the South by the collision of the Amotape Block against the NO peruvian margin during the Early Campanian (E. Jaillard pers. comm.) provoking its rotation and accretion. The collision continues to the North with the accretion of the Santa Elena Peninsula during the Paleocene. The Coastal Block to the North of the Colonche Fault and the Cordillera Occidental were accreted at the end of the Middle Eocene.

The third stage or post-collision stage started in the Late Eocene developing the present forearc basins which underwent a stronger subsidence period during the Miocene and locally during the Pliocene-Pleistocene. The main deformation in this stage is atributed to transcurrent faulting due to the partition phenomena of the Nazca Plate oblique subduction. The collision and subduction of the Nazca (12 Ma) and Carnegie (2 Ma) ridges have locally and temporarily affected the sedimentation buy they have not produced very deep transformations in the forearc region.

The invoked mechanism capable to provoke the collisions is the installation during the Campanian of a second East dipping subduction zone paralell to the ancient cretaceous system subsisting to the West, which followed the marginal basin axis then located between the cretaceous island-arc and the Southamerican continent. Both subduction systems might have funcioned simultaneously until the Middle-Upper Eocene. From the Oligocene it survives only the more ancient and more occidental subduction system which envolves during the Neogene to its present condition.

# BASEMENT FAULTING AND INVERSION OF THE NW NEUQUÉN BASIN, ARGENTINA.

Jacqueline L.M.Booth and Mike P.Coward

Department of Geology, Imperial College, Prince Consort Road, London SW7 2BP, England.

**KEYWORDS :** Inversion, Backthrusting, Los Molles Formation, Cordillera del Viento.

## INTRODUCTION.

The Neuquén Basin lies to the immediate east of the Andean Cordillera in Argentina, between the latitudes of 35° and 41°S. It formed as a back-arc extensional basin during the Late Triassic and Early Jurassic, open to the Pacific at its northwestern margin. The Mesozoic and Cenozoic sedimentary infill reaches a thickness of 7km (Vergani et al., 1995), a lengthy period of thermal subsidence (Aalenian to Albian) succeeding the initial rifting (Norian to Toarcian). Inversion of the generally north-south trending normal faults in the western half of the basin began in the Eocene, uplifting several sizable basement blocks above surface level. One of the largest of these blocks is the Cordillera del Viento in the northernmost part of Neuquén Province. The results of field studies, the analysis of seismic lines and Landsat TM images, and palaeomagnetic data from around this range and to the north in Mendoza Province will be presented here.

## STRATIGRAPHY

Recent works on the stratigraphy have analyzed it using sequence stratigraphic divisions (e.g. Legarreta and Gulisano, 1989). The Jurassic to Early Tertiary succession can be separated into ten mesosequences, the first two of which make up the Norian to Toarcian synrift, lying on a basement of Carboniferous to mid-Triassic volcanics (Choiyoi) and clastics. The mesosequences begin with a continental clastic unit, then a transgression to give platform and deeper basin deposits, followed by gradual progradation of marginal facies from the south and east towards the northwest. The termination of several mesosequences reveal basin dessication and hypersalinity, the evaporite horizons having since been utilized as detachments during inversion.

Sediment thicknesses increase greatly towards the northwest of the basin, a large depocentre originally being located in the Chos Malal area (Figure 1), although amalgamation of the isolated half-grabens in response to thermal subsidence did not occur until the mid Jurassic (Vergani et al., 1995). Following the subsidence during the later Mesozoic, the loading by the Andean magmatic arc in the Tertiary produced a narrow foreland basin along the Chilean border.

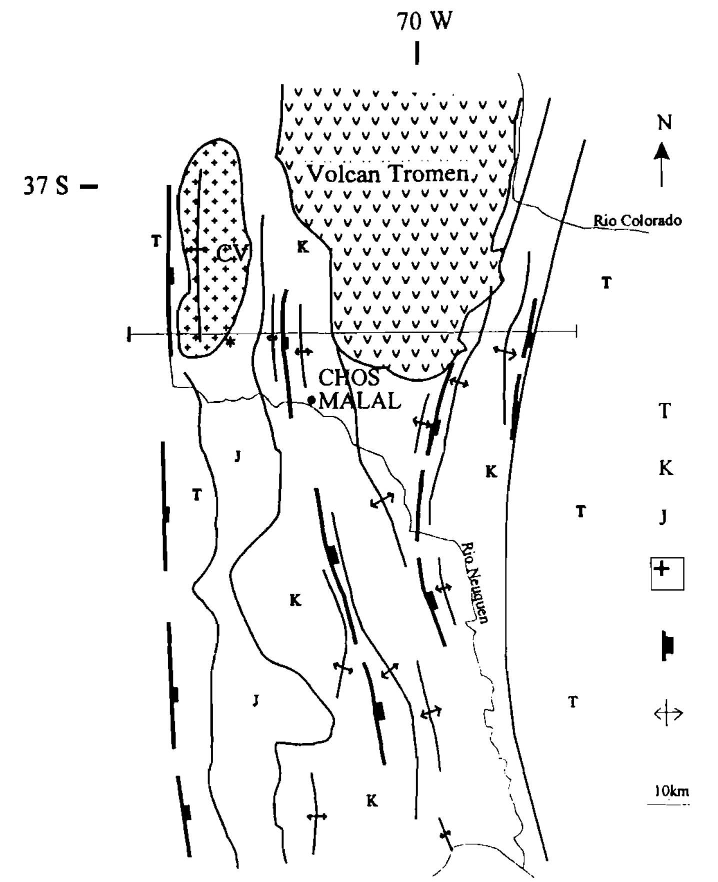


**Figure 1.** Sketch map of the Chos Malal area of Neuquén Province, Argentina, based on Landsat™ image. Section line for Fig.2 marked, * shows locality of outcrops shown in Fig. 3.

## STRUCTURE

A variety of structural styles are observable in the area around Chos Malal (Figures 2&3). Field sections made across this region show large-scale basement involvement in the compression, but in a thick rather than thin-skinned style (which would utilize low-angled thrusts); significant changes in fold wavelength; multiple detachments and backthrusting.

The Cordillera del Viento is interpreted as an inversion of a large west dipping half graben in which significant increases in the synrift Los Molles Formation (Toarcian) thickness occur. Uplift of the basement on high angle reverse faults (50°-70°) has produced a broad anticline, movement on the west-dipping thrust passing into backthrusts at the base of Los Molles. At the outcrop scale a brecciated band, 15m thick, of these shales is found above the basement (Choiyoi Group), with top-to-the-west shear sense in highly deformed beds. Structures here show mesoscale inversions (Figure 3) which provide a good analogue for the Cordillera del Viento anticline. Why forward propagation of the thrust should be transferred to antithetic motion here at the pre to synrift boundary may be explained by the elasto-plastic, non-viscous nature of overpressured shales (Los Molles is one of the source rocks for the overlying sandstones), in which localized shear zones can form but complete decoupling around the fault cannot (Verschuren et al., 1996). It is equally feasible that these backthrusts represent inversion of secondary normal faults, formed during the Pliensbachian-Toarcian rift phase, giving an inherited weakness to this unit.

Fifteen kilometres to the east along section, and less well constrained, is the Las Macinas anticline. This can be related to the structural inversion of another smaller half-graben of similar polarity (normal displacement approximately 500m). Thrust movement has been transferred from the steep palaeo-normal fault to footwall

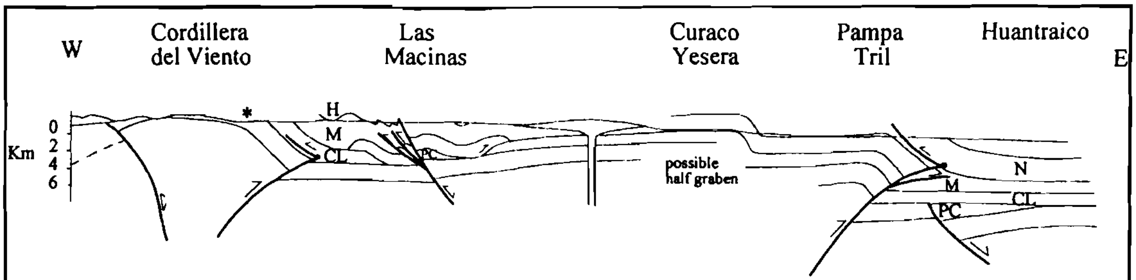


**Figure 2.** Sketch section showing the structures along a W-E transect from the Cordillera del Viento to Filo Morado (see Fig. 1 for location). Sequences - PC: Pre-Cuyo; CL: Cuyo and Lotena; Mendoza Supersequence; N: Neuquén, (all are mesosequences unless stated). * marks location of outcrops shown in Fig.3. No vertical exaggeration.

shortcuts, evidenced by overturned folds at the surface in the Huitrín Formation. Foreland-directed thrusting out of the graben occurs at the pre-synrift boundary, possibly in response to back-rotation of the normal fault about an horizontal axis.

To the east of Las Macinas there is a change from west to east fold vergence and an increase in fold

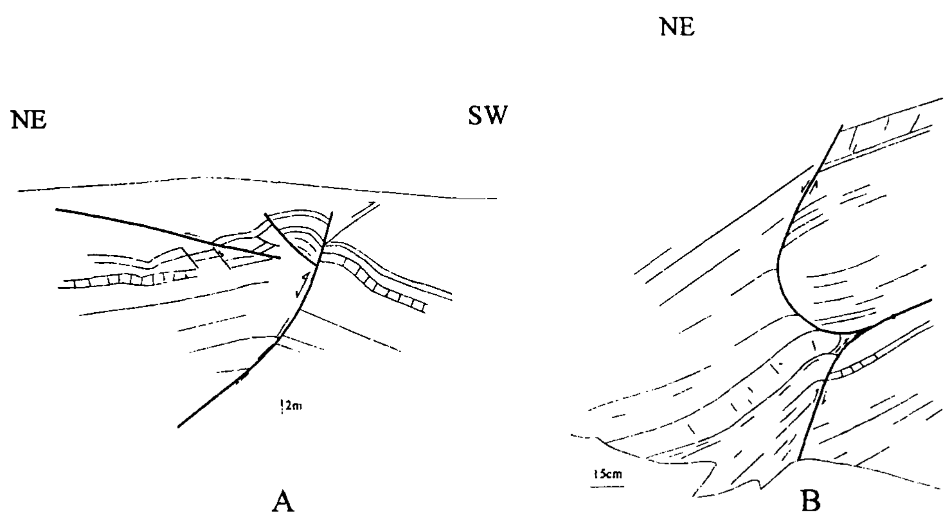


**Figure 3.** Meso-scale inversion structures within the Los Molles Formation. A: Inverted normal fault showing expulsion of the hanging-wall, with possible reworking of earlier antithetic faults. B: Incipient Ile flottante footwall shortcut of a palaeo-normal fault. Footwall cut-offs on lower thrusted segment are 70° - 80°, identical to those preserved in the uninverted fault.

wavelength and asymmetry, reflecting a change in inversion style. The Curaco Yesera del Tromén and Pampa Tril monoclines have very gently dipping backlimbs of 10-15km length and short, hooked forelimbs. Wells drilled through Pampa Tril show basement at a depth of 1470m (Viñes, 1990). This fold may have formed as a basement-involved fault propagation fold localized on the underlying normal fault - the short Huantraico Rift, beneath the syncline of the same name. Earlier interpretations of this structure have reconstructed it with hidden duplexes in the triangle zone between the two folds, (Viñes, 1990, and Ploszkiewicz, 1987). The Huitrín salt horizon which forms the top of the seventh mesosequence (Aptian) becomes active as a detachment in this structure. It acts as a slip horizon backthrusting the western limb of the Huantraico syncline over the monocline forelimb.

This is the eastern limit of the Andean deformation front, the undeformed external parts of the basin lying in the foreland. Basement involved thrusting of similar geometry is also characteristic of the fold and thrust belt margin to the north towards Malargüe in Mendoza Province.

## CONCLUSIONS

The role of basement in affecting the structural style of the Neuquén fold and thrust belt has been significant. Shortening across the area has been in the order of 20%, and occurred mostly during the Oligocene and Miocene in response to easterly-directed compression from the Andean chain, though possibly including a component of ridge-push from the South Atlantic ridge.

## ACKNOWLEDGMENTS

J.Booth wishes to thank Daniel Boggetti for help and advice in the field, and GAMSA in Mendoza for logistical support and the Landsat data.

## REFERENCES

Legeretta L., and Gulisano C.A., 1989. Análisis estratigráfico secuencial de la cuenca neuquina (Triásico Superior - Terciario Inferior), Argentina, in G.A.Chebli and L.A.Spalleti, eds., *Cuencas Sedimentarias Argentinas:* Serie Correlación Geológica 6, 221-243.

Ploszkiewcz J.V., 1987. Las zonas triangulares de la faja fallada y plegada de la cuenca Neuquina, Argentina. *Decimo Congreso Geologico Argentino, San Miguel de Tucuman,* Actas I: 177-180.

Vergani G.D., Tankard A.J., Belotti H.J., and Welsink H.J., 1995. Tectonic evolution and paleogeography of the Neuquén Basin, Argentina, in A.J.Tankard, R.Suárez S., and H.J.Welsink, *Petroleum basins of South America*: AAPG Memoir 62, 383-402.

Verschuren M., Nieuwland D., and Gast J., 1996. Multiple detachment levels in thrust tectonics: sandbox experiments and palinspastic reconstruction, in P.G.Buchanan and D.A.Nieuwland, eds., *Modern developments in structural interpretations, validation, and modelling,* Geological Society Special Publication No.99, 227-234.

Viñes R.F., 1990. Productive duplex imbrication at the neuquina basin thrust belts, Argentina, in J.Letouzey, ed., *Petroleum and tectonics in mobile belts*: Paris, Edition Technip, 69-80.

# SUPERPOSED STRUCTURAL STYLES OF THE MARACAIBO BASIN, VENEZUELA

Emilio Bueno R.

Maraven, S.A.
Caracas 1010 A, Venezuela
Apartado 829

KEY WORDS: Maracaibo basin, structural evolution, Caribbean plate collision, Lara nappes obduction, Eocene foreland basin, superposed tectonics

## INTRODUCTION

The Maracaibo basin, which is located between two andean chains, the Merida Andes and the Sierra de Perija (fig. 1), has been subjected to several deformation styles during its geologic evolution.
The objective of this paper is the explanation of the different tectonic phases which deformed the sediments of the Maracaibo basin. This structural evolution was constructed from the interpretation of a transect of 2D and 3D seismic lines, which cross the basin from NW to SE (fig. 2).

Fig 1. The Maracaibo Block

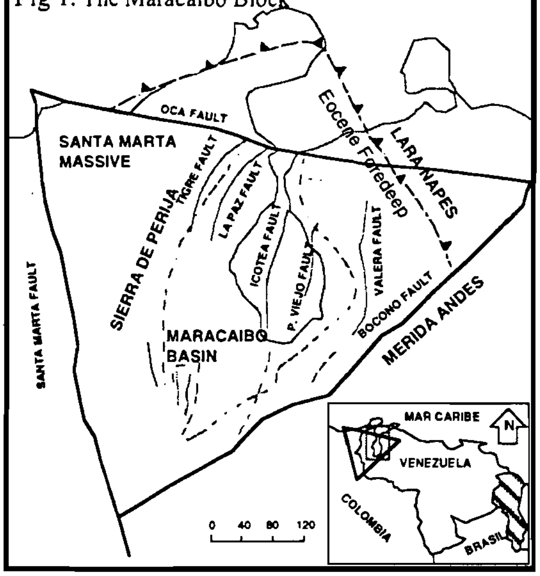


## STRUCTURAL FRAMEWORK

The actual Maracaibo basin is located inside a triangular tectonic block (fig.1), bounded by the Bocono fault, in the Merida Andes, the Santa Marta fault, located west of the Sierra de Perija in Colombia, and the E-W striking Oca fault, running parallel to the boundary with the Caribbean plate.
Before the uplift of the Merida Andes, the basin included the Barinas-Apure basin, located south of the Andes.
Inside the triangular tectonic block, one can differentiate two fault systems: a N to NE striking fault system, which experienced compressional deformation by episodic pulses, and an extensional W to NW striking fault system. The N to NE striking system consist of two main faults (fig. 3). A lower fault, which is a thrust propagated at basement and Cretaceous levels and generally absorbed by the Colon shales (Upper Cretaceous). This fault is converted into a drape fold structure at Paleocene levels. The upper fault is a normal growth fault at the Eocene level and strikes opposite to the overprinted thrust

## STRUCTURAL EVOLUTION

During the breakup of Pangea (Triassic-Jurassic times), the North and South American plates separated from each other forming a belt of rift-grabens (Pindell, 1990), opening the space for the depositional history of the Maracaibo basin. The graben system extended from the Gulf of Venezuela to the south-

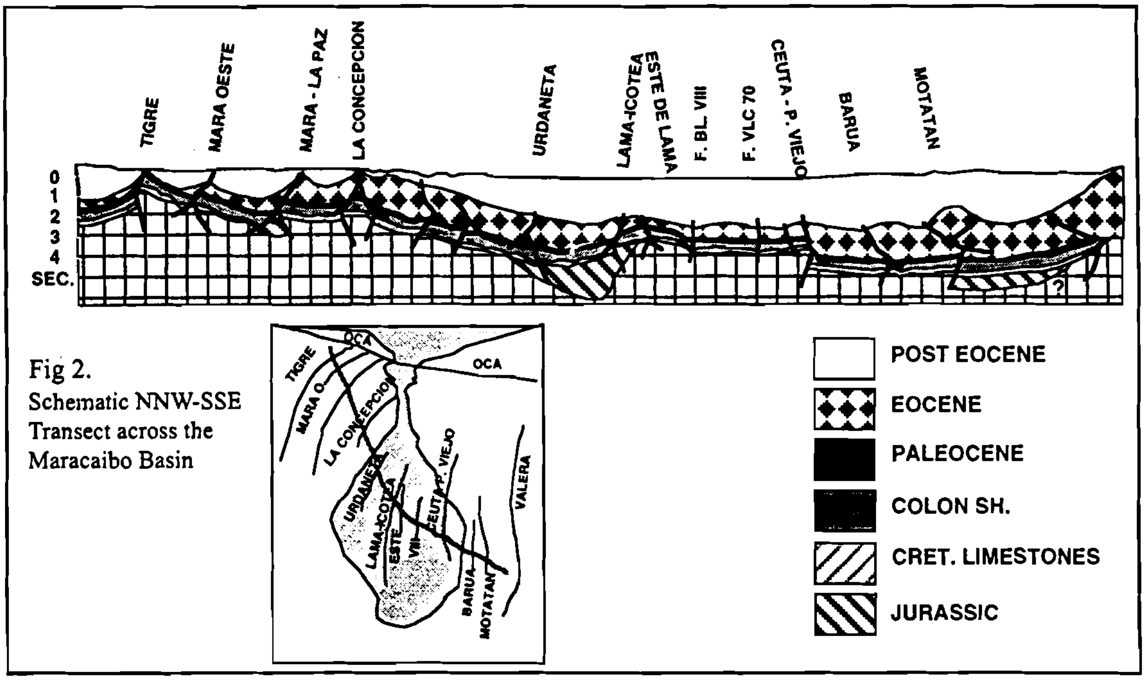


Fig 2.
Schematic NNW-SSE Transect across the Maracaibo Basin

reaching Ecuador (Bartok, Reijers and Juhasz, 1981).
The Jurassic La Quinta formation filled the grabens with volcano-sedimentary sequences. Some of these grabens are buried under the thick sediments of the Maracaibo basin and others are outcropping both in the Merida Andes and the Sierra de Perija

The graben system that developed from extension changed to a compressional phase presumably during Upper Jurassic to Lower Cretaceous times. Subsequently, the sediments were folded and faulted culminating in a partial to total erosion (Stephan, 1980).

During the Cretaceous , the sediments were deposited in a passive margin setting (Pindell, 1990) under broad subsidence . After the basal Rio Negro sands thick sequences of the Cogollo group carbonates were deposited (Lower Cretaceous). This was followed by the black bituminous limestones of La Luna formation, which is considered as the main source rock for oil in the basin. The Upper Cretaceous was characterized by the shaly Colon formation, set behind the arch environment (Bartok et al., 1981).

Up to the end of Paleocene and during Eocene the basin area faced an eastward moving Caribbean plate across its northern edge. The encounter with this Pacific-derived plate caused two different kinds of events. To the northwestern part of the basin ocurred a collision and subduction. But, the northeastern edge underwent an obduction.

The oblique collision with the Caribbean plate caused a subduction under the Santa Marta Massive in Colombia, which

Fig 3. E-W Section across the Icotea Structure

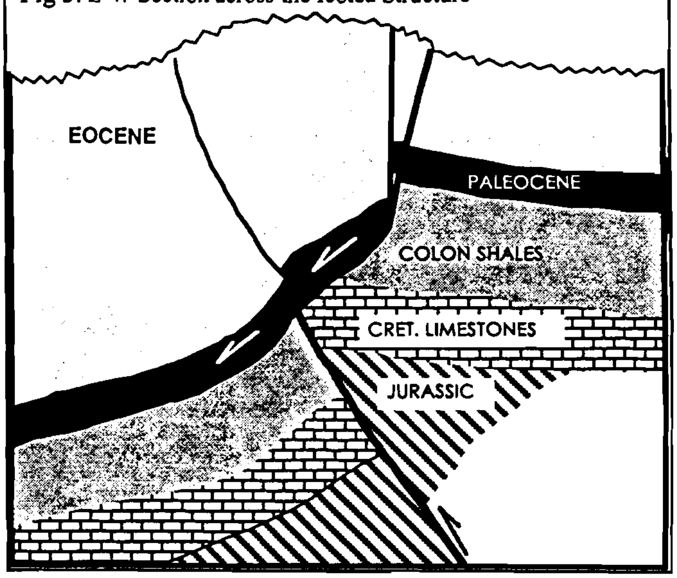

extended under the Maracaibo basin (van der Hilst, 1993). The resulting compression created a thrust belt in the Sierra de Perija and a foreland tectonic province in the Maracaibo basin. The thrust belt is characterized by faults in a thin-skinned setting, while the foreland area developed basement-involved faults.
In the foreland tectonic province set in the Maracaibo basin, the compression caused thrust propagation along old N to NE oriented Jurassic grabens and related structures. The thrusts extended across the basement and Lower Cretaceous carbonates, but once reaching the Upper Cretaceous Colon shales, the reverse faulting detoured and was absorbed. At Paleocene levels, the thrusts were developed into drape fold structures. In the foreland province of the Rocky Mountains in Wyoming, one can observe similar drape fold structures (Lowell. 1985). The resulting high and low areas were filled by Eocene tectono-sedimentary sequences and bounded by normal growth faults dipping opposite to the overprinted thrusts. The compressional deformation took place though episodic pulses. Each tectono-sedimentary sequence began with a sediment deposition under extensional regime. After a compressional pulse the sediment wedges were shortened, slightly folded, inverted and sometimes slightly eroded. A new deposition began once the compresional pulse ended, began a new deposition. Seismic lines of the Mara field (in the western part of the basin) define three different tectono-sedimentary sequences for the Eocene and another three for post-Eocene times (fig. 5).

Fig 4.
Eocene Structural Duality
(Compression /Extension)

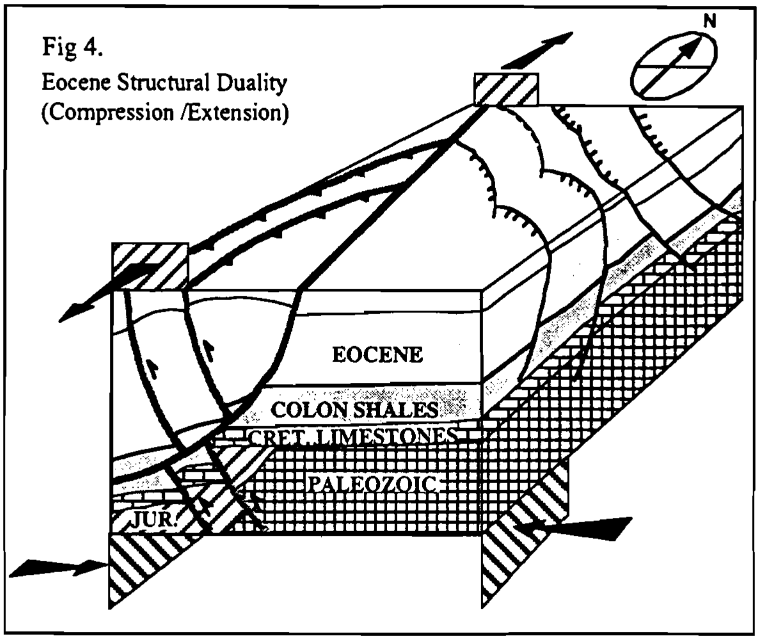


The compressional Eocene deformation involved only faults striking N to NE, while taking into account that the main shortening axis was oriented NW-SE (figs. 3 & 4).

The extensional deformation was opposite to the compressional forces (fig. 4). As the Caribbean plate appeared along the northern edge of the Maracaibo basin, its charge produced a flexural deformation, resulting in a foredeep located close to the allochtonous body. The foredeep advanced eastwards together with the Caribbean plate.
This event transformed the area of the Maracaibo basin into a foreland basin (Lugo and Mann, 1993). To accomodate to this new situation, the old sedimentary passive margin platform completed a lithospheric bend toward the foredeep. In this extensional environment were normal faults striking W to NW, allowing for a stepweise descent into the foredeep.
Towards the central part of the lake (during Lower Eocene times) was located a high, which was presumably a reactivation of the Merida High - active during the Paleozoic. Large normal growth faults bound the northern and southern edges of this high.
The eastward migration of the Caribbean plate lead to an obduction. The Lara nappes were pushed over part of the actual Falcon and Lara areas (Stephan, 1977,1980). The foredeep was located close to the obduction zone in the northeastern part of the basin.

The combination of NW oriented compression with the eastward foredeep migration which merged with the Caribbean plate) resulted in a clockwise rotation of the main blocks of the Maracaibo basin. This action caused sinistral strike-slips along the main faults striking N to NE.

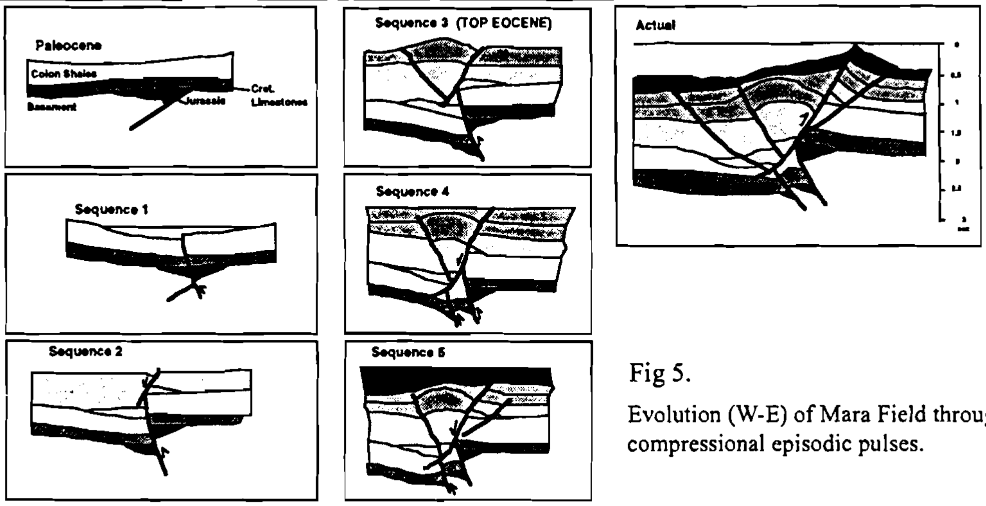


Fig 5.
Evolution (W-E) of Mara Field through compressional episodic pulses.

CONCLUSIONS

The structural styles that have ocurred in the Maracaibo basin were heavily influenced by plate tectonics. The breakup of Pangea opened the space for Jurassic sediment deposition, followed by a quiet Cretaceous passive margin. Once the Caribbean plate appeared in the northern edge of the area during the Upper Paleocene, the environment changed to a foreland tectonic province. During the Eocene, the oblique collision with the Caribbean plate in the northwestern edge of the basin (and the following subduction) produced a NW-SE compression. This caused thrust propagation at the border of old jurassic grabens. While in the opposite quadrant a foredeep produced by the charge of the allochton and later, by the obduction produced in the northeastern basin edge, gave place to an extensional deformation in a foreland basin setting. The resulting normal faults strike E-W to NW-SE.
Additionally, the combination of the NW oriented compression with the eastwards foredeep migration (which merged with the Caribbean plate) resulted in a clockwise block rotation. Thus causing sinistral strike-slips along the main faults striking NNE.

REFERENCES

**Bartok, P., Reijers, T.L.A. and Juhasz, I., 1981**:
Lower Cretaceous Cogollo Group, Maracaibo Basin, Venezuela: Sedimentology, Diagenesis and Petrophysics. Am. Ass. Petrol. Geol. Bull., v 65p. 1110 -1134.
**Lowell, J.D., 1985**:
Structural Styles in Petroleum Exploration. OGCI Publications, Tulsa.
**Lugo, J. and Mann, P., 1993**:
Tectonic implications of Paleocene-Eocene foreland basin. Lake Maracaibo, Venezuela. A.A.P.G. Bull. 77. 331.
**Pindell, J.L. and Barret, S.F., 1985**:
Geological Evolution of the Caribbean . A Plate-Tectonic Perspective, in: Dengo, G. and Case, J.E., eds., The Geology of North America, Boulder, Colorado, p. 405-432.
**Stephan, J.F., 1977**:
El Contacto Cadena Caribe-Andes Merideños entre Carora y El Tocuyo (Edo. Lara). Observaciones sobre el estilo y la edad de las deformaciones cenozoicas en el occidente venezolano. V Congreso Venezolano de Geología, Caracas, v.2, p. 505-530.
**Stephan, J.F., Beck, C., Bellizzia, A. et Blanchet, R., 1980**:
La Chaine Caraibe du Pacifique à l'Atlantique. 26th. Geological International Congress. Abstracts C.t. p. 38-59.
**Van der Hilst, R. and Mann, P., 1993**:
Tectonic Implications of Tomographic Images of Subducted Lithosphere beneath Northwestern South America. A.A.P.G./S.V.G, International Congress and Exhibition, Caracas.

# THE RED BEDS OF THE SAN JERONIMO GROUP (CUZCO PERU) MARKER OF THE INCA 1 TECTONIC EVENT

Víctor CARLOTTO(1), Gabriel CARLIER (2), José CARDENAS(3) Willy GIL(3), Richard CHAVEZ(3)

(1) Universidad Nacional San Antonio Abad del Cuzco (Peru) and Laboratoire de Géodynamic des Chaînes Alpines Grenoble (France)
(2) ORSTOM, TOA, UR 1H, 213 rue La Fayatte, 75480 Paris,France.
(3) Universidad Nacional San Antonio Abad del Cuzco Av. de la Cultura s/n Cuzco-Peru.

**KEY WORDS:** San Jeronimo Group, Middle-Eocene- Early Oligocene, Inca 1 Tectonic, Cuzco, Peru.

## RESUMEN

Las Capas Rojas del grupo San Jerónimo eran consideradas de edad Cretácica superior y su origen estaba relacionada a la fase Tectónica Peruana. Sin embargo, la sucesión estratigráfica, observaciones de campo, correlàciones y una datación radiométrica, muestran que esta unidad abarcaría desde el fin del Eoceno medio hasta el fin del Oligoceno inferior y que la sedimentación estaría relacionada al evento Tectónico Inca 1, que en la región se traduce como un *continuum* tectónico compresivo, desarrollando fallas de rumbo, sobre las que se formaron cuencas *pull-apart*.

## INTRODUCTION

A red series of continental origin which is more than 5,000 meters thick, which is known with the name of Red Beds (Marocco, 1978) or San Jeronimo Group (Córdova,1986), widely crops out in the region of Cusco and Sicuani. In Cuzco, the San Jerónimo Group has been divided in 3 Formations, Kayra (3000 m), Soncco (1600 m) and Punacancha (1700 m) (Córdova, 1986).

Former Studies had considered to the Red Beds of the San Jerónimo Group, as the Latest Cretaceous-Tertiary age (Marocco, 1978; Córdova, 1986).The Maastrichtian times, given to the Kayra and Soncco Formations,was based first on the charopytes presence near the Kayra base, which indicate The Maastrichtian age and then for the "dinosaur tracks" presence near the top of the Soncco Formation (Córdova, 1986; Noblet et al 1987). Then the Punacancha Formation would be Tertiary, this disconformably overlies the Soncco Formation. Further studies (Carlotto, 1992), have demonstrated that the San Jerónimo Group overlies on the paleontologycally dated series, which is of The Paleocene-Earliest Eocene times (Quilque and Chilca Formations) (Fig. 1A), that is why it was considered the overthrust in order to explain the supposed abnormal superposition (Carlotto 1992; Jaillard et al 1993).

The field works, the tectonic sections analysis and the stratigraphic correlations gave the benefit of the doubt to the overthrust existence, that is why, it was important to review and look for other ways of datation for the Red Beds. To the South-east of Cuzco, in the SW anticline limb, we have the type section of the San Jerónimo Group where the volcanic tuffs, which were found under the "dinosaur tracks", were sampled to be submitted to a radiometric datation. These samples gave a K/Ar age of 29.9±1.4 Ma (Carlotto et al 1995).

This age, plus the stratigraphic succession, the correlations and structural sections, indicate that the Red Beds of the San Jeronimo Group are before to the Late Oligocene times (28 Ma) and discard the Latest Cretaceous age based in supposed dinosaur tracks. Therefore, they also discard its relation with the Peruvian Tectonic Event.

## SEDIMENTARY EVOLUTION AND STRUCTURAL SETTING

The obtained datation only lets us know the top's age of this unit. However, the Red Beds overlie on disconformity to the Chilca Formation of Late Paleocene-Earliest Eocene age. On the other hand, Noblet et al (1987) has made sedimentation rate calculations of the Sicuani's Red Beds (near Cuzco), where by comparisons with the pull-apart and the rift basins, he indicates that these Red Beds could have been deposited in 15 Ma approximately. If we consider these data as valid the Red Beds' base would be of the final Middle Eocene (≈43 Ma).

The sedimentary evolution of the Red Beds is divided in two coarsening upward sequences (Kayra and Soncco Formations) (Fig. 1A). The deposit means are characterized by floodplains that are flown by braided rivers (Córdova, 1986). The first sequence (Kayra Formation) corresponds to the basin opening related to the strike-slip faults, where the coarsening upward sequences indicate that the fluvial sedimentation progrades especially from South to North (Córdova ,1986). The volcanic activity seems weak and null. In the second sequence (Soncco Formation), the rivers proceed preferably from the SE (Córdova, 1986). The development of progressive unconformities predominates in different places, beginning from the inferior limit of this sequence and it is associated to the compression. The volcanic activity becomes more important. The dated sample is located at the top of this Formation, in other words, it is found on the last levels of the progressive unconformities. Synsedimentary tectonic features has been already recognized within the Cuzco-Sicuani basins by Noblet (1985) and Cordova (1986).

Red Bed outcrops appear in the Cuzco region, to the north of a curved structure (Fig. 1B), to the limit between the NE border of the South Peruvian Western Trough and the Cuzco-Puno Swell. These outcrops can be divided in 3 different sectors: In the NW Sector there are folds NE-SW (Fig. 1B), while in the East Sector, the folds have a NW-SE, N-S and E-W direction, it is in this last system, where more spectacular progressive unconformities can be seen. Finally in the Central Sector, mainly gypsum, silts, and limestones crop out in a diapir fashioned way, on which little isolated bodies of the Red Beds appear. Inside of this evaporitic body there are thrustings that make the gypsum levels repeat. Nevertheless, the evaporites also appear in the other sectors delimiting the folds that affect the Red Beds.

What is essential of the structuration as it is observed now, has been acquired during the sedimentation of the Red Beds. The later tectonic effects have not greatly modified it.(Córdova,1986).

## GEODYNAMIC CONTEXT

The Inca 1 Tectonic crisis of the Middle Eocene (44-42 Ma) is defined as a short duration event (Soler, 1991). This event corresponds to the anomaly 18 (≈43 Ma) (Pilger, 1983) that indicates an abrupt velocity increase of the Pacific SE and a slight direction modification of the convergence. Also, for the Pacific SE, the anomaly 13 (Pilger, 1983) corresponds to a change of convergence direction between the Farallon and South America plates and a net velocity decrease. The convergence direction passes from N45° (Anomalies 13 - 16) and N70° (Anomalies 13-12).

According to this geodynamic context, we think that the so called Inca 1 Tectonic crisis would be responsible of the beginning of the Red Bed basin functioning and that this would not have behaved only as a short duration crisis, but as a continuum tectonic. Thus the tectonic evolution of the 3 formerly described sectors can be explained considering the average vector of convergence between the Farallon and South America plates of N45°, before the anomaly 13 (Pilger, 1983) and N70°, that is posterior to this anomaly. A senestral strike-slip movement is produced with the NE vector in the fault segment in the NW Sector. This movement controls the opening of the NE-SW pull apart basin and its posterior evolution, evidenced now by the NE-SW folds. In the East Sector, which is the most complex, the different direction folds seem to define pull-apart basins controlled by old accidents (Cordova 1986). The origin of these pull-apart basins would be related to regional dextral strike-slip motions. In this East Sector, the main efforts NE (N45° to N70°), can produce locally senestral strike-slip faults. Indeed, the progressive unconformities of the Ancaschaca zone and the Occopata one (Fig. 1), can be explained by senestral motions, controlled by old accidents. The progressive unconformities not only had a tectonic control but also they seem to have been controlled by diapirisim phenomena, which have synchronically worked. In the Central Sector, the regional strain NW-SE, produces thrusting. In front of them type Dome structure of evaporites are formed, which explains the great gypsum abundance (Fig. 1C). Little Red Bed bodies are placed over the evaporites and in front of the thrust.

## CONCLUSIONS

The Red Beds sedimentation of the San Jeronimo Group, corresponds to the pull-apart basins, controlled by strike-slip faults, as it was previously interpreted (Córdova, 1986; Noblet, 1987). These faults are inherited structures of the Pre-Mesozoic and Mesozoic paleogeography, to the boundary between the Cuzco-Puno Swell and the NE border of the South Peruvian Western Trough. In this compressive context the Cusco region, presented a curved zone with the NW-SE and E-W faults propense to the strike-slip fault development.

The sedimentological evolution, the synsedimentary tectonic structures (progressive unconformities, faults, clastic dykes, etc), clearly show that the Red Beds of the San Jerónimo Group have been deposited under a constant tectonic regime. In a first moment the pull-apart basins individualize themselves and important progressive unconformities are developed right after. This is explained by the regional changes of strain related to the convergence of the plates. All of this is interpreted as the result of the Inca 1 Tectonic Event that starts in the Middle Eocene Times (44-42 Ma) and continues as a tectonic continuum until the end of the Early Oligocene times.

## REFERENCES

Carlotto V.1992. Relations entre sédimentation, paléogéographie et tectonique dans la région de Cuzco (Sud du Pérou) entre le Jurassique superieur et le Paléocène. DEA University of Grenoble, 73 p.

Carlotto V., Carlier G., Cárdenas J. 1985. La edad de las Capas Rojas del Grupo San Jerónimo (Region de Cusco) y su significado tectónico. Seminario Taller Evolución de la Litósfera en los Andes Peruanos y sus márgenes, Lima. 2p.

Cordova E.1986. Un bassin intramontaneux andin péruvien. Les Couches Rouges du bassin de Cuzco (Maastrichtien-Paléocène). Thesis Third Cycle University of Pau, 272 p

Jaillard E., Carlotto V., Cardenas J., Chavez R., Gil, W. 1993. La "Nappe des Couches Rouges" de Cuzco (Sud de Pérou): Mise en évidence stratigraphique, interprétations tectoniques et paléogéographiques. *Comptes Rendus de l' Académie des Sciences, Paris*, 316: 379-386

Noblet C., Marocco R., Delfaud J. 1987. Analyse sédimentologique des "Couches Rouges" du bassin intramontagneux de Sicuani (Sud du Pérou). *Bulletin de l'Institut Francais d'Etudes Andines*, 16: 55-78. Lima

Marocco R. 1978. Estudio Geológico de la Cordillera de Vilcabamba. *Boletín del Instituto de Geología y Minería*, D, 4; 157 p. Lima.

Soler P. 1991. Contribution a l'étude du magmatisme associé aux marges actives-Pétrographie, géochimie et géochimie isotopique des roches intrusives sur un transect des Andes du Pérou Central-Implications géodynamiques et métallogéniques. Dr Thesis University of Paris VI, Paris, 950 p

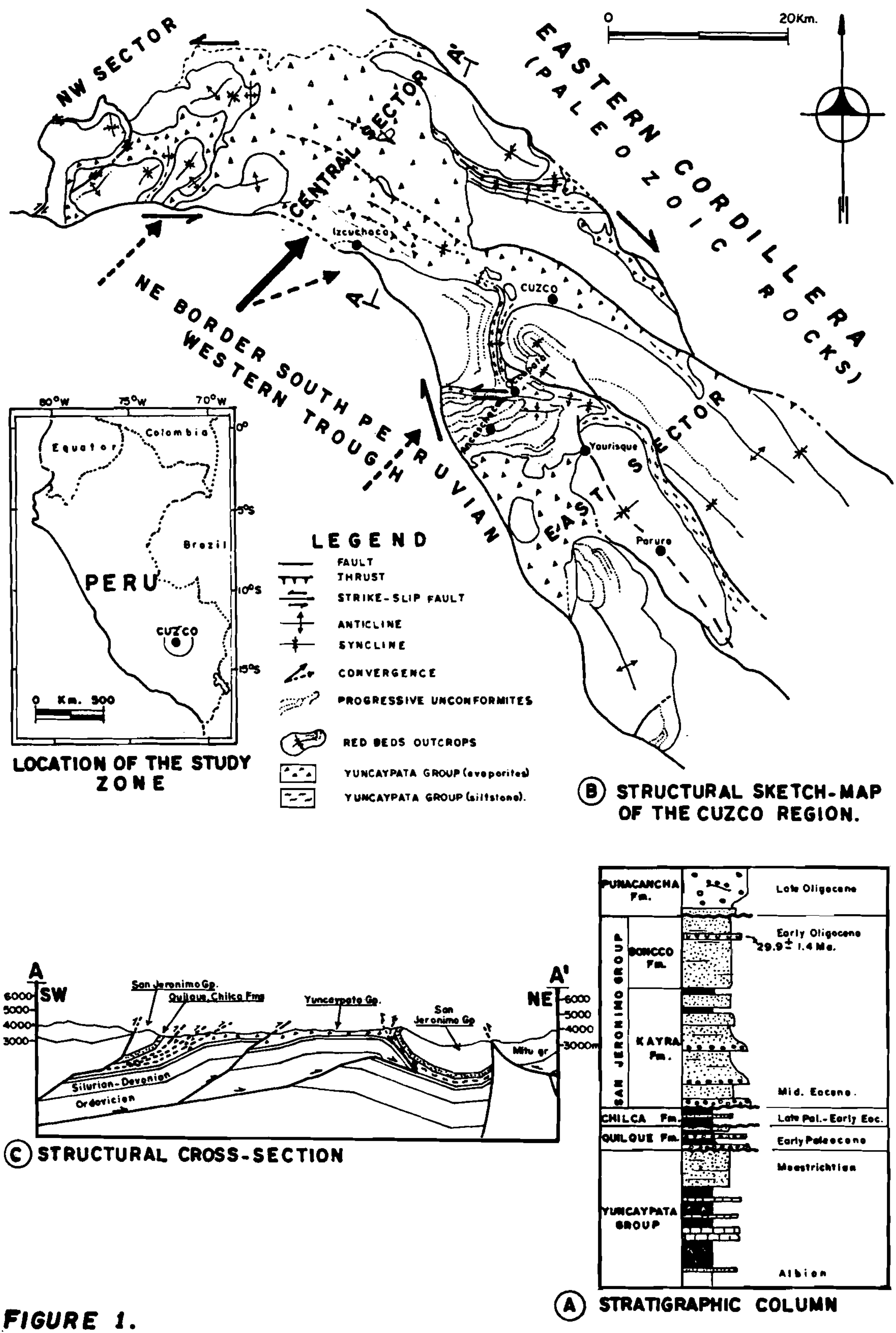
NW SECTOR
CENTRAL SECTOR
EASTERN CORDILLERA (PALEOZOIC ROCKS)
EAST SECTOR
NE BORDER SOUTH PERUVIAN WESTERN TROUGH
0 20Km.
Izcuchaca
CUZCO
Yaurisque
Paruro
A
A'
LEGEND
FAULT
THRUST
STRIKE-SLIP FAULT
ANTICLINE
SYNCLINE
CONVERGENCE
PROGRESSIVE UNCONFORMITES
RED BEDS OUTCROPS
YUNCAYPATA GROUP (evaporites)
YUNCAYPATA GROUP (siltstone).
80°W 75°W 70°W
Colombia
Equator
Brazil
PERU
CUZCO
0 Km. 500
0°
5°S
10°S
15°S
LOCATION OF THE STUDY ZONE
B STRUCTURAL SKETCH-MAP OF THE CUZCO REGION.
A SW
A' NE
6000
5000
4000
3000
San Jeronimo Gp.
Quilque, Chilca Fms
Yuncaypata Gp.
San Jeronimo Gp
Mitu gr
Silurian-Devonian
Ordovician
C STRUCTURAL CROSS-SECTION
PUNACANCHA Fm.
Late Oligocene
SONCCO Fm.
Early Oligocene
29.9 ± 1.4 Ma.
SAN JERONIMO GROUP
KAYRA Fm.
Mid. Eocene.
CHILCA Fm.
Late Pal.-Early Eoc.
QUILQUE Fm.
Early Paleocene
Maastrichtian
YUNCAYPATA GROUP
Albian
A STRATIGRAPHIC COLUMN

FIGURE 1.

# TECTONIC MODEL OF THRUSTS AND IMBRICATED THRUSTING WEDGE ON THE NORTHWESTERN FLANK OF THE MERIDA ANDES BETWEEN TORONDOY AND VALERA (VENEZUELA)

José Tomas CASTRILLO (1, 2) and Yves HERVOUET (1)

(1) Lab. Géologie structurale et télédétection, I.P.R.A.-C.U.R.S., Avenue de l'université, 64000 PAU, FRANCE.

(2) Escuela Ingeneria, Universidad de Los Andes, Mérida, VENEZUELA.

---

**KEY WORDS :** Thrusts, Back Thrusts, Remote Sensing, Modelization, Recent Compression, Venezuelan Andes.

A new model to explain the tectonic evolution and present structural configuration of the North-Andean Flanck (Torondoy-Caja Seca-Valera; Figure 1) is presented. The deformation style is based on the geometry of flexure folds applied to thrusting areas. The geometry is formed by ramps and flats associate to fault-bend folds (Suppe; 1983), wich evolve into fault-folds (Figure 2 and Figure 3).

In the study area, this deformation is the cause of complex imbricated thrusting and intercutaneus thrusting wedge system, which are consequence of distinct tectonic events. These events have affected the Andean Flank since the Oligocene-Miocene period until recent Pleistocene. The Virtudes Thrust (Figure 2) is the main expression of this system.

The system has developped in two phases: the first event (Figure 3-1 to 3-3), Pre-Pliocene in age, is developped over a ramp 3-4 km long dipping about 30-35 to the south-east, towards the Boconó Fault. A second event, Plio-Pleistocene in age, with a ramp of 3-4 km and dipping 55-60 to the south-east is formed on the upper flat of the first ramp (Figure 3-4).

Andean basement rocks have been overthrusted up to 34-36 km into the Maracaibo Basin. It is the cause of the Cretaceous and Tertiary rocks decollements over the fault-bend fold. The decollements of the Meso-Cenozoic cover are situated within the shaly units of the Upper Cretaceous Formations (Luna-Colon) and also within the Mio-Plio-Pleistocene Betijoque Formation.

This complex thrusting is associated (Figure 2) with strike slip faults, dextral (Piñango Fault) in the south or senestral (Rio Momboy and Rio Motatan Faults) in the east.

In agreement with Hospers and Van Wijnen (1959), Kellogg and Bonini (1982, 1985), Giegengack (1984), Kohn *et al.* (1984) and De Toni and Kellogg (1993), this work, based on remote sensing studies, field observations and cross-section modelizations, suggests that the Venezualan Andes uplift is caused by crustal shortening along two generations of complex southeast dipping thrust faults.

REFERENCES:


ANONYMOUS .- Mapa geologico de Valera a la escala de 1/100000, *Min. Energia y Minas*, Venezuela, 1988.

CHARLESWORTH H. & JAHANS P. .- Thrust: a program to model strata affected by thrusts, 1992.

DE TONI B. & KELLOGG J. .- Seismic evidence for blind thrusting of the Northwestern flank of the Venezuelan Andes. *Tectonics*, vol. 12, n 6, 1393-1409, 1993.

GIEGENGACK R. .- Late Cenozoic tectonic environments of the Central Andes, *Mem. Geol. Soc. Am.*, 162, 343-364, 1984.

HOSPERS J. & VAN WIJNEN J. C. .- The gravity field of the Venezuelan Andes and adjacent basins. *Versl. Gewone Vergad. afd. Natuurkd. K. Ned. Akad. Wet.*, 23, 1-95, 1959.

KELLOGG J. & BONINI W. E. .- Subduction of the Carribean plate and basement uplifts in the overriding South American plate. *Tectonics*, 1, 251-276, 1982.

KELLOGG J. & BONINI W. E. .- Reply. *Tectonics*, 4, 785-790, 1985.

KOHN B.P., SHAGAM R., BANKS P.O., BURKLEY L.A. .- Mesozoic-Pleistocene fission track ages on rocks of the Venezuelan Andes and their tectonic implications. *Mem. Geol. Soc. Am.*, 162, 365-384, 1984.

SUPPE J. .- Geometry and kinematics of fault-bend fold. *Am. J. Sci.*, 283, 684-721, 1983.


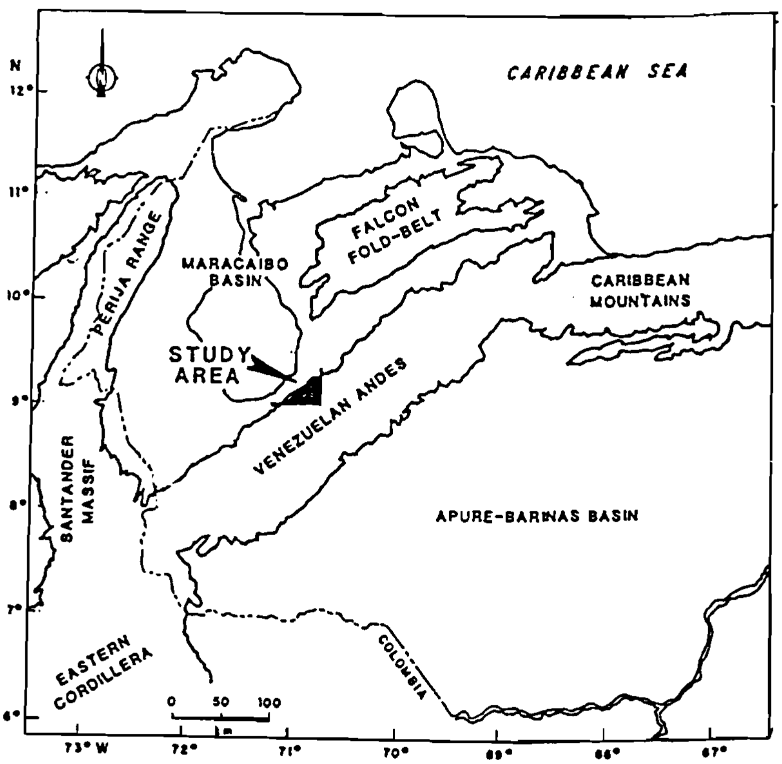


Figure 1: Location map of the study area (slightly modified from De Toni and Kellogg, 1993).

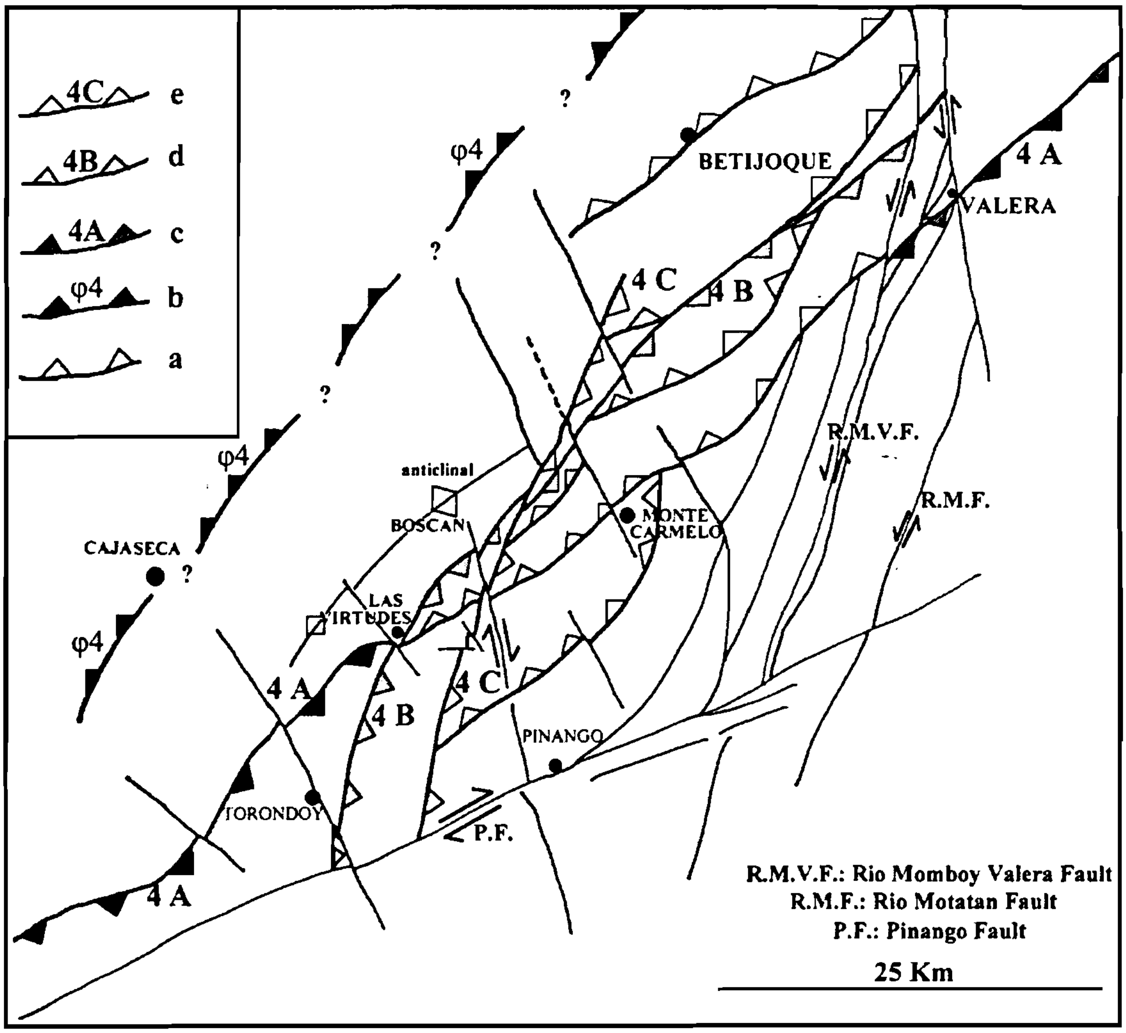


Figure 2: Structural analysis using remote sensing data (Landsat TM path 006-row 054) and landscape observations.

a: Pre-Pliocene back thrusts (figures 3-1 to 3-3); b: Plio-Pleistocene back thrust (figure 3-4); c, d & e: Synthetic thrusts, Plio-Pleistocene in age (not modelled on figure 3); c: Las Virtudes thrust (Plio-Pleistocene); d: Ancient Pleistocene thrust; e: Recent Pleistocene thrust and back thrust.

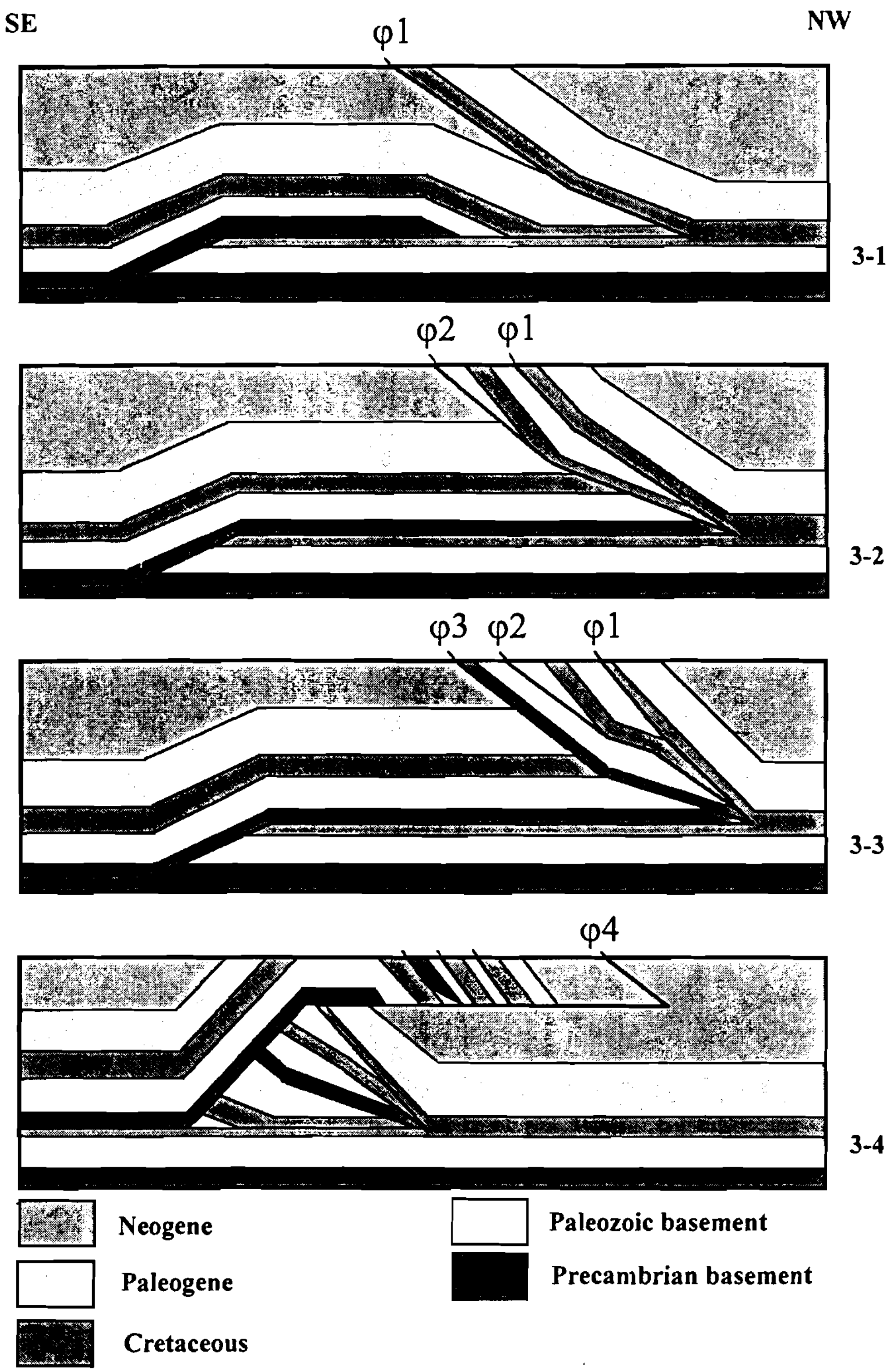


Figure 3: Modelled cross-sections of the Northwestern flank of the Venezuelan Andes using program "Thrust" (Charlesworth and Jahans, 1992).

3-1 to 3-3: Pre-Pliocene events; 3-4: Plio-Pleistocene event.

# NATURE AND TIMING OF CENOZOIC INTRA-ARC DEFORMATION, SOUTHERN CHILE.

Jose CEMBRANO[1], Elizabeth SCHERMER[2], Alain LAVENU[3], Francisco HERVE[1], Sergio BARRIENTOS[4], Bill McCLELLAND[5] and Gloria ARANCIBIA[1]

(1) Departamento de Geologia, Universidad de Chile, Casilla 13518, Santiago, Chile
(2) Geology Department, Western Washington University, Bellingham WA 98225, USA
(3) ORSTOM, casilla 53 390, Correo central, Santiago 1, Chile.
(4) Departamento. de Geofisica, Universidad de Chile, Casilla 2777, Santiago, Chile.
(5) Department of Geological Sciences, University of California, Santa Barbara, CA93106, USA.

**KEY WORDS:** Andes, Southern Chile, kinematics, Cenozoic, Magmatic arc.

## INTRODUCTION

Regional-scale long-lived shear zones spatially associated with ancient and present-day magmatic arcs provide a unique opportunity to address the link between tectonics and magmatism at a crustal scale, both in the long and short-term. Valuable information concerning the tectonics of magmatic arcs also comes from the study of the regional-scale trend of dike swarms, spatial distribution of volcanic centers and focal mechanisms of intra-arc crustal earthquakes. The nature of deformation partitioning of the convergence vector at subduction zones may also be assessed through constraining the kinematics and timing of intra-arc deformation and its correlation with coeval plate motions.

The Cenozoic geodynamic setting of the southern Chilean Andes is well constrained showing relatively steady right-oblique subduction of the Farallon (Nazca) plate beneath South America since 48Ma, with the exception of nearly orthogonal convergence during the 26-20 Ma time span, following the breakup of the Farallon plate (Pardo-Casas and Molnar, 1987). During the last 14 Ma the Nazca-South America-Antarctica triple junction has migrated northward from Tierra del Fuego to its present position at the southern end of the Southern Andes Volcanic Zone (Cande and Leslie, 1986). Both oblique subduction and ridge subduction have been proposed to be driving mechanisms for intra-arc shear (Beck, 1991; Nelson et al., 1994).

We propose that the long-term and short-term kinematics of the Cenozoic magmatic arc in southern Chile are recorded in: (1) Pre-Eocene(?) and Miocene-Pliocene ductile shear zones and Miocene-Pliocene brittle faults of the intra-arc Liquine-Ofqui fault zone (LOFZ) (Herve et al. 1979; Lavenu and Cembrano, 1994; Cembrano et al. 1996) ; (2) Eocene-Miocene dike swarms (Herve et al. 1995); (3) spatial distribution of Holocene volcanic centers (Nakamura, 1977, Lopez-Escobar et al. 1995); and (4) a few, intra-arc crustal earthquakes (Chinn and Isaacks, 1983; Barrientos and Acevedo, 1992) (Figure 1).

In this work we present the results of systematic field and petrographic observations in several E-W transects across the intra-arc northeast-trending LOFZ which extends for more than 1000 km northward from the Nazca-South America-Antarctica triple junction. Geological observations together with new and published geochronological data suggest marked differences in kinematics, physical conditions and possible age of deformation in the magmatic arc of the southern Chilean Andes for the Cenozoic (Figure 1). The spatial distribution of dike swarms and volcanic centers in southern Chile is also addressed to help constraining the intra-arc tectonics.

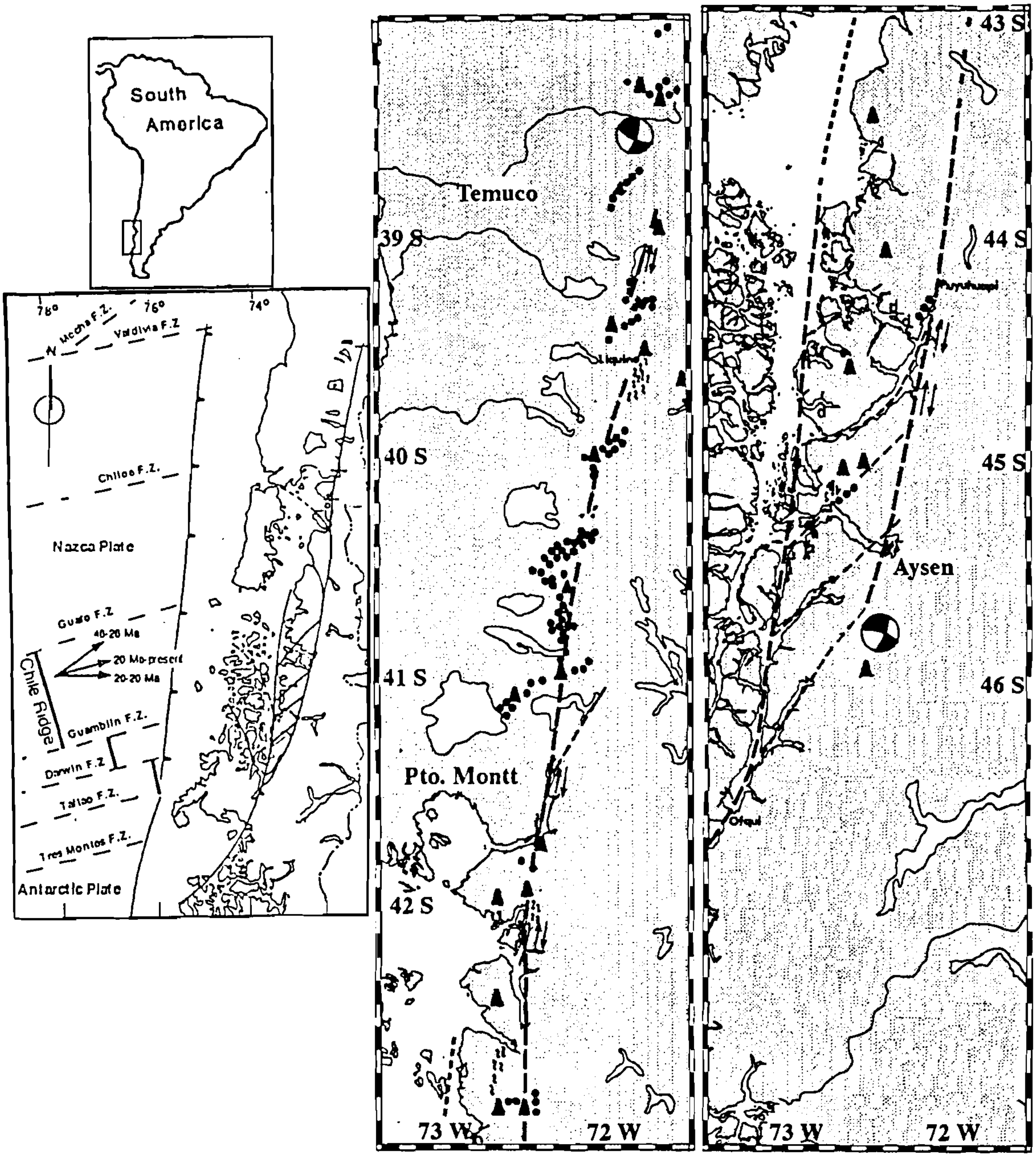


Figure 1. Regional scale sketch map showing the main tectonomagmatic features of the Cenozoic magmatic arc of the southern Chilean Andes (compiled from Barrientos and Acevedo, 1992; Chinn and Isaacks, 1983; Cembrano et al. 1995; Herve et al. 1979; Herve et al. 1995; Lopez-Escobar et al. 1995).

Pre-Eocene(?) to Miocene-Pliocene ductile shear zones

Holocene basaltic minor eruptive centers

d Eocene-Miocene dike swarms

Holocene stratovolcanoes

Miocene-Pliocene brittle faults

Crustal intra-arc earthquakes

Main lineaments of the Liquine-Ofqui fault zone

## NATURE AND TIMING OF INTRA-ARC DEFORMATION

Pre-Eocene (?) mylonitic strips up to one km in width document sinistral transpressional ductile deformation near the northern end of the LOFZ (Liquine, 39°S). This is in contrast with post-Miocene ductile to brittle dextral strike-slip deformation further south (Figure 1). At 42°S, new U-Pb zircon ages from one synkinematic and one prekinematic pluton are 9.9±0.6 and 135±12, respectively. Published K-Ar and Ar-Ar ages are mostly ~9-13 Ma in hornblende and ~6-3 Ma on biotite, indicating either uplift and cooling or pervasive thermal resetting of Cretaceous plutons during Miocene time. New Ar-Ar ages on biotite from both ultramylonitic shear zones and less deformed plutonic rocks range from 3.59±0.01 to 3.78±0.01. Microstructural observations suggest the latest ductile fabrics in plutonic rocks formed at greenschist facies conditions (300-350°C) similar to biotite Ar closure temperature.

Work in progress at 44°-46°S near the southern end of the LOFZ (Puyuhuapi-Aysen area, figure 1), shows that brittle faulting predominates over ductile deformation along north and northeast-trending lineaments making up a strike-slip duplex (Cembrano and Herve, 1993). Ductile dip-slip along with dextral strike-slip kinematics has been inferred from fabric studies on meter wide mylonitic shear zones occurring within the Patagonian Batholith and metamorphic wallrock. Kinematic analysis of fault slip data shows transpressional to compressional deformation of possible Miocene-Pliocene age. Eocene-Miocene mafic dike swarms (Figure 1) have a predominant northeast trend over an area of several hundred square km., which is consistent with an overall dextral strike-slip kinematics at the time of emplacement. Likewise, the spatial distribution of Holocene basaltic minor eruptive centers between 38°S and 46°S is mostly restricted to northeast, en echelon, alignments (Figure 1), which are believed to document rapid magma ascent through subvertical tension fractures within a transpressional dextral strike-slip volcanic arc. Previously published seismic data for the southern Andes volcanic arc is limited to only two earthquakes (Chinn and Isaacks, 1983; Barrientos and Acevedo, 1992), both having dextral strike-slip focal mechanism (Figure 1)

## CONCLUSIONS

Available long-term and short term data show that the magmatic arc of the southern Chilean Andes has been undergoing transtensional to transpressional dextral strike-slip deformation for several million years. This tectonic regime has exerted a major control in the long-term and short-term magma ascent and emplacement as shown by synkinematic Eocene-Miocene dike swarms, Miocene plutonic rocks and present-day volcanic centers. Different degrees of deformation partitioning of the Farallon (Nazca)-South America convergence vector into arc-parallel shear and arc-orthogonal shortening has likely been responsible for the existence of episodic and/or coeval dextral-strike-slip and dip-slip deformation along the arc.

**Acknowledgements**

Fondecyt projects 1930496 and 1950497 to JC have funded most of this research. This abstract was written while the main author was at Dalhousie University under a Killam fellowship. We thank G. Lopez, K. Lein and A. Sanhueza for help during fieldwork.

## REFERENCES

Barrientos, S. and Acevedo, P. 1992. Seismological aspects of the 1988-1989 Lonquimay (Chile) volcanic eruption. *Journal of Volcanology and Geothermal Research*, 53, 73-87.

Beck, M.E., 1991. Coastwise transport reconsidered: lateral displacements in oblique subduction zones, and tectonic consequences, *Physics of the Earth and Planetary Interiors*, 68, 1-8.

Cande, S.C. and Leslie R.B. Late Cenozoic tectonics of the Southern Chile Trench. Journal of Geophysical Research, 91, 471-496.

Cembrano J. and Herve, F., 1993. The Liquine-Ofqui fault zone: a major strike-slip duplex in the southern Andes. *Second Symposium International "Geodynamique Andine" Oxford (UK)*, p.175-178. ORSTOM editions.

Cembrano, J,, Herve, F. and Lavenu, A. 1996. The Liquine-Ofqui fault zone: A long-lived intra-arc fault system in southern Chile. *Tectonophysics* special issue on Andean Geodynamics (in press)

Chinn, D.S., and Isaacks B.L., 1983. Accurate source depths and focal mechanisms of shallow earthquakes in western South America and in the New Hebrides island arc. *Tectonics*, 2, 529-563.

Herve, F., Araya, J.L., Solano, A., 1979. Edades radiometricas y tectonica neogena en el sector costero de Chiloe Continental., X region. *in Actas Segundo Congreso Geologico Chileno*, v1, p F1-F8, Santiago.

Herve, F., Pankhurst, R.J., Drake, R. and Beck, M., 1995. Pillow metabasalts in a mid-Tertiary extensional basin adjacent to the Liquine-ofqui fault zone: the Isla Magdalena area, Aysen, Chile. *Journal of South American Earth Sciences*, 8, 33-46.

Lavenu, A. and Cembrano, J., 1994. Neotectonica de rumbo dextral en la zona de falla Liquine-Ofqui: Geometria, cinematica y tensor de esfuerzo. in *Actas VII Congreso Geologico Chileno*, 81-85.

Lopez-Escobar, L., Cembrano, J. and Moreno, H. Geochemistry and tectonics of the Southern Andes basaltic Quaternary volcanism (37°-46°S). *Revista Geologica de Chile* ,22, 2,219-234.

Nakamura, K. 1977. Volcanoes as possible indicators of tectonic stress orientation: principle and proposal. *Journal of Volcanology and Geothermal Research*, 2, 1-16.

Nelson, E., Forsythe, R. and Arit, I., 1994. Ridge collision in terrane development. *Journal of South American Earth Sciences*, 7, 271-278.

Pardo-Casas, F. and Molnar, P., 1987. Relative motion of the Nazca (Farallon) and South American plates since Late Cretaceous times. *Tectonics*, 6, 233-248.

# STRUCTURE OF THE ANDEAN FOOTHILLS, CHOS MALAL REGION, NEUQUEN BASIN, ARGENTINA

Vincent CHAUVEAU(1), Bertrand NIVIERE(1), Peter R. COBBOLD(1), Eduardo A. ROSSELLO(2), Jean-François BALLARD(3) and Herbert T. EICHENSEER(3)

(1) Géosciences-Rennes, 35042 Rennes, France.
(2) CONICET y Universidad de Buenos Aires, 1425 Buenos Aires, Argentina.
(3) Elf Aquitaine Production, C.S.T.J.F., av. Larribau, 64018 Pau, France.

**KEY WORDS** : Andean foothills, structure, Chos Malal, Neuquén Basin, Argentina.

## INTRODUCTION

The Neuquén Basin of West-Central Argentina (Fig. 1) was formed in the late Paleozoic to early Mesozoic as a result of continental rifting (Legarreta and Uliana, 1991; Uliana and Legarreta, 1993; Urien and Zambrano, 1994; Vergani *et al.*, 1995). During the Mezosoic and Cenozoic, more than 7 km of sediments were deposited, including marine, continental and volcanoclastic units.

In general, the Neuquén Basin has been well studied, because it produces petroleum (Uliana and Legarreta, 1993; Urien and Zambrano, 1994). However, the western reaches in the Andean foothills are less well known.

We have studied the Chos Malal region, where well-exposed sections provide insights into basin development, inversion and the formation of Andean structures.

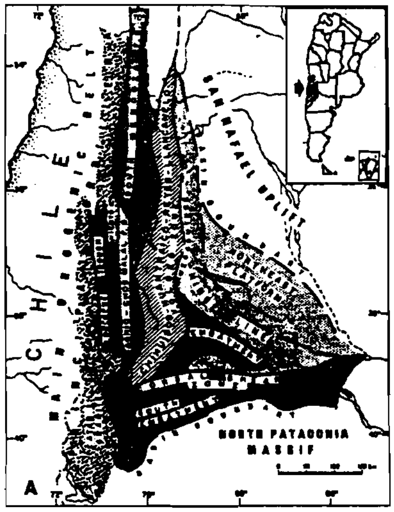


Fig. 1. The Neuquén Basin (after Urien and Zambrano, 1994).

## DEVELOPMENT OF THE NEUQUEN BASIN

In the western Neuquén Basin, late Paleozoic volcanic units (Andacollo and Choiyoi groups, Fig. 2) form the top of economic basement (Urien and Zambrano, 1994). They were deposited in an intra-arc setting. From the Triassic to the Early Cretaceous, a phase of extensional tectonics resulted in half-grabens, trending NNE to N (Manceda and Figueroa, 1995; Urien and Zambrano, 1994; Uliana *et al.*, 1995; Vergani *et al.*, 1995). Two major marine cycles (Jurásico and Andico) occurred between the Liassic and the end of the Albian, while the basin was in a back-arc position (Legarreta and Uliana, 1991). Each cycle resulted in thick black shales, passing upwards into sandstones or evaporites (Fig. 2). Near the base of the Jurásico cycle, the Los Molles Fm. contains many layers of tuff and a major turbidite, indicating strong tectonic control on the development of the basin, which was near a volcanic arc.

From the Cenomanian to the Paleogene, continental sandstones of the Riograndico cycle appear to have been deposited in a foreland basin (Barrio, 1990; Vergani *et al.*, 1995). During the Cenozoic, abundant volcanoclastics show that the basin was in an intra-arc setting.

## STRUCTURE OF THE CHOS MALAL AREA

Our structural map (Fig. 3) and cross-sections (Fig. 4), drawn on the basis of fieldwork, Landsat images and subsurface data, show two structural domains: one north of Chos Malal, dominated by thick-skinned thrusting; the other, south of Chos Malal, showing only thin-skinned structures.

In the northern domain, two mountains nearly 3000 m high (the Cordillera del Viento and the Tromen volcano) have formed above eastward-verging blind thrusts (Uliana *et al.*, 1993; Urien and Zambrano, 1994; Uliana *et al.*, 1995). The Cordillera del Viento, which started as a ramp anticline and became a pop-up, brings late Paleozoic basement to outcrop. Further east, the Pampa de Tril thrusts detach within Paleozoic basement. Here, the cover has been backthrust westwards (Viñes, 1990), detaching on Aptian evaporites (Huitrín Fm.). The resulting triangle zone forms the current mountain front.

In the southern domain, the basement does not crop out. Thin-skinned structures include thrusts and folds. Anticlines are typically box folds with km-scale wavelengths and their hinges can be followed for several tens of kilometers along strike. Synclines tend to be wider, reaching 15 km in the south. In general, fold axes trend N160° to N170° throughout the area, but there are some anomalies (Fig. 3): (i) the southern edge of the Cordillera del Viento anticline trends N060°, instead of N170° elsewhere; (ii) around Tromen volcano, folds swing from N to NE on the southeastern side and from N to NW on the southwestern side; (iii) SE of Collipili, fold axes trend N060°.

Within the cover sequence, there are several detachments. The uppermost is in the Aptian Huitrín Fm. (Viñes, 1990; Vergani *et al.*, 1995), where up to 300 meters of halite are known from subsurface data (Gabriele, 1993). Other detachments are in thick black shales of the Los Molles and Vaca Muerta formations (see Vergani *et al.*, 1995). On reaching the Los Molles, the basement thrust ramp of the Cordillera del Viento passes upwards into a flat, visible on a seismic line. As for the Vaca Muerta shales, they fill the cores of detached anticlines in the southern domain (Fig. 4b) and anomalous thicknesses have been encountered locally in wells. In general, the shales are overpressured (Vergani *et al.*, 1995).

We have measured fault-slip data at 6 localities in Late Cretaceous rocks (Fig. 3) and 19 localities in Jurassic rocks. The data were analyzed using the method of right dihedra (Angelier and Mechler, 1977). In Late Cretaceous rocks, the principal direction of shortening is sub-horizontal. For localities 1, 2 and 3, the principal shortening trends N070°, sub-perpendicular to regional fold trends and sub-parallel to the convergence direction of the Nazca plate since 49 Ma (Pardo-Casas and Molnar, 1987). In contrast, for localities 4, 5 and 6, the principal shortening trends N170°. The significance of this result is not clear. In Jurassic rocks west of Chos Malal, the principal shortening is either sub-vertical (associated with normal faults) or sub-horizontal (associated with strike-slip faults). The principal extension trends NE, but varies with age (from N020° before the Kimmeridgian to N100° in the Kimmeridgian). Negative flower structures and synsedimentary faults are common. The latter show stratigraphic thickness variations (growth) or evidence for burial in the last stages of faulting. Thus the tectonic context was extensional or transtensional during much of the Jurassic.

There is evidence for basin inversion during the Late Cretaceous and Tertiary. 1. On seismic evidence, most eastwards-verging thrust flats and ramps are reactivated Jurassic normal faults (see Manceda and Figueroa, 1993; Urien and Zambrano, 1994; Uliana *et al.*, 1995; Vergani *et al.*, 1995). 2. West of Chos Malal, we have found at outcrop several examples of listric normal growth faults, reactivated as reverse faults. 3. The southern edge of the Cordillera del Viento was a lateral thrust ramp during Andean compression, but may have been an extensional transfer fault during the Jurassic. 4. In the southern domain, linear belts with anomalous northeasterly fold trends may also be reactivated Jurassic transfer faults. Tertiary volcanic sills around Collipilli have two main trends (Llambias and Malvicini, 1978), one parallel to regional fold axes, the other at N040° to N060°, parallel to anomalous fold trends.

As for the fold axis deviations around the southern edge of the Tromen volcano, we suggest that they are due to gravitational collapse during the Tertiary.

On seismic evidence, Andean compression began during the Late Cretaceous (Vergani *et al.*, 1995). It reached a paroxysm during the late Paleocene and early Eocene (Manceda and Figueroa, 1993; Vergani *et al.*, 1995). Thus the Sierra Mayal (Zollner and Amos, 1973), an intrusive andesitic porphyry of Eocene age, cuts a large anticline. The cross-cutting Collipilli volcanic sills are also Eocene in age (Llambias and Rapela, 1989). Deformation induced by collapse of the Tromen volcano appears to be later than Pleistocene-Holocene basalts.

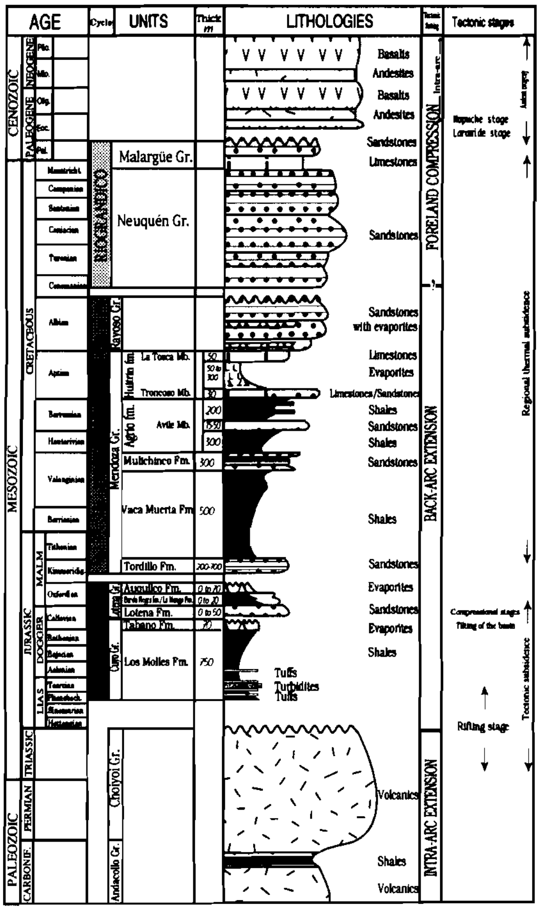


Fig. 2: Stratigraphic chart for the western part of the basin.

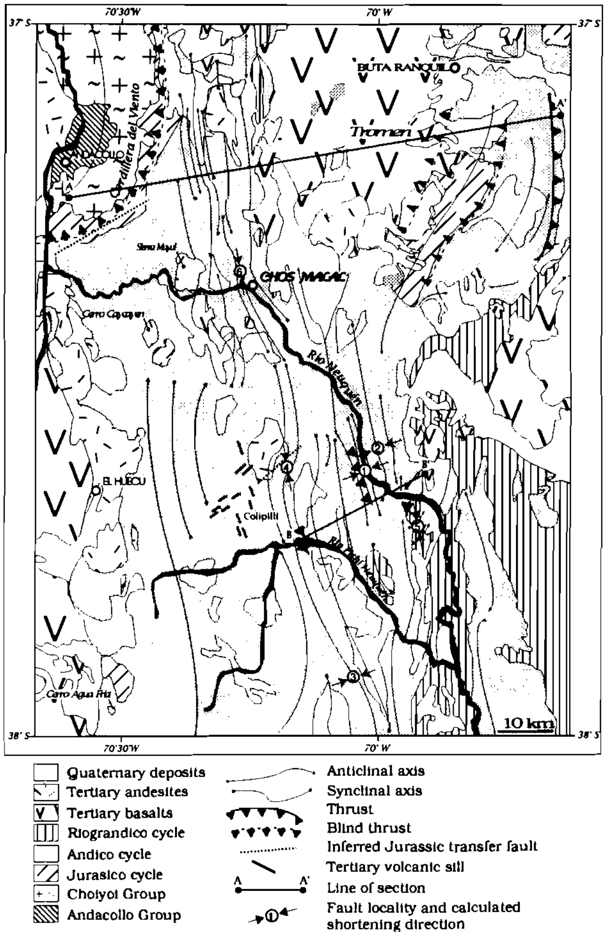


Fig. 3: Simplified geological and structural map of the Chos Malal area.

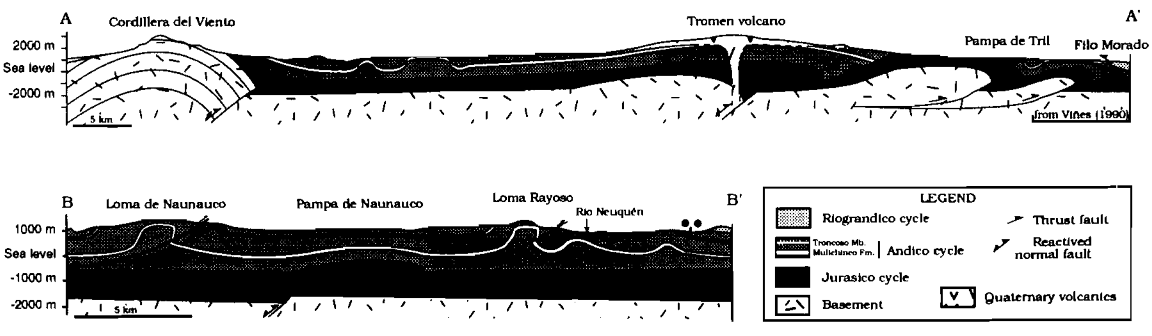


Figures 4a and 4b: Structural cross sections of the Neuquén Basin foothills (see Fig. 3 for section lines).

## CONCLUSIONS

In the Chos Malal area, Andean shortening of Paleogene age is responsible for thin-skinned deformation of the Mesozoic sedimentary cover on at least three levels of detachment. In the northern domain, thick-skinned deformation involved eastwards-verging basement thrusts, formed by reactivation of Jurassic normal faults. Jurassic transfer faults, striking NE, were also reactivated and may be responsible for anomalous fold trends and lateral thrust ramps. The main Andean deformation ended before the Oligocene. The Tromen volcano, formed during the Quaternary, locally modified the structural pattern.

## REFERENCES

Angelier, J. and Mechler, P. 1977. Sur une méthode graphique de recherche des contraintes principales également utilisable en tectonique et séismologie: la méthode des dièdres droits. Bull. Soc. Géol. France, 7: 1309-1318.

Barrio, C.A..1990. Late Cretaceous - Early Tertiary sedimentation in a semi-arid foreland basin (Neuquén basin, western Argentina). Sed. Geol., 66: 255-275.

Delpino, D. and Desa, M. 1995. Mapa geológico y de recursos minerales de la provincia del Neuquén, República Argentina, escala 1:500.000. Secretaría de Minería, Dirección Nacional del Servicio Geológico, Buenos Aires.

Gabriele, N.A. 1993. Azufre nativo vinculado a estratos evaporíticos de la formación Huitrín (Cretácico inferior). Rev. Asoc. Geol. Argentina, 48: 265-276.

Legarreta, L. and Uliana, M.A. 1991. Jurassic-Cretaceous marine oscillations and geometry of back-arc basin fill, central Argentine Andes. In: McDonald, D.I.M. (ed.), Sedimentation, tectonics and eustasy, Int. Ass. Sedimentol. Sp. Publ., 12: 429-450.

Llambías, E.J. and Malvicini, L. 1978. Geología, petrología y metalogénesis del area de Collipilli, provincia del Neuquén, Argentina. Rev. Asoc. Geol. Argentina, 4: 257-276.

Llambías, E.J. and Rapela, C.W. 1989. Las volcanitas de Collipilli, Neuquén (37°S) y su relación con otras unidades paleógenas de la cordillera. Rev. Asoc. Geol. Argentina, 44: 224-236.

Manceda, R. and Figueroa, D. 1995. Inversion of the Mesozoic Neuquén rift in the Malargüe fold and thrust belt, Mendoza, Argentina. In: Tankard, A.J., Suárez Soruco, R. and Welsink, H.J. (eds.), Petroleum Basins of South America, AAPG Mem., 62: 369-382.

Pardo-Casas, F. and Molnar, P. 1987. Relative motion of the Nazca (Farallon) and South America plates since late Cretaceous time. Tectonics, 6: 233-248.

Uliana, M.A. and Legarreta, L. 1993. Hydrocarbon habitat in a Triassic-to-Cretacous sub-Andean setting: Neuquén basin, Argentina. J. Petrol. Geol., 16: 397-420.

Uliana, M.A., Arteaga, M.E., Legarreta, L., Cerdán, J.J. and Peroni, G.O. 1995. Inversion structures and hydrocarbon occurence in Argentina. In: Buchanan, J.G and Buchanan, P.G. (eds.) Basin inversion, Geol. Soc. London Spec. Publ., 88: 211-233.

Urien, C.M. and Zambrano, J.J. 1994. Petroleum systems in the Neuquén basin, Argentina. In: Magoon, L.B. and Dow, W.G., The petroleum system - from source to trap, AAPG Mem., 60: 513-534.

Vergani, G.D, Tankard, A.J., Belotti, H.J. and Welsink, H.J. 1995. Tectonic evolution and paleogeography of the Neuquén Basin, Argentina. In: Tankard, A.J., Suárez Soruco, R. and Welsink, H.J. (eds.), Petroleum basins of South America, AAPG Mem., 62: 383-402.

Viñes, R.F. 1990. Productive duplex imbrication at the Neuquén basin thrust belt front Argentina. In: J. Letouzey (ed.), Petroleum and tectonics in mobile belts, Editions Technip, Paris: 69-80.

Zollner, W. and Amos, A.J. 1973. Descripción geológica de la hoja 32b, Chos Malal, provincia del Neuquén. Servicio Nacional de Geología y Minería, Buenos Aires, Boletin, 143: 91 pp.

# THE ALTIPLANO-EASTERN CORDILLERA LIMIT IN THE URUBAMBA REGION (CUZCO-PERU)

Richard CHAVEZ(1) Willy GIL(1),Víctor CARLOTTO(2), José CARDENAS(1), Etienne JAILLARD(3)

(1) Universidad Nacional San Antonio Abad del Cuzco Av. de la Cultura s/n Cuzco-Peru.
(2) Universidad Nacional San Antonio Abad del Cuzco (Peru) and Laboratoire de Géodynamic des Chaînes Alpines Grenoble (France)
(3) ORSTOM, TOA, UR 1H, 213 rue La Fayatte, 75480 Paris,France.

**KEY WORDS**: Altiplano, Eastern Cordillera, tectonic, Urubamba, Cuzco, Peru

## RESUMEN

El límite Cordillera Oriental-Altiplano en la región de Urubamba (Cuzco-Perú) esta dado por un alto estructural, controlado por fallas de rumbo, donde convergen cabalgamientos del Altiplano con vergencia NE y cabalgamiento de la Cordillera Oriental con vergencia SW. El Alto estructural corresponde al Umbral Cuzco-Puno que controló la sedimentación, paleogeografía y la tectónica, por lo menos a partir del Paleozoico superior.

## GEOLOGICAL SETTING

The Urubamba region is located between two morpho-structural units: The NE border of the Altiplano and the SW border of the Eastern Cordillera, limited by the valley of the Urubamba river which represents aproximately an Intermediate Domaine.

In the Eastern Cordillera of the study zone, a lot of stratigraphic units crop out. Stratigraphic units sach as: The Silurian-Devonian, the Early Permian (Copacabana Group), the Permian-Triassic (Mitu Group) and scarcely the Mesozoic (Huancane Formation and Yuncaypata Group). This domaine is characterized by the NW-SE thrusts, which make the Mitu group to repeat and put the Silurian-Devonian rocks in contact with the Mitu Group. These thrusts have a vergence towards the SW.

The Altiplano domaine is represented by the Huancane Formation (Neocomian), The Yuncaypata Group (Albian-Maastrichtian), the Quilque and Chilca Formations (Paleocene-Early Eocene), and finally by the Red Beds of the San Jeronimo Group (Middle Eocene-Early Oligocene).These units are affected by thrusts and fault propagation folds. The folds are plurikilometric of WNW-ESE to NW-SE direction, with axial plane slightly bent to the south (Piuray Anticline).The anticline west limit is cut by evaporite domes (Maras domes, Marocco, 1978). Gypsum seems to come from fhe Lower part of the Yuncaypata Group.

The Intermediate Domaine is given by strike-slip faults and it is here where two thrusting systems converge. Eastern Cordillera thrusts with SW vergence and the Altiplano thrusts with NE vergence. The strike-slip fault is probably of a dextral motion that takes out Lower Paleozoic rocks to outcrop in flower structure way. Paleogeographically this Intermediate Domaine would correspond to an structural height (Cuzco-Puno Swell). Various quaternary shoshonite bodies locate along this strike-slip fault system.

All of these domaines are affected by a posterior folding of NE-SW direction and by N-S and NE-SW faults.

A chronology of phases has been deducted from the geological plane analysis. Thus we have that the NW-SE system of folds that really constitute the fault propagation folds, has been originated in the first place in the Altiplano Domaine. After that the thrusts have been formated with SW vergence of the Eastern Cordillera. The strike-slip fault system of the Intermediate Domaine has moved later on; however, this system is older, because it has controlled the sedimentation and the synsedimentary deformation of the Red Beds of the San Jerónimo Group. Finally a NE-SW folding and N-S and NE-SW faults affect the three domaines.

## GEOMETRIC ANALYSIS

Semi-balanced cross sections have been constructed out of the superficial geology (AA' Section) restoring it in a no-deformed state and considering the location of the syn-orogenic sedimentation (San Jerónimo Group) (BB' Section).

A common detatchment in the Altiplano and the Eastern Cordillera is located in the Lower Paleozoic (Ordovician) which is deadened in the Intermediate Domaine, in front of a structural height, that is originated by the strike-slip fault presence (AA' Section). A superior detatchment has also been recognized into the Yuncaypata Group in the Altiplano Domaine. In both domaines it is possible to see fault propagation folds, differenciated by their vergence. Asymetric synclines are developed in the San Jeronimo Group, which present greater thicknesses toward the eastern limbs (AA' Section). In the Altiplano, the structures with vergence to the NE are limited by the structural height (Cuzco-Puno Swell), and mainly affect the whole sedimentary cover. In this domaine, intercutaneous thrust wedge are observed which are associated to a passive backthrust (AA' Section). In the Eastern Cordillera the structures with SW vergence deform the Paleozoic, Permo-Triassic, and Mesozoic rocks, and they are also limited by the structural height of the Intermediate Domaine.

From the construction of the semi-balanced cross section (AA' Section)), a structural shortening of 35% has been calculated.

## KINEMATIC ANALYSIS AND INTERPRETATION

The possible ausence of the Copacabana Group in the Altiplano and its presence in the Eastern Cordillera, can explain the existence of a positive zone that controlled and limited the Permian-Carboniferous basin which could be the precursor structural element of the Cuzco-Puno Swell. A very intense distensive tectonic activity developped during the Permian-Triassic, originated the Mitu basin individualization that limits in its western part with the Cusco-Puno Swell, developping variable and more important thicknesses to the NE (BB' Section). During the Late Permian-Early Triassic a positive zone (Cusco-Puno Swell) seems to be already well differenciated. The Eastern Cordillera behaves inestably and contemporarily granitic bodies are placed possibly through normal faults, intruding rocks of the Mitu Group.

The Neocomian sedimentation (Huancané Formation) is established in the three domaines. Neverthless, the Intermediate Domaine behaved as a high depth with reduced sedimentation.The tectonic regime for this time was more estable.

The Yuncaypata Group is developped over the Intermediate Domaine (Cuzco-Puno Swell)

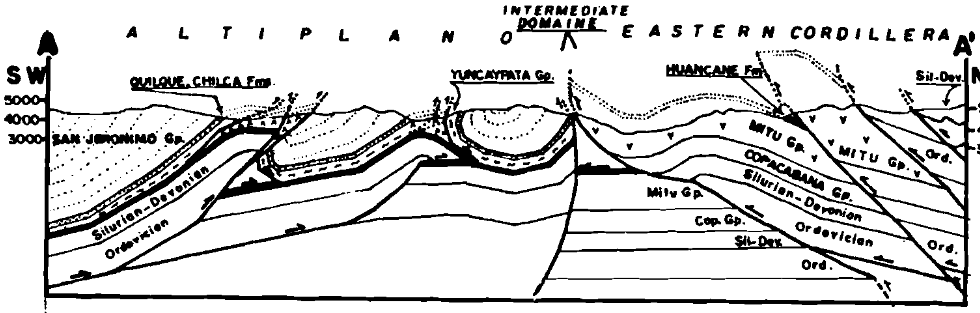


SEMI-BALANCED CROSS-SECTION

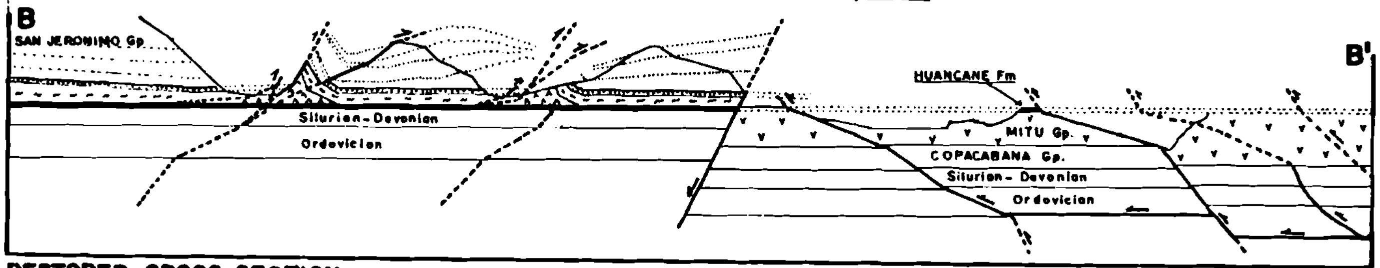


RESTORED CROSS-SECTION

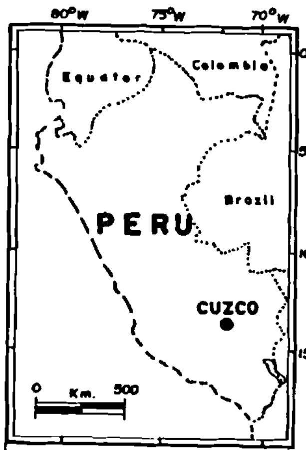


LOCATION OF THE STUDY ZONE

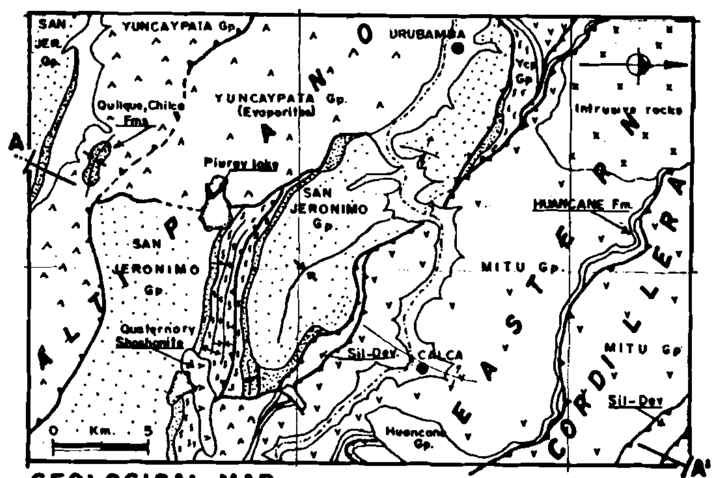


GEOLOGICAL MAP

spreading toward the Altiplano and being more restricted toward the Eastern Cordillera.

The Quilque and Chilca formations, mainly spread in the Altiplano, the structural height controlled and avoided a greater extension towards the Eastern Cordillera. The thickness of these units is more or less constant, but regionally it seems to increase to the SW.

The San Jerónimo Group, is also restricted to the NE border of the Altiplano ,this has been deposited in pull-apart basins of NO-SE direction, controlled to the North by strike-slip faults of the Intermediate Domaine. progressive unconformities can be seem inside these basins.

In the Cuzco region the Inca 1 Tectonic event (≈44-28Ma) seems to manifest by a compressive regime that originated a tectonic front with possible vergence to the NE. In front of this structural element developped the San Jerónimo Group sedimentation (Middle Eocene-Early Oligocene) (Carlotto et al 1995). The movement of strike-slip faults of the Intermediate Domaine that partly controlled the sedimentation, seems to be Paleogeographic pre-Mesozoic accidents. The progressive unconformities seem to be the result of thrusts, strike-slip faults and diapiric phenomena, that sinchronically worked (Chavez, 1995)

The folding that comes after to the deposit of the San Jeronimo Group, the development by fault propagation folds of NE and SW vergences, the functioning of intercutaneous wedges that originate a passive backthrust and the possible reactivation of the strike-slip faults, could be explained by the tectonic crisis of the Early Oligocene (Quechua Phase 0 ≈28-26Ma). The strike-slip fault reactivation and an important activity of thrusts with SW vergence of the Eastern Cordillera, seem to be caused by the Quechua Phase 3 (≈7-6 Ma) (Chavez, 1995).

## CONCLUSIONS

The Altiplano-Eastern Cordillera, in the Urubamba Region (Cuzco-Peru) is given by an structural height controlled by a strike-slip fault, where the Altiplano domaine thrusts converge with NE vergence and the Cordillera domaine thrusts with SW vergence, The structural height corresponds to the Cusco-Puno Swell that controls the sedimentation, the paleogeography and the tectonic at least since the Upper Paleozoic. The present structure shows that the andean deformations first affected the Altiplano Domaine and then the SW border of the Eastern Cordillera, and they are linked mainly to the Inca and Quechua tectonic events.

## REFERENCES

Carlotto V., Carlier G., Cárdenas J. 1985. La edad de las Capas Rojas del Grupo San Jerónimo (Region de Cusco) y su significado tectónico. Seminario Taller Evolución de la Litósfera en los Andes Peruanos y sus márgenes, Lima. 2p.

Chávez R. 1995. Geología, Estratigrafía y Tectónica de la Región Calca-Urubamba.Thesis University of Cusco, 143p.

Marocco R. 1978. Estudio Geológico de la Cordillera de Vilcabamba. *Boletín del Instituto de Geología y Minería*, D, 4; 157 p. Lima.

# TECTONIC INHERITANCE AND STRUCTURAL STYLES IN THE MERIDA ANDES (WESTERN VENEZUELA).

Bernard COLLETTA(1) , François ROURE(1) Bruno DE TONI(2), Daniel LOUREIRO(2) Herminio PASSALACQUA(2)and Yves GOU(3).

(1)Institut Français du Pétrole, BP311, 92506 Rueil-Malmaison, France
(2)Intevep, Apartado 76343, Caracas 1070-A, Venezuela
(3)Beicip Franlab, 92506 Rueil-Malmaison, France

**KEY WORDS:** Venezuela, Merida Andes, tectonic inversion, crustal scale balanced sections

## INTRODUCTION

Unlike the adjacent Caribbean and Central Andean orogens, the Merida Andes (Fig. 1) do not relate to direct interactions between the South American craton and either arc terranes or oceanic domains, but represent only minor intraplate readjustements between the Eastern Cordillera in the south and the South Caribbean transform margin in the north.Although no deep seismic profiling has yet been attempted across the Venezuelan Andes, a large set of conventional seismic reflection profiles has been recorded by the petroleum industry in the Maracaibo and Barinas-Apure basins, respectively along the North and South Andean foothills. In addition, isolated refraction and magnetotelluric data are available. However, only the gravimetric coverage is really complete, thus providing a relatively coherent image of the basement architecture.

## STRUCTURE OF THE SOUTH ANDEAN FLANK

The Barinas-Apure basin extends from the Andean foothills in the northwest to the Guyana shield in the southeast, thus encompassing most of the drainage area of the Rio Apure, a tributary of the Orinoco River. Southwards, it connects directly with the Llanos basin in Colombia. The Barinas basin hardly compares with a flexural basin. It is largely dominated by either north- or south-verging basement-involved structures. The tectonic inheritance is obvious, as Paleogene normal faults are locally inverted and early emplaced Paleogene Caribbean nappes are frequently reactivated or refolded by younger oblique Neogene Andean structures. Seismic profiles in this area also attest to the strong Neogene structural inversion of Upper Jurassic-Lower Cretaceous grabens. Seemingly, Paleozoic, Hercynian or more likely Caledonian structures were reactivated during both the Tethyan rifting and the Andean deformations, and account for local pre-existing crustal heterogeneities.

## STRUCTURE OF THE NORTH ANDEAN FLANK

Tectonic inheritance is less obvious along the North Andean flank, with most structures being exclusively derived from the Neogene Andean compressions. Although outcrop conditions are rather poor, numerous seismic lines and exploration wells also provide good control of the overall architecture of this part of the orogen. In the north, a flexural basin developed in Neogene times between the Andes and the Lake Maracaibo. North-verging thrusts are mainly detached in the pre-Cretaceous substratum and form a deeply buried antiformal stack, whereas secondary décollement levels occur either in the Upper Cretaceous or Tertiary strata, accounting for the passive roof thrust of a conventional frontal triangle zone.

## CRUSTAL ARCHITECTURE OF THE MERIDA ANDES

Although no deep seismic and only scarce refraction data are yet available, two trans-Andean regional profiles (Fig. 1 and Fig. 2) have been balanced and constrained by an inversion of the gravimetric data. Both sections fit with a progressive deepening of the northern Moho and require minimum south-dipping subduction of the infra-continental lithospheric mantle of the Maracaibo microplate. The shortening for both sections averages 60 km.

Palinspastic restorations assume a relative cylindricity for the deep crustal architecture of the Andes and minimize the possible effects of a progressive right-lateral escape of the Maracaibo microplate with respect to stable South America along the Bocono Fault. Due to strain partitioning, the Neogene oblique convergence induced surficial thrust fronts parallel to the plate boundary, strike-slip motion in the allochthon along the Bocono Fault, and an asymmetric subduction (wedging) at depth.

## CONCLUSIONS

The Venezuelan Andes constitute a Neogene transpressional feature. In detail, however, the tectonic inheritance of older structures accounts for contrasting structural styles along the strike of the North Andean flank, or between the northern, central and southern segments of the orogen:

Pre-existing Paleozoic thrusts account for the asymmetry observed during the subsequent Jurassic episode of rifting, as well as for the localization of intra-crustal southeast-verging Neogene conjugate backthrusts.

Pre-existing late Paleozoic or Jurassic extensional structures account for a pre-orogenic thinning of the Maracaibo lithosphere in the southern Andean segment, resulting in its presently moderate reliefs. In addition, the Neogene inversion of Jurassic grabens controls locally the structural culminations, especially in the southern part of the Barinas basin.

By contrast, pre-existing Paleogene normal faults and reactivated Eocene Caribbean thrusts are essentially restricted to the northern part of the North Andean foothills, in the Barinas basin.

An estimate of 60 km of Neogene shortening results from the construction of crustal-scale balanced cross sections. Constant along the strike of the Venezuelan Andes, this value precludes any major rotation of the Maracaibo microplate with respect to the stable South American craton.

The Merida Andes are a key example of an intercratonic orogenic belt, developed in response to oblique convergence between two independent continental lithospheric blocks. In this case, only the northwestern foreland develops as a conventional flexural basin. The surficial asymmetry of the orogen is effectively highly significant of what is happening at depth. Unlike the coastal Caribbean belt in eastern Venezuela and Trinidad, or farther south in the true Andean Cordillera, the South American lithosphere is not subducted beneath the Merida Andes. By contrast, it is the Maracaibo lithospheric microplate that is progressively involved in a southeast-dipping A-subduction.

The understanding of these particular and contrasted structural styles is of major importance for petroleum exploration. Numerous prospects indeed appear to postdate the major episodes of hydrocarbon generation and migration, and thus would not be of any interest unless a remigration of early entrapped hydrocarbons occurred.

Hopefully, this is frequently the case, as attested to by numerous discoveries in the Barinas basin, and the oil seeps that frequently occur along the North Andean foothills.

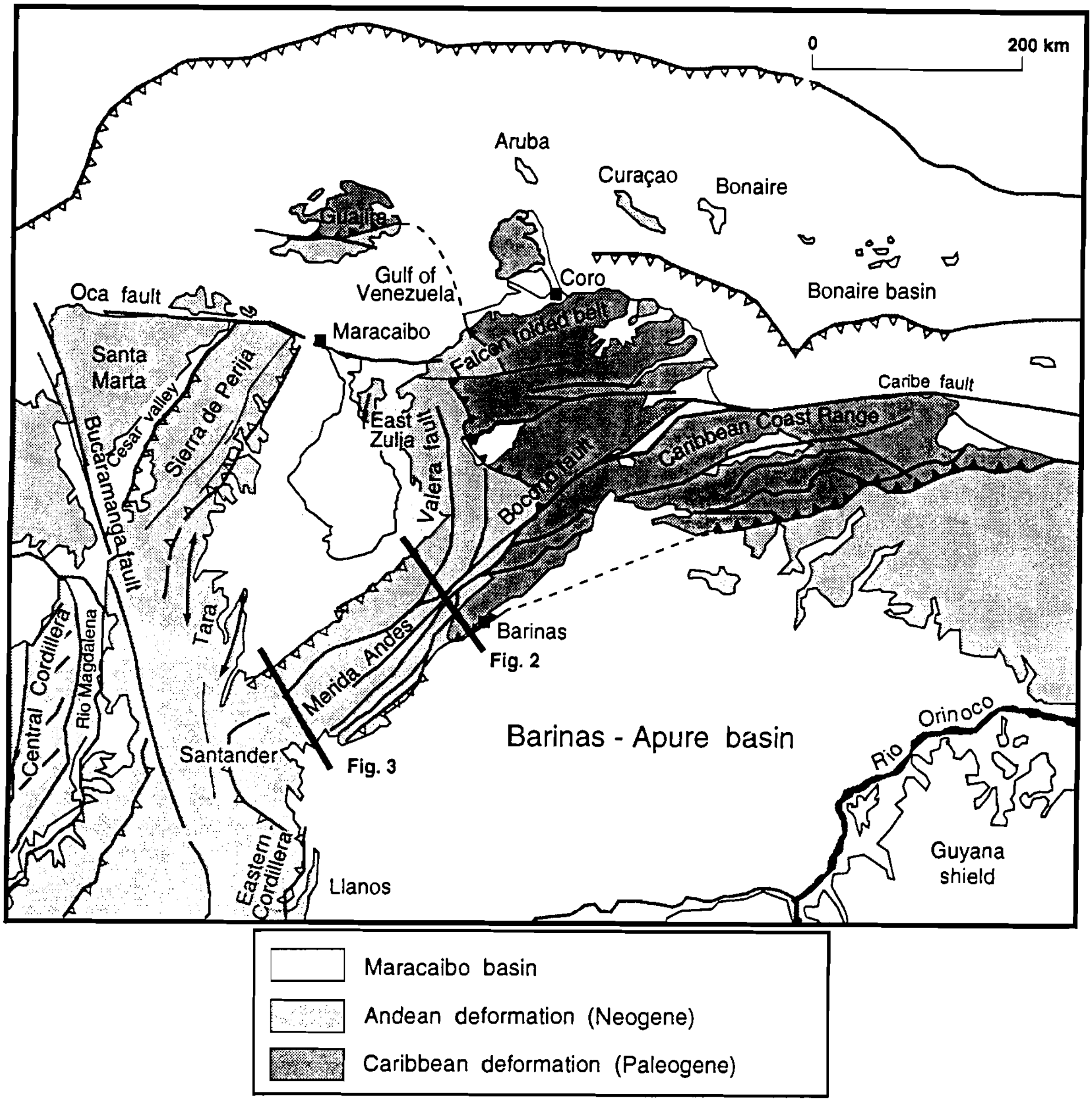


**Figure 1:** Structural map of the northwestern part of South America, imaging the Merida Andes, the Bocono Fault and their relationships with the Colombian Andes in the south, the Caribbean allochthon in the north-east.

**Figure 2:** Crustal-scale balanced section across the Central Andes. Notice the progressive underthrusting of the Maracaibo lithosphere (upper mantle) beneath the South American plate, and the progressive wedging of the upper crust. See Fig. 1 for location.

**Figure 3:** Crustal-scale balanced cross-section in the Southern Andes. Notice the relative thinning of the lithosphere in the restored section (Jurassic rifting), in place of the future Andes. For location, see Fig. 1.

Fig. 2

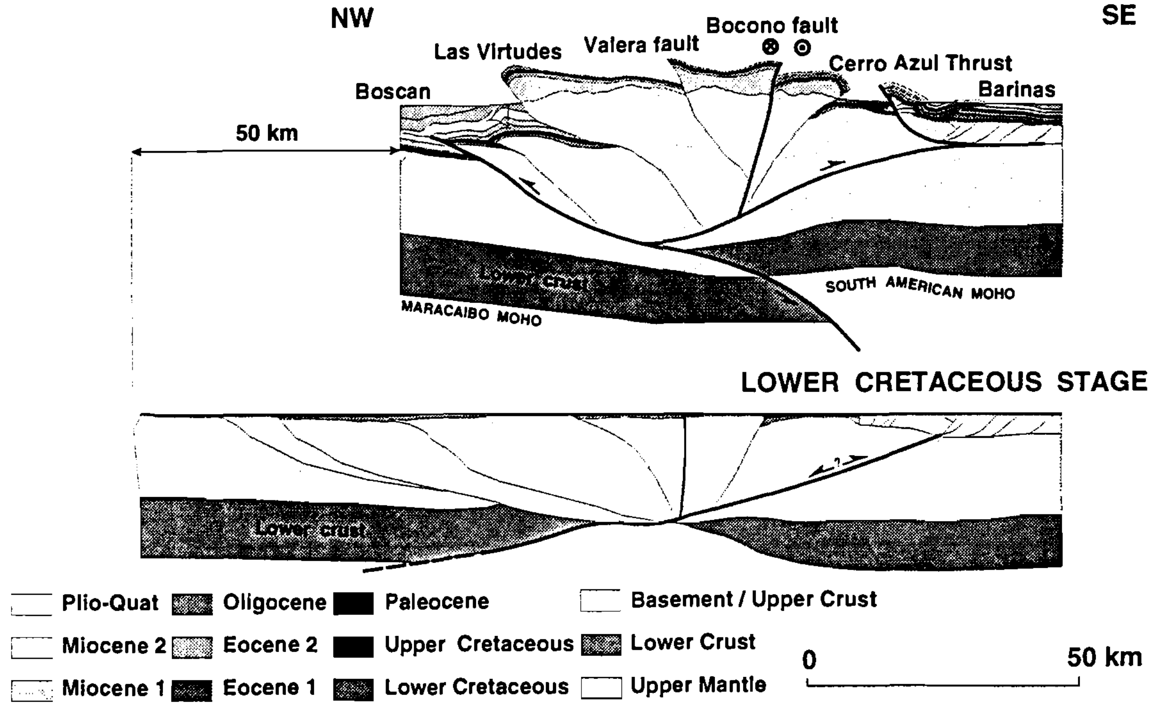
PRESENT STAGE
NW
SE
Las Virtudes
Valera fault
Bocono fault
Cerro Azul Thrust
Boscan
Barinas
50 km
Lower Crust
SOUTH AMERICAN MOHO
MARACAIBO MOHO
LOWER CRETACEOUS STAGE
Lower crust
Plio-Quat
Oligocene
Paleocene
Basement / Upper Crust
Miocene 2
Eocene 2
Upper Cretaceous
Lower Crust
Miocene 1
Eocene 1
Lower Cretaceous
Upper Mantle
0
50 km

Fig. 3

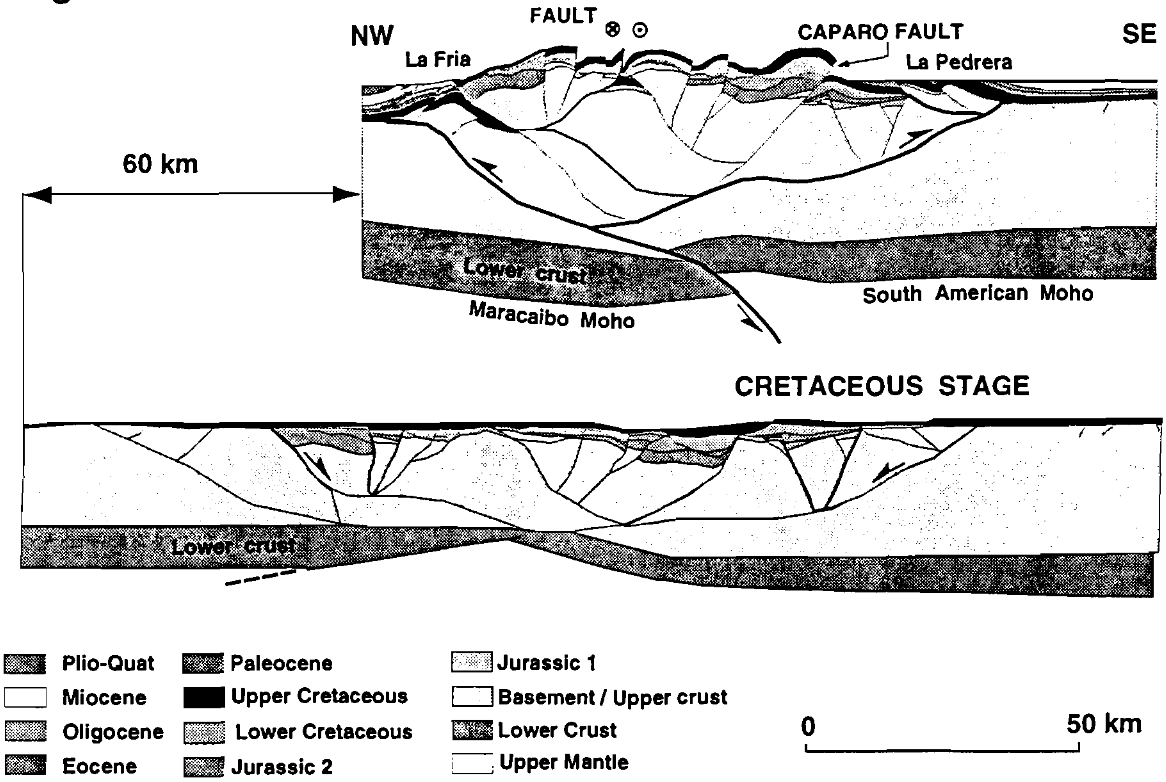
PRESENT STAGE
RIO MOCOTIES FAULT
NW
SE
La Fria
CAPARO FAULT
La Pedrera
60 km
Lower crust
South American Moho
Maracaibo Moho
CRETACEOUS STAGE
Lower crust
Plio-Quat
Paleocene
Jurassic 1
Miocene
Upper Cretaceous
Basement / Upper crust
Oligocene
Lower Cretaceous
Lower Crust
Eocene
Jurassic 2
Upper Mantle
0
50 km

# SUBSIDENCE HISTORY OF THE NORTH PERUVIAN ORIENTE (MARAÑON BASIN) SINCE THE CRETACEOUS.

Carlos CONTRERAS(1), Etienne JAILLARD(2) and Medardo PAZ(3).

(1) Convenio ORSTOM-PETROPERÚ, Av. Paseo de la República 3361, Apdo 3126, Lima, Peru.
(2) ORSTOM, Institut Dolomieu, 15, rue Maurice-Gignoux, 38031 Grenoble cedex, France.
(3) PETROPERÚ S.A., Av. Paseo de la República 3361, Apdo 3126, Lima, Peru.

KEY-WORDS : Cretaceous, Tertiary, subsidence, Andean tectonics, pericratonic basin, foreland basin.

## INTRODUCTION, GEOLOGICAL FRAMEWORK

A study of the subsidence history of the northern Oriente of Perú (Marañon Basin) has been undertaken using the backstripping method (Steckler & Watts 1978, Sclater & Christie 1980, Allen & Allen 1990). This study highlights the tectonic evolution of this distal backarc area during Cretaceous and Tertiary times (Contreras 1994, 1996).

The Cretaceous cycle began with transgressive sandstones (Cushabatay Fm), which rest disconformably on Paleozoic to earliest Cretaceous rocks. Their base is strongly diachronous from West (Valanginian ?, Tarazona 1984) to East (Albian). Marine shales of early Late Albian age were deposited all over the basin (Raya Fm). They are overlain by regressive deltaic to fluvial sandstones (Agua Caliente Fm), the top of which is strongly diachronous, being dated of Late Albian to Early Turonian age from West to East (Kummel 1948). The overlying marls, limestones and scarce sandstone beds of Turonian to Santonian age (Chonta Fm) express a major transgression. Disconformable sandstones are dated as Campanian and Early Maastrichtian (Vivian Fm, Salas 1991). A short-lived marine transgression of early Maastrichtian age (Cachiyacu Fm) is then followed by the deposition of fine-grained red beds of Maastrichtian age (Huchpayacu Fm, Mathalone & Montoya 1995).

The Tertiary series begins with fine-grained continental red beds of Paleocene age (Yahuarango Fm). They are disconformably overlain by disconformable marine to brackish shales and marls, and red siltstones and sandstones of Eocene age (Pozo Fm, Mathalone & Montoya 1995). After a probable hiatus of most of the Oligocene, red beds with local coal measures and evaporites were laid down during the Early Miocene (Chambira Fm). They are followed by a new short-lived, restricted marine transgression of late Early to early Middle Miocene age (Pebas Fm, Hoorn 1993). Red beds with conglomerate intercalations ascribed to the Late Miocene and Pliocene (Marañon Fm) are overlain by coarse-grained fluvial sandstones and conglomerates of mainly Pleistocene age (Corrientes Fm).

## METHOD AND RESULTS

Thirty wells have been selected, on the base of their geographic location, suitable depth, good quality electric records and micropaleontological and stratigraphic data. They are scattered throughout the northern part of the Oriente basin of Peru (Marañon Basin).

The age of the formation boundaries was determined using the paleontological data available in published works and confidential industrial reports (fig. 1). However, biostratigraphic revisions of the cretaceous ammonites of Peru are in progress, and some ages will need emendments. The importance and duration of sedimentary hiatuses were often approximated and/or extrapolated. Conversion to absolute ages was made using the time-scale and eustatic chart of Haq et al. (1987).

Corrections for eustatic variations through time were made on the base of the relative sea-level estimates of Haq et al. (1987). Paleobathymetric corrections were estimated following the indications of faunal assemblages and the determination of sedimentary environments.

Data processing was performed with the software "Back" version 01 (Contreras 1996), inspired

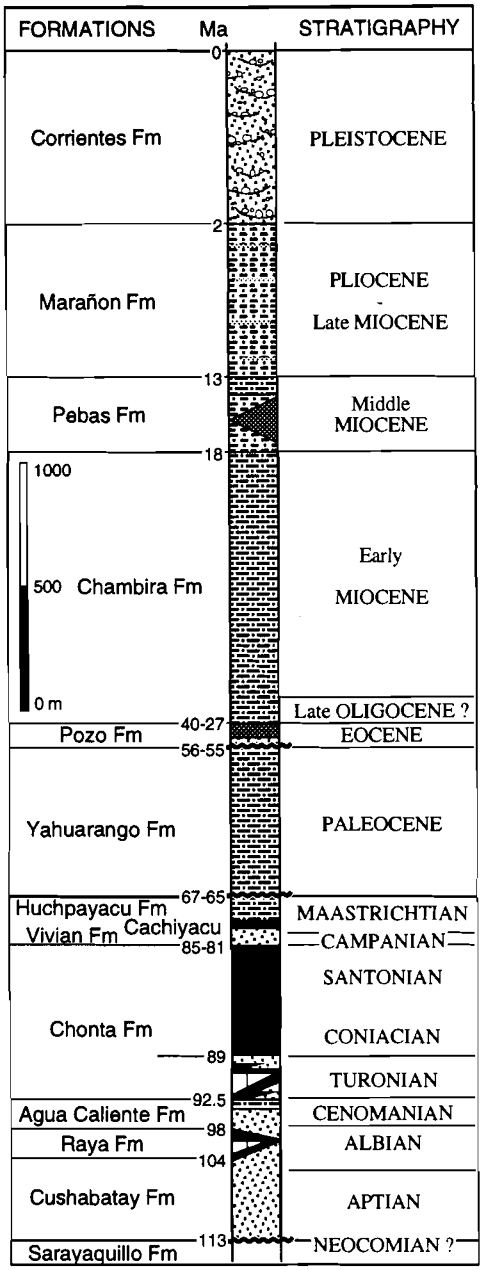


*Fig. 1 : Composite stratigraphic log of the Cretaceous and Tertiary series of the Oriente of northern Peru.*

from the algorythms elaborated by Stam et al. (1987). "Back" restaures the original thickness of the formations, taking into account the depth-porosity relations obtained from electric logging.

As a whole, tne tectonic subsidence of the Peruvian Oriente is low. Total tectonic subsidence since the Aptian vary from 1.6 km in the Southeast and 3.9 km in the Western part of the basin, with an average rate of tectonic subsidence of ≈ 35 m/Ma (Contreras 1994, 1996). This value is higher than that of the Ecuadorian Oriente (5 to 10 m/Ma, Berrones 1992, Thomas et al. 1995), and lower than that of northwestern Peru during the Cretaceous (30 to 75 m/Ma, Jaillard 1993).

During the Cretaceous, average decompacted sedimentation rates vary between 5 m/Ma (Casa Blanca Fm) to 15 m/Ma (Raya Fm), and 75 m/Ma to 56 m/Ma (Upper Chonta Fm). During the Tertiary and Quaternary, sedimentation rate is maximum during the deposition of the Corriente (160 m/Ma) and Chambira Fms (125 m/Ma) and minimum during the Eocene (9 m/Ma, Pozo Fm).

During the Cretaceous, the average subsidence rates vary between 1 m/Ma (Casa Blanca Fm) to 4 m/Ma (lower Vivian Fm), and 43 m/Ma (Cushabatay Fm). During Tertiary and Quaternary times, they range from 101 m/Ma (Chambira Fm) to 9 m/Ma (Corrientes Fm).

The subsidence rates also vary in space, evidencing a decreasing trend towards the East, SE and NE. During Late Albian and Cenomanian (Agua Caliente Fm), the subsidence rate in the western areas locally reached 35 m/Ma, whereas it is only of 6 m/Ma near the eastern border (fig. 3). During the Paleocene, subsidence rate varied from more than 90 m/Ma in the West to less than 10 m/Ma in the East of the basin. Finally, during the Early Miocene, subsidence rate was more than 160 m/Ma in the northwest, and less than 20 m/Ma in the southern part of the studied area (fig. 3).

## TECTONIC HISTORY : INTERPRETATION AND DISCUSSION.

Three major tectonic periods can be distinguished in the evolution of the basin. Each period begins with a high subsidence stage followed by a slowdown or uplift (fig. 2).

The first period corresponds to the Cretaceous (113-65 Ma). The initial subsidence (Aptian-Albian) coincides with the Mochica tectonic period (≈ Albian, Mégard 1984), whereas the uplifts and very weak average subsidence observed during latest Cretaceous times are partially coeval with the Peruvian compressional period (Coniacian-Campanian, Steimann 1929, Jaillard 1993, fig. 2). The depocenter is located near the center of the basin (fig. 3). Detailed analysis suggests that NE and NW-trending paleogeographic structures controlled the subsidence pattern. The low average subsidence rate (≈ 12 m/Ma) and the lack of significant initial subsidence suggest that there was no significant crustal stretching, the Oriente Basin behaving as a stable pericratronic, distal back-arc basin.

The second period (65-28 Ma, Paleogene) began with a drastic increase of the tectonic subsidence (Paleocene) and ended with a slight but long-termed uplift (Oligocene hiatus, fig. 2). During this stage, the depocenters migrated toward the West or Northwest, expressing the flexure of the continental crust due to the incipient crustal shortening and thickening of the paleo-Andes (fig. 3). The subsidence pulse of the beginning of this stage is poorly understood. It could be related to the end of the Peruvian compressional phase. The basal disconformity of the Pozo Fm coincides with the Late Paleocene-Early Eocene contrac-

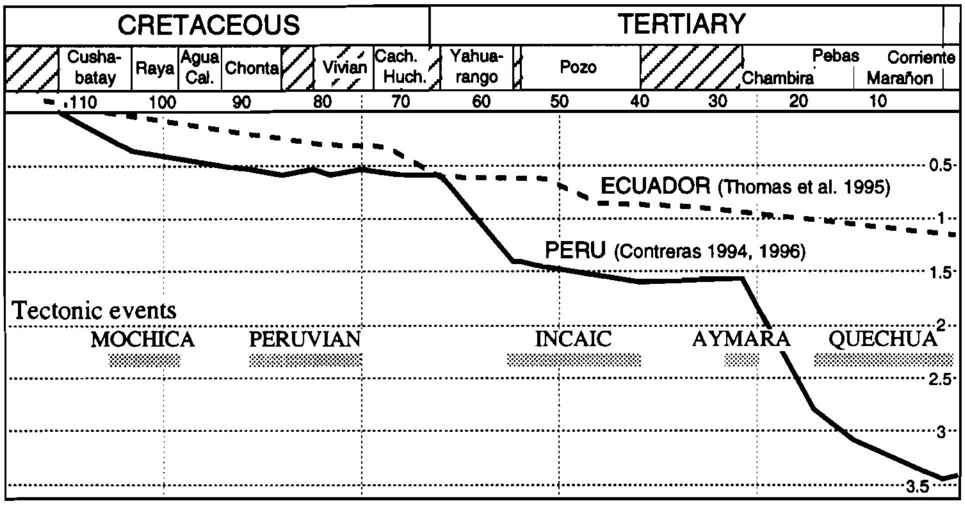


*Fig. 2 : Average tectonic subsidence of the Oriente Basin of northern Peru and Ecuador.*

tional Incaic phase. The moderate average subsidence rate (≈ 27 m/Ma), the link between subsidence and compressional tectonic phases and the pattern of the isosubsidence curves suggest that the Oriente basin was submitted to a flexural subsidence regime. This period is regarded as intermediate between the former pericratonic and the subsequent foreland periods.

The third period (28-0 Ma, Neogene) recorded a dramatic acceleration of the tectonic subsidence (Early Miocene), followed by a slowdown of subsidence (Middle Miocene-Pliocene) and then an uplift of the basin (Pleistocene). The beginning of this period coincides with an important compressive tectonic phase (Sébrier et al. 1988, Sempéré et al. 1990) and with the creation of the Miocene Andean intermontane basins (Marocco et al. 1995). The uplift recorded in the latest Pliocene-Pleistocene could correspond to the general and fast uplift of the whole andean chain since ≈ 6 Ma (Sébrier et al. 1988, Laubacher & Naeser 1994). On maps, the pattern of isosubsidence curves is disturbed, due to the incipient deformation of the subandean zone, located on the western border of the basin (fig. 3). The relatively high average subsidence rate (≈ 67 m/Ma) indicates that flexural subsidence dominates, and that the Oriente basin of Peru has become a foreland basin.

Thomas et al. (1995) identified comparable periods in the Oriente Basin of Ecuador. Their first period (108-72 Ma) seems to correspond to our first stage. However, Thomas et al. (1995) ascribed the whole Tena Fm to the Maastrichtian, while it most probably spans the Maastrichtian and Paleocene stages (Jaillard et al. 1995). Therefore, they determined a strong subsidence rate for the Maastrichtian (35-40 m/Ma) which they include into the second stage, and a hiatus during the Paleocene, which appears as a period of high subsidence in Peru (fig. 2). The age discrepancy about the beginning of the second stage (fig. 2) probably arises from the poor stratigraphic constraints about the Oligocene times. In the Oriente of Peru, the badly documented Oligocene hiatus has been mostly assumed on regional considerations (Contreras 1994).

Our results are in agreement with the interpretation of Thomas et al. (1995) of a flexural mechanism for the subsidence, typical of a foreland basin, from the beginning of the second period onwards. However, problems remain unsolved. (1) There are growing evidences of Senonian contractional deforma-

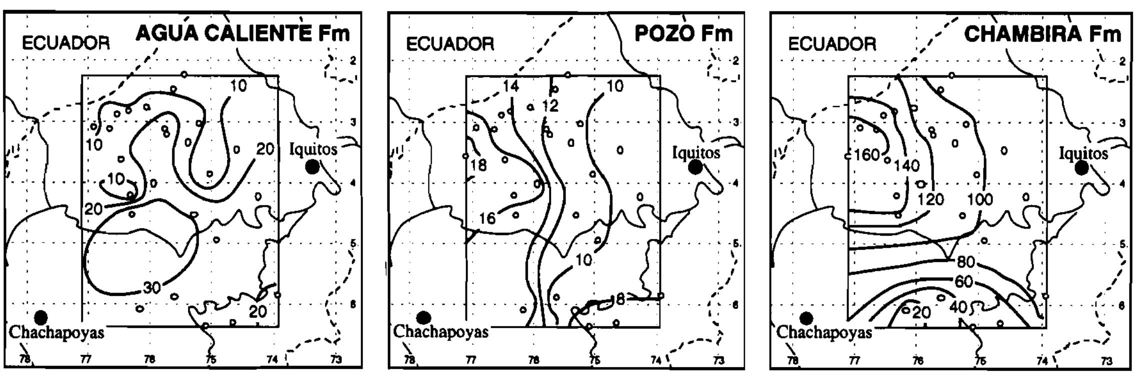


*Fig. 3 : Tectonic subsidence rates during Middle Cretaceous, Eocene and Early Miocene times.*

tions in the forearc zones, which are not recorded in the subsidence history of the Oriente basins of northern Peru and Ecuador. (2) The hiatuses that follow the subsidence pulses occur in most parts of the Oriente basins and are more frequent and important on their western border. Therefore, it seems difficult to interpret them as due to the migration of the flexural forebulge (Thomas et al. 1995). (3) In Ecuador, the subsidence seems to have not increased during the third stage (fig. 2), which is a period of rapid shortening in the subandean zone.

Therefore, it is necessary to specify the age and tectonic significance of the Tertiary deposits of the Oriente basins, in order to check wether a simple flexural model can account for the subsidence history of the Andean eastern basins at this time.

## REFERENCES


Allen, P.A. & Allen, J.R. 1990. *Basin Analysis. Principles and applications.* Blackwell, 450 p., Oxford.

Berrones, G. 1992. Estudio de la subsidencia de la Cuenca oriental ecuatoriana entre el Jurásico superior y el Reciente. *Simp. Nacion. «Investigación y desarrollo tecnológico en el área de hidrocarburos»*, Conuep & Petroproducción, eds., 2, 937-968, Quito.

Contreras, C. 1994. *Subsidencia tectónica durante el Terciario en la cuenca Marañon.* Orstom-Petroperú technical agreement, unpubl. report, 19 p., Lima.

Contreras, C. 1996. *Subsidencia tectónica durante el Cretáceo en la cuenca Marañon.* Thesis Universidad Nacional Mayor de San Marcos, 190 p., unpubl., Lima.

Haq, B.U., Hardenbol, J. & Vail, P.R. 1987. Chronology of fluctuating Sea levels since the Triassic. *Science*, 235, 1156-1167.

Hoorn, C. 1993. Marine incursions and the influence of Andean tectonics on the Miocene depositional history of northwestern Amazonia : Results of a palynological study. *Palaeogeogr., Palaeoclim., Palaeoecol.*, 105, 267-309.

Jaillard, E. 1993. L'évolution tectono-sédimentaire de la marge péruvienne au Crétacé supérieur et Paléocène et ses relations avec la géodynamique. *Bull. Soc. géol. France*, 164, 819-830.

Jaillard, E. et al. 1995. *Síntesis estratigráfica y sedimentológica del Cretáceo y Paleógeno de la cuenca oriental del Ecuador.* Convenio Orstom-Petroproducción, unpubl. report, abstract, 25 p., Quito.

Kummel, B. 1948. Geological reconnaissance of the Contamana region, Peru. *Geol. Soc. Am. Bull.*, 59, 1217-1266.

Laubacher, G. & Naeser, C.W. 1994. Fission-track dating of granitic rocks from the Eastern Cordillera of Peru : evidence for late Jurassic and Cenozoic cooling. *J. Geol. Soc., London*, 151, 473-483.

Marocco, R., Baudino, R. & Lavenu, A. 1995. The intermontane Neogene continental Basins of the Central Andes of Ecuador and Peru : Sedimentologic, tectonic and geodynamic implications. *Am. Ass. Petrol. Geol. Mem.*, 62, 597-613.

Mathalone, J.M.P. & Montoya, M. 1995. Petroleum geology of the Sub-andean Basins of Peru. *Am. Ass. Petrol. Geol. Memoir*, 62, 423-444.

Mégard, F. 1984. The Andean orogenic period and its major structures in Central and Northern Peru. *J. Geol. Soc., London*, 141, 893-900.

Salas, G. 1991. Factores geológicos de control de acumulación de hidrocarburos en las cuencas del Oriente peruano. *IV Simp. Bolivar. "Exploración petrolera en las cuencas subandinas"*, 2, 15 p., Bogotá.

Sclater, J.G. & Christie, P.A.F. 1980. Continental stretching: an explanation of the past-mid-Cretaceous subsidence of the central North Sea basin. *J. Geophys. Res.*, 85 (B7), 3,711-3,739.

Sébrier, M., Lavenu, A., Fornari, M. & Soulas, J.-P. 1988. Tectonics and uplift in Central Andes (Peru, Bolivia and Northern Chile) from Eocene to present. *Géodynamique*, 3, 85-106, Paris.

Sempéré, T., Hérail, G., Oller, J. & Bonhomme, M. 1990. Late Oligocene-early Miocene major tectonic crisis and related basins in Bolivia. *Geology*, 18, 946-949.

Stam, B., Grandstein, F., Lloyd, P. & Gillis, D. 1987. Algorythms for pororsity and subsidence history. *Comput. Geosci.*, 13, 317-349.

Steckler, M.S. & Watts, A.B. 1978. Subsidence of the Atlantic-type continental margin off New York. *Earth Planet. Sci. Lett.*, 41, 1-13.

Steinmann, G. 1929. *Geologie von Peru.* Karl Winter ed., Heidelberg, 448 p.

Tarazona, A. 1985. Palinología de la Formación Cushabatay del Pongo de Tiraco, Oriente peruano. *I Simp. Nac. Carbón*, 20 p., Lima.

Thomas, G., Lavenu, A. & Berrones, G. 1995. Evolution de la subsidence dans le Nord du bassin de l'Oriente équatorien (Crétacé supérieur à Actuel). *C. R. Acad. Sci., Paris*, 320, IIa, 617-624.

# STRUCTURE AND KINEMATICS OF A FOOTHILLS TRANSECT, LAGO VIEDMA, SOUTHERN ANDES (49° 30' S)

I. Coutand(1), Y. Le Dez(1), M. Diraison(1), P.R. Cobbold(1), D. Gapais(1), E.A. Rossello(2) and M. Miller(3)

(1) Géosciences Rennes (UPR 4661, CNRS), 35042 Rennes Cédex, France
(2) CONICET y Dpto. de Ciencias Geológicas, Universidad de Buenos Aires, República Argentina
(3) Compañía General de Combustibles, Dávila 350, 1007 Buenos Aires, República Argentina

**KEY WORDS** : Southern Andes, Lago Viedma, fold-and-thrust belt, right-lateral wrenching.

## INTRODUCTION

The Southern Patagonian Cordillera lies between 46°30' S and 55° S (Fig. 1). It first formed as a result of rapid convergence between the oceanic Nazca plate and continental South America. From 49 Ma to 25 Ma, the vector of relative motion trended approximately N010°. Since then, it has remained steady at N080° and the rate of convergence has been about 9 cm/a (Cande and Leslie, 1986; Pardo-Casas and Molnar, 1987). However, the Chile ridge collided with the Chile trench west of Tierra del Fuego at about 14 Ma (Cande and Leslie, 1986; Ramos and Kay, 1992) and rapidly moved towards the North. The Southern Patagonian Cordillera is now in the zone of convergence between the Antarctic and the South America plates. This convergence has been slower (about 2 cm/a) and directed more nearly East-West (Cande and Leslie, 1986).

Lago Viedma is a glacial lake (Fig. 1), on the eastern side of the mountains and at the northwestern edge of the Magellan Basin. This basin first formed during a Triassic rifting event (Uliana et al., 1989). It further developed as a foreland basin during Andean compression, from Albian to Oligocene times (Dott et al., 1982). A fold-and-thrust belt developed in the foothills at its western edge (Katz, 1972; Winslow, 1982; Ramos, 1989; Kraemer, 1993; Alvarez-Marrón et al., 1993).

Between Lago Argentino and Lago Viedma (Fig. 1), the main structures within the fold-and-thrust belt trend N to NNE and alternatively verge eastwards or westwards (Kraemer, 1993). Between 47° and 49°S, Ramos (1989) described passive roof duplexes, where a Paleozoic sequence underthrusts overlying Jurassic and Cretaceous sequences without emerging at the surface.

From changes in the associated pattern of sedimentation, deformation in the westernmost parts of the area could have started in the early Cenomanian (Riccardi and Rolleri, 1980; Wilson, 1983, 1991). In easternmost parts, deformation may have started in the Eocene, reaching a paroxism in the early to middle Miocene, when the Chile ridge collided with South America (Ramos, 1989; Ramos and Kay, 1992).

We have mapped a transect and drawn a section across the fold-and-thrust belt. It runs for 40 km along the northern shore of Lago Viedma, from the Miocene granitic intrusion of Monte Fitzroy (El Chaltén) in the West, to the undeformed foreland in the East (Fig. 2). The transect crosses Upper Paleozoic to Pliocene sediments. It yields new information on the structure of the fold-and-thrust belt and on the kinematics and timing of deformation.

## LAGO VIEDMA TRANSECT

In section, folds and thrusts are thick-skinned in the West and thin-skinned in the East (Fig. 2). Between Cerro Fitzroy and the Rio de las Vueltas, Paleozoic marine sediments (Bahia La Lancha Formation), Jurassic volcanics (Tobífera or El Quemado Formation), Early Cretaceous marine shales (Rio Mayer Formation) and the Fitroy granitic intrusion have all been uplifted to the surface on steeply-dipping faults with reverse components, associated with folds of km-scale wavelengths. Exhumed Early Cretaceous shales display a low-grade slaty cleavage.

Eastwards from Cerro Faldeo, folds and thrusts within unmetamorphosed Cretaceous marine sandstones are thin-skinned, above a detachment within Rio Mayer shales, about 30 km long. The top of the Tobífera volcanics is inferred to be flat-lying beneath the shale detachment. There is no surface evidence for basement duplexes underlying the eastern part of our transect.

The folds in the Cretaceous sandstones are of chevron, kink or concentric styles, typical of flexural slip between regular layers. Structures verge either eastwards or westwards. Towards the eastern end of the section, fold wavelengths tend to be larger and amplitudes smaller, recording a decrease in the intensity of shortening. Depocentres in synclines and condensed sequences over anticlines and hangingwalls of associated reverse faults, all indicate that folding was synchronous with ongoing sedimentation. Shortening was thus already underway in the Middle to Late Cretaceous.

Magmatic rocks provide further constraints on the timing of deformation. In the hinterand, the Fitzroy granitic pluton is a shallow-level, syntectonic, multiple intrusion. A cooling age of 18 ± 3 Ma (Miocene) has been obtained by the method of K/Ar on biotites (Nullo et al., 1978). The edges of the pluton are vertical, but an associated granitic sheet has been thrust over intensely folded Rio Mayer shales. In the foreland, Pliocene plateau basalts, capping the sedimentary sequence, are flat-lying or only slightly tilted. However, basaltic feeder dykes, cutting Early Cretaceous shales, are sequentially offset to the east by slip between sandstone layers, indicating that deformation continued to accumulate after the Pliocene.

Evidence for active tectonics is provided by sharp escarpments associated with major reverse faults in the hinterland.

Restoration of sections, assuming both line and area balancing, yields an estimated shortening of only 6% for the Middle to Upper Cretaceous sandstones, but as much as 37% for the Early Cretaceous shales. This difference may reflect the way deformation has accumulated throughout time, or it may indicate an eastwards attenuation in space. However, such restorations should be treated with great caution, because of probable motions into or out of the plane of section.

There are several lines of evidence in favour of right-lateral wrenching parallel to the strike of the mountain belt. In the foreland, major faults are low-angle thrusts, trending NNW, obliquely to the mountain front; whereas, towards the West, faults become of higher angle and they curve into parallelism with the mountain belt. Of the folds in the sedimentary sequence, some are flat-lying, whereas others are upright. Flat-lying folds tend to have horizontal axes trending NNW, whereas upright folds tend to have steep axes and axial surfaces trending more nearly N. These features are characteristic of wrenching in a layered sequence (Odonne and Vialon, 1983). Further evidence for wrenching is provided by flat-lying striations with right-lateral senses on steeply-dipping fault planes, especially at the mountain front (Fig. 2). Finally, the mountain front itself is a very sharp topographic feature and deformation decays rapidly away from it.

## CONCLUSIONS

In the Lago Viedma area, the Andean foothills form a fold-and-thrust belt. Between Cerro Fitzroy and the Rio de las Vueltas, thick-skinned reverse faults bring Jurassic volcanics, Paleozoic sediments and the Fitzroy granite to the surface. Further East, thin-skinned folds in Cretaceous sandstones detach on flat-lying Early Cretaceous shales.

Growth folds indicate that shortening started in the Middle Cretaceous. It appears to have continued to the Present. Fold geometries and orientations, fault striations, sharp relief and steep gradients of deformation, all provide evidence for a component of right-lateral wrenching along strike.

We suggest that the observed kinematics and the timing of deformation are due to oblique convergence of the Nazca and South American plates during the Late Cretaceous and Tertiary.

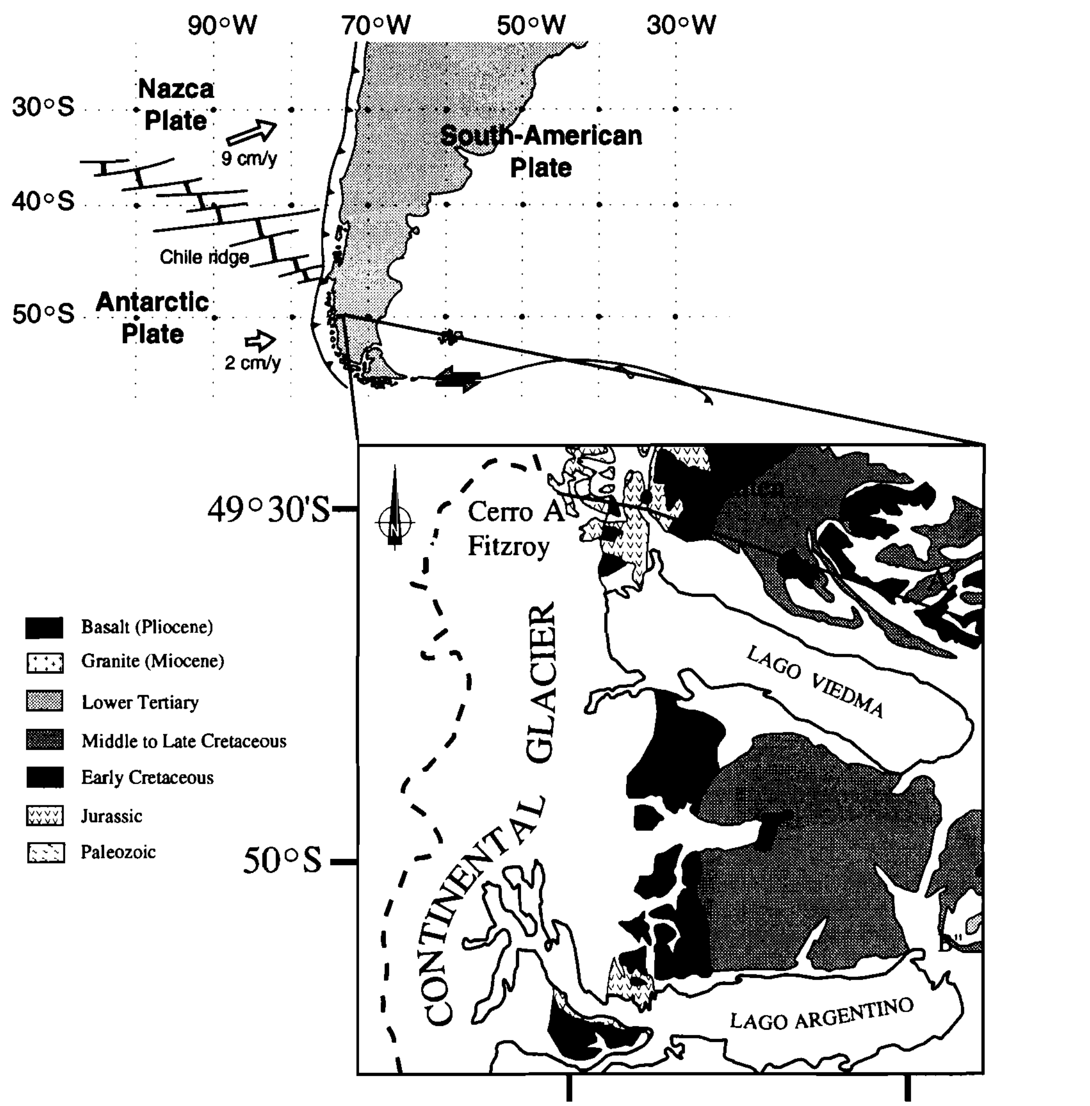


**Figure 1.**

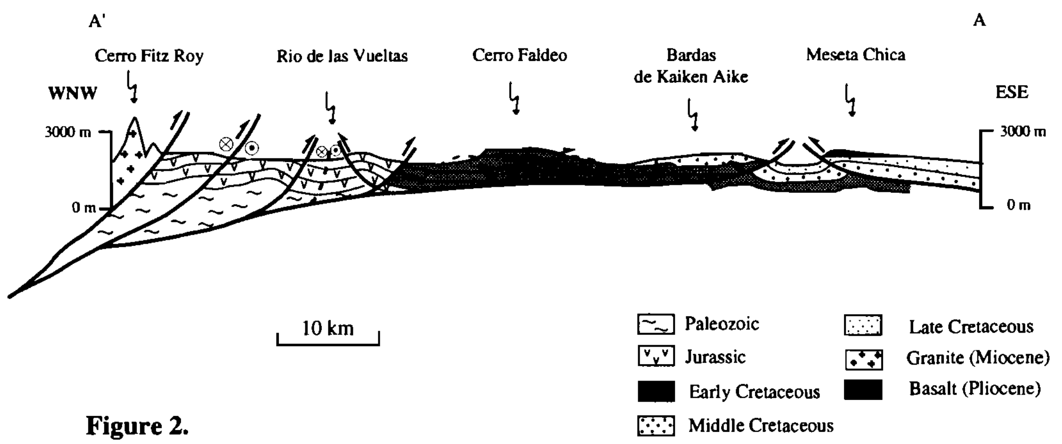


**Figure 2.**

## REFERENCES


Alvarez-Marrón, J., McClay, K.R., Harambour, S., Rojas, L. and Skarmeta, J. 1993. Geometry and evolution of the frontal part of the Magallanes foreland thrust and fold belt (Vicuña Area), Tierra del Fuego, Southern Chile. A.A.P.G. Bull., 77: 1904-1921.

Cande, S.C. and Leslie, R.B. 1986. Late Cenozoic tectonics of the southern Chile trench. J. Geophys. Res., 91: 471-496.

Dott, R.H., Jr., Winn, R.D., Jr. and Smith, C.H.L. 1982. Relationship of late Mesozoic and early Cenozoic sedimentation to the tectonic evolution of the southernmost Andes and Scotia Arc. In: Antarctic Geoscience (edited by C. Craddock), University of Wisconsin Press, Madison, Wisconsin, USA, 193-203.

Katz, H.R. 1972. Plate tectonics-orogenic belts in the southern Pacific. Nature, 237: 331.

Kraemer, P.E. 1993. Perfil estructural de la Cordillera Patagónica Austral a los 50° L.S, Santa Cruz. XII Cong. Geol. Argentino y II Cong. Explor. Hydrocarburos, Actas, 7: 119-125.

Nullo, F.E., Prosperio, C. and Ramos, V.A. 1978. Estratigrafía y tectónica de la vertiente este del Hielo Continental Patagónico. Argentina-Chile. VII Cong. Geol. Argentino, Actas, 1: 455-470

Odonne, F. and Vialon, P. 1983. Analogue models of folds above a wrench fault. Tectonophysics, 99: 31-46.

Pardo-Casas, F. and Molnar, P. 1987. Relative motion of the Nazca (Farallón) and South American Plates since Late Cretaceous time. Tectonics, 6: 233-248.

Ramos, V.A. 1989. Andean foothills structures in the northern Magallanes basin, Argentina. A.A.P.G. Bull., 73: 887-903.

Ramos, V.A. and Kay, S.M. 1992. Southern Patagonian plateau basalts and deformation: backarc testimony of ridge collisions. Tectonophysics, 205: 261-282.

Riccardi, A.C. and Rolleri, E.O. 1980. Cordillera patagónica austral. II Simp. Geol. Reg. Argentina, Acad. Nac. Ciencas, Cordoba, 2: 1173-1306.

Uliana, M.A., Biddle, K.T. and Cerdan, M. 1989. Mesozoic extension and the formation of Argentine sedimentary basins. A.A.P.G. Mem., 46: 599-614.

Wilson, T.J. 1983. Stratigraphic and structural evolution of the Ultima Esperanza foreland fold-thrust belt, Patagonian Andes, southern Chile. PhD Thesis, Univ. Colombia, New York, 360 pp.

Wilson, T.J. 1991. Transition from back-arc to foreland basin development in the southernmost Andes: Stratigraphic record from the Ultima Esperanza District, Chile. Geol. Soc. Am. Bull., 103: 98-111.

Winslow, M.A. 1981. Mechanisms for basement shortening in the Andean foreland fold and thrust belt of southern South America. In: Thrust and Nappe Tectonics (edited by K.R. McClay and N.J. Price), Geol. Soc. London Spec. Publ., 9: 513-528.

Winslow, M.A. 1982. The structural evolution of the Magallanes basin and neotectonics in the southernmost Andes. In: Antarctic Geoscience (edited by C. Craddock), University of Wisconsin Press, Madison, Wisconsin, USA, 143-154.

# BASIN INVERSION IN THE EASTERN CORDILLERAS

Michael P. COWARD(1) and Alison RIES(2)

(1) Department of Geology, Imperial College of Science, Technology & Medicine, London SW7 2BP, UK
(2) Ries-Coward Associates Ltd, 70 Grosvenor Road, Caversham, Reading, Berks., RG4 0ES, UK

KEY WORDS: basin-inversion, fault reactivation, basin modelling.

## INTRODUCTION

The sub-Andean basins show excellent examples of the geometry and kinematics of structural basin inversion, illustrating the processes by which half-grabens rotate and shorten, with coeval expulsion of the basin-fill. Fig. 1 shows an example from one of the basins in northern Peru. The original extensional fault may be locally and partially reactivated as a steep reverse fault, curving to develop a new flatter thrust profile upwards. The basin fill may be expelled in moderate to low-angle antithetic thrusts, which may form triangle zones with their own backthrust systems. Footwall shortcuts may develop, synthetic to the original normal fault and these may form their own triangle zones and back-thrust systems. The result is a thickening of the syn-rift and post-rift succession above the original half-grabens. Without seismic data or regional modelling, it is often difficult to determine the location and original position of the normal fault. Many structural interpretations ignore the basin inversion and concentrate on the thin-skinned aspects of the deformation, even sometimes attributing the deformation to salt migration.

The same arguments apply to the larger inverted basins forming the Eastern Cordilleras of Colombia, Ecuador, Peru and Bolivia. The original basins range in age from Ordovician to Cretaceous; the sharp curvature of the Andes in northern Peru is due to reactivation of two sets of orthogonal rift systems.

## EASTERN CORDILLERA OF BOLIVIA

The eastern edge of the Altiplano Basin in Bolivia displays an excellent example of large-scale basin inversion. Cretaceous source rocks are essentially confined to this basin; knowledge of its geometry is therefore critical for modelling subsequent oil maturation and migration.

The northern part of the Eastern Cordillera is characterised by a major E-dipping normal fault system of Paleozoic age, reworked to form a Cretaceous basin which, when reactivated by Andean compression, forms a series of E-dipping, W-verging thrusts, formed on the footwall of the original extensional fault (Fig. 2). However, to the S, the extensional structures had a different polarity. Here the Andean structure involved back-steepening of the basin-bounding W-dipping fault and westward tilting of the Paleogene and Neogene sediments towards the Altiplano. There was only small-scale basement fault reactivation on the flanks of the Eastern Cordillera.

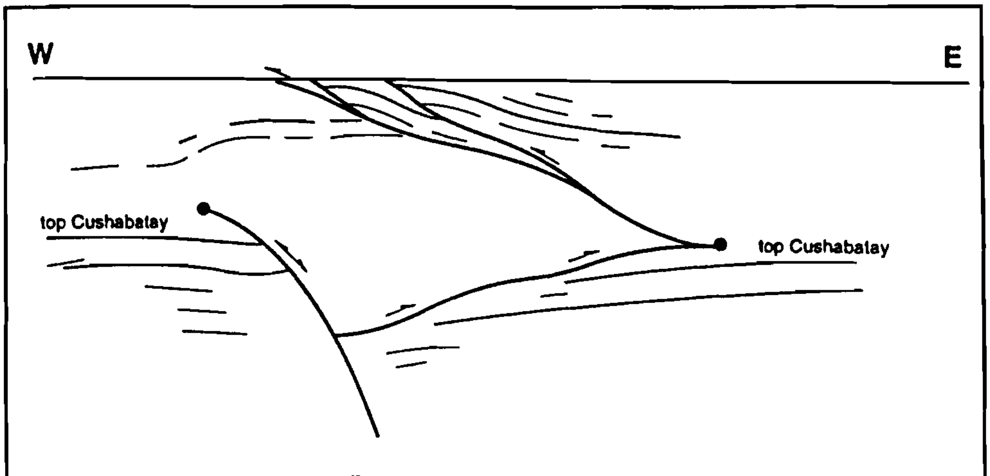


*Fig.1: Inverted half-graben, northern Peru.*

The thrusts along the western edge of the Cordillera are clearly Paleogene structures, reactivated during the Neogene. There is no outward migration of the mountain front and the structures locally back-step. Paleogene shortening exceeds Neogene shortening so that the Paleogene sections of the thrusts are longer than their reworked Neogene sections and many of the Paleogene folds and thrusts in the eastern Altiplano are unconformably overlain by only gently tilted Neogene sediments.

Thrusts along the eastern edge of the Cordillera are thin-skinned but modified by basement reactivation and local basin inversion. The thin-skinned structures can be modelled in terms of the eastward expulsion of the basin-fill, away from the main depocentre in the western part of the Cordillera. However, the amount of overthrusting across the Chaco Basin does not balance total crustal deformation without some large lateral eastward translation of the original rift basin. The deeper parts of the Eastern Cordilleran rift system probably underlie the Altiplano.

Fig. 2. Section through the western bounding fault of the Eastern Cordillera , Bolivia

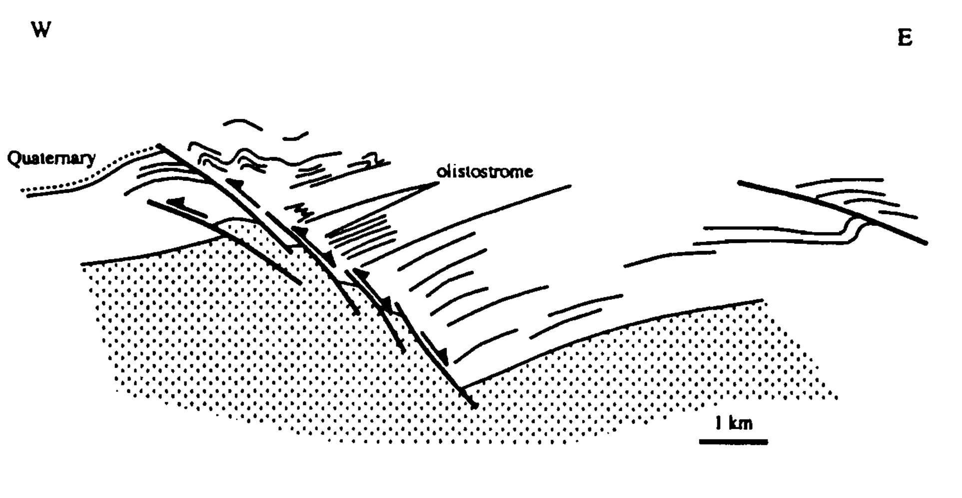

## EASTERN CORDILLERA OF COLOMBIA

Many of the recent structural sections through the Eastern Cordillera of Colombia have emphasised the importance of thin-skinned deformation and shown how the surface structures can be modelled in terms of fault bend and fault propagation folds. Thin-skinned models are clearly applicable to the eastern edge of the Cordillera in the Yopal-Cusiana area. However, there are two arguments against the general thin-skinned footwall-propagating thrust model:

(i) There is no general migration of the thrust structures or foreland basin depocentre eastwards away from the Cordillera; several of the structures appear to cut back and the flexural basin has grown in situ rather than migrated. It does not fit a typical Alpine or Himalayan model for a foreland basin.

(ii) Along strike of main part of the Eastern Cordillera, the structures can be traced into the Upper Magdalena Basin, where they clearly involve basin inversion. Many of the original normal faults dip east. antithetic to the thin-skinned thrusts on the eastern margin of the Cordillera. Shortening of the half-grabens has involved displacements along bedding-parallel detachments in the syn-rift Viletta Formation shales.

The simplified composite structural section in Fig. 3 illustrates the reinterpreted structure and essentially incorporates aspects of previous thin-skinned (Colletta et al., 1990) and thick-skinned models (Dengo and Covey, 1993). Fig. 4 illustrates a simplified reconstruction.

Fig. 3. Simplified west-east section through the Eastern Cordillera, north of Bogota

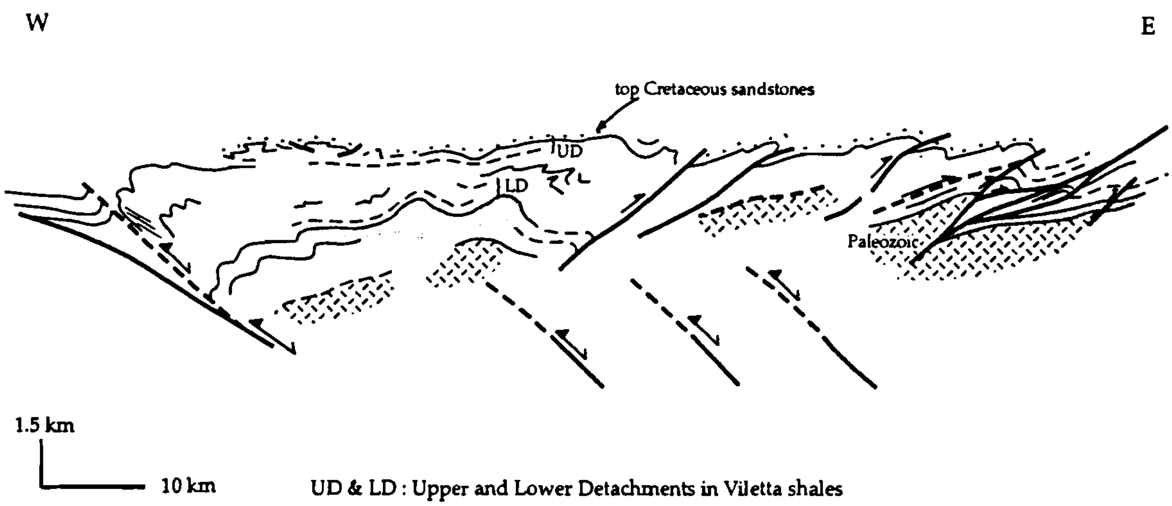


UD & LD : Upper and Lower Detachments in Viletta shales

## CONCLUSIONS

The interpretation of seismic data as well as field data in many parts of the Eastern Cordillera and sub-Andean basins has allowed new or modified interpretations to be made of the structure. These interpretations may be combined with regional tectonic data to develop models for whole crustal deformation in the eastern Andes. The new models are critical for understanding basin evolution, particularly involving hydrocarbon source rock location, maturation and subsequent hydrocarbon migration. The inverted basin concept allows the different hydrocarbon kitchen areas to be located and modelled through time.

## REFERENCES

Colletta, B., Hebrand, F., Letonzey, J., Werner, P. and Rudkiewicz, J.L., 1990. Tectonic style and crustal structure of the Eastern Cordillera (Colombia) from a balanced cross section. In: J. Letonzey (Ed), *Petroleum and Tectonics in Mobile Belts*, Paris, 81-100.

Dengo, C.A. and Covey, M.C., 1993. Structure of the Eastern Cordillera of Colombia: Implications for trap styles and regional tectonics. *A.A.P.G. Bulletin*, 77, 1315-1337.

Fig. 4. Simplified reconstruction of section shown in Fig. 3.

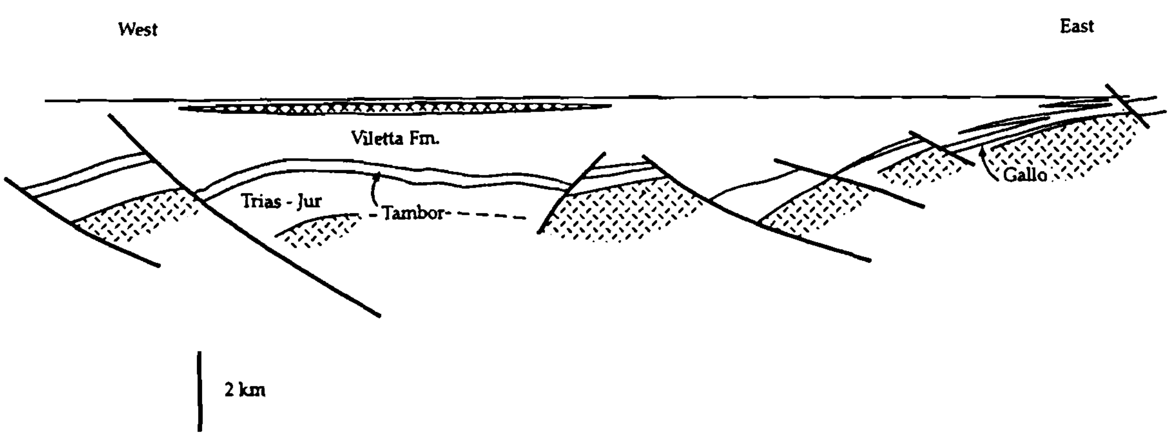

# RELATIONSHIPS BETWEEN THE STRUCTURE AND THE FORELAND BASIN IN THE HIGH ANDES NEAR 32°S, ARGENTINA

Ernesto O. Cristallini (*), Daniel J. Pérez (**)

Departamento de Ciencias Geológícas, Universidad de Buenos Aires.
Ciudad Universitaria Pabellón II.
(1428) Capital Federal, Argentina.
(*) ernesto@tango.gl.fcen.uba.ar
(**) daniel@tango.gl.fcen.uba.ar

KEYWORDS: High-Andes, Ramada-Espinacito, Manantiales, Foreland Basin, Structure, Unroofing

The Cenozoic structural evolution of the High Andes of San Juan, Argentina, near 32°00'S and 70°00'W along the international border with Chile is the result of three deformation stages (Cristallini et al., 1994) (see figure 1). The first one started with NNW trending structures detached in upper Jurassic gypsum, and is typical of a thin-skinned fold and thrust belt. In the second stage the basement is involved by the tectonic inversion of Triassic normal faults producing a thick-skinned fold and thrust belt characterized by the refolding of the old structure, and consequently a passive and ductile deformation of post Jurassic deposits took place. The deformation of the basement with high angle reverse faults at the Ramada-Espinacito Massif, produced a sticking point in the foreland propagation of the thrust belt (see figure 1). This is responsible for the third stage, characterized by NNW out-of-sequence-thrusts developed in the westernmost sector. These three stages contribute to the development of La Ramada fold and thrust belt (Ramos et al., 1995).

The erosion of these cordilleras provide the fill of the Manantiales foreland basin located to the east (Pérez, 1995) (see figure 1). Unroofing studies made in this basin constitute the main constrains to establish the timing of the structural evolution. These deposits are represented by the Chinches Formation (Mirré, 1966) consisting of seven different members (TC0-TC6) (Pérez, 1995). In each one is possible to correlate different composition with the lithology of the Mesozoic sequences that outcrop in La Ramada fold and thrust belt. These Tertiary deposits can be divided in three sections. The lower one is composed of red sandstones and conglomerates with clasts of rhyolites, carbonates and piroxene bearing andesites indicative of the Cordillera del Límite uplift. The middle of the sequence is represented by shales, sandstones and conglomerates composed of clasts of limestones and red sandstones and it is indicative of the Cordillera del Medio uplift. These two sequences represent the first deformation stage of the fold and thrust belt. The top of the Tertiary foreland sequence is represented by conglomerates and breccias bearing big blocks of rhyolitic composition that indicate the beginning of the basement uplift (Cordillera de Santa Cruz, Cordón del Espinacito). This latter represents the second stage of deformation developed in the western part of the region. Quaternary deposits unconformably overlying the Chinches Formation are composed by granitic and rhyolitic blocks in the conglomerates, that represent the final uplift of the basement, and may be related with the last stage of the fold and thrust belt development.

The unroofing studies of the Tertiary sequences have proved that the clasts have been derived from the main Cordillera. Combining the information of Tertiary sequences and structural relationships it was possible to established the timing of the deformation in the High Andes at this latitude. The base of the Tertiary deposit can be dated about 20 Ma (Pérez, 1995). This suggests that the deformation begun in the area at the Lower Miocene. Andesitic lavas dated in 9.2 ±0.3 (Cristallini and Cangini, 1993) to 10.7 ±0.7-12.7±0.7 (Pérez, 1994, 1995) unconformably overlaid the structure of La Ramada fold and thrust belt. These constrain the High Andes uplift among 20 and 10 Ma at this latitude. The unconformity between Tertiary and Quaternary deposits, suggest the a find uplift at Pliocene-Pleistocene.

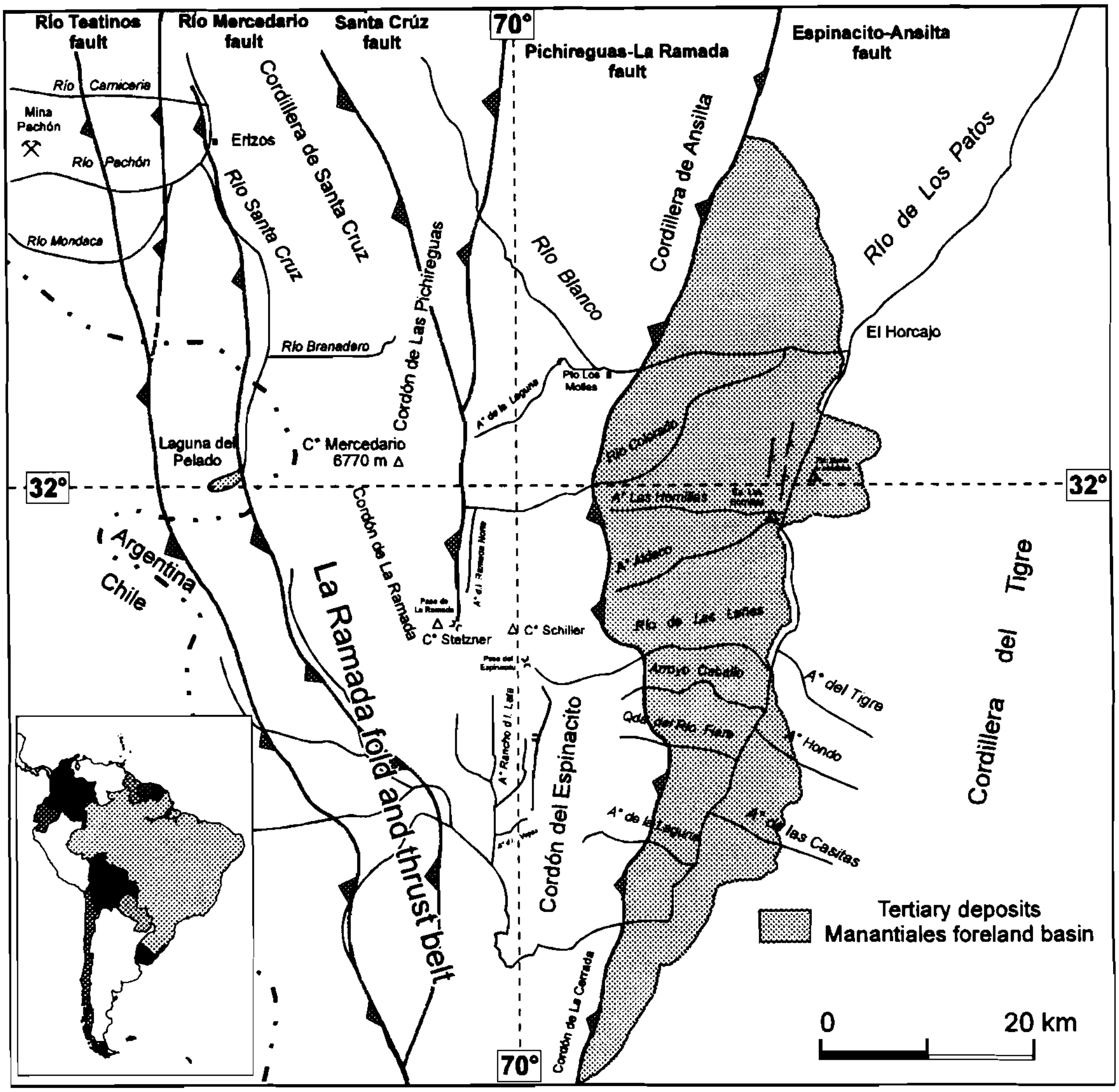


Figure 1: Geological map of the location the Chinches Formation and the main structure of the La Ramada and fold and thrust belt.

## REFERENCES

CRISTALLINI, E.O., A. MOSQUERA, V. A. RAMOS, 1994. Estructura de la Alta Cordillera de San Juan. Revista de la Asociación Geológica Argentina, 49 (1-2): 165-183.

CRISTALLINI, E. O. and A. H. CANGINI, 1993. Estratigrafía y estructura de las nacientes del río Volcán, Alta Cordillera de San Juan. XII Congreso Geológico Argentino y II Congreso de Exploración de Hidrocarburos, Actas. 3:85-92, Buenos Aires.

MIRRE, J. C., 1966. Geología del valle del río Los Patos entre Barreal y las Hornillas. Revista de la Asociación Geológica Argentina, Tomo 21, No. 4, p.211.

PEREZ, D.J., 1994. Estratigrafía y estructura del paso de las Pichireguas, Alta Cordillera de San Juan. 7° Congreso Geológico Chileno. Actas 1: 514-518. Concepción

PEREZ, D.P., 1995. Evolución geológica de la región del cordón del Espinacito, provincia de San Juan, Argentina. Universidad de Buenos Aires, Facultad de Ciencias Exacta y Naturales, Tesis Doctoral, 262p, (inédito) Buenos Aires.

RAMOS, V.A, M. CEGARRA, E.O. CRISTALLINI, 1995. Cenozoic Tectonics of the High Andes of West- Central Argentina (30°-36° S latitude). Tectonophysics, in press.

# TECTONIC INSTABILITY RELATED WITH THE DEVELOPMENT OF THE PALEOZOIC FORELAND BASIN OF THE BOLIVIAN CENTRAL ANDES (14-22°S)

Enrique DIAZ[1], Rodrigo LIMACHI[2], Víctor Hugo GOITIA[2], Daniel SARMIENTO[2], Oscar ARISPE[3] and Rubén MONTESINOS[4]

(1) ORSTOM, Casilla 9214, La Paz, Bolivia
(2) YPFB, Casilla 1659, Santa Cruz, Bolivia
(3) UMSA, La Paz, Bolivia
(4) UATF, Potosí, Bolivia

KEYWORDS : Gravity flows, Paleozoic, foreland basin, tectonic instability, Bolivia.

## INTRODUCTION

The revision of many type stratigraphic sections of the Bolivian Paleozoic Cordilleran cycle in the Altiplano, Eastern Cordillera and Subandean region revealed frequent gravity-flow deposits within the sequence. While their presence is not new, their revision and interpretation is of interest in order to corroborate the latest interpretations of the Paleozoic evolution of the Bolivian Central Andes. This work summarises the principal findings with respect to gravity-flow deposits of a 7-month-long revision of most of the type stratigraphic sections of the Silurian through Mid-Carboniferous of Bolivia, and draws conclusions on their relation with the tectonic setting during that time.

## STRATIGRAPHY AND TECTONICS

Basic stratigraphy for the Paleozoic of Bolivia has been recently revised and published under the YPFB-ORSTOM scientific cooperation agreement (Sempere, 1995; Oller, 1992). The Lower Paleozoic (Cambro-Ordovician) Tacsarian sequence mostly reflects the development of a backarc basin, which was followed by a Silurian to mid Carboniferous foreland successor basin (Sempere, 1989, 1995; Isaacson and Díaz, 1995). The Cordilleran cycle (Suárez, 1989) represents the infill of this basin (see figure 1 for reference).

1. Initiation of the foreland successor basin: the Cancañiri Fm.

This unit has been dated as Early Silurian (Llandovery) based on the latest (more recent) non-resedimented fauna present in it (Suárez, 1995). The Cancañiri Fm. presents all types of evidence for submarine sediment instability, including mass slides, rafted beds, slumps, debris flows, mud flows and turbidites. Slided and rafted beds may reach thicknesses exceeding 50 m and widths exceeding several kms. Grain-size of the resedimented material varies greatly, leading to many different lithologies depending on the degree of mixture. Evidence for glaciation of the source area is indicated by the presence of large outsized granitoid clasts, and faceted and striated clasts found within the debris flow deposits. However, there is no evidence for subglacial deposits (tillites, pavements), and it is here suggested that glaciation was local and temporarily reached the basin margins as tidewater glaciers. The thickness of this unit varies greatly from a few meters or absent, to more than 1 km in western areas. Several different events of catastrophic resedimentation can be identified, together with intermediate phases of "normal" deposition. It is probable that these events affected different areas at different times, beginning in the late Ashgillian and ending in the Wenlockian. To the west, the Cancañiri Fm. lies within two deep-marine shaly units: the Tokochi and Huanuni Fms. The overlying Llallagua Fm. consists of turbidites with a western source area, and the common depocenter area hosting the Tokochi, Cancañiri, Huanuni and Llallagua Fms. probably corresponds to the foredeep of the basin in response to tectonic deformation and piling of thrusted blocks to the west and south.

2. The Siluro-Devonian shallow-marine sedimentary fill of the foreland basin

Beginning in the Wenlockian with the Uncía and Kirusillas Fms., and ending in the Famennian with the Colpacucho and Iquiri Fms., the filling of the mid-Paleozoic retroarc foreland basin of the Bolivian Central Andes took place as a wave- and storm-dominated shallow-marine platform (epeiric sea). The high subsidence rates and sediment-supply rates kept pace with global sea-level changes, allowing for the recognition of at least three third-order cycles with variably-developed systems tracts. The depocenters and areas of maximum subsidence progressively shifted to the east and north from the Ordovician to the Carboniferous (Montemurro, 1994). This trends are related with an active deformational front located to the south and west. Higher degrees of erosion and wider pre-Cretaceous gaps in the same direction corroborate this inference. Evidence for sediment instability can be found in all the units, specially towards the southern and western areas (Figure 2). As with the Cancañiri Fm., all the different stages of submarine gravity flows are present in the Siluro-Devonian sequence, from massive slides, rafted slabs, slumps, debris flows, mudflows and turbidites. Figure 2 summarises the geographic location and the distribution in the stratigraphic column of the most important events.

3. End of the foreland setting and change of tectonic regime in the Carboniferous

The gradual shallowing-upwards and regressive tendency of the Late Devonian units is abruptly cut by a marked deepening and the initiation of resedimentation in the latest Famennian (Strunian). The Cumaná and Itacua Fms. overlie a short and poorly-preserved deepening event, followed by high clastic influx and deposition of the Ambo Group in the northern Altiplano, and the Macharetí and Mandiyutí groups in the central and southern Sub-Andes and Chaco. As with the Cancañiri Fm., evidence for a glaciated source area is indicated by the presence of large outsized granitoid clasts and frequent faceted and striated clasts found within the debris flow deposits or as dropstones. However, there is no evidence for subglacial deposits (tillites, pavements) in Bolivia, and it is suggested that glaciation was only local and temporarily reached the basin margins as tidewater glaciers (Díaz and Isaacson, 1994). Displacement of the region to lower latitudes during the Carboniferous led to important climatic changes (Sempere, 1995; Isaacson and Díaz, 1995). Serpukhovian regression set the end of the foreland basin development and the beginning of a new tecto-sedimentary cycle with erosion of relict reliefs and deposition of the Titicaca and Cuevo Groups in a different tectonic setting.

## CONCLUSIONS

Two major periods of instability events and resedimentation initiate and terminate respectively the development of the Cordilleran cycle. These two periods (latest Ordovician-Early Silurian and latest Devonian-Early Carboniferous) are characterized by resedimented units locally exceeding 1-km thickness each, which provide evidence for a tectonic imprint on the global eustatic cycles affecting the Central Andean basin. Widening of stratigraphic gaps to the south and west, and progressive displacement of the foredeep (maximum subsidence areas) and depocenters towards the east and north, are probably related with propagation of the deformational front in this latter direction. Variable-sized gravity-flow deposits throughout the sequence evidence tectonic instability during the whole Cordilleran cycle (Figure 2). Tectonic piling in the deformational front was the probable cause for the increased subsidence, sediment supply and tectonic instability which facilitated sediment failure, as well as for the development of reliefs leading to local glaciation during periods of cold climate and favourable orientation (late Ashgill-Llandovery and late Famennian-Tournaisian).

REFERENCES


Díaz E. and P.E. Isaacson 1994. Late Devonian glacially-influenced marine sedimentation in western Gondwana: the Cumaná Formation, Altiplano, Bolivia. *CSPG Memoir*, 17, 511-522.

Isaacson P.E. and E. Díaz 1995. Evidence for a Middle-Late Paleozoic foreland basin and significant latitudinal shift, Central Andes. *AAPG Memoir*, 62, 231-249.

Montemurro G. 1994. Estratigrafía y ambiente sedimentario del Silúrico y Devónico en la cuenca del Chaco boliviano. 11° Congr. Geol. Boliviano. *Memorias*, 151-160.

Oller J. 1992. Cuadro cronoestratigráfico de Bolivia. YPFB internal document.

Sempere T. 1989. Paleozoic evolution of the Central Andes (10-26°S). 28th Int. Geol. Congr., Washington D.C.. *Abstracts*, 3, 73.

Sempere T. 1995. Phanerozoic evolution of Bolivia and adjacent regions. *AAPG Memoir*, 62, 207-230.

Suárez R. 1989. El Ciclo Cordillerano (Silúrico-Carbonífero inferior) en Bolivia y su relación con países limítrofes. *Revista Técnica YPFB*, 10 (3/4), 233-243.

Suárez R. 1995. Comentarios sobre la edad de la Formación Cancañiri. *Revista Técnica YPFB*, 16 (1-2), 51-54.


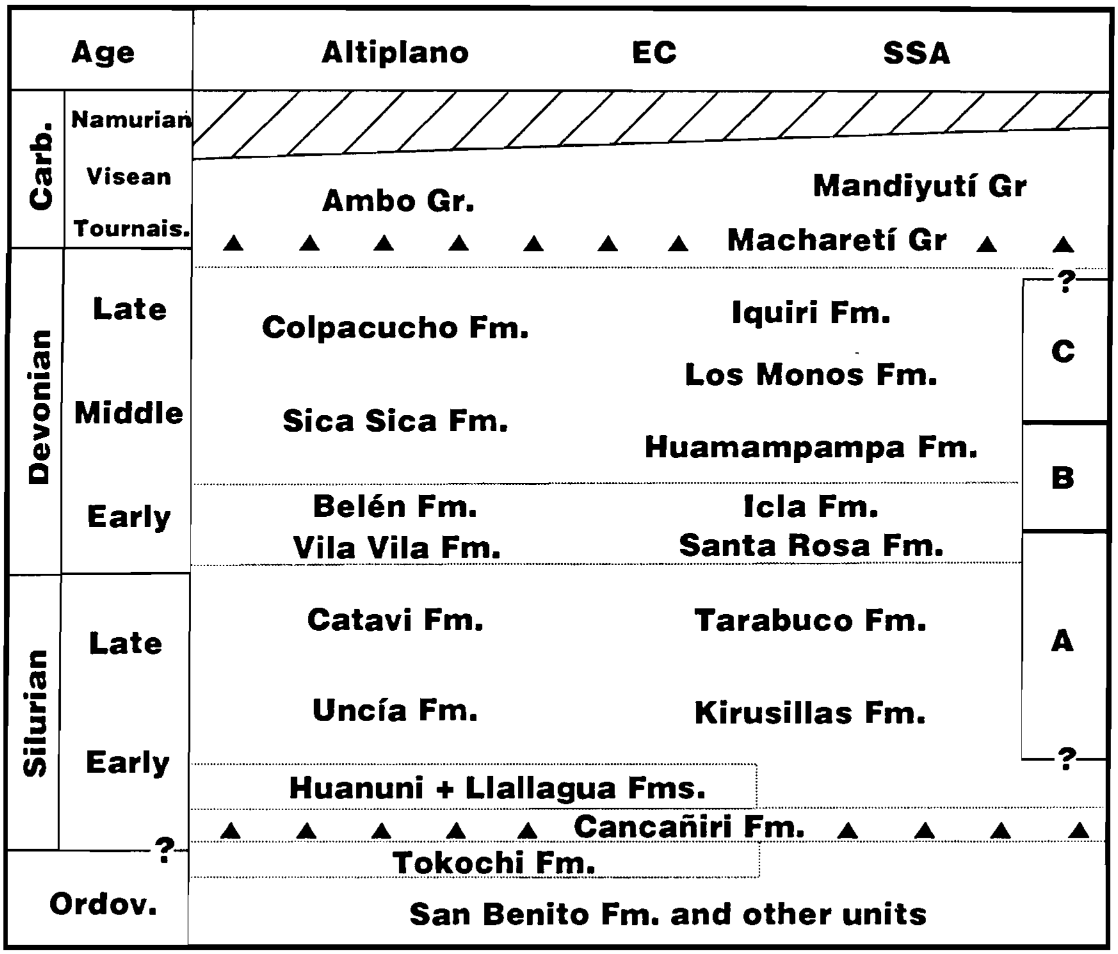


Figure 1: Simplified stratigraphy and correlation of the Paleozoic Cordilleran cycle (Silurian-early Carboniferous) of the Bolivian Central Andes. Triangles indicate the two major events of tectonic instability and resedimentation. A, B, C: main third-order cycles. EC: Eastern Cordillera, SSA: southern Sub-Andes.

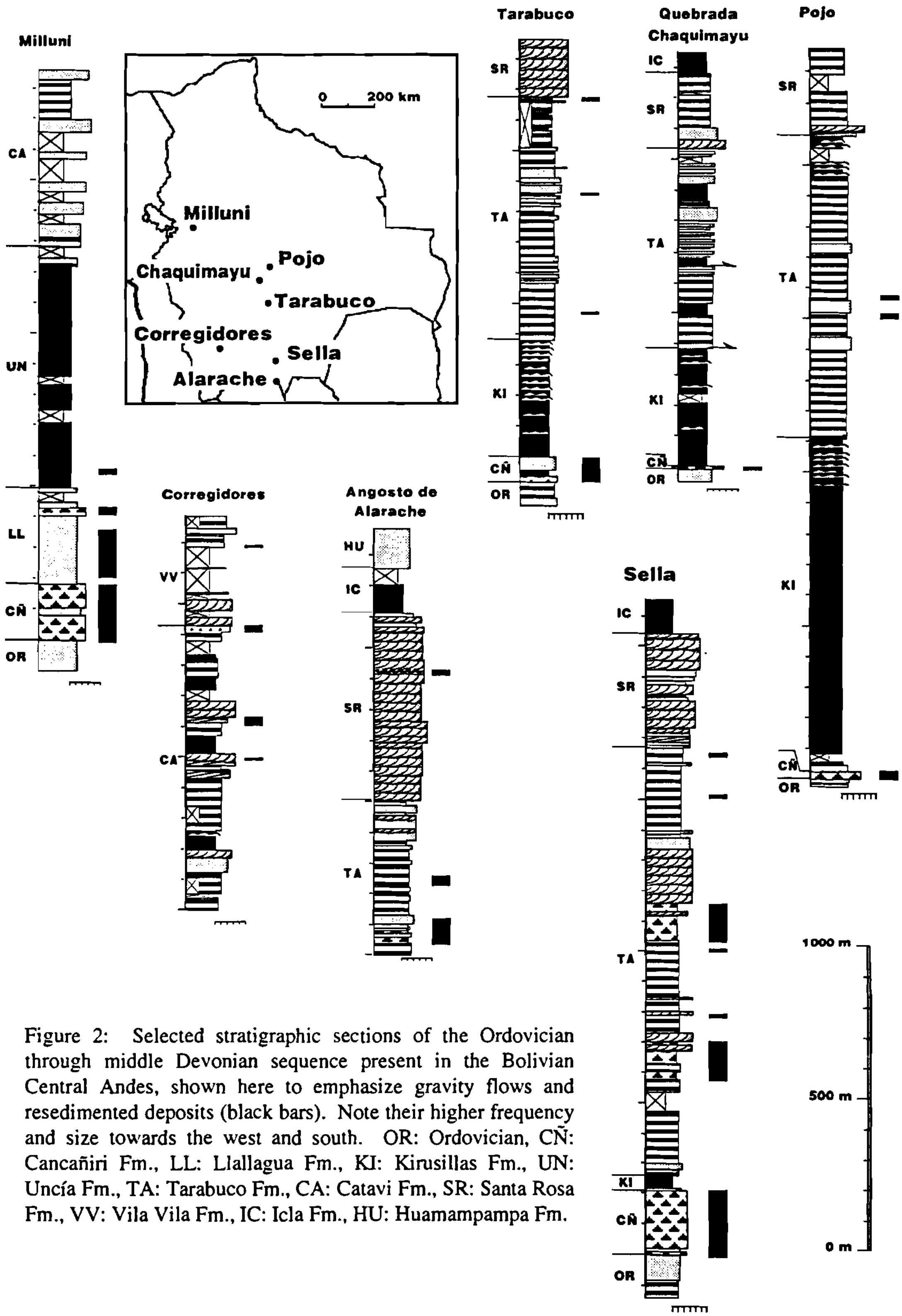


Figure 2: Selected stratigraphic sections of the Ordovician through middle Devonian sequence present in the Bolivian Central Andes, shown here to emphasize gravity flows and resedimented deposits (black bars). Note their higher frequency and size towards the west and south. OR: Ordovician, CÑ: Cancañiri Fm., LL: Llallagua Fm., KI: Kirusillas Fm., UN: Uncía Fm., TA: Tarabuco Fm., CA: Catavi Fm., SR: Santa Rosa Fm., VV: Vila Vila Fm., IC: Icla Fm., HU: Huamampampa Fm.

# TERTIARY KINEMATICS OF THE SOUTHERN ANDES AND THE DEVELOPMENT OF THE MAGELLAN FORELAND BASIN (PATAGONIA).

Marc DIRAISON[1], Peter R. COBBOLD[1], Denis GAPAIS[1], Eduardo A. ROSSELLO[2]

[1] Géosciences-Rennes (UPR 4661 du CNRS), Université de Rennes I, 35042 RENNES Cedex, France
[2] CONICET and Universidad de Buenos Aires, Departamento de Ciencias Geológicas, Ciudad Universitaria, 1428 Buenos Aires, República Argentina

**KEY WORDS:** Southern Andes, Magellan Basin, Fault kinematics, Modelling.

## INTRODUCTION AND GEOLOGICAL SETTING

Between the Patagonian Cordillera (trending N-S) and the Darwin Cordillera (trending E-W), the Southern Andes form an arc. This bounds the Magellan Basin on its western and southern sides (Fig. 1). Both arc and basin result from complex tectonics at the southwestern margin of Gondwana since the Late Triassic (Rapela & Pankhusrt, 1992, Storey, 1993). The basin has been through three main stages. First, a stage of regional extension (Triassic to Early Cretaceous), contemporaneous with early opening of the Southern Atlantic, formed a rift system trending NNW and led to opening of the Magellan back-arc basin (Dalziel, 1974). Second, during the Late Cretaceous, closure of the back-arc basin coincided with changes in the plate tectonics. The closure was associted with uplift of the Cordillera and thermal subsidence of the Magellan Basin (Nelson, 1982). Third, during the Tertiary, the Magellan Foreland Basin formed and deformation propagated cratonward, via a fold-and-thrust belt (Winslow, 1982, Alvarez-Marrón et al., 1993). The sedimentary infill of the basin, synchronous with deformation, is locally as much as 8 km thick. The distribution of Tertiary sediments shows a degree of mirror symmetry about the Magellan Straits (Fig. 1).

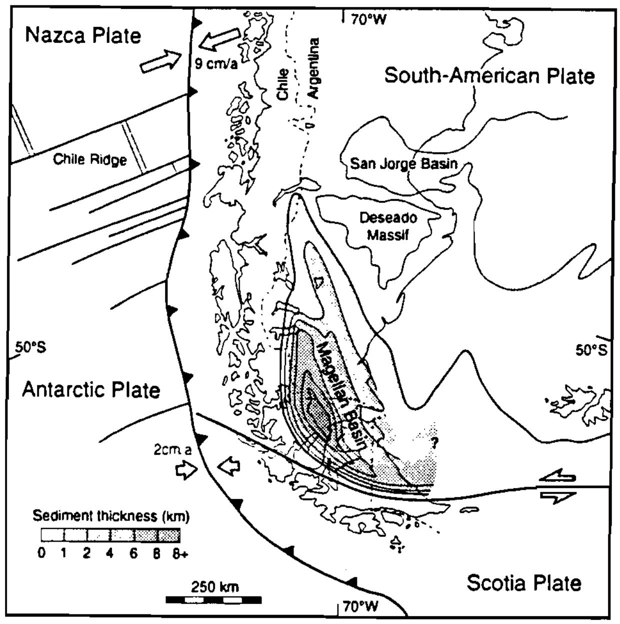


**Figure 1:** Map of southern South America showing tectonic setting with adjacent oceanic plates. Grey arrows indicate relative motions between plates. Sediment thicknesses in Magellan Basin are indicated in shades of grey (modified from Ramos, 1989).

We present a structural interpretation of the area, based on field observations, satellite imagery, kinematic analysis of fault data and analogue models.

## FAULT KINEMATICS

We have measured over 1500 striated fault planes at 74 localities between lake Buenos Aires and Tierra del Fuego (Fig. 2). Localities are either in basement rocks or in their Mesozoic and Cenozoic cover and they are mainly along the southwestern edge of the basin. A graphical and kinematic method has been used to analyse fault-slip data. Results show that (1) the principal directions of shortening are sub-horizontal and strike sub-perpendicularly to the Cordillera, (2) the principal directions of extension are also sub-horizontal and (3) strain ellipsoids are estimated to be mainly of plane-strain to flattening type at regional scale (Fig. 2).

At outcrop scale, fault-slip data provide information on the relative proportions of strike-slip and dip-slip faulting. Strike-slip is dominant, either right-lateral and trending N along the Patagonian Cordillera or left-lateral and trending E along Cordillera Darwin. These observations are consistent with strike-slip faults interpreted on satellite imagery. We have also found normal faults trending perpendicularly to the Cordillera, especially along lakes Viedma and Argentino, and, most important, along the Magellan Straits.

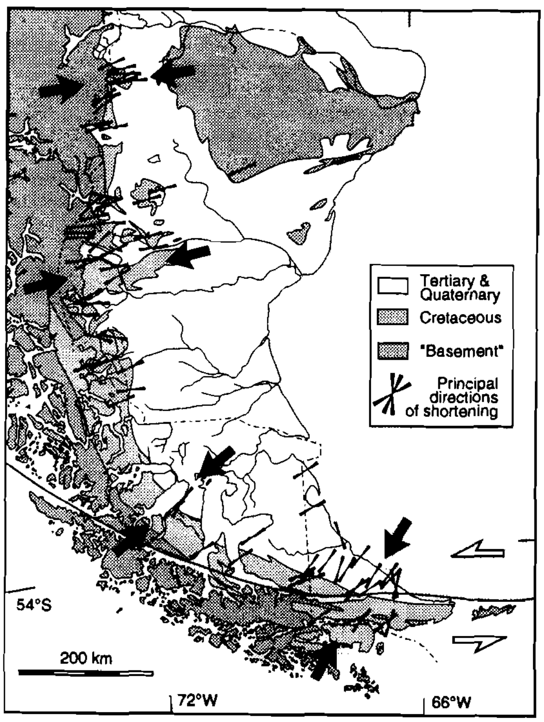


**Figure 2:** Schematic geological map with results of kinematic fault analyses at 74 localities. Small black arrows indicate calculated shortening directions. Large dark arrows summarize regional trends.

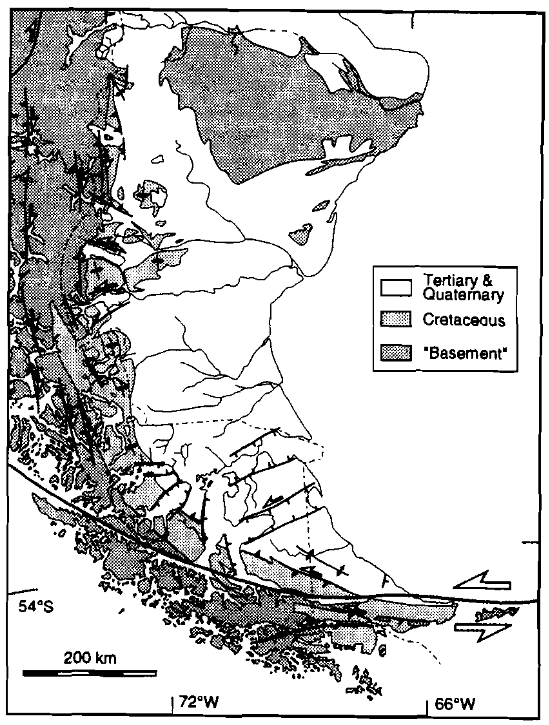


**Figure 3:** Schematic geological and structural map of studied area. Major reverse faults in Chilean Cordillera are partly from Landsat interpretation.

## REGIONAL STRUCTURES

Major folds and thrusts have long been recognized in the Cordillera and its foothills next to the Magellan Basin (Servicio Nacional de Geología y Minería, 1980). Strike-slip faults have been less documented. A few left-lateral ones have been described in Cordillera Darwin (Cunningham, 1993, Klepeis, 1994) and the right-lateral Liquiñe-Ofqui fault system has been documented in the field and from satellite imagery in the Patagonian Andes north of latitude 45° S. Our own studies have revealed other strike-slip fault systems, including left-lateral ones, both ductile and brittle, in the Cordillera of Tierra del Fuego (Argentina) and right-lateral ones in the foothills of the Patagonian Cordillera. Using geological maps, satellite images and field observations, we have compiled a schematic map of major faults and folds (Fig. 3). Major thrusts are sub-parallel to the Cordillera but have strike-slip components. Of greatest novelty are grabens and half-grabens of Tertiary age which accommodate extension in directions sub-parallel to the Cordillera. Prominent examples lying along the Magellan Straits have partially separated Tierra del Fuego from the mainland. Some normal faults also have components of strike-slip, depending on their trends.

Some of the major Tertiary structures are reactivated faults of Mesozoic age or possibly older.

## ANALOGUE MODELS

We have investigated the plate tectonics of southern South America and the possibility of inducing deformation at its southern tip, using analogue models at fully lithospheric scale. Brittle upper crust was modelled with dry sand; ductile lower continental crust and lithosperic mantle, with silicone putties of appropriate viscosities and densities. For oceanic lithosphere, the ductile lower crust was omitted. The model lithosphere floated on a less viscous asthenosphere. Continental South America was given a rectangular shape with a rounded corner. Horizontal forces and velocities were applied in a given direction to the oceanic plate, to simulate spreading at a mid-oceanic ridge.

During the experiments, subduction initiated spontaneously at the western continental margin sub-perpendicular to the applied convergence. The oceanic plate subducted at a low angle and the adjacent continent became folded at lithospheric scale. In contrast, at the southern margin, deformation was transpressive and more localized. In some experiments, rifts developed at the corner of the continent and the blocks between them underwent rotations about vertical axes. These preliminary results are consistent with structural observations made in the field and with our analyses of fault-slip data.

## CONCLUSIONS

In the southern Andes and Magellan Basin, the observed structural pattern is consistent with the complex tectonic context of southern South America. Deformation within the continent is due to relative motions between the Nazca, Antractic, Scotia and South American plates. The deformation includes shortening in directions subperpendicular to the mountain belts and also components of strike-slip: right-lateral along the Southern Patagonian Andes and left-lateral along Cordillera Darwin. Between them, stretching along the arc has resulted in the formation of rift valleys.

## REFERENCES

Alvarez-Marrón, J., McClay, K.R., Harambour, S., Rojas, L. and Skarmeta, J. 1993. Geometry and Evolution of the Frontal Part of the Magallanes Foreland Thrust and Fold Belt (Vicuña Area), Tierra del Fuego, Southern Chile. Am. Assoc. Petrol. Geol. Bull., 77: 1904-1921.

Bruhn, R.L. 1979. Rock structures formed during back-arc basin deformation in the Andes of Tierra del Fuego. Geol. Soc. Am. Bull., 90: 998-1012.

Cunningham, W.D. 1993. Strike-slip faults in the southernmost Andes and the development of the Patagonian Orocline. Tectonics, 12: 169-186.

Dalziel, I.W.D., de Wit, M.J. and Palmer, F.K. 1974. Fossil marginal basin in the southern Andes. Nature, 250: 291-294.

Klepeis, K. 1994. Relationship between uplift and the metamorphic core of the southernmost Andes and shortening in the Magallanes foreland fold and thrust belt, Tierra del Fuego, Chile. Tectonics, 13: 882-904.

Nelson, E.P. 1982. Post-tectonic uplift of the Cordillera Darwin orogenic core complex: Evidence from fission track geochronology and closing temperature-time relationship. J. Geol. Soc. London, 130: 755-762.

Ramos, V.A., 1989. Andean foothills structures in Northern Magallanes Basin, Argentina. Am. Assoc. Petrol. Geol. Bull., 73: 887-903.

Rapela, C.W. and Pankhusrt, R.J., 1992. The granites of northern Patagonia and the Gastre fault system in relation to the break-up of Gondwana. In: Magmatism and the Causes of Continental Break-up. Geol. Soc. London Spec. Publ., 68: 209-220.

Servicio Nacional de Geología y Minería 1980. Geological map of Chile. Scale: 1: 1, 000, 000. Six sheets.

Storey, B.C., 1993. Tectonic controls on Gondwana break-up models: Evidence from the Proto-Pacific margin of Antartica. Tectonics, 10: 1274-1288.

Winslow, M.A., 1982. The structural evolution of the Magallanes Basin and neotectonics in the southernmost Andes. In: C. Craddock (Editor), Antartic Geoscience. University of Wisconsin, Madison, WI: 143-154.

# CENOZOIC THRUSTING AND RIGHT LATERAL WRENCHING IN THE BARILOCHE AREA, SOUTHERN ANDES.

Marc DIRAISON [1], Peter R. COBBOLD [1], Eduardo A. ROSSELLO [2] and Arturo J. AMOS [3]

[1] Géosciences-Rennes (UPR 4661 du CNRS), Université de Rennes I, 35042 RENNES Cedex, France
[2] CONICET and Universidad de Buenos Aires, Departamento de Ciencias Geológicas, Ciudad Universitaria, 1428 Buenos Aires, República Argentina
[3] PROGEBA, San Carlos de Bariloche, República Argentina

**KEY WORDS:** Southern Andes, Fault kinematics, Digital image, Right-lateral transpression.

## INTRODUCTION AND GEOLOGICAL SETTING

In Northern Patagonia, the Andean chain is made of several structural and topographic units (Cingolani et al., 1991): the Coastal Ranges (an accretionary prism), the Central Valley, the main Cordillera (containing the current volcanic arc) and the Sub-Andean zone (Fig. 1). These units formed during subduction of the Nazca plate along the Chilean trench. The plate boundary between Nazca and South America is oblique to the direction of relative plate convergence (Fig. 1).

The Bariloche area straddles the eastern part of the main Cordillera and Tertiary sediments of the Sub-Andean zone between 40° and 42°S. The area includes the northern part of the Ñirihuau Basin, south of lake Nahuel Huapi (41°S).

The eastern part of the main Cordillera is made of metamorphic and intrusive rocks (Cazau et al., 1989) and remnants of Mesozoic sedimentary basins which are inverted grabens. Early Tertiary volcano-clastic rocks (Huitera and Ventana formations), a product of the volcanic arc, have been incorporated into the main Cordillera north of lake Nahuel Huapi.

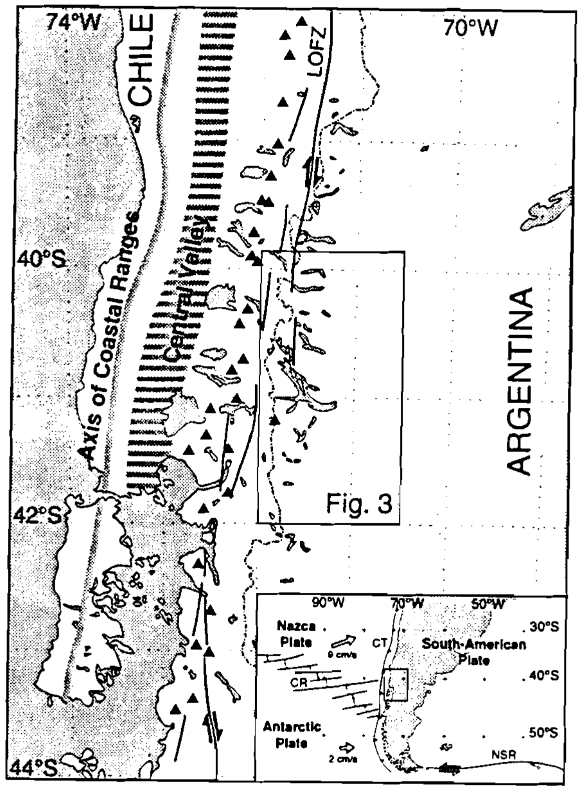


**Figure 1:** Schematic map showing location of area studied. Inset shows tectonic setting of southern South America with adjacent oceanic areas. White arrows, indicating relative motion between plates, are from model NUVEL-1 of Gripp and Gordon (1990). CR: Chile Ridge, CT: Chile Trench, NSR: North Scotia Ridge. Main map shows Central Valley (dashed zone) between Coastal Ranges (grey line) and main Andean Cordillera. Altitudes over 1000 m. are shaded (grey). Solid triangles indicate volcanoes. The Liquiñe Ofqui Fault Zone (LOFZ) is a set of right-lateral fault segments (black lines with opposing arrows) visible on Landsat images (after Dewey and Lamb, 1992).

In the Late Tertiary, volcanic activity diminished and the Ñirihuau Basin developed in a back-arc context. It contains shallow-marine and fluviatile sediments (Ñirihuau Formation, Lower to Middle Miocene), followed by continental sediments with some volcanics (Collon Cura Formation, Upper Miocene and Pliocene ).

Our structural interpretation of the area is based on field observations, digital data and a kinematic analysis of fault-slip data.

## REGIONAL STRUCTURES

A digital topographic image shows the general northerly trend of the Andes and its sharp eastern boundary (Fig. 2). Major transverse valleys are occupied by Quaternary glacial lakes. A close correlation between topography and regional structures is revealed by superimposing digital geological and topographic maps. Major structures follow two main trends (Fig. 3). Reverse faults trend SE, as along lake Nahuel Huapi. High-angle oblique-slip fault systems (reverse, right-lateral) trend N, as in the valley north of El Bolsón and within both basement and Tertiary sediments north of 41°S.

## FAULT KINEMATICS

We have mesured striated fault planes at 33 outcrop localities, located in both basement and cover rocks (Fig. 4) and have analysed the fault-slip data using graphical and kinematic methods. The principal direction of shortening is sub-horizontal and strikes between NNE and ENE at regional scale; the principal direction of extension is also sub-horizontal (Fig. 4). Strain ellipsoids are estimated to be mainly of plane-strain to flattening type.

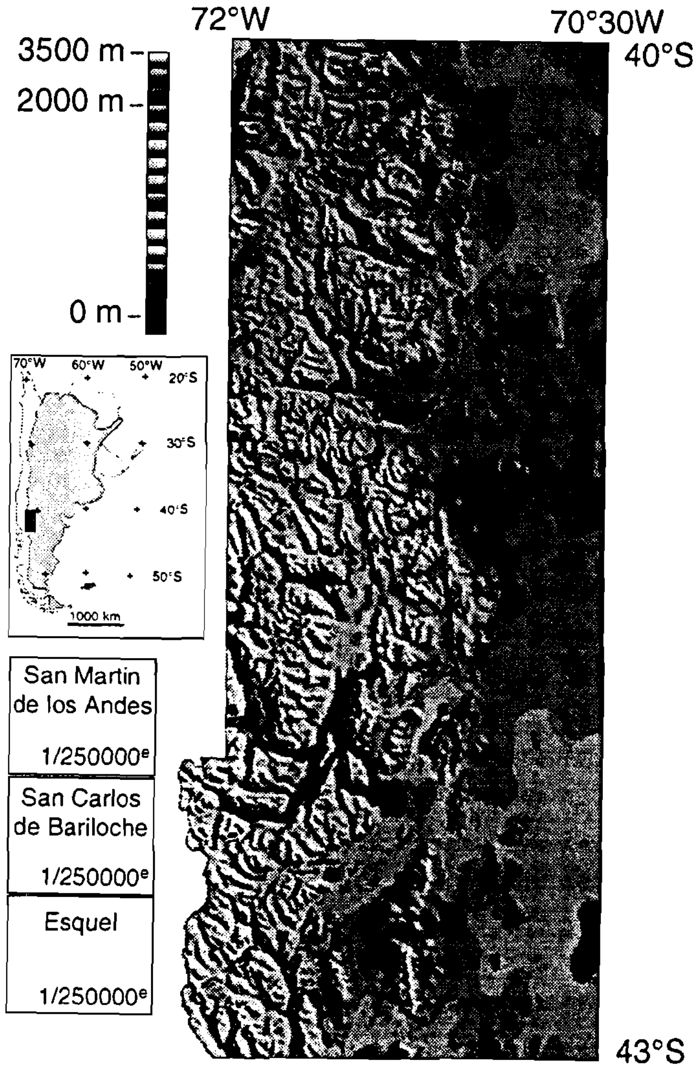


**Figure 2:** Digital topographic image, compiled from the following maps edited by the Instituto Geogrâphico Militar Argentino at 1/250 000: San Martín de los Andes (4172-II), San Carlos de Bariloche (4172-IV) and Esquel (4372-II and 4372-I). Artificial illumination is from the NE.

At outcrop scale, fault-slip data provide information on the relative proportions of crustal thickening and strike-slip faulting. Predominant are faults with components of right-lateral strike-slip trending N or conjugate left-lateral strike-slip trending E.

## CONCLUSIONS

Throughout the area, major reverse faults and thrusts trend SE, forming the edges to Cenozoic basins of foreland or ramp styles. Some of these are inverted grabens of Mesozoic age. The dominant strike-slip faults are right-lateral and trend nearly N, parallel to the Andean chain. Conjugate left-lateral faults trend nearly E.

From the fault-slip data, the principal direction of shortening trends NE. It is compatible with the oblique direction of convergence between the Nazca and South America plates. However, we also infer a regional component of right-lateral wrenching. This tectonic style seems to have lasted throughout the Neogene.

## REFERENCES

Cazau, L., Mancini, D., Cangini, J. and Spalletti, L. 1989. Cuenca de Ñirihuau. Cuencas Sedimentarias Argentinas: 299-318.

Cingolani, C.,Dalla Salda, L., Hervé, F., Munizaga, F., Pankhurst, R.J., Parada, M.A. and Rapela, C.W. 1991. The magmatic evolution of Northern Patagonia; new impressions of pre-andean and andean tectonics. Geological Society of America. Special Paper, 265: 29-43.

Dewey, J.F. and Lamb, S.H. 1992. Active tectonics of the Andes. Tectonophysics, 205: 79-95.

Gripp, A.E. and Gordon, R.G. 1990. Current plate velocities relative to the hotspots incorporating the NUVEL-1 global plate motion model. Geophysical Research Letters, 17: 1109-1112.

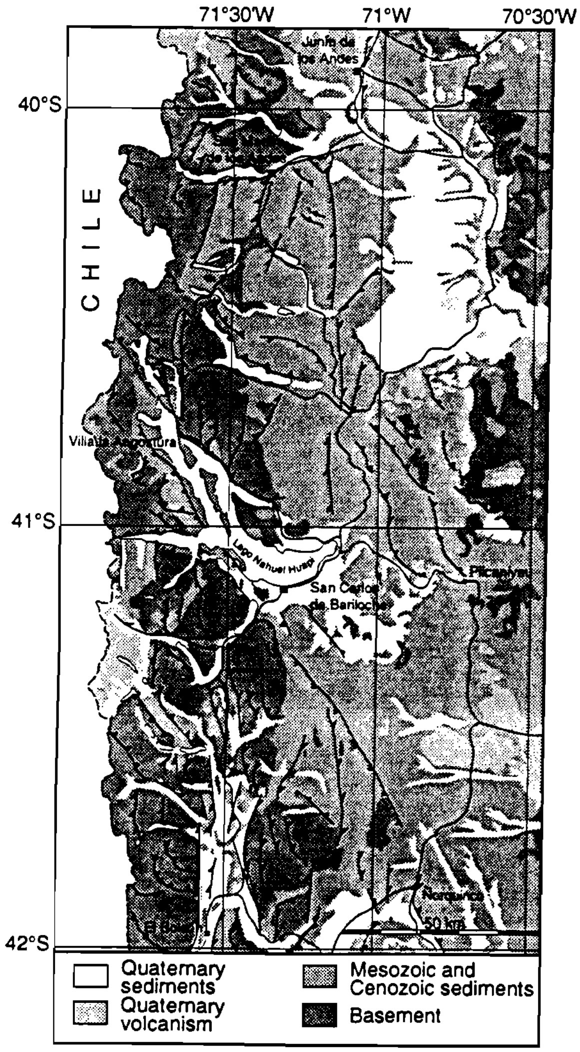


Figure 3: Schematic structural and geological map (Mercator projection) of area studied. Major reverse faults are from Landsat interpretation and from superimposed geological maps and digital topographic data (see Fig.3). Black triangles point in directions of underthrusting.

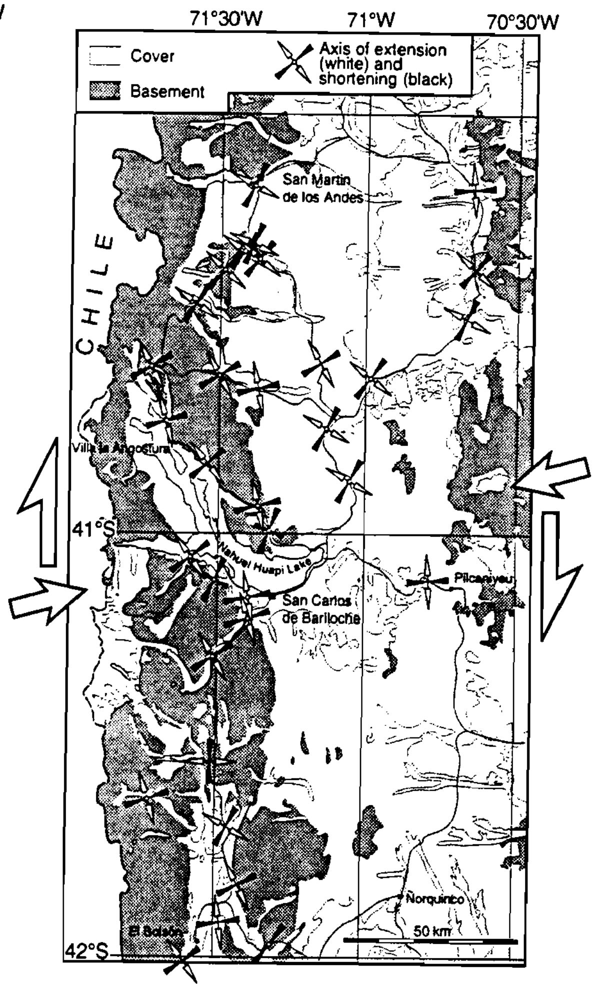


Figure 4: Results of kinematic fault analyses. Map shows directions of shortening (black arrows) and extension (white arrows for horizontal extension, white circles for vertical extension) at 33 localities.

# CLOCKWISE ROTATIONS IN NORTHERN CHILE: OROCLINAL BENDING AND IN SITU TECTONIC ROTATIONS?

G. DUPONT-NIVET[1], P. ROPERCH[2,1], P. GAUTIER[1], A. CHAUVIN[1], M. GÉRARD[3] AND G. CARLIER[4]

1 Géosciences Rennes, Campus de Beaulieu, Rennes, France
2 ORSTOM and Universidad de Chile, Santiago, Chile
3 Centre ORSTOM, Bondy, France
4 ORSTOM et MNHN, Paris, France

KEY WORDS: Paleomagnetism, Tectonics, Rotation, Orocline, Chile

## INTRODUCTION

The pioneer paleomagnetic work carried by a Japanese team (Kono et al., 1985) did show clockwise rotations of the Chilean forearc, counterclockwise rotations in Peru and evidence for a tectonic origin of the bending of the Central Andes. Later, Isacks (1988) proposed that mountain building in the Central Andes, characterized by differential along-strike shortening, has enhanced the development of the Bolivian orocline (see also Watts et al., 1995). Recently however, some authors have questioned the origin of the rotations, observed mostly in Mesozoic rocks, along the forearc of northern Chile. Forsythe and Chisholm (1994) and Grocott et al. (1994) indicate that clockwise rotations recorded in Jurassic-lower Cretaceous rocks are linked to the sinistral motions along the Atacama fault system during the Early Cretaceous. On the other hand, they discard the possibility that a significant amount of clockwise rotations is associated to oroclinal bending. In contrast, we interpret the general clockwise sense of rotation as evidence for a dextral shear and oroclinal bending effect during the Tertiary.

In this study we report new paleomagnetic results based on an extensive sampling (100 sites) from 22°S to 26°S. During our last fieldwork in February 1996, the paleomagnetic sampling was mostly done in lower Tertiary volcanics east of the Mesozoic arc in order to have a better control on the timing and spatial distribution of the rotations.

## PALEOMAGNETIC SAMPLING

The forearc of northern Chile is principally composed by north-south trending features. The coastal magmatic arc with Mesozoic intrusives and volcanics (La Negra formation) is longitudinally cut by the Atacama fault system. The ductile deformation along this fault system is of lower Cretaceous age (Marinovic et al., 1995) and clearly shows a sinistral sense of shear. Some of the faults have been reactivated during the Late Tertiary - Quaternary and they mostly show normal scarps. The late Cretaceous and early Tertiary volcanics outcrop east of the Mesozoic magmatic arc and west of the Domeyko fault system and they usually show little deformation. Most of the Andean deformation in northern Chile is observed across the Domeyko fault system. The tectonic style is complex and involved E-W shortening with successive dextral and sinistral shear (Mpodozis et al. 1993; Reutter et al., 1991).

We sampled the Jurassic La Negra formation near Tocopilla (12 sites), Antofagasta (16 sites) and Taltal (9 sites). Six sites were drilled in Mesozoic intrusives. In the central valley, east of Taltal, we sampled Paleocene-Eocene volcanics. About 200 Km further north, we sampled upper Cretaceous and lower Tertiary volcanics and sediments near Baquedano and Quebrada del Buitre. West of the Salar de

Atacama, we drilled two sections in the Tonel-Purilactis red sandstones and interbedded sills and one site in the Oligo-Miocene Paciencia red beds.

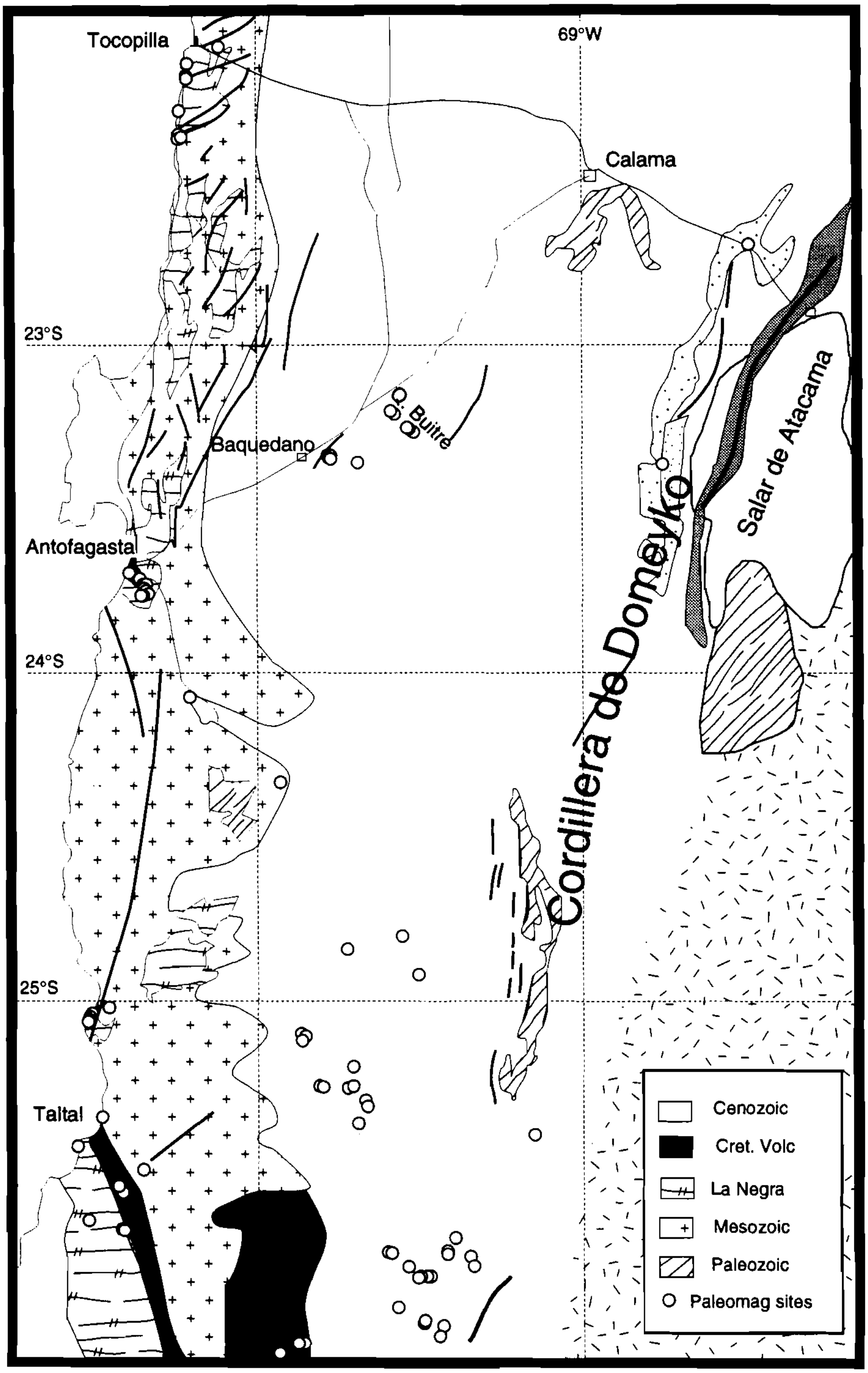


Figure 1: Simplified geological map from northern Chile and paleomagnetic sampling

PALEOMAGNETIC RESULTS

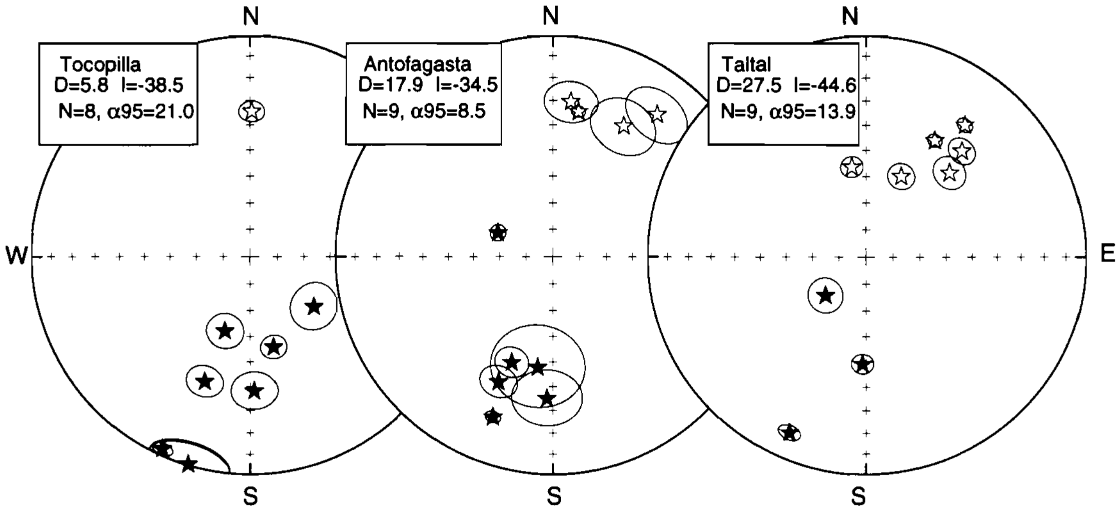


Figure 2: Paleomagnetic results from the Mesozoic arc.

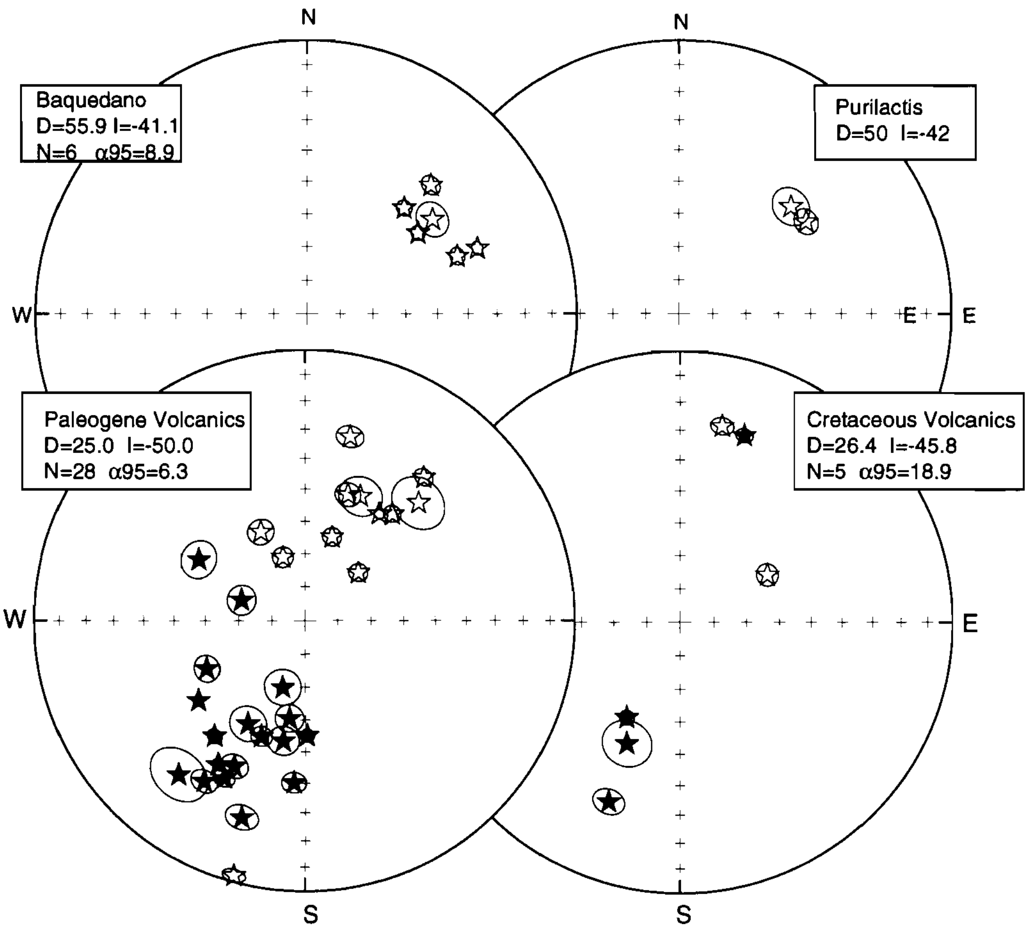


Figure 3. Paleomagnetic results from the area in between the Atacama and Domeyko faults system

**The Jurassic volcanics**

Magnetic susceptibility is usually high to very high (up to 0.1SI). Multidomain magnetite and maghemite is often the main magnetic carrier and secondary magnetizations are widespread. In the

Antofagasta area, in many cases, normal and reverse polarity magnetizations are found within the same flow. This behavior is likely associated to low temperature metamorphism during burial of the thick volcanic sequence. After detailed thermal and AF demagnetizations we were however able to determine a characteristic magnetization for several sites (Fig. 2).

**Upper Cretaceous and Tertiary**

*Baquedano and Purilactis formation*

East of Baquedano, about 70 Km NE of Antofagasta, the characteristic magnetization in the sediments and interbedded lavas corresponds to a remagnetization associated to an oxidizing event of possible hydrothermal origin. This remagnetization is however well defined and in good agreement with the primary magnetization recorded in a ryolitic lava located 10 km east of the Baquedano section. On average these sites record a clockwise rotation of about 60°. We sampled also 5 sites in the Quebrada Buitre but there is a large scatter between the sites. Only one section in the red sandstones and interbedded sills in the Tonel-Purilactis formation gave reliable paleomagnetic results; this section also documents large clockwise rotation (Fig. 2) and this result is in good agreement with a previous study in the same formation and located further north (Hartley et al., 1992).

*Central Valley (East of Taltal from 24°45' to 26°)*

For all sites, the characteristic magnetization was determined precisely with the majority of the samples showing univectorial magnetizations (Fig.3). After removal of 3 directions which are at more than 2 standard deviations from the mean, the mean declination is 25°. This result demonstrates that clockwise rotations are not restricted to the coastal domain.

Our new paleomagnetic results provide additional evidence for a tectonic process involving large clockwise rotations in northern Chile during the Tertiary. The differential along-strike shortening model of Isacks (1988) implies clockwise rotations during the Late Cenozoic by about 10°. Paleomagnetic results obtained in Bolivia (Butler et al., 1995; Roperch et al, this volume) suggest that the largest rotations occurred before 20Ma. Thus, the difference between the observed and expected (from the Isacks model) rotations emphasizes the importance of early-middle Tertiary tectonics in the structuration of the Central Andes.

**Acknowledgments**. Discussions about the geology and tectonics of Northern Chile with C. Mpodozis, P. Cornejo and A. Tomlinson have been very helpful to prepare the paleomagnetic field sampling.

REFERENCES

Forsythe, R., and L. Chisholm, 1994. Paleomagnetic and structural constraints on rotations in the North Chilean Coast Ranges, *Journal of South American Earth Sciences*, *7*, 279-295.

Grocott, J., G.K. Taylor, P.J. Treloar, and J. Wilson, 1994. Magmatic arc fault systems and the emplacement of mesozoic plutonic complexes in Northern Chile, *7° Congreso Geologico Chileno, II*, 1360-1364.

Hartley, A., E. Jolley and P. Turner, 1992. Paleomagnetic evidence for rotation in the Precordillera of northern Chile: structural constraints and implications for the evolution of the Andean forearc, *Tectonophysics*, 205, 49-64.

Isacks, B.L.; 1988. Uplift of the central Andean plateau and bending of the Bolivian orocline, *J. Geophys. Res.*, 93, 3211-3231.

Kono, M., K. Heki and Y. Hamano, 1985. Paleomagnetic study of the Central Andes: counterclockwise rotation of the Peruvian block, *J. Geodyn.*, 2, 193-209.

Marinovic, N., I. Smoje, V. Maksaev, M. Hervé and C. Mpodozis, 1995. Hoja Aguas Blancas, *Carta geologica de Chile, 1/250000, Serv. Nat. Geol. Min.*, Vol 70, 150pp.

Mpodozis, C., N. Marinovic, and I. Smoje, 1993. Eocene left lateral strike slip faulting and clockwise block rotations in the cordillera de Domeyko, west of Salar de Atacama, Northern Chile, *second International Symposium on Andean Geodynamics*, 225-228.

Reutter, K.J., E. Scheuber, and D. Helmcke, 1991., Structural evidence of orogen parallel strike slip displacements in the Precordillera of Northern Chile, *Geologische Rundschau, 80*, 135-153.

Watts, A.B., S.H. Lamb, J.D. Fairhead and J.F. Dewey, 1995, Lithospheric flexure and bending of the Central Andes, *Earth Planet. Sci. Lett.*, 134, 9-21.

# THE CENOZOIC FOREARC EVOLUTION IN NORTHERN CHILE: THE WESTERN BORDER OF THE ALTIPLANO OF BELEN (CHILE)

Marcelo GARCIA*, Gérard HERAIL*,Reynaldo CHARRIER*.

* Convenio ORSTOM-Departamento de Geología, Universidad de Chile, Casilla13518, Correo 21, Santiago.

KEY WORDS: Andes, Altiplano, Tectonic, Chile.

## INTRODUCTION

The Altiplano is a 3.500 - 4.500 m high plateau located between 15° and 27° South latitude. This mosphostructural unit characterize the Bolivian Orocline in the Central Andes. It is composed by thick Tertiary continental, detritic sedimentary series, which were deformed under compressive stresses (Semperé et al., 1990). The Altiplano is not an homogeneous back arc bassin ( i.e. Lavenu, 1986; Semperé et al., 1990; Hérail et al., 1992; Kennan et al., 1995). In the eastern border the remaining sedimentary series are rather thin (less than one to few kilometers) and remmants of erosion surfaces attain the Eastern Cordillera. Deformation occurred essentially before 13-10 Ma. In the Central Altiplano the deposits reach thicknesses of more than 10.000 m in the Corque-Rosapata syncline (Meyer and Murillo, 1961), their source beeing the uplifted margins of the basin after compressive deformation. Highest reliefs and bigger structural displacement are located to the East (Rochat et al., 1996).

The composition and structure of the sedimentary infill evolve from east to west (Rochat et al., 1996). In Bolivia, these structures can only be described partially on the basis of seismic information. In Chile, on the West margin of the Altiplano, good exposures permit a more complete analysis of the stratigraphic series that register the tectonic evolution of this side of the plateau. In this paper we describe the structure of the West margin of the Altiplano in the region near Belén (Fig. 1) and intend to reconstruct the chronology of its tectonic evolution.

## THE DEFORMED SERIES

*a) The substratum and the Cenozoic volcanic series.* The basement outcroping in this region is the Belén Metamorphic Complex (Complejo Metamórfico de Belén = CMB) consisting of metamorphic and magmatic units (Montecinos, 1963; Pacci et al., 1980), dated at 1.000 Ma (Pacci et al., 1980). Recent age determinations indicate early Paleozoic ages and a complex evolution (Basei et al., 1995, 1996). The CMB is unconformably covered by sandstones of the Jurassic Livilcar Formation (Muñoz et al., 1988), which were deposited on the East margin of the Jurassic backarc basin (Muñoz and Charrier, 1993).

The Cenozoic stratigraphic series begins with the accumulation of volcanic deposits and some volcano detritic intercalations. The approximately 500 m thick Oxaya Formation (Montecinos, 1963; Salas et al., 1996; García, 1996) is a dacitic to ryolithic, welded ignimbrite, with several kinds of fluidal structures and containing big pumice fragments, some of which attain 20 cm in diameter. All xenoliths are of volcanic origin. A K/Ar age on a biotite from the upper part of the formation gave ages between 19.0±0.6 and 19.9±1.1 Ma (Naranjo and Paskoff, 1985; Aguirre, 1990; Muñoz and Charrier, in press). A K/AR age on biotite from an ignimbrite level located 300 m below the top of the series gave 21±0.6 Ma (Table 1, Fig. 1).

The 1.500 m thick Lupica Formation, defined by Montecinos (1963), was assigned a Cretaceous age. García (1996) differenciated three members in this unit: a lower member composed of breccious and porphyric andesites with tuffaceous intercalations, a middle member composed of ignimbrites and volcaniclastic intercalations, and a mainly sedimentary upper member consisting of sandstones, shales, limestones, and andesitic and tuffaceous intercalations. The lava flows and breccias of the lower member were deposited in an extensional environment. In fact, East of Belén (Fig. 1) the lower part of this

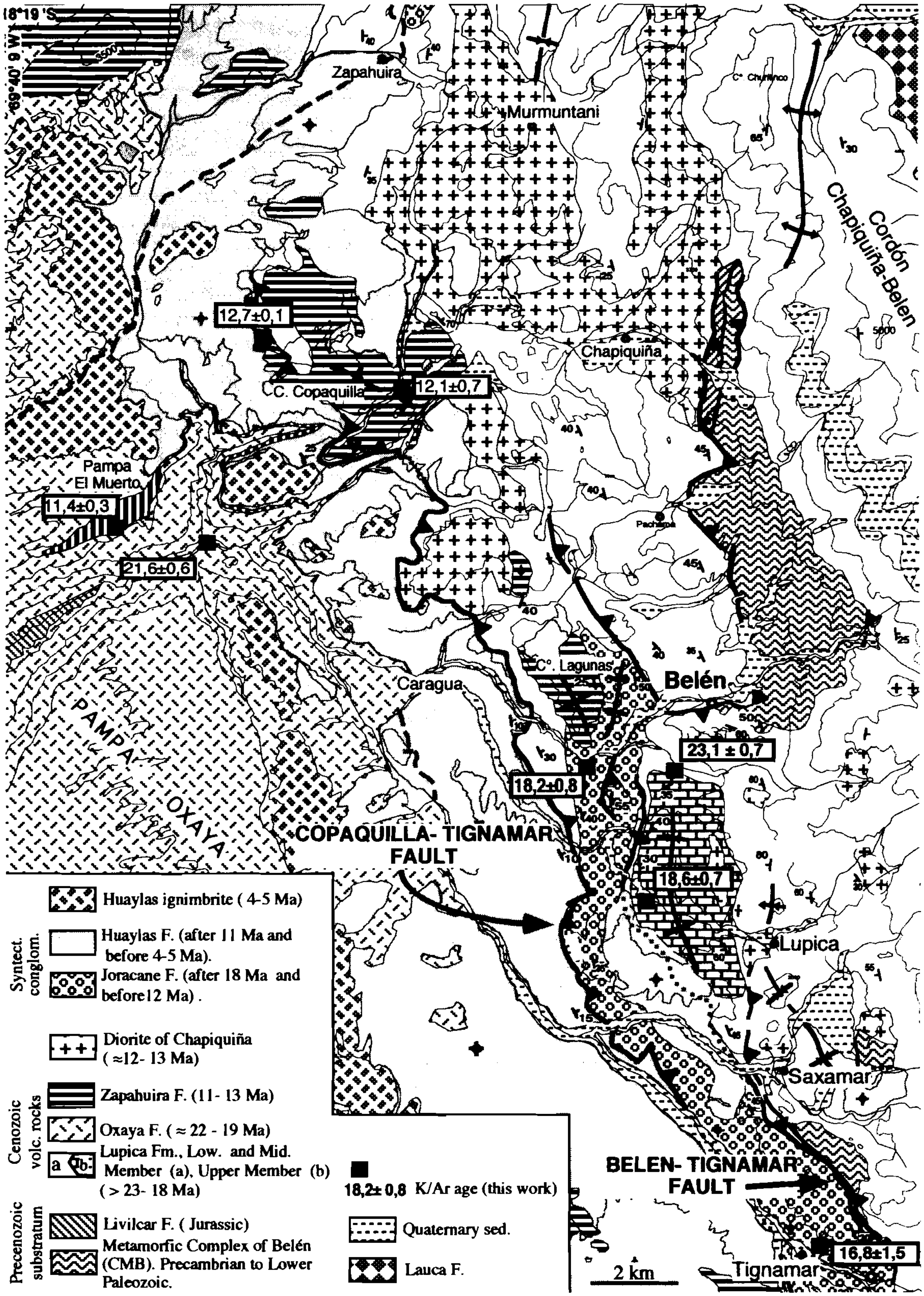


Figure 1: Geological map of the Belen Altiplano border.

member is in tectonic contact with the CMB. The lower layers of the Lupica Formation are more deformed than the upper ones. This indicates syntectonic deposition during extensional conditions and suggests that deformation ceased during deposition of the Lupica Formation. The presence of lacustrine deposits in this unit is an evidence for endoreic basins developed in active volcanic environments, probably caused by collapse of a caldera. These events occurred between 23±0.7 Ma and 18±0.7 Ma ago according to radioisotopic ages obtained in an ignimbrite layer from the floor of the middle member, and a tuff from the middle part of the upper member. We finally conclude that the Oxaya and Lupica Formations are coeval and that they were deposited during a long lasting episode of explosive volcanism and caldera development.

The Zapahuira Formation (García, 1996) forms an approximately 500 m thick series composed of andesitic, basaltic lavas and laharic flows of similar composition, that unconformably overlie the Oxaya and Lupica Formations, and the syntectonic conglomerates of the Joracane Formation. Three ages obtained in this newly defined unit fall between 11.4±0.3 and 12.7±0.1 Ma.

*b) The syntectonic conglomerate deposits.* The Joracane Formation (García, 1996) is composed by nearly 1.600 m thick conglomerates and rare volcanic intercalations. To the East, this unit is westwardly thrusted by the Lupica Formation and the CMB, while to the West it thrusts also westwardly the Huaylas Formation (Fig. 1). These conglomerates are essentially composed by volcanic fragments of the Lupica Formation; calcareous clasts of the upper member of the Lupica Formation are locally present, as well as clasts of theCMB (Tignámar region). The conglomerates are of fluvial origin. They form metric to more meters thick, rather soft, layers. Measures of imbrication and the granulometric pattern indicate a sediment supply from areas located to the East. These areas were uplifted by activation of the Belén-Ticnamar. K-Ar ages on biotites from tuff levels intercalated in this conglomeratic series gave 18.2±0.8 and 16.8±1.5 Ma.

The Huaylas Formation (Salas et al., 1966) consists of conglomeratic deposits that unconformably overlie the Oxaya Formation and cover with progressive unconformity the units located to the East of the Copaquilla-Tignámar fault; to the west the Huaylas Formation onlap the Oxaya Formation. These conglomerates are also of fluvial origin. The sediment supply directions and the clast composition indicate a western provenance and an origin from the Lupica Formation and the CMB. The lower levels of this unit are deformed by the Copaquilla-Belén fault, while the upper levers are not deformed and extend to the East of the fault (Fig. 1). The Huaylas Formation lies over the Pampa El Muerto basalts which were dated 11.4±0.3 Ma and contains Huayquerian fauna (Salinas et al., 1991). It is covered with strong angular unconformity by the 30 m thick Huaylas ignimbrite dated at 4.4±0.3 and 4.8±0.3 Ma (Naranjo and Paskoff, 1985).

## AGE AND SEQUENCE OF THE CENOZOIC DEFORMATION

The early Miocene deposits lie directly on top of the Precambrian-early Paleozoic metamorphic complex and the marine Jurassic deposits. Cretaceous as well as early Cenozoic rocks, well exposed on the East side of the Altiplano, are not present in this region. It is, therefore, possible to conclude that the West margin of the Altiplano remained elevated and exposed to erosion for most of the Mesozoic and the early Tertiary. Early Miocene deposits accumulated in an extensive tectonic regime (most probably a caldera environment). After approximately 18 Ma the western border of the Altiplano was subjected to compressive deformation. The compresive episode, that came to an end between 8 Ma and 4-5 Ma, caused a series of westvergent folds and thrusts, and triggered the deposition of syntectonic conglomerates: Joracane and Huaylas Formations (Fig. 1).

The Joracane Formation is associated to activity of the Belén-Tignámar fault. This fault cuts across the conglomeratic series and no progressive unconformity was observed, suggesting a late reactivation phase. The activity of the Belén-Tignámar fault started at 18 Ma and stopped around 12 Ma.

The Huaylas Formation is associated to the Copaquilla-Tignámar fault. The activity of this fault began after 11 Ma and ended before 4-5 Ma, but well after 8 Ma. The synsedimentary deformation in this unit is well developed; its lower levels are folded and thrusted, while the subhorizontal upper levels cover with erosional unconformity the upthrusted block. The conglomeratic filling has been strongly eroded and an erosional level 100 to 150 m below the top of these conglomeratic series is sealed by the Huaylas ignimbrite. The remmants of the ignimbrite East of the Copaquilla-Tignámar fault (NW of Cerro Copaquilla) lie nearly one hundred meters above the general level of the ignimbrite, suggesting a late reactivation of the fault after 4-5 Ma.

The thrust faults, Belén-Tignámar, to the East, and Copaquilla-Tignámar, to the West are developed in sequence.

REFERENCES.

BABY, P., HÉRAIL, G., LOPEZ, M., LOPEZ, O., OLLER, J., PAREJA, J., SEMPERE, T. et TUFIÑO, D., 1989. Structure de la zone subandine de Bolivie : influence de la géométrie des séries sédimentaires antéorogéniques sur la propagation des chevauchements,*C. R. Acad. Sci. Paris*, 309, Série II, p. 1717-1722.
BABY, P., SEMPERE, T., OLLER, J., BLANCO, J., ZUBIETA, D. et HÉRAIL,G., 1992. Evidence for major shortening on the eastern edge of the Bolivian Altiplano: the Calazaya nappe, *Tectonophysics*, 205, 1-3, p. 155-169.
BASEI, M.A., CHARRIER, R.and HERVE, F. 1995. New ages ( U-Pb, Rb-Sr, K-Ar) from supposed Pre-cambrian units in Chile: Some geotectonic implication. ( Abstract). IGCP Project N° 376 Anual Meeting, 23-24 October 1995, Salta, Argentina.
GUBBELS, T., ISACKS, B., FARRAR, E., 1993. High-level surfaces, plateau uplift and foreland development, Bolivian Central Andes. *Geology,* 21: 695-698.
HÉRAIL, G., SOLER, P., BONHOMME, M., LIZECA, J. L., 1993. Evolution géodynamique du contact Altiplano - Cordillère Orientale au Nord d'Oruro (Bolivie) - Implications sur le déroulement de l'orogénèse andine, *C.R. Acad. Sci.* , 317,série II, p. 512-522.
KENNAN, L., LAMB, S., RUNDLE, C. 1995. K/Ar dates from the Altiplano and Cordillera Oriental of Bolivia: implications for Cenozoic stratigraphy and tectonics. *J. of South American Earth Sciences,* 8,2, p.163-186.
LAVENU,A. , 1986, Etude néotectonique de l'Altiplano et de la Cordillère Orientale de Bolivie, *Thèse de Doctorat d'Etat-ès-Sciences*, Univ. Paris Sud, Orsay, 434 p.
MARTINEZ, C., 1980. Structure et évolution de la chaîne hercynienne et de la chaîne Andine dans le nord de la Cordillère des Andes de Bolivie. *Trav. et Doc. ORSTOM*, n°119, 352p.
MEYER, H. C. et MURILLO, J., 1961. Sobre la geologia de las Provincias Aroma, Pacajes y Carangas, *Bol. Depto. Nat. Geol. La Paz-Bolivia*, 1, 47 p.
MUNOZ, N. and CHARRIER, R.1993. Jurassic-Early Cretaceous facies distribution in the western Altiplano ( 18°-21° 30' S.L.). Implications for hydrocarbon exploration. *2° Symp. Intern. "Géodynamique Andine" ( Oxford)* , ed. ORSTOM, Paris , p. 307-310.
MUNOZ, N. and CHARRIER, R. in press. Uplift of the western border of the Altiplano on a west-vergent thrust system, Northern Chile. *J. of South American Earth Sciences.*
NARANJO, J.A. and PASKOFF, R. 1985. Evolución cenozoica del piedemonte andino en la Pampa del Tamarugal, norte de Chile ( 18°-21° S). *Actas IV Congreso Geol. Chil.* 5. p.149-164.
ROCHAT, Ph. et al. 1996. Geometry and kinematics of the northern Bolivian Altiplano within the Central Andes. *ISAG 96*, this volume.
SALAS, R., KAST R., MONTECINOS F., SALAS, I. 1966. Geologia y recursos minerales del Departamento de Arica, Provincia de Tarapacá. *Inst. de Inv. Geol.*, Bol. 21. 130p.
SALINAS, P., VILLAROEL C., MARSHALL, L., SEPULVEDA, P., MUÑOZ, N. 1991. Typotheriopsis sp. ( Notongulata, Mesotheridae), Mamifero del Mioceno Superior en las cercanias de Belen, Arica, Norte de Chile. *Actas VI Congreso Geol. Chil. . p.314-317.*
SEMPERE, T., HÉRAIL, G., OLLER, J., et BONHOMME, M., 1990. Late Oligocene-early Miocene major tectonic crisis and related basins in Bolivia, *Geology*, 18, p. 946-949.
SEMPERE,T. , HÉRAIL,G. , OLLER,J. , BABY, P.,BARRIOS,L. et MAROCCO,R. 1990. The Altiplano: a province of intermontane foreland basins related to crustal shortening in the Bolivian Orocline area, *1° Symp. Intern. "Géodynamique Andine" ( Grenoble)*, ed. ORSTOM, Paris , p. 167-170.

# THE CONTINUUM TECTONIC DURING THE CRETACEOUS-PALEOCENE TIMES IN THE ANDEAN NORTH-PERUVIAN FORELAND BASIN (MARAÑON BASIN)

Willy GIL (1), Patrice BABY (2) and Medardo PAZ (3)

(1) Convenio PETROPERU-ORSTOM
(2) ORSTOM, TOA, UR 1H, 213 rue La Fayatte, 75480 Paris,France.
(3) PETROPERU

**KEY WORDS**: Marañon Basin, Foreland, Tectonic Inversion, Continuun Tectonic, Cretaceous-Paleocene, Peru

## GEOLOGICAL SETTING

The Marañon basin is located in the NE slope of the Peruvian andean mountains.This basin, is part of the estructural depression that spreads from Colombia to Argentina and it is found between the Guyan-Brazilian Craton and the Andean Cordillera.Morpho-estructurally, it can assume arbitrary boundaries (Fig. 1).Its south boundary is given by the Contaya-Cushabatay Arc, that is characterized by having a little depression topography. The north border is limited by the Conanaco Arc that divides the Marañon Basin from the Napo basin of Ecuador. Its eastern portion is limited by the Iquitos Arc. This positive structural element.that borders the Brazilian and Guyan Cratons joins both cratons, which are separated by the Amazon graben (Morales 1959). Its western portion is limited by the sub-andean thrust belt, that is characterized by having an accidented, thrusting and folding topography, as a product of the Andean orogeny. The Marañon basin contains a thick series of sedimentary rocks that go from the Paleozoic to the Quaternary times. They overlie a substratum of Precambrian granitic rocks (Fig. 3). All of this group of rocks is affected by compressional reactivations of paleozoic and mesozoic extensional faults (tectonic inversions). Laurent and Pardo (1974) had already evidenced extensional paleozoic phenomena that originated uplifted blocks crumbled down towards the Nor-East and South-East of the basin. These apparently extensional phenomena continued to the Triassic-Jurassic times originating like this the Pucará and Sarayaquillo basins. This extensional tectonics was alterned by regional and local uplifts, which were originated either by compressional and/or isostatic phenomena (Gil,1995). A slight erosional unconformity between the Pucara Group (Upper Triassic-Early Jurassic)), seems to show an uplift phenomenon, possibly originated by Flexuring. A slight disposition in onlap towards the base of the Sarayaquillo Formation, which was observed in the Cretaceous Charnella zone, can indicate that this one already constituted a structural height during the jurassic sedimentation. This would evidence a flexuring as a consecuence of the subduction beginning in the peruvian margin (Gil, 1995). An erosion surface located between the Sarayaquillo (Late Jurassic) and Chusabatay Formations (Early Cretaceous) indicate a regional uplift, which is syn and/or post-Sarayaquillo but ante-Cushabatay. The Cretaceous is characterized by the tectonic inversions essencially located in the eastern and central part of the basin. These structures are controlled by the pre-cretaceous paleogeography. Most of them correspond to tectonic inversions of paleozoic half-graben or graben, located at the eastern border, and Triassic-Jurassic in the Central and Western zone. In the Tertiary, an asimetrical foreland basin is evidenced which depocentre migrated to the East, at the same time as the Orogenic Front's (Marocco 1994). In the Neogene series, three important coarsening upward sequences have been observed, which constitute the sedimentary response to 4 continuum tectonic periods: 28-26 - 10Ma, 10 - 7Ma, 7 - 2.7 Ma and 2.7 - 0Ma (Marocco, 1994). The actual structures present an homogeneous deformation of all the Neogene sedimentary series, indicating a late structuration. In the North-East extreme of the Marañon basin, the Cretaceous rocks lie over blocks apparently of Precambrian and Paleozoic age. In the central part and SW over the Jurassic series. The contact with the Paleozoics is in an strong angular unconformity, while the contact with the Jurassic is in a weak unconformity, which is becoming concordant toward the East.

## TECTONIC EVOLUTION

For the kynematic analysis of the 8 (Fig. 2) studied structures, tectonic evolution (Palinspastic restoration) sketches were made determining extensional and compressive events (tectonic inversions) (Fig. 4 and 5).

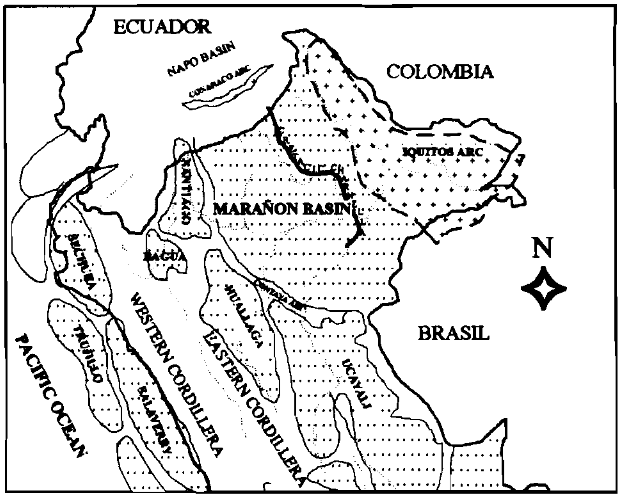


FIG. 1 BASINES LOCATION MAP OF PERU

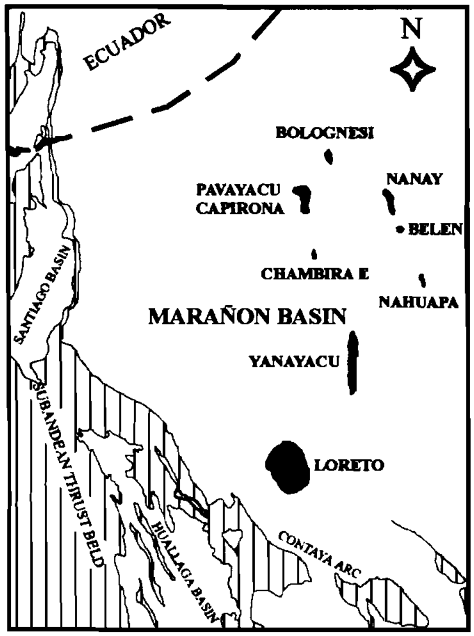


FIG. 2 STRUCTURES LOCATION MAP OF THE MARAÑON BASIN

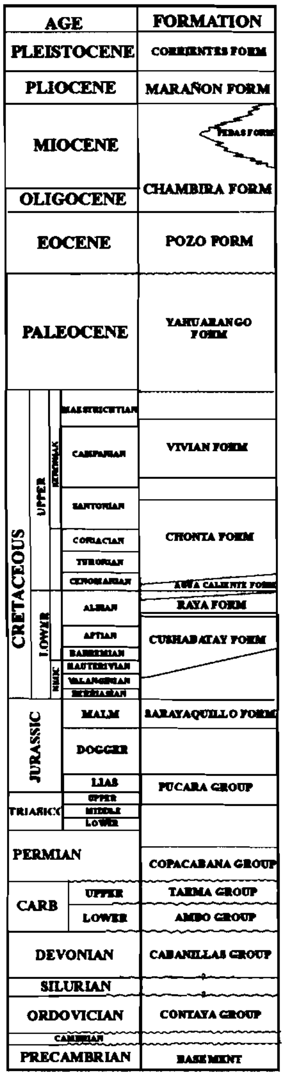


FIG. 3 STRATIGRAPHIC COLUMN OF THE MARAÑON BASIN

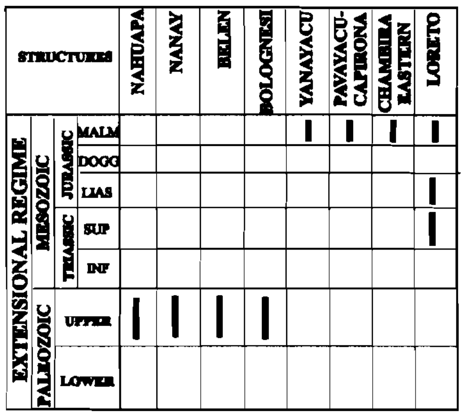


FIG. 4 STRUCTURES EXTENSIONAL REGIME

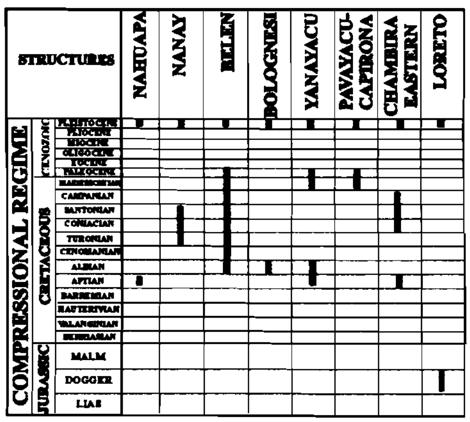


FIG. 5 STRUCTURES COMPRESSIONAL REGIME

**Extensional Tectonic.** Extensional events of the Late Paleozoic times are registered by the Nanay, Nahuapa, Belen and Bolognesi structures. These structures show very deformed units in sometimes roll-over blocks that directly underlie to the Cretaceous in angular unconformity. Extensional events of the Triassic and Jurassic are evidenced in the Loreto structure where an extensional regime contemporarily happened to the Pucara Group sedimentation (Upper Triassic-Early Jurassic). In the Late Jurassic, the Sarayaquillo Formation is also developped in an extensional general regime, which is evidenced in the Loreto, Yanayacu, Capirona-Pavayacu and East Chambira structures.

**Uplift and Flexuring**

Uplift and tectonic inversion of the Middle Jurassic inversion (Dogger): Apparently, a first compressive event manifested by a tectonic inversion appears in the Middle Jurassic before the sedimentation of the Sarayaquillo Formation. This phenomenon is evidenced in the Loreto Structure, in which it is possible to distinguish an erosion surface between the Pucara Group and the Sarayaquillo Formation.

Uplift by flexuring of the Latest Jurassic- Earliest Cretaceous: This uplift phenomenon, possibly originated by flexuring, is evidenced by the erosion surface, between the Sarayaquillo and Cushabatay Formations. It is about a regional uplift mainly located in the Cretaceous Chamella zone.

## TECTONIC INVERSION OF CRETACEOUS TIMES

Tectonic inversion of the Aptian: The Nahuapa, Yanayacu, and East Chambira structures present little tectonic inversions contemporary to the sedimentation of the Cushabatay Formation.
Tectonic Inversion of the Albian: The Belen, Bolognesi and Yanayacu structures present tectonic inversion synchronically developped to the sedimentation of the Raya Formation (Middle-terminal Albian),and Agua Caliente Formation (Late Albian- Cenomanian). In the Belen Structure, this compressive event apparently spread at least to the Paleocene.
Tectonic Inversion of the Early Turonian: The Belen structure presents a tectonic activity for this time.
Tectonic Inversion of the Turonian-Coniacian: This compressive event is evidenced during the sedimentation of the Chonta Formation and is registered in the Nanay, Belen and East Chambira structures. In the Nanay and Chambira East structures, this compressive phenomenon prolongates until the Santonian, while the Belen Structure, shows a reactivation until the Early Eocene. The Nanay Structure shows a good sign of this deformation, and besides, it presents the absence of the Late Turonian (ROBERTSON, 1990).
Tectonic Inversion of the Santonian: During this period the Nanay and Belen Structures show a tectonic activity.
Tectonic Inversion of the Campanian: Campanian marine deposits are covered in unconformity by Maastrichtian sandstones (Vivian Formation). This erosion is apparently produced at the same time as the tectonic inversions, which are manifested in the Belen and East Chambira structures.
Tectonic Inversion of the Maastrichtian-Paleocene: They are noticed in the Belen, Yanayacu and Capirona-Pavayacy structures.

## TECTONIC INVERSION OF TERCIARY TIMES.

All the terciary sedimentary column is locally deformated by tectonic inversions. It is impossible to evidence a syn-sedimentary tectonic in the 3 Neogene sequences. Apparently, the tectonic inversions that affect the tertiary foreland sediments of the Marañon basin are very late, of the Pliocene or Quaternary times.

## DISCUSSION

In the peruvian margin, the Aptian is characterized by the absence of vulcanism and by a general regimen in distension (Jaillard, 1993), neverthless, compressive and contemporary events to the Cushabatay Formation are registered in the Marañon basin. In the Late Aptian-Early Albian a slight distension is registered in the peruvian margin (Jaillard 1993), it is impossible to differenciate this phenomenon in the Marañon basin. In the Albian, the activity of a very important volcanic arc is accompanied by the Coastal Batholit location. This period is marked by thick volcanic efusions located in the western part of the peruvian margin and the south of Ecuador, and abruptly end in the Cenomanian. At the same time a very important tectonic phase of compressive character is developped, which corresponds to the Mochica phase (Megard, 1984; Vicente, 1989);

Jaillard, 1994). It is possible that the eustatic regression of the Late Albian-Early Cenomanian could have been reinforced by this tectonic event.
An stratigraphic hiatus of the Early Turonian (ROBERTSON, 1990), restrincted in the eastern border of the Marañon basin (proximal part) could have been originated by a tectonic uplift, it is also posssible that this statigraphic hiatus is originated by later erosions associated to a eustatic emersion (Jaillard 1994).
In the Late Turonian an stratigraphic hiatus is also registered in the Marañon basin, which covers a greater area than the Early Turonian indicating an increasing erosion to the East. According Jaillard (1994) it would be originated by tectonic events at great scale and reinforced the contemporary eustatic regression.
The peruvian phase appears in the Andean Mountains (Jaillard, 1993) culminating the Late Campanian. This deformation is restrincted to the eastern portion of the basin.
Then an importan regression is registered in Central and South Peru as well as in Bolivia. Which explains the almost general absence of all the deposits of the Late Santonian in the peruvian East. This eustatic regression (Haq, 1987), is reinforced by the effects of the Peruvian tectonic.
In the Marañon basin, the marine deposits of the Campanian are covered in unconformity with the sandstones in the Vivian Formation (Maastrichtian), which points out the Late Campanian erosions ocurrence. The same thing has been noticed in the East of Ecuador (Jaillard, 1994).
In the Upper Campanian the greatest peruvian phase is well determined and it is reponsible of greater events such as the Cincha-LLuta overthrusting in the Arequipa zone (Vicente, 1989; Jaillard, 1993). The definite general emersion of all the peruvian andean mountains and of the sedimentary hiatus of the Late Campanian in most of the part of the peruvian margin. This greater event occurs in the Eastern basin, possibly in the Maastrichtian-Paleocene times, due to the fact that some studied structures (Belen, Yanayacu and Capirona-Pavayacu) present a tectonic inversion in this time interval.
The Neogene series of the Marañon basin, present three great coarsening upward sequences that can be correlated to the Quechua 1, 2 and 3 tectonic phases, that reactivate the sedimentation (Marocco, 1994). Besides it is well kown that the litostatigraphic organization in three coarsening upward sequences is also common in the eastern slope of the Ecuatorian and Bolivian andean mountains (Marocco, 1994).

## CONCLUSION

In the Marañon basin, tectonic inversions have been produced since the Aptian to the Paleocene. It is impossible to talk about tectonic phases, but of a deformation continuum that is distributed in an heterogeneous way in all the basin. Only the Belen structure seems to have registered the whole deformation continuum. These conclusions agree with Marocco's observations (1990) .Indeed, according Morocco, the Central Andean Mountains initiate their emersion in the Santonian. In the superficial zones of the crust, this compression happens through a tectonic continuum that produces, according the local conditions, fracturation, ductile deformation, or active basin's formations. During the Neogene, a typical basin of foreland basin instalates. A second period of tectonic inversion of pre-cretaceous faults appear during the Pliocene and probably the Quaternary.

## REFERENCES

Gil W. 1995. Tesis Universidad Nacional San Antonio Abad del Cusco
Haq. B. U., Hardenbol J. & Vail P. R. 1987. . Science 235.
Jaillard E. 1993 Bull. Soc. Géol. France, T 164 N° 6.
Jaillard E. 1994 Convenio Orstom-Petroperu. Inf inédito Petroperu. Lima.
Laurent H. & Pardo A. 1974. III Congreso Peruano de Geológia. Lima, Perú.
Marocco R. 1993. III INGEPET, Lima Perú.
Marocco R. & Delfault J. 1990. Inter. Symp. Andean Geodyn. (ISAG), Grenoble, Abstrac ORSTOM Paris.
Megard F. 1984. J. Geol. Soc. London 141
Morales L.G. 1959. 5th Worl Petrol. Congr. N. Y. proc sec.1 paper 51.
ROBERTSON RESEARCH 1990. Inf. inédito Petroperu Robertson Research.
Vicente J. C. 1989. In G. E. Ericksen, M. T. Cañas Pinochet & J. A. Reinemund Eds., Geology of the Andes and its relations to energy and mineral resources. - Circum-Pacific Council Energy Min. Resources, Earth Sci. Ser. Houston 11.

# GEOLOGIC AND PETROLEUM EVOLUTION IN OLLEROS BLOCK SANTA BARBARA SYSTEM - SALTA - ARGENTINE

**R.GÓMEZ OMIL(1)*, L.ALBARIÑO (2)*.**

**(1) (2) PLUSPETROL S.A. - La Rioja 301,Buenos Aires,Argentina (1214)**

**KEY WORDS: Phanerozoic Sedimentation, Poliphasic Tectonic, Petroleum System.**

## INTRODUCTION

The studied area is located in the Province of Salta, in the nothwest of Argentine, covering an area of 6300 km2. It belongs to the " Santa Bárbara Tectonic System" where many geological studies were performed during the last decades. The results obtained with the wildcats drilled during the 70's - 80's (more than 10 dry wells) associated with geochemistry studies, both indicated that no oil generation had existed regarding Yacoraite Fm (Upper Cretaceous). After this negative exploration stage two shallow oil fields were discovered, both related to structural traps (faulted anticlines), Cuchuma and Lumbreras, productive from fractured limestones in the Yacoraite Fm. (Figure 1). To explain their existence, new sedimentary and tectonic models were developed and a most accurate petroleum system is also suggested

## STATIGRAPHY AND TECTONIC

The stratigraphic column is conformed by rocks that involve ages between Precambrian and Quaternary with a total approx. thickness of 8000m. (Figure 2).

**Precambrian (Puncoviscana Fm. Turner1960):** mainly composed of slates, its real thickness is unknown, and is highly deformed by several tectonic events.

**Paleozoic:** (Meson Gr .Turner 1960, Mojotoro Fm, Cachipunco Fm. Hagerman 1933) (Cambrian to Devonian). Marine quartzites and shales (Vistalli C.1987) with a total approx. thickness of 2500m. Affected by the compressive stages (thick skinned) related to the orogenic Oclóyica (Base Silurian) and Chánica (Base Carboniferous) .

**Cretaceous, Paleocene, Lower Tertiary (Salta Group - Turner 1959):**This sedimentary cycle represents a Synrift stage.( Bianucci et al 1982) (Pirgua Subgroup.Reyes et a 1973. Lower-Upper Cretaceous), and Postrift (Balbuena - Moreno 1970 and Santa Bárbara Subgroups - Moreno 1970). The total thickness has approx. 2500m and is composed of fluvial and eolian sandstones and conglomerates in the Synrift, whereas the Postrift stage is represented by limestones shales, sandstones and evaporites deposited in shallow lacustrine, playa lake and eolian environments.(Gómez Omil et al 1987.)

**Neogene(Oran Group - Russo 1975)(Upper Miocene to Pliocene):**They represent the synorogenic sediments. The oldest are fluvial distal facies and the youngest local fluvial facies mainly **fanglomerates,** with a maximun thickness about 5000m(Gebhard J.et al 1974). At least three compressive tectonic events have been recognised (thick and thin skinned) during this time interval. The first happened around 17 M years related to tectonic inversion (Grier M.1990;Letouzey 1990)(Sosa Gómez et al 1993) (Salfity et al 1994) (Quichua phase I-Middle Miocene),the second around 10 M years (Quichua phase II,Upper Miocene),and the third in the Pliocene (Diaguita phase)(Jordan T.1984).Due to it simportant deformation many different types of structures could be defined: fault propagation fold,out of the graben thrust faults,and also tensional faults (Syn rift) and strike slip faults. Most of the anticlines are related to grow structures and have a strong sedimentary control mainly developed since the upper Miocene (Quichua phase II).(Medwedeff D.1989)(Suppe J.et al.1992)

**PETROLEUM SYSTEM**

**Source Rock:** The only stratigraphic unit with good source potential is the lacustrine Yacoraite Fm (Upper Cretaceous),related with the post rift stage.Shales with TOC values between 1 to 6% and type II-III kerogen has been described.The maximun source rock thickness is about 40m in the studied area.

**Maturity:** Based on vitrinite reflectance values from surface samples and in Basin Mod analysis, mature areas are located just in some synclines where the total subsidence over the Yacoraite Fm was more than 3500m. In all the cases this subsidence happened in the upper Miocene and Pliocene, related to growth anticlines. The difference in thicknesses between the synclines and the anticlines for the upper Miocene and Pliocene is about 2000m.The main oil generation could have begin at 5.5 MM years.

The present geothermal gradient in the region according to wells is about 2.6 to 3° C /100m.

**Migration:** A very short and local migration has been stablished with no more than 10 km from the kitchen located in the synclines to the nearest anticlines (Cuchuma and Lumbreras) .

**Carriers:** There are no good carrier with enough porosity as sandstones or limestones related to the source rock Yacoraite Fm. It is possible that fractures could be the main carriers that connect the kitchen to the final trap.

**Seal:**The shales and evaporites that represent the initial post rift sequences (Olmedo Fm) which cover the main reservoir, have a thickness about 40m and also a regional distribution. It's the proved seal in oilfields Cuchuma and Lumbreras.

**Reservoir:**The reservoir in both oil fields is related to fractured limestones.

**Trap:** The discovered traps are in both cases anticlines with four-way clossure, conformed in different timing each.

The Petroleum System herein defined is deficient because the discovered oil fields are filled up about 10% of its structural clossure ,and also many other structures drilled are dry. The main problem could be related to the restricted and isolated kitchen so the area of effective drainage is very little.

## CONCLUSIONS

A poliphasic tectonic and also a sedimentary evolution are defined since the Precambrian to the present. The Petroleum System is analysed. The behavior of both subjects together allows to explain the existence of the only two oil fields found in the region (Cuchuma and Lumbreras), the bad results obtained in the oil exploration (10 well dry) in past decades,as well as to focus the exploration efforts in specifical areas.

## REFERENCES


Allmendinger R.W.,Ramos V.,Jordan T.,Isacks B.1983.Paleogeography and Andean structural geometry,northwest Argentina.Tectonic.2,1-16 Washington.

Bianucci H.y Homovc J.1982.Tectogénesis de un sector de la cuenca del Subgrupo Pirgua.Noroeste Argentino.V Congreso Geológico Argentino.Acta I .539-546.

Ghebard J.,Giudicci A.,y Oliver Gascón J.1974.Geologia de la Comarca entre el río Juramento y el arroyo las Tortugas. Prov.de Salta y Jujuy.Rep.Argentina.R.A.G.A.Rev.XIX (3) 359-375.

Gómez Omil R.,Boll A.,Hernández R.1987.Cuenca Cretácico-Terciaria del Noroeste Argentino.(Grupo Salta).Cuencas Sedimentarias Argentinas.Serie de Correlación Geológica 6.Tucumán..

Grier M.1990.(Tesis Cornell University)The influence of the Cretaceous Salta Rift Basin on the development of Andean Structural Geometries,NW Argentine Andes.

Jordan T.1984.Cuencas,vulcanismo y acortamientos Cenozoicos Argentina -Bolivia -Chile.20°-28° Latitud Sur.IX Congreso Geológico.Acta II .7-24.

Letouzey,J.1990.Fault reactivation,inversion and fold thrustbelt.Petroleum and Tectonics in Mobile Belts.Paris.101-128.

Medwedeff D.1989.Grow fault bend folding at Southeast Lost Hills ,San Joaquin Valley,California.A.A.P.G Bull.73 (1)54-64.

Suppe J.,Chou G.,Hook C. 1992.Rates of folding and faulting determined from grow strata.In Mc Clay Thrust Tectonics.105-140.

Vistalli C.1987.Cuenca Siluro-Devónica del Noroeste .Cuencas Sedimentarias Argentinas,Serie de Correlación Geológica 6.

FIGURE 1

STRATIGRAPHIC COLUMN

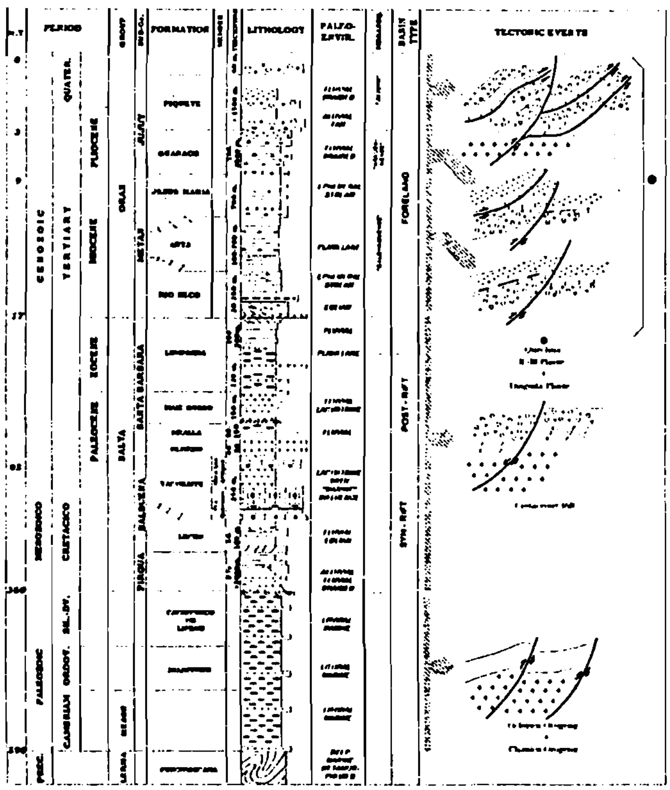

## GEOLOGIC MAP

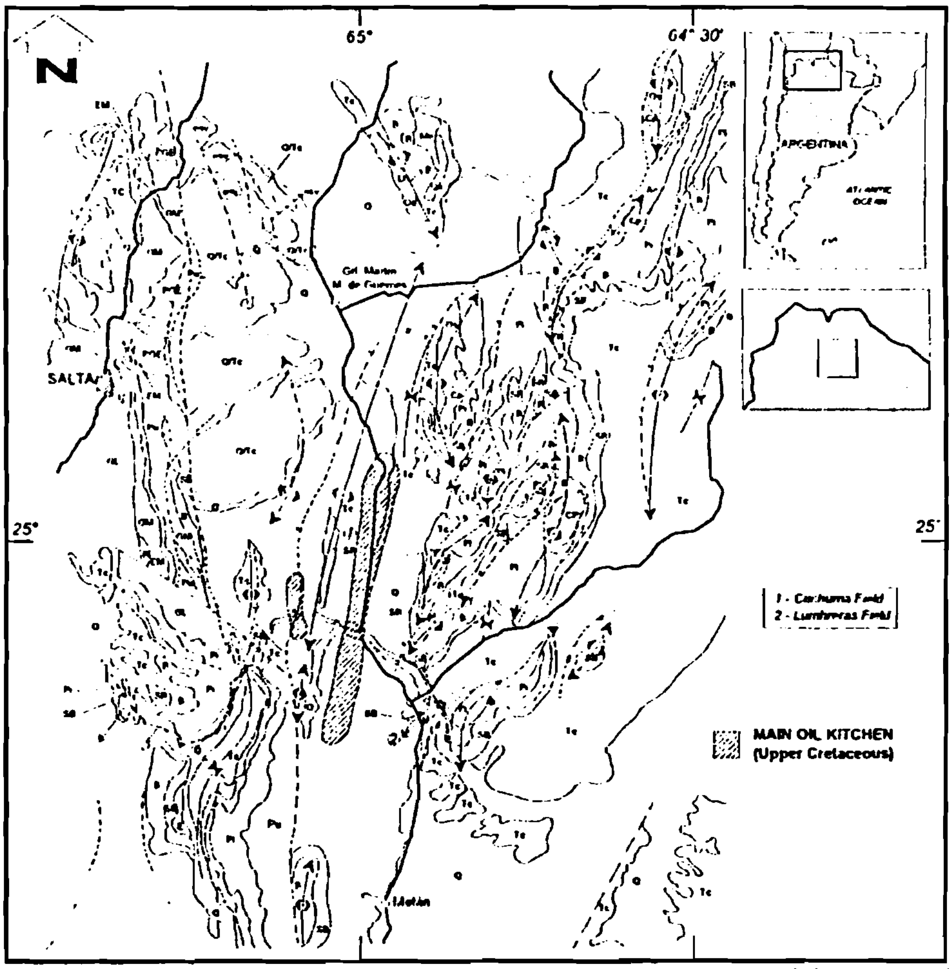


Modif.: F. Garrasino 1984

| | | |
|---|---|---|
| Q/Tc | QUATERNARY - TERTIARY | |
| Q | QUATERNARY | NEOGENE |
| Tc | TERTIARY SEDIMENTITES | NEOGENE |
| SB | Sta. BARBARA SubGr. | NEOCRETAC. PALEOGENE |
| B | BALBUENA SubGr. | NEOCRETAC. PALEOGENE |
| Pi | PIRGUA SubGr. | NEOCRETAC. PALEOGENE |
| Li | LIPEON Fm. | SILURIAN DEVONIAN |
| Cp | CACHIPUNCO Fm. | SILURIAN DEVONIAN |
| Me | MENDIETA Fm. | SILURIAN DEVONIAN |
| Ac | A° COLORADO Fm. | SILURIAN DEVONIAN |
| GM | MOJOTORO Gr. | ORDOVICIAN |
| OSV | Sta. VICTORIA Gr. | ORDOVICIAN |
| EM | MESON Gr. | CAMBRIAN |
| Pu | PUNCOVISCANA Fm. | PRE CAMBRIAN |
| GL | LERMA Gr. | PRE CAMBRIAN - LOWER CAMBRIAN |
| PGE | METAMORPHITES | LOWER CAMBRIAN |

# EMPLACEMENT OF PLUTONIC COMPLEXES, STRAIN AND STRAIN PARTITIONING IN THE COASTAL CORDILLERA, (25°- 27°S), N CHILE

John GROCOTT and Jeff WILSON

School of Geological Sciences, Kingston University, Kingston-upon-Thames, Surrey KT1 2EE, U.K.

KEY WORDS: Pluton emplacement; strain partitioning; magmatic arc; northern Chile

## INTRODUCTION

Emplacement of plutonic complexes in the Coastal Cordillera was associated with deformation in ductile shear zones. Undeformed plutonic rocks and mylonites in adjacent wall rocks yield $^{40}Ar/^{39}Ar$ hornblende and muscovite cooling ages and zircon ages for the undeformed pluton that are, within error, identical. Therefore: (1) plutons were emplaced at high level and cooled rapidly; (2) heat to allow ductile deformation advected to high levels within the arc during magmatism. To account for arc asymmetry defined by east-younging plutonic rocks and east-down displacements in associated shear belts, Grocott and others (1994) proposed that Lower Jurassic to Lower Cretaceous plutons were emplaced as sheets at dilational jogs in an east-dipping extensional fault system. They identified also a change in arc kinematics during Early Cretaceous time (c130 Ma) when ductile deformation became dominated by sinistral strike slip. Farther north in the Cordillera, authors report a Late Jurassic to Early Cretaceous transtensional regime partitioned into arc-normal and arc-parallel sinistral strike-slip components (Scheuber et al. 1995). Recent research on granite emplacement has emphasised that it is not necessary to create space at a dilational site within a fault system to emplace plutonic complexes. Rather, magma pressure is capable of dilating any fracture where it exceeds the regional normal stress component acting across it allowing intrusions to be emplaced as sheets by magma wedging (Ingram & Hutton, 1994). Successively emplaced sheets may build into composite bodies of batholithic proportions (McCaffrey and others 1996). Here, we re-evaluate emplacement models for plutonic complexes in the Coastal Cordillera in the light of this new work, and use new AMS (anisotropy of magnetic susceptibility) data to demonstrate strain partitioning during emplacement of the Lower Cretaceous Las Tazas plutonic complex.

## PERMIAN AND TRIASSIC (P-T) PLUTONIC COMPLEXES

These tonalite to leucogranite plutonic complexes are N-S elongate, composite sheets folded by upright, low amplitude, large wavelength E-W open folds and earlier, inclined, close to tight NE-trending folds. They are located close to the present-day coast (Fig. 1) and have map dimensions typically 30km x 10km and thicknesses >1 km. Plutons were emplaced into strongly deformed Devonian-Carboniferous metasedimentary rocks. Structures within the metasediments include SW-vergent major recumbent folds and mylonite belts. The plutonic complexes were emplaced sub-parallel to the pre-existing foliation and have gentle dips imposed by later folding. Where composition was appropriate, andalusite and muscovite mark a narrow contact aureole, though little ductile deformation is present in the country rocks. Neither magmatic state nor crystal-plastic fabrics have been recorded in the plutons. The main upper and lower contacts are well-defined but there is interleaving of thin, concordant granitoid sheets with metasedimentary country rock above and below the main contacts. Laterally, the plutons interfinger with country rocks in the manner described by McCaffrey and others (1996) for the Lake District batholith, N England. At the edges of the intrusions contacts are steeply-dipping implying that sheet edges are blunt rather than tapered. We conclude that P-T plutons were emplaced as composite, sub-horizontal sheets parallel to the anisotropy of the metasedimentary rocks. Their orientation, absence of direct association with faults and lack of internal and external deformation are consistent with emplacement by dilation of sub-horizontal, mode 1 fractures induced by magma pressure.

## LOWER (LJ) AND UPPER JURASSIC (UJ) PLUTONIC COMPLEXES

Evidence from LJ tonalitic to granodioritic plutons (Fig. 1) has provided strong arguments for emplacement at dilational jogs in an east-dipping extensional fault system fed by a dyke-transport magma ascent mechanism (Dallmeyer, et al., 1996). Plutons were emplaced within mylonitic metasedimentary rocks and are now exposed at roof level. The mylonites contain both pre- and syn-tectonic contact-metamorphic muscovite and andalusite and this implies that Palaeozoic shear zones were reactivated during emplacement. Stretched andalusite defines an WNW-ESE extension lineation associated with top-east shear sense indicators that appear to confirm low-angle normal-slip displacements linked to pluton emplacement.

A dioritic UJ plutonic complex (Las Animas) lies inboard of the LJ plutonic rocks. It is elongate N-S and passes upward into a folded sill complex that cuts arc volcanic rocks of the La Negra Formation (Fig. 1). In exposure, pluton margins are steep though the wide aureole implies that the pluton is a moderately east-dipping sheet. A narrow belt of high temperature mylonites with steep extension lineations is present in country rock along the western margin of the complex and has the same $^{40}Ar/^{39}Ar$ cooling age as the pluton. Farther W, vertical, NE-SW trending swarms of basaltic andesite yield similar $^{40}Ar/^{39}Ar$ ages to the plutonic complex and may be representative of dyke feeder(s) of the UJ plutonic and the sill complexes. The emplacement mechanism for this pluton is uncertain and we have no data on its internal structure. There is however, no specific evidence pointing to emplacement at a dilational jog. Instead, the steep high temperature shear zone at the western margin is consistent with emplacement as an east-dipping sheet within a dip-slip shear zone.

## LOWER CRETACEOUS (LK) PLUTONIC COMPLEXES

Las Tazas plutonic complex (Fig. 1) was emplaced at c.130 Ma inboard of the UJ plutonic complex and is bounded by the western and central branches of the Atacama Fault Zone (AFZ). The complex contains two plutons, one of which is a composite N-S trending vertical sheet with dimensions 60km x10km. Along the western margin of this sheet a broad N-S belt of high-temperature mylonite has vertical foliation and steeply pitching stretching fabric. The vorticity vector (Robin & Cruden, 1995) is perpendicular to the stretching lineation and deformation non-coaxial with a kinematic vorticity number approaching 1. Kinematic indicators demonstrate east (pluton)-side-down displacements. Again, $^{40}Ar/^{39}Ar$ are similar for the mylonites and the pluton indicating that cooling rates for both pluton and mylonites were rapid. The western margin of the pluton cuts the mylonitic rocks and we suggest that deformation partitioned immediately into the magma as it was emplaced. Late syn-plutonic strain, reflected by anisotropy of magnetic susceptibility (AMS) and magmatic state fabrics, is characterised by a margin-parallel flattening with a weak, steeply south-pitching, linear element. The AMS data show that the late-synplutonic deformation of the pluton was characterised by a coaxial strain partitioned into the pluton with a weak, oblique-slip non-coaxial component. Locally developed low-temperature crystal-plastic fabrics within the pluton also reveal east-down displacements parallel to a steep stretching fabric. Major and trace element geochemistry shows that the pluton was emplaced from west to east as a sequence of vertical sheets. The south-pitching linear element of the AMS fabric becomes shallower eastward in the younger sheets due to an increasing dextral component in the non-coaxial portion of the strain. In the eastern country rocks of the complex mylonitic deformation was polyphase. Dextral kinematic indicators on horizontal sections are overprinted by low-temperature (greenschist facies) mylonites with sinistral strike-slip displacements associated with a sub-horizontal stretching lineation. According to Grocott and others (1994), Las Tazas complex was emplaced at a dilational jog in an extensional fault system. The new AMS data does not support this interpretation and the pluton may simply have dilated the north-south trending belt of mylonitic rocks now exposed at its western margin when magma pressure overcame the normal stress acting across the ductile shear belt.

Remolino plutonic complex (Fig. 1) covers an area of 130km x 40km. The internal structure of the pluton is unknown. At its eastern margin a broad belt of greenschist facies, sinistral strike-slip mylonitic rocks has the same $^{40}Ar/^{39}Ar$ hornblende cooling age (c.125 Ma) as the undeformed pluton. This mylonite belt can be traced south for at least 60km on the western side of the Lower Cretaceous batholith (Arévalo, 1995). The eastern country rock of the pluton is characterised by a narrow belt of high-temperature mylonite with a vertical N-S trending foliation and a down-dip stretching fabric. This shows that, although sinistral strike-slip is the dominant style of ductile deformation in the magmatic arc post-c.130 Ma, dip-slip deformation continues to be associated with the early stages of the emplacement of arc plutonic complexes.

La Borracha pluton has a $^{40}Ar/^{39}Ar$ hornblende cooling age of c.106 Ma and is the youngest plutonic complex we have so far dated in the Lower Cretaceous batholith. Like Las Tazas and Remolino complexes it appears to be a vertical sheet emplaced along the AFZ. Its dimensions are 100km x 10 km, it trends NNW-SSE and cuts the sinistral shear belt at the margin of Remolino complex (Fig. 1). In a shear zone developed in country rock at the western margin of the pluton, steeply pitching stretching lineations with east-down kinematic indicators are present. Locally, low temperature sinistral strike-slip mylonitic deformation was superimposed on the dip-slip fabric. The trend and shape of the pluton and dip-slip mylonites imply emplacement at a releasing bend in the AFZ (Fig. 1).

## CONCLUSIONS

Re-evaluation of pluton emplacement mechanisms in the Coastal Cordillera between 25°-27°S indicates that P-T plutonic complexes were emplaced as sub-horizontal sheets at high crustal levels. LJ, UJ and earliest LK plutons were mainly emplaced as sheets by magma wedging rather than at specific dilational sites in fault systems. The plutons were emplaced in an extensional arc with an increasing strike-slip component through time and transtension certainly provides the most satisfactory setting for the youngest LK plutonic complex studied (La Borracha). However, we now have AMS evidence for at least local arc-normal shortening during emplacement of the earliest LK plutons at 26°S.

## REFERENCES

Dallmeyer, R.D., Grocott, J., Brown, M., Taylor, G.K., & Treloar, P.J. 1996. Mesozoic magmatic and tectonic events within the Andean plate boundary zone, 26°-27°30'S, North Chile: constraints from $^{40}Ar/^{39}Ar$ mineral ages. Journal of Geology, 104, 19-40.

Grocott, J., Brown, M., Dallmeyer, R.D., Taylor, G.K. & Treloar, P.J. 1994. Mechanisms of continental growth in extensional arcs: an example from the Andean plate boundary. Geology, 22, 391-394.

Ingram, G.M. & Hutton, D.H.W. 1994. The Great Tonalite Sill: emplacement into a contractional shear zone and its implications for Late Cretaceous to early Eocene tectonics in southeastern Alaska and British Columbia. Geological Society of America Bulletin 106, 715-728.

McCaffrey, K.J.W., Evans, D.J. & Petford, N. 1996. Scale-invarient geometry of tabular sheet intrusions. Geology (In review).

Robin, P-Y F. & Cruden, A.R. 1994. Strain and vorticity patterns in ideally ductile transpression zones. Journal of Structural Geology 16, 447-466.

Scheuber, E., Tomislav, B., Jensen, A. & Reuter, K-J. 1994. Tectonic development of the North Chilean Andes in relation to plate convergence and magmatism since the Jurassic. In: Reutter, K-J & Scheuber, E. (eds.) Tectonics of the Southern Central Andes, 121-139.

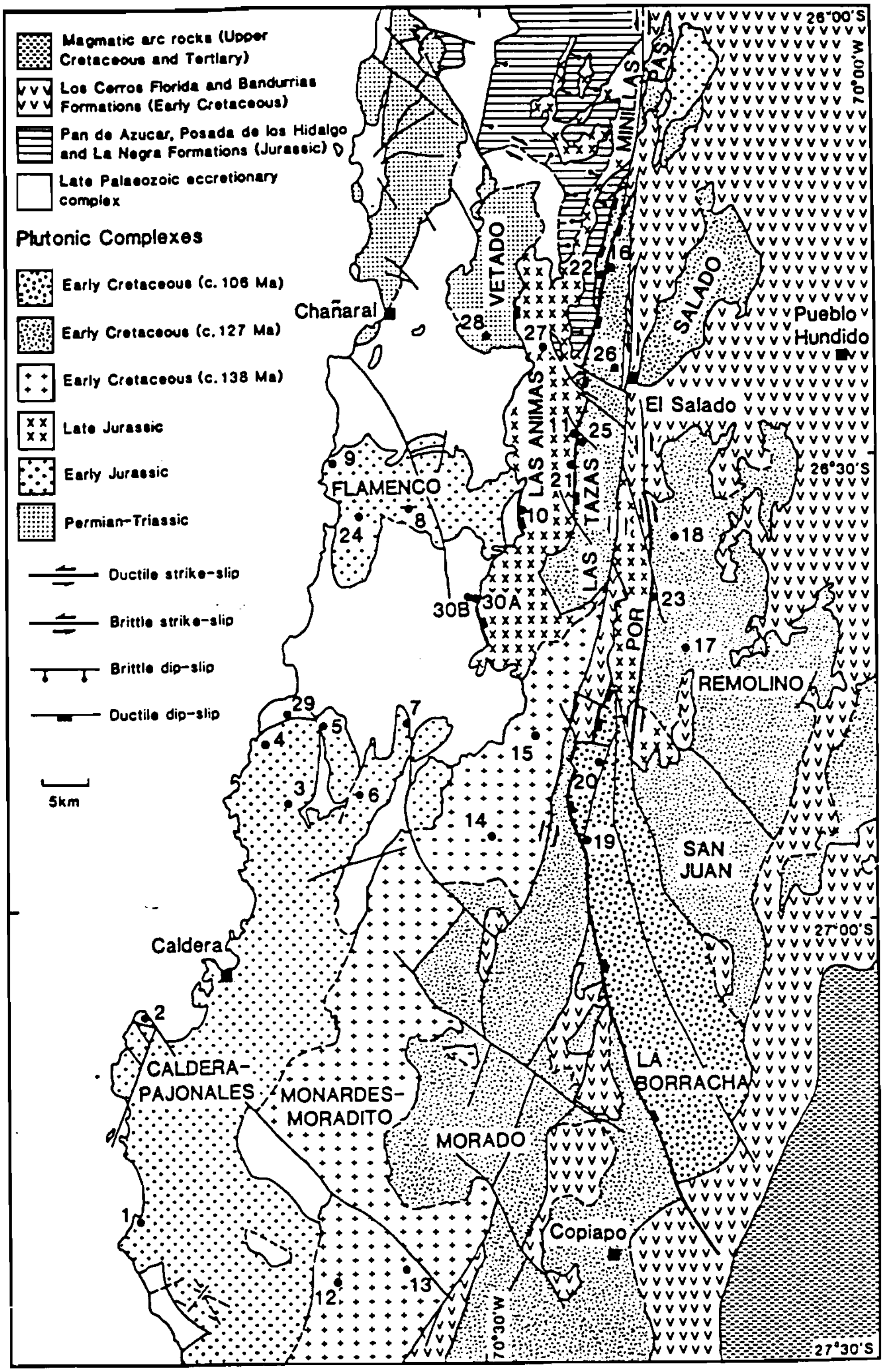


Figure 1. Detailed geological map of the area between 26°S and 27°30'S, Atacama Region, North Chile showing the plutonic complexes and main zones of ductile and brittle deformation referred to in the text. $^{40}Ar/^{39}Ar$ sample localities of Dallmeyer *et al* (1996) are indicated. POR is the Porvenir plutonic complex, PAS is the Pastenes plutonic complex. (From Dallmeyer *et al*, 1996)

# CENOZOIC TECTONO-STRATIGRAPHIC EVOLUTION OF THE ANDEAN FOREARC NORTHERN CHILE

Adrian J. HARTLEY[(1)], Geoffrey MAY[(1)], Stephanie J. KAPE[(2)],
Peter TURNER[(2)] and Guillermo CHONG[(3)].

(1) Department of Geology & Petroleum Geology, King's College, University of Aberdeen, Aberdeen AB9 2UE, U.K.
(2) School of Earth Sciences, University of Birmingham, Edgbaston, Birmingham, U.K.
(3) Departamento de Ciencias Geologicas, Universidad Catolica del Norte, Av. Angamos 0610, Casilla 1280, Antofagasta, Chile.

**KEY WORDS:** Cenozoic, northern Chile, forearc, tectono-stratigraphy, basin analysis

## INTRODUCTION

It has been suggested that during the Cenozic the tectonic regime along the Pacific margin of South America was controlled by the angle and rate of convergence at the subduction zone (Pardo-Casas & Molnar, 1987). Periods of rapid convergence (>100 mm/a) correspond to phases of compressional deformation and periods of relatively slow convergence (<50 mm/a) correspond to intervals of tectonic quiescence. The angle of convergence is considered to have controlled the amount of strike-slip deformation, an increase in obliquity resulting in an increase in transpressional/transtensional deformation. A number of deformation phases have been determined for the Cenozoic of the Central Andes which have become relatively widely accepted in the literature (e.g. Jordan & Alonso 1987) these include: the Late Eocene Incaic, an Early Miocene phase, the Late Miocene Quechua and the Pliocene Diaguita phases. The Incaic and Quechua deformation phases correspond with periods of increased convergence (Pardo-Casas & Molnar, 1987). The Central Andean margin appears, therefore, to have been subject to a compressional tectonic regime throughout much of the Cenozoic, interspersed with periods of tectonic quiescence. However, the structural and sedimentological expression of these tectonic regimes varies considerably. Here we examine the Cenozoic structural and stratigraphic evolution of the north Chilean forearc using new and published data in a traverse across the forearc through the Coastal Cordillera, Central Depression, the Precordillera and the Preandean Depression. We suggest that compressional episodes were interspersed with periods of active transtensional basin formation and that Late Miocene extension of the Coastal Cordillera is related to crustal flexure and extensional collapse. In addition, much of the palaeomagnetically determined rotation which has affected the north Chilean forearc can be attributed to localised strike-slip deformation associated with these periods of deformation, and not oroclinal flexure.

## TECTONO-STRATIGRAPHIC EVOLUTION

Following the Late Eocene Incaic Orogeny a period of 'tectonic quiescence' was associated with pluton emplacement and development of a regional pediplain across northern Chile. The post-Incaic evolution of the forearc is detailed for distinct morphotectonic zones.

**Preandean Depression**

Deposition in the Preandean Depression (Salar de Atacama) commenced in the Early Oligocene (30 Ma) following Incaic deformation at approximately 40 Ma. Sedimentation was continuous until at least the Early Miocene (19 Ma). In a southerly sub-basin, 800 m of sandflat, playa and sheetflood sediments were deposited between 30 and 24 Ma. At 24 Ma an abrupt influx in coarse grained detritus produced 600 m of alluvial fan sheetflood and debris flow deposits up to 19 Ma (Kape, 1996). In the northern sub-basin 500 m of distal sheetflood sediments were deposited before 24 Ma, prior to deformation and development of an unconformity between 24 and 15 Ma (Kape, 1996). Elsewhere, sedimentation did not commence until approximately 10 Ma when deposition of the 'Hollingworth gravels' took place unconformably over the Early Miocene succession at approximately 10 Ma (Naranjo et al., 1994). A thick sequence of ignimbrites and interbedded gravels were deposited between 10 and 4 Ma (San Bartolo Group) followed unconformably by deposition of Plio-Pleistocene sheetflood and lacustrine sediments (Vilama Formation) which in turn were locally deformed prior to the Holocene.

**Precordillera**

Sedimentation in the Precordillera took place within the Calama Basin. The basin forms a link between the Preandean and Central Depressions and is located within the Cordillera de Domeyko. Following Incaic deformation, sedimentation commenced in the ?Late Eocene to Early Oligocene with deposition of 500 m of alluvial fan deposits (?35-?28 Ma). Deformation in the Late Oligocene to early Miocene took place prior to deposition of 100 m of fluvial and playa deposits in the Early to Mid-Miocene (?21-?14 Ma). Deposition of 115 m of alluvial-lacustrine sediments (interrupted by localised deformation) took place in the Late Miocene (9-3 Ma) following Mid-Early Late Miocene deformation and non-deposition. Sedimentation recommenced in the Late Pliocene to Pleistocene with deposition of 30 m of fluvio-lacustrine sediments, minor deformation and incision.

**Central Depression**

Deposition within the Central depression followed Incaic deformation (after 42 Ma) in the Late Eocene to Early Oligocene (?35 Ma). Approximately 1000 m of alluvial fan and lacustrine sedimentation took place throughout the Oligocene and Miocene (the Sichal Formation) up to 11 Ma (Jensen et al. 1995)(although it should be noted that exposure is poor over this interval). A hiatus between 11 and 7 Ma was followed by deposition of volcanics (Ichuno Formation) and alluvial-lacustrine sediments of the Quillagua Formation up to the Late Miocene-?Early Pleistocene (Saez, 1995).

**Coastal Cordillera**

Up to 120 m of interbedded shallow marine and alluvial fan sediments were deposited along the western flank of the Coastal Cordillera from the Late Miocene onwards (La Portada and Mejillones formations). Sedimentation was largely conformable with localised unconformities developed adjacent to active faults, and has taken place in active half-grabens or topographic lows carved in Jurassic volcanics and granodiorites.

## SYNTHESIS: BASIN FORMATION AND DEFORMATION

Comparison of the stratigraphic sections from the studied areas reveals the following sequence of events:

1) Commencement of alluvial fan and playa sedimentation across the area in the Late Eocene/Early Oligocene following regional deformation associated with the Incaic Orogeny. The Calama Basin and Preandean Depression almost certainly formed part of a single basin.

2) End Oligocene/Early Miocene deformation in the Calama Basin and northern part of the Salar de Atacama. Whether deformation took place in the Central Depression is difficult to ascertain due to the lack of detailed information.

3) Continuation of alluvial fan and playa sedimentation from the Early to Mid/Late Miocene.

4) Regional deformation associated with the Quechuan orogeny which affected the Central Depression, Calama Basin and Preandean Depression.
5) Commencement of sedimentation in the Late Miocene across the forearc with ignimbrite emplacement dominant in the Preandean Depression and alluvial-lacustrine sedimentation in the Calama Basin and Central Depression. The latter two basins were linked after localised deformation in the latest Miocene. Initiation of sedimentation on the western side of the Coastal Cordillera and development of extensional tilted fault blocks.
6) Localised Late Pliocene to Pleistocene deformation in the Calama Basin and Preandean Depression synchronous with localised sedimentation and incision.

## DISCUSSION

It is suggested that following the Incaic deformation phase, the Oligocene period of tectonic quiescence was represented by transtensional basin formation recorded by virtually synchronous sedimentation in the Central Depression, Calama Basin and Preandean Depression. Changes in sediment thicknesses adjacent to large-scale faults (e.g. Precordilleran Fault system) suggest these faults were active (Jensen et al. 1995). The development of a transtensional tectonic regime could be due to extensional collapse of the Incaic Orogen following a decrease in convergence rate. A significant deformation phase took place at the end Oligocene/Early Miocene. The regional extent of this phase is difficult to constrain, however, the amount of deformation appears to have been greatest in the Calama Basin - a feature which suggests deformation associated with movement along the Precordilleran Fault System (May et al. this volume). Alluvial fan and playa sedimentation in transtensional basins continued up to the end of the Mid-Miocene across the study area prior to the regional Quechuan deformation phase. The full extent of sedimentation in the Preandean Depression during this time period is difficult to quantify due to post-depositional uplift and erosion associated with the Quechuan Orogeny.

A significant change in deposition took place from the Late Miocene to Late Pliocene. The products of the volcanic arc swamped the Preandean Depression, whilst diatomite and carbonate lacustrine sedimentation dominated over much of the Calama Basin and Central Depression. Interestingly, this lacustrine sedimentation is coincident with a change from a semi-arid to hyper-arid climate (Alpers & Brimhall, 1988). A series of localised deformation phases affected the forearc during the Late Pliocene and Pleistocene which may correspond to the Diaguita phase of deformation (Jordan & Alonso, 1987). Throughout much of the Tertiary it appears that the Central Andes were subject to periods of intense compressional-transpressional deformation interspersed with periods of fault-controlled subsidence. Subsidence is likely to have been related to a transtensional tectonic regime generated by periods of crustal collpase and stress relaxation. Localised deformation appears to have continued throughout much of the basin-fill and may be related to movement on individual faults. This cycle of compression and relaxation could account for much of the tectono-stratigraphic development of what is now the Andean forearc.

An extensional collapse process may also explain the Late Miocene development of the Coastal Cordillera. The leading edge of the South American Plate is represented by a series of extensional graben and half-graben (Moberly et al. 1982; Padilla & Elgueta, 1992) which have an inferred Miocene fill. It is proposed that stress relaxation following uplift associated with the Quechuan deformation phase has resulted in extensional collapse of the leading edge of the continental plate, possibly due to a decreased convergence rate and/or less effective coupling with the Nazca Plate. This process could explain why synchronous extensional and compressional deformation has affected the forearc.

A number of palaeomagnetic studies have been undertaken on rocks of different ages from throughout the north Chilean forearc. The studies have frequently found evidence for block rotation which is commonly interpreted in terms of Oroclinal bending. It is possible that many of the palaeomagnetically determined rotations simply reflect localised deformation associated with transpressional/transtensional fault movement.

## REFERENCES

Alpers, C.N. & Brimhall, G.H. 1988. Middle Miocene climatic change in the Atacama Desert, northern Chile: evidence from supergene minerlization at La Escondida. Bulletin of the Geological Society of America, 100, 1640-1656.

Jensen, A., Dorr, M.J., Gotze, H.J., Kiefer, E., Ibbeken, H. & Wilke, H. 1995. Subsidence and sedimentation of a forearc-hosted, continental pull-apart basin: The Quillagua Trough between 21°30 and 21°45 S, northern Chile. Recent and Ancient Lacustrine Systems in Convergent Margins, GLOPALS - IAS Meeting, Antofagasta, Abstract, p. 5-6.

Jordan, T.E. & Alonso, R.N. 1987. Cenozoic stratigraphy and basin tectonics of the Andes Mountains, 20-28o South latitude. Bulletin of the American Association of Petroleum Geologists, 71, 49-64.

Kape, S.J. 1996. Basin Analysis of the Oligo-Miocene Salar de Atacama, northern Chile. Unpublished PhD Thesis, University of Birmingham, U.K.

Moberly, R., Shepherd, G.L. & Coulbourn, W.T. 1982. Forearc and other basins, continental margin of northern and southern Peru and adjacent Ecuador and Chile. In: Legget, J.K. (ed), Trench-Forearc Geology, Special Publication ofthe Geological Society, London, 10, 171-189.

Naranjo, J.A., Paskoff, R. & Ramirez, C.F. 1994. Morphostratigraphic evolution of the northwestern margin of the Salar de Atacama Basin (23°S-68°W). Revista Geologica de Chile, 21, 91-103.

Padilla, H. & Elgueta, S. 1992. Neogene marine deposits of Caleta Patillos, northern Chile: their relationship with Neogene sediments of the Peninsula de Mejillones. Revista Geologica de Chile, 19, 83-89.

Pardo-Casas, F. & Molnar, P. 1987. Relative motion of the Nazca (Farallon) and South American plates since Late Cretaceous time. Tectonics, 6, 235-248.

Saez, A. 1995. Cenozoic and Quaternary lacustrine systems in northern Chile (Central Andes, arc and fore-arc zones). Recent and Ancient Lacustrine Systems in Convergent Margins, GLOPALS - IAS Meeting, Antofagasta. Excursion guidebook.

# STRUCTURE OF THE ARGENTINE ANDEAN CORDILLERA BETWEEN 30° 30' AND 31° 00' S

N.Heredia (1), L.R. Rodriguez Fernández (2) & D. Ragona (3)

(1) Instituto Tecnológico Geominero de España, Avda. República Argentina, 30, 1º B, 24004 León
(2) Instituto Tecnológico Geominero de España, C/ Rios Rosas, 23, 28003 Madrid
(3) Servicio Geológico Argentino, Avda. Julio A. Roca, 651, 1322 Capital Federal

**Key Words:** Andean Cordillera, Gondwanic Orogen, Andean Orogen, normal faults, inversion tectonic.

## Introduction

In the Argentine Andean Cordillera between latitude 30° 30' and 31° 00' (fig.1), two main tectonostratigrafic groups can be defined : a Paleozoic (Gondwanic) basement with a characteristic thin skinned tectonic structure and the Andean cover with remarkable extensional structures inverted by Tertiary compressional tectonic event.

The Gondwanic basement is constituted by Silurian?, Devonian and Permo-Carboniferous marine sedimentary units, generally deposited in carbonate or siliciclastic sedimentary platforms, intruded by Upper Paleozoic granitoid rocks ( Tocota pluton ). The most important structures related with Gondwanic Orogenic Cycle are thrust and related folds, with transport direction to the East and remarkable shortening.

The Andean cover discordant over the Gondwanic basament has a volcanic and volcanoclastic origin with some interbedded continental sedimentary rocks. Two tectonostratigraphic groups can be also defined: a preorogenic sequence linked with an extensional tectonic event, and a synorogenic sequence linked with a compressional tectonic event producing the inversion of the previous extensional features. The lower units (Choiyoi Group and Vizcachas Fm. of Permian and Triasic age) are affected by normal faults with downtrow of the Western blocks and are intruded by Triasic granodioritic rocks. These faults involve the Gondwanic basement in a typical thick skinned tectonic style and are grouped in bands with a N-S direction. The uppermost units (Melchor and Olivares groups of Tertiary and Plio-Quaternary ages) are also discordant over the last ones. The normal faults were inverted in the Upper Miocene by an elevation of the West blocks, deforming the lower and upper units in a compressional context during the Andean Orogenic Cycle.

### The Gondwanic Orogenic Cycle

The Gondwanic Orogenic Cycle goes from the upper Devonian to the lower Permian. The preserved structures linked to this Orogenic Cycle in this area were generated during San Rafaelic phase at lower Permian (Ramos, 1988). The deformation characteristics are of thin-skinned type: almost complete absence of metamorphism and schistosity, and the presence of numerous thrust levels, with folds related to thrust surface geometry.

Usually, the thrust surfaces are placed on favorable levels —as the Silur-Devonian limestones situated on the bottom of the Paleozoic succession. The main geometric structures at different scales (m to km) are imbricate fans or duplexes. The observation of different kinematic criteria shows an East tectonic transport direction for all Gondwanic thrusts.

Some folds at different scales appear to be related to the Gondwanic thrusts. The folds have different geometric features. Asymmetric folds are the most common type depicting interlimb angles lower than 70º and the axial plane dipping 20º to 40º W. The folds are facing towards the E or the SE. Generally, they are cylindrical folds, but sometimes we can find folds with non cylindrical shapes.

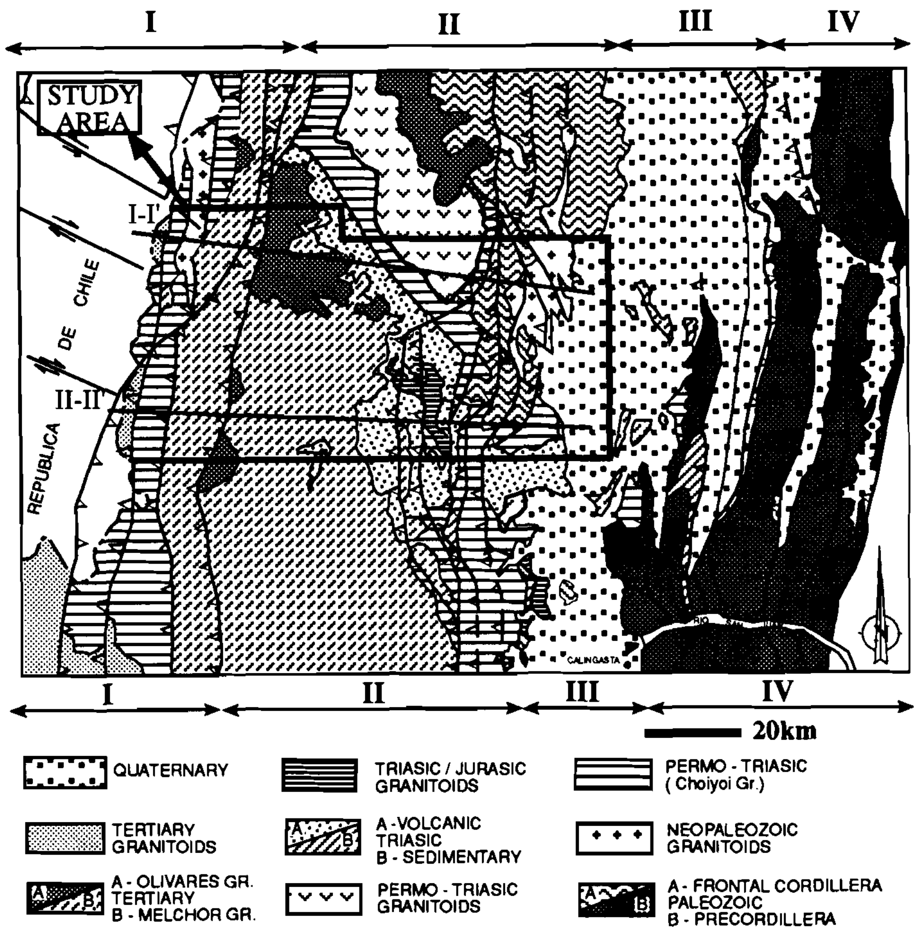


**Fig.1.- Geological sketch map with location of study area.**
**I-Principal Cordillera. II- Frontal Cordillera. III- Rodeo-Calingasta Basin.**
**IV- Precordillera**

Although it was not possible to restore the Gondwanic deformation, we were able to estimate the shortening of some minor structures. The calculated shortening is up to 70% in some duplex structures in the Atutia river area using a bed-length balance method. The calculated shortening must not be too different from the regional shortening generated by the Gondwanic deformation.

## The Andean Orogenic Cycle

The Andean Orogenic Cycle (Ramos, 1988) is the ultimate responsible of the tectonic construction of the Andean Cordillera. In this cycle we can distinguish two main stages: the first one is an extensional tectonic episode, starting in upper Permian and concluding in the lower Cretaceous; the second one is a compressional tectonic episode, which goes from the upper Cretaceous to the Quaternary.

## The extensional stage

In the upper Permian starts an important extensional stage, which generates a significant volcanism (Choiyoi volcanic episode). From the Triassic to the lower Jurassic, this process accelerates, but it slows down in the rest of the Jurassic and the lower Cretacic, and the first marine deposits appear. The deposition area and the Mesozoic sedimentation depocenters migrate to the W, conditioned by the extensional deformation migration in the same direction.

The structures related to the Andean extensional tectonic process are normal faults grouped in bands with a N-S direction (fig. 1). Sometimes we can find normal faults with a NO-SE direction, which represent transfer zones.

The normal faults are listric, mergin to a common detachment level dipping to the W. In the cross section I-I' and II-II' (fig.2) we can observe the Andean extensional prism geometry, with the

Gondwanic basement dipping to the W, and at the same time, each fault-block dipping to the E. This geometrical configuration defines a half-graben model and determines the existence of an important Gondwanic basement outcrop in the E of the studied area (Tocota Horst). We must remark the presence of Jurassic sediments in the W side of the Cortadera Fault (fig. 2). This fact shows that the Cortadera Fault represents the limit between the two main paleogeographical and structural domains of the Andean Cordillera in this area: the Cordillera Frontal and the Cordillera Principal.

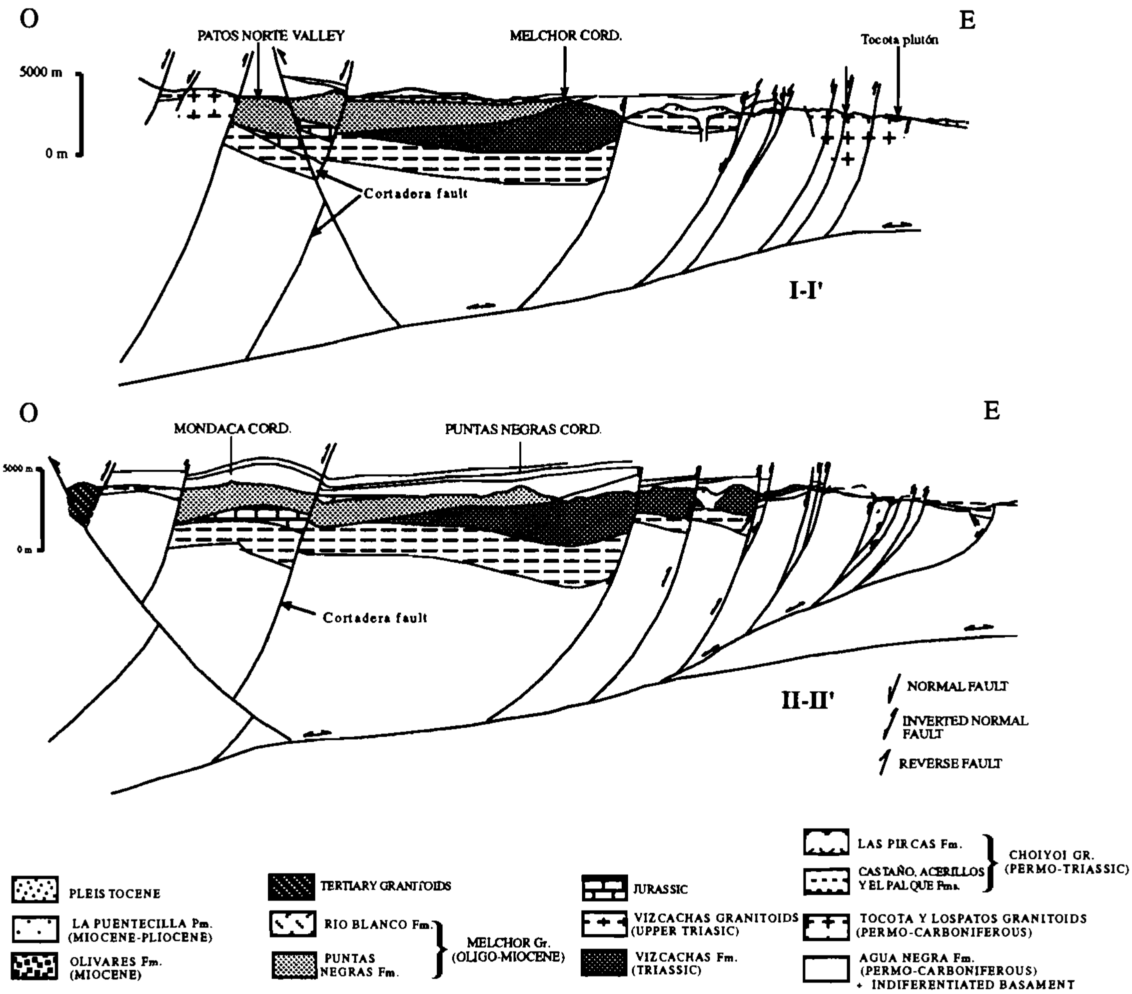


**Fig. 2.- Geological cross sections. For location see Fig. 1.**

## The compressional stage

The Andean compressional stage starts in the upper Cretaceous in the same latitude in Chile (Legarreta and Uliana, 1991). However, in the studied area, it probably starts in the Oligocene, which is the age of the first synorogenic sediments (Melchor Group). The Melchor Group lays unconformabily over the preorogenic successions and the Gondwanic basement (fig. 2), and its depocenters migrate from the W to the E, opposite to the extensional stage depocenters. The geometrical configuration of the Melchor Group is determined by the extensional structure and the erosion surfaces developed over the different fault-blocks from the Jurassic to the Oligocene. In the upper edge of the fault blocks the Melchor Group rests on the lower Andean units (cross sections I-I' and II-II', fig. 2); and in the E of the studied area, it even rests on the Gondwanic basement.

The most important compressional structures are reverse faults and thrusts, and scarce related folds. Most of the faults are generated by the inversion of the extensional faults during compressional tectonics process. However, some faults formed later cut the pre-existing faults (fig. 1 and 2). The observation of different kinematic markers shows an East tectonic transport direction for the Andean compressional structures.

The inversion ratio of the reverse fault measured in the Tertiary sinorogenic rocks is usually less than 1 km. The crustal shortening calculated in the cross section I-I' and II-II' (fig. 2) is of about 8%. This fact contrasts with the more than 50% calculated shortening of the Precordillera unit (Gosen, 1992). All this shows that most of the crustal shortening of the Andean Cordillera at the compressional stage has been transferred to the Precordillera unit through the lower detachment fault. This facts also show that the Cordillera Frontal unit is an uplift block in which the estensional structures have been preserved, and that the Rodeo-Calingasta basin is of piggy back type.

## References

Gosen, W. von (1992).-. *Jour. Struct. Geol.*, 14 (6), 643-667.

Legarreta, L. y Uliana, M.A. (1991).- *Spec. Publ. Int. Assoc. Sed.*, 12, 429-450.

Ramos, V. A. (1988).- Processes in Continental Litospheric Deformation, S. Clark and D. Burchfiel (Eds.). *Geol. Soc. Amer., Spec. Paper*, 218, 31-54.

# SEQUENCE OF LATE OLIGOCENE-MIOCENE FOLD-THRUST DEFORMATION AND DEVELOPMENT OF PIGGYBACK BASINS IN THE EASTERN CORDILLERA, SOUTHERN BOLIVIA

Brian HORTON

Department of Geosciences, University of Arizona, Tucson, Arizona 85721 USA

**KEY WORDS:** Bolivia, thrust-belt kinematics, piggyback basins

## INTRODUCTION

Late Oligocene-Miocene piggyback basins in the Eastern Cordillera of southern Bolivia developed on top of the evolving Andean thrust belt. These orogenic wedge-top basins contain progressive unconformities and have been folded and cut by thrust faults. Field mapping, measured stratigraphic sections, and $^{40}Ar/^{39}Ar$ isotopic dates reveal the sequence of fold-thrust deformation in the region. In general, out-of-sequence thrusting within an east-directed thrust system led to the development of fault-propagation and fault-bend folds that flank individual piggyback basins.

## GEOLOGIC SETTING

Three north-trending basins, referred to as the Estarca, Tupiza, and Nazarano basins (from west to east), are separated by mountain ranges that average ~4 km elevation. The basins themselves are ~10 km wide by ~80 km long and situated at elevations of ~3 km. In southern Bolivia, the Eastern Cordillera is part of the thrust-belt hinterland consisting of a thick section of penetratively deformed, low-grade metamorphosed Ordovician rocks with subvertical slaty cleavage and narrow north-trending synclinal belts of modestly deformed, unmetamorphosed Cretaceous rocks. Cenozoic fold-thrust deformation in the hinterland thus affected a geologic column consisting of a pre-existing "slate belt" of Ordovician rocks and a few isolated occurrences of Cretaceous rocks. This complex pre-thrusting geometry may have inhibited development of continuous regional decollements in specific stratigraphic horizons and favored development of both east- and west-vergent structures.

## BASIN STRATIGRAPHY

The piggyback basins contain nonmarine clastic deposits of late Oligocene-Miocene age. Rapid lateral facies changes and stratigraphic pinch-outs within and among the basins have led to differing stratigraphic interpretations (Montano, 1966; Herail et al., 1996). The Tupiza basin consists of three north-trending outcrop belts representing three distinct piggyback basins. The oldest deposits, herein named the Bella Vista unit, are exposed in a syncline in the eastern outcrop belt. This unit consists of a 400-600 m thick alluvial-fan conglomerate dominated by clasts of Ordovician shale on the east limb of the syncline and clasts of Cretaceous sandstone on the west limb. The eastern section and underlying Ordovician rocks were folded prior to deposition of the overlying Tupiza Formation volcanic rocks. The 300 m thick Tupiza Formation volcanic rocks overlie the eastern Bella Vista section with a highly angular unconformity and conformably overlie the western Bella Vista section. The Tupiza volcanic rocks and probable equivalents to the north have been dated at 22.7 +/- 0.6 Ma and 29.9 +/- 0.9 Ma (K/Ar ages; Herail et al., 1996).

The oldest deposits of the central outcrop belt of the Tupiza basin are the Catati Formation, a 400 m thick section of floodplain/lacustrine shale with thin gypsum layers deposited with slight angular unconformity on Ordovician strata. Paleocurrent indicators show that a basal conglomerate/sandstone with predominantly Cretaceous sandstone clasts was derived from the west and ripple-cross-stratified sandstones from the uppermost Catati were derived from the southeast. The Catati Formation is correlated with similar lithologies at the top of the Tupiza volcanic rocks of the eastern outcrop belt and is thus early Miocene in age. The Tupiza Formation conglomerate is a red alluvial-fan deposit conformably overlying the Catati Formation in the central outcrop belt and the Tupiza volcanic rocks in the eastern outcrop belt. The Tupiza conglomerate, about 500 m thick in the eastern belt and 1000 m thick in the central belt, exhibits an unroofing sequence in which basal strata are dominated by Cretaceous sandstone clasts and upper strata contain mainly clasts of Ordovician shale. Large clasts of Tupiza volcanic rocks are present only in the eastern belt. A tuff near the base of the eastern belt of the Tupiza conglomerate yielded an $^{40}Ar/^{39}Ar$ age of 16.14 +/- 0.06 Ma. Clast-size variations and cross-stratified conglomerate/sandstone in both outcrop belts reveal paleoflow toward the east.

The Nazareno Formation, the oldest deposit in the western outcrop belt of the Tupiza basin, is up to 1000 m thick and is typically in unconformable contact or fault contact with Ordovician rocks. A basal, 200 m thick red conglomerate dominated by clasts of Ordovician shale pinches out eastward, suggesting that it could not have been continuous with the Tupiza conglomerate. The rest of the Nazareno Formation is composed of shale and fine-grained sandstone. A tuff within the Nazareno Formation has been dated at 18.0 +/- 0.5 Ma (K/Ar; Herail et al., 1996). The Oploca Formation is a 600 m thick section of braided-fluvial conglomerate/sandstone that unconformably overlies Nazareno and Ordovician strata. Conglomerate clast compositions include Ordovician shale and Tertiary volcanic rocks. Sediment transport was dominantly along the basins's north-trending axis, with a probable Ordovician source terrane to the west and volcanic sources to the north. A tuff near the base of the Oploca Formation yielded an $^{40}Ar/^{39}Ar$ age of 13.33 +/- 0.15 Ma. A tuff near the top is 8.28 +/- 0.74 Ma (K/Ar age; Herail et al., 1996).

The Estarca basin is composed of an eastward-coarsening and thickening section of conglomerate, sandstone, and shale. The basin deposits overlie Ordovician strata with a highly angular unconformity and are up to 800 m thick. The section is dominated by Ordovician detritus and is presumably the temporal equivalent to the Nazareno and Oploca Formations of the Tupiza basin.

The Nazareno basin contains a fining-upward, shale-dominated section up to 800 m thick. Conglomerate horizons contain clasts of Ordovician shale and Tertiary volcanic rocks. A 20.9 +/- 0.6 Ma tuff near the base (K/Ar age; Herail et al., 1996) and a 12.79 +/- 0.12 Ma tuff near the top ($^{40}Ar/^{39}Ar$ age; Gubbels et al., 1993) reveal a Miocene age for the basin.

## SEQUENCE OF DEFORMATION

Progressive unconformities, provenance characteristics, and cross-cutting thrust relationships involving Tertiary deposits define a pattern of out-of-sequence thrusting within an overall east-vergent thrust belt.

(1) A late Oligocene west-directed thrust on the eastern margin of the Tupiza basin provided an eastern source of Ordovician detritus for the Bella Vista unit. This thrust folded the conglomeratic unit in a footwall syncline prior to unconformable overlap by the late Oligocene-early Miocene Tupiza volcanic rocks. Syndepositional deformation west of the Bella Vista unit is suggested by interbedded Cretaceous-clast conglomerates derived from the west.

(2) Early middle Miocene east-directed thrusting and associated growth of a fault-propagation fold and fault-bend fold is linked to deposition of the lower-middle Tupiza conglomerate (16.14 +/- 0.06 Ma;

$^{40}Ar/^{39}Ar$ age). A progressive unconformity in the eastern strata suggests syndepositional growth of a structure on the western margin of the eastern outcrop belt. The central outcrop belt lacks progressive unconformities, suggesting no nearby structures with actively rotating limbs. However, both the central and eastern belts of Tupiza conglomerate record unroofing of a major sediment source to the west. The eastern belt also contains clasts of Tupiza volcanic rocks reworked from the area between the central and eastern belts. These provenance indicators and growth strata suggest growth of a fault-propagation fold with active limb rotation within the Tupiza conglomerate depositional area. This feature provided minor amounts of Tupiza volcanic rocks to the east. A fault-bend fold that lacks evidence for rotating limbs is present on the west flank of the Tupiza conglomerate depositional area; this structure was the primary source of sediment. Both folds are consistent with an east-directed thrust system with a ramp-flat geometry.

(3) Late middle Miocene-late Miocene east-directed, out-of-sequence thrusting and fold growth is associated with deposition of the upper Tupiza conglomerate and lower Oploca Formation (13.33 +/- 0.15 Ma; $^{40}Ar/^{39}Ar$ age). In the central outcrop belt, a progressive unconformity in upper strata of the Tupiza conglomerate suggests a growing structure to the west. In the western outcrop belt, a progressive unconformity in the lower Oploca Formation suggests a growing structure to the east. A fault-propagation fold at the tip of an east-directed out-of-sequence thrust accounts for both progressive unconformitites and a mapped thrust on the west margin of the central outcrop belt which places Ordovician rocks on the upper Tupiza conglomerate. This break-back thrust may have cut up from the footwall ramp of the pre-existing fault-bend fold on the west margin of the Tupiza conglomerate depositional area.

(4) Post-middle Miocene (post Tupiza conglomerate) folding and thrusting characterized the eastern outcrop belt of the Tupiza basin. Tight folding of the Tupiza conglomerate may be related to reactivation of the west-directed thrust on the eastern basin margin, which cuts the upper Tupiza conglomerate, and potential reactivation of a thrust between the central and eastern outcrop belts.

(5) Late Miocene fault-bend fold growth post-dates the Oploca Formation and deposits of the Estarca and Nazareno basins. The eastern Estarca deposits, western Oploca deposits, and western Nazareno deposits lack significant progressive unconformities and have been tilted approximately parallel to the slopes of their adjacent range fronts. These features are consistent with growth of two fault-bend folds separating the Estarca, Tupiza, and Nazareno basins during translation along a deeper decollement.

## CONCLUSIONS

Late Oligocene-Miocene deformation within the predominantly east-vergent hinterland portion of the Andean thrust belt led to isolation of individual piggyback basins. Shortening within this ramp-flat thrust system produced fault-bend folds that served as major sediment source areas and fault-propagation folds with actively rotating limbs which led to growth of progressive unconformities in adjacent deposits. Out-of-sequence thrusting within the Eastern Cordillera of southern Bolivia from late Oligocene to late Miocene time may represent a prolonged phase of subcritical thrust-wedge conditions such that the thrust front could not migrate eastward. By late Miocene time (~10 Ma) thrust-wedge taper had apparently increased enough to initiate thrusting farther east in the Subandean Zone.

## ACKNOWLEDGMENTS

Supported by an NSF Graduate Fellowship and grants from GSA, AAPG, Sigma Xi, and the University of Arizona. I am grateful to P. Copeland for the $^{40}Ar/^{39}Ar$ dates, and C. Gorman and Ugo Palmito for field assistance.

**REFERENCES:**

Gubbels, T., Isacks, B., and Farrar, E., 1993, High-level surfaces, plateau uplift and foreland development, Bolivian Central Andes: *Geology*, 21, 695-698.

Herail, G., Oller, J., Baby, P., Bonhomme, M., and Soler, P., 1996, Strike-slip faulting, thrusting and related basins in the Cenozoic evolution of the southern branch of the Bolivian Orocline: *Tectonophysics*, in press.

Montano., D., 1966, Estudio geologico de la region de Tupiza-Estarca-Suipacha (Ph.D., thesis): Universidad Mayor de San Andres, La Paz, 76 p.

# NEOGENE FISSION-TRACK STRATIGRAPHY OF SOUTHERN ECUADORIAN BASINS: IMPLICATIONS FOR REGIONAL TECTONIC HISTORY

Dominik HUNGERBUEHLER, Michael STEINMANN, Wilfried WINKLER and Diane SEWARD

Geological Insitute ETH Zürich, Sonneggstr. 5, CH-8092 Zürich, Switzerland

KEY WORDS: Ecuador, Miocene, basin analysis, zircon fission track

## INTRODUCTION

Uplift and deformation of the Andes are related to the subduction of the Nazca plate underneath the South American continent. The Ecuadorian Andes consist of two parallel N–S striking mountain chains separated by the Interandean valley. The Cordillera Real in the east consists of Paleozoic and Mesozoic metamorphic rocks and the Cordillera Occidental in the west of Cretaceous to Neogene volcanics. In the Interandean zone several sedimentary basins developed during the Neogene. Uplift and deformation events are recorded in the mostly continental basin fill series, revealing a detailed Neogene history of the Ecuadorian Andes.
The project consists of a detailed analysis of stratigraphy, sedimentology and deformation of several basins in southern Ecuador (Fig. 1, Cuenca, Nabón, Girón, Santa Isabel, Loja, Malacatos-Vilcabamba, Catamayo-Gonzanamá, Playas and Zumba). The stratigraphic framework and the timing of basin fill deformation is established by fission-track age determinations in intercalated pyroclastics. A study of microfossil and facies patterns allows the reconstruction of depositional environments.

## BASIN STRATIGRAPHY

The geological frame of the sedimentary basins is hardly known, except for that of Nabón (Hungerbühler et al., 1995). Earlier studies focused on the Cuenca basin, resulted in a geological map and established the stratigraphy. Timing of the basin fill was based on two K-Ar analysis of intercalated pyroclastics (Lavenu et al., 1992). Correlation from other basins to the Cuenca basin was based purely on lithological similarities (Putzer, 1968). However, our fission-track ages as well as fossil mammal data (Madden et al., 1994) show considerable variability in timing of sedimentation from basin to basin.

In the Nabón basin (Winkler et al., 1993; Hungerbühler et al., 1995) the continental fill (about 600 m) consists of primary and reworked volcaniclastic sediments. A detailed stratigraphic analysis with 12 fission-track ages and paleomagnetic stratigraphy showed that the sedimentation took place during a very short period of time (8.5 – 7.9 Ma). High sedimentation rates of dominantly volcaniclastic material in the Nabón basin relates to the acidic volcanic activity at the time. Synsedimentary compressional deformation features (growths folds and sedimentary wedges) in the scale of several 100 m indicate a WNW-ESE shortening, perpendicular to the basin axes.

In the other basins the fill series consist of alluvial and lacustrine sediments derived mainly from the Cordillera Real and coeval volcanics. The sediments rest unconformably on a volcanic unit (Late Oligocene – Early Miocene) and turbidite series (Late Cretaceous) in the northern region and on metamorphic units (Devonian) and volcanic series (Paleogene) in the south. Most of the basins were developed in a half graben setting during extension. There is evidence for a marine or brackish environment (ostracods, shrimps) at the base of the series of Cuenca and Malacatos-Vilcabamba. Deposition took place during relatively short time ranges in the Middle and Late Miocene and sediment accumulation was rapid: Malacatos-Vilcabamba (1500 m) 4 Ma, Loja (1000 m) 3 Ma and Cuenca (2700 m) 7 Ma. Facies distribution, transport directions and metamorphic pepple components in the sediments indicate an eastern source area for all the basins. There is almost no input derived from the West. Therefore, there is no evidence for a pronounced positive relief of a western mountain chain (Cordillera Occidental) during the time of sedimentation.

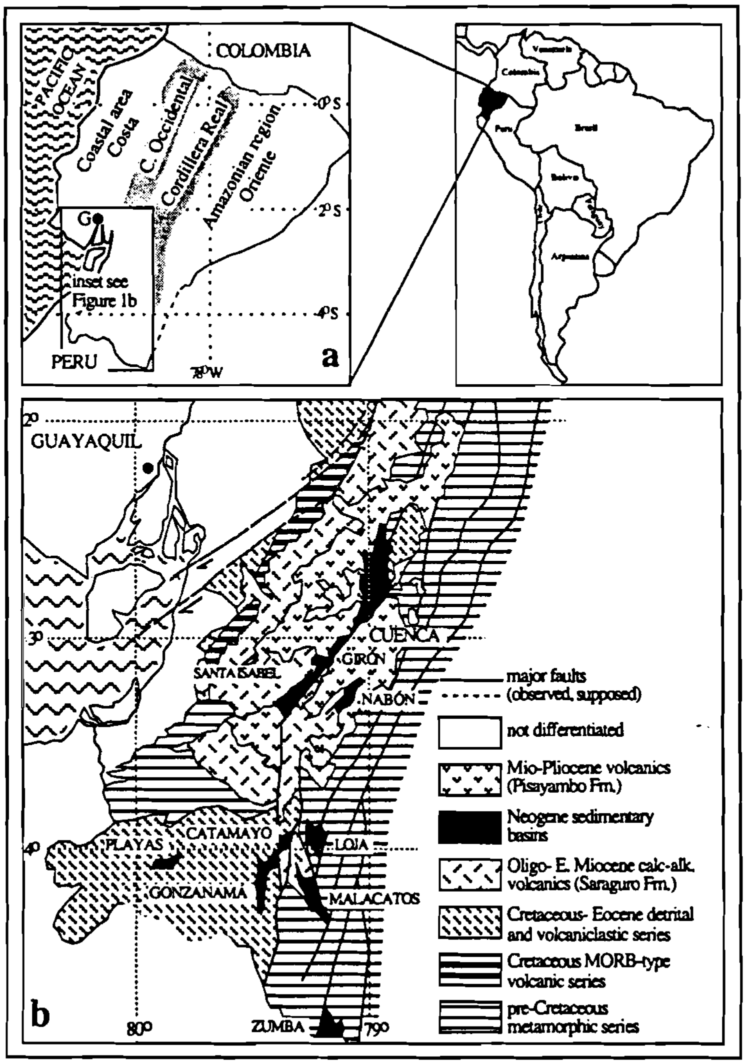


**Fig. 1.** Simplified maps of Ecuador, a) Morphotectonic areas of Ecuador, b) Geological map of southern Ecuador with position of the main Neogene sedimentary basins (after Litherland et al., 1993).

Zircon fission-track ages of volcanic horizons are the first age determinations of Neogene sediments in southern Ecuador on a regional scale. They indicate much younger and shorter periods of sedimentation in the basins than previously assumed. The obtained chronostratigraphy is summarised in Fig. 2, which is based on about 80 fission-track age determinations. The data show synchronous sedimentation of basin fill in Cuenca, Malacatos-Vilcabamba, Santa Isabel and Loja, the oldest preserved sediment being 15-14 Ma. Basal sediments in Girón are clearly older than in the other basins. Sedimentation was continuous within individual basins but was variable in time between them. Airfall deposits from the top of the Loja and Malacatos-Vilcabamba basin series give an age of about 11 Ma, assuming a shorter sedimentation period than in the Cuenca basin (top at 8 Ma). The basin fill of Nabón is clearly younger than in all other basins. The basin series are often sealed by young pyroclastics of an age between 6 and 2 Ma, indicating regional volcanic events in southern Ecuador. Where these young pyroclastics are missing it is difficult to estimate how much sediment has been removed by denudation.

Together with the zircons, coeval apatites have been dated. Since apatite has a blocking temperature of 100±5°C (Harrison, 1985) some estimation of burial depth can be obtained by measuring the amount of annealing, both through the age determination as well as track length measurements.

There are major unconformities in the sequences with good correlation from basin to basin, implying regional activity rather than local events. The basal unconformity between the volcanic basement and the basin fill series represents a long time gap (4 to 15 Ma). In addition several minor discordances are present in all fill series. The angular unconformity at around 8 Ma marks a younger regional tectonic event which can be observed in the northern part of the studied area.

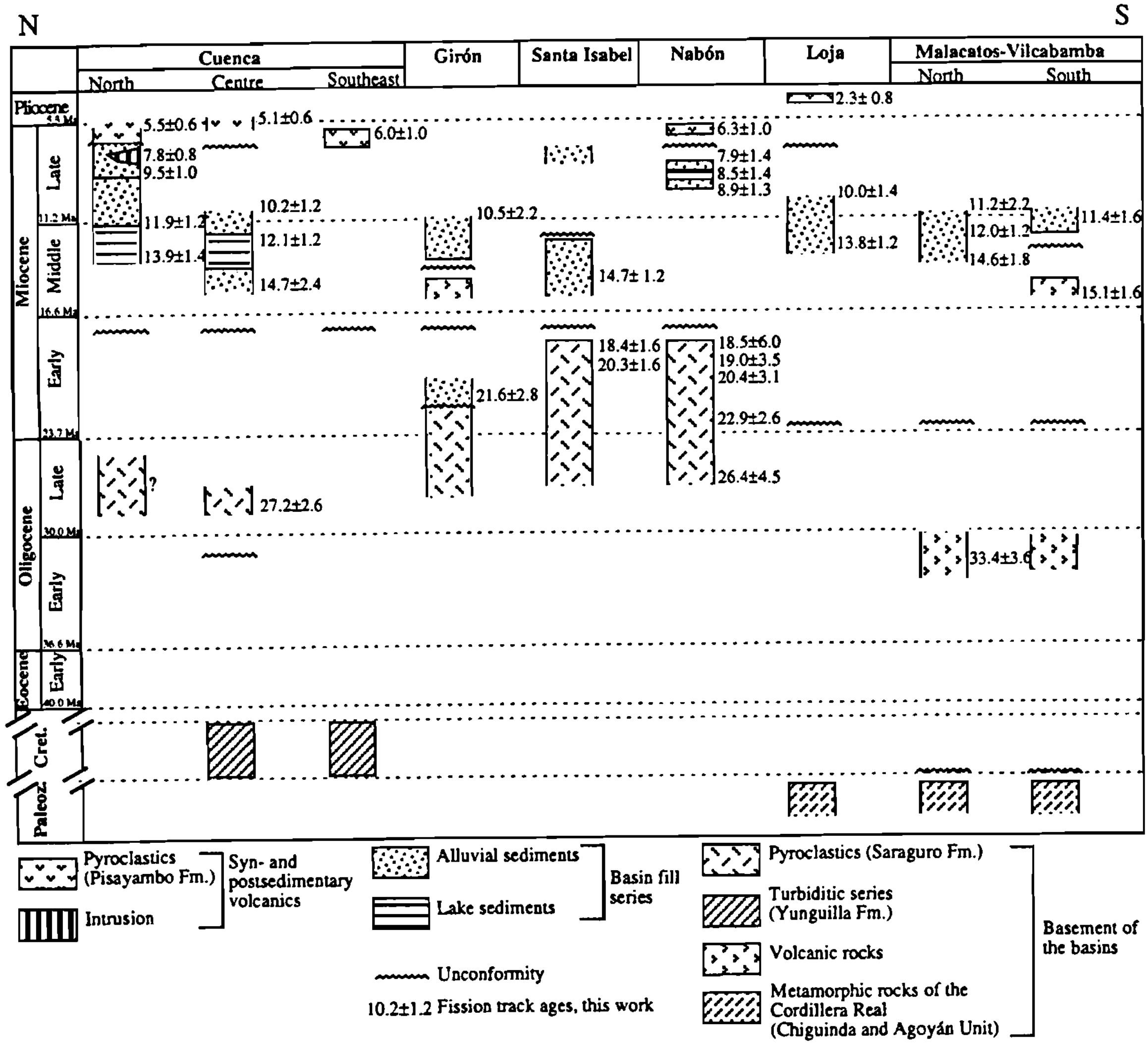


**Fig. 2.** Chronostratigraphic correlation chart of basement and fill of the Miocene basins in southern Ecuador, based on about 80 zircon fission-track age determinations. These ages were determined using the external detector method. The zircons were extracted using standard separation techniques and were mounted in teflon and polished. Etching was carried out at 210°C in a eutectic melt of KOH and NaOH for 36 - 100 h. Samples were irradiated together with Fish Canyon Tuff age standard and glass dosimeter (CN1 and NBS SRM 612). All ages were determined using the zeta approach. Errors are expressed as 2 σ.

## DEFORMATION OF THE BASIN FILL SERIES

Most of the basin series suffered dominant, postsedimentary deformation in an E–W compressional regime which is related to the convergence of the Nazca plate. This deformation is characterised by large scale thurst faulting, inverse faults and folding. The timing of the postsedimentary deformation is provided by fission-track ages of undeformed sediments which unconformably overlie the basin series. A Latest Miocene age is indicated.

In particular the strong postsedimentary E-W shortening in the Cuenca basin caused west and east vergent thrust faulting. The faults can be traced in N-S strike direction over more than 80 km. The timing of the deformation can be clearly determined. It postdates the depositon of the Mangán Formation (uppermost basin fill, 9.5 Ma) and was completed before the intrusion of the Cojitambo dacite (7.8 Ma), which cuts the deformed sediments discordantly. Coeval compressional synsedimentary deformation is restricted to the basins of Nabón and to the top of Malacatos-Vilcabamba series. A major pulse of uplift during this deformation event can be assumed.

## CONCLUSIONS

Sedimentation in the individual basins took place during relatively short periods in the Middle and Late Miocene. Two major unconformities indicate periods of higher tectonic activity between 18 - 15 Ma and around 8 Ma.

Sedimentological features such as evidence for flow direction from the basins, fragmentary facies relations and discordant basin sediments outside of the main basin domains suggest that the preserved sedimentary series represent only relicts of larger basinal areas.

Observed half graben configurations confirm early extensional settings during basin development. There is no evidence for synsedimentary transpressional tectonics as assumed, except in the young Nabón basin.

Most of the basin series suffered a dominant, postsedimentary deformation around 8 Ma, in an E-W compressional regime, which correlates to the synsedimentary deformation in the Nabón basin.

The marine or brackish facies at the base of some basin fills and the strong volcanic input suggest perhaps that the older basins were formed in a volcanic arc environment at or below sealevel. Only the young Nabón basin shows clear evidence for a truly intermontane setting.

A dominant eastern source area and marine or brackish ingressions from the West indicate a younger age for the uplift of the Cordillera Occidental (Steinmann et al., 1996) than generally assumed.

## REFERENCES

Harrison T.M., 1985. A reassessment of fission-track annealing behaviour in apatite. Nuclear Tracks, 10, 329-332.

Hungerbühler D., Steinmann M., Winkler W., Seward D., Egüez A. and Heller F. 1995. An integrated study of fill and deformation in the Andean intermontane basin of Nabón (Late Miocene, southern Ecuador). *Journal of Sedimentary Geology*, 96, 257-279.

Lavenu A., Noblet C., Bonhomme G., Egüez A., Dugas F. and Vivier G. 1992. New K-Ar age dates of Neogene to Quaternary volcanic rocks from the Ecuadorian Andes: Implications for the relationship between sedimentation, volcanism and tectonics. *Journal of South American Earth Sciences*, 5 (3-4), 309-320.

Litherland M., Egüez A. and Zamora A. 1993. Mapa geológico del Ecuador, escala 1:1'000'000. Quito: CODIGEM, BGS.

Madden R.H., Burnham R., Swisher C.C.III., Carlini A.A. and Walton A.H. 1994. Mammalian paleontology, paleobotany and geochronology of the Miocene intermontain basins of Southern Ecuador. *Journal of Vertebrate Paleontology*, in press.

Putzer H. 1968. Tertiäre Lignite im interandinen Graben von Ecuador als Beispiel für synorogene Kohlenbildung in intermontanen Becken. *Geologisches Jahrbuch, Hannover*, 85, 461-488.

Steinmann M., Seward D. and Hungerbühler D. 1996. Thermotectonic history of the Andes, south Ecuador: Evidence from fission-track dating. *Third International Symposium on Andean Geodynamics*, Saint-Malo, 17-19 September 1996, this volume.

Winkler W., Egüez A., Seward D., Ford M., Heller F., Hungerbühler D. and Steinmann M. 1993. A short-lived compression related sediment fill in the intermountain basin of Nabón (Late Miocene, southern Ecuador). *Symposium International "Geodynamique Andine"*, Oxford, 21-23 September 1993, edited by ORSTOM, 321-324.

# LATEST CRETACEOUS TO PALEOGENE RED BEDS OF PERU, AND THE EARLY STAGES OF THE ANDEAN DEFORMATION.

Javier JACAY [(1)], Etienne JAILLARD [(2)] and René MAROCCO [(2)]

(1) Institut Français d'Études Andines, Contralmirante Montero, Casilla 18-1217, Lima 18, Peru.
(2) ORSTOM, TOA, UR 13, 209-213 rue La Fayette, 75480 Paris cedex 10, France.

KEY-WORDS : Late Cretaceous, Paleogene, continental deposits, eustatism, uplift, shortening.

## INTRODUCTION

The Peruvian Andes are considered an orogenesis related to the subduction of the Pacific oceanic plate beneath the continental margin of South America. During late Cretaceous and Paleogene times, the Peruvian margin can be divided into several palaeogeographic zones, trending parallel to the trench. These are, from West to East :

- The volcanic arc (Soler 1991) was active mainly during the Albian and was the site of repeated batholith intrusions during late Cretaceous times. This zone seems to have been deformed and partly or episodically emergent since the late Albian-Cenomanian.
- The Western Trough is mobile and subsident basin filled by a thick shallow-marine series (Benavides 1956, Mégard 1978). Compressional tectonics occurred since the Senonian and led to the progressive emergence of this zone, which became the late Cretaceous-Paleogene paleo-Andes.
- A positive threshold ("Marañon Geanticline") received a reduced sedimentation (Wilson 1963, Mégard 1978), and was deformed mainly during Paleogene and Neogene times.
- The Eastern Basin, with moderate subsidence, is characterized by a mixed, marine-continental sedimentation, and was deformed mainly during the Neogene.

The Red Beds of Central and Northern Peru were deposited on the eastern edge of the Western Trough. Their stratigraphy was established by Benavides (1956), Wilson (1963) and Mégard (1978). For the Paleogene succession, Noble et al. (1990), Naeser et al. (1991) and Jacay (1994) specified the stratigraphy and proposed tectonic interpretations.

## STRATIGRAPHY OF THE LATE CRETACEOUS-PALEOGENE SUCCESSION IN PERU.

In Central and Northern Peru, the late Cretaceous - Paleogene succession can be subdivided into three main sedimentary cycles (Jaillard 1994) : Coniacian - Campanian (Celendín Fm) ; Late Campanian - Paleocene (Casapalca and Fundo el Triunfo Fms) ; and latest Paleocene - Eocene (Chota and Rentema Fms, upper Mb of the Sacapalca Fm = El Carmen Conglomerate).

### Coniacian - Middle (?) Campanian

During early Senonian times, Central Peru was the site of deposition of marls and evaporite (Celendín Fm), the top of which has been dated as Coniacian (Romani 1982) or Santonian (Wilson 1963). Farther North, marine fossiliferous marls and limestones of the Celendín Fm were dated as Santonian in the Cajamarca area (Benavides 1956) and as middle Campanian in the Bagua syncline (Mourier et al. 1988). The end of the marine sedimentation in Peru is, therefore, diachronous from South to North. However, a major sedimentary hiatus occurred between the Santonian and Middle Campanian marine transgressions, which can be due to mild tectonic uplift or eustatic regression.

**Late Campanian - Paleocene**

This period is marked by predominantly fine- to medium-grained, continental red deposits of alluvial plain environment. Short-lived marine incursions are indicated by the occurrence of marine foraminiferas and brackish algae at the base of the Sacapalca Fm of Central Peru (Mabire 1961, Bizon et al. 1975, Jacay 1994), and by selachians and mesohaline ostracods at the base of the Fundo el Triunfo Fm of Northern Peru (Mourier et al. 1988). In the latter area (Bagua), selachians, dinosaur bones and charophytes indicate a Late Campanian-Maastrichtian age for the red beds (Mourier et al. 1988). In the Sacapalca Fm, Mégard (1978) quoted Maastrichtian charophytes (Jaillard et al. 1994).

**Late Paleocene - Eocene**

This period began with unconformable coarse-grained deposits. The El Carmen Conglomerate of Central Peru overlies the lower part of the Sacapalca Fm with local angular unconformity (Mégard written comm. 1996). It is interpreted as deposited on a proximal alluvian fan with local and/or episodic lakes, whereas the coarse-grained sandstones and microconglomerates of the Rentema Fm of Northern Peru were deposited by braided streams in a middle alluvial fan environment (Jacay 1994). In Northern Peru, tuffs associated with the Rentema Fm yielded 54.2 ± 6.4 Ma F/T ages (Naeser et al. 1991). Farther west, the unconformable volcanic Llama and conglomeratic Chota Fms were dated by K/Ar as 54.8 ± 1.8 and 49.5 ± 2 Ma, respectively (Noble et al. 1990). Thus, the age of the basal unconformity nay be considered as close to the Paleocene-Eocene boundary. In Central Peru, the El Carmen Conglomerate is unconformably overlain by the "Carlos Fransisco volcanics", which yielded late Middle Eocene K/Ar ages of 39 ± 1.9 Ma (Noble et al. 1979) and 39.8 Ma (Mégard, written comm. 1996). Vertebrates remains are currently under study.

## TECTONIC INTERPRETATIONS

In the Western Trough of Central and Northern Peru, the marine sedimentation ceased between Late Coniacian and Middle Campanian times (Celendín Fm) and gave way to continental red bed deposits of late Campanian - Maastrichtian age (Fundo el Triunfo and Casapalca Fms). The fine-grained clastic supply recorded from the Coniacian onwards and the progressive emergence of the Western Trough result from Senonian contractional deformations and crustal thickening of the westernmost areas of the margin (Peruvian phase; Steimann 1929, Jaillard 1994). However, the eustatic sea-level drop of Late Santonian-Early Campanian age (Haq et al. 1987) can account for a substantial part of the marine regression.

In the studied areas, the basal unconformity of the Chota and Rentema Fms, and El Carmen Conglomerate evidences an erosional hiatus of most of the Paleocene, which is also recorded on the western edge of the Eastern Basin of Southern Peru (Jaillard et al. 1993) and Ecuador (Faucher et al. 1971). This indicates that uplift and, therefore, shortening occurred in the former Western Trough during part of the Paleocene.

The deposition of unconformable coarse-grained conglomerates and sandstones of latest Paleocene and/or Early Eocene age can be ascribed to the compressional early Incaic phase of late Paleocene - Early Eocene age (Noble et al. 1990). Since these deposits are widespread in the Eastern Basin, the early Incaic phase affected the whole western areas.

## REFERENCES


Benavides, V. 1956, Cretaceous system in Northern Peru. *Am. Mus. Nat. Hist. Bull.*, New York, 108, 352-494.

Bizon, G., Bizon, J.-J., Fourcade, E. & Vachard, D. 1975, Nouvelle description d'*Archaias (perouvianella* nov. sub-gen.) *peruviana* (Steinmann) 1929, Foraminifère (Peneroplidae) du Sénonien du Pérou. *Bull. Soc. géol. Fr.*, (7) 17, 1157-1167.

Faucher, B., Vernet, R., Bizon, G., Bizon, J.J., Grekoff, N., Lys, M. & Sigal, J. 1971, *Sedimentary Formations in Ecuador. A stratigraphic and micropaleontological survey.* Bureau Études Indust. Coop. Inst. Franç. Pétrole (BEICIP), 220 p., 3 vol..

Haq, B.U., Hardenbol, J. & Vail, P.R. 1987, Chronology of fluctuating Sea levels since the Triassic. *Science*, 235, 1156-1167.

Jacay, J. 1994, *Evolution sédimentaire de la marge andine: le Crétacé supérieur des Andes du Pérou central et septentrional.* DEA thesis, Univ. Grenoble I, 97 p.

Jaillard, E. 1994, Kimmeridgian to Paleocene tectonic and geodynamic evolution of the Peruvian (and Ecuadorian) margin. *in:* J.A. Salfity, ed., *Cretaceous tectonics in the Andes*, 101-167, Earth Evolution Sciences, Fried. Vieweg & Sohn, Braunschweig/Wiesbaden.

Jaillard, E., Cappetta, H., Ellenberger, P., Feist, M., Grambast-Fessard, N., Lefranc, J. P. & Sigé, B. 1993, The Late Cretaceous Vilquechico Group of Southern Peru. Sedimentology, paleontology, biostratigraphy, correlations. *Cretaceous Res.*, 14, 623-661.

Jaillard, E., Grambast-Fessard, N., Feist, M. & Carlotto, V. 1994 Senonian-Paleocene charophyte succession of the Peruvian Andes, *Cretaceous Res.*, 15, 445-456.

Mabire, B., 1961, La "Serie de Capas Rojas" Cretáceo-Terciarias en los Andes centrales del Perú. *Bol. Soc. geol. Perú*, 36, 151-185.

Mégard, F. 1978, *Etude géologique des Andes du Pérou central.* Mém. ORSTOM, 86, 310 p., Paris.

Mourier, T., Bengtson, P., Bonhomme, M., Buge, E., Cappetta, H., Crochet, J.-Y., Feist, M., Hirsch, K., Jaillard, E., Laubacher, G., Lefranc, J.-P., Moullade, M., Noblet, C., Pons, D., Rey, J., Sigé, B., Tambareau, Y. & Taquet, P. 1988, The Upper Cretaceous-Lower Tertiary marine to continental transition in the Bagua basin, Northern Peru. *Newslett. Stratigr.*, 19, 143-177.

Naeser, C.W., Crochet, J.-Y., Jaillard, E., Laubacher, G., Mourier, T. & Sigé, B. 1991, Tertiary Fission-Track ages from the Bagua syncline (Northern Peru). Stratigraphic and tectonic implications. *J. South Amer. Earth Sci.*, 4, 61-71.

Noble, D.C., McKee, E.H. & Mégard, F. 1979, Early Tertiary "Incaic" tectonism, uplift and volcanic activity, Andes of Central Peru. *Geol. Soc. Am. Bull.*, 90, 903-907.

Noble, D.C., McKee, E.H., Mourier, T. & Mégard, F. 1990, Cenozoic stratigraphy, magmatic activity, compressive deformation, and uplift in Northern Peru. *Geol Soc. Am. Bull.*, 102, 1105-1113.

Romani, M. 1982, *Géologie de la région minière Uchucchacua-Hacienda Otuto, Pérou.* Thesis 3rd cycle, Univ. Grenoble, 176 p.

Soler, P. 1991, *Contribution à l'étude du magmatisme associé aux zones de subduction. Pétrographie, géochimie et géochimie isotopique des roches intrusives sur un transect des Andes du Pérou Central. Implications géodynamiques et métallogéniques.* Dr Thesis, Univ. Paris VI, 950 p.

Steinmann, G. 1929, *Geologie von Peru.* Karl Winter ed., Heidelberg, 448 p.

Wilson, J.J. 1963, Cretaceous stratigraphy of central Andes of Peru. *Am. Ass. Petrol. Geol. Bull.*, 47, 1-34.

# SEDIMENTARY MODEL FOR THE ORIENTE BASIN OF ECUADOR DURING THE CRETACEOUS.

Etienne JAILLARD (1)

(1) ORSTOM, TOA, UR 13, 209-213, rue La Fayette, 75480 Paris cedex 10, France.

KEY-WORDS : Cretaceous, palaeogeography, climate, depositional sequence, accomodation space.

During the Cretaceous, the Andean margin of Peru and Ecuador comprised arc and forearc zones, a subsident western trough, an axial threshold, and a shallow marine to continental eastern basin, often named the Oriente basin. Therefore, the latter represented the easternmost marine area of the active margin.

The mainly marine Albian-Maastrichtian succession of the Oriente Basin of Ecuador (Napo Gp, fig.) is marked by four conspicuous facies (Jaillard et al. 1995). The first one consists of massive transgressive, often glauconitic sandstones with erosional base. The second one is made of thin-bedded bioclastic limestones with erosional base, deposited in an open marine shallow shelf environment. The third one is constituted by unbioturbated laminated black shales deposited in a marine, very low-energy, disoxic to anoxic environment. The fourth facies is represented by massive laminated and unbioturbated limestones deposited on a very low energy, disoxic marine shelf. Other facies include open marine marls, marine sand sheets and prograding sandstones.

Such a facies succession express the alternation of open marine environments with moderate energy, and restricted low-energy depositional periods. This alternation can be explained through the dynamics of the marine Cretaceous sedimentation of the Oriente basin, controlled by palaeogeographic and climatic features, and by the creation rate of accomodation space.

## CHARACTERISTICS OF THE ORIENTE BASIN OF ECUADOR

**Palaeogeography**. The Oriente basin is located on the eastern side of the South American continent. It was therefore protected from the eastward blowing dominant winds and eastward migrating tropical storms (Whalen 1995). This situation was also responsible for the occurrence of upwellings currents that induced a high planctonic productivity zone and, therefore, an $O_2$ depleted layer in the water column (Arthur & Sageman 1995). This latter could invade the neighbouring shallow platform, namely the Andean basins, during important sea-level rises, provoking the deposit of anoxic beds (Wignall 1991). Finally, the upwelling of cold water contributed to the inhibition of sedimentary production, and thus favoured the preservation of the organic matter. Several types of topographic thresholds protected the Oriente Basins from the open marine influences. During at least Albian times, a locally emergent volcanic arc developed. During Senonian times, contractional movements produced the emergence of part of the present-day coastal areas. Finally, paleogeographic highs, such as the "Marañon geanticline" acted as efficient thresholds during most of the Cretaceous. These barriers limited significantly the oceanic influences. Most of the marine Cretaceous deposits of the basin are of shallow marine environment. Therefore, the basin was very shallow and its average slope was very low. This feature probably favoured the damping out by friction over the sea-bottom of the open marine factors such as swell, tides, storms and currents. In contrast, the very low gradient may have induced local high velocity tidal currents, since tide surges covered large horizontal distances, even with microtidal regime (Tucker & Wright 1990).

These characteristics altogether explain that the basin was generally protected from the oceanic energetic factors, and that most of the sediments were deposited in very low-energy conditions (Irwin 1965, Friedman & Sanders 1978).

**Climate**. "Middle" and early Late Cretaceous times were a period of greenhouse climate (Hallam

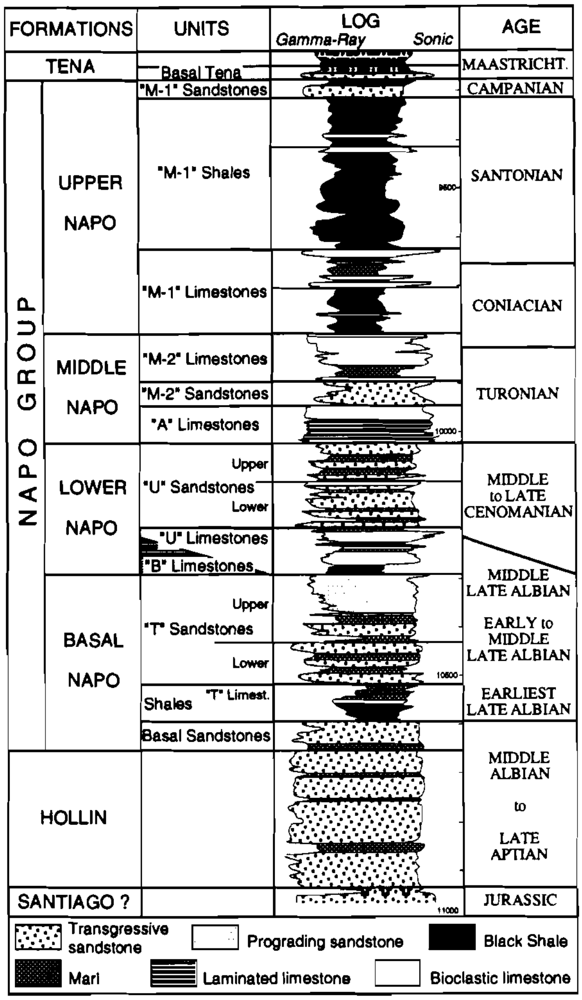


*Cretaceous series of the Oriente Basin of Ecuador.*

1985). At this time, the Oriente Basin of Ecuador located in the equatorial zone (Ross & Scotese 1988), was probably submitted to a wet and hot climate. The latter was responsible for the development of a dense vegetal cover on the continental areas that inhibited mechanical erosion, explaining partly the scarcity of coarse detrital particles in the Cretaceous sedimentation.

The hot temperatures induced the formation of a superficial layer of warm, low density water. Heavy rains fed large rivers that flowed into the basin, inducing the formation of a superficial wedge of hyposaline, low density water, reinforcing the density contrast due to the temperatures. Because the lack of significant energetical factors prevented the mixing of this superficial layer with the denser deep waters, the water column was then marked by a thermo-haline stratification that limited or even inhibited the circulation and oxygenation of the lower layer.

**Tectonics**. The Oriente Basin experienced a low tectonic subsidence rate during the Cretaceous, ranging from 4 to 10 m/Ma, according to the areas (Berrones 1994, Thomas et al. 1995).

Late Albian is a period of contractional deformation in Peru, which can explain the arrival of noticeable clastic amounts in the Oriente Basin («T» sandstones). Coniacian-Santonian times coincide with the beginning of the Peruvian compression that must have triggered the flexural subsidence of the Eastern basins. The high sedimentation rate observed in the Maastrichtian can be related to the renewal of flexural subsidence due to the Campanian tectonic event. The latter can account for the arrival of clastic sediments during Campanian and Maastrichtian times.

**Eustatism**. When subsidence is low as in the case of the Oriente basin of Ecuador, the accomodation space variations are nearly coeval with the sea-level changes (Jervey 1988). In the same way, if the sediment input is low, the sedimentary accumulation is low and the facies evolution roughly reflects the thickness of the water column (Jervey 1988).

The high-energy, open marine facies are restricted to the transgressive deposits. During eustatic trangressions, marine influences (swell, currents, tides) were able to enter into the basin, because of its flat topography, and of the low sedimentation rate that did not allow the rapid fill of the accomodation space. This gave way to the reworking and deposition of relatively high energy nearshore sands (Nummedal & Swift 1987), or to the sedimentation of shallow open marine limestones. Both types of deposits overly erosional surfaces formed during the previous emergence period and/or by nearshore wave activity.

## DEPOSITIONAL SEQUENCES OF THE CRETACEOUS MARINE SUCCESSION

Two end-member types of depositional sequences can be recognized in the Oriente Basin.

**Retrograding sandstone sequences** are characterized by an erosional base (SB+TS), an important clastic fraction generally represented by glauconitic sandstones, a clear transgressive vertical facies succession (TST), a shaly maximum flooding (MF), a reduced thickness (2-10 m) and the lack or reduction of prograding deposits (HST). They are interpreted as deposited during periods of low creation rate of accomodation space (Cenomanian, Late Santonian-Early Maastrichtian). Because of the lack of subsidence, only the major eustatic rises reached the basin. The lack of creation of accomodation space provoked the emergence of the basin early in the eustatic cycle, and prohibited the deposition of prograding HST. The

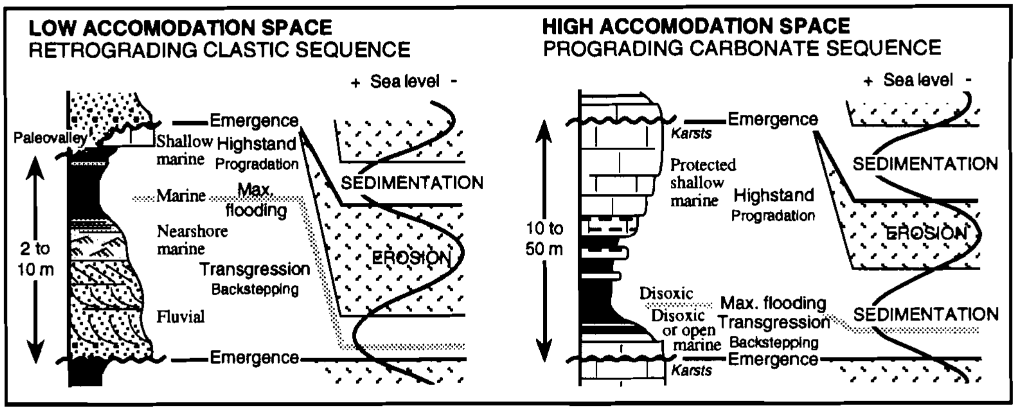


*Main types of depositional sequences in the Cretaceous marine series of the Oriente Basin.*

abundance of clastic material can be due to the long emergence periods that allowed the progradation of continental clastic systems, and to erosion and reworking of the marine or continental former deposits. Tectonic activity and subsequent rejuvenation of reliefs (Late Albian, Campanian) can also have increased the clastic supply, which inhibited the production of carbonate sediments. Good examples are represented by the "T" (lower part), "U", "M-2"?, "M-1" and Basal Tena sandstones.

**Prograding carbonate sequences** are relatively thick (10-50 m), predominantly carbonated sequences with erosional base (SB). The TST can be either thin and constituted by calcarenites and/or bioclastic marls, or thick and made up of laminated, anoxic carbonates, depending on the subsidence and sea-level rise rates. The MF is expressed by disoxic marls or shales, and the HST is represented by thick limestones made of stacked shallowing upward parasequences. They are interpreted as deposited during periods of relatively rapid creation of accomodation space (Late Albian, Turonian-Early Santonian). The high relative sea-level provoked the continentward shift of the shoreline, the retrogradation of the continental clastic systems and allowed the carbonate production. Substantial accomodation space allowed the deposition, before emergence, of HST much thicker than the TST. Relatively short emergence hiatuses allowed the preservation of the HST and minimized the production of detrital particles. Good examples of these sequences are the lower "T", "A" and "M-2" limestones. During major sea-level rises (Late Albian, Early Turonian), the $O_2$-depleted waters of the outer shelf overwhelmed the basin, provoking deposition of dysoxic to anoxic carbonated TST ("B", "A" limestones).

**Intermediate cases** are represented by two types of sequences. (1) Thick prograding clastic sequences formed during periods of high rate of creation os accomodation space, and of important clastic supply. Both parameters seem to have been controlled by tectonic events (Late Albian Mochica phase for the «T» sandstones, Senonian Peruvian phase for the Tena Fm). (2) Aggradational stacks of thin retrogradational carbonated parasequences («C», upper "T", "U" limest.) seem to correspond to periods of low rate of creation of accomodation space and relatively high average sea level. Due to the reduced accomodation space, the TST is well-expressed, but only the basal HST is preserved below the SB erosional surface. The relatively high sea level account for the scarcity of detrital material and the development of carbonates.

## PALAEOECOLOGY OF THE ORIENTE BASIN

Because of palaeogeographic and climatic features, the sedimentological behaviour of the Oriente epeiric basin of Ecuador was comparable to that of a closed shallow sea and shares some features with lakes. The Oriente Basin was protected from oceanic influences by paleogeographic and topographic features. Climatic factors were responsible for the density stratification of the water-column. Wind waves, local storms and the O2-rich river water were able to oxygenate only the superficial water layer. As a consequence, in stable conditions, the isolated cold, saline, dense deep waters could become rapidly anaerobic and promoted anoxic deposits.

Stratification of the water column can also account for the peculiar biota of distal parts of the Andean Basin. During sea-level rise, the thickness of the hyposaline superficial layer was probably minimum, due to the entry of marine energetic factors, and the reduction of continental areas and correlative decrease of fresh water sources ; the fauna was dominantly marine. During highstands, the upper water wedge developed, inducing the development of euryhaline, or mixed, hyposaline and marine faunas. During sea-level drops, the upper low-density water wedge thickened due to the decraese of marine influences, the enlargement of drainage areas and increase of fresh water sources; fresh water to brackish fauna was dominant. Finally, the beginning of lowstand periods could be marked by a lacustrine stage, due to the disappearance of the saline wedge and predominance of the fresh water input. To consider such peculiar conditions may contribute to solve recent controversies about the palaeoecology of some Andean basin fauna (e.g. Gayet et al. 1993, Rouchy et al. 1995).

## CONCLUSIONS

The low-energy character of the Cretaceous deposits of the Oriente Basin of Ecuador can be accounted for by mainly paleogeographic factors (western margin of a continent, topographic barriers, gradient of the basin). These, together with climatic factors due to the equatorial latitude (temperature, heavy rains, large rivers) induced an environment protected from the open marine influences and a thermohaline stratification of the water column, which favoured the deposition and preservation of organic matter.

The low subsidence rate and a low sediment supply recorded in the Oriente Basin influenced the nature of the depositional sequences. On one hand, a high (respectively low) rate of accomodation space creation controlled the deposition of mainly progradational (respectively retrogradational) sequences. On the other hand, a high (respectively low) relative sea level and/or a weak (respectively important) tectonic activity induced a low (respectively important) clastic supply, and the deposition of carbonate (respectively clastic) sequences.

## REFERENCES

Arthur, M.A. & Sageman, B.B. 1994. Marine Black Shales: depositional mechanisms and environments of ancient deposits. *Ann. Rev. Earth Planet. Sci.* 1994, 22, 499-551.

Berrones, G. 1992. Estudio de la subsidencia de la Cuenca oriental ecuatoriana entre el Jurásico superior y el Reciente. *Simp. Nac.: Investigación y desarrollo tecnológico en el área de hidrocarburos*, Conuep-Petroproducción, eds., tomo 2, 937-968, Quito.

Friedman, G.M. & Sanders, J.E. 1978. *Principles of sedimentology*. J. Wiley & Sons, New York, 792 p.

Gayet, M., Sempéré, T., Cappetta, H., Jaillard, E. & Levy, A. 1993. Conséquences paléogéographiques de la présence d'une faune marine variée dans le Maastrichtien des Andes de Bolivie, du Sud péruvien et du Nord-Ouest de l'Argentine. *Palaeogeog., Palaeoclim., Palaeoecol.*, 102, 283-319.

Hallam A. 1985. A review of Mesozoic climates. *J. geol. Soc. London*, 142, 433-445.

Irwin, M.L. 1965. General theory of epeiric clear water sedimentation. *A.A.P.G. Bull.*, 49, 445-459.

Jaillard, E. et al. 1995. *Síntesis estratigráfica y sedimentológica del Cretáceo y Paleógeno de la cuenca oriental del Ecuador*. Orstom-Petroproducción techn. agreem., unpubl. report, 2 vol., Quito.

Jervey, M.T. 1988. Quantitative geological modelling of siliciclastic rock sequences and their seismic expression. *Soc. Econ. Paleont. Miner. Spec. Publ.*, 42, 47-69.

Mello, M.R., Koutsoukos, E.A. & Erazo, W.Z. 1993. The Napo Formation, Oriente basin, Ecuador: hydrocarbon source potential and paleoenvironmental assessment. *A.A.P.G. Mem.*, 56, 167-181.

Swift, D.J.P. & Thorne, J.A. 1991, Sedimentation on continental margins, I : A general model for shelf sedimentation. *Int. Ass. Sed. Spec. Publ.*, 14, 3-31.

Ross, M.I. & Scotese, C.R., 1988. A hierarchical tectonic model of the Gulf of Mexico and Caribbean region. *Tectonophysics*, 155, 139-169.

Rouchy, J.-M., Camoin, G., Casanova, J. & Deconinck, J.-F. 1993. The central paleo-Andean basin of Bolivia (Potosi area) during late Cretaceous and early Tertiary : reconstruction of ancient saline lakes using sedimentological, paleoecological and stable isotope records. *Palaeogeogr., Palaeoclim., Palaeoecol.*, 105, 179-198.

Thomas, G., Lavenu, A. & Berrones, G. 1995. Evolution de la subsidence dans le Nord du bassin de l'Oriente équatorien (Crétacé supérieur à Actuel). *C. R. Acad. Sci., Paris*, 320, IIa, 617-624.

Tucker, M.E. & Wright, V.P. 1990. *Carbonate Sedimentology*. Blackwell Scient. Publ., Oxford, 482 p.

Whalen, M.T. 1995. Barred basins: a model for eastern ocean basin carbonate platforms. *Geology*, 23, 7, 625-628.

Wignall, P.B. 1991. Model for transgressive black shales ?. *Geology*, 19, 167-170.

# STRATIGRAPHY OF THE WESTERN «CELICA BASIN» (SW ECUADOR).

Etienne JAILLARD(1), Peter BENGTSON(2), Luc BULOT(3),
Annie DHONT(4), Gérard LAUBACHER(1) and Emmanuel ROBERT(5).

(1) ORSTOM, TOA, UR 13, 209-213 rue La Fayette, 75480 Paris cedex 10, France.
(2) Geol.-Paläont. Institut, Univ. Heidelberg, Im Neuenheimer Feld 234, D-69120 Heidelberg, Germany.
(3) Institut Dolomieu, 15 rue Maurice-Gignoux, 38031 Grenoble Cedex, France.
(4) Institut Royal des Sciences Naturelles de Belgique, 29 rue Vautier, B-1040 Bruxelles, Belgium.
(5) Labo. Géol. Sédim. Paléont., Univ. P. Sabatier, 39 allée Jules-Guesde, 31062 Toulouse cedex, France.

KEY-WORDS : Late Cretaceous, Paleocene, forearc zone, turbidites, unconformity, Peruvian phase.

## INTRODUCTION

The Celica basin is a turbiditic trough of Late Cretaceous age located in southwesternmost Ecuador and northwesternmost Peru, where it is named Lancones Basin. The sediments rest on the Paleozoic Amotape-Tahuin Massif (A-T Massif) to the West, and on the Celica volcanic arc to the East (fig.). Hence, the sediments of the basin are mainly siliciclastic toward the West and volcaniclastic toward the East.

In Ecuador, the cover of the A-T Massif has been defined as a single formation of Cretaceous age (Puyango Gp or Cazaderos Fm, Kennerley 1973, Bristow & Hoffstetter 1977) that would grade laterally into the eastern series. In Peru, stratigraphic and sedimentological studies of the A-T Massif cover (Copa Sombrero Gp) resulted in the definition of several stratigraphic units (e.g. Iddings & Olsson 1928, Olsson 1934, Fisher 1956, Morris & Alemán 1975, Reyes & Caldas 1987).

Stratigraphic data on the Eastern series of the Celica Basin have been published previously (Jaillard et al. 1996). This paper presents new stratigraphic results obtained from the western part of the Celica Basin of southwestern Ecuador, i.e. the Cretaceous sedimentary cover of the A-T Massif.

## STRATIGRAPHY

**Basal Conglomerates**. In Ecuador, greywackes and shales bearing silicified woods unconformably overly the A-T Massif basement. Then, conglomeratic quartzites with silicified tree-trunks are overlain by shales and fine-grained sandstones with thin intercalations of limestone and tuff. From poorly specified layers, Shoemaker (1982) determined Auracariaceae of Early Cretaceous age (fig.). Tuffs yielded reset K/Ar ages of 75±9 and 64±6 Ma (Shoemaker 1982). In Peru, similar quartzose conglomerates that unconformably rest on the Paleozoic A-T Massif are ascribed to the Albian (Gigantal conglomerate, Reyes & Vergara 1987).

**Lower limestones.** Overlying the siliciclastic rocks are grey to black, laminated bituminous marls and limestones. In Ecuador, unprecised beds yielded *?Hypacanthoplites* sp., *Parahoplites* sp., *Brancoceras aegoceratoides, Desmoceras latidorsatum, Hysteroceras orbignyi, Oxytropidoceras (?Laraiceras)* sp. and *Ox. (Venezoliceras) commune* of early to early late Albian age (Bristow & Hoffstetter 1977). In Puyango, we collected bivalves (*Ceratostreon* sp. *Cucullaea* sp., heterodonts), and the ammonite *Epicheloniceras s.l.* sp. of late Aptian to earliest Albian age (fig.). In Peru, comparable limestones are dated as Albian by foraminiferas, inoceramids and ammonites (Pananga and Muerto Fms, Iddings & Olsson 1928, Chalco 1955, Zuñiga & Cruzado 1979, Reyes & Caldas 1987). In both countries, the limestones are overlain by a thick clastic series made up of dark shales interbedded with sandstones and greywackes deposited by turbidity currents (Copa Sombrero Gp of Peru, Morris & Alemán 1975, Reyes & Caldas 1987).

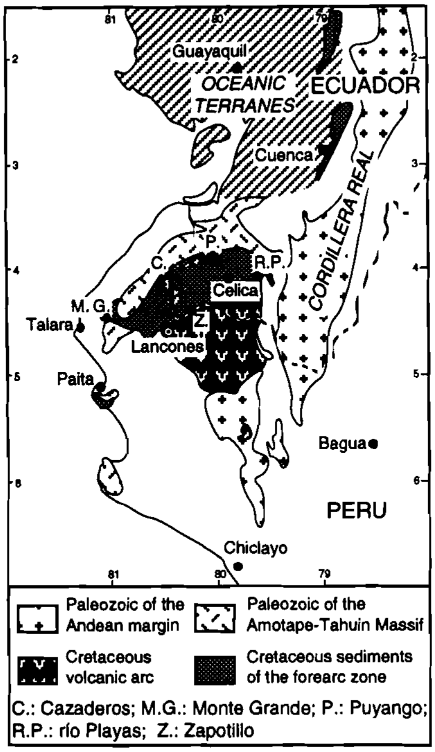


*Location of the studied area.*

**Copa Sombrero Group.** In Ecuador, a calcareous nodule or a block from the base of the succession yielded the ammonite *Brancoceras* sp. of early middle Albian age (fig.). Higher in the succession, in shales and greywacke turbidites, we found post-Albian ammonites, which are currently studied. In Peru, the lower part of the succession consists of black shales and calcareous siltstones, with sandstone and pyroclastite intercalations, interpreted as basin plain to slope deposits (Huasimal Fm, Reyes & Caldas 1987, Reyes & Vergara 1987, Morris & Alemán 1975, Chávez & Nuñez del Prado 1991). It yielded ammonites of middle to late Albian (Fisher 1956), and early Cenomanian age (Olsson 1934).

In Ecuador, the upper part of the turbidite succession includes two thick, unfossiliferous quartzose conglomerate layers correlated with the Jahuay Negro and Tablones formations of Peru, respectively. It contains numerous unidentifiable inoceramids. The upper part of the Copa Sombrero Group of Peru contains also two conglomeratic layers interpreted as upper to middle fan deposits (Chávez & Nuñez del Prado 1991). The lower one (Jahuay Negro Fm) contains scarce Cenomanian ammonites and Cenomanian-Turonian inoceramids (Reyes & Vergara 1987, Reyes & Caldas 1987). The upper conglomerate has been correlated either with the «middle Conglomerates» of Olsson (1934) (Chalco 1955), or with the Tablones Formation ascribed to the Campanian (Reyes & Caldas 1987). They are separated by a shaly unit with thin interbeds of arkosic sandstones bearing scarce inoceramids (Encuentros Fm, Morris & Alemán 1975, Reyes & Caldas 1987, Chávez & Nuñez del Prado 1991). From the Copa Sombrero Group, cf.*Barroisiceras haberfellneri* of early Coniacian age (Petersen 1949) and Senonian microfauna (Weiss 1955) were reported.

**Unconformable limestones and marls.** In Ecuador, in the northern part of the studied area (Puyango), thick-bedded, sandy coarse-grained limestones with large bivalves unconformably rest on the Albian black laminated limestones or on the overlying turbidites. A loose ammonite of unknown origin found on these outcrops is a *Vascoceras* ex gr. *cauvini* Chudeau, 1909 of latest Cenomanian age. These limestones grade upwards into yellow marls interbedded with light-coloured, skeletal and oolithic limestones. A whorl fragment of Texanitinae ? gen. sp. indet. found in these marls suggests a late Santonian to Campanian age (fig.). These carbonated units are only locally present. The Campanian foraminiferal assemblage mentioned by Sigal (1968, Bristow & Hoffstetter 1977) may proceed from these beds.

In the Lancones Basin of Peru, Morris and Alemán (1975) consider the Campanian Tablones Formation to be an unconformable shallow-water deposit, that postdates the emergence and deformation of the Copa Sombrero Group. In the Talara Basin, transgressive sandstones and conglomerates of Campanian age rest unconformably on Paleozoic rocks or on the Albian limestones (Redondo Fm, Weiss 1955, González 1976). Farther south, in the Paita area, shales, calcareous sandstones, massive limestones and subordinate conglomerates of probable Campanian age, rest unconformably on Paleozoic rocks (La Mesa Fm, Olsson 1944). These units express a regional transgression in open shallow marine shelf to nearshore environments (Olsson 1934, 1944, Morris & Alemán 1975, and obs. pers.).

**Overlying deposits.** In Ecuador, the uppermost unit of the Celica Basin consists of black shales with calcareous nodules and thin-bedded sandstone turbidites. Toward the West (Cazaderos), we found the inoceramid *Platyceramus* sp. of Senonian age and poorly preserved ammonites among which *Acanthoscaphites* sp., Pachydiscidae indet. and two specimens of *Diplomoceras* sp. indicate a late Campanian to Maastrichtian age (fig.). Farther southeast (Zapotillo), thick black siliceous shales are characterized by numerous *Platyceramus* sp. and may be coeval with the late Campanian-Maastrichtian deposits.

In the Lancones Basin of Peru, the upper shaly unit (Pazul Fm) is considered as Coniacian (Fisher 1956), Campanian (Morris & Alemán 1975), or Maastrichtian to Paleocene in age (Reyes & Caldas 1987), according to the authors. It is regarded as a lower fan or basin plain deposit (Chávez & Nuñez del Prado 1991).

On the A-T Massif of the Talara area, black shales (Clavulina shales, Olsson 1934) rest on the Copa Sombrero Group, and are overlain by coarse-grained quartzose conglomerates (Monte Grande Fm, Iddings &

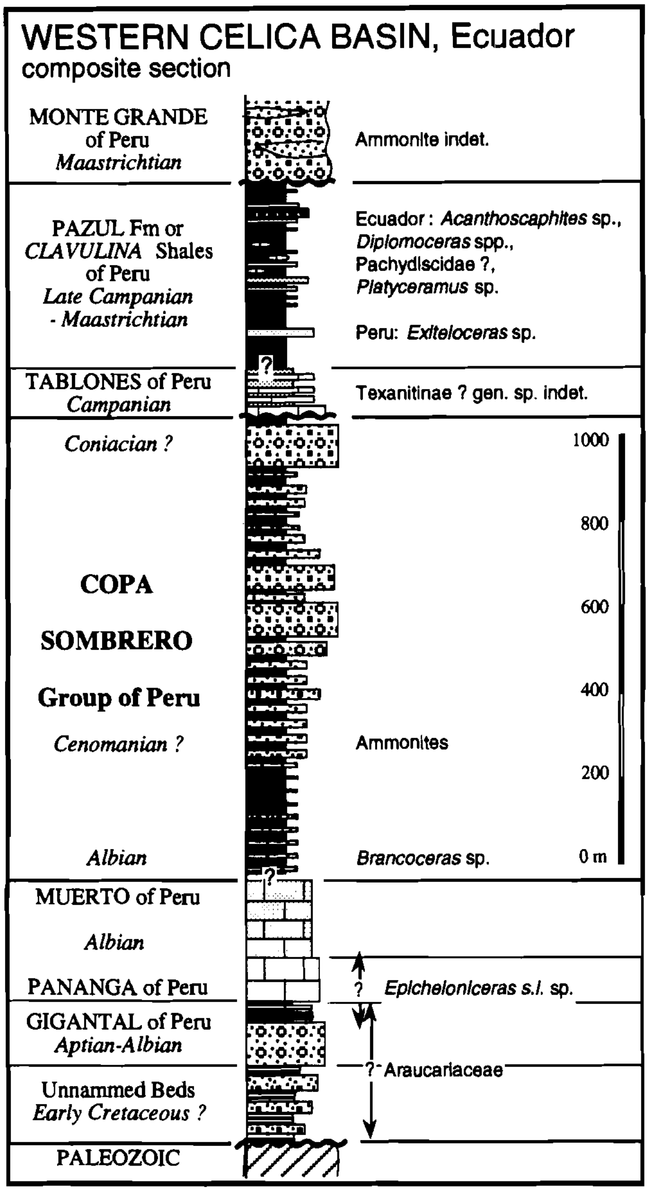


Olsson 1928, Olsson 1934). In these black shales, we found *Exiteloceras* sp. of late Campanian to Maastrichtian age, whereas the overlying conglomerates only yielded an unidentifiable ammonite (fig.). In the Talara Basin, the Maastrichtian and Paleocene stages are represented by marine black shales (González 1976). Near Paita (NW Peru), the transgressive deposits are overlain by coarse-grained conglomerates of Maastrichtian age that mainly contain clasts of metamorphic rocks (La Tortuga Fm, Olsson 1944). In Río Playas (SW Ecuador), coeval conglomerates contain clasts of mainly volcanic origin (Casanga Fm, Jaillard et al. 1996). In Bagua (fig.) red beds of coastal and alluvial plain environment are dated as Maastrichtian (Mourier et al. 1988, Naeser et al. 1991).

## EVOLUTION OF THE WESTERN CELICA BASIN.

During the early and middle Albian, the A-T Massif was a stable area of the Andean forearc zone.

The Celica Basin was created during the late middle to early late Albian. Its formation was associated with a strong synsedimentary tectonic instability expressed by slumps, olistolites, clastic dykes, and turbidite flows (Morris & Alemán 1975, Reyes & Caldas 1987, Chávez & Nuñez del Prado 1991). This event can be related to the Mochica tectonic phase of Peru, marked by an alternation of contractional and extensional deformations (Mégard 1984), probably due to a dextral shear regime (Soler 1991, Jaillard 1994).

The conglomerate intercalations (Cenomanian-Turonian?) indicate that the tectonic activity was going on, and that the A-T Massif was submitted to intense erosion. Some times after the Turonian or Coniacian, the Celica Basin was deformed and became emergent. This tectonic event is coeval with part of the Peruvian contractional phases of Coniacian to Campanian age (Steimann 1929, Jaillard 1994).

The unconformable limestones postdate the deformation and emergence of the Celica Basin. These deposits indicate an important shallow marine transgression, which we propose to correlate with the Campanian transgressive beds recognized on the eastern side of the Celica Basin of Ecuador (part of El Naranjo Fm of Río Playas, Jaillard et al. 1996), in the Talara Basin (Weiss 1955, González 1976) and the Paita area of northwestern Peru (Olsson 1944) and in the Bagua syncline of northern Peru (Mourier et al. 1988, Naeser et al. 1991). They express the creation of a wide forearc basin of late Campanian-Maastrichtian, possibly Paleocene age. Although field evidences are still lacking, it appears that this basin extended NNE-ward throughout Ecuador, where black shales and turbidites (Yunguilla Fm) yielded the ammonites *Sphenodiscus peruvianus*, *Solenoceras* sp. and microfaunas of Maastrichtian age (Faucher & Savoyat 1973, Bristow & Hoffstetter 1977). The Yunguilla «Flysch» is presently tectonically pinched between accreted terranes and the continental Andean margin (fig.).

In northwestern Peru and southwestern Ecuador, the coarse-grained conglomerates of Maastrichtian age express an important tectonic event of late Campanian-early Maastrichtian age (?) that rejuvenated volcanic (Ecuador) or metamorphic reliefs (Peru) and contributed to the emergence of the Bagua area.

## REFERENCES


Bristow, C.R., & Hoffstetter, R. 1977. *Ecuador.* Lexique Stratigr. Internat., V, 5a2, 410 p., CNRS ed., Paris.

Chalco, R. A. 1955. Estudio geológico preliminar de la región Sullana-Lancones. *Bol. Técn. Empr. Petrol.*, fasc. 3, Minist. Fom. Publ., Lima.

Chávez, A. & Nuñez del Prado, H. 1991. Evolución vertical de facies de la serie turbidítica cretácea (Grupo Copa Sombrero) en el perfil-tipo Huasimal-Encuentros (Cuenca Lancones en el Noroeste del Perú). *Bol. Soc. geol. Perú*, 82, 5-21.

Faucher, B. & Savoyat, E. 1973. Esquisse géologique des Andes de l'Equateur. *Rev. géog. phys. géol. dyn.*, (2), 15, 115-142.

Fisher, A.G. 1956. Desarollo geológico del Noroeste peruano durante el Mesozóico. *Bol. Soc. geol. Perú*, 30, 177-190.

Iddings, A. & Olsson, A.A. 1928. Geology of Northwest Peru. Bull. *Am. Ass. Petrol. Geol.*, 12, 1-39.

Jaillard, E. 1994. Kimmeridgian to Paleocene tectonic and geodynamic evolution of the Peruvian (and Ecuadorian) margin. *in*: J.A. Salfity, ed., *Cretaceous tectonics in the Andes*, 101-167, Earth Evolution Sciences, Fried. Vieweg & Sohn, Braunschweig/Wiesbaden.

Jaillard, E., Ordoñez, M., Berrones, G., Bengtson, P., Bonhomme, M., Jiménez, N. & Zambrano, I. 1996. Sedimentary and tectonic evolution of the arc zone of Southwestern Ecuador during Late Cretaceous and Early Tertiary times. *J. South Am. Earth Sci.*, in press.

Kennerley, J.B. 1973. Geology of the Loja Province, Southern Ecuador. *London Inst. Geol. Sci.*, Rep. 23, 34 p.

Morris, R.C. & Alemán, A.R. 1975. Sedimentation and tectonics of middle Cretaceous Copa Sombrero formation in Northwest Peru. *Bol. Soc. geol. Perú*, 48, 49-64.

Mourier, T., Bengtson, P., Bonhomme, M., Buge, E., Cappetta, H., Crochet, J.-Y., Feist, M., Hirsch, K., Jaillard, E., Laubacher, G., Lefranc, J.-P., Moullade, M., Noblet, C., Pons, D., Rey, J., Sigé, B., Tambareau, Y. & Taquet, P. 1988. The Upper Cretaceous-Lower Tertiary marine to continental transition in the Bagua basin, Northern Peru. *Newslett. Stratigr.*, 19, 143-177.

Naeser, C.W., Crochet, J.-Y., Jaillard, E., Laubacher, G., Mourier, T. & Sigé, B. 1991. Tertiary Fission-Track ages from the Bagua syncline (Northern Peru). Stratigraphic and tectonic implications. *J. South Am. Earth Sci.*, 4, 61-71.

Olsson, A.A. 1934. Contributions to the Paleontology of Northern Peru. The Cretaceous of the Amotape region. *Bull. Am. Paleont.*, 20, 104 p..

Olsson, A.A. 1944. Contributions to the Paleontology of Northern Peru. Part VII: The Cretaceous of the Paita region. *Bull. Am. Paleont.*, 28, 113 p..

Petersen, G. 1949. Condiciones geográficas y geológicas de la Cuenca del río Zarumilla. *Soc. Geol. Perú, Vol. Jubilar*, fasc. 7, 1-40, Lima.

Reyes, L. & Caldas, J. 1987. Geología de los cuadrángulos de Las Playas, La Tina, Las Lomas, Ayabaca, San Antonio, Chulucanas, Morropon, Huancabamba, Olmos y Pomahuaca. *Bol. Inst. Geol. Min. Metal.*, (A), 39, 83 p., Lima.

Reyes, L. & Vergara, J. 1987. *Evaluación geológica y potencial petrolífero de la Cuenca Lancones.* Petroperú, unpubl. rep., 57 pp., Lima.

Shoemaker, R.E. 1982. Fossil leaves from the Lower Cretaceous Ciano Formation, Southwestern Ecuador. *Palaeontographica Abt. A*, 180, 120-132.

Sigal J. 1968. *Estratigrafía micropaleontológica del Ecuador, datos anteriores y nuevos.* Inst. Francés Petróleo, Serv. Nac. Geol. Min., internal report, Quito.

Soler, P. 1991. *Contribution à l'étude du magmatisme associé aux zones de subduction. Pétrographie, géochimie et géochimie isotopique des roches intrusives sur un transect des Andes du Pérou Central. Implications géodynamiques et métallogéniques.* Dr Thesis, Univ. Paris VI, 950 p.

Steinmann, G. 1929. *Geologie von Peru.* Karl Winter ed., Heidelberg, 448 p.

Weiss, L. 1955. Planktonic index foraminifera of northwestern Perú. *Micropaleontology*, 1, 301-319.

Zuñiga, F. & Cruzado, C. 1979. Bioestratigrafía del Noroeste Peruano. *Bol. Soc. geol. Perú*, 60, 219-232.

# ALONG-STRIKE SEGMENTATION OF THE ANDEAN FORELAND

Jonas KLEY[(1)], César R. MONALDI[(2)] and José A. SALFITY[(2)]

[(1)] Geologisches Institut, Universität Karlsruhe, P.O. Box 6980, D-76128 Karlsruhe, Germany
[(2)] Universidad Nacional de Salta-CONICET, Buenos Aires 177, 4400 Salta, Argentina

**KEY WORDS:** Foreland deformation, thin-skinned thrust belts, thick-skinned thrust belts, basement thrusts

## INTRODUCTION

Along most of its 8000 km length, the eastern flank of the Andean orogen is underlain by thrust belts of Tertiary (mostly Neogene) age. Structural styles, however, vary greatly along strike. It has been shown that the segmentation of Andean foreland deformation coincides both with the segmented geometry of the downgoing slab and with stratigraphic and structural inhomogeneities of the upper plate (northern Argentina; Allmendinger et al., 1983; Jordan et al., 1983). Here, we describe the varying styles of foreland deformation along the entire orogen and discuss the relative importance of the different controlling factors proposed.

## TYPES OF FORELAND DEFORMATION

Three principal types of foreland deformation can be distinguished: (1) Thin-skinned fold-and-thrust belts with a basal décollement within the sedimentary cover (Fig. 1a). Shortening of the cover in the foreland belt is balanced by extensive overthrusts of basement sheets in the internal zones of the thrust belt. (2) Thick-skinned thrust belts with a décollement at mid-crustal depths. Some of these belts occur at the orogenic front in a position similar to thin-skinned belts (Fig. 1b), but others lie at a large distance from the orogen. (3) Laramide or Pampeanas-type basement thrusts which possibly affect the entire crust (Fig. 1c). The widely spaced thrusts usually occur in irregular, anastomosing patterns.

None of these structural styles are mutually exclusive, and the transitions between them are sometimes gradual (Fig. 2). Areas of thin-skinned thrusting may later become affected by thick-skinned thrusting as a result of the piggy-back propagation of basement-cover thrusts (e.g. Cordillera Oriental of Colombia; Interandean Zone of southern Bolivia; Fig. 1a). The structural style can also switch from thin-skinned to thick-skinned and vice versa in both space and time as deformation propagates cratonward. Deep-seated basement thrusts are the exclusive style of deformation in eastern Colombia and western Venezuela (Sierra Nevada de Santa Marta, Sierra de Perijá, Mérida Andes). In northwestern Argentina, however, the basement thrusts of the Sierras Pampeanas are coeval with thin-skinned thrusting in the Precordillera. Foreland basement thrusts may also pass laterally into basement nappes of the internal belt (Shira uplift and Cordillera Oriental in southern Peru).

## FACTORS CONTROLLING STYLE VARIATIONS

Many regional studies suggest that stratigraphy and the pre-Neogene tectonic history of individual areas exert an important control on the development of distinct structural styles. Thin-skinned Fold-and-thrust belts depend on the existence of a more or less undisturbed sedimentary cover at least some 2-3 km thick, and in some cases on a particularly weak basal layer. Many, if not all, basement-involved thrust belts result from the inversion of Mesozoic rift basins (e.g.Colletta et al., 1990; Grier et al., 1991; Salfity et al., 1993; Uliana et al., 1995). The conditions for the development of Pampeanas-type

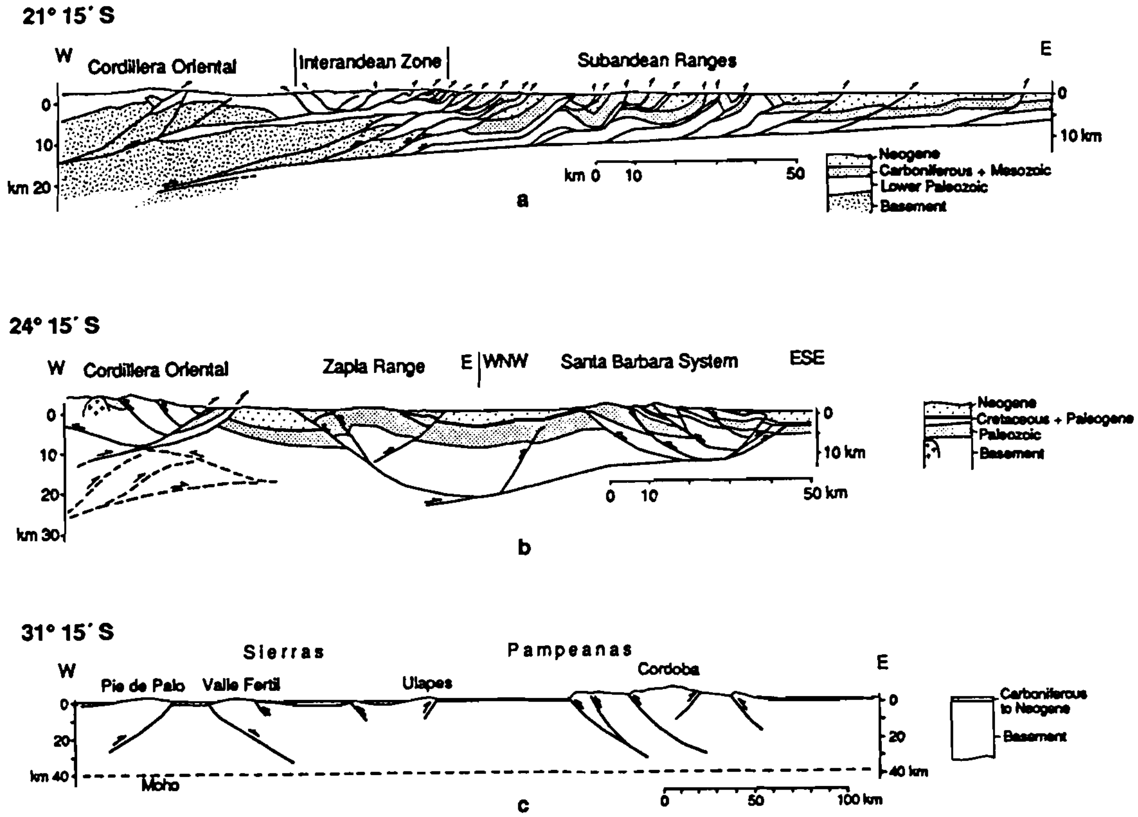


**Fig. 1:** Examples for the different styles of foreland deformation. Cross-sections are located in Fig. 2.
a) The Subandean Ranges in southern Bolivia, a well-developed thin-skinned thrust belt (structure from Baby et al., 1992, and Dunn et al., 1995, slightly modified). The Interandean Zone is a thin-skinned belt carried piggy-back on younger basement thrusts.
b) Zapla Range and Santa Barbara System of northern Argentina, a thick-skinned thrust belt developed from a Cretaceous rift. Depth to detachment is estimated from cross-section balancing. Deep structure of Cordillera Oriental is hypothetical.
c) The Sierras Pampeanas, Argentina. Names refer to individual ranges. Depth of faulting under Sierra Pie de Palo and Sierra del Valle Fértil from earthquake hypocenters (Jordan & Allmendinger, 1986).

basement thrusts are probably least understood. The boundary of the Sierras Pampeanas with the thick-skinned thrust belt of the Santa Barbara system is transitional. Reactivation of earlier normal faults does play a role in the development of some of the Sierras Pampeanas (Schmidt et al., 1995), but apparently not in all of them.

The correlation of subducted slab geometry and structural style is strongest in the foreland from 20° to 33° S (southern Bolivia and northern Argentina). It is less evident on an orogen-wide scale, where a well-developed thin-skinned belt occurs over a flat slab (Santiago and Huallaga belts of northern and central Peru) and deep-seated basement thrusts occur over a slab which dips at 25-30° at present (eastern Colombia and western Venezuela; Laubscher, 1987; Malavé and Suárez, 1995). If the coincidence of segmentation in the lower plate with an older segmentation of the upper plate in northern Argentina is not merely by chance, then we are forced to conclude that in some way the properties of the upper plate have influenced the development of the flat slab segment between 27° and 33° S. Isacks (1988) pointed out that a stiff upper plate will tend to flatten the slab dip if plate convergence is rapid. North of 22° S, thick Silurian shales unaffected by Cretaceous extension permitted the development of a wide thin-skinned fold-and-thrust belt, with internal basement thrust sheets advancing far over the craton. Farther south,

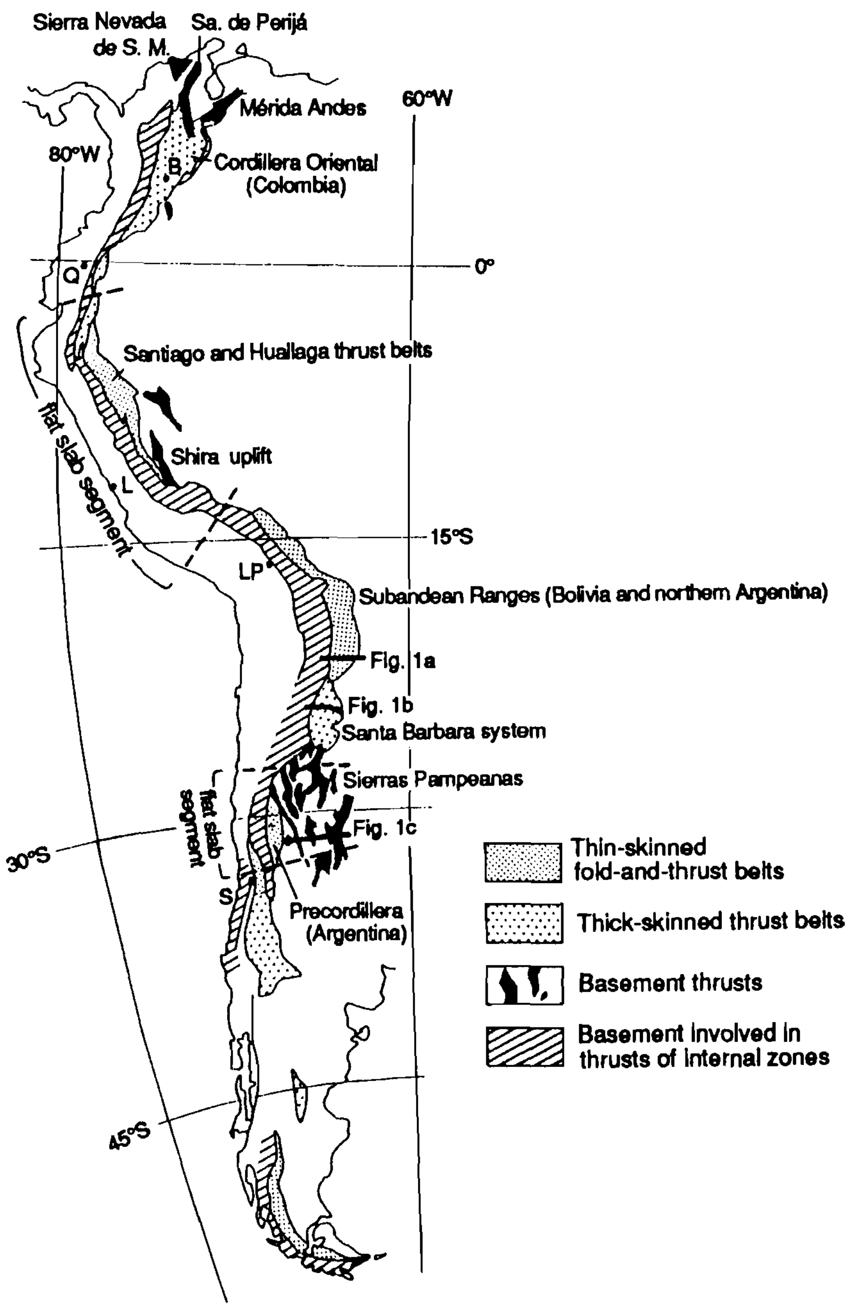


**Fig. 2:** The distribution of different styles of foreland deformation along the Andes. The extent of flat subducting segments of the Nazca plate is also shown. Only the structural units mentioned in the text are labeled.

where the Andean front impinges on the Cretaceous rift, a thick-skinned foreland belt developed, which eventually grades into the basement thrusts of the Sierras Pampeanas. These changes in structural style reflect an increasingly rigid upper plate, with shortening decreasing southward. The difference in shortening is not sufficient to explain the full downdip extent of the flat slab, but it might represent the trigger for its development.

## CONCLUSIONS

Different styles of Andean foreland deformation are characterised by the way basement is involved in thrusting: Basement thrusts with large displacements are typical for the internal zones bordering thin-skinned belts. In thick-skinned thrust belts and provinces of Pampeanas-type basement thrusts, the displacement on individual thrusts usually does not exceed a few kilometers. Apparently, it is the development of a basal décollement in the overlying sedimentary cover that allows large slip to accumulate on a single basement thrust. The frequent link of thick-skinned belts with former rift areas might thus be explained by two factors: First, potential décollement levels can be offset by normal faults, and second, reactivation of earlier normal faults may be easier than the evolution of a new décollement. Outside the rift areas, the lack of a thick sedimentary cover may prompt basement-involved thrusting which possibly affects the entire crust.

## REFERENCES


Allmendinger, R.W., Ramos, V.A., Jordan, T.E., Palma, M., and Isacks, B.L., 1983, Paleogeography and Andean Structural Geometry, Northwest Argentina: Tectonics, 2, 1-16.

Baby, P., Herail, G., Salinas, R., and Sempere, T., 1992, Geometry and kinematic evolution of passive roof duplexes deduced from cross section balancing: example from the foreland thrust system of the southern Bolivian Subandean zone: Tectonics, 11, 523-536.

Colletta, B., Hebrard, F., Letouzey, J., Werner, P., and Rudkiewicz, J.L., 1990, Tectonic style and crustal structure of the Eastern Cordillera (Colombia) from a balanced cross-section, in: Letouzey, J., ed., Petroleum and Tectonics in mobile belts: Editions Technip, 81-100, Paris.

Dunn, J.F., Hartshorn, K.G., and Hartshorn, P.W., 1995, Structural Styles and Hydrocarbon Potential of the Subandean Belt of Southern Bolivia, in: Tankard, A.J., Suárez Soruco, R. and Welsink, H.J., eds., Petroleum Basins of South America, AAPG Memoir 62, 523-544.

Grier, M.E., Salfity, J.A., and Allmendinger, R.W., 1991, Andean reactivation of the Cretaceous Salta rift, northwestern Argentina.: Journal of South American Earth Sciences, 4, 351-372.

Isacks, B.L., 1988, Uplift of the Central Andean Plateau and Bending of the Bolivian Orocline: Journal of Geophysical Research, 93, 3211-3231.

Jordan, T., Isacks, B., Allmendinger, R.W., Brewer, J.A., Ramos, V.A., and Ando, C.J., 1983, Andean tectonics related to geometry of subducted Nazca plate: Geological Society of America Bulletin, 94, 341-361.

Jordan, T.E., and Allmendinger, R.W., 1986, The Sierras Pampeanas of Argentina: A modern analogue of Rocky Mountain foreland deformation: American Journal of Science, 286, 737-764.

Laubscher, H.P., 1987, The kinematic puzzle of the Neogene Northern Andes, in: Schaer, J.-P., and Rodgers, J., eds., The Anatomy of Mountain Ranges, Princeton, New Jersey, Princeton University Press, 211-227.

Malavé, G., and Suárez, G., 1995, Intermediate-depth seismicity in northern Colombia and western Venezuela and its relationship to Carribean plate subduction: Tectonics, 14, 617-628.

Salfity, J.A., Monaldi, C.R., Marquillas, R.A., and Gonzáles, R.E., 1993, La inversión tectónica del Umbral de los Gallos en la cuenca del grupo Salta durante la Fase Incáica, XII. Congreso Geologico Argentino y II. Congreso de Exploración de Hidrocarburos, Tomo III: Mendoza, Argentina, 200-210.

Schmidt, C.J., Astini, R.A., Costa, C.H., Gardini, C.E., and Kraemer, P.E., 1995, Cretaceous Rifting, Alluvial Fan Sedimentation, and Neogene Inversion, Southern Sierras Pampeanas, Argentina. in: Tankard, A.J., Suárez Soruco, R. and Welsink, H.J., eds., Petroleum Basins of South America, AAPG Memoir, 62, 341-358.

Uliana, M.A., Arteaga, M.E., Legarreta, L., Cerdán, J.J., and Peroni, G.O., 1995, Inversion structures and hydrocarbon occurrence in Argentina, in: Buchanan, J.G., and Buchanan, P.G., eds., Basin Inversion, Geological Society Special Publication, 88, 211-233.

# REGIONAL BALANCED CROSS SECTION IN THE PATAGONIAN ANDES OF TIERRA DEL FUEGO (Argentina and Chile)

Pablo E. Kraemer

Department of Geology and Geophysics. Guyot Hall. Princeton University. Princeton N.J. 08540.

**KEY WORDS: Structure-Balanced cross section-Patagonian Andes.**

## INTRODUCTION

The Patagonian Andes are divided into the External and Internal Tectonic Domains. The External Tectonic Domain is characterized by structures developed in the sedimentary cover, scarce basement outcrops, low temperature deformation (usually not above green schist facies) and almost absent calcalcaline magmatism. The Internal Tectonic Domain is characterized by low to high grade polydeformed metamorphic rocks emplaced as basement thrust sheets, basic rocks with oceanic crust affinities, and abundant calcalkaline magmatism. These two descriptive domains can be mapped regionally and the boundary is a transitional zone with basement thrust and basement cored anticlines. Here I show a regional balanced cross section through the Patagonian Andes which goes from Tierra del Fuego island to the Pacific ocean (Figure 1-A). It was constructed using the fault-bend folding theory [Suppe, 1985]. The cross section presents a new interpretation linking the structures of the External and Internal domains. The rocks of the Internal domain are interpreted as alocthonous thrust sheets transported hundreds of kilometers along a basal decollement. The deformation propagates from the Internal to the External domain since Mid Cretaceous to Cenozoic.

### External Domain

The External Domain is characterized by a thick folded and thrusted sedimentary cover. Fault related folds are the typical structures to the north and imbricated thrust systems to the south (Figure 1-A). The frontal folds are interpreted as fault bend folding structures related to three decollements, D1-D2 and D3 located near the top, middle and bottom of Eocene-Oligocene clastic deposits (Figure 1-B) [Cagnolatti et al., 1989; Alvarez Marrón et al., 1993]. The age of deformation of the frontal fold belt is post (S4) and can be related to a Miocene regional event of deformation. The shortening in the frontal zone is partially transfered to a back-thrust (BT) which is the limit of the frontal folds. south of this backthrust there is an imbricated system of five thrusts sheets composed of Upper Jurassic-Lower Cretaceous rocks (S1) and Upper Cretaceous rocks (S2). These thrust are related to a decollement located at the top of the Jurassic volcanics of Tobifera Formation (D4) described in surface at the Cerro Verde anticline by Klepeis [1994]. At the north edge of the imbricated thrust system, the Vicuña thrust (VT) and a back-thrust (BT) define the triangular zone described by Alvarez Marrón et al (1993). The Cerro Verde anticline (CV), affected by Quaternary strike slip faults, is the first outcrop of Tobifera Formation along the section. It is interpreted here as two stacked basement thrust sheets which are connected to the basal decollement of the orogen (D5) by a 15° ramp under the Darwin Cordillera (DC) (Figure 1-A). The shortening produced by the displacement of the basement thrust sheets along the top of Tobifera volcanics (D4) and top of Upper Cretaceous-Lower Tertiary rocks (D3) account for most of the Tertiary shortening of the fold belt east of the Deseado thrust. The Cerro Verde anticline refolds the deformed cover due to the activation of a lower decollement in the basement. This is a possible mechanism for thickening the orogenic wedge and to propagate the deformation toward the foreland during consecutive events of deformation. The fact that the low grade basement thrust sheet (BT) at the north end of Darwin Cordillera was emplaced out of sequence during the Paleocene-Eocene [Klepeis, 1994], suggest a post Mid Cretaceous (age of the main deformation in southern Darwin Cordillera) and pre Eocene event of cover deformation during Maastrichtian-Paleocene.

**Internal Domain.**
The Darwin Cordillera is the most important basement outcrop in Tierra del Fuego, metamorphosed during the Upper Cretaceous as a consequence of the Mid Cretaceous compressive deformation [Kohn, 1995]. Along the profile three basement thrusts were mapped [Mingramm, 1982; Caminos et al., 1981]. Here they are interpreted as an east vergent imbricated thrust system with more than 200 km of shortening and rooted in the basal decollement (D5) at 30 km below sea level (Figure 1-A). The southern limit of Darwin Cordillera is a tectonic boundary associated with an abrupt metamorphic grade change from chlorite-biotite grade to kianyte grade along the Beagle Channel fault [Kohn,1995]. This metamorphic jump is not recognized 20 kilometers toward the east in the section because the rocks on either the north coasts of Dumas Peninsula (DP) or the south coast of the Beagle Channel (BCH) are in chlorite-biotite grade (GS in Figure 1-A). This lateral changes probably reflect variable crustal shortening and uplift along the irregular margins of the back arc basin deformed during the Mid Cretaceous. The outcrops of the Upper Jurassic volcanics (Tobifera) in depositional contact below basic rocks of the back arc basin (Tortuga Complex) along the coast of Dumas Peninsula [Suarez et al, 1985], are here interpreted as transitional crust of the north side of the back arc basin thrusted over continental crust of Darwin Cordillera. The basic rocks of Tortuga Complex are an incomplete ophiolite sequence outcroping extensively south of the Beagle Channel. They are composed by pillow lavas, sheeted dikes and gabbros representing the upper levels of the oceanic crust formed in a Mesozoic marginal basin [Suarez et al, 1985]. The metamorphism and geochemistry of these rocks support an origin related to a spreading center [Stern and Elton, 1979] but no ultrabasic rocks were found yet in the Tortuga Complex neither in the Sarmiento Complex toward the north. south of the Beagle Channel fault in Dumas Peninsula (PD) and Pasteur Peninsula (PP) several thrusts merge to a decollement located 5 kilometers below the top of the basic rocks and two more decollements are infered at the bottom and top of the Upper Jurassic-Lower Cretaceous sedimentary rocks. The southermost thrust transport Upper Jurassic-Lower Cretaceous rocks associated to the activity of a magmatic arc located on the southern margin of the basin.
It is proposed here that the basic rocks are alocthonous thrust sheets emplaced over continental crust and transported hundreds of kilometers toward the foreland along D5. Most of the deformation south of the Beagle Channel is related to a Mid Cretaceous compressive event between 87-90 Ma and 100-110 Ma [Halpern and Rex, 1972].

## CONCLUSIONS

The Patagonian Andes of Tierra del Fuego are divided into an External and Internal Tectonic Domains, each one having different style of structures and rock association. The structures of the External Domain are related to four main decollements (D1-4) located in the sedimentary cover and the deformation migrates toward the foreland in at least three events of shortening during the Maastrichtian-Paleocene, Eocene and Miocene. The emplacement of basement thrusts that fold or cut the previously deformed cover is a possible mechanism for thickening the orogenic wedge and to propagate the deformation toward the foreland during consecutive events of deformation.
The structures of the Internal zone in Darwin Cordillera are basement thrusts rooted in a basal decollement (D5) located at 30 kilometers below sea level and a 15° ramp link the basal decollements of the Internal and External domains. The structures south of Darwin Cordillera are related to a basal decollement located in the oceanic crust of the back arc basin. This basic rocks are interpreted as alocthonous thrust sheets emplaced over continental crust and transported hundreds of kilometers toward the foreland. The main episode of deformation in the Internal domain is Mid Cretaceous age sustaining the general propagation of the deformation toward the foreland since then.

## REFERENCES


Alvarez Marrón, J., K.R. Mc Clay ., S. Harambour., L. Rojas and J. Skarmeta.1993. Geometry and evolution of the frontal part of the Magallanes foreland thrust and fold belt (Vicuña area), Tierra del Fuego, Southern Chile, *AAPG Bull.*,77(11), 1904-1921.

Cagnolatti, M., G.Covellone., J Erlicher y F.Fantin.1987. Fallamiento y plegamiento de cobertura al suroeste del rio Grande, Cuenca Austral- Tierra del Fuego., *X Congreso Geologico Argentino*, 1, 149-152,Tucuman.

Caminos, R., M.J. Haller., O.Lapido., A. Lizuain., R.Page and V.Ramos.1981 Reconocimiento Geologico de los Andes Fueguinos. Territorio Nacional de Tierra del Fuego., *VII Congreso Geológico Argentino*, 3, 759-786,San Luis.

Halpern, M., and D.C. 1972.Rex,Time of folding of the Yahgan Formation and age of the Teckenika bed, southern Chile, South America, *Geol. Soc. Am. Bull.*,83,1881-1886.

Klepeis, K. A.,1994.Relationship between uplift of the metamorphic core of the southermost Andes and shortening in the Magallanes foreland fold and thrust belt, Tierra del Fuego, Chile, *Tectonics.*,13(4), 882-904.

Kohn, M. J., F.S. Spear., T.M. Harrison and I.W.D Dalziel, 1995.$^{40}Ar/^{39}Ar$ geochronolgy and P-T-t paths from the Cordillera Darwin metamorphic complex, Tierra del Fuego, Chile, *J. Metamorph. Geol.*,13,251-270.

Mingramm, A. R. G. 1982. Evolution scheme of Fueguian Andes along Los Cerros - Pla Hardy section., *Rep. E.P./A.R.G. M / E.P Draw N G00618. Shell, Holanda.*

Stern, C. R. and D. Elthon.1979.Vertical variation in the effects of hidrothermal metamorphism in Chilean ophiolites; their implications for ocean floor metamorphism, *in Processes at mid ocean ridges*, editor J. Francheteau,Tectonophisics, 55(1-2),179-313.

Suppe, J.1985. *Principles of Structural Geology*, 537., Prentice-Hall,Inc, Englewood Cliffs, New Jersey.


Figure 1-A Regional cross section in the Patagonian Andes of Tierra del Fuego. VT: Vicuña thrust; DT: Deseado thrust; CV: Cerro Verde anticline; BT:Basement thrust; BCH:Beagle Chanell; DP:Dumas Peninsula ; PP:Pasteur Peninsula; PO:Pacific ocean.

1-B.S1-S4:tectostratigraphic units bounded by unconformities, J:Jurassic unconformity, MK:Mid Cretaceous unconformity, MP: Maastrichian - Paleocene unconformity, E:Eocene unconformity; M:Miocene unconformity. D1-5: Decollements.

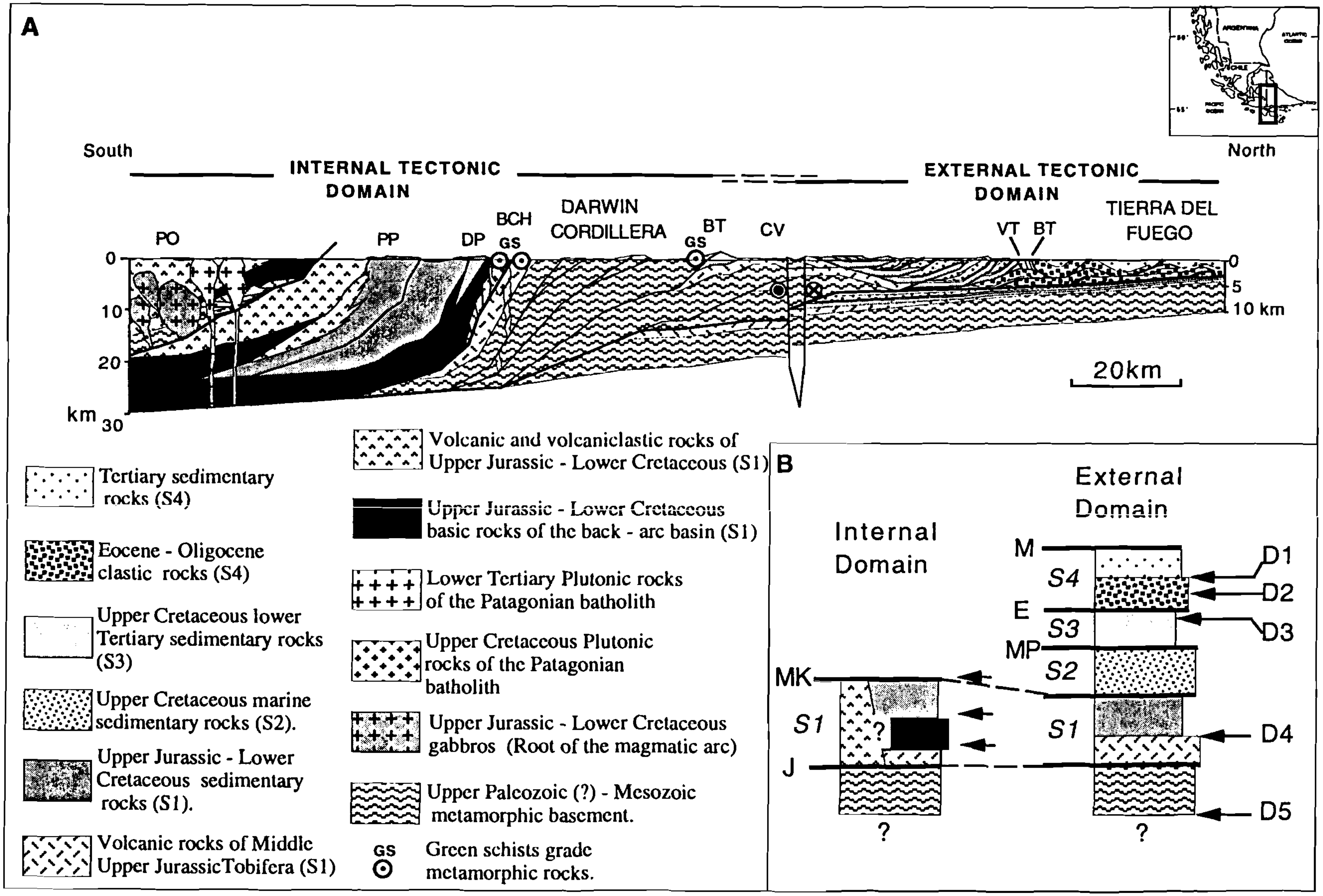
A
South
North
INTERNAL TECTONIC DOMAIN
EXTERNAL TECTONIC DOMAIN
PO
PP
DP
BCH
GS
DARWIN CORDILLERA
GS
BT
CV
VT
BT
TIERRA DEL FUEGO
0
10
20
km 30
0
5
10 km
20km
Tertiary sedimentary rocks (S4)
Eocene - Oligocene clastic rocks (S4)
Upper Cretaceous lower Tertiary sedimentary rocks (S3)
Upper Cretaceous marine sedimentary rocks (S2).
Upper Jurassic - Lower Cretaceous sedimentary rocks (S1).
Volcanic rocks of Middle Upper JurassicTobifera (S1)
Volcanic and volcaniclastic rocks of Upper Jurassic - Lower Cretaceous (S1)
Upper Jurassic - Lower Cretaceous basic rocks of the back - arc basin (S1)
Lower Tertiary Plutonic rocks of the Patagonian batholith
Upper Cretaceous Plutonic rocks of the Patagonian batholith
Upper Jurassic - Lower Cretaceous gabbros (Root of the magmatic arc)
Upper Paleozoic (?) - Mesozoic metamorphic basement.
GS Green schists grade metamorphic rocks.
B
Internal Domain
External Domain
M
E
MP
MK
J
S4
S3
S2
S1
S1
D1
D2
D3
D4
D5
?
?

# THE JURASSIC-EARLY CRETACEOUS ARC OF THE CHILEAN COASTAL CORDILLERA NEAR TALTAL: AN ASSEMBLAGE OF CRUSTAL SLIVERS

D. KURTH, E. SCHEUBER and K.-J. REUTTER

FU Berlin, Institut f. Geologie, SFB 267, Teilprojekt C1, Malteserstr. 74-100, D - 12 249 Berlin

**key words: Jurassic magmatic arc, terranes, crustal slivers**

## INTRODUCTION

The north Chilean Coastal Cordillera represents the first magmatic arc (Jurassic to early Cretaceous) of the Andean cycle. This arc is composed of > 5 km of arc volcanics (mainly basaltic andesites) and gabbroic to granodioritic intrusives. The main structure of the Coastal Cordillera is the > 1000 km long arc-parallel Atacama Fault Zone (AFZ) which was activated in the early Cretaceous as a trench-linked strike-slip fault. South of Taltal (25°24.100 S / 70°29.100 W) the Atacama Fault Zone separates two blocks of strongly different geological and tectonical development, the Cifuncho-Block to the west and the Pingo-Block to the east.

The CIFUNCHO - BLOCK is made up of an assemblage of different crustal slivers represented by three fault-bounded sub-blocks. These are from W to E:

- a western block consisting entirely of Palaeozoic rocks, strongly folded phyllites and quartzites, outcropping mainly along the coast, which were intruded by granites of the Permian Cifuncho Pluton.
- a middle block consisting of ~ 1500 m of a coarse to medium grained continental sedimentary sequence, locally containing intermediate volcanic intercalations of late Triassic age, Lower Jurassic marine sediments overlain by a Lower Jurassic volcanosedimentary sequence
- an eastern block composed entirely of arc volcanics, ~ 5000 m of the Jurassic La-Negra Formation and ~ 800 m of the likewise volcanic Lower Cretaceous Aeropuerto Formation

The stratigraphic record of the PINGO - BLOCK bordering the Cifuncho-Block to the east is strongly reduced. Triassic and Jurassic formations are lacking: Palaeozoic sediments and plutonic rocks are overlain only by the magmatic arc volcanics of the Lower Cretaceous Aeropuerto Formation. The Pingo-Block was intruded by gabbros to granodiorites of the Cerro del Pingo plutonic group in early Cretaceous times.

THE CHILEAN COASTAL CORDILLERA SOUTH OF TALTAL

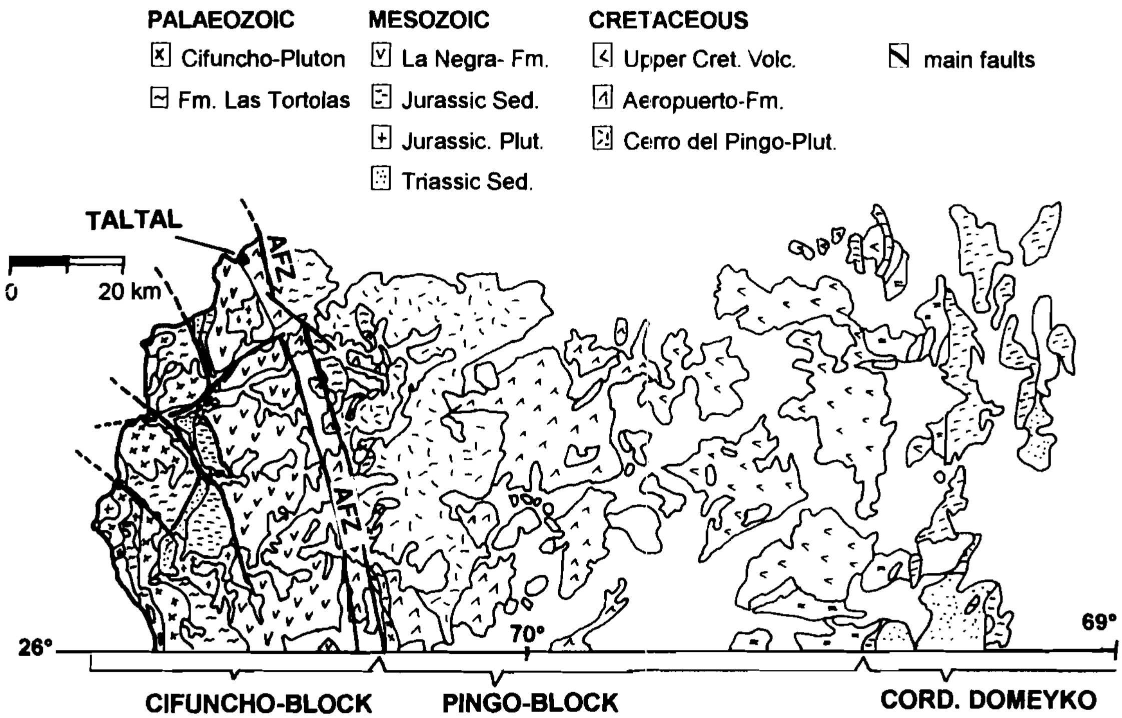


**TECTONICS**

In general the structures of the <u>Cifuncho-Block</u> were formed in an arc-parallel (N-S) sinistral transtensional regime in late Jurassic times. The following types of structures can be observed:

a) N-S trending **strike-slip faults** occur mainly at the boundaries of the sub-blocks. Fault rocks are fault gouge and breccia. Displaced marker horizons and microstructures indicate a mainly sinistral sense of displacement
b) **Folds and thrusts** occur only in the Triassic-Lower Jurassic sediments. Fold axes and thrust planes trend ~ ENE: vergencies are directed towards NNW and SSE.
c) **N - S to NNW - SSW striking normal faults**
d) **NE trending dextral strike-slip faults**. Along these faults the Cifuncho-Block has been fragmented into smaller parts

The age of deformation is constrained by predeformative dioritic sills and stocks (K-Ar in Hornblende: 155 $\pm$ 5 Ma) and by post-deformative andesitic dikes. N of Antofagasta similar dikes gave a cooling age of 147 $\pm$ 6 Ma (K-Ar in hornblende). This time-lag corresponds to the final stage of igneous activity in the Cifuncho Block which cooled below 100°C at 77 $\pm$ 7 Ma (fission track on apatite)
The different composition of the Pingo-Block poses the question whether this block, before it became part of the early Cretaceous magmatic arc, was covered by Jurassic marine backarc sediments in a similar way as the areas east of it (Cordillera Domeyko) or if it was an elevated area during that time. In

the first case exhumation of the Paleozoic rocks must have occurred during the late Jurassic or early Cretaceous, perhaps at the time of the intrusion of the Pingo-Pluton (~ 120 Ma). Deformation concentrated on the Atacama Fault Zone which separates the Pingo-Block from the Cifuncho-Block. Here a ~ 500 m wide mylonitic belt developed. Numerous kinematic indicators uniformly reveal a sinistral sense of shear. Two mylonitic zones could be distinguished: an older one, developed in a late Jurassic diorite yielded 141 $\pm$ 6 Ma (K-Ar in hornblende), a younger one developed in an early Cretaceous granodiorite yielded 123 $\pm$ 3 Ma (K-Ar in biotite). Thus, also in the Pingo block deformation was contemporaneous to magmatic activity. The Palaeozoic rocks fell short of the 100°C-isotherme at 134 $\pm$ 9 Ma and the Cretaceous granodiorite at 90 $\pm$ 9 Ma.

## CONCLUSIONS

The Pingo-Block and the Cifuncho-Block as well as its subblocks are all bounded by major strike slip faults and show great differences in their respective geological evolution. Thus, these blocks could be interpretated as "terranes" which, according to Coney (1989) are "geologic entities of regional extent with a coherent stratigraphic sequence different from the cratone nearby and bounded by a major fault". It can be shown, however, that these blocks owe their origin to the special conditions of magmatic arc tectonics and the movement of the forearc with respect to the upper plate so that the term "terrane" may be not adequate for this phenomenon. The following facts have to be considered:

a) The blocks were originally part of the upper plate and were affected by arc magmatism.
b) The mobility of these blocks depends entirely on igneous activity in the arc which, by advective heat transfer, leads to a weakening of the crust of the arc. This weakening results in a decoupling of the forearc from the remaining upper plate. Decoupling in turn allows the forearc slivers to move parallel to the arc. When magmatism stops, the crust of the arc becomes rigid and the forearc slivers become locked.
c) The overall movements of the blocks are constrained essentially to directions parallel to the arc along trench linked strike slip faults.

The described lateral movements were a consequence of strongly oblique plate convergence towards SE (JAILLARD 1986). This oblique convergence caused the movement of the Cifuncho-Subblocks relative to the Pingo-Block. Although the amount of the lateral displacement cannot be determined at the moment, the described contrasting stratigraphic records of the two blocks are an indication of large-scale displacements.

## REFERENCES

Coney, P.J., (1989): Structural aspects of suspect terranes and accretionary tectonics in western North America. - J. Struct. Geol., 11, p. 107 - 125

Jarrard, R.D., (1986): Relations among subduction parameters. - Rev-. Geophys., 24, p. 217-284

This work is part of the Sonderforschungsbereich 267 - Deformationsprozesse in den Anden supported by the DFG (German research foundation) and FU Berlin

# ARC AND FOREARC BRITTLE DEFORMATION IN TRANSPRESSIVE REGIME OF THE LOWER CRETACEOUS, COASTAL RANGE (26°-27°S), CHILE: Microtectonics antecedents

Luis LARA (1), Sergio GELCICH (1), Julio Carrasco (2) y Alejandro DIAZ (1)

(1) Servicio Nacional de Geología y Minería. e-mail: sernageo@reuna.cl Santiago, Chile.
(2) Departamento de Geología. Universidad de Chile. Casilla 2777. Santiago, Chile.

**KEY WORDS:** Brittle deformation, Atacama Fault System, strain partitioning, microtectonic analysis.

## INTRODUCTION

The inversion of microtectonics data, obtained from mesoscopic faults associated with the main alignements of a structural system, allows to make a more thorough description of the kinematics and interpret it in the regional setting. In this work we compute stretching and shortening axis *(strain)* (e.g. Marret y Allmendinger, 1990) for a set of structures contained in the domain of Atacama Fault System (AFS) (Saint Amand, 1960), "El Salado" segment (Naranjo, 1987), particularly between 26° and 27°S.

These antecedents, jointly with available paleomagnetic data, magmatism ages and mineralization characteristics associated with AFS, allows to apply for a partition model of deformation for the discussed area.

## MICROTECTONIC DATA

*NS alignments* : represented by the AFS main traces, relevant to anastomosic cleavage areas and occasionally to *sensu stricto* faults with subhorizontal striae. The kinematics indicators describe a generally sinestral lateral displacement. *(Fig.1)*

*NE-SW alignments* : of little frequency, thogh with lengths surpassing 10 km, are remarkedly associated to mineralization occurrences of Fe-Cu. In the Cerro Negro mining district, mainly normal mesoscopic faults defining a NW-SE maximun stretching axis and a subvertical shortening axis.

*NW-SE alignments* : represented in the forearc region, AFS west, for a set of mainly sinestral displacement faults and wich would be linked to the clockwise block rotation. In jurassic rocks, this rotation reaches 35° with no important latitudinal displacement (Taylor, 1994). In the AFS domain this set is recorded too, particularly well exposed in the Manto Verde Fault (MVF) (Linsay *et al.*, 1994), in the los Pozos-Manto Verde mining district. The MVF, displayed at aproximately 30° between the AFS central and eastern branches, relevant to a group of mainly normal or sinestral-normal displacemet mesoscopic faults. Said kinematics defines a maximun NE-SW horizontal stretching axis and vertical shortening axis.

## DEFORMATION MODEL

The geometry of the structural system and the described kinematics, allows to infer a domain of arc where the deformation would be partitioned in a simple shear component, without greater displacement in the borders of the shear zone (AFS main alignments), and with extension associated to NW-SE

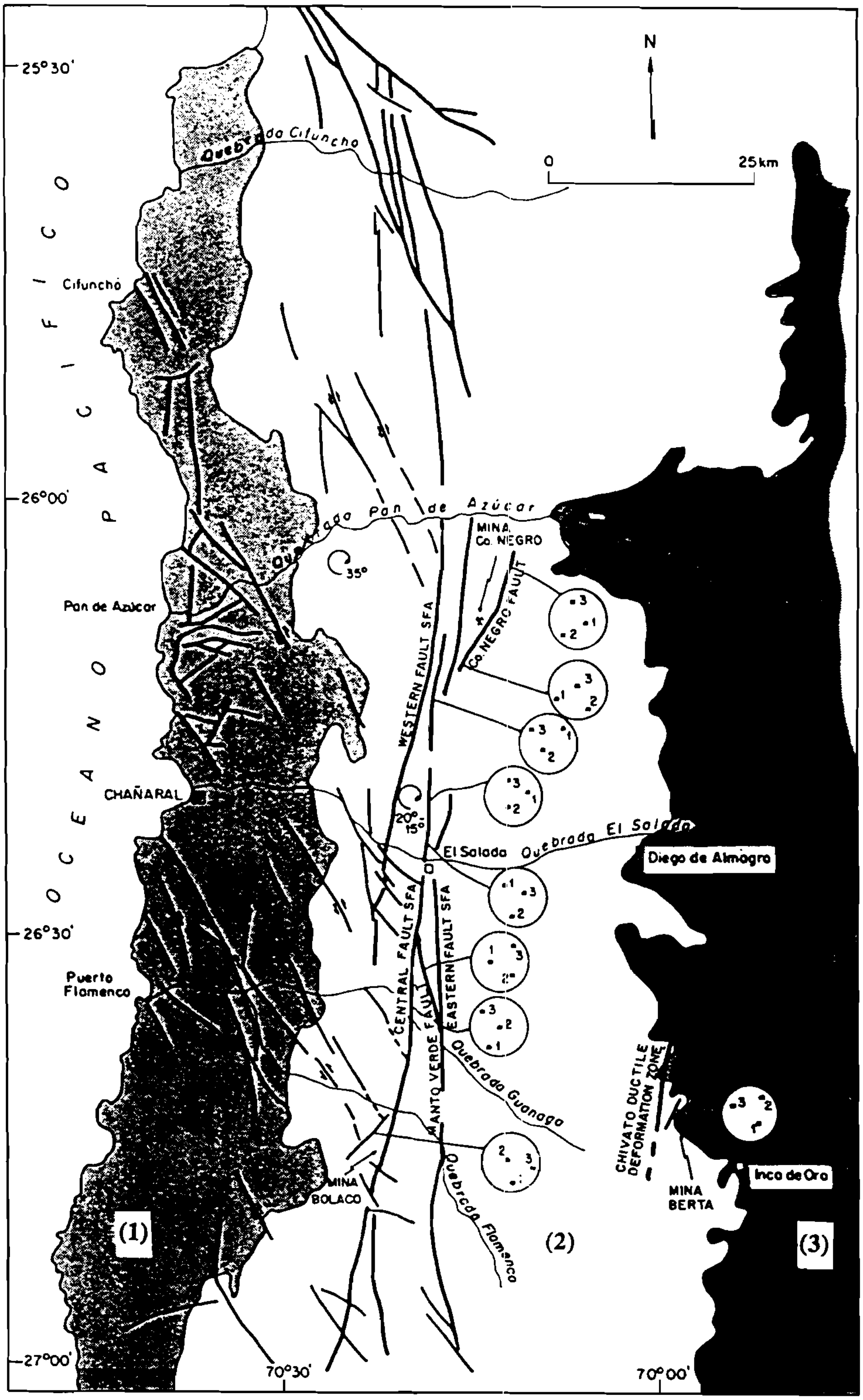


**Fig.1.** Geologic sketch that shows three major units, from west to east: (1) Paleozoic Basement including Devonian-Carboniferous metamorphic rocks and Permian-Triassic and Triassic granitoids, (2) Mesozoic Magmatic Arc and (3) Tertiary-Quaternary Alluvial, Coluvial and Pediplain Deposits. Major structural systems are displayed and its corresponding stereoplot, with strain axis, are shown too.

structures (MVF). A simultaneous component of pure shear is justified by the low angle of the MVF and the borders of the shear zone taken in to account. On the other hand, the forearc domain would reflect the remaining pure shear fraction absorved with leakage of blocks or "slivers" in the NW-SE structures, developed in a sector of coast prortruding towards west. Moreover, the NE-SW structures could be linked to the first and solve space
problems associated with the blocking rotations. The reduced component of lateral displacement described, as well the geometric display of structures in the arc and forearc, allow to assume a transpressive deformation system of "pure shear dominated" (Tikoff y Teyssier, 1995) associated with a slanting subduction of important component (convergency angle greater than 20o).

Chronologic relationships, though imprecise, allows to describe the following sequence of events:

_Jurassic-Lower Cretaceous (156-125 Ma)_ : Extensional (Grocott _et al._, 1994), or transtensional arc. First clockwise rotation ($15^{o}$-$20^{o}$) (Taylor _et al._, 1993) of jurassic rocks through preceding structures of NW-SE direction in the forearc domain. Said event could be related to a very low spreading rate in the Phoenix-Farallon ridge and the reducedconvergency velocity resulting from considering fixed the Sudamerican plate, previous to the Atlantic ridge opening (Uyeda y Nakamori, 1979, Mpodozis y Allmendinger, 1992).

_Valanginian-Cenomanian (125-115 Ma)_ : Change of tectonic regime. Ductile deformation in the sinestral transpresive regime in the central and eastern branches of the AFS. Fe mineralization in the AFS main branches, associated with the upper structural level. Fe-Cu mineralization on the arc domain (Manto Verde-Los Pozos district) associated with the same level.

This deformation events would only be initially related to the important spreading rate of the Pacific ridge (125 Ma) with convergency direction towards the SE. Indeed, it is empirically accepted the inconsistency of intraarc megafaults and "extensional" subduction regimes (or "Mariana" type by Uyeda y Nakamori, 1979) (Jarrard, 1986), as the one generated as from this period. Instead this, an important extension in the backarc region is developed. This event would be registered in the full development of marginal basins in the continental margin. Therefore, after the initial deformation of the period, the AFS would provisionally abandoned.

_Aptian-Albian (115-100 Ma)_ : Pure-simple shear in the arc domain. Reactivation of NW-SE (MVF) extensional structures displacing mineralized bodies. Pure shear in the forearc domain with NW-SE structures reactivation and clockwise rotations ($20^{o}$-$15^{o}$) (Taylor _et al._, 1993).

These transpressive deformation events coincide with the opening of Atlantic ridge (somewhat subsequent to the 115 Ma, in this latitude) (Rabinowitz y La Brecque, 1979). Though the Pacific ridge spreading continued, the displacement of Southamerican plate generate less favorable conditions for the backarc subsidence (Uyeda y Nakamori, 1979; Mpodozis y Allmendinger, 1992).

_Albian-Santonian (100-85)_ : Extension in the backarc region. This event would be related to the extinguishing of the Phoenix-Farallon ridge at 100 Ma by reducing the speed of the subducted plate. This would cause the reactivation of the marginal basin area and the new abandonement (?) of the AFS. The period could end with the inversion phase of the basin (pre-Santonian) followed by a new Upper Cretaceous-Paleocene regional extension.

The microtectonic analysis in progress, as well as the dynamic models subject to built on it, added to a better chronologic constrain of the deformative events, will contribute with antecedents concerning the evolution of the continental margin, expressed in the arc and forearc domains, during part of the Lower Cretaceous.

## REFERENCES

1. Grocott, J., Brown, M., Dallmeyer, R., Taylor, G. y Treloar, P. 1994. Mechanisms of continental growth in extensional arcs: an example from Andean plate-boundary zone. Geology V22, pp.391-394.

2. Jarrard, R. 1986. Terrane motion by strike-slip faulting of forearc slivers. Geology V14., pp.780-783.

3. Lindsay, N., Vila, T. y Zamora, R. 1995. Geology of the Mantoverde Copper Deposit, a hidrothermal-tectonic breccia related to the Atacama Fault Zone. Actas VII Congreso Geolóogico Chileno, Concepción. pp. 1580-1584.

4. Marrett, R. y Allmendinger, R. 1990. Kinematics analysis of fault-slip data. Journal of Structural Geology V12., No8. pp.973-986.

5. Mpodozis, C. y Allmendinger, R. 1992. Extensión cretácica a gran escala en el Norte de Chile (Puquios-Sierra de Fraga, 27°S): significado para la evolución tectónica de los Andes. Revista Geológica de Chile V19, No2, pp.167-197.

6. Naranjo, J. 1987. Interpretación de la actividad cenozoica superior a lo largo de la zona de falla Atacama, norte de Chile. Revista Geológica de Chile V31, pp.43-55.

7. Rabinowitz, P. y La Brecque, J. 1979. The mesozoic South Atlantic Ocean and evolution of its continental margins. Journal of Geophysical Research, No.84, pp.5973-6002.

8. Saint Amand, P. y Allen C. 1960. Strike-slip faulting in Northern Chile. Geological Society of America Bulletin V71, pp.1965.

9. Taylor, G., Randall, D., Grocott, J. y Treloar, P. 1993. Paleomagnetic studies of fault block rotations in relation to transtension on the Atacama Fault System and granite emplacement. Actas Second ISAG, Oxford (UK). pp.253-254.

10.Tikoff,B. y Teyssier, C. 1994. Strain modeling of displacement-field partitioning in transpresional orogens. Journal of Structural Geology V16, No 11, pp.1575-1588.

11. Uyeda, S. y Kanamori, H. 1979. Back-Arc opening and the mode of subduction. Journal of Geophysical Research V84, No.B3, pp.1049-1061.

# PIGGY-BACK BASINS OF THE SUBANDEAN ZONE (BOLIVIA) : A VIEW FROM NUMERIC AND ANALOGUE MODELS.

P. Leturmy[1], J.L. Mugnier[1], P. Vinour[2], P. Baby[3], B. Colletta[2].
[1] ESA CNRS 2055, Université J. Fourier, Laboratoire de géodynamique des Chaînes Alpines, 15 rue Maurice Gignoux, 38031 Grenoble Cedex, France.
[2] Institut Français du Pétrole Rueil Malmaison, France.
[3] ORSTOM, San Ignacio 805 y Humboldt, Apartado 17.11.6596, Quito, Ecuador.

KEY WORDS: thrust, piggy-back basin, sedimentation, erosion, Sub Andean zone, Bolivia.

## INTRODUCTION

The Eastern zone of the Andean chain is formed by the Subandean belt. The syn-orogenic sedimentation in this zone is located in either a flexural through or in large and deep piggy-back basins. We want to understand the role of the superficial mass transfer on the kinematical evolution of this thrust belt. It has already been shown that superficial processes are of great importance in the evolution of a thrust wedge considered at large scale, but can erosion and sedimentation control tectonics at a smaller scale, and what are the consequences of this control on the final geometry of a thrust system? To investigate those interactions, two kind of modellisations are proposed.

The first approach consists in "sand-box" models which have been scaled to have a realistic mechanical behaviour. The second approach uses numerical models in which forward kinematical models are coupled to erosional processes.

## GEOLOGICAL SETTING

The Subandean Zone of Bolivia forms the external border of the Andean chain. This zone is 140-150 Km large, and is bound at the east by the CFP ("Cabalmiento Frontal Principal"), and at the west by the present foreland basin. Shortening structures separate Tertiary basins more than 25 Km large and more than 6000 m thick. This zone was characterised since Oligocene by sedimentation ahead of the Andean belt. Its deformation is not very important until 6 Ma, (Baby, 1995): only a few anticlines began their growth in the Sub Andean zone whereas thrust tectonics mainly affects the Eastern

Cordillera from 21 Ma to 9 Ma. After 6 Ma the structuration is intense in the Subandean Zone, and the average shortening velocity is about 7 mm/yr. in southern Bolivia and in northern Bolivia.

The variation from north to south of the thickness and lithologies of the series implies some differences in deformation style (Baby and *al.*, 1989). In the northern part of the Bolivian Subandean Zone, the basal detachment is located in the Ordovician formation. In the southern part, the basal detachment is located at the base of the Silurian formation. These variations in the sedimentary wedge from north to south also implies a variation in the basal detachment slope. In the north, its dip is about 5°, while in the south it is only 2°. The topographic slope of the Subandean belt also varies from 1.4-1.7° in the north to 0.6-1.3° in the South.

## ANALOGUE SANDBOX EXPERIMENTS

Analogue sandbox experiments were undertaken to investigate interaction between sedimentation, erosion and tectonics. Initial geometry, shortening rate and sedimentation rate have been defined from the regional studies of the Subandean Zone.

Modelling has been realised in a normal gravity field with the "Structurator" sandbox. It conception was especially realised by IFP (Institut Français du Pétrole) to fall in the investigation field of an X-ray tomograph (medical scanner). The apparatus is formed by a basal rigid plate associated with two step by step motors that respectively moves a lateral border and tilts the basal rigid plate. Experiments were made using 4 materials: glass micro beads, silicone, sand, and pyrex. The model is constituted, from bottom to top, by : one glass micro beads layer for the basal decollement, one sand layer for the lower competent series, one layer of silicone for an intermediate decollement, one sand layer for the upper competent series.

Four experiments have been performed to investigate erosion, sedimentation and tectonic interactions: we made one experience with basement tilting, without erosion and without sedimentation; one with basement tilting, sedimentation and without erosion; two with erosion and sedimentation and respectively with and without basement tilting.

## A NUMERICAL MODELLING

This numerical method is based on a forward kinematical model, a progressive tilting of the basement, a superficial short range transport and a Coulomb wedge theory. This code (Chalaron et *al.*, 1995) allows to study a wide range of parameters.

The mechanical parameters has been fixed from the equilibrium study of the critical taper of northern Bolivia. The best fit to fill the basins of north Bolivia is obtained, from a trial and error procedure, with a high value of transport capacity (500 $m^2$/yr.).

During this experiment, two piggy-back basins develops above the wedge and have different evolutions.

The extension of the external basin is nearly the same from the beginning to the end.

The extension of the internal basin always reduces during the deformation. In the eastern part of the basin, sediments are continuously eroded, whereas in the western part some onlaps are preserved from erosion. Toplaps mark a very extended unconformity related to change in the thrust sequence and in the development of duplexes.

## CONCLUSION

Concerning the modellisations:

1) The two approaches show that the evolution of a thrust wedge considered at large scale is controlled by the growing of a shortened Coulomb wedge. The change imposed along it upper boundary by surface transport influences the nucleation of ramps, the propagation of decollement along weak layers and partitioning of displacement along the fault system.

2) Analogue models without surface transport are characterised by a forward breaking sequence for the ramps in the duplex between the two decollement levels, and by a forward breaking sequence for the emergent faults. Displacement mostly occurs along the outer and deeper trajectory of the thrust system when there is no surface transport.

3) Analogue models show that superficial processes are important for the nucleation of new faults and for the partitioning of displacement along the fault system. Erosion favours tectonic indentation that restrains the forward propagation of the thrust system. This tectonic indentation is induced by the development of major emergent back-thrusts, and out-off sequence reactivation in the duplex between the two decollement.

4) Wedge shaped sedimentation, induced by the increase of subsidence from the foreland to the front of the thrust belt, favours a forward shift of this front. This shift occurs abruptly when the tilt of the basement reaches a given value, and is followed by out-of sequence reactivation.

5) Anteorogenic wedge shaped body located above a weak layer could propagate deformation far in the foreland and a backward sequence reduces the backward topographic slope created at the back limb of the frontal ramp anticline.

6) Numerical models show that several duplexes develop in a thrust system where three decollement levels are linked by irregularly spaced ramps. In this case, several independent culminations bump the topographic surface, and delimit depressions. Out-of sequence reactivations attempt to reduce the bumpy aspect of the topography, but the culminations persist at the hanging-wall of the ramps that transfer displacement from deep decollements to higher decollements. The out-off sequence reactivation could even increased the high of the inner culmination.

7) Numerical models show that the superficial processes smooth the topography by erosion of the antiforms and sedimentation in the depressions. Augmentation of the efficiency of surface transport increases the erosion rate and the sedimentation rate until

a state where all the depressions are filled and the topographical effects of the culminations are nearly hidden. greater augmentation have no more influence.

Piggy-back-basin development could be induced by: 1) the increase of the foreland basin taper; 2) the incorporation of an ante-orogenic wedge taper in the thrust belt; 3) relative depression between two independent anticlines related to two ramps located along a unique thrust trajectory; 4) a change in mechanical parameters and most probably increase of fluid pressure.

Concerning the thrust belt of the Subandean Zone of Bolivia:

1) Angular unconformity of growth strata above fold structures in the Southern Subandean Zone show that a strong sedimentation is synchronous with the tectonics, and the piggy-back basins are separated from foreland by weak relief. The development of the piggy-back basins could be linked to the progressive tilting of the basement, and/or to the increase of the pressure along the decollement zone during a phase of hydrocarbon generation due to tertiary deposits.

2) In the Subandean Zone of North Bolivia, this study suggests that the Tertiary sediments presently located above the thrust belt were deposited in a piggy-back basin separated from the foreland by a relief affected by erosion since 10 Myr (Quendeque formation).

Reflectors evidenced in the inner piggy-back basin seems comparable to the large unconformity that marks in the numerical models a change in the thrust sequence.

The cause of the early development of the piggy-back-basin is the wedge-shaped Silurian-Ordovician rocks. Furthermore, this study supports the interpretation, still debated, that the displacement related to the duplex at the boundary between Subandean zone and Eastern Cordillera, is transferred eastward to the external thrust system of the Subandean belt, whereas back-thrusts at the roof of this duplex are minor structures.

REFERENCES

Baby, P., G. Herail, J.M. Lopez, O. Lopez, J. Oller, J. Pareja, T. Sempere, et D. Tufino, 1989. Structure de la Zone Subandine de Bolivie: influence de la géométrie des séries sédimentaires antéorogéniques sur la propagation des chevauchements. C. R. Acad. Sci., 309 (II): 1717-1722.

Baby, P., 1995. Importance du raccourcissement et de la sédimentation synorogénique dans la structuration des zones d'arrière arc des Andes centrales (Orocline bolivien), Mémoire d'habilitation à diriger les recherches, Université de Grenoble.

Chalaron, E., J.L. Mugnier, and G. Mascle, 1995. Control on thrust tectonics in the himalayan foothills: Aview from a numerical model. tectonophysics, 248 (1-2): 139-163.

# METAMORPHIC BASEMENT AND THE STRATIGRAPHY OF OVERLYING VOLCANO-SEDIMENTARY ROCKS AT 18°S : IMPLICATIONS FOR STYLE AND TIMING OF ANDEAN DEFORMATIONS

Judith Lezaun (1), V. Heber (1), A. Beck (1), K. Hammerschmidt (2) , G. Wörner (1)

1) Geochemisches Institut, Goldschmidtstr. 1, 37077 Universität Göttingen; email: Gwoerne@gwdg.de
2) Freie Universität Berlin, Institut für Geologie, FR Geochemie, Boltzmannstr. 18-20, 14195 Berlin

**Keywords**: Northern Chile, Central Andean Uplift, Metamorphic Basement, Cretaceous/Tertiary, Ar-Ar Ages, Compressional and Extensional Deformation

## Introduction

Uplift and crustal thickening in the Central Andes occurred in Miocene to Recent times. However, the cause, processes and timing of uplift is still poorly constrained and has led to conflicting interpretations.We present new observations from the Chilean Western Escarpment of the Central Andes at 18°S relating to the tectonic style and timing of deformation of the Andean metamorphic basement rocks and their overlying Cretaceous to Tertiary volcano-sedimentary cover.

## Belén Metamorphic Basement and overlying Cretaceous to Tertiary rocks

Exposures of amphibolite-facies metamorphic basement rocks near Belén and Tignámar have long been known (Salas et al., 1966, Pacci, 1980). A very rough protolith age between 1.5 to 2.0 Ga was determined by Nd model ages and Sm-Nd by Damm et al. (1986) and Basel et al. (1995). A younger metamorphic overprint between uplift and cooling is documented by K-Ar ages on micas and amphiboles in the range of 490 to 500 Ma. The youngest (and most reliable ??) ages of 360 to 390 Ma on the basement metamorphic age (orthogneiss) is given by Lucassen (1994). Intrusions occurred also between 475 and 507 Ma (Basel et al., 1995). Damm et al. (1994) reported one fission track age of 75 Ma on zircon, indicating a Lower Cretaceous uplift or reheating event.

Detailed mapping at a scale of 1:15.000 over the entire range of basement exposures and its deformed overlying volcano-sedimentary units to the N of the village of Belén led to the following observations:

The Belén basement is overlain unconformably by a basal sequence of basement conglomerates and breccias grading into finer-grained sandstones and siltstones. Carbonate rocks are rare and conspiciously rich in detrital material. The carbonates contain brachiopodes of Permian age, while in the basal conglomeratic sandstone we found poorly preserved gastropods. This basal sequence is irregularly distributed indicating a varied shallow marine environment close to a shoreline.

Andesitic conglomerates, breccias, lava flows and quartz-bearing ignimbrites (c. 700 m, Lupica Formation, Salas et al., 1966) overly the basal sequence. Volcanic and volcanoclastic rocks are rarely intercalated by coarse-grained fluvial sediments. Sedimentology and reddish-green alteration suggest a

terrestrial, low elevation environment for deposition. Salas et al. (1966) included fine-grained fluvial and lacustrine sediments of volcano-detritical origin to the south and north as an upper member into the Lupica Formation for which he suggested an Upper Cretaceous to Oligocene age. The latter fluvio-lacustrine sediments could represent a shallow and quiet water environment equivalent to the upper part of the coarse-grained member of the Lupica Formation N of Belén, but may also well be significantly younger (up to only 25 Ma, Muñoz, 1991). This unit is overlain conformably by a series of slightly welded ignimbrites consisting of eight flow units with an estimated total thickness of 500 m ("Belén-Ignimbrites"), and a series of mafic aphyric andesite scoria and breccias. Ignimbrites and breccias are almost entirely unaltered and distinct from the breccias and ignimbrites of the "Lupica Formation". Lupica Formation, Belén-Ignimbrites and younger andesite scoria and breccia are variably folded from open folds in the E to tightly folded in the W with vertical fold planes.
Silicified, xenolith-rich and flat lying ignimbrites disconformably overly these folded Cretaceous/Tertiary strata at elevations between 4300 m and > 5000 m up to the crest of the Western Cordillera which is strongly dissected by glacial kars ("Kar-Ignimbrites"). These ignimbrites are quartz rich and show only limited distribution. They may be related to silicic post tectonic intrusions into the Lupica Formation which are abundant further N between Zapahuira and Putre.
Younger rocks, which are not exposed in the immediate working area, belong to the Oxaya Formation, of which the uppermost welded ignimbrite has been dated at about 19 Ma (Naranjo & Paskoff, 1985; Walfort et al., 1995). These plateau-forming ignimbrites occur from the Altiplano (Condoriri Ignimbrite) to the coast near Arica ( Schröder & Wörner, this meeting), and show large vertical displacements due to a second major phase of uplift and a resulting episode of erosion and basin sedimentation (Uhlig et al., this meeting). Our interpretation here, however, is mainly concerned with the older, pre-Miocene history.

Our stratigraphic framework and ages for the different volcanic units and their deformational history suggests an episode of crustal shortening and compressive tectonics in pre-Miocene times which led to an initial stage of uplift, erosion and sedimentation. The metamorphic basement rocks are involved into the compressional tectonic movements: At several places the boundary (i.e. the old land surface) between basement rocks and overlying strata is cut by flat to steeply E-dipping reverse faults and thrusts. Individual basement blocks are found to overthrust the basal sequence and the andesitic breccias of the Lupica Formation, often by not more than 100 m. The western boundary of the Belén basement block is in reverse fault contact to the younger, folded sediments. By contrast, the eastern boundary of Belén metamorphic rocks, which is exposed at elevations between 3595 m and 4000 m, is marked by a N-S trending vertical fault uplifting of the basement in the W against the Lupica Formation in the E (Fig. 1). Both, the W-vergent thrust in the W and the vertical fault in the E can be traced clearly along most of the basement exposure.

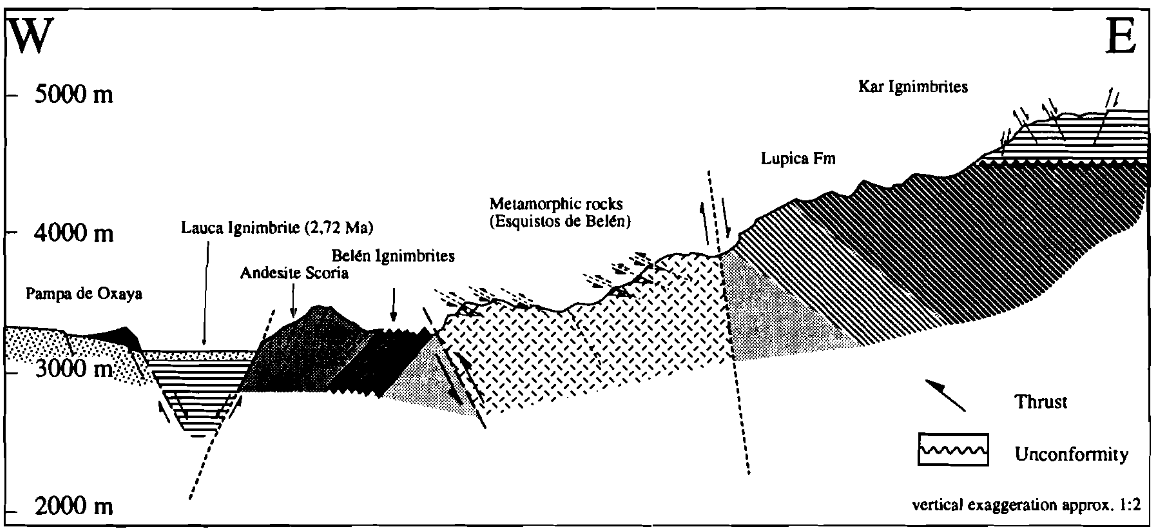


Fig. 1 Schematic W-E cross section through tht Western Escarpment of the Altiplano near Belen

Overlying silicified Kar-Ignimbrites are not affected by this folding but show evidence for extensional movements which could be due to either gravitational subsidence near the oversteepened escarpment or to younger extensive movements related to normal faulting of the >19 Ma Oxaya Formation.

Significant crustal shortening in Eocene to Oligocene times involved the metamorphic basement. Distinctly more intense style of folding in the volcano-sedimentary rocks (Lupica Formation) to the W of the Belén basement exposure indicates the possibility of the rigid basement blocks acting as a tectonic back stop or ramp against the more easily deformed sediments. The age of deformation must be older than the Kar-Ignimbrites (which are older than 19 Ma). New Ar-Ar ages of the Kar-Ignimbrites and the folded Belén-Ignimbrites will put a narrow bracket on this compressive movements of the first phase of Andean uplift in this area.

These compressive movements are clearly older than the age and deformation of the Oxaya Formation which is normally faulted resulting in the large Oxaya block. Elevation difference between this block and correlated exposures of ignimbrites from the Altiplano indicate realative movements of at least 1500m.

## Conclusions

Field investigations in the vicinity of the Belén basement inlyers provide evidence for style and timing of Cretaceous to Tertiary Andean deformations. Permian brachiopodes in carbonates and clastic sediments overlying the basement indicate exposure and erosion of the metamorphic basement during the Upper Paleozoic. The younger Lupica Formation; which can be correlated to many other occurences of similar facies in Northern Chile, is strongly folded. Contacts between the basement and overlying strata range from purely sedimentary to tectonic. The volcanic to volcanoclastic Lupica Formation was observed to be overthrusted by the metamorphic basement along W-vergent thrusts. These deformations are related to an early phase of Andean uplift which was clearly compressive in style. Degree and style of folding of the Cretaceous/Tertiary Lupica Formation differ regionally. We explain this by the basement block acting as rigid ramps at the base of the Lupica Formation in Belén.
Normal faulting and lateral extensional displacement of the Miocene Oxaya Formation represents a second major phase of Andean uplift (Uhlig et al. this meeting).

## References

M. Basel, R. Charrier and H. F (1995). New ages (U-Pb, Rb-Sr, K-Ar) from supposed precambrian units in Northern Chile: Some geotectonic implications. IGPC-Project 376 Laurentia-Gondwana Connections before pangea Field conference, San Salvador de Jujuy, Argentina.

F. Lucassen, H. Wilke, G. Franz, E. Medina and J. Infanta (1994). Paleozoic metamorphic rocks from the Preandean basement of Northern Chile (18-24° S): Regional geology, metamorphic history, age constraints and position in the crustal structure. Arbeitsbericht TU Berlin, Berlin, pp 245 -262.

Muñoz N (1991). Marco geologico y estratigraphia de un sistema fluvio-lacustre, Paleogeno. Altiplano de Arica, Norte de Chile. Actas, VI Congreso Geologico Chileno, Servicio Nacional de Geologia y Mineria, Santiago de Chile, pp 201-204.

Naranjo JA, Paskoff R (1985). Evolucion cenozoica del piedemonte Andino en la Pampa del Tararugal, Norte de Chile (18°-21°S). Actas, IV Congreso Geologico Chileno, Servicio Nacional de Geologia y Mineria, Santiago de Chile, pp 149-165.

Pacci D, Hervé F, Munizaga F, Kawashita K, Cordani U (1980). Acerca de la edad Rb/Sr precámbrica de rocas de la Formación Esquistos de Belén, Departamento de Parinacota, Chile. Revista Geológia de Chile 11: 43-50.

Salas R, Kast RF, Montecinos F, Salas I (1966). Geología y recursos minerales del departmento de Arica. Provincia de Tarapacá, Boletín, Universitad de Chile, Santiago.

Walfort B, Hammerschmidt K, Wörner G (1995). New Ar/Ar ages from Tertiary volcanics in the North Chilean Andes (18 S) : Implication for tectonic and magmatic evolution. EUG-meeting Strasburg, April 1995. Terra Abstracts, Terra Nova 7, 354.

# FALLA OESTE FAULT SYSTEM : RECORD OF ITS REGIONAL SIGNIFICANCE AS EXPOSED IN THE CHUQUICAMATA OPEN PIT, NORTHERN CHILE

Darryl D. Lindsay(1), Marcos Zentilli(1) and Guillermo Ossandon(2)

(1) Department of Earth Sciences, Dalhousie University, Halifax, NS, B3H 3J5, Canada
(2) Superintendencia de Geologia, CODELCO- Chuquicamata, Chuquicamata, Chile

KEY WORDS : tectonics, extension, strike-slip faults, left-lateral, fault gouge, mineralization

## INTRODUCTION

Late Eocene subduction related magmatic arc tectonics produced orogen-normal shortening and dextral orogen-parallel strike-slip motions in the Precordillera of northern Chile (Scheuber and Reutter, 1992). This Incaic tectonic phase, within the Precordillera, formed the Domeyko Fault System along which numerous Eocene-Oligocene intrusive complexes bearing porphyry copper mineralization were emplaced.

The Falla Oeste is often referred to as the essential branch of the Domeyko (Maksaev, 1990) or Precordilleran (Reutter et al., 1991) Fault System in northern Chile. The Falla Oeste is best defined as a fault system of regional scales ,with individual branches or sub-systems of faults that record approximately 40 m.y. of regional deformation.

Within the Chuquicamata district the Falla Oeste fault system is comprised of the Mesabi, Estanques Blancos, Balmaceda, Nor-Oeste, Este, Americana, Calderones, West Fissure, Chucos, San Lorenzo, Zaragoza, C2 and several important un-named faults and fault systems. The regionally important Falla Oeste, which has tectonic significance, must be differentiated from the district scale fault that traverses the Chuquicamata open pit, herein, the West Fissure, as displayed on original district and deposit scale maps (see Lopez, 1939).

Differences in the kinematics of the Domeyko fault system (right-lateral, unknown total displacement) with those of the West Fissure (left-lateral, estimated 35-40 km (Ambrus, 1979)) have been explained by a tectonic inversion of the fault system (Reutter et al., 1993).

Due to poor surface exposure along its length, little is known about the relationships between the fault systems and alteration/mineralization processes. The open pit of the Chuquicamata porphyry copper deposit offers an unprecedented lateral (3.3 km) and vertical (0.55 km) surface exposure of the West Fissure and all of the related faults of the Falla Oeste fault system (Figure 1). This exposure enables a detailed examination of the fault systems their relative timing relationships and association with multiple alteration-mineralization events.

The Mesabi fault, probably the oldest in the Falla Oeste system, is concentrated within and along a Triassic through Cretaceous(?)volcano-sedimentary package. This mylonitic, N10-30$^{o}$ fault consistently displayes a right-lateral sense of displacement. Mineralization along this fault (magnetite bodies) appears restricted to zones of intersection with later faults, such as those of Estanques Blancos. Ductile deformation fabrics, such as foliations, lineations, and mylonitic shear zones are irregularly distributed throughout the open pit and to the north east, being increasingly more common as the Mesabi fault is approached. It is expected that a similar fault may be located on the western side of the Chuquicamata intrusive complex but this fault has not been recognized. The ductile nature of these shear zones indicates that dextral deformation at relatively high temperatures continued during or just after intrusion (~33-34 Ma) of the complex. Newly discovered thrust zones within the

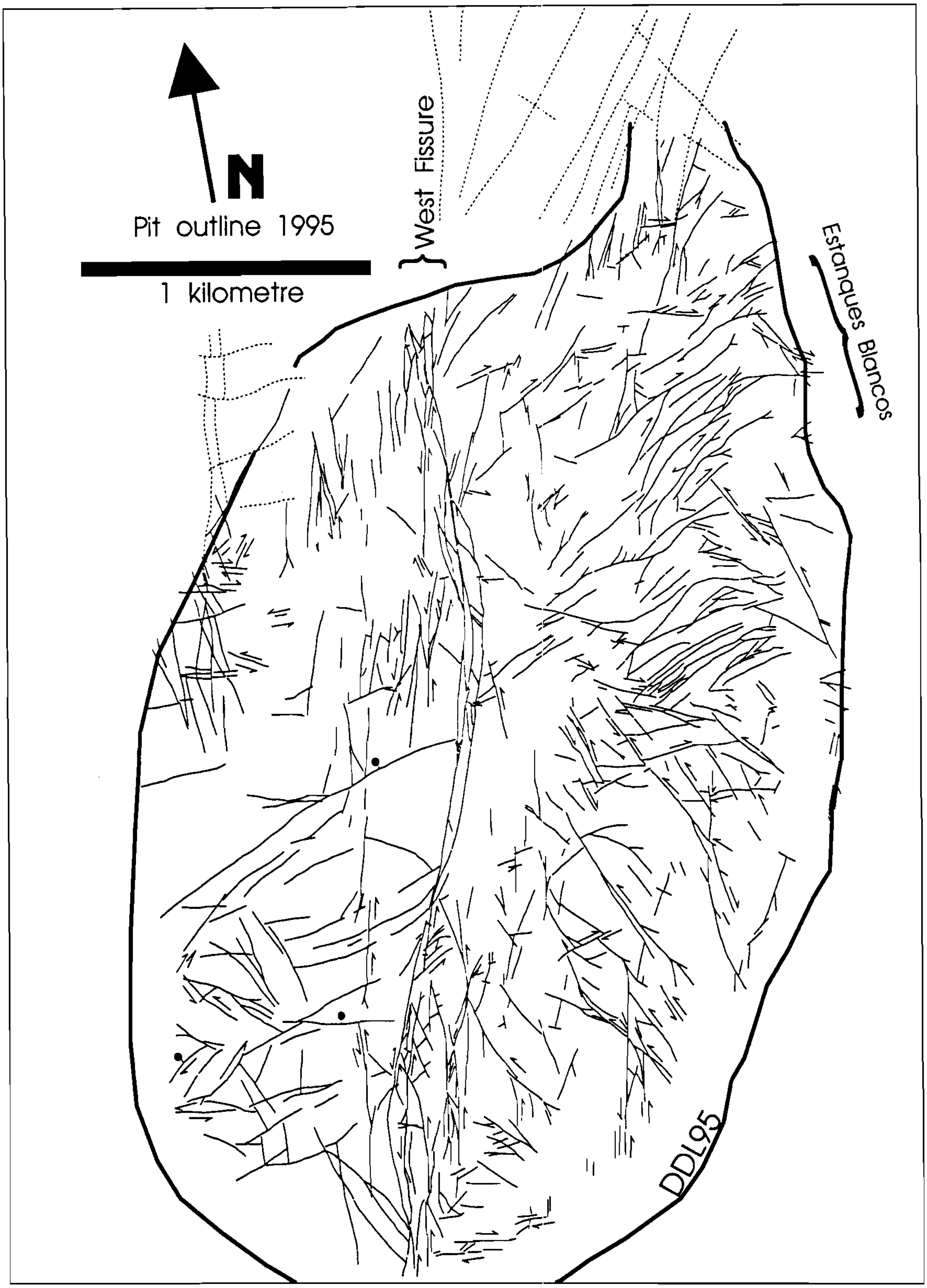


Fig.1. Distribution of mapped faults and fault-veins found within and adjacent to the Chuquicamata open pit. All faults are within the domain of the Falla Oeste fault system. The West Fissure can be seen to be comprised of a number of distinct but inter-related fault branches. Sense of displacement shown.

Chuquicamata complex support a NE-SW directed compressive stress regime at this time. Late magmatic alteration and porphyry copper mineralization took place as the intrusive cooled. Plate tectonic reconstructions and estimates of relative plate velocities indicate that a dextral transpressive tectonic regime was likely active during Eocene-Oligocene times (Pardo-Casas and Molnar, 1987; Pilger, 1984).

The Estanques Blancos fault system is within a domain that contains an array of streaming veins and veinlets indicating a structural control and anisotropy of mineralization. The dominant faults are all brittle features bearing breccia and fault gouge containing dextral shear sense indicators. In a number of cases the gouges are almost completely composed of the sulfides chalcocite and pyrite. The majority of these faults have sericite alteration halos. Recent $^{40}Ar$-$^{39}Ar$ radiometric dating indicates this alteration-mineralization event occurred at ~31 Ma. This fault system dextrally displaces the Mesabi fault system approximately 500 m. These faults although having displacements along strike may also have a substantial normal component of slip.

Field mapping, geochemical traverses and grain size analysis show the West Fissure to have undergone periodic, multiple, weakly oblique strike-slip events beginning after mainstage mineralization. Original cross-sections based on drillcore intersections with the fault illustrated a geometry incapable of large strike-slip motions. Relogging and interpretation of this fault in drillcore shows a system of inter-related branches capable of the previously hypothesized tens of kilometres (35-40 km) of displacement (Ambrus, 1979). Different metals concentrate within different fault branches indicating distributed displacements and increasing the potential for displaced mineralized fault slivers, or side wall rip-outs. Although some of the faults in the Falla Oeste fault system show structural fabrics inversion (Reutter et al., 1993); (eg. Mesabi), a detailed study of the West Fissure shows no indication of inversion and shows no evidence of high temperature ductile deformation within, or adjacent to, the present fault zone.

## CONCLUSIONS

The superb exposure of the Falla Oeste fault system outcropping in the Chuquicamata open pit allows one to observe early deep ductile emplacement and pre- to syn-mineralization structural features through late upper crustal brittle features and their relationships to multiple mineralization events. Conclusions that can be drawn from mesoscopic to microscopic analyses of structural features are as follows :

- The Falla Oeste is a large fault system that has been active in northern Chile since the Eocene. Different faults and fault systems within the Falla Oeste can be differentiated and evaluated with respect to mineralization and alteration events.
- Earliest deformation is associated with the emplacement of the Chuquicamata intrusive complex and continued transpressive deformation associated with the late Eocene Incaic tectonic phase.
- Main stage mineralization occurred after the peak of the Incaic tectonic phase and prior to the development of the West Fissure.
- The Estanques Blancos fault system had formed and was active during the latest alteration-mineralization event ~31 Ma.
- The West Fissure is a late upper crustal structure that played no part in the emplacement of the Chuquicamata intrusive complex, or the initial development of the associated porphyry copper deposit. However, it played an important role in the control of mineralization during the ~31 Ma and the supergene mineralization events.

## REFERENCES

Ambrus, W.J., 1979. Emplazamiento y mineralizacion de los porfidos cupriferos de Chile. Unpublished Ph.D. Thesis, Universidad de Salamanca, Spain, 313p.

Lopez, M.V., 1939, The primary mineralization at Chuquicamata, Chile, S.A. Economic Geology, v. 65, p. 674-711.

Maksaev, V., 1990. Metallogeny, Geological Evolution and Thermochronology of the Chilean Andes Between

Latitudes 21° and 26° South, and the Origin of Major Porphyry Copper Deposits. Unpublished PhD thesis, Dalhousie University, 354 pages.

Reutter K.J., Scheuber, E., and Helmcke, D., 1991, Structural evidence of orogen-parallel strike-slip displacements in the Precordillera of northern Chile: Geol. Rdsch. v. 80, p. 135-153.

Reutter K.J., Chong, G., and Scheuber, E., 1993. The "West Fissure" and the Precordilleran fault system of northern Chile: In Andean Geodynamics, ISAG 1993, ORSTROM/Oxford University, Oxford, U.K., p 237-240.

Scheuber, E. and Reutter, K.J., 1992, Magmatic arc tectonics in the Central Andes between 21° and 25° South: Tectonophysics, v.205, p. 127-140.

Tomlinson, A.J., Mpodozis, C., Cornejo, P.C. and Ramirez, C.F., 1993.Structural geology of the Sierra Castillo-Agua Amarga fault system, Precordillera of Chile, El Salvador-Potrerillos: In Andean Geodynamics, ISAG 1993, ORSTROM/Oxford University, Oxford, U.K., p 259-262.

# SKARN FORMATION BENEATH LASCAR VOLCANO, N CHILE: EVIDENCE FOR THE WESTERN CONTINUATION OF THE YACORAITE FORMATION (LATE CRETACEOUS) OF NW ARGENTINA

Rosa A. MARQUILLAS(1) & Stephen J. MATTHEWS(2)

(1) Facultad de Ciencias Naturales, CONICET-Universidad Nacional de Salta, Buenos Aires 177, 4400 Salta, Argentina.
(2) Department of Geology, University of Bristol, Wills Memorial Building, Queens Road, Bristol BS8 1RJ, UK.

**KEY WORDS:** Central Andes, Puna-Altiplano, Lascar, skarn, Late Cretaceous, limestone.

## INTRODUCTION

We report the occurrence of skarn xenoliths in the eruption products of Lascar volcano, N Chile. These rocks are samples of a chemically zoned metamorphic-metasomatic skarn body developed around the subvolcanic magma chamber. This skarn system is still actively developing at present. Using a variety of geochemical techniques we have identified the host rock as impure limestones and carbonate-cemented sandstones belonging to the Late Cretaceous Yacoraite formation, which outcrops extensively in NW Argentina, thus proving that this unit extends a considerable distance westwards beneath the young volcanic zone in this area.

## YACORAITE FORMATION

In the Early Cretaceous several rift troughs opened in northwest Argentina and surroundings, thus starting the accumulation of the Salta Group basin and equivalents. During Mid-Eocene times the Inca diastrophism inverted the basin and interrupted sedimentation (Marquillas and Salfity, 1988; Salfity and Marquillas 1994). The Yacoraite Formation (Maastrichtian-Eopaleocene) is an extensive, partly dolomitic limestone of the postrift accumulations of the Salta Group. This unit has developed not only over the former synrift troughs but also over the San Pablo high and other structural highs (Figure 1). In the Argentinian Puna the limestone lies on Ordovician basement at the northern El Toro Lineament, and on Precambrian basement in the south. In the Puna the outcrops are scarcer and more isolated than in other areas. The development of these accumulations also affected the territories of Bolivia and very probably the north of Chile. The Yacoraite Limestone was deposited by epeiric flooding, in a frame of tectonic quiescence; deposition occurred under shallow water conditions, with frequent subaerial exposure. These transgressive deposits are mainly ooid grainstone, packstone, stromatolites, sandstone, and in the relatively deep facies, shales and the calcareous mudstones. A maximum thickness of 200 m has been recorded.

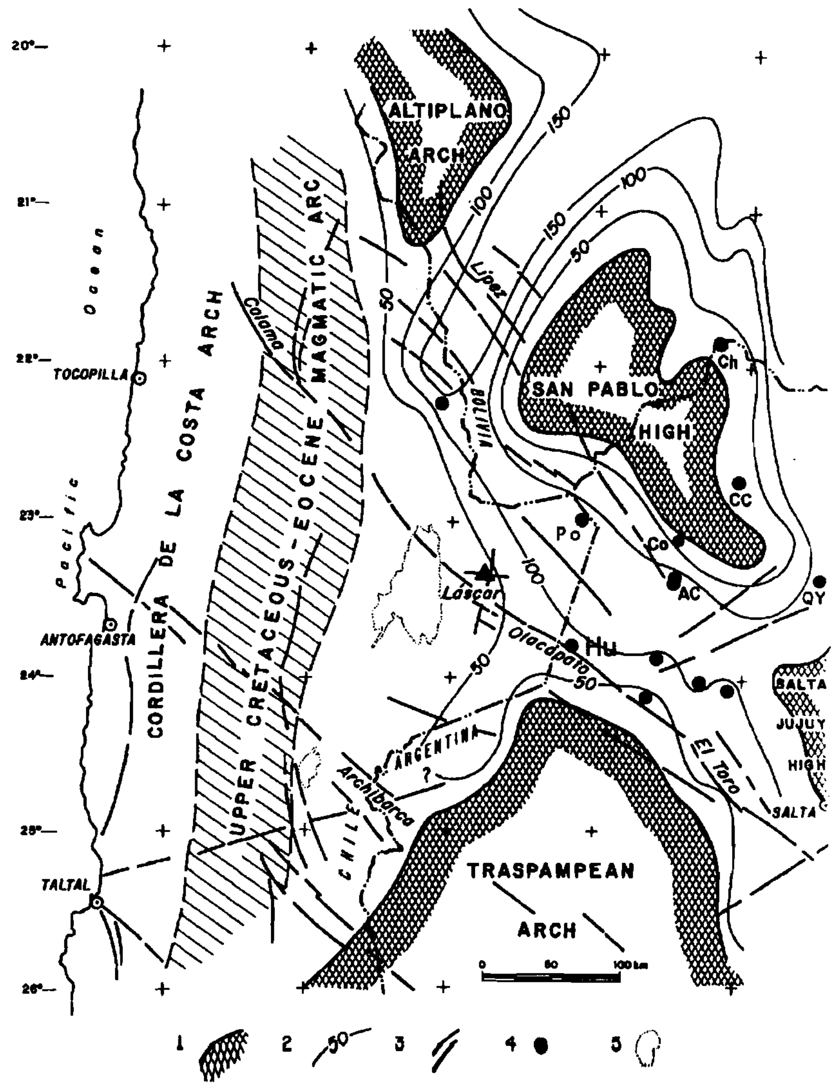


Figure 1. Isopach map of the Yacoraite formation, showing the position of Lascar volcano. 1: Basement high. 2: Isopach in metres. 3: Fault or lineament. 4: Isopach control point. 5: Salar. Hu = Huaytiquina, Po = Poquis, Ch = Chaupiorco, CC = Casa Colorada, Co = Coranzuli, QY = Quebrada Yacoraite, AC = Abra Calvario.

## LASCAR VOLCANO

Lascar is a composite calc-alkaline stratovolcano located on the volcanic front in NE Chile (5,592m, 23°22'S, 67°44'W). Its eruption products are medium- to high-K andesitic to dacitic rocks in the form of lavas and pyroclastic flows (Matthews *et al.*, 1994a). The magmas are the product of combined magma mixing, fractional crystallization and assimilation of country rocks. The dominant magmas are 2-pyroxene andesites although 2-pyroxene dacites and hornblende- and biotite - rich dacites are also important. Lascar magmas are highly oxidized, containing anhydrite phenocrysts, and this has been attributed to $fO_2$ buffering by a coexisting $SO_2$ - $H_2S$ rich gas phase (Matthews *et al.*, 1994b).

## SKARN XENOLITHS

Skarn xenoliths are common throughout the stratigraphy of the volcano (Matthews *et al.*, 1994a; 1996). They have a variety of mineralogies, ranging from contact-metamorphic wollastonite-rich rocks to pyroxene-garnet and magnetite-pyroxene-rich samples which are interpreted as the product of Fe-Mn-Mg-Ti-Al metasomatism. These xenoliths originated in a zoned skarn system around the subvolcanic magma chamber of the volcano. Retrograde alteration by magma-derived acid sulphate fluids produced secondary carbonate veins and sulphate alteration.

## RELATIONSHIPS WITH THE YACORAITE FORMATION

Skarn xenoliths from Lascar are interpreted as fragments of a zoned skarn body around the subvolcanic magma chamber. The protolith has been identified as the Yacoraite formation on the basis of whole-rock major element and REE compositions. Following normalization of the whole rock major elements in both the xenoliths and samples of Yacoraite rocks by removal of the $CO_2$ from the analyses (e.g. CaOn = CaO X TOTAL / (TOTAL - $CO_2$), the wollastonite skarns fall in the range of Yacoraite compositions. Other skarn types can be related to the Wollastonite skarns by metasomatic addition of Fe, Mn, Mg, Ti and Al. Examples are shown in Figure 2.

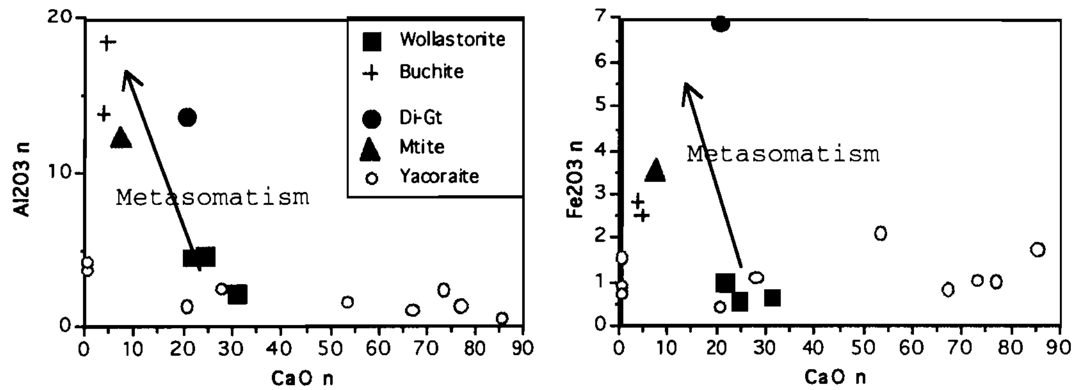


Figure 2. Plot of normalized whole-rock $Al_2O_3$ and $Fe_2O_3$ showing the relationship between various types of Lascar skarn xenoliths and rocks of the Yacoraite formation. The wollastonite skarns are the product of thermal metamorphism.

Chondrite-normalized REE spiderplots of Yacoraite samples are similar to those of the skarn xenoliths (light REE enrichment, positive and negative Eu anomalies). The slopes of the plots for both Yacoraite samples and the skarn xenoliths fall in the same range. The wollastonite skarns have a negative Ce anomaly of variable size which can be traced to late-stage retrograde calcite veins. REE and stable isotopic data ($^{13}C$ and $^{18}O$) indicate that this calcite was dissolved from Yacoraite country rocks and redeposited in the skarn by magma-derived acid fluids (Matthews *et al.*, 1996).

## CONCLUSIONS

Lascar volcano is underlain by a zoned skarn body developed within impure limestones which have been identified on geochemical grounds as belonging to the Yacoraite formation. The limestone protolith was geochemically similar to outcropping Yacoraite rocks along the Chile-Argentina border, indicating that similar facies are likely to underlie Lascar. This confirms previous interpretations that this unit extends a considerable distance westward beneath the Puna of NE Chile. It is likely that the subvolcanic intrusions beneath the volcanic zone in this area have developed an extensive field of skarn orebodies and that the volcanoes represent the surface expression of such an orefield.

## REFERENCES

Marquillas, R.A. & Salfity, J.A., 1988. Tectonic framework and correlations of the Cretaceous-Eocene Salta group, Argentina. In: Bahlburg, H., Bretkreuz, Ch. & Giese, P. (Eds.). *The Southern Central Andes: Lecture Notes in Earth Sciences,* **17,** Springer-Verlag Berlin Heidelberg, 119-136.

Matthews, S.J., Jones, A.P. & Gardeweg, M.C., 1994a. Lascar Volcano, Northern Chile; Evidence for Steady-State Disequilibrium. *Journal of Petrology,* **35,** 401-432.

Matthews, S.J., Jones, A.P. & Beard, A.D., 1994b. Buffering of melt oxygen fugacity by sulphur redox reactions in calc-alkaline magmas. *Journal of the Geological Society, London,* **151,** 815-823.

Matthews, S.J., Marquillas, R.A., Kemp, A.J., Grange, F.K. & Gardeweg, M.C., 1996. Active Skarn Formation Beneath Lascar Volcano, Northern Chile: A Petrographic and Geochemical Study of Xenoliths in Eruption Products. *Journal of Metamorphic Geology* (In Press).

Salfity, J.A. & Marquillas, R.A., 1994. Tectonic and sedimentary Evolution of the Cretaceous-Eocene Salta Group Basin, Argentina. In: Salfity, J.A. (Ed.). *Cretaceous tectonics of the Andes.* Earth Evolution Sciences, Freidr. Vieweg & Sohn, Braunschweig-Wiesbaden, 266-315.

# OLIGOCENE-RECENT SEDIMENTARY AND TECTONIC EVOLUTION OF THE CALAMA BASIN, N. CHILEAN FOREARC

Geoffrey MAY (1), Adrian J. HARTLEY (1) and Finlay M. STUART (2)

(1) Dept. of Geology & Petroleum Geology, King's College, University of Aberdeen, AB9 2UE, UK.
(2) Scottish Universities Research & Reactor Centre, East Kilbride, Glasgow, G75 0QF, UK.

**KEY WORDS:** Forearc basin, $^{40}Ar/^{39}Ar$ dating, Stratigraphy, Tectonic evolution, West Fissure.

## INTRODUCTION

The Calama Basin is located between 22°S and 23°S in the forearc of N. Chile (Fig. 1). It forms one of the pre-Andean basins of the region that are situated between the Pre-Cordillera (Cordillera de Domeyko) to the west and the current volcanic arc (Western Cordillera) to the east. Sediments within the basin have been poorly constrained stratigraphically but were thought to comprise 3 unconformable successions of lower(?) Miocene to Pleistocene age (Naranjo & Paskoff, 1981). New data is presented that shows the basin fill to be older and more complex and recording a number of deformation phases which appear to correlate well with known movements on the West Fissure fault system.

## BASIN STRATIGRAPHY

The basin is filled with over 700 m of continental sediments that form 5 unconformable successions of Oligocene to Quaternary age (Fig. 2). Newly obtained $^{40}Ar/^{39}Ar$ ages (Table 1) from ash horizons interbedded within each succession has allowed constraints to be placed on the timing of sedimentation and intervening deformation events.

A summary of the basin stratigraphy is shown in Figure 2. Up to 500(?) m of alluvial braidplain conglomerates comprise the lowest succession in the basin. They unconformibly overlie the Cretaceous to Eocene Purilactis Group along the eastern margin of the basin and contain a 30.15±0.26 Ma ash near the top of the succession, thereby constraining their age as lower Oligocene. These are unconformably

| Sample | Site | Location | Age (Ma) |
|---|---|---|---|
| EK19-A-34 | 1 | Quebrada Yalqui | 30.15±0.26 |
| EK19-A-26 | 2 | Quebrada Yalqui | 19.62±0.36 |
| Sifon Ign* | 3 | Various | 8.33±0.15 |
| EK19-A-20 | 4 | Angostura | 7.82±0.10 |
| EK19-A-7 | 5 | West of Calama | 5.76±0.10 |
| EK19-A-10 | 6 | Angostura | 3.37±0.06 |

Table 1. $^{40}Ar/^{39}Ar$ ages for volcanic deposits within the Calama Basin. The site numbers correspond to the stratigraphic positions shown in Figure 2. *indicates average age (K-Ar) of the Sifon Ignimbrite obtained by De Silva (1989).

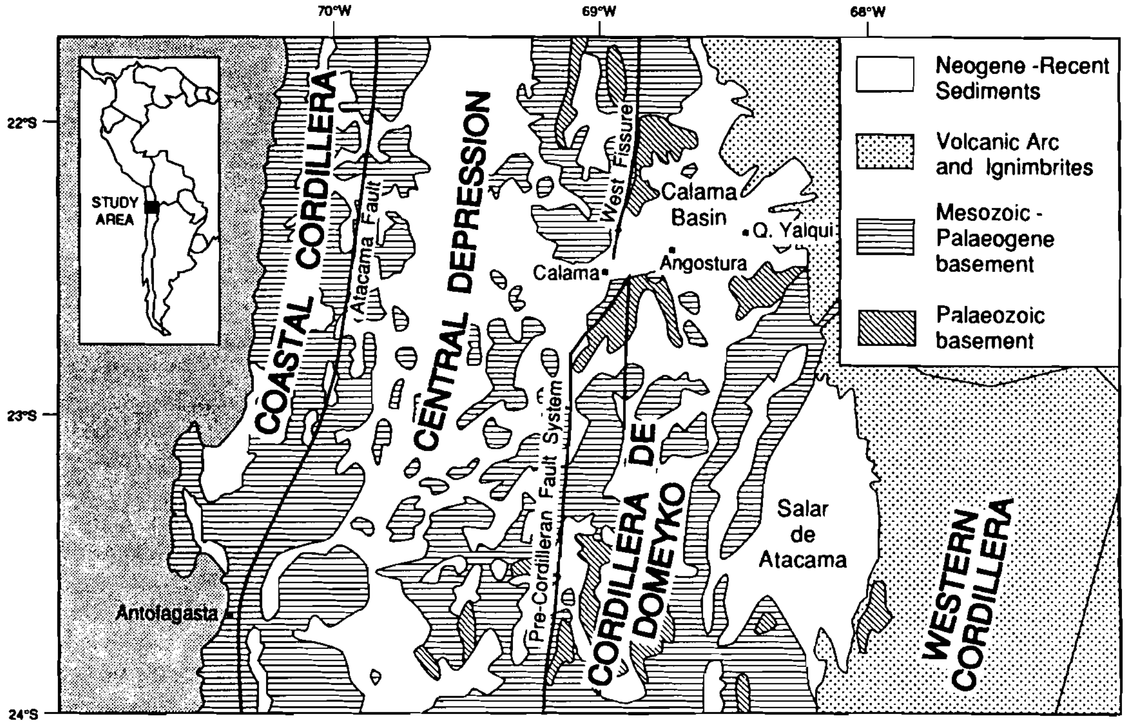


Figure 1. Location of the Calama Basin within the N. Chilean forearc.

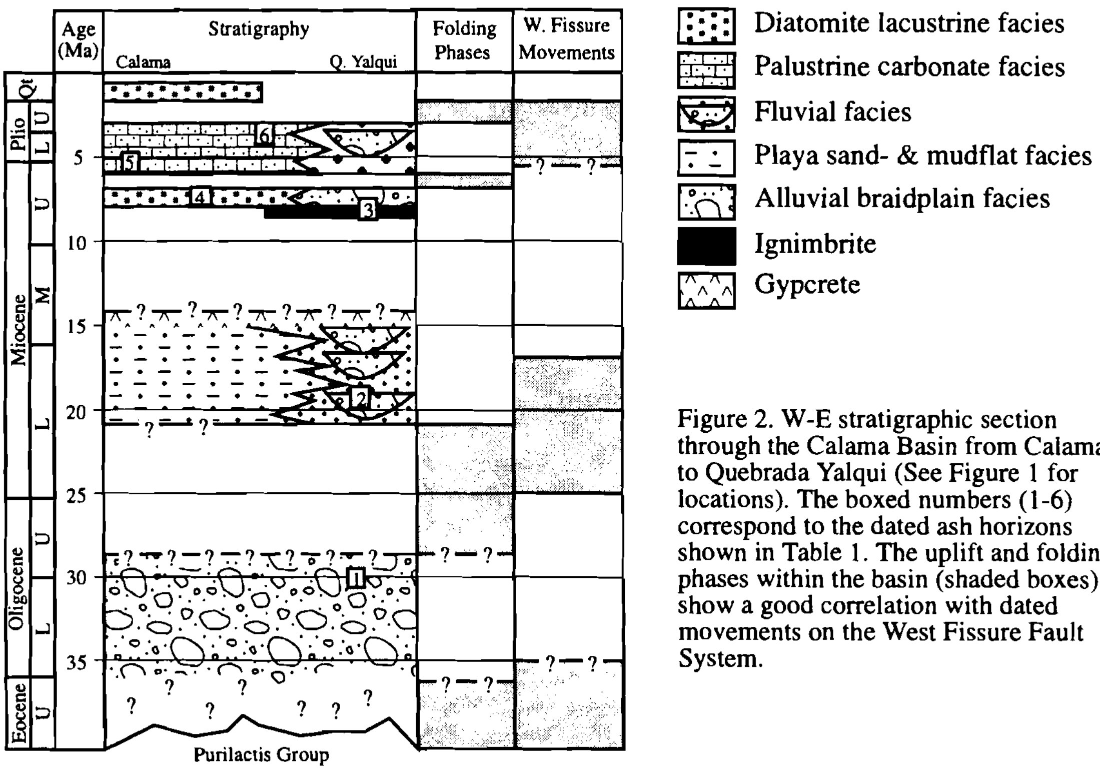


Figure 2. W-E stratigraphic section through the Calama Basin from Calama to Quebrada Yalqui (See Figure 1 for locations). The boxed numbers (1-6) correspond to the dated ash horizons shown in Table 1. The uplift and folding phases within the basin (shaded boxes) show a good correlation with dated movements on the West Fissure Fault System.

overlain by approximately 100 m of fluvial and playa sediments. An ash towards the base of this sequence has yielded an age of 19.62±0.36 Ma placing sedimentation within the Lower Miocene. An upper age is uncertain but the development of thick gypcretes suggests a significant time gap prior to resumption of sedimentation in the Upper Miocene. The Upper Miocene to Recent stratigraphy comprises 3 unconformable successions (May *et al.*, in review). Between 8.3 and 7 Ma 30 m of alluvial fan sediments, passing basinwards to lacustrine diatomites were deposited. These were locally folded prior to the deposition of up to 85 m of palustrine carbonates between 6 and 3 Ma. A widespread episode of folding followed, before the deposition of 20 m of localised Quaternary(?) fluvio-lacustrine sediments.

Phases of uplift and deformation within the basin are constrained as occurring during the upper Eocene, upper Oligocene-lower Miocene, upper Miocene and upper Pliocene. The cessation of sedimentation during the middle Miocene is presumably related to the regional change to hyper-arid conditions at this time (Alpers & Brimhall, 1988) and not tectonic uplift as the strata are conformable with overlying successions.

## DISCUSSION AND CONCLUSIONS

The onset of sedimentation during the lower Oligocene is mirrored in sediments of the Paciencia Formation in the Salar de Atacama Basin (Kape, 1996) and the Sichal Formation in the Central Depression (Jensen, 1992). Therefore, subsidence following the end of the Eocene Incaic phase of Andean deformation is seen across the forearc of the region. Phases of deformation on the West Fissure system (Fig. 1) occurred as dextral strike-slip during the Eocene (Reutter *et al.*, 1993), sinistral strike-slip during the lower Miocene (25-17 Ma: A. Tomlinson, pers. comm., 1995) and as post upper Miocene transpression. These tectonic phases correlate well with the observed deformation, and subsequent sedimentation, periods within the Calama Basin (Fig. 2).

## REFERENCES


Alpers C.N. & Brimhall G.H. 1988. Middle Miocene climatic change in the Atacama Desert, northern Chile: Evidence from supergene mineralization at La Escondida. *Geol. Soc. Am. Bull.*, 100, 1064-1656.

De Silva S.L. 1989. Geochronology and stratigraphy of the ignimbrites from the 21°30'S to 23°30'S portion of the Central Andes of northern Chile. *J. Volcanology and Geothermal Res.*, 37, 93-131.

Jensen P.A. 1992. *Las cuencas aluvio-lacustres Oligoceno-Neogeno de la region de ante-arco Chile Septentrional entre los 19° y 23° Sur.* Unpublished PhD thesis, University of Barcelona, Spain.

Kape S.J. 1996. *Basin Analysis of the Oligo-Miocene Salar de Atacama, Northern Chile.* Unpublished PhD thesis, University of Birmingham, UK.

May G. Hartley A.J. Stuart F.M. Turner, P. & Chong, G. In Review. Distinguishing between climatic and tectonic signatures in arid continental basins: an example fro the Upper Miocene-Pleistocene, Calama Basin, northern Chile.

Naranjo J.A. & Paskoff R.P. 1981. Estratigrafia de los depositos Cenozoicos de la region de Chiuchiu-Calama, Desierto de Atacama. *Revista Geologica de Chile,* 13-14, 79-85.

Reutter K.J., Chong G. & Scheuber E. 1993. The "West Fissure" and Precordilleran fault system of northern Chile. *Second International Symposium Andean Geodynamics, Oxford (UK),* 1, 237-240.

# STRUCTURAL STYLES IN THE DOMEYKO RANGE, NORTHERN CHILE

Susie M$^{c}$ELDERRY[1], Guillermo CHONG DIAZ[2],
David J. PRIOR[1] and Stephen S. FLINT[1]

(1) Department of Earth Sciences, University of Liverpool, P O Box 147, Liverpool L69 3BX, UK.
(2) Departamento de Geología, Universidad Católica del Norte, Antofagasta, CHILE.

**KEY WORDS:** Domeyko fault system, strike slip faults, thrust faults, kinematics

## INTRODUCTION

In the North of Chile, the Domeyko Range forms the Precordillera of the Andes, situated between Longitudinal Valley and the Western Cordillera. The Domeyko Fault System, otherwise known as the West Fissure Fault System, is located within the Domeyko Range (Figure 1). The fault system is known to extend for some 800km, from 21°S to 28°S. It can be divided into segments, based on the fault patterns and continuity. In between each segment is an area of non exposure (Mpodozis et al 1993). The northernmost segment extends 200km from Quebrada Blanca to Chuquicamata. Immediately to the south, from Chuquicamata to Limon Verde, the Calama Basin hides any exposure of the Domeyko Fault system. The central fault segment passes 300km from Limon Verde to Vaquillas and is limited to the south by 50km of non- exposure. The southern segment is about 200 km long and begins near El Salvador passing to Quebrada Carrizalillo. Considerable effort has been expended in the analysis of satellite imagery. As such, the traces of major structures are well known. All three accessible segments have been mapped and to some extent three dimensional geometric models have been developed. Kinematic analyses of these fault systems are rather rarer. Very detailed kinematic studies have been completed in particular mines but there are few data across more extensive regions of the Domeyko Fault system. This paper presents preliminary kinematic data from the southern portion of the central segment of the Domeyko Fault system and outlines some of the problems associated with collecting such data from the Domeyko region.

Faulting activity in the Andes, broadly corresponds temporally and spatially with the activity of the magmatic arc. Faulting is thought to relate to the emplacement of the porphyry bodies in the Eocene (Coira et al 1982, Scheuber et al 1994). The present high Cordillera has not always been the site of the magmatic arc. The locus of the magmatic arc in the Latest Cretaceous to Oligocene corresponded to today's Precordillera. It is believed that hot fluids in the crust, corresponding to the magmatic arc, raise crustal temperatures and pore-fluid pressures. These factors contribute to a weakening of the crust at the site of the arc. As the magmatic arc migrated east over time, so the deformation centres (generally fault systems) have also migrated east over the same time. The age of individual faults and the relationships between individual faults however remains obscure.

## STRUCTURE OF THE DOMEYKO RANGE

The structure of the Domeyko range is characterised by a core Palaeozoic rocks, mainly intrusives, flanked with igneous extrusives and volcanogenic sediments thought to be of Triassic age (Chong, 1973), some Triassic reefal sediments, Jurassic marine rocks and Cretaceous continental clastics.

There are later Tertiary sediments and ignimbrites further away from the range. The contacts between the core, Triassic and Jurassic and younger units are mainly tectonic, commonly thrusts (as exemplified by La Escondida fault). Typically at any latitude in a section across the Precordillera, the faults comprise one major strike slip fault and smaller thrust faults or vice versa (Tomlinson et al, 1993). The structure of this hill range has been interpreted as both an anticline (Reutter et al , in press) and a positive flower structure( Mpodozis et al, 1993).

The Domeyko Fault system was active during the Incaic tectonic event (Reutter et al., in press: Maksaev, 1990: Dobel et al, 1992) and the emplacement of the main copper porphyries is dated in the same time period. The fault system is interpreted to have accommodated a transpressional regime (cf. Sanderson and Marchini, 1981). Work carried out by Maksaev suggests a dextral sense to the main faults, whilst work by Reutter et al suggests a dextral sense for the system until 33Ma, when, after a change in the orientation of active faults from north south to NE-SW and back again, the sense changed to sinistral. This is based upon textural studies in altered rocks in the Chuquicamata region. The faulting has been interpreted as responding to the transmitted stresses from the subduction interface. From the relative plate motion vectors (Pardo-Casas and Molnar, 1987 ) this would lead to an expectation of a dextral sense from 49-35 Ma, followed by a more compressive phase until 26Ma then later sinistral compressive stresses.

In the southern portion of the central fault segment the main strike slip fault is the Sierra de Varas (SdV) fault. Abutting this are the Profeta thrust and the La Escondida fault. This study concerns the area to the south of the intersection of the SdV fault and the Profeta thrust (figure 1). Immediately to the north, the La Escondida fault and the SdV fault define a shear lozenge (Mpodozis et al, 1993b). The area of study may be the northern part of a similar lozenge. Here, the SdV fault provides the eastern limit of the fault system. The limit of the fault system in the west is a reverse fault juxtaposing Jurassic and Tertiary units in contact.

Passing from west to east, across the system, the first evidence of deformation is the fault bounding the Jurassic units. The fault dips to the east. In the north of the study area the fault is shallow, carrying Jurassic calcareous siltstones over poorly lithified Tertiary conglomerates. In Quebrada Profeta, also in the north of the study area, this fault occurs along an evaporite horizon of varying width, generally of the order of 10's of metres. In Quebrada Las Mulas, further to the south, the fault occurs over a much smaller width (~5m), cutting through an intrusive ignimbrite. The fault emplaces Jurassic rocks against younger Tertiary units to the west. The fault plane is sub-vertical with very well developed, mainly down dip slickenlines. The slickenlines are contained in seams of a few mm thickness comprising a fine grained, dark coloured material.. Profile views of many of these seams show offsets. Across approximately 5 metres perpendicular to the fault, these seams form a complex network. Cross cutting relationships indicate a complex local deformation history involving rather more than the simple down-dip movements. The mechanism of deformation here is clearly different to that in the evaporites, presumably a result of the presence of the ignimbrite with a different rheology and possibly higher temperature of deformation. These seams provide some of the freshest fault rock material from the Domeyko range and detailed laboratory investigations will be completed to constrain better the local kinematic history and the conditions of deformation.

Passing into the Jurassic marine rocks to the east, there are a variety of deformation structures. There are folds on 10's metres scale throughout the Jurassic and small scale faults. The folds have hinge lines orientated NE-SW, with shallow plunges. In the north of the area, there is a substantial evaporite horizon (Oxfordian - Kimmeridgian) which has folded in a complex manner. This evaporitic material is contained within a fault bound wedge which dies out to the south. The hinge lines of folds lie sub parallel to the Profeta thrust to the east suggesting that the folding and this structure may be related.

The Jurassic is limited to the east by the Profeta thrust. Interactions with topography clearly show that this dips shallowly to the east. The Profeta thrust emplaces andesites, probably of Triassic age, above the Jurassic marine rocks. No outcrop scale kinematic indicators have been observed associated with the Profeta thrust.

In Quebrada Las Mulas, at the south of the studied area, andesites, probably of Triassic age, have been mapped in detail, at scales of 1:500, in an attempt to unravel the structural history. The andesites exhibit primary structures such as flow banding and are cut by a series of breccia bands, of 2-20cm thickness. The significance of these breccia bands is somewhat ambiguous. The primary fabrics form a cluster when plotted as poles on a stereonet. The breccia bands at the eastern margin have a single intersection. Further west however the breccia bands have a seemingly random distribution. It is uncertain whether they represent some tectonic disturbance. If treated as Andersonian structures the intersection may represent the intermediate stress axis. Alternatively the breccias may be depositional, possibly forming around "tongues" of andesite as it flowed. To resolve this, sample analysis and geometrical modeling are being undertaken.

To the east the SdV fault is poorly exposed. It is assumed to be vertical, from its interaction with topography, and is covered by a lower Miocene ignimbrite which it offsets with a dextral sense by a few 10's of metres (Mpodozis et al, 1993b).

## OUTSTANDING PROBLEMS

The different lithostratigraphic units of the Domeyko Range have responded differently to the deformation associated with the Domeyko fault system. Kinematic information is slight, but it is clear that there are variations in kinematics and kinematic histories on several scales. It is clear that different lithologies will have had different rheologies and will have responded differently in deformation. This is particularly important if there were significant thermal differences, such as those generated by intrusions concomitant with deformation. However, at this stage, it is not clear how much of the differences in deformation style and kinematics can be attributed to partitioning in a single deformation episode as opposed to the superposition of discrete events with different kinematics and perhaps at different conditions.

One practical problem is in obtaining good kinematic information from desert exposures. Whilst lack of vegetation is a clear advantage for remote sensing and large scale mapping it is a hindrance to detailed kinematic analyses. Good exposures are rare, especially in the case of important contacts. Where exposure is observed one has to fairly pervasive fracturing related to very recent tectonics, unroofing and weathering.

In order to add as much detailed information as possible about the chronology, absolute timing, sense and conditions of deformation, further work is being carried out on numerous samples. Dating, stable isotope work (to identify source and mobilisation of fluids), microstructural analysis (to identify deformation mechanisms and senses of movement) and geometrical modeling are all being undertaken.

## REFERENCES

Chong, G. 1973, Reconocimiento geológico del area Catalina, Sierra de Varas y estratigrafía del Jurásico del Profeta. Memoria, Universidad de Chile, Fac Ciencias Fis. y Mat.

Coira B., Davidson J., Mpodozis C. & Ramos V. 1982. Tectonic and Magmatic evolution of the Andes of North Argentina and Chile. Earth Science Reviews , 18, 303-332.

Dobel R., Friedrichsen H., & Hammerschmidt K. 1992. Implication of Ar/Ar dating of early Tertiary volcanic rocks from the north Chilean Precordillera. Tectonophysics, 202 55-81.

Maksaev V. 1990. Metallogeny, geological evolution and thermochronology of the Chilean Andes between latitudes 21° & 26° south and the origin of major porphyry copper deposits. PhD thesis, Dalhousie University,Halifax, Nova Scotia, Canada.

Mpodozis C., Marinovic N.,Smoje I. 1993a. Eocene left lateral strike slip faulting and clockwise block rotations in the Cordillera de Domeyko, West of the Salar de Atacama, Northern Chile. 2nd ISAG,Oxford (UK) 21-23/9/1993

Mpodozis C., Marinovic N., Smoje I., Cuitino. 1993b. Estudio Geologico estructural de la Cordillera Domeyko entre Sierra Limon Verde y Sierra Mariposas: Region de Antofagasta. Report.

Pardo-Casas F. & Molnar P. 1987. Relative plate motion of the Nazca (Farallon) and South American plates since Late Cretaceous time. Tectonics v6 : 233-248.

Prinz P., Wilke H.-G., Hillebrandt A. V. 1994. Sediment accumulation and subsidence history in the Mesozoic marginal basin of Northern Chile. Tectonics of the southern Central Andes. Eds, Reutter K.-J., Scheuber E., Wigger P. J.

Reutter K.-J., Scheuber E., Chong G. in press. The Precordilleran Fault System of Chuquicamata, Northern Chile: evidence for reversals along arc-parallel strike slip faults. Tectonophysics.
Sanderson D. J. & Marchini R. D. 1981. Transpression. Journal of Structural Geology, v 6 (5)449-458.
Scheuber E., Bogdanic T., Jensen A., Reutter K.-J. 1994. Tectonic development of the North Chilean Andes in relation to plate convergence and magmatism since the Jurassic. Tectonics of the Southern Central Andes, Eds; Reutter K.-J., Scheuber E., Wigger P. J.
Tomlinson A. J., Mpodozis C., Cornejo P. C., Ramirez C. F. 1993. Structural Geology of the Sierra Castillo - Agua Amarga fault system, Precordillera of Chile, El Salvador - Potrerillos. 2nd ISAG, Oxford (UK), 21-23/9/1993.

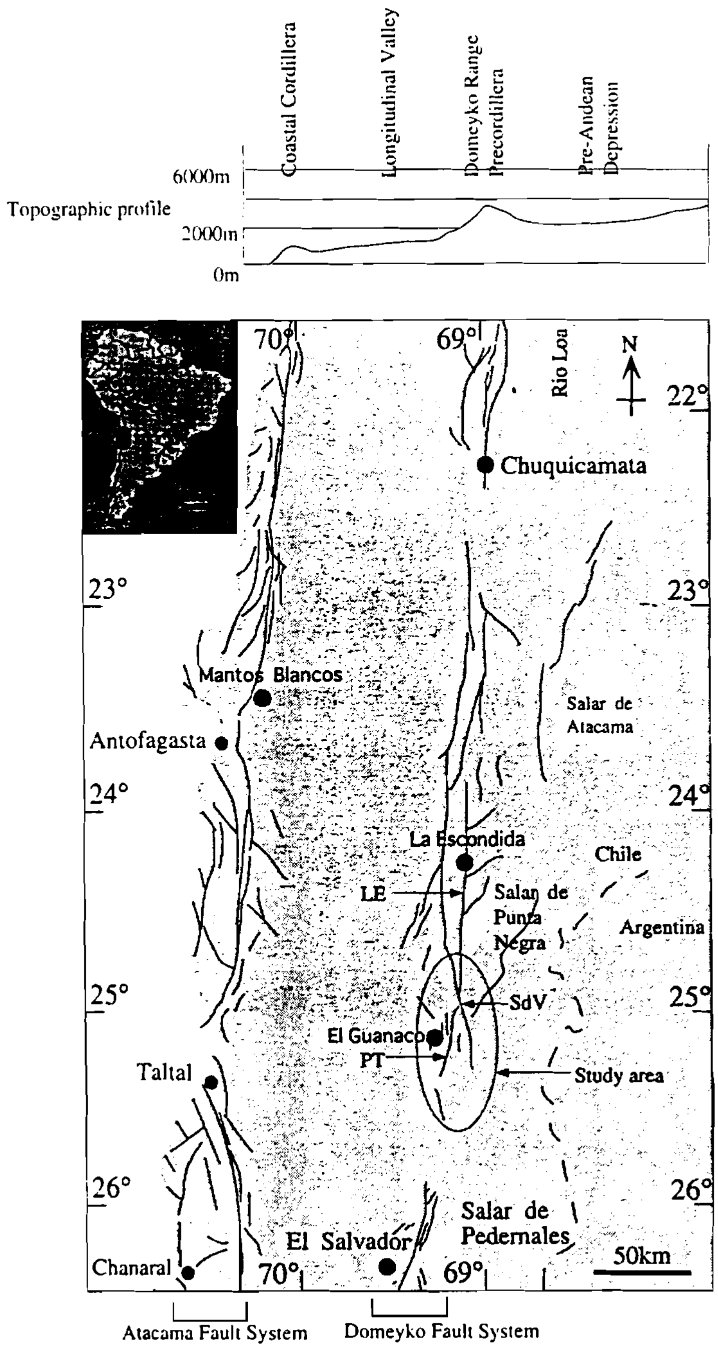


Figure 1, (modified from Prinz et al 1994), showing location, fault system and topographic profile. PT : Profeta Thrust. LE : La Escondida Fault SdV : Sierra de Varas Fault

# STRUCTURE OF THE EASTERN CORDILLERA IN NORTHERN ARGENTINA

Ricardo MON

Facultad de Ciencias Naturales, Universidad Nacional de Tucumán; Miguel Lillo 205, 4000 Tucumán, Argentina.

**KEY WORDS** Andes basement - involved folding thrusting Plio-pleistocene

## INTRODUCTION

The structure of the most southerly segment of the Eastern Cordillera, located between 22° and 27° S in northern Argentina, clearly distinguish it from those extending northward in Perú and Bolivia. This segment of the Eastern Cordillera developed over an ancient west-verging faultbelt belonging to the Ocloyic orogen (late Ordovician-Silurian) and over Cretaceous rift basins which are oblique to the strike of the Cenozoic Cordillera, therefore it shows notable along-strike differences in its stratigraphy and structure. The Proterozoic basement was intensely involved in Cenozoic folding. It is a foldbelt where most of the anticlines, cored by Proterozoic basement (Figures 1-A and 1-B), were thrust and imbricated by the younger than 1,5 Ma Diaguita movements. Some of the early Paleozoic and the late Cretaceous structures were reactivated and inverted, and sometimes transported pasively to the surface by the Cenozoic thrusts, therefore some of the structural complications are inherited from older tectonic orogenies.

## STRUCTURE

Between 22° and 24° S lat the Eastern Cordillera is a fold and thrust-belt with a predominantly eastward vergence (Figure 1-1). The west verging structures croping out at its west border are in fact older Ocloyic structures transported passively to the surface (Figure 1-2). This segment consists mainly of folds of Precambrian basement covered unconformably by thick Cambrian (Meson Group) and Ordovician (Santa Victoria Group) marine strata (Turner, 1960) (Figure 1-A and 1-B). The Tertiary and late Cretaceous successions are scarcely developed. South of 24° S lat, the Eastern Cordillera displays double-vergence, its western edge is thrust over the tectonic depression of the Calchaquí Valley and its eastern edge is thrust over the Subandean Ranges. South of 25° S lat, the Eastern Cordillera undergoes a pronounced change: the Proterozoic basement plunges under the late Cretaceous (Salta Group) successions; the early Paleozoic strata thinned out and the Cretaceous strata are lying directly over the Proterozoic basement. The Cretaceous-Tertiary continental rocks attain a combined thickness greater than 4000 m. This part of the chain consists of major folds developed in these Cretaceous and Tertiary continental successions. It coincides with a pronounced structural depression where the axis of the basement- involved folds located northward are plunging to the south and those located southward plunge to the north. The southern end of the Eastern Cordillera (south of 26° S lat) is an anticlinorium which plunges at its both ends, made up of basement folds with a thin Cretaceous-Tertiary cover (Figure 1-A).

The shortening decreases southward from 40%, measured in some cross-sections of the Quebrada de Humahuaca, to 25% at its southern end. The reconstructions of the deep structure based on surface data and on interpretation of seismological data allow to postulate a regional décollement surface about 20 km deep. (Grier 1990; Cahill et al. 1992). The décollement surface of the Subandean Ranges seems to be higher , therefore it could be a ramp below the boundary between Eastern Cordillera and Subandean Ranges (Figure 1-3).

The present-day structure is the result of several superposed tectonic movements, starting in late Cretaceous, and the reactivation of ancient Paleozoic structures. This chain developed over a west verging fault belt belonging to the foreland of the Ocloyic orogen (Mon, 1993). Probably the Ocloyic faults were partially reactivated coinciding with the west-verging backthrusts of the western edge of the Eastern Cordillera. It seems that there is a correlation between the west-verging tendency and the intensity of the Ocloyic deformation. The Ocloyic deformation decreases northward in the same way as does the double vergence. The Cretaceous successions cover unconformably the older rocks; they are lying over the Precambrian basement and different Paleozoic levels. Because of the long stratigraphic hiatus it is impossible to establish the age of the movements represented by this unconformity, which may be attributed to the Ocloyic movements as well as to the younger Precretaceous movements. Upper Miocene red beds lie unconformably over the late Cretaceous beds and the older rocks indicating a folding episode between the Upper most Cretaceous and the Upper Miocene. They can be attributed to the Pehuenche movements ( Salfity et al. 1984; Jordan & Alonso, 1987). The most intense movements occurred between Upper Pliocene and Pleistocene, when the pronounced uplifting of the chain produced the sedimentation in intramontane basins of thick fanglomerates beds yielding isotopic ages of 1,5 Ma (Marshall et al. 1982). These beds are overriden by Cretaceous and Proterozoic basement plates. That signifies that these segments of the Eastern Cordillera were thrust over the products of its own erosion at very recent time. These last movements belong to the Diaguita orogeny. Probably the folding of the Eastern Cordillera started with fault-propagation folds which later were dislocated by the younger Diaguita thrusts. After Marrett et al.(1994) and Claudohous et al. (1994) this young thrusting episode is not represented northward of 22° 30' where it is replaced by normal and strike slip faults. This cinematic change could be associated to major crustal variations (Allmendinger et al. 1993; Whitman et al. 1993).

The Eastern Cordillera rides over the cover of the Subandean Ranges by major thrusts set en echelon (Figures 1-A; 1-3). This tectonic edge coincides with a paleogeographic boundary represented by the west termination of the Silurian and Devonian successions of the Subandean Ranges. These successions are absent in the Eastern Cordillera. North of 24° S lat, the west margin of the Eastern Cordillera is marked only by a morphological change with the Puna. The Puna has internal drainage and the drainange of the Eastern Cordillera flows to the Atlantic basins. South of 24° S lat, the west edge of the Eastern Cordillera is thrust over the Tertiary succssesions filling the tectonic depression of the Calchaquí Valley. Southward the eastern belt of the Eastern Cordillera has a sudden termination at 27° S lat, the west belt has a transitional passage with the Pampean Ranges (Figure 1 A).

## CONCLUSIONS

Southward of 22° S lat, near the boundary between Argentina and Bolivia, the Proterozoic basement reaches the surface and becomes the main component of this part of the chain. The sedimentary cover, made-
up of Paleozoic, Cretaceous and Tertiary beds, was folded together with the basement. Folding took an important part in the deformation of this segment of the Eastern Cordillera. Major thrusting is related to the late movements of the tectonic evolution, dislocating the folds already formed. In this segment of the Eastern Cordillera there are not major décollements and lateral tectonic transport as those described northward, in Bolivia (Sempere et al, 1988; Kley & Gangui, 1993). Probably this segment represents the outcrops of the deep basement thrust sheets postulated by Kley & Gangui, 1993 in the subsurface of southern Bolivia. The tectonic movements become younger from north to south; the late Oligocene-early Miocene movements described in Bolivia (Sempere et al. 1990) are replaced southward by late Miocene-Pliocene movements. The 9 Ma thrusting episode reported by Cladohous et al. 1994 in the Altiplano continued until 1,5 Ma or even younger times (Mon et al. 1993; Marrett et al. 1994). The

major thrust designated as "Cabalgamiento Andino Principal" (Semp[ere et al. 1988) was not identified in the surface southward of 22° S lat, but the "Cabalgamiento Frontal Principal" (Sempere et al. 1988} can be clearly recognized, it represents the boundary between the Eastern Cordillera and the Subandean Ranges.

**FIGURE 1.** 1 - A. Regional schematic map. 1 - B. Map of basement-involved folds at both sides of the Humahuaca valley. 1-1; 1-2 and 1-3 cross-sections of the east-verging segment of the Eastern Cordillera, in cross-section 1-2 are represented west verging ocloyic (Lower Paleozoic) structures transported passively to the surface. Proterozoic basemet, horizontal lines; undifferentiated Lower Paleozoic, solid points; Upper Cretaceous, vertical lines; Tertiary, open points.

## REFERENCES


Allmendinger, R.W., Gubbels, T., Isacks, B. & T. Claudohous, T., 1993. Lateral variations in late Cenozoic deformation, Central Andes, 20 - 28° S. Second International Symposium Andean Geodynamics, 1: 155-158. Oxford.

Cahill, T., Isacks, B.L., Whitman, D., Chatelain, J.L.. Perez, A., Mong, Chiu, J., 1992. Seismicity and tectonics in Jujuy province, northwestern Argentina. Tectonics, 11: 944-959.

Cladouhos, T.T., Allmendinger, R.W., Coira, B y Farrar, A., 1994. Late Cenozoic deformation in the Central Andes: fault kinematics from the northern Puna, northwestern Argentina and southwestern Bolivia. Journal of South American Earth Sciences, 7:209-228.

Grier, M.E., 1990. The influence of the Cretaceous Salta rift basin in the development of Andean structural geometries, NW Argentina Andes. Ph.D. disertation Cornel University, Ithaca, New York. Unpublished.

Jordan, T.E. & Alonso, R.N., 1987. Cenozoic stratigraphy and basin tectonics of the Andes mountains, 20 - 28° South latitude. The American Association of Petroleum Geologists, 71:49-64.

Kley, J. & Gangui, A., 1993. Basement-involved thrusting in the Eastern Cordillera Subandean transition zone southern Bolivia: evidence from cross-section balancing and gravimetric data. Second International Synposium Andean Geodynamic, 1:203-206. Oxford.

Marrett, R.A., Allmendinger, R.W., Alonso, R.N. & Drake, R.E., 1994. Late Cenozoic tectonic evolution of the Puna Plateau and adjacent foreland, northwestern Argentine Andes. Journal of South American Earth Sciences, 7: 179-207.

Marshall, L.G., Buttler, R.L., Drake, R.E. & Curtis, G.H.1982. Geochronology of Type Uquian (later Cenozoic) land mammal age, Argentina. Science, 216: 986-988.

Mon, R., 1993. Influencia de la orogenia Oclóyica en la segmentación andina en el norte argentino. Actas Décimosegundo Congreso Geológico Argentino, 3:65-71. Buenos Aires.

Mon, R., Rahmer, S. y Mena, R., 1993. Estructuras superpuestas en la Cordillera Oriental, provincia de Jujuy, Argentina. Actas del Décimosegundo Congreso Geológico Argentino, 3:48-54.

Salfity, J.A., Gorustovich, S.A., Moya M.C. y Amengual, R. 1984. Marco tectónico de la efusividad cenozoica en la Puna argentina.. Actas del Noveno Congreso Geológico Argentino, 1:539-554. Buenos Aires.

Sempere, T., Hérail, G., & Oller, J., 1988. Los aspectos estructurales del oroclino boliviano. Quinto Congreso Geológico Chileno, 1A:127-142. Santiago.

Sempere, T., Hérail, G., Oller, J. & Bonhomme, M.G., 1990. Late Oligocene-early Miocene major tectonic crisis and related basins in Bolivia. Geology, 18: 946-949.

Turner, J.C.M., 1960. Estratigrafia de la sierra de Santa Victoria y adyacencias. Boletín Academia Nacional de Ciencias, 2: 163-196.

Whitman, D., Isacks, B. L. & Mahlburg Kay, S., 1993. Lithospheric structure and along-strike segmentation of the central Andean plateau., 17-29° S. Second International Symposium Andean Geodynamics, 1: 41-44. Oxford.

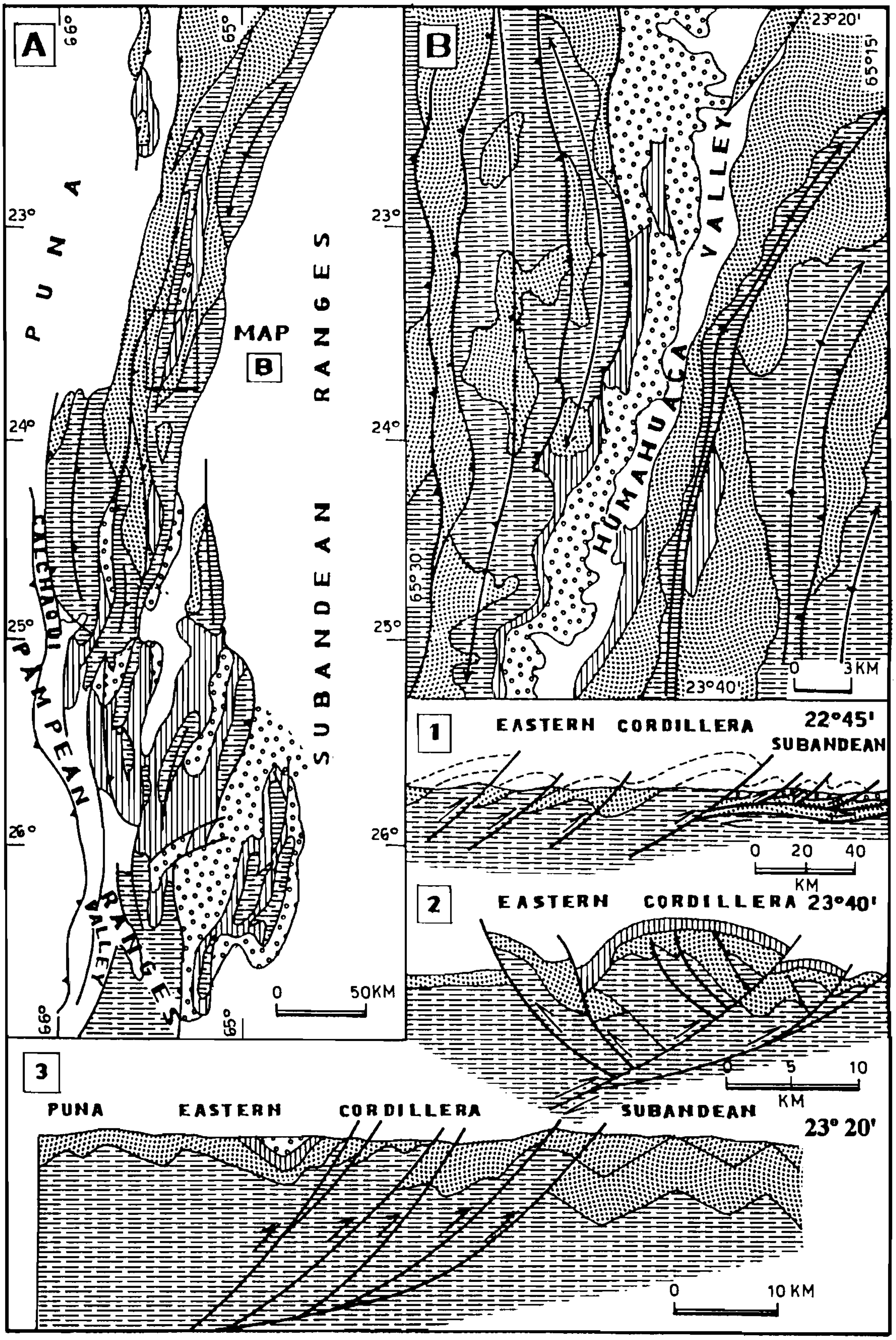
A
PUNA
MAP
B
SUBANDEAN RANGES
PAMPEAN RANGES
CALCHAQUI VALLEY
0 50KM
B
HUMAHUACA VALLEY
23°20'
65°15'
65°30'
23°40'
0 3KM
1
EASTERN CORDILLERA
22°45'
SUBANDEAN
0 20 40
KM
2
EASTERN CORDILLERA 23°40'
0 5 10
KM
3
PUNA
EASTERN CORDILLERA
SUBANDEAN
23° 20'
0 10 KM

# THRUST FRONTS IN THE LERMA VALLEY (SALTA, ARGENTINA) DURING THE PIQUETE FORMATION DEPOSITION (PLIOCENE-PLEISTOCENE)

César R. MONALDI*, Raúl E. GONZALEZ* and José A. SALFITY*

* Universidad Nacional de Salta - CONICET. Buenos Aires 177 (4400) Salta, Argentina.

**KEY WORDS**: Thrust fronts, Foreland basin, Tertiary, NW Argentina.

## INTRODUCTION

Once the stages of mechanical and thermal subsidence that controlled the accumulations in the rift basin of the Salta Group (Cretaceous-Eocene) had finished, compressional episodes took place in succession, which resulted in the inversion of the basin. At the same time, they set the structural framework of accumulation for the post-Eocene sequences.

The East migration of the thrust front is described here, together with the progressive incorporation of the Tertiary foreland basin deposits to the fold and thrust belt.

## THRUST FRONT MIGRATION

Even though precise chronology of the different compressional episodes and post-Eocene Tertiary units is not yet available, it is inferred that the first compressional stage started in the Eocene (Incaic Phase), while the Lumbrera Formation deposited (Vergani and Stack 1989, Monaldi et al. 1993).

This episode originated low structural relief, which was probably linked to blind thrusting.

Later on, a new compressional episode (Lower-Middle Miocene), more intense than the previous one, resulted in a fold and thrust belt whose deformation front was located West of the present Calchaqui valley, whereas a foreland basin was generated on the East (Figure 1a). In the fold belt (present Puna), the Pastos Grandes Group deposited in intermontane basins (of piggy-back type?), whereas in the foreland basin the accumulations of the Oran Group and equivalent ones succeeded (Monaldi et al. 1993).

In the region of the Lerma valley, the Oran Group is formed, from base to top, by the Metán Subgroup (Río Seco, Anta and Jesus María Formations) and by the Jujuy Subgroup (Guanaco and Piquete Formations). These units deposited in eolian, ephemeral and braided fluvial, lacustrine and alluvial fans environments (Vergani and Starck 1989; Gonzalez et al. 1995).

When the deformation spread towards the East, the sedimentary wedge of the foreland basin was progressively incorporated to the fold belt and began to be a supply source for the syntectonic deposits that accumulated in its front. The presence of small limestone clasts from the Yacoraite Formation in the conglomerates of the Guanaco Formation (Upper Miocene), suggests that some positive structures had already generated in the foreland basin during the deposition of the Guanaco Formation and that erosion levels got to affect its substratum constituted by the Salta Group.

During the deposition of the Piquete Formation (Pliocene-Pleistocene), two conspicuous thrust fronts existed already in the foreland basin, as inferred from the mapping analysis carried out in the Lerma valley and adjacent regions. One of them was located in the western flank of the Lerma valley, whereas the remaining one was situated on the western border of the Metán valley (Figure 1b and 2).

The synorogenic deposits of the Piquete Formation show, towards the thrust fronts mentioned above,

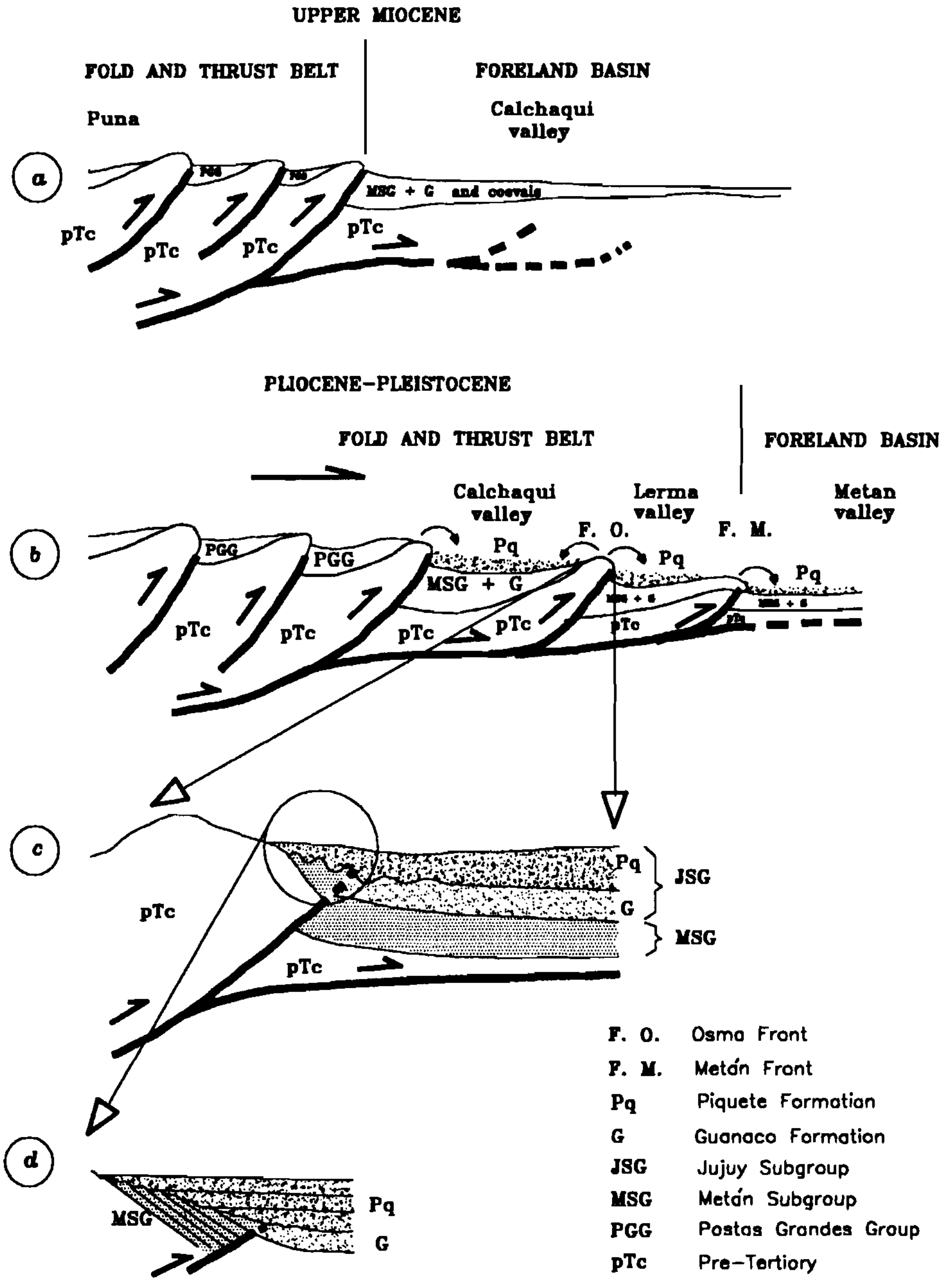


**Figure 1:** Schematic cross sections (not to scale)

typical geometry of growth strata, with onlap arrangement on the different underlying units, which in turn are affected by erosive truncations of its strata (Figure 1c and 1d). Far away from the fronts, the Piquete Formation lies in apparent concordance on the underlying Guanaco Formation. The structural and topographic relief of deformation fronts was a factor that controlled the preservation of the Oran Group units deposited before the Piquete Formation (Metan Subgroup and Guanaco Formation). In this way, units mentioned above were, in some cases, eroded against the frontal ramps of the thrusts that constitute

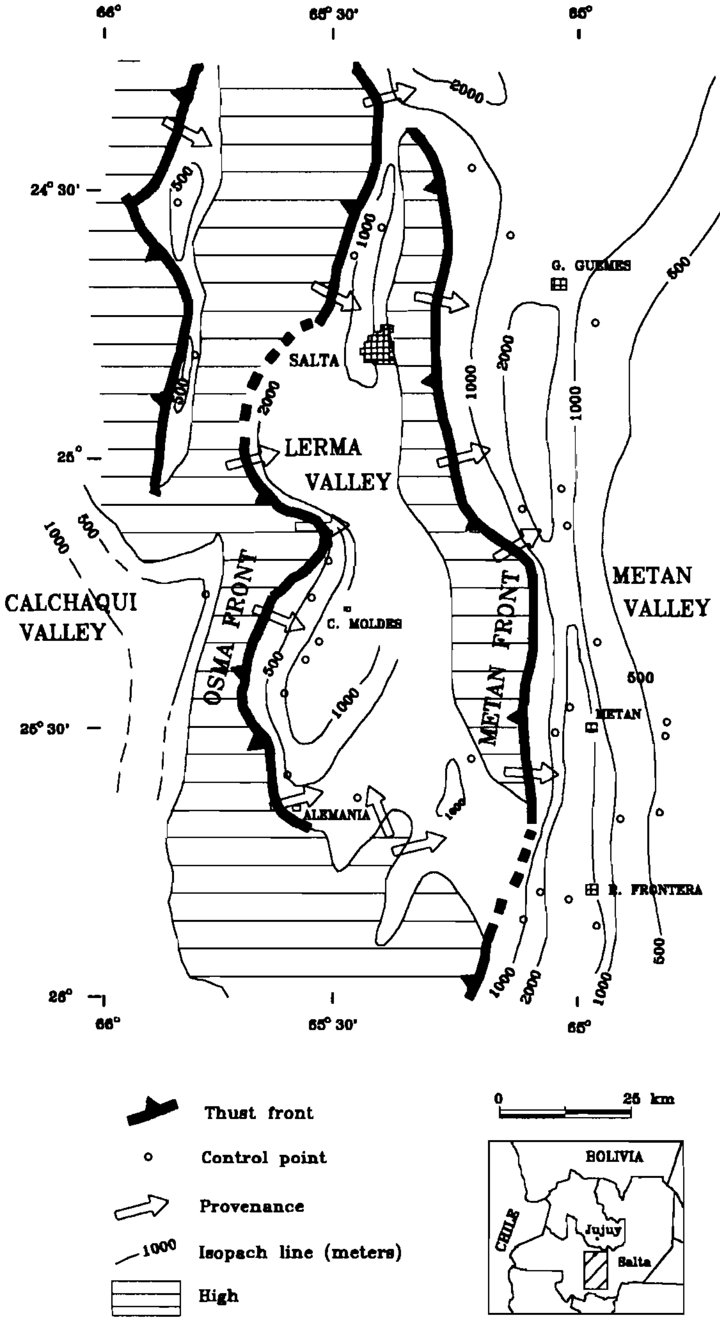


**Figure 2:** Piquete Formation and coevals (Upper Pliocene-Pleistocene). Isopach map.

the deformation fronts. Thus the Piquete Formation deposited on stratigraphic terms belonging to the Salta Group. There was more preservation in areas with lower structural relief or against lateral or oblique ramps. The composition of synorogenic deposits of the Piquete Formation shows the unroofing of the deformation fronts, with clasts originating from the Salta Group in the lower levels and progressive increase of detritus originating from the basement in the upper levels. On the other hand, their thicknesses are much greater towards the thrust fronts (Figure 2).

Locally, the thrust fronts provided greater quantities of sediments as compared to the higher hinterland. However, the erosion products of the latter might have reached the basin (or basins) of the Piquete Formation, either crossing the deformation fronts or laterally surrounding them, following structural depressions along them.
Finally, a new deformation episode (Diaguita phase) folded the synorogenic deposits of the Piquete Formation, originating the morphology that, without major changes, can be observed at present. This episode ocurred after 1,3 Ma (González et al 1995, Malamud et al. 1995) and might still be active, if the seismicity of the region is taken into consideration.

## CONCLUSIONS

In the Valle de Lerma Region, the East migration of the thrust fronts during Late Pliocene-Pleistocene incorporated the deposits of the Neogene foreland basin (Metan Subgroup and Guanaco Formation) to the fold and thrust belt. At the same time, the new thrust fronts exerted control on the composition, geometry and thickness of the Piquete Formation synorogenic deposits.
After 1.3 Ma, the deposits of the Piquete Formation were faulted and folded, thus originating the morphology that can be observed at present.

## REFERENCES

González R. E. , B. D. Malamud y C. I. Galli, 1995. "Paleoambiente y cronología en el tramo superior de la cuenca neogena de antepaís en el noroeste argentino (valle de Lerma): la Formación Piquete". Evolución tectónica y sedimentológica de cuencas de antepais, Asociación Argentina de Sedimentología. San Juan, Resumen.

Malamud B. D., T. Jordan, R. Alonso, E. Gallardo y R. González, 1995. "Four new Quaternary ash and tuff ages, Lerma valley, NW Argentina". American Geophysical Union, Fall Meeting, V22b-12, Abstracts.

Monaldi, C. R., J. A. Salfity, N. Vitulli y A. Ortiz, 1993. Estructuras de crecimiento episodico en el subsuelo de la laguna de Guayatayoc, Jujuy, Argentina. XII Congreso Geologico Argentino, Actas III: 55-64. Mendoza.

Vergani, G. y D. Stark, 1989. Aspectos estructurales del valle de Lerma, al sur de la ciudad de Salta. Boletin de Informaciones Petroleras, YPF, 20: 2-9. Buenos Aires.

# Petroleum Potential of the Bolivian Altiplano

I. Moretti (1) and O. Aranibar (2)

(1) Convenio YPFB-ORSTOM, Casilla 4875, Santa Cruz, Bolivia
Permanent address: IFP, BP 311, 92506 Rueil Malmaison, France
(2) GXG-YPFB, Casilla 1659, Santa Cruz, Bolivia

Key Word: Bolivia, Altiplano, Source Rock, Petroleum potential,

## *Introduction:*

Petroleum exploration in the Bolivian Altiplano has been active in the 70's years without any commercial success and started again in 95 with three wells drilled by YPFB and EXXON. This new phase began with a complete re-evaluation of the zone based on seismic interpretation and field studies. A more coherent structural interpretation has been proposed and the source rocks content has been quantified. We will present here an evaluation of the petroleum potential of Altiplano based of the structural sketch proposed by the YPFB's geologists and the ORSTOM's ones P. Baby and Ph Rochat (Univ. of Grenoble)

## *Source rock:*

The two main source rocks on the Bolivian Altiplano are the Paleozoic (Silurian + Devonian) and the Upper Cretaceous (Chaunaca Fm, Santanian, and El Molino Fm., Maastrichtian to Danian).

The Lower Paleozoic contains some rich organic levels. It is overmature in the Eastern Cordillera as well as in the Sub Andean Zone, but may eventually play some role on the western part of the Altiplano, where the Middle to Upper Paleozoic is supposed to have been thinner, or missing as in the San Andres well. The Middle Paleozoic is the main source rock on the Sub Andean Zone (Moretti et al., 1994, Fig 1) and, at least in the Eastern part of the Altiplano, shows similar facies to the ones known on the Sub Andean Zone (Moretti et Aranibar, 1995). It is a marine source rock with a rather low but constant petroleum potential (Initial S1+S2 around 5 mg HC/g, Fig 2). The main dubiousness concerning the influence of this source rock is its thickness in the Altiplano. The Silurian and Devonian reach a total thickness of up to 4000 meters on the Sub Andean Zone, as opposed to the Altiplano, which may correspond more or less to the western border of the Silurian-Devonian foreland basin. Southward, from the Uyuni-Kheuany faults, the Devonian is missing

The Permian and Carboniferous are present in the north, around the Titicaca Lake, but are missing in the south due to pre-Jurassic erosion (Diaz, 1994). The Lower Carboniferous is characterised by a progradational deltaic sequence and does not present a high potential except very locally. The Upper Carboniferous and Lower Permian Copacabana Fm. is an excellent source rock on the northern part of the Sub Andean Zone (Lliquimuni area, Moretti et al., 1994) and, by reputation, it is the source rock of the Pirín field in Peru, but organically rich and thick facies have not been recognized in the Bolivian Altiplano area, where the Copacabana Fm. is mainly calcareous.

The El Molino Fm. could locally present very high potential (S2 up to 20 mg HC/g, Aranibar et al., 1995), but the data are rather inhomegeneous. The best values are from the Eastern Cordillera, where the Cretaceous is immature (Fig 1). On the Altiplano, Cretaceous outcrops are numerous on the eastern part and lead to various debates in terms of depositionnal environment (Gayet et al., 1993, Blanc-Valleron et al., 1994). Westward, only the Tertiary is outcropping, and a lot of uncertainties remain on the facies and even on the units existing on subsurface, the existence of an Ordovician source rock as well as some Jurassic ones, related to the Chilean back arc opening, is not to preclude but remains hypothetical.

## *Tectonic setting*

The Pacific subduction started in early Mesozoic times, first in an extensional context (various backarc basins may be recognized from Jurassic to Cretaceous over the whole margin from Venezuela to south Chile, and then in a compressional context (Jaillard, 1994). The change from extension to compression is not synchronous along the margin, and in Bolivia is late compared with neighboring regions. The Cretaceous is still extensional and the Paleogene is characterized by large and deep half grabens which may correspond to strike-slip faults. The first definitively inverse faulting started at the end of the Oligocene (27 My, Sempere et al., 1990), with thrusting and uplift in the modern Eastern Cordillera. Nevertheless the compression may have started before late Oligocene (Butler et al., 1995). Late Oligocene also corresponds to the formation of the Altiplano as an isolated basin, limited to the east by the Eastern Cordillera and to the west by the Western Cordillera, formed by the Andean volcanoes. The erosion of the Eastern Cordillera induced conglomeratic deposits along the east (Coniri Fm.) when the western part is mainly volcano-detritic. The previously formed half grabens were then progressively inverted on the Altiplano and subsidence continued in some basins. This phase of compression took place at the end of the Miocene, and is contemporaneous with the eastward migration of the compressional front of the Sub Andean Zone, where the thrusts are dated from 14 Ma to recent (Baby, 1995). The current phase starting in the Pliocene is also compressive (Baby et al., 1990, 1992), and leads to the uplift and strong erosion of the eastern part of the Altiplano (Geise, 1994). The very rapid vertical movements which started presumably at the Upper Miocene, are due to deep processes: crustal thickening (James, 1971) and lithospheric thinning (Wigger, 1993) and are accommodated by high-angle faults.

*Thermicity:*

The current heat flow is very high, the average value reaches 100 $mW/m^2$ (Henry et Pollack, 1988). These data are compatible with the already mentioned lithospheric thinning and lead to a shallow oil window (around 2500 meters). One may correlate this heat flow to the present desequilibrium (-400 mgal on the Bouguer gravity anomaly) and uplift of the area. We suggest to date the increase from a normal heat flow (around 60 mW/m2) to 100 $mW/m^2$ at the Upper Miocene coeval with the increase of uplift rate in the area.

*Timing of HC generation and migration*

Supposing that the Middle Paleozoic source rock did not mature during the Late Paleozoic, the generation of HC from both Paleozoic and Cretaceous source rocks started in the Oligocene, at the end of the Potoco-Tihuanacu deposits, and it is mainly active during Miocene time. The speculated reservoirs are Cretaceous to early Tertiary, so the traps are all connected to the Neogene evolution of the area. Recent structures (end of Miocene to present) are risky because they are more recent than the increase of subsidence. One of the main risk, is also the lack of reservoir, for instance the Toledo-X1 well drilled by EXXON in the northern part of the Poopo lake found the Paleozoic below the Miocene without proving any reservoirs since the Cretaceous and Paleogene were missing due to erosion at the top of the structure.

*Current exploration:*

The Altiplano is a frontier zone where only 8 wells have been drilled, 5 between 1970 and 1976 and 3 between 1995 and 96. Three of them were badly located (salt domes or basement structures). The southern one (Vilque) was drilled on a Paleozoic high and showed that the Cretaceous is very thin and not organically rich in this part. Large quantities of methane and nitrogen have been reported. The methane seems to indicate the presence of an overmature source rock, and the nitrogen has not been explained. The northern well, San Andrés de Machaca, is also dry and does not record any source rock potential. The Precambrian basement has been found directly under a sandy Cretaceous leading to very negative conclusions for the northern western part of Altiplano. The oil seeps are all on the eastern part, except the Rio Mauri one. The origin of each one is still a matter of debate.

*Conclusions*

From a structural point of view, the Altiplano may be divided in two parts. The eastern part is thursted by the Eastern Cordillera and affected by strong compressional features. The western part is characterized by Early Tertiary deep half-grabens that may still be recognized and have been slightly inverted during the Miocene. Eastward, many of the structures involved evaporites from the Cretaceous and Early Paleogene, as can be seen on outcrops and in numerous seismic lines.

From a geochemical point of view, the eastern part is rather well known: the Paleozoic source rocks exist from north to south (to the Uyuni-Khenayani Fault) and the Cretaceous (El Molino Fm. & Chaunaca Fm.) presents an excellent potential. Nevertheless, the Chaunaca Fm. is too thin ( 5 meters of source rock) for an active participation to the petroleum system, and the true thickness of source rock in the El Molino Fm. is still poorly known (from 30 to 100 meters). To the north, the Permian and Carboniferous source rocks are present, but are also very thin, and the outcropping Cretaceous does not show any high HC potential. To the south, the same fact has been recorded, the El Molino Fm. reduces its potential and becomes thinner and more sandy. Eastward everything is speculative and there is no proven source rock. Hopefully, a new well in this part will allow a better knowledge of the area on the coming months.

From a timing point of view, the best structures are the oldest ones, and this means the highest part of the Early Paleogene halfgrabens (as Santa Lucía to the west), or the first compressive one related to the Late Oligocene phase (they are numerous on the Poopo Lake area).

*This study has been done through the YPFB-ORSTOM convention. The data comes from the YPFB-GXG data base and some additional samples has been collected during field studies made with the TOTAL geologists J.L. Pittion and M. Specht. We thanks the YPFB colleagues (J. Jarandilla, E. Martínez y G. Navarro) for many helpfull discussions and the YPFB exploration managment, Ings. M. Cirbián y M. López, for help and autorization to publish.*

**References:**

ARANIBAR O., CIRBIAN M. y TALUKAR, S., 1995.The Molino-Tertiary petroleum system in the southern and central Altiplano and adjacent Eastern Cordillera, Bolivia. AAPG Annual Convention, Houston (Texas), Marzo 1995.

BABY P., SEMPERE T., OLLER J., BARRIOS L., HÉRAIL G. y MAROCCO R. (1990). - Un bassin en compression d'âge oligo-miocène dans le sud de l'Altiplano bolivien. *C. R. Acad. Sci. Paris*, t. 311, Série II, p. 341-347.

BABY P., SEMPERE T., OLLER J. y HÉRAIL G. (1992). - Evidence for major shortening on the eastern edge of the Bolivian Altiplano: the Calazaya nappe. *Tectonophysics*, 205, 1-3, p. 155-169.

BABY P., 1995. Structuration des Andes centrales. Thèse d'habilitation. Univ Grenoble.

BLANC-VALLERON M. M., SCHULER M., RAUSCHER R., CAMOIN G. Y ROUCHY J.-M. (1994). - La matière organique des séries d'âge Crétacé supérieur-Tertiaire inférieur du bassin de Potosi (Cordillère orientale, Bolivie): apports stratigraphiques et paléogéographiques. *C. R. Acad. Sci. Paris.*, t. 319, Série II, p. 1359-1366.

BUTLER R., RICHARDS D., SEMPERE T., MARSHALL L., (1995) Paleomagnetic determinations of vertical-axis tectonic rotations from late Cretaceous and Paleogece strata of Bolivia. Geology, v 23, 799-802.

DIAZ E. (1994). - Upper Devonian and Carboniferous of the Altiplano of Bolivia: stratigraphy, sedimentology and paleogeographic evolution. PhD, Univ. of Idaho, 208 p.

GAYET M., SEMPERE T., CAPPETTA H., JAILLARD E. y LÉVY A. (1993). - La présence de fossiles marins dans le Crétacé terminal des Andes centrales et ses conséquences paléogéographiques. *Palaeogeog., Palaeoclim., Palaeoecol.*, 102, p. 283-319.

GEISE P., (1994) - Geothermal structure of the Central Andean crust - Implications for heat transport and rheology. In Tectonics of the southern central Andes, Springer-Verlag, p 69 - 76.

HENRY S. Y POLLACK H. (1988). - Terrestrial heat flow above the Andean Subduction Zone in Bolivia and Peru. *J. Geophys. Res.*., v 93, n B12, p.15153-15162.

JAILLARD E. (1994). - Tectonic evolution of the Peruvian margin between Kimmeridgian and Paleocene times. *in* : Salfity J.A., éd., Cretaceous tectonics in the Andes, Viewing Pub., Braunschweig/Wiesbaden (Allemagne), Earth Evolution Sciences, Monograph series, 1, p. 101-167.

JAMES D. (1971). Andean crustal structures. JGR, v 76, 3246-3271.

MORETTI I. & ARANIBAR O, (1994). Evaluación del potencial petrolero del Altiplano de Bolivia. Técnica de YPFB, v 15 (3-4), 327-352.

MORETTI I., BABY P., ARANIBAR O. y ROCHAT P., (1995). Evaluación del potencial petrolero del Altiplano de Bolivia. Informes YPFB-ORSTOM-TOTAL.

MORETTI I., DIAZ MARTINEZ E., AGUILERA E, MONTEMURRO G. y M. PEREZ, (1994). - Las rocas madre de Bolivia y su potencial petrolífero: Subandino - Madre de Dios - Chaco. Revista Técnica de YPFB, v 15 (3-4), 293-317.

ROCHAT P., HÉRAIL G. & BABY P. (1995). - Analyse géométrique et modèle tectono-sédimentaire de l'Altiplano nord Bolivien. CRAS, Submitted.

ROCHAT P., (1996) These, Université de Grenoble, en prep.

SEMPERE T., HÉRAIL G., OLLER J. y BONHOMME M. (1990a). - Late Oligocene-early Miocene major tectonic crisis and related basins in Bolivia. *Geology*, 18, p. 946-949.

SEMPERE T. (1994). - Kimmeridgian? to Paleocene tectonic evolution of Bolivia. *in* : Salfity J.A., éd., Cretaceous tectonics in the Andes, Viewing Pub., Braunschweig/Wiesbaden (Allemagne), Earth Evolution Sciences, Monograph series, p. 168-212.

WIGGER P. J., SCHMITZ M., ARANEDA M., ASCH G., BALDZUHN S., GIESE P., HEINSOHN W. D., MARTINEZ E., RICALDI E., RÖWER P. Y VIRAMONTE J. (1994). - Variation in the Crustal Structure of the Southern Central Andes Deduced from Seismic Refraction Investigations. *in* : K.-J. Reutter E. Scheuber P.J. Wigger, éd., Tectonics of the Southern Central Andes - Structure and Evolution of an Active Continental Margin, Springer-Verlag, Berlin, 1, p. 23-48.

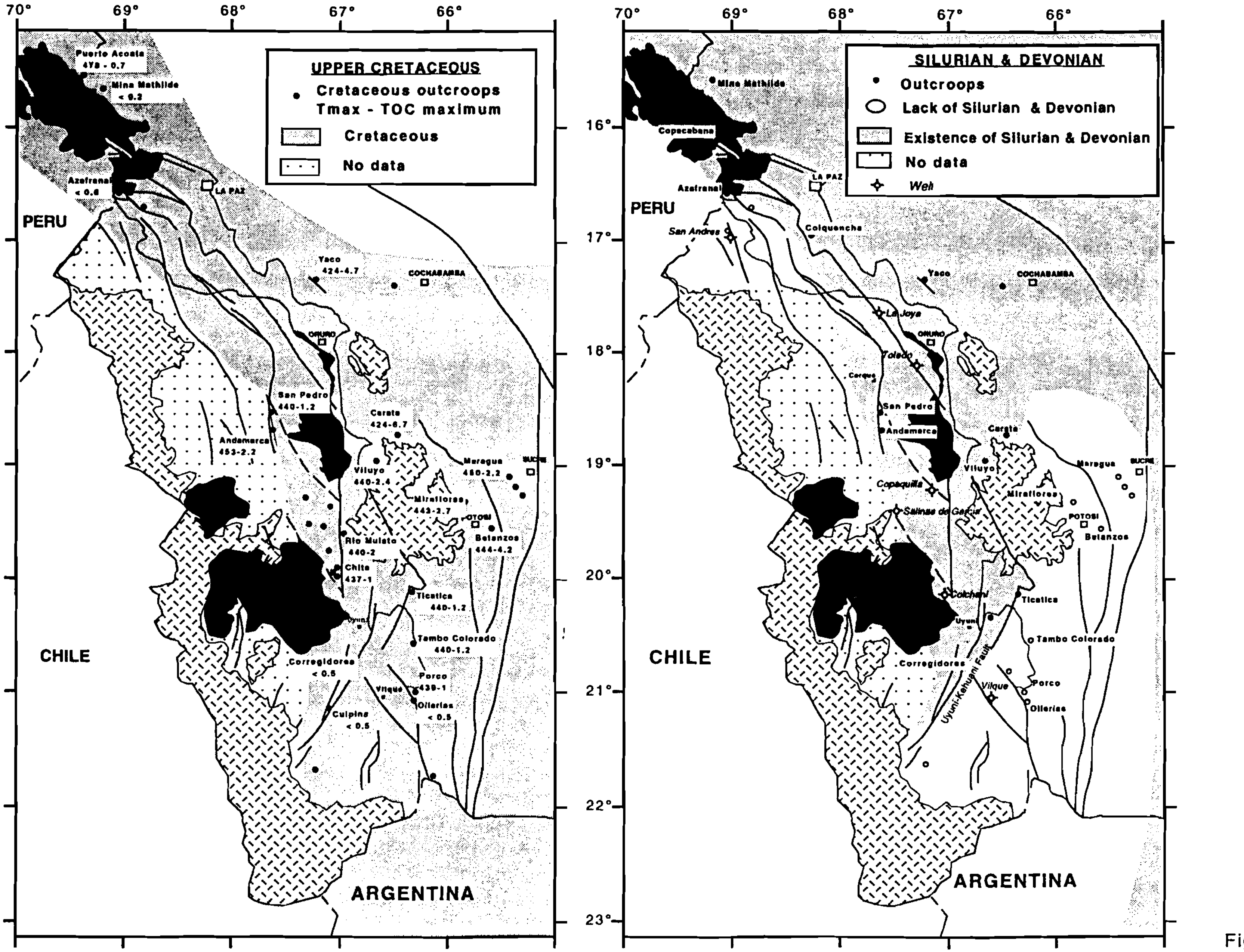

UPPER CRETACEOUS
Cretaceous outcroops
Tmax - TOC maximum
Cretaceous
No data
Puerto Acosta
478 - 0.7
Mina Mathilde
< 9.2
Azafranal
< 0.6
LA PAZ
PERU
Yaco
424-4.7
COCHABAMBA
ORURO
San Pedro
440-1.2
Carata
424-6.7
Andamarca
453-2.2
Viluyo
440-2.4
Maragua
480-2.2
SUCRE
Miraflores
443-2.7
POTOSI
Belanzos
444-4.2
Rio Mulato
440-2
Chita
437-1
Ticatica
440-1.2
Uyuni
Tambo Colorado
440-1.2
CHILE
Corregidores
< 0.5
Porco
439-1
Vilque
Ollerias
< 0.5
Culpina
< 0.5
ARGENTINA
SILURIAN & DEVONIAN
Outcroops
Lack of Silurian & Devonian
Existence of Silurian & Devonian
No data
Well
Mina Mathilde
Copacabana
Azafranal
LA PAZ
PERU
San Andres
Colquencha
Yaco
COCHABAMBA
La Joya
ORURO
Toledo
Corque
San Pedro
Andamarca
Carata
Viluyo
Maragua
SUCRE
Copaquilla
Salinas de Garci
Miraflores
POTOSI
Belanzos
Colchani
Ticatica
Uyuni
Tambo Colorado
CHILE
Corregidores
Uyuni-Kehuani Fault
Vilque
Porco
Ollerias
ARGENTINA
70°
69°
68°
67°
66°
16°
17°
18°
19°
20°
21°
22°
23°


Fig 1

# PRELIMINARY STRUCTURAL RESULTS ON THE NORTH PATAGONIAN BATHOLITH (CHILE, AYSEN, 44°-45°30' S)

Anne NEDELEC (1) and Alejandro SANHUEZA (2)

(1) Pétrophysique, UMR 5563 CNRS, Univ. P. Sabatier, 38 rue des 36-ponts, 31400 Toulouse, France
(2) Departamento de Geologia, Universidad de Chile, plaza Ercilla 803, Santiago, Chile

**KEY WORDS** : AMS, pluton emplacement, shear zone, Miocene, peraluminous granite

## INTRODUCTION

The southern Andes are characterised by a huge calc-alkaline batholith whose northern part between 39 and 47° S is called the North Patagonian Batholith (NPB). A roughly north-south lineament system, the Liquine-Ofqui Fault Zone (LOFZ), extends along the axial part of the NPB. It is regarded as a dextral strike-slip fault zone related to the oblique convergence of the Nazca and South America plates in this area (Dewey & Lamb, 1992). The youngest plutonic activity (Miocene) occurred near the LOFZ, whereas the rest of the batholith yielded mainly Cretaceous ages (Pankhurst & Hervé, 1994). Despite the the difficult field conditions, structural mapping has been attempted between 44 and 45°30 S (Fig. 1a) by systematic anisotropy of magnetic susceptibility (AMS) measurements from orientated sampling in Aysén region between 44 and 45 ° 30 S (Fig. 1a).

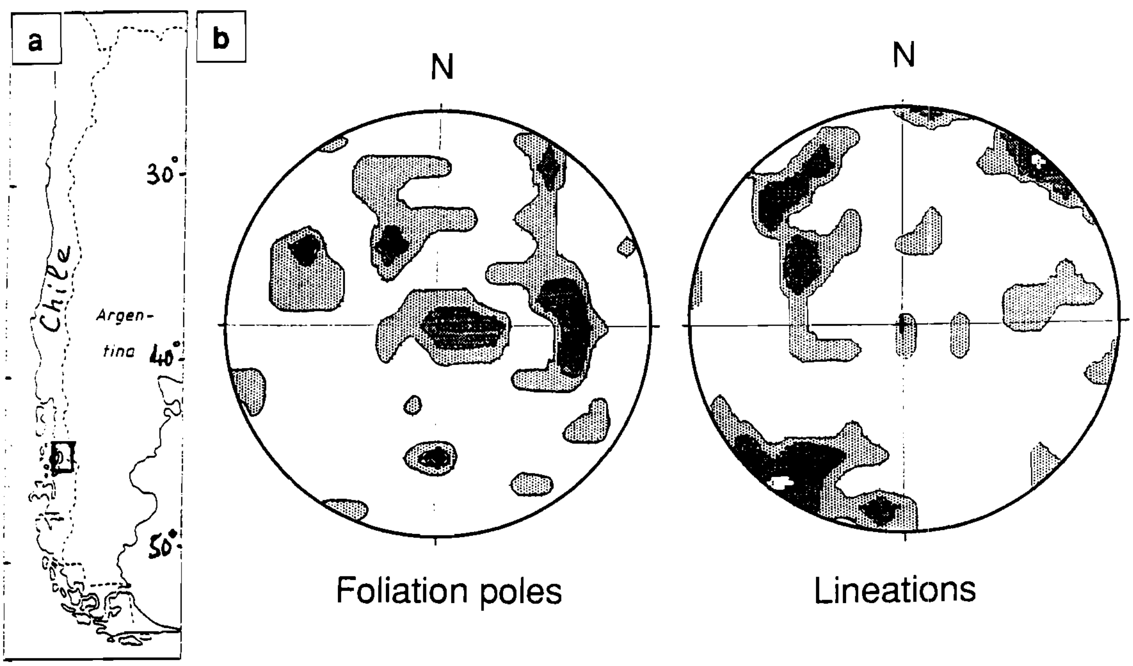


Fig. 1. a. Location of the studied area. b. Orientation diagrams of magnetic structures (equal area; lower hemisphere; n = 32; contour interval = 2%).

## PETROSTRUCTURAL DATA

The continental part of the NPB in Aysén is mainly made of tonalites with abundant mafic bodies along the coast and dominant granodioritic rocks towards the east. They are separated by granitic units roughly aligned along a north-south trend. Samples were picked out from all these domains. All samples display magmatic textures in thin sections, with the sole exception of the peraluminous granite east of Puerto Cisnes (see below). The high level emplacement conditions of the eastern granodiorites are deduced from the common occurrence of microgranular and granophyric facies.

Magnetic susceptibility intensities range from 7 to 11058 x $10^{-5}$ SI. Most values are typical of ferromagnetic rocks. Magnetic structures (Fig. 1b) mostly represent magmatic fabrics. Foliations are subhorizontal or variously dipping, often towards the west. There are two main lineation orientations: subhorizontal lineations with a N40 strike and lineations plunging toward the north-west at a low to moderate angle.

The peraluminous granite east of Puerto Cisnes (Fig. 2) yielded a Rb-Sr whole rock isochron age of 10 Ma (Hervé et al., 1993). It deserves special attention owing to its uncommon mineralogy (garnet - aluminosilicates - muscovite) and to its texture typical of incipient to pronounced solid-state deformation. The highly foliated samples display shear planes characterized by quartz ribbons, sillimanite and late muscovite, together with submagmatic fractures in feldspars. Magnetic foliations are roughly north-south and steeply dipping to the west. Lineations plunge at a very low angle to the south. These features suggest syntectonic emplacement along a north-south strike-slip shear zone, very likely the LOFZ.

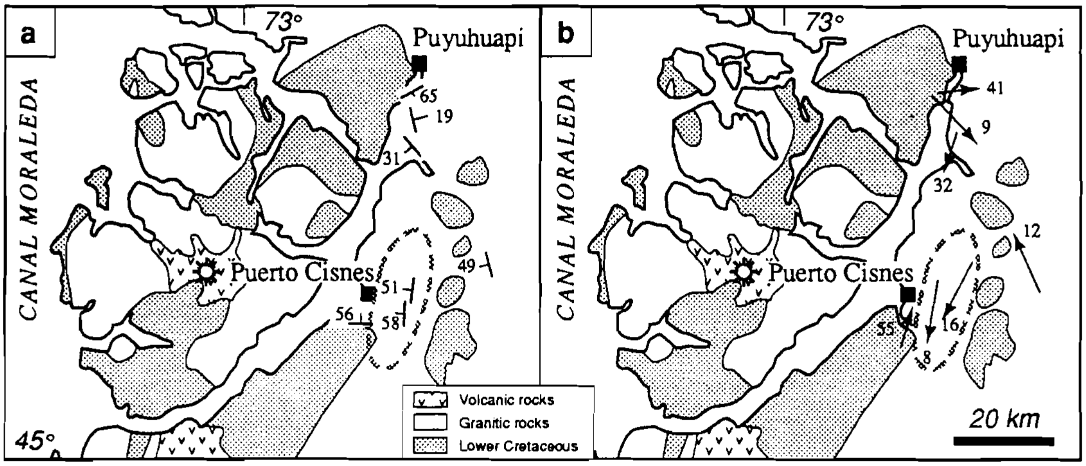


Fig. 2. Detailed foliation (a) and lineation (b) maps with 10 Ma-old syntectonic granite (dashed contour).

## CONCLUSIONS

Most plutonic rocks of the NPB display magmatic textures, with the exception of an Upper Miocene peraluminous granite that was syntectonically emplaced in a strike-slip regime related to the LOFZ. Work in progress will unravel the P-T conditions along this fault and propose a tectonic interpretation for the structures of the other plutonic units.

*Acknowledgements*. Financial support was received from the ECOS-CONICYT Program, from the European Project CI1*-CT93-0033 and from the UMR 5563. Technical assistance by C. Cavaré-Hester, P. Lespinasse and A.M. Roquet, and scientific discussion with J.L. Bouchez are greatly acknowledged.

## REFERENCES

Dewey J.F. & Lamb S.H., 1992. Active tectonics of the Andes. *Tectonophysics*, 205, 79-95.

Hervé F., Pankhurst R.J., Drake R., Beck M.E. Jr & Mpozodis C., 1993. Granite generation and rapid unroofing related to strike-slip faulting, Aysén, Chile. *Earth Planet. Sci. Lett.*, 120, 375-386.

Pankhurst R.J. & Hervé F., 1994. Granitoid age distribution and emplacement control in the North Patagonian batholith in Aysén (44° - 47° S). *Actas 7o Congreso Geol. Chileno*, II, 1409-1413.

# AN AREA-BALANCED MODEL OF THE LATE CENOZOIC TECTONIC EVOLUTION OF THE SOUTHERN BOLIVIAN ARC AND BACK-ARC

Nihal OKAYA, Sohrab TAWACKOLI & Peter GIESE

FU Berlin, Institut für Geologie, Geophysik und Geoinformatik, Malteserstr. 74-100, 12249 Berlin, Germany

KEY WORDS: area-balancing, late Cenozoic, southern Bolivia, tectonic evolution.

## INTRODUCTION

Newly available geological and geophysical data yield new constraints on the late Cenozoic evolution of the southern Bolivian central Andes (Fig. 1) and motivate re-evaluation and refinement of former tectonic models (e.g. Suàrez et al., 1983; Isacks, 1988; Roeder, 1988; Sheffels, 1990; Schmitz, 1992). The main purpose of this effort is to quantitatively unravel the detailed tectonic evolution in consistency with geological and geophysical data at hand. Such a model allows to study the relevance of other processes suggested for Andean orogeny, i.e. thermal uplift (Froidevaux & Isacks, 1984) and magmatic addition (Thorpe et al., 1981; de Silva, 1989). Furthermore, the model provides a guideline for further quantitative modelling studies in which the thermal and mechanical aspects of the suggested tectonic model can be examined.

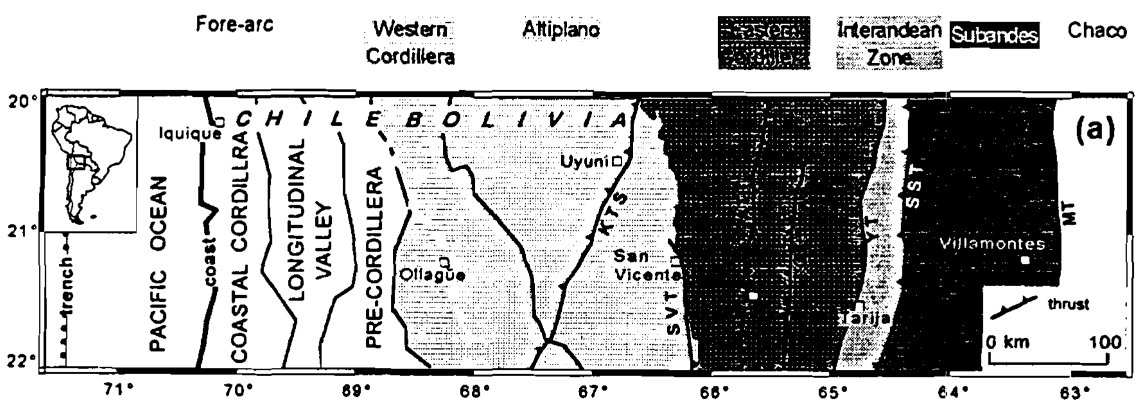


FIGURE 1: Map of the 20°-22°S section of the Central Andes showing the main tectonic units, and major thrusts in the region between the Altiplano and the Chaco (KTS: Khenayani Thrust System; SVT: San Vicente Thrust System, ATT: Aquile-Tupiza Thrust, CTT: Camargo-Tojo Thrust, YT: Yunchará Trust, SST: San Simón Thrust; MT: Mandeyapecua Thrust).

METHOD & DATA BASE

Based on different geological and geophysical data a plausible scheme of the crustal evolution from late Oligocene to present (27-0 Ma) along an idealised cross-section reaching from the Western Cordillera to the Chaco foreland (20°-22°S) (Fig. 1) is synthesised in an area-balance model. The tectonic evolution is described by relating upper-crustal thrusting to crustal-scale deformation. The amount of isostatic uplift is included by Airy isostasy. The reordered upper crustal convergence is balanced by a corresponding mantle-lithospheric shortening. In the model thermal and rheological arguments are used to distinguish between pure and simple shear deformation.
The model is constraint by and tested against the following geological and geophysical data. Estimates of upper crustal shortening together with age data (e.g. Baby et al., 1992, 1990, 1989; Gubbels et al., 1993; Kley, 1996; Kley et al., 1996) supply the detailed deformation history along a continuos section through the southern Bolivian Andes. Evidence on the timing of crustal thickening along the profile is derived from data on the uplift history (e.g. Jordan & Alonso, 1987; Sempere et al., 1990; Gubbels et al., 1993). The present-day deep seismic structure (Wigger et al., 1993) yields clues to tectonic processes at depth and confines the crustal structure of the model at 0 Ma. The magmatic activity (Davidson et al., 1990; Avila-Salinas, 1991) is associated with a region of thinned mantle-lithosphere (Isacks, 1988).

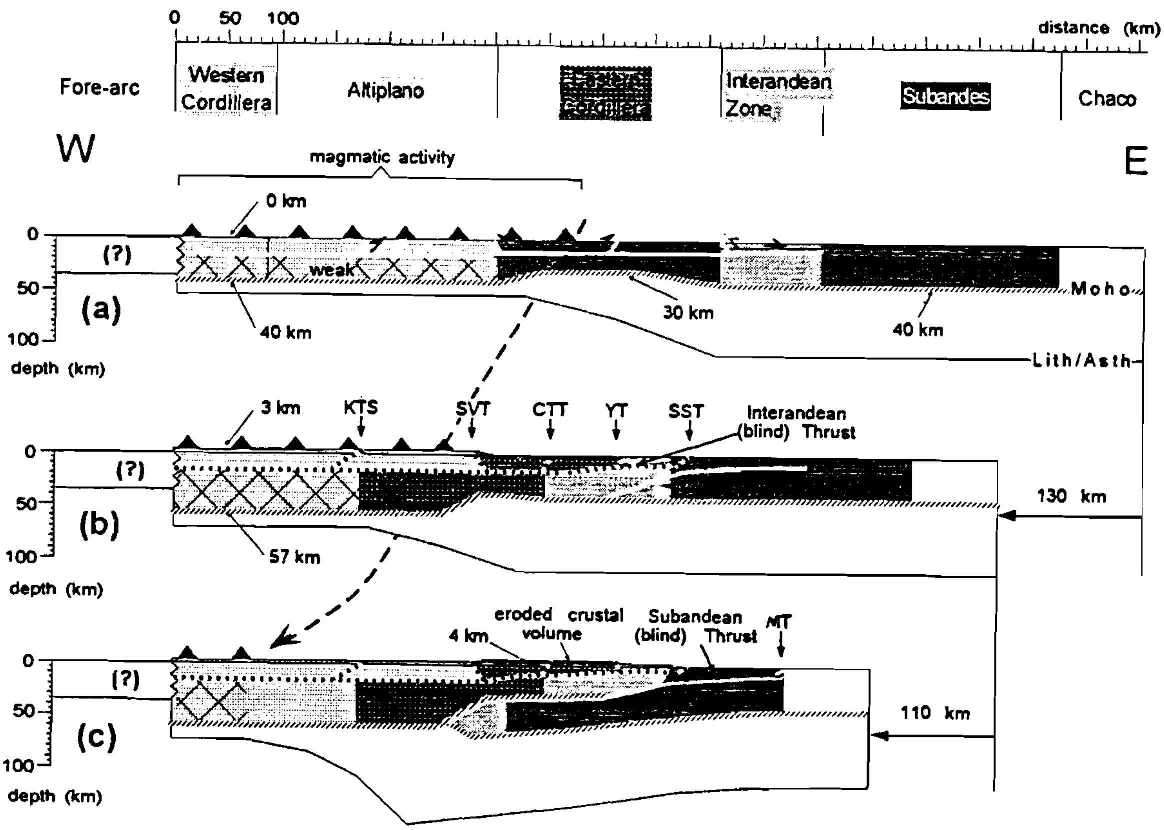


FIGURE 2: Area-balanced model of the 27-0 Ma phase of the tectonic along an idealised cross-section reaching from the Western Cordillera to the Chaco foreland. The Figure shows snapshots of the model (a) at 27 Ma, (b) at 5 Ma, and (c) at 0 Ma. Motions are indicated by black half arrows; active thrusts are shown in white lines, inactive thrusts are shown in dashed black-white lines. The area of magmatic activity is outlined by black triangles. The hatched line indicates the initial Moho at 27 Ma followed through time.

## AREA-BALANCED MODEL OF THE TECTONIC EVOLUTION

At the on-set of deformation (~27 Ma) the initial state of the Chaco, the Subandes, the Interandean Zone, the Altiplano and the Western Cordillera (Fig. 2a) is characterised by a largely uniform crustal thickness of 40 km (Isacks, 1988, Schmitz, 1994). The eastern part of the Eastern Cordillera is assumed to mark the eastern transition to the thinned, 30 km thick crust of the western Eastern Cordillera where Cretaceous rifting events are documented (e.g. Avila-Salinas, 1991). The width of the individual tectonic units is restored according to the recorded shortening amounts. These are in the Altiplano ~20 km (Baby et al., 1990), at the western margin of the Eastern Cordillera ~35 km (Kley et al., 1996; Baby et al., 1990), in the Eastern Cordillera ~30 km (Kley et al., 1996), in the Interandean Zone ~45 km (Kley, 1996), and in the Subandes ~110 km (Kley, 1996; Baby et al., 1992, 1989). The thinned mantle lithosphere of ~10 km thickness corresponds to the area of late Oligocene magmatism reaching from the Western Cordillera to the western Eastern Cordillera; further east the mantle-lithospheric thickness amounts to ~60 km.
Based on the data summarised above the late Cenozoic tectonic evolution of the southern Bolivian Andes is suggested to be due to two major thickening mechanisms for crustal convergence.
During the ~27-5 Ma phase (Fig. 2a and b) upper crustal shortening of ~130 km in the Altiplano, the Eastern Cordillera and the Interandean Zone is adapted along a major detachment (future "Interandean blind thrust"; Kley, 1996) which follows the brittle-ductile transition at upper-crustal level beneath the Eastern Cordillera and at mid-crustal level beneath the Altiplano. At depth the cold (rigid) middle and lower crust of the Eastern Cordillera thrust under the Altiplano and the heated (ductile) lower crust of the Altiplano and the Western Cordillera thicken by pure shear. In the Western Cordillera and the Altiplano, this phase accounts for thickening (~57 km) and for major uplift (~3 km). The Eastern Cordillera is only affected by minor thickening (~40 km) and uplift.
During the ~5-0 Ma phase (Fig. 2b and c) a new major detachment ("Subandean blind thrust"; Kley, 1996) establishes. The Subandean crust thrust under the crust of the Eastern Cordillera by simple shear deformation. This process accounts for upper crustal shortening of ~110 km in the Subandean fold-thrust belt, and thickening, uplift and erosion in the Eastern Cordillera. This deformation could be responsible for the distinct change from rugged, deeply incised topography of the Eastern Cordillera to valley-and-ridge topography of the Subandean fault-thrust belt.

## CONCLUSIONS

(1) In the suggested model the present-day crustal volume of the seismic structure is well reproduced east of the San Vicente thrust indicating that tectonic shortening played the dominant role in the eastern part of the orogen. West of the San Vicente thrust, under the Western Cordillera and the Altiplano, crustal volume is missing. This volume would correspond to an additional shortening of ~80 km in the area between the Altiplano, Eastern Cordillera and Interandean Zone.
(2) The model suggest that additional processes are responsible for crustal uplift and thickening in the Western Cordillera and Altiplano. Magmatic addition would require ~2500 km$^2$ of magma intrusion. Thermal uplift would demand delamination of the lower lithosphere at the eastern margin of the Altiplano. An update of the chronology of magmatic activity could yield constraints on the relevance of this processes in Andean orogeny.
(3) A distinct characteristic of the tectonic model is the different uplift mechanism for the Altiplano and Eastern Cordillera. The Western Cordillera and Altiplano rose uniformly by pure shear thickening of the lower crust whereas the Eastern Cordillera uplifted stepwise with inception at its eastern border and westward migration with time. Geochronological data giving constraints on the timing and amount of exhumation are necessary to confirm this pattern.
(4) In comparison with the model by Isacks (1988) and Gubbels et al. (1993) our model accounts for the observed Interandean and Subandean thrusts (Kley, 1996). The "Quechua" phase (~14-10 Ma) leading to compressive deformation in the Altiplano (Jordan & Gardeweg, 1989) affects in southern Bolivia the eastern Eastern Cordillera whereas deformation in the Altiplano is predated to ~27-19 Ma.

REFERENCES

Avila-Salinas, W., 1991. Petrological and tectonic evolution of the Cenozoic volcanism in the Bolivian western Andes, in Harmon, R.S. & Rapela, C.W., eds., Andean magmatism and its tectonic setting: Boulder, Colorado, Geological Society of America Special Paper, 265.

Baby, P., Herail, G., Lopez, J.M., Lopez, O., Oller, J., Pareja, J., Sempere, T. & Tufiño, D., 1989. Structure de la zone Subandine de Bolivie: influence de la géometrie sédimentaires antéorogéniques sur la propagation des chevauchements: C.R. Acad. Sci. Paris, Série II, v. 309, pp. 1717-1722.

Baby, P., Sempere, T., Oller, J., Barrios, L., Hérail, G. & Marocco, R., 1990. Un basin en compression d'age Oligo-Miocène dans le sub de l'Altiplano Bolivien: C. R. Académie des Sciences Comptes Rendue París, Série II, v. 311, p. 341-347.

Baby, P., Hérail, G., Salinas, R. & Sempere, T., 1992. Geometry and kinematic evolution of passive roof duplexes deduced from the foreland thrust system of the Southern Bolivian Subandean Zone: Tectonics, v. 11, p. 523-536.

Davidson & 5 other, 1990. The Nevados de Payachata volcanic region (18° S/ 69° W, N. Chile) II. Evidence for widespread crustal involvement in Andean magmatism: Contributions to Mineralogy and Petrology, 105, pp. 412-432.

De Silva, S.L., 1989. Altiplano-Puna complex of the Central Andes: Geology, v. 17, pp. 1102-1106.

Froidevaux, C. & Isacks, B.L., 1984. The mechanical state of the lithosphere in the Altiplano-Puna segment of the Andes. Earth and Planetary Science Letters: v. 71, p. 305-314.

Gubbels, T.L., Isacks, B.L. & Farrar, E., 1993. High-leval surface, plateau uplift, and foreland development, Bolivian central Andes: Geology, v. 21, p. 695-698.

Isacks, B.L., 1988. Uplift of the central Andean plateau and bending of the Bolivian orocline: Journal of Geophysical Research, v. 93, p. 3211-3231.

Jordan, T.E. & Alonso, R.N., 1987. Cenozoic stratigraphy and basin tectonics of the Andes Mountains, 20°-28° south latitude: American Association of Petroleum Geologists Bulletin, v. 71, p. 46-64.

Jordan, T.E. & Gardeweg, M., 1989. Tectonic evolution of the late Cenozoic central Andes (20-33°S), in Ben-Avraham, Z., ed., The Evolution of the Pacific Ocean Margins, Oxford University Press, New York, p. 193-206.

Kley, J., 1996. Transition from basement-involved to thin-skinned trusting in the Cordillera Oriental of southern Bolivia: Tectonics, in press.

Kley, J., Müller, J., Tawackoli, S., Jacobshagen, V. & Manutsoglu, E., 1996. Pre-Andean and Andean-age deformation in the Eastern Cordillera of southern Bolivia: Journal of South American Earth Sciences, submitted.

Roeder, D., 1988. Andean-age structure of the Eastern Cordillera (Province of La Paz, Bolivia): Tectonics, v. 7, p. 23-29.

Schmitz, M., 1994. A balanced model of the south central Andes: Tectonics, v. 13, p. 484-492.

Sempere, T., Hérail, G., Oller, J. & Bonhomme, M.G., 1990b. Late Oligocene-early Miocene major tectonic crisis and related basins in Bolivia: Geology, v. 18, p. 946-949.

Sheffels, B.M., 1990. Lower bound on the amount of crustal shortening in the central Bolivian Andes: Geology, v. 18, p. 812-815.

Suàrez, G., Molnar, P. & Buchfield, B.C., 1983. Seismicity, fault plane solutions, depth of faulting, and active tectonics of the Andes of Peru, Ecuador, and Southern Columbia: Journal of Geophysical Research, v. 88, p. 10403-10428.

Thorpe, R.S., Francis, P.W. & Harmon, R.S., 1981. Andean andesites and crustal growth: Royal Society of London Philosophical Transactions, ser. A, v. 301: p. 305-320.

Wigger, P. & 10 others, 1993. Variation of the crustal structure of the southern central Andes deduced from seismic refraction investigations, in Reutter, K.J. et al., eds., Tectonics of the Southern Central Andes: New York, Springer-Verlag, p. 23-48.

# TERTIARY TECTONICS OF NORTHERN PATAGONIA: THE EVIDENCE OF CHILEAN BASIN REMNANTS

David J. Prior[(1)], Francesca M. Ray[(1)] and Stephen S. Flint[(1)]

(1) Department of Earth Sciences, University of Liverpool, L69 3BX, U.K.
email: davep@liverpool.ac.uk

**KEY WORDS**: Tertiary Basins, Ridge subduction, Patagonia

## INTRODUCTION

The tectonic setting of Northern Patagonia is unique and provides one of the most exiting tectonic field laboratories in the world. The South American continent has been bounded by a subduction margin throughout the Tertiary. Today a mid oceanic ridge segment is in the process of subduction at 46°30'S latitude (Cande & Leslie, 1986; Behrmann, Lewis et al., 1992) and ridge subduction has operated intermittently for 14 million years (Cande & Leslie, 1986). Another ridge subduction event may have occurred in the Eocene (Cande & Leslie, 1986). Geophysical data has been used to suggest that subducted ridge segments, or the slab windows postulated to form at the locus of subducted spreading centres, continue to be tectonically active several hundred kilometres east of the trench (Murdie et al., 1993; Murdie et al, in review). Detailed investigations in Argentina have attributed Tertiary basalts, Tertiary molasse basin sedimentation and development of a foreland thrust belt to the history of ridge subduction and slab window development (Ramos & Kay, 1991; Ramos, 1989). Within Chile there are significant topographic and related climatic variations which correspond to the change from the continental margin affected by ridge subduction (south of the Chile Triple Junction) and the margin unaffected by ridge subduction immediately to the north (Forsythe & Prior, 1992). The Chilean segment of Northern Patagonia is pivotal to the tectonic understanding of this region, providing the link between the trench and the region comprising the foreland thrust belt, molasse basin and plateau basalts. Structural analysis of this region is particularly complex since many of the units have a considerable pre-Tertiary tectonic history. This is particularly true of the Palaeozoic basement (Hervé et al, 1987) which has enjoyed significant poly-phase deformation during the Palaeozoic. The Mesozoic volcanic successions (Skarmeta, 1978) provide a poor stratigraphic template. Remnants of Tertiary sedimentary basins provide the best opportunity for a first order analysis of the Tertiary structure and history of this region. This paper presents a summary of work completed on the Tertiary Basin systems of Chile between 46°30' and 47°30'S, expresses the significance of these data and suggests future research directions. Figure 1 shows the location of the main basin remnants.

## BASIN TEMPLATE

The Tertiary basins are variably unconformable upon Mesozoic volcanics or Palaeozoic basement. A schematic stratigraphy of the Tertiary of Chile South of 46°30'S is shown in figure 2. Locally the clastic sediments lie conformably over an acidic volcanic succession which is itself unconformable upon the Upper Cretaceous Divisidero/ Cardiel formation. The status of this younger volcanic formation remains unclear; it has been assigned to the Divisidero/ Cardiel by the geological survey (Skarmeta 1978; Niemeyer et al., 1984) whilst Niemeyer (1975) assigned these to a separate formation, the Chile Chico formation and suggested that these volcanics may be Tertiary in age. Although there is no independent evidence for the Tertiary status of these volcanics we also assign them to the Chile Chico Fm.

The Guadal/ Centinela Formation is the lowermost recognized unit within the Tertiary sedimentary succession. We have distinguished a continental clastic succession usually assigned to the base of the Guadal. This is sufficiently distinct to deserve formation status and we have named this the San Jose Formation. The San Jose formation comprises alluvial-fluvial facies in the west, in the Cosmelli Basin. The San Jose formation of the Cerro Rocoso basin comprises fluvial and perhaps deltaic facies. Palaeocurrents within the San Jose are generally to the East.

The Guadal Formation comprises marine and marginal marine facies. Faunal constraints are poor but suggest an age between Eocene and Miocene. In the Cosmelli basin marginal marine facies of the lowermost and uppermost Guadal sandwich a thin more open marine facies. The lowermost marginal facies, including significant oysterbanks, is of regional significance, being clearly identifiable at Lago Posades in Argentina. Palaeocurrents in the Marginal facies of the Cosmelli basin are dominantly N-S. In the Cerro Rocoso basin the Guadal is restricted to a thin layer within Plateau basalts. The basalts lie conformably above the San Jose formation. here the uppermost San Jose includes a significant coal horizon.

The Guadal is overlain by the Galera/Santa Cruz Formation. The nature of this contact is a little cryptic but in general seems to be erosive. The Santa Cruz is an extensive Molasse type fluvial facies system extending several hundred km into Argentina. Palaeocurrents are dominantly to the east. In Argentina further plateau basalts of Pliocene age lie above the Santa Cruz. Mammalian fossils and K/Ar ages of tuffs have been used to constrain the ages of the Santa Cruz between 22 and 12Ma, with younger ages in the north.

## BASIN STRUCTURE

Fold and fault structures are identified in both the Cosmelli and Cerro Rocoso basins. These structures accommodate E-W shortening and almost certainly connect to the foreland thrust belt identified to the south and east in Argentina. An east dipping fault defines the west margin of the Cosmelli basin. In both the south and north of the Cosmelli basin this structure has a thrust like geometry, although emplacing Tertiary over older strata. In the north of this basin, the latest movements recorded on the western basin margin fault have a significant N-S strike slip component. The Cosmelli basin has an overall synformal form. In the west of the basin the San Jose and Guadal formations are stacked in a complex imbricate fan suggesting thrusting to the east. The structural complexity decreases up stratigraphy so that the lowermost Galera is only gently folded. Internal disconformities and palaeocurrent patterns suggest that this structure was growing during the sedimentation of the uppermost Guadal.

In Cerro Rocoso the Chile Chico, San Jose, basalts and Guadal are carried by a large scale east directed thrust over the top of lowermost Galera fluvial sediments. The Chile-Chico to basalt stratigraphy now defines a hanging-wall antiform structure. Soft sediment deformation within the lowermost Galera show identical kinematics to the major structure and suggest that the structure was active here during deposition of the lower Galera. An unusual recumbent fold structure in sills within the plateau basalt complex is geometrically comparable to other folds.

The Patagonian fold and thrust belt is thought to have propagated from South to North through time (Ramos, 1989; Ramos & Kay unpublished data). Data from the Chilean Tertiary basins also suggests an overall propagation from west to east, so that tectonic activity in the Cosmelli basin occurred during Guadal deposition , whereas deposition further to the east in the Cerro Rocoso basin occurred during Galera deposition. The latest strike-slip movements of the fault bounding the Cosmelli basin may also suggest that there is a component of superposed northward propagation.

## TECTONIC SIGNIFICANCE

Ramos (1989) and Ramos & Kay (1991) have suggested that the Patagonian molasse basin and the foreland thrust belt relate to the history of ridge subduction. The degree of coincidence of continental topographic, sedimentation and deformation patterns with the region which has experienced ridge subduction is a powerful suggestion of a link between these processes. However, the majority of the dating information suggests that the molasse basin sedimentation and at least some of the deformation initiated before the first ridge collision so that the link between continental plate processes and the plate margin is not so simplistic. It is possible that the initial generation of topography and the molasse basin was in response to subduction of younger and more buoyant crust as the ridge approached.

Further qualification of these models requires an analysis of how the topography and deformation have evolved with time along the margin. The key obstacle to this is the unraveling of Tertiary structures in the Mesozoic and Palaeozoic. In the Mesozoic an understanding of the spatial distribution of volcanic facies and the identification of any regional marker horizons is crucial. In the Palaeozoic it is important to understand fully the Palaeozoic deformation history to establish what has been superposed on this.

## REFERENCES

Behrmann, J.H., Lewis, S., Musgrave, R., & shipboard party. 1992. Proceedings of the Ocean Drilling Program. 141, Initial Results.

Cande, S.C., & Leslie, R.B., 1986, Late Cenozoic tectonics of the southern Chile trench: Journal of Geophysical Research, 91, 471-496.

Forsythe, R.D. & Prior, D.J. 1992. Cenozoic continental geology of South America and its relations to the evolution of the Chile Triple Junction. In: Behrmann, J.H., Lewis, S., & Musgrave, R., (eds.,). Proceedings of the Ocean Drilling Program. 141, Initial Results, 23-31.

Hervé, F., Godoy, E., Parada, M.A., Ramos, V., Rapela, C., Mpodozis, C., & Davidson, J., 1987, A general view on the Chilean-Argentine Andes, with emphasis on the early history: In Monger, J.W.H., & Francheteau, J., (eds) Circum-Pacific orogenic belts and evolution of the Pacific Ocean basin: *American Geophysical Union Geodynamics Series*, 18, 97-113.

Murdie R.E., Prior D.J., Styles P., Flint S.S., Pearce R.G. & Agar S.M. 1993 Seismic responses to ridge-transform subduction: Chile triple junction. Geology v.21, p.1095-1098.

Murdie, R.E., Prior, D.J., Styles, P., Flint, S.S., & Agar, S.M.. In review. The fate of subducted mid-oceanic spreading ridges: the implications of new gravity data from southern Chile. Bulletin of the Geological Society of America.

Niemeyer, H. 1975. Geología de la regiòn comprendida entre el lago General Carerra y el Río Chacabuco, Provincia de Aisén, Chile. Memoria, Universidad de Chile, Fac Ciencias Fis. y Mat.

Niemeyer, H., Skarmeta, J., Fuenzalida, P., Espinosa, W., 1984, Hojas peninsula de Taitao y Puerto Aisen: *Carte Geologica de Chile* No 60-61.

Ramos V.A. & Kay S.M., 1992 Southern Patagonian plateau basalts and deformation: backarc testimony of ridge collisions. Tectonophysics v.205, p.261-282.

Ramos V.A., 1989 Foothills structure in Northern Magellenes Basin, Argentina. American association of petroleum geologists, 73, 887-903.

Skarmeta, J., 1978. Regioncontinental de Aisén entre el lago General Carerra y la Cordillera Castillo. *Carte Geologica de Chile* No 29.

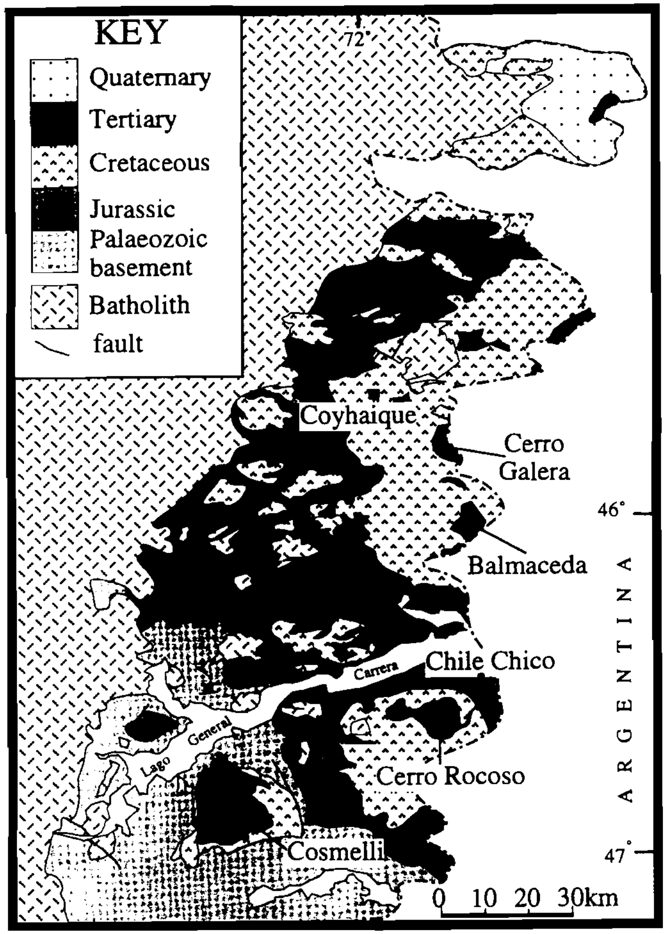
KEY
Quaternary
Tertiary
Cretaceous
Jurassic
Palaeozoic basement
Batholith
fault
72°
Coyhaique
Cerro Galera
46°
Balmaceda
Chile Chico
Carrera
General
Lago
Cerro Rocoso
Cosmelli
47°
A R G E N T I N A
0 10 20 30km

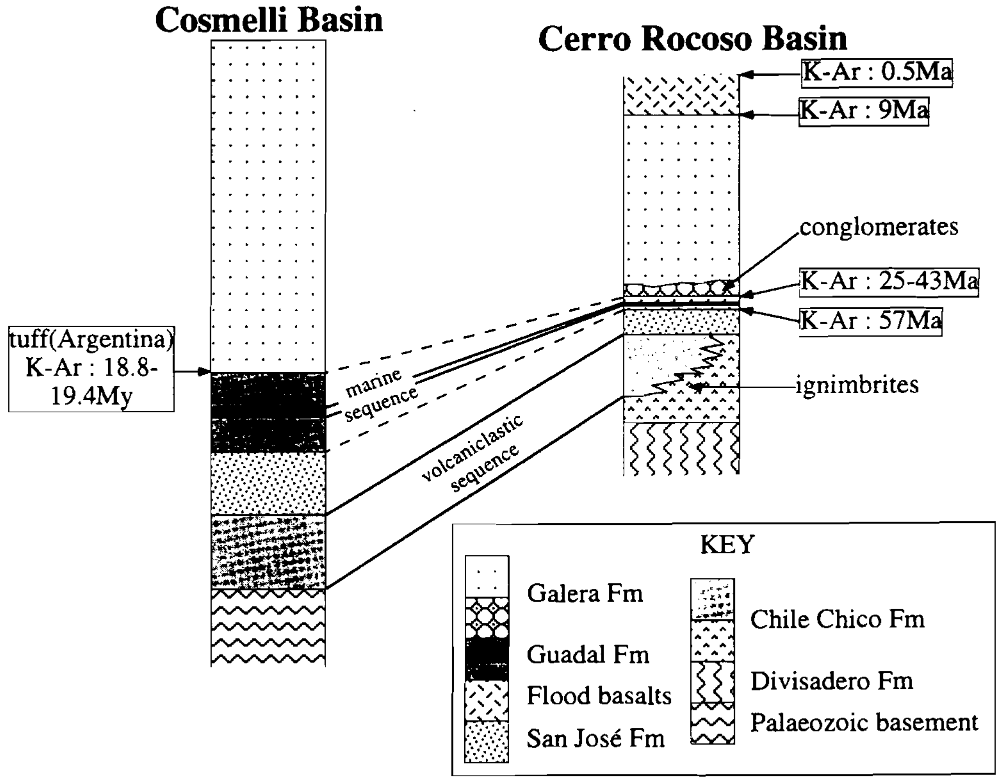
Cosmelli Basin
Cerro Rocoso Basin
tuff(Argentina) K-Ar : 18.8-19.4My
K-Ar : 0.5Ma
K-Ar : 9Ma
conglomerates
K-Ar : 25-43Ma
K-Ar : 57Ma
ignimbrites
marine sequence
volcaniclastic sequence
KEY
Galera Fm
Guadal Fm
Flood basalts
San José Fm
Chile Chico Fm
Divisadero Fm
Palaeozoic basement

# TECTONIC EVOLUTION OF THE MAIN CENTRAL ANDES AT PASO PIUQUENES (33°30'S), ARGENTINA AND CHILE

Victor A. RAMOS [1], Estanislao GODOY [2], Verónica GODOY [1] and Francisco PÁNGARO [3]

[1] Laboratorio de Tectónica Andina, Universidad de Buenos Aires, Ciudad Universitaria, 1428 Buenos Aires, Argentina (email andes@gl.fcen.uba.ar)
[2] Servicio Nacional de Geología y Minería, Avda. Santa María 0104, Santiago, Chile
[3] YPF S.A., Cutralcó, Neuquén, Argentina

KEY WORDS: Tectonics, Andes, Crustal thickness, Arc volcanics, Cenozoic, Structure.

## INTRODUCTION

The Piuquenes pass along the border between Argentina and Chile is one of the classic localities first described by Darwin in 1835 during his celebrated world trip. His precise stratigraphic descriptions were the first geological observations in the Central Andes. The excellent exposures of the Aconcagua fold and thrust belt as well as the widespread development of the Cenozoic volcanism made this area an interesting target to analyze the relationship between volcanism and tectonics through Cenozoic times which is the aim of the present study.

The area is located east of the city of Santiago de Chile, and west of Tunuyán city in Argentina. The access in the Chilean side is by road up to 10 kilometers of the Piuquenes pass while from Argentina the pass is more than 30 kilometers away from a secondary road and is reached after two days walk.

The original description of Darwin (1846) recorded the first fossiliferous Mesozoic marine sequence of the Central Andes. But, perhaps more important for the scope of this work is the description of the Tunuyán Conglomerates where he analyzed the provenance of the clasts. He mentioned the occurrence of large clasts of crystalline basement in these conglomerates that should have been derived from an eastern source. More than a century latter, the regular survey of the region by Polanski (1964) was the only other published reference of the geology of the area. In recent years, the laboratory of Andean Tectonics of the University of Buenos Aires surveyed the area in detail at both slopes of the Andes.

## GEOLOGIC SETTING

The area has a Proterozoic metamorphic basement emplaced by Carboniferous to Permian arc-related granitoids. These rocks are unconformably covered by the Choiyoi Group volcanic sequence. These Permo-Triassic rocks range from basalts, andesites to rhyolites and record the transition from a subduction related volcanism at the base to a widespread extensional intraplate volcanism in the uppermost rhyolites during Triassic times.

The Mesozoic sedimentary sequence is composed by marine and continental deposits and has been the object of different studies (Polanski, 1964, Thiele, 1980). The lower detachment is controlled by a Middle Jurassic gypsum and is responsible for the presence of Callovian rocks in the core of the Yeguas Muertas anticline in the Chilean side (Godoy, 1993). The eastern slope of the Andes is characterized by an imbrication of thrust slices detached from the Auquilco Gypsum (Oxfordian). As a result of that, red beds, black shales, and carbonates of Tithonian to Neocomian age are repeated and deformed along the axis of the fold and thrust belt. These sequences interfingered to the west with volcaniclastic and volcanic products derived from the arc.

## THE SYNOROGENIC DEPOSITS

A series of shales and fine sandstones of lacustrine to low energy fluvial facies represent the distal synorogenic deposits of Paleogene age. The overlying Tunuyán Conglomerates, which are correlated with the Santa María Conglomerates of the Aconcagua region, located further north, range in age from 20 to 8 Ma. The Tunuyán Conglomerates are a coarsening up sequence, deposited in alluvial fans and breaded proximal rivers, and reached up to 1,300 m. Most of their clasts are derived from the different lithologies deformed and uplifted in the fold and thrust belt, west of the thrust front of Cerro Palomares. These conglomerates are covered by the Butaló Formation (Polanski, 1964), which consists of fine sandstones and clays, with reworked tuffs and thin limestones and shales with fossil gastropods. Fine conglomerates of this unit record the first clasts of crystalline basement that show an east provenance, probably derived from the Cordón del Portillo.

## THE CENOZOIC VOLCANICS

There are three major volcanic episodes in the region. The Contreras Formation is the lowermost unit at the base of the Tunuyán Conglomerates. It consists of lava flows and basaltic breccias, covered by andesitic pyroclastic flows. All these rocks have been folded and thrust during deformation of Tunuyán conglomerates. These rocks are correlated with the 22 Ma old Máquinas Basalt in the flat subduction segment (Ramos et al., 1989). The geochemical analyses of Contreras volcanics indicate a typical retroarc or intraplate setting (Fig. 1).

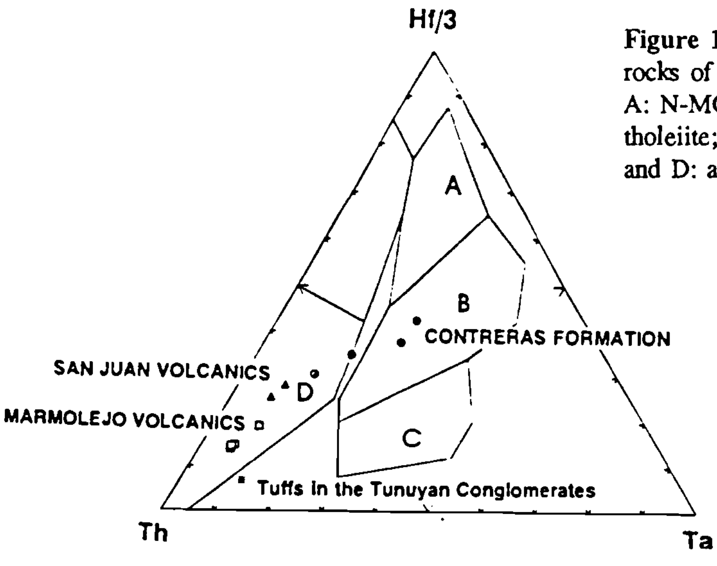


**Figure 1**: Woods diagram of the volcanic rocks of the Piuquenes Pass region.
A: N-MORB; B: E-MORB & within-plate tholeiite; C: within-plate alkaline basalt, and D: arc volcanics.

The second volcanic sequence corresponds to the andesites and dacites of the Marmolejo volcanic center. These rocks are separated by an angular unconformity from the deformed Mesozoic sequences. They are typical calcalkaline volcanic rocks formed in a magmatic arc setting (Fig. 1). These volcanics are assigned to the Late Miocene-Early Pliocene. The volcanic rocks are tilted by an out-of-sequence thrust.

The third volcanic episodes is represented by andesites and dacites erupted from the San Juan Volcano. These arc related rocks (Fig. 1) are unconformably covering the previous structures and rocks, and are assigned to the Pliocene.

## TECTONIC EVOLUTION

The structure of the area has a minimum orogenic shortening of 50 km, produced during the Miocene in a thin skinned fold and thrust belt (Pángaro et al., 1995). The analysis of the structure indicate a piggy-back order for the major thrusts that cannibalized part of the synorogenic deposits. The last episode recorded is an out-of-sequence thrust that west-tilted the base of Marmolejo volcanics, during the Late Miocene-Early Pliocene. This OST may be related to a sticking point produced by the uplift during the Upper Miocene of Cordon del Portillo basement in the Frontal Cordillera. The Pliocene San Juan volcanics postdated all the thrusts in the Principal Cordillera.

An interesting relationship is seen when the geochemical data from the volcanic sequences are introduced in the structural evolution of the area. The REE slope inferred from the La/Yb ratio, were plotted against the relative enrichment of the light REE assumed by the La/Sm (see Fig. 2). As proposed by Kay et al. (1991) in the flat segment there is a clear trend of increasing these ratios during time. This increase was correlated by different authors with the thickening of the crust. Striking similarities are found when the magmatic and tectonic evolution in this normal subduction segment at the latitude of Piuquenes Pass (33°30'S) is compared with the evolution in the flat slab segment (Kay et al., 1987). It is evident that although in both segments the tectonic and magmatic histories are similar there some important differences. The timing of deformation is younger and the degree of crustal thickening is smaller in the southern segment.

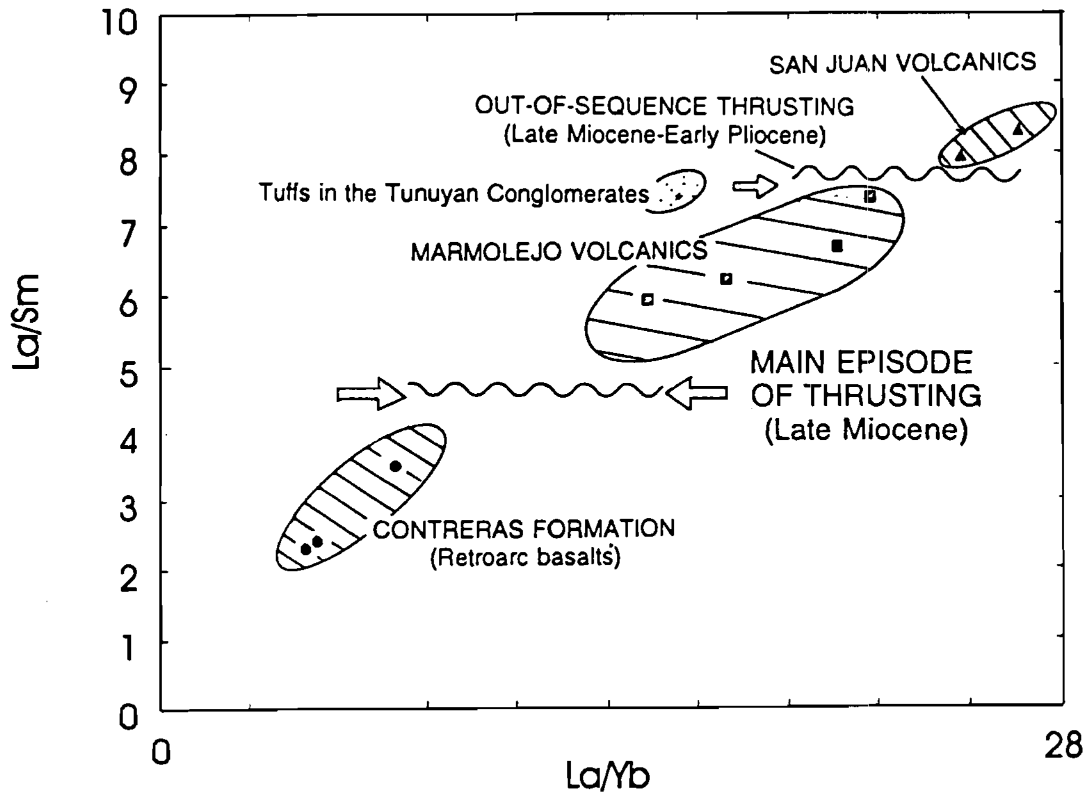


**Figure 2**: La/Sm and La/Yb ratios of the different volcanic suites of the Piuquenes Pass.

## CONCLUDING REMARKS

The integrated survey of the Chilean and Argentine slopes of the Principal Andes shows:

- The tectonic evolution of this segment of the Andes begun with a retroarc basaltic volcanism of Early Miocene age, that is interfingered with the first synorogenic deposits. At this time the crustal thickness was normal or sligthly attenuated.
- The orogenic front migrated from the Chilean side in the Lower Miocene to the Argentine side in the Middle-Upper Miocene. Consequently, thickenning of the crust was followed by an expansion of the westerly derived synorogenic deposits to the east.
- The Marmolejo volcanics during the Late Miocene-Early Pliocene unconformably covered the deformed rocks of the Aconcagua fold and thrust belt. The volcanic front have migrated at that time from the Chilean side to the present international border.
- The uplift of the Frontal Cordillera may have generated a sticking point in the normal piggy-back order of thrusting to the foreland in the Principal Andes. As a result of that an out-of-sequence thrust in the inner previously deformed area tilted the Marmolejo Volcanics.
- During the Pliocene the region became stable, and the andesites and dacites of San Juan Volcano unconformably overly the structure of the fold and thrust belt.

The relationship between the structural evolution, and the magmatic arc trend, indicates that crustal thickening derived from some geochemical parameters tightly matched the thickness obtained through balanced structural cross-sections.

## ACKNOWLEDGMENTS

The financial support of Fundación Antorchas and the UBACYT grant Ex-132 made this work possible.

## REFERENCES

DARWIN, CH.R., 1846. Geological observations on South America. Being the third part of the Geology of the voyage of the Beagle, during the years 1832 to 1836. Smith, Elder & Co., 1-279, London.

GODOY, E., 1993. El Caloviano del Estero Yeguas Muertas, Río Yeso del Maipo, Chile: implicancias tectónicas y paleogeográficas. XII° Congreso Geológico Argentino, Actas II: 104-107, Buenos Aires.

KAY, S.M., V. MAKSAEV, R. MOSCOSO, C, MPODOZIS and C. NASI, C.E. GORDILLO, 1987b. Tertiary Andean magmatism in Chile and Argentina between 28°S and 33°S: Correlation of magmatic chemistry with a changing Benioff zone. Journal South American Earth Sciences 1(1):21-38.

KAY, S.M., C. MPODOZIS, V.A. RAMOS and F. MUNIZAGA, 1991. Magma source variations for mid to late Tertiary volcanic rocks erupted over a shallowing subduction zone and through a thickening crust in the Main Andean Cordillera (28-33°S). Geological Society of America, Special Paper 265: 113-137.

PÁNGARO, F., E. GODOY and V.A. RAMOS, 1995. Structural balanced cross section of the Aconcagua folded and thrust belt at 33°25' of South Latitude. ICL Andean Thrust Tectonics Symp. 34-35 p., San Juan.

POLANSKI, J., 1964. Descripción geológica de la Hoja 25a Volcán San José, provincia de Mendoza. Dirección Nacional de Geología y Minería, Boletín 98: 1-94, Buenos Aires.

RAMOS, V.A., S. M. KAY, R.N. PAGE and F. MUNIZAGA, 1989. La Ignimbrita Vacas Heladas y el cese del volcanismo en el Valle del Cura, provincia de San Juan. En Simposio Vulcanismo Andino, B. Coira (ed.) Asociación Geológica Argentina, Revista XLIV(1-4): 336-352, Buenos Aires.

THIELE, R., 1980. Hoja Santiago. Región Metropolitana. Carta Geológica de Chile. Escala 1:250.000. Instituto de Investigaciones Geológicas 39: 1-51, Santiago.

# CRETACEOUS-PALEOGENE STRATIGRAPHIC SEQUENCES AND THE EARLY ANDEAN OROGENIC EVENTS IN THE ECUADORIAN ORIENTE BASIN

Marco V. RIVADENEIRA M.

PETROPRODUCCION P. O. Box No 17-10-7019. Quito Ecuador.

**KEY WORDS:** Oriente basin. Cretaceous-Paleogene Sedimentation. Andean orogeny.

## INTRODUCTION

The stratigraphic sequence of the Ecuadorian Oriente Basin, is strongly influenced by the early Andean orogenic events, which were weak until the Santonian-Campanian. During this time, minor erosional surfaces developed. In the younger parts of the section (Paleocene-Oligocene), the unconformities become stronger and the first molasse deposits appear in response to the western Andean emersion.

## GEOLOGICAL EVOLUTION

### Aptian - early Albian

The Hollin Formation unconformably overlies the Preaptian eroded and deformed formations (Fig. 1). It comprises a sequence of coarse sandstone fining and thining upward, with minor carbonaceous claystone, siltstone and coal interlayers. It thins to the east and pinchs out near the Ecuadorian-Peruvian border.

This period is characterized by a relative tectonic quiescense. The braided Cretaceous river flowed into the basin, carring the basal sandstones. Later deposition was the result of marine transgresion (estuarine, and tidal enviroments ). The main bulk of sandstones seems to be derived from the Paleoamazon system , but an important source was the higlands of the Brasilian-Guyana Shield located in the east and northeast .

### Middle Albian - Campanian.

The Napo Formation comprises four members : sandy-shaly Napo Basal, sandy Napo Inferior, limy Napo Medio and shaly-sandy Napo Superior (fig. 1).

The Napo epicontinental marine basin, was characterized by restricted circulation , creating anoxic conditions during the middle Albian, Turonian and Coniacian times. Black and dark organic rich grey shales, marls and limestones were deposited under those conditions. To the east, the rivers flowed into the basin forming deltas and estuaries.

During the Albian - Santonian times, minor synsedimentary movements and reactivations of older faults occured.

For the late Turonian - early Coniacian times, in the outcrop of the Mirador Anticline located in Central Subandean Zone Jaillard E. (1995) reported an unconformity at the top of the Turonian M2 limestones. It's the first indication of an uplift of the Subandean Zone. This event is characterized by reactivation of numerous faults.

In the middle-late Campanian, the Andean uplift, caused by the Macuchi-Continent plate collision (Odin & Odin 1995), is recorded in the uplift of the Subandean Zone, mainly in the Central part of that zone ("Napo Uplift" and " Pastaza Depression" ). The Campanian section was almost completely removed by erosion in the North Subandean (ten-twenty feet) of Coniacian sediments. In the Southwest of the Zone (Jaillard E. 1995) the erosion is minimum, and the Campanian deposits (M1 sandstone) are preserved as in the eastern part of the basin.

These facts show a differentiated important uplift of the Subandean Zone. The uplift was stronger in the central area, where the eastern terrains were dragged up. It reached the area of Cononaco and Rumiyacu fields (where the Campanian deposits are almost complete eroded) located in the western flank of the basin. In the Subandean Zone important regional extent oblique tectonic elements seem to control its dynamics.

A small NNO foreland basin formed back to the stronger uplifted zone. It shows that the uplift began at the late Santonian, and some of the paleocurrents began to have eastern directions. An important group of faults were reactivated during the Coniacian - Santonian and their related folds were formed.

**Maastrichtian-Paleocene.**

The Tena Formation unconformably overlies the Napo Formation in the west, were an important thikness of the Napo Superior was eroded (fig. 1). But to the east, the unconformity changes into a conformity . It comprises a medium-coarse to conglomeratic transgresive basal sandstone and multicoloured claystones and siltstones. This formation gradually thins to the east.

The uplift of western Andean domain caused the withdrawal of the sea from the basin , and set the new west-east directions of fluviatile system. The Guayana-Brazilian Shields continued as a secundary source of sediments during Maastrichtian-Paleocene times (Jaillard E. 1995).

**Eocene**

As a result of the uplift and erosion of the ancestral Andean ranges, Tiyuyacu conglomerates and coarse sandstones, claystones and siltstones were laid down in the basin . The axis of Eocene basin was almost the same that the present basin axis.

The Andean mountains experimented a multiepisodic uplift, which produced at least two conglomeratic secuences. The main conglomeratic depositation laid down along the northwestern and northcentral areas of the Oriente Basin in alluvial fans and plains.

The preferential deposition in the northwestern portions of the basin is probably due to the Andean ranges, which were nearest in the north than in the south (the altitude was higer in the north). Campbell C. J. (1970) explains the absence of coarse clastic sediments in the Marañon area by the continued existence of the Marañon Portal to the west.

A group of reverse faults and related folds formed . The basin structured in this time, and two subbasins developed: the northern Napo Subbasin narrower than the soutern Pastaza Subbasin , with high density of faulting and folding, which decreases toward the Pastaza Subbasin. The increased structural deformation is the result of Jurassic-Cretaceous extension and subsecuent Tertiary compression being taken up by a more limited rock volume (Jenks 1956 in Dashwood M. F. & Abbots,1990). The faults reactivated at this time, and related folds, together with those reactivated in the Turonian-Campanian, are the more important in the hidrocarbon history.

After Tiyuyacu sedimentation occured diastrophic events related to Andean orogeny wich provoked erosion of those sediments, reaching 5.800 feet at the eastern portion of the basin (Tiputini 1 well. Llerena M. G. 1991)

**Oligocene**

At the late Eocene the Andean source area were reduced by erosion, and progressively finer sediments were deposited in the basin. A short transgression took place. The Orteguaza deposited (fig. 1). It consists of green shales and sandstones. Afterwards the Chalcana Formation which comprises brown-redish claystones, with subordinate sandstones and conglomerates, deposited under continental to marginal-marine conditions.

There is no evidence of tectonic activity at this time, only sporadic andean uplfting laid down minor conglomerates in the Chalcana formation.

## CONCLUSIONS

The first indications of Andean compresion are evidenced by the Santonian-Campanian uplift of the "Napo Uplift" and "Pastaza Depression" in the Subandean Zone.

The basin is almost definetly structured at the Eocene, when the andean compression formed two regional structures: the northern Napo Subbasin, more structured than the southern Pastaza Subbasin.

The Albian-Eocene is a critical time for the hydrocarbon sistem. The productive structures began to develop, the reservoirs rocks and potential source rocks were depositing.

## REFERENCES

Almeida T. 1992. Estudio Regional de la formación Tiyuyacu. Universidad Central del Ecuador. Tesis de grado

Campbell C. J. 1970. Guide to the Puerto Napo Area, eastern Ecuador with notes on the regional geology of the Oriente Basin. Ecuadorian Geological and Geophysical Society.

Dashwood M. F. & Abbots I. L. 1990. Aspects of the petroleum geology of the Oriente Basin, Ecuador.Geological Society Special Publication No 50, pp 89-117.

Jaillard E. 1995. Síntesis estratigráfica y sedimentológica del Cretáceo y Paleógeno de la Cuenca Oriental del Ecuador. Orstom-Petroproducción. Informe Interno.

Llerena M. G. 1991. Estudio de la compactación de las lutitas de la Cuenca Oriental. Universidad Central del Ecuador. Tesis de Grado.

Odin G. S. & Odin Ch. 1990. Echelle numérique des temps géologiques. B.R.G.M. Geochronique No 35

Rivadeneira M. Dávila C. Toro J. 1996. La arenisca M1 en la Cuenca Oriente Ecuatoriana. Petroproducción. Informe Interno.

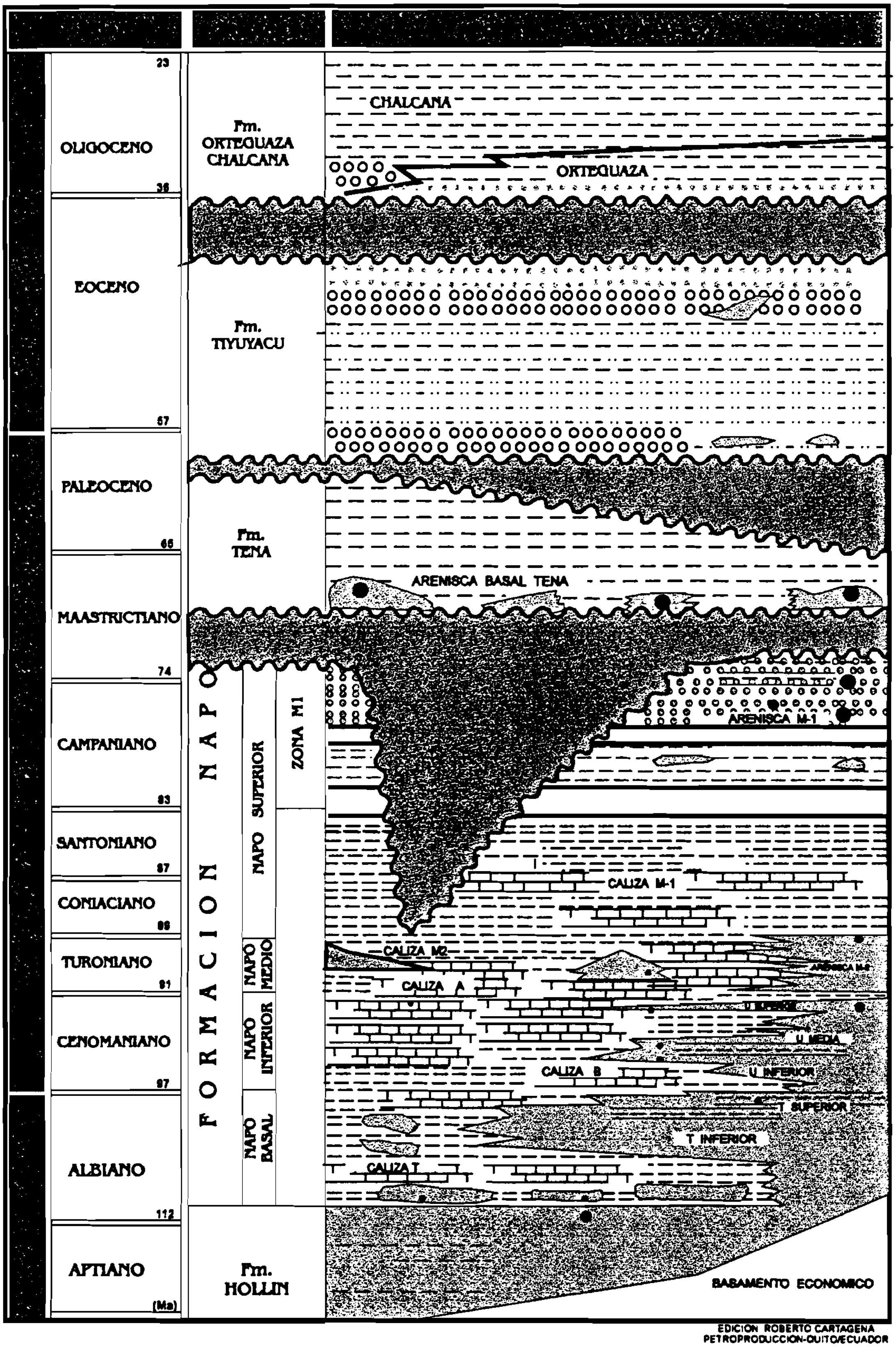


FIGURE : 1

CRETACEUS AND PALEOGENE CHRONOSTRATIGRAPHIC DIAGRAM OF THE ECUADORIAN ORIENTE BASIN.

● YACIMIENTO DE PETROLEO

# GENESIS AND KINEMATIC OF THE NORTHERN BOLIVIAN ALTIPLANO

Philippe ROCHAT (1), Patrice BABY (2), Gérard HÉRAIL (3), Georges MASCLE (1), Oscar ARANIBAR (4), Bernard COLLETTA (5)

(1) UPRES-A. 5025, Instut Dolomieu, 15 rue M. Gignoux, 38031 Grenoble - France
(2) ORSTOM Ecuador, cc 17 11 6596, Quito - Ecuador
(3) ORSTOM Chile, cc 53390, Santiago 1 - Chile
(4) YPFB. cc 1659 Santa Cruz - Bolivia
(5) IFP. 1 avenue de Bois-Préau, BP 311, 92506 Rueil Malmaison cedex - France

KEY WORDS: Altiplano, thrusts, inversion, syntectonic sedimentation, erosion.

## INTRODUCTION

The Altiplano is an enigmatic high plateau of the Central Andes, characterized by a thick crust about 70 Km (Wigger et al., 1994, Beck et al. 1996). Recent seismologic data show that magmatic accretion did not cause this crustal thickening (Dorbath et al., 1992), and numerous authors have emphasized the importance of horizontal shortening in the Altiplano structuration (Roeder 1988; Baby et al., 1992; Hérail et al., 1993). New seismic data available in YPFB as well as recent field works allow us to present a new geometrical model of the northern Altiplano, and to discuss its sedimentary evolution characterized by thick accumulations of Tertiary continental sediments (10.000 m).

## STRUCTURAL SETTING

Recent field's works and analyses of seismic perfiles reflexions available in YPFB permit us to propose a new tectonic setting.
The northern Bolivian Altiplano can be divided in three structural domains (fig. 1 § 2)
- domain 1: At the eastern edge, the La Joya-Toledo plain forms the northern extremity of the Poopo basin, where late Tertairy and Quaternary deposits overlay the SW verging thrusts system of the Cordillera Oriental (Coniri Fault system). This plain is limited to the west by the Chuquichambi thrust, which forms the oriental flank of the Corque syncline. More to the north, in the Corocoro area where the Coniri limit is outcropping, synsedimentary structures prove a compressionnal activity of the Coniri fault as a thrust west verging system. This generation of structures is fold latter with a transpresionnal geometry showing a strike slip movement along this limit.
- domain 2: In the central area, the Corque syncline (2A) corresponds to the eastern part of an inverted half-graben. In the central part of the syncline, reflexion siesmic data show a thickness of 10 000 meters of Tertiary deposits, whithin which no erosionnal surfaces are observed. Its oriental flank represents the hanging wall of the Chuquichambi thrust, whereas its occidental flank is carried on the Turco thrust. The sole thrust is located in the base of the Tertiary series characterized by evaporitic layers. Little lenght wawe of structures located in the western flank are compatible with a thin skin tectonic and show that the basement is not impliquated in the compressive structures. In the central part of the northern altiplano, at the Andamarca latitude, the eastern edge of the Corque hemi-graben (not inverted) is N-S oriented, and reactived with a dextral strike-slip movement. More to the south at the east of the continuation of the Chuquichambi trend fault, Salinas de Garcia Mendoza area, oblique and sygmoide folds developped into Cretaceous deposits provide a transpresionnal regime induced by the dextral movement along the Chuquichambi limit.
- domain 3: The western edge is characterized by undeformed Pliocene and Pleistocene formations. These sediments seal: to the east, the preserved part of the Corque basin (2B), and to the west, a hemi-graben

(3), limited at its eastern edge by the Villa Flor fault, which is the continuation of the Mauri basin outcropping to the North in the Berenguela area. Tectonic style is reactivation of vertical faults well constrained by seismic perfiles.

## TERTIARY SEDIMENTARY SEQUENCES

Using recent new datations (Swanson et al., 1987; Lavenu et al., 1989; Marshall et al., 1992, Kennan and al, 1995), we characterize five major depositional sequences which regroup all the previously sedimentary formations defined on the Altiplano (Hochstatter 1972; Cheroni, 1968 for example):

- Sequence 1 (Eocene-Oligocene: Tihuanacu Fm., Berenguela Fm., Turco Fm.), is formed by an alternance of red sandstones and argilites, characterized in its upper part by lenses of west-proceeding fluvial conglomerates (Sempere et al., 1990). This sequence does not outcrop in the Cordillera Oriental; it is 3000 m thick in the domain 2 and 2200 m thick in the domain 1.
- Sequence 2 (basal Upper Oligocene - Lower Miocene: Coniri Fm., Kollu Kollu Fm., Azurita and Huayllapucara Fm., Mauri 1-5 Fm.) is characterized by coarse conglomeratic layers, which are composed of Paleozoic rocks pebbles coming from the East (Coniri Fm), in domain 1, and red granites and gneiss pebbles coming from the West, in domain 3. In the Corque syncline (domain 2), the sequence consists of sandy sediments. Near the Coniri fault (domain 1), the sediments show progressive unconformities recording the uplift of the Cordillera Oriental. The base of the Coniri Fm has been dated at 25,5±1,7 My (Sempere et al., 1990) and the base of the Mauri Fm at 25,2±1 My (Lavenu, 1989).
- Sequence 3 (Middle Miocene) overlies the Oligo-Miocene on the domain 2, and an erosional surface on domains 1 and 3. It is 5000 meters thick in the center of the Corque syncline and thinner to the west. The base is characterized by sandstones, thin conglomerates and argillite (Caquiaviri Fm.), and the top by argillites and local evaporites (Rosapata Fm.). In the Mauri basin, the sediments (base of Mauri 6 Fm) are volcano-detritic and pinch out to the West. In domain 1, the sediments are thinner and pinch out to the East.
- Sequence 4 (Upper Miocene: Pomata Fm.) shows progressive unconformities and overlies the Middle Miocene with the Callapa tuff dated at 9,03±0,007 My (Marshall et al.,1992). This sequence is composed of argillites and lenses of conglomerates with Paleozoic rocks pebbles in domains 1 and 2, with some volcano-detritic sediments to the West. The domain 3B is characterized by greywackes.
- Sequence 5 (Pliocene) dated at its base at 5,34±0,003 My ( Marshall et al., 1992), unconformably overlies the Upper Miocene. This sequence is composed of lacustrine sandy loam with lenses of east-prograding conglomerates, in domain 1, and volcano-detritic sediments, in domains 2 and 3.

## BALANCED CROSS SECTIONS

Four sections have been constructed using the kink method. For each one's, structures are built with hypothesis of a mimimun shortening. The main detachments are located in the base of the Ordovician, base of the Silurian, base of the Devonian and base of the Tertiary rocks; In Salinas de Garcia Mendoza area, base of the Cretaceous is a decollement surface permitting the expulsion of an cretaceous basin. The thrust system geometry is characterized by fault progation folds of 1° generation (sometimes reactivacted), fault bend folds and duplex structures. The eastern limit of the Corque basin was built as a normal fault reactivacted in the north and creation of short cut (deformation of the footwall) in the south. These mecanisms of inversion are well imaged by tomographic images resulting of analog sand box experiments realised and analysed by tomography in IFP.

In our balanced cross section,the value of shortening ranges between 25 km to 60 km. Shortening is bigger in the south where the Poopo basin is well developped.

CONCLUSIONS: KINEMATIC MODEL AND CRUSTAL GEOMETRICAL MODEL

A combined study of the structural geometry and depositional sequences allow us to propose a tectonosedimentary evolution :

During Eocene-Lower Oligocene times, the Altiplano corresponded to a basin filled up by a low detritism coming from the West. The Chuquichambi trend could control the sedimentation during this period, and induce the difference of thickness between domains 1 and 2 and the depot center of evaporitic layers present at the base of the first sequence.

During the Oligo-Miocene, the Altiplano started to structure and corresponded to a compressional basin thrusted by the Eastern Cordillera. Erosive surfaces in domains 1, 2B and 3 show that the basin boundaries were deformed and eroded, while the central part of the basin (2A) was undeformed and filled by sediments, due to the erosion of the Eastern Cordillera and the western Precambrian basement.

The Middle Miocene is characterized by very high rates of sedimentation in two north-south elongated hemi-graben: the Mauri basin and the Corque basin. This period corresponded with a gentle tectonic activity along the thrusts of the Coniri system (Hérail et al. 1993). Geometry of the synsedimentary deformation, recorded within the upper Miocene sequence in the Corque syncline and Poopo basin, show that the Corque hemi-graben suffered the tectonic inversion and that in the same time Coniri system was reactivacted with a strike slip component.

During the Lower Pliocene, in domains 3 and 2, the Upper Miocene structures were peneplaned and sealed by volcano-detritic sediments. The Poopo basin (1) corresponded to a terrigene basin controlled by the development of the Chuquichambi thrust, which becomė a ridge between two Pliocene basins. At the same time, the Subandean zone was structured (Baby et al., 1989); crustal shortening increased and produced an uplift of the Cordillera and the Altiplano.

Combinning our regional studies of the Altiplano and Subandean zone and surface mapping of the Eastern Cordillera provided by the Bolivian Oil Company YPFB, we purpose two crustal balanced cross sections with a shortening of 191 km for the 18° transect and 231 km for the 22° transect (Baby and al, this issue). At this crustal scale the Altiplano take characteristics of a piggyback basin and corresponds to the bigest detritic basin of the andean chain.

REFERENCES:

BABY, P., SEMPERE, T., OLLER, J., BLANCO, J., ZUBIETA, D. and HÉRAIL,G., 1992. Evidence for major shortening on the eastern edge of the Bolivian Altiplano: the Calazaya nappe, *Tectonophysics*, 205, 1-3, p. 155-169.

BECK, S., ZANDT, G., MYERS, S., WALLACE, T., SILVER, P. and DRAKE, L., submitted. Crustal Thickness Variations in the Central Andes, *Geology.*

CHERRONI, C., 1968. Geologia de la Serrania de Berenguela, *Informe YPFB (GXG-1338).*

DORBATH, C., GRANET, M., POUPINET, G. and MARTINEZ, C., 1993. Teleseismic study of the Altiplano and the Eastern Cordillera in northern Bolivia: new constraints on a lithospheric model, *J. Geophys. Res.*, 98, B6, p. 9825-9844.

HÉRAIL, G., SOLER, P., BONHOMME, M. and LIZECA, J. L., 1993. Evolution géodynamique du contact Altiplano - Cordillère Orientale au Nord d'Oruro (Bolivie) - Implications sur le déroulement de l'orogénèse andine, *C.R. Acad. Sci.*, 317,série II, p. 512-522.

HOCHSTATTER, H., 1972. Informe sobre la region NE del Altiplano septentrional, *Informe YPFB (GXG-1792).*

KENNAN, L., LAMB, S. and RUNDLE, C., 1995. K/Ar dates from the Altiplano and Cordillera Oriental of Bolivia, impliquations for Cenozoic stratigraphy and tectonic, *J. South Amer. Earth Sci.*, 8, 2, p. 163-186.

LAVENU, A., BONHOMME, M., VATIN-PERIGNON, N. and de PACHTERE, P., 1989. Neogene magmatism in the Bolivian Andes between 16° and 18° S. Stratigraphy and K-Ar geochronology, *J. South Amer. Earth Sci.*, 2, 1, p. 35-47.

MARSHALL, L. G., SWISHER, C., LAVENU, A., HOFFSTETTER, R. and CURTIS, G., 1992. Geochronology of the mammal-bearing late Cenozoic on the northern Altiplano, Bolivia, *J. South Amer. Earth Sci.*, 5, 1, p. 1-19.

ROEDER, D.,1988. Andean age structure of eastern Cordillera, *Tectonics*, 7, 1, p. 23-39.
SEMPERE, T., HÉRAIL, G., OLLER, J. and BONHOMME, M., 1990. Late Oligocene-early Miocene major tectonic crisis and related basins in Bolivia, *Geology*, 18, p. 946-949.
SWANSON, K. E., NOBLE, D. C., McKEE, E. H., SEMPERE, T., MARTINEZ, C. and CIRBIAN, M., 1987. Major revisions in the age of rock units and tectonic events in the northern Altiplano basin of Bolivia, *GSA Meeting*, Abstracts with Programs, 19, p. 456.
WIGGER, P., SCHMITZ, M., ARANEDA, M., ASCH, G., BALDZUHN, S.,GIESE, P., HEINSOHN, W., MARTINEZ, E., RICALDI, E., ROWER, P. and VIRAMONTE, P., 1994. Variation in the Crustal structure of the Southern Central Andes deduced from Seismic Refraction Investigation, *in : Reutter ,K.J., Scheuber ,E .et Wigger ,P.J, éd., Tectonics of the Southern Central Andes,* p. 23-48.

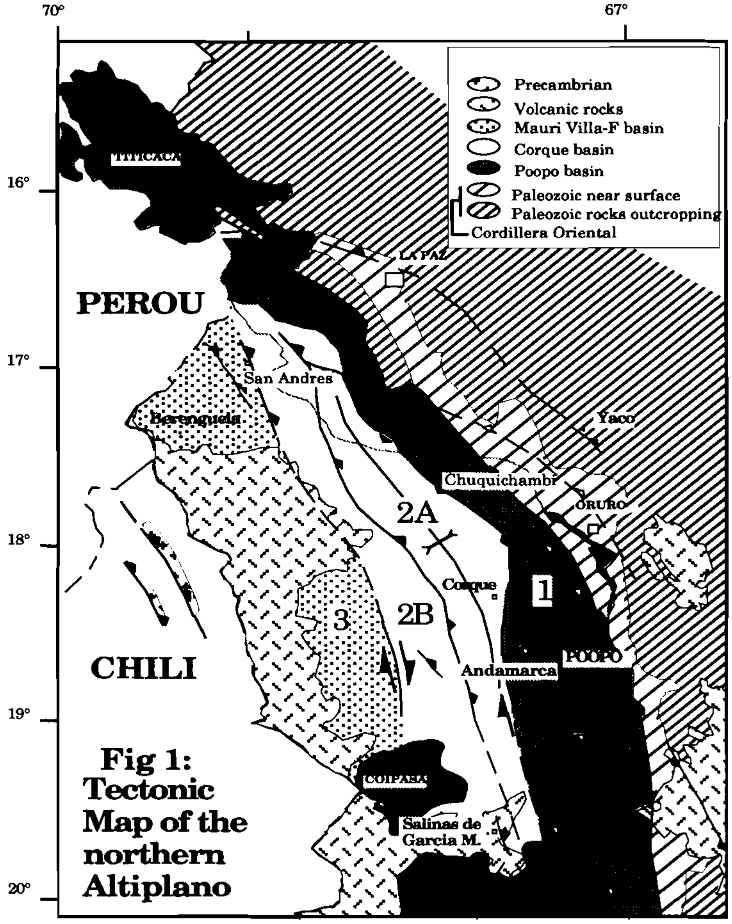


**Fig 1: Tectonic Map of the northern Altiplano**

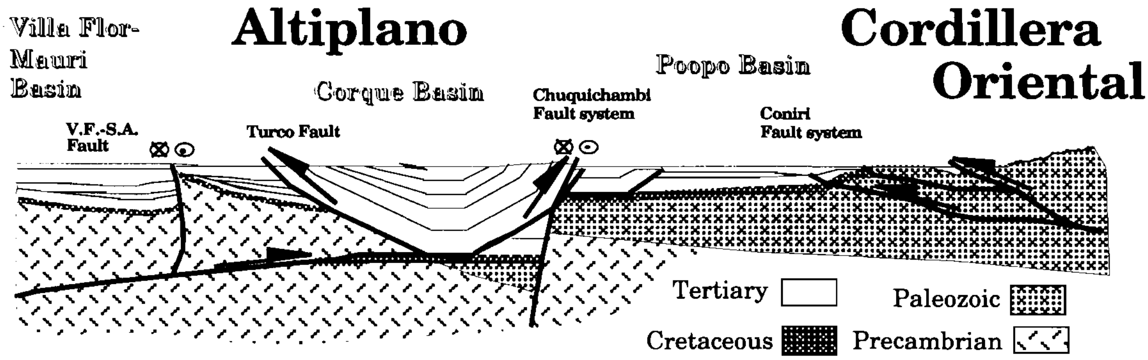


Fig 2: Schematic section of the northern Altiplano

# MAGNETOSTRATIGRAPHY AND PALEOMAGNETIC ROTATION OF THE NORTH-CENTRAL BOLIVIAN ALTIPLANO BASIN

P. ROPERCH[1,3], L. AUBRY[1], G. HERAIL[1], M. FORNARI[2] and A. CHAUVIN[3]

(1) ORSTOM and Dep. Geologia, Univ. Chile, Santiago
(2) ORSTOM, La Paz, Bolivia
(3) Géosciences Rennes, Campus de Beaulieu, 35042 Rennes cedex.

KEY WORDS: Paleomagnetism, Magnetostratigraphy, Tectonic rotations, Bolivian Altiplano

## INTRODUCTION

Magnetostratigraphic dating can be a very powerful tool in the study of continental basins. In the Andes, for example, magnetostratigraphic studies have brought important constrains in the understanding of the development of the foreland basins of the Sierras Pampeanas [Johnson et al., 1986].In this study, we report an attempt to use paleomagnetism to determine sedimentation rates in one of the thickest Andean Tertiary sedimentary basins located in the north-central Bolivian Altiplano [Kennan et al., 1995; Rochat et al., this volume].

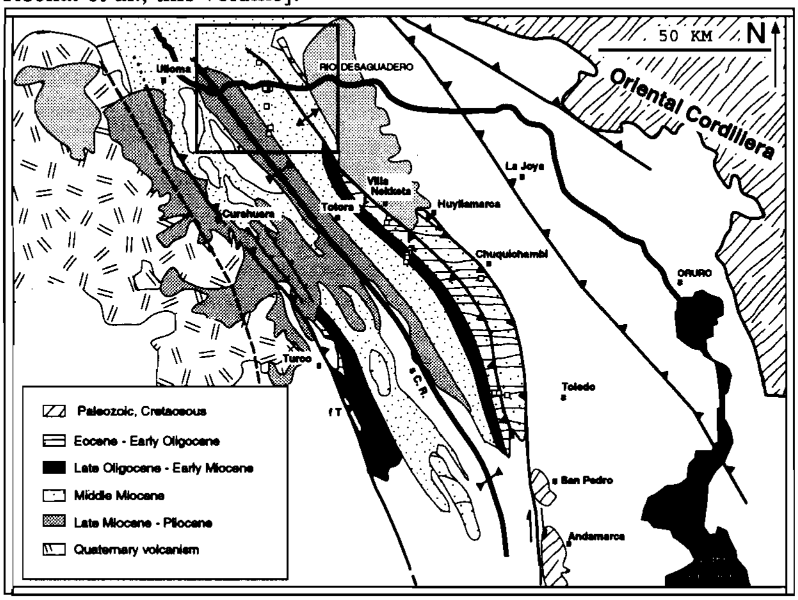


Figure 1: Simplified geologic map of the Central Bolivian Altiplano (modified from Rochat et al., in press). Squares correspond to the paleomagnetic sampling.

The sequence of Tertiary continental deposits is well exposed within the Corque syncline (Fig. 1). This structure is oriented N150 and its axis can be traced for more than 100 km. The lowest sedimentary sequence is the Eocene-Oligocene Tihuanaku formation which is well exposed on the eastern border of the basin. The age of this formation is poorly constrained because of the lack of fossils or interbedded volcanic units. This sequence is followed by the more conglomerate Coniri formation of Late Oligocene- Early Miocene age. The middle Miocene Totora formation overlay conformably the Coniri formation. Most of the deformation took place in late Miocene and the main tectonic structure is the curved Chuquichambi thrusts system.

We first did a paleomagnetic survey to determine the stability of the magnetization and evidence of a reliable magnetostratigraphic record.. Most of the successful studies in the Neogene basins of NW

Argentina deal with sediments rich in volcanoclastic and the remanent magnetization carried by magnetite. In contrast, the central Altiplano basin is mostly filled by red beds deposits.

The Tihuanaku formation (also named Huayllamarca) is mainly composed of consolidated fine red sandstones with interbedded red claystones. The sandstones do not record a stable magnetization and only the claystones have a stable remanence carried by hematite. The red claystones record in sequence normal or reverse polarity and this observation indicates a detrital or early diagenetic origin for the hematite. However, the lack of fresh exposure of a sufficiently continuous sequence has so far prevented the acquisition of a magnetostratigraphic record in the Tihuanaku formation. The Totora formation is mainly composed of poorly consolidated sandstones with interbedded claystones. After removal of 10 to 20 cm of weathered clays, instead of taking oriented blocks, we choose to drill the soft sediments with air-cooling; a technique which enables to collect a large number of samples (997 cores in this study).

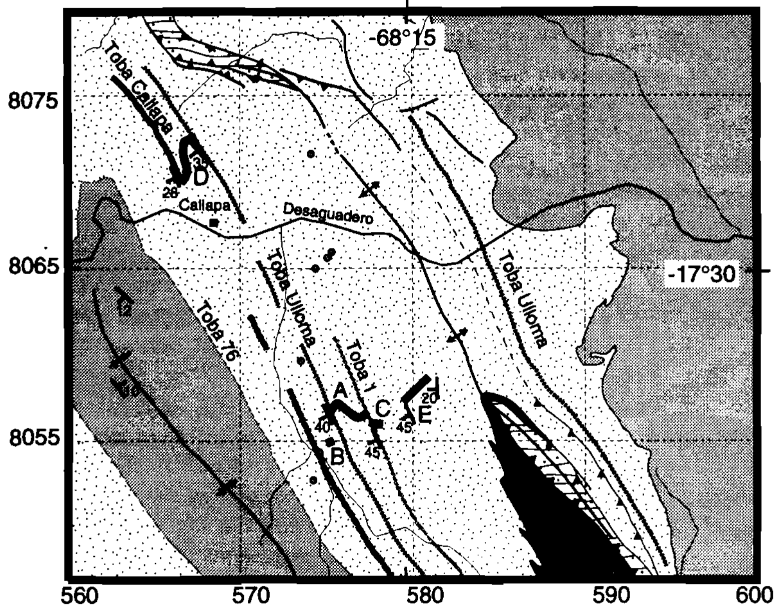


Figure 2: Map showing the locations of the magnetostratigraphic sections

MAGNETOSTRATIGRAPHY OF THE TOTORA FORMATION:

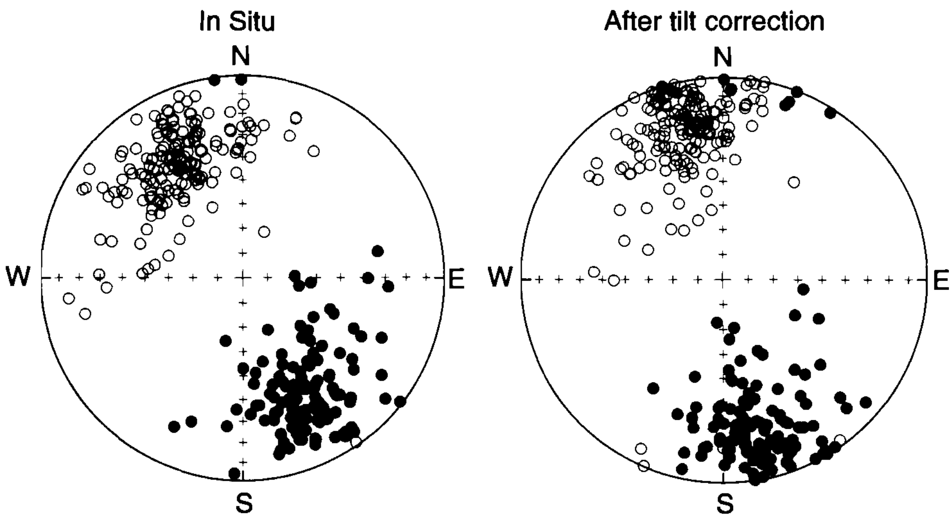


Figure 3: Equal-area projections of the characteristic magnetizations for section D in in situ and after tilt correction. Open (filled) symbols correspond to negative (positive) inclinations. In in situ coordinates the observed magnetizations are significantly different from the present day field. Normal and reverse polarity magnetizations are also antiparallel..

The Totora formation is a thick formation which outcrops largely on the eastern limb of the Corque Syncline with layers dipping to the west from about 45° to 30° (Figure 2). An other important feature of the Totora formation is the existence of numerous tuff layers and two of them have been previously dated by K-Ar and $Ar^{39-40}$ radiometric dating. The Callapa and Ulloma tuffs are also well recognized in the field and they provide straightforward stratigraphic markers. We sampled four main sections (A, C, D and E). It was almost impossible to perform an E-W traverse perpendicular to the strike of the sedimentary sequence. The positions of the sampling sites were obtained by GPS positioning and the complete thickness of our magnetostratigraphic sequence was calculated according to the strike and dip of the structure. We arbitrarily put the base of our sequence at the base of section E. Sampling between the Ulloma and Callapa tuffs was performed north of the Callapa village. From the base of section E to the top of section D (Tuff Callapa), the sequence is about 4600m thick. The large sampling gap between sections E and C and the absence of radiometric control in the lower part of the section do not permit magnetostratigraphic dating of the lower part. We will only report the interpretation of the composite section (C+A+D). Normal and reverse polarities are observed. The magnetization is carried by magnetite and hematite. There is a slight increase in magnetic susceptibility toward the top of the sequence (from 2-3 $10^{-4}$ to $10^{-3}$ SI) indicating the volcanism input in the sediments. The tilt toward the west of the sedimentary strata provides a good control on the age of the magnetization and we can discard the effect of viscous overprints in the present day field (Figure 3). The numerous radiometric datings of the Callapa and Ulloma tuffs indicate that this part of the magnetostratigraphic record should be correlated to the geomagnetic reversal polarity timescale [4] (GRPTS) in the time interval 8-11 Ma. The correlation of the observed magnetic record with the GRPTS shows that sediments were deposited from about 11.7 Ma to 9 Ma with an almost constant sedimentation rate of 0.97Km/Ma. Using this mean rate of sedimentation, the Ulloma tuff is dated at 10.23 Ma and the Callapa tuff at 9.17Ma. These estimates are in excellent agreement with the best ages given by Marshall et al. (1992) of 10.35±0.06 and 9.03±0.07Ma.

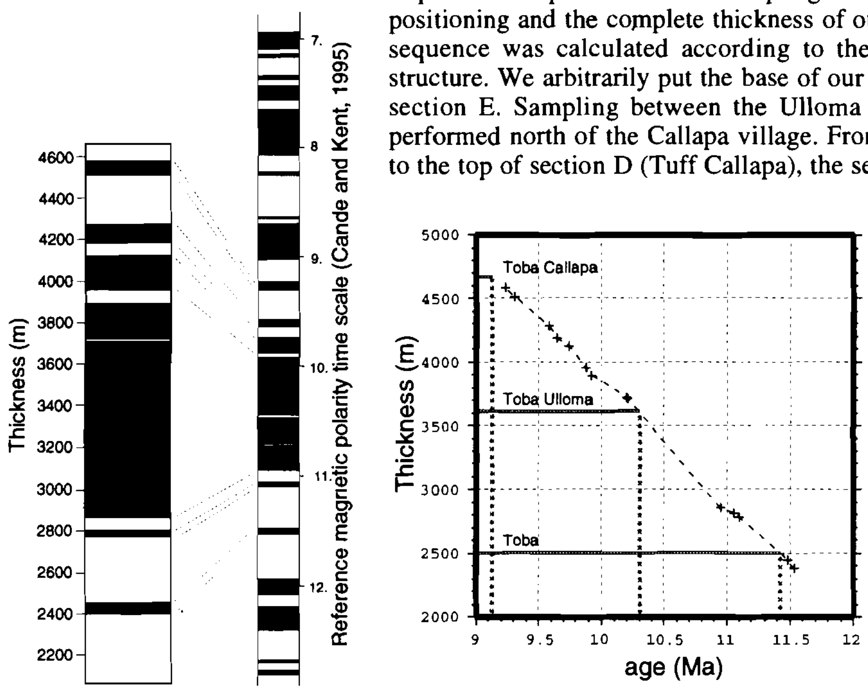

Figure 4: Correlation of the observed record with the GRPTS

TECTONIC ROTATION OF THE CENTRAL ALTIPLANO BASIN.

The Chuquichambi thrust system is characterized by its curved structure. This curved shape is possibly inherited or was enhanced during deformation. Nine paleomagnetic sites (129 cores) were drilled where the structures are NW oriented and 5 sites (71 cores) further south in the north trending structures. The mean declination for the northern sites is deflected from the expected direction by about 30° while the southern sites give 20° suggesting that most of the Chuquichambi curvature is possibly due a paleogeographic feature (Fig. 5). The two populations are however not statistically different. An additional sampling is needed to ensure the 10° difference between the two branches of the Chuquichambi structure. Nevertheless, our paleomagnetic study indicates that the whole Chuquichambi struture is rotated counterclockwise by about 20°

The paleomagnetic results from the dispersed sampling within the Totora formation as well as those from sections A,B and C and D (Fig.6) also confirm the existence of a counterclockwise rotation greater than 10° after 9 Ma. The consistency of the paleomagnetic results over several tens of kilometers demonstrates that the Central Altiplano basin rotated about 10° since the late Miocene. The respectively 20° and 10°

rotations are likely related to the shortening observed across the eastern cordillera and subsequently in the subandes.

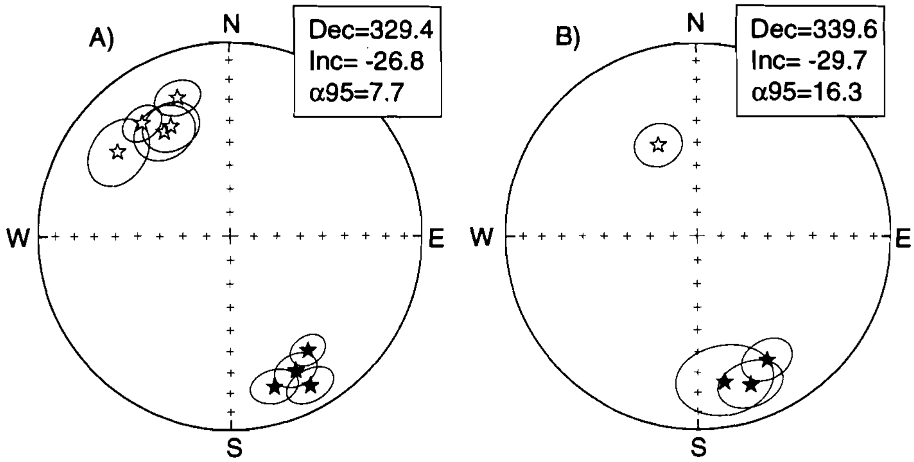


Figure 5: Paleomagnetic results from the Chuquichambi structure. A) northern branch, B) southern sites

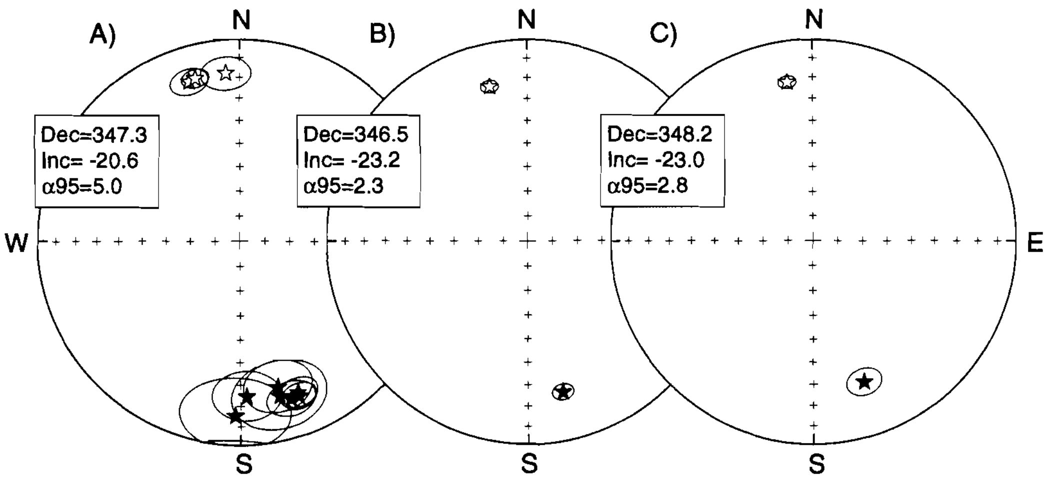


Figure 6: Paleomagnetic results from the Totora formation. A: dispersed sampling; B: section D mean 298 samples ; C: sections A+B+C mean 272 samples

**Acknowledgements**: We thank Marco Kapak, Seferino Gonzales, Ricardo Frontanilla, Marcelo Adunate and Ricardo Molinero for their help in the field.

REFERENCES

Cande, S.C., and D.V. Kent, 1995. Revised calibration of the geomagnetic polarity timescale for the Late Cretaceous and Cenozoic, *J. Geophys. Res.*, *100* (B4), 6093-6096.

Johnson, N.M., T.E. Jordan, P.A. Johnsson, and C.W. Naeser; 1986. Magnetic polarity stratigraphy, age, and tectonic setting of fluvial sediments in an eastern Andean foreland basin, San Juan Province, Argentina, in *Foreland basins: International Association of Sedimentologists Special Publication,* edited by P. a. A. Homewood P. eds, pp. 223-235.

Kennan, L., S. Lamb and, C. Rundle; 1995. K-Ar dates from the Altiplano and Cordillera Oriental of Bolivia: implications for Cenozoic stratigraphy and tectonics; *J. S. Am. Earth Sci.*, 8, 163-186.

Marshall, L.G., Swisher, C., Lavenu, A., Hoffstetter R. and Curtis, G., 1992. Geochronology of the mammal-bearing late Cenozoic on the northern Altiplano, Bolivia, *J. South Amer. Earth Sci.*, 5, 1, p. 1-19.

# THE VALLE FÉRTIL FLOWER STRUCTURE AND ITS RELATIONSHIPS WITH THE PRECORDILLERA AND PAMPEAN RANGES, (30-32°S, ARGENTINA).

Eduardo A. Rossello [1,2], Marcos E. Mozetic [1,3], Peter R. Cobbold [4], Marc de Urreiztieta [4], Denis Gapais [4] & Oscar R. López-Gamundí [5]

[1] Dpto. de Ciencias Geológicas, Universidad de Buenos Aires, Pabellón II, 1428 Buenos Aires, Argentina.
[2] CONICET
[3] BHP Petroleum Argentina Inc.
[4] Géosciences-Rennes (UPR 4661-CNRS) Campus de Beaulieu, 35042 Rennes Cédex, France.
(5) TEXACO Inc., Central Exploration Department. 4800 Fournace Place, Bellaire 77401-2324 Texas, USA.

**KEY WORDS:** Valle Fértil, Argentina, flower structures, ramp basins, Andean foreland.

## INTRODUCTION

The Andes result from oblique subduction of the oceanic Nazca plate beneath the continental South America plate (Fig. 1). Between 27°S and 32°S, the Andean Cordillera trends N-S and lies above a subhorizontal segment of the descending Nazca plate (Fig. 1). From the Chile trench towards the foreland, the mountain belt consists of a series of N-S trending structural units: the Coastal Cordilleras, the Principal Cordillera (inactive volcanic arc), the Frontal Cordillera, the Precordillera and the Sierras Pampeanas. This work deals with the foreland basin geometry between the Precordilleran fold and thrust belt and the westernmost basement uplifts of the Sierras Pampeanas.

Between 29° and 33° S, East of the Precordilleran thrust front, the NW-SE trending Desaguadero-Valle Fértil fault marks the western boundary of the Pampean ranges (Fig. 1, VF). In the foreland, in successive compressional basins alternate with basement uplifts, bounded by high-angle thrusts (Jordan & Allmendinger, 1986). Five structural domains can be identified from West to East (Rossello *et al.*, 1995): (1) the Precordilleran thrust front, (2) a proximal foreland basin, (3) the intervening Valle Fértil basement high, (4) a distal foreland basin and the Pampean Ranges. Our description of compressional structures is based on field observations and seismic data.

## PRECORDILLERAN THRUST FRONT

In the Precordillera (Fig. 2) a series of east-verging thrust sheets involving Early to Lower Paleozoic sediments, overthrust intercalated Neogene deposits (Beer *et al.*, 1990). The amount of bulk regional shortening across this segment of the Andes may 65-70% (Allmendinger *et al.*, 1990). Asymmetric anticlines westwards verging alternate with tight synclines. On the western margin of the Precordillera, the upper Tertiary cover (younger than 15 Ma., Beer *et al.*, 1990) reaches a thickness of 4 km within the Valle de Iglesia. The Precordilleran front is thrust over the Tertiary foreland detrital deposits (Fig. 2).

## PROXIMAL FORELAND BASIN

The immediate foreland basin (Bolsón Bermejo, Fig. 2) is filled with Neogene syn-orogenic deposits reaching a thickness of 7,000 m (confirmed by wells). These 14-2.3 Ma detrital sequences are upward coarsening (Johnson *et al.*, 1987, Beer & Jordan, 1989). The Neogene sedimentary cover forms fault-propagation folds and lies unconformably, either on the Paganzo Group sequences (to the East) or on lower Paleozoic sediments (to the West). The Bermejo basin is a roughly symmetric ramp basin. It deepens towards the West under the Precordilleran front (Zapata & Allmendinger, 1996) and is overthrust on its eatern margin by the Valle Fértil Ranges. Furthermore, in the middle of the basin the top of the crystalline basement is symmetrically kinked (Fig. 2) and emerges locally at the surface in the Sierra Pie de Palo area (Fig 1, PL).

## INTERVENING BASEMENT HIGH, VALLE FÉRTIL-SIERRA MORADA

Within the foreland, the Valle Fértil Range has an anomalous NW-SE trend. It is an assemblage of crystalline basement blocks, locally covered by folded Paleozoic rocks to the North (Paganzo Group). These blocks are bounded to the West by high-angle westward verging thrusts. In detail, the structure consists of (1) *en échelon* N 170 trending left-lateral thrusts, (2) associated N-S fold hinges and culminations, (3) conjugate right-lateral faults trendin N 070 and (4) normal faults trending N 120. Hence, the eastern margin of the Valle Fértil system is a major transpressional left-lateral wrench zone. Faulting involves the crystalline basement and can be interpreted in cross-section as a positive flower structure (Harding, 1990), verging towards the West. This structure probably reactivated Triassic normal faults. Along the abrupt western margin of the Valle Fértil Ranges, the vertical offset of the top of the basement is at least 7,000 m according to seismic information (Fig. 2). On the eastern margin, an erosional surface exposed on the top of the range (Jordan *et al.*, 1989) dips gently eastwards, beneath the sediments of the Villa Unión-Pagancillo Basin.

## DISTAL FORELAND BASIN

East of the Valle Fértil Range is the distal domain of the Andean foreland. The Villa Unión-Pagancillo basin is filled with Neogene detrital sequences which rest unconformably on the upper Paleozoic deposits of the Paganzo Group. This asymmetric ramp basin deepens eastwards, the base sloping 10° to 15°, from the Sierra Valle Fértil-Sierra Morada to the Famatina-Sañogasta Ranges. The depocenter reaches a depth of 4,000 m. Surface geology (Malizia *et al.*, 1995) and sub-surface data indicate a thinning of the Tertiary sequences towards the East. The eastern edge of the basin is bounded by a thrust fault along the Famatina-Sañogasta Ranges.

## PAMPEAN RANGES

The Sierra de Famatina-Sañogasta are made of crystalline basement. The interface between the basement and the sedimentary cover is the erosional surface mentioned above. This interface is locally overlained by sequences of the Paganzo Group and sedimentary remnants attributed to the Neogene. Thick-skinned tectonics characterize the Pampean Ranges. Uplifted blocks of basement are bounded by high-angle thrusts (Jordan & Allmendinger, 1986). These regional faults results in large vertical offsets of the top of the basement. The highest basement outcrops are on the Famatina range (6,250 m a.s.l.). In surrounding Neogene basins, sediments reach thicknesses of several thousand meters (10 km in Quebreda la Troya basin). Consequently, the vertical offset locally exceeds 10 kilometers.

## CONCLUSIONS

The foreland basin, 200 km wide between 29° and 32°S, is of ramp type. The eastern margin is against the Famatina-Sañogasta Ranges. The central sector is uplifted and emerges at the surface along the left-lateral Valle Fértil wrench zone. This major regional fault divides the foreland into two asymmetric basins. According to the geometry and sedimentary characteristics of the Neogene cover, the Andean foreland basin is of typical ramp style (Cobbold *et al.*, 1993).

## ACKNOLEDGEMENTS

This study was carried out as part of (1) a research program funded by the EEC : "Andean tectonics of Argentina" (CI1*-CT93-0091 AR) and (2) a research project of the University of Buenos Aires UBA 1994-1997 (Ex 003).

## REFERENCES

**Allmendinger, R.W., D. Figueroa, D. Snyder, J. Beer, C. Mpodozis & B.L. Isacks, 1990.** Foreland shortening and crustal balancing in the Andes at 30 S Latitude, Tectonics, 9 (4), 789-809.

**Beer & Jordan 1989.** The effects of Neogene thrusting on deposition in the Bermejo Basin, Argentina. Journal of Sedimentary Petrology, v. 59, 330-345.

**Beer, J.A., R.W. Allmendinger, D.E. Figueroa & T.E. Jordan, 1990.** Seismic stratigraphy of a piggyback basin, Argentina. AAPG Bull 74 (8), 1183-1202.

**Cobbold, P.R., P. Davy., D. Gapais,, E.A. Rossello., E. Sadybakasov, J.C. Thomas, J.J. Tondji Biyo, M. de Urreiztieta.** Sedimentary basins and crustal thickening. In: S. Cloetingh, W. Sassi, F. Horvath and C. Puigdefabregas (Editors), Basin Analysis and Dynamics of Sedimentary Basin Evolution. Sedimentary Geology, 86 (1993) 77-89.

**Harding, T.P., 1990.** Identification of wrench faults using subsurface structural data: criteria and pitfalls. AAPG, Bull. 74 (10), 1590-1609.

**Johnson, A.T., T.E. Jordan, N.M. Johnson, & C.W. Naeser, 1987.** Magnetic polarity stratigraphy, age, and tectonic setting of fluvial sediments in the eastern Andean foreland basin, San Juan province, Argentina. International Association of Sedimentologists, Special Publication, 8, 63-75.

**Jordan, T.E. & R.W. Allmendinger, 1986.** The Sierras Pampeanas of Argentina: a modern analogue of Rocky Mountain foreland deformation. American Jour.nal of Sciences, 286, 737-764.

**Jordan, T.E., P. Zeitler, V. Ramos & A.J.W. Gleadow, 1989.** Thermochronometric data on the development of the basement peneplain in the Sierras Pampeanas, Argentina. Journal of South American Earth Sciences, 2 (3). 207-222.

**Malizia, D.C., J.H. Reynolds & K.D. Tabbutt, 1995.** Chronology of Neogene sedimentation, stratigraphy, and tectonism in the Campo de Talampaya region, La Rioja province, Argentina. Sedimentary Geology 96, 231-255.

**Rossello, E.A., M.E. Mozetic, P.R. Cobbold & M. de Urreiztieta, 1995.** El límite entre Precordillera y Sierras Pampeanas (Andes centrales de Argentina): consecuencias tectónicas y topográficas regionales. *IX° Congreso Latinoamericano de Geología (Caracas).* Actas Microregistradas.

**Zapata, T.R. & R.W. Allmendinger, 1996.** Thrust-front zone of the Precordillera, Argentina: a thick skinned triangle zone. AAPG Bull , 80 (3), 359-381.

**Figure 1.**

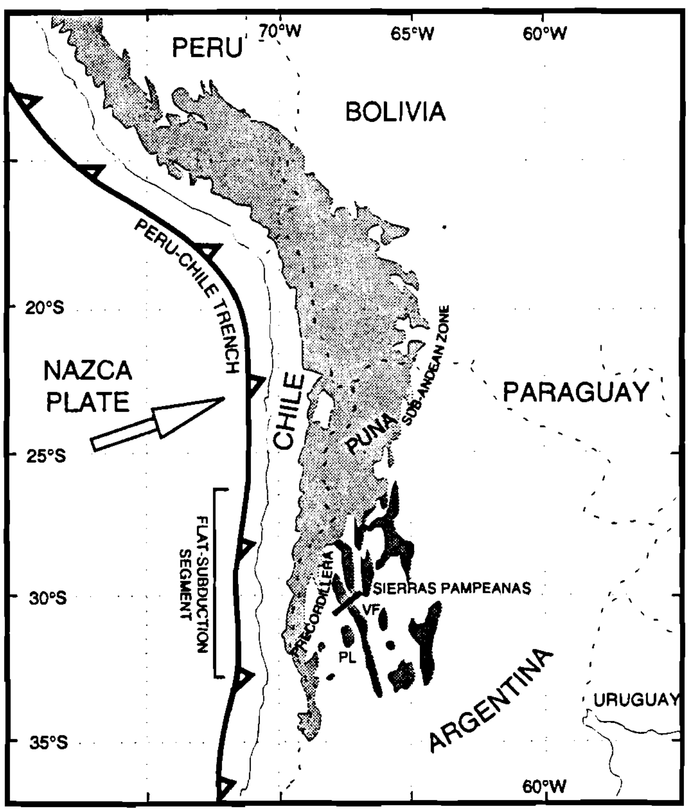

**Figure 2.**

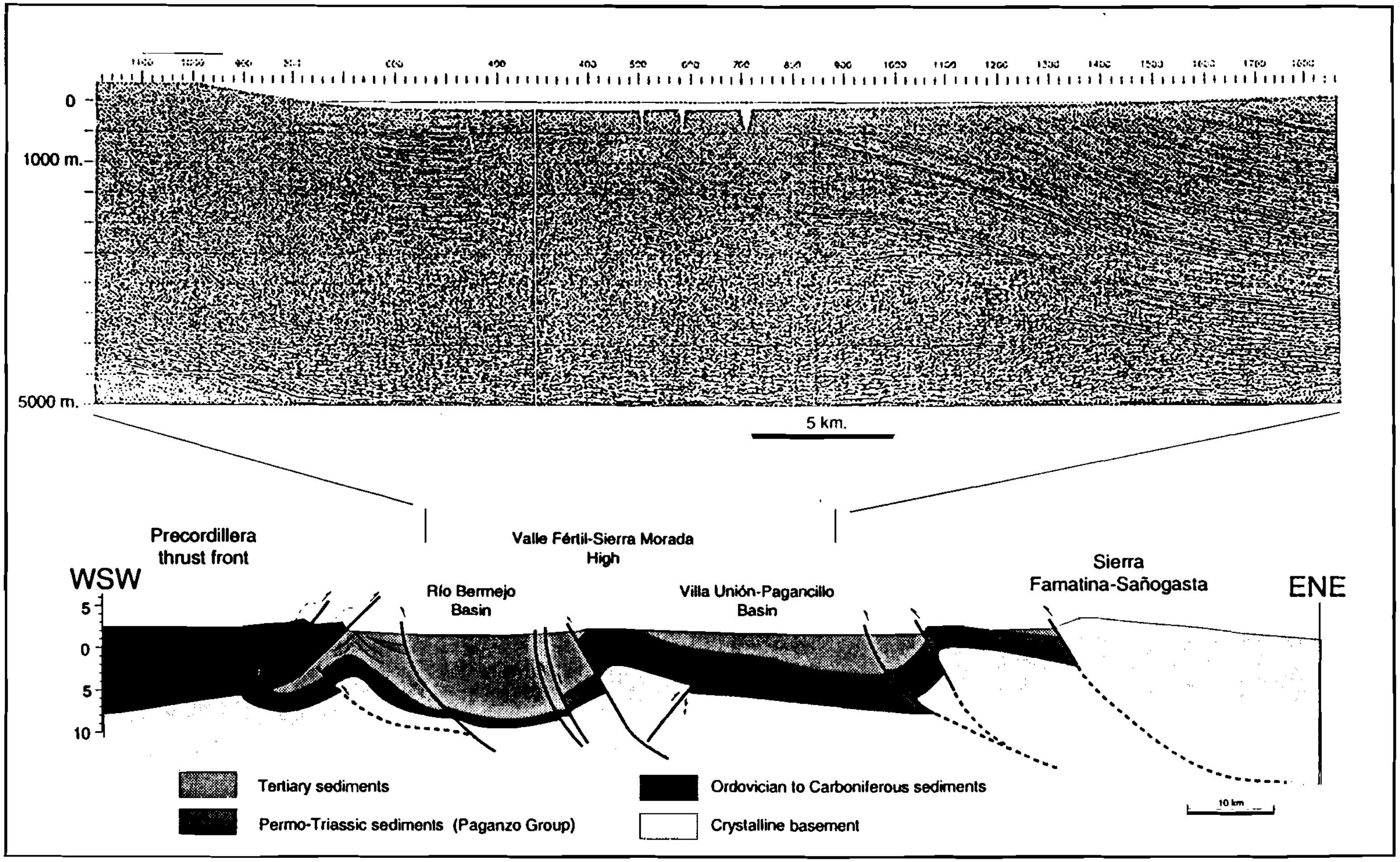
0
1000 m.
5000 m.
5 km.
Precordillera
thrust front
WSW
Valle Fértil-Sierra Morada
High
Río Bermejo
Basin
Villa Unión-Pagancillo
Basin
Sierra
Famatina-Sañogasta
ENE
5
0
5
10
Tertiary sediments
Permo-Triassic sediments (Paganzo Group)
Ordovician to Carboniferous sediments
Crystalline basement
10 km

# POST-EOCENE BASINS OF THE ARGENTINE CENTRAL ANDES

J.A. SALFITY*, S.A. GORUSTOVICH*, R.E. GONZÁLEZ*, C.R. MONALDI*, R.A. MARQUILLAS*, C.I. GALLI* and R.N. ALONSO*

*Universidad Nacional de Salta-CONICET, Buenos Aires 177, 4400 Salta, Argentina.

**KEY WORDS**: Basins, Tertiary, Central Andes, Argentina

## INTRODUCCION

The Neogene sedimentary basins of Argentine Central Andes and neighbouring regions developed into different tectonic frameworks; therefore, they were of different geologic origins.
This paper deals with the tectonic setting and regional distribution of the Tertiary basins developed in the Argentine Central Andes (22°-36° LS) during post-Incaic (post-Middle Eocene) and pre-Diaguita (Late Pliocene-Early Pleistocene) times.
The meaning of Neogene is here used in its widest sense. The sedimentary history of these Neogene basins began from Miocene times on, or before from late Eocene up to Oligocene. These sedimentary episodes are also named "Tertiary".

## STRUCTURAL HIGHS

The available information about the present-day distribution and the thicknesses of Tertiary deposits -in outcrops as well as in subsurface- let Yrigoyen (1969) draw the isopach lines of the main Argentine depocenters.
The region considered in this paper includes the Argentine Central Andes between the southern end of the Central Volcanic Arc (AC) and the northern end of the Southern Volcanic Arc (AS).
It is possible to distinguish the following structural highs:
**El Desierto High**, located in the northern part of the Chaco-Paranense basin.
Domeyko Arch. It was the western edge of the Atacama Tertiary basin of northern Chile. The Tertiary deposits lay in angular unconformity on the Cretaceous-Eocene Purilactis Group.
**San Rafael High**, in the southern end of the region. Over this arc basaltic retroarc flows will take place during Pliocene-Pleistocene times.
**Central Andean Arch and Southern Andean Arch**. Both archs were the host rock of the Miocene-Pliocene volcanic arcs. The Central one has transverse volcanic belts into de Argentine Puna.
**Pampean Arch**. It was the western edge of the marine Paraná Formation ingression; nevertheless, a westward dispersion of this ingression between 28-30°SL has been proposed.
**Cordillera Frontal-Precordillera Occidental High**, where piggyback like basins developed.
Other structural highs, that were in force during Paleozoic and Mesozoic times, remain buried by Tertiary basins. They are:
**Michicola Arch**. It is located on the northern wedge of Olmedo Sag and governed pre-Tertiary basins from the Carbonifeorus up to Paleocene times.
Quirquincho Arch. It was buried by upper Cretaceous-Paleogene posrift deposits and also by Neogene strata.
**Traspampean Arch**. There developed sedimentary basins separated by Ordovician transverse structural

highs. From Miocene times, these highs were the host rock of transverse volcanic belts of the Argentine Puna.

**Pie de Palo Arch**, was a part of the Sierras Pampeanas Occidentales during pre-Oligocene times. Neogene deposits buried this arc completely, except for the present-day Sierra de Pie de Palo that emerged since the Quechua diastrofism..

## DEPOCENTER DISTRIBUTION

The post-Incaic orogenic front originated the foreland basins of the region (Figure 1). This front is a series of en echelon thrusts of N-S Andean trending; the northern thrusts are displaced eastward and the southern ones westward.

The main Neogene depocenters are divided according to their with regard to the orogenic front (Figure 1): **a**) Andean depocenters located westward, and **b**) foreland and extra-Andean depocenters, some of them at the subsurface, located eastward the orogenic front.

The distribution of depocenters, their sedimentary history, and the geologic nature and structural framework of the pre-Oligocene basement, let us distinguish the following regional tectonic domains where the Tertiary sedimentary basins developed:

**Northern Foreland**: Includes the sub-Andean System of northern Argentina, developed to the east of Cordillera Oriental and Puna Austral. This foreland is the southern end of the Bolivian sub-Andean Neogene belt. The sedimentary filling (Orán Group) consists of foreland deposits at the base and taphric synorogenic basins at the top.

**Olmedo Sag**. Post-Incaic strata of Orán Group inherited the extensional tectonic framework, with thermal subsidence, that governed into the underlying Salta Group basin during Campanian-Eocene times. Thus, the sedimentary processes would have been able to be continuous between both Salta and Orán groups; Cenozoic Andean tectonics did not reach the Olmedo rift.

These deposits buried the previous Cretaceous basin and covered northward the Paleozoic basement of Michicola arch. In these regions the Neogene deposits overburdened and matured Devonian (Los Monos Formation) and Cretaceous (Yacoraite Formation) sources oil rocks.

**Famatina Forleand**. The Famatina foreland and associate basins developed in the transition area between southern Puna and northwestern Sierras Pampeanas, and between Northern Foreland and Cuyo Foreland. The sedimentary succession has a thick coarsening-upward stratigraphic column.

**Cuyo Foreland**. Post-Incaic coarsening-upward successions accumulated overlying the Precambrian basement, Lower and Upper Paleozoic, and non-marine Triassic and Cretaceous basins. The triangular geometry is curiously symmetrical to that of Northern Foreland-Olmedo Sag, in both cases located between the orogenic front, and Valle Fértil and Aconquija-Los Blancos lineaments, respectively.

**Backarc tectonic troughs of the Puna**. Since the Middle Eocene isolated troughs originated because of fragmentation of the Ordovician basement. These troughs are separated by WNW-ESE trending horsts. The first stage of filling is thinning-upward and was accumulated before the Miocene-Pliocene volcanic arc. In this way, the troughs developed between Central Andean Arch and the Northern Foreland. The Miocene-Pliocene volcanic arc had a great influence on the upper sedimentary succession.

**Atacama Forearc** (Chile). In this basin the angular unconformities in the base and top of Paciencia Group (Oligocene-Lower Miocene) are clearly distinguished. This group lies on Purilactis Group (Cretaceous-Paleogene) and underlies San Bartolo Group (Miocene). The sedimentary succession is thinning-upward, like the ones in the Puna backarc basins. In both cases there was magmatic quiescence. The Atacama basin was separated from the Puna's basins by the Central Andean Arch.

**Basins over Pampean Region**. They are intermontane basins mainly in the subsurface, of less thickness than in the Andean basins. They developed over Precambrian basement and over Upper Paleozoic, Triassic, and Cretaceous non-marine basins.

**Chaco-Paranense Marine Platform**. The Upper to Middle Miocene Atlantic marine ingression (Paraná Formation) reached the Northern Foreland, probably the Olmedo Rift, the Paraguayan Chaco and the Bolivian sub-Andean system.

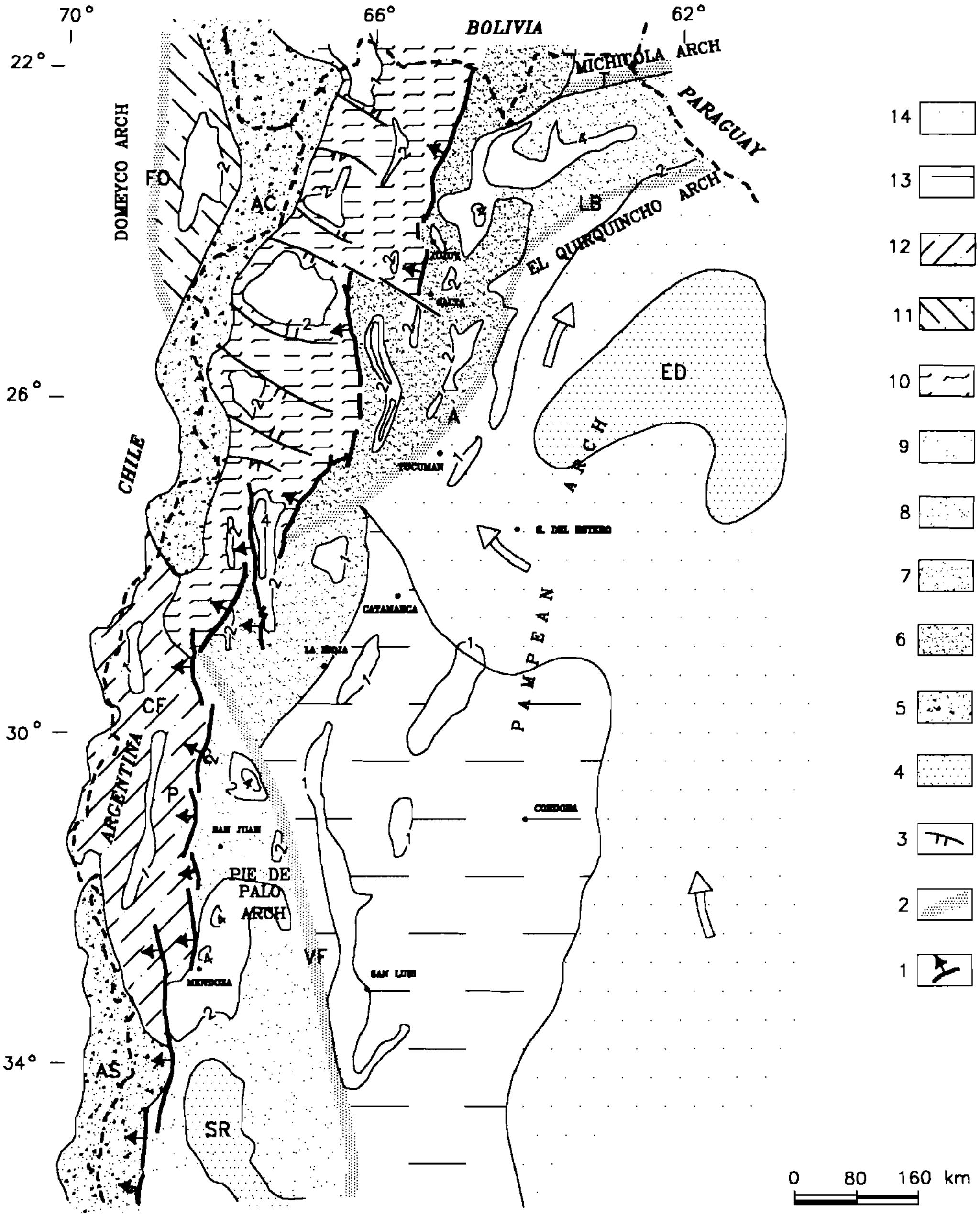


**FIGURE 1**: Present-day location of the main post-Incaic depocenters. Isopachs lines in km (white).

**1**, Post-Incaic thrust. **2**, Faults and lineaments: T, Tomasito; LB, Los Blancos; FO, Western Fault; A, Aconquija; VF, Valle Fértil. **3**, Assumed faults of the Puna's horsts. **4**, Main structural highs: ED, El Desierto; SR, San Rafael. **5**, Structural highs (Central -AC- and Southern -AS- Andean archs) where the Neogene volcanic activity took place. Basin tectonic framework: **6**, Northern Foreland. **7**, Olmedo Sag; **8**, Famatina Foreland; **9**, Cuyo Foreland. **10**, Puna's Backarc troughs. **11**, Atacama Forearc Basin (Chile). **12**, Cordillera Frontal (CF)-Western Precordillera (P) block, where piggyback basins developed. **13**, Intermontane basins over Pampean region. **14**, Marine platform of the Chaco-Paranense basin (arrows denote ingression path).

## CONCLUSIONS

Present-day distribution and tectonic setting of the post-Incaic basins of the Argentine Central Andes let to classify them in the following tectonic domains: Northern Foreland, Olmedo Sag,
Famatina Foreland, Cuyo Foreland, Backarc Troughs of the Puna, Atacama Forearc Basin (Chile), Cordillera Frontal-Precordillera High where piggyback bassins developed, Pampean Region Basins, and Chaco-Paranense Marine Platform.
The post-Incaic orogenic front separates the western Andean basins and the eastern foreland basins. This front is a series of en echelon thrusts of N-S Andean trending.
The main structural highs were El Desierto High, Cordillera Frontal-Precordillera High, and San Rafael High as the southern end of the Cuyo Foreland.
The Central and Southern Andean archs would be structural highs coevally with early Neogene basin evolution. These structural highs were the host rocks of the volcanic arcs, that began their evolution from middle Miocene.

## REFERENCES

Yrigoyen, M.R., 1969. Problemas estratigráficos del Terciario de Argentina. Ameghiniana, 4: 315-326.

# TERTIARY EXTENSIONAL FAULTING AT THE LOWER LOA VALLEY, NORTHERN CHILE (21-22°S)

Pere SANTANACH [1], David SERRAT [1], Alberto SÁEZ [1], Lluís CABRERA [1] and Guillermo CHONG [2]

(1) Grup de Geodinàmica i Anàlisi de Conques. Dpt. de Geologia Dinàmica, Geofísica i Paleontologia, Universitat de Barcelona. C. Lluís Solé Sabarís s/n, 08028-Barcelona, Spain.
(2) Departamento de Ciencias Geológicas, Universidad Católica del Norte, Avda. Angamos 0610-casilla 1280, Antofagasta, Chile.

**KEY WORDS:** Central Andes, extensional faulting, Tertiary.

## INTRODUCTION

The ductile strike-slip movements of the Atacama Fault System during Jurassic and Cretaceous are well documented (Hervé 1987b, Scheuber and Andriessen 1990, Scheuber *et al.* in press). On the contrary, the Tertiary kinematics of this fault system is less known, although some studies have been done (Armijo and Tiehle 1990, Hervé 1987a, Naranjo 1987, Véliz 1994). The aim of this contribution is to furnish new data regarding the Tertiary activity of the Atacama Fault System in its northern part (fig.1), both in the Coastal Cordillera (Salar Grande) and the western margin of the Longitudinal Valley (Salar de Llamara area, along the Lower Loa Valley). Special attention will be paid to the relationships between fault movements and stratigraphic units.

## STRATIGRAPHIC UNITS

Uncomformably over the Paleozoic and Mesozoic rocks of the Coastal Cordillera four main stratigraphic units have been distinguished along the Lower Loa Valley (Cabrera *et al.* 1995):

1) At the bottom, covering a strong paleorelief, the **Loa Canyon Breccias Unit** crops out along the Loa Canyon and reaches a maximum observable thickness of 400 m. Clasts are heterometric, angular and of local provenance.

2) A **Red Alluvial Sandy-conglomeratic Unit** with interbedded anhydritic layers (Sáez *et al.* 1994) reaches several tens of m in thickness near Quillagua. This unit corresponds to distal alluvial fan deposits related to the Precordillera, and therefore it is part of a transverse alluvial system. It wedges out to the West. Jensen (1992) named this unit Hilaricos Fm. and tentatively correlated it to Sichal Fm. which is supposed to be Oligocene(?)-Miocene in age.

3) The **Diatomitic Fluvio-lacustrine Unit**, defined by Rieu (1975), is extensively described as Quillagua Fm. in Sáez *et al.* (1994) and Cabrera *et al.* (1995). Its detritic deposits have a southern origin and constitute a longitudinal fluvial system. The maximum observed thickness is 55 m. A cineritic level (**Aduana Cinerite**) related to the volcanism developed in the Alta Cordillera is found at the bottom of this unit. It is 6.8 My old (K/Ar method, Kiefer *et al.*, in press). Units 2 and 3 correspond to Quillagua Fm. from Jensen (1992).

4) The **Upper Evapotitic Unit** (Soledad Fm., Bobenrieth 1979) includes all the evaporites (anhYdrites and halites) which are found at the top of the sequence, and comprises those infilling Salar Grande. The age of this unit may range from Oligocene(?) to Plio-Pleistocene.

## STRUCTURE

From the survey carried out in the Salar Grande area and along the Loa Canyon the following features should be pointed out:

The structure of the Salar Grande basin is a N-S elongated half-graben defined by an extensional fault system. The main faults run along its western margin and the salt infilling the basin lies on the tilted and down thrown eastern block. The Salar Grande forms part of a tilted block structure which is well imaged by the present-day morfology; the N-S oriented hills have a steep eastern slope and a gentle western one (fig.2). The salt layers are horizontal and partially fill up the paleo-relief created by the mentioned N-S normal faults. Probably they lie on local breccias, like those outcropping SW of Salina Guanillos, which possibly may be correlated to the Loa Canyon Breccias Unit.

Along the Loa Canyon, from the coast to few km south of Quillagua, the described stratigraphic units are undeformed, filling up a vigorous paleo-relief developed on basement (Paleozoic and Mesozoic) rocks. This paleo-relief is asymmetric: steep slopes an gently inclined ones. This paleomorphology is interpreted as the result of an extensional event which produced a tilted block system, the steep slopes corresponding to normal faults. The prevalent trends of the normal faults along the Loa Canyon are aproximately N-S and E-W resulting in a complex block system. Most part of the Loa Canyon Breccias Unit is undeformed. However, the lowest beds outcropping in the canyon close to an E-W fault show internal low-angle unconformities (fig. 3), evidencing their syntectonic deposition. Thus, it is concluded that the E-W extensional event, which individualized the Longitudinal Valley and the Coastal Cordillera, and also some smaller basins like Salar Grande in the Coastal Cordillera, occurred at the beginning of the sedimentatin of the Loa Canyon Breccias and stopped during the deposition of this unit (Oligocene-Early Miocene [?]).

The structures related to the described extensional event are cut by the normal fault system which defines the coastal scarp. Since the oldest marine terraces are Pliocene (Hartley and Jolley 1995), this faulting event probably occurred at the Miocene-Pliocene boundary. The small basin filled with breccias SW of Salar Grande, near Salina Guanillos, constitutes an example of early extensional structures cut by the coastal scarp system during latest Miocene times.

Some of the faults outcropping in the surveyed area show neotectonic or even present-day activity. However, most of the faults which led to the formation of the western margin of the Longitudinal Valley (Quillagua basin) and the Salar Grande basin developed mainly at the beginning of Loa Canyon Breccias deposition. Since then they have remained unactive as shown by the undisturbed younger deposits that seal them.

## CONCLUSIONS

The relationships between the stratigraphic units and the normal faults evidence two main extensional phases during Tertiary:

The first one (Oligocene (?)-Miocene) developed in the Coastal Cordillera and Longitudinal Valley. It resulted in a tilted block structure which steps down towards the East. This phase is responsible for the formation of the western margin of the Longitudinal Valley and the associated lacustrine basins (Quillagua basin, Salar Grande).

The second one (Miocene-Pliocene) developed more to the West and gave rise to the Coastal Scarp Fault which throws down the western block.

Thus, during Tertiary, the E-W extensional activity migrated towards the West.

The preset-day Coastal Cordillera is a horst resulting from the superposition of both described brittle phases.

This contribution is part of the DGICYT PB94-0901 project and has been partially financed by the Comissionat per Universitats i Recerca, Generalitat de Catalunya (GRQ94-1048).

Fig.1.- Setting of the surveyed area.

A. F. S. Atacama Fault System
1. Salar Grande
2. Salar de Llamara
3. Quillagua

A and B: Cross-sections of fig.2.
Rectangle: Figure 3.

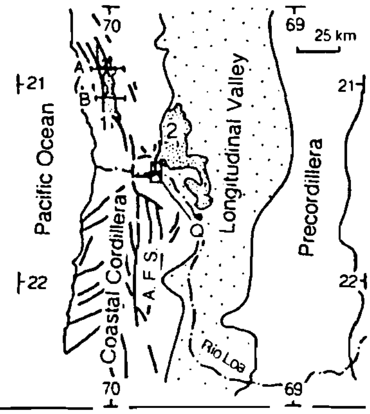


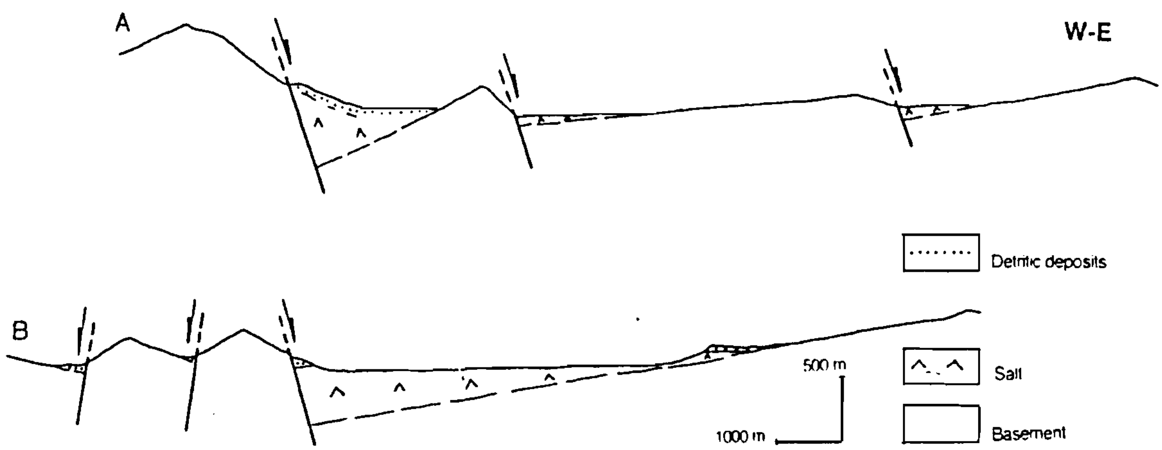


Fig.2.- Sections across Salar Grande (see location in fig.1).

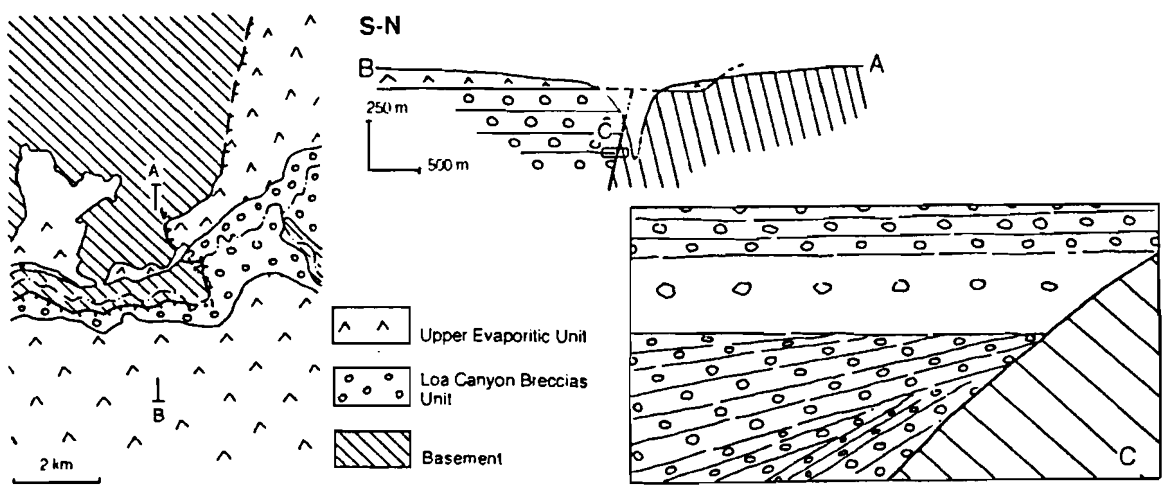


Fig.3.- Map and cross-section of the Loa Canyon (see location in fig.1). C. Internal low-angle unconformities in the Loa Canyon Breccias Unit (sketch after a photograph).

## REFERENCES

Armijo R. and Tiehle R. 1990. Active faulting in northern Chile: ramp stacking and lateral decoupling along a subduction plate boundary? *Earth and Planetary Science Letters*, 98, 40-61.

Bobenrieth L. 1979. *Geología de los cuadrángulos Cerro Desamparado y Cerro Soledad. Proyecto Cordillera de la Costa Tocopilla-Río Loa, escala 1:50000*, 97 pp., Instituto Investigaciones Geológicas.

Cabrera L., Chong G., Jensen A., Pueyo J.J., Sáez A. and Wilke H.G. 1995. *Cenozoic and Quaternary lacustrine systems in northern Chile (Central Andes, Arc, and Fore-Arc zones).* Excursion Guidebook, Recent and Ancient Lacustrine Systems in Convergent Margins GLOPALS-IAS Meeting, 77 pp., A. Sáez ed., Antofagasta (Chile).

Hartley A. J. and Jolley E. J. 1995. Tectonic implications of Late Cenozoic sedimentation from the Coastal Cordillera of northern Chile (22-24° S). *J. Geol. Soc.* London, 152, 51-63.

Hervé A. M. 1987a. Movimiento normal de la falla Paposo, zona de falla Atacama, en el Mioceno, Chile. *Revista Geológica de Chile*, 31, 31-36.

Hervé A. M. 1987b. Movimiento sinistral en el Cretácico inferior de la zona de falla Atacama al norte de Paposo (24°S), Chile. *Revista Geológica de Chile*, 31, 37-42.

Jensen A. 1992. *Las cuencas aluvio-lacustres oligoceno-neógenas de la región de Ante-Arco de Chile septentrional.* Tesis doct., 217 pp., Universitat de Barcelona.

Kiefer E., Dörr M.J., Götze H.-J. and Ibbeken H. submitted. Gravity-based mass-balance of an alluvial-fan giant: The Arcas Fan, northern Chile. *Geology*.

Naranjo J.A. 1987. Interpretación de la actividad cenozoica superior a lo largo de la zona de falla Atacama, Norte de Chile. *Revista Geológica de Chile*, 31, 43-55.

Rieu M. 1975. Les formations sedimentaires de la Pampa del Tamarugal et le Río Loa (norte Grande du Chili). *Cahiers Orstrom, Sér. géol.*, VIII(2), 145-164.

Sáez A., Jensen A., Cabrera L. and Chong G. 1994. Secuencias fluvio-lacustres de la Fm. Quillagua. Plioceno de la región de Antearco del N de Chile. *II Congreso Español del Terciario*, 1994, Comunicaciones, 263-266.

Scheuber E. and Andriessen P.A. 1990. The kinematic and geodynamic significance of the Atacama fault zone, northern Chile. *J. Struct. Geol.*, 12, 243-257.

Scheuber E., Hammerschmidt K. and Friedrichsen H. in press. $^{40}Ar/^{39}Ar$ and Rb-Sr analyses from ductile shear zones from the Atacama fault zone, northern Chile: the age of deformation. *Tectonophysics*.

Véliz G. H. 1994. Deformación frágil del sistema de fallas de Atacama al noreste de Antofagasta, Cordillera de la Costa del norte de Chile. *7° Congr. Geol. Chileno 1994, Actas*, I, 210-214.

# INFLUENCE OF REGIONAL TECTONICS ON MIOCENE VOLCANIC CALDERA FORMATION IN THE PUNA ALTIPLANO, NW OF ARGENTINA: THE AGUAS CALIENTES CALDERA COMPLEX

Carles Soriano(1), Joan Martí(1), Ivan Petrinovic(2), José Viramonte(2)

(1) Institute of Earth Sciences "Jaume Almera" (CSIC), c/ LLuis Sole Sabaris s/n 08028 Barcelona, Spain
(2) Universidad Nacional de Salta, Instituto Geonorte, c/ Buenos Aires, 177, 4400 Salta, Argentina

**KEY WORDS:** caldera collapse, reverse faults, strike-slip faults

## INTRODUCTION

Large volcanic caldera complexes, up to 30 km in diameter, of Miocene age are located in a region with active strike-slip tectonics and reverse faulting, the Puna Altiplano of northwestern Argentina. Strike-slip tectonics is produced by the oblique subduction of the Nazca plate beneath the South American plate (Fig. 1) (de Silva, 1989). The Puna Altiplano is placed east of the present magmatic arc and west of the active foreland fold and thrust belt, the Santa Barbara System (Fig. 1). N-S reverse faults as well as WNW-ESE sinistral strike slip faults are being active in the Puna during all the Cenozoic times (Allmendinger et al. 1983). Superimposed on the former tectonic setting caldera collapse events developed starting in Middle Miocene and ending in Upper Miocene.

Miocene volcanic complexes are located between 3500 and 5000 meters above sea level and are thought to represent part of an ancient magmatic arc (Viramonte & Petrinovic, 1990). Volcanism is typically orogenic, i.e. calc-alkaline type (Harmon & Barreiro, 1984), and is closely related to the strike-slip tectonics and reverse faulting developed in the Puna. After caldera formation strike-slip and reverse faulting masked some of the geomorphologic features produced by caldera collapsing. In order to evaluate the effects of pervasive strike-slip and reverse faulting on short-lived caldera collapse dynamics a detailed study of the Aguas Calientes caldera complex has been carried out (Fig. 2 and 3).

### *The Aguas Calientes caldera complex*

The Aguas Calientes complex is a 10 Ma old caldera located between two major WNW-ESE strike-slip faults (Fig.2), the Calama-Olacapato-El Toro fault and the Pastos Grandes fault. Both faults can be traced throughout the Puna following major satellite lineaments and also volcanoes and sag ponds alignments (Fig. 2). The eastern part of the Aguas Calientes caldera wall can be seen as a fault scarp that trends N-S and bends to E-W in the southern part of the caldera (Fig. 2 and 3). The fault scarp is located in the south block of the Calama-Olacapato-El Toro fault in a zone where the trend of this fault slightly bends to the ENE yielding a transtensive fault bending (Fig. 2). Adjacent to the caldera fault scarp the caldera floor is depressed, but further east it is elevated up to 1000 m above the fault scarp. This elevation is thought to be caused by a thermal resurgence of caldera floor after caldera collapse (Petrinovic, 1995).

The stratigraphy in the Aguas Calientes area is composed of pre-caldera Ordovician granites, welded syn-caldera ignbimbrites with a strong columnar jointing and quaternary post-caldera deposits represented by lava flows of shoshonitic composition and alluvial fan deposits (Fig. 3). Pre-caldera rock exposures are located outside the caldera depression, whereas syn-caldera and post-caldera deposits crop out either inside and outside the caldera depression (Fig. 3) (Petrinovic, 1995).

The Calama-Olacapato-El Toro fault extends from Calama in northern Chile to El Toro in northwestern Argentina and is expressed as a major lineament in satellite images. Segments of this fault link two shoshonitic volcanic cones of 200 ka to 400 ka near San Antonio de los Cobres and are the northern end of the Aguas Calientes caldera (Fig. 2 and 3). In this zone the sinistral movement on the Calama-Olacapato-El Toro fault has displaced about 10 km a post-Cretaceous thrust that places Precambrian rocks over alluvial fan Cretaceous deposits (Fig.2), whereas east of San Antonio de los Cobres the displacement observed on the syn-caldera ignimbrite is 2 Km. A broad, spaced (cm to dm) and steep cleavage has developed adjacent to the Calama-Olacapato-El Toro fault plane on the syn-caldera deposits (Fig. 3a) in the northern part of the Aguas Calients caldera.

The Pastos Grandes fault links three WNW-ESE aligned volcanoes of Lower Pliocene age south of the Salar del Rincón and can be traced from the former volcanoes to Santa Rosa de Pastos Grandes (Fig. 2). South of this fault another WNW-ESE fault can be traced along several step over fault segments that produce small Quaternary sag ponds. Some of the fault segments are transpressive step over segments which indicate a sinistral shear movement (Fig. 2). A weak, spaced and steep cleavage can be observed adjacent to the fault plane on the Aguas Calientes syn-caldera ignimbrite near Santa Rosa (Fig. 2).

Structures with a N-S trend that bound uplifted zones of Ordovician and Precambrian rocks and depressed zones filled up with Quaternary alluvial fan deposits and N-S elongated Quaternary salars are commonly observed in the Aguas Calientes area (Fig. 2). Most of these structures are interpreted as N-S trended reverse faults being the fault plane either dipping to the E or to W (Allmendinger et al. 1983). Northeast of the Aguas Calientes caldera N-S reverse faults bend to the SW as a result of sinistral movement on the Calama-Olacapato-El Toro fault (Fig. 2).

In the northern boundary of the Aguas Calientes caldera one of the former N-S reverse faults is trending NNE-SSW, dipping 45° to the WNW, and is displacing two fault blocks of syn-caldera ignimbrite (Fig.3b). The fault plane is characterized by a 10 m thick hydrothermally altered zone in the footwall and by a closely spaced cleavage in the hangingwall as well as in the footwall (Fig. 3). Cleavage displays a sigmoid geometry that indicates a reverse movement on the fault plane. This fault is buried by a shoshonitic lava flow extruded from a vent located on the Calama-Olacapato-El Toro fault plane (Fig. 3).

The Aguas Calientes caldera fault scarp and caldera depression have been extensively studied in order to find evidences on the influence of regional tectonics in caldera dynamics. Hydrothermal alteration postdates caldera formation since it has been observed in the syn-caldera ignimbrite along the fault scarp and along E-W and NW-SE fault planes located inside the caldera depression (Fig. 3). The Aguas Calientes caldera wall is interrupted to the north by a segment of the Calama-Olacapato-El Toro fault (Fig.2, 3). North of this strike-slip fault no geomorphological signature of the caldera wall can be observed and minor exposures of syn-caldera ignimbrite occur (Fig. 3). Striated surfaces on fault planes inside the caldera depression and on the caldera wall indicates a poliphase kinematic history that postdates caldera collapse. Therefore most fault planes have at least two sets of striae, one of them indicating a strike-slip and other a dip slip movement (Fig. 3c and 3d). Strike-slip may be either dextral or sinistral, whereas dip slip striae clearly postdates strike-slip ones but no sense of movement has been possible to deduce from them.

## CONCLUSIONS

The location of the Aguas Calientes caldera in the context of the regional tectonics in the Puna Altiplano suggest that caldera collapse dynamics is closely controlled by a network of previous fault planes. This caldera is located south of a transtensive bend of the Calama-Olacapato-El Toro fault and only minor erupted volcanics crop out north of this fault. Thus, we suggest that the former strike-slip fault was reactivated as a normal fault during caldera collapse allowing the extrusion of volcanic material. After the volcanic event strike-slip movement continued as demonstrated by fault cleavage and fault displacement observed in the syn-caldera deposits either on the Calama-Olacapato-El Toro fault and on other faults located inside the caldera. Dip slip sets of striae on the former faults postdates collapse events are likely to be related to the thermal resurgence. Movement on reverse faults outside the caldera also continued after caldera collapse as demonstrated by cleavage and fault displacement observed in syn-caldera deposits. Thus, after the short-lived caldera collapse events the regional strike-slip and reverse faulting that dominate the Aguas Calientes area continued.

## REFERENCES

Allmendinger, R.W., Ramos, V.A., Jordan, T.E., Palma, M., Isacks, B.L. 1983. Paleogeography and andean strucutral geometry, northwest Argentina. Tectonics, 2 (1), 1-16.

de Silva, S.L. 1989. Altiplano-Puna volcanic complex of the central Andes. Geology, 17, 1102-1106.

Harmon, R.S. & Barreiro, B.A (Eds.). 1984. Andean magmatism, chemical and isotopic constraints. Shiva publishing limited, 1-236

Petrinovic, I.A. 1995. The Aguas Calientes volcanic complex. Unpublished PhD thesis. Universidad de Salta, Argentina, 1-274.

Viramonte, J.G. & Petrinovic, I.A. 1990. Cryptic and partially buried calderas along strike-slip fault system in the central Andes. International Symposium of Andean Geodynamics, I: 318-320. Grenoble

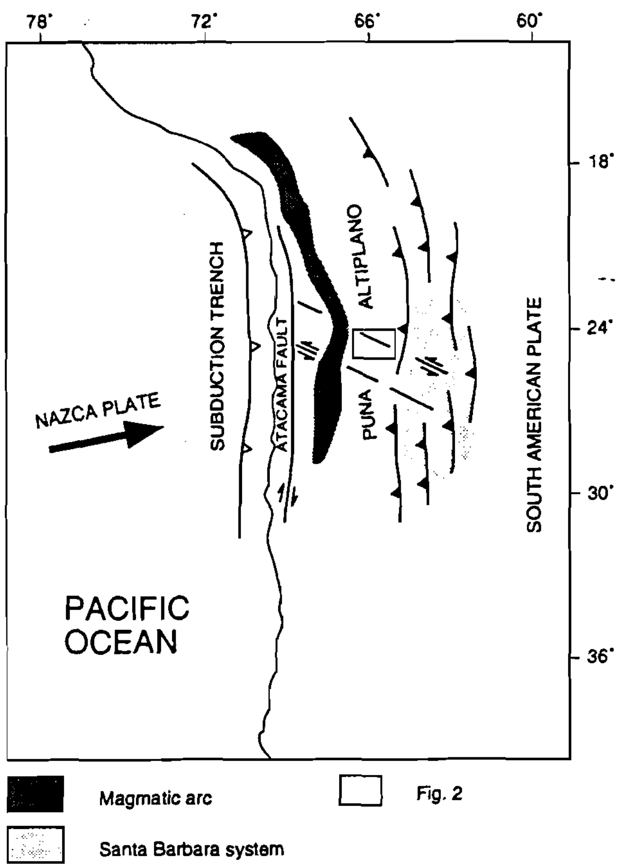


*Fig. 1. Simplified tectonic map of the central Andes in northwestern Argentina showing oblique subduction of the Nazca plate beneath the South American plate and location of the studied area.*

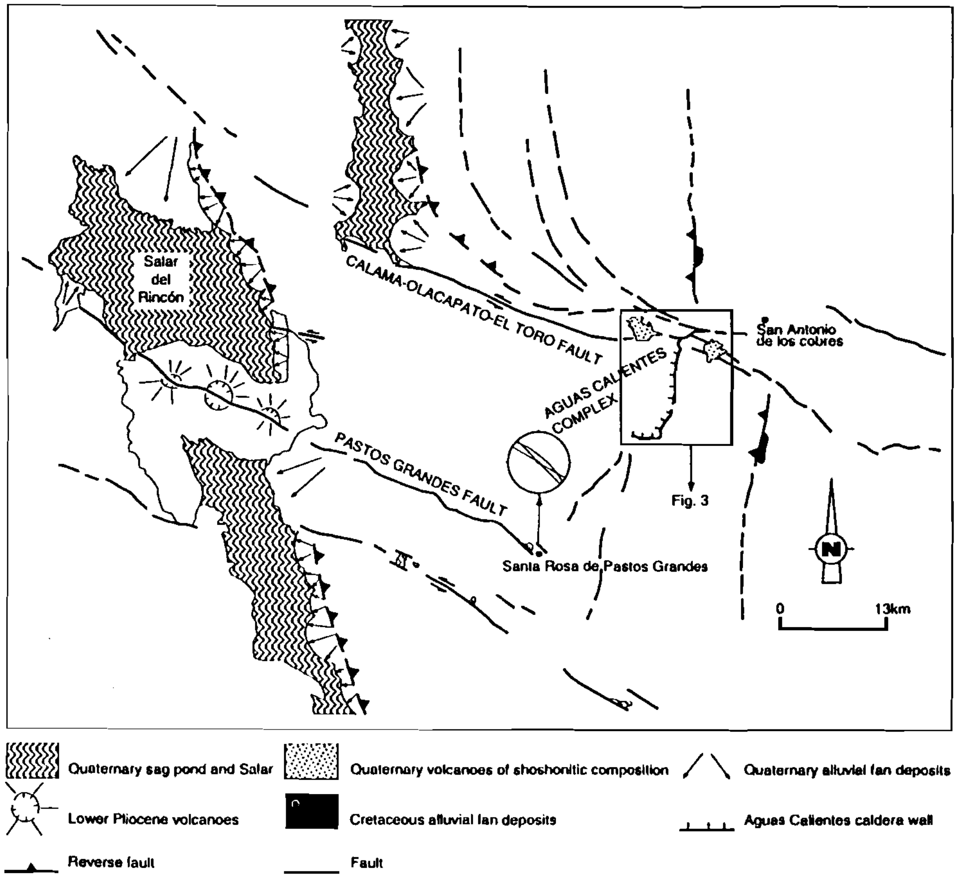


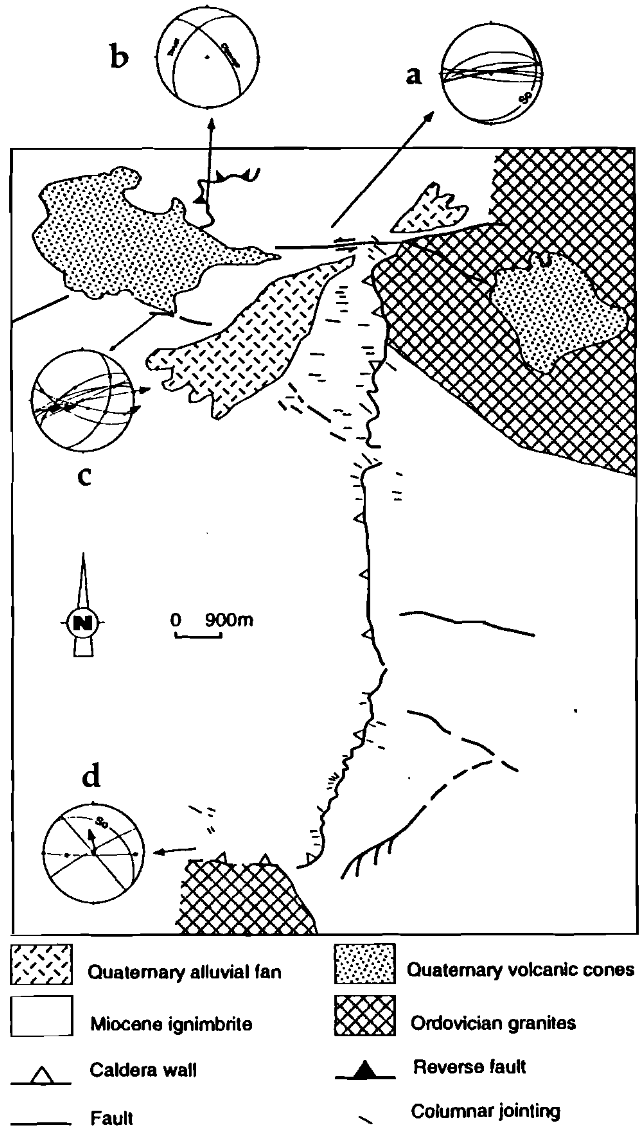


*Fig. 2. Geological map of the Puna Altiplano in the Aguas Calientes area. Major tectonic and geomorphologic features have been drawn from unpublished Landsat satellite images and from field data. Lower hemisphere equal area plots of cleavage planes on the Pastos Grandes fault are also shown.*

*Fig. 3. Geological map of the Aguas Calientes caldera fault scarp showing lower hemisphere equal area plots of several structural elements and sense of movement on fault planes (see text for explanation).*

# MESOZOIC PALAEOGEOGRAPHY OF SOUTHERN SOUTH AMERICA

Luis A. Spalletti and Juan Franzese

Centro de Investigaciones Geológicas, Universidad Nacional de La Plata, CONICET. Calle 1 n° 644, 1900 La Plata, República Argentina.

**KEY WORDS**: Palaeogeography, South America, Mesozoic, Patagonia.

Different palaeogeographic reconstructions of southern South America have been reported by Harrington, 1962; Camacho, 1967; Riccardi, 1987, Uliana and Biddle, 1987, 1988; Macellari, 1988 and Urien et al., 1995. Our study was specifically designed to develop eight palaeogeographic maps of Patagonia, between the Late Triassic and the Late Cretaceous in 15 to 30 Ma steps. More than 300 references relevant to the interval 210-75 Ma were selected to compile a palaeogeographic database including stratigraphic, structural, sedimentologic, geotectonic and palaeoenvironmental information.

In the Late Triassic Patagonia was an almost positive land with narrow and isolated continental rifts, filled with volcaniclastic sediments (Fig. 2a). Calc-alkaline intrusions (Central Patagonian Batholith) and the Comallo volcanics are emplaced at the NW end of the Gastre Fault System.

The 180 Ma map (Fig. 2b) shows the opening of the Neuquén and the Pampa de Agnia basins, characterized by shallow to deep marine deposits related to a palaeopacific transgression. A dominantly acidic volcanism (Marifil Complex) covers large areas of northern Patagonia. The older evidence of an Andean magmatic arc occurs at the southern margin of the Pampa de Agnia depocenter.

During the Bathonian-Callovian transition (165 Ma), most of the Patagonian region to the south of the Gastre Fault System is characterized by the (Chon Aike and Tobífera) bimodal volcanism. In central and southern Patagonia several NW-SE and NNW-SSE trending grabens formed as a result of widespread extensional tectonism. Transcurrent displacement along the Gastre Fault System controlled the Cañadón Asfalto depocenter in north-central Patagonia.

The Late Jurassic map (150 Ma, Fig. 2d) shows significant palaeogeographic changes. The Río Mayo-San Jorge and the Magallanes basins are enterely developed, and the silicic volcanism is restricted to SW Patagonia, where submarine rhyolite-flows intercalate with deep marine siliciclastics. The Andean magmatic arc reaches the 50 ° S.L. The early rift continental deposits of the San Jorge Basin laterally grade into continued shallow marine sediments in the intra-backarc Río Mayo basin. Shallow marine facies in most of the Magallanes basin indicate the onset of widespread extension, and to the west, deep marine deposits suggest an effective connection between the Magallanes basin and the Pacific Ocean.

At 135 Ma (Fig. 3a) the Andean magmatic arc extends along the whole western Patagonian margin. However, the Pacific connection of the Magallanes basin persists, and the marginal Rocas Verdes basin, floored by oceanic crust, develops in a backarc position.

The Aptian (120 Ma, Fig. 3b) was a time of transition. Continental red beds are widespread in the Neuquén and San Jorge basins. The topographic barrier of the magmatic arc produced the closure of the Río Mayo basin. To the south, several paths through the volcanic chain connect the Magallanes basin with the Pacific Ocean.

During the Cenomanian-Turonian (90 Ma, Fig. 3c), the Neuquén and the San Jorge basins are integrated in a single continental depocenter. In northeastern Patagonia, the newly opened Colorado rift is also filled up of continental deposits. Along the western margin of southern South America the Andean magmatic arc chain separates Patagonia from the Pacific Ocean. In the Magallanes basin, a foreland stage causes strong detrital contributions from the west and progressive migration of the depocenter to the east.

The 75 Ma map (Fig. 3d) shows a widespread transgressive episode embracing the Colorado basin and the North Patagonian platform. The San Jorge basin becomes again a large and isolated continental depocenter. A general regression is recorded in the Magallanes basin, caused by both renewed uplift along the Andean margin and a marked NNW to SSE fluvio-deltaic progradation.

## REFERENCES

Camacho, H. 1967. Las transgresiones del Cretácico superior y Terciario de la Argentina. Asociación Geológica Argentina Revista 22, 253-280.

Harrington, H. 1962. Paleogeographic development of South America. American Association of Petroleum Geologists Bulletin 46, 1773-1814.

Macellari, C. 1988. Cretaceous paleogeography and depositional cycles of western South America. Journal of South American Earth Sciences 1, 373-418.

Riccardi, A. 1987. Cretaceous paleogeography of southern South America. Palaeogeography, Palaeoclimatology, Palaeoecology 59, 169-195.

Uliana M. & Biddle K. 1987. Permian to Late Cenozoic evolution of northern Patagonia, main tectonic events, magmatic activity, and depositional trends. in McKenzie (Ed.) Gondwana six: structure, tectonics and geophysics. AGU Geophysical Monograph 40, 271-286.

Uliana M. & Biddle K. 1988. Mesozoic-Cenozoic paleogeographic and geodynamic evolution of southern South America. Revista Brasileira de Geociencias, 18, 172-190.

Urien, C., Zambrano, J. & Yrigoyen, M. 1995. Petroleum basins of southern South America: an overview. in Tankard, A., Suárez, R. & Welsink, H. (Eds.) Petroleum basins of South America. American Association of Petroleum Geologists Memoir 62: 63-77.

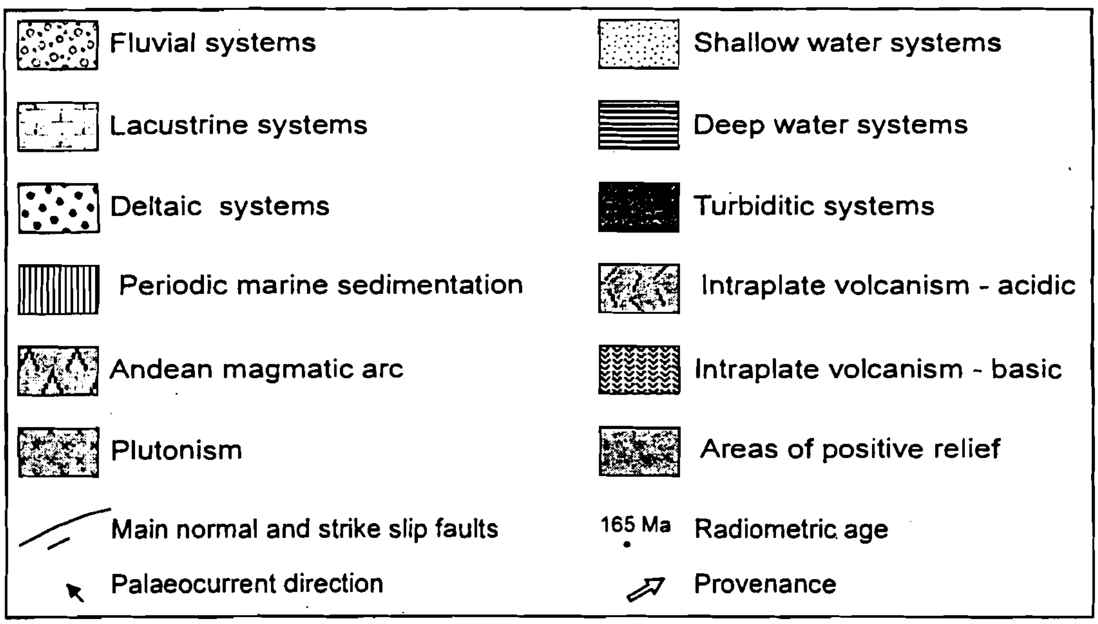


Figure 1. Legend to palaeogeographic maps shown in figures 2 and 3.

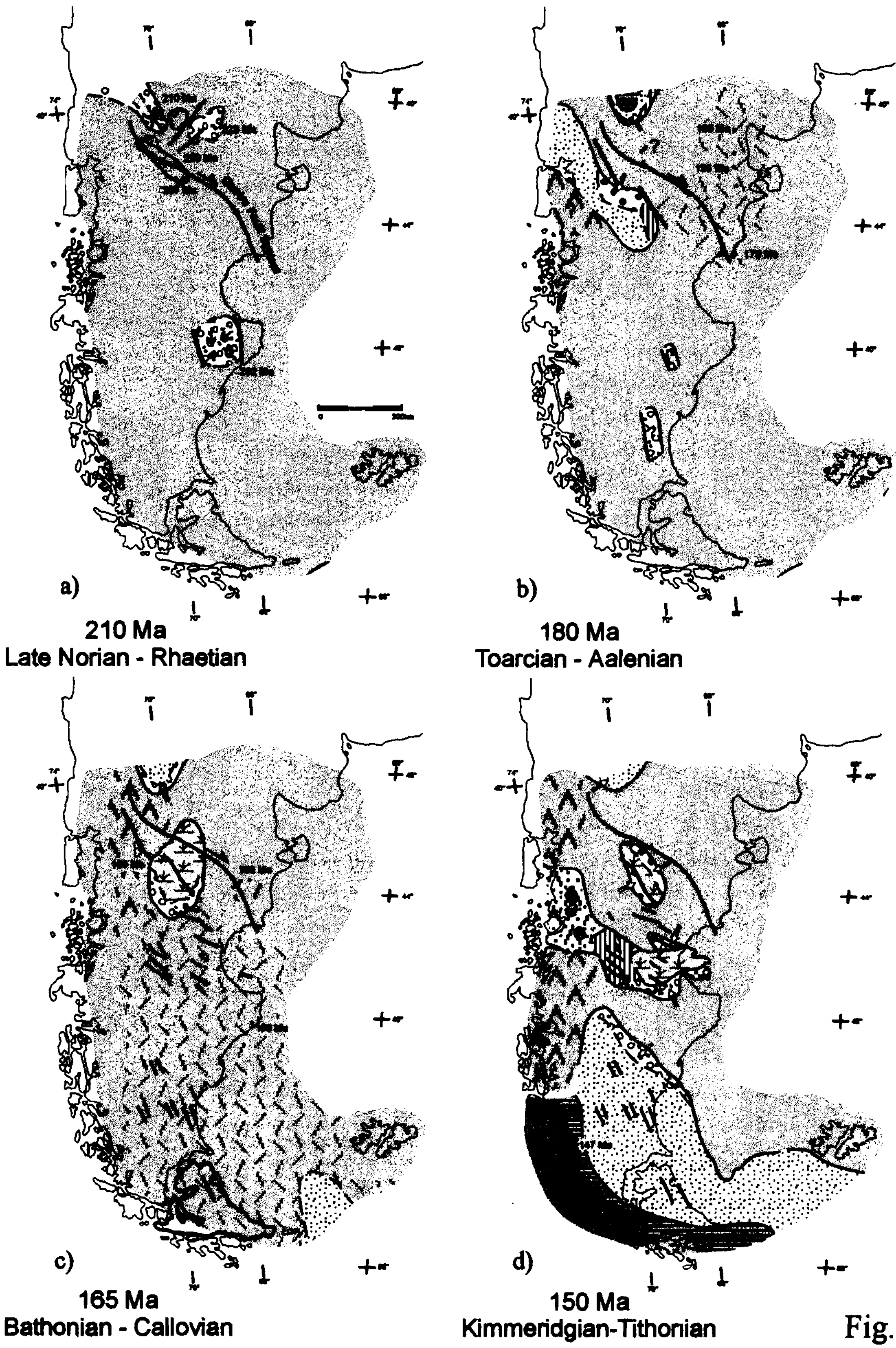
a)
210 Ma
Late Norian - Rhaetian
b)
180 Ma
Toarcian - Aalenian
c)
165 Ma
Bathonian - Callovian
d)
150 Ma
Kimmeridgian-Tithonian

Fig.2

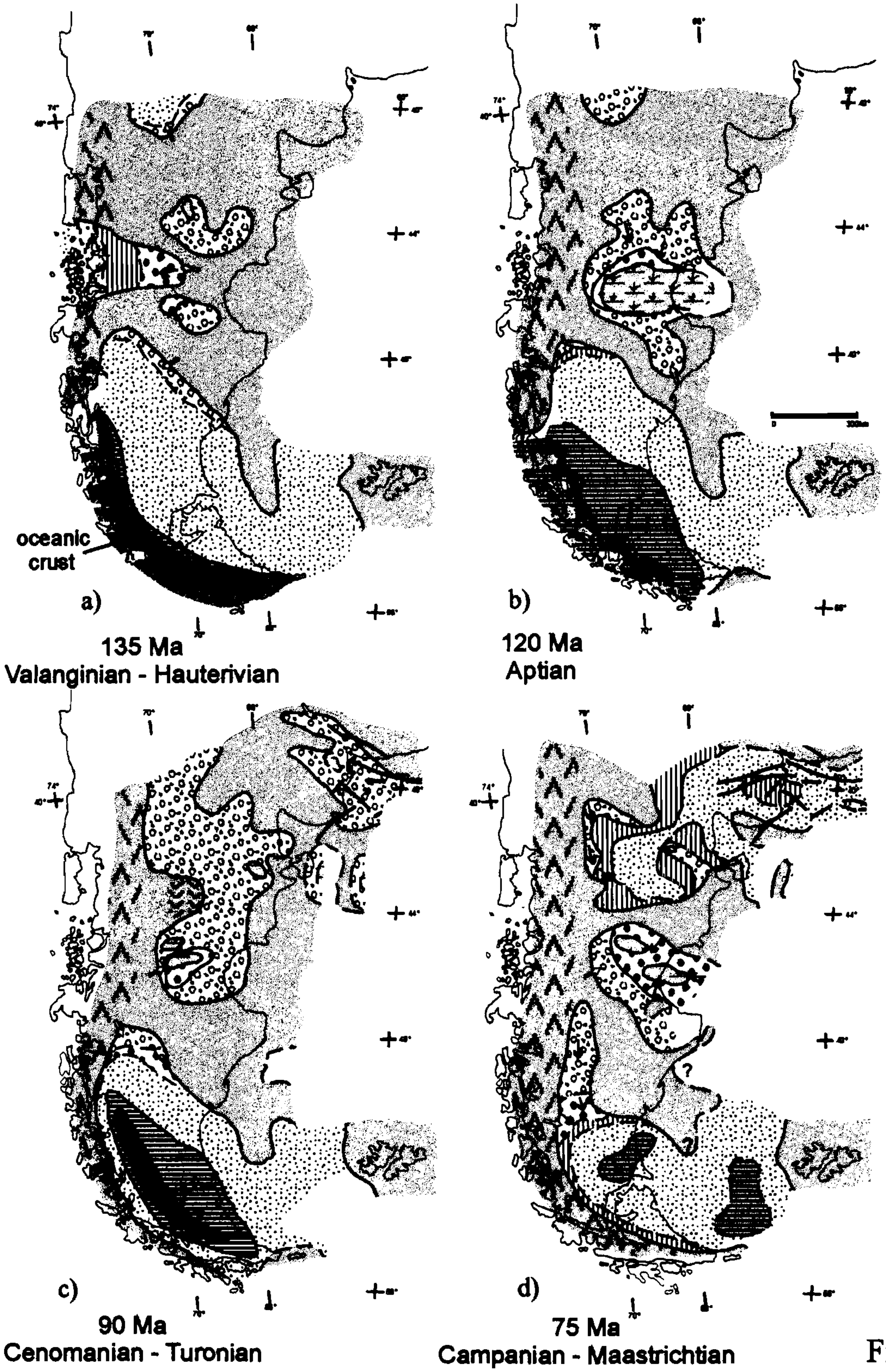
oceanic crust
a)
135 Ma
Valanginian - Hauterivian
b)
120 Ma
Aptian
c)
90 Ma
Cenomanian - Turonian
d)
75 Ma
Campanian - Maastrichtian

Fig.3

# THERMOTECTONIC HISTORY OF THE ANDES, SOUTH ECUADOR: EVIDENCE FROM FISSION-TRACK DATING

Michael STEINMANN, Diane SEWARD and Dominik HUNGERBUEHLER

Geologisches Insitut ETH Zürich, Sonneggstr. 5, CH-8092 Zürich, Switzerland

**KEY WORDS:** Ecuador, Cretaceous, Miocene, basin analysis, fission track, exhumation, Andean uplift.

## INTRODUCTION

A study of the thermo-tectonic history and assessment of the amount of uplift and exhumation in the Ecuadorian Andes yields information that helps one to reconstruct the paleogeography. The uplift event of Late Miocene and Early Pliocene age was described by Kennerley (1980) as "the Andean Event", which caused differential vertical movement in the Sierra and folding and thrusting of the Subandean zone in the Oriente. Uplift and deformation events are also recorded in the fill series of Neogene basins in the Interandean zone of southern Ecuador (Hungerbühler et al., 1996). In the Cordillera Real, an earlier uplift event during Late Cretaceous, was shown through radiometric age determinations on metamorphic rocks (Aspden et al., 1992). In the current, ongoing study, samples from the "basement" rocks of southwest Ecuador, in an east west profile from 3000 m to sea level, have been collected for fission-track analysis to determine exhumation rates.

## METHODOLOGY

The fission-track technique is now a widely used dating method with particular application to thermo-tectonic histories of mountain belts. Since the blocking temperature of apatite is quite low (approximately 105° C, Parrish, 1983), relative to other dating methods, it has become particularly applicable for evaluating low temperature thermal histories. Thermal history information can be obtained not only from the ages but also from length measurements of the etched tracks. From the age and track length distribution, time temperature paths experienced by the apatite can be estimated. Modelling using genetic algorithmus can sometimes refine the interpretation. This application of apatite fission-track technique is a very useful tool in the analysis of tectonic evolution of mountains, including exhumation, unroofing and/or cooling histories, locating and determining amount of vertical movement of major faults, and provenance studies of sedimentary sequences that have not seen the required temperatures to erase the initial detrital grain ages. In addition, dating of zircon, with a higher blocking temperature, allows cooling histories to be extended back in time. Current temperatures for zircon are approximately 240° C, (Yamada et al., 1995).

The concept of a single unique blocking temperature for fission tracks has had to be extended to a range of temperatures since, as a rock sequence passes upwards and / or cools down, there is a range of temperature over which the tracks begin to both form and disappear (anneal); this is called the partial annealing zone. This temperature range is generally accepted as between 120°C and 60°C for apatite. Below 60° C one can assume for all essential purposes that the tracks that are formed are retained.

By measuring track lengths in apatites insight into the rate of exhumation and the thermal history of the rock can be estimated. Only tracks in grains in which the c-axis is parallel to the polished surface of the grain are measured. Further the tracks must be beneath the surface having been etched through cracks or through other tracks (Bhandari et al., 1971). In order to measure full lengths, only those horizontal to the plane of the surface are measured. Such tracks are termed confined horizontal tracks. The form of the tracks-length histogram and associated statistics allow more detailed information regarding the history of a rock.

England and Molnar (1990) pointed out the confusion between exhumation or uplift of rocks with tectonic uplift. They define the relationship as:

tectonic (surface) uplift = uplift of rock - exhumation

It is well to keep this in mind when interpreting fission-track data.

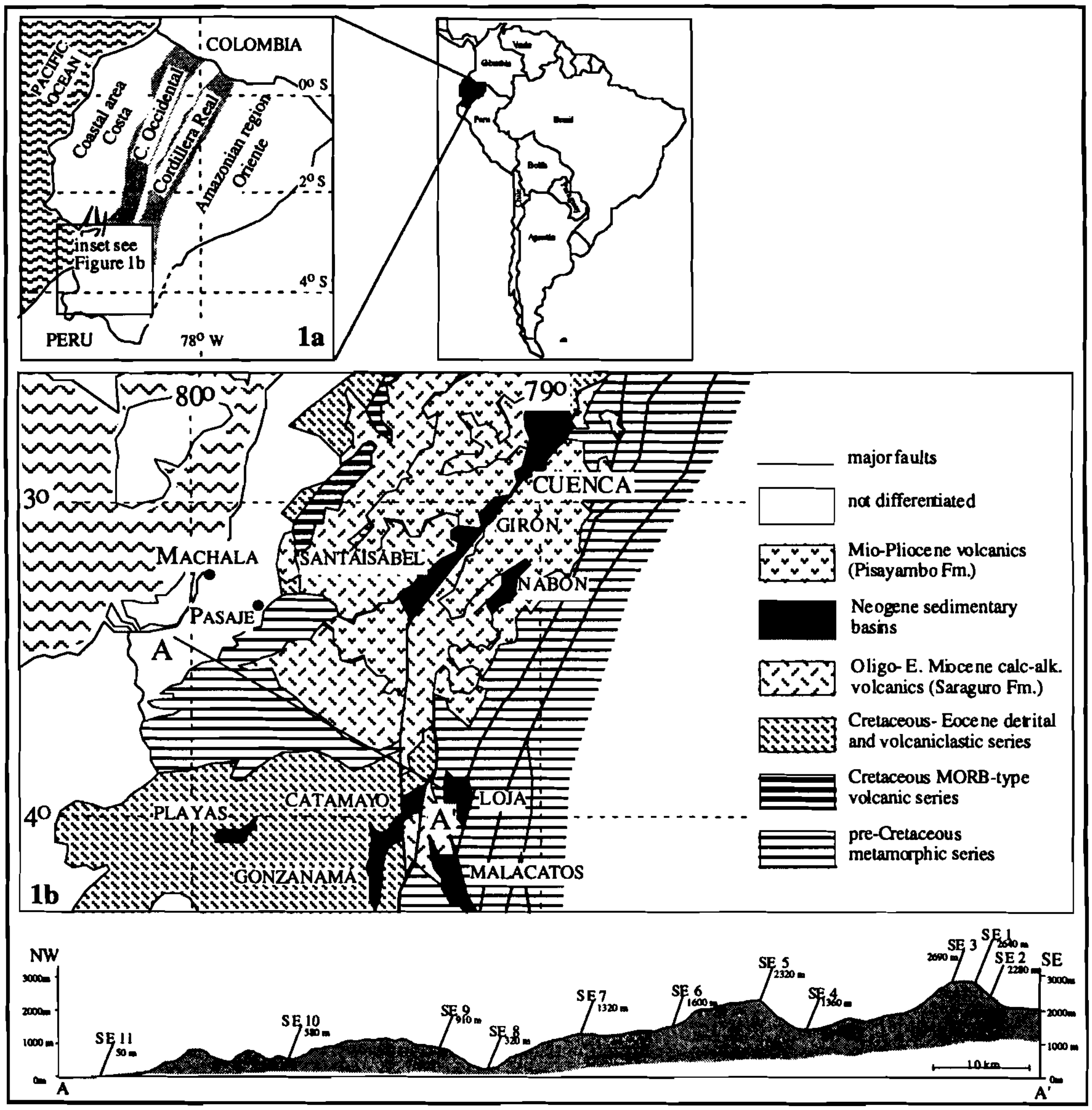


Fig. 1 Simplified geological map of southwestern Ecuador (after Litherland et al., 1993). The NW-SE cross-section (A-A') shows the sample location and the altitude above see level (v.e. = 3x).

## GEOLOGICAL SETTING AND INITIAL RESULTS

Southern Ecuador is composed of three major geological zones (Fig. 1): 1) Paleozoic to Mesozoic metamorphic series in the Cordillera Real and in the El Oro Province; this El Oro metamorphic belt separates 2) Cretaceous to Eocene detrital volcaniclastic series in the southwest from 3) Cretaceous to Eocene MORB typ and island arc volcanic series in the north (Cordillera Occidental).

Fourteen samples from these "basement" rocks and from granitic intrusions were collected in roadcuts from Loja to Machala and from Pasaje to Girón. 12 zircons and 11 apatites samples were separated, 1 from the San Lucas intrusion (Eocene), two from the metamorphic Chiguinda Unit (Paleozoic?), two from the Alamor Group (Cretaceous), six from Jurassic to Miocene intrusions and one from the Yunguilla Fm. (Cretaceous). The Loja - Machala section crosses several terranes which were accreted during Mesozoic collisional events (Aspden and Litherland, 1992). The fission-track analysis of this section will demonstrate if the terrane boundaries were reactivated during the Cenozoic.

Initial zircon ages range from Cretaceous to Miocene; apatites range from Palaeocene to Miocene. Mean confined track lengths in the apatites lie between 13 and 14 µm with unimodal distributions, implying a simple exhumation/cooling history, from a depth of 3-4 km, over this period.

## REFERENCES

Aspden J.A. and Litherland M., 1992. The geology and Mesozoic collisional history of the Cordillera Real, Ecuador. *Tectonophysics* 205, 187-204.

Aspden J.A., Harrison S.H. and Rundle C.C. 1992. New geochronological control for the tectono-magmatic evolution of the metamorphic basement, Cordillera Real and El Oro Province of Ecuador. *Journal of South American Earth Sciences* 6 (1-2), 77-96.

Bhandari N., Bhat S.G., Lal D., Rajagopalan G., Tamhane A.S.J. and Venkatavaradan V. 1971. Fission fragment tracks in apatite: recordable track lengths. *Earth and Planetary Science Letters* 13, 191-199.

England P. and Molnar P. 1990. Surface uplift, uplift of rocks, and exhumation of rocks. *Geology* 18, 173-177.

Hungerbühler D., Steinmann M., Winkler W. and Seward D., 1996. Neogene fission-track stratigraphy of southern Ecuadorian basins: Implications for regional tectonic history. *Third International Symposium on Andean Geodynamics*, Saint-Malo, 17-19 September 1996, this volume.

Kennerley J.B., 1980. Outline of the geology of Ecuador. *Overseas Geology and Mineral Resources*, Institute of Geological Sciences (UK), 55, 17 p.

Litherland M., Egüez A. and Zamora A. 1993. Mapa geológico del Ecuador, escala 1:1'000'000. Quito: CODIGEM, BGS.

Parrish R. 1983. Cenozoic thermal evolution and tectonics of the Coast Mountains of British Columbia 1, fission-track dating, apparent uplift rates, and patterns of uplift. *Tectonics*, 2, 601-631.

Yamada R., Tagami T., Nishimura S. and Ito H. 1995. Annealing kinetics of fission tracks in zircon: an experimental study. *Chemical Geology (Isotope Geoscience Section)*, 122, 249-248.

# THE EASTERN CORDILLERA OF SOUTHERN BOLIVIA: A KEY REGION TO THE ANDEAN BACKARC UPLIFT AND DEFORMATION HISTORY

Sohrab TAWACKOLI[1], Volker JACOBSHAGEN[1], Klaus WEMMER[2], Paul A.M. ANDRIESSEN[3]

(1) FR Geologie, Freie Universität Berlin, Malteserstr. 74-100, D-12249 Berlin, Germany
(2) IGDL, Universität Göttingen, Goldschmidtstr. 3, D-37077 Göttingen, Germany
(3) Laboratorium voor Isotopengeologie z.w.o., De Boelelaan 1085, 1081 HV Amsterdam, Netherlands

KEY WORDS: Eastern Cordillera,Southern Bolivia, fission track, K/Ar ages, uplift, deformation

## INTRODUCTION

The back-arc region of Southern Bolivia comprises three major units (fig. 1): The Altiplano, forming a high plateau at about 4000m, is an intramontaneous basin with Cenozoic infill. The Eastern Cordillera (EC), reaching more than 5000m altitude, is built up mainly of a very thick pile of Ordovician anchimetamorphic sediments. In places, it is covered by Cretaceous and Paleogene or Neogene sediments, respectively, among which continental ones prevail. To the W the EC is overthrust upon the Altiplano. The Subandean ranges with Late Paleozoic to Neogene rocks, form part of an E-verging fold-and-thrust belt, together with the eastern part of the EC (Interandean). As the Altiplano and the Subandean units have been subject of oil prospection, geological exploration was much more intensive, there, than in the EC. Looking, however, for a geodynamic model of the back-arc evolution in Meso- and Cenozoic times, the EC plays a key role. In this view we present new results from extensive field work in the western part of the southern EC (Tupiza Region) combined with K/Ar and apatite fission track dating. The onset of major deformation phases, deformation style and progress can be well outlined herein through Cenozoic times.

## GEOLOGICAL FRAMEWORK

The EC is bound to the adjacent physiographic provinces by a pair of divergent thrust systems. To the west the Paleogene-Neogene sediment infill of the Altiplano basin is overthrust at the San Vicente thrust system by turbiditic rocks of Llanvirn-Caradoc age (Erdtmann et al., 1995) whereas at the eastern border of the EC, accomodated thin-skinned folding and thrusting in Cambrian to Triassic strata of the Interandean zone refer to a basement involved thrust (Kley, in press).
The oldest Mesozoic rocks of the Southern EC are swarms of mafic dikes and sills intruding Ordovician strata. These rocks are exposed in the area of Cornaca, 50 km N of Tupiza. A sample of a dike N of Cornaca yielded an Early Jurassic age of 184.0±4.9 Ma (K/Ar, whole rock). The emplacement of these magmatic rocks is due to extensional processes that culminated east of South America in the opening of the South Atlantic.
Predominantly continental Cretaceous sediments of the Puca Group are completely recorded for the timespan ?Kimmeridgian to Paleocene in a back-arc rift setting. In the southern part of the high fragmentated Potosi basin discontinuous Cretaceous successions from the N-trending synclines of Tupiza and Camargo reflect active rifting processes accompanied by normal faults and alkaline basaltic

volcanism. In the syncline of Tupiza Coniacian basanitic lava-flows of the Aroifilla Fm. (Sempere, 1994) are the youngest Cretaceous strata. However, Tertiary conglomeratic rocks of the Tupiza region include Pucalithus limestone fragments of the El Molino Fm. (Maestrichtian) which does not crop out in the area, at present.

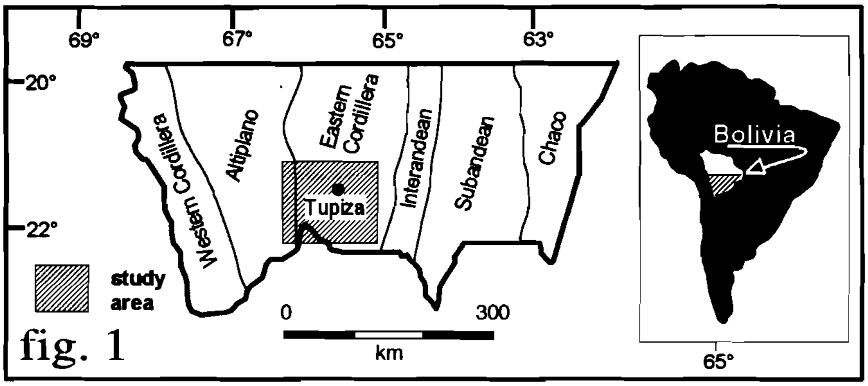


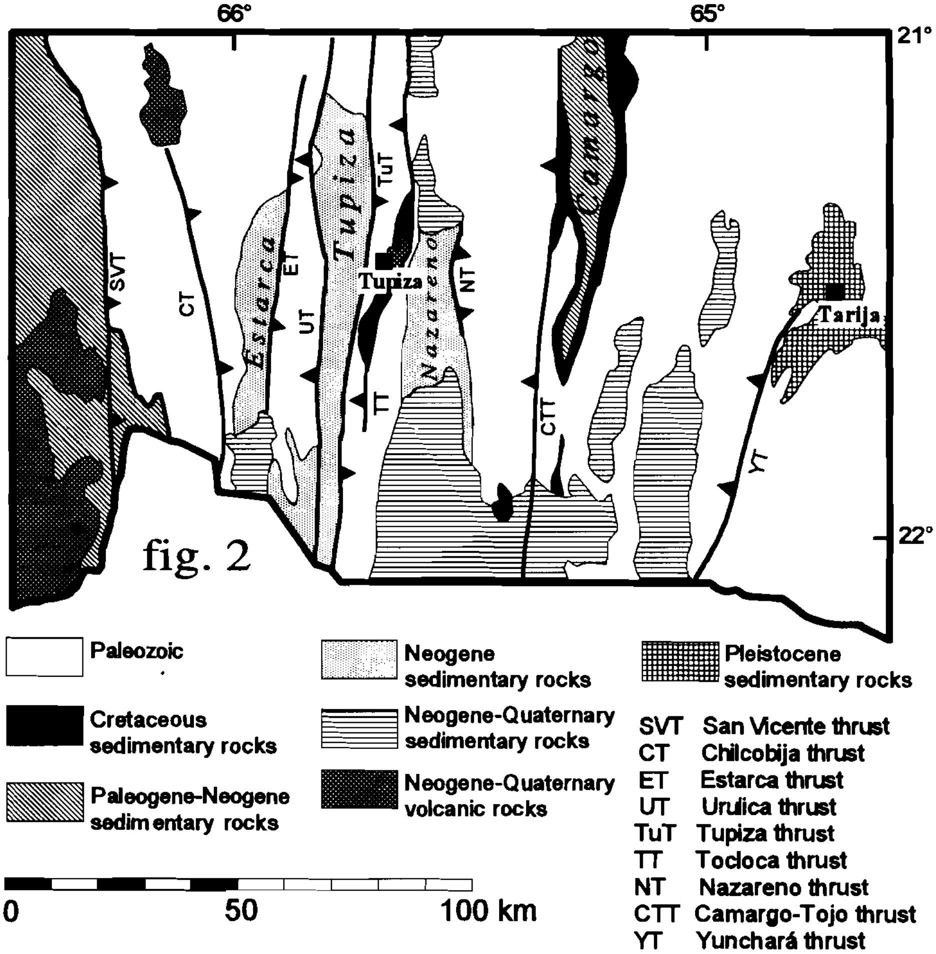


Fig. 1: Major physiographic and structural provinces of the Southern Bolivian Andes.
Fig. 2: Generalized geological map of the Tupiza-Tarija region, Southern Bolivia.

Tertiary continental strata occuring in the EC are conserved in a twofold record. In the Camargo syncline Paleogene to probably Oligocene deposits represent a paleo-foreland basin, whereas fault-related Late Oligocene to Middle Miocene deposits in the area of Tupiza have been developed within intramontaneous basins (fig. 2). Here the sedimentary infill is mainly conglomeratic and composed of fragments of the underlying Ordovician and Cretaceous rocks and trachyandesitic volcanics, which intruded into Cretaceous and lowermost Tertiary strata.
Deformation in the backarc has migrated eastward since late Oligocene times and is essentially chracterized by a major eastward shift from the Altiplano and the EC to the Subandean Ranges at about 10 Ma (Kley et al., in press).

## CENOZOIC BASINS OF TUPIZA

The Tertiary redbeds of the Tupiza area are preserved in three distinct N-trending depressions called the Tupiza, Estarca and Nazareno basin.
The Tupiza basin is a complex of four partly overlapping Tertiary basins being affected by syn- and postsedimentary thrusting. Here the oldest Cenozoic sediments belong to the tightly folded Catati Fm. and the transitionally overlapping first "member" of the Tupiza Fm. (m1). Both successions are bounded to the east by the W-vergent Tupiza thrust . The base of the Catati Fm. is marked by a sharp angular unconformity to the Ordovician basement.
Since no datable materials and no upper contact to the following members exist, the age of these deposits can only be predated by the rhyodacitic intrusion of Kharachi Orkho, which breaks through these strata. A whole-rock sample from this locality yielded a K/Ar age of 21.4±0.5 Ma. The lowermost stratigraphic limit can be considered as post-Cretaceous because of the numerous limestone pebbles included in the Tupiza Fm. m1.
In the syncline of Cerro Bolivar (S of Tupiza) the Tupiza m2 can be subdivided into two parts. The lower conglomeratic part contains only pebbles of the underlying Ordovician rocks. Eastward directed paleocurrents indicate that these conglomerates were deposited in a basin separate from that of Tupiza m1. The upper part consists of 250 m thick trachyandesitic lava-flows. A basal sample from the western hinge of the syncline obtained a biotite K/Ar age of 21.7±0.4 Ma. N of Tupiza identic lava-flows overlie the Ordovician, forming a wide anticline. Previous assumptions that these lavas are much younger than those of Cerro Bolivar can definitely be denied, as a sample collected at the eastern hinge of the anticline (E of Estancia Tolonias) yielded a biotite K/Ar age of 21.6±0.4 Ma. The source of these lava-flows is assumed to be the subvolcano of Mojon Pampa (E of Tupiza), because of its central position and the geochemical composition of its rocks.
The overlying Tupiza m3 consists of polymictic conglomerates containing clasts of trachyandesites from its base. The outcrops are restricted to the east of Rio Tupiza and demonstrate a separate basin configuration with a southward dipping basin axis. Biotites from a dacitic pyroclastic tuff from the lower parts close to Tupiza yielded a K/Ar age of 17.6±0.5 Ma.
The westernmost part of the Tupiza basin is covered by conglomerates of the Oploca Fm.. Coglomerates similar to the Tupiza Fm. m3 are locally preserved beneath the Oploca Fm.. This basin-infill is embraced to the east by the W-vergent Oploca thrust located W of the Tupiza thrust and to the west by the E-vergent Urulica thrust. Both thrusts have caused gentle folding at the basin margins where lower strata come to light. Biotites from thick pyroclastic intercalations from the western margin (S of Chifloca) gave a K/Ar age of 17.0±0.4 Ma. In a small area (N of Palquisa) at the eastern margin the Oploca Fm. unconformably overlies a folded gipsyferous silty to sandy succession with tuffaceous layers in its lower parts. Biotites from these tuffs have been dated with a K/Ar age of 24.3±0.6 Ma.
The Estarca basin contains essentially Ordovician clast bearing fanglomerates of the similar named formation bound to the east by the W-vergent Estarca thrust. The lack of volcanogenic material suggests that the Estarca Fm. is coeval with the upper parts of the Oploca Fm.. This assumption can be supported by the simultaneous development of the Urulica thrust as the backthrust of the Estarca thrust later than about 17 Ma.
Conglomerates of the Nazareno Fm. are located east of the Cretaceous syncline of Tupiza in the Nazareno basin. Undeformed tuffaceous layers from the fine grained upper parts were dated at

12.79±0.12 Ma (Ar/Ar) by Gubbels et al. (1993). This upper section consists of fluvial and pediment deposits which are connected with the origin of the San Juan del Oro peneplain. The southern prolongation of this surface at the Argentinian boarder covers also the Tupiza and the Estarca basins. Lava-flows from the Tupiza Fm. m2 locally enter the basin at its western edge (Rancho Chuchuli) in a basal position. Biotites from a trachyandesitic sample from this locality yielded a biotite K/Ar age of 21.3±0.4 Ma. Here ongoing conglomeratic sedimentation is recorded by progressive angular unconformities which demonstrate synsedimentary folding. The eastern limit of the basin is marked by the westvergent Nazareno thrust.

## APATITE FISSION TRACK DATA

Two Oligocene ages have been obtained from apatites of magmatic rock samples of pre-Cenozoic origin. Coniacian basanitic lava-flows from the top of the Aroifilla Fm. exposed near Tupiza yielded an age of 32.1±4.9 Ma. Apatites from an Early Jurassic dike intruded into the Ordovician rocks in the area of Cornaca have been dated with 29.7±2.7 Ma. These data testifie to an early Tertiary uplift of the EC.

## CONCLUSIONS

The fission track data point to an Early Oligocene uplift of the EC, which may have caused erosion of the Cretaceous-Paleocene cover. This event was followed by the deposition of the probably Late Oligocene Catati and Tupiza m1 Fms..

Neogene basin development started with a major tectonic pulse at 24-22 Ma which effected an angular unconformity at their bottom. The basins are mainly controled by W-verging overthrusts, which probably pass into a deep-seated detachment plane near the brittle/ductile transition zone. Within the single basins compressive deformation is heterogenous. In the Nazareno basin, continuous deformation is recorded from 22 to 12 Ma, whereas in the Tupiza and Estarca basins thrust activity happened later than 17 Ma.

## REFERENCES

Erdtmann, B.-D., Kley, J., Müller, J., and Jacobshagen, V., 1995, Ordovician basin dynamics and new graptolite data from the Tarija region, Eastern Cordillera, south Bolivia, VIIth International Symposium on the Ordovician System: Las Vegas.

Gubbels, T.L., Isacks, B.L., and Farrar, E., 1993, High-level surfaces, plateau uplift, and foreland development, Bolivian Central Andes: Geology (Boulder), v. 21, p. 695-698.

Kley, J., in press, Transition from basement-involved to thin-skinned thrusting in the Cordillera Oriental of southern Bolivia: Tectonics.

Kley, J., Müller, J., Tawackoli, S., Jacobshagen, V., and Manutsoglu, E., in press, Pre-Andean and Andean-age deformation in the eastern Cordillera of southern Bolivia: Journal of South American Earth Sciences.

Sempere, T., 1994, Kimmeridgian? to Paleocene Tectonic Evolution of Bolivia, *in* Salfity, J.A., ed., Cretaceous Tectonics of the Andes: Braunschweig, Wiesbaden, Vieweg, p. 168-212.

# PALEOMAGNETISM, STRIKE-SLIP FAULT SYSTEMS AND CRUSTAL ROTATION IN THE REGION 25-27ºS OF NORTHERN CHILE.

Graeme TAYLOR [1], Darren RANDALL[1] and John GROCOTT[2]

(1) Department of Geological Sciences, University of Plymouth, Plymouth, Devon PL4 8AA, U.K.
(2) School of Geological Sciences, University of Kingston, Kingston-Upon-Thames, KT1 2EE, U.K.

KEY WORDS: Palaeomagnetism, Rotation, Fault Systems, Northern Chile

## INTRODUCTION

The Coastal Cordillera, Central Depression and PreCordillera of northern Chile between 25-27ºS are separated or dissected by major strike-slip fault systems, namely the Atacama Fault Zone, the Central Valley Shear Zone and the La Ternera-Domeyko fault systems (Figure 1). These fault systems are dominantly sinistral (Brown et al., 1993; Cornejo et al., 1993). Palaeomagnetic data from geological units affected by these fault systems indicate substantial clockwise crustal rotation upto ~47º (Randall et al., in press). In general the palaeomagnetic data appear to show a decrease in rotation eastward across the whole region, but are difficult to reconcile with previously proposed large scale models developed to explain the observed change in sense of rotation about the Bolivian Orocline.

## THE FAULT SYSTEMS

The oldest strike-slip fault system which affects the Coastal Cordillera is the Atacama Fault Zone (AFZ), which is characterised as a ductile sinistral, trench-linked, strike-slip fault system which had previously developed as an extensional fault system (Grocott et al., 1994). $Ar^{40}$-$Ar^{39}$ dating indicates that the ductile motion on the fault zone was Early Cretaceous in age and was intimately associated with the emplacement of granitic plutons during the period 132-126 Ma and motion may have continued until 106 Ma (Dallmeyer et al., 1996). Recent field mapping by ourselves and others (Arévalo 1995), coupled with Landsat interpretation shows that the principal fault zone is not a continuous feature, as previously thought, but is segmented and cross-cut by major sinistral NW trending faults. These faults cut the youngest pluton in this region (106 Ma), and appear to sole into a N-S to NE-SW trending fault zone which separates the Coastal Cordillera from the Central Depression. This shear zone we term the Central Valley Shear Zone (CVSZ) which, together with the NW trending strike-slip faults, define an Atacama Fault System. This fault system affects the entire width of the Coastal Cordillera and appears traceable from at least 29 to 25ºS (Taylor et al., in press). In the region around Inca de Oro, the CVSZ is a transpressive strike-slip fault zone which is intruded by syn-tectonic plutons dated to ~80 Ma (Sylvester & Palacios, 1992) while east of Copiapo it is a narrow fold and thrust belt dissected by a sinistral mylonite zone (Arévalo, 1995) which affects Late Cretaceous sedimentary units.

The structure in the east of the area is dominated by the La Ternera-Domeyko fault system which is again a major transpressive sinistral strike-slip fault system. Detailed field studies and geochronology reveal that this fault system was active during the period 42-33 Ma when it was kinematically linked to the fold and thrust belt of the Porterillos-El Salvador area in the north and to a set of NW trending sinistral faults to the south of Porterillos (Cornejo et al., 1993). Clockwise rotation of crustal blocks was predicted from the structural geometry and has been confirmed palaeomagnetically.

## PALAEOMAGNETISM AND ROTATION

Table 1 lists published palaeomganetic results from the region and adjacent areas and two new results, one from layered gabbros at Caldera (Early Jurassic) and the second from volcanics and intrusives of the Sierra de Duchasa Fm. (Late Cretaceous) which crop out 15 km east of Copiapo, east of the CVSZ (Table 1). Work is in progress on a range of units from this latter area and from near Inca de Oro. One problem in defining the amount of rotation observed at any location is the reference directions with which the observed data are compared. We have rotated African data into S. American co-ordinates to supplement the available data from the S. American plate and have selected poles on the basis of reliability criteria (Table 2). The most doubtful of these reference directions is that for the Early Jurassic which is markedly different from the younger directions and must either imply rapid plate motion at this time or that the available poles are inaccurate.

## CONCLUSIONS

The data show a general W-E decrease in the magnitude of the rotations across the major fault systems. Previous models used to explain rotations in the S. American margin include oroclinal bending, dextral shear crustal shear, differential shortening across a pre-existing bend and block rotation in a transpressive sinistral fault system (Figure 2a-d) (references in Randall et al., in press). The oroclinal bending and dextral shear zone hypotheses are rejected as the observed geology in this part of northern Chile does not support such models. The differential shortening model, as originally proposed, would not lead to the variation in rotation observed nor to rotations greater than 20º or so. We favour a model involving repeated deformation and rotation in a series of sinistral transpressive fault systems, due to oblique convergence at an advancing subduction boundary, which have migrated eastward through time. and may incorporate a lesser component of rotation due to differential shortening in Neogene times.

## REFERENCES


Arévalo, C. 1995. Mapa Geologico de la Hoja Copiapo, Region de Atacama. Documentos de Trabajo, 8, Servicio Nacional de Geologia y Mineria, Chile.

Brown, M., Diáz, F. & Grocott, J. 1993. Displacement history of the Atacama fault system 25°00'S-27°00'S, northern Chile. Geol. Soc. America. Bull, 105, 1165-1174.

Cornejo, P., Mpodozis, C., Ramirez, C. & Tomlinson, A., 1993. Estudio geologica de la region de Portrerillos y El Salvador (26-27° Lat. S). Servicio Nacional de Geologico y Mineria.

Dallmeyer, R.D., J. Grocott, M. Brown, G.K. Taylor & P.J. Treloar, 1996. Mesozoic magmatic and tectonic events within the Andean Plate Boundary Zone, 26º-27º30'S, North Chile: Constraints from $^{40}Ar/^{39}Ar$ Mineral Ages. Jnl. of Geology, 104, 19-40.

Grocott, J., Brown, M., Dallmeyer, R.D., Taylor, G.K. & Treloar, P.J., 1994. Mechanisms of continental growth in extensional arcs: an example from the Andean plate boundary. Geology, 22, 391-394.

Randall, D.E., Taylor, G.K. & Grocott, J., in press. Major crustal rotations in the Andean Margin: Paleomagnetic results from the Coastal Cordillera of northern Chile. Jnl. of Geophys. Res.

Taylor, G.K., Grocott, J., Pope, A. & Randall, D.E. Mesozoic fault systems, deformation and fault block rotation in the Andean forearc 25°-27°S: A crustal scale strike-slip duplex in the Coastal Cordillera of Northern Chile. Submitted to E.P.S.L.

Sylvester, H. & Palacios, C., 1992. Transpressional structures in the Andes between the A. F.Z. and the West Fissure System at 27ºS, III Region, Chile. Zentralblatt für Geologie und Paläontolgie, 6, 1645-1658.

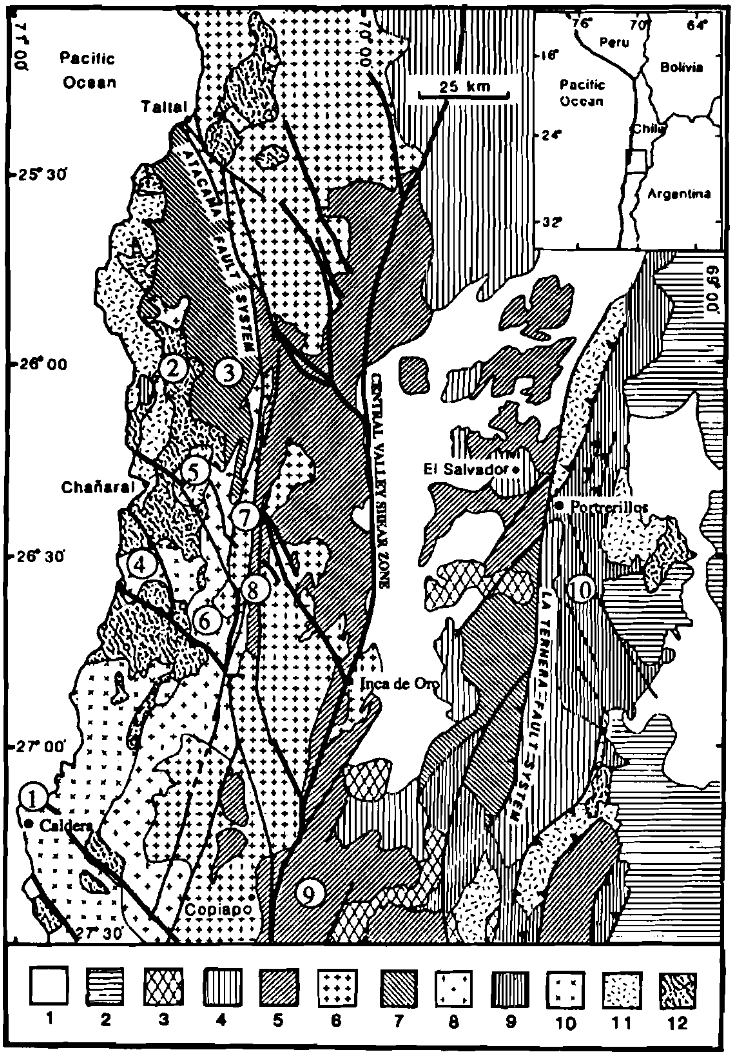


Figure 1. Generalized geological map of northern Chile. Inset shows location with respect to the western margin of South America. 1, Late Cenozoic continental sedimentary rocks; 2, Miocene-Oligocene plutonic rocks; 3, Early Tertiary plutonic rocks; 4, Palaeocene-Eocene volcanic and sedimentary rocks; 5, Cretaceous volcanic and sedimentary rocks; 6, Cretaceous plutonic complexes; 7, Jurassic volcanic rocks; 8, Early Cretaceous-Late Jurassic plutonic rocks; 9, Jurassic-Triassic sedimentary rocks in the east; 10, Early Jurassic plutonic rocks; 11, Triassic-Permian plutonic complexes; 12, Palaeozoic pre-arc basement. Numbers in circles refer to sampled sites (Table 1).

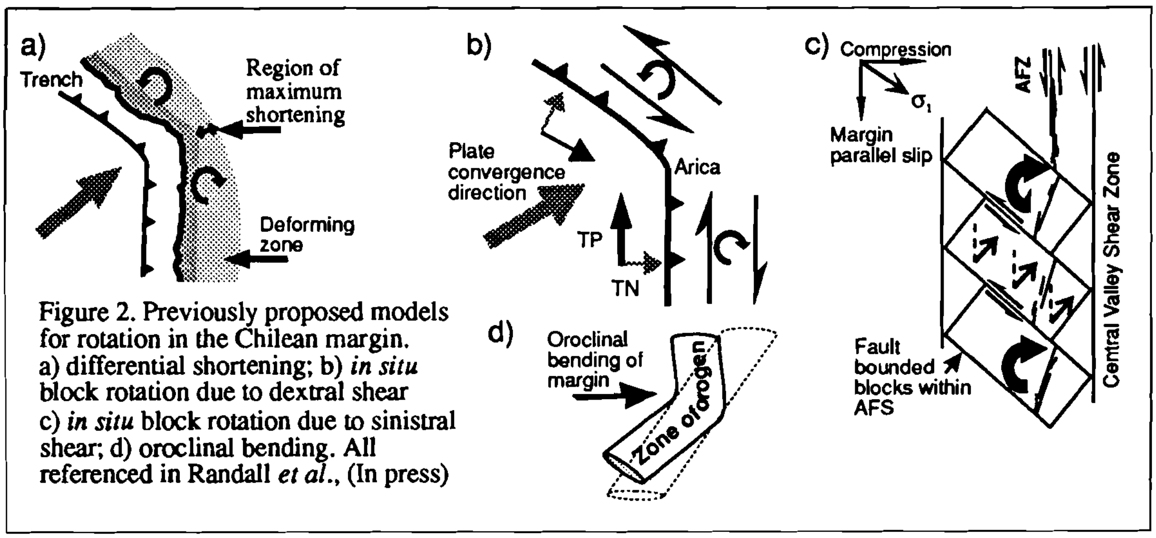


Figure 2. Previously proposed models for rotation in the Chilean margin. a) differential shortening; b) *in situ* block rotation due to dextral shear c) *in situ* block rotation due to sinistral shear; d) oroclinal bending. All referenced in Randall *et al.*, (In press)

**TABLE 1. PALAEOMAGNETIC ROTATIONS RECORDED BETWEEN 22.5° AND 27.6°S, NORTHERN CHILE**

| Locality | Age Ma | Lat.°S | Long.°W | No. | Dec. (°) | Inc. (°) | $\alpha_{95}$ (°) | Rotation | Flattening | Ref. |
|---|---|---|---|---|---|---|---|---|---|---|
| **WEST OF ATACAMA FAULT ZONE** | | | | | | | | | | |
| Caldera gabbros[1] | 192 | 27.1 | 71.0 | 8 | 35.1 | -30.4 | 14.5 | 15.1±16.8 | -25.6±12.9 | 1 |
| La Negra Fm.[2] | M. Jur | 26.0 | 70.6 | 14 | 42.0 | -35.5 | 9.6 | 40.0±11.5 | -7.5±9.1 | 2 |
| Cifuncho Fm.[3] | ? M. Jur | 25.6 | 70.6 | 11 | 36.6 | -50.0 | 9.6 | 34.6±13.7 | 7.0±9.1 | 3 |
| Flamenco dykes[4] | M. Jur | 26.3 | 70.6 | 5 | 45.6 | -43.0 | 8.8 | 43.6±11.7 | 0.0±8.5 | 2 |
| Vetado dykes[5] | M .Jur | 26.2 | 70.4 | 6 | 48.9 | -49.6 | 12.1 | 46.9±16.5 | 6.6±10.8 | 2 |
| Las Animas dykes[6] | 155 | 26.2 | 70.4 | 5 | 44.0 | -48.6 | 11.2 | 42.0±15.2 | 5.6±10.2 | 2 |
| Las Tazas dykes[7] | 132-126 | 26.3 | 70.4 | 7 | 38.7 | -41.5 | 12.0 | 39.7±13.8 | -6.5±10.1 | 2 |
| **WEST OF CENTRAL VALLEY SHEAR ZONE** | | | | | | | | | | |
| Remolino dykes8 | < 126 | 26.3 | 70.3 | 13 | 37.2 | -39.3 | 11.6 | 38.2±13.0 | -8.7±9.8 | 2 |
| **WEST OF LA TERNERA FAULT ZONE** | | | | | | | | | | |
| Sierra La Dichusa volcanics[9] | 77-62 | 27.2 | 70.1 | 7 | 29.3 | -42.1 | 8.0 | 33.3±10.7 | -8.9±7.5 | 1 |
| **EAST OF LA TERNERA FAULT ZONE** | | | | | | | | | | |
| Cerrillos Fm. (CEG locality) | ? E. Tert. | 27.6 | 69.8 | 6 | 21.6 | -48.5 | 22.9 | 32.6±31.4 | -6.5±19.7 | 4 |
| Quebrada Monardes Fm. | E. Cret | 27.6 | 69.6 | 8 | 23.7 | -40.9 | 14.1 | 27.7±15.3 | 5.9±11.5 | 4 |
| Quebrada Monardes Fm.[10] | E. Cret | 26.7 | 69.4 | 7 | 22.7 | -44.9 | 12.2 | 26.7±14.2 | 9.9±10.1 | 5 |
| La Ternera Fm. | L. Triass | 27.6 | 69.4 | 18 | 33.1 | -51.1 | 6.5 | 13.1±13.1 | -4.9±7.6 | 4 |
| Lipiyoc | Miocene | 22.5 | 67.0 | 17 | 2.6 | -44.4 | 7.9 | 2.6±8.9 | -0.6±6.4 | 6 |

**TABLE 2. PALAEOMAGNETIC REFERENCE DIRECTIONS**

| Time period | No. | Dec. (°) | Inc. (°) | $\alpha_{95}$ (°) |
|---|---|---|---|---|
| Miocene-Recent | - | 0 | -45 | 1 |
| Early Cenozoic | 3 | 349 | -55 | 9 |
| Late Cretaceous | 12 | 356 | -51 | 5 |
| mid-Cretaceous | 13 | 359 | -48 | 4 |
| Early Cretaceous | 5 | 356 | -39 | 3 |
| Late Jurassic | 1 | 16 | -51 | 12 |
| Middle Jurassic | 5 | 2 | -43 | 6 |
| Early Jurassic | 7 | 17 | -58 | 8 |

Table 1. Numbers on localities refer to Figure 1. Lat. and Long. are position of sampling site; No. is number of sites; Dec. and Inc. are declination and inclination of palaeomagnetic vector; $\alpha$95 is 95% confidence circle. Rotation and flattening calculated according to Beck (1980) with correction of Demarest (1983). References are; 1, This study; 2, Randall *et al.* (In press); 3, Forsythe et al. (1987); 4, Riley *et al.* (1993); 5, Randall (1996); 6, Somoza *et al.* (In press). All referenced in (2).

Table 2. Headings as in Table 1.

# MESOZOIC AND CENOZOIC ACRETIONARY EVENTS IN THE COLOMBIAN ANDES

Jean Francois TOUSSAINT and Jorge Julian RESTREPO

Facultad de Minas - Universidad Nacional de Colombia - Sede Medellin

KEY WORDS : Colombian Andes, Terranes, Accretion, Dispersion, Exotic blocks.

## INTRODUCTION

New results have been obtained recently ( Desmet, 1995; Estrada, 1995; Toussaint and Restrepo, 1994, in print) about the tectonics, geochemistry and the paleomagnetism of the Western part of Colombia. They confirm that the Northern Andes are composed of a mosaic of aloctonous Terranes accreted to the Amazonian Craton (Fig. 1).

This information allows to determine the geodynamic settings of the terranes with oceanic crust, diverse types of sutures and the several accretion ages.

## THE SITUATION AT THE BEGINNING OF THE MESOZOIC

At the beginning of the Mesozoic, Eastern Colombia was formed by the collage of a continental terrane (The Chibcha Terrane) to the Llanos Orientales which are part of the Amazonian Craton.

However, at that time, no terrane of Western Colombia was accretioned, being possible that the Tahami Terrane wich continental crust, was localized South of its actual position.

Its possible that during the Triassic and Jurassic situation, various terranes at present time located in Central America (Chortis and Maya Terranes) were situated West of the Eastern Colombia. These Terranes were separated from South America Plate at late Jurassic.

## FORMATION AND ACCRETION OF THE OCEANIC TERRANES.

During the Cretaceous was when the formation of the terranes with oceanic basement started. Above a oceanic crust of which are some ophiolites, a great quantity of Plateaux basalts were poured out. These basalts show an ecuatorial paleolatitud (Estrada, 1995). This volcanism is attributed at the beginning of the Hot Spot activity of the Galapagos Islands. In other regions of the ocean, it also formed some volcano-sedimentary sequences of Insular Arcs (Desmet, 1995).

During Early Cretaceous, a oceanic Terrane (Calima Terrane) was amalgamated by means of ophiolitic suture with eastern vergency to a continental Terrane that was located South of its actual position (Tahami Terrane). The tectonic characteristics of this amalgamation are marked by an important overthrusting and by a metamorphism of medium and high pressure.

The Composite Calima-Tahami Terrane was united to the Eastern Colombia at Late Cretaceous period by means of the dextral Otu-Pericos fault. This movement is directly related with the movement in the same direction of the Caribbean Plate in relation to South America.

The Cauca-Romeral fault system is not a cretaceous suture; it is a dextral wrench system which disperses terranes that was previously joined. These dispersion movements continued during all the Cenozoic Era.

During the Miocene period, two oceanic terranes (Gorgona and Cuna Terranes) was accreted to the Andean Block. The last collision was marked by an overthrusting with eastern vergency and by some ultrabasic rocks. The collision of the Cuna Terrane had an effect in all the Colombian Andes and permitted the formation of the Eastern Cordillera.

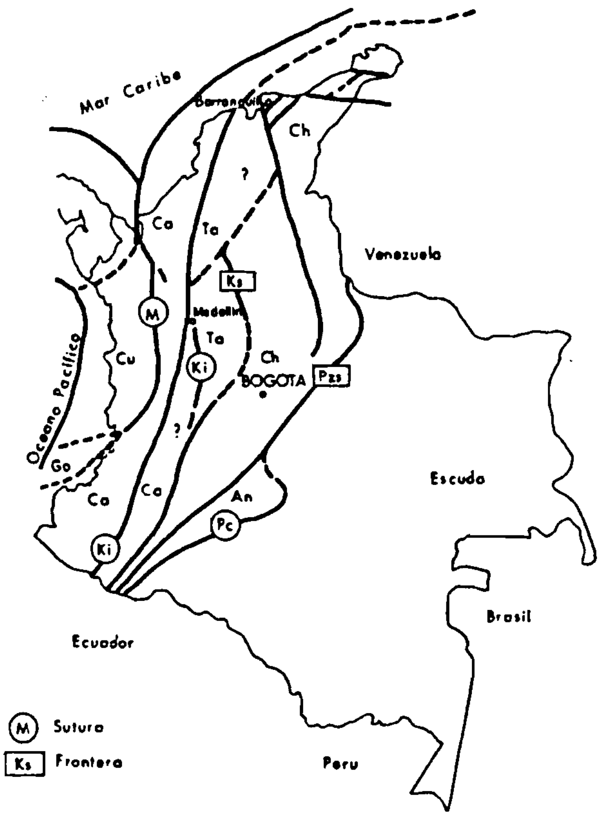


Fig. 1: Schematic map of the main terranes of Colombia according to Toussaint and Restrepo (1988 and 1994).
An: Andaqui Terrane, Ch: Chibcha Terrane, Ta: Tahami Terrane, Ca: Calima Terrane, Go: Gorgona Terrane, Cu: Cuna Terrane. PC: Precambrian suture, Pzs: late Paleozoic boundary fault, Ki: Early Cretaceous suture, Ks: Late Cretaceous boundary, M: Miocene suture.

In the present time, the Colombian Andes are located between three great plates which converge to it. The actual instability of this zone is a consequence of this situation.

The Cuna Terrane is affected by a dispersion fault which overthrusts the Panama Terrane over the Colombian Andes. This dispersion is marked by an important seismic node. Another fault, the dextral striking Guaicaramo fault, produces the dispersion of the Colombian Andes in relation to the South American Plate.

## CONCLUSIONS

This results show that the geodynamic processes that permit the formation of the Northern Andes are different from those who had influence in the Central Andes. With this course, the formation of this part of the Andes is similar to the western margin of North America.

## REFERENCES

Desmet A. 1995. Ophiolites et series basaltiques cretacees des regions caraibes et norandines: bassins marginaux, dorsales ou plateaux oceaniques? These Univ. H. Pioncare, Nancy, 1 - 597.

Estrada J.J. 1996. Paleomagnetism and Accretion events in the Northern Andes. These. State Univ. New York at Birnimgham, 1 - 170.

Etayo F. et al. 1986. Mapa de terrenos geologicos de Colombia. Ingeominas. Bogota. 14,1 - 235.

RestrepoJ.J. and Toussaint J.F. 1988. Terranes and continental Accretion in the Colombian Andes. Episodes, 11, 189 - 193.

Toussaint J.F. and Restrepo J.J. 1994. The Colombian Andes during Cretaceous Times. In: Cretaceous tectonics of The Andes. Ed: Vieweg, 61 - 100.

Toussaint J.F. 1995. Evolucion Geologica de Colombia. Medellin, Colombia, Tomo 1, 1 - 229 and Tomo 2, 1 - 94.

# RESTORATION IN MAP VIEW OF THE PAMPEAN RANGES PROVINCE, SOUTHERN EDGE OF THE PUNA PLATEAU, ARGENTINA.

Marc de URREIZTIETA [1], Olivier BOURGEOIS [1], Denis GAPAIS [1], Peter R. COBBOLD [1], Claude LE CORRE [1], Eduardo A. ROSSELLO [2], & D. ROUBY [1].

[1] Géosciences Rennes, CNRS (UPR.4661), 35042 Rennes Cedex, France.
[2] CONICET y Dpto. de Ciencias Geológicas, Universidad de Buenos Aires, República Argentina.

**KEY WORDS** : Restoration, Neogene kinematics, Pampean Ranges

**RESUMEN** : En el Noroeste Argentino (27°S), el límite meridional de la Puna es una zona transpresiva dextral : la zona de transición de Tucumán. Las estructuras regionales neógenas se desarollaron como consecuencia de las variaciones de la intensidad de deformación continental entre dos segmentos corticales. En el sector Norte (Puna), el accortamiento neógeno y el espesor cortical son importantes. Al Sur, en las Sierras Pampeanas, la deformación continental es menor. Un método numérico de reconstrucción en mapa nos permite estimar los desplazamientos y el campo de deformación producidos por la tectónica neógena a través de la zona.

## INTRODUCTION :

The Sierras Pampeanas of Argentina are located in the Central Andes at the southern edge of the Altiplano-Puna (27°S). The boundary between the high plateau and the northernmost Pampean Ranges is a major dextral transpressional zone : the Tucumán transfer zone (Jordan et al., 1983; Urreiztieta et., al, 1996). A variation in the style of deformation within the foreland occurs across this transition zone (Allmendinger et al., 1983). The Sub-Andes are affected by thin-skinned deformation whereas the Pampean Ranges, located further South, are characterized by thick-skinned deformation. Deformation within the Pampean Ranges involves faulting and basement uplifts associated with block rotations about vertical axes. The study area consists of alternating Neogene compressional basins and ranges of Pre-Mesozoic crystalline basement. Ramp basins and basement uplifts are bounded by high angle thrusts and result from the bulk subhorizontal shortening and crustal thickening of the area since Miocene times (Gonzalez Bonorino, 1950). The Neogene detrital cover lies unconformably on an erosional surface which is exhumed on the tops of most crystalline basement ranges. This interface is easily identified both on the ranges (via topography and satellite images) and at the base of the basins (via seismic profiles). This plane of reference and the regional fault pattern were used to estimate the overlaps along major faults and to draw a mosaic of fault-bounded blocks throughout the Pampean Ranges area (Fig. 1). We have restored the crustal rigid block geometry using a numerical method of reconstruction in map view in order to compute the field of finite displacements associated with the fault network. We compare the numerical results with previous interpretations based on structural and paleomagnetic studies and discuss the regional tectonic patterns across the Pampean Ranges.

## PRINCIPLE OF THE METHOD

To estimate the Neogene kinematics within the Pampean Ranges we used a numerical restoration method applicable in map view to non cylindrical compressional structures (Rouby *et al.*,

**Figure 1.**

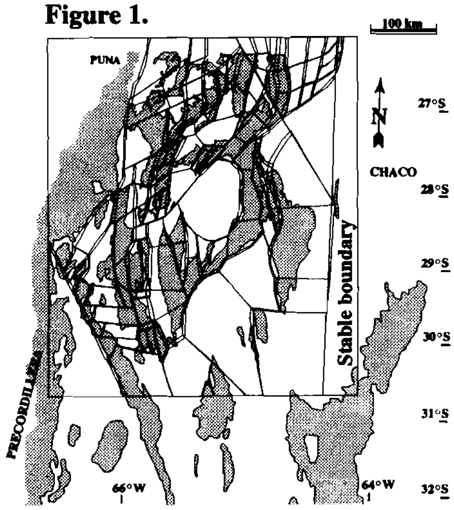


**Figure 2.**

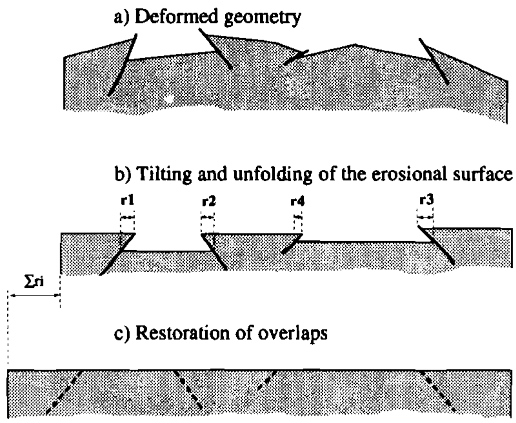


**Figure 3.**

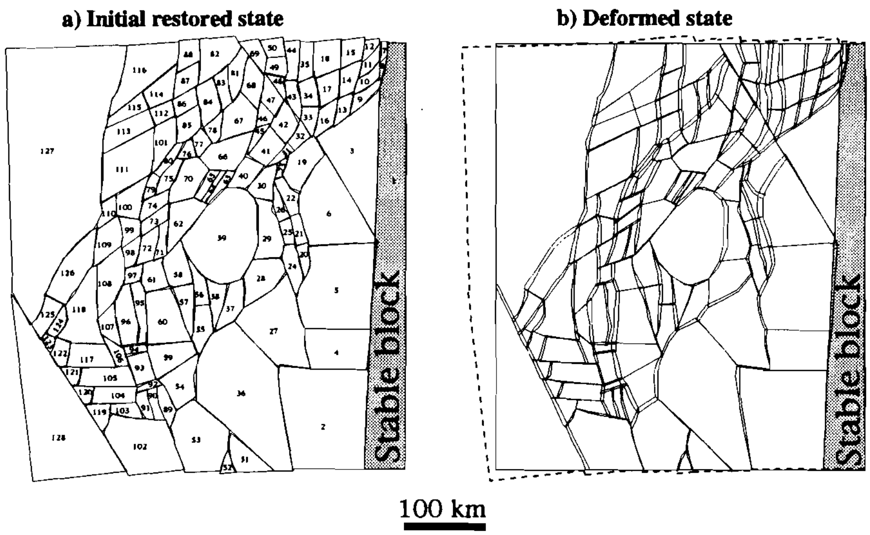


**Figure 4.**

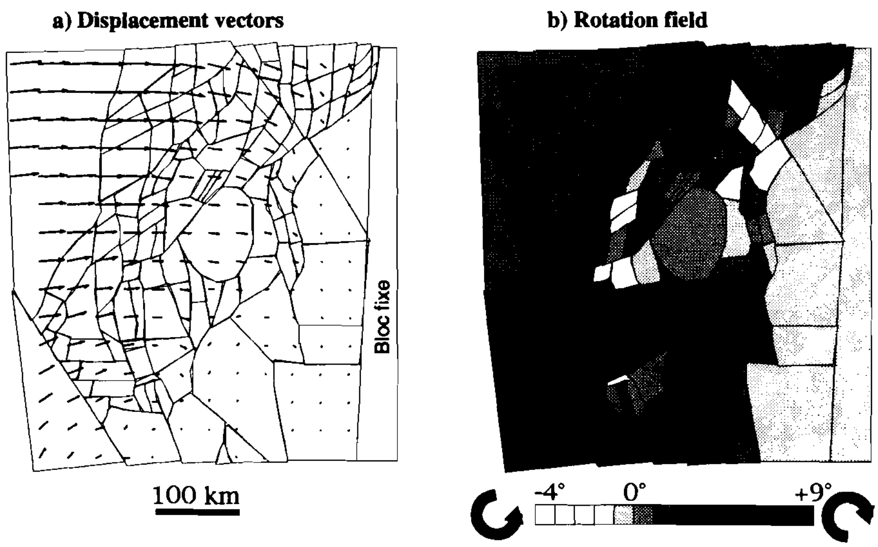

1993; Bourgeois, 1994). The principle of restoration is to compute the initial undeformed state of an horizontal reference surface, assuming that displacement on the faults is achieved by rigid translations and rotations of the fault blocks. The initial data is a mosaic of fault bounded blocks overlaping each other along compressional structures (Fig. 1). The width of the overlaps is equal to the horizontal component of the amount of overthrusting corrected by the folding and tilting of the reference surface (Fig. 2). The displacement on the fault is inverted by minimizing gaps and overlaps at block boundaries using a series of rigid body translations and rotations about vertical axes centered at the block centroids. In doing so, we assume that internal strain of blocks is negligible with respect to the displacement along faults. The comparison between restored and deformed states gives the fields of finite displacements, finite block rotations and finite strain.

## RECONSTRUCTION OF THE PAMPEAN RANGES

For the study area, the reference plane is the erosional surface (interface between Neogene cover and crystalline basement). We assume that it was horizontal before deposition of the Neogene cover. The carving of the area into 128 fault-bounded blocks fits the regional fault pattern (Fig.1). The dip of fault planes is arbitrarily chosen at 45°. The amount of overthrusting along regional faults is estimated using field observations and seismic surveys and corrected by untilting and unfolding of the reference surface (Fig. 2). The blocks are adjusted against the stable easternmost boundary (equivalent to the Andean foreland; Fig. 1). After numerical fitting, gaps and overlaps between rigid blocks remain but they are negligible with respect to the overall area.

## FIELDS OF FINITE DISPLACEMENTS, ROTATIONS AND STRAIN

Displacement vectors are the finite displacements of points of a regular grid attached to the block mosaic between the initial and final stages (Fig. 3). Displacements increase away from the stationary boundary (Fig. 4a). Furthermore, displacements increases from the South towards the Northwest, defining two sectors limited by a NE-SW trending strip (equivalent to the Tucumán transition zone). This pattern suggests that the absolute motion of the blocks towards the East is greater in the Puna. Rigid blocks in the vicinity of the plateau were translated twenty kilometers towards the NE. This finite displacement field (Fig. 4a) and the geometry of the regional fault pattern are compatible with a dextral component along the NE-SW trending Tucumán transfer zone (TTZ).

Individual rigid block rotations calculated by the reconstruction are mostly clockwise (Fig. 4b). Rotations reach maximal values (9°) within the TTZ, where *en échelon* blocks bound the plateau. This pattern of bulk clockwise rotations is compatible with a regional component of dextral wrenching along the southeastern edge of the Puna. The clockwise block rotations are consistent with paleomagnetic measurements along the southeastern edge of the Puna (Roperch et al., 1996). Paleomagnetic results within Cretaceous to Pliocene sequences also confirm the bulk clockwise pattern of block rotations (up to 29° within the TTZ). The magnitudes of rotations calculated by the restoration are smaller than the measured paleomagnetic rotations. This suggests that we have probably under-estimated the strike-slip components along major faults.

The finite element analysis of the displacement field gives the orientations of the principal shortening and stretching axes within each cell of a regular grid. We have compared the orientations of the principal axes of deformation with the orientations of axes obtained from the analysis of fault populations measured at 72 localities in the field (Fig. 5). The fault population analysis shows that the shortening directions are sub-horizontal at most localities and are therefore comparable with the horizontal shortening directions obtained by restoration. Both methods show a substantial scattering of the orientations of shortening axes throughout the area (Fig. 5). There is a good consistency between both sets of results (Fig. 5). Two main shortening directions are represented. The first shortening orientation is widespread and trends roughly E-W. The second shortening orientation is locally observed in the vicinity of the Puna within the TTZ and strikes NW-SE. Furthermore, unlike field observations, restoration estimates the amount of dextral wrenching parallel to the TTZ (Fig. 6). The dextral component along the southern edge of the Puna appears to be significant (bulk dextral shearing is about $\gamma = 0{,}20$.) It is combined with a NW-SE regional shortening of 10%.

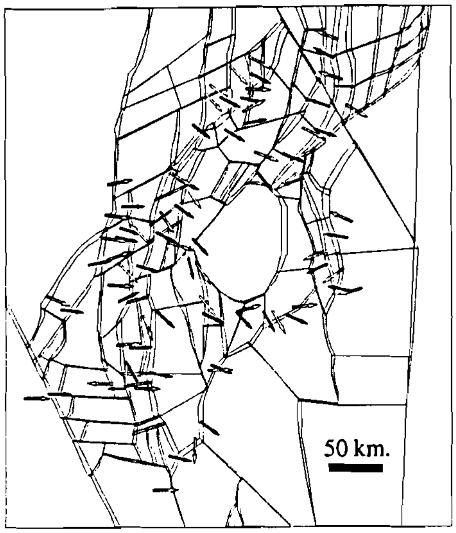


**Figure 5.**

Shortening axes from fault kinematics

Shortening axes from restoration

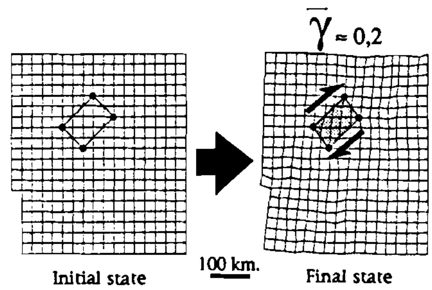


**Figure 6.**

## CONCLUSIONS

The finite displacement, rotation and strain fields calculated by restoration are consistent with the results of (1) the fault populations analysis, and (2) the paleomagnetic study.

The displacement field confirmes a dextral component along faults parallel to the TTZ and indicates an overall dextral motion along the TTZ of 20 km. The clockwise rotations associated with the motion along regional faults are maximal within the TTZ. Furthermore, we confirm that the NW-SE regional shortening across the TTZ is at least 15 km. Fault population analysis and restoration show a strong consistency. The scattering of shortening directions measured in the field is also shown by the numerical restoration. Across the Tucumán Transfer Zone, results of both methods reflect the superimposition of two main deformation fields: (1) a ENE-WSW to E-W subhorizontal shortening probably related to bulk convergence between Nazca and South America plates, and (2) a NW-SE subhorizontal shortening consistent with dextral wrenching along the TTZ and with southeastward expansion of the high plateau. The resulting bulk strain is locally of constrictional type, with subvertical principal extension.

The finite displacement and strain field calculated by the reconstruction method does not take into account the history of deformation. However, the remarkable correlation between the results of this numerical method and other independant methods suggests that the complex strain field accumulated in the area probably results from a progressive deformation.

## REFERENCES

**Allmendinger, R.W., Ramos, V.A., Jordan, T.E., Palma, M. & Isacks, B.L., 1983.** Paleogeography and Andean structural geometry, NW Argentina. Tectonics, v. 2: No.1: 1-16.

**Bourgeois, O., 1994.** Restauration numérique en plan de la déformation discontinue dans les domaines en compression. Application à la dépression Tadjik, Asie Centrale. Mémoire de D.E.A. (unpublished), Université de Rennes 1.

**González Bonorino, F., 1950.** Algunos problemas geológicos de Las Sierras Pampeanas. Rev. Assoc. Geol. Argentina., V: 81-110.

**Jordan, T.E., Isacks, B.L., Ramos, V. & Allmendinger, R.W., 1983.** Mountain building in the Central Andes. Episodes, 1983: 20-26.

**Rouby, D., Cobbold, P.R., Szatmari, S., Coehlo, D. & Rici, J.A., 1993.** Least-squares palinspastic restoration of regions of normal faulting-application to the Campos Basin (Brazil). Tectonophysics, 221: 439-452.

**Urreiztieta, M. de, Gapais, D., Le Corre, C., Cobbold, P.R. & Rossello, E., 1996.** Cenozoic dextral transpression and basin development at the southern edge of the Altiplano-Puna, NW Argentina. Tectonophysics (In Press).

**Roperch, P., Aubry, L., Urreiztieta, M. de, Rossello, E.A., & Chauvin, A., 1996.** New paleomagnetic constraints on Andean tectonics along the southeastern edge of the Altiplano-Puna. (N-W Argentina). Journal of Geophysical Research (accepted).

# THE APTIAN-LATE ALBIAN MARINE TRANSGRESSION IN THE ORIENTE BASIN OF ECUADOR.

Rommel VILLAGÓMEZ[1], Etienne JAILLARD[2], Luc BULOT[3], Marco RIVADENEIRA[4] and Ramon VERA[5].

(1) ORSTOM, San Ignacio 805 y Humboldt, Apartado 17-11-6596, Quito, Ecuador.
(2) ORSTOM, Institut Dolomieu, 15, rue Maurice-Gignoux, 38031 Grenoble cedex, France.
(3) Institut Dolomieu, 15, rue Maurice-Gignoux, 38031 Grenoble cedex, France.
(4) PETROPRODUCCIÓN, Juan León Mera y Orellana, Quito, Ecuador.
(5) Escuela Politécnica Nacional, Ladrón de Guevara s/n, Quito, Ecuador.

KEY-WORDS : Aptian, Albian, biostratigraphy, facies, transgression, backstepping.

## INTRODUCTION

In the Oriente Basin of Ecuador, the early Cretaceous marine transgression begins with the deposition of poorly dated continental to marine sandstones (Hollin Fm), which disconformably overly Paleozoic to earliest Cretaceous rocks (Tschopp 1953, Bristow & Hoffstetter 1977, White et al. 1995). The overlying Basal Napo Formation of Albian age comprises from base to top (Faucher et al. 1971, Bristow & Hoffstetter 1977, Jaillard et al. 1995, fig. 1) : marine, glauconitic shales and sandstones ("Basal Sandstones"), locally capped by thin massive limestones ("C Limestones"); marine black shales ("Basal Napo Shales"); open shelf limestones ("T Limestones"), and marine to deltaic sandstones ("T Sandstones").

Recent biostratigraphic data demonstrate that this succession is strongly diachronous through the basin (Villagómez 1995). It express the progressive backstepping of continental to marine strata onto the border of the basin, the facies sequence reflecting the large-scale Cretaceous transgression in the Andean Basin.

## VERTICAL FACIES SUCCESSION

According to most authors (Kummert & Casal 1986, Souza Cruz 1988, White et al. 1995), the lower part of the Hollin Formation, is characterized by coarse-grained, cross-bedded sandstones, conglomeratic beds and plant remains (amber, coal measures), deposited by braided stream in a continental environment. The upper part of the formation, made up of medium-grained sandstones with gentle trough cross-bedding was deposited by meandering fluvial systems, or in estuarine to shoreline environments (fig. 1). The Guianese shield is believed to have been the source-area (Villagómez 1995).

The Basal Napo Sandstones (Upper Hollin of some authors) begin with massive cross-bedded sandstones, fine-grained rippled sandstones and shales of shoreline environment (Souza Cruz 1988, White et al. 1995, fig. 1). The upper part of the unit is made of glauconitic sandstones, shales, marls and sandy limestones with thick shelled bivalves, interpreted as deposited in an open marine shallow clastic shelf environment, in a transgressive context (White et al. 1995, Jaillard et al. 1995). They are capped by the glauconitic "C Limestones", which contain echinoderms, algae and bivalves, of open marine shelf environment. The latter often present thin layers of ammonite-bearing limestone separated by erosional surfaces, expressing stacked flooding events separated by emergence periods (Jaillard et al. 1995, fig. 1).

The Basal Napo Shales are unbioturbated, black laminated shales. They contain abundant inoceramids, ammonites and foraminifers (few Ticinella, some Hedbergella) at the base, and restricted planctonic (Hedbergella, few fish remains) and benthic associations (Cibicides, Praebulimina) in the upper part. The base of the unit represents a major maximum flooding, whereas its upper part express a progradation in a low energy, disaerobic marine environment (Jaillard et al. 1995, fig. 1).

This vertical facies succession evidence a large-scale marine transgression.

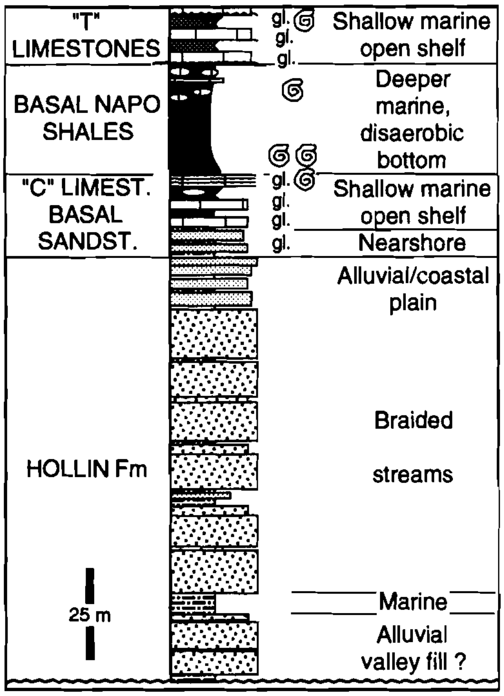


*Fig. 1 : Lithostratigraphy of the Aptian-Albian transgression in the northern part of the Oriente Basin of Ecuador (adapted from White et al. 1995).*

BIOSTRATIGRAPHY

Biostratigraphic data available from wells and field sections allow to define three chronostratigraphic units.

Undetermined dwarf ammonites, inoceramids and *Hedbergella* cf. *delrioensis* obtained from marine shales at the base of the Hollin Formation indicate a post-Early Aptian age (Tiguino-1, Mills 1971). A comparable, though undated, marine shale has been mentioned within the Hollin Formation (Zorro-1, Lammons 1975). In other places, micropaleontological associations of probable Late Aptian age have been obtained from part of the Hollin Formation (río Misahualli, Faucher et al. 1971; Villano-3, Stratigraphic Service 1995). Thus, the base of the Hollin Formation appears to be of «middle» or Late Aptian age. Yet, Robertson Research (1988) ascribed to the Early Aptian the association of *Hedbergella delrioensis*, *H.* cf. *gorbachikae*, *H.* cf. *sigali*, *Nannoconus globulus*, *Rhagodiscus achlyostaurion*, *Rh. angustus*, *Callialasporites trilobatus* and *Inaperturopollenites curvimuratus* found at the top of the formation in Cowi-1 (fig. 2). This would imply an Early Aptian or older age for the Hollin Formation at this place. However, the results of recent biostratigraphic studies suggest that this association can be younger.

Early to Middle Albian micropaleontological assemblages have been identified in the upper part of the Hollin Formation in the northern and central part of the basin (Pungarayacu-30, Ordoñez et al. 1994; Tiwae-1, Arai et al. 1990; Villano-3, Stratigraphic Service 1995, fig. 2). They include *Prediscosphaera columnata*, *Callialasporites trilobatus*, *Classopolis echinatus*, *Elaterosporites klaszi*, *Perotriletes pannuceus*, *Sofrepites legouxae* and tricolpate pollens of angiosperms. In the Southwest, however, an ammonite assemblage of earliest Middle Albian age with *Mirapelia* sp., *Brancoceras aegoceratoides* and *Lyelliceras* gr. *ulrichi* occurs at the top of the massive "C Limestones" and at the base of the Basal Napo Shales (Chinimbimi, Bulot & Jaillard 1995, Jaillard et al. 1995, fig. 2).

Late Albian palynomorph markers (*Elaterosporites protensus*, *E. verrucatus*) are common in the

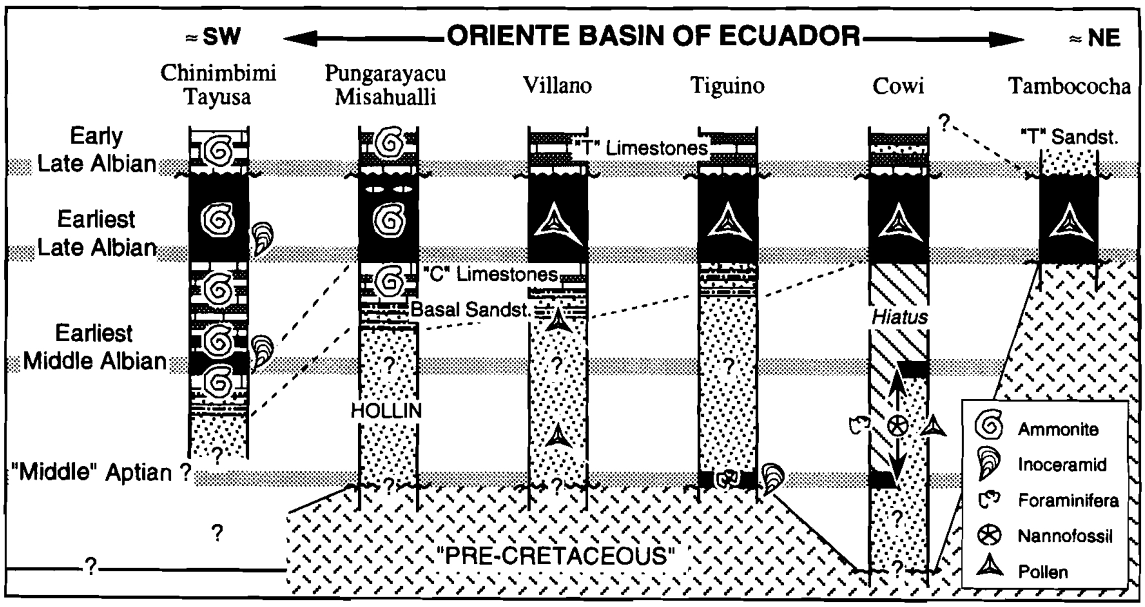


*Fig. 2 : Biostratigraphic data for the Aptian-Albian transgression from selected wells and field sections.*

Basal Napo Shales of the northwestern and central parts of the basin (Pungarayacu-30, Ordoñez et al. 1994; río Misahualli, Faucher et al. 1971, Jaillard et al. 1995; Tivacuno-1, Ordoñez et al. 1989; Tiwae-1, Arai et al. 1990; Cowi-1, Robertson Research 1988; Villano-3, Stratigraphic Service 1995; fig. 2). On the eastern border, however, they occur in marine shales overlying directly the pre-Cretaceous basement, below the "T Sandstones" (Tambococha-1, Zambrano et al. 1994), thus indicating the lack of Late Aptian to Middle Albian sandstones (fig. 2). In the northwestern part of the basin, an ammonite assemblage of earliest Late Albian age with *Dipoloceras* gr. *bouchardianum* and *Venezoliceras (Venezoliceras)* cf. *venezolanum* was found at the base of the Basal Napo Shales (Pungarayacu-30, río Misahualli, Bulot & Jaillard 1995, Bulot et al. in press). In the South, a similar association occurs in the upper part of the Basal Napo Shales (Chinimbimi, Bulot & Jaillard 1995, Bulot et al. in press, fig. 2).

## INTERPRETATIONS AND CONCLUSIONS

In the Oriente Basin of Ecuador, the Early Cretaceous transgression is marked by at least two important Maximum Floodings representing useful time-lines. "Middle"to Late Aptian marine shales are locally present, and predate the deposition of sandstones of Late Aptian to Albian age. The major Maximum Flooding of early Late Albian age occurs at the base of the Basal Napo Shales in the northern part of the basin, and within its upper part in the South. Other Maximum Floodings of probable Early Albian (Basal Sandstones) and earliest Middle Albian age (Basal Shales) were identified in the southwestern part of the basin (Chinimbimi, fig. 2 and 3). However, additional studies are necessary to correlate them with other sections.

These biostratigraphic data demonstrate that the Aptian-Albian marine transgression resulted in a large-scale backstepping of the facies and thus, in an important diachronism of the lithological units. As an example, the disconformable continental sandstones would be of Late Aptian to Early Albian age in the central-southern part of the basin, of Late Aptian to Middle Albian age in its northern and central parts, and of Late Albian age in its northeastern border of the basin, where they are, therefore, coeval with the "T Sandstones" of the rest of the basin. In this interpretation, the Hollin facies represents the coastal onlap deposits of the "middle" to Late Aptian Maximum Flooding. In the same way, the Basal Napo Shales facies is of earliest Middle Albian age in the Southwest, and of early Late Albian age in most of the basin.

During the Early Cretaceous transgression, the lateral facies succession in the basin comprised (1) continental sandstones deposited by braided streams; (2) glauconitic sandstones and shales of shallow shelf to nearshore environment; (3) fossiliferous limestones of open marine, shallow-shelf environment; and (4) deeper marine, disaerobic black shales (see also White et al. 1995). These lithofacies are strongly diachronous. In the westernmost part of the Andean basin (Lima area, Peru), the transgressive Early Cretaceous sandstones are of probably Early Valanginian age (Rivera et al. 1975, Benavides 1956, Jaillard & Sempéré 1989). As a consequence, the Early Cretaceous transgression displays a diachronism of nearly 30 Ma across the whole Andean Basin. Therefore, chronostratigraphic correlations cannot be established in the transgressive deposits of the Andean basin, without previous careful biostratigraphic studies.

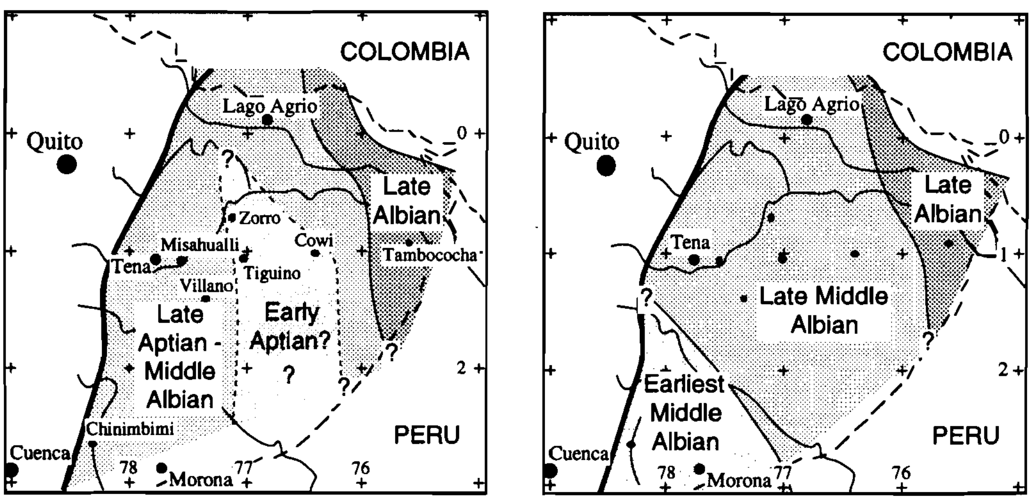


Age of transgressive sandstones    Age of marine shales or limestones

*Fig. 3 : Paleogeography of the Aptian-Albian transgression in the Oriente Basin of Ecuador.*

REFERENCES


Arai, M., Pedrão, E., Viviers, M.C. & Antunes, R.L. 1990. *The biostratigraphy and paleoenvironments of the Tiwae-1 well Oriente basin (Ecuador).* Petrobras, unpubl. report, 20 p., Quito.

Benavides, V. 1956. Cretaceous system in Northern Peru. *Am. Mus. Nat. Hist. Bull.*, 108, 352-494.

Bristow, C.R., & Hoffstetter, R. 1977. *Ecuador.* Lexique Stratigr. Internat., V, 5a2, 410 p., CNRS ed., Paris.

Bulot, L. & Jaillard, E. 1995. Stratigraphic significance of the Albian ammonite fauna from the Oriente of Ecuador. *2nd International Symposium on Cretaceous Stage Boundaries*, Bruxelles, Abstracts, 3 p..

Bulot, L., Robert, E. & Jaillard, E. in press. Population dynamics of the Albian ammonite faunas of Northern Peru and Ecuador. *Palaeogeog, Palaeoclim., Palaeoecol.,*.in press.

Faucher, B., Vernet, R., Bizon, G., Bizon, J.J., Grekoff, N., Lys, M. & Sigal, J. 1971. *Sedimentary Formations in Ecuador. A stratigraphic and micropaleontological survey.* Bureau Études Indust. Coop. Inst. Français Pétrole (BEICIP), 220 p., 3 vol..

Haq, B.U., Hardenbol, J. & Vail, P.R. 1987. Chronology of fluctuating Sea levels since the Triassic. *Science*, 235, 1156-1167.

Jaillard, E. & Sempéré, T. 1989. Cretaceous sequence stratigraphy of Peru and Bolivia. *in*: L.A. Spalletti, ed., *Contribuciones de los Simposios sobre el Cretácico de América latina*, A1-A27, Buenos-Aires.

Jaillard, E., Caron, M., Dhont, A., Ordoñez, M., Andrade, R., Bengtson, P., Bulot, L., Cappetta, H., Dávila, C., Díaz, R., Huacho, J., Huamán, C., Jiménez, D., Jiménez, N., Montenegro, J., Néraudeau, D., Rivadeneira, M., Toro, J., Villagómez, R. & Zambrano, I. 1995. *Síntesis estratigráfica y sedimentológica del Cretáceo y Paleógeno de la cuenca oriental del Ecuador.* Orstom-Petroproducción technical agreement, unpubl. report, 2 vol., Quito.

Kummert, P. & Casal, C. 1986. Granulometría de areniscas cementadas con sílice, aplicación a la determinación de los ambientes de sedimentación de la Formación Hollin del campo Bermejo Sur. *IV Cong. Ecuat. Geol. Min. Petról.*, II, 149-162, Quito.

Lammons, J.M. 1974. *Palynological study of some samples of the Zorro-1 well.* Anglo-Ecuadorian Oilfields Ltd, Zorro-1 well unpubl. report, 1 p., Quito.

Mills, S.J. 1972. *A review of micropaleontological evidence from the Ecuadorian Oriente.* Anglo-Ecuadorian Oilfields Ltd, Ecuad. Oriente geol. note, 26, 21 p., unpubl., Quito.

Ordoñez, M., Jiménez, N., Zambrano, I., Suárez, J. & Ricaurte, J. 1989. *Análisis bioestratigráfico y paleoecológico del pozo Tivacuno-1.* Petroproducción-Guayaquil, unpubl. report, Quito.

Ordoñez, M., Jiménez, D. & Zambrano, I. 1994. *Estudio geológico del pozo Pungarayacu-30.* Petroproducción-Guayaquil, unpubl. report, 4 vol., Quito.

Rivera, R., Petersen, G. & Rivera, M. 1975. Estratigrafía de la Costa de Lima. *Bol. Soc. geol. Perú*, 45, 159-196.

Robertson Research 1988. *The biostratigraphy, palaeoenvironment and petroleum geochemistry of the interval 8330'-10120' in the Conoco Ecuador Ltd, Cowi-1 well, Oriente Basin, Ecuador.* unpubl. report, Quito.

Souza Cruz, C.E. de 1988. Cretaceous sedimentary facies and depositional environments, Oriente Basin, Ecuador. *III Cong. And. Indust. Petrol.*

Stratigraphic Service 1995. *Biostratigraphy of the Villano-3 well from the Oriente of Ecuador.* Arco Oriente, unpubl. report, 35 p. + anexos, Quito.

Tschopp, H.J. 1953. Oil explorations in the Oriente of Ecuador. *Am. Ass. Petrol. Geol. Bull.*, 37, 2303-2347.

Villagómez, R. 1995. *Estudio de la Formación Hollín y la transgresión albiana en la subcuenca Napo del Oriente ecuatoriano.* Tésis Ing. Geol., Esc. Polit. Nac., 96 p. + anexos, unpubl., Quito.

White, H., Skopec, R.A., Rámirez, F., Rodas, J. & Bonilla, G. 1995. Reservoir characterization of the Hollin and Napo Formations, Western Oriente Basin, Ecuador. *in:* A.J. Tankard, R. Suárez & H.J. Welsink, eds., Petroleum basins of South America, *Am. Ass. Petrol. Geol. Memoir*, 62, 573-596.

Zambrano, I., Ordoñez, M. & Jiménez, D. 1993. *Estudio litoestratigráfico y micropaleontológico del pozo Tambococha-1.* Petroproducción-Guayaquil, unpubl. report, 53 p., Quito.

# FAULT REACTIVATION IN THE ESPINAL BLOCK, COLOMBIA

P.J. Wheeler[1], M.P.Coward[1] and R. Gillcrist[2]

1. Department of Geology, Imperial College of Science, Technology and Medicine, Prince Consort Road, London, SW7 2BP
2. Lasmo Oil (Colombia) Ltd,Calle 72, No 8-24, Piso 8, Bogota, Colombia

**KEYWORDS**: Fault reactivation, Inversion

## INTRODUCTION

The Magdalena valley and the Eastern Cordillera represent, to varying intensities, an inverted Mesozoic rift system. The inversion has been achieved by extensional fault reactivation and back rotation. The rift system runs approximately NE-SW, coincident with the Carboniferous Caledonian collisional fabric.

Two stages of fault reactivation are apparent, namely the Permian to Jurassic extensional reactivation of the Caledonian fabric, recorded in the syn-rift deposits, and the Cenozoic compressional reactivation of this extension which is recorded in numerous inversion structures. This is an example of the positive feedback process that often occurs in continental reactivation. The Espinal block provides a clear example of the inversion (Fig.1).

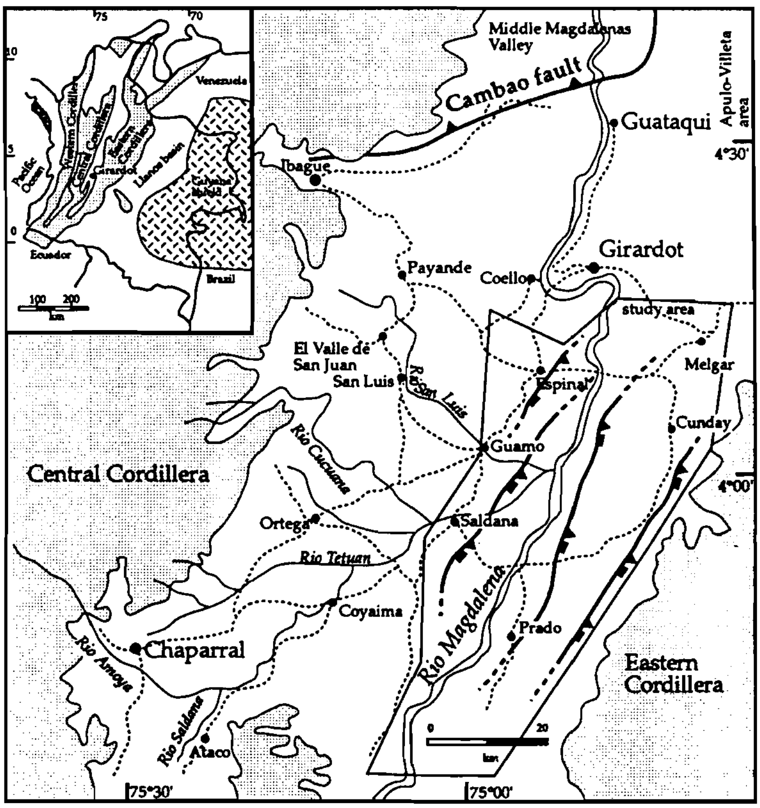


Fig.1 Location of study area showing the trend of the inverted extensional faults. Base map modified from Barrio and Coffield 1992

## CHRONOLOGY OF INVERSION

A late Palaeocene to early Eocene series of thrusts has imbricated the Villeta, Guadalupe and Guadas formations and has then been erosionally truncated. It is postulated that these imbricates represent the tip of a gravitationally driven detachment forming at the base of the thick overpressured shale formation, the Villeta (Fig.2). Deformation at this time was mainly restricted to the Western and Central Cordilleras and is driven by the highly oblique dextral accretion of the Western Cordillera to Colombia. It is thought that a minor uplift of the Eastern Cordillera occurred during this time, for the following reasons. With convergence rates of around 200mm/yr (Daly 1989) and taking a force balance approach (McCaffrey 1992) dextral motions in southern Colombia of approximately 125mm/yr would have to be accommodated there. Due to the curvature of the Colombian margin the obliquity (the angle between the trench normal and convergence direction) rapidly decreases at $4^0$N, the same latitude as the Espinal block; As a result no dextral motion would be expected in Northern Colombia the oblique convergence being accommodated in the subduction zone. This would cause a very high stress gradient around $4^0$N and this may have driven an early, minor uplift of the Eastern Cordillera producing enough of a gravitational potential to cause slip along an overpressured horizon. This stress has also driven the oblique reactivation of the most westerly Jurassic fault that is included in the area of study (Fig.1). This has folded the syn-rift deposits producing a doubly plunging anticline which has been erosionally truncated, with the imbricate slip system, in the Late Palaeocene/Eocene.

The areas central extensional fault is reactivated in the Mid-Eocene producing a prominent inversion anticline, folding of the earlier imbricates and thrusting in the Cretaceous/Palaeocene post-rift and was active until the beginning of the Miocene (Fig.3). Reactivation of this steep primary fault is an effective way of producing vertical motion but not horizontal shortening. This has led to the formation of a footwall propagating shortcut thrust that is kinematically and mechanically more favourable for accommodating large scale horizontal displacement. An imbricate of the shortcut thrust active during the Oligocene has caused the uplift and erosion of growth and pre-growth strata (the Doima, Porterillo and Chicoral formations, the Gualanday group) producing a mid/late Oligocene unconformity. This shows that the fold growth rate was much greater than the sedimentation rate. Deeper footwall shortcuts have propagated along the decollement horizon that exists at the stratigraphic and mechanical boundary of the Villeta shales and the underlying Caballos quartzarenite-conglomerates. This has produced fault propagation folding during the early/mid-Miocene, folding the Cira and Honda formations and refolding the Gualanday group. A dimensionless growth rate (Suppe et al 1990) of 0.56 indicates that sedimentation rates in the fluvial Honda formation were high compared to the rate of fold growth. The absolute growth rate is unknown as stratigraphic horizons have not been accurately dated.

Folding of the Eocene imbricate system has inhibited the easy movement along it so that when the third and most easterly extensional fault is reactivated in the Late Miocene/Pliocene the motion was accommodated by the development of large overthrusting (Fig.4). The displacement on the overthrust would be the sum of the displacement on the inverted extensional fault (A) and the early Eocene slip plane (B). However, minor reactivation of the earlier imbricates has occurred tilting the Miocene strata so the overthrust displacement would in fact underestimate the motion on the extensional fault and slip plane. Reactivation of the extensional fault has folded the slip plane in this region so that it would now act as a buffer to strain propagation hence raising the possibility that overthrusting will occur in the region of this perturbation if another fault reactivated to the east.

## CONCLUSIONS

The Espinal block provides an excellent example of the intimate relationship between the Mesozoic rift system and the subsequent Andean deformation as the extensional faults have been sequentially inverted from west to east. The study area may also indicate a Palaeocene uplift of the Eastern Cordillera that should be looked for elsewhere.

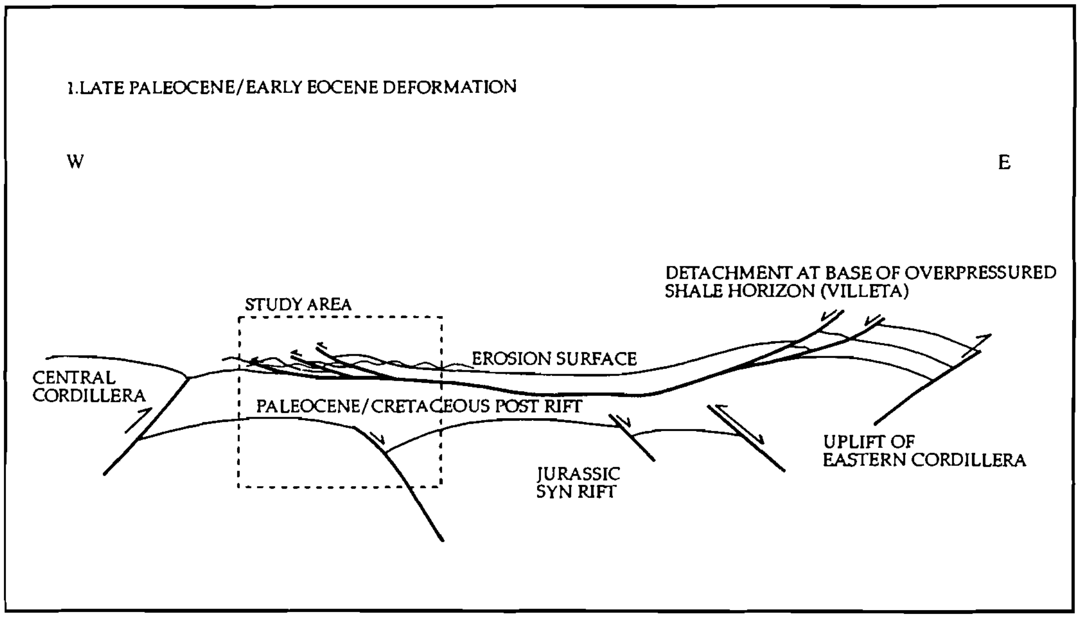


Fig.2 Phase 1- Detachment at base of Villeta driven by Eastern Cordillera uplift

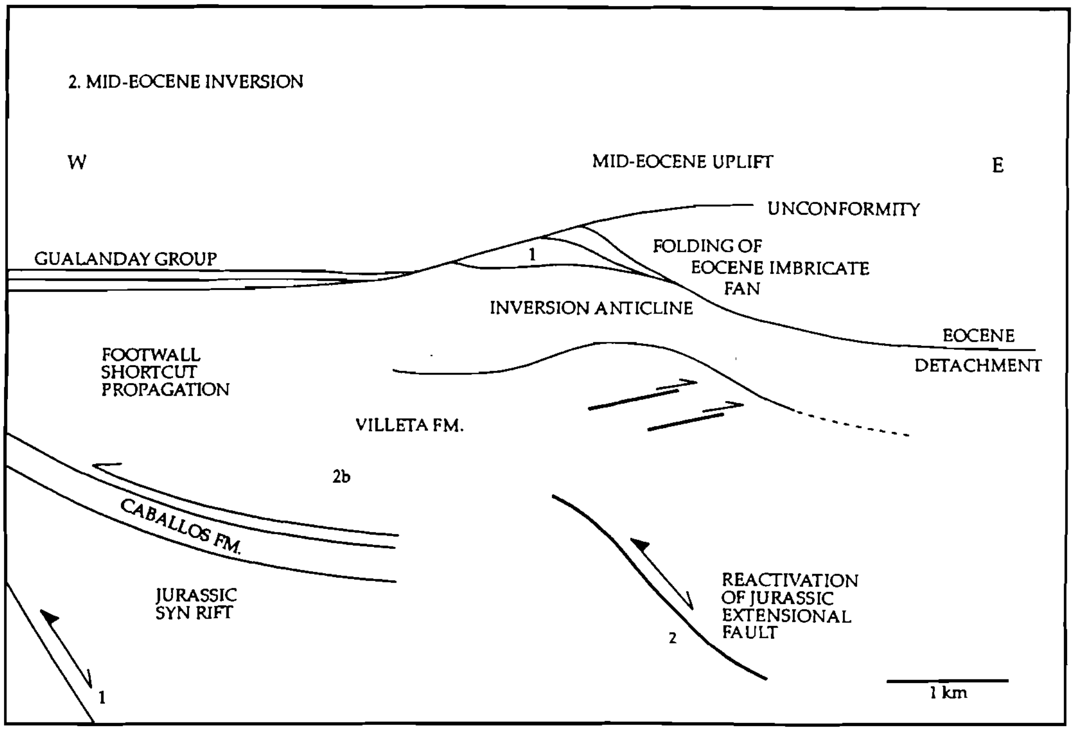


Fig.3 Phase 2- Reactivation of extensional fault
Phase 2b- Propagation of footwall shortcut along tilted Caballos/Villeta boundary. Tilting was driven by Phase 1 reactivation of westerly extensional fault

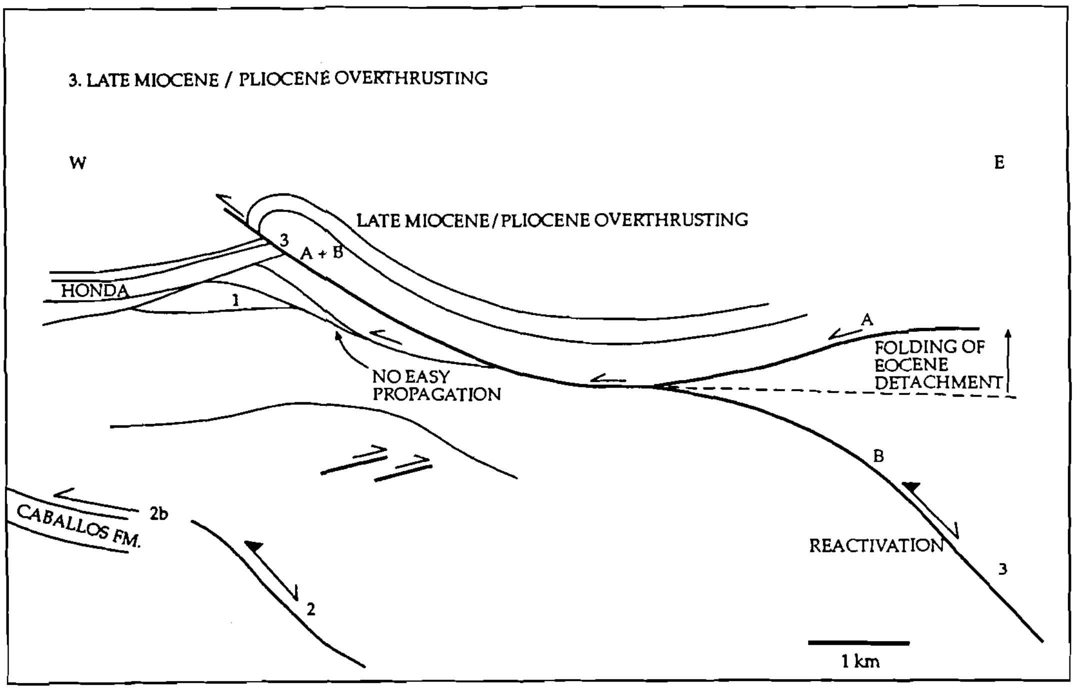


Fig.4 Phase 3-Reactivation of easterly fault drove overthrusting and folded earlier Villeta detachment

## REFERENCES

Barrio C. and Coffield D. 1992 Late Cretaceous stratigraphy of the Upper Magdalena Basin in the Payande-Chaparral segment (western Giradot sub-basin), Colombia. *Journal of South American Earth Sciences* Vol.5, No.2, 123-139

Daly M. Correlations between Nazca/Farallon plate kinematics and forearc basin evolution, Ecuador. *Tectonics* Vol.8 No.4 769-790

McCaffrey R. 1992 Oblique plate convergence, Slip vectors and forearc deformation *Journal of Geophysical Research* Vol.97 No.B6 8905-8915

Suppe J.Chou G. Hook S. 1990 Rates of folding and faulting determined from growth strata *In* McClay K. (ed.) *Thrust Tectonics* Chapman and Hall 105-121

# CENOZOIC EVOLUTION OF THE ANDEAN FORELAND BASIN BETWEEN 15°30' AND 22°00'S

David ZUBIETA ROSSETTI[1], Patrice BABY[2] and Jean Louis MUGNIER[3]

(1) YPFB, Casilla 4875, Santa Cruz, Bolivia.
(2) ORSTOM, Casilla 17-11-6596, Quito, Ecuador.
(3) Inst. Dolomieu, 15 rue Maurice Gignoux, 38031 Grenoble, France.

KEY WORDS: Foreland basin, Cenozoic, deformation, sedimentation, Bolivia.

## INTRODUCTION

The Andes mountain belt began its main uplift during the Cenozoic through several deformational phases (Röeder, 1988; Sempere et al., 1990; Herail et al., 1990; Baby et al. 1992). Along the eastern external border of the orogen developed the Andean foreland basin, hosting thousands of meters of clastic sediments, most of them continental. Foreland basins such as those of the Andes are characterized by an asymmetrical geometry with a greater thickness of sediments deposited closer to the deformational front, and important lateral facies changes within the sequences due to the diminution of depositional energy (Flemings and Jordan, 1989). During the Late Oligocene, Miocene and Pliocene, the Central Andean foreland basin was filled with clastic supply from the west. Tectonic pulses at different time intervals alternate with periods of tectonic quiescence reflected in the changes of depositional style from aluvial fans to fluvial and lacustrine environments.

This work presents the preliminary results of a study of part of the basin occupying the Subandean deformational belt and the Beni and Chaco plains, between 15°30' and 22°00'S. The objective is to identify the distribution and lateral facies changes of the sedimentary sequences that filled the basin from the Late Oligocene to present times, as well as thickness variations and their relation with tectonic events and deformation during the Cenozoic.

## BASIN DEVELOPMENT

As the deformation in the Eastern Cordillera advanced eastwards and the Subandean belt began to develop, the basin received an important clastic supply from the west. It is at the front of the active thrust belt where the bulk transport direction is toward the evolving basin (Allen et al., 1986). Along the proximal margin of the basin, the base of the sequence is represented by the sandstones and conglomerates of the Petaca and Bala Formations of Late Oligocene-Middle Miocene age (Sempere et al., 1990; Marshall and Sempere, 1993). Along the distal edge of the basin, this unit unconformably onlaps sediments of alleged Maastrichtian-Paleocene? age (Zubieta Rossetti and Sandi, 1994). Over these units, a period of relative tectonic quiescence of Middle Miocene age is represented in the distal part of the basin by the fluvial and lacustrine sequence of the Yecua Formation, which includes evidence for marine influence (Marshall and Sempere, 1993). The model for deposition of fine-grained sediment as an indicator of tectonic reactivation in foreland basins (Blair and Bilodeau, 1988) may be applied to this sequence (Yecua-Tariquía and Quendeque Formations), which presents an overall thickening and coarsening trend. The transition to the Tariquía Fm. is marked by fluvial deposits representing relative tectonic quiescence and progradation as a result of the erosion of reliefs. A tectonic reactivation began in the Late Miocene, with

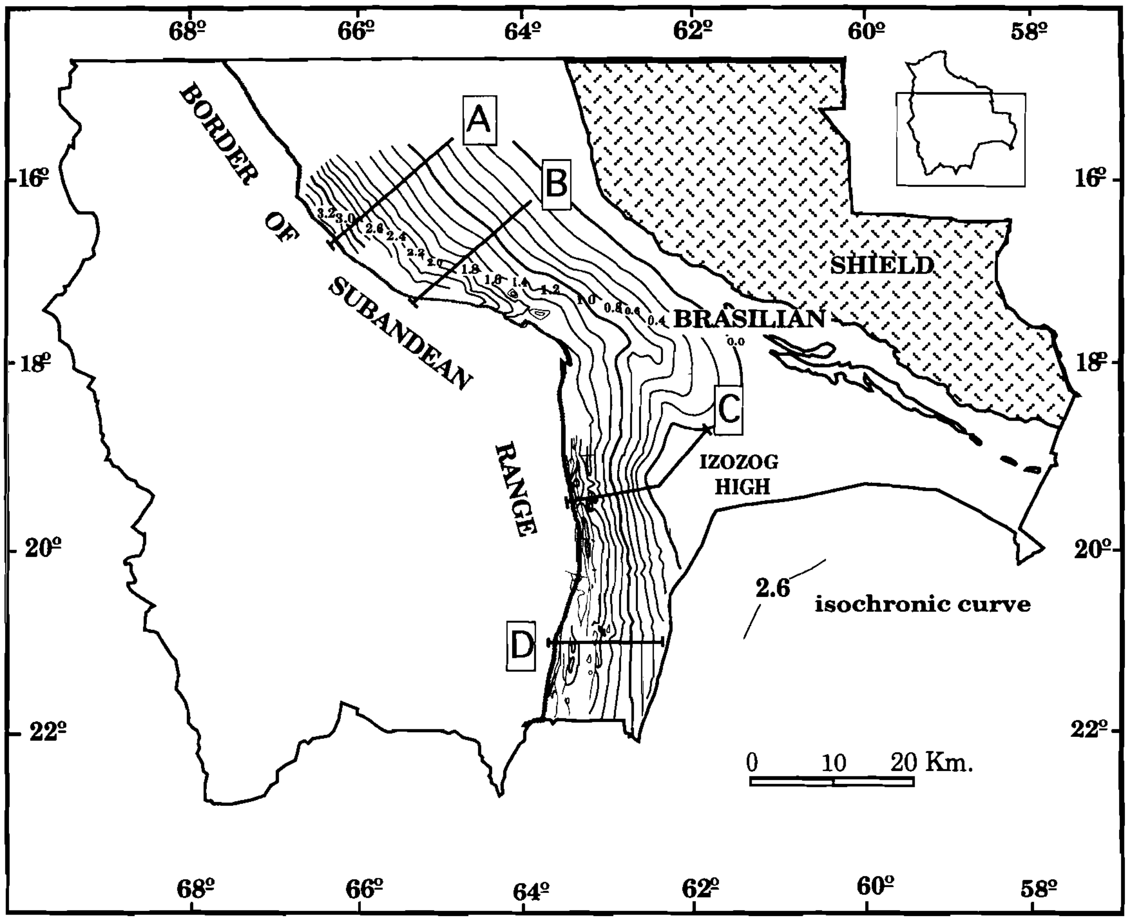


Figure 1: Isochrone map of depth to base of Tertiary in the Bolivian Andean foreland (Chaco and Beni plains). Sections represent seismic lines of Figure 2. Isochrones are in seconds. Western limit is the external border of the Andean deformational front.

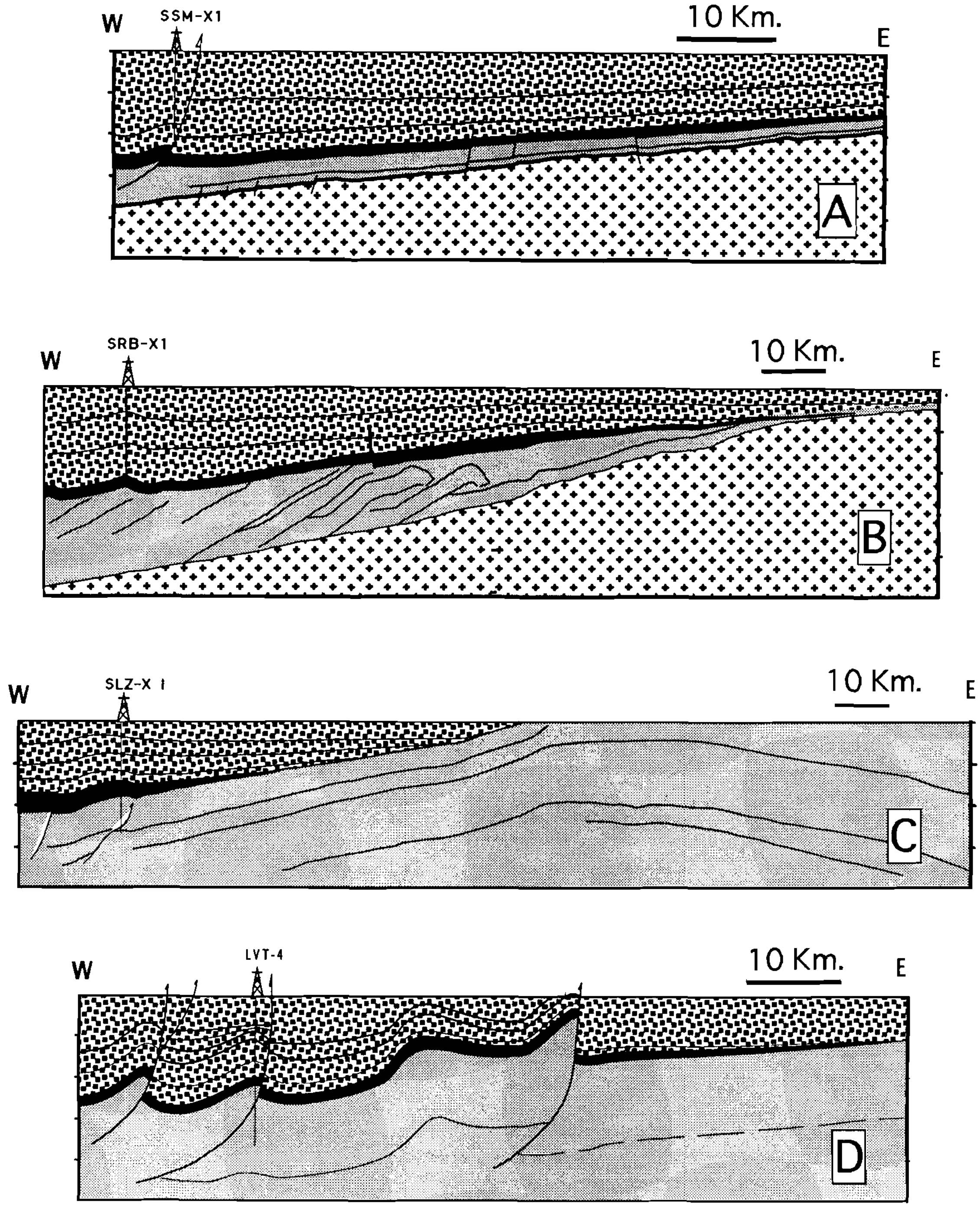


Figure 2: Interpreted seismic sections showing the geometry of the Cenozoic sedimentary fill of the Andean foreland basin, and the structural style of the Andean deformational front at different latitudes. See location in Figure 1. Note the different horizontal scales. Vertical scale is in seconds. Dotted: Cenozoic; black: Mesozoic; gray: Paleozoic; crosses: basement.

renewed coarse-grained sedimentation interpreted as a result of the migration of the deformation front towards the east, and leading to synorogenic deposition of the Guandacay and Charqui Formations. The deposition of the Emborozú and Tutumo Formations in the Pliocene correspond to the last most intense tectonic phase of Andean deformation in the Subandean region.

## CONCLUSIONS

Clastic sediments deposited in the Central Andean foreland basin during the last 27 Ma have a direct genetic relationship with the uplift of the Eastern Cordillera and Subandean ranges. The isochrone map of the base of the Cenozoic (Figure 1) shows the geometry of the sediments accummulated in the basin as they relate with the interactive processes of deformation, erosion, transport and deposition. Seismic sections at different latitudes (Figure 2) show that the structural style is related with the geodynamic evolution of the deformational front, and with the presence of pre-Andean structural elements, such as the Madidi, Chapare and Izozog highs.

## REFERENCES

Allen, P., Homewood, P. and Williams, G., 1986. Foreland basins: an introduction. Spec. Publs. int. Ass. Sediment., 8, 3-12.

Baby, P., Hérail, G., Salinas, R. and Sempere, T., 1992. Geometry and kinematic evolution of passive roof duplexes deduced from cross-section balancing: examples from the foreland thrust system of the southern Bolivian Subandean Zone. Tectonics, vol. 11, no. 3, p. 523-536.

Blair, T.C. and Bilodeau, W.L., 1988. Development of tectonic cyclothems in rift, pull-apart, and foreland basins: Sedimentary response to episodic tectonism. Geology, 16, 517-520.

Flemings, P. and Jordan, T., 1989. A synthetic stratigraphic model of foreland basin development. Journal of Geophysical Research, 94 (B4), 3851-3866.

Hérail, G., Baby, P., Oller, J., López, M., López, O., Salinas, R., Sempere, T., Beccar, G. and Toledo, H., 1990. Structure and kinematic evolution of the Sub-Andean thrust system of Bolivia. First Int. Symp. Andean Geodyn., Grenoble, 179-182.

Marshall, L. and Sempere, T., 1993. The Petaca (Late OLigocene-Middle Miocene) and Yecua (Late Miocene) Formations of the Subandean-Chaco Basin, Bolivia, and their tectonic significance. Docum. Lab. Lyon, 125, 291-301.

Röeder, D., 1988. Andean-age structure of Eastern Cordillera (Province of La Paz, Bolivia). Tectonics, 7 (1), 23-39.

Sempere, T., Herail, G., Oller, J. and Bohnomme, M., 1990. Late Oligocene-Early Miocene major tectonic crisis and related basin in Bolivia. Geology, 18, 946-949.

Zubieta Rossetti, D. and Sandi, R., 1994. Consideraciones estratigráficas del área Boomerang-Chapare. Rev. Téc. YPFB, 15 (3-4), 319-325.

# MAGMATISME, PETROLOGIE
# MAGMATISM, PETROLOGY
# MAGMATISMO, PETROLOGIA

# LOW-GRADE METAMORPHISM OF MESOZOIC AND CENOZOIC VOLCANIC SEQUENCES OF PATAGONIA (43° - 46°S), CHILE

Luis AGUIRRE(1), Joaquín A. CORTES(2), Diego MORATA(3) and Francisco HERVE(1)

(1) Departamento de Geología, Universidad de Chile, Casilla 13518, Correo 21, Santiago de Chile
(2) Servicio Nacional de Geología y Minería (SERNAGEOMIN), Casilla 10465, Santiago de Chile
(3) Departamento de Cristalografía, Mineralogía, Estratigrafía, Geodinámica, Petrología y Geoquímica. Universidad de Cádiz, 11510 Puerto Real, Cádiz, España

**KEY WORDS** : Patagonia, volcanic rocks, low-grade metamorphism, metamorphic facies, P-T conditions

## INTRODUCTION

Results of a petrological reconnaissance of Mesozoic and Cenozoic volcano sedimentary rock sequences of Patagonia (43° - 46°SLat) are reported with the aim to describe and discuss the characteristics of very low and low-grade metamorphic phenomena affecting these rocks.The sequences cover from the middle-late Jurassic to the Neogene and correspond to the Ibáñez Formation (Jurassic) and some coeval units, to the Divisadero Formation (Cretaceous), to the Estratos de Las Juntas (Paleogene?), and to younger lava flows (Neogene) (Fig.1). The Mesozoic extrusive activity is mainly represented by calcoalkaline volcanic arcs composed of andesitic strato volcanoes, dacitic domes and rhyolitic ignimbrites (De La Cruz *et al.* 1994) with minor basalt and basalt andesite flows. The Paleogene rocks represent arc deposits and flood basalts of back-arc or continental intraplate type (Prieto and Cortés, 1995). The Neogene rocks correspond mainly to eroded volcanic centres in the Puyuhuapi area.

## LITHOLOGY

The **Jurassic** rocks comprise: (a) amygdaloidal, porphyritic, andesite and andesitic basaltic flows; (b) porphyritic dacite flows with albitized plagioclase and altered amphibole phenocrysts in a felsitic groundmass; and (c) dacitic ignimbrites with chloritized "fiamme". The **Cretaceous** rocks correspond to: (a) porphyritic, partly amygdaloidal, andesite flows and flow-breccias with plagioclase phenocrysts in an intersertal groundmass of plagioclase and iron oxides ; (b) amygdaloidal olivine basalts with partially albitized phenocrysts of plagioclase and olivine (ghosts) in a fine-grained groundmass of plagioclase microliths, clinopyroxene (augite), and iron oxides. Among the **Tertiary** rocks, those belonging to the Estratos de Las Juntas are represented by: (a) poorly amygdaloidal basaltic andesites with plagioclase and clinopyroxene phenocrysts; (b) porphyritic andesite flows and; (c) lapilli tuffs with abundant diabasic clasts.Those of Neogene age mainly correspond to: (a) porphyritic, highly amygdaloidal olivine basalts with plagioclase and fresh olivine (Fo80-Fo85) phenocrysts in a hyalopilitic groundmass, and (b) fine to medium-grained, amygdaloidal basaltic flows with quench textures.

## METAMORPHISM

All the rocks are strongly altered which is reflected in high $H_2O$ contents (0,3 to 8,0%, mean = 3,8%, $\sigma$= 2,6 for 9 rocks analyzed chemically) and in the presence of a variety of secondary minerals. These appear as replacement of primary minerals, filling amygdales and veinlets, and as patchy alteration of glassy and intergranular groundmass. The secondary associations found in the *c.* 80 sections studied (microscope, EPMA, XRD) are combinations of the 18 phases shown in Fig.2. Associations typical of the zeolite, prehnite-pumpellyite, prehnite-actinolite and greenschist facies are represented and no deformational features are recorded, the metamorphic transformations being purely mineralogical.

The ***Tertiary rocks*** have been mainly metamorphosed in the zeolite facies. Low temperature parageneses including zeolites, smectites, interstrafied smectite/chlorite (S/C), and celadonite are common, notably in the Neogene lavas. Among the zeolites, analcite, natrolite-mesolite and phillipsite are represented. In some amygdale cores, tobermorite, a Ca-Al hydrous silicate, has been found rimmed by phillipsite. Mafic phyllosilicates in these Tertiary rocks are mainly interestrafied S/C with average X% (=chlorite content) between 56 and 89; the highest X% values are found in lavas of the Estratos de Las Juntas with compositions corresponding to pycnochlorite. The temperatures of formation of these phyllosilicates, according to the Cathelineau & Nieva (1985) thermometer, are of *c.* 280°C for the Estratos de Las Juntas and of *c.*150°C for the Neogene basalts. The albitization of plagioclase is strong in flows of the Estratos de Las Juntas whereas in the Neogene basalts the original calcic compositions are preserved or only slightly modified. Aragonite filling amygdales was found in Paleogene basalts located 12 km NW of Balmaceda.

In the ***Cretaceous rocks***, the main metamorphic assemblages include pumpellyite, prehnite, epidote, chlorite, and albite. The almost total absence of zeolites , the scarcity of smectites and the considerable amount of chlorite contrast with the features observed in the Tertiary lavas. Pumpellyites have total iron as $Fe_2O_3$ higher than 10% with $XFe^{3+}$ in the interval 18-33, typical of Fe-pumpellyites in sub-greenschist facies. $Fe^{3+}$ partitioning between pumpellyite, prehnite and epidote in these assemblages takes place with $XFe^{3+}$epi > $XFe^{3+}$pum > $XFe^{3+}$prh. Mafic phyllosilicates (mainly pycnochlorite) with X% between 90 and 100 predominate indicating temperatures of formation of 220° - 330°C. Albitization of the plagioclase phenocrysts is intense in most samples with compositions approaching the albite pole; however, relictic plagioclase is found as patches of $An_{48}$ composition.. Titanite contained in some samples is $Al_2O_3$-rich (4,2-7,3%), a feature diagnostic for subgreenschist facies.

Mineral associations in the ***rocks of Jurassic age*** are those of highest grade. The common presence of secondary actinolite, and of biotite in some associations, indicate temperatures of the greenschist facies. Pumpellyite is practically absent, only recorded as tiny flakes in some narrow epidote-rich veinlets. Amphibole is the most representative secondary phase. In the classification diagram (Leake, 1978) two amphibole groups are apparent in relation with the value of the ratio $Mg/(Mg+Fe^{2+})$ (Fig. 3). The first, richer in Mg, corresponds to locality 1 in the Futaleufú area and the second, richer in Fe, to locality 12 near La Tapera (Fig.1). In both groups, a linear variation exists with compositions displayed from the actinolite to the ferro-tschermakite-hornblende field. Three areas are identified in the Leake(1978) diagram (Fig.3): (a) weakly altered primary ferro-hornblende; (b) partially transformed primary Mg-hornblende, and (c) metamorphic actinolite and actinolite-hornblende. The very low NaM4 contents in the Ca-amphiboles of the Jurassic rocks indicate (Brown,1977) pressures below 2kb for their formation.These values, added to temperatures as high as 340°C obtained with the chlorite thermometer in these same rocks, indicate metamorphic conditions similar to the Californian Sierra Nevada region (see Brown,1977 and references therein) where batholithic intrusions have strongly influenced the regional thermal gradients.

## CONCLUSIONS AND FINAL REMARKS

All the rocks, from Jurassic to Neogene, are affected by non deformative, very low and low-grade metamorphism. The secondary mineral phases and their associations are indicative of the zeolite, prehnite-pumpellyite, prehnite-actinolite and greenschist facies. Differences in metamorphic grade related to the age of the sequences have been established. Thus, zeolite-bearing associations are present in the youngest, Neogene,rocks; pumpellyite coexisting with prehnite and epidote is characteristic in the Cretaceous volcanic rocks, whereas the presence of actinolite, in places related to biotite, has been only recorded in the Jurassic rocks. The temperatures inferred for these metamorphic assemblages go from *c.* 120° to near 350°C with pressures probably not exceeding 2 kb. The metamorphism of the Cretaceous rocks is the most pervasive and probably took place in a fairly thick subsiding pile under a slowly rising thermal gradient in an environment with a high fluid/rock rati (extensive albitization, formation of chlorite *s.s.*, presence of pumpellyite, etc.). The batholithic intrusions with ages around 95 Ma (see Pankhurst and Hervé,1994) exposed close to or immediately adjacent to the Cretaceous outcrops, have not disturbed the low-grade pattern of the Cretaceous rocks, one which stands close to that of hydrothermal burial metamorphism. Recent estimations of the age of the Divisadero Formation indicate a minimum age of 102 Ma (Belmar, 1996). In central Chile, dating of the low-grade metamorphic phenomena that affected lower Cretaceous rocks has shown that these phenomena occurred about 15 Ma after deposition of the sequence (Aberg *et al.* 1984). If a similar interval could be envisaged for the Aysén region, the metamorphism of the Divisadero Formation could be as young as 87 Ma, that is subsequent to the main batholithic intrusions in the region. This would explain the preservation of the low-grade metamorphic pattern observed. Contrasting with the previous case, the greenschist metamorphism of the Jurassic rocks bears the imprint of a rapidly imposed thermal regime with a low fluid/rock ratio and selective fluid circulation. These characteristics resulted in metastable equilibrium of some primary minerals and patchy growth of secondary phases, *e.g.* partial albitization of plagioclase, partial transformation of primary amphibole into actinolite, persistence of S/C phyllosilicates, sporadic biotite formation. The thermal influence of the Cretaceous batholithic intrusions on the Jurassic sequence is thus quite apparent and could be partly explained by the screen position of the main belts of these rocks in the region (Fig.1). It is possible, however, that this batholith-related thermal metamorphism overprinted a pre-existent burial pattern as suggested by the rare presence of pumpellyite in two of the Jurassic rocks studied.

A tentative sequence of events in the region would be: (1) deposition of the Jurassic units followed by a burial metamorphic episode; (2) deposition of the Divisadero Formation (from the Hauterivian to *c.* 102Ma according to Belmar, 1996); (3) batholithic intrusion at *c.* 95 Ma overprinting and obliterating the Jurassic low-grade pattern ; (4) burial hydrothermal metamorphic phenomena affecting the Divisadero Formation (*c.* 87 Ma?); (5) deposition and metamorphism of the Estratos de Las Juntas and metamorphism, mainly hydrothermal, of the Neogene volcanic rocks.

## AKNOWLEDGEMENTS

This research has been funded by FONDECYT Projects 92 0914 and 1950544, by the CNRS-CONICYT agreement and by the CE Project CT1I (00.33) all of which are duly thanked.

## REFERENCES

Aberg ,G., Aguirre , L.,Levi , B. and Nyström , J.O., 1984. Spreading-subsidence and generation of ensialic marginal basins: an example from the early Cretaceous of central Chile. In: Marginal Basin Geology (eds. Kokelaar, B.P. & Howells, M.F.). *Geol. Soc. London, Sp. Pub.*, 16, 185-193. Blackwell Sc. Pub., Oxford.

Belmar , M. 1996. Geología de los cuadrángulos Balmaceda y C° Farellón Norte, Región de Aysén. *Taller de Título II (unpublished)*, Departamento de Geología, Universidad de Chile, 83p.

Brown , E.H., 1977. The crossite content of Ca-amphibole as a guide to pressure of metamorphism. *J. Petrol.*, 18, 53-72.

Cathelineau, M. and Nieva, D., 1985. A chlorite solid solution geothermometer. The Los Azufres geothermal system (Mexico). *Contrib. Min. Petrol.*, 91, 235 - 244.

De La Cruz, R., Suárez, M. and Demant, A., 1994. Facies volcánicas del Mesozoico de Aisén (sector noreste), 44° - 47° lat.S.,Chile (Formaciones Ibáñez y Divisadero).*7° Cong. Geol. Chileno,* Concepción, Actas, v.1, 27-3.

Leake, B.E., 1978. Nomenclature of amphiboles. *Can. Mineral.*, 16, 501- 520.

Pankhurst, R.J. and Hervé, F., 1994. Granitoid age distribution and emplacement control in the North Patagonian batholith in Aysén (44°-47°S). *7° Cong. Geol. Chileno*, Concepción. Actas, v.1, 1409-1413.

Prieto, X. and Cortés, J.A., 1995. Geología del sector oriental de la Hoja Río Cisnes (71° a 72°20' LW y 44° a 45° LS,), Región de Aysén. Informe de Avance (unpublished). Convenio Gobierno Regional XI Región-SERNAGEOMIN. Proyecto Aysén NE. 50p.

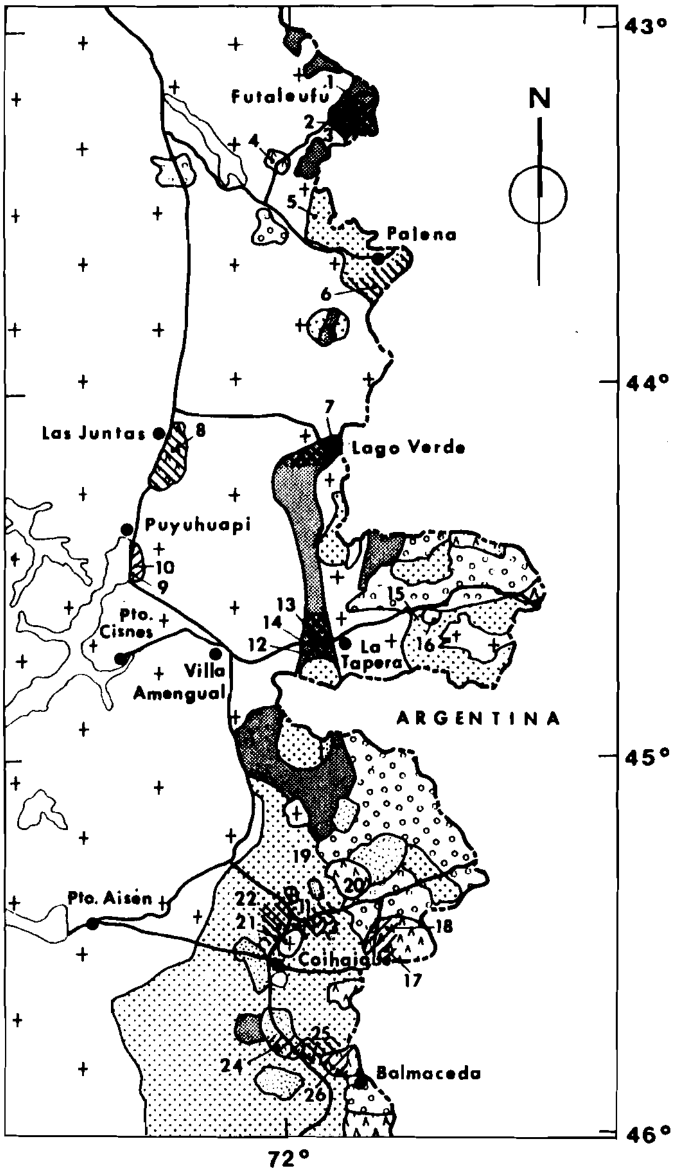


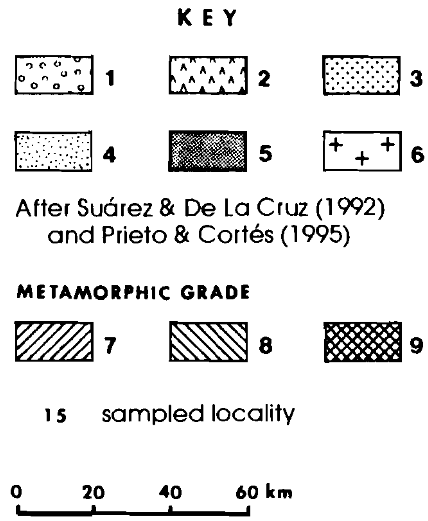


**Figure 1.** Geology of the Patagonian region (43º-46ºS) showing distribution of metamorphic facies and localities sampled.

1.- Quaternary sediments, 2.-Tertiary sedimentary rocks and basalts; 3.- Upper Cretaceous rhyolitic and dacitic tuffs, andesitic lava flows; 4.- Lower Cretaceous marine sedimentary rocks; 5.- Jurassic rhyolitic and dacitic tuffs, andesitic lava flows; 6.-Patagonian Batholith: granitoids and metamorphic rocks; 7.- Zeolite facies; 8,- Prehnite-pumpellyite facies; 9.- Greenschist facies.

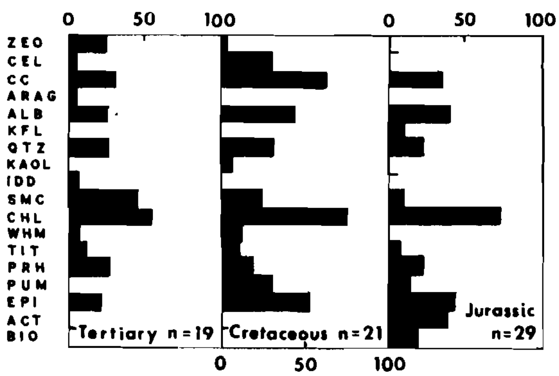


**Figure 2.**-Frequency of metamorphic minerals in the Mesozoic and Cenozoic volcanic rocks of Patagonia (43º-46ºS)

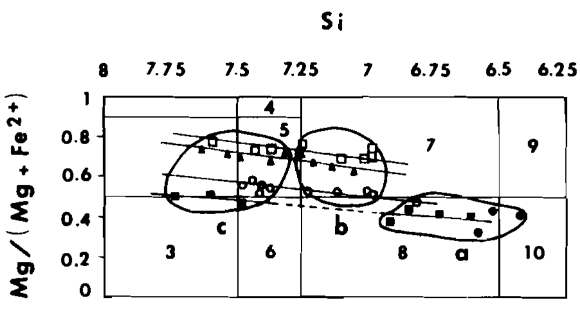


**Figure 3.**-Composition of amphiboles in rocks of Patagonia (43º-46ºS). Classification and fields according to Leake, 1978.

# Na-RICH IGNEOUS ROCKS AND CRUSTAL THICKENING IN THE ANDES

Michael P. Atherton[(1)], Nick Petford[(2)]

(1) Department of Earth Sciences, University of Liverpool, The Jane Herdman Laboratories, Brownlow Street, Liverpool, L69 3BX.
(2) School of Geological Sciences, Kingston University, Penrhyn Road, Kingston-upon-Thames, Surrey, KT1 2EE.

**KEY WORDS:** Na-rich rocks, Crust, Archaean TTG.

Na-rich plutonic and volcanic rocks are not uncommon in the Andes. They vary in age from Lower Palaeozoic to Tertiary. The Na-rich volcanic rocks described so far include those in North Chile of Quaternary age (Feeley & Hacker, 1995), which overlie the thickest part of the crustal keel (>70km, Fig. 1). Compositionally similar rocks are also present in the Miocene/Quaternary volcanoes of Tupungato and Marmolejo, east of Santiago again over thick crust. Plutonic rocks with similar chemistry can be divided into two groups. The first, those in a similar setting to the volcanic rocks form Tertiary plutons (Eocene, Miocene and possibly Pliocene) which also lie along the spine of the Andes, where crustal thickness ≥50km (Fig.1). They include the Cordillera Blanca, Peru, El Abra, N. Chile and a series of small Tertiary plutons in Chile near the Chile/Argentina border which extend southwards to the latitude of Santiago at least.

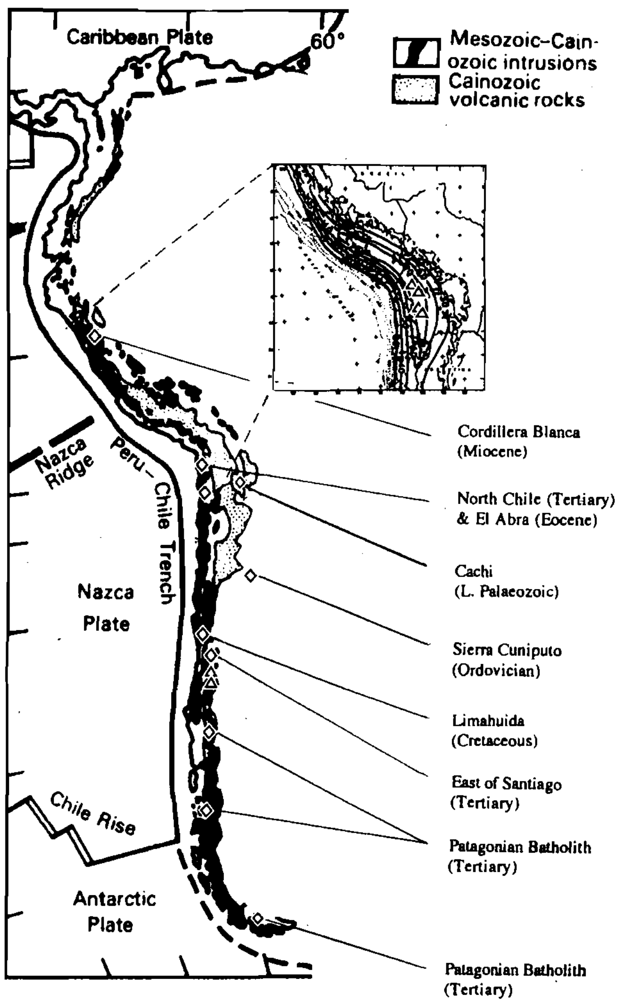


Fig. 1. Map of the Andes showing locations of Na-rich plutons (diamonds) and Quaternary volcanic rocks (triangles) in north Chile (inset) and east of Santiago.

The second group, with poorly understood geotectonic settings are of Ordovician to Tertiary age eg, Tertiary plutons in the Patagonian Batholith and Lower Palaeozoic plutons such as Cachi in Argentina Fig.1. This group intrudes crust where structure and history is unclear.

Rocks from these plutons and volcanoes have high $(La/Yb)_N$, Sr/Y ratios, high $Na_2O$ contents and low Y and Yb values, compared to the more voluminous Cordilleran Batholithic plutons such as the Coastal Batholith, Peru (Fig.2 and Atherton & Petford, 1993).

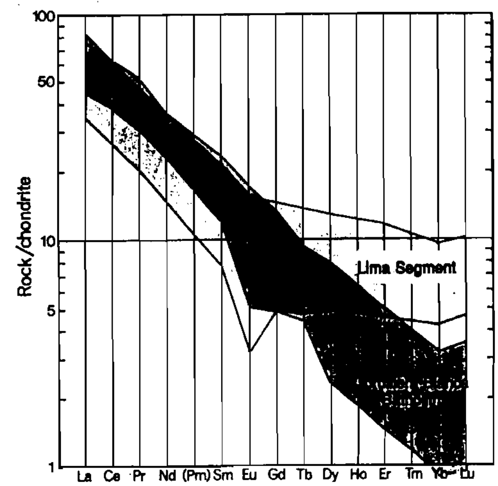


Fig. 2

Consideration of the Miocene Cordillera Blanca Batholith in north central Peru, for which we have considerable data and a good understanding of the crustal structure below the Batholith, indicates that together with the characteristics outlined above there is also a marked decrease in FeO, MgO, $TiO_2$ and CaO in the granites, compared to the more basic rocks. Furthermore the values are lower than rocks with similar $SiO_2$ contents (70-75%) from the Coastal Batholith (Fig.3), which were derived by shallow partial melting or high level fractional crystallization (Atherton, 1990). The 'dramatic' decrease in these elements and increase in $SiO_2$ in partial melts when garnet was stabilised at 12-18 kb was first described by Rushmer (1993) in experiments on melting hydrated basalt. Chemical modelling of the Cordillera Blanca rocks is compatible with this, with melts leaving residues of pyroxene + garnet ± hornblende ± plagioclase (Petford & Atherton, in press). Such residues are present in the experiments and are typically found in mafic lower crustal xenoliths (Rushmer, 1993).

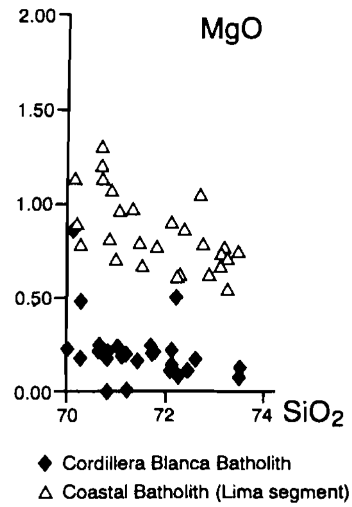


Fig. 3

Rocks similar in many respects to those described here ie, high $(La/Yb)_N$, Sr/Y ratios, high $Na_2O$ contents and low Y, Yb values have been considered to characterise Archaean high grade gneiss terrains eg. TTG (Tonalite Trondhjemite Granodiorite) suites (Fig.4). A common interpretation of the data and thermal considerations suggest that they were melts of hydrated subducted ocean crust (see Atherton & Petford, 1993 for brief review). Indeed such a genesis is attractive considering the importance and longlife of subduction along the Andean margin. However it is clear the rocks of the Cordillera Blanca Batholith formed by melting of *thickened* crust as the slab is too old, cold and dehydrated to melt (Atherton & Petford, 1993). As the age of the batholith rocks youngs systematically with increasing acidity over the period 13-5 Ma the marked decrease in the major elements described above marks the incoming of garnet as a major component in the source mineralogy. This relates to the well documented Miocene thickening of the crust below the batholith.

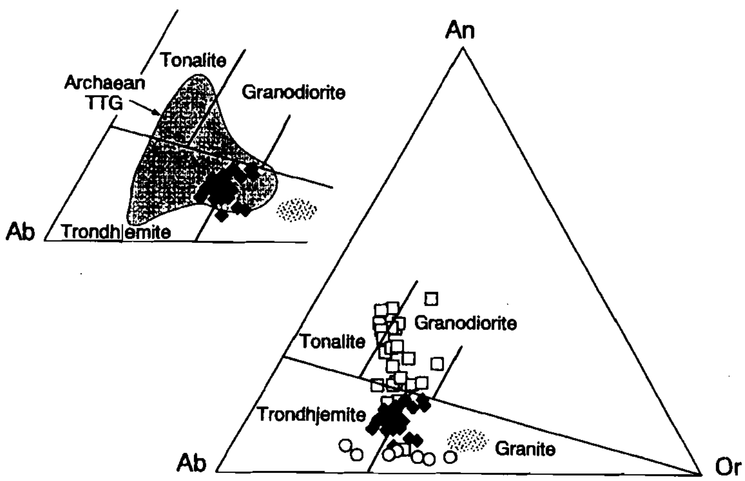


Fig. 4 An - Ab - Or diagram showing Cordillera Blanca tonalities + granodiorites (squares), leucogranodiorites (black diamonds) and pegmatites (circles), with the Coastal Batholith granite field (dotted) shown for comparison. In set shows Archaean TTG field with Cordillera Blanca leucogranodiorites.

The *thickened* crust melting model may, we think, be extended to the rest of the Na-rich rocks above the Andean keel (Group 1) reflecting the thickening of the Andean crust during the Tertiary. It may also relate to the second group of plutons, where information on crustal thickness is absent or where, in the case of the older plutons, it may have changed due to delamination or lower crustal erosion.

If this is the case, the intrusion/extrusion of these Na-rich rocks in the Andes marks periods of major crustal thickening and their absence periods of quiescence.

Finally, the presence in the Andes, of Na-rich rocks with a chemistry similar to Archaean, apparently slab derived melts, but here formed by lower crustal melting of hydrated basalt, suggests the origin of Archaean TTG rocks is still problematic.

**REFERENCES**

Atherton M.P. 1990. The Coastal Batholith of Peru: the product of rapid recycling of new crust formed within rifted continental margin. *Geological Journal*, 25, 337-349

Atherton M.P. & Petford N. 1993. Generation of sodium-rich magmas from newly underplated basaltic crust. *Nature*, 362, 144-146.

Feeley T.C. & Hacker M.D. 1995. Intracrustal derivation of Na-rich andesitic and dacitic magmas: an example from Volcán Ollagüe, Andean Central Volcanic Zone. *Journal Geology*, 103, 213-225.

James, D.E. 1971. Andean crustal and upper mantle structure. *Journal of Geophysical Research*, 76, 3246-3271.

Rushmer T. 1993. Experimental high pressure granulites: some applications to natural mafic xenolith suites and Archaean granulite terranes. *Geology*, 21, 411-414.

Thorpe, R.S., Francis, P.W. & Harmon, R.S. 1981. Andesites in crustal evolution. *Philosophical Transactions of the Royal Society*, 301, 305-320.

Acknowledgements. Figure one was adapted from James (1971) and Thorpe et al. (1981).

# PETROGENESIS OF THE ECUADORIAN MAGMATIC ARC, A GEOCHEMICAL TRAVERSE ACROSS THE NORTHERN ANDES: PETROLOGY, GEOCHEMISTRY AND ISOTOPIC OBSERVATIONS

**R Barragan Talentti**[1], D. J. Geist[2]

[1] Oryx Ecuador Energy Company, P.O.Box 17-11-6545, Quito, Ecuador
[2] Geology Dept., University of Idaho, Moscow, ID 83844, USA

**KEY WORDS:** slab, incompatible elements, LIL/HFSratios, crustal assimilation

## INTRODUCTION

The Andes in Ecuador contains one of the most complete records of igneous activity available for the western margin of South America. They display a strong geochemical and petrological zoning from west to east and provide a good opportunity to test the nature and the effects of subduction, crustal thickness and upper-plate structure on the genesis and evolution of magmatic arcs.

The Ecuadorian Andes lie in two parallel north-striking belts. Besides, several isolated volcanoes lie behind the arc in the subandean zone. There are some fundamental differences in the tectonic setting of the volcanic belts of Ecuador eastward from the trench that could influence cross-strike differences in the magmas from these volcanoes: The Benioff zone drops from about 100Km to 200 Km (?). Successively older and chemically different basement exists. The western (trenchward) belt lies on Cretaceous to Tertiary terranes of oceanic affinity. The eastern volcanic chain lies on strongly metamorphosed Mesozoic. The back-arc volcanoes lie on a thick Phanerozoic sedimentary sequence that overlies the Amazon craton and are not associated with any extensional structures. The crust thickens from 40 to 60 Km between the Western and Eastern Cordilleras, then thins back to 30 Km (Feininger et al., 1983). Besides these complications, the volcanoes from Ecuador lie above the subducting Carnegie ridge.

A study of the entire volcanic chain would obviously be an overwhelming task. Therefore, a few well-suited volcanoes have been selected for detailed study because they are aligned perpendicular to the trench, are representative of their geologic setting and each has had Holocene activity. These volcanoes from west to east are Atacazo from the Western Cordillera, Antisana from the Real or Eastern Cordillera and Sumaco from the back arc basin (Fig. 1). Because this transect is parallel to the convergence of the Nazca and South American plates, variables that are associated with different features of the subducted slab should be eliminated. Instead, this study is focused on the effects of magmatism respect to depth of the subducted slab and the effects of magma production and evolution in different crustal settings.

## GEOCHEMICAL CHARACTER

As is typical of most arcs, lavas from the Ecuadorian volcanoes are progressively richer in potassium away from the trench, ranging from medium-K andesites and dacites at Atacazo to high-K andesites and dacites at Antisana to tephriphonolites at Sumaco (Fig. 2).

The absolute concentrations of most of the incompatible trace elements increase inland (Table. 1), so that Sumaco volcano is the richest and Atacazo the poorest in these elements, despite the fact that the lavas are, on average progressively less siliceous. All three volcanoes are characterized by anomalously low concentrations of HFS elements relative to LIL elements, although the size of the anomaly decrease inland from the trench (Fig. 3). The depletion of HFS vs LIL elements is a nearly obiquitous feature of subduction-related lavas and is thought to be inherited from fluids derived from the subducted lithosphere (Hickey et al., 1986). These characteristics are also well displayed on the diagram of LIL/HFS vs. LIL (i.e., Ba/Nb vs. Ba) (Fig. 4). Although the Sumaco lavas are most strongly enriched in all incompatible elements, they have the lowest LIL/HFS ratios (Table. 1), suggesting less slab contribution. In contrast, Antisana and Atacazo volcanoes have progresively lower incompatible element concentrations but higher LIL/HFS ratios, suggesting relatively more slab contributions

Sr isotope ratios range from 0.7042 to 0.7043 at Atacazo, 0.7045 to 0.7047 at Antisana, and 0.7042 to 0.7043 at Sumaco. The slightly higher $Sr_{87}/Sr_{86}$ of Antisana magmas is best explained by assimilation, because of the very thick crust there. Presumably, the cratonic crust beneath Sumaco has the most radiogenic Sr, but the lavas there do not show evidence of extensive assimilation, which is also apparent in the low silica contents of those lavas.

TABLE. 1

Sinthesis of major, trace element abundances and Sr isotopic ratios for volcanoes in study

| | ATACAZO Occidental Cord. | ANTISANA Eastern Cordillera | SUMACO Oriente Basin |
|---|---|---|---|
| | (%) | (%) | (%) |
| SiO2 | 57.65-66.4 | 55.64-64.15 | 43.24-54.22 |
| K2O | 0.87-1.26 | 1.55-3.14 | 3.96-4.43 |
| Na2O | 3.68-4.61 | 3.72-4.65 | 6.33-6.93 |
| | (ppm) | (ppm) | (ppm) |
| Zr | 88-129 | 145-189 | 396-406 |
| Ba | 353-600 | 611-764 | 2390-2640 |
| Rb | 17-28 | 38-122 | 96-125 |
| Sr | 335-430 | 580-885 | 2542-2624 |
| Y | 6-16 | 12-19 | 34-49 |
| Nb | 1-4 | 7-12 | 53-82 |
| La | 4.63-10.8 | 8-21 | 27-31 |
| Ce | 12-18 | 38-68 | 183-285 |
| Th | 1.07-1.55 | 6-17 | 28-30 |
| U | 0.5-0.7 | 1.5-6.4 | 7.3-10.7 |
| Nd | 3.65-11.2 | 22.9-55.9 | 86.3-121 |
| Sm | 1.4-2.8 | | 13.7-18.5 |
| Eu | 0.72-0.83 | 1.06-2.41 | 3.65-5.03 |
| Tb | 0.21-0.44 | 0.4-0.78 | 1.07-1.59 |
| Yb | 0.48-1.5 | 1.03-1.97 | 3.38-4.67 |
| Lu | 0.06-0.22 | 0.17-0.28 | 0.5-0.63 |
| Hf | 2.25-2.85 | 3.16-6.05 | 5.65-6.91 |
| Ta | 0.19-0.25 | 0.42-0.94 | 2.60-3.54 |
| Ba/Nb | 114-223 | 76-125 | 31-53 |
| La/Sm | 3.3-4.3 | 1.83-2.08 | 1.67-1.97 |
| Ba/Sm | 214.3-230.7 | 139.8-150.7 | 152-187 |
| $Sr_{87}/Sr_{86}$ | 0.7042-0.7043 | 0.7045-0.7047 | 0.7042-0.7043 |

## CONCLUSIONS

On the basis of the major, trace element evidence and Sr isotope ratios, there are some possible explanations for the systematic compositional trends in the Andes of Ecuador:

- The volcanoes are supplied by similar parental magmas, which undergo different amounts of crustal interaction. Specifically, Sumaco's alkaline magmas may have assimilated more alkali-rich crustal material than the trenchward volcanoes. However, the thickest crust underlies Antisana volcano (60 km). Also, most of the exposed basement in the North Andes zone is siliceous, and Sumaco lavas are notably silica poor, suggesting that this hypothesis is invalid.

- The volcanoes are supplied by similar parental magmas, but they assimilate different kinds of crust. Namely, the terranes underlying the volcanoes are older and have stronger continental affinity away from the trench and younger and of oceanic affinity towards the coast. However, the obvious lack of siliceous contaminants in Sumaco's lavas and the isotopic data suggests this model is not correct either.

- The parental magmas for each volcano come from fundamentally different sources. The magmas of Atacazo and Antisana have both been strongly effected by assimilation in the lower crust, Atacazo less because of the thinner crust and its oceanic affinity. Sumaco is mostly unrelated to the other volcanoes and results from melting of recently enriched alkalis continental lithosphere. This may be related to the depth of the Benioff zone and therefore different pressure conditions in the melting region beneath each volcano. Alternatively, there may be an ancient enriched lithospheric component. In this case.

-Crustal assimilation, although detectable with Sr isotopes, does not strongly alter the major and trace elements in the magmas. Therefore, fundamental differences in the melting regime in the source cause different extents of partial melting. Atacazo magmas (low ITE, high LIL/HFS) result from large input of the slab component and large extent of melting. Sumaco magmas (high ITE contents, low LIL/HFS) result from a small slab contribution and small degree of melting. We presently prefer the latest model, because the Sr isotopes do not correlate with any other geochemical parameters.

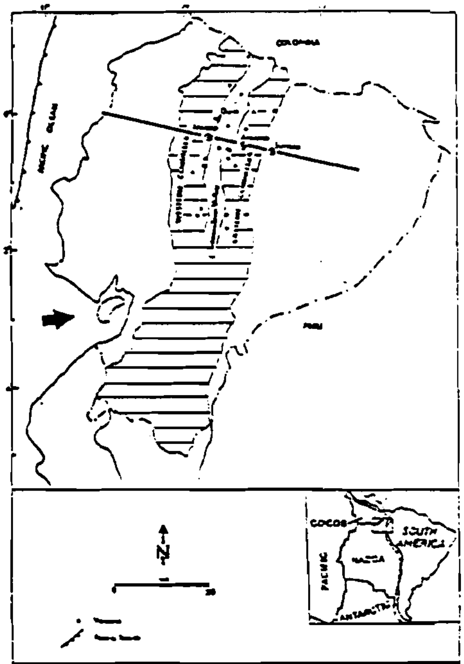


Figure 1. Location of the study area. A petrologic transect of the Ecuadorian Andes

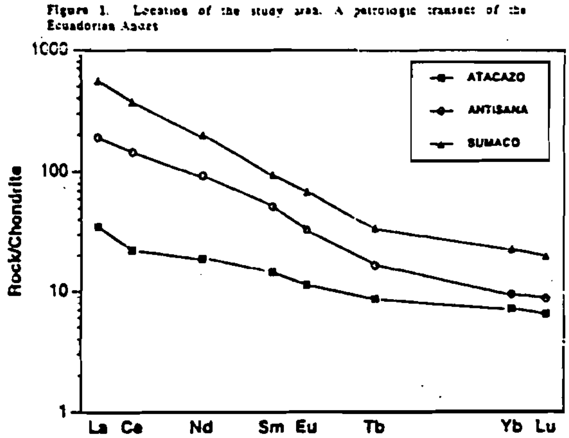


Figure 3 Normalized rare-earth elements of average lavas from Atacazo, Antisana and Sumaco with respect to chondrite values.

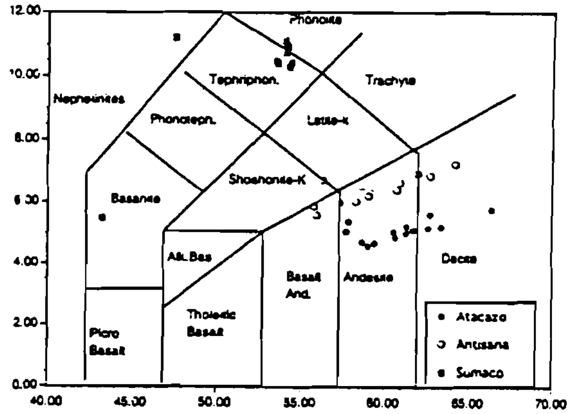


Figure 2 Silica versus total alkalis for lavas from the three volcanic centers. Compositional fields of cal-alkaline and alkaline rocks were taken from Le Maitre (1984), in Wilson (1989)

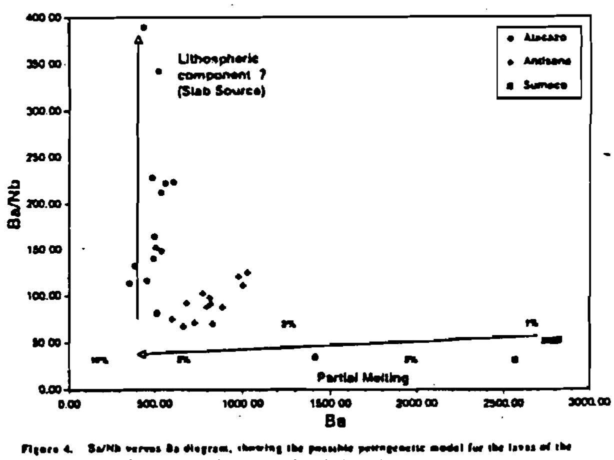


Figure 4. Ba/Nb versus Ba diagram, showing the possible petrogenetic model for the lavas of the Ecuadorian Andes. 1 to 10% partial melting are hypothetical values

REFERENCE

Barragán, R., and Geist,D., 1993. A petrologic transect of the Ecuadorian Andes, Eos, **Transactions, AGU**, p. 637.
Feininger, T. and Seguin, M.K., 1983. Simple Bouguer gravity anomaly field and the inferred crustal structure of continental Ecuador. **Geology**, 11, 40-44.
Hawkesworth, C. J., Gallagher, K., Hergt, J., and McDermott, F., 1993. Mantle and slab contributuions in arc magmas. **Annu. Rev. Earth Planet. Sci.**, 21: 175-204.
Hickey, R., Frey, F., Gerlach, D., and Lopez-Escobar, l., 1986. Multiple sources for basaltic arc rocks from the southern volcanic zone of the Andes (34°-41°S): trace element and isotopic evidence for contributions from subducted oceanic crust, mantle and continental crust. **Journal of Geoph. Reser.**, 91, p.5963-5982
O'Brien, H., Irving, A., and McCallum, I. S., 1991. Eocene potassic magmatism in the Highwood Mountains, Montana: Petrology, geochemistry and tectonic implications. **Journal. Geophys. Res.** 96, No B8: 13237-13260.
Wörner, G., Moorbath, S., and Harmon, R., 1992. Andean cenozoic volcanic centers reflect basement isotopic domains. **Geology**, 20,:1103-1106.

# CHEMICAL CLASSIFICATION OF GABBROIC-DIORITIC ROCKS, BASED ON $TiO_2$, $SiO_2$, $FeO_{tot.}$, MgO, $K_2O$, Y AND Zr

Ludwig BIERMANNS

Universität Tübingen, Institut und Museum für Geologie und Paläontologie, Sigwartstraße 10, D - 72076 Tübingen, EU.

**KEY WORDS:** Gabbros; geochemistry; genesis; tectonic setting; major elements; trace elements.

## INTRODUCTION

As chemical classifications of gabbroic-dioritic rocks from the Andes (e.g. Argentine, Chile, Peru) also contribute to the genesis of this mountain range, the topics of this paper is the presentation of geochemical diagrams, based on $TiO_2$, $SiO_2$, $FeO_{tot.}$, MgO, $K_2O$, Y and Zr of this rock group, which allow the classification of the geotectonic positions from recent ages to Precambrium.

The presented diagrams are based on 60 references with 287 critically selected data sets where data with secondary alterations of all kind, or data interpretations which permit two or more different possibilities were strictly omitted.

The same geotectonic position of gabbroic-dioritic rocks as of their volcanic or subvolcanic varieties (basaltic-dioritic rocks) is often revealed by *different* quantities of major and trace elements. Some examples shall explain this. The $TiO_2$ content of basaltic-andesitic rocks hardly exceeds 3.2 wt.% (Miyashiro & Shido, 1975; Ikeda & Yuasa, 1989). Among gabbroic-dioritic rocks, however, $TiO_2 > 3.2$ wt.% is of no scarcity. On the contrary, $TiO_2$ quantities of 2 to > 5 wt.% are characteristic of ocean-island cumulate *gabbros* (fig. 1). Island-arc basalts (IAB), according to Pearce (1983), are characterized by Zr = 13 to 280 ppm. Typical of island-arc *gabbros* (fig. 2), however, is the quantity of this trace element which ranges between 2.5 and 80 ppm only. Among n-type mid-ocean ridge basalts (n-type MORB), Zr amounts to 30 - 150 ppm (Shervais & Hanan, 1989); n-type mid-ocean ridge *gabbros*, in their turn, reveal a range of Zr from 15 to 200 ppm. Mid-ocean ridge basalts (MORB) contain Y of 15 - 60 ppm (Pearce et. al., 1984). Unfortunately, the term "MORB" is not classified more detailed. The n-type mid-ocean ridge *gabbros*, however, which reach a Y quantity of 5 - 30 ppm, are a remarkable example for gabbroic-dioritic rocks to be investigated by means of geotectonic classification diagrams which are defined specially for this rock group.

## CONCLUSIONS

The following classification diagrams can be used for all the diorites and gabbroic rocks which are defined by Streckeisen (1978). The $SiO_2$ contents of the gabbroic-dioritic rocks which are investigated by the user are less than 62 wt.% (Gulson, 1972) and higher than 36 wt.%. For the explanation of the following diagrams, instead of "gabbroic-dioritic rocks", only the term "gabbros" is given.

In the field "ocean-floor gabbros" of the $TiO_2$ - $SiO_2$ diagram (fig. 1), the data are characteristic of MgO > 10 wt.% (in extreme cases, MgO > 30 wt.%) and of CaO < 9 wt.%. $Na_2O + K_2O$ often do not amount to more than 1.0 wt.% of the whole rock composition. Cr shows a quantity between 400 and 1000 ppm. These data show that predominantly primitive gabbroic rocks are to be found in this field

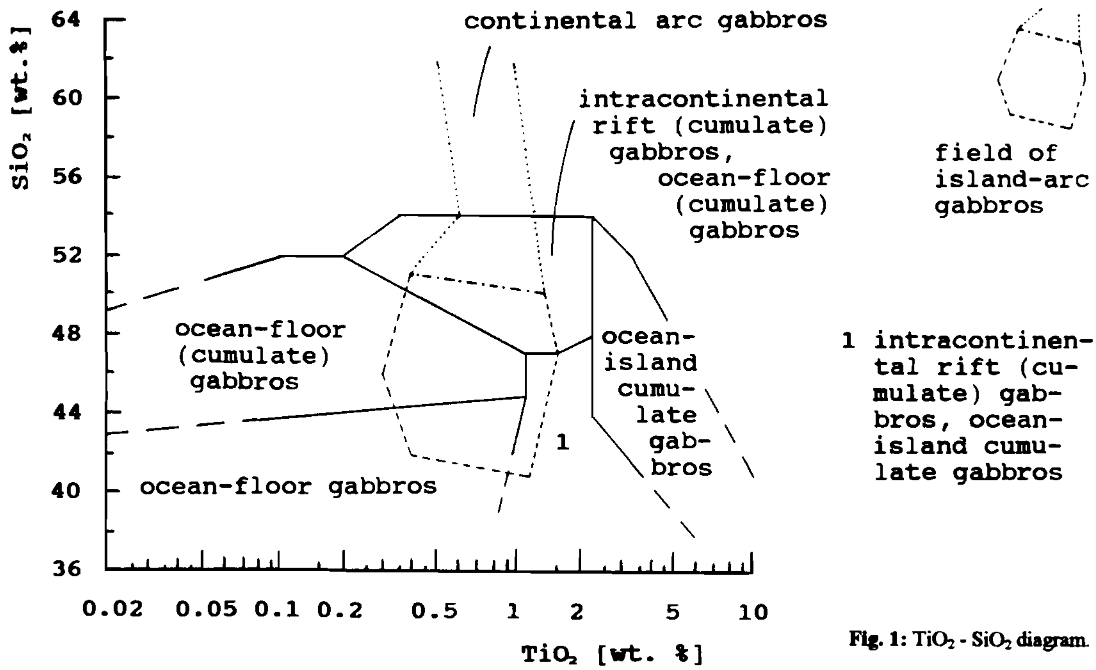


**Fig. 1:** $TiO_2$ - $SiO_2$ diagram.

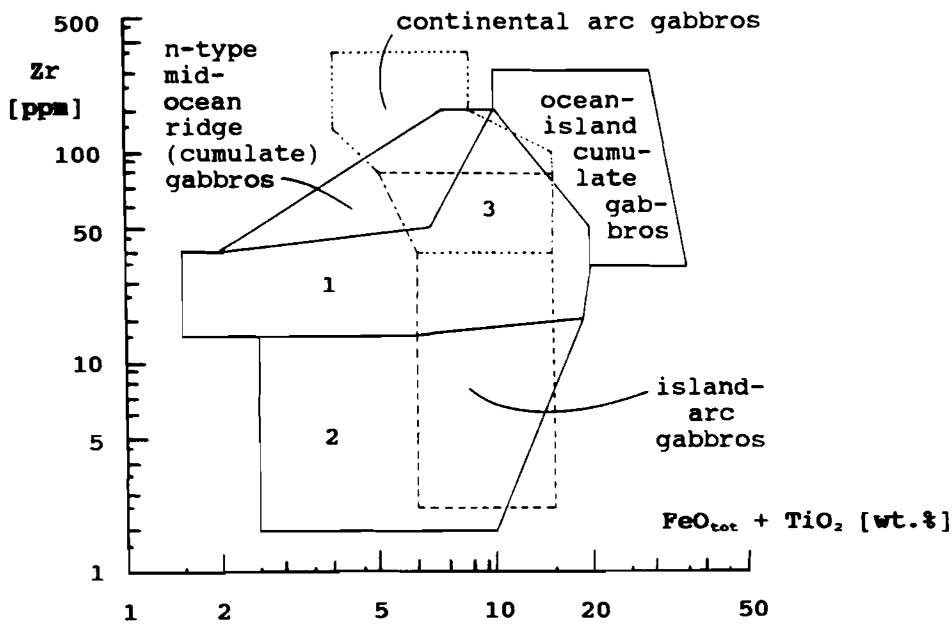


1 n-type mid-ocean ridge (cumulate) gabbros, intracontinental rift (cumulate) gabbros

2 primitive mid-ocean ridge (cumulate) gabbros, n-type mid-ocean ridge (cumulate) gabbros

3 island-arc gabbros, continental arc gabbros

**Fig. 2:** Diagram on $FeO_{tot}$ + $TiO_2$ vs. Zr.
As these two diagrams show a broad variety in the tectonic settings of the gabbroic-dioritic rocks, they should be used prior to one of the following diagrams (figs. 3 and 4).

with the focus on a high share of MgO. In the field "ocean-floor (cumulate) gabbros", however, 15 wt.% CaO and 2 wt.% $Na_2O + K_2O$ are nothing unusual. Primitive mid-ocean ridge gabbros which also occur in this field are normally characterized by such a high CaO quantity. $Na_2O + K_2O$ up to 3.5 wt.%, Cr < 150 ppm and a higher amount of Zr emphasize a more evolved stage of the ocean-island cumulate gabbros as compared with the ocean-floor gabbros. Apart from their increased quantity of $SiO_2$ to > 60 wt.%, the continental arc gabbros are characterized by < 150 ppm Cr, and $Na_2O + K_2O$ often amount to > 5 wt.%. A strong variation from 3.5 to 11 wt.% shows CaO.

In the diagram $FeO_{tot.} + TiO_2$ vs. Zr (fig. 2), the continental arc gabbros are noticeable for their high Zr quantitiy up to 350 ppm. Among the ocean-island cumulate gabbros, this trace element shows a variation from 35 to 200 ppm. The minimum amount of $FeO_{tot.} + TiO_2$ is 10 wt.%, more than 25 wt.% of these element oxides also ocur within this tectonic position.

The diagram $MgO/TiO_2$ vs. Zr (fig. 3) only shows the ocean-floor related rocks: the primitive mid-ocean ridge gabbros are characterized by a high $MgO/TiO_2$ ratio as a consequence of a high amount of MgO, and a low quantity of $TiO_2$ (and of $FeO_{tot.}$) which decrease as low as 0.02wt.% (1.5 wt.%). Zr is characteristic of a variation between 2 and 20 ppm. A broader range in Zr take the n-type mid-ocean ridge (cumulate) gabbros from 8 to 200 ppm. The field "primitive island-arc gabbros" which can be separated relatively well from the other fields reveal a lower $MgO/TiO_2$ ratio as compared with the primitive mid-ocean ridge gabbros. Zr quantities of less than 3 ppm and not more than 30ppm is also characteristic of this tectonic setting.

For ocean-floor gabbros, ocean-island cumulate gabbros and island-arc gabbros:

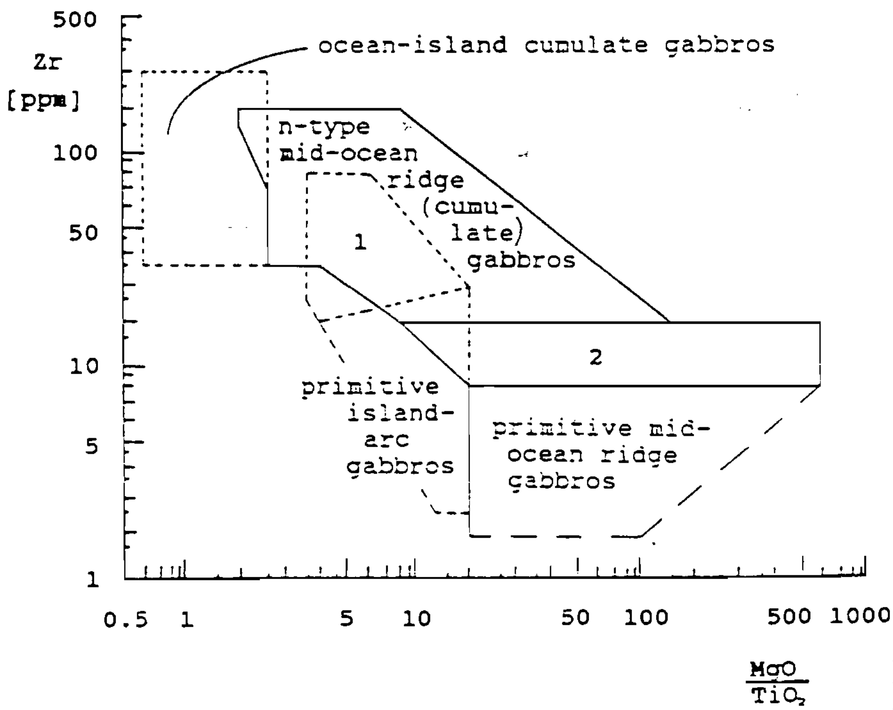


**Fig. 3:** Diagram on $MgO/TiO_2$ vs. Zr for ocean-floor related gabbros. For the continent-related gabbros, the diagram in fiig. 4 is applied.

1 primitive island-arc gabbros, evolved island-arc gabbros

2 primitive mid-ocean ridge (cumulate) gabbros, n-type mid-ocean ridge (cumulate) gabbros

occur. The reason for the low $MgO/TiO_2$ ratio for the ocean-island cumulate gabbros, of course, is not only the high amount of $TiO_2$, but also the low share of MgO, often decreasing to < 5 wt.%. The $TiO_2$ - Y/20 - $K_2O$ triangular diagram for arc and continental gabbros (fig. 4) gives the user following details: the field "intracontinental rift (cumulate) gabbros" has a decreased share of Y as compared with arc-related and continent-continent collisional gabbros (strictly speaking also arc-tectonic setting gabbros). Indeed, the typical amount of Y for intracontinental rift (cumulate) gabbros varies between 2 and 10 wt.%. The continent-continent collision gabbros are typical of high $K_2O$ in comparison with the gabbros from the other tectonic settings. $K_2O$ often amounts to more than 2.5 wt.%. Summarizing, the diagrams also can be used for metamorphic rocks up the higher amphibolite facies metamorphism. For volcanic rocks (basaltic and andesitic rocks), however, they cannot be applied. $K_2O$ should be interpreted with care if a higher metamorphism has affected the user's investigated rocks because of its low stability.

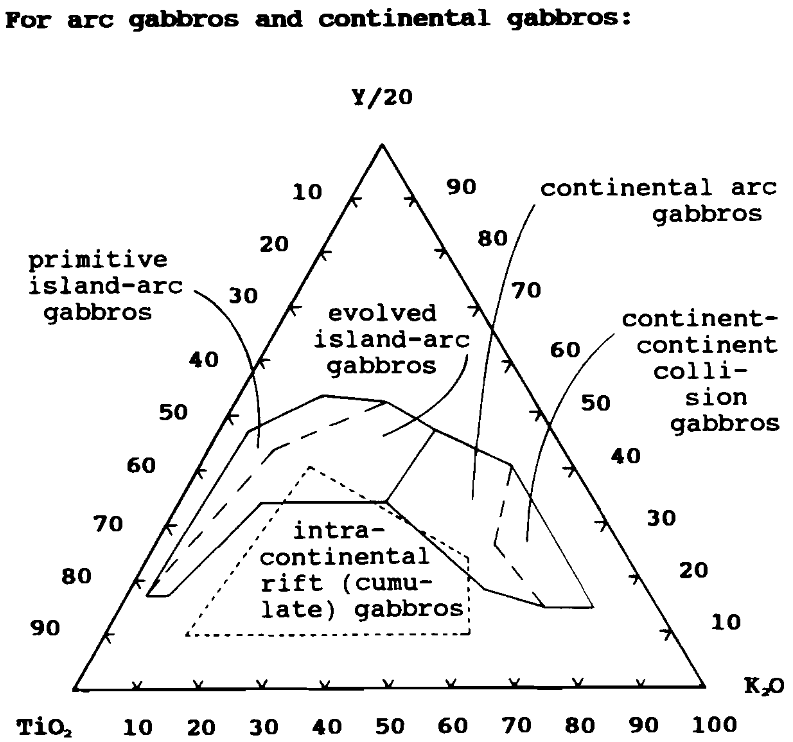


Fig. 4: $TiO_2$ - Y/20 - $K_2O$ triangular diagram for arc gabbros and continental gabbros.

## REFERENCES

Gulson, B.L. 1972. The high-k diorites and associated rocks of the Yeoval diorite complex. Contributions to Mineralogy and Petrology , 35, 173 - 192.

Ikeda, Y. & Yuasa, M. (1989). Volcanism in nascent back-arc basins behind the Shichito Ridge and adjacent areas in the Izu-Ogasawara arc, northwest Pacific: evidence for mixing between E-type MORB and island-arc magmas at the initiation of back-arc rifting. Contributions to Mineralogy and Petrology, 101, 377 - 393.

Miyashiro, A. & Shido, F. 1975. Tholeiitic and calc-alkaline series in relation to the behavior of titanium, vanadium, chromium and nickel. American Journal of Science, 275, 265 - 277.

Pearce, J.A. 1983. A user's guide to basalt dicrimination diagrams. In: Tarrey (ed.) Shiva Publ.

Pearce, J.A., Lippard, S.J. & Robberts, S. 1984: Characteristics and tectonic significance of Supra-subduction zone ophiolites. Geological Society Special Publications, 16, 77 - 94.

Shervais, J.B. & Hanan, B.B. 1989. Jurassic volcanic glass from the volcanic complex, Franciscan Assemblage, Northern CaliforniaCoast Range. Geology, 17, 510 - 514.

Streckeisen, A. 1976. To each plutonic rock it proper name. Earth Science Revue, 12, 1 - 33.

# A REAPPRAISAL OF THE CENOZOIC INNER ARC MAGMATISM IN SOUTHERN PERU : CONSEQUENCES FOR THE EVOLUTION OF THE CENTRAL ANDES FOR THE PAST 50 Ma.

Gabriel CARLIER[1-2], Jean Pierre LORAND[2], Michel BONHOMME[3] and Victor CARLOTTO[4].

[1] ORSTOM, UR 13, 213, rue La Fayette, 75010 PARIS, FRANCE
[2] CNRS, URA 736, Laboratoire de Minéralogie, Muséum National d'Histoire Naturelle, 61, rue Buffon, 75005 PARIS, FRANCE
[3] CNRS, URA 69, Laboratoire de Géologie, Université Joseph Fournier, 15, rue Maurice Gignoux, 38031 GRENOBLE CEDEX, FRANCE
[4] Departamento de Geología, Universidad Nacional San Antonio Abad del Cusco, CUSCO, PERU.

KEY WORDS : Southern Peru, lamproite, shoshonite, calc-alkaline, peraluminous magmatism.

## INTRODUCTION

The Altiplano, a high plateau 200 km-wide and 1500 km-long is undoubtely the major feature of the Central Andes. One of its most characteristic feature is the presence of varied magmatic events, referred to as the Inner Arc Magmatic Domain by Clark et al. (1990). This magmatism started about 48 Ma ago and shows a greater diversity compared to the Main Arc Domain of the Western Andean Cordillera. Several occurrences of phlogopite lamproites, phlogopite-diopside-sanidine lamproites and ultrapotassic minettes have recently been discovered (Carlier et al., 1996) in addition to the peraluminous magmatism of dominantly crustal origin and high-K calc-alkaline to shoshonitic volcanism previously identified (Pichavant et al., 1988; Clark et al., 1990). This led to a reappraisal of the Cenozoic Inner Arc magmatism in Southern Peru, which is presented here along with new age determinations and geochemical data on the ultrapotassic lavas, the high-K calc-alkaline to shoshonitic volcanism and the calc-alkaline plutons. These data provide important informations on the evolution of Central Andes for the past 50 Ma.

## LOCATION, AGE AND NATURE OF THE ALTIPLANO CENOZOIC MAGMATISM

The South Peruvian Altiplano (SPA) constitutes the northern ending of the Bolivian Altiplano. It is progressively pinched northward and disappears in the Abancay region (Fig. 1). Like the Bolivian Altiplano, the SPA is divided into a Western Domain and an Eastern Domain separated by the Sicuani-Huancane sinistral active fault system (SHF). The Western Domain is structured by N- to NE-verging thrust fault systems, i.e. from the north to the south the Paruro-Acomayo fault (PAF), the Langui Lake fault (LF), the Calapuja fault (CF) and the Mañazo fault (MF).

The Cenozoic Inner Arc magmatism always occurs in the vicinity of the different thrust fault systems defined above. It started at about 48 Ma, in the Northernmost part of the Western Domain by gabbro-diorite plutons intruding the southern area of the Paruro-Acomayo thrust fault (Fig. 1). These are the Acomayo and Pomacanchi plutons dated at 48-34 Ma and 44-37 Ma respectively, and coeval with the large Andahuaylas-Yauri batholith which intruded the eastern margin of the Western Cordillera. All these rocks have textural and geochemical features of calc-alkaline cumulates crystallized at the bottom of shallow magmatic chambers. The outcropping of cumulates indicates a period of uplift and erosion of the southern margin of the PAF and the eastern margin of the Western Cordillera before the intrusion of calc-alkaline dacitic and trachydacitic subvolcanic plugs dated at 34 and 32 Ma. The erosion products of this calc-alkaline magmatism filled the Cusco and Sicuani molassic basins (CMB and SMB, Fig. 1).

Magmatism becomes widespread between 30 Ma and 27 Ma, affecting both domains of the SPA. Significant changes in its composition and its location are observed in the Western Domain (Fig. 1). Sparse alkaline syenite dykes occur in the Abancay area, in the northern part of this domain. Alkaline lavas of similar ages are observed along the Calapuja thrust fault. These are the Ayaviri leucite-bearing basanite-phonotephrite-trachyte suite which coexist with high-K monzograbbroic subvolcanic intrusions. Meanwhile, a calc-alkaline magmatism (subvolcanic intrusions) still persists along the Mañazo thrust fault, to the south of the studied area (Clark et al., 1990). During the same period, the Eastern Domain was the locus of a peraluminous magmatism, the earliest cordierite-bearing peraluminous monzogranite intrusions being dated at 28 Ma (Clark et al., 1990). Numerous small peraluminous cordierite-bearing monzogranitic stocks and cordierite-muscovite-sillimanite-bearing dacitic and rhyolitic peraluminous ash-flow tuffs have been recognized over a distance of 200 km, in close association with shoshonites (Laubacher et al., 1988; Pichavant et al., 1988). The most important feature of this domain is the occurrence of potassic to ultrapotassic minettes with diagnostic features of Spanish phlogopite lamproites, i. e. orthopyroxene-bearing phenocryst assemblages, low CaO contents (<2wt%), strong enrichments in large-ion lithophile elements -LILE (Ba=1550-6550 ppm, Zr=217-779 ppm, $La_N/Yb_N$=17-65), Mediterranean C1-normalized REE patterns ($La_N/Nd_N$<1.5; Eu/Eu*<1) and negative high field strength elements -HFSE, Ba and Sr anomalies in primitive mantle-normalized multi-element patterns (Carlier et al., 1996). These minettes, dated at 24-20 Ma, are interpreted as Al-rich phlogopite lamproites contaminated to various degrees by partially crystallized peraluminous granites.

The peraluminous magmatism of the Eastern domain becomes increasingly important during the Miocene. The last peraluminous magmatic events give ages of about 4 Ma. Meanwhile, in the Western Domain, the calc-alkaline magmatism recognized along the Mañazo fault reaches its major development (Clark et al., 1990) and other evidences of calc-alkaline magmatism of similar ages are known along the Calapuja thrust fault. An important shoshonitic event dated at 5-6 Ma is also known along the Mañazo thrust fault, in the Puno department (Lefèvre, 1979).

For the past 3 Ma, the magmatic activity was focussed along the Abancay-Curahuasi-Anta, Cusco and Sicuani-Huancane fault systems which separate the Western Domain from the Eastern one and the Eastern Cordillera. Previously identified as only shoshonitic (c.f. Lefevre, 1979), the Plio-Quaternary Inner Arc Magmatism is in fact composed of shoshonites, minettes, lamproites and even peraluminous rhyolites and dacites. Shoshonites can be sub-divided into a hornblende-bearing Pliocene suite in the Abancay-Anta area, a phlogopite-bearing Quaternary shoshonitic suite in the Cusco area and a pyroxene-bearing Quaternary shoshonite suite in the Sicuani-Ayaviri area. Peraluminous rhyolites and dacites showing minettes inclusions ($K_2O/Na_2O$=1.5-1.7, Ba=4930-5170 ppm, Sr=2370-2700 ppm, $La_N/Yb_N$=36-46) are closely related to the Sicuani-Ayaviri shoshonite suite. In addition, phlogopite-diopside-sanidine-K-richterite lamproites dykes, dated at 2.3 Ma, have been identified in the Cusco and Ayaviri areas (Carlier et al., in prep.). These lavas resemble the Leucite Hill phlogopite lamproites in having very high LILE contents (Ba=4750-12400ppm, La=$6.10^2$ x CI-chondrites) and no negative HFSE anomaly (La/Nb=1.1-1.2) in primitive mantle-normalized multi-element patterns.

## CONCLUSION

For the last 34 Ma., the Western Domain of the SPA has experienced a general N- to NE-trending compressional regime. In this domain, the Cenozoic magmatism is mainly composed of calc-alkaline suites which are related to the subduction of Nazca plate beneath the South America Plate. Alkaline and shoshonitic suites documented local extensional regimes at about 28-30 Ma and 5-6 Ma.

The lamproite occurrences provide petrologic evidence of the existence of a thick lithosphere, undoubtedly the western margin of the Brazilian Craton, beneath the Eastern Andean Cordillera and the Northern Altiplano. The westward displacement of this ultrapotassic magmatism from the Eastern Domain to the Western Domain during the last 25 Ma suggests a north-eastward thrusting of the Altiplano (and probably the Western Cordillera) above the Brazilian Craton. A consequence of the Altiplano thrusting is a local fusion of its lower crust that produces the peraluminous magmatism.

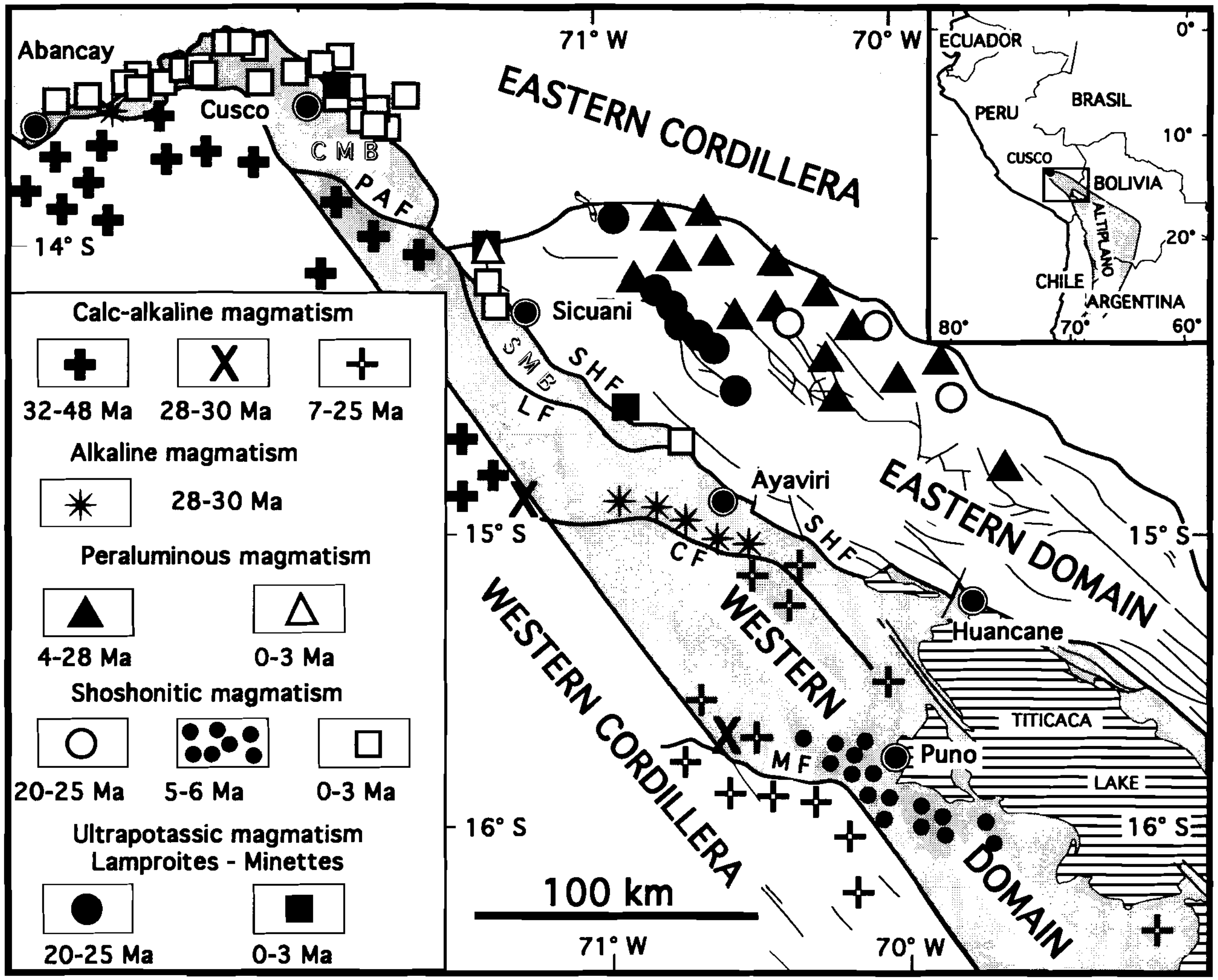


**FIGURE 1** : Location, age and nature of the Southern Peruvian Altiplano Cenozoic magmatism.

Structural and magmatic features of the SPA could be explained by the progressive northward migration and counterclockwise rotation of the Western Cordillera during the Eocene-Miocene times then followed by its south-eastward displacement along the the active sinistral Abancay-Curahuasi-Anta, Cusco and Sicuani-Huancane fault systems. Such displacements of Western Cordillera and Altiplano deduced from the study of the Inner Arc Cenozoic magmatism in Southern Peru are consistent with the directions commonly assumed for the convergence between the Nazca plate and the South America Plate since the Eocene (Pardo-Casas & Molnar, 1987).

## REFERENCES

Carlier, G., Lorand, J. P., Audebaud, E. & Kienast, J. R. 1996. Petrology of an unusual orthopyroxene-bearing minette suite from southeastern Peru, Eastern Andean Cordillera. Al-rich lamproites contaminated by peraluminous granites. *Journal of Volcanological and Geothermal Research*, in press.

Clark, A. H., Farrar, E., Kontak, D. J., Landgridge, R. J., Arenas, M. J., France, L. J., McBride, S. L., Woodman, P. L., Wasteneys, H. A., Sandeman, H. A. and Archibald, D. A. 1990. Geologic and geochronologic constraints on the metallogenic evolution of the Andes of Southeastern Peru. *Economic Geology*, 85, 1520-1583.

Laubacher, G., Sébrier, M., Fornari, M. & Carlier, G. 1988. Oligocene and Miocene continental sedimentation, tectonics, and S-type magmatism in the Southeastern Andes of Peru (Crucero basin) : Geodynamic implications. *Journal of South American Earth Science*, 1, 225-238.

Lefèvre, C. (1979). Un exemple de volcanisme de marge active dans les Andes du Pérou (sud) du Miocène à l'Actuel (zonation et pétrogenèse des andésites et shoshonites). *Thèse USTL*, Montpellier, 555pp.

Pardo-Casas, F. and Molnar, P. 1987. Relative motion of the Nazca (Farallon) and South America Plate since late Cretaceous times. *Tectonics*, 6, 233-248.

Pichavant, M., Kontak, D. J., Briqueu, L., Valencia Herrera, J. and Clark, A. H. 1988. The Miocene-Pliocene Macusani Volcanics, SE Peru. II Geochemistry and Origin of a felsic peraluminous magma. *Contributions to Mineralogy and Petrology*, 100, 325-338.

# GEOCHEMISTRY OF EARLY TERTIARY BACK-ARC BASALTS FROM AYSÉN, SOUTHERN CHILE (44-46° S): GEODYNAMIC IMPLICATIONS.

Alain DEMANT [1], Francisco HERVÉ [2], Robert J. PANKHURST [3], Manuel SUAREZ [4]

[1] Laboratoire de Pétrologie Magmatique, CNRS URA 1277 et FU 17, CEREGE, BP 80, Aix-en-Provence Cedex 04, France
[2] Departamento de Geología, Universidad de Chile, Casilla 13518, Correo 21, Santiago, Chile
[3] British Antarctic Survey, c/o NERC Isotope Geosciences Laboratory, Keyworth, Nottingham NG12 5GG, U.K.
[4] Sernageomin, Casilla 10465, Correo 09, Avenida Santa María 0104, Santiago, Chile

**KEY WORDS**: Chile, Patagonia, Tertiary basalts, extension, geochemistry, geodynamic

## INTRODUCTION

The geology of the Aysén region (44-47° S) is dominated by the presence of a huge calc-alkaline batholite, the North Patagonian Batholite (NPB), which constitute the spine of the chain. This 200 km wide plutonic complex intruded to the west the Chonos Late Paleozoic metamorphic complex, and to the east, Paleozoic and Mesozoic volcanic and sedimentary units (Pankhurst and Hervé, 1994). The Mesozoic stratigraphy comprises two main subduction-related volcanic episodes, the Middle to Upper Jurassic Ibañez Formation and the Middle Cretaceous Divisadero Formation. The Lower Cretaceous marine Coyhaique Group, deposited in a back-arc basin, provides a useful stratigraphic marker between the volcanic successions (Bell et al., 1994; De la Cruz et al., 1994). Volcanic activity resumed after a period of quiescence in Eocene time. Mesa basalts, situated in a back-arc position, crop out in the Balmaceda and Río Cisnes regions. Pliocene and Quaternary andesitic stratovolcanoes and monogenetic basaltic centres of the volcanic arc are located westward, near the Liquiñe-Ofqui fault zone (LOFZ), a 1000 km long, trench parallel, dextral strike-slip duplex, which has been active at least since the mid-Tertiary (Cembrano and Hervé, 1993).

## GEOLOGICAL SETTING

A basaltic succession, approximately 150 m thick, composed of subhorizontal lava flows with frequent columnar jointing, outcrops in the Balmaceda basin. The flows tend to be thicker toward the top (up to 10 m). The first eruptions occurred in a subaqueous environment as revealed by the presence of pillow lavas with interstitial hyaloclastites and sediments, or finely stratified surtseyian-type surge deposits exposed in the Río Oscuro valley. In this last locality, the basaltic sequence lies above poorly-welded tuffs which are probably also Tertiary (Suárez et al., 1994). The Balmaceda basalts were overlaid by Miocene to Pliocene continental sediments with intercalated acidic pyroclastic units. Base upon a whole rock K/Ar radiometric age (46 ± 2 Ma; Baker et al., 1981), an Eocene age can be assigned to the Balmaceda basalts. Some zeolites are visible in hand specimen, and were identified as heulandite clinoptilolite in the pillows, and chabazite in the massive flows. Two basaltic plugs with abundant fresh

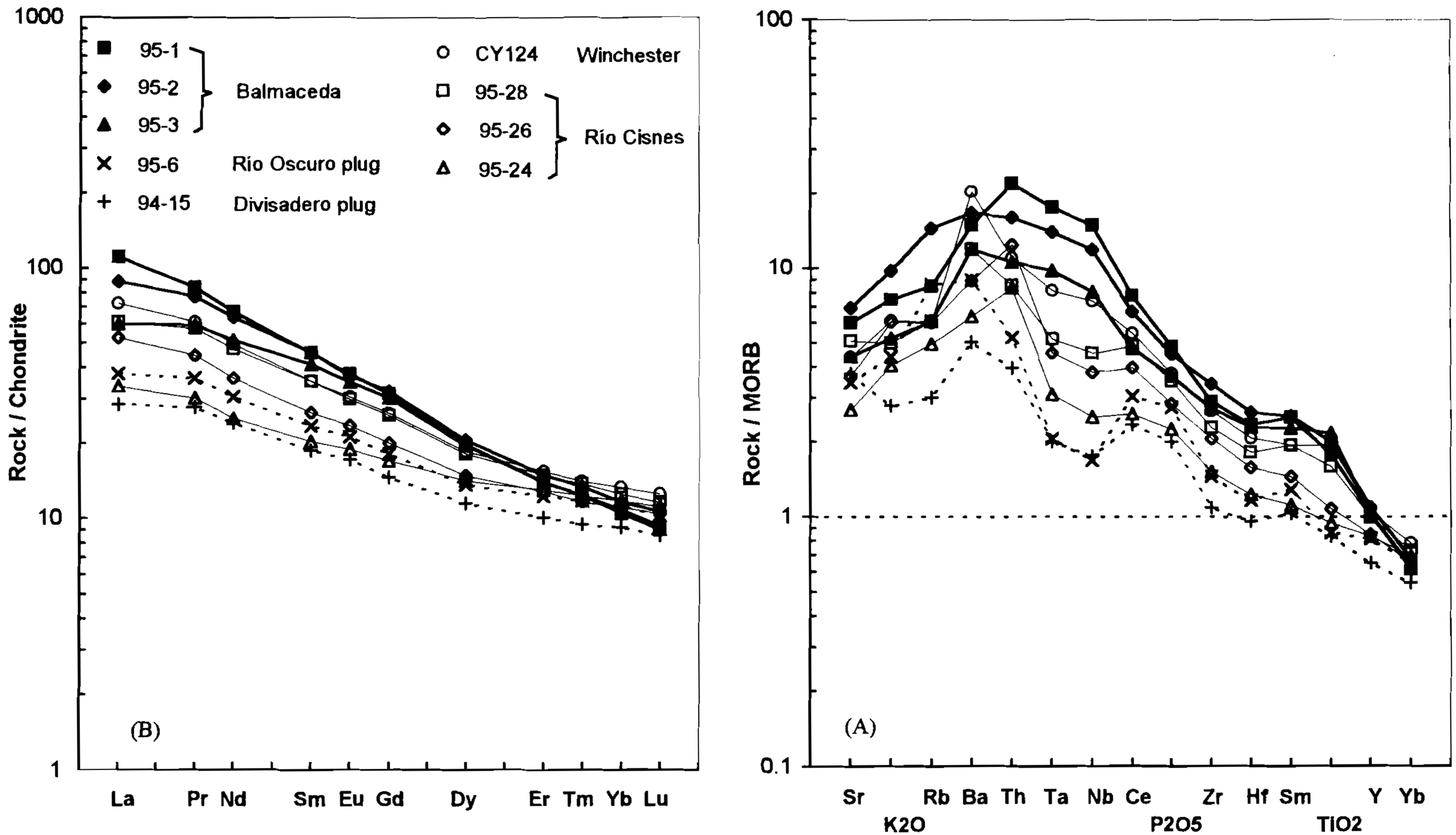


Fig. 1 : MORB-normalised element abundances (B) and Chondrite normalised rare-earth patterns (A) of Early Tertiary basalts from the northern Patagonian Andes. The following observations can be enhanced: (1) progressive fading of the Ta-Nb anomaly for the Río Cisnes and Río Winchester basalts; (2) absence of this anomaly, typical of OIB, for the Balmaceda basalts; (3) progressive enrichment in light-REE and (La/Yb)n ratios (B) from the basaltic plugs through the Río Cisnes and Balmaceda basalts.

olivine were also sampled; one east of Cerro Divisadero (94-15), the type locality for the Cretaceous volcanic succession, and the other in the upper part of the Río Oscuro valley (96-6). These basaltic bodies intruded the ignimbrites and are, therefore, probably also Eocene.

Flat lying mesa basalts also occurred, 200 km north of Balmaceda, in the Río Winchester and Río Cisnes valleys. The Río Cisnes sequence (about 100 m thick) shows a progressive decrease of the thickness of the lava flows (from 20 m for sample 95-28 to 1 m for 95-24) and an increasing oxidation, as revealed by the iddingsitisation of olivine phenocrysts, toward the top of the volcanic pile. Most of these flows are olivine-rich basalts. Peralkaline rhyolitic domes (El Chueco) are associated with the basalts. No radiometric ages are available on these basalts but overlying Lower Miocene continental sediments (Río Frías Formation, Marshall and Salinas, 1990) and Upper Miocene to Pliocene glacial or fluvio-glacial deposits clearly post-date the volcanic activity which can be considered as broadly contemporaneous with the Balmaceda sequence.

## GEOCHEMISTRY

The Early Tertiary Patagonian basalts are fairly uniform in mineralogy. Olivine is the principal component, but some flows also contain few clinopyroxene and/or plagioclase phenocrysts. The twenty-one new chemical analyses presented here contribute to define the geochemical signature of these Plateau basalts. All the basalts are olivine normative (48-50 wt % silica); only four contain some nepheline (less than 1%) in the norm. They have the composition of continental tholeiites. Basalts from Balmaceda are more differentiated (Mg# ~ 55) than the Río Cisnes ones (Mg# ~ 64); the basaltic plugs of Cerro Divisadero and Río Oscuro are proximate to a primitive pole with Mg# ~ 68. The geochemical characteristics of the basalts and their spatial evolution are discussed based on Fig. 1. The MORB-normalised trace element abundances, expressed on the Pearce (1983) spidergram, show clear differences between the Balmaceda and Río Cisnes basalts. The later, and the basalts from the Divisadero and Río Oscuro plugs, are enriched in incompatible elements (above all Ba and Th) and present a negative anomaly in Ta and Nb, less pronounced for the Río Winchester basalt. This kind of trend is interpreted either as the result of crustal contamination or as indicative of an origin from the enriched sub-continental lithosphere (Hawkesworth et al., 1990; Arndt and Christensen, 1992; Arndt et al., 1993; Turner and Hawkesworth, 1995). Low Ba/Zr ratios, as defined for the Early Tertiary basalts from south-east Greenland (Fitton et al., 1995), indicate that contamination does not play any role, while low La/Nb and Zr/Nb ratios characterise an enriched lithospheric mantle source. The Balmaceda basalts have a different trend which doesnot exhibit Ta and Nb anomalies and, therefore, more akin to OIB signatures. REE patterns of the Balmaceda basalts are slightly more enriched and the (La/Yb)n ratios higher (5.7 to 10.2) than that of the Río Cisnes basalts (2.5 to 5.4).

## CONCLUSION

Early Tertiary basalts from Balmaceda and Río Cisnes are related with incipient extensional tectonism responsible for the generation of back-arc basins. These basalts, of probable Eocene age, correspond to the mostly tholeiitic Early Patagonian plateau basalts (Baker et al., 1981; Stern et al., 1990). More recent (25 Ma to recent) undersaturated alkali basalts extended further East in the Cosmelli basin, on the southern side of Lago General Carrera (Flint et al., 1995), and in Argentina. Differences in the geochemical signatures between the Río Cisnes and Balmaceda basalts, particularly the fading of the Ta-Nb anomaly, remind the widely studied evolution observed in the Basin and Range province of south-western United States and north-western Mexico, interpreted as a typical exemple of progressive decrease of the influence of the lithospheric mantle source during crustal thinning, and the correlative increase of an asthenospheric component (Fitton et al., 1988 and 1991; Kempton et al., 1991). The geodynamic context is fairly similar and corresponds to the progressive cessation of subduction, as a result of the collision of an oceanic ridge with a continental plate (Ramos and Kay, 1992), and the corresponding development of a slab window (Hole et al., 1995) and back-arc extension.

## REFERENCES

Arndt N.T. & Christensen U. 1992. The role of lithospheric mantle in continental flood volcanism: thermal and geochemical constraints. *J. Geophys. Res.*, 97, 10967-10981.

Arndt N.T., Czamanske G.K., Wooden J.L. & Fedorenko V.A. 1993. Mantle and crustal contributions to continental flood volcanism. *Tectonophysics*, 223, 39-52.

Baker P.E., Rea W.J., Skarmeta J., Caminos R., & Rex D.C. 1981. Igneous history of the Andean cordillera and Patagonian plateau around latitude 46° S. *Phil. Trans. R. Soc., London,* A303, 105-149.

Bell C.M., Townsed M.J., Suárez M., & De la Cruz R. 1994. The depositional environments of the Lower Cretaceous Coyhaique Group, Aysén Basin, southern Chile (45°-46°). *7° Congr. Geol. Chileno (Concepción),* extended abstracts, 402-403.

Cembrano J., & Hervé F. 1993. The Liquiñe - Ofqui Fault zone: a major Cenozoic strike slip duplex in the southern Andes. *Second ISAG (Oxford),* extended abstracts, 175-178.

De la Cruz R., Suárez M., & Demant A. 1994. Facies volcanicas del Mesozoico de Aisén (sector noroeste), 44°-47° Lat. S., Chile (Formaciones Ibañez y Divisadero). *7° Congr. Geol. Chileno (Concepción),* extended abstracts, 27-31.

Fitton J.G., James D., Kempton P.D., Ormerod D.S., & Leeman W.P. 1988. The role of lithospheric mantle in the generation of Late Cenozoic basic magmas in the western United States. *J. Petrol.*, Special Lithosphere issue, 331-349.

Fitton J.G., James D., & Leeman W.P. 1991. Basic magmatism associated with Late Cenozoic extension in western United States: Compositional variations in space and time. *J. Geophys. Res.*, 96, 13693-13711.

Fitton J.G., Saunders A.D., Larsen L.M., Fram M.S., Demant A., Sinton C., & Leg 152 shipboard scientific party 1995. Magma sources and plumbing systems during break-up of the SE Greenland margin: preliminary results from ODP Leg 152. *J. Geol. Soc. London*, 152, 985-990.

Flint S.S., Prior D.J., Agar S.M., & Turner P. 1994. Stratigraphic and structural evolution of the Tertiary Cosmelli Basin and its relatioship to the Chile Triple junction. *J. Geol. Soc. London*, 151, 251-268.

Hawkesworth C.J., Kempton P.D., Rogers N.W., Ellam R.M. & Calsteren P.W. 1990. Continental mantle lithosphere and shallow level enrichment processes in the Earth's mantle. *Earth Planet. Sci. Lett.*, 96, 256-268.

Hole M.J., Saunders A. D., Rogers G., & Sykes M.A. 1995. The relationship between alkaline magmatism, lithospheric extension and slab window formation along continental destructive plate margins. *In* Smellie J.L. (ed.), « Volcanism associated with extension at consuming plate margins », *Geol. Soc. Sp. Publi.*, 81, 265-285.

Kempton P.D., Fitton J.G., Hawkesworth C.J., & Ormerod D.S. 1991. Isotopic and trace elements on the composition and evolution of the lithosphere beneath the southwestern United States. *J. Geophys. Res.*, 96, 13713-13735.

Marshall L., & Salinas P. 1990. Stratigraphy of the Río Frías Formation (Miocene), along the Alto Río Cisnes, Aisén, Chile. *Rev. Geol. de Chile,* 17, 57-87.

Pankhurst R.J., & Hervé F. 1994. Granitoid age distribution and emplacement control in the North Patagonian batholith in Aysén (44°-47° S), *7° Congr. Geol. Chileno (Concepción),* extended abstracts, 1409-1413.

Pearce J.A. 1983.The role of sub-continental lithosphere in magma genesis at destructive plate margins. *In* C.J. Hawkesworth and M.J. Norry (eds), «Continental basalts and mantle xenoliths», 230-249, Shiva.

Ramos V.A., & Kay S.M. 1992. Southern Patagonian plateau basalts and deformation: backarc testimony of ridge collision. *Tectonophysics,* 205, 261-282.

Stern C.R., Frey F.A., Futa K., Zartman R.E., Peng K. & Kyser T.K. 1990. Trace-element and Sr, Nd, Pb and O isotopic composition of Pliocene and Quaternary alkali basalts of the Patagonian Plateau lavas of southernmost South America. *Contrib. Mineral. Petrol.*, 104, 294-308.

Suárez M., Prieto X., Belmar M., & Quiroz D. 1994. Estratigrafía terciaria del sector nororiental de Aysén (44°-46° L. S.), Chile. *7° Congr. Geol. Chileno (Concepción),* extended abstracts, 533-537.

Turner S., & Hawkesworth C.J. 1995. The nature of the sub-continental mantle: constraints from the major-element composition of continental flood basalts. *Chem. Geol.*, 120, 295-314.

# BASALTS OF THE CHILEAN ALTIPLANO, SOUTH-CENTRAL ANDES

Bernard DÉRUELLE[1], Oscar FIGUEROA A.[2] and Stephen MOORBATH[3]

(1) Laboratoire de Magmatologie et Géochimie Inorganique et Expérimentale, Université Pierre et Marie Curie, 4, Place Jussieu, Paris, France, e-mail : bd@ccr.jussieu.fr.
(2) Departamento de Ciencias de la Tierra, Universidad de Concepción, Casilla 3-C, Concepción, Chile.
(3) Department of Earth Sciences, University of Oxford, Oxford, OX1 3PR, U.K.

**KEY WORDS** : Basalts, Chilean Altiplano, South-Central Andes.

## INTRODUCTION

Six basalts have been sampled on the Chilean Altiplano, along the Calama–Olacapato–El Toro lineament, in the Central Volcanic Zone (CVZ) of the Andes (fig. 1). This is the first record of occurrence of basalts ($SiO_2$ < 53 wt %) upon the Chilean Altiplano in South-Central Andes (SCA), whereas basalts have already been sampled in northermost Chile as parasitic cones of Nevados de Payachata volcanic complex (Wörner *et al.*, 1988; Davidson *et al.*, 1990) in Peru (Lefèvre *et al.*, 1973; Kontak *et al.*, 1986) Bolivia (Soler and Jimenez, 1993; Davidson and de Silva, 1995) and Argentina (Hörmann *et al.*, 1973; Viramonte, unpublished). The Chilean basalts are undoubtedly of Recent age and occur as small lava flows, some of them being accompanied by a small (< 0.01 $km^3$) unnamed pyroclastic cone near the Argentina–Chile boundary. It is noteworthy that these basalts are exposed East of large stratovolcanoes (e.g. Miscanti, Lascar) classically made of andesites and dacites but nearby minor eruptive centers (e.g. Cordón Puntas Negras, Volcan Puntas Negras, Déruelle, 1994).

## PETROGRAPHY AND MINERALOGY

The basalts have a typical microlitic porphyritic texture with phenocrysts of plagioclase (An 53.2–70.4) sometimes in disequilibrium, of olivine (up to Fo 86.8), diopside and augite (Wo 42.2–47.4), magnetite and chromite (38.4 < $Cr_2O_3$ wt % < 44.8; 12.0 < $Al_2O_3$ wt % < 21.9) in a groundmass of plagioclase, augite, magnetite and chromite. These basalts contain neither orthopyroxene nor ilmenite. Their mineralogy is quite different from that of alumina basalts that frequently occur in Meridional Andes (Southern Volcanic Zone) and contain phenocrysts of plagioclase, olivine, and scarce augite in a groundmass of plagioclase, augite, and Fe-Ti oxides sometimes accompanied with microcrysts of olivine (Déruelle,1982).

The occurrence of chromite as phenocrysts is uncommon in Chilean basalts. Chromite is not rare as tiny inclusions in olivine phenocrysts in Andean alumina basalts and basaltic andesites (Déruelle, unpublished) as well as in peridotite xenoliths occurring in alkali basalts (Xu *et al.*, 1993).

## GEOCHEMISTRY

Chilean Altiplano basalts have similar $TiO_2$, $Fe_2O_3$, CaO and $Na_2O$ contents as SVZ alumina basalts but have lower $Al_2O_3$ and higher MgO and $K_2O$ contents (fig. 2a, b). They contain higher Rb,

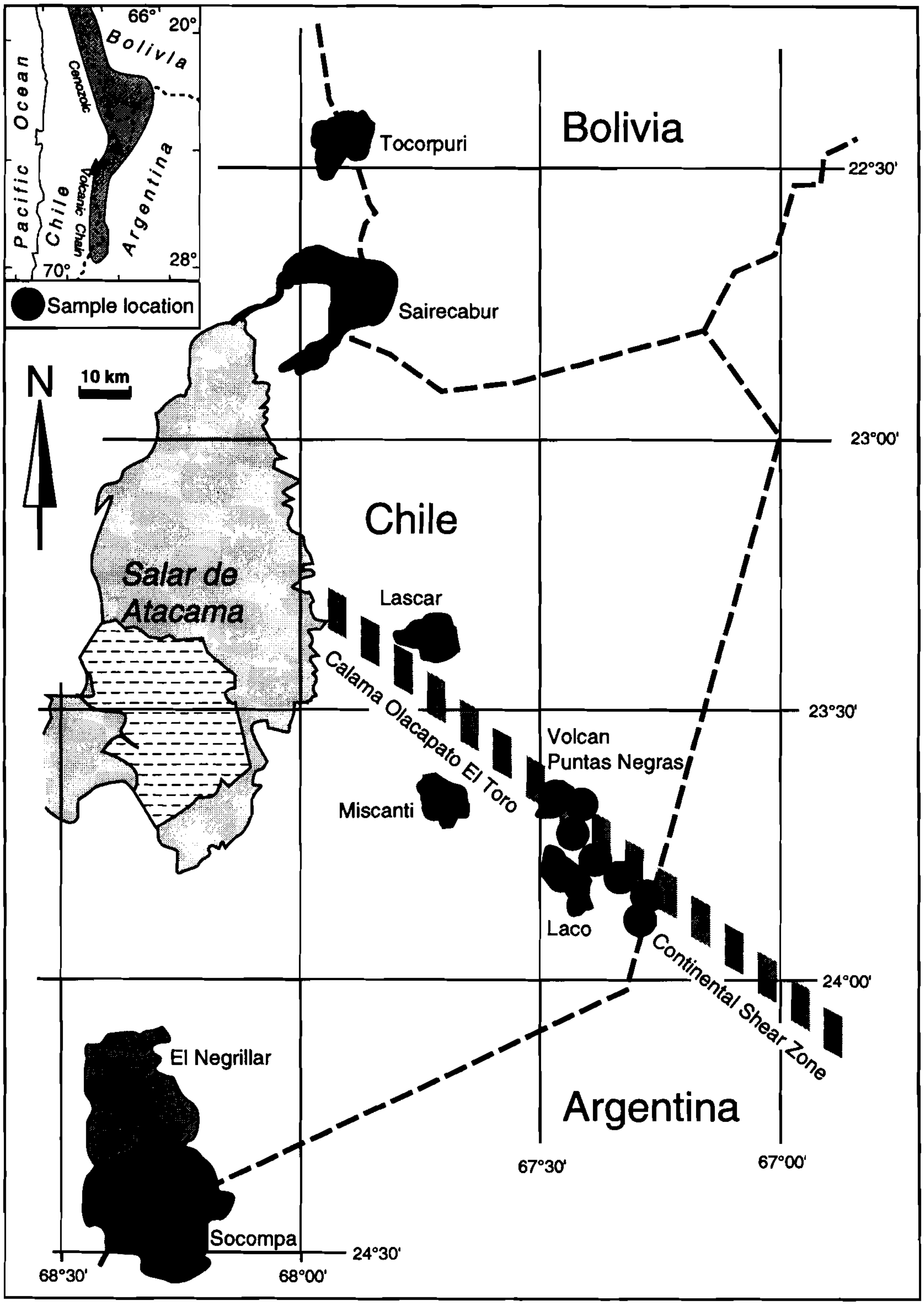


Fig. 1. Location the Chilean Altiplano basalts

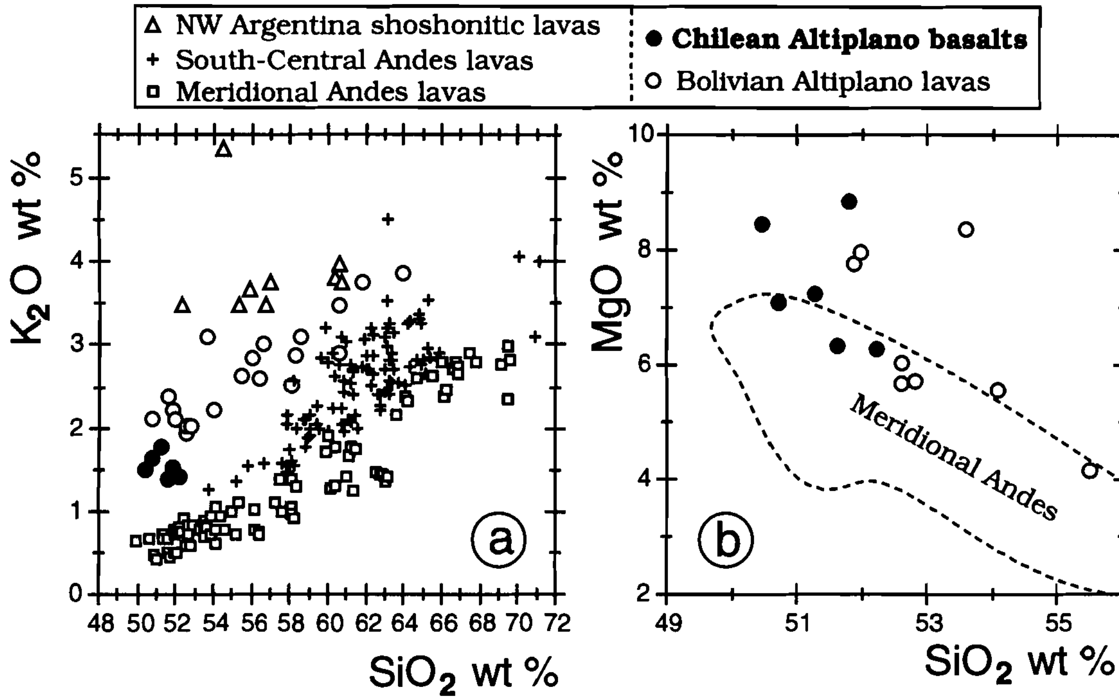


Fig. 2. $SiO_2$ *vs* $K_2O$ (a) and MgO (b) diagrams (all data after Déruelle, 1982, 1991, except Bolivian Altiplano lavas, after Davidson and de Silva, 1995).

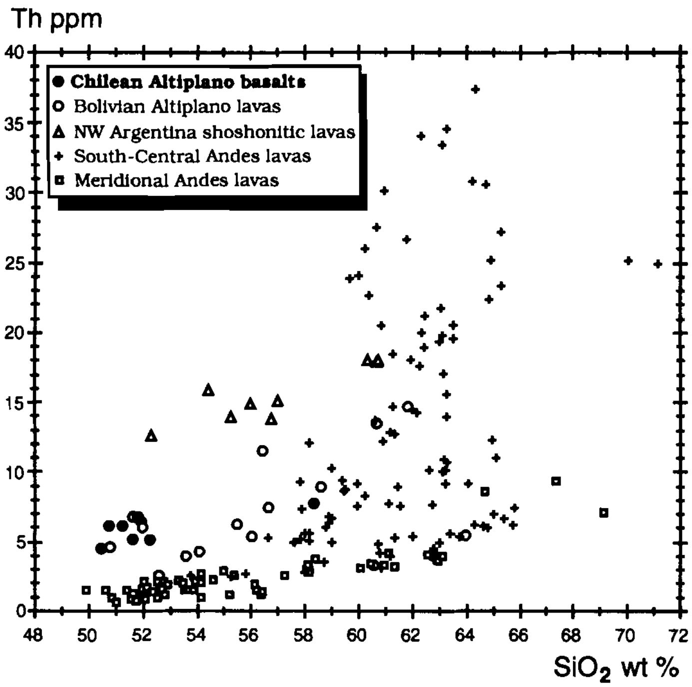


Fig. 3. $SiO_2$ *vs* Th diagram (same data source as in fig. 2).

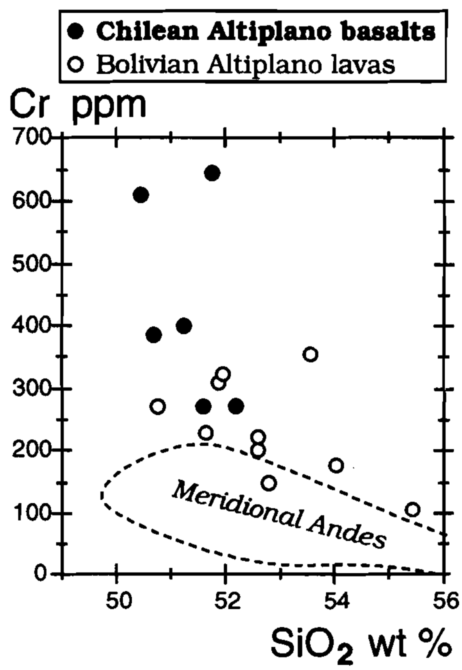


Fig. 4. $SiO_2$ *vs* Cr diagram (same data source as in fig. 2).

Sr, Ba, Ta, Th, U and rare-earth elements (fig. 3). They are also richer in Cr (fig. 4) and Ni. Their $^{87}Sr/^{86}Sr$ ratios (0.7057-0.7063) are in the same range as those of lavas from El Negrillar minor eruptive centers in SCA (Déruelle et al, 1982) but are by far higher than those measured in SVZ alumina basalts (< 0.7045, Déruelle *et al.*, op. cit.).

## DISCUSSION AND CONCLUSIONS

On the one hand, it is first noteworthy that the basalts studied here are the only ones recorded up to date upon the Chilean Altiplano of SCA, where stratovolcanoes are only made of andesites and dacites. On the other hand, it is clear that Chilean Altiplano basalts are different from those that built up SVZ stratovolcanoes. They are also different from NW Argentina shoshonites and furthermore to alkali basalts occurring farther East, away from the subduction zone. On the contrary they present similarities with Late Cenozoic basalts of the Bolivian Altiplano (Davidson and de Silva, 1995). They are characterized overall by very high chromium contents.

Their magmatic specificity is probably related to a deep origin, and their eruption has been controlled by the Calama–Olacapato–El Toro shear zone. Nevertheless their deep source is probably of lithospheric nature (high Cr and moderate Ta contents) and a crustal contamination may have played a role in their genesis, as attested by their high $^{87}Sr/^{86}Sr$ ratios when compared to those of extra-Andean Argentinian alkali basalts.

## REFERENCES

Davidson J.P., McMillan N.J., Moorbath S., Wörner G., Harmon R.S. and Lopez-Escobar L. 1990. The Nevados de Payachata volcanic region (18° S, 69° W, N. Chile) II. Evidence for widespread crustal involvement in Andean magmatism. Contrib. Mineral. Petrol., 105, 412-432.

Davidson J.P. and de Silva S.L. 1995. Late cenozoic magmatism of the Bolivian Altiplano. Contrib. Mineral. Petrol., 119, 387-408.

Déruelle B. 1982. Petrology of the Plio-Queaternary volcanism of the South-Central and Meridional Andes. J. Volcanol. Geothermal Res., 14, 77-124.

Déruelle B., Moorbath S. and Harmon R.S. 1982. Combined Sr–O isotope relationships and petrogenesis of Andean volcanics of South America. Nature 302, 814-816.

Déruelle B. 1991. Petrology of Quaternary shoshonitic lavas of northwestern Argentina. *In*: R.S. Harmon and C.W. Rapela (eds), Andean magmatism and its tectonic setting. *Geol. Soc. Amer. Spec. Paper*, 201-216

Déruelle B. 1994. Volcan Puntas Negras and Cordón Puntas Negras (northern Chile) : petrology and geochemistry of minor eruptive centers. 7° Congr. Geol. Chileno, Concepción, Univ . Concepción, 1029-1033.

Hörmann P.K., Pichler H. and Zeil W. 1973. New data on the young volcanism in the Puna of NW-Argentina. Geol. Rundsch. 62, 397-418.

Kontak D.J., Clark A.H., Farrar E. and Pearce T.H. 1986. Petrogenesis of a neogene shoshonite suite, Cerro Moromoroni, southeastern Peru. Canadian Mineral. 24, 117-135.

Lefèvre C. 1973. Les caractères magmatiques du volcanisme plio-quaternaire des Andes dans le sud du Pérou. Contrib. Mineral. Petrol. 41, 259-272.

Soler P. and Jimenez Ch. N. 1993.Magmatic constraints upon the evolution of the Bolivian Andes since late Oligocene times. Second ISAG, Oxford (UK), ORSTOM Ed., Coll. Colloques et Séminaires, Paris, 447-452.

Wörner G., Harmon R.S., Davidson J.P., Moorbath S., Turner D.L., McMillan N.J. and Nye C. 1988. The Nevados de Payachata volcanic region (18° S, 69° W, N. Chile) I. Geological, geochemical and isotopic observations. Bull. Volcanol. 50, 287-303.

Xu Y.-G., Ross J.V. and Mercier J.-C. 1993. The upper mantle beneath the continental rift of Tanlu, Eastern China: evidence for the intra-lithospheric shear zones. Tectonophysics 225, 337-360.

# LICANCABUR, AN ANDESITIC VOLCANO OF THE SOUTH-CENTRAL ANDES

Oscar FIGUEROA A.(1) and Bernard DÉRUELLE(2)

(1) Departamento de Ciencias de la Tierra, Universidad de Concepción, Casilla 3-C, Concepción, Chile.
(2) Laboratoire de Magmatologie et Géochimie Inorganique et Expérimentale,
Université Pierre et Marie Curie, 4, Place Jussieu, Paris, France.

KEYWORDS : Licancabur volcano, Andesites, South-Central Andes, magma mixing.

## INTRODUCTION

Licancabur volcano (22°56' S, 67°53' W) is located in the Central Volcanic Zone (CVZ) of the Andes, on the Chilean-Bolivian boundary (fig. 1). It looks like a 1500 m high almost perfect cone, 9 km base diameter, and a constant slope of 30°. The total volume of the cone is 35 $Km^3$. Due to its location on the border of the Altiplano which dips in Chile towards the Salar de Atacama pull-apart basin, the western flank is better developed than the eastern one. Although this volcano is one of the most famous in Chile and Bolivia, it has not been yet the object of a detailed geological study (Déruelle, 1979; Marinovic and Lahsen, 1984; De Silva and Francis, 1991).

## GEOLOGY

A sketched geological map (fig. 2) based on field work and photo interpretation has been established. Licancabur is built upon Chaxas and La Pacana ignimbrite formations (Gardeweg and Ramirez, 1987). No historical activity has been recorded. Nevertheless all the lava flows are well-preserved and were not affected by glaciations. Some of them present pristine levees and ridges. The oldest lava flows (OLF) occur West and North and are partially covered by the lava flows that built up the cone (CLF). Some OLF are underbedded with pre-caldera Sairecabur lava flows. Avalanche deposits occur west of the cone. Numerous N130° faults, parallel to the Calama–Olacapato–El Toro lineament, affect the Licancabur and Sairecabur basement.

## PETROGRAPHY

The most common phenocryst phase is plagioclase. Orthopyroxene phenocrysts predominate over clinopyroxene ones. Scarce subhedral olivine phenocrysts and/or amphibole, with some Fe-Ti oxides are also present. The basaltic andesite contains olivine phenocrysts (up to 6 mm) which are generally rimmed by orthopyroxene. No biotite has been found at Licancabur.

## MINERALOGY

Olivine phenocrysts generally present normal zoning, with Fo 82 cores and Fo 69 rims. Orthopyroxene phenocrysts are also zoned with En 78 cores and En 70 rims. Clinopyroxene phenocrysts

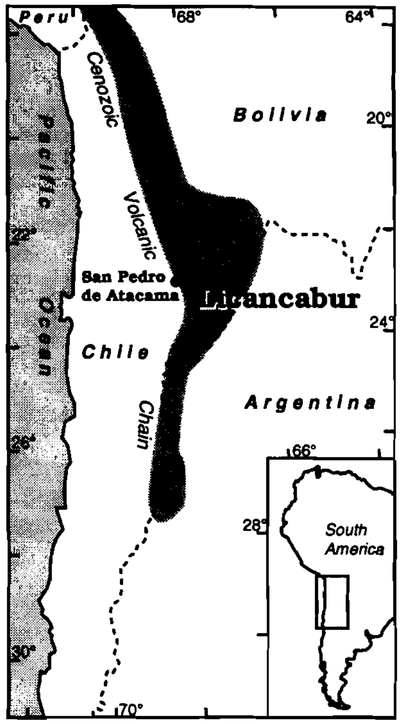


Fig. 1. Location of Licancabur volcano in the Central Volcanic Zone.

Fig. 2. Geological sketch map of Licancabur volcano.

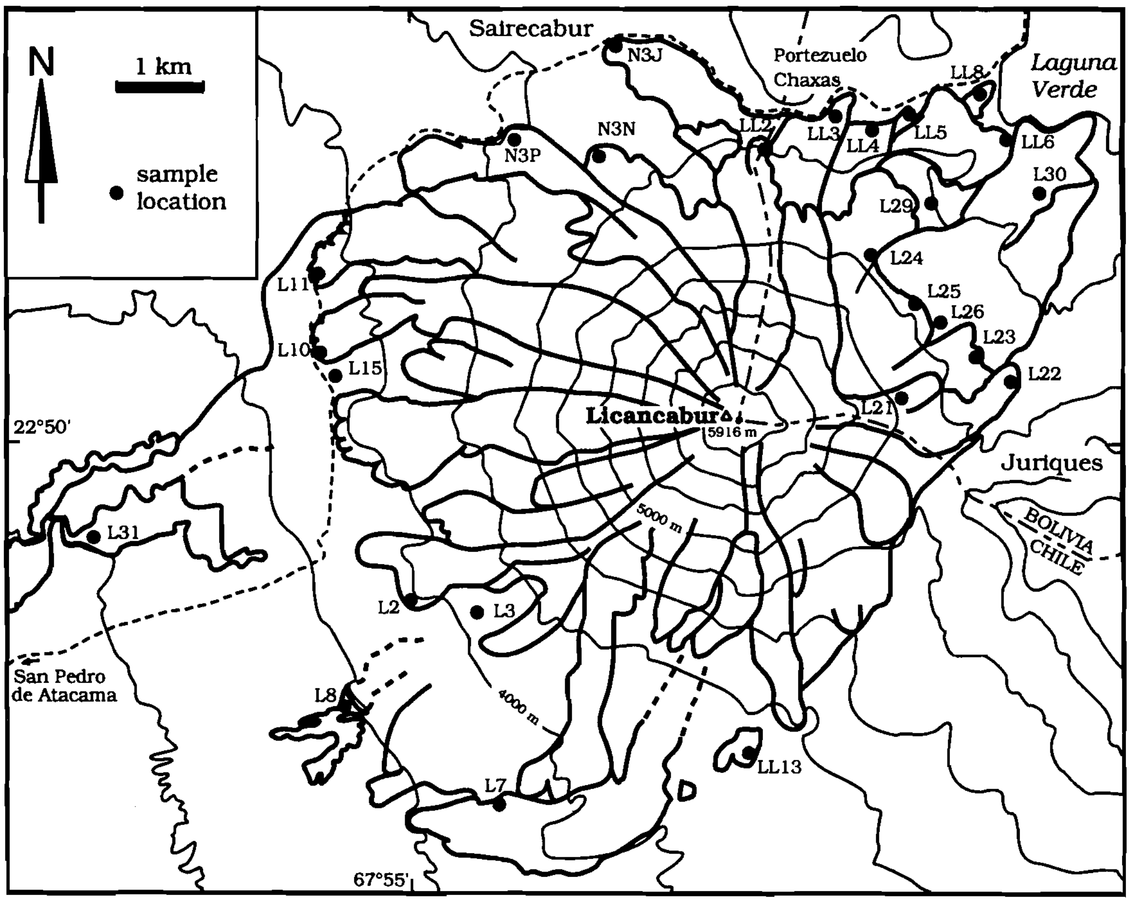

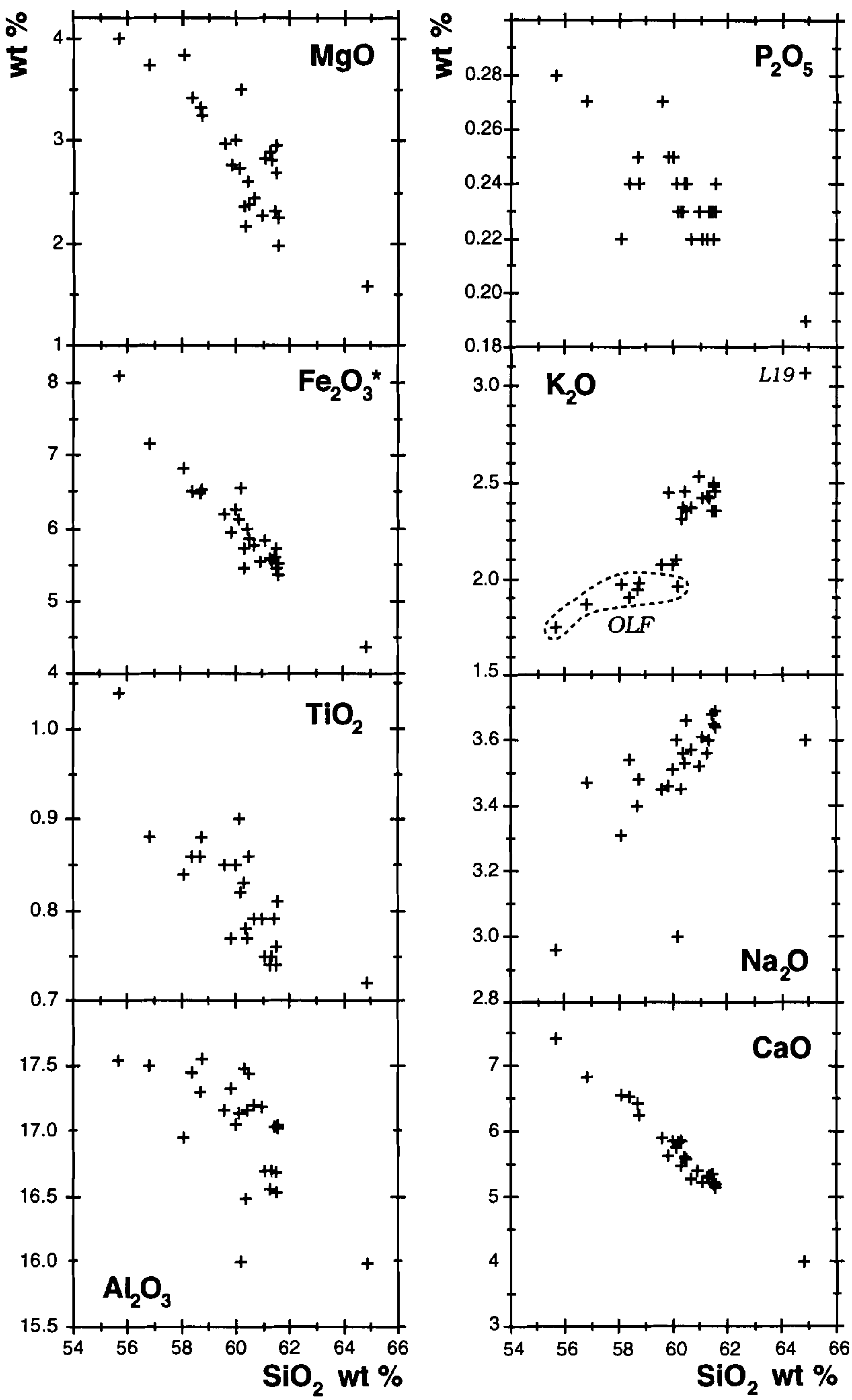


Fig. 3. Harker diagram for Licancabur lavas.

are mainly augite and scarce diopside. Plagioclase phenocryst compositions vary from An 78 to An 52 (core) and An 74 to An 48 (rim). Scarce Mg-hornblende phenocrysts occur in some andesites and the dacite and are commonly rimmed with Fe-Ti oxides, plagioclase and pyroxene crystals. Phenocrysts of titanomagmetite are common whereas ilmenite ones are rare.

## GEOCHEMISTRY

CLF are only andesites (56 < $SiO_2$ wt % < 63) and one dacite (L19, 64.84 $SiO_2$ wt %). OLF are andesites and one basaltic andesite (L31, 55.69 $SiO_2$ wt %). In a Harker diagram (fig. 3), CaO and $Fe_2O_3$ distributions define a clear trend for all the lavas. On the contrary, $TiO_2$, $Al_2O_3$, $Na_2O$, and $P_2O_5$ show a rather scattered distribution. MgO contents permit to well distinguish between OLF (with higher MgO) and CLF. OLF present a good differentiation trend for $K_2O$ (from 1. 7 to 2.2 wt %), whereas CLF are gathered around 2.5 $K_2O$ wt %, except the dacite which has higher $SiO_2$ and $K_2O$ contents. Transition element (Co, Cr, Ni) contents also allow to distinguish between OLF and CLF (fig. 4).

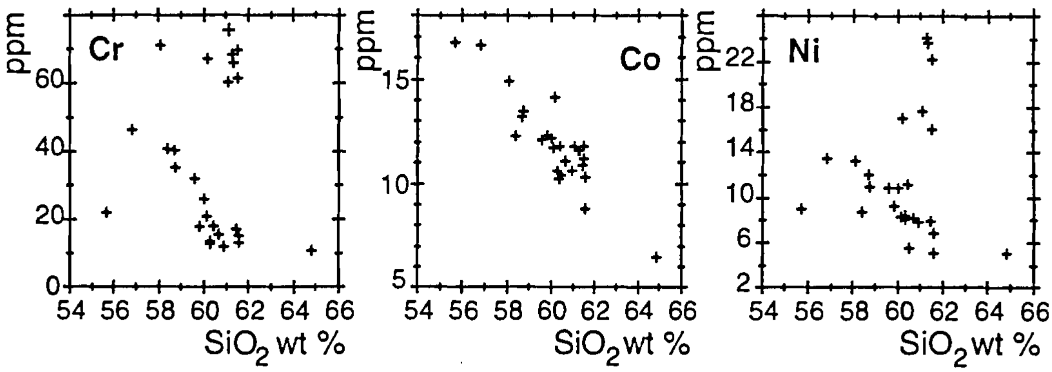


Fig. 4. $SiO_2$ - Cr, - Co, and - Ni diagrams for Licancabur lavas.

## DISCUSSION AND CONCLUSIONS

The geochemical data confirm that OLF and CLF are distinct. OLF are somewhat similar to oldest Sairecabur lavas (Déruelle, 1982) and also to shoshonitic lavas of NW Argentina, which erupted along the Calama–Olacapato–El Toro lineament, and were recognized as the result of magma mixing (Déruelle, 1991). OLF are more basic and richer in transition elements than CLF. An origin of CLF as the result of various steps of mixing between OLF and L15 dacite magmas (see fig. 3, $K_2O$-$SiO_2$) is proposed.

## REFERENCES

Déruelle B. 1979. Pétrologie d'un volcanisme de marge active: Atacama et Andes Méridionales. Thèse Doct. Etat, Univ. Paris-Sud, Orsay, 417 pp.

Déruelle B. 1982. Sairecabur volcano, a Plio-Quaternary calc-alkaline massif of the Andes of Atacama: petrology. Tercer Congr. Geol. Chileno, Depto. Geociencias, Univ. Concepción, Chile, D 20-40.

Déruelle B. 1991. Petrology of Quaternary shoshonitic lavas of northwestern Argentina. *In*: R.S. Harmon and C.W. Rapela (eds), Andean magmatism and its tectonic setting. *Geol. Soc. Amer. Spec. Paper*, 201-216.

De Silva S.L. and Francis P.W. 1991. Volcanoes of the Central Andes, Springer-Verlag, Berlin, 216 pp.

Gardeweg M. and Ramirez C.F. 1987. La Pacana caldera and the Atana ignimbrite—a major ash-flow and resurgent caldera complex in the Andes of northern Chile. *Bull. Volcanol.*, 49, 547-566.

Marinovic N. and Lahsen A. 1984. Hoja Calama, Carta Geol. Chile, 58, Sernageomin, Santiago.

# LATE OLIGOCENE EARLY MIOCENE ALKALINE MAGMATISM IN THE CENTRAL ALTIPLANO OF BOLIVIA

Michel FORNARI (1), Felix ESPINOZA (2), Eddy BALDELLON (2), Pierre SOLER (1)

(1) ORSTOM, UR 13, 213 rue La Fayette, 75480 Paris cedex 10, France
(2) GEOBOL, Servicio Geológico de Bolivia, La Paz, Bolivia

**KEYWORD** : Bolivia, Altiplano, Oligocene, Alkaline, Magmatism

## INTRODUCTION

The Late Oligocene - Early Miocene basic Tambillo lavas are located in the central Altiplano, between the Miocene to Recent subduction related volcanic arc and the Late Miocene–Pliocene peraluminous ignimbritic fields of Morococala and Los Frailes in the Cordillera Oriental (fig. 1). The Tambillo lavas extend for over 80 km, within a NNW–SSE belt, at the Eastern side of the Salar de Uyuni. Nevertheless, equivalent volcanic formations extend as far north as the Bolivia/Peru border. The petrography, and major and trace element characteristics of the lavas evidence alkaline affinities which suggest particular processes in magma generation.

## GEOLOGY AND MINERALOGY

The Tambillo lavas consist mainly of sills, dykes and lava flows; varying from basaltic to andesitic compositions. The hornblendite of Cerro Poke (23.6±1.3Ma) and the andesitic intrusive stock of Yarhui Koya (22.1±0.5Ma) correspond to the same magmatic event.
The sill thickness varies from about 50 cm to 120 m; in the Serrania de Urachata (fig. 2) 15 sills are currently mapped, with a total thickness of 500 m. The sills extend laterally from several kilometers to several tens of kilometers. Each sill shows very homogeneous mineralogy and grain size. Most of the sills are porphyritic; with pyroxene (± 1.5 cm) or plagioclase phenocrysts up to 3 cm.
The dykes strike to the north–east and to the east and rarely to the north. Generally they show finer grain size than the sills; however, sometimes, they contain phenocrysts of

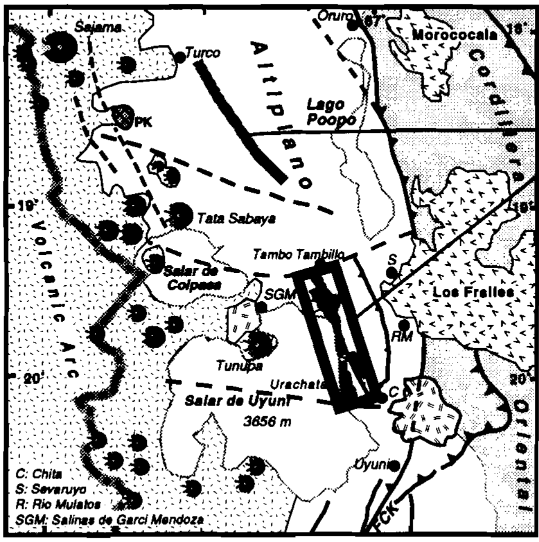


**Fig. 1: Location of the studied area**

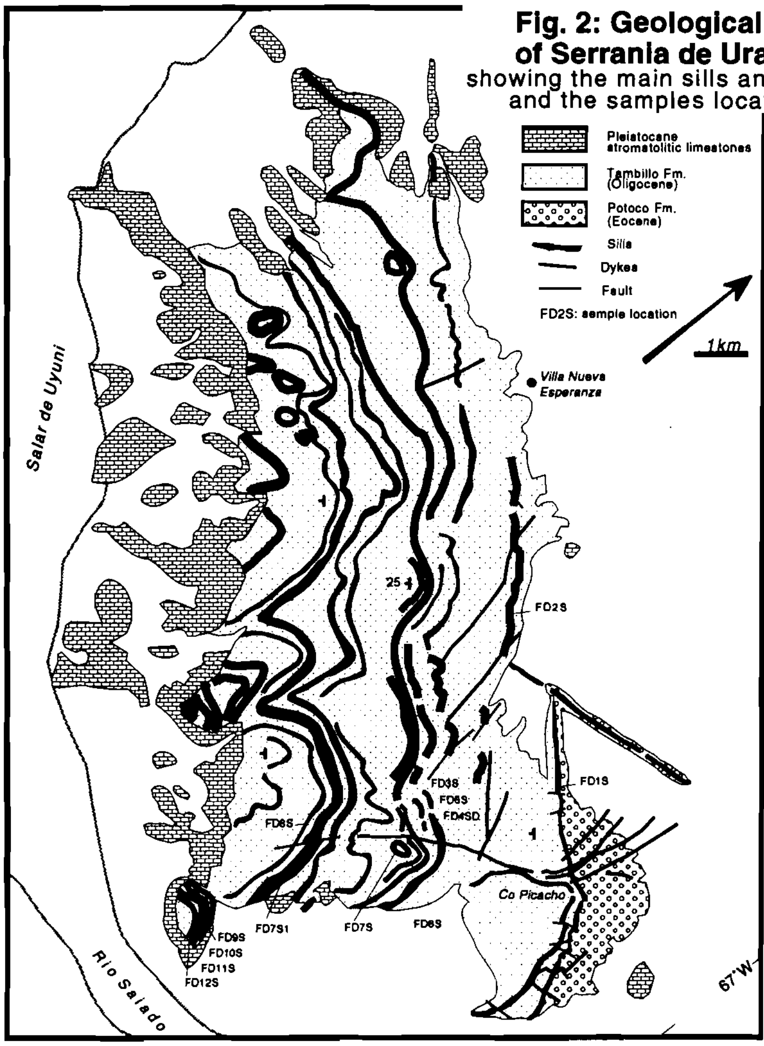


**Fig. 2: Geological map of Serrania de Urachata**
showing the main sills and dykes and the samples location.

pyroxene or biotite up to 1 cm long. Some of the dykes contain millimetric to centrimetric mafic enclaves.

The mineralogy indicates changes with the degree of differentiation; the Tambillo lavas contain abundant olivine in the most basic rocks, augite, calcic plagioclase, opaque minerals, apatite; biotite (phlogopite) and hornblende are more abundant in andesitic lavas. The lavas contains cumulus minerals, which may show resorption borders, evidencing disequilibrium and change during the stages of crystallization.

## GEOCHEMISTRY

The rocks are silica undersatured, olivine- and nepheline-normative with high $K_2O$ (1.2–6%), $TiO_2$ (0.7–2.25%), $P_2O_5$ (0.6–0.9%). The most basic rocks are relatively undifferentiated whereas some sills and dykes define trends with diverse ranges of differentiation, mainly by crystal fractionation.

Incompatible LIL elements rare strongly enriched (up to 1300 ppm of Ba), but the element ratios (e.g., La/Nb, Ba/Nb) and Nb/Y versus Zr/P plot, suggest alkaline affinity rather than subduction related compositions (fig. 3).

The chondrite-normalized patterns of the RRE show enrichment of LREE relative to HREE ($La/Lu_N$ 9–20) with relative flat HREE segment ($Sm/Lu_N$ 2–5) (fig. 4).

## DISCUSSION

Most of the samples show comparable patterns in the normalized spidergram which suggests a derivation from basic parent magmas with small degrees of partial melting of a garnet-bearing lherzolitic mantle source. Trace element compositions apparently preclude large amount of crustal contamination.

As indicated by mineral zoning, cumulus phases, and trends in compatible element plots, etc., the Tambillo lavas result from variable degrees of fractional crystallization of relatively homogeneous magmas.

The presence Oligocene alkaline magmatism located eastward of the calc-alkaline arc appears to be related to particular tectonic setting, with transtensional conditions.

## REFERENCES

Espinoza R.F. 1995. Geologia al Nor Este del Salar de Uyuni. Petrología de las rocas igneas de la Formaci6n Tambillo. Tesis, UMSA, La Paz, Bolivia.

Espinoza R.F., Soler P., Baldellon P. E., Fornari M. 1984. Observaciones de campo, analisis petrografico y geoquimico de las lavas Tambillo. Memorias, XI Congr. Geol. Bol. 282–292

**Fig. 3: normalized incompatible element spidergram of Tambillo lavas**

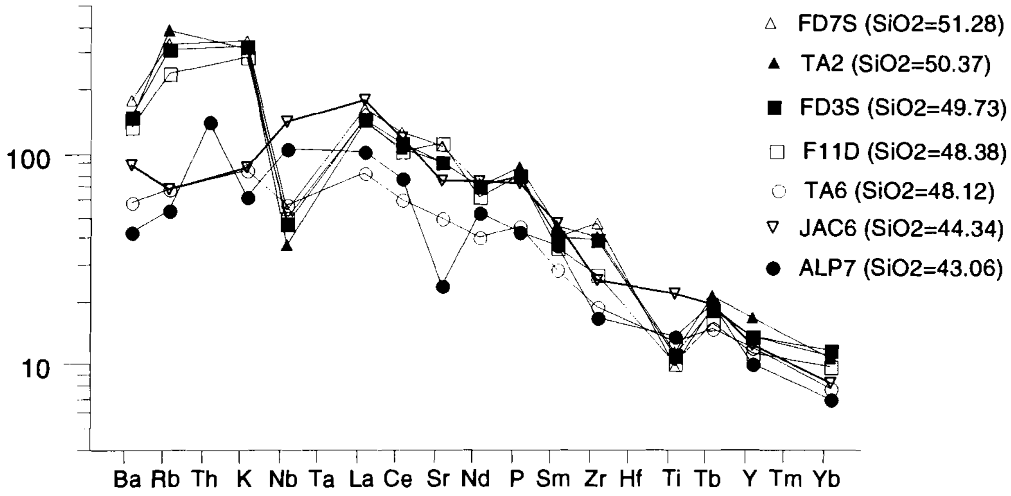


**Fig. 4: REE normalized spidergram of Tambillo lavas**
(note the similarity between samples)

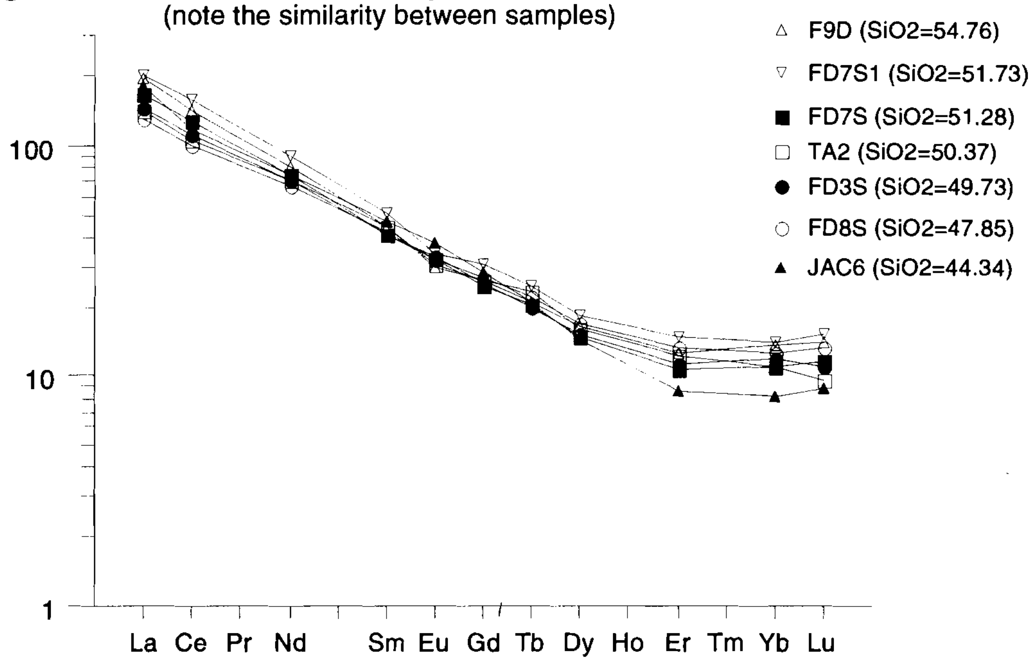

# CHEMICAL CONSTRAINTS ON NEOGENE SLAB WINDOW MAFIC MAGMATISM IN SOUTHERN PATAGONIA

Matthew L. GORRING (1), Suzanne M. KAY (1), and Victor A. RAMOS (2)

(1) Department of Geological Sciences, Snee Hall, Cornell University, Ithaca, NY 14853 USA
(2) Departamento Ciencias Geológicas, Universidad de Buenos Aires, Ciudad Universitaria, 1428 Buenos Aires, Argentina

KEY WORDS: Slab windows, backarc volcanism, ridge collision, Neogene, trace elements, isotopes

## INTRODUCTION

Extensive Neogene Patagonian plateau lavas (46.5° to 49.5°S; Fig. 1) are related to progressive opening of asthenospheric "slab-windows" associated with collisions of segments of the Chile Rise with the Chile Trench at 12 Ma and 6 Ma. Temporal and spatial variations in trace elements (Fig. 2), volumes of erupted magma, and Sr-Nd-Pb isotope ratios (Fig. 3) are consistent with a model in which variable melting percentages are produced by upward flow of an OIB-like, asthenospheric mantle through a northeastward migrating "slab-window" (Fig. 4). The asthenospheric mantle must have been anomalously hot and/or contained volatiles that lowered its melting point to explain the observed melt volumes and the high percentages of partial melting.

## TECTONIC SETTING AND RADIOMETRIC AGE CONSTRAINTS

Abundant Neogene Patagonian mafic plateau lavas occur southeast of the modern Chile Triple Junction (46.2°S), about 100 to 400 km east of the volcanic arc gap between the Southern (SVZ) and Austral Volcanic Zones (AVZ) (Fig. 1). The Late Cenozoic tectonic history of the Chilean margin has been punctuated by the collision of Chile Rise segments with the Chile Trench (Fig. 1). Reconstructions of the oceanic tectonic history (Cande and Leslie, 1986), radiometric age dating of plateau lavas, and kinematic modeling of the subducting Nazca and Antarctic Plates (Ramos and Kay 1992; Gorring et al. submitted) support a model in which these lavas erupted in response to the opening of asthenospheric slab windows that accompanied ridge collisions at 12 and 6 Ma (Figs. 1 and 4). Estimates of Neogene absolute plate motion vectors for South America (Minster and Jordan 1978; Cande and Leslie, 1986) indicate that these lavas do not represent a hotspot track produced by a deep mantle plume. Slab window magmatism is best developed in the backarc where ridge collision occurred at 12 Ma (Fig. 1). In this region, two sequences of slab window lavas have been identified: 1) a voluminous, tholeiitic, Late Miocene to early Pliocene "main-plateau" sequence, and 2) a less voluminous, alkaline, latest Miocene to Quaternary "post-plateau" sequence. A 2 to 5 Ma hiatus separates main- from post-plateau sequences. Both main- and post-plateau lavas postdate ridge collision and become systematically younger (11 to 5 Ma and 7 to 2 Ma, respectively) to the northeast (Fig. 4). The geophysical, geochemical, and radiometric age data fit a slab window model in which main-plateau lavas track the passage of the trailing Nazca Plate edge, and are produced by strong asthenospheric flow into the opening slab window. Post-plateau lavas are produced by weak, upward flow in the slab window when it has fully developed (Fig. 4). Slab windows inferred to have existed south 49.5°S that were associated with mid-Miocene ridge collisions did not produce similar sequences of main-plateau lavas.

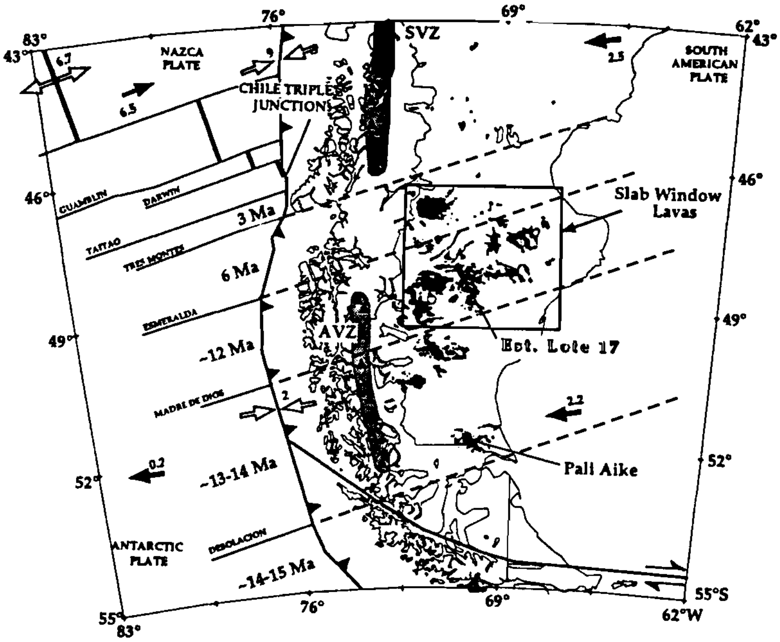


FIGURE 1 - Tectonic map of southern South America showing the distribution of Neogene slab window lavas (boxed area), and relative to other important tectonic features. Timing of ridge collisions (Cande and Leslie 1986) and projected borders of individual slab windows are shown (dashed lines). Important xenolith localities (Pali Aike and Estancia Lote 17) are also shown. Plate motion vectors (open = relative; filled = absolute) from Minster and Jordan (1978).

## TRACE ELEMENT CONSTRAINTS ON SLAB WINDOW MELTING

Main- and post-plateau slab window lavas have OIB-like trace element characteristics ($(La/Yb)_n > 1$, $La/Ta < 20$), are unlike MORB or SVZ arc lavas, and show little evidence for crustal contamination. Both sequences have similar incompatible trace element ratios (Th/La = 0.1 to 0.2, Th/U = 3 to 5), suggesting that the mantle source had relatively homogeneous trace element characteristics, therefore, trace element modeling can provide constraints on source region chemistry and spatial and temporal variations in melting percentages. In order to investigate source chemistry and chemical variability generated by melting percentages, trace element characteristics of these lavas are compared with nonmodal, incremental batch melting models (Fig. 2A-B). A trace element-enriched garnet lherzolite, with 2 to 3x chondritic trace element abundances was used as the source. Trace element content of magmas were corrected for crystal fractionation by adding equilibrium olivine and clinopyroxene until major element compositions were in equilibrium with olivine of $Fo_{90}$, and thus, represent the inferred trace element content of primary magmas. Fractionation-corrected samples match the trend of the melting model well, consistent with an enriched mantle source region with relatively homogeneous trace element characteristics (Fig. 2A).

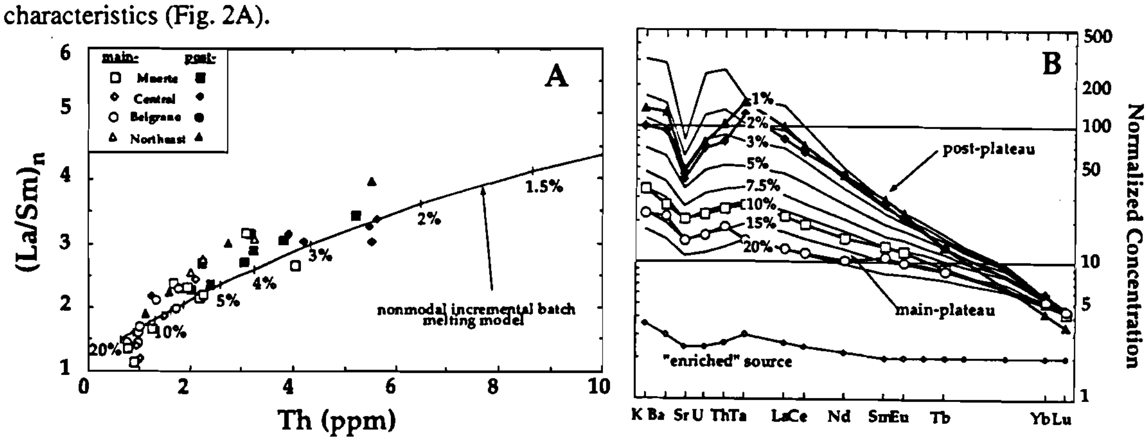


FIGURE 2A-B - Plots showing trace element systematics of fractionation-corrected slab window lavas compared to a nonmodal, incremental batch melting model. Samples in B from the Meseta de la Muerte.

Main- and post-plateau lavas show systematic temporal and spatial chemical variations (Fig. 2A) in a SW-NE transect across the backarc northeast of the 12 Ma ridge collision (Fig. 1). Main-plateau lavas from the southwest and central regions (Mesetas de la Muerte, Central, and Belgrano) can be modeled by the highest melting percentages (6 to 15%), whereas, post-plateau lavas can be modeled by much lower melting percentages (2 to 5%). In contrast, both sequences in the Northeast Region can be modeled by low to intermediate melt percentages (2 to 8%). Major elements ($SiO_2$, $TiO_2$, $K_2O$) correlate well with the trace element variations and with observed eruptive volumes. Depleted HREE signatures indicate garnet is an important residual phase, even at high melting percentages. Melting within the garnet stability field and FeO contents of 9 to 11.5 wt% are consistent with melt generation depths in the 70 to 100 km range based on experimental and theoretical studies in the literature.

## ISOTOPIC CONSTRAINTS ON SLAB WINDOW MAGMA SOURCE REGIONS

Sr, Nd, and Pb isotopic ratios of southern Patagonian slab window lavas have strong affinities with southern hemisphere OIBs with positive Dupal Pb anomalies (Fig. 3A-B) that are interpreted to reflect the OIB-like mantle source. Ranges of isotope ratios are similar for main- and post-plateau lavas ($^{87}Sr/^{86}Sr$ = 0.7036 to 0.7047, $\varepsilon_{Nd}$ = +4.8 to -0.5, $^{206}Pb/^{204}Pb$ = 18.28 to 18.87, $^{207}Pb/^{204}Pb$ = 15.58 to 15.65, and $^{208}Pb/^{204}Pb$ = 38.2 to 38.8). Regionally distinctive features are higher $^{87}Sr/^{86}Sr$ and lower $\varepsilon_{Nd}$ and $^{206}Pb/^{204}Pb$ ratios than for both Neogene slab window lavas from the Antarctic Peninsula (Hole et al. 1995), and Plio-Pleistocene lavas from Pali-Aike (Fig. 1; Stern et al. 1990). Patagonian slab window lavas also have lower $^{87}Sr/^{86}Sr$ ratios at a given $\varepsilon_{Nd}$ than most mafic arc lavas of the southern SVZ (Lopez-Escobar et al. 1993), consistent with the lack of significant contamination by subduction-related fluids. Evidence for crustal components is also lacking in that Sr and Nd isotope ratios do not correlate with parameters sensitive to crustal processes (i.e. $SiO_2$, MgO, Th/La). However, both main- and post-plateau lavas from the east-central backarc have consistently lower $^{206}Pb/^{204}Pb$ ratios than lavas from the western backarc (Fig. 3B). This may reflect minor assimilation of lower crustal components that have distinct Pb isotopic compositions due to variations in basement age. The lack of evidence for large amounts of crustal components indicates that the OIB isotopic signature of these lavas is subcrustally derived. Based on the relatively "depleted" Sr-Nd isotopic signature of southern Patagonian mantle xenoliths thought to represent the lithosphere (Stern et al. 1989; Fig. 3A), the "enriched", OIB-like signature is most likely derived from the asthenosphere.

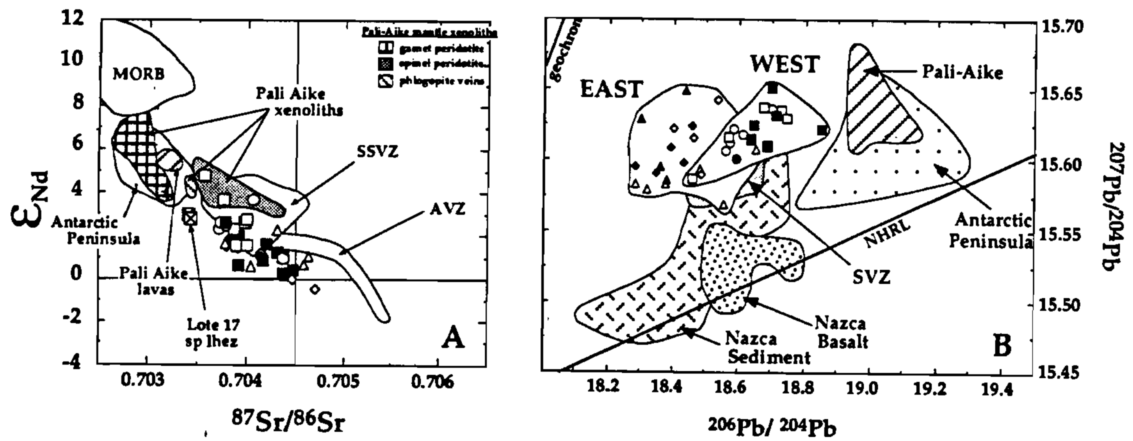


FIGURE 3A-B - Plots showing Sr, Nd, and Pb isotopic data for slab window lavas (symbols as in Fig. 2). Fields for other volcanics and lithospheric xenoliths are from the literature and our unpublished data. NHRL is the Northern Hemisphere Reference Line.

## IMPLICATIONS FOR THE SOUTHERN PATAGONIAN SLAB WINDOW MODEL

The geochemical data fit a slab window model in which main-plateau lavas track the passage of the trailing Nazca Plate edge and are produced by strong asthenospheric flow (Fig. 4). Spatial and temporal variations in major and trace elements document a northeastward decrease in percent partial melting, total volumes of melt produced, and average depth of melting that generated the main-plateau sequence. This is consistent with 1) thicker lithosphere beneath the eastern backarc, and 2) suppression of slab window flow as the plate edge is subducted to greater depths. Post-plateau lavas erupt when the slab window is fully developed and are produced by weaker, residual slab window flow (Fig. 4) and show little significant spatial or temporal variation, suggesting that percentages and depths of melting were similar across the backarc. Based on trace element modeling and FeO contents, and estimates of lithospheric thicknesses, melt generation and final equilibration would have occurred in the asthenosphere, at depths of 70 to 100 km. Thus, the Sr, Nd, and Pb isotope ratios of southern Patagonian slab window lavas are interpreted to reflect a dominant OIB-like, asthenospheric source. Two models could explain OIB-like asthenospheric mantle beneath southern Patagonia: 1) the entrainment of a pre-existing, weak plume-like feature (Fig.

4), or 2) ambient OIB-like asthenosphere. The plume entrainment model simultaneously solves the OIB-like asthenospheric chemistry, high temperatures required for anhydrous, high-P magma generation, the large volumes of high percentage melts, and the lack of mid-Miocene slab window lavas south of 49.5°S. In contrast, an ambient OIB-like asthenosphere model eliminates the need for plumes, but requires a $H_2O$- or $CO_2$-bearing mantle source to produce melts of peridotite at normal mantle temperatures. In this case, asthenosphere south of 49.5°S would have been relatively cool and dry compared to the north in order to explain the lack of mid-Miocene slab window lavas there.

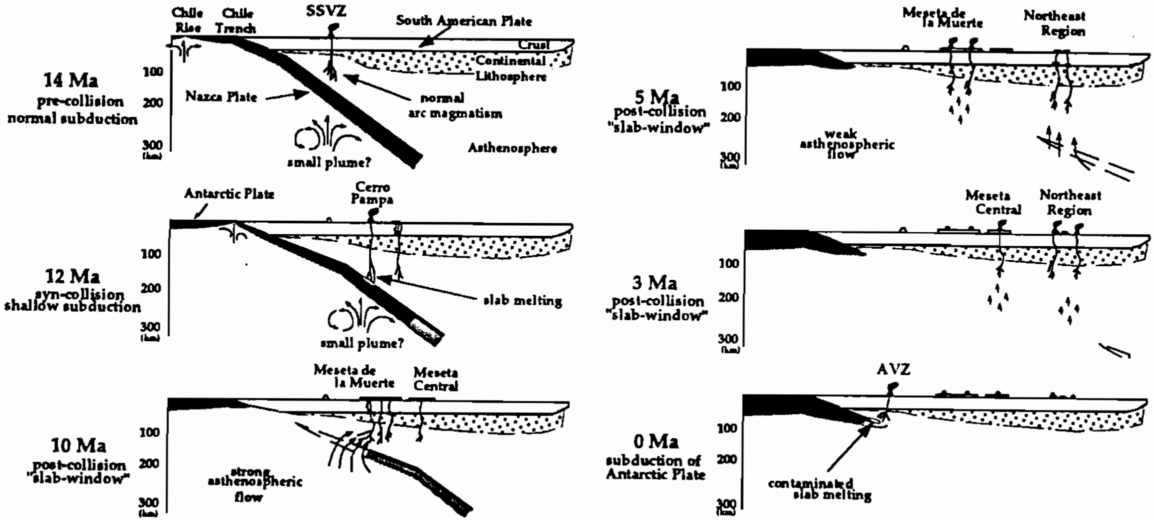


FIGURE 4 - Cross-sections showing slab window magmatic evolution for the region northeast of where the Chile Rise collided at 12 Ma. Active and inactive main- and post-plateau sequences are shown as filled and open surface features, respectively (rectangles = main-plateau; cones = post-plateau).

## REFERENCES


Cande, S.C., R.B. Leslie, 1986. Late Cenozoic tectonics of the Southern Chile Trench. *J. Geophys. Res.*, 91, 471-496.

Gorring, M.L., S.M. Kay, P.K. Zeitler, V.A. Ramos, 1995. A slab window origin for Neogene Patagonian plateau lavas (46.5° to 49.5°S). submitted to Tectonics

Hole, M. J., A.D. Saunders, G. Rogers, M.A. Sykes, 1995. The relationship between alkaline magmatism, lithospheric extension and slab window formation along continental destructive plate margins. in Volcanism associated with Extension at Consuming Plate Margins, Geol Soc. Lond. Spec. Pub. 81, edited by J.L. Smellie, p. 265-285.

López-Escobar, L., R. Kilian, P.D. Kempton, M. Tagiri, 1993. Petrography and geochemistry of Quaternary rocks from the Southern Volcanic Zone of the Andes between 41°30' and 46°00', Chile. *Rev. Geol. Chile*, 20, 33-55.

Minster, J.B., T.H. Jordan, 1978. Present-day plate motions. *J. Geophys. Res.*, 83, 5331-5354.

Stern, C. R., S. Saul, M.A. Skewes, K. Futa, 1989. Garnet peridotite xenoliths from the Pali-Aike alkali basalts of southernmost South America. in Kimberlites and Related Rocks, edited by J. Ross et al., Perth, Blackwell Scientific, p. 735-744.

Stern, C. R., F.A. Frey, K. Futa, R.E. Zartman, Z. Peng, T.K. Kyser, 1990. Trace element and Sr, Nd, Pb, and O isotopic composition of Pliocene and Quaternary alkali basalts of the Patagonian Plateau lavas of southernmost South America. *Contrib. Min. Petrol.*, 104, 294-308.

Ramos, V. A., S.M. Kay, 1992. Southern Patagonian plateau basalts and deformation: backarc testimony of ridge collision. *Tectonophys.*, 205, 261-282.


This project supported by the US National Science Foundation (EAR-9219328), the Geological Society of America (5156-93), the Servicio Geológico Nacional de Argentina, and the Cornell Chapter of Sigma Xi. This paper is a contribution to IGCP project 345.

# MAGMATIC RESPONSES TO ACTIVE SPREADING RIDGE SUBDUCTION : MULTIPLE MAGMA SOURCES IN THE TAITAO PENINSULA REGION (46°-47°S, CHILE TRIPLE JUNCTION).

Christèle GUIVEL (1), Yves LAGABRIELLE (1), Jacques BOURGOIS (2), René MAURY (1), Hervé MARTIN (3), Nicolas ARNAUD (3), Joseph COTTEN (1).

(1) URA 1278, Université de Bretagne Occidentale, 6, Avenue Le Gorgeu, 29287 Brest Cédex, France.
(2) CNRS, Université Pierre et Marie Curie, Boîte 119, 4, place Jussieu, 75252, Paris Cedex 05, France.
(3) URA 10, Université Blaise Pascal, 5, rue Kessler, 63038, Clermont-Ferrand, France.

**KEY WORDS :** Ridge subduction, forearc magmatism, contamination, slab melting sources.

## INTRODUCTION

During the Pliocene, the subduction of the Chile ridge beneath the South American margin was coeval with the emplacement of magmatic suites and possible ophiolite obduction close to the trench axis (Taitao Peninsula). The chemical characteristics of the plutons and volcanic rocks indicate that magmas originated either from mantle sources, or from slab melting, or directly from the subducted spreading center interacting with the overlying Chile margin continental crust.
Based on field data and geochemical characteristics, 5 categories of magmatic products can be distinguished among the plutonic-volcanic suites exposed in the Taitao region.

**1. The Bahia Barrientos ophiolite.** The Bahia Barrientos ophiolite includes mantle peridotites, gabbros and rare doleritic dikes. The gabbros show depleted N-MORB REE pattern (i, fig.2). Precise geochronological data from the ophiolitic rocks are not available yet, 2 K/Ar ages around 13 Ma and 6 Ma have been obtained on a hornblendite vein and a doleritic dike respectively (Bourgois et al., 1993; Le Moigne, 1994). Elements of the ophiolite complex are also found as exotic fragments of various size included in later intrusions. Gabbros and doleritic lenses are included in the Seno Hoppner pluton. Dolerites are present as inclusions in granodiorite magmatic breccias well exposed along the western coast of the Tres Montes Peninsula. Numerous decametric fragments of gabbros and dolerites are included in the acidic dike complex exposed in the central part of the Taitao Peninsula.
**2. The volcano-sedimentary units.** The Pliocene Chile Margin unit (CMU) (Fig. 1), 4-6 km thick, consists of interbedded sedimentary and volcanic material showing numerous evidences for deposition in shallow-water environment. It unconformably overlies the pre-Jurassic metamorphic basement of the Chile margin. The Main Volcanic Unit (MVU) consists of pillow-lavas and associated sediments that accumulated also in a shallow water environment. It differs from the CMU by a well developped greenschist metamorphic overprint and the lack of pyroclastic material. The MVU and CMU flows show a large range of composition including N-MORB, E-MORB, and calc-alkaline lavas (h,k,l, fig. 2). The MVU and CMU volcanic suites result of eruptions of magmas originating from the downgoing active spreading center buried at shallow depths, and uprising through the Chilean continental basement. These magmas were affected by various degrees of upper crustal contamination coupled with fractional crystallization during their ascent and possible storage within the Chilean continental crust (Lagabrielle et al., 1994).
**3. The acidic dike complex (central area).** A sheeted dike complex is exposed in the central part of the Taitao Peninsula. The dikes intruded the gabbros and associated dolerites of the Bahia Barrientos

ophiolite. They show dacitic to rhyolitic compositions and have REE pattern typical of calc-alkaline series (g, fig.2). Polymict volcanic breccias with a rhyolitic matrix exposed in the central part of the dike complex were emplaced subsequently above the previously eroded dikes. They include angular fragments of granite and subordinate coarse grained ophiolitic dolerites (Fig.1).

**4. The Taitao plutonic intrusions.** The plutonic suite includes 5 plutons (Cabo Raper, Seno Hoppner, Bahia Barrientos, Estero Cono and Tres Montes). Contact between intrusions and surrounding units are tectonic at many localities, but primary magmatic relationships are preserved locally. Granite fragments present within the rhyolite breccias (Fig. 1) belong to the plutonic suite. The Cabo Raper pluton, located less than 17 km landward from the trench axis, is a biotite and hornblende bearing granodiorite. K/Ar data on separate biotite from two samples yield ages of 5±1 Ma and 4.8±0.3 Ma. The chemical characteristics of the Cabo Raper pluton and samples from the Tres Montes intrusives are similar to those of adakitic or TTD suites which are believed to derive from partial melting of metabasalts under amphibolite-eclogite transition PT conditions (Kay et al., 1993). The Seno Hoppner pluton is a fine to medium grained granite. It displays typical characteristics of calc-alkaline series and most probably originated from the partial melting of the forearc mantle wedge. K/Ar ages obtained from biotite and feldspar are 5.9±0.5 Ma and 6.8±0.2Ma respectively. The present day location of the intrusions at less than 30 km from the trench axis is a possible result of strong tectonic erosion in relation with ridge-subduction (Bourgois et al, in press).

**5. The Pliocene volcanic edifices.** Volcanic and hypo-volcanic edifices (volcanoes, stocks, calderas) are present in the eastern part of the studied area in a region lacking extensive deformation. Radiometric ages obtained on two edifices (Pan de Azucar, the Fiordo San Pedro Caldera) range from 3.8±0.8 Ma to 5.1±1.3 Ma (Mpodozis, 1985). The geochemical compositon of the Pan de Azucar and Fiordo San Pedro volcanoes are similar to that of the Cabo Raper pluton with typical HREE low values.

## CONCLUSION

The Mio-Pliocene Taitao magmatic suites are characterized by a wide range of chemical affinities and display a large number of possible sources (MORBs, contaminated MORBs, slab melting-derived magmas, calc-alkaline magmas). The origin of the various magmatic component is closely linked to the active ridge subduction which occured between 6 and 2 Ma. The Taitao Peninsula units allow to better constrain (1) the sources of near-trench plutons and associated volcanic rocks, (2) the massive removal of forearc material from the overriding plate, both being two major consequences expected from spreading-ridge subduction.

## REFERENCES


Bourgois, J., Martin, H., Lagabrielle, Y., Le Moigne, J., and Frutos Jara, J., Subduction-erosion related to spreading-ridge subduction : Taitao Peninsula (Chile margin triple junction area). *Geology*. in press.

Bourgois, J., Lagabrielle, Y., Le Moigne, J., Urbina, O., Janin, M.C., and Beuzart, P., 1993a, Preliminary results of a field study of the Taitao ophiolite (Southern Chile): Implications for the evolution of the Chile triple junction: Ofioliti, v. 18, p. 113-129.

Cande, S.C., and Leslie, R.B., 1986, Late Cenozoic tectonics of the southern Chile trench: Journal of Geophysical Research, v. 91, p. 471-496.

Forsythe, R.D., Nelson, E.P., Carr, M.J., Kaeding, M.E., Hervé, M., Mpodozis, C.M., Soffia, M.J., and Harambour, S., 1986, Pliocene near trench magmatism in southern Chile: A possible manifestation of ridge collision: Geology, v. 14, p. 23-27.

Lagabrielle, Y., Le Moigne, J., Maury, R.C., Cotten, J., and Bourgois, J., 1994, Volcanic record of the subduction of an active spreading ridge, Taitao peninsula (southern Chile): Geology, v. 22, p. 515-518.

Le Moigne, J., 1994. Subduction d'une dorsale océanique active : géologie des ophiolites de Taitao (point triple du Chili). Thèse de doctorat, Universté de Bretagne Occidentale, Brest.

Mpodozis, C.M., Hervé, M., Nasi, C., Soffia, M.J., Forsythe, R.D., and Nelson, E.P., 1985, El magmatismo plioceno de Peninsula Tres Montes y su relacion con la evolucion del punto triple de Chile austral: Revista Geológica de Chile, v. 25-26, p. 13-28.

Kay, S.M., Ramos, V.A., and Marquez M., 1993, Evidence in Cerro Pampa volcanic rocks for slab-melting prior to ridge-trench collision in southern south America: The Journal of Geology, v. 101, p. 703-714.

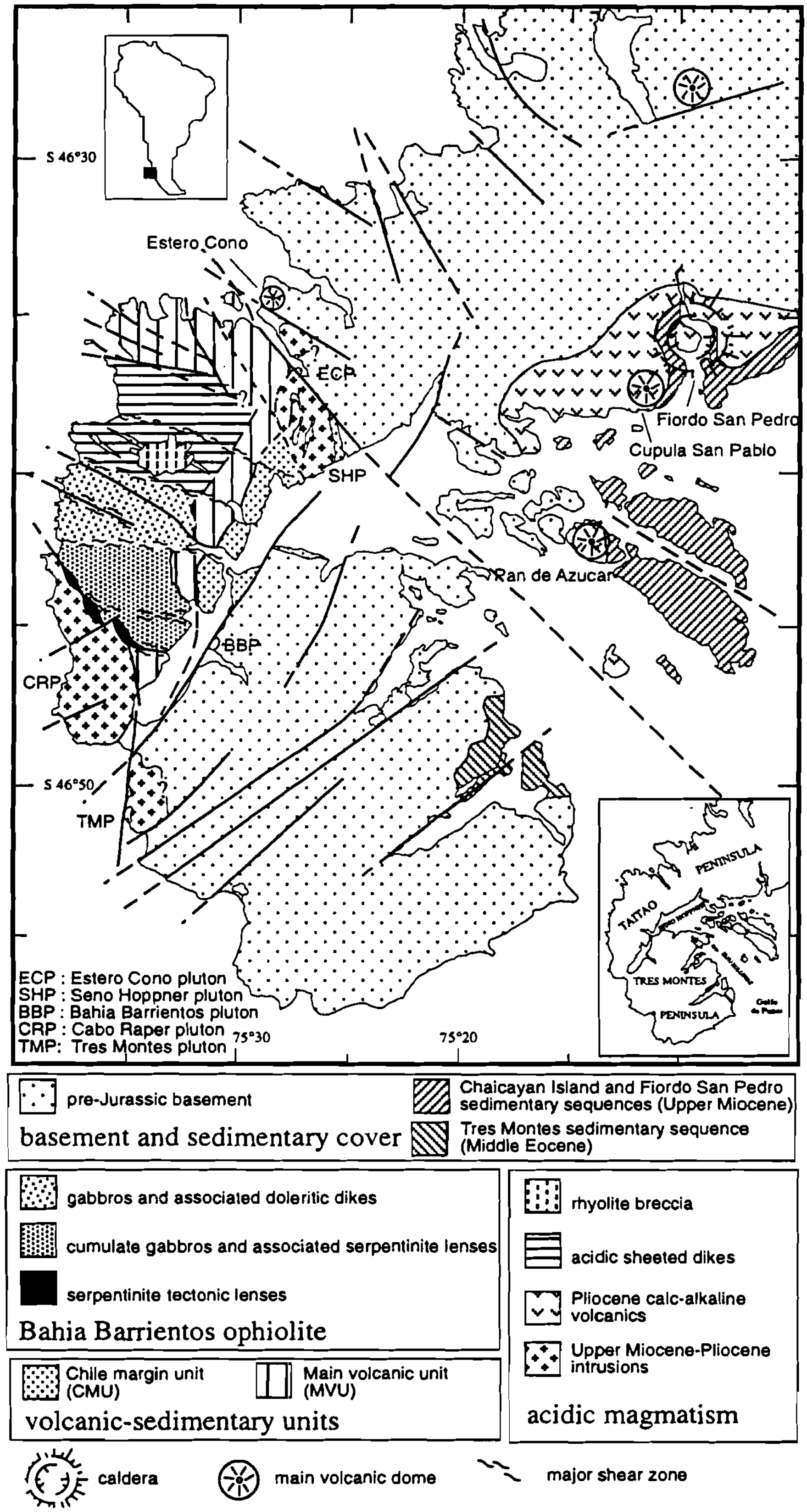


Fig. 1 : Preliminary geological map of the Taitao and Tres Montes Peninsula.

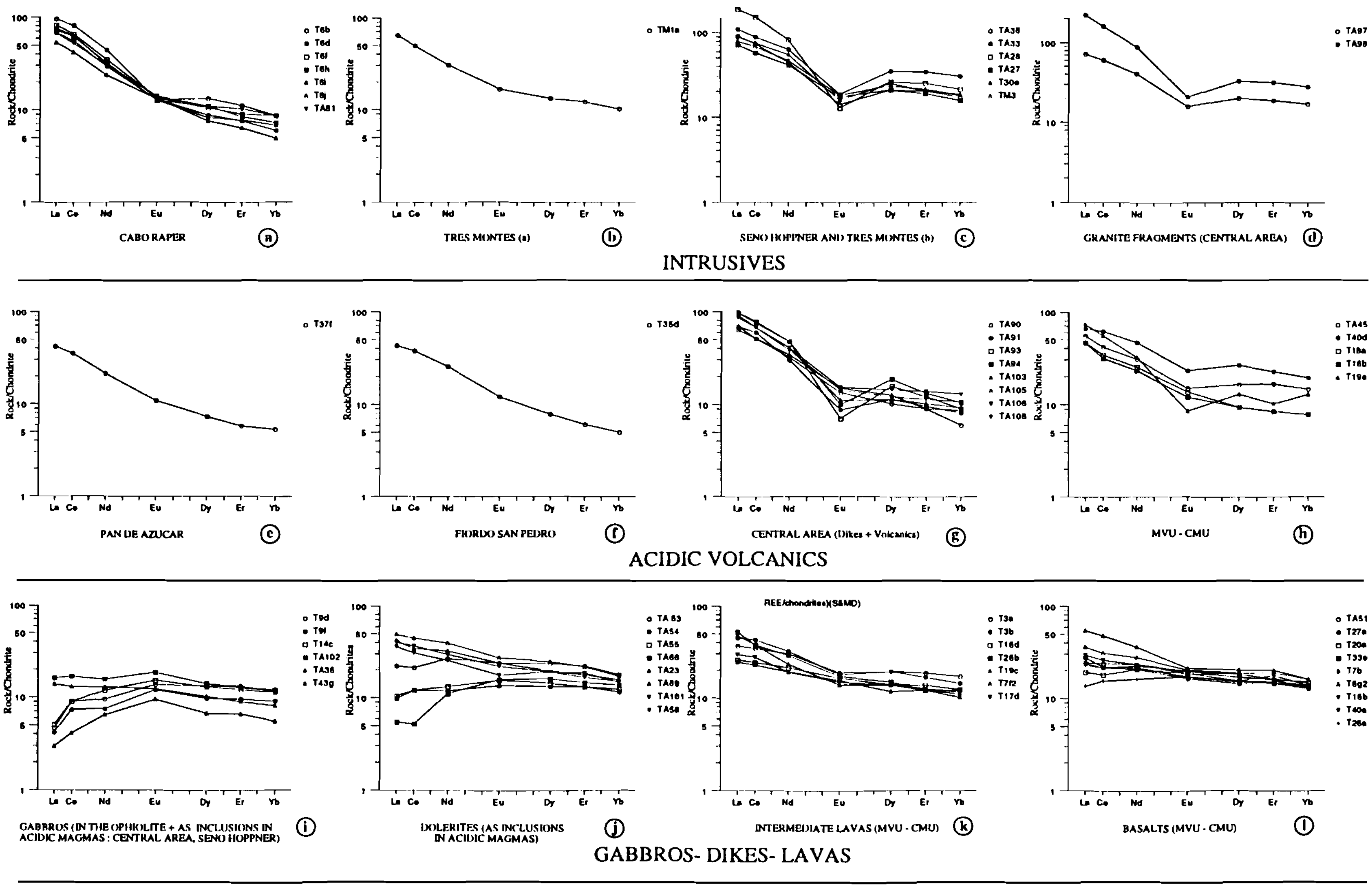


Fig. 2 : Rare Earth Element diagram

Normalization values : Sun and Mac Donough, 1989

# AGE AND Al-IN-HORNBLENDE GEOBAROMETRY IN THE NORTH PATAGONIAN BATHOLITH, AYSEN, CHILE.

Francisco HERVE (1), Robert PANKHURST (2), Alain DEMANT (3), Elisa RAMIREZ (1)

(1) Departamento de Geología, Universidad de Chile, Casilla 13518, Correo 21, Santiago-CHILE
(2) British Antarctic Survey, High Cross, Cambridge CB3 0ET, UK
(3) Laboratoire de Petrologie Magmatique-URA 1277 CNRS, Université de Marseille III, FRANCE

**KEY WORDS**: North Patagonian Batholith, Aysén, geochronology, geobarometry, uplift-rates

## Introduction

The North Patagonian Batholith is a complex elongated batholith in the Andes of Southern Chile, parallel to the continental margin and forming the basement of the present day volcanic arc. In the Aysén region (43° to 47°S Lat.), it is >100 km wide, and exhibits a marked E–W age zonation. Pressures of crystallization, determined mainly by the Al-in-hornblende geothermometer, are presented and compared with the ages of crystallization determined by the Rb-Sr whole-rock method. The pattern of calculated uplift/denudation rates is related to the tectonics of the continental margin.

## Geochronology

A summary of available geochronological data for the granitoids of Aysén was presented by Pankhurst and Hervé (1994), revealing a systematic spatial distribution of ages within the batholith. The western margin of the batholith is of Early Cretaceous age, particularly in the southern part of the area. The eastern margin of the batholith is mainly mid-to-Late Cretaceous, although Early Cretaceous ages are also present in the northern area and plutons with ages close to 10 Ma also occur as satellite bodies to the east of the main batholith. The median zone is characterised by plutonic events at ca. 45 Ma, 25–15 Ma and 10 Ma or less, representing discrete stages in the establishment of the present-day subduction regime (Pankhurst et al., 1995).

## Geobarometry

Crystallization pressures were calculated from electron microprobe analysis of hornblendes from 18 samples (Schmidt, 1992). All samples contained the buffer mineral association prescribed for valid calibration of the method. Geothermometric determination (Blundy and Holland, 1990) indicated essentially magmatic temperatures of mineral equilibration in all samples (600–774°C). Spatial distribution of samples was limited by the compositional and sampling restrictions. The results are shown in

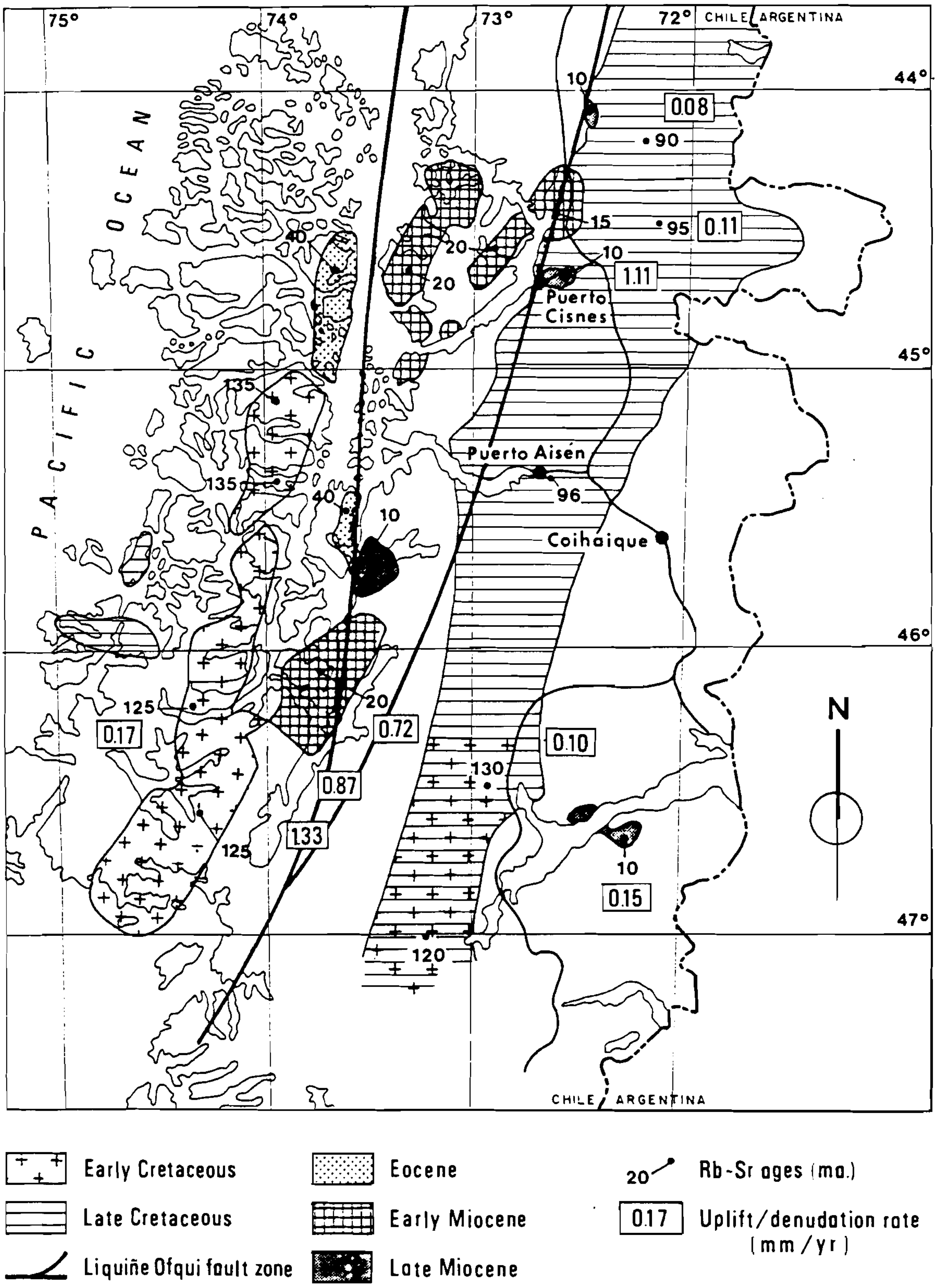
75°
74°
73°
72°
CHILE ARGENTINA
44°
45°
46°
47°
PACIFIC OCEAN
Puerto Cisnes
Puerto Aisén
Coihaique
N
0.08
0.11
1.11
0.10
0.15
0.17
0.72
0.87
133
Early Cretaceous
Late Cretaceous
Liquiñe Ofqui fault zone
Eocene
Early Miocene
Late Miocene
Rb-Sr ages (ma.)
Uplift/denudation rate (mm/yr)

Table 1, together with calculated average uplift rates asuming the indicated ages of crystallization of the magmas. The suggested error in calculated pressures is ±0.5 kb (i.e. 1.9 km in terms of depth). Most of the samples were collected at sea level, those inland were at altitudes less than 0.7 km.

| | Pressure (kb) | Depth (km) | Age (Ma) | Uplift/ denudation rate (mm/yr) |
|---|---|---|---|---|
| **Eastern Margin** | | | | |
| Lago Verde | 1.9 | 7.0 | 88 | 0.08 |
| Rio Toqui | 2.8 | 10.4 | 96 | 0.11 |
| Rio Murta | 3.5 | 12.9 | 130 | 0.10 |
| Las Llaves | 0.4 | 1.5 | 10 | 0.15 |
| **Central Part** | | | | |
| Rio Cisnes | 3.0 | 11.1 | 10 | 1.11 |
| Bahia Erasmo | 4.7 | 17.4 | 20 | 0.87 |
| Bahia Erasmo | 7.2 | 26.6 | 20 | 1.33 |
| Bahia Exploradores | 3.9 | 14.4 | 20 | 0.72 |
| Rio Palena* | 4.2 | 15.5 | 5 | 3.11 |
| Cholgo* | 4.8 | 17.8 | 10 | 1.78 |
| Rio Mariquita* | 2.3 | 8.5 | 10 | 0.85 |
| **Western Margin** | | | | |
| Estero Vidal | 5.6 | 20.7 | 124 | 0.17 |

**Table 1.** Pressure, depth and uplift/denudation rates as determined in this study. Pressures are averages for 2 to 6 hornblende analyses for each sample (Lago Verde is an average of 5 samples). Pressure for Rio Cisnes was derived on phengite. An asterisk (*) denotes samples from north of the area of Fig. 1.

## Discussion and conclusions

The crystallization pressures obtained are within middle to upper crustal range, consistent with the epizonal to mesozonal characteristics of the studied intrusive rocks. The shallowest intrusions are those of Lago Verde and Paso Las Llaves, both of which have well developed miarolitic cavities, considered indicative of shallow emplacement. Pressures determined by fluid inclusion analysis in the Paso Las Llaves pluton (Vargas and Hervé, 1995) are consistent with the Al-in-hornblende results. The rest of the plutons were emplaced at depths greater than 10 km and some more than 20 km.

The average uplift/denudation rates obtained are around 0.1 to 0.2 mm/yr for both western and eastern marginal zones of the batholith. Deeper emplacement of plutons in the western margin is in keeping with their intrusion into Late Palaeozoic metamorphic rocks, whereas those of the eastern margin intrude volcanic sequences deposited over such basement. Thus, the present day exposed margins of the batholith represent different levels of emplacement and erosion.

Average uplift rates one order of magnitude higher (0.7 to 3.1 mm/yr) were calculated for the Tertiary plutons in the central zone of the batholith. Deeper levels of emplacement are also indicated for these plutons (average 16 km) compared to those of the Late Cretaceous eastern margin (10 km). The Miocene plutons are spatially related to the Liquiñe-Ofqui Fault Zone, where tectonic activity has been effective from at least

Mid-Tertiary times (Hervé et al., 1995). Igneous bodies were differentially transported upwards at high rates along this dextral strike slip fault zone in the Late Cenozoic, a feature characteristic of "flower" structures in transpressive environments. This central zone with rapid uplift rates coincides with the present main topographic range of the Andes, for which Holocene uplift rates of 4–10 mm/yr have been independently suggested (Hervé & Ota, 1993).

Uplift/denudation rates for the last 20 Ma are much higher in the Andes of Aysén than in the main Andean cordillera near Santiago (0.15–0.26 mm/yr; Skewes & Holmgren, 1993). In contrast, the height of the range is much greater in the latter area (6 km) than in Aysen (3 km). If subduction parameters were comparable in both areas, climatic difference may have been a factor in allowing and sustaining higher uplift/ denudation rates in Aysén.

**Acknowledgements.** EPMA mineral analysis were performed at Université de Montpellier under the guidance of C. Merlet. The research is part of the project "Evolution of Meso-Cenozoic magmatism and metamorphism in the North Patagonian Andes" (CE contract CII-CT93-0033) and FONDECYT Project 1950544. This is a contribution to Project IGCP 345 "Andean Lithospheric Evolution".

## REFERENCES

Blundy, J.D. & Holland, T.J.B. (1990). Calcic amphibole equilibra and new amphibole-plagioclase geothermometer. Contributions to Mineralogy and Petrology, 104, 208-224.

Hervé, F. & Y. Ota (1993). Fast Holocene uplift rates in the Andes of Chiloé, Chile. Revista Geológica de Chile, 19, 15-23.

Hervé, F., Pankhurst, R.J., Drake, R. & M. Beck (1995). Pillow metabasalts in a mid-Tertiary extensional basin adjacent to the Liquiñe-Ofqui fault zone: The Isla Magdalena area, Aysén, Chile. Journal of South American Earth Sciences, 8, 33-46.

Pankhurst, R.J. & F. Hervé (1994). Granitoid age distribution and emplacement control in the North Patagonian batholith in Aysen, Southern Chile. VII Congreso Geológico Chileno, Concepción. Actas II, v. II, p. 1409-1413.

Pankhurst, R.J., Weaver, S.D. & Hervé, F. (1995). Mesozoic-Miocene granitoid evolution and petrogenesis in Southern Chile. U.S. Geological Survey Circular, 1129, 111.

Schmidt, M. (1992). Amphibole composition in tonalite as a function of pressure: an experimental calibration of the Al-in-hornblende barometer. Contributions to Mineralogy and Petrology, 110, 304-310.

Skewes, M.A. & Holmgren, C. (1993). Solevantamiento andino, erosión y emplazamiento de brechas mineralizadas en el depósito de cobre porfídico Los Bronces, Chile Central (33°S): aplicación de geobarometría de inclusiones fluidas. Revista Geológica de Chile, 20, 71-84.

Vargas, G. & Hervé, F. (1995). Emplazamiento hipabisal mioceno tardío del stock de Paso de Las Llaves en la región de tras arco, Aysén. Universidad de Chile, Depto de Geología, Comunicaciones, No. 46, 3-15.

# CENTRAL ANDEAN MANTLE-DERIVED BASALTS AND NEOGENE MANTLE ENRICHMENT BENEATH THE PUNA PLATEAU

Suzanne Mahlburg KAY(1), Constantino MPODOZIS(2), and Beatriz COIRA(3)

(1) Dept. of Geological Sciences, Snee Hall, Cornell University, Ithaca, NY 14853 USA
(2) Servicio Nacional de Geologia y Mineria, Casilla 10465, Santiago, Chile
(3) CONICET and Universidad Nac. de Jujuy, Casilla 258, (4600) S. S. de Jujuy, Argentina

KEY WORDS: Andean lithosphere, Puna plateau, plateau uplift, primitive magmas, subduction

## INTRODUCTION

A barrier to understanding Andean magmatic source regions and processes in the Puna-Altiplano plateau has been a lack of chemical constraints from primitive and near-primitive mantle-derived magma. The observation is that Miocene and younger magmas erupted through the thickened crust of the plateau show enriched isotopic and trace element signatures. These chemical signatures have been variably ascribed to old enriched mantle, subducted sediment, subducted tectonically eroded forearc crust, in situ crustal contamination, or some combination of these processes (see review by Kay and Abbruzzi 1996). The purpose here is to address the nature and evolution of the mantle source region by examining the chemistry of primitive Plio-Pleistocene and Oligocene mafic magmas from the southern Central Volcanic Zone (CVZ). The data indicate that the Puna mantle has been enriched through the subduction process since the Late Oligocene. The existence of primitive Plio-Pleistocene mafic magmas in the region of highest average elevation in the Central Andes also raises questions as to how dense magmas rise through thickened crust.

## TECTONIC SETTING OF THE MAFIC MAGMAS

The lavas considered here outcrop in the reion of the southernmost CVZ near 27° S (Fig. 1). The Oligocene lavas occur in the forearc of the modern CVZ in the Segerstrom belt (26° 52', 68° 49'). They sit backarc to the main andesitic-dacitic Oligocene volcanic arc (see Kay et al. 1994) and are among the early lavas erupted in the modern Andean magmatic cycle. These lavas constitute one of the scattered occurrences of Oligocene backarc mafic lavas that extend from at least 30° S to 22° S latitude. Two samples yield whole rock K/Ar ages of 24.0±0.9 and 24.3±0.9 Ma. The Plio-Pleistocene magmas erupted some 50 km to the east in the modern CVZ volcanic arc from mafic cinder cones on the flanks of the Incahuasi (top at 6610 m) and San Francisco volcanic centers near 26.9° S, 68.25° W latitude. Their young morphology and their superposition over dacitic lavas on San Francisco dated at 1.2±0.7 Ma limit their age to < 2 Ma. The cinder cones are at a minimum elevation of 5000 m.

These Pleistocene lavas as well as other young Puna basaltic and basaltic andesite lavas have erupted from cinder cones and fissure flows associated with normal/strike slip fault zones. The fault zones separate major crustal blocks and are major zones of crustal weakness. The San Francisco and Incahuasi region flows are some of the mafic flows near the northeast-trending fault zone which includes the Escarpe Robertson fracture of Gonzalez-Ferran et al. (1985) and extends northward towards the elongate, fault-controlled Salar de Antofalla. The most mafic Puna flows are Late Miocene to Pleistocene in age and overlap the most recent period of motion on these

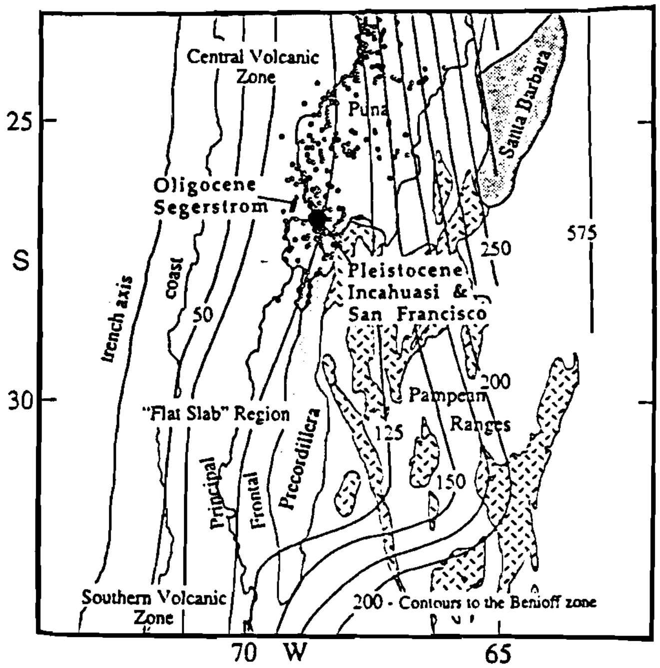


Figure 1. Map of central Andes showing mafic lava sample sites relative to modern tectonic framework. Circles are representative Neogene volcanic centers. Modern active Central Volcanic Zone terminates at Ojos de Salado volcano on southern edge of dot marking location of Incahausi and San Francisco volcanoes.

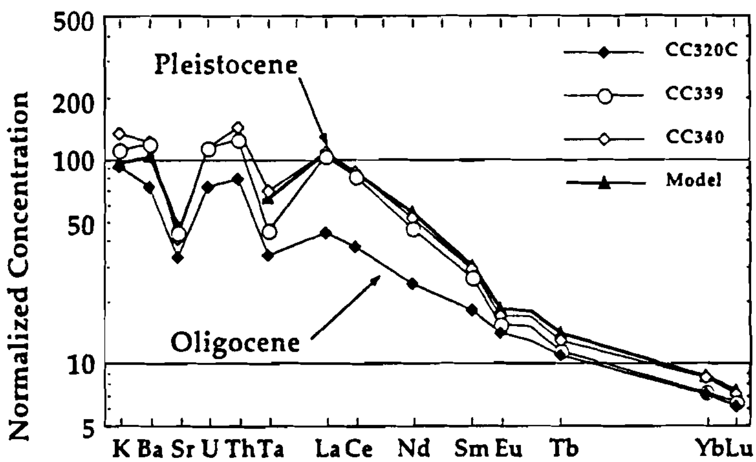


Figure 2 - Extended trace element patterns normalized to MORB for volatile elements and chondrites. Factors (ppm): K (116), Ba (3.77), Sr (14), U (0.015), Th (0.05), Ta (0.02), La (0.378), Ce (0.976), Nd (0.716), Sm (0.23), Eu (0.0866), Tb (0.589), Yb (0.249) and Lu (0.0387). Data in Table 1.

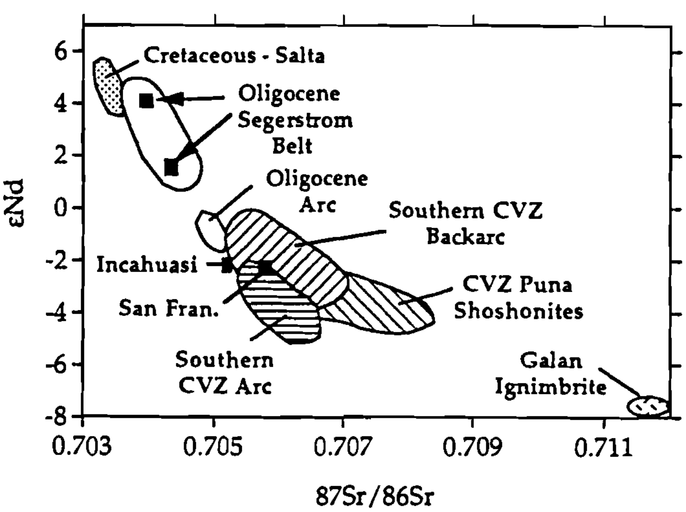


Figure 3 - Plot of $\epsilon$Nd versus $^{87}Sr/^{86}Sr$ for Oligocene Segerstrom and Pleistocene Incahuasi and San Francisco lavas relative to Cretaceous alkaline, Oligocene arc, southern CVZ mafic (<60% $SiO_2$) and Puna shoshonitic lavas, and Cerro Galan ignmibrite to east. Note Incahuasi and San Francisco data overlap southern CVZ mafic lavas. Data from Kay et al. (1994), Kay and Abbruzzi (1996), Francis et al. (1989) and references therein.

faults. Kay et al. (1994) have proposed that this fault motion is genetically linked with catatrophic loss ("delamination") of continental Puna lithosphere since the Late Miocene.

## CHEMISTRY OF THE MAFIC LAVAS: EVIDENCE FOR NEOGENE MANTLE ENRICHMENT AND MIXING WITH PONDED SILICIC MAGMA IN THE THICKENED CRUST

The primitive nature of the Oligocene and Pleistocene lavas whose analyses are shown in Table 1 is indicated by their low FeO/MgO ratios, their high MgO (>9%), Cr (500 to 690 ppm) and Ni (155-200 ppm) concentrations, and their phenocryst populations. In detail, the most mafic Oligocene basalt (CC320c - 49% $SiO_2$) has a higher FeO/MgO ratio (1.0 versus 0.8) and less primitive phenocrysts (olivine - Fo82; clinopyroxene - En46Fs9Wo45; plagioclase - AN72) than the Pleistocene lavas (CC339 and CC340). The Pleistocene lavas are characterized by about 53% $SiO_2$, primitive FeO/MgO ratios (0.77-0.82), primitive phenocrysts (olivine: FO88-89; clinopyroxene: En48Fs8Wo44 - CC339 only) that are in equilibrium with a magma of the whole rock composition, and a lack of plagioclase phenocrysts.

Table 1 - COMPOSITIONS OF NEAR PRIMITIVE PUNA MAGMAS

| | Oligocene | Pleistocene | | | |
|---|---|---|---|---|---|
| | Segerstrom | Incahuasi | San Fran. | Model* | L. Verde |
| SAMPLE | CC320C | CC339 | CC340 | Magma | LV364 |
| $SiO_2$ | 49.18 | 53.55 | 53.08 | 48.49 | 74.00 |
| $TiO_2$ | 1.24 | 0.90 | 1.19 | 1.39 | 0.30 |
| $Al_2O_3$ | 15.32 | 14.80 | 14.81 | 15.12 | 13.39 |
| FeO | 9.64 | 7.22 | 7.40 | 8.72 | 1.28 |
| MnO | 0.14 | 0.13 | 0.15 | 0.17 | 0.06 |
| MgO | 9.09 | 9.36 | 8.99 | 10.88 | 0.36 |
| CaO | 10.18 | 8.33 | 8.36 | 9.91 | 1.29 |
| $Na_2O$ | 2.73 | 2.97 | 3.14 | 2.96 | 3.97 |
| $K_2O$ | 1.29 | 1.57 | 1.86 | 1.36 | 4.16 |
| $P_2O_5$ | 0.31 | 0.28 | 0.31 | 0.35 | 0.15 |
| Volatiles | 0.43 | | | | 0.45 |
| Total | 99.55 | 99.11 | 99.29 | 99.35 | 99.41 |
| La | 16.9 | 39.1 | 40.9 | 41.4 | 38.4 |
| Ce | 36.5 | 79.9 | 83.7 | 85.0 | 77.6 |
| Nd | 17.8 | 33.3 | 37.0 | 39.7 | 24.9 |
| Sm | 4.22 | 6.07 | 6.77 | 7.11 | 5.2 |
| Eu | 1.23 | 1.37 | 1.49 | 1.65 | 0.75 |
| Tb | 0.654 | 0.681 | 0.770 | 0.839 | 0.456 |
| Yb | 1.78 | 1.81 | 2.13 | 2.20 | 1.82 |
| Lu | 0.243 | 0.254 | 0.279 | 0.291 | 0.228 |
| Sr | 471 | 618 | 579 | 675 | 141 |
| Ba | 276 | 450 | 460 | 396 | 750 |
| Cs | 0.57 | 0.93 | 0.92 | | 9.8 |
| U | 1.1 | 1.7 | 1.7 | | 10.4 |
| Th | 4.0 | 6.2 | 7.2 | | 29.7 |
| Hf | 3.0 | 4.0 | 4.1 | 4.1 | 4.4 |
| Ta | 0.69 | 0.90 | 1.4 | 1.3 | 2.1 |
| Sc | 31.7 | 23.4 | 23.6 | 28.0 | 3.0 |
| Cr | 689 | 602 | 507 | 618 | <1 |
| Ni | 155 | 197 | 188 | 229 | <1 |
| Co | 46 | 37 | 37 | 45 | 1 |
| FeO/MgO | 1.06 | 0.77 | 0.82 | 0.80 | 3.55 |
| Ba/La | 16.4 | 11.5 | 11.2 | 9.6 | 19.5 |
| La/Sm | 4.0 | 6.4 | 6.0 | 5.8 | 7.4 |
| La/Yb | 9.5 | 21.6 | 19.2 | 18.8 | 21.1 |
| Eu/Eu* | 0.92 | 0.79 | 0.76 | 0.83 | 0.55 |
| La/Ta | 24 | 43 | 29 | 32 | 18 |
| Th/U | 4.0 | 3.6 | 4.2 | | 2.9 |
| $^{143}Nd/^{144}Nd$ | 0.512857 | 0.512538 | 0.512525 | 0.512544 | 0.512389 |
| $\epsilon Nd$ | +4.3 | -2.0 | -2.2 | -1.8 | -4.9 |
| $^{87}Sr/^{86}Sr$ | 0.703978 | 0.705230 | 0.705797 | 0.705782 | 0.706500@ |
| $^{206}Pb/^{204}Pb$ | | 18.979 | 18.890 | | 18.90 |
| $^{207}Pb/^{204}Pb$ | | 15.618 | 15.631 | | 15.67 |
| $^{208}Pb/^{204}Pb$ | | 38.976 | 39.008 | | 39.04 |

*Model - composition calculated by subtracting 18% of Laguna Verde Ignminbite LV364 from San Francisco lava CC340.

@Isotopic composition approximated from other ignimbrites in region. Referenced to $\epsilon$Nd.

Comparison of the Oligocene and Pleistocene magmas suggests that the Pleistocene magmas are from a more enriched mantle source then the Oligocene magmas. Evidence comes from higher $^{87}Sr/^{86}Sr$ and lower $^{143}Nd/^{144}Nd$ ratios (Fig. 3) and higher normalized light REE and Ba levels (Fig. 2) at roughly the same heavy REE level. As discussed below, this "enriched" component is difficult to explain solely by crustal contamination in the thickened Puna crust. The data support an enriched mantle source as predicted by modeling of less primitive CVZ back-arc lavas by Francis et al. (1989), Mantovani and Hawksworth (1990), and Kay et al. (1994).

That is not to say that no crustal contaminants enter the Pleistocene magmas as they ascend. In fact, their relatively high $SiO_2$ contents (53%), their negative Eu anomalies despite a lack of plagioclase phenocrysts and high Sr contents (>600 ppm), and their sparse feldspar and quartz xenocrysts are best explained by a crustal contaminant (see also Kay et al. 1994). Addition of ≈ 18% of a silicic crustal melt like the nearby Pliocene Laguna Verde ignimbrite (74-77% $SiO_2$; Table 1 and Fig. 2), seems a likely process. Removing such a component from the Pleistocene lavas results in a primitive magma (Table 1) that differs primarily in having lower $SiO_2$ (48.5%), $K_2O$ (1.36%), U, and Th, and higher MgO (10.9%) and CaO (9.9%) concentrations. Importantly, the "enriched" source signals of the Pleistocene lavas - high $^{87}Sr/^{86}Sr$ and low $^{143}Nd/^{144}Nd$ ratios and REE pattern (Figs. 2 and 3) - are little modified by such a process. The model is not perfect as too much U and Th is removed and a negative Eu anomaly remains. The model is somewhat improved by a silicic component with a larger Eu anomaly and lower U and Th contents. However, the lower Sr and REE contents of such a contaminant would have even less effect on the "enriched" signal of the mantle-derived magma.

The best explanation is that the Pleistocene magmas are primitive mantle-derived magmas that mixed on ascent with pockets of silicic melts ponded at levels in the crust where both feldspar and quartz were crystallizing. The presence of only sparse olivine phenocrysts and the near primitive character of the San Francisco lava shows that only a small amount of fractionation occurred and that ascent was rapid. This is more consistent with contamination being primarily through mixing with ponded silicic magmas rather through fractionation-assimilation (AFC) processes. Even extreme AFC models like that of Aitcheson and Forrest (1994) have problems producing these magmas if the Laguna Verde ignimbrite is representative of the contaminant. The conclusion of an enriched mantle beneath the southern Puna in the Pleistocene seems inescapable.

The Late Oligocene Segerstrom basalts put a timescale on this mantle enrichment as they are derived from a less enriched mantle. Other support for at least post middle Cretaceous enrichment comes from the depleted isotopic signatures (modern day ratios - $^{87}Sr/^{86}Sr \approx 0.7033$; $\epsilon Nd \approx +5$) in ≈ 85 Ma lavas from the Salta region east of the Puna (Kay et al. 1994). The mechanism of mantle enrichment must thus be linked to the Neogene subduction process.

## REFERENCES

Aitcheson, S.J., and Forrest, A.H., 1994. Quantification of crustal contamination in open magmatic systems. Jour. Petrology, 35, 461-488.

Gonzalez-Ferran, O., Baker, P.E., and Rex, D. C. 1985, Tectonic-volcanic discontinuity at latitude 27° South, Andean Range, associated with Nazca plate subduction. Tectonophysics 112: 423-441.

Francis, P.W., Sparks, R.S.J., Hawkesworth, C.J., Thorpe, R.S., Pyle, D.M., Tait, S.R., Mantovani, M.S., and McDermott, F., 1989, Petrology and geochemistry of volcanic rocks of the Cerro Galan caldera, northwest Argentina. Geol. Mag. 126: 515-147.

Kay, S.M. and Abbruzzi, J.A., 1996, Magmatic evidence for Neogene lithospheric evolution of the central Andean "flat-slab" between 30° and 32° S, Tectonophysics: in press.

Kay, S. Mahlburg, Coira, B., and Viramonte, J., 1994, Young mafic back-arc volcanic rocks as guides to lithospheric delamination beneath the Argentine Puna Plateau, Central Andes. J. Geophys. Res. 99: 24323-24339.

Kay, S.M., Mpodozis, C., Tittler, A., and Cornejo, P., 1994, Tertiary magmatic evolution of the Maricunga mineral belt in Chile, International Geology Review 36: 1079-1112.

Mantovani, M.S. and Hawkesworth, C., 1990, An inversion approach to assimilation and fractional crystallization processes in the Central Andes. Contrib. Mineral. Petrol. 105: 289-302.

## APPENDIX - ANALYTICAL METHODS

Major elements by electron microprobe at Cornell Univ. (CC339, CC340) and by atomic absorption and wet methods at Chilean survey (CC320c; LV364). Trace elements by Instrumental Neutron Activation Analyses (INAA) and isotopic ratios on VG Sector mass spectrometer at Cornell University. Sr normalized to $^{86}Sr/^{88}Sr = 0.1194$. Standard values: $^{87}Sr/^{86}Sr$ on NBS987 = 0.710265 (±.000036) and $^{143}Nd/^{144}Nd$ on La Jolla + 0.511847(±0.000036). $\epsilon Nd$ based on La Jolla at -15.15. Within-run $2\sigma$ errors = ± 0.000005 to 0.000007. Pb ratios corrected for mass fractionation using $^{206}Pb/^{204}Pb = 16.937$, $^{207}Pb/^{204}Pb = 15.493$, and $^{208}Pb/^{204}Pb = 36.705$ for NBS SRM981.

This project was supported by the US National Science Foundation (EAR-9508023) and the Chilean FONDECYT (1950025). The paper is a contribution to IGCP project 345.

# Composition and P-T-conditions of the sub-andean mantle wedge: Constraints from Southern Andes (50°S) mantle xenoliths

**Rolf Kilian**

Mineralogisches Institut, Universität Heidelberg, Im Neuenheimer Feld 236, 69120 Heidelberg
Tel. 49-6221-546015; E-mail: rkilian@classic.min.uni-heidelberg.de

**Key words:** Southern Andes, mantle xenoliths, geochemistry, P-T equilibrium.

## Introduction

Mantle xenoliths derived from the sub-arc mantle have been erupted with Quaternary basalts at the Cerro del Fraile, 25 km to the east of the Holocene Andean volcanic front in the Southern Andes (50°S). Their petrographical and chemical investigation provide information on the composition and thermal structure, and on metasomatic and magmatic processes of the mantle wedge beneath the Southern Andes.

This study reports the major and trace element chemistry of 20 characteristic xenolithes as determined by XRF and ICP-MS analyses. The major element composition of mantle minerals in 20 selected xenoliths was investigated by electron microprobe.

## Results

On the basis on their mineral and chemical composition the mantle xenoliths can be devided into three groups: (1) Spinel-harzburgites are chemically depleted compared to a primitive mantle (Hofmann 1988). They have low contents of CaO (< 2 wt.%) and $Al_2O_3$ (> 2 wt.%), high Mg# (>90) and relatively low contents of Y (< 1.2 ppm), HRE (e.g. Yb <0.15 ppm) and HFS elements. Compared to the HFS element content (Ta, Nb, Ti) the LIL element concentrations (Ba, Rb, K, Sr) are significantly higher suggesting a metasomatic overprint. Geothermometry (Brey & Köhler 1990) indicate that these rocks equilibrated at pressures from 0.7 to 2.1 GPa and at temperatures between 900°C and 1040°C. (2) Spinel-lherzolites are chemically less depleted than harzburgites (higher contents of CaO, $Al_2O_3$, REE and HFS elements). The mineral texture is often heterogeneous and the mineral chemistry variable suggesting local enrichment processes at different scales. Veins in the lherzolites are composed of clinopyroxene, apatite, phlogopite and rutile. Some lherzolites contain tiny patches of glass forming interconnected networks along grain boundaries. The melt from which the glass derived reacted selectively with lherzolitic clinopyroxene and spinel. The glass is tonalitic in composition and not in chemical equilibriuum with olivine or clinopyroxene. Chemically it can not be inherited from the host basalt. (3) Olivine websterites and pyroxenites which are chemically and mineralogically variably enriched compared to primitive mantle. Peridotitic components in the websterites are chemically comparable to the harzburgites. Relictic chemical equilibria indicate temperatures between 950°and 1040°C, which are comparable to those of the harzburgites

## Conclusion

The trace element budget of the harzburgites can be explained by 20-25% melt extraction of a fertile N-MORB mantle (Pearce et al. 1995). The LIL element enrichmet in the harzbugites is due to a metasomatic process probably related to the subduction of the Antarctic plate under the most southern Andes.

Chemical and petrographical evidences of spinel lherzolites suggest that they were formed by different magmatic and metasomatic enrichment processes (different melt types and fluids) modifying previously depeleted peridotites. The chemical disequilibrium in most lherzolites may suggest that the enrichment process is relatively young (Tertiary ?). Patches of tonalitic glass observed in some lherzoliths may by be due to melt infiltration from a deeper, probaly eclogitic source (Antarctic Plate: Stern & Kilian 1996). The glass composition (60.0 wt.% $SiO_2$, 5 - 6 wt.% $Na_2O$, 5 - 7 wt.% CaO, 19-21 wt.% $Al_2O_3$; Mg# 82-87) can be inherited from a trondhjemitic melt (with low Mg# 25-40, and low $CaO/Na_2O$ <1 ) derived from the subducted Antarctic plate which has selectively assimilated 20-25% clinopyroxene, 10-12% spinel, 3% olivine and 3% orthopyroxene (relative to the mass of the primary melt) during ascent trough the mantle wedge.

Olivine websterites and pyroxenites were formed by basaltic melts infiltrating the peridotitic mantle.

## References

Brey, G. P. & Köhler, T. (1990): Geothermobarometry in Four-Phase Lherzolites: I. Experimental results from 10 to 60 kb.- J. Petrol., 31: 1313-1352.

Hofmann, A. 1988. Chemical differentiation of the Earth: the relationship between mantle, continental crust, and oceanic c rust. EPSL 90: 297-314.

Pearce J.A., Baker P.E., Hrvey P.K. & Luff I.W. (1995): Geochemical evidence for subduction fluxes, mantle melting and fractional crystallization beneath the south Sandwich Island Arc. J. Petrol. 36: 1073-1109.

Stern C. & Kilian R. 1996. The role of subducted slab, mantle wedge and continental crust in the generation of adakites from the Andean Austral Volcanic Zone. Contrib. Mineral. Petrol. 123 (3): 263-282.

# GEOCHEMICAL CONSTRAINTS ON CRUSTAL STRUCTURE FROM NEOGENE VOLCANIC ROCKS OF THE SALAR DE ANTOFALLA VOLCANIC FIELD AND ADJACENT ANDEAN CORDILLERA (24°-26°S, 67°-69°W)

Bernhard Kraemer [1], Raphael Wittenbrink [1], Knut Hahne [2], Heinz Gerstenberger [2]

(1) Institut für Geologie, Geophysik und Geoinformatik, Freie Universität, Malteser Str. 74 - 100, 12249 Berlin, Germany
(2) GeoForschungsZentrum Potsdam, Telegrafenberg, 14473 Potsdam, Germany

**KEY WORDS**: Southern Central Andes, Salar de Antofalla, Volcanics, Isotopes (Sr, Nd, Pb), crustal structure

## INTRODUCTION

The Salar de Antofalla volcanic field (SAF) is a huge area of Miocene to recent calcalcaline volcanism located in NW Argentina ( about 26° S, 67° W) at the southern end of the Andean Central Volcanic Zone (CVZ) (Fig. 1). It is emplaced within the southern part of the Puna high plateau and belongs to the back arc region of the CVZ. Volcanic structures comprise large Middle Miocene - Pliocene stratovolcanic complexes with andesitic to dacitic rocks and Pliocene - Pleistocene monogenetic mafic scoria cones and associated lava flows. Whereas the younger mafic cones are structurally controlled and affected by N-S and NNW-SSE trending strike-slip and normal faults, the older stratovolcanoes are aligned with a NW-SE-lineament but are not affected by true faulting. It is one of the lineaments transverse to the Andean mountain chain which segment the southern argentine Puna (Alonso et al., 1984).

Currently detailed age and geochemical information on the stratovolcanic complexes is lacking whereas data of the monogenetic mafic rocks are interpreted in terms of delamination processes (Kay et al., 1994) and to show both subduction and within-plate geochemical signatures (Thorpe et al., 1984).

Here we discuss new geochemical data on the stratovolcanoes and scoria cones in relation to contemporaneous volcanic rocks of the Andean cordillera in the west.

## SAMPLE LOCATIONS, PETROGRAPHY AND AGE

Three stratovolcanic complexes (Cerro Archibarca, Tebenquicho, Beltran) have been sampled which are aligned together with Cerro Galan at the NW-SE trending Archibarca-lineament (Salfity et al., 1985). They consist of andesitic to dacitic domes and flows constructed above a basal platform (Tebenquicho, Beltran) or associated with an older ring structure (Archibarca). Sampling covered both platforms as well as flows and domes. Age relations are constrained by erosional state and by two K-Ar age determinations. Tebenquicho is the oldest complex (12.0 Ma, Gonzales, 1983), followed by Beltran (7.7 ± 0.2 Ma, K-Ar on biotites) and Archibarca volcanics. Additionally to the Archibarca lineament volcanics (ALV) the basal andesitic lava flow of Cerro De La Aguada volcano has been sampled which forms part of the contemporaneous Antofalla stratovolcanic complex 30 km to the south of ALV.

The predominant mineral assemblage of all volcanics is plagioclase-biotite-hornblende-magnetite with minor quartz-apatite-(Beltran: titanite) in the dacites and minor orthopyroxene-clinopyroxene in the andesites. Fe-Ti-oxides are common to all samples. Disequilibrium textures comprise resorbed quartz and plagioclase grains.

The monogenetic mafic rocks sampled are localized predominantly at the eastern side of the Salar de Antofalla but also occur at its southern end and to the northwest. They are basaltic to andesitic in composition and have typically a microcrystalline/glassy matrix with 5-10 vol-% phenocrysts. These comprise olivine, clinopyroxene and orthopyroxene in basalts/basaltic andesites and mostly plagioclase with olivine, clinopyroxene and orthopyroxene as microlites in the andesites. As noted by former workers (Pichler & Zeil, 1972, Kay et al., 1994) quartz and plagioclase often occur as xenocrysts up to 2 cm showing disequilibrium textures as pyroxene rims and embayment by resorption.

The oldest rocks of this type overlying discordantly folded evaporites were dated with 5,6 ± 0,3 Ma (K-Ar on whole rock sample).

## WHOLE ROCK GEOCHEMISTRY

### 1. Major and trace elements

According to their whole rock composition the volcanic rocks of the SAF region classify as high-K calcalcaline basalts to dacites. Major and trace elements show similar ranges and trends displayed by the Cerro Galan complex (Francis et al., 1989). Archibarca rocks show at given silica content enrichment in $Al_2O_3$ relative to Beltran and Tebenquicho rocks. This correlates with slightly higher CaO and Sr contens and has to be interpreted as a higher plagioclase content. Archibarca rocks show also higher HFSE (Zr, Nb, Ta, Y) and lower compatible element (Sc, Ni, Cr, V) contents and have a tendency to higher La/Sm and lower La/Yb ratios relative to Beltran and Tebenquicho rocks. This could be due to variation in source composition, crystal fractionation or magma mixing.

At given $SiO_2$ or $K_2O$ values Ba contents are higher in Archibarca rocks but Th, Pb, Rb and Cs are lower. It has to be noted that potassium feldspar is absent in ALV rocks. Furthermore in a plot Nb/Ta vs Zr/Hf which tries to avoid fractionation effects of biotite/hornblende and zircon, each volcanic complex displays a distinct range (Fig.2). Both facts points to variation of source composition rather than fractionation effects.

### 2. Isotopes

Monogenetic mafic rocks (50 - 60 wt% $SiO_2$) of SAF area have $i^{87}Sr/^{86}Sr$ = 0,7051 - 0,7089 and ALV rocks (59 - 65 wt% $SiO_2$) have $^{87}Sr/^{86}Sr$ = 0,7077 - 0,7091 and $^{143}Nd/^{144}Nd$ = 0,51231 - 0,51243 (ALV rocks have not been time corrected due to uncertain age. However, age corrected values would not be far outside the error limits), which is within the range of basaltic to andesitic rocks of the CVZ. The Pb isotopic data of mafic and ALV rocks fall in the typical range of the southern CVZ: $^{208}Pb/^{204}Pb$ 38,446 - 39,167, $^{207}Pb/^{204}Pb$ 15,594 - 15,703, $^{206}Pb/^{204}Pb$ 18,551 - 18,988.

The $^{87}Sr/^{86}Sr$ initial ratios of mafic rocks correlate with $SiO_2$, which is commonly interpreted as a feature of open system AFC processes (Francis et al., 1989) in which crustal components are melted and assimilated by parental mantle magmas. Sr and Nd isotopic ratios of ALV rocks are within the range of the monogenetic rocks and can be interpreted also as mixed or AFC melts triggered by injection of mantle melts. This is indicated also by the $d^{18}O$ value = 7,92 of a dacitic lava sample of Cerro Beltran.

We compare these data with Sr, Nd and Pb isotopic compositions of four contemporaneous stratovolcanoes of the Andean Cordillera 50 - 90 km to the west (Azufre, Cordon del Azufre, Lastarria, Llullaillaco) (Fig. 3, Fig. 4). As pointed out by Wittenbrink & Kraemer (1996) intermediate to acid lavas from these centers were derived by interaction of already altered basaltic andesites and crustal melts during their ascent within the middle crust.

Andesites - rhyolites of the Cordillera reach lower Sr and Pb and higher Nd isotopic ratios compared to rocks of SAF region (0,7059 - 0,7071, $^{208}Pb/^{204}Pb$ 38,634 - 38,827, $^{207}Pb/^{204}Pb$ 15,627 - 15,638, $^{206}Pb/^{204}Pb$ 18,688-18,873, 0,51253 - 0,51242 respectively). At given Pb and $SiO_2$ contents the volcanics of the SAF region are displaced to higher Pb isotopic composition than arc rocks. The enriched

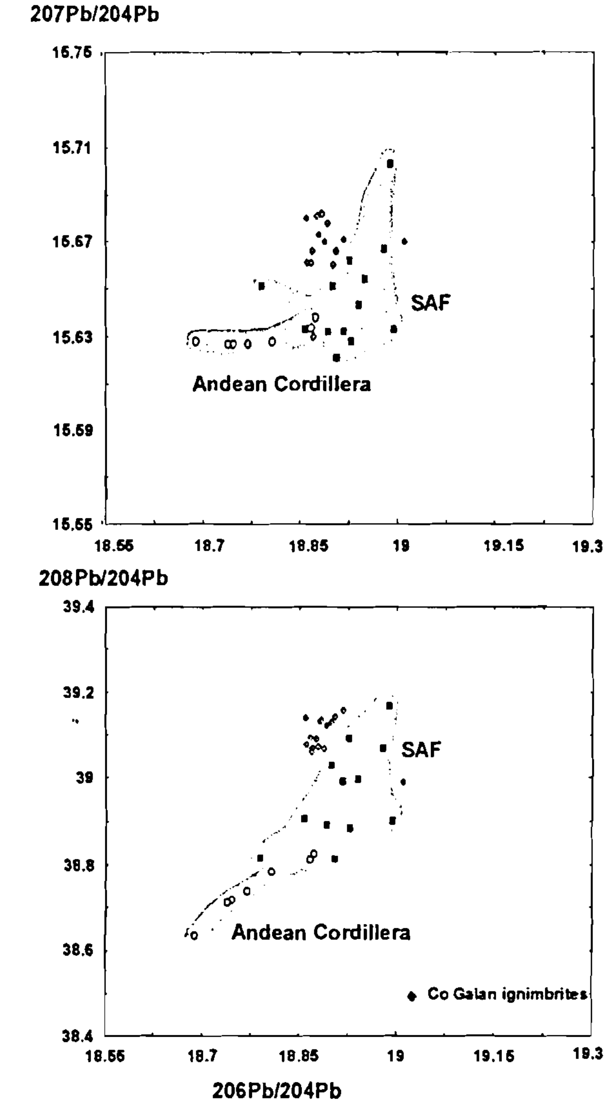


Fig. 4 Pb istopic ratios in Salar de Antofalla volcanic region and adjacent Andean arc

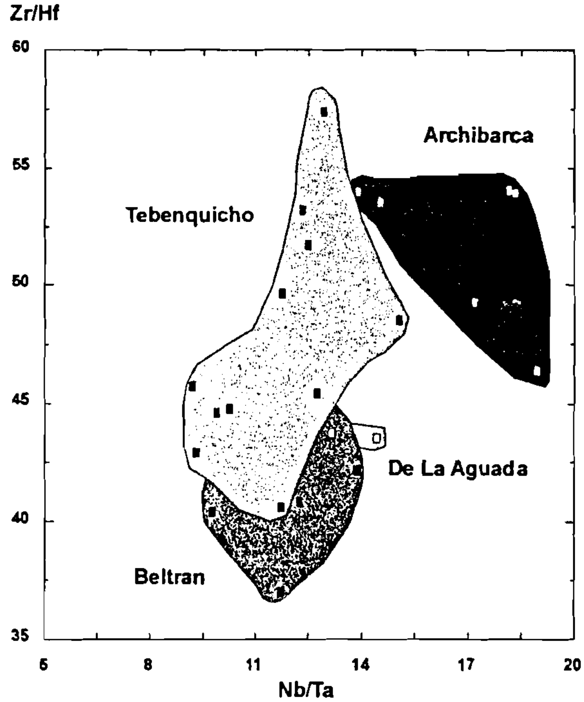


Fig. 2 HFS element ratios in Archibarca lineament rocks

Fig. 1 Location sketch map

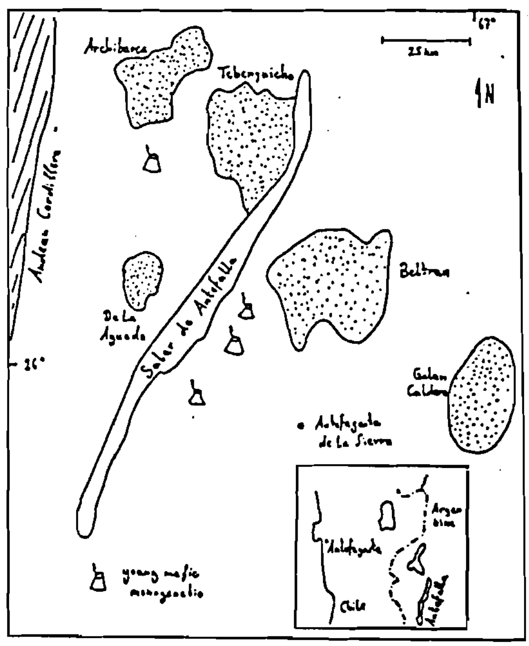


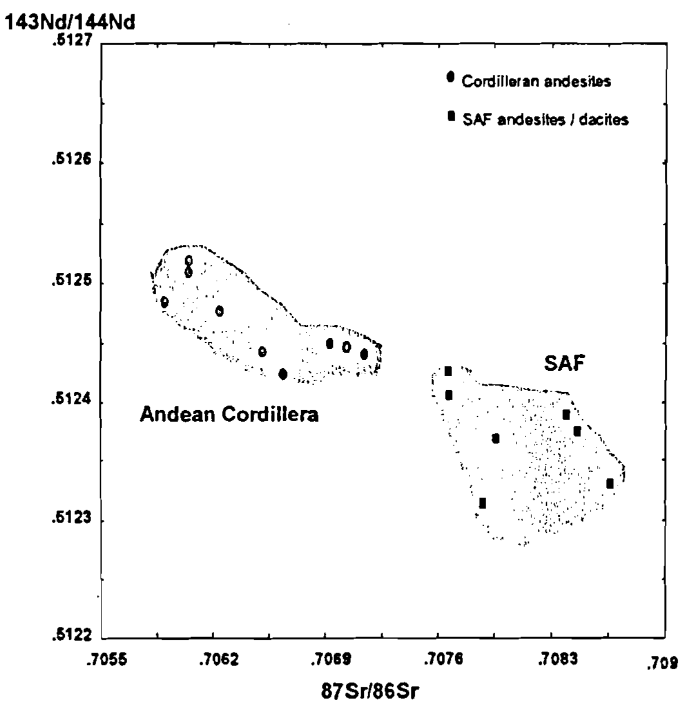


Fig. 3 Sr-Nd isotopic ratios

isotopic ratios of the SAF back arc region can be explained by higher Th/Pb-, U/Pb-, $^{87}Sr/^{86}Sr$ and lower $^{143}Nd/^{144}Nd$ ratios of contaminant(s).

This could be interpreted as variable age and/or composition of the underlying basement rocks. Ramos (1986) postulated two allochthonous terranes of Precambrian and Paleozoic age to have been accreted between the two regions. However, new data on high-grade metamorphic rocks of basement outcrops in N Chile and NW Argentina show similar conditions of metamorphism and a peak-metamorphism age of 500 Ma. This does not support the idea of terrane accretion (Lucassen et al., 1996) and, thus, the isotopical zonation can not be explained by basement rocks of different age.

As noted by Feeley & Davidson (1995) at Ollague volcano assimilation processes in upper crustal regions are of minor importance in the magmagenesis of andesites and dacites. Thus, we conclude that compositional variation within the deep crustal precambrian basement block is most probably to account for the isotopical zonation between the SAF back arc region and the Andean Cordillera. The trace element pattern of ALV rocks also indicates the stated variation of source rock composition.

## CONCLUSIONS:

Andesitic to dacitic rocks which extruded at stratovolcanoes of the Archibarca lineament have crustal sources of variable composition mixed with ascending basaltic mantle melts. Compared to contemporaneous intermediate to acid volcanic rocks from the Andean Cordillera 50 - 90 km in the west they reach higher Pb and Sr and lower Nd isotopic ratios.

The zonation of isotopic composition between these two regions is attributed to variation of underlying precambrian rocks of the same crustal basement block. It is not due to allochthonous terranes which have been postulated elsewhere.

## REFERENCES:

**Alonso, R. et al. (1984)** Puna Austral - Bases para el subprovincialismo geologico de la Puna Argentina. IX Congr. Geol. Arg., Bariloche, Actas I, 43 -63 **Feeley, T.C. & Davidson, J.P. (1995)** Petrology of Calc-Alcaline Lavas at Volcan Ollague and the Origin of Compositional Diversity at Central Andean Stratovolcanoes. J. Petrol., 35, 1295 - 1340. **Francis, P.W. et al. (1989):** Petrology and geochemistry of volcanic rocks of the Cerro Galan caldera, northwest Argentinia. Geol. Mag. 126, 515-547. **Gonzales, O. E. (1983)** Geologia, Alteracion Hidrotermal y Edad del Cerro Tebenquicho, Dep. Antofagasta de la Sierra, Catamarca. Asoc. Geol. Argentina Rev., 38, 49 -59. **Kay, S.M. et al. (1994)** Young mafic back arc volcanic rocks as indicators of continental lithospheric delamination beneath the Argentine Puna plateau, central Andes. J. Geophy. Res., 99, 24323 - 24339 **Lucassen et al. (1996)** The Paleozoic Basement of the Central Andes (18° - 26° S) - A metamorphic view. III Int. Symp Andean Geodynamics, this volume. **Pichler, H. & Zeil, W. (1972)** The Cenozoic rhyolite-andesite association of the Chilean Andes. Bull. Volcanol., 35, 424 - 452. **Ramos, V.A. (1988)** Late Proterozoic-Early Paleozoic of South America - A collisional history. Episodes, 11, 168-174 **Salfity, J. A. (1985)** Lineamentos transversales al rumbo andino en el noroeste argentino. IV Congr. Geol. Chil., Antofagasta, Actas 2, 119 - 137. **Thorpe, R.S. et al. (1984)** Relative roles of source composition, fractional crystallization and crustal contamination in the petrogenesis of Andean volcanic rocks. Phil. Trans. R. Soc. Lond., A310, 675-692 **Wittenbrink, R & Kraemer, B. (1996)** Variation in time and space of magmagenesis of neogene to recent volcanic rocks in the southern Central Volcanic Zone (CVZ) of the Andes (24°-26°S, 67°-69°W). VI Goldschmidt Conference, Heidelberg, 31.3.-4.4.1996, Abstracts.

# Geochemical evolution of Triassic and Jurassic volcanic successions in Northern Chile between 20° and 26°30' latitude south

Wolfgang KRAMER(1) and Ralph EHRLICHMANN(2)

(1) GeoForschungsZentrum Potsdam, Telegrafenberg C2, D-14473 Potsdam, Germany
(2) Kuhnertstraße 20, D-13595 Berlin, Germany

**Key words :** Subduction volcanism, geochemistry, Jurassic, Triassic, Coastal Range, Precordillera

## INTRODUCTION

Triassic volcaniclastic and intermediate to acid volcanic remainders can be found in some small graben-like structures whereas preserved volcanic successions of a Jurassic magmatic arc/back arc system are widespread in Northern Chile between around 20° and 26°30' latitude south within the Coastal Range and subordinate in the Precordillera.
Interbedded lava flows, pyroclastica, and other sediments with fossil content on places allow biostratigraphic age-correlations as shown in Table 1. New findings and analytical results characterize the Mesozoic volcanic successions of Northern Chile as rather variable in space and time.

## OCCURRENCES AND SOME GEOLOGICAL-VOLCANOLOGICAL FEATURES

The pyroclastica-lava series of Upper Triassic graben-like structures from the Coastal Range are calc-alkaline and of intermediate to acid character, different from the Triassic Paramillos volcanic complex of the Cuyo basin, West-Argentina. This is made up by alkaline basalts (cf. Ramos & Kay 1991).
Predominant pyroclastic rocks and lavas, which are concentrated around eruptive centers, appear in the Lower Jurassic (Sinemurian) *Posada de los Hidalgos-Formation* south of Taltal. They are calc-alkaline intermediate rocks.
The volcanic successions, chiefly formed in the Middle Jurassic, are predominant mafic and may reach great thicknesses, e.g. up to more than 5 km near Antofagasta (cf. Palacios 1978). They are built up by lava flows and may be intruded by porphyritic and doleritic sills and dykes. Partly they were extruded submarine, forming pillow lavas, e.g. in the *Caleta Ligate-* and *El Godo-Formations*, and comprise trachydacitic to rhyolitic lavas or ignimbrites. Often the successions form laterally extensive lava flows, in part composed by finger-like flows as within the *La Negra-Formation* near Antofagasta and Taltal.
More than 300 m thick basaltic andesitic series occur in the Quebrada Tranquita area, Precordillera. They correspond to the basaltic andesitic to trachyandesitic La Negra volcanics of the Coastal Range between Taltal and Antofagasta by their chemical character. They have no analogy immediately westward in the Coastal Cordillera.
Around 22° longitude south volcanics of the La Negra-Formation appear in the Coastal range near Tocopilla (cf. Palacios 1978), but alkaline olivine basalts have been recognized as intercallation into sediments of the Cerro Jaspe, Precordillera.
The youngest volcanic succession investigated, according to Thomas (1970) is of Lower Cretaceous age. It is part of the *Puntas Barancos-Formation* and comprises trachydacitic to rhyolitic lavas as well as pyroclastic- and tuff-breccias.

Table 1: Preliminary results on the occurrence of Triassic to Upper Jurassic/Lower Cretaceous volcanic successions from volcano-sedimentary formations of the Northern Chilean Coastal Range and Precordillera, simplified. Age correlation on biostratigraphic base according to Kossler (1996), Prinz et al. (1994) and Thomas (1970). Abreviations: c-alk: calk-alkaline, alk: alkaline, LREE: light rare earth elements

| | | **Coastal Range** | | | **Precordillera** | |
|---|---|---|---|---|---|---|
| | | Taltal - Chanaral | Antofagasta - Tocopilla | Iquique | Quebrada Tranquita Sierra Candeleros | Cerro Jaspe |
| Lower Cretaceous | | | | **Punta Barrancos-Form.** *Trachydacite, Rhyolite,* weak alk, high Th, La/Yb and LREE | | |
| Upper Jurassic | Lower Oxfordian | | | ? ? ? | | |
| Middle Jurassic | Callovian Bathonian | ? ? ? **La Negra-Formation** *Basaltic Andesite, Andesite, Trachybasalt (Rhyodacite),* | | **El Godo-Formation** *Basalt, Basaltic Andesite* c-alk to weak alk, medium LREE, | *Basaltic Andesite, Basalt, Trachyandesite,* medium LREE, low & medium Ti | |
| | Bajocian | predominant c-alk, weak alk, medium LREE ? ? ? | | **Caleta Ligate-Form.** see El Godo-Formation + *(Trachydacite, Rhyolite)* **Oficina Viz-Formation** | | *Alkaline Basalt,* negative Nb-Ti-anomalies missing |
| Lower Jurassic | Sinemurian | **Posada de los Hidalgos-Formation** *Trachyandesite,* alk, c-alk, low LREE | Quillagua: *Andesite, Trachyandesite,* c-alk, alk, high LREE | *Basalt, Bas. Andesite,* c-alk, low LREE ? ? ? | | |
| Triassic | | **Cifuncho-Form.** *Trachydacite, Dacite, Rhyolite,* c-alk, low REE | Cerro de Cuevitas: *Rhyolite* | | | |

## TRACE ELEMENT TRENDS

Figure 1 gives a first glance over the hygromagmatophile (incompatible) element abundances. It shows different LILE(large ion lithophile elements)/HREE(heavy rare earth elements) ratios with the highest concentrations of LILE in the Cretaceous dacites and lowest HREE in the Triassic volcanics.
All the investigated Triassic to Lower Cretaceous volcanic rocks which occur along the Costal Range and in the Precordillera around 27° latitude south display negative Nb-P-Ti anomalies and are primarily calc-alkaline which is characteristic for collisional or subductional areas.
Recorded by the contents of $SiO_2$, MgO, Cr and other trace elements, the Jurassic volcanics are predominantly mantle-derived mafic rocks (cf. also Lucassen & Franz 1994), and they are crustal-influenced as indicated by variable Th/Nb and La/Sm ratios. A negative Eu-anomaly becomes more significant in the course of the Bajocian to the Lower Callovian time resulting from increasing fractionation of plagioclase. Indicated by Th/Nb and La/Sm ratios, there is an increasing crustal contamination within mafic and intermediate volcanics with time.
The hygromagmatophile element abundances of the alkaline Cerro Jaspe basalt show convex-up pattern which are typical of asthenospheric mantel provenance.

## CONCLUSIONS

As shown by the interdigitation of biostratigrafically dated sediments, volcaniclastics and lava flows, on principle, the volcanic activities are lasting and quite intensive during Jurassic times in Northern Chile, beginning in the Sinemurian (e.g., Posada de los Hidalgos-Formation) and extending up into the Callovian (El Godo-Formation). A coastal profile south of Iquique verifies volcanic eruptions throughout the Bajocian, Bathonian and Callovian. The distribution of the calc-alkaline basaltic andesites and trachyandesites south of Taltal and in the Quebrada Tranquita area, Precordillera, hint at a possible eastwards-dislocation of the volcanic arc around 27° latitude south.
The Jurassic, especially Middle Jurassic, magmatism procured a huge input of melts from the mantle wedge into the arc crust. It may have triggered acid crustal melting (ignimbrites). The Jurassic volcanism is clearly bimodal by those intercalated acid lavas and ignimbrites. Triassic and part of Lower Jurassic precursors of intermediate to acid character have predominant crustal sources. Until now we know one Jurassic alkaline basalt complex (Cerro Jaspe) with an asthenospheric source within the study area. These may be due to a slab 'window', caused by either rift subduction or a flattening slab.
The chemical changes (increasing crustal influence) up to the Upper Jurassic/Lower Cretaceous reflect a development towards the maturation stage of the Mesozoic volcanic arc.

## REFERENCES

Hofmann A.W. 1988. Chemical differentiation of the earth: the relationship between mantle, continental crust and oceanic crust. *Earth Planet. Sci. Lett.*, 90, 243-262.
Kossler A. 1996. Bajocian (Middle Jurassic) volcano-sedimentary sequences in the Coastal Cordillera of Northern Chile. *Zbl. Geol. u. Paläont.*
Palacios-Monasterio C. 1978. The Jurassic Paleovolcanism in Northern Chile. *Dissertation, Eberhard-Karls-Universität Tübingen.*
Lucassen F. & Franz G. 1994. Arc related Jurassic igneous and meta-igneous rocks in the Coastal Cordillera of northern Chile/region Antofagasta. *Lithos*, 32, 273-298.
Prinz P., Wilke H.G., Hillebrandt A.v. 1994. Sediment accumulation and subsidence history in the Mesozoic marginal basin of Northern Chile. In: Reutter K.J., Scheuber E., Wigger P. (eds.). Tectonics of the Southern Central Andes, Springer, 219-232.
Ramos V.A. & Kay S. 1991. Triassic rifting and associated basalts in the Cuyo basin, central Argentina. Geol. Soc. Amer. Spec. Pap., 265, 79-91.
Thomas A. 1970. Quadrángulos Iquique y Caleta Molle, Provincia Tarapacá. *Carta Geol. de Chile*, 21.

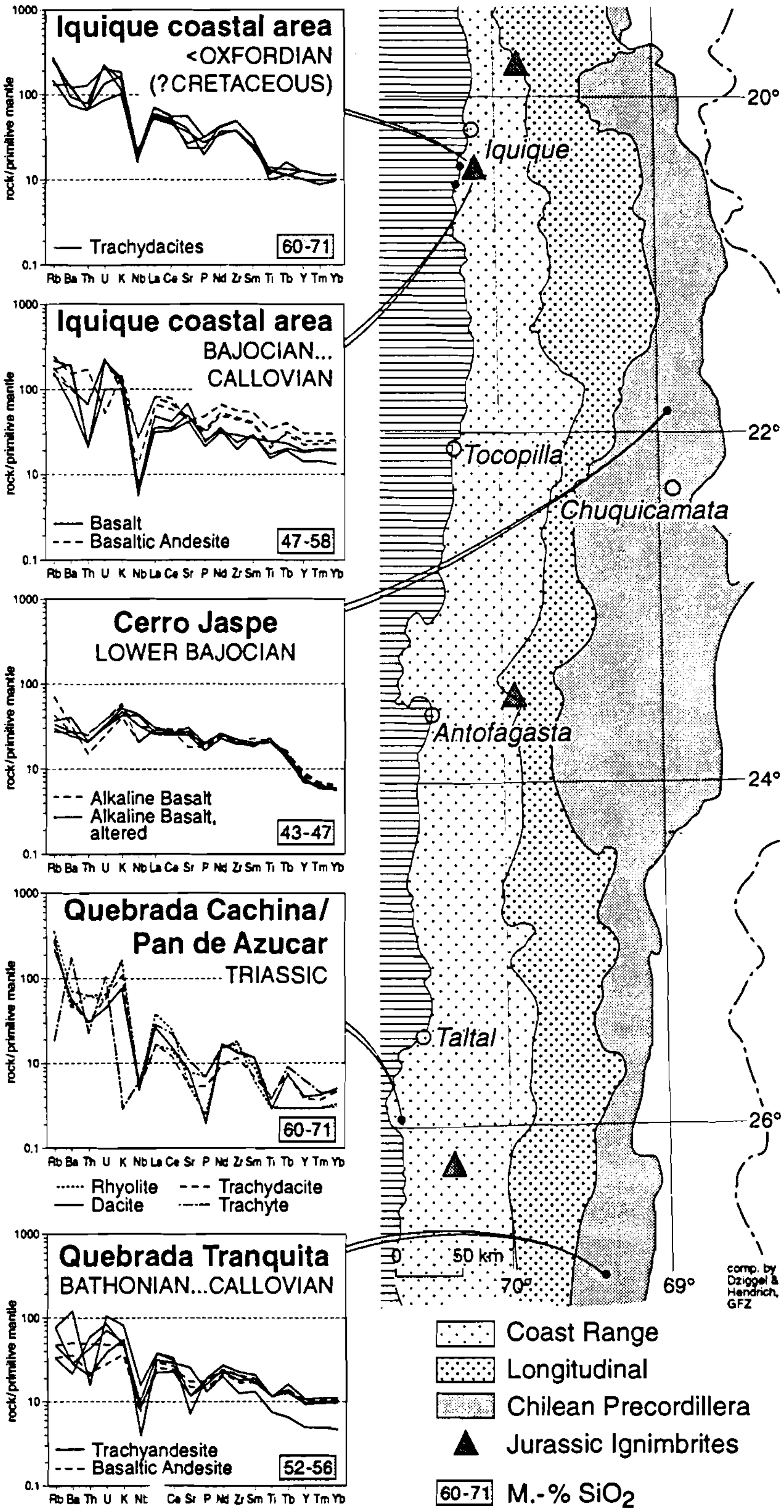


Figure 1. Ske.ch map of the study area in North Chile and hygromagmatophile element abundances normalized to primitive mantle according to Hofmann (1980). The selected examples may nearly represent the variability of the abundances in mafic to intermediate Mesozoic volcanites.

# THE HIGH-K NEOGENE BACK-ARC VOLCANISM OF THE BOLIVIAN ALTIPLANO : A COMPLEX PETROGENETIC STORY.

Pascale LEGROS [1], Pierre SOLER [2], Alain DEMANT [1], Christian COULON [1] and Michel FORNARI[3]

[1] Laboratoire de Pétrologie Magmatique, URA CNRS 1277 et FU 17, CEREGE, BP 80, 13545 AIX-en-Pce Cedex 04, France.
[2] ORSTOM, Département TOA, 211 rue Lafayette, 75480 PARIS Cedex 10, France.
[3] Institut de Géodynamique URA 1279, Université de Nice-Sophia Antipolis, Parc Valrose, 06108 NICE Cedex 02, France.

**KEY WORDS** : Bolivia, Neogene, Back-arc, Volcanism, Assimilation, Magma mixing

## INTRODUCTION

The high-K back-arc volcanism which was emplaced on the Bolivian Altiplano during the Neogene differs from the Andean Cordillera Central Volcanic Zone (CVZ) arc activity in the small volumes of lavas emitted by minor monogenetic centers instead of stratovolcanoes, and its close relations with the tectonic regime on the Altiplano. But its genesis seems to be linked to complex processes as in the arc. Try to decipher the story of these small magma batches, using mineralogical and isotopic evidences, is the purpose of this study.

## GEOLOGICAL SETTING

Since the Upper Oligocene period, a peculiar volcanism was emplaced on the Bolivian Altiplano, in a back-arc situation, East of the CVZ subduction-related volcanic arc (400 km from the trench), above a very thick continental crust of about 70 km. This volcanism is characterized by a temporal alternation of mainly two types of minor events, distributed along major fractures, essentially in the northern and central parts of the Altiplano (Fig.1) : acidic phenocryst-rich domes (andesitic to dacitic in composition) on the one hand, mafic aphyric flows on the other hand. According to available radiochronological data (K/Ar method), this alternation seems to be related to tectonic episodes (Soler & Jimenez, 1993) : during periods of compressive deformation, domes were emplaced whereas, during extensive or transtensive short-lived episodes, the lavas were erupted as reduced flows. These volcanic events represent small volumes of magma (between $10^{-3}$ and $10^{-1}$ $km^3$ ) compared to the large volumes emitted by active stratovolcanoes of the volcanic arc. This observation leads to suppose that these monogenic centers erupted from small crustal reservoirs (or conduits?) rather than large magma chambers. The edifices concerned by this study are Early to Late Miocene domes and Middle Miocene and Quaternary flows. The whole-rock geochemistry of the two types of events is quite similar, excepted for $K_2O$ contents which are higher in the lava flows, classified for this reason as "shoshonitic" flows instead of "high-K calc-alkaline" for the domes.

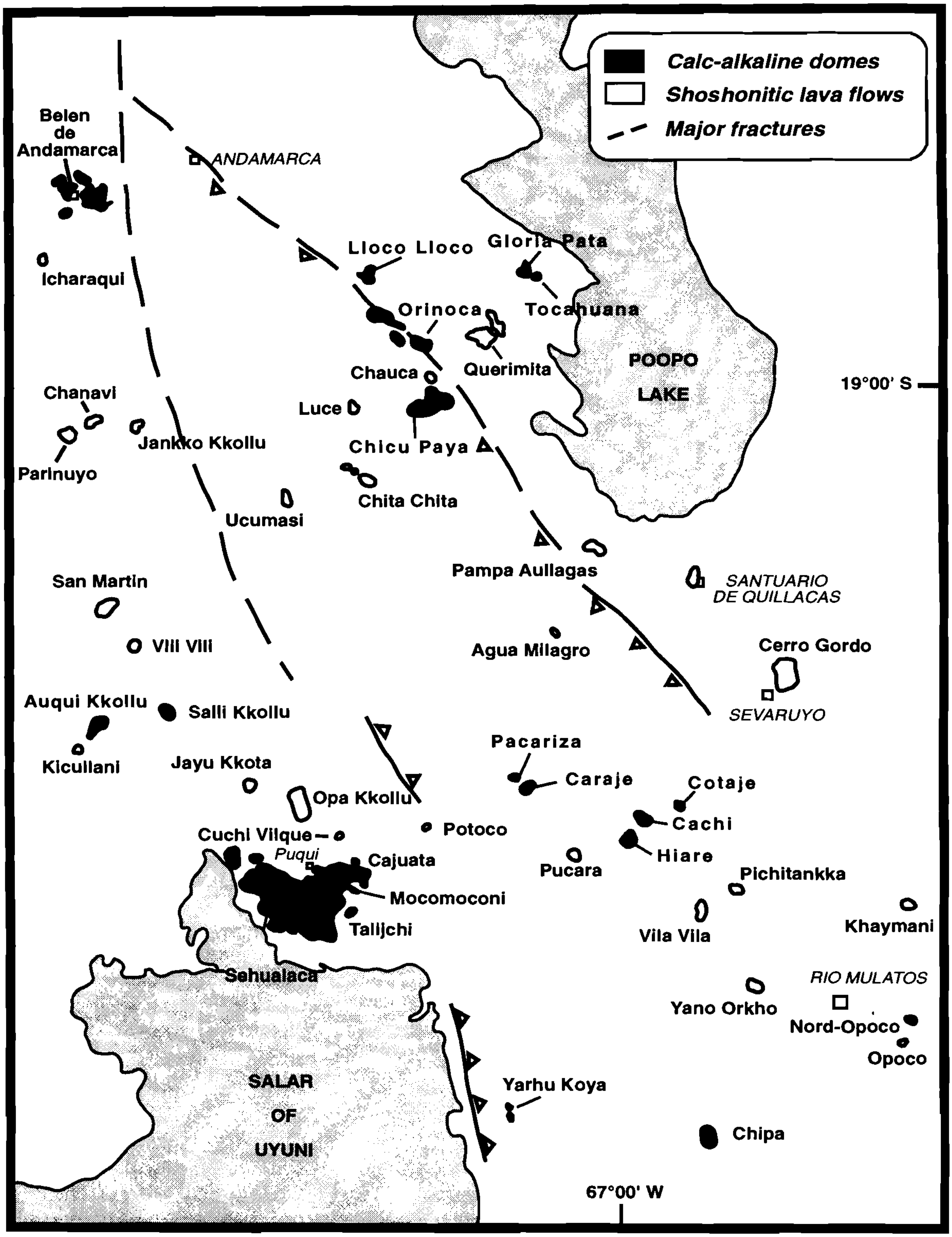


**FIG.1 : Location map of miocene to quaternary back-arc volcanic minor centers of the central Bolivian Altiplano.**

## COMPLEX MINERALOGICAL ASSOCIATIONS

Domes and lava flows, though differing in their type and time of emplacement and their amount of phenocrysts, share complex mineralogical associations and show xenoliths of crustal and magmatic origin.

The two main petrogenetic processes highlighted by this unusual mineralogy are crustal assimilation and magma mixing. For both processes, we can observe two kinds of evidences : complete xenoliths and/or xenocrysts (with reaction rims) coming from disaggregated or digested xenoliths.

- **Crustal assimilation.** Some lava flows contain numerous metamorphic crustal xenoliths of granulite to amphibolite facies. These xenoliths, millimetric to centimetric in size, are partially digested but exhibit a well-preserved schistosity. The most frequent xenolith type corresponds to a sillimanite and biotite-bearing gneiss, probably extracted at lower crustal level since this part of the crust is supposed to be composed of high-grade crystalline metamorphic rocks, instead of sedimentary, volcanic and plutonic rocks as in the upper crust (Gill, 1981). Domes sometimes contain amphibolite xenoliths coming certainly from the same crustal depth as the gneiss xenoliths.

However, the majority of our samples (domes and flows) only present metamorphic xenocrysts with reaction rims. The most frequent xenocrysts are : garnet rimmed by plagioclase and orthopyroxene, sillimanite, kyanite replaced by green spinel, quartz with undulatory extinction and clinopyroxene rim... Biotite and feldspars (plagioclase and K-feldspar) of metamorphic origin are microscopically distinguishable from the host-rock magmatic phenocrysts by their degree of alteration or destabilisation (with or without rims).

The only possibility to explain the occurrence of such minerals in volcanic rocks is the involvement of crustal assimilation during magma ascent through the continental crust (Maury & Bizouard, 1974 ; Pognante, 1990). According to the nature of the xenoliths and preserved xenocrysts, this process probably occurred in the lower crust, at a depth between 20 and 70 km.

Major elements contents show that these rocks are not peraluminous and then cannot be interpreted as crustal melts, such as Macusanites (Pichavant et al. 1988).

Isotopic data (Soler et al., 1993) confirm the importance of crustal contamination and, more precisely, the role of the lower crust Precambrian gneiss. We can indeed see, on a $^{143}Nd/^{144}Nd$ versus $^{87}Sr/^{86}Sr$ diagram, that isotopic values of our rocks tend towards the deep crustal end-member represented by a quartz-sillimanite gneiss xenolith found in one of the lava flows (Pampa Aullagas) from the central Altiplano (Davidson & de Silva, 1995). Even the most mafic flows (with Mg# between 61 and 64) are contaminated and cannot provide informations on the nature of the mantelic source.

- **Magma mixing.** In the same way, we can find in both domes and flows rounded dark basaltic xenoliths with vacuolar hyalodoleritic texture, composed of large acicular hornblende crystals, around olivine and pyroxenes cores. Plagioclase (sometimes with skeletal shapes) and Fe-Ti oxides occur as microcrystals in a glassy groundmass. All these characteristics are typical of quenched basaltic liquids (Coulon et al., 1984) and imply that these xenoliths formed by mixing of a hot basaltic magma with a more acidic and cooler one.

Domes and flows more often exhibit xenocrysts in disequilibrium originated from the mafic magma : olivine rimmed by orthopyroxene, clino- and orthopyroxene aggregates rimmed by amphibole microcrystals, or scattered hornblende phenocrysts with pyroxene cores. Host-rock felsic phenocrysts can also develop reaction textures such as sieve-textures for plagioclase (systematically with an inverse zoning) or clinopyroxene rim around quartz...These features were already recognized as the result of a magma mixing phenomenon by several authors (Paz,1992 ; Stimac & Pearce, 1992 ; Matthews et al., 1994). Exceptionally, in some lava flows, there are evidences of two mixing episodes, one with a more basic magma, and the other with a more felsic (i.e. rhyolitic) magma.

The problem is to determine at what crustal level this process happened. Since the mixing occurred between a basaltic and a more felsic, i.e. cristallized magma, it probably took place in small shallow reservoirs, where the acidic magma was trapped. After the basaltic intrusion in the reservoir, mixing occurred between the two different magmas and probably triggered the eruption of the hybrid mixing product (Sparks et al, 1977).

Fractional crystallization is supposed to have occurred during the last part of the ascent, in small chambers.

## CONCLUSIONS

We can conclude from the petrographical, mineralogical and isotopic data available on the domes and lava flows that mantle-derived parental magmas have undergone at least one episode of crustal assimilation and magma mixing during their ascent through the thick continental crust under the Bolivian Altiplano. The petrogenetic story can be as follows : primary magmas, generated by partial melting of a mantelic source that is still not well defined, first arised in the lower continental crust where they sampled and partly digested ancient granulitic crustal rocks, such as sillimanite and biotite gneiss found as xenoliths in some lava flows. Then, parental magmas continue their ascent and mix with more acid magmas stocked in shallow reservoirs, triggering the eruption of small volumes hybrid magmas, emplaced as high-K calc-alkaline domes under compressive tectonic conditions or as shoshonitic flows under transtensive or extensive conditions.

## REFERENCES


Coulon C., Clocchiatti R., Maury R.C. & Westercamp D. 1984. Petrology of Basaltic Xenoliths in Andesitic to Dacitic Host Lavas from Martinique (Lesser Antilles) : Evidence for Magma Mixing. *Bull. Volcanol.*, 47-4 (1), 705-734.

Davidson J.P. & de Silva S.L. 1995. Late Cenozoic magmatism of the Bolivian Altiplano. *Contrib.Mineral.Petrol.*, 119, 387-408.

Gill J.B. 1981. Orogenic andesites and plate tectonics. *Berlin-Heidelberg ; Springer-Verlag*, 390 pp.

Matthews S.J., Jones A.P. & Gardeweg M.C. 1994. Lascar Volcano, Northern Chile; Evidence for steady-state disequilibrium. *J. Petrol.*, 35, part 2, 401-432.

Maury R.C. & Bizouard H. 1974. Melting of Acid Xenoliths into a Basanite : an Approach to the Possible Mechanisms of Crustal Contamination. *Contrib.Mineral.Petrol.*, 48, 275-286.

Paz Moreno F. 1992. Le volcanisme mio-plio-quaternaire de l'état du Sonora (nord-ouest du Mexique) : évolution spatiale et chronologique ; implications pétrogénétiques. *Thèse d'Université*, Université Aix-Marseille III, 196p.

Pichavant M., Kontak D.J., Briqueu L., Valencia Herrera J. & Clark A.H. 1988. The Miocene-Pliocene Macusani Volcanics, SE Peru. II. Geochemistry and origin of a felsic peraluminous magma. *Contrib. Mineral. Petrol.*, 100, 325-338.

Pognante U. 1990. Shoshonitic and ultrapotassic post-collisional dykes from northern Karakorum (Sinkiang, China). *Lithos*, 26, 305-316.

Soler P. & Jimenez N. 1993. Magmatic constraints upon the Evolution of the Bolivian Andes since Late Oligocene times. *Second ISAG*, Oxford (UK), 21-23/9/1993, 447-451.

Soler P., Carlier G., Aitcheson S.J. & Fornari M. 1993. Sr, Nd and Pb isotopic constraints upon the origin of the Quaternary shoshonitic lavas and the deep structure of the Central Altiplano of Bolivia. *EUG VII, Strasbourg (France), Terra Abstracts, Abstract suppl. N°1 to Terra Nova*, 5, 584-585.

Sparks S.R.J., Sigurdsson H. & Wilson L. 1977. Magma Mixing : a Mechanism for Triggering Acid Explosive Eruptions. *Nature*, 267, 315-318.

Stimac J.A. & Pearce T.H. 1992. Textural evidence of mafic-felsic magma interaction in dacite lavas, Clear Lake, California. *Amer.Mineral.*, 77, 795-809.

# ADAKITES FROM ECUADOR: PRELIMINARY DATA

Michel MONZIER (1), Jean-Philippe EISSEN (2), Jo COTTEN (3), Minard L. HALL (4), Claude ROBIN (1) and Pablo SAMANIEGO (4)

(1) ORSTOM, Apartado postal 17-11-6596, Quito, Ecuador (e-mail: monzier@orstom.ecx.ec)
(2) ORSTOM, Centre de Brest, BP 70, 29280 PLOUZANE cedex, France (e-mail: eissen@ifremer.fr)
(3) Département des Sciences de la Terre, CNRS - URA n°1278, Université de Bretagne Occidentale, B. P. 809, 29285 Brest, France (e-mail: Jo.Cotten@univ-brest.fr)
(4) Instituto Geofisico, Escuela Politecnica Nacional, Apartado postal 17-01-2759, Quito, Ecuador (e-mail: mhall@instgeof.ecx.ec)

**KEY WORDS:** volcanology, geochemistry, adakites, Ecuador

## INTRODUCTION

Adakites are andesites-dacites-rhyolites (but mainly dacites) with peculiar characteristics such as relatively high Al and Na contents, very low Y and Yb contents, and high La/Yb and Sr/Y ratios, that are not associated with parental basalts. They are usually considered to be derived from the partial melting of metamorphosed basalts (amphibolite and eclogite) at high pressure, leaving garnet or amphibole in the residues, thus giving them their unusual geochemical characteristics (Defant and Drummond, 1990; Defant, et al., 1991; Drummond and Defant, 1990; Atherton and Petford, 1993; Defant and Drummond, 1993; Sajona et al., 1993). It is generally accepted that adakitic magmas form where young (<25 Ma), hot oceanic crust is subducted and melts at 23-26 kbar (75-85 km) and 700-775°C (Drummond and Defant, 1990), i.e. near the corner of the mantle wedge. Accordingly, adakitic volcanoes should lie quite close (≈ 80 km) to the trench. However, Atherton and Petford (1993) presented evidence that the partial melting of basaltic material of the lower crust at ≈50 km depths by newly underplated hot magmas (generated in the underlying asthenospheric wedge) should be considered as an additional way to generate adakite, when 1/ subducting oceanic crust is too old and cold, 2/ volcanism is very far from the trench, and 3/ local heat flow is high.

## ECUADORIAN ADAKITES

Young oceanic lithosphere (<20 Ma) formed along the Cocos-Nazca spreading axis is being subducted under central and northern Ecuador since at least the early Pliocene with a rate of convergence of ≈ 8 cm/y (Fig. 1). The Benioff plane dips ≈ 25° eastward, attaining ≈130-150 and ≈150-175 km depths under the Quaternary volcanoes of the ecuadorian Western and Eastern Cordilleras, respectively (Winter, 1990). The Eastern Cordillera constitutes the eastern edge of the Andean Block (AB), a wedge between the Nazca (NAZ) and South American (SAM) plates presently affected by an E-W compressive state of stress (Ego et al., 1995). The collision-subduction of the Carnegie Ridge in front of Ecuador (Pennington, 1981) or, more certainly, the oblique NAZ-SAM convergence in the Ecuador-Colombia area (Ego et al., 1995) would explain the northeastward motion of the AB, along the great NE-SW right-lateral transpressive faults of the East Andean Front Fault Zone.

ORSTOM (French Scientific Research Institute for the Development in Cooperation) and the Geophysical Institute of the National Polytecnical School of Quito are collaborating since 1994 in a joint volcanological program which includes studies on several volcanoes of Ecuador, namely Cotacachi, Fuya Fuya, Mojanda, Pululahua, Cayambe, Cotopaxi, Tungurahua, Sangay... (Fig. 2) We present here the first results in geochemistry (see also Robin et al. and Samaniego et al., this volume). To date, all the rocks sampled within the framework of this joint program have $SiO_2$ contents > 55%; they are mainly medium-K basic andesites to rhyolites, and a few high-K acid andesites to rhyolites (Fig. 3; all values LOI free and recalculated to 100%). For comparison, basaltic rocks clearly predominate in a typical

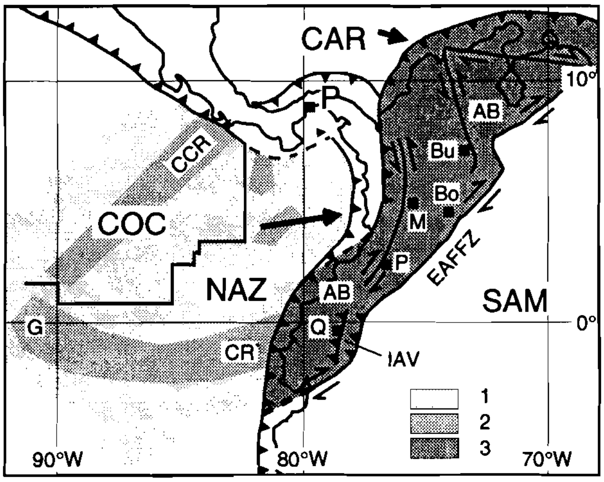


**Fig. 1**

Geodynamics of the Andean Block.
COC= Cocos Plate;
NAZ= Nazca Plate;
CAR= Caribbean Plate;
1= Galapagos Gore; 2= oceanic ridges:
CCR= Cocos Ridge, CR= Carnegie Ridge; 3= Andean Block (AB);
G= Galapagos Islands.
Large arrows= NAZ and CAR plate convergence with respect to SAM fixed.
IAV= Inter Andean Valley;
EAFFZ= East Andean Front Fault Zone;
Q= Quito, P= Popayan, M= Manizales, Bo= Bogota, Bu= Bucaramanga, P= Panama. After Pennington (1981) and Ego et al. (1993).

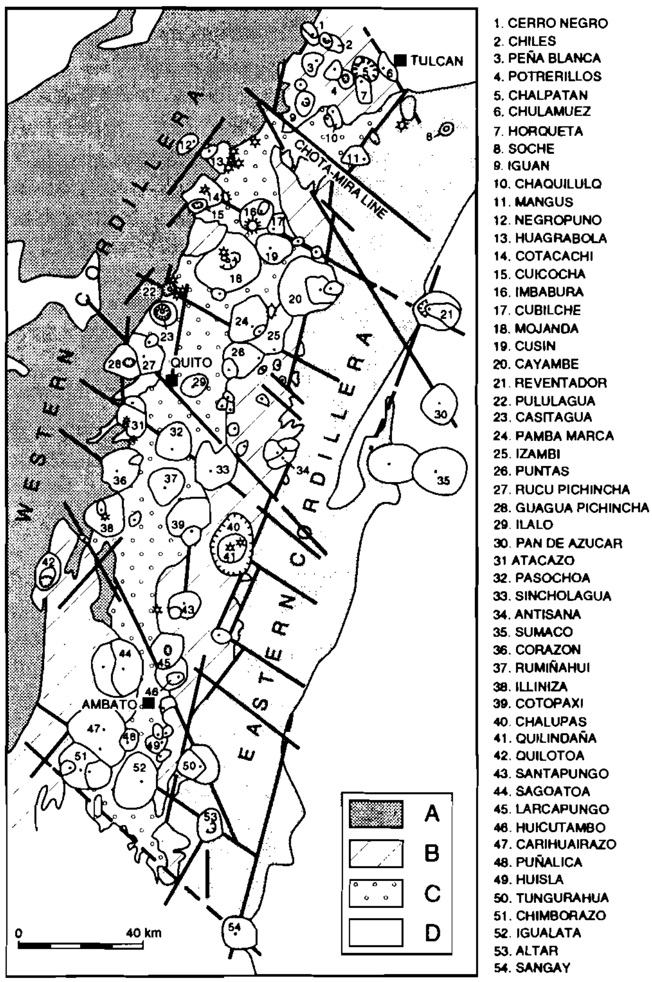


**Fig. 2**

Quaternary volcanoes and main tectonic lineations of the Ecuadorian Andes from 1° N to 2° S (from Barberi et al., 1988).

A= Western Cordillera: Macuchi Formation and Cretaceous-Eocene clastic deposits;
B= undifferentiated basal volcanic complex (Late Miocene-Quaternary);
C= volcanic and volcano-sedimentary deposits filling the Interandean Depression;
D=Eastern Cordillera: mainly metamorphites.

island-arc, such as the New Hebrides arc (Southwest Pacific; Monzier et al., in prep.). A marked increase of K2O content is also obvious in the volcanic products from the Western Cordillera to the Eastern Cordillera, an observation already noted by Barberi et al. (1988). Another striking difference between the rocks from the two cordilleras is the value of the Ba/La ratio (LILE / HFSE), >49 in the Western Cordillera and <49 in the Eastern Cordillera (Cayambe, Chacana, Cotopaxi, Tungurahua), an observation which may reflect a greater slab contribution in the magmas of the Western Cordillera. Diagrams of Sr/Y vs. Y and La/Yb vs. K2O (Fig. 3) emphasize the very high Sr/Y and La/Yb ratios of recent Cayambe dacites, a characteristic signature of dacitic melts derived from metamorphosed basalts, i. e. adakites. These adakites from Cayambe clearly follow a broad melting trend on the La/Yb vs. K2O diagram, fractionation being only of minor importance. Contrarily, in the Tungurahua suite fractionation is the dominant process. Sr/Y ratios and Y contents of adakites from Cayambe and Mount St Helens (Defant and Drummond, 1993) are very similar. Lastly, it should be stressed that samples from the old part of Cayambe are not adakitic. All samples from Cushnirumi and Fuya Fuya also have a strong adakitic character, whereas only some of the rocks from Cotacachi, Pululahua, Quilotoa, Cotopaxi and Tungurahua volcanoes are adakites. Conversely, all Mojanda samples are calc-alkaline.

## PRELIMINARY CONCLUSIONS

At this point of the program, it appear that adakites are common in Ecuador, in both cordilleras. They can appear either during a given period of the history of a single volcano (Cayambe: Samaniego et al., this volume) or simulteanously with calc-alkaline rocks at two close volcanic centers (Fuya Fuya and Mojanda: Robin et al., this volume), which entail some interesting volcanological questions. The question of the basaltic source, i. e. slab or lower crust melting, remains unsolved for the moment, but as ecuadorian adakitic volcanoes (especially Cayambe) lie far from the trench, it is perhaps more reasonable to contemplate a crustal origin than a slab one, even if the subducting crust is young (<20 Ma). Regional crustal modeling and heat flow measurements would be very convenient to solve this question as well as detailed studies on the mode of subduction below Ecuador and the role of the Carnegie Ridge in this process.

## REFERENCES


-Atherton, M. P. and Petford, N., 1993. Generation of sodium-rich magmas from newly underplated basaltic crust. *Nature*, 362, 144-146.

-Barberi, F., Coltelli, M., Ferrara, G., Innocenti, F., Navarro, J.M. and Santacroce, R., 1988. Plio-Quaternary volcanism in Ecuador. *Geol. Mag.*, 125, 1, 1-14.

-Ego, F., Sebrier, M., Lavenu, A., Yepez, H. and Eguez, A., 1993. Quaternary state of stress in the northern Andes and the restraining bend model for the ecuadorian Andes. Second ISAG, Oxford (UK), 21-23/9/1993, extended abstracts, Editions de l'ORSTOM, Paris 1993, p. 89-92.

-Ego, F., Sébrier, M. and Yepes, H., 1995. Is the Cauca-Patia and Romeral fault system left or rightlateral? *Geophys. Res. Let.*, 22, 1, 33-36.

-Defant M. J. and Drummond, M. S., 1990. Derivation of some modern arc magmas by melting of young subducted lithosphere. *Nature*, 347, 662-665.

-Defant M. J. and Drummond, M. S., 1993. Mount St. Helens: potential example of the partial melting of the subducted lithosphere in a volcanic arc. *Geology*, 21, 547-550.

-Defant, M. J., Richerson, P. M., De Boer, J. Z., Stewart, R. H., Maury, R. C., Bellon, H., Drummond, M. S., Feigenson, M. D. and Jackson, T. E., 1991. Dacite genesis via both slab melting and differentiation: petrogenesis of La Yeguada volcanic complex, Panama. *J. Petrol.*, 32, 6, 1101-1142.

-Drummond, M. S. and Defant, M. J., 1990. A model for trondhjemite-tonalite-dacite genesis and crustal growth via slab melting: Archean to modern comparisons. *J. Geophys. Res.*, 95, B13, 21503-21521.

-Monzier, M., Robin, C., Eissen, J. P. and Cotten, J. (in prep.). Geochemistry of the volcanic New Hebrides Central Chain (Southwest Pacific). *J. Volcanol. Geotherm. Res.*,...

-Pennington, W. D., 1981. Subduction of the eastern Panama Basin and seismotectonics of northwestern South America. *J. Geophys. Res.*, 86, B11, 10753-10770.

-Sajona, F. G., Maury, R. C., Bellon, H., Cotten, J., Defant, M. J., Pubellier, M. and Rangin, C., 1993. Initiation of subduction and the generation of slab melts in western and eastern Mindanao, Philippines. *Geology*, 21, 1007-1010.

-Smith D. R. and Leeman, W. P., 1987. Petrogenesis of Mount St Helens dacitic magmas. *J. Geophys. Res.*, 92, B10, 10313-10334.

-Winter, T., 1990. Mécanismes des déformations récentes dans les Andes équatoriennes. Thèse Paris XI, Orsay, France, 205p.

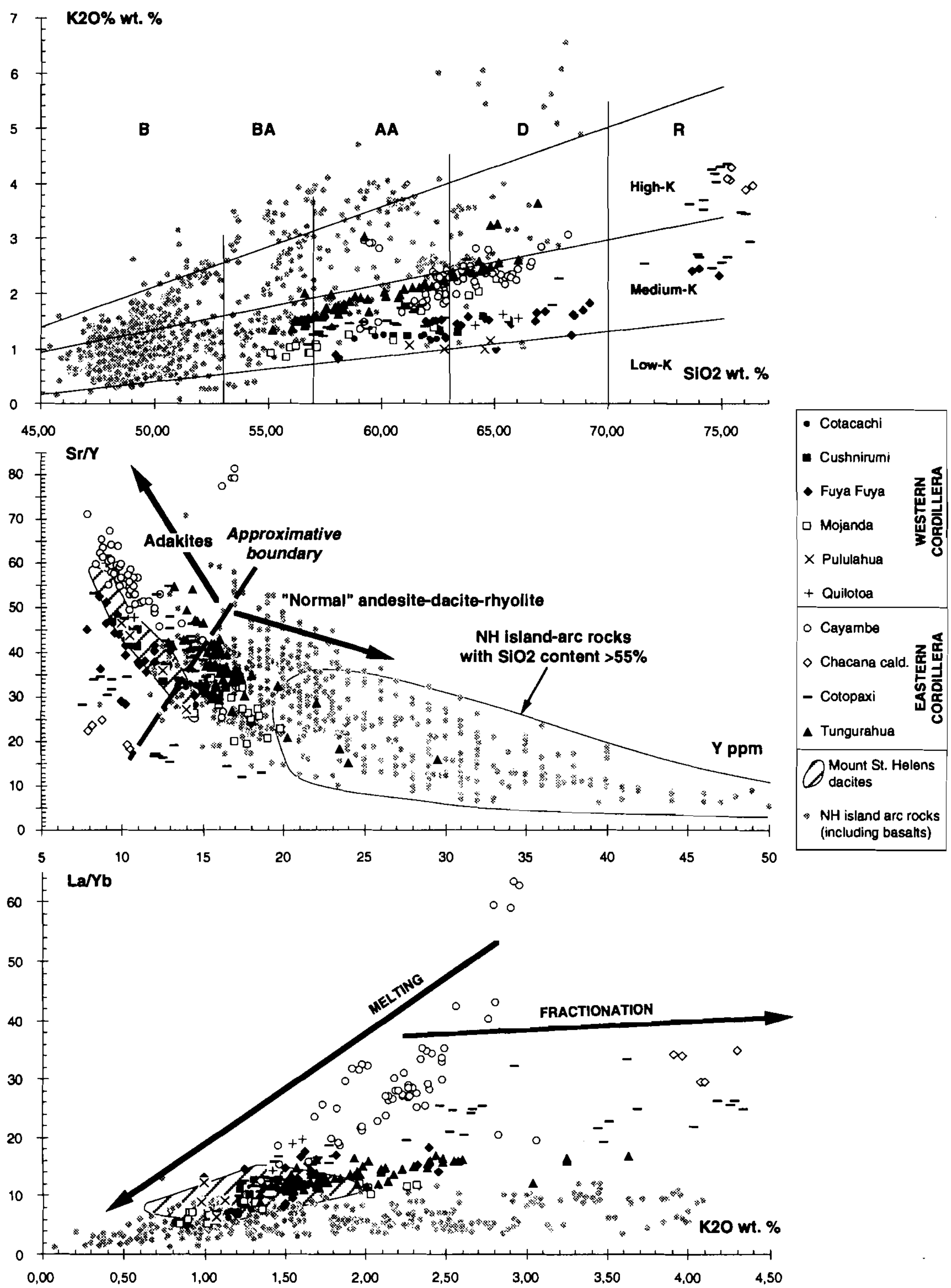


**Fig. 3** K2O vs. SiO2, Sr/Y vs. Y and La/Yb vs. K2O diagrams for volcanic rocks from Ecuador. Mount St Helens dacites (Smith and Leeman, 1987) and New Hebrides island arc rocks (Monzier et al., in prep.) are given for comparison. An approximative boundary between adakites and "normal" rocks is also presented, but its exact location is questionable.

# CHEMICAL CHARACTERISTICS OF METAMORPHIC MINERALS IN LOWER CRETACEOUS BASIC FLOWS FROM THE COAST RANGE, CENTRAL CHILE.

Diego MORATA(2), Mario VERGARA(1), Luis AGUIRRE(1), José CEMBRANO(1) & Encarnación PUGA(3)

(1) Dpto. Geología . Facultad de Ciencias Físicas y Matemáticas. Universidad de Chile. Casilla 13518. Correo 21. Santiago de Chile (Chile).
(2) Dpto. Cristalografía y Mineralogía, Estratigrafía, Geodinámica, Petrología y Geoquímica. Facultad de Ciencias del Mar. Universidad de Cádiz. 11510 Puerto Real, Cádiz. Spain
(3) Instituto Andaluz de Ciencias de la Tierra. CSIC-Universidad de Granada. Fac. Ciencias. Avda. Fuentenueva s/n. 18002 Granada (Spain).

**KEY WORDS:** Burial metamorphism, pumpellyite, K-rich minerals, Coast Range, Central Chile.

## INTRODUCTION

The Lower Cretaceous Ocoite Group (Aguirre *et al.* 1989) with a thickness of 3-13 km constitutes a *c.* 1000 km long belt of volcanic rocks in the Coast Range of central Chile. Predominant rock types are basic lava flows characterized by high K content which classify as high-K calcalkaline basalts and basaltic andesites with shoshonitic affinity (Levi *et al.*, 1982, 1988; Vergara *et al.*, 1995). They present porphyritic textures with abundant phenocrysts of plagioclase and minor clinopyroxene. Very low to low-grade burial metamorphism affects them with development of quartz,albite,K-feldspar, prehnite, pumpellyite, epidote, actinolite, white mica, chlorite, calcite and zeolites present as pseudomorphs of primary minerals, as groundmass replacement and filling amygdales. Metamorphism increases in grade with stratigraphic depth in the rock pile from zeolite facies at the top to greenschist facies at the base (Levi, 1969;Levi *et al.* 1982).

Here we study the chemical composition of some of the secondary minerals present in the basic lavas of the Ocoite Group from the Bustamante Hill area located *c.* 35 km west of Santiago. In this area the Cretaceous lavas are well exposed with the presence of unaltered levels in which the primary mineralogy and the chemistry are preserved. The aim of this work is to show the chemical variations of some of the secondary minerals, both at a macro and microdomains.

## MINERAL CHEMISTRY

In order to avoid the influence of microdomain chemistry in the composition of the metamorphic phases, the study was largely restricted to minerals filling amygdales among which K-feldspar, chlorite, epidote and pumpellyite are the most representative phases. Minor prehnite, albite and quartz appear in some lavas. Most commonly,primary plagioclase phenocrysts are partially or totally replaced by albite, epidote and white mica, with some relict primary patches of composition between $An_{56}Ab_{40}Or_4$ to $An_{70}Ab_{28}Or_2$ (figure 1a).

Chemical analyses were performed in a CAMECA-CAMEBAX microprobe (20kV, 10nA, 10μ) at the University of Granada, Spain.

*K-feldspar*

K feldspar ($Or_{67}$ to $Or_{98}$ with An $\leq$ 4) appears as patches replacing primary plagioclase phenocrysts as well as filling amygdales (figures 1a and 1b). K-feldspar replacing primary plagioclase phenocrysts are characterized by a BaO content ranging from 0.30 to 0.56% (figure 1b). On the other hand secondary feldspar in amygdales is mainly adularia ($Or_{97}Ab_3$) with BaO contents up to more than 2.5% (figure 1b) and varying in composition from core to rim in a same crystal.

*Pumpellyite*

Pumpellyite in amygdales presents strong chemical variations in terms of $Fe_2O_3$ and $Al_2O_3$ (figure 2) with $XFe^{3+}$ values (= $100Fe^{3+}/(Fe^{3+} + Al_t)$) ranging from 12 to 33% and increasing from the top levels to the bottom, a tendency already pointed out by Levi *et al.*(1982). We have studied pumpellyite chemical variations at the scale of a single crystal in different amygdales finding that a similar variation, characterized by increasing $Fe_2O_3$ and decreasing $Al_2O_3$ from core to rim, exists in these crystals. This chemical variation is strong and accounts for high point spreading in the Al-Fe-Mg diagram where compositions in a same crystal plot in different reference fields (which could be interpretated as generated at different metamorphic facies!).

*Chlorite*

Chlorite also presents remarkable compositional variations from top to bottom of the Ocoite Group. The general trend is characterized by an increase in chlorite molecular component (%*Xc*) from top to bottom (figure 3) accompanied by the increase of the temperature value obtained from the Cathelineau geothermometer (Cathelineau & Nieva, 1985). At the level of one amygdale, an increase in chlorite component, and consequently of the temperature of formation, exists from rim to core

*Epidote*

Epidote compositional variations in amygdales are very similar from top to bottom in the pile, with no particular trends being observed. Largest variations of the $XFe^{3+}$ observed cover the interval 22 to 37%.

## DISCUSSION

The presence of secondary minerals rich in K and Ba (adularia and white mica) replacing primary plagioclase phenocrysts and filling amygdales can be interpreted as being conditioned by a primary high K whole rock composition or as produced by K and Ba being introduced to the system during burial metamorphism. In this respect, it is worth noting that in the Mesozoic magmatism of central Chile, only those rocks with a shoshonitic affinity include adularia in the secondary assemblages. The $K_2O$ contents in whole rock analyses of unaltered aphanitic samples from the studied region range from 1.18% (in basalts) to 3.90%(in andesites) (Vergara *et al.*, 1995). Considering the maximum $K_2O$ content found in primary Ca-rich plagioclase (*c.* 0.6%) and taking 30% as the modal percentage of plagioclase phenocrysts in the rocks, the $K_2O$ content of the groundmass can be calculated applying simple mass balance. Thus, the $K_2O$ contents could vary from *c.* 1.0% in basalts to *c.* 3.7% in andesites. These contents of primary K could account for the presence of secondary adularia in patches of primary plagioclase phenocrysts due to internal remobilization of K. More chemical work is needed to determine if the K available in the system suffices to explain the presence of abundant adularia in amygdales. Concerning Ba, calculations are more complex due to the fact that only some phenocrysts are partially replaced by adularia and, in these cases, the BaO content of this adularia is very minor.

The compositional variations from top to bottom found in pumpellyites, with an increase of the $XFe^{3+}$ contents, could be related to the metamorphic gradients (Levi *et al.*, 1982). Moreover, the strong compositional variations observed in a same amygdale, with increase in $Fe_2O_3$ from core to rim, must be interpreted as due to local variations in $fO_2$ in thermodynamic conditions of disequilibrium. These dramatic variations in the pumpellyite chemistry are a major limitation in using the composition of this mineral for qualitative estimations of the metamorphic grade. Variations in the $XFe^{3+}$ in single crystals of epidote and pumpellyite from a particular amygdale are also taken as a consequence of disequilibrium conditions, at least at the amygdale scale.

Chemical variations observed in chlorites agree with the general metamorphic pattern determined by Levi *et al.* (1982), with an increase in the chlorite component from top to bottom. Variations into a single amygdale also agree with the general trend characterized by a rising chlorite component from rim to core. For the lower levels of the volcanic pile studied, the calculated temperatures coincide with the temperatures usually assigned to the prehnite-pumpellyite to greenschist facies.

## CONCLUSIONS

Two main conclusions can be drawn based on the chemical variations described. These variations largely fit in the regional metamorphic pattern already established by Levi *et al.* (1982). However, the compositional trends found for some index minerals, *i.e.* chlorite and notably pumpellyite, reflect highly heterogeneous conditions during this burial metamorphism, at least at the scale of a same lava flow. This heterogeneity can result from severe variations in $fO_2$ from top to bottom in a same lava flow during the formation of the pumpellyites and the mafic phyllosilicates. Thus, conclusions concerning metamorphic grade based on the compositional reference fields of the Fe-Al-Mg diagram should be critically assesed.

Concerning the presence of abundant Ba-rich adularia in amygdales, further detailed work must be carried out to clarify its origin, either primary or metasomatic.

## ACKNOWLEDGEMENTS

This research has been carried out under a C.S.I.C. - Universidad de Chile cooperation project. Other financial support came from the Spanish Research Project PB92-0952 and the Universidad de Chile DTI-2834-9445 Project.

## REFERENCES

Aguirre, L. 1993. Compositional variations of Cretaceous pumpellyites along the western margin of South America and their relation to an extensional geodynamic setting. *J. metamorphic Geol.*, 11, 437-448.

Aguirre, L.; Levi, B. and Nystr_m, J.O., 1989. The link between metamorphism, volcanism and geotectonic setting during the evolution of the andes. in: Daly, J.S., Cliff, R.A. & Yardely, B.W.D., eds., Evolution of metamorphic belts. *Geol. Soc. London Sp. Pub.*, 43, 223-232.

Cathelineau, M. and Nieva, D., 1985. A chlorite solid solution geothermomether. The Los azufres geothermal system. *Contrib. Mineral. Petrol.*, 91, 235-244.

Levi, B. 1969. Burial metamorphism of a Cretaceous Volcanic sequence West from Santiago, Chile. *Contrib. Mineral. Petrol.*, 24, 30-49

Levi, B.; Aguirre, L. and Nystr_m, J.O., 1982. Metamorphic gradients in burial metamorphosed vesicular lavas: comparison of basalt and spilite in Cretaceous basic flows from Central Chile. *Contrib. Mineral. Petrol.*, 80, 49-58.

Levi, B.; Nystr_m, J.O.; Thiele, R. and Aberg, G. 1988. Geochemical trends in Mesozoic-Tertiary volcanic rocks from the Andes in central Chile and tectonic implications. *J. South Amer. Earth Sci.*, 1, 63-74.

Vergara, M.; Levi, B.; Nystrom, J. and Cancino, A. 1995. Jurassic and Early Cretaceous island arc volcanism, extension, and subsidence in the Coast Range of central Chile. *Gel. Soc. Amer. Bull.*, 107, 1427-1440.

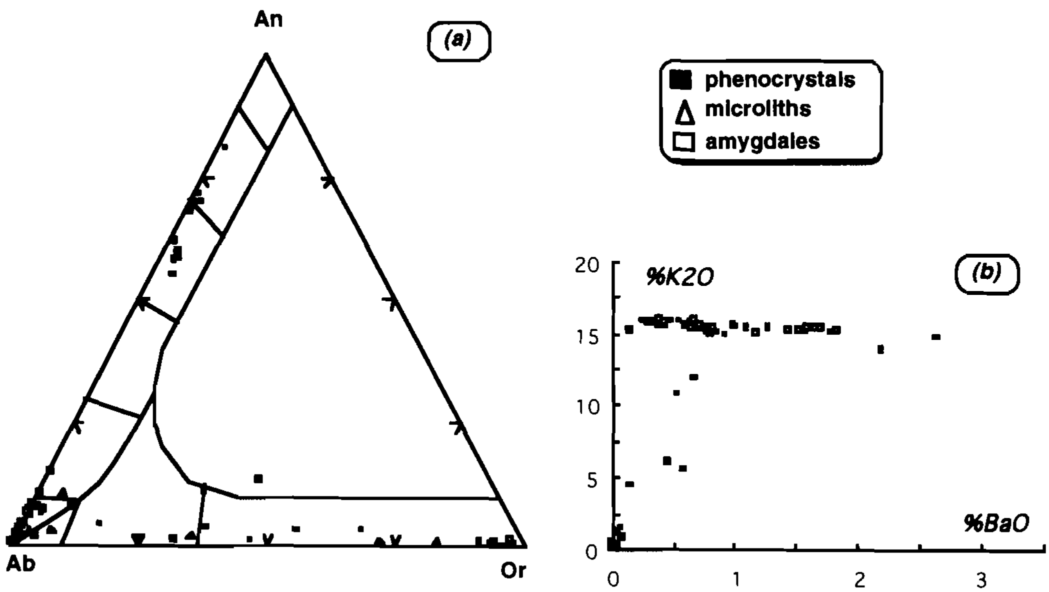


*Figure 1.- Feldspar compostional variations in Cretaceous lavas from the Coast Range, Central Chile.*

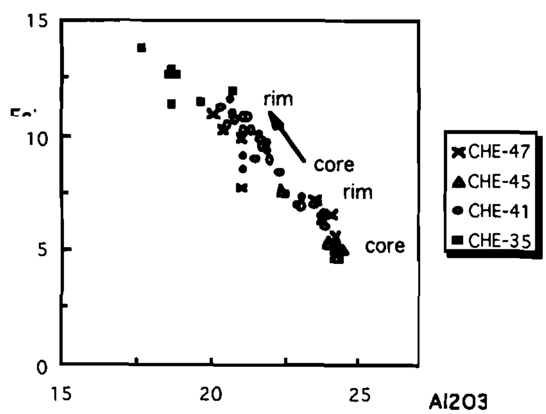


*Figure 2.- $Al_2O_3$ vs $Fe_2O_3$ in pumpellyites from amygdales. Samples in legend are stratigraphically ordered from top (sample CHE-47) to bottom (CHE-35).*

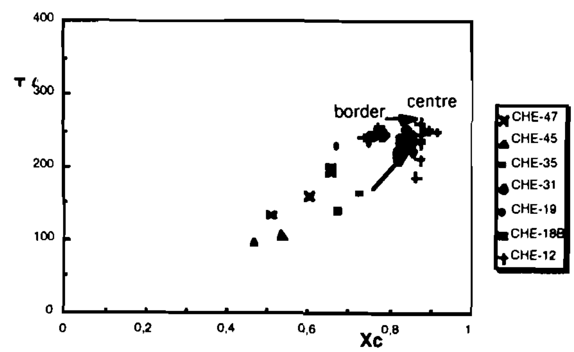


*Figure 3.- %Xc vs T (° C) in chlorites from amygdales. Samples in legend are stratigraphically ordered from top (sample CHE-47) to bottom (CHE-12).*

# The Geochemistry of Huaynaputina Volcano, Southern Peru

**Richard A. OLIVER[1], Nicole VATIN-PERIGNON[2], Pierre GOEMANS[3] and Francine KELLER[2]**

[1] Institut Laue Langevin, Avenue des Martyrs, Grenoble, France.
[2] Institut Dolemieu, UJF Grenoble, France
[3] Simecsol, Agence de Crolles, Crolles, France

## INTRODUCTION

The Central Volcanic Zone (CVZ) of the Peruvian and Chilean Andes is an active, convergent margin, continental arc, but with a highly thickened crust (up to 75 km) which is thicker than any other subduction zone. This gives rise to volcanic suites which are chemically and isotopically distinct from those erupted in other parts of the Andean arc, where the continental crust is of normal thickness (Thorpe et al., 1984; Harmon et al., 1984; Wörner et al., 1992). A quantity of data exists for young volcanic rocks south of 17°S (Wörner et al., 1992) but data from volcanic centres above this latitude are scarce. We detail here some data from the volcanic centre of Huayanaputina in Southern Peru.

The Volcano Huaynaputina is situated at 16°35'03" S: 70°52'00"W in the province of Moquegua, Southern Peru at approximately 80 km east of the town of Arequipa. The last recorded eruption from this volcano was in 1600 when a series of large plinean type eruptions took place lasting for approximately one month. From contemporaneous accounts, the ash and pumice fall out from this series of eruptions was extremely heavy, and resulted in a large loss of life over a fairly wide area. At the same time records also show that large pyroclastic flows descended the valley of the Rio Tambo (Figure 1.) reaching the coast some 130 km from the source.
In this paper we detail the geochemistry of the products from this last eruption together with rocks from earlier eruptions and attempt to show the geochemical evolution of this typical CVZ calc-alkaline volcano.

## GEOLOGICAL SETTING:

The Volcano rises to a maximum elevation of 4800 metres but the actual volcanic edifice is much smaller than this having an approximate elevation of less than 1000m. The volcano is situated on a plateau with an average elevation of 4200 meters which has been deeply incised by the Rio Tambo and the eastern side of the volcano falls away into the gorge (Figure 2). The volcano is built on volcanics and sediments of the Barroso formation, which lie unconformably over, to the west gneisses and granites of the Precambrian basement, which have been faulted to the surface, these have been intruded by basic and acidic dykes but it is not known if this was a contemporaneous episode. To the south the rocks are formed of sediments of the Yura (Upper Jurrassic-Lower Cretaceous) formation whilst to the east the rocks are of the Toquepala (Cretaceous) formation which have been intruded by tonalites and granodiorites which have been Rb/Sr dated to 22.8 +/- 2Ma (Oliver et al. 1993).

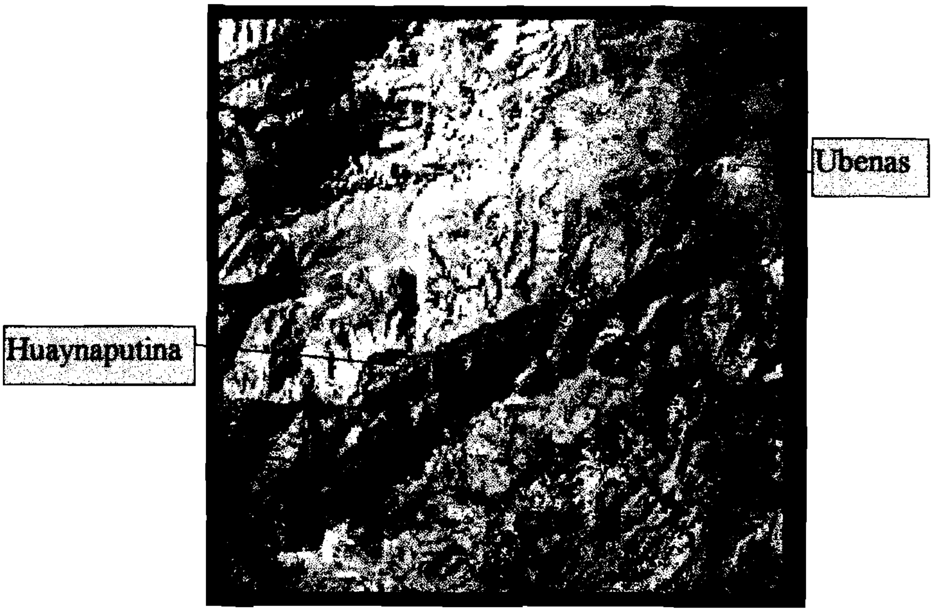


**Figure 2. Landsat photo of Huaynaputina volcano (centre left) with Ubenas volcano (top right).**

## GEOCHEMISTRY

Rock types from the Huaynaputina volcano range from andesites to dacitic pumices ($SiO_2$ wt% from 57-67.8), Fig 3 and as with other examples from the northern part of the CVZ fall into the high-K field of volcanic rocks. Relative to high-K calk-alkaline rocks the Huaynaputina lavas are indistinguishable from andesites from Solimana, (Vatin Perignon et al., 1992) and Coropuna, (Venturelli et al., 1978).
Multi-element discriminant diagram patterns are almost identical to other centres from this region (Figure 4.), although some samples show a distinct negative anomaly for Ta. This possibly indicates an increasing contamination by crustal components (Davidson et al., 1988).

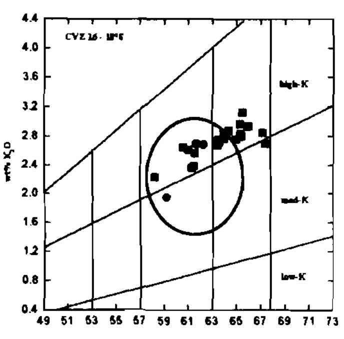


**Figure 3. Plot of wt% $K_2O$ versus wt% $SiO_2$ for rocks from the Huaynaputina volcano, S. Peru**
(circle is field for other CVZ rocks (Wilson,1989)

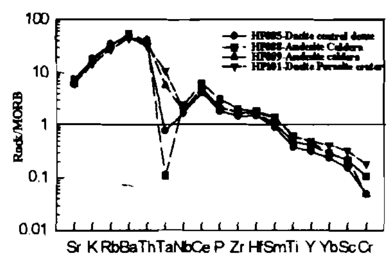


**Figure 4. Multi-element discriminant diagram for representative samples from Huaynaputina volcano**

This is born out by a plot of Th versus Ta (Figure 5) where samples from Huaynaputina lie both in the field of subduction zone magmatism and Orogenic related magmatism indicating the crustal contamination of these volcanics. However it is also evident that some crystal fractionation has taken place which is shown by a plot of Zr versus Hf (Figure 6.) where the lavas follow a trend away from mantle values.

The variation of Sr isotopes with $SiO_2$ For Huaynaputina volcano is compared with other data from the CVZ. The variation of $^{87}Sr/^{86}Sr$ ratios is fairly small varying from 0.70637 to 0.70692

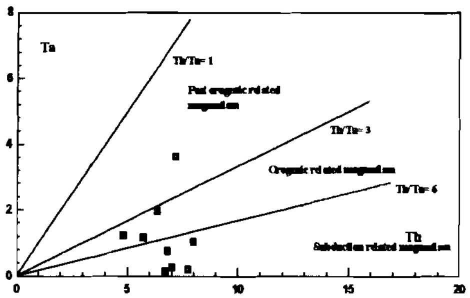


**Figure 5. Plot of Th versus Ta for Huaynaputina volcanics.**
**(fields are from Cabanis et al., 1990)**

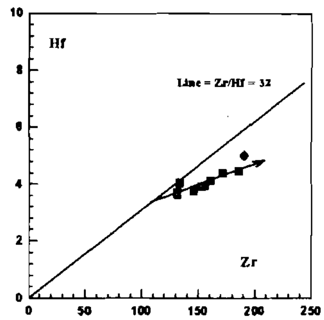


**Figure 6. Plot of Zr versus Hf for Huaynaputina volcanics.**

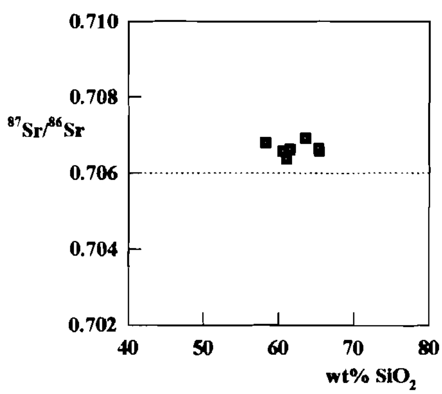


**Figure 7. Plot of Sr isotope ratios versus $SiO_2$ for andesites and dacites from the Huaynaputina volcano compared to data from (A) San Pedro-San Pablo. N. Chile (Thorpe et al., 1976), (B) Solimana, S. Peru, (Goemans, 1986).**

These values fall within the fields described for the San Pedro-San Pablo complex, N. Chile, field A on Figure 7., and Solimana volcano, S. Peru, field B. This indicates similar source types as for other volcanic centres within the region with similar amounts of crustal contamination. This is born out by a slightly negative correlation for $\varepsilon_{Sr}$ with increasing Sr content.

## CONCLUSIONS

The geochemistry of the Huaynaputina volcano is shown to be typical for the CVZ, with andesitic to dacitic magmas showing evidence for both crystal fractionation and crustal contamination.

## REFERENCES

Cabanis B., Cocheme J.J., Vellutini P.J., Joron J.L and Treuil M., 1990, Post collisional Permien volcanism in northwestern Corsica: an asessment based on mineralogy and trace-element geochemistry. *J. Volc. Geotherm. Res.*, 44, 51-67.

Davidson J.P., Ferguson K.M., Colucci M.T. and Dungan M.A., 1988. The origin and evolution of magmas from the San Pedro Pellado volcanic complex, S. Chile: multicomponent sources and open system evolution. *Contrib. Mineral. Petrol.*, 100, 429-445.

Goemans P., 1986, Pétrogéochimie du volcan Solimana, Sud Pérou. (Géochimie comparée de quelques édifices des Andes centrales et septentrionales). *Mem. DGUG, UJF de Grenoble*, 114p, (unpublished)

Harmon R.S., Barreriro B.A., Moorbath S., Hoefs J., Francis P.W., Thorpe R.S., Deruelle B., McHugh J. and Viglino J.A., 1984, Regional O-, Sr and Pb isotope relationships in late Cenozoic calc-alkaline lavas of the Andean Cordillera., *J. Geol. Soc., London*, 141, 803-822.

Oliver R.A., Vatin Perignon N., Keller F. and Salas G., 1993, Geochemical constraints on the evolution of the Southern peruvian Coastal Batholith: Toquepala segment. (abst). *Proceedings of 2nd ISAG, Oxford, England.*

Thorpe R.S, Potts P.J. and Francis P.W., 1976, Rare earth data and petrogenisis of andesites from the North Chilian Andes., *Contrib. Mineral. Petrol.* 54, 66-75.

Thorpe R.S., Francis P.W. and O'Callaghan L.et al., 1984, relative roles of source composition, fractional crystallisation and crustal contamination in the petrogenisis of Andean volcanic rocks., *Phil. Trans. R. Soc. Lond.*, A310, 675-692.

Vatin Perignon N., Oliver R.A., Goemans P., Keller F, Briqueu L. and Salas G., 1992, Geodynamic interpretaions of plate subduction in the northernmost part of the Central Volcanic Zone from the geochemical evolution and quantification of the crustal contamination of the Nevado Solimana volcano, Southern Peru., *Tectonophysics*, 205, 329-355.

Venturelli M., Frangipane M, Weibel M. and Antiga D., 1978, Trace element distribution in the Cenozoic lavas of the Nevado Coropuna and Andagua valley, central Andes of Southern peru. *Bull. Volcanol.*, 41, 213-228.

Wilson M.,1989, Igneous Petrogenesis, Unwin Hyman, London.

Wörner G., Moorbath S. and Harmon R.,1992, Andean Cenozoic volcanic centers reflect basement isotopic domains. *Geology*, 20, 1103-1106.

# PETROLOGY AND EMPLACEMENT OF FRONTAL CORDILLERA GRANITOIDS, MENDOZA PROVINCE, WESTERN ARGENTINA (33-34°S)

H. M. Orme[1], N. Petford[1], M. P. Atherton[2], D. Gregori[3], M. A. Ruvinos[3], S. G. Pugliese[1]

[1]School of Geological Sciences, Kingston University, Kingston upon Thames, Surrey, UK.
[2]Department of Earth Sciences, University of Liverpool, Brownlow Street, Liverpool, UK.
[3]Departamento de Geologia, Universidad Nacional del Sur, San Juan 670, 8000 Bahia Blanca, Argentina

**KEY WORDS:** Granite, defromation, emplacement

The area discussed is a 30 km transect along the Mendoza City to Santiago de Chile road in western Mendoza Province, Argentina (32°25'-33°10', 69°- 69°20). The most southerly point on the map (Fig. 1) is situated 30 km west of Mendoza City. Previous work by Caminos (1965) showed that two stocks of granitic rocks, Guido and Cacheuta, lie in a NNE/SSW trending basin of mainly acidic volcanic rocks of the Choi Yoi Lower Triassic, and syn and post rift sedimentary rocks of Upper Triassic age. Although both stocks intrude the Choi Yoi, they remain to be dated isotopically. Sedimentary rocks of Carboniferous and Devonian age crop out in the area, as well as a faulted basement slice. To the south of Cacheuta Stock is an contact between granitic and older dioritic rocks. Dykes of basalt and basaltic andesite intrude both stocks. All older lithologies have been affected subsequently by extensive brittle deformation.

## GRANITE PETROLOGY

### Guido Stock

Guido Stock has an ellipsoid outcrop pattern with a long axis parallel to the trend of the sedimentary basin the separates the stock from Cacheuta Stock (Fig. 1). It covers an area of approximately 60 km$^2$ and forms a mountainous terrane of peaks mostly over 2000m above sea level. Guido Stock granitic rocks can be subdivided into discrete facies (see Fig. 1) on the basis of petrological evidence. These are: 1) *Quartz-rich granitic rock*, 2) *Coarse k-spar-rich granitic rock* and 3) *Xenolithic granitic rock*. Enclave size ranges from 1-10cm in diameter, and undeformed examples tend to be roughly circular in shape and occur with a frequency of 0-10 m$^2$. A narrow band of xenotilths occurs along the road at the southern contact with a hornfelsed lithology of as yet unidentified age. Magmatic enclaves are also present in this facies.

### Cacheuta Stock

Cacheuta Stock is ellipsoid in outcrop pattern with a NNE/SSW trending long axis; its area is approximately 90km$^2$ with peaks up to 2500m. Cacheuta Stock can also be subdivided into 2 discrete granite facies: 1) *Rapakivi granitic rock* and 2) *'Normal' granitic rock* containing coarse k-spar, quartz and plagioclase, with biotite flakes and occasional fine euhedral hornblende (Fig. 1).

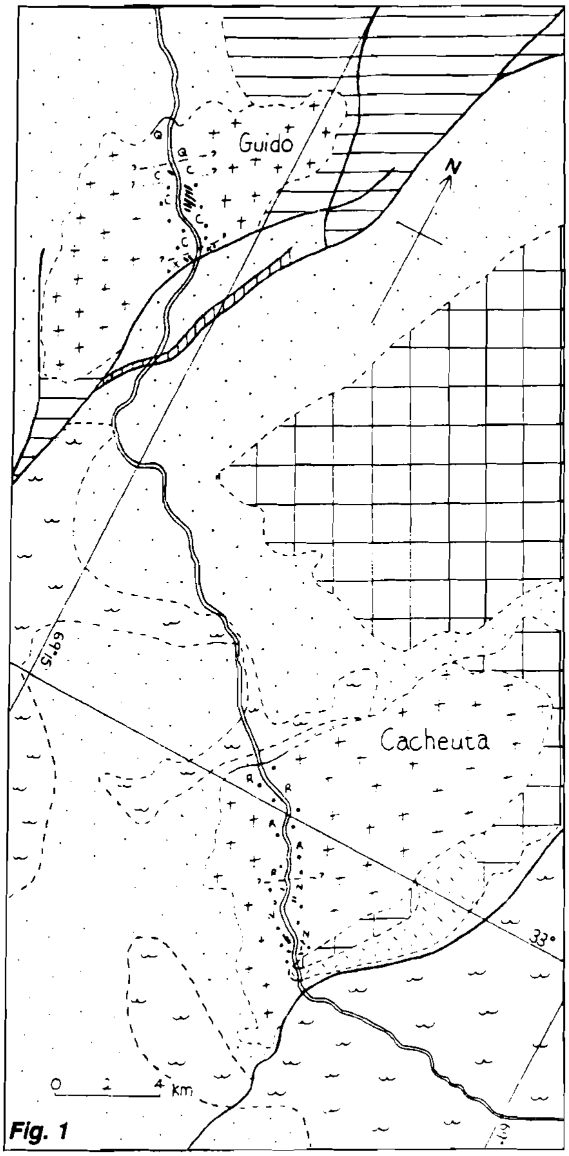


Fig. 1

### Cacheuta & Guido Granitic Stocks and the Geology of the Surrounding Area.

**Key:**

- Quaternary & recent deposits
- Basalt & basaltic andesite dykes
- Undifferentiated granitic rocks
- Quartz rich granitic rocks
- Coarse K-spar granitic rocks
- Xenolithic granitic rocks
- Rapakivi granitic rocks
- 'Normal' granitic rocks
- Granodiorite / diorite
- Volcanic and sedimentary rift deposits (Trias & Tert)
- Carboniferous sediments
- Devonian sediments
- Phyllitic basement

- Geological boundary
- Fault
- Predicted geol. boundary
- Granite facies transition
- Enclave transition
- Enclaves present (overlay)

**Fig. 2** Guido Dyke Trends

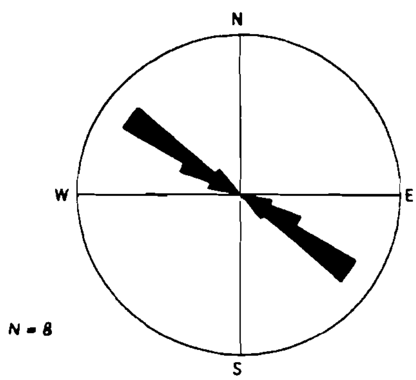


**Fig. 3** Cacheuta Dyke Trends

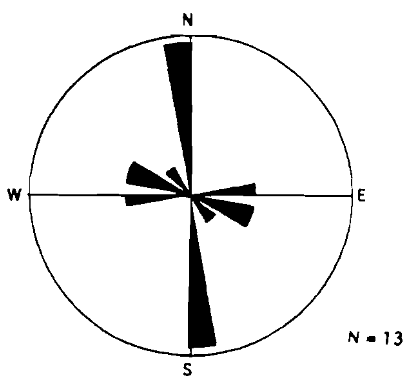

## GRANITE STRUCTURES

Metric scale faults bisect the intrusions with orientations parallel to the main joints. Later fault movement has occurred along some planes. Abundant cataclasites were found in the *xenolithic* granitic rocks. Near the southerly contact of Guido Stock they have shallow dip angles with strikes ranging from N/S to NE/SW dipping to the W and NNE. Most importantly, brittle shearing on both the centimetric and metric scale was observed in both stocks. Shallow angle roof and sole faults of duplexes occurring in the *xenolithic* and *rapakivi* granitic rocks gave a dextral shear sense (Fig. 4).

## DYKES

Both stocks are cut by dykes of more mafic compositions; Guido by basaltic andesite, and Cacheuta by basalt. The near vertical dykes vary in width from 0.5 - 22 m. All dykes exhibit a marked sinuosity in their outcrop pattern, although dyke-granite contacts are sharp, indicating that they intruded at a late syn-plutonic stage. The dykes of both plutons have a common orientation with those of Guido clustering around trends approximately NW/SE, whilst those of Cacheuta Stock cluster around orientations between E/W and NW/SE and also have a marked occurrence of N/S trends (Figs. 2 and 3). It is likely that the dykes are exploiting structures formed in relation to the large NNE/SSW trending faults of the area, and their significance will be discussed along with the granite emplacement.

## GRANITE EMPLACEMENT

By combining field data from both stocks with regional structures around 33°S, a tentative model for the emplacement of the Frontal Cordillera granitoids can be made (Fig. 4). Regional fault sets trending NW/SE intersect major N/S fault lineaments at approximately 75° and are thought to define $R_1$ Riedel shears. Dextral movement along these faults is consistent with an overall sinistral shear sense along the major faut axis. Dyke orientations within the plutons reflect emplacement during extension associated with 'P'shearing and granitoid emplacement (eg. Tikoff &Teyssier, 1992). We conclude that the grainitc rocks of the Frontal Cordillera were emplaced during a period of left-lateral strike-slip motion concurrent with regional plutonism.

## REFERENCES

Caminos, R. 1965. Geologia de la vertiente oriental del Cordon del Plata, Cordillera Frontal de Mendoza. ASOCIACION GEOLOGIA ARGENTINA, Revista XX (3), pp. 351 - 392.

Davis, G. H. & S. J. Reynolds. 1996. Structural geology of rocks and regions. John Wiley & Sons. p. 367.

Segun et al. 1967. Bosquejo Geologico del area entre Uspallata y Cacheuta, (Provincia de Mendoza). First International Symposium on Gondwana Stratigraphy and Palaeontology.

Tikoff, B & Teyssier, C. 1992. Crustal-scale en echelon "P-shear" tensional bridges: A possible solution to the batholith space problem. GEOLOGY 20, No 10, pp. 927-930.

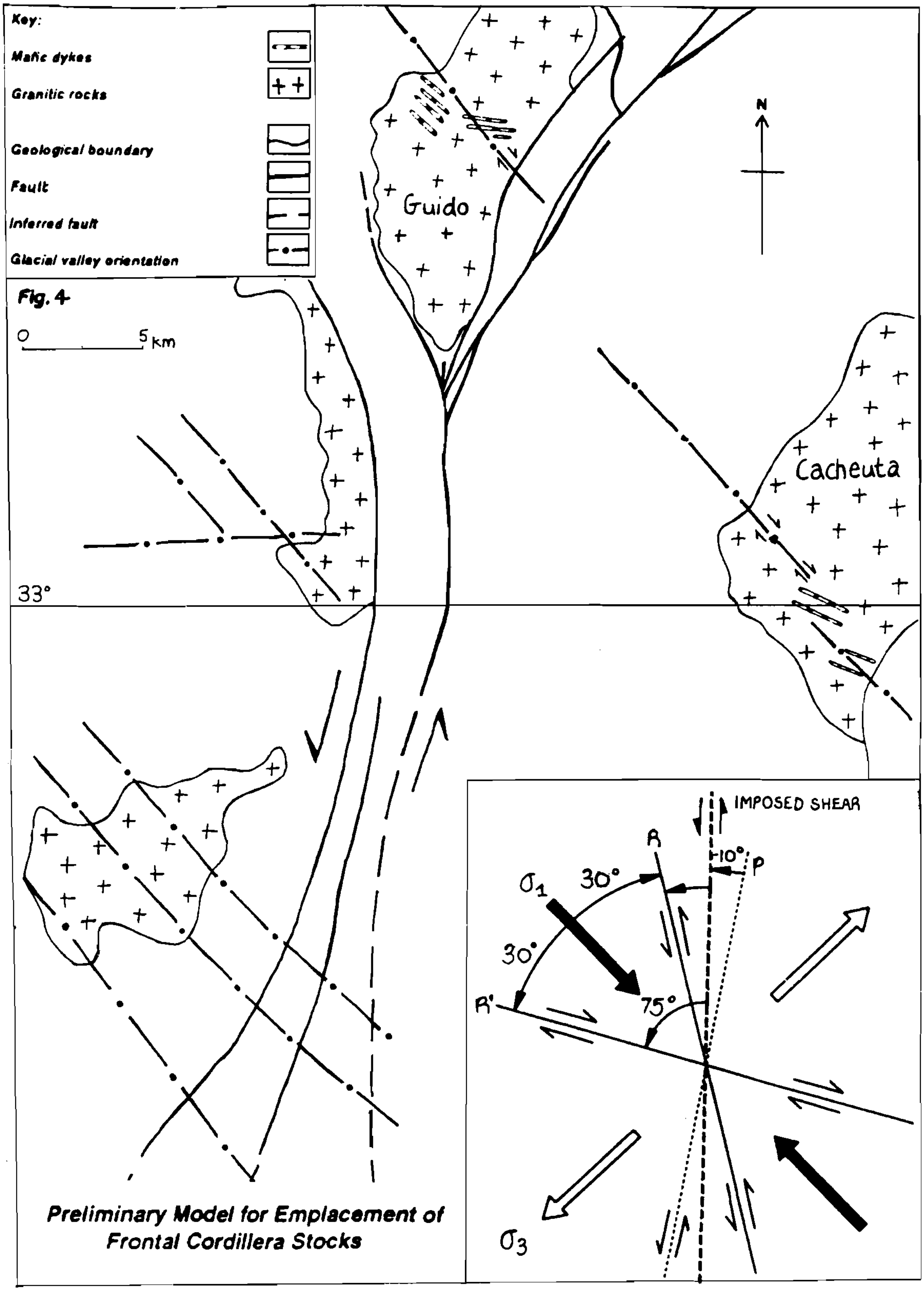
Key:
Mafic dykes
Granitic rocks
Geological boundary
Fault
Inferred fault
Glacial valley orientation
Fig. 4
0 5 km
N
Guido
Cacheuta
33°
IMPOSED SHEAR
R
10°
P
σ1
30°
30°
R'
75°
σ3
Preliminary Model for Emplacement of Frontal Cordillera Stocks

# MAGMATIC EVOLUTION OF THE EASTERN PART OF THE CHILEAN PATAGONIA (AYSEN REGION): GEOCHRONOLOGICAL AND GEOCHEMICAL CONSTRAINTS

Miguel A. PARADA, Alfredo LAHSEN and Carlos PALACIOS

Departamento de Geología, Universidad de Chile, Casilla 13518 correo 21, Santiago, Chile

**KEY WORDS:** magmatism, geochronology, geochemistry, Chilean Patagonia

## INTRODUCTION

Numerous studies have been done in the Northern Patagonian Batholith (NPB) in order to characterize the accross-NPB temporal and compositional variations (Halpern & Fuenzalida, 1978; Hervé, 1984; Bartholomew & Tarney, 1984; Bruce et al., 1991; Pankhurst & Hervé, 1994). A large number of radiometric dates obtained with different method (Rb-Sr, K-Ar and Ar-Ar) indicate that the Meso-Cenozoic plutonism have developed in a more stationary condition than the eastward migrating plutonism developed in the Andes of central Chile (cf. Drake et al., 1982; Parada et al., 1988). This study includes rocks of the NPB and rocks of the poorly dated volcanic units developed further east. The Liquiñe - Ofqui Fault Zone (LOFZ), is the western boundary of this study. It represents a major dextral srtike-slip fault system along which important displacements of the western block of the continental margin are not ruled out (Cembrano & Hervé, 1993). Based on publihed and 34 new ages together with geochemical and isotopic data, we attempt to characterize the main Meso-Cenozoic magmatic events. This study was carried out in three areas: i) eastern part of the NPB at about 44° 30' S; ii) eastern part of the Aysén Region, between Coihaique and Balmaceda (45° 30' - 46°S), and iii) along the rivers Rio Chacabuco and Rio Baker (47° - 47°30'S).

## TRANSVERSE AGE VARIATIONS IN THE NPB AT ABOUT 44° 30' S.

At a regional scale the spatial age distribution in the NPB gives rise to across-batholith zonation in which the youngest ages (Miocene) are in the central part adjacent to the LOFZ (Hervé, 1984; Pankhurst & Hervé, 1994). To the east of the LOFZ the plutons are Cretaceous in age, whereas to the west, Jurassic to Eocene intrusions are recognized (Bartholomew & Tarney, 1984; Bruce et al., 1991; Pankhurst & Hervé, 1994) forming poorly-defined belts. At 48° S, the NPB do not exhibit regular unidirectional migration of the intrusions with time (Weaver et al., 1990). Sixteen Ar-Ar ages were obtained accross the eastern part of the NPB. They confirm the previous documented regional scale age zonation characterized by Upper Miocene plutons at the LOFZ, Lower Miocene rocks further east and extensive Lower Cretaceous intrusions in the easter part of the NPB.

At the local scale, three age ranges emerge from the data of the Miocene event: 15 - 18 Ma, 9 - 11 Ma and 5 - 7 Ma. The first range is documented with a whole-rock Rb-Sr isochron (Pankhurst & Hervé, 1994) and three new Ar-Ar hornblende ages obtained in samples from the El Queulat diorite located 10 Km east of the LOFZ. Three new Ar-Ar biotite ages obtained in the same samples of the El Queulat diorite, and previous whole-rock Rb-Sr isochron and Ar-Ar ages obtained in three different garnet granite plutons (Hervé et al., 1993), define the second range. The third range is given by three Ar-Ar ages in garnet granites plutons. In addition, ages of 5.5 Ma were obtained in biotite and muscovite of three milonite samples from the LOFZ near Puerto Cisnes.

The emplacement of one Miocene plutonic unit appears to trigger the uplift and subsequent cooling of the previous unit. The first age range represents the plutonic emplacement of the El Queulat diorite. The second range includes emplacement ages of the garnet granite intrusions and cooling ages of the El Queulat diorite emplaced during the first range. The third range represents cooling ages of the garnet granite pluton. The ages of the milonite fall within the third age range and suggest that the subsolidus cooling of the garnet granites was produced by the youngest activity of the LOFZ recorded in the area.

Accross the Cretaceous plutonic belt of the NPB between 44° and 44° 30' S, an eastward decreasing ages emerge from the previous radiometric data and 4 new Ar-Ar ages. Those ages range from 124 to 75 Ma.

## AGES OF VOLCANIC ROCKS IN THE AREA BETWEEN COIHAIQUE AND BALMACEDA

Based on previous and new (11) radiometric dates (Ar-Ar in biotite and plagioclase and whole-rock K-Ar), three volcanic events can be recognized between 115 - 40 Ma. The oldest event is formed by abundant felsic tuffs, minor amount of basalts and small plutons that crop out along the foothill of the Patagonian Andes between Coihaique and Balmaceda. Rocks of this event have Ar-Ar and K-Ar ages between 100 and 115 and were assigned to the Cerro Divisadero Volcanic Complex (Belmar, 1996). The second event corresponds to a bimodal association (basalt and rhyolite) which developed to the east of the former event. Previous and new (5) age determinations define a range between 90 and 75 Ma, with the exception of one Ar-Ar age of 96 Ma. Basalts and rhyolitic tuffs from the Alto Rio Coihaique, as well as pilow basalts and associated rhyolitic tuffs near Balmaceda, form part of this event. A sequence of olivine basalts represents the last volcanic event, which have K-Ar ages of 46 and 55 Ma (cf. Belmar, 1996). A new whole-rock K-Ar age of 49 Ma was obtained for a basalt from a sequence located 5 Km north of Balmaceda.

## AGES OF MAGMATIC ROCKS ALONG THE RIVERS RIO CHACABUCO AND RIO BACKER

Three magmatic episode are recognized in this area: Middle Jurassic, Cretaceous and Eocene. The volcanic products of each episode were deposited over polymetamorphic and polydeformed schist and phyllites of a Paleozoic basement.

The Middle Jurassic event has been dated in two areas. In the Alto Rio Chacabuco, near the Chile - Argentina boundary, rhyolitic tuffs of a felsic volcanic sequence have Ar-Ar biotite and plagioclase ages of 160 and 144 Ma respectively. This sequence is intruded by a granitic pluton around which an argillic alteration developed at about 130 Ma. U-Pb and Ar-Ar biotite ages of about 155 and 158 Ma respectively, were obtained in two plutons intruding a volcanic sequence in the El Faldeo area, south of Cochrane. These jurassic ages represent the oldest mesozoic magmatic event in the studied segment of the Chilean Patagonia and correspond to the volcanism of the Ibáñez formation. At Levicán Peninsula in the General Carrera lake (~ 46° 30'S) a rhyolitic tuff of the Ibáñez formation gave an Ar-Ar biotite age of about 130 Ma.

Two Cretaceous ages of 104 and 92 Ma (K-Ar and Ar-Ar respectively) were obtained from a volcanic-sedimentary sequence developed to the west of the Jurassic volcanics of the Rio Chacabuco. The older age was obtained in a rhyolite located near the confluence of the rivers Rio Chacabuco and Rio Backer, whereas the younger age was obtained in an andesite located 20 Km further east. A sample of hornblende tonalite from the easternmost part of the NPB of these latitudes, gave an Ar-Ar hornblende age of 114 Ma.

An Eocene volcanic-sedimentary sequence, developed along the NNW-SSE segments of the rivers Rio Backer and Rio El Salto, is documented by two K-Ar ages of about 47 Ma obtained from rhyolitic tuffs The sequence also includes sedimentary breccias, basalts and felsic sills.

## GEOCHEMISTRY

Compositional variations have been observed accross the NPB at about 44° 30' S. Within the Tertiary granitoids near the LOFZ, two types of granitoids were recognized: garnet-muscovite granite and hornblende-biotite diorite. This plutonic association differs from that of hornblende-biotite granite and tonalite, which characterize the Cretaceous granitoids developed further east. All the analyzed NPB granitoids have VAG signatures. However, more fractionated REE patterns and LIL element enrichment are observed in the Cretaceous granitoids than in the Tertiary diorites.

The volcanic events recognized in the studied area are characterized by an association of abundant rhyolitic tuffs, and minor basaltic to andesitic lavas. The exception is the poorly known Jurassic event, in which only felsic material have been recognized. Similarities among the rhyolitic tuffs of the different events are recognized. These rocks have La/Yb between 5 and 20 and negative Eu anomalies. In addition they have near constant HREE enrichment of about 10 x chondrite values, precluding the garnet participation as a residual phase. Likewise the rhyolitic tuffs, the basaltic materials do not show significant differences. Compared with basalts of the Southern Volcanic Zone, most of the analyzed basalts show high LILE and moderate HFSE enrichment respect to MORB. Some of the Eocene basalts have OIB signatures.

Sr and Nd isotope data were obtained for representative samples from the Jurassic, Lower Cretaceous, Upper Cretaceous and Eocene magmatic events. Most of the rhyolitic - dacitic samples have initial Sr ratios between 0.705 and 0.712 and εNd values between 0.0 and -4.6, which suggest and important crustal contribution. Sr and Nd isotopic values within the same ranges have been obtained for Middle Jurassic granitoids south of Cochrane.

## CONCLUSIONS

The studied segment of the NPB represents a portion of the magmatic arc developed during the Cretaceous and Upper Tertiary. The jump of the plutonism to the LOFZ indicates that this structure became in the locus of the magmatism and constituted the uplifted Neogene margin north of the collision of the Chile ridge with the trench at 47° S. Taking all the avilable radiometric data, an age correlation exists between plutonism and volcanism. However, the plutonic counterparts for the Middle Jurassic, Upper Cretaceous volcanism are poorly represented.

Unlike the plutonism, the Mesozoic - Early Cenozoic volcanism generated a bimodal magmatism. The felsic materials exhibit geochemical and isotopic similarities regardless the age, suggesting a common origin. According to the published Sr isotopic data, the NPB and Southern Patagonian Batholith (SPB) have comparatively lower values than theirs volcanic counterparts. In the SPB at 48°S, the initial Sr ratios increase with increasing age (from Middle Jurassic to Eocene), indicating that the crustal contribution decreases with time (Bruce et al., 1991). Such coherent age - crustal contribution relationship is not observed in the Mesozoic - Paleogene volcanic rocks. On the contrary, the crustal contribution appears to be ubiquitous in the origin of the studied felsic volcanic rocks.

## ACKNOWLEDGMENTS

This study was financed by the FONDEF Project MI-15.

## REFERENCES

Bartholomew, D. S. & Tarney, J. (1984). Crustal extension in the southern Andes (45° - 46° S). In: B. P. Kokelaar, M. F. Howells & R. A. Roach (eds). Volcanic processes in marginal basins. Spec. Publ. Geol. Soc. Lond., 195-205.

Belmar, M. (1996). Geología de los cuadrángulos Balmaceda y Cerro Farellón Norte, Región de Aisén. Unpublished Tesis, Dept. de Geología, Univ. de Chile, Santiago, 83p.

Bruce, R. M., Nelson. E. P., Weaver, S. G. & Lux, D. R. (1991). Temporal and spatial variation in the southrern Patagonian batholith; Constraints on magmatic arc development. In Harmon, R. S. & Rapela, C. W. (eds). Andean magmatism and its tectonic setting. Boulder Colorado, Geol. Soc. Am. Spec. Paper 265, 1-12.

Cembrano, J. & Hervé, F. (1993). The Liquiñe-Ofqui Fault Zone: a major Cenozoic strike slip duplex in the southern Andes. Extended abstract; Second International Symposium on Andean Geodynamic, Oxford, 175-178.

Drake, R. E., Vergara, M., Munizaga, F. & Vicente, J. C. (1982). Geochronology of Mesozoic-Cenozoic magmatism in central Chile, Lat 31° - 36° S. Earth Sci. Reviews, 18, 353-363.

Halpern, M. & Fuenzalida, R. (1978). Rubidium - Strontium geochronology of a transect of the Chilean Andes between latitudes 45° and 46° S. Earth Planet. Sci. Lett., 41, 60-66.

Hervé, F. (1984). Rejuvenecimiento de edades radiométricas y el sistema de fallas Liquiñe-Ofqui. Comunicaciones 35, 107-116.

Hervé, F., Pankhurst, R. J., Drake, R., Beck, Jr. M. E. & Mpodozis, C. (1993). Granite generation and rapid unroofing related to strike-slip faulting, Aysén, Chile. Earth Planet. Sci. Lett. 120, 375-386.

Pankhurst, R. J. & Hervé, F. (1994). Granitoid age distribution and emplacement control in the North Patagonian batholith in Aysén (44° - 47° S). 7° Congreso Geológico Chileno, Concepción, Volumen II, 1409-1413.

Parada, M. A. and 9 others. (1988). Mesozoic and Cenozoic plutonic development in the Andes of central Chile (30° 30' - 32° 30' S). Jour. South Am. Earth Sci. 1, 249-260.

Weaver, S. G., Bruce, R., Nelson, E. P., Brueckner, H. K. & LeHuray, A. P. (1990). The Patagonian batholith at 48° S latitude, Chile; Geochemical and isotopic variations. In Kay, S. M. & Rapela, C. W. (eds). Plutonism from Antarctica to Alaska. Boulder, Colorado, Geological Society of America Special Paper 241, 33-50.

# THE PLIO-HOLOCENE MAGMATIC ARC BETWEEN 36° - 39° S: CONTROLS OF THE BENIOFF GEOMETRY

**Abel Hector Pesce**

Secretaria de Mineria e Industria, Subsecretaria de Mineria
Dirección Nacional del Servicio Geológico, Departamento de Geotermia
Av. Julio A. Roca 651 Piso 8ª Sector 10
(1322) Buenos Aires, Argentina

**KEY WORDS:** Tectonics - Volcanism - Shoshonites - Plio-Holocene

## INTRODUCTION

Within the global tectonic frame, the occidental edge of South America is an active continental margin product of the convergence betwen the Nazca and Antartica plates and the south American continental plate (Le Pichon, 1968; Isacks and Oliver, 1968; Janes, 1971; Stauder, 1973; Menjard and Philip, 1976) originating an igneous activity (Volcano-tectonic) that remains at present time. The convergence plane (Benioff Zone) presents angle variations along the active margin (Barazangi and Isacks, 1976; Isacks and Barazangi, 1977; Bevis and Isacks, 1984; Jordan et al., 1983, etc.).

During the past decade, numerous studies have increased the knowledge about the Benioff Zone behaviour and geometry. In function of distribution and features of magmatic sequences which have been developed during the Plio Holocene, this work, with the support of studies and geophysical information localized at the south Andin region, interprets and postulates a geometrical model of the descending plane in the zone included between 36° and 39° S latitude.

Gathering the geological, geophysical and volcanic evidences, complementind with petrogenetic concepts (particularly those related to the Shoshonitic magma generation hypothesis) and together with the analysis of registered seisms between 36° and 39° South Latitude during 1906-1980, a theoretical model of oceanic plate descending evolution from Pliocene up to Holocene is proposed.

The first data group allows us to distinguish three subductin areas in the plate, separated by fractures which are approximately located between parallel 33° and 37° SL; 37° and 38° 30' S; 38° 30' and 45° / 46° S, triple point (Figure 1).

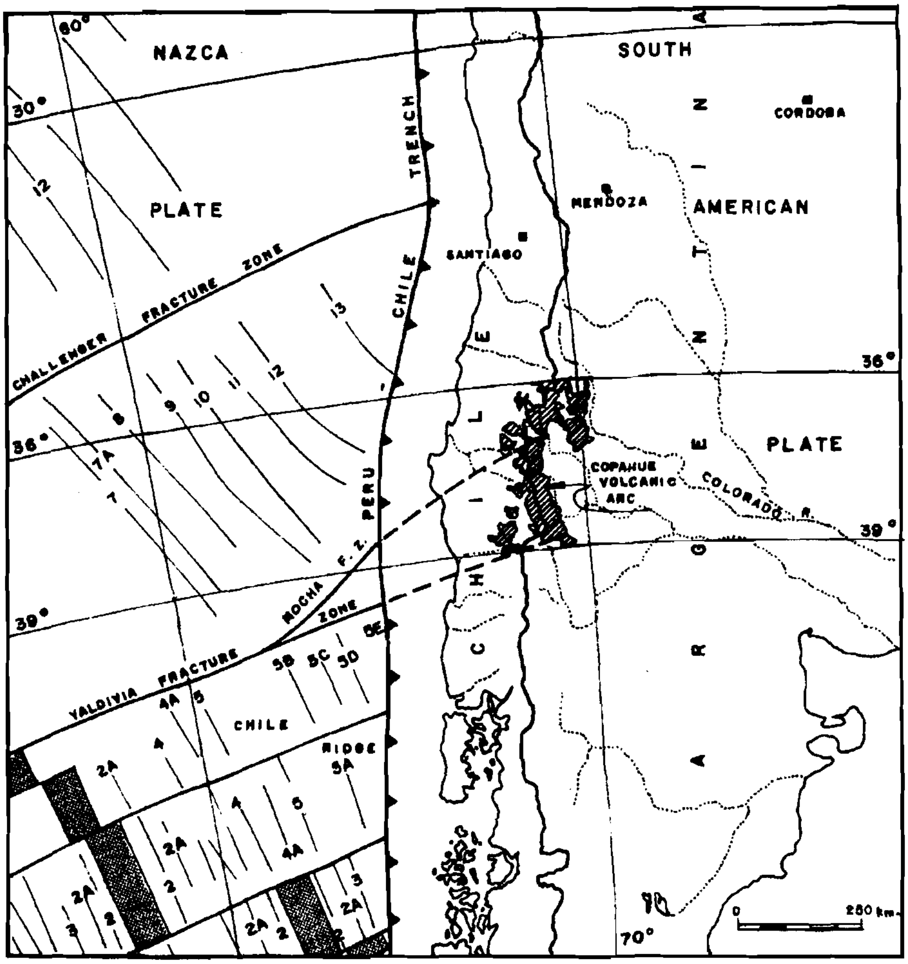


Figure 1: Map showing the fracture zone of the Oceanic Plate and extensions of the Mocha and Valdivia Factura Zones onto the continental margin, reinterpretation of its outlines after Herron (1981). The map also shows the location of Chile Ridge and Perú-Chile Trench and volcanic activity during the Pliocene-Holocene, between 36° and 39° lat. S.

Based on the information exposed in the study, the following conclusions can be extracted from:

**a)** At 37° and 38° 30' SL the subducted plate is segmented because of the interaction with the South American plate. The fracture area at North is represented by Mocha Fracture (37° SL) and it is defined at the South by Valdivia Fracture 38° 30'. These fracture zones delimit an area that outlines the limits between a crust which, at Trench sector, has different ages and structures (Herron, 1981) and in the continental area reflects in surface unequal volcanic characteristics, related to evolution, distribution and composition aspects.

**b)** The fracture zones pointed out above, allow us to interpret the existence of a "splinter or microplate". This splinter corresponds to the separationof a minimum portion of Nazca plate, at SE, in the contact area with Chile Ridge. This small fraction with a N 80° E pushing direction (Stauder, 1973) different than the one at the North of 37° SL (N 85° E, Stauder, op. cit.) has a penetration front with a N 10° W general direction. This disposition is probably due to the unequal penetration speed since the edges have different contact surfaces (the contact area is greater at North whilst at the South it is reduced by interaction with Chile Ridge). At the same time, its reduced size decreases the pushing force, being this a probable cause for major inflexion of penetration angle.

c) The efusive centers, which are the origin of the Plio-Holocene calcoalkaline and shoshonitic magmatic sequences, have an unequal distribution.

At North of 37° the calcoalkaline front extends up to 69° 45' and to the South up to 70° 30' and the distribution surface of the shoshonitic (?) magmatic sequences hase an extension of 60 km. to the North of 37° SL in EW direction, and this area is restricted to a narrow fringe of 10 km. to the South. At the same time, there is a concordance between the volcanic distribution areas in surface, the data information about the seismic profiles and the magma generation zones, which is approximately 80 to 100 km. depth for calcoalkaline magmas (Hanus and Veneck, 1978) and 150 km. for shoshonitic magmas (Deruell, 1982).

## CONCLUSIONS

This set of data allows the postulation of a theoretical model of the subduction plane geometry since the Pliocene to the Holocene (Figure 2). The most remarkable characteristics of the theoretical model are:

I) At North of 37° SL, the subduction (?) plane gets deeper through a 28° to 30° plane (Swift and Carr, 1974) and penetrates slowly to 150 to 160 km. depth. Its influence in surface should have been extended up to 69° 45' WL minimum.

II) Between 37° and 38° 30' in the area close to the Trench, the "splinter or microplate" gets deeper with a small angle of 20° approximately (Plafker, 1972). From 72° 30' / 72° 15' the oceanic microplate penetration angle increases. This change of angle and higher depth is corroborated with the location of active calcoalkaline volcanism at 71°, 71° 30' WL. Furthermore the Andean Andesitic primary magmas generation areas can be found at these latitudes in coincidence with seismic profile data. It is interpretated that this penetration angle remains up to a depth of 130 to 150 km. approximately (Shoshonitic magmas generation area) since the extension of efusive centers of this sequence at surface is limited by a narrow fringe of 10 km. approximately.

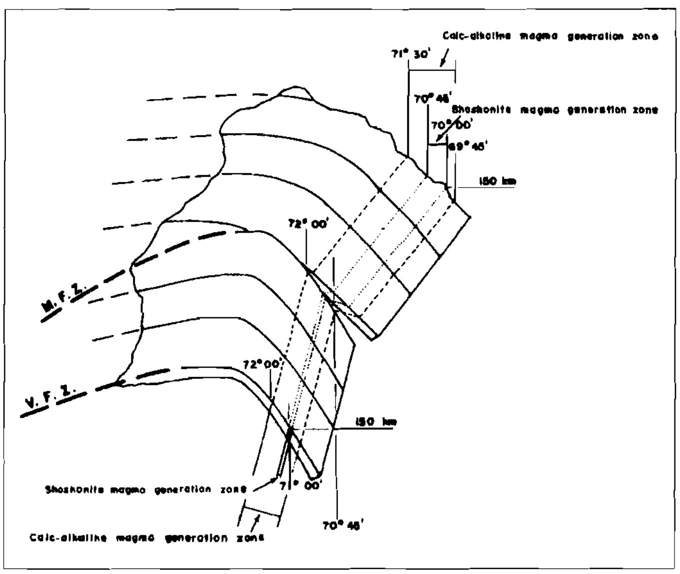


Figure 2: Interpretation of the oceanic plate geometry in the continental area between 36° - 39° last. S. During Pliolocene - Holocene, in function to volcanic evidence.

**REFERENCES**

Barazangi, M. Isacks, B. 1976. Spatial distribution of earthquakes and subduction of the Nazca plate beneath South America. Geology V.4, :686-692.

Bevis, M. Isacks B. 1984. Hypocentral Trend Surface Analysis: Probing the Geometry of Benioff Zones. Journal Geophys. Resear. V. 89, N B7:6153-6170.

Hanus, V. and Vanek, J. 1976. Intermediate aseismicity of Andean Subduction Zone and Recent Andesitic Volcanism. Jur. Geophy.42:219-223.

Herron, M and Hayes D. 1969. A Geophysical Study of the Chile Ridge. Earth Planet. Scienc. Letter. 6*77-83.

Isacks, B. and Oliver, J. 1968. Seismology and the New Global Tectonics. Jurnal Geophys. Resear. V. 73, N.18:5855-5899.

Isacks, B. and Barazangi, M. 1977. Geometry of Benioff Zones: Lateral segmentation and downwards bending of the subducted lithosphere. in Talwani, M. and Pitman, W. eds., Island arc deep sea trenches and back-arc basins: American Geophysical Union Ewing Serie I, :99-114.

James, D. 1971. Plate Tectonic Model for the Evolution of the Central Andes. Geolog. Societ. Americ. Bullet. V 82:3325-3346.

s of the central Andes. Geolog. Socie. Americ. Memor. 154.

Jordan. T.E., Isacks, B.L., Allmendinger, R.W., Brewer, J.A., Ramos, V.A. and Ando, C.J., 1983. Andean tectonics related to geometry of subducted Nazca Plate. Geological Stud. Americ. Bollet. V. 94:341-361.

Le Pichon, X. 1968. Sea-floor spreading and continental drift. Jour. Geophys. Resear. V.73, N.12:3661-3697.

Plafker, G.1972. Alaskan Earthquake of 1964 and Chilean Earthquake of 1960 Implications for arc tectonics. Jurna. Geophys. Researc. V. 77, N.5:901-925.

Stauder, W. 1973. Mechanism and Spatial Distribution of Chilean Earthquakes with Relation to Subduction the Oceanc Plate. Journal Geophys. Researc. V. 78,N23:5033-5061.

Swift, S. and Carr, M. 1974. The segmented nature of the Chilean seismic zone. Physic. Eart. Planet. Inter. 9:183-191.

# RECONNAISSANCE 40Ar-39Ar AGE AND PALAEOMAGNETIC STUDY OF IGNEOUS ROCKS AROUND COYHAIQUE, S. CHILE (45'30-47°S)

N. PETFORD[(1)] & P. TURNER[(2)]

(1) School of Geological Sciences, Kingston University, Kingston KT1 2EE, UK
(2) School of Earth Sciences, University of Birmingham, Birmingham B15 2TT, UK

**KEY WORDS:** Age dating, Palaeomagmetism, Patagonia

From Eocene times onwards southern-central Patagonia has been the site of a number of ridge-trench collisions (Cande & Leslsie, 1986; Ramos and Kay, 1992). Subduction of a spreading oceanic ridge beneath continental lithosphere is a rare event and the potential effects of ridge subduction on the overriding South American plate are still poorly understood. In order to better constrain the timing of igneous activity and the possible effect of tectonic rotations formed in response to ridge subduction events, $^{40}Ar$-$^{39}Ar$ radiometric age dating and palaeomagnetic studies of key outcrops were undertaken in the region south of Coyhaique between 45'30 and 47°S.

## REGIONAL GEOLOGY

The regional geology of the study area is summarised in Figure 1. The oldest rocks exposed in the region are Palaeozoic basement shales and phillites, overlain unconformably by volcanic arc rocks of the Jurassic Ibanez and Cretaceous Divisidero Formations (Suarez et al., 1994). During this time, the bulk of the Patagonoan batholith was believed to have been emplaced, although recent K-Ar and Rb-Sr ages (Pankhurst & Herve, 1994), supported by new data presented here, suggest that granitoid magmatism continued well into the Tertiary. A major phase of igneous activity began at the end of the Cretaceous with the extrusion of the voluminous Patagonian flood basalts and associated minor intrusives (Petford et al, this volume).

## COYHAIQUE DYKE AND GRANITOID STOCK

### $^{40}$Ar-$^{39}$Ar ages

Eight samples (five whole-rock and two mineral separates) were selected for age dating. All quoted ages and related MSWDs are $^{36}Ar/^{40}Ar$-$^{39}Ar/^{40}Ar$ isochron ages. Errors (in Ma) are quoted at $\pm$1s.

Figure 1 shows plots of the %39Ar gas release spectra, ages and geographical location of three whole-rock basalt samples SC 59, SC 13 and SC 11, along with two biotite separates SC 31 and SC 32 from the Patagonian batholith. The oldest rock dated in this study was the basaltic andesite dyke SC located 15 kilometres south east of Coyhaique. The dyke is part of a well exposed vertical swarm trending generally NNE-SSW that intrude into local black shales of the Cretaceous Divisidero Formation. The sample yields a well defined gas release spectrum, with a whole-rock (isochron) age of 61 $\pm$

**Fig. 1.** $^{40}Ar$-$^{39}Ar$ gas release spectra for three basalts (whole-rock) and two mineral separates (biotites) from the Patagonian batholith around Coyhaique (45°30-47°00S). Samples SC 59, 32 and 31 are $^{36}Ar/^{40}Ar$-$^{39}Ar/^{40}Ar$ isochron ages ± 1σ. SC 13 and SC12 show minimum estimated total gas ages (TGA).

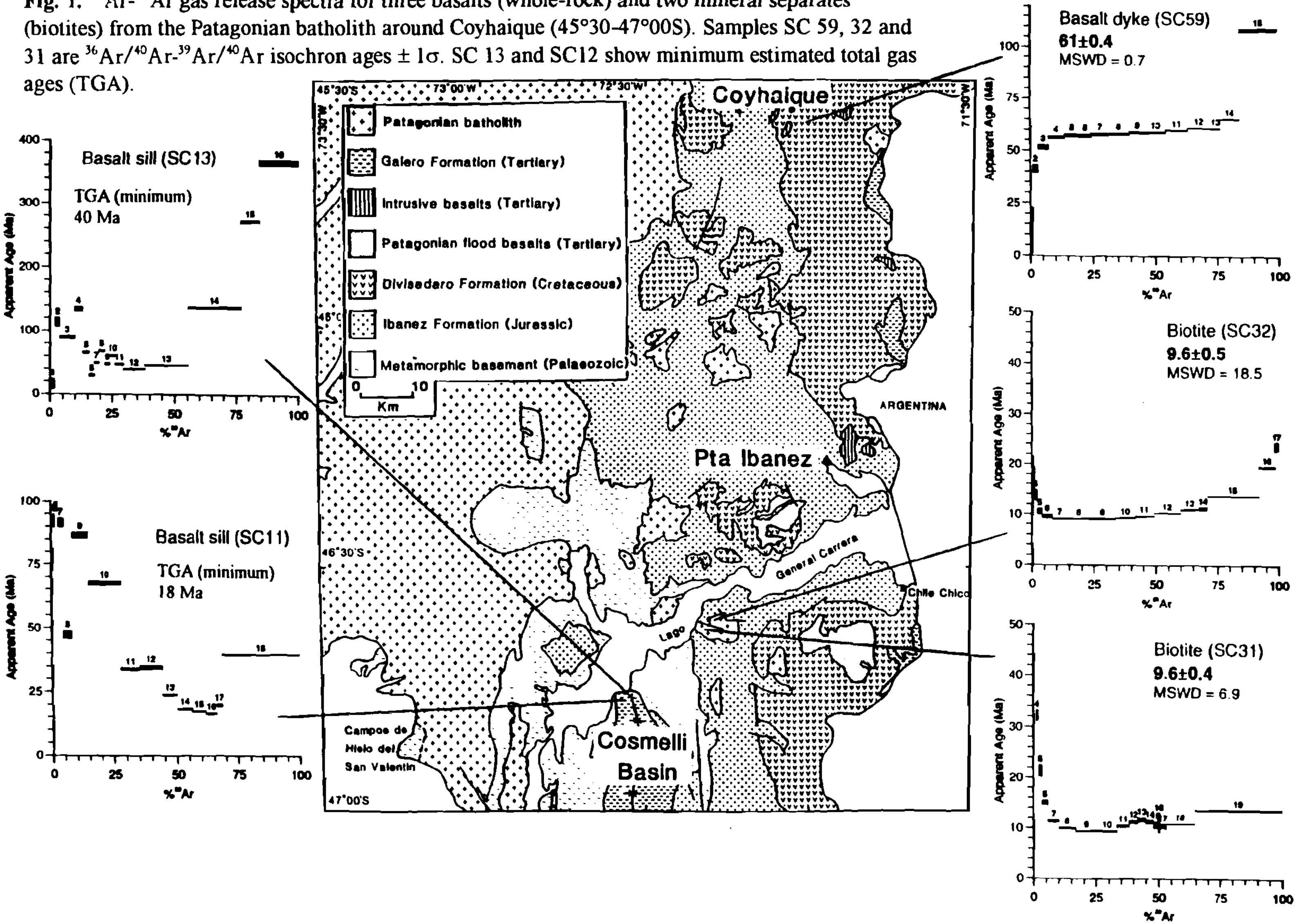

0.4 Ma (MSWD = 0.7) similar to the total gas age of 61.6 ± 0.6 Ma indicative of a true cooling age undisturbed by any subsequent thermal resetting.

Samples SC 32 and SC 31 are biotite fractions from a granitoid stock located to the east of the main Patagonian batholith that intrudes into volcanic rocks of the Ibanez Formation. The rocks are dioritic with $SiO_2$ contents of 52.49 and 54.63 wt% respectively. Biotite 40Ar-39Ar mineral isochron ages are identical within error at 9.6 Ma. This unexpectedly young age places the stock in the Mid Miocene, and is further evidence for a young component within the Patagonian batholith. Although their total gas ages are broadly similar (9.6 ± 0.5 and 10.4 ± 0.4 Ma), their relatively high MSWDs of 6.9 and 18.5, and slightly erratic gas release spectra indicate mild disturbance may have occurred during or after cooling.

**Palaeomagnetic Results**

Palaeomagnetic results for samples 59 (Coyhaique dykes) and, 31 and 32 (granitoid stock) are characterized by initial NRM direction with steep negative inclinations. During partial thermal demagnetization over 80% of the remanence is lost on heating to 350°C. Above this temperature there are no systematic directional changes and vector analysis indicates that the characteristic remanence lies in the temperature range 100-400°C.There are insufficient palaeomagnetic data to calculate a realistic virtual geomagnetic pole for the Coyhaique dykes.

The granitoid stock shows more complex palaeomagnetic properties than the Coyhaique dykes. The initial NRM directions have southerly declinations with a relatively steep positive inclination (reversed polarity). During thermal demagnetization a low blocking temperature component is removed between 0 and 100°C. Above this temperature there is usually a slight relative increase in NRM intensity followed by a sharp drop near the Curie temperature of magnetite (580°C). Vectorial analysis indicates that the NRM comprises two major components, one with a lower unblocking temperature spectrum between 100-400°C has a north easterly declination.and shallow negative inclination. The mean direction of *Dec*: 182; *Inc*: 64; *n* 5 ;$\alpha_{95}$ 6.9. The direction corresponds to a Virtual geomagnetic Pole at *Lat*: 88S *Long*:160 SE with *Dp* 8.8 and *Dm*11.0.

**INTRUSIONS IN THE COSMELLI BASIN**

The Cosmelli basin is located above a segment of continental crust that has experienced several ridge subduction events over the last 15 Ma. Recently, Flint et al., (1992) have interpreted the Cosmelli basin as a foreland basin that formed in response to ridge subduction processes.

**$^{40}$Ar-$^{39}$Ar ages**

Comparison with the other sample spectra in Figure 1 shows that the gas release spectra of two basaltic sills SC 13 and SC 11 intruding the Cosmelli basin sediments are severely disturbed. Indeed, it was not possible to obtain an isochron plot for either sample, due to the high degree of scatter of individual gas fraction ages. Such scatter is characteristic of rocks that have undergone extensive isotopic resetting of radiogenic argon after initial cooling, with the 'U'-shaped gas release spectra of both samples diagnostic of excess radiogenic argon. Total gas ages (the sum of all the individual gas fractions) comparable with ages that would be obtained by K-Ar dating are 146 Ma for SC 13 (Tithonian) and 31.6 Ma for SC 11 (Oligocene). Clearly the older of these ages is at odds with established stratigraphic correlations within the Cosmelli basin, although they do show the advantage of $^{40}Ar$-$^{39}Ar$ technique over K-Ar dating in identifying samples that have had their primary ages reset. Taking the total gas age of the *lowest age steps* from both spectra gives some indication of the *possible maximum age* of the sample. This is about 40 Ma for SC 13 (steps 7, 9, 11,12,13) and about 18 Ma for SC 11 (steps 14-17). Although no significant emphasis should be placed on these age estimates (they account for approximately 35 and 20% of total 39Ar released), they are nevertheless closer to assumed stratigraphic ages based on correlations between intercalated sediments.

## Palaeomagnetism

Palaeomagnetic data for the basalt sills is different. The Lower Sill (SC 11) has reversed polarity whereas the Upper Sill (SC 13) is of normal polarity. There are also important directional differences between the two. The initial NRM of SC 11 has a northerly declination with steep negative inclination. During partial; thermal demagnetization there is a near exponential decay of the NRM intensity and above 150°C there is only a single component of magnetization. The lower sill shows a smooth demagnetization trend with a slight concave-up curve. The median destructive field lies at about 200mT. The othogonal vector plot shows the presence of only a single component of magnetization consistent with those seen in the partial thermal demagnetization. The mean direction calculated for the combined data is *Dec*: 155 *Inc*: 71 $n$ 12 $\alpha_{95}$ 7.3 The corresponding VGP is *Lat*: 72S *Long* 339E with *Dp*11.1 and *Dm* 12.7

## References

Baker, P.E., Rea, W.J., Skarmeta, J., Caminos, R. & Rex, D.C. 1981. Igneous history of the Andean cordillera and Patagonian plateau around latitude 46S. Phil. Trans. R. Soc. London, 303, 105-149.

Cande, S.C. & Leslie, R.B. 1986. Late Cenozoic tectonics of the Southern Chile trench. JGR, 91, 471-496.

Charrier and others, 1979. K-Ar ages of basalt flows of the Meseta Buenos Aires in southern Chile and their relation to the southeast Pacific triple junction. Geology, 7, 436-439.

Flint, S., Prior, D., Agar, S.M. & Turner, P. 1994. Stratigraphic and structural evolution of the Cosmelli basin and its relationship to the Chile triple junction. J. Geol. Soc. London, 151, 251-268.

Pankhurst, R.J. & Herve, F. 1994. Granitoid age distribution and emplacement control in the Northern Paragonian batholith in Aysen (44-47°S). 7 Congresso Geologico Chileno, 2, 1409-1413.

Ramos, V.A., & Kay, S.M. 1992. Southern Patagonian plateau basalts and deformation: backarc testimony of ridge collisions. Tectonophysics, 205, 261-282.

Suarez, M., Prieto, X., Belmar, M. & Quiroz, D. 1994. Estratigraphica Terciaria del sector nororiental de Aysen. 7 Congresso Geologico Chile, 1, 533-537.

# AGE AND ORIGIN OF SOUTHERN PATAGONIAN FLOOD BASALTS, CHILE CHICO REGION (46°45'S)

N. PETFORD[1], M. CHEADLE[2] & B. BARREIRO[3]

(1)School of Geology, Kingston University, Kingston, KT1 2EE, UK
(2)Department of Earth Sciences, University of Liverpool, Liverpool, L69 3BX, UK
(3)NIGL, Keyworth, Nottingham,NG12 5G, UK

**KEY WORDS**: Basalts, Patagonia, Slab Window, Plumes

New chemical and age data from the Chile Chico region (ca. 46°S), located within the current Andean volcanic arc gap are reported from a detailed traverse 250 m through an exposed lower plateau basalt sequence of Hy-normative olivine tholeiites. $^{40}Ar/^{39}Ar$ ages of 51.7 ± 0.7 to 51.8 ± 0.9 imply an eruption time of ca. 0.1 Ma and confirm the similarity in age of these rocks with the neighboring Posadas basalts in Argentina. Ages less than 10 Ma in an upper sequence of Ne-normative alkali olivine basalts confirm the wide range in ages reported in earlier K-Ar reconnaissance studies of the region, and show that flood basalt magmatism occurred throughout most of the Tertiary (ca. 50 Ma) in this region of Patagonia. The minimum estimated volume of the lower sequence and surrounding Miocene basalts exposed between 46-49°S is ca. 2 x $10^4$ $km^3$, giving an average magma eruption rate of 0.2 $km^3$ yr, comparable with the Parana lavas.

The basalts are OIB-like (Ba/La < 15, La/Nb < 1.6) with Mg numbers up to 67, epsilon Nd values of +6 to +2 and $^{87}Sr/^{86}Sr$ ratios of 0.7030-0.7045. Correlation between La/Nb, $TiO_2$ and sotopic composition between the lower and upper sequence basalts suggest a switch in source region from predominantly asthenospheric to lithospheric mantle with time.

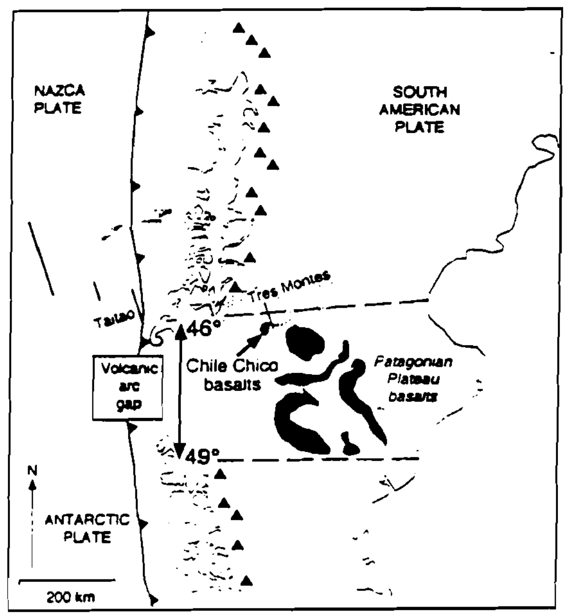


Fig. 1. Present day plate tectonic setting of the Patagonian flood basalt provence (after Murdie et al., 1993).

## LOCAL GEOLOGY

The Chile Chico basalts (ca. 46'30°-46'45°S) are located on a plateau (Meseta) at a mean elevation of 2000 m, close to the Chilean-Argentinean boarder (Fig 1). The plateau is itself an extension of the larger Meseta Buenos Aires (ca. 500 $km^2$) located mainly in Argentina, but which has been deeply dissected by the Rio Heinemeni which marks the boarder between both countries in this region. They form a sequence of basalt lavas and occasional sills and intercalated sediments covering an area of approximately 300 km$^2$ where they rest upon Mesozoic-Tertiary volcaniclastic rocks and marine sediments. The orientation of the well exposed lower sequence lavas ranges from subhorizontal to ca. 25° SW/140°. The estimated current thickness of the lower sequence is about 250 m, giving a minimum estimated volume of 75 km$^3$. However, the pile is cut by volcanic necks and plugs (including the nodule-bearing Cerro Lapiz) which acted as feeders for younger surface cones and flows, indicating the basalt pile was once much thicker. The minimum estimated volume of the lower sequence and surrounding Miocene basalts exposed between 46-49°S is > 10$^4$ km$^3$

## $^{40}Ar/^{39}Ar$ BASALT AGES

The $^{40}Ar/^{39}Ar$ age spectra and stratigraphic position of analysed basalts in the Chile Chico lower sequence are shown in Figure 2. $^{40}Ar/^{39}Ar$ Ages from the base and upper part of the sequence are within error, indicating extrusion rates of the order of 0.1 Ma. $^{40}Ar/^{36}Ar$-$^{39}Ar/^{40}Ar$ isochron ages range from 51.7 ± 0.7 Ma at the base of the sequence to 51.8 ± 0.9 just beneath the plateau surface, both comparable with the minimum K-Ar age of Charrier et al (1979) from Cerro Lapiz.

The youngest rock dated in this study is a basaltic dyke that cuts up through the Chile Chico lower sequence. Its isochron age of 8.5 ± 0.2 Ma coincides with early Miocene to Pliocene ages reported by Charrier et al (1979) for the upper unit of the Mestea Buenos Aires at Chile Chico, and is a likely feeder dyke for these younger rocks. Taking the estimated minimum basalt volume of Eocene basalts in Patagonia we obtain an average (minimum) eruption rate of 0.2 km$^3$ yr, comparable with the Parana flood basalts.

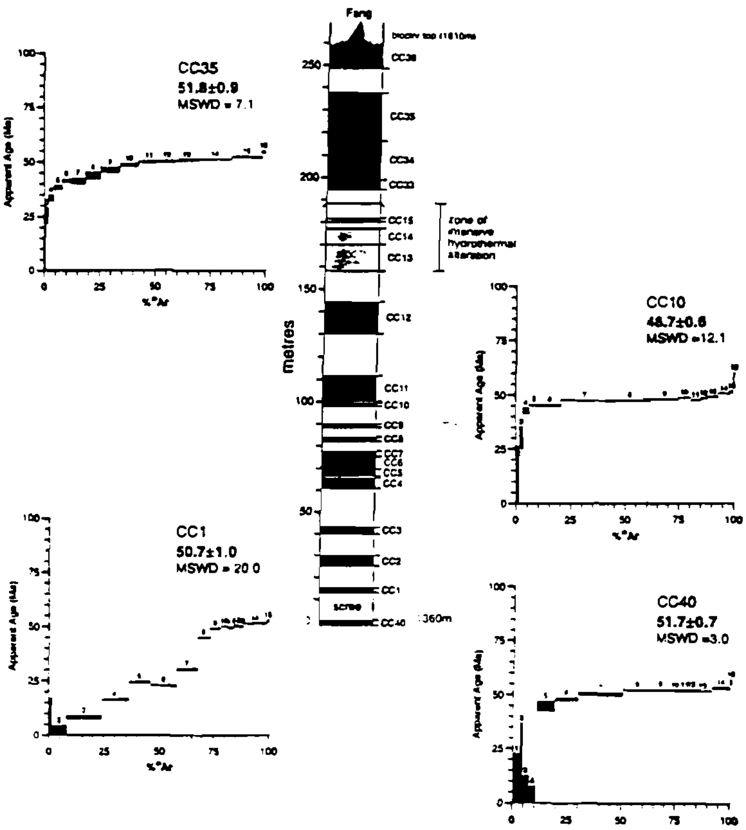


Fig. 2. Composite log through the lower sequence basalts showing position and thickness of each basalt unit sampled. Quoted errors are ± 1 sigma.

## BASALT CHEMISTRY

Half the Chile Chico basalts have Mg numbers > 60 similar to primary mantle-derived liquids. The upper and lower sequence basalts can be subdivided according to $TiO_2$ contents into a high Ti-group ($TiO_2$ > 2 wt%) and a low-Ti group ($TiO_2$ < 2 wt%). Incompatible element abundances are similar to the Eocene Posadas basalts (Ramos and Kay, 1992), with a general enrichment of HFSE over LILs (Fig. 3). Low Ba/La (< 15) and La/Nb (< 1.5) ratios similar to those reported in previous studies are further evidence for the OIB-like nature of the Patagonian flood basalts. Although εNd (+6 to +2) and $^{87}Sr/^{86}Sr$ ratios (0.7035-0.7045) suggest derivation from a relatively depleted mantle source, in detail their are important differences in the chemical and isotopic compositions of both groups (Fig. 4). Eocene Lower Sequence basalts have εNd values of +5 to +4, 2-3 wt% $TiO_2$ and Nb/La > 1, while the post-Eocene Upper Sequence basalts have more evolved εNd values of +3.5 to +2, 2-1 wt% $TiO_2$ and Nb/La ratios < 1, consistent with a switch from asthenospheric to lithospheric mantle source regions with time (cf. Columbia River basalts).

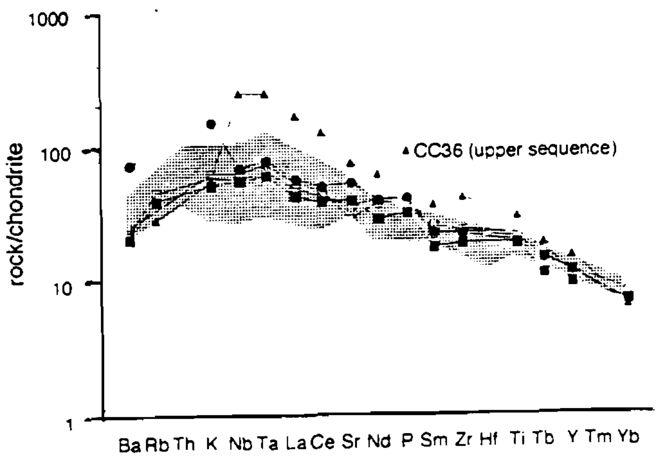


Fig. 3. Incompatible element plot for Chilr Chico basalts. Posadas basalts (shaded) shown for comparison.

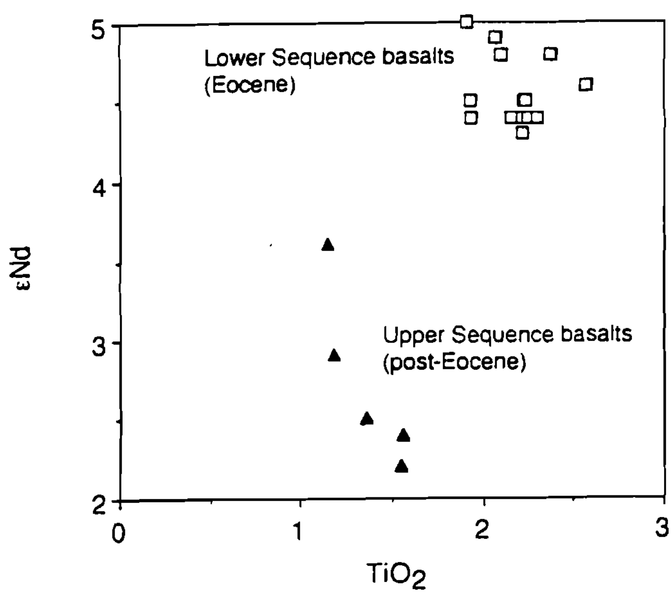


Fig. 4. εNd v $TiO_2$ plot for Lower and Upper sequence basalts showing a shift towards lower Ti and more enriched (lithospheric) isotopic compositions with time.

## ORIGIN OF EOCENE BASALTS

Ramos and Kay (1992) have proposed that the Eocene Posadas basalts are closely related to the collision of the Aluk-Farallon ridge with the Andean subduction zone between 52 and 42 Ma and the subsequent formation of an asthnospheric slab window. Significantly, the new $^{40}Ar$-$^{39}Ar$ ages for the Posadas basalts at Chile Chico (51.8 Ma) coincide nicely with the predicted onset of Eocene ridge-trench collision. Major and trace element modelling (Cheadle & Petford, 1993) suggests that the Eocene age Chile Chico magmas originated by ca. 5% melting of an anomalously hot mantle source at between 80-90 km depth, at a mantle potential temperature of 1400-1450°C (Fig. 5). Although the subducting slab normally prohibits hot mantle from rising to melting depths, slab windows within the subducting oceanic lithosphere may provide temporal and spatial opportunities for hot, relatively depleted to OIB-like subcontinental mantle, to rise to more shallow depths where melting can occur. Whether the mantle heat source is deep seated or shallow remains an important open question (King & Anderson, 1996).

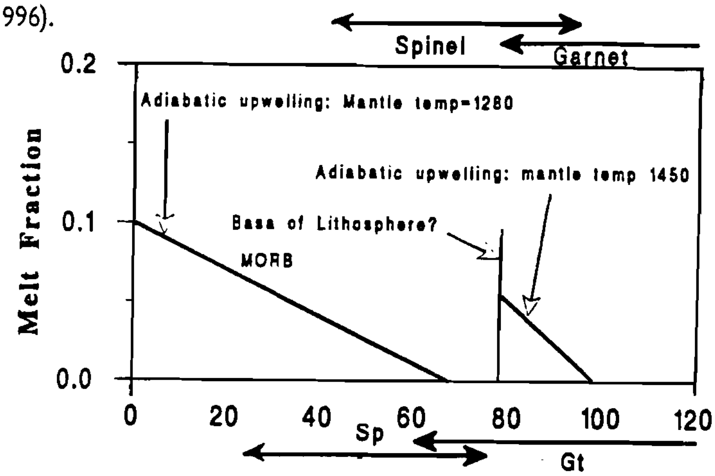


Fig. 5. Melt fraction v depth. Up-welling of hot mantle (Tp 1450°C) at base of 80 km-thick lithsphere produces 5% melt.

## REFERENCES


Baker, P.E., Rea, W.J., Skarmeta, J., Caminos, R. & Rex, D.C. 1981. Igneous history of the Andean cordillera and Patagonian plateau around latitude 46S. Phil. Trans. R. Soc. London, 303, 105-149.

Charrier and others, 1979. K-Ar ages of basalt flows of the Meseta Buenos Aires in southern Chile and their relation to the southeast Pacific triple junction. Geology, 7, 436-439.

Cheadle, M. & Petford, N. 1993. Origin of Patagonian flood basalts. EOS, 74, p.663.

McKenzie, D & O'Nions, R.N., 1995. The source regions of ocean island basalts .J. Pet, 36, 133-159.

Ramos, V.A., & Kay, S.M. 1992. Southern Patagonian plateau basalts and deformation: backarc testimony of ridge collisions. Tectonophysics, 205, 261-282.

Stern, C.R, and others, 1990. Trace element and Sr, Nd,Pb and O isotopic composition of Pliocene and Quaternary alkali basalts of the Patagonian plateau lavas of southernmost Aouth America. Contrib. Miner. Petrol., 104, 294-308.

King, S.D. & Anderson, D.L. 1996. An alternative mechanism of flood basalt formation. Earth. Plenet. Sci. Lett., 136, 269-279.

Murdie, R. E., Prior, D.J., Styles, P., Flint, S.S., Pearce, R.G. & Agar, S.M. 1993. Seismic responses to ridge-transform subduction: Chile triple junction. Geology, 21, 1095-1098.

# MINERALOGICAL AND GEOCHEMICAL CHARACTERIZATION OF MIDDLE CRETACEOUS TO PALEOCENE OCEANIC AND CONTINENTAL VOLCANIC ROCKS FROM SOUTHWESTERN ECUADOR.

Cédric REYNAUD(1), Henriette LAPIERRE(1), Etienne JAILLARD(1,2), Stalin BENITEZ(3), Gerardo BERRONES(3) and Georges MASCLE(1).

(1) LGCA, UPRES-A-5025, 15 rue Maurice-Gignoux, 38031 Grenoble cedex, France.
(2) ORSTOM, TOA, UR 13, 209-213 rue La Fayette, 75480 Paris cedex 10, France.
(3) Petroproducción, km 6,5 vía a la Costa, casilla 10829, Guayaquil, Ecuador.

KEY-WORDS : Late Cretaceous, Paleogene, oceanic plateau, island arcs, continental arc, geochemistry.

## INTRODUCTION AND GEOLOGICAL SETTING

Southwestern Ecuador includes oceanic terranes of Cretaceous age accreted to the continental Andean margin between late Cretaceous and late Eocene times (Goossens & Rose 1973, Feininger & Bristow 1980, Jaillard et al. 1995). The oceanic floor, known as the **Piñón Fm**, yielded 110-100 Ma K/Ar ages (Aptian-Albian, Goossens & Rose 1973). It is thought to constitute the basement of the whole coastal area of Ecuador, and bears three distinct island arcs. In the Guayaquil area, the thick volcaniclastic deposits of the **Cayo Fm** of Cenomanian?-Campanian age are believed to represent the products of an island arc (≈95-75 Ma, Bristow & Hoffstetter 1977, Jaillard et al. 1995). It overlies the Piñón Fm through a thin but distinctive volcanic layer referred to as the **Las Orquídeas beds**. The presently NE trending **San Lorenzo Fm** is represented by conglomerates and greywackes intercalated with lava flows, which crop out NW of a fault system that separates it from the Cayo Fm (Manta area, fig. 1). It yielded consistent late Santonian-Paleocene ages (85-53 Ma, Goossens & Rose 1973, Lebrat et al. 1987, Wallrabe-Adams 1990). The **Macuchi Fm** of early to middle Eocene age crops out in the NNE-trending Western Cordillera.

The continental Andean margin of southernmost Ecuador includes various volcanic units. The **Celica Fm** consists of submarine, mainly andesitic lava flows, agglomerates and tuffs that crop out near the Peruvian border. It is usually interpreted either as a continental arc (Lebrat et al. 1987, Wallrabe-Adams 1990). Since it is crosscut by the Tangulla granite which yielded inconsistent 114 to 49 Ma K/Ar ages, an early Cretaceous age was inferred for the Celica Arc (Kennerley 1980). However, its extension in Peru is dated by Albian to Cenomanian fossils. The Celica Fm is overlain by the **Alamor Fm** made of coarse-grained greywackes and intercalated volcanics of early late Cretaceous age (Jaillard et al. 1996). Farther East, the **Sacapalca Fm** consists of subaerial agglomerates, tuffs and lavas, interpreted as a continental volcanic arc (Mamberti 1995). Since it is crosscut by plutons, which range in age from 26-21 Ma to 59-51 Ma or even 66-61 Ma, the Sacapalca Fm would be of early Eocene-Paleocene, or even late Cretaceous age (Jaillard et al. 1996).

The aim of this paper is to present preliminary results about the mineralogy, geochemical composition and geodynamic significance of the middle Cretaceous to Paleocene volcanic units of both, oceanic and continental origins.

## MAGMATIC AFFINITIES

All the volcanic-rocks of southern Ecuador are affected by a low grade hydrothermal alteration with preserved magmatic textures. Clinopyroxene and plagioclase are replaced by smectites and calcite + epidote, respectively. The groundmass is always replaced by smectites while prehnite + pumpellyite + smectites fill vacuoles. The samples analyzed for this study are relatively fresh with preserved clinopyroxene and plagioclase.

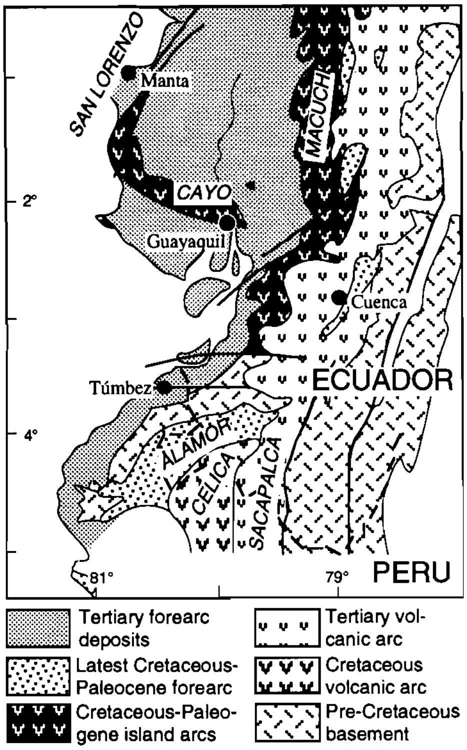


*Fig. 1 : Location of the studied area.*

The volcanic rocks of **oceanic origin** (Piñón and San Lorenzo Fms, Las Orquídeas beds) show mafic (MgO>5%) to intermediate compositions and are mainly dolerites, basalts and andesites. Basalt is the main rock type of the Piñón Fm and Las Orquídeas beds. Dolerites occur in the Piñón and San Lorenzo Fms while andesites are only found in the San Lorenzo Fm. All these rocks are formed of plagioclase, clinopyroxene and Fe-Ti oxides. The crystallization sequence in the basalts and dolerites of Pinon and Las Orquídeas Fms. is: plagioclase -> cpx -> oxides while in the rocks of the San Lorenzo Fm, Fe-Ti oxides crystallize before plagioclase. Orthopyroxene is uncommon. Plagioclase predominates (50 to 80 % of modal composition) in all the rock-types and shows normal zoning with labradorite core ($An_{75}$) and oligoclase rim ($An_{10}$). Clinopyroxene exhibits augite composition ($En_{45}$, $Fs_{12}$, $Wo_{43}$). In the San Lorenzo andesite, clinopyroxene shows diopside core rimmed by augite. Oxides are Ti-rich ($TiO_2$ ~ 5%) magnetites.

Basalts and dolerites of the Piñón Fm show E.MORB affinities with flat REE patterns [0.9<(La/Yb)C <1.3, fig. 2A) and Nb, Hf, and Ta enrichments relative to N.MORB (fig. 3A). They cluster in the E.MORB field in the Hf/3-Th-Ta diagram (Wood 1980, fig. 4). Basalts, dolerites, andesites of the Las Orquídeas beds and San Lorenzo Fm differ from the E.MORB of the Piñón Fm by LREE enriched patterns [2.31<(La/Yb)C<3.9, fig. 2B] and a depletion in Nb, Hf, and Ta relative to N.MORB (fig. 3B). They are enriched Ba, Rb, Sr relative to N.MORB (fig. 3B). All these rocks fall in the calc-alkaline field in the Hf/3-Th-Ta diagram (fig. 4). The REE abundance of the basalts and dolerites of the Las Orquídeas beds is 10 times the chondritic abundance and markedly lower than that of the San Lorenzo rocks. Moreover, the igneous rocks of Las Orquídeas beds show a significantly depletion in HREE, Zr, Ti, and Y, compared to the calc-alkaline rocks of San Lorenzo and more generally to the calc-alkaline mafic rocks of oceanic arcs (Wilson 1989).

The Piñón E.MORB tholeiite is characterized by an εNd, back calulated at 110 Ma, of +7 (fig. 5) which falls in the range of Oceanic Island Basalts. The Las Orquídeas calc-alkaline rocks show similar εNd ratios, back calulated at 110 Ma, that range between +6 and +7 (fig. 5). These εNd ratios fall in the range of oceanic arcs. In contrast, the initial ($^{87}Sr/^{86}Sr$)i ratios of the E.MORB tholeiite and calc-alkaline lavas, back calculated at 110 Ma exhibit a wide range of values (-4.2<εSr<+4.2). The enrichment of both rocks in radiogenic Sr is probably linked to hydrothermal alteration experienced by these submarine lavas.

Thus, the basalts and dolerites of the Piñón Fm display E.MORB tholeiitic affinities, very similar to those of oceanic plateau basalts (Floyd 1989). Moreover, they share in common with the Late Cretaceous tholeiites from Curaçao (Kerr et al. 1996) and the Cenomanian-Coniacian E.MORB tholeiitic basalts from Hispaniola (Dupuis 1995), flat REE patterns, Ta, Nb, Hf enrichments relative to N.MORB and εNd ratios of +6/+7. The Las Orquídeas and San Lorenzo calc-alkaline rocks display petrological and geochemical features of intra-oceanic arc-rocks. The low HREE and Y contents of the Las Orquídeas rocks suggest the presence of residual garnet in the mantle source.

The lavas exposed on the **continental margin** (Celica, Alamor and Sacapalca Fms) show contrasting petrological and geochemical features with respect to the E.MORB tholeiites and calc-alkaline rocks. They occur as flows or fragments in pyroclastic breccias. They show intermediate to felsic compositions. Dacite is the most common rock-type. Mafic to acidic andesites are also present. Plagioclase is the most abundant mineral (30 to 80% of phenocrysts) and exhibits anorthite composition ($An_{90}$). Two groups of rocks may be distinguished on the basis of the nature of the ferro-magnesian phenocrysts. The lava in flows and pyroclastic breccias of the Celica Fm are clinopyroxene- and orthopyroxene-phyric, respectively. The andesites and dacites of the Alamor and Sacapalca Fms are amphibole- phyric. The dacites include quartz phenocrysts. Amphibole is always zoned ; it is a K-poor ($K_2O$<1%) hornblende. Fe-Ti are $TiO_2$ (4 to 6%) rich magnetite and crystallize before the plagioclase and clinopyroxene.

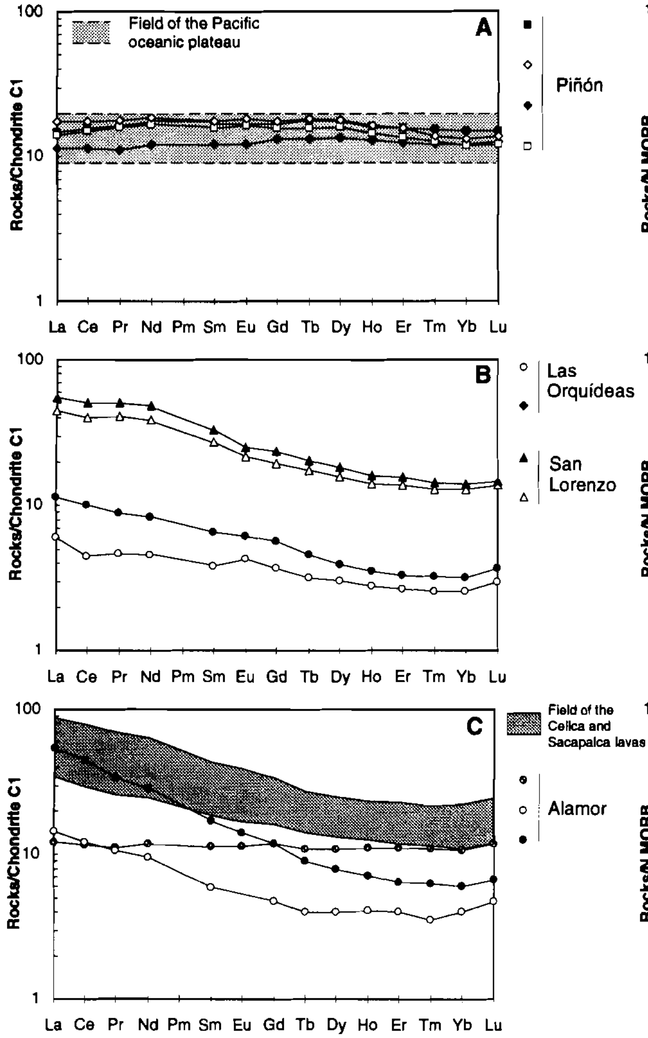


Fig 2 : Rare Earth Element normalized abundance normalized to C1 chondritic meteorite values (Normalisation values : Sun and Mc Donough, 1989).
A : Piñón Fm.
B : San Lorenzo Fm. and Las Orquídeas Beds.
C : Celica, Alamor and Sacapalca Fms.

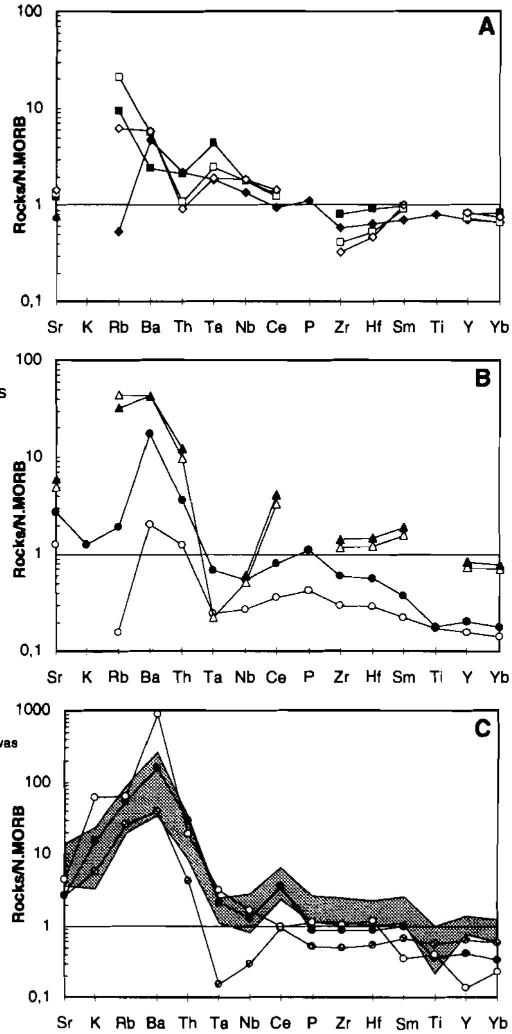


Fig 3 : N.MORB-normalized spiderdiagrams (Normalisation values : Sun and Mc Donough, 1989).
A : Piñón Fm.
B : San Lorenzo Fm and Las Orquídeas Beds.
C : Celica, Alamor and Sacapalca Fms.

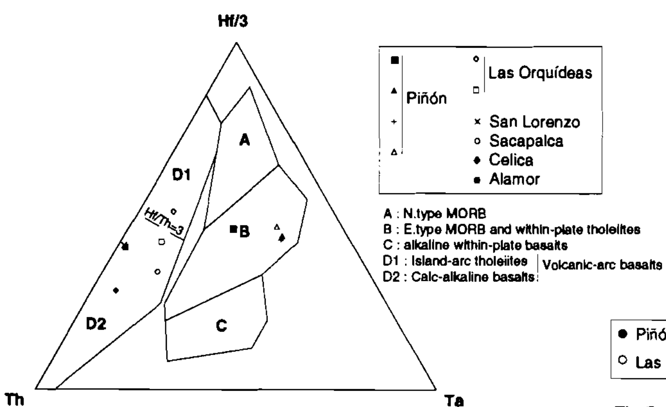


Fig 4 : Hf/3-Th-Ta discrimination diagram (after Wood, 1980).

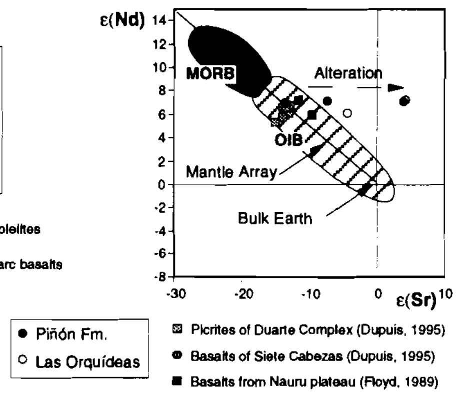


Fig 5 : ε(Nd) vs ε(Sr) isotopique correlation diagram showing the position of the Piñón and Las Orquídeas samples (calculated at t=110 My).

All the lavas show LREE enriched patterns [1.5<(La/Yb)C<3.11, fig. 2C], except for a volcanic fragment in a breccia of the Alamor Fm, which shows a flat REE pattern [(La/Yb)C=1.06]. A dacite of the Alamor Fm differs by lower REE concentrations (10 times the chondriitic abundance), but his REE pattern is of calc-alkaline type. The trace element patterns normalized to N.MORB are enriched in LILE and depleted in Ti and Nb (fig. 3C). In the Hf/3-Th-Ta diagram (fig. 4), these rocks fall in the volcanic arc basalt field, and more specially in the calc-alkaline field. Their Th levels are relatively high (2.31<Th ppm<4). This suggests a crustal contamination.

Thus, the lavas of the Celica, Alamor and Sacapalca Fms show calc-alkaline affinities. The predominance of dacites, the presence of hornblende and the high content in Th suggest that they were developed in an active continental margin setting.

## CONCLUSIONS

The Piñón Fm may represent part of a Cretaceous Caribbean-Colombian Pacific-derived oceanic plateau. This would explain whyit could not be subducted and was part of the terranes accreted to the North and South American cratons sometimes during the late Cretaceous-early Eocene. Because of its oceanic plateau nature, the Piñon basement constituted the upper plate of successive intra-oceanic subduction systems. The overlying Las Orquídeas and San Lorenzo calc-alkaline rocks developed in island-arc setting. A calc-alkaline volcanism developed on the continental margin of southern Ecuador during late early Cretaceous (Celica Fm), late Cretaceous (Alamor Fm) and Paleocene (?) times (Sacapalca Fm).

## REFERENCES

Bristow, C.R. & Hoffstetter, R., 1977, *Ecuador.* Lexique Stratigr. Internat., V, 5a2, 410 p., CNRS ed..

Dupuis, V., 1995, *Les séquences d'arc crétacées et leur substratum de type plateau océanique des Grandes Antilles.* DEA thesis, Univ. Nice Sophia-Antipolis, 39 p.,unpubl..

Feininger, T. & Bristow, C.R., 1980, Cretaceous and Paleogene history of coastal Ecuador. *Geol. Rundsch.*, 69, 849-874.

Floyd, P.A, 1989, Geochemical features of intraplate oceanic plateau basalts, *Geol. Soc. London, Spec. Publ.*, 42, 215-230.

Goossens, P.J. & Rose, W.I., 1973, Chemical composition and age determination of tholeitic rocks in the basic Cretaceous Complex, Ecuador. *Geol. Soc. Am. Bull.*, 84, 1043-1052.

Jaillard, E., Ordoñez, M., Benítez, S., Berrones, G., Jiménez, N., Montenegro, G. & Zambrano, I., 1995, Basin development in an accretionary, oceanic-floored forearc setting : southern coastal Ecuador during late Cretaceous to late Eocene times. *Am. Ass. Petr. Geol. Mem.*, 62, 615-631.

Jaillard, E., Ordoñez, M., Berrones, G., Bengtson, P., Bonhomme, M., Jiménez, N. & Zambrano, I., 1996, Sedimentary and tectonic evolution of the arc zone of Southwestern Ecuador during Late Cretaceous and Early Tertiary times. *J. South Am. Earth Sci.*, in press.

Kennerley, J.B., 1980, Outline of the geology of Ecuador. *Overseas Geol. Min. Resources*, 55, 1-16.

Kerr, A.C, Tarney, J., Marrimer, G. F., Klaver, G.Th., Saunders, A.D. & Thirwall, M.P., 1996, The geochmistry and petrogenesis of the late-Cretaceous picrites and basalts of Curaçao, Netherlands Antilles: a remnant of an oceanic plateau. *Contrib. Mineral. Petr.*, in press.

Lebrat, M., Mégard, F., Dupuy, C. & Dostal, J., 1987, Geochemistry and tectonic setting of pre-collision Cretaceous and Paleogene volcanic rocks of Ecuador. *Geol. Soc. Am. Bull.*, 99, 569-578.

Mamberti, M., 1995, *Premier essai de caractérisation de l'environnement géodynamique des formations du Crétacé-Paléocène de l'Equateur par la pétrologie et la géochimie des matériels ignés.* Maitrise Mem., Univ. Grenoble, 42 p., unpubl..

Sun, S.S. & Mc Donough, W.F., 1989, Chemical and isotopic systematics of oceanic basalts : implications for mantle composition and processes, *Geol. Soc. London, Spec. Publ.*, 42, 313-345.

Wallrabe-Adams, H.-J., 1990, Petrology and geotectonic development of the Western Ecuadorian Andes: the Basic Igneous Complex. *Tectonophysics*, 185, 163-182.

Wilson, M., 1989, *Igneous petrogenesis. A global tectonic approach.* Chapman & Hall, 466 pp.

Wood, D.A., 1980, The application of a Th-Hf-Ta diagram to problems of tectonomagmatic classification and to established the nature of crustal contamination of basaltic lavas of the British Tertiary volcanic province. *Earth Planet. Sci. Lett.*, 50, 11-30.

# CONTRASTED ERUPTIVE STYLES AND MAGMATIC SUITES (ANDESITIC VS. ADAKITIC) AT MOJANDA VOLCANO, ECUADOR.

Claude ROBIN[1,2], Miguel JIMENEZ[2], Minard HALL[2],
Patricio ESCOBAR[2], Michel MONZIER[1,2], Jo COTTEN[3]
and Jean-Philippe EISSEN[4]

(1) ORSTOM, UR 14, A.P. 17-11-6596, Quito, Ecuador (e-mail robin@orstom.ecx.ec)
(2) Instituto Geofisico, Escuela Politecnica Nacional A.P. 17-01-2759, Quito, Ecuador (e-mail mhall@instgeof.ecx.ec)
(3) Département des Sciences de la Terre, CNRS-URA 1278, Université de Bretagne Occidentale, BP 809, 29285 Brest, France (e-mail JoCotten@univ-brest.fr)
(4) ORSTOM Centre de Brest, 29 280 Plouzané, France (e-mail eissen@ifremer.fr)

KEY WORDS : composite volcano, eruptive dynamics, Plinian activity, andesites, adakites, Ecuador.

## INTRODUCTION

In Ecuador, Mojanda volcano, located 50 km Northeast of Quito, is one of the most voluminous volcanoes in the Interandean Depression which separates the western Cordillera from the Cordillera Real. Very little information (Hall 1977) is available about this edifice which was previously thought to be a single volcano, truncated by a small summit caldera, 2.2 x 2.8 km wide. The volcanic complex consists of two contemporaneous volcanoes. Here, we emphasize the striking differences between these volcanoes, concerning their history, eruptive styles and magmatic characteristics, despite their proximity.

## MAIN PHASES OF DEVELOPMENT AND ERUPTIVE STYLES

The Mojanda volcanic complex is 26 km in diameter and rises to a maximum elevation of 4263 m from its base, between 2200 and 3000 m elevation. The orientation and convergence of lava flows and other deposits indicate the existence of two volcanic centres, located only 4 km apart : the Mojanda ss and the Fuya Fuya (Fig. 1).

**Mojanda ss centre.** This volcano experienced two caldera events. The truncation of a basal, essentially effusive edifice (Mojanda I), observed between 3750 and 4000 m elevation, suggests a former caldera, 5 km in diameter, around the previously recognized small summit caldera. Mojanda I consists of a monotonous series of andesitic and siliceous andesitic lava-flows and breccias (56-63% $SiO_2$).

Mojanda II : Except for pyroclastic deposits and a series of lavas that flowed to the North, this new cone did not extend over the limits of the caldera. Four volcanic units comprise this cone :

1- Lava flows from Yanaurco (unit MII-1), composed of diopside and olivine basaltic andesites (55-56% $SiO_2$).

2- Scoria flow deposits (56-58% $SiO_2$) containing bombs and vitric blocks, found on the SE and N flanks (unit MII-2). These deposits suggest eruptive episodes in an open-conduit regime. Dense juvenile blocks also indicate that andesitic domes emplaced in the summit area were destroyed by strong explosive activity.

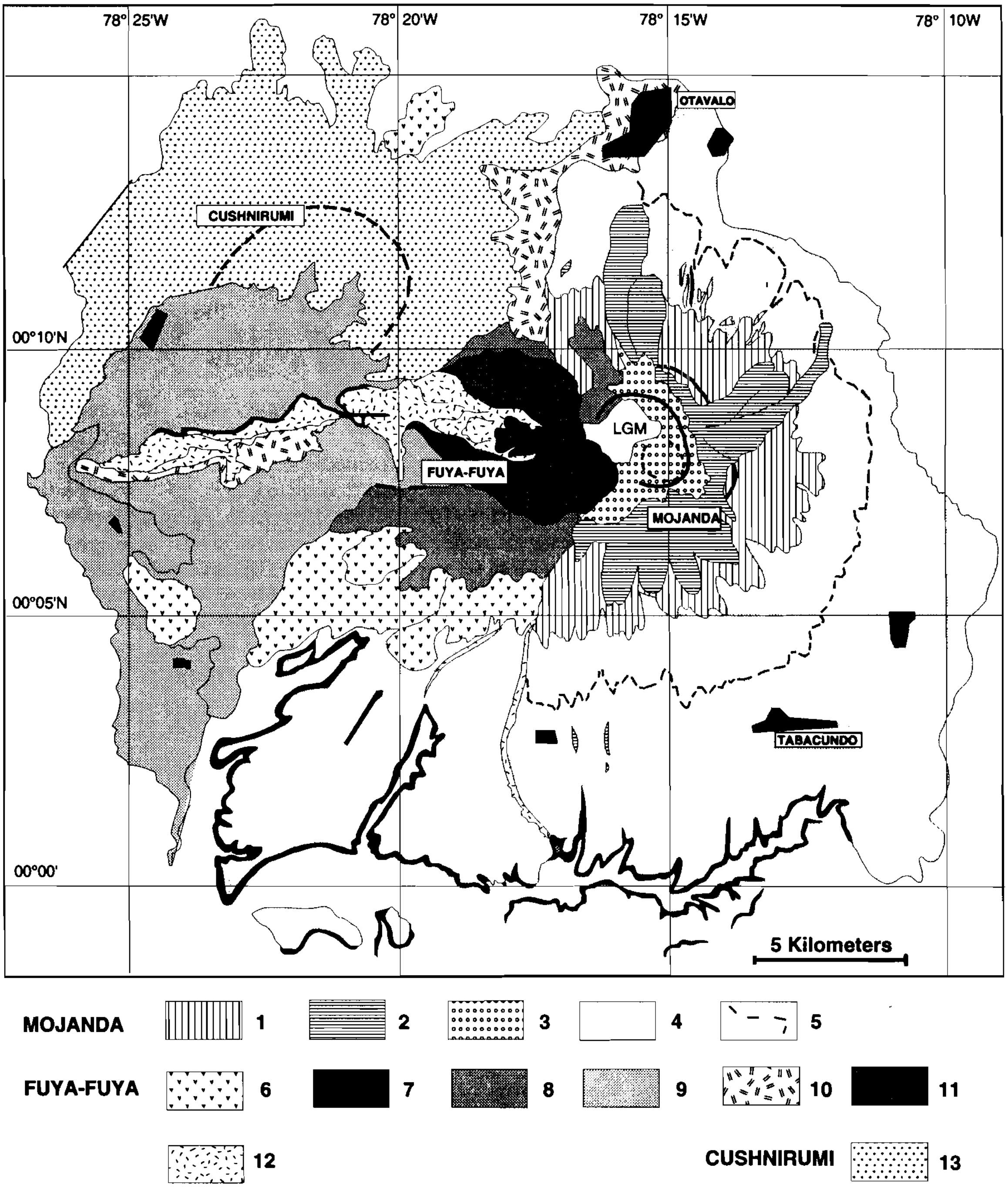


Figure 1. Simplified geological map of the Mojanda volcanic complex. **Mojanda volcanic centre** : 1- Basal edifice (MOJ I, mainly lava flows). 2- Post-caldera edifice (mainly mafic with scoria flows; MOJ II-III). 3- Yanaurcu breccias (MOJ IV). 4- Undifferentiated pyroclastic deposits from Fuya-Fuya and Mojanda (mainly ash and pumice fallout deposits), epiclastic deposits and superficial reworked ashy deposits (Cangahua). 5- Limit of flowage of lavas from MOJ I.
**Fuya-Fuya volcanic centre** : 6- Basal lavas and domes. 7- Outcrop zones of pyroclastic deposits related to the Plinian and dome activity (especially the thick rhyolite pumice layers R1 and R2, ash and bloc pyroclastic flow deposits and associated lahars). 8- San Bartolo volcanic cone (lava flows). 9- Avalanche deposits. 10- Ahs and pumice flows following the avalanche event. 11- Summit complex ofFuya-Fuya (lava flows and domes). 12- Recent pyroclastic flows related the summit domes.
**Cushnirumi** : 13- undifferentiated deposits (mainly lava flows) from Cushnirumi. Heavy lines represent the limit of calderas. LGM = Laguna Grande de Mojanda.

**3**- A 300 m thick unit of basic andesite to andesite breccias forming the upper part of the cone around Laguna de Mojanda (unit MII-3). These breccias, bearing abundant quenched vitric clasts, have hydromagmatic characteristics.

**4**- A sequence of Plinian and phreatoplinian deposits (ash and lapilli beds) of basaltic andesite and andesite. These products have been ejected during a major eruption or series of eruptions responsible for the formation of the small summit caldera. Mafic dykes which cross the caldera in a N-S orientation are associated with this phase.

**Fuya-Fuya volcanic centre.** Upon the western flank of Mojanda I, thick andesitic to dacitic lavas and lava domes were extruded, forming the Fuya-Fuya basal edifice. Thick sequences of Plinian and dome collapse deposits are related to this stage of development. The interpretation of numerous sections of pyroclastic deposits on the outer south slopes (block and ash flow deposits, block rich lahars, Plinian ashfalls and extensive pumice fall deposits), clearly indicate that, during this period, the activity of Fuya Fuya was strongly explosive, constantly related to acid magmatism from a gas-rich shallow magma chamber and acid extrusions.

Six major Plinian deposits interbedded with deposits of dome activity and emitted during two long magmatically and volcanically cycles are observed. Each cycle began with a voluminous Plinian eruption resulting in a thick rhyolite pumice deposit (70-71% $SiO_2$), which was followed by episodes of dome construction and collapse, and minor emissions of ash and/or pumice.

The two main rhyolite pumice deposits, R1 and R2, at the base of each sequence, have been recognized as far away as Quito. The lower pumice R1, 4 m thick at 15 km SW of Fuya Fuya centre, is divided into two layers. The lower one is progressively enriched towards the top in andesitic ($SiO_2$ = 60%) juvenile clasts (cauliflower bombs and scoria). Both deposits R1 and R2 represent cataclysmal Plinian eruptions, probably responsible for the opening of large vents in the summit area.

The intermediate construction stage of Fuya-Fuya is represented by the San Bartolo cone, formed by a pile of andesitic and acid andesite lava flows covering the remnants of the summit domes. A large Mount St Helens collapse event was then responsible for the loss of the major volume of this new cone and part of Fuya-Fuya's basal lavas and dome extrusions. The collapse also affected the western flank of the Mojanda II edifice (Fig.1). Voluminous dacitic pyroclastic flows, overlying the avalanche deposits, followed the avalanche event.

During the Late Pleistocene and Holocene, a new complex consisting of viscous lava flows and domes formed in the Fuya-Fuya avalanche caldera. Its eruptive activity is mainly represented by pyroclastic deposits directed to the west by the drainage and prevailing winds. Unglaciated Colangal and Panecillo domes are the last extrusions of this complex.

## GEOCHEMISTRY.

48 analyses of major and trace elements have been made other the whole volcanic complex. Both Mojanda and Fuya-Fuya volcanic centres show remarkably distinct chemical characteristics on diagrams using both major as well as trace elements. Both suites lie in the medium-K calc-alkaline field, but the Mojanda series is clearly more K-enriched than the Fuya Fuya series. The Mojanda suite has higher contents of Ti, Fe and Ca, and consequently is less silicic. A discriminant diagram to differentiate the two series is the Sr/Y vs Y diagram. On figure 2, rocks from Fuya-Fuya fit within the adakite field, while the Mojanda suite shows characteristics of the normal continental andesite-dacite calc-alkaline rocks. In this diagram, rocks from Cushnirumi volcano, a third, nearby older volcano, greatly destroyed by an avalanche and dissected by erosion (Fig. 1), also appear as adakites (Monzier et al, this volume).

## DISCUSSION AND CONCLUSIONS

Two major closely associated volcanic centres form what was previously considered as Mojanda volcano. Although completely contemporaneous and only 4 km apart, these centres developed different histories and eruptive styles.

At Mojanda, an andesitic basal edifice ended with a caldera collapse. A new cone began with basaltic andesite lava flows, which later turned to andesites with explosive dynamics characterized by magma-water interactions. The volcanic history of this cone ended with the last phreatoplinian eruption

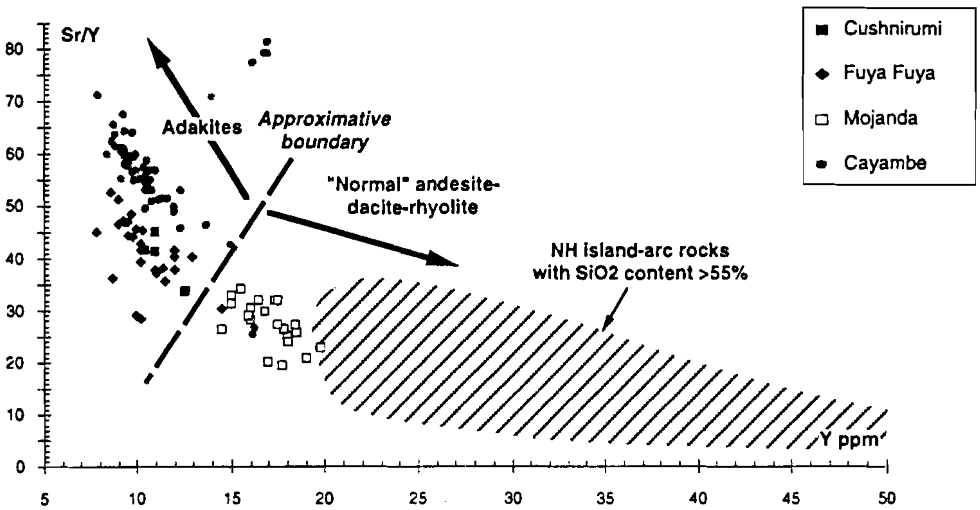


Fig. 2. Sr/Y vs. Y diagram for rocks from Fuya Fuya, Mojanda and Cushnirumi volcanoes, Ecuador. Analyses from Volcan Cayambe (East of Mojanda) are also reported. New Hebrides island arc rocks field is given for comparison. An approximative boundary between adakites and "normal" rocks is presented.

producing the summit caldera. At each evolution stage of Fuya Fuya, explosive activity related to silicic magmas was dominant. Climactic explosive dynamics occurred during two major cycles which began with a cataclysmal rhyolitic Plinian eruption and died out with acid andesite / dacite dome extrusion. Explosive volcanism related to silicic magmas continued during and after a large sector collapse of the volcano. Lastly, the avalanche caldera was occupied by a later dome complex.

These opposite types of development are related to two drastically different magmatic suites and indicate the existence of two magma reservoirs. Although both magmatic suites fall into the medium-K calc-alkaline field in a K2O Vs SiO2 diagram, the Mojanda suite is more K-enriched than the Fuya-Fuya suite which also demonstrates obvious adakitic characteristics. Adakites are andesite-dacite-rhyolite sequences (but mainly dacites) that are not associated with parental basalts, and are considered as being derived from the partial melting of amphibolite or eclogite at high pressure. They are characterized by relatively high contents of Al and Na, very low Y and Yb, and high La/Yb and Sr/Y ratios (Defant and Drummond, 1990; Dummond and Defant, 1990). Below the Mojanda volcanic complex, the slab is ~ 130-150 km deep. At this deph, the P-T conditions exceed those normally proposed for adakitic magma generation (23-26 kbars; 700-775°C). Thus, the presence of the Fuya-Fuya adakites agrees better with a hypothesis that implies their formation by partial melting of newly underplated (magmatic accreted) basaltic material than by a melted slab hypothesis. The simultaneous presence of two distinct magmatic suites at the same place stress an interesting volcanological question. Another question is the possible interaction between both volcanoes, since the juvenile andesitic magma within the R1 deposit from Fuya-Fuya is not adakitic but clearly belongs to the Mojanda series (Fig 2) and thus may have come from the Mojanda magma reservoir. More geochemical studies are in progress in order to answer these questions.

## REFERENCES

Defant M. J. and Drummond M.S. 1990. Derivation of some modern arc magmas by melting of young subducted lithosphere. Nature, 347, 662-665.
Dummond M. S. and Defant M. J. 1990A model for trondhjemite-tonalite-dacite genesis and crustal growth via slab melting: Archean to modern comparisons. J. Geophys. res., 95, B13, 21503-21521.
Hall M. L., Publ. del I.P.G.H., Seccion Nacional del Ecuador, 1977, 119 p.

# WITHIN-PLATE VOLCANISM IN UPPER TRIASSIC TO LOWER JURASSIC PUCARÁ GROUP CARBONATES (CENTRAL PERU)

Silvia ROSAS(1), Lluís FONTBOTÉ(2) and Wolfgang MORCHE (3)

(1) Escuela de Ingeniería Geológica, Universidad Nacional de Ingeniería, Av. Túpac Amaru s/n, San Martín de Porres, Lima, Peru.
(2) Département de Minéralogie, 13, rue des Maraîchers, CH-1211 Genève 4, Switzerland.
(3) INGEMMET, Av. Canadá 1470, San Borja, Lima, Peru.

KEY WORDS: Triassic, Jurassic, Pucará, within-plate volcanism, rifting, Peru.

## INTRODUCTION

The Pucará Group platform carbonates (Upper Triassic - Lower Jurassic) were laid down in northern and central Peru in a NNW-SSE elongated basin (Fig. 1). They represent the first sediments of the Andean cycle, the beginning of which is marked by a Norian transgression (Mégard, 1978). The sedimentary evolution of the Pucará Group can be explained in terms of a large transgressive/regressive second order sequence which consists of predominantly shallow water carbonates including a maximum flooding period represented by ammonite-bearing bituminous calcareous shales.

Detailed investigations in the southern part of the basin show that the Pucará Group thickens progressively from west to east in the form of a half-graben (Fig. 2). This can be explained by asymmetrical subsidence during sedimentation such being assisted by contemporaneous faulting along the eastern margin of the basin (permitting rapid subsidence) and a stable hinge zone to the west. Synsedimentary tectonics at the eastern edge led to the formation of discrete structural blocks with extreme variations in thickness and facies. It has been suggested that, during burial diagenesis, these faults served as channelways for the basinal brines responsible for MVT-mineralization (Fontboté et al., 1995, Spangenberg, 1995, and Moritz et al., 1996).

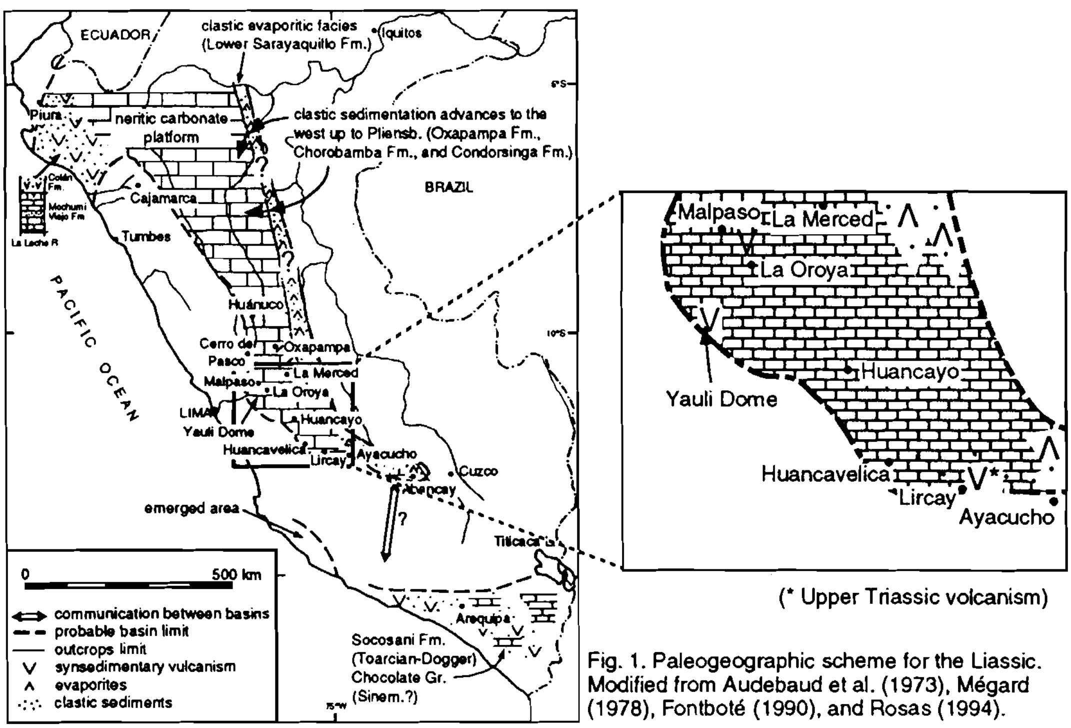


Fig. 1. Paleogeographic scheme for the Liassic. Modified from Audebaud et al. (1973), Mégard (1978), Fontboté (1990), and Rosas (1994).

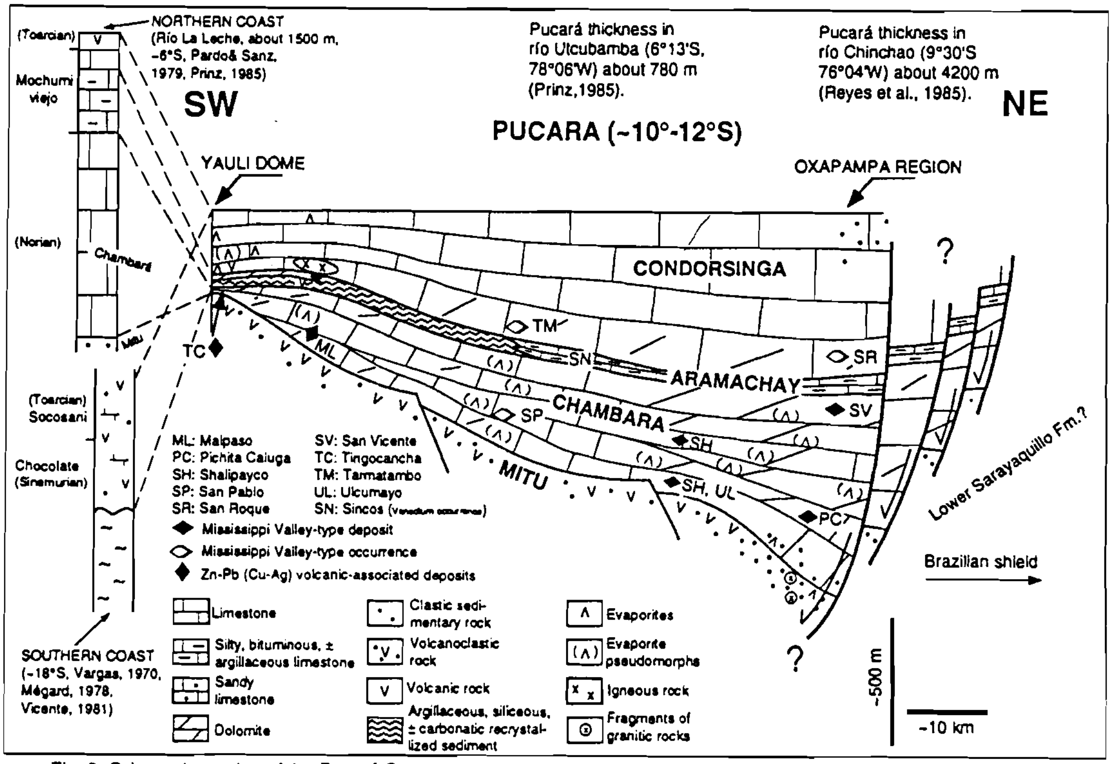


Fig. 2. Schematic section of the Pucará Group and its western equivalents. The location of some MVT and volcanic-associated deposits is shown (from Rosas & Fontboté, 1995)

Table 1. XRF-analyses of magmatic rocks intercalated in the Pucará Group.

| Unit | Montero volcanic rocks in Condorsinga Fm. (Liassic) | | | | | Tuffs in Aramachay Fm. (Liassic) | | | Volcanic rocks in Chambará Fm. (Triassic) | | |
|---|---|---|---|---|---|---|---|---|---|---|---|
| Section | Yauli Dome | | | | | Yauli D. | Malpaso | | Lircay | | |
| Sample | PB-51 | PB-53 | PB-54 | PB-55 | PB-56 | PB-22 | PA-103 | PA-107 | HU-17 | HU-21 | HU-23 |
| height (m) | 127.7 | 126.0 | 129.5 | 135.0 | 149.5 | 33.3 | 350.2 | 366.0 | (2 analyses) | | |
| % | | | | | | | | | | | |
| $SiO_2$ | 53.55 | 53.71 | 51.55 | 53.47 | 41.78 | 56.93 | 72.28 | 72.02 | 46.36 | 44.25 | 47.01 |
| $TiO_2$ | 2.23 | 1.76 | 2.26 | 2.30 | 2.16 | 0.89 | 0.51 | 0.26 | 2.64 | 1.71 | 2.19 |
| $Al_2O_3$ | 13.94 | 10.60 | 13.81 | 14.10 | 13.71 | 22.11 | 14.25 | 10.82 | 14.76 | 15.32 | 15.16 |
| $Fe_2O_3$ | 11.78 | 8.37 | 15.54 | 11.68 | 10.36 | 1.04 | 0.83 | 0.41 | 10.88 | 9.43 | 10.21 |
| MnO | 0.14 | 0.06 | 0.18 | 0.18 | 0.16 | 0.01 | bdl | bdl | 0.21 | 0.46 | 0.15 |
| MgO | 4.12 | 0.14 | 3.55 | 4.10 | 2.04 | 0.77 | 0.88 | 0.58 | 6.43 | 5.27 | 6.62 |
| CaO | 6.54 | 10.26 | 5.35 | 6.33 | 11.37 | 5.44 | 2.13 | 6.20 | 7.90 | 7.86 | 9.30 |
| $Na_2O$ | 3.00 | 5.02 | 4.04 | 3.76 | 4.41 | 0.06 | bdl | 0.39 | 4.05 | 4.66 | 3.02 |
| $K_2O$ | 2.21 | 1.63 | 2.53 | 1.78 | 1.79 | 1.53 | 1.99 | 1.99 | 2.06 | 1.82 | 1.73 |
| $P_2O_5$ | 0.57 | 0.40 | 0.51 | 0.37 | 0.31 | 0.18 | 0.12 | 0.16 | no data | 0.29 | 0.93 |
| LOI | 2.42 | 8.11 | 1.20 | 1.50 | 10.64 | 10.96 | 6.87 | 7.03 | 4.50 | 8.64 | 2.73 |
| ppm | | | | | | | | | | | |
| Ba | 427 | 194 | 427 | 381 | 302 | 151 | 38 | 84 | 384 | 399 | 732 |
| La | 20 | 13 | 15 | 10 | 30 | 34 | 18 | 17 | no data | 31 | 32 |
| Ce | 56 | 44 | 39 | 41 | 51 | 75 | 55 | 60 | no data | 37 | 91 |
| Cr | 20 | 13 | 19 | 19 | 24 | <5 | 6 | <5 | no data | 322 | 294 |
| Ni | 11 | <5 | 12 | 17 | <2 | 7 | <5 | <5 | no data | 250 | 419 |
| Rb | 67 | 29 | 54 | 46 | 30 | 51 | 53 | 55 | 22 | 40 | 34 |
| Sr | 200 | 96 | 352 | 333 | 114 | 467 | 224 | 250 | 157 | 284 | 963 |
| Y | 59 | 47 | 47 | 54 | 36 | 31 | 57 | 26 | no data | 21 | 27 |
| Zr | 301 | 244 | 193 | 212 | 198 | 447 | 323 | 152 | 186 | 124 | 217 |
| Nb | 14 | 13 | 8 | 9 | <5 | 19 | 14 | 6 | no data | 23 | 50 |
| V | 376 | 312 | 420 | 435 | 422 | 67 | 15 | 10 | no data | 215 | 188 |
| Co | 56 | 24 | 65 | 59 | 31 | bdl | bdl | bdl | no data | 50 | 40.00 |
| Cu | 49 | 70 | 12 | 17 | <4 | 18 | 20 | 16 | no data | 13 | 49 |
| Pb | 7 | 22 | 6 | 4 | <2 | 18 | 2 | 33 | no data | 41 | 118 |
| Zn | 95 | 105 | 70 | 78 | 64 | no data | bdl | bdl | no data | 198 | 113.00 |
| TOTAL (%) | 100.68 | 100.18 | 100.69 | 99.74 | 100.51 | 100.06 | 99.94 | 99.93 | 99.83 | 99.91 | 99.39 |

bdl= below detection limit, LOI=lost on ignition

A sequence analysis of the western margin of the southern part of the basin, together with the westward thinning of the sequence, point to the existence of a structural high at the western margin of the basin and to a connection between the Pucará basin and open ocean in the north-western part of Peru (see also discussion in Rosas, 1994 and Rosas & Fontboté, 1995). This contrasts with previous interpretations (Loughman & Hallam, 1982) which on the basis of the relatively large amounts of phosphate in the middle part of the Pucará Group, suggested that the Pucará basin was a carbonate shelf unrestrictedly open to the paleo-Pacific to the west. As an explanation for this phosphate formation, they proposed an upwelling of phosphate-rich waters from deep ocean. However, according to Calvert & Price (1971), upwelling of water from great ocean depths is not strictly necessary for phosphate formation, and according to Bentor (1980), Pevear (1966), and Föllmi (1993) the origin of phosphates of this type is in any case not necessarily related to upwelling. This makes Loughman & Hallam's assumption unnecessary.

Intercalated in Pucará sediments are known a number of volcanic occurrences (Rosas, 1994, Kobe, 1995). The purpose of this contribution is to present geochemical data of selected volcanic rocks in order to determine the possible geotectonic setting(s) during deposition.

## VOLCANIC INTERCALATIONS IN THE PUCARA GROUP

Upper Triassic volcanic intercalations are unknown in the occidental series. However, evidence of Upper Triassic volcanic activity has been reported in central regions of the basin. They are basic and quartz-dacitic altered lava flows and tuffaceous layers in Atacocha (Hirdes & Amstutz, 1978, Hirdes, 1990) and alkaline olivine basalts in Lircay (Rangel, 1978, Mégard et al., 1983, Morche et al., 1996). The geochemistry of these rocks (Table 1) is not indicative of volcanic arc activity but of within-plate volcanism (Fig. 4). Tuffaceous layers have been described at the lower part of the Pucará succession in the Yauli Dome by Dalheimer (1990), but they can not unequivocally be ascribed to the Upper Triassic.

Younger intercalations of lava have been observed in a few places. One of these is in the Yauli Dome where several dark-brown lava flows are intercalated with Liassic carbonates over a thickness of 40 m. These lavas are known as the "Montero Basalt" and show an aphanitic texture with vesicles and amygdales filled with calcite, chlorite, and zeolites. Incipient flow-banding has also been recognized. Geochemical studies, including trace element analyses (Table 1), indicate an andesite basalt composition (Fig. 2) and a clear within-plate signature for these rocks (Fig. 4).

Relatively thin (<3 m) intercalations of acid tuffs have been studied in the lower Liassic series of the Yauli Dome and in the Malpaso region. They consist of greenish altered fine-grained rocks, which trace elements indicate to be of rhyodacitic, dacitic, or trachyandesitic composition (Fig. 3).

In the north-western part of Peru, Pardo & Sanz (1979) and Prinz (1985) describe Upper Liassic volcanic rocks in a succession of tuffaceous graywackes, red beds and bedded cherts. They are known as the Colán Formation. The volcanic components of this unit have been studied geochemically by Romeuf (1994), from which she concludes a calc-alkaline basaltic composition and a volcanic arc setting.

In the southern coastal area of Peru volcanic rocks occur in the middle Liassic (Benavides 1962, James, et al., 1975, Vicente et al., 1982, Boily et al., 1984). They are known as the Chocolate Formation and consist of between 900 and 3000 m of andesites, subordinate dacites, volcanic agglomerates and breccias which could represent early stages of volcanic-arc activity.

## DISCUSSION AND CONCLUSIONS

Audebaud et al. (1973) proposed the existence of a western volcanic arc contemporaneous with Pucará sedimentation. However, the above data suggest that within-plate volcanism characterized the Pucará basin during Upper Triassic times as well as up into middle Liassic times. The volcanic arc started its activity in the northwest and south of Peru during Liassic times, as it did also in northern Chile where Hillebrandt et al. (1986) dated Hettangian and Sinemurian marine carbonates below the calc-alkaline basalts and basaltic andesites of the La Negra Formation. The influence of the volcanic arc elsewhere in the Pucará Basin is not revealed in the lithofacies described in Rosas (1994) and Rosas & Fontboté (1995).

In conclusion, the Pucará Basin possibly formed mainly as a result of aborted rifting at the western margin of the Brazilian shield. Some within-plate volcanism accompanied this stage. The western volcanic arc developed only coetaneously with the uppermost part of the Pucará Group and had little if any influence in the sedimentary record of the central part of the basin.

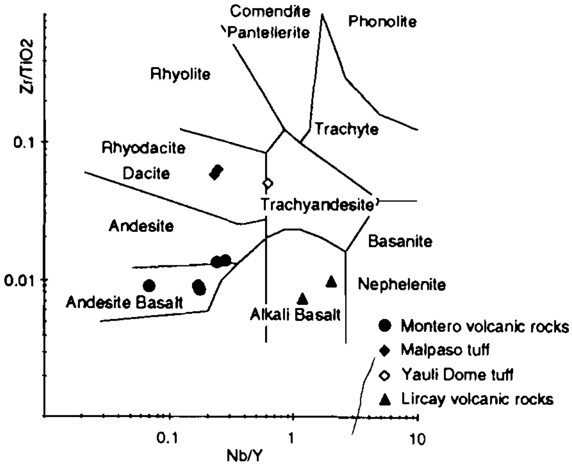


Fig. 3. Nb/Y vs Zr/TiO diagram (after WINCHESTER & FLOYD, 1977) for classification of magmatic rocks.

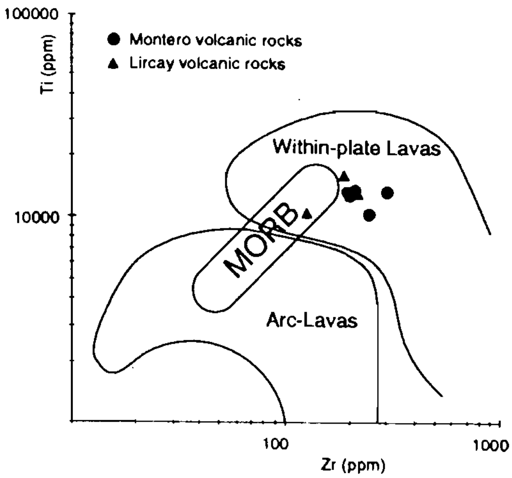


Fig. 4. Ti vs Zr diagram (after PEARCE, 1982) for interpretation of the origin of magmatic rocks.

REFERENCES

Benavides, V. (1962) Estratigrafía preterciaria de la regi6n de Arequipa. Bol. Soc. geol. Perú, 38, p. 5-63.

Bentor, Y.K. (1980) Phosphorites — The unsolved problems. in: Bentor, Y.K. [ed.] Marine phosphorites. Soc. econ. Paleont. Mineralog. Spec. publ., 29, p. 3-18.

Boily, M., Brooks, C. & James, D.E. (1984) Geochemical characteristics of the late Mesozoic Andean volcanics. In: Harmon, R.S. & Barreiro, B.A. [eds.] Andean magmatism: chemical and isotopic constraints. Shiva, Cheshire, p. 191-202.

Calvert, S.E. & Price, N.B. (1971) Upwelling and nutrient regeneration in the Benguela current, October, 1968. Deep-sea Res., 18, p. 505-523.

Dalheimer, M. (1990) The Zn-Pb-Ag deposits Huaripampa and Carahuacra in the mining district of San Cristobal, central Peru. in: Fontboté, L., Amstutz, G.C., Cardozo, M., Cedillo, E. & Frutos, J. [eds.] Stratabound ore deposits in the Andes. Springer, Berlin-Heidelberg, p. 279-291.

Föllmi, K.B. (1993) Phosphorus and phosphate-rich sediments, an environmental approach. Chem. Geol., 107, p. 375-378.

Hirdes, W. (1990) Machcán Mine: A Pb-Zn Ore Deposit in Pucará Sediments of the Atacocha District, Central Peru. in: Fontboté, L., Amstutz, G.C., Cardozo, M., Cedillo, E. & Frutos, J. [eds.] Stratabound ore deposits in the Andes. Springer, p. 293-303.

James, D.E., Brooks, C. & Cuyubamba, A. (1975) Early evolution of the central Andean volcanic arc. Carnegie Inst. Yearbook, 74, p. 247-250

Kobe, H.W. (1995) Evaporitas y volcánicos, Grupo Pucará, Perú central, componentes volcánicos, evaporíticos y sedimentos metalíferos en la parte occidental de ola cuenca del Grupo Pucará, Perú central. Volumen Jubilar Alberto Benavides, Soc. geol. Perú, p. 179-191

Morche, W., Larico, W., Narváez, S, & Guevara, C. (1996) Geología del Cuadrángulo de Huancavelica. Bol. Inst. geol. min. metal., serie A, in press.

Moritz, R., Fontboté, L., Spangenberg, J. Rosas, S., Sharp, Z. & Fontignie, D. (1996) Sr, C, and O isotope systematics in the Pucará basin, central Peru: Comparison between Mississippi Valley-Type deposits and barren areas. Min. Dep., 31, p. 147-162.

Pearce, J.A. (1982) Trace elements of lavas from destructive plate boundaries. In: Thorpe, R.S. [ed.] Andesites: Orogenic andesites and related rocks. Wiley, p. 525-548.

Pevear, D.R. (1966) The estuarine formation of United States Atlantic coastal plain phosphorites. Econ. Geol., 61, p. 251-256.

Romeuf, N. (1994) Volcanisme Jurassique et metamorphisme en Equateur et au Perou. P.h.D. Thesis Universite de Marseille. Faculte des Sciences et Techniques de St-Jerome, 305 p.

Rosas, S. & Fontboté (1995) Evolución sedimentol6gica del Grupo Pucará (Triásico superior - Jurásico inferior) en un perfil SW-NE en el centro del Perú. Volumen Jubilar Alberto Benavides, Soc. geol. Perú, p. 279-309.

Spangenberg, J. (1995) Geochemical (elemental and isotopic) constraints on the genesis of the Mississippi Valley-type zinc-lead deposits of San Vicente, central Peru. Terre & Environment 1, 123p.

Vicente, J.C., Beaudoin, B., Chávez, A. & Leon, I. (1982) La cuenca de Arequipa (Sur Peru) durante el Jurásico-Cretácico inferior. 5° Congr. Latinoam. Geol, Argentina, ACTAS, 1, p. 121-153.

Winchester, J.A. & Floyd, P.A. (1977) Geochemical discrimination of different magma series and their differentiation products using immobile elements. Chem.Geol., 20, p. 325-343.

Other references can be found in Rosas & Fontboté (1995).

# Widespread Cenozoic ignimbrites in N-Chile, W-Bolivia and S-Peru (17°-20°S/71°-68°E): Stratigraphy, extension, correlation and origin.

Wolfgang SCHRÖDER and Gerhard WÖRNER

Geochem. Institut, Georg August Universität Göttingen, Goldschmidtstr. 1, 37077 Göttingen; Germany
email: wschroe@ugcvax.dnet.gwdg.de

**KEY WORDS**: Northern Chile, Central Andes, Miocene, ignimbrites, pumice, correlation, extension, source area.

## INTRODUCTION

Large volume monotonous ignimbrites in N-Chile, W-Bolivia and S-Peru (17°-20°S/71°-68°E) represent one of the worldwide largest silicic provinces in the Cenozoic. Several pyroclastic outflow-sheets >1.000 $km^3$ were deposited during Miocene and Pliocene. These magmas are interpreted as a result of large scale crustal melting in response to events of crustal thickening (~70 km) in the last 25 Ma and may represent a similar event as the "ignimbrite flare up" (deSilva, 1989) in the Salar de Atacama region (21°-24°S). The working area is distinct from the Salar de Atacama region with respect to the considerably older age of the ignimbrites, and the Andean crust showing a different style of tectonism and uplift. We present data on the timing and volume of the two major ignimbrite events in northernmost Chile and western Bolivia in Miocene and Pliocene times. These events are related to the timing and style of uplift of the Andes in this region.
At 18°S we distinguish four main phases of ignimbrite volcanism:

### (1) Pre-Miocene Ignimbrites

The metamorphic basement near Belén is overlain by a sequence up to 700 m thickness of altered lava flows, lava breccias and silicified ignimbrites. These tectonized volcanics and intercalated ignimbrites are associated with proximal pyroclastic and volcaniclastic, as well as fluvio-lacustrine sediments. This sequence was correlated by Salas et al. (1966) to the Lupica-Formation at North and South (Upper Cretaceous/ Tertiary). Ignimbrites in this formation are altered and strongly folded. Within the upper member of the Lupica Formation, we found a series of 8 strongly folded unwelded and only slightly altered ignimbrites to th N and W of Belén (~500 m). These "Belén-Ignimbrites" underly an equally folded series of mafic andesite breccia and flows of large lateral distribution. Clearly the breccia and Belen-Ignimbrites are younger than the Lupic-Ignimbrites, and older than the stratigrafically higher "Kar-Ignimbrites"

A series of lithic-rich, strongly silicified ignimbrites disconformably overly these folded Cretaceous-Tertiary strata and form the highest crests of the Western Cordillera with altitudes between 4.300 and 5.200 m where they are glacially disseccted by kars ("Kar-Ignimbrites"). These ignimbrites have only local distribution and can be correlated to abundant post-tectonic silicic intrusions into the Lupica-Formation further N between Zapahuira and Putre.
This succession is composed of eight outflow-sheets with a thickness of 500 m. To the top this sequence changes to unaltered layers of andesite scoria and -breccias. The volume of these older ignimbrites cannot be determined.

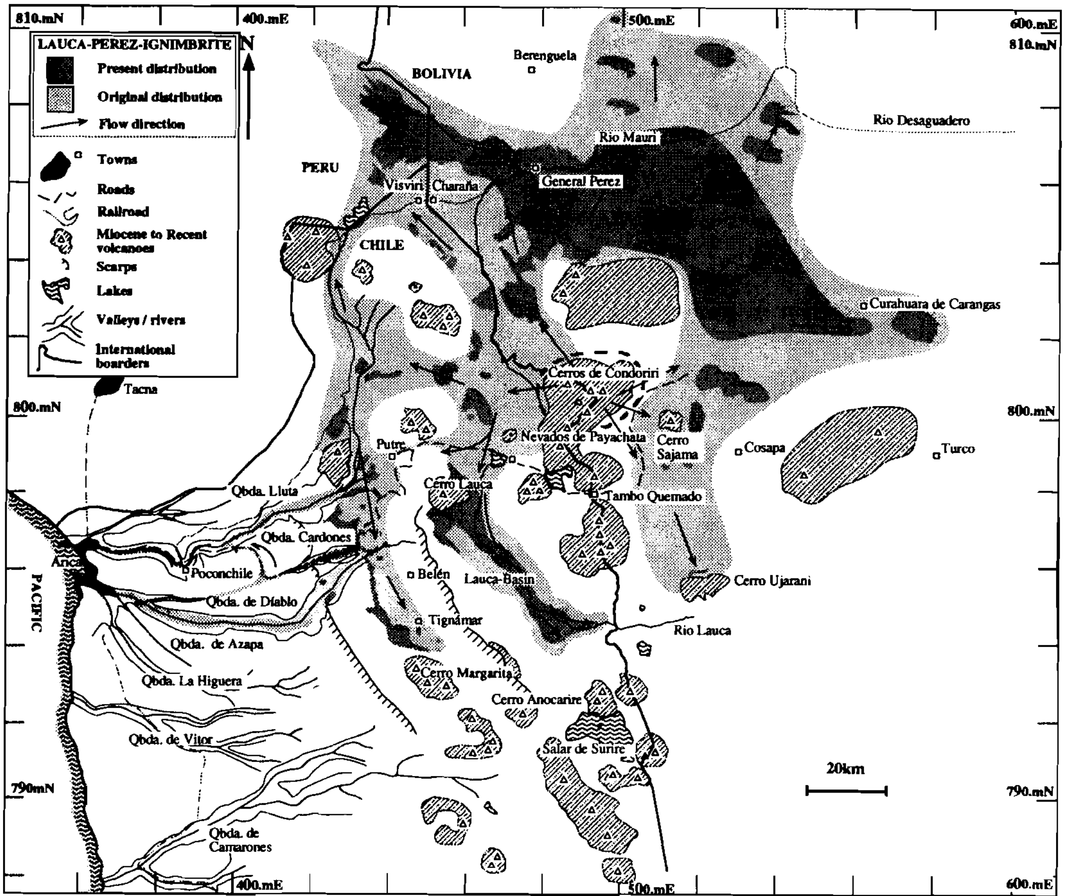

Fig. 1: Distribution of the Lauca-Perez ignimbrite (E-Bolivia: unpublished data of GEOBOL)

## (2) Oxaya-Ignimbrites (20-19 Ma)

**Monotonous large volume ignimbrites** (~**19 Ma**) at 18°S form the inclined West-Andean slopes in northernmost Chile and are suggested to result from an event of extended crustal melting around 19 Ma. These ignimbrite sheets with a total thickness of up to 900 m together with the underlying >1.000 m of monotonous alluvial, fluviatile and lacustrine sediments form the Oxaya-Formation. This association suggests that the Miocene ignimbrites post-date a first major phase of crustal thickening, uplift, erosion and sedimentation.
The Oxaya ignimbrites are subdivided into four main outflow-sheets (members 1-4) with a combined maximum thickness of 930 m in the Quebrada Cardones. The uppermost welded Oxaya-Ignimbrite gave an Ar/Ar sanidine step heating age of 19.38±0,01 Ma. (Walfort et al., 1995). The Oxaya-Ignimbrites can be traced in E-W direction over a distance of 130 km from the Western-Cordillera (~4.600 m/Lago Chungará) to the Coastal Cordillera. Corrleated occurrences on the Altiplano have been assigned the name "Condoriri"-Ignimbrite by Salas et al (1966). Closer to the coast and, presumably, more distally, the ignimbrites are less welded but still reach 300 m at the coast near Arica.
Satellite images, air-potographs and field data show that the Oxaya ignimbrites can be correlated 300 km along the continental margin, from Southern-Peru (~17°S) to the Chilean Camarones valley (~20°S). This areal extent and measured thickness suggest total volumes of of the Oxaya ignimbrites of >3.000 km$^3$. The source area of the Oxaya ignimbrites is still unknown.

There is no indication of a significant time span between the individual ignimbrites because erosion between the out-flow sheets is limited. Only distally and towards the coast, the ignimbrites are intercalated by a fluvio-lacustrine sedimentary succesion up to 200-400 m thick in the Camarones valley. Nevertheless, the ignimbrites represent a large volume of silicic (crustal ?) melts erupted within a geologically short period around 19 Ma.

### (3) The Lauca-Pérez ignimbrite (Huaylas-Fmt, 2,72±0,01 Ma)

A younger post-tectonic ignimbrite of the Huaylas-Formation ("Lauca-Iignimbrite")was dated by the Ar-Ar-method to 2.7±0,01 Ma (Walfort et al. 1995) and can thus be correlated with the ignimbrite of the "Pérez-Formation" which covers wide areas in western Bolivia and southern Peru.
The source area was identified by regional distribution and topography on Landsat satellite images as well as field-work to underly younger stratovolcanoes of the Cerros de Condoriri complex just E of the border between Chile and Bolivia, and NE of the Nevados de Payachata volcanoes. The caldera itself is not recognized by satellite images. However, the thickness increases up to >100 m on a flat ramp descending from the Cerro Condorir area. We also observe a higher degree of welding in an upper flow unit rich in fiamme which only occurs near the Cerro Condoriri area. These obeservations are evidence for a proximal position. Chemical data, Ar-Ar ages as well as petrographic and field correlations clearly show that the Lauca-Ignimbrite in northern Chile correlates to the Pérez-Ignimbrite 2.2-3 Ma (K-Ar, Everden et al. 1977) and 3 Ma (K-Ar, Lavenu et. al. 1989) in western Bolivia. We therefore use the name Lauca- Peréz Ignimbrite.

Today, the Lauca-Peréz Ignimbrite is strongly dissected by erosion. The initial total areal extend of ~200 km is estimated from widely distributed erosional remnants to about 15.000-20.000 km$^2$, with most of the area covering the flat-lying Bolivian Altiplano (Fig. 1). The maximum distance traveled is ~130 km, one of the largest distances demonstrated for an ignimbrite, comparable with the Taupo ignimbrite in New Zealand (Wilson et al., 1995). The aspect ratio (ratio of average thickness of a deposit to the diameter of a circle that covers the same area) is ~1:3.500 (Wilson 1995). A bulk volume is estimated to >775 km$^3$. From the relationship between caldera dimensions and the size of the associated ignimbrite the caldera to the Lauca/Pérez ignimbrite is expected to be in the order of 15-25 km wide. Such a caldera would well fit under the extensive Cerro de Condoriri stratovolcano complex.

The Lauca-Pérez ignimbrite fills in morphological depressions and valleys, onlaps and/or passes over higher topography, and thus serves as a reliable morphological and stratigraphic marker in northernmost Chile and Western Bolivia.

We subdivide the Lauca-Pérez ignimbrite into a groundsurge of 10-50 cm thickness at the base and three flow units. The lower, first flow unit is fine-grained with typical phenocryst-poor fibrous pumice 0.5 to 2 cm in size. This unit is in some places restricted to morphological lows whereas the second flow unit appears to have been more mobile. The second layer is characterized by an abundance of large qurtz-beraring pumices in its upper part. These reach diameters of 20 to 50 cm typically in the most distal parts (Alcérreca, Cerro Ujarani in Bolivia) near to the termination of the flow (see also: Wright et al. 1981). The uppermost youngest flow unit occurs only near the source area and shows evidence of intense welding (fiamme-structures). This petrographic variation and the occurrence of white-grey heterogeneous lapilli suggests magma mingling and eruption from a chemically zoned magma chamber.

The Lauca-Pérez ignimbrite flowed radially from its source but encountered the flat-lying Altiplano only to the N, W and S. This resulted in the widespread distribution of the Peréz-Ignimbrite and the mesa-like occurence on the Bolivian Altiplano. Here, the total thickness of the outflow-sheets amounts to 20-100 m in proximal areas, depending on underlying morphology. A major portion, however, flowed to the west and filled the depression between the volcanic front and the Western Cordillera (Chilean Altiplano). One large part of the flow continued S over 80 km into the Lauca-Basin (Kött et al, 1995). Another part of the flow started its descent to the coast after passing through narrow valleys and passes cutting through the Western Cordillera (Upper Lluta Valley, Portezuelo Las Quevas, Portezuele Chapiquiña). The ignimbrite descended the extreme morphology from 4.500 m to about 3000 m onto the the Pampa de Qxaya block (Uhlig et al, this meeting) where the flow again separated into different lobes. One lobe followed the half-graben along the Pampa de Oxaya 70 km to the south reaching Cerro Margarita. Several other flows concentrated into several valleys (Lluta-, Cardones-, Diablo-, Azapa- and Cerro Ujarani) and continued over a distance of 90 km to the Pacific Ocean, near the city of Arica. At the narrow passage of the Lluta-valley entrance the thickness of the ignimbrite-deposits increases strongly to over 100 m due to ponding effects.
In the deeply incised Lluta- and Azapa-valleys remains of the Lauca-Pérez ignimbrite between 600 and 20 m above the present valley-bottom. This places constraints on the amount of valley incision in the past 2,7 Ma (Uhlig et al. this meeting).

The Lauca-Pérez ignimbrite suffered only minor, mostly normal faulting indicating that since about at least 2,7 Ma there was no major tectonic activity in the area, except possibly for large regional movements unrelated to small scale faulting.

### (4) Local small volume ignimbrites (Pleistocene/Pliocene)

Local small-scale ignimbrites are also observed, but can be distinguished from for example the Lauca-Pérez Ignimbrite by their chemical and petrographic composition. These local ignimbrites are related to the stratovolcanoes of the volcanic front (Miocene to Recent).

## CONCLUSIONS

The occurrence of ignimbrites at 18°S in the Andes mark a major episode of crustal melting at around 19 Ma which is preceeded by extensive erosion and deposition of sediment. Normal faulting with high vertical offsets in a second pulse of uplift resulted in a stair-case topography locally overprinting large-scale anticlines. This steep topography was formed between <19 Ma and about 10 Ma, and has since not been changed significantly by either erosion or subsequent tectonics (Uhlig et al., this meeting). A second, minor pulse of ignimbrite magmatism occurred at 2,7 Ma.

Timing and relative volumes of the ignimbrite volcanism at 18°S are thus quite distinct from the Salar de Atacama region. This region is mostly characterized by strike-slip displacements with strike-slip transpression and local pull-apart tectonics. Resulting dissection and crustal extension may have favoured the ascent of crustal melts and consequently the eruption of extensive ash-flow tuffs. In this region voluminous ignimbrite volcanism is observed between 4 and 10 Ma.

In the Arica area, however, large strike slip movements are absent since at least Miocene times One reason could be that only in the Arica bend area at 18°S the convergence between Nazca and South American plates is normal whereas further south the convergence is oblique.

Miocene ignimbrites at 18°S representing large magma volumes (>1.000 $km^3$) can be correlated over large areas, and thus be used to characterize and date the tectonic and erosional events. The "young" Lauca-Pérez ignimbrite (2,7 Ma) overlies and seals as a marker horizont the older topography. It represents a widespread ignimbrite flow and -emplacement from a high topographie with altitudes of 4.600 m over a large distance from the Bolivian Altiplano down the coastal valleys into the Pacific Ocean.

## REFERENCES


Cas R.A.F. & Wright J.V. 1993. Volcanic successions: modern and ancient. *Chapman & Hall*, London.

deSilva S.L. 1989. Altiplano-Puna volcanic complex of the central Andes. *Geology* v.17, p.1102-1106.

Everden J.F. et. al. 1977. Potassium-argon ages of some Bolivian rocks: *Economic Geology*, v.72., p.1042-1061.

Kött A. et.al. 1995. Miocene to Recent history of the western Altiplano in northern Cile revealed by lacustrine sediments of the Lauca Basin (18°15'-18°40'/69°30'-69°05'W). *Geol. Rundschau* , 84: 770-780.

Lavenu A. et.al. 1989. Neogene magmatism in the Bolivian Andes between 16°S and 18°W: stratigraphy and K/Ar geochronology. *Journal of Latin American Earth Science*, v.2, p.35-47.

Salas et al. 1966. Geología y recursos minerales del departamento de Arica; Provincia de Tarapacá, *Boletín*, Universidad de Chile, Santiago.

Walfort B., Hammerschmidt K., Wörner G. 1995. New Ar/Ar ages from Tertiary volcanics in the North chilean Andes (18°S): Implication for tectonic and magmatic evolution. *Terra Abstracts, Terra Nova* 7, 354.

Williams H. et al. 1979. *Volcanology*. San Francisco: Freeman, Cooper.

Wilson C.J.N. et.al. 1995. An exceptionally widespread ignimbrite with implications for pyroclastic flow emplacement. *Nature* v.378, p.605-607.

Wright J.V.et al. 1981. Towards a facies model for ignimbrite forming eruptions. *In Self & Sparks* 433-439.

# Rare-earth and trace element abundances of the Neogene volcanism of the Farellones Formation and the WE Montenegro-Cerro Manquehue Lineament (Central Chile)

Nicole VATIN-PERIGNON[1], Sergio RIVANO G.[2], Mario VERGARA M.[2] and Francine KELLER[1]

[1] Université Joseph-Fourier de Grenoble, UFR de Géologie & Laboratoire de Géodynamique des Chaînes Alpines UPRES -A 5025 CNRS, 15, rue Maurice Gignoux, 38031 Grenoble cedex, France

[2] Facultad de Ciencias Fisicas y Matematicas, Dep tamento de Geología y Geofisica, Universidad de Chile, Casilla 13518, correo 21, Santiago, Chile

**KEY WORDS**:

Basalts, andesites, fractional crystallization, parental magma, Miocene, Chile

## INTRODUCTION

Miocene volcanics of the *Farellones Formation* are located at the north of the río Aconcagua, east of the Oligocene-Miocene magmatic belt and west of the present volcanic arc in the Central Chilean Andes (Vergara *et al.*, 1988; Rivano *et al.*, 1990; Rivano & Sepúlveda, 1991). Deposits of this period form a N/S trending chain of 400 km long to 25-65 km wide between 31°30 and 34°S. This segment of the calc-alkaline magmatic arc is cross-cutted by an equivalent age localized mafic to intermediate magmatism forming a *W/E Lineament* with a discordant orientation. The stratigraphy and detailed chronology established for this Formation have been given by Beccar *et al.* (1986), Rivano *et al.* (1990, 1993) and the isotopic character of lavas by López-Escobar *et al.* (1991). More recently, Stern and Skewes (1995) show that lower and upper plate parameters may have the same importance for producing spatial and chemical segmentation of the Andean arc.

Miocene Farellones activity is characterised by calc-alkaline volcanic rocks ranging from basalt through andesite and dacite to high-silica rhyolite. The *Montenegro-Cerro Manquehue Lineament* provides outstanding exposures of lava necks and domes ranging from basalts to dacites, extruded during the same period and commonly aligned along a W-E fault zone. We use trace element and rare earth element (REE) abundances, petrography and mineral chemistry to « fingerprint » eruptive products and to describe the compositional distinctions between the volcanic series. The purpose of our contribution is to clarify the relationships between ignimbrites, andesites and the transversal basaltic lineament.

## GEOLOGIC SETTING

The volcanic sequences at Cerro La Gloria (type locality) can be divided into two major episodes. The *Lower Member* is composed mainly of rhyolitic welded and non-welded ignimbrites and air-fall deposits interbedded with lacustrine sediments and its thickness varies from 1 m to about 300 m. $^{40}Ar/^{39}Ar$ ages indicate an age of about 26.7 Ma for the oldest phase of the *Farellones Fm.* (Rivano & Vergara, 1996). The well defined history of multiple eruptions begins about 20 Ma. The *Upper Member* consists mostly of andesitic to dacitic lavas (up to 1500 m) with minor dacitic tuffaceous beds, erupted between 19 and 8 Ma, and associated with several riodacitic domes and dykes extruded during this period.

Basaltic necks and dacitic domes of the *W/E Montenegro-Cerro Manquehue Lineament* are part of isolated Miocene volcanic rocks and plutons which intruded the foothills of the Central Chilean Andes. The basaltic neck of Cerro Huechún has been dated at 20.2 and 20.3 Ma and the dacitic dome of Chacabuco at 18.4 Ma by K-Ar method (Rivano *et al.*, 1993).

The Portezuelo del Azufre unit is formed by small dacitic to rhyodacitic intrusions which are Miocene in age (18 Ma, Rivano *et al.*, 1993) and in relation with volcanics of the *Upper Member* of the Farellones Fm.

## PETROGRAPHY AND MINERAL CHEMISTRY

Rhyolites (70-75% $SiO_2$) represent about 95% of the total eruptives of the *Lower Member* and are variably porphyritic with plagioclase (oligoclase-andesine) as dominant phase and quartz usually present. The greatest petrographic variation lies in the subordinate assemblage of biotite ± hornblende ± Fe-Ti oxides.

The most mafic rocks of the *Upper Member* are basalts and basaltic andesites but plagioclase-two-pyroxene andesites make up the dominant group. Basalts and basaltic andesites are variably porphyritic and generally contain phenocrysts of plagioclase and clinopyroxene in a granular to subophitic groundmass of plagioclase, pyroxene and magnetite. Olivine ($Fo_{55-62}$) and plagioclase ($An_{73-75}$) occur as phenocrysts and microphenocrysts in the most primitive lavas (<5o wt% $SiO_2$ ). Augites show relatively little compositional variation ($Wo_{40-42}$ $En_{41-42}$ $Fs_{15-18}$). Plagioclase phenocrysts often display core to rim zonations ($An_{81-46}$ ) and augite ($Wo_{45-47}$ $En_{41-45}$ $Fs_{10-20}$) and pigeonite ($Wo_3$ $En_{74}$ $Fs_{22}$) increase in relative abundance. In more evolved compositions, andesites contain hornblende, biotite and glomerocrysts.

Phenocryst assemblages of basaltic andesites of the *W/E Lineament* are characterised by plagioclase ($An_{92-75}$), orthopyroxene ($Wo_{2-3}$ $En_{53-70}$ $Fs_{27-40}$), clinopyroxene ($Wo_{40-45}$ $En_{43-45}$ $Fs_{9-15}$), magnetite and rare olivine. Microlites ($An_{50-57}$ ) and intersertal groundmasses change in composition. Dacitic domes are sparsely porphyritic with plagioclase ($An_{40-47}$ ), augite ($Wo_{42}$ $En_{37}$ $Fs_{21}$), pigeonite, Fe-Ti oxides and contain vesiculated mafic inclusions.

## RARE-EARTH AND TRACE ELEMENT GEOCHEMISTRY

Contents of REE and trace elements in representative Farellones and W/E Lineament lavas are given in Table 1.

Chondrite-normalized rare-earth-element (REE) profiles for the rhyolites of the *Lower Member* and for andesites of the *Upper Member* are very similar. Andesites and rhyolites have evolved patterns and show low LREE/HREE factionation ($La/Yb_n$ = 5 - 7) and negative Eu anomalies increasing with differentiation. These characteristics are consistent with lavas formed mainly through crystal fractionation. Basaltic andesites of the *Upper Member* are comparable with those of the *W/E Lineament* showing less evolved and regular REE patterns and only a slight enrichment of LREE relative to the HREE.($La/Yb_n$ = 2 - 3). The relative parallelism of their patterns confirm their genetic relationship. Dacites exhibit maximal variations in REE abundances and have no Eu anomalies. These lavas are characterized by higher LREE/HREE fractionation and have among the highest $La/Yb_n$ (14-19) of all Farellones lavas.

Table 1. Major and trace element analyses of representative Farellones samples

| *N°* | 1 | 2 | 3 | 4 | 5 | 6 | 7 | 8 | 9 | 10 | 11 | 12 | 13 |
|---|---|---|---|---|---|---|---|---|---|---|---|---|---|
| *sample* | *CH95-13* | *1801-B* | *CH95-16* | *CH95-14* | *CH95-9B* | *2801-09* | *15-14* | *CH95-18* | *CH95-3A* | *CH95-4* | *CH95-1* | *1301-04* | *2801-01* |
| *SiO2* | 70,33 | 75,52 | 49,82 | 51.24 | 56,86 | 59,10 | 61,55 | 62,54 | 50,26 | 50,39 | 51,51 | 62,80 | 63,92 |
| *TiO2* | 0,26 | 0,28 | 1,53 | 1,41 | 1,11 | 0,96 | 0,76 | 0,64 | 0,89 | 0,90 | 0,61 | 0,56 | 0,64 |
| *Al2O3* | 13,14 | 11,89 | 19,43 | 19,02 | 19,36 | 16,51 | 16,99 | 17,82 | 18,46 | 18,51 | 19,04 | 15,67 | 17,04 |
| *Fe2O3t* | 1,48 | 1,41 | 9,00 | 8,35 | 6,16 | 7,19 | 5,24 | 4,55 | 8,90 | 8,84 | 7,92 | 2,67 | 3,37 |
| *MnO* | 0.06 | 0.03 | 0,14 | 0,18 | 0,11 | 0,14 | 0,11 | 0,05 | 0,13 | 0,13 | 0,13 | 0,08 | 0,06 |
| *MgO* | 0,26 | 0,16 | 4,04 | 3,24 | 1,76 | 3,16 | 1,79 | 1,59 | 4,84 | 4,74 | 6,32 | 0,31 | 1,81 |
| *CaO* | 2,54 | 2,35 | 8,86 | 8,05 | 4,97 | 4,93 | 4,65 | 4,15 | 9,48 | 9,43 | 10,68 | 7,90 | 4,32 |
| *Na2O* | 1,68 | 1,59 | 3,48 | 3,83 | 4,46 | 2,96 | 4,15 | 5,85 | 3,08 | 3,11 | 2,64 | 3,74 | 4,62 |
| *K2O* | 5,19 | 3,77 | 2,20 | 2,32 | 3,31 | 1,59 | 1,87 | 1,39 | 0,84 | 0,85 | 1,11 | 1,74 | 1,96 |
| *P2O5* | 0,01 | 0,04 | 0,32 | 0,31 | 0,28 | 0,11 | 0,16 | 0,07 | 0,36 | 0,37 | 0,08 | 0,06 | 0,10 |
| *L.O.I.* | 4,06 | 3,60 | 1,68 | 0.99 | 1,75 | 3,85 | 2,18 | 1,29 | 2,50 | 2,47 | 0,77 | 4,85 | 1,31 |
| *Total* | 99.01 | 100,64 | 100,50 | 98,94 | 100,13 | 100,50 | 99,45 | 99,94 | 99,74 | 99,74 | 100,81 | 100,38 | 99,15 |
| *Ba* | 473 | 335 | 323 | 382 | 512 | 515 | 380 | 331 | 314 | 323 | 266 | 830 | 581 |
| *Rb* | 173 | 187 | 42 | 59 | 85 | 45 | 65 | 21 | 17 | 21 | 11 | 58 | 53 |
| *Sr* | 45 | 128 | 496 | 455 | 469 | 318 | 441 | 544 | 749 | 784 | 752 | 586 | 658 |
| *Y* | 26 | 22 | 33 | 32 | 31 | 20 | 19 | 8 | 18 | 18 | 13 | 10 | 8 |
| *Zr* | 179 | 207 | 215 | 239 | 306 | 157 | 193 | 170 | 92 | 96 | 55 | 131 | 112 |
| *Nb* | 10 | 7 | 9 | 12 | 15 | 5 | 5 | 3 | 5 | 5 | 2 | 5 | 4 |
| *Cs* | 4,13 | 11,20 | 1,94 | 1,89 | 3,52 | 1,54 | 1,55 | 0,55 | 0,65 | 0,89 | 0,64 | 8,85 | 2,19 |
| *Hf* | 6,54 | 6,45 | 5,93 | 6,85 | 8,52 | 4,35 | 5,26 | 2.01 | 2,34 | 2,38 | 1,59 | 3,18 | 2,99 |
| *Ta* | 0,85 | 0,81 | 0,59 | 0,75 | 0,94 | 0,40 | 0,46 | 0,23 | 0,30 | 0,31 | 0,08 | 0,40 | 0,40 |
| *Th* | 21,00 | 24,20 | 5,44 | 7,10 | 8,31 | 6,21 | 11,10 | 2,18 | 2,56 | 2,53 | 1,43 | 5,31 | 4,54 |
| *U* | 5,35 | 5,58 | 1,53 | 1,82 | 2,14 | 1,88 | 3,44 | 0,53 | 0,79 | 0,80 | 0,45 | 1,66 | 1,44 |
| *La* | 21,14 | 24,73 | 21,07 | 23,08 | 28,21 | 15,89 | 17,85 | 10,24 | 16,09 | 16,39 | 6,78 | 24,33 | 18,39 |
| *Ce* | 49,12 | 54,42 | 49,33 | 53,26 | 66,76 | 35,18 | 37,47 | 22,31 | 35,01 | 36,82 | 16,43 | 47,76 | 38,35 |
| *Pr* | 5,92 | 6,51 | 6,59 | 6,99 | 8,80 | 4,70 | 4,77 | 2,83 | 4,60 | 4,71 | 2,32 | 5,62 | 4,72 |
| *Nd* | 22,43 | 23,96 | 28,26 | 29,48 | 36,24 | 19,75 | 19,69 | 11,00 | 18,78 | 18,81 | 10.27 | 20,11 | 18,75 |
| *Sm* | 4,88 | 5,06 | 6,41 | 6,48 | 7,73 | 4,53 | 3,89 | 2,02 | 4,18 | 4,17 | 2,57 | 3,61 | 3,55 |
| *Eu* | 0,72 | 0,51 | 1,62 | 1,59 | 1,76 | 1,22 | 0,96 | 0,64 | 1,27 | 1,32 | 0,88 | 0,96 | 1,02 |
| *Gd* | 3,98 | 4,13 | 6,11 | 6,13 | 6,81 | 3,86 | 3,39 | 1,80 | 3,41 | 3,58 | 2,32 | 2,63 | 2,55 |
| *Tb* | 0,65 | 0,67 | 0,91 | 0,90 | 0,97 | 0,62 | 0,55 | 0,23 | 0,54 | 0,55 | 0,36 | 0,36 | 0,31 |
| *Dy* | 4,00 | 3,71 | 5,28 | 5,23 | 5,38 | 3,56 | 3,13 | 1,21 | 3,34 | 3,24 | 2,16 | 1,92 | 1,63 |
| *Ho* | 0,83 | 0,87 | 1,09 | 1,08 | 1,07 | 0,79 | 0,71 | 0.24 | 0,69 | 0,70 | 0,47 | 0,37 | 0,31 |
| *Er* | 2,45 | 2,23 | 3,02 | 2,97 | 2,90 | 1,89 | 1,66 | 0,64 | 1,72 | 1,78 | 1,30 | 0,99 | 0,76 |
| *Yb* | 2,73 | 2,63 | 2,77 | 2,71 | 2,64 | 1,88 | 1,82 | 0,62 | 1,84 | 2,00 | 1,31 | 0,99 | 0,67 |
| *Lu* | 0,41 | 0,42 | 0,42 | 0,41 | 0,39 | 0,28 | 0,29 | 0,10 | 0,26 | 0,26 | 0,20 | 0,16 | 0,09 |

XRF analyses for major elements (in wt.%) and ICP-MS analyses for trace elements (in ppm) at the Geological Department of the University Joseph-Fourier of Grenoble.
Analytical procedures for trace element and REE concentrations following those of Barrat et al. (1996).
Farellones Fm: lower Member: anal. 1 to 2, upper Member: anal. 3 to 8, Montenegro-Cerro Manquehue lineament: anal. 9 to 12. Miocene dacitic intrusion (Portezuelo del Azufre) associated with the Farellones volcanics: anal. 13.

On a multi-element diagram normalized to N-MORB, rhyolites of the *Lower Member* and andesites of the *Upper Member* show typical patterns for evolved subduction related magmas with marked enrichment of the large-ion lithophile (LIL) elements ( e.g. K, Rb, Th) with the exception of Ba and Sr (and Eu) indicating the effects of feldspar and accessory mineral fractionation. The negative anomaly of Ba may be also an indication of a refractive mineral phase, possibly phlogopite, in the source material. Ti and P show marked negative anomalies for rhyolites, this is general for all the analysed rhyolites and is very typical for arc magmas indicating the early fractionment of ilmenite or

Ti-magnetite and apatite. Nb also least some of the magma is of mantle origin. Decreases of Zr and Ba in these rocks may be explained by fractionation of biotite. Rhyolites have patterns much like those of high-silica rhyolites with Nb and Ti depleted relative to the REE and a pattern of high field strengh (HFS) elements (Ta, Nb, Zr, Hf) typical of arc magmas. Basaltic andesites of the *W/E Lineament* are the most mafic compositions erupted and display a low range in concentrations including the relative enrichement of the LIL elements and depletions of HFS elements relative to the REE. their patterns are different of those of basaltic andesites of the *Upper Member*, especially one basaltic andesite (CH95-1) in having all the elements depleted . Dacites are enriched in Ba and in common with Yb, Y decreases and the overall decrease in these elements may be probably due to hornblende fractionation.

All of the lavas have a high Th/Ta ratio: 25-35 for rhyolites, 15-24 for dacites, 10-15 for andesites and 8-9 for basaltic andesites. In general, Th vs Ta trends are very coherent for basaltic andesites and andesites of the *Upper Member* and the *W/E Lineament* whereas rhyolites of the *Lower Member* and dacitic domes are very different. Compositional variations show also coherent trends for basaltic andesites and andesites on binary element-element diagrams for a number of other elements (e.g. Zr vs Hf, Yb vs Ce) and show that these lavas have the same parental magma and their evolution may be largely dominated by crystal fractionation. The differences in REE and trace element compositions for rhyolites and dacitic intrusions may be attributed to source heterogeneity of lavas.

## CONCLUSIONS

The volcanism of the *Farellones Fm.* and the *W/E Lineament* is characterized by the relative enrichments of the LREE accompanied by. enrichments of LIL elements. Mafic magma of the *W/E Lineament* and andesites of the *Upper Member* of the Farellones Fm. can be related to each other by crystal fractionation. REE and trace element concentrations show coherent trends which may reflect a relatively homogeneous magma source. Compositions of rhyolites and ash flow tuffs of the *Lower Member* and dacitic intrrusions are very different and may reflect large components of continental crust formed or reworked in a subduction-related environment.

## REFERENCES

Barrat, J.A., Keller, F., Amossé, J., Taylor, R.N., Nesbitt, R.W. & Hirata, T. Determination of rare earth elements in sixteen silicate reference samples by ICP-MS using a Tm addition and an ion-exchange chromatography procedure. *Geostandards Newsletter* (submitted), 1996.

Beccar, I., Vergara, M., Munizaga, F. 1986. Edades K-Ar de la Formación Farellones en el cordón del Cerro La Prava, Cordillera de los Andes de Siantago, Chile. *Revista Geológica de Chile*, 28-29:109-113.

López-Escobar, L., Kempton, P.D., Harmon, R.S. & Vergara, M. 1991. Isotopic character of Miocene lavas 33-35°S, central Chile. *EOS, American Geophysical Union*, 72, 44,

Rivano, S., Godoy, E., Vergara, M. & Villarroel, R. 1990. Redefinición de la Formación Farellones en la Cordillera de los Andes de Chile central (32-34°S). *Revista Geológica de Chile*, 17: 205-214.

Rivano, S. & Sepúlveda, P. 1991. Hoja Illapel, Región de Coquimbo, Chile. *Servicio Nacional de Geologia y Mineria*, Carta geológica de Chile n° 69, 1/250 000°, 120 p.

Rivano, S., Sepúlveda, P., Boric, R., & Espiñeira, D. 1993. Hojas Quillota y Portillo. *Servicio Nacional de Geologia y Mineria*,Carta geológica de Chile n°73, 1/250 000°, 147 p.

Rivano, S. & Vergara, M. 1996. La discordancia basal de Farellones: un ejemplo del relieve premioceno. *Servicio Nacional de Geologia y Mineria*, Carta geológica de Chile.

Stern, C.R. & Skewes, M.A. 1995. Miocene to present magmatic evolution at the northern end of the Andean Southern Volcanic Zone, Central Chile. *Revista Geológica de Chile*, 22: 261-272.

Vergara, M., Charrier, R., Munizaga, F., Rivano, S., Sepúlveda, P., Thiele, R. & Drake, R. 1988. Miocene volcanism in the central Chilean Andes (31°30 - 34°35 S). *J.South American Earth Sciences*, 1: 119-209.

# GEOCHEMICAL FEATURES OF THE SOUTHERN ANDES OLIGOCENE-MIOCENE VOLCANISM IN THE PRECORDILLERAN REGION OF TALCA-LINARES (35°20'-35°50'S)

Vergara, M. (*), López-Escobar, L. (**), and Beccar, I.(*)

(*) Departamento de Geología, Universidad de Chile, Casilla 13518, Santiago 21, Chile.

(**) Instituto de Geología Económica Aplicada, Universidad de Concepción, Casilla 4107, Concepción 3, Chile.

**KEYWORDS**: Oligo-Miocene volcanism, Geochemistry, Southern Andes.

## INTRODUCTION

Tertiary volcano-sedimentary sequences constitute an important geological unity that covers a large part of the Andean Cordillera at least between latitudes 33°S and 37°S. However, Tertiary volcanic outcrops are scarse between 37°S and 40°S, being restricted to the Longitudinal Depression (Central Valley) and Coastal Range. Deep drilling projects, carried out by ENAP (Chilean Oil Company), have allowed to determine the distribution and thickness of this unity in the latter region.

This report discusses the stratigraphy and geochemistry of the Tertiary volcanism that outcrops in the Andean precordillera between latitudes 35°20'S and 35°50'S, that is between the latitudes of the Chilean cities of Talca and Linares.

## GEOLOGY

In the Andean precordillera between Talca and Linares, Beccar (1966) defined a 1500 m thick Tertiary unit mainly consisting of volcanic rocks. Its base is represented by a sequence of basaltic lava flows showing amygdules of zeolite, pyroclastic tuffs, pyroclastic flows (ignimbrites) and volcanoclastic sediments. Overlying this sequence there is a thick sequence of volcanic detritus flows, tuffs and volcanic sediments of fluvial, alluvial and lacustrine origin. The latter sediments, that represent about 70% of this column, consist of turbidity deposits, volcanoclastic deposits with normal and/or inverse gradation, planar lamination and traction structures. This sequence also shows deposits of detritus flows and lahars related to the synchronous volcanic activity. On the basis of K/Ar age determinations, the basaltic lava flows from the base of this unit are Upper Oligocene (Karzulovic et al., 1979). A 39Ar/40Ar age obtained in plagioclase from a basal weldge tuff gave 27.4 Ma. (Fig. 1). On its eastern side, this Tertiary unit is intruded by the Rio Melado granodioritic stock, dated at 23 Ma by Drake et al. (1982). On its western side, this unit is overlain by ignimbrites, rhyolitic domes and basaltic lava-breccia flows of Miocene age (17 Ma). Dyke clusters and volcanic plugs of Miocene age are also found on the western part of the Andean precordillera. Beccar (1996) has described an intense alteration with zeolite minerals such as wairakite and laumontite. This suggests the existence of a high paleogeothermal gradient associated with paleogeothermal fields.

## GEOCHEMISTRY

Lava flows from the base of the Tertiary unit are mainly Cpx basalts, Cpx+Opx basaltic andesites and, in less proportion, Opx + Amph andesites. Basalts and basaltic andesites are prophyrytic with phenocrysts of plagioclase (An54-An60), augite-type clinopyroxene (En41Fs18Wo41) and orthopyroxene inmersed in a groundmass whose texture varies from intergranular to hyalophitic. Analyzed samples have a relatively low K content, being tholeiitic according to the Peccerillo and Taylor (1976) classification criteria. Their location in the AFM diagram also confirm their tholeiitic affinity. However, their MgO contents are low (3.8-4.2%), indicating that they are quite differentiated. Compared with most Southern Andes Quaternary volcanic rocks, Tertiary basalts from the Talca-Linares region exhibit low (La/Yb)n (1.5-2.2; Fig. 2) and (La/Sm)n ratios (0.97 to 1.42), and slightly positive Eu anomaly (probably due to plagioclase accumulation). Their (La/Yb)n and (La/Sm)n ratios are similar to those presented by island arc tholeiitic series (Pearce et al., 1995). Samples N° 9 and 12 are basalts with 45 and 47% $SiO_2$ respectively; samples 10 and 11 are basaltic andesite and andesite respectively.

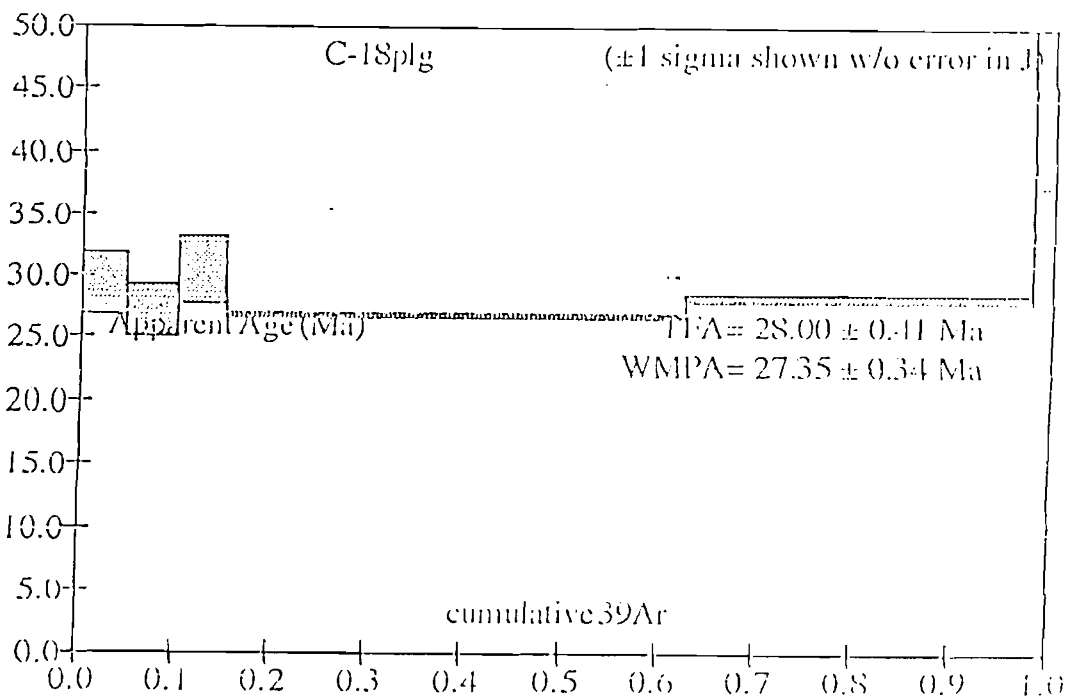


Fig. 1. Ar/Ar plateau age.

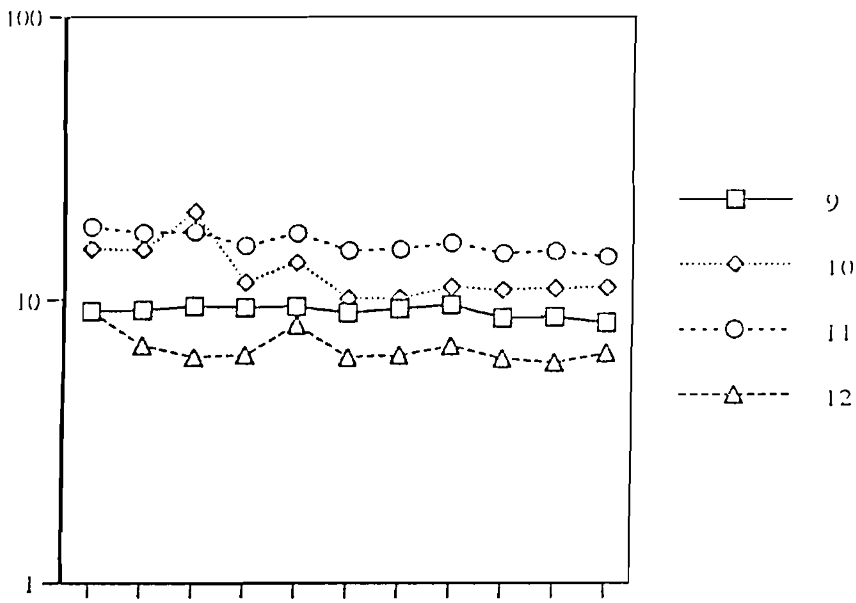


Fig. 2. Chondrite normalized REE abundances for Oligoce-Miocene lavas of the Talca-Linares precordillera.

## CONCLUSIONS

The Oligocene-Miocene volcanic rocks from the Andean precordillera of Talca-Linares are representative of a magmatism that is more tholeiitic than the magmatism that gave origin to Quaternary basalts from the Southern Andes. This magmatism was probably associated with a thin crust and a relatively high geothermal gradient (as suggested by the alteration mineralogy of these rocks). The Upper Oligocene-Miocene volcanic rocks from further north (latitudes 33-34°S) also present tholeiitic affinities and their Sr and Nd- isotope ratios (López-Escobar et al., 1991; Nyström et al., 1993; Stern and Skewes,1995) are more primitive than those exhibited by Quaternary basalts from the Southern Andes.

## ACKNOWLEDGEMENTS

This work was supported by the following grants; FONDECYT-CHILE N°195-0568 and DTI (Universidad de Chile) N° E28349655.

## REFERENCES

Beccar, I. 1996. Geología del área Colbún-Machicura, precordillera de Talca-Linares. Thesis, Universidad de Chile, Departamento de Geología. In prep.

Drake, R.; Vergara, M.; Munizaga, F.; Vicente, J.C. 1982. Geochronology of Mesozoic magmatism in central Chile, Lat. 31°-36°S. Earth-Science Reviews, Vol. 18, p. 353-363.

Karzulovic, J.; Hauser, A.; Vergara, M. 1979. Edades K/Ar en rocas volcánicas e intrusivas del área de los proyectos hidroeléctricos Colbún-Machicura, ENDESA. In Congreso Geológico Chileno, N° 2, Actas, Vol. 4, p. J127-J133.

López-Escobar, L.; Kempton, P.D.; Harmon, R.S.; Vergara, M. 1991. Isotopic character of Miocene lavas 33-35°S, central Chile. EOS, American Geophysical Union, Transactions, Vol. 72, N° 44, p.520.

Nyström, J.O.; Parada, M.A.; Vergara, M. 1993. Sr-Nd isotope composition of Cretaceous to Miocene volcanic rocks in central Chile: A trend toward a MORB signature and a reversal with time. In Symposium on Andean Geodynamics, N° 2, Extended Abstracts, p. 411-414. Oxford, England.

Pearce, J.A.; Baker, P.E.; Harvey, P.K.; Luff, I.W. 1995. Geochemical evidence for subduction fluxes, mantle melting and fractional crystallization beneath the South Sandwich island arc. Journal of Petrology, Vol. 36, N° 4, p. 1073-1109.

Peccerillo, A.; Taylor, S.R. 1976. Geochemistry of Eocene calc-alkaline volcanic rocks from Kastamonu area, northern Turkey. Contributions to Mineralogy and Petrology, Vol. 58, p. 63-81.

Stern, C.R.; Skewes, M.A. 1995. Miocene to present magmatic evolution at the northern end of the Adean Southern Volcanic Zone, Central Chile. Revista Geológica de Chile, Vol. 22, N° 2, p.261-272.

# DEEP CRUST AND MANTLE XENOLITHS, GRANATÍFERA TUFF, SW COLOMBIA - IMPLICATIONS FOR ANDEAN MAGMATISM

Marion B.I.Weber[1], John Tarney[1], Ray Kent[1] and Pamela D. Kempton[2]

[1] Department of Geology, University of Leicester, Leicester. LE2 1YB
[2] NERC Isotope Geoscience Laboratory, Keyworth, Nottingham NG12 5GG, UK

**Key Words:** melting, adakites, restites, subduction, underplating, oceanic plateau

## INTRODUCTION

The Andean cordillera represents a major zone of continental crustal growth, but the details of the mechanisms remain controversial. One concern is the balance between *lateral accretion* through subduction-accretion processes, which tectonically intermixes continental detritus with scraped-off anomalous ocean floor, and *vertical accretion* through emplacement of mantle- or subducting slab-derived granitoids, or through basaltic underplating. A critical point is the nature of the deep crust beneath the Andean margin, which is commonly invoked as a component source in granitoid magmas, but there is little firm information available as to its major or trace element or isotopic character. Whereas xenolith suites brought up in volcanic breccia pipes provide such information on the composition of the deep crust and upper mantle, these are mostly available from the interior of cratons, or in back-arc regions (e.g. Pali-Aike, Patagonia) with only a few examples from *active continental margins* (e.g. Itinome-gata, Japan; Calbuco, S. Chile; Kodiak Island, Alaska). The Granatífera tuff-breccia, located east of Mercaderes, SW Colombia, provides a rich assemblage of mantle and deep crustal nodules essentially from beneath an active volcanic arc, and so provides a valuable window into the deep crust and crustal accretion processes. Is it possible to evaluate the contribution to Andean crustal growth?

## PETROLOGY OF THE GRANATÍFERA XENOLITHS

The Granatífera tuff-breccia, located in SW Colombia (Figure 1), contains a rich assemblage of deep crust and mantle xenoliths. These include garnet peridotites, garnet pyroxene rocks, pyroxenites, garnet amphibolites and garnet granulites (cpx-gt-plg-qz). A proportion of the mantle xenoliths have deformation fabrics, the garnet peridotites in particular showing sheared mosaic porphyroclastic textures (Harte 1977), whereas the garnet pyroxenites show fine grained recrystallisation textures at grain boundaries. Thermobarometry on the deformed garnet peridotites provides estimates of pressures in the excess of 18 kb and temperatures over 860°C for the mantle rocks. Temperatures for the crustal rocks range from 890 to 1000°C for the garnet pyroxene rocks, 994 to 1048°C for the granulites, and 727 to 1036°C for the amphibolites, calculated at 10 kb. Pressures estimated for a garnet amphibolite are 12 to 13 kb. Other xenoliths (bombs) found in the Granatífera Tuff, are basaltic andesites and dacites, and amphibolitic pegmatites. Additionally there are low grade slates and schists representing upper crust compositions.

There is every reason to believe that this rich assemblage of rock types enclosed in an basltic andesitic to andesitic host (but with much comminuted crystalline debris) may be representative of the crust and

## TRACE ELEMENT AND ISOTOPE GEOCHEMISTRY

Compositionally there is a complete range of rock types from ultramafic, through mafic and intermediate to silicic but, as with many other xenolith suites, there is a high proportion of basic rocks. The crucial issue is the petrogenetic relationships between these rocks.

Many of the andesitic and pegmatitic rocks have moderately high $Al_2O_3$ (> 15wt%), high Sr, very low Rb/Sr ratios, low Y, high K/Rb and low Nb, giving prominent *negative* Nb anomalies and *positive* Sr anomalies, as shown in Figure 2. The trace element characteristics are found in adakitic volcanics, generally linked with zones of ridge subduction (see Drummond and Defant, 1990), but are also found in much greater volume in Precambrian tonalite-trondhjemite-granodiorite ("TTG") suites (Martin 1994; Tarney & Jones 1994). There is a consensus that such trace element characteristics result from partial melting of a mafic source with hornblende and/or garnet in the residual assemblage. The conditions are most easily attained through partial melting of young, hot, subducting lithosphere (during ridge subduction), though are not necessarily unique to that environment. Additionally the majority of these xenoliths have low $^{87}Sr/^{86}Sr$ ratios (0.7035–0.7053). The isotopic characteristics imply that the mafic material must have a relatively short crustal residence time and not have suffered significant ridge hydrothermal activity or permeation by subduction fluids.

An additional petrogenetic factor is that the region to the west of the Mercaderes-Río Mayo area comprises a thick pile of mafic rocks, believed to be part of an accreted Cretaceous (ca. 88 Ma) oceanic plateau (Kerr *et al.* 1996). Although the upper altered parts of the plateau have clearly been imbricated, scraped-off and obducted, the deeper parts of this plateau may have "subcreted" beneath the continental margin, and suffered diverse dehydration-melting events to produced the extensive volcanism present at the surface, as well as that at depth, leaving behind a restite of amphibolitic to granulitic composition. Experimental studies and modelling of the melting of basaltic amphibolites has shown that restites include garnet amphibolites and granulites (cpx-gt±plg±hbl) (Rushmer 1993; Peacock *et al.* 1994; Sen and Dunn 1994). The more mafic crustal xenoliths of the Granatífera Tuff could represent these restitic materials; so the potential exists within the xenolith suite to evaluate and demonstrate these relationships.

## REFERENCES


Drummond, M.S. and Defant, M.J. 1990. A model for trondhjemite-tonalite-dacite genesis and crustal growth via slab melting: Archean to modern comparisons. *Journal of Geophysical Research* **95**, 21,503-21,521.

Harte, B. 1977. Rock nomenclature with particular relation to deformation and recrystallization textures in olivine bearing xenoliths. *Journal of Geology* **85**, 279-288.

Kerr, A.C., Tarney, J., Marriner, G.F., Nivia, A., Klaver, G.T. and Saunders, A.D. 1996. The geochemistry and tectonic setting of late Cretaceous Caribbean and Colombian volcanism. *Journal of South American Earth Sciences* (in press)

Martin, H. 1993. The mechanisms of petrogenesis of the Archaean continental crust – comparison with modern processes. *Lithos* **30**, 373-388.

Peacock, S.M., Rushmer, T. and Thompson, A.B. 1994. Partial melting of subducting oceanic crust. *Earth and Planetary Science Letters* **121**, 227-244.

Rushmer, T. 1993. Experimental high-pressure granulites: Some applications to natural mafic xenolith suites and Archean granulite terranes. *Geology* **21**, 411-414.

Tarney, J. and Jones, C.E. 1994. Trace element geochemistry of orogenic igneous rocks and crustal growth models. *Journal of the Geological Society, London* **151**, 855-868.

Sen, C. and Dunn, T. 1994. Dehydration melting of a basaltic composition amphibolite at 1.5 and 2.0 GPa: implications for the origin of adakites. *Contributions to Mineralogy and Petrology* **117**, 394-409.

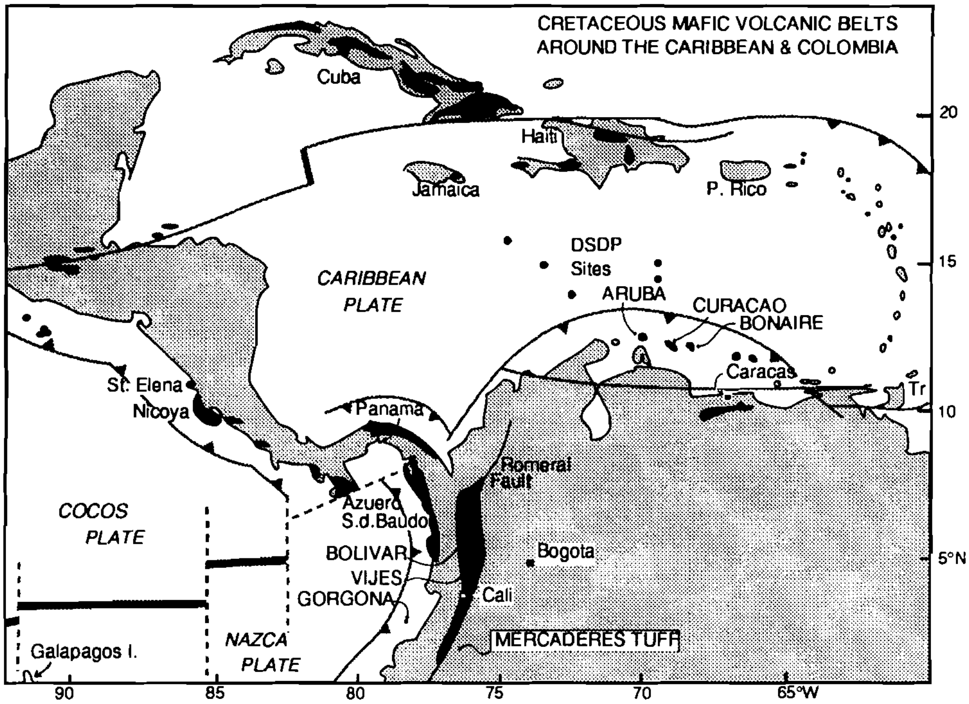


Fig. 1. Sketchmap showing location of Granatífera (Mercaderes) tuff, together with outcrops of accreted obducted mafic oceanic plateau sequences in Colombia and the Caribbean.

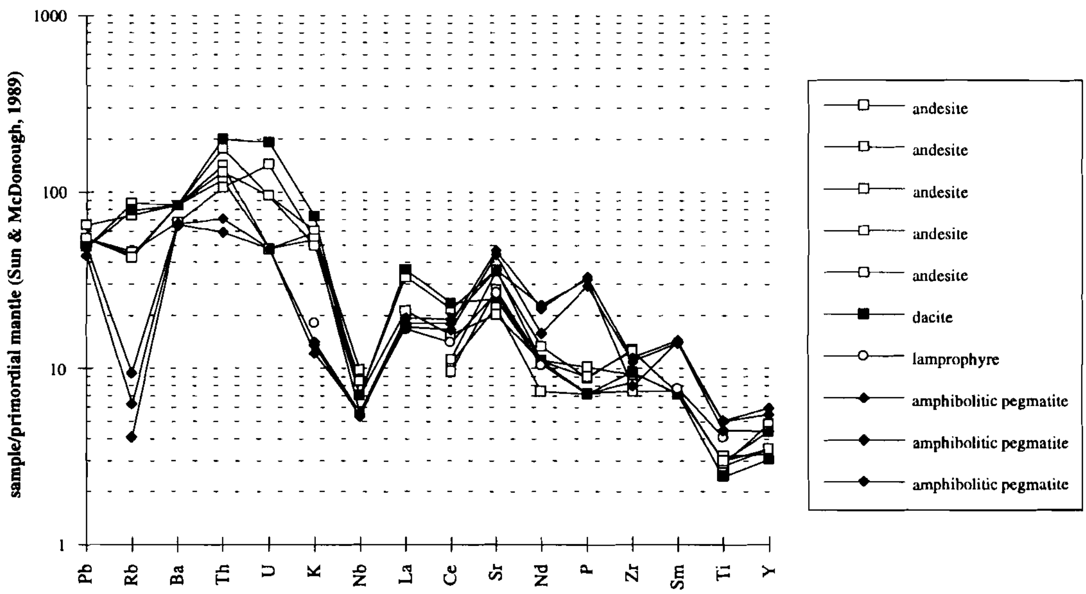


Fig. 2. Multi-element diagram (normalised to primordial mantle) of the volcanic and pegmatitic xenoliths from the Granatífera Tuff.

# THE GENESIS OF PRIMITIVE TONALITES ASSOCIATED WITH AN ACCRETING CRETACEOUS OCEANIC PLATEAU: THE ARUBA BATHOLITH AND THE ARUBA LAVA FORMATION

Rosalind V. WHITE [1], John TARNEY [1], Gerard Th. KLAVER [2], and Arminda V. RUIZ [3]

[1] Department of Geology, University of Leicester, Leicester, LE1 7RH, UK
[2] Rijks Geologische Dienst, Richard Holkade 10, 2000 AD Haarlem, The Netherlands
[3] Geoscience Section, Archaeological Museum, Oranjestad, Aruba, Netherlands Antilles

**KEY WORDS**: Aruba batholith, tonalite, oceanic plateau sequence, amphibolite melting, imbrication

## INTRODUCTION

Andean batholiths are usually dominated by tonalite, but the nature of the source components and the petrogenetic mechanisms in generating tonalite still need to be resolved. Lower crust, subducted mafic crust or magmatically underplated mafic crust are all possible sources; but each has thermal problems. Some tonalites however appear to be generated entirely within the oceanic environment and so the number of possible sources and the tectonic and thermal regimes under which tonalite may be generated are much reduced. Here we describe the occurrence, relationships and geochemistry of the tonalitic batholith on Aruba, Netherlands Antilles (Figure 1), which appears to have been generated as the thick mafic crust of an ocean plateau was being imbricated, obducted and underplated. The batholith has both the trace element and isotopic characteristics ($^{87}Sr/^{86}Sr_i$ = ~0.7036, Klaver, unpubl. data) that indicate a

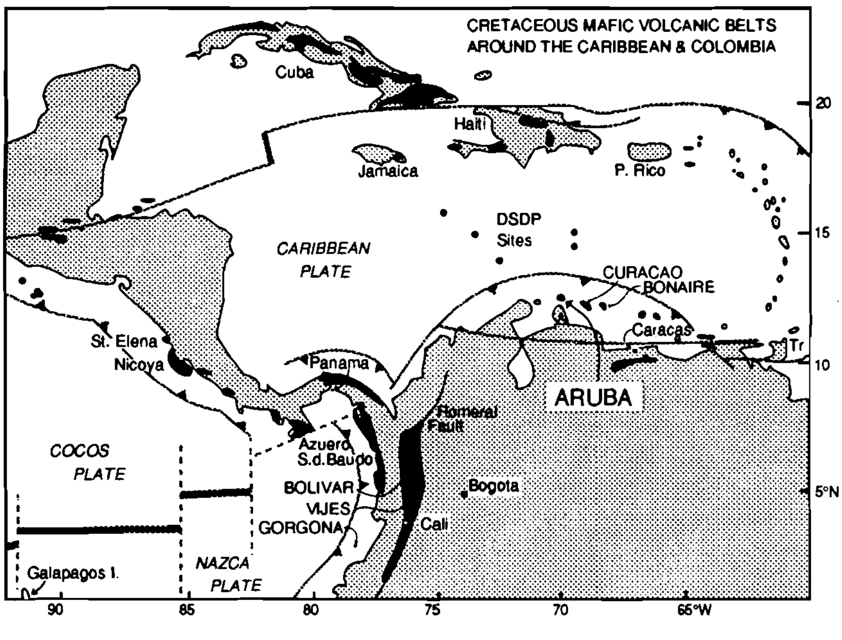


**Figure 1**: Location map showing the position of Aruba relative to other obducted fragmants of the oceanic plateau sequence of the Caribbean Plateau.

primitive source with short crustal residence time. The results are relevant to the generation of Precambrian tonalites (Martin, 1993).

## FIELD RELATIONSHIPS

The Cretaceous batholith that crops out on the island of Aruba comprises dominant tonalite with subordinate trondhjemite, diorite, gabbro and notably melanocratic magma type ("hooibergite") that forms small plugs within the batholith. The batholith is bordered by mafic rocks of the plateau sequence, the Aruba Lava Formation, that comprises pillow basalts, dolerite sills, tuffs and minor sediments, and has chemical affinities with the sequence of pillow basalts and picritic flows exposed on the adjacent island of Curaçao (Klaver, 1987). The Aruba Lavas may represent a stratigraphically higher member of the plateau sequence because of the greater proportion of tuffs exposed, indicating a shallower eruption depth, and the presence of calc-alkaline tuffs but few picrites. The Curaçao and Aruba Lava Formation basalts have a transitional (T-MORB) signature.

Important shear zones, up to 1 km wide, transect the Aruba Lava Formation, and are interpreted as zones where the plateau began to imbricate as it collided with the S. American continental margin subduction zone. Some are high-grade (amphibolite) and must have been exhumed. The plateau, being unusually thick (c. 15km from seismic evidence), and possibly still hot, and would have resisted subduction. One lower-grade shear zone has small tonalitic intrusions within it that have been boudinaged by subsequent shearing, thus dating the tonalite intrusion as syn-deformation. In the high-grade shear zone the amphibolite is net-veined by silicic melts. Examination of small-scale structures reveals that the amphibolite is in fact melting, but there is a considerable volumetric component of melt just "passing through" the amphibolite, with agmatitic textures requiring that this melt was at high magma pressure. These melts are dominantly trondhjemitic, but there are also tonalites and more dioritic rock types cutting the amphibolites that have no chilled margins, and were clearly emplaced into hot rock.

Complex cross-cutting relationships exist between the various rock types of the batholith, and again, chilled margins are very rare, suggesting that the timing between successive episodes of intrusion was not enough for the first magma type to completely cool. Up to five phases of intrusion can be identified in exposures of just $1m^2$, and the order of intrusion is not necessarily the same in different exposures, implying that intrusion of the different magma types occurred in a short time period.

The earliest and latest intrusive phases are the most mafic: gabbro being followed by the dominant tonalite/diorite intrusion, and finishing with the spectacular melanocratic hooibergites. The latter magma was clearly wet enough to crystallise abundant hornblende, but was also hot enough to trigger re-melting of the surrounding tonalites, and acid back-veining of the hooibergite in various rheological states is observed. The hooibergite may represent either melting of the amphibolitic residue remaining after tonalitic and trondhjemitic liquids had been extracted, or melts with a significant mantle component. In either case this requires a later thermal pulse. A late thermal pulse is also indicated by the numerous mafic dykes cross-cutting the batholith, but are chilled against it.

## GEOCHEMISTRY

The Aruba Lava Formation, like that on Curaçao, is dominated by mafic rocks that are less-depleted with respect to light REE and other incompatible elements than normal MORB (Kerr et al. 1996), perhaps a consequence of entrainment processes in the ascending plume head. Effectively, this leaves it a more fertile source for tonalite production than normal oceanic crust. The tonalites have many compositional similarities with modern adakites and with Precambrian tonalite-trondhjemite-granodiorite (TTG) suites: low Y, high Sr and Ba, low Rb and with high Sr/Y and K/Rb ratios, but with prominent negative Nb anomalies and small positive Sr and Ba anomalies on multi-element mantle-normalised spidergrams. These characteristics would be compatible with melt generation from a mafic source similar to that of the host amphibolites. The low initial Sr isotopic ratios (0.7036) and positive Nd would be compatible with this.

## THE ROLE OF HYDROUS FLUIDS

Water seems to have played an important role in promoting the development of shear zones (greenschist- to amphibolite-facies) within the relatively fresh Aruba Lava Formation, penetration of hydrous fluids being aided by the imbrication of the plateau. With dehydration-melting of amphibolite-facies assemblages, high field strength elements such as Nb and Ta may have been retained in residual titanite or rutile, and Y and the heavy REE in residual garnet or hornblende during tonalite generation. Further melting under higher temperature conditions during the later thermal pulse may have released water (i.e. anhydrous residues) leading to emplacement of the wet melanocratic magmas (hooibergites) that are characterised by extensive sub-solidus hornblende growth, and which promoted hydrous remelting of the tonalites to cause back-veining and production of hornblendic pegmatites.

## COMPARISON WITH ARCHAEAN and OTHER TONALITES

There are a number of interesting similarities with Archaean tonalites. The association of tonalites, trondhjemites and granodiorites, with abundant mafic enclaves, is very similar to that of Archaean TTG suites (the melanocratic hooibergite resembles more closely Scottish Caledonian appinites), The correspondence extends to the late stage emplacement of abundant mafic dykes. Greenstone belts have been likened to oceanic plateaus (Storey et al., 1991; Kusky and Kidd, 1992) because of the occurrence of spinifex komatiitic or picritic flows in obducted Cretaceous plateaus (cf. Gorgona: Kerr et al, 1996c). Precambrian greenstone belt mafic sequences are commonly associated with pene-contemporaneous voluminous tonalites (TTG), and hence it is possible these may have formed in exactly the same way as on Aruba.

## CONCLUSIONS

The association of a primitive tonalite suite with an accreting oceanic plateau implies that voluminous silicic crustal compositions can be generated during imbrication and thrust stacking of thick mafic volcanic sequences. There are implications for Archaean greenstone belts and for mechanisms of crust generation.

## REFERENCES

Kerr, A.C., Tarney, J., Marriner, G.F., Nivia, A., Klaver, G.T. and Saunders, A.D. 1996a. The geochemistry and tectonic setting of late Cretaceous Caribbean and Colombian volcanism. *Journal of South American Earth Sciences* (in press)

Kerr, A.C., Marriner, G.F., Arndt, N.T., Tarney, J., Nivia, A., Saunders, A.D., & Duncan, R.A. 1996b. The petrogenesis of Gorgona komatiites, picrites and basalts: new field, petrographic and geochemical constraints. *Lithos* **486**, (in press)

Kerr, A.C., Tarney, J., Marriner, G.F., Klaver, G.Th, Saunders, A.D. and Thirlwall, M.F. 1996c. The geochemistry and petrogenesis of the late-Cretaceous picrites and basalts of Curaçao, Netherlands Antilles: remnant of an oceanic plateau. *Contributions to Mineralogy and Petrology* (in press)

Klaver, G.Th., *The Curaçao lava formation an ophiolitic analogue of the anomalous thick layer 2B of the mid-Cretaceous oceanic plateaus in the western Pacific and central Caribbean*, Ph.D. Thesis, Univ. Amsterdam, 1987.

Kusky, T.M., and Kidd, W.S.F. 1992. Remnants of an Archean oceanic plateau, Belingwe greenstone belt, Zimbabwe, *Geology*, **43**, 43-46.

Martin, H. 1993. The mechanisms of petrogenesis of the Archaean continental crust – comparison with modern processes. *Lithos* **30**, 373-388.

Storey, M., Mahoney, J.J., Kroenke, L.W. and Saunders,, A.D. 1991. Are oceanic plateaus sites of komatiite formation? *Geology*, **19**, 376-379.

# HYDROTHERMALISME / MINERALISATIONS
# HYDROTHERMALISM / MINERALIZATIONS
# HIDROTERMALISMO / MINERALISACIONES

# SPACE-TIME EVOLUTION OF THE HYDROTHERMAL ACTIVITY IN A VOLCANIC DOME : THE CERRO BONETE EPITHERMAL TYPE MINERALIZATIONS (BOLIVIA)

Laurent BAILLY[1], Jacques L. LEROY[1]

(1) Univ. Henri Poincaré-Nancy 1, LESH, BP 239, F-54506 Vandoeuvre cedex

**KEY WORDS** : andean volcanism, fluid-rock interactions, fluid circulation, T-space-time evolution

In a volcanic system, part of the activity corresponds to the circulation of hot fluids, which are responsible for the alteration of the percolated rocks and the transfert of chemical elements (metals or not). Thanks to accurate studies of the minerals developped during these fluid-rocks interactions (mineral composition, geothermometers, related fluid inclusions), it is possible to define the characteristics and the space-time evolution of this hydrothermal activity in a cooling volcanic dome.

The Cerro Bonete massif in Bolivia (near the Argentinian border) (fig.1) belongs to the Early Cenozoic magmatic belt, which extends all along the Bolivian orocline. In the area, the oldest volcanic formation is the Rondal formation, which corresponds to high-K, meta-aluminous andesites and andesi-basalts After erosion, they are followed by the intermediate to acid volcanics of the Quehua formation. It consists of voluminous (up to 700 m) pyroclastics flows cut and overlain by coalescent lava domes, flow breccias and lava flows. They are high-K, peraluminous rhyodacites (Fornari et al, 1993 ; Bailly, 1994). These domes host several mines and prospects known as the "Bolivian polymetallic veins", mined out for some of them during the spanish times (Sugaki et al, 1986 ; Richter et al, 1992). Two of them were studied (Bailly, 1994). Bolivar mine (Ag, Bi, Pb, Zn, Cu) consists of a subvertical E-W vein emplaced in an extrusive dacitic volcanic dome, whereas Lipeña mine (Sb) was mined in the Rondal lavas.

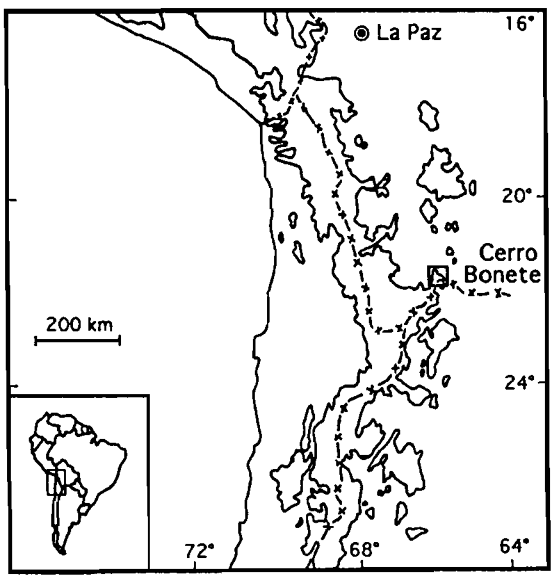


fig.1 - Location of the Cerro Bonete area on eastern border of the cenozoic volcanic belt

In Lipeña mine, the mineralization (pyrite, marcasite, stibnite, realgar, orpiment) precipitation in the vein is related to the replacement, in the wall-rocks, of the primary igneous assemblage (olivines, pyroxenes, plagioclases) by montmorillonites (± marcasite, pyrite) and farther from the vein by mixed-layered minerals (± jarosite). These mineralogical transformations are geochemically characterized by a strong leaching of Ca, Mg, Mn, Na, trace and rare earth elements.

In Bolivar mine, in getting farther away from the vein, the dominant illite - subordinate chlorite (chamosite) association is replaced by a dominant chlorite (brunsvigite)-subordinate illite one. In the same way, a decrease of the $X_{Fe}$ ratio for both illite and chlorite (fig.2) and an increase of the phengitic substitution rate of the illites occur.

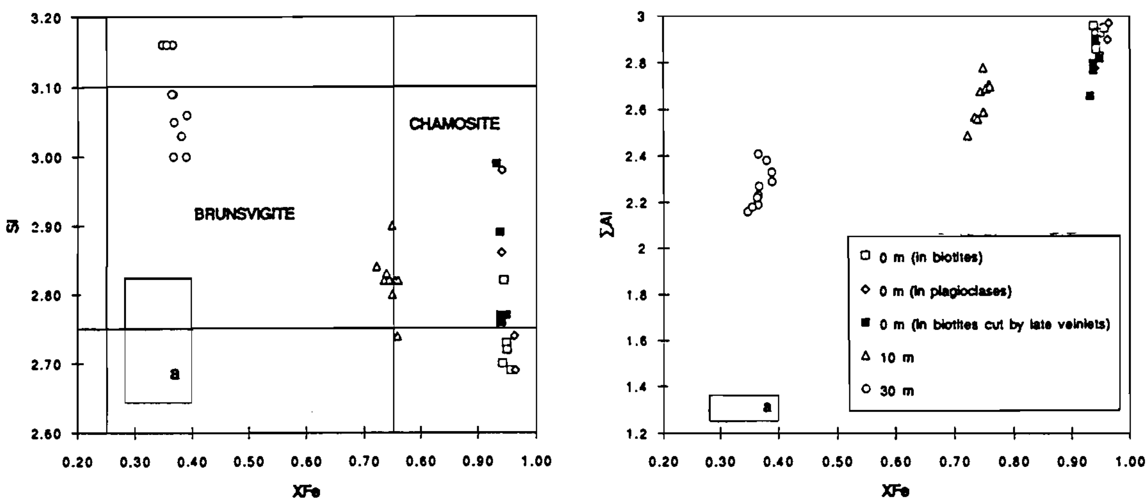


fig.2 - $\Sigma$Al and Si vs XFe diagrams for the chlorites developped in the wall-rocks according to their distance to the vein. The box (a) corresponds to the composition of the unaltered biotites in the reference sample.

During the alteration, Na and Ca are strongly leached, whereas large amounts of Fe and K are added. In the vein, the chlorites are the only alteration minerals observed in close association with each stage of mineralization deposition. Even if they are all chamosites, significant chemical variations occur between the different generations. Both chlorites and illites are used in order to estimate the water/rock ratios during fluid circulation and the fluid temperatures in the vein and the wall-rocks. Combined with fluid inclusion studies, they lead to a multi-staged, space-time evolution of the hydrothermal activity during the volcanic dome cooling (fig.3).

Stage 1 is initiated by the raising, towards shallow levels, of deep, hot (around 350°C), moderately salted (4.9 to 16.8 wt % eq. NaCl) and reduced hydrothermal fluids. The arsenopyrite-pyrite assemblage precipitates in fractures created in the dome by the fluid pressure. Simultaneously a pervasive chloritization of the biotites is observed up to at least 30 m from the vein. At 30 m, the water/rock ratio is low, the chlorite composition is controlled by the composition of the former minerals and there is a thermic equilibrium between the fluids and the cooling dome around 260 °C. After this first pulsation, the illites crystallization occurs in the previously fractured dome, in response to mixing of colder and less salted fluids, probably of meteoritic origin, with the previous ones.

Stage 2 corresponds to a second pulsation of hot (250-190°C) fluids. They are associated to the polymetallic mineralization (Bi-Ag-Pb-Zn-Cu).The percolated volume is smaller due to an increasing fluid channelization in a colder dome (around 190°C ?)

The last stage (stage 3, sulfides-carbonates) corresponds to a third pulsation of more hot (230-290°C) and Ca-enriched fluids. This stage is only observed within the vein. A possible continuity of the hydrothermal activity between stages 2 and 3 seems to be argued by the progressive increase of the fluid salinities and temperatures.

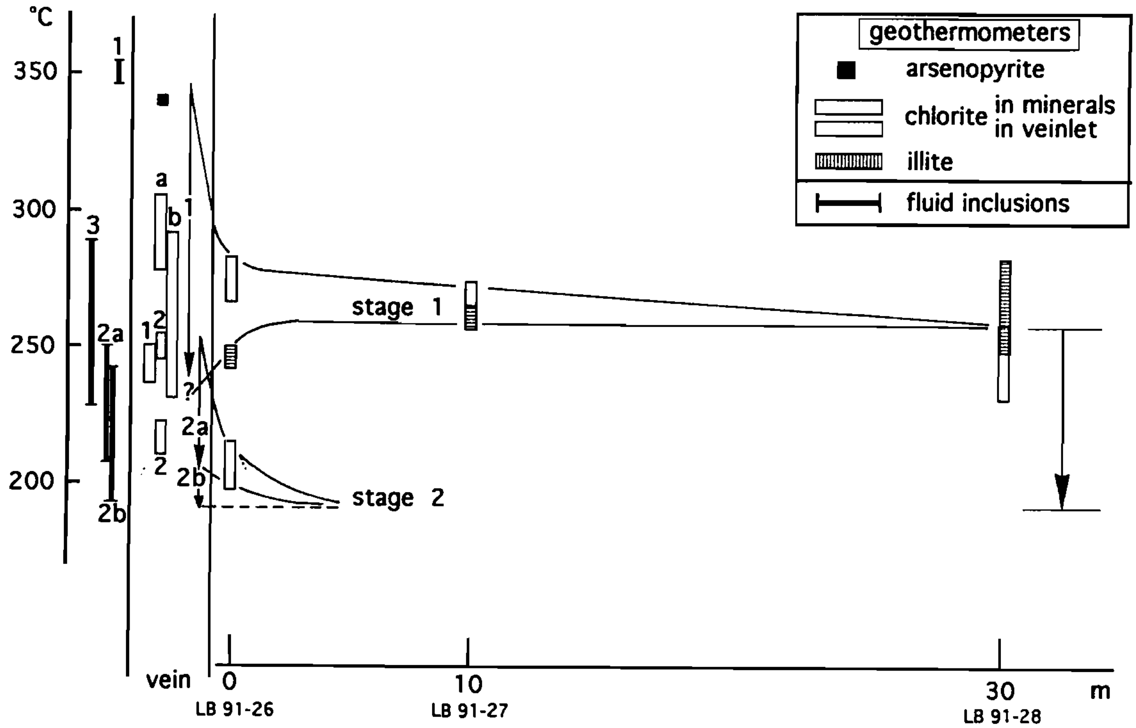


fig.3 - Space-time evolution of the fluid temperature and of the percolated volume in the Bolivar dome during its cooling.

Such a space-time fluid evolution with several pulsations of hot volcanic fluids and mixing with dilute meteoritic fluids, is often described for the epithermal-type ore deposits related with volcanic activity (Hedenquist et al, 1992 ; Hedenquist and Lowenstern, 1994 ; Marcoux, 1995).

## REFERENCES

Bailly L. 1994. Le secteur minéralisé du Cerro Bonete (sud-ouest Bolivie) : Etude du magmatisme, des minéralisations et des altérations associées. Essai de localisation de la source des métaux. *Thèse Univ. Henri Poincaré-Nancy 1*, 301 p.

Fornari M., Pozzo L., Soler P., Bailly L., Leroy J. and Bonhomme M. 1993. Miocene volcanic centres in the southern Altiplano of Bolivia, the Cerro Morokho and Cerro Bonete area (Sur Lipez). *ISAG 93, ORSTOM Edit.*, 363-366.

Hedenquist J.W. and Lowenstern J.B. 1994. The role of magmas in the formation of hydrothermal ore deposits.. *Nature*, 370, 519-527.

Hedenquist J.W., Reyes A.G., Simmons S.F. and Taguchi S. 1992. The thermal and geochemical structure of geothermal and epithermal systems : a framework for interpreting fluid inclusion data. *Eur. J. Mineral.* , 4, 989-1015.

Marcoux E. 1995. Gold and volcanoes : epithermal gold deposit, a review. *C.R.Acad.Sci. Paris*, 321, IIa, 723-735.

Richter D.H. et al. 1992. Cerro Bonete area. *in* "Geology and mineral resources of the Altiplano and Cordillera Occidental, Bolivia". *U.S.G.S.*, 1975, 166-174.

# A STRUCTURAL MODEL FOR THE DEVELOPMENT OF FE-CU MINERALISATION WITHIN THE ATACAMA FAULT SYSTEM, (25°00' S - 27°15' S), NORTHERN CHILE.

Christopher G. BONSON, John GROCOTT & Andrew H. RANKIN

School of Geological Sciences, Kingston University, Kingston-upon-Thames, Surrey KT1 2EE. U.K.

KEY WORDS: fault systems, Fe-Cu mineralisation, northern Chile

## INTRODUCTION

The Coastal Cordillera of the Central Andes, northern Chile hosts extensive hydrothermal base- and precious-metal mineralisation of late Mesozoic - early Cenozoic age. Detailed field, petrologic and structural investigation of selected mineral deposits within the Atacama fault system has enabled a structural model for the mineralisation to be constructed and has allowed two styles of hydrothermal Fe mineralisation to be assigned to different phases of tectonism within the Andean margin.

## ATACAMA FAULT ZONE

The Atacama fault zone, a 1000 km long, trench-linked, predominantly left-lateral, strike-slip fault zone (Brown *et al.*, 1993) is the dominant structural feature of the Coastal Cu-Fe belt. The fault zone is comprised of NNE-SSW trending fractures formed during late Jurassic to early Cretaceous times, as a response to south-easterly directed, oblique subduction of the Aluk plate. Initial ductile shearing, associated with the emplacement of the main lower Cretaceous batholith, *circa* 130-125 Ma (Dallmeyer *et al.*, 1996), was followed by arc abandonment and cooling. This lead to the development of a brittle fault system which acted as a conduit for circulating hydrothermal fluids.

## MAGNETITE-DOMINATED MINERALISATION

The NNE oriented fractures, which comprise the Atacama fault zone, host numerous occurrences of magnetite-dominated mineralisation, collectively referred to as the Cretaceous (Atacama-Coquimbo) Iron Belt. Magnetite-dominated deposits, pertaining to two styles of magnetite mineralisation, were studied in the Coastal Cordillera of the Lower Cretaceous batholith.

Kiruna-type, *magnetite-apatite* mineralisation was studied at Mina Fresia and Mina Carmen (Fig. 1). These mineral deposits comprise lenticular bodies with a principal mineralogy of magnetite (>60%), and variable amounts of haematite, apatite, actinolite and scapolite. Quench textures, fine vein networks and large volumes of propylitised wall-rocks, suggest that the magnetite fluid had a low viscosity which is attributed to an abundance of volatiles. It is thought that these mineral deposits formed during the pegmatitic stage of crystallisation.

Two examples of magnetite-actinolite-chalcopyrite mineralisation were studied at Mina Las Adrianitas and Mina Cerro Negro Norte, to the south of the field area (Fig. 1). These deposits comprise andesitic composition volcanics (Bandurrias Formation) replaced by magnetite, and are irregular in form. The replacement magnetite is cut by quartz veins and fracture controlled actinolite, and is sometimes found in microbreccias. In addition, disseminated pyrite and chalcopyrite occurs throughout the mineral

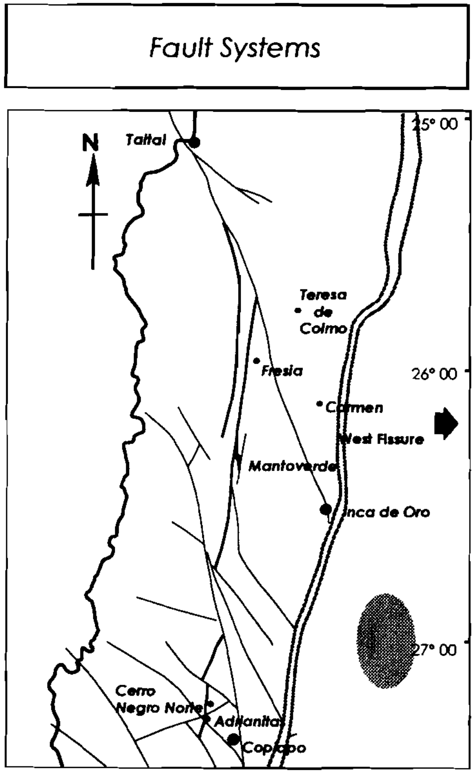


- Atacama Fault Zone
- Atacama Fault System NW Faults
- Central Valley Fault Zone
- Approximate location of extensional tectonics (Mpodozis & Allmendinger, 1993), Sierra de Fraga.

Fig. 1 Simplified map illustrating the different generations of fractures that comprise the Atacama fault system.

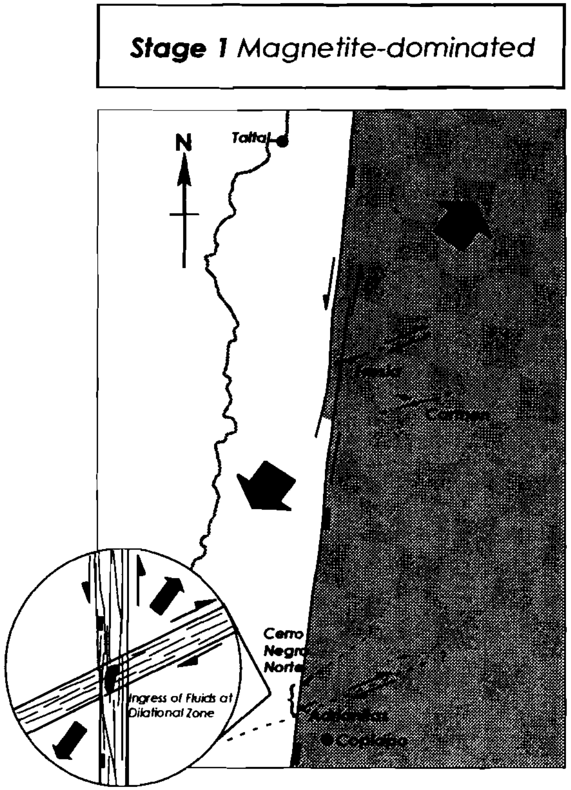


- Trace of the Atacama Fault Zone
- Transfer faults (transtensional)
- Intra- and back-arc volcanic basin

Fig. 2 Tectonic setting of magnetite-dominated mineralisation in the Lower Cretaceous. AFZ fault comprises the western margin to the back- or intra-arc basins, with the ENE trending fracture zones representing transfer zones in the faulted margin.

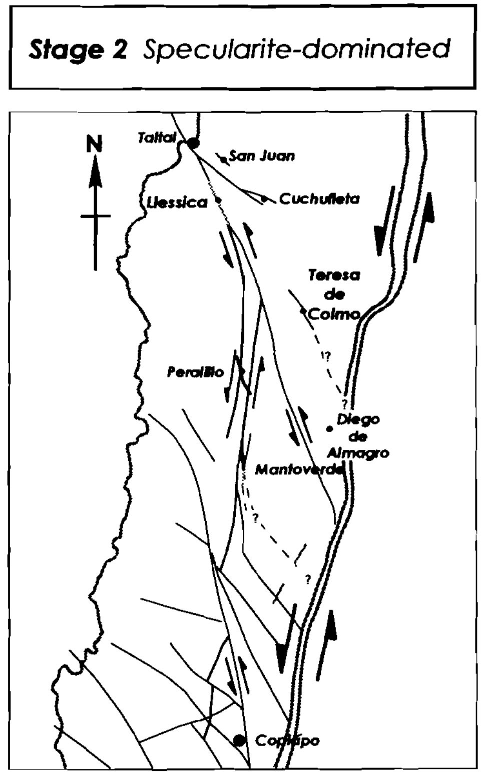


- Trace of the Atacama Fault Zone
- Reactivated and mineralised AFZ trace
- Trace of Atacama Fault System Faults
- Speculated Trace of AFS Faults
- Trace of the Central Valley Fault Zone
- Approximate trace of Ince de Oro Fault Zone

Fig. 3 Tectonic setting of specularite-dominated mineralisation in the Mid-Upper(?) Cretaceous. Mineralisation occurs in dilational fault structure (jogs or bends) along NW AFS faults or along reactivated segments of the AFZ.

deposits, as well as minor apatite. By analogy with the Punta del Cobre Cu(Fe) deposit (Marschik & Fontboté, 1995), these deposits probably represent examples of hydrothermal mineralisation associated with deep seated plutons, with temperatures of formation around 400°-500° C.

The Atacama fault zone may have acted as the western bounding fault of the Neocomian intra- and back-arc basins (Thiele & Pincheira, 1987). The stress regime in the back-arc was probably similar to the transtensional environment in which many lower Cretaceous arc-plutons are emplaced (Grocott *et al.*, 1994). The mineralisation at magnetite-dominated mines generally has a N-S (010-020°) orientation, related to the Atacama fault zone, and/or a ENE-WSW orientation related to a set of transfer faults in the Atacama fault zone which seem to have been important ENE-WSW lineaments during the arc/ back-arc development. (Fig. 2). The location of magnetite-dominated deposits at the intersection of the two fault sets suggests that these zones were important in the focusing of crustal fluids. The shear sense of the transfer structures would be right-lateral under a sinistral transtensional regime (Fig. 2), explaining the common observation of ENE-NE oriented faults offsetting the Atacama fault zone along its length. Mina Fresia lies very close to one such right-lateral zone. It is inferred that magnetite-rich fluids (and their source magmas ?) utilised the N-S Atacama fault zone fractures and the ENE oriented fracture zones (displacement transfer structures ?) as conduits, and that transtensional displacements created dilational zones within the areas of fracture intersection, where the mineralising fluids were focused (Fig. 2).

Published ages of the magnetite-dominated mineral deposits, close to the Atacama fault zone, range in age from 128 Ma at Boqueron Chañar (Oyarzún, 1990), south of the field area, to *c.* 102 Ma at Cerro Imán, Copiapó (Zentilli, 1974).

## ATACAMA FAULT SYSTEM

The Andean margin has been affected by extensional tectonics until *c.* 80 Ma (see Mpodozis & Allmendinger, 1993; Arévalo & Grocott, this conference), after which it is thought that the margin became dominated by transpression. Post *c.* 80 Ma, magmatic and structural activity stepped towards the east, with the formation of the recently recognised Central Valley Fault Zone (Taylor *et al., in review*), thought to be a terrane boundary between the Coastal Cordillera and Precordillera (Fig. 1). As a result of displacements along the Central Valley fault zone, large NW-trending sinistral shears propagated through the forearc, cutting and displacing the Atacama fault zone (Fig. 1) and the lower Cretaceous batholith. These faults are referred to collectively as the Atacama fault system. Sinistral displacements along the NW Atacama fault system shears caused clockwise block rotations with *circa* 35° of rotation (Randall *et al., in press*).

## SPECULARITE-DOMINATED MINERALISATION

Numerous small-medium sized specularite-dominated mineral deposits occur throughout the Coastal Cordillera. The mineralisation typically takes the form of hydrothermal breccias, cemented with a matrix of specularite, or as fault-hosted specularite veins. Specularite is the principal mineral within the breccia matrixes and veins. In addition, Cu sulphides (and supergene Cu minerals) are found distributed throughout, as well as minor magnetite.

Specularite-chalcopyrite mineralisation frequently occurs in hydrothermal implosion breccias at dilational jogs along NW trending, sinistral strike-slip faults, inboard (towards the E) of the Atacama fault zone, e.g. Teresa de Colmo (Fig. 3). The NW trending host faults belong to the Atacama fault system and are probably associated with the accommodation of crustal scale fault block rotation, and therefore fault block shape change. However, this style of mineralisation is also found along the N-S trending Atacama fault zone. It is inferred that mineralising hydrothermal fluids (and their sub-volcanic sources ?) utilised re-activated segments of the Atacama fault zone as transport pathways and were focused into fault-hosted dilational structures. For example, the Mantoverde deposit comprises a hydrothermal breccia located along a dilational bend of a Mantoverde fault, which transfers displacement between two reactivated segments of the Atacama fault zone (Fig. 3). The extent of Atacama fault zone reactivation is unclear, but was geometrically necessary to accommodate the shape change during crustal scale block rotation.

Dates for the age of mineralisation are, at present, constrained by structural arguments alone. An upper age for the specularite mineralisation during the AFS development is *tentatively* thought to be 80

Ma. This argument is based on the premise that displacements on low-angle extensional fault systems in the Sierra de Fraga (Mpodozis & Allmendinger, 1993)(Fig. 1) are incompatible with sub-vertical sinistral strike slip displacements in the Atacama fault system. Therefore, the AFS is thought to post-date the phase of mid-Cretaceous extensional tectonics.

## CONCLUSIONS

1. Magnetite dominated mineralisation appears to be strongly linked to the Atacama fault zone and an ENE trending fault set, which are likely to have been important in the development of the volcanic intra- and back-arc basins, during the lower Cretaceous.

2. Specularite-chalcopyrite mineralisation took place during the development of the Atacama fault system during the Upper Cretaceous. Mineralising fluids were focused into dilational fault structures associated with NW trending shears of the Atacama fault system and along reactivated segments of the Atacama fault zone.

## REFERENCES

Arévalo C. & Grocott J. this conference. Jurassic to Lower Eocene extensional tectonics in the arc and back-arc of the Atacama Region, Chile.

Dallmeyer R.D., Brown M., Grocott J., Taylor G.K. & Treloar P.T. 1996. Mesozoic magmatic and tectonic events within the Andean Plate Boundary Zone, 26°-27° 30' S, North Chile: Constraints from $^{40}Ar/^{39}Ar$ mineral ages. *Journal of Geology*, 104, 19-40.

Grocott J., Brown M., Dallmeyer R.D., Taylor G.K. & Treloar P.J. 1994. Mechanisms of continental growth in extensional arcs: an example from the Andean plate boundary zone. *Geology*, 22, 391-394.

Marschik R. & Fontboté L. 1995. Superimposed alteration and volcanic-hosted Cu(-Fe) mineralization in the Punta del Cobre Belt, northern Chile: A new type of intrusion related deposit ? In: Kribek & Zak (Eds), *Mineral Deposits*, Pasava, Balkema, Rotterdam, 477-481.

Oyarzún J.M. 1990. The Metalliferous Ore Deposits of Chile and Argentina, and their Geologic Framework. In: Fontboté L., Amstutz G.C., Cardozo M., Cedillo E. & Frutos J. (Eds) *Stratabound Ore Deposits in the Andes*, Springer-Verlag, 61-78.

Randall, D. & Taylor, G.K. in press. Major crustal rotations in the Andes: Paleomagnetic results from the Coastal Cordillera of northern Chile. *Journal of Geophysical Research.*

Taylor G.K., Grocott J., Randall D. & Pope A. in review. Mesozoic fault systems, deformation and fault block rotation in the Andean forearc 25°-27° S: A crustal scale strike-slip duplex in the Coastal Cordillera of Northern Chile. *Earth and Planetary Science Letters.*

Thiele R. & Pincheira M. 1987. Tectónica transpresiva y moviemento de desgarre en el segmento sur de la zona de Falla Atacama, Chile. *Revista Geológica de Chile*, 31, 77-94.

Zentilli M. 1974, Geological evolution and metallogenic relationships in the Andes of northern Chile between 26° and 27° south (Ph.D. thesis): Ontario, Canada, Queens University, 446 p.

# EVIDENCES OF COMPRESSIVE STRUCTURES IN THE MUZO AND COSCUEZ EMERALD DEPOSITS, EASTERN CORDILLERA OF COLOMBIA

Yannick BRANQUET [(1)], Bernard LAUMONIER [(2)], Benoît LOPES [(3)], Alain CHEILLETZ [(4,1)], Gaston GIULIANI [(5,1)] and Felix RUEDA [(6)]

(1) CRPG-CNRS, BP 20, 54520 Vandœuvre-lès-Nancy, France
(2) EMN-INPL, 54042 Nancy cedex, France
(3) BRGM, PO BOX 1492, JEDDAH, 21431KSA, Arabia Seoudita
(4) ENSG-INPL, BP 452, 54001 Vandœuvre-lès-Nancy, France
(5) ORSTOM, 213 rue La Fayette, 75480 Paris cedex 10, France
(6) MINERALCO S.A., calle 32, No 13-07, Santafe de Bogotá, Colombia

**KEY WORDS**: emerald deposit, Colombia, thrusts, duplex, hydrothermalism, Eocene-Oligocene boundary

## INTRODUCTION

This paper presents the results of structural studies (Branquet, 1995; Lopés, 1995) realized on two major emerald deposits of Colombia located in the western border of the Eastern Cordillera (EC) (Fig. 1). These studies have been motivated by the recognition of the sedimentary-hydrothermal origin and the syn-tectonic nature of the mineralization in the eastern border of the EC (mining district of Chivor) (Giuliani et al., 1992; Giuliani et al., 1995; Cheilletz and Giuliani, 1996). A new tectonic model emerges from this study.

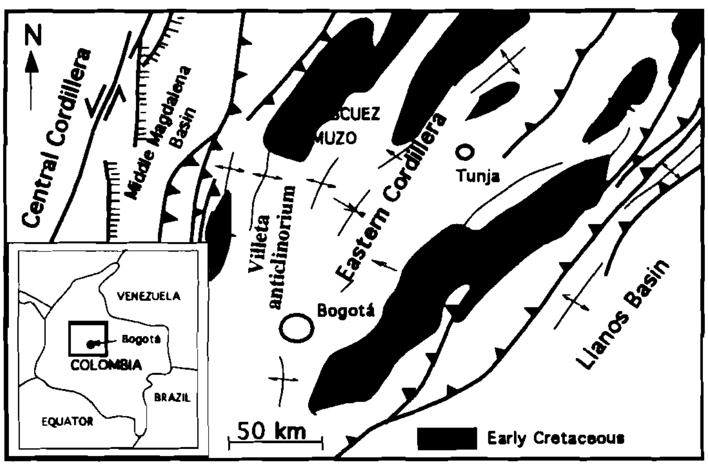


**Figure 1**. Location of the Muzo and Coscuez emerald deposits in the Villeta anticlinorium in the EC (Schamel, 1991, modified).

## GEOLOGICAL SETTING

Between subduction-related Western and Central cordilleras and the Llanos foreland, the EC is supposed to have originated in the inversion since Upper Miocene (except for Middle Eocene folds, Cooper et al., 1995) of a Triassic-Paleogene basin, with development of thrusts, ramp folds and reverse faults verging eastwards over the Llanos foreland but also westwards over the middle Madgalena basin (Colleta et al., 1990; Dengo and Covey, 1993; Roeder and Chamberlain, 1995). In the west of the EC, emerald deposits are hosted within the lower part of Early Cretaceous series, which cores kilometric scale anticlines forming the Villeta anticlinorium (Fig. 1). The formations outcropping in the deposits are, from bottom to top: (i) dolomitic limestones (at Coscuez only); (ii) carbonated black shales (CBS), hosting the emerald mineralization; (iii) siliceous black shales (SBS); (iv) argilites.

## THE COSCUEZ DEPOSIT

A N35°E trending fault (Coscuez fault) separates a western domain characterized by thrusts (or reverse faults) and ESE-ward vergent N25°E folds, from an eastern one (including the mine) presenting a main thrust (Coscuez thrust) superposing SBS and CBS units. The eastern domain shows E-W, northward vergent, horizontal folds and thrusts with white hydrothermal tectonic breccias (HTB) cemented by carbonates and pyrite, younger N-S folds and N30°E cleavage. The Coscuez thrust is outlined by a HTB and cuts the E-W folds. In the Coscuez mine, thrusts are proved by greatly truncated strata and the presence of an HTB. Two deformational events are recognizable: (i) a NNE-ward vergent D1, especially in the eastern domain (firstly E-W folds and lastly Coscuez thrust); (ii) a ESE-ward vergent D2 presenting N25°E folds, especially in the western domain. The Coscuez fault, outlined by a HTB, acted firstly as a tear senestral fault during D1 and then as the reverse fault during D2, when the western domain moved moderatly onto the eastern one.

## THE MUZO DEPOSIT

The Muzo deposit is exploited in two mines: the Quipama mine on the southside of the N135°E trending Itoco fault and the Tequendama mine on the other side. The Muzo deposit is mainly characterized by thrusting which is demonstrated by CBS over SBS superposition, HTB, and truncated strata.

The Quipama mine have a complex structure in which the 3D geometry of the tectonic units limited by thrusts, can be precisely described. According to this geometry, using folds as kinematic indicators and establishing a chronology based on the folding of thrusts, two deformational events can be identified: (i) D1, characterized by N130°E folding and thrusting which presents a N30°E transport axis (vergency undeterminated); (ii) D2, characterized by ESE-ward folding and thrusting.

At Tequendama, the same D1 and D2 structures occurred, but a D3 event has deeply reworked them. The D3 event is marked by the development of a red HTB (cement of ankerite). D3 is also characterized by an hectometric scale NW-ward vergent fold and a reverse fault. Relatively to D2, D3 was a backthrusting and backfolding event linked to the Itoco fault which was clearly a senestral tear-fault. During these three phases, first thrusts can be folded by a later phase, they can also be reactivated with a different transport axis.

## DISCUSSION AND CONCLUSION

If a duplex is defined by an array of thrust horses bounded by a floor thrust at the base and by a roof thrust at the top (McClay, 1992), the emerald deposits are two -or (at Tequendama) three-phase duplexes which have induced structural highs determinated by NNE-SSW and NW-SE lineaments, hence the limited extend of the CBS and emerald mineralization, except northwards at Tequendama; hidden structures probably exist that seem worth being prospected. The three deformational events were associated with an hydrothermalism (responsible for emerald precipitation) which generated under-compacted levels and enhanced high rate deformation (thrusts) besides the low rate one which produced folds and cleavages.

The age of the tectonic phase is the same as the radiometric age of the hydrothermalism: Cheilletz et al. (1994) determined for the Coscuez and Muzo deposits an Upper Eocene-Lower Oligocene age, respectively 38 Ma and 32 Ma. Motion is parallel to the trend of the EC (NNE-SSW) during D1. During D2 and D3 the motion is orthogonal to the EC global trend, the change of transport direction between D1 and D2-D3 is not explained yet, as is the age itself which is older than the supposed age of the chain formation (Middle-Upper Miocene). These results should be accounted for in any reappraisal of EC genesis.

## REFRENCES

Branquet Y. 1995. Etude structurale de la mine d'émeraude de Coscuez, Cordillère Orientale, Colombie. *Mem. D.E.A non publié, INPL et CRPG, Nancy*, 80 p.

Cheilletz A., Féraud G., Giuliani G. and Rodriguez C.T. 1994. Time-pressure-temperature constraints on the formation of Colombian emeralds: a laser-probe and fluid inclusion study. *Econ. Geol.*, 89, 361-380.

Cheilletz A. and Giuliani G. 1996. The genesis of Colombian emeralds: a restatement. *Mineralium Deposita*, in press.

Colleta B., Hebrard F., Letouzey J., Werner P. and Rudkiewicz J. L. 1990. Tectonic style and crustal structure of the Eastern Cordillera (Colombia) from a balanced cross-section, *in Letouzey J. ed., Petroleum and tectonics in Mobile Belts*, Paris, Technips, 81-100.

Cooper M. A., Addison F. T., Alvarez R., Coral M., Graham R. H., Hayward A., B., Howe S., Martinez J., Naar J., Pulham A., J. and Taborda A. 1995. Basin Development and Tectonic History of the Llanos Basin, Eastern Cordillera, and Middle Magdalena Valley, Colombia. *AAPG. Bull.*, 79, 10, 1424-1443.

Dengo C.A. and Covey M.C. 1993. Structure of the Eastern Cordillera of Colombia: Implications for Trap Styles and Regional Tectonics. *AAPG. Bull.*, v.77, No. 8, 1315-1337.

Giuliani G., Sheppard S. M. F., Cheilletz A. and Rodriguez C. T. 1992. Contribution de l'étude des phases fluides et de la géochimie isotopique $^{18}O/^{16}O$, $^{13}C/^{12}C$ à la genèse des gisements d'émeraude de la Cordillère Orientale de la Colombie. *C. R. Acad. Sci. Paris*, 314, II, 269-274.

Giuliani G., Cheilletz A., Arboleda C., Carillo V., Rueda F. and Baker J. 1995. An evaporitic origin of the parent brines of Colombian emeralds: fluid inclusion and sulfur isotope evidence. *Eur. Journal of Mineralogy*, 7, 151-165.

Lopés B. 1995. Etude structurale des mines d'émeraude de Muzo, Cordillère Orientale de Colombie. *Mem. D.E.A non publié, INPL et CRPG, Nancy*, 80 p.

McClay K. R. 1992. Glossary of thrust tectonics terms. *In McClay K. R., ed., Thrust tectonics, Chapman & Hall*, 419-433.

Roeder D. and Chamberlain R. L. 1995. Eastern Cordillera of Colombia: Jurassic-Neogene evolution. *AAPG mem.*, 62, 633-645.

Schamel S. 1991. Middle and Upper Magdalena basins. *In Biddle K. T. ed., Active margin basins, AAPG mem.*, 52, 283-303.

# MINERALOGY AND GEOCHEMISTRY OF THE SALAR GRANDE SALT ROCK (I Región de Tarapacá, Chile). GENETIC IMPLICATIONS

Javier GARCIA-VEIGAS[(1)], Guillermo CHONG[(2)] and Juan José PUEYO[(3)]

[(1)] Serveis Científico-Tècnics. Universitat de Barcelona. Zona Universitaria de Pedralbes. 08028 Barcelona.
[(2)] Departamento de Geología. Universidad Católica del Norte. Avda.Angamos, 6810. Casilla 1280. Antofagasta.
[(3)] Facultat de Geología. Universitat de Barcelona. Zona Universitaria de Pedralbes. 08028 Barcelona.

**KEYWORDS:** salar, halite rock, halite textures, minor elements, interstitial brines, paleohydrology.

## INTRODUCTION

The Salar Grande (Fig. 1), located about 80 km at the South of Iquique (70°00' W, between 20°45' and 21°45' S latitude), is the only significant intermontane evaporitic basin in the Coastal Range of Chile. It is some 45 km long (in N-S direction) and 5 km wide. The altitude of the salar surface ranges from 640 to 750 m.a.s.l.

The salar basin is located in a tectonic depression controlled by one branch of the Atacama Fault System. This fault controls the Salar Grande basin on the SE, W, and NW edges. The fault generates several blocks (in the northern part of the salar) displaying level differences of several hundreds of meters. The Atacama Fault cuts the salar obliquely, producing a sharp scarp. E-W faults control the eastern edge, generating creeks perpendicular to the salar shoreline.

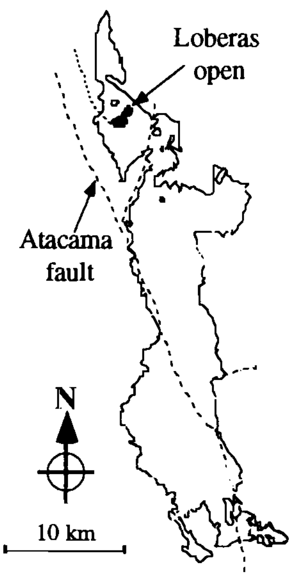


**Fig.1.** The Salar Grande

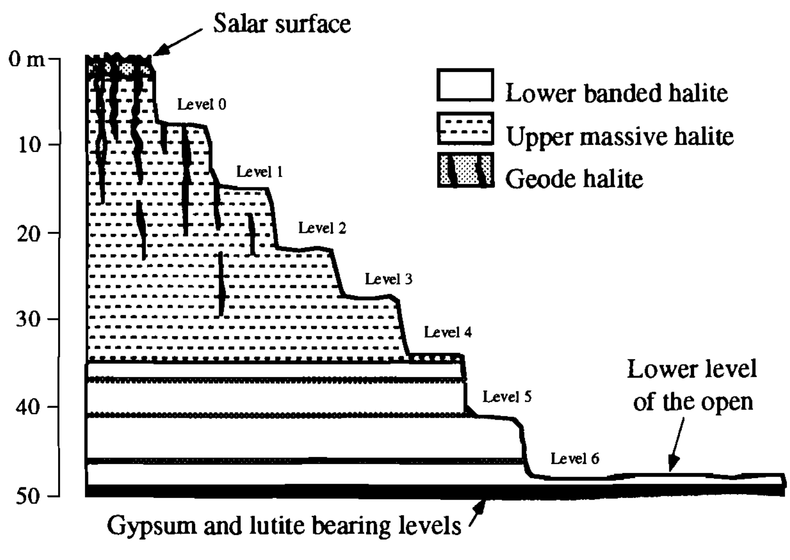


**Fig. 2.** Mina Loberas. North end of Salar Grande.

The Salar Grande, still not covered by younger sediments, is an ancient salar (Chong, 1984) that has lost its brines and whose sedimentary infill is composed of very pure halite, with very scarce amounts of sulphates, and no clear evidence of bull-eye facies distribution, as expected in a salt lake. The salar surface shows thick saline crusts with polygonal cracks. The effects of deflation, dissolution, and capillar processes (produced by the effect of local fog *-camanchaca-*) are evident. Large blocks, probably related to substrate fractures, are visible in aerial and satellite images.

## BASIN INFILL CHARACTERISTICS, MINERALOGY, AND PETROLOGY

Several open pits (mainly in the northern part) and four boreholes (made towards the center and the southern part) are the only available sources of information about the substrate composition of the salar. These sources reveal that their sedimentary infill is composed of a massive halite body, reaching about 100 m in thickness. Their composition is homogeneous, without significant detrital (or other) sediments. The extremely scarce interlayers (cm- to mm- thick) are black and brown altered volcanic ashes.

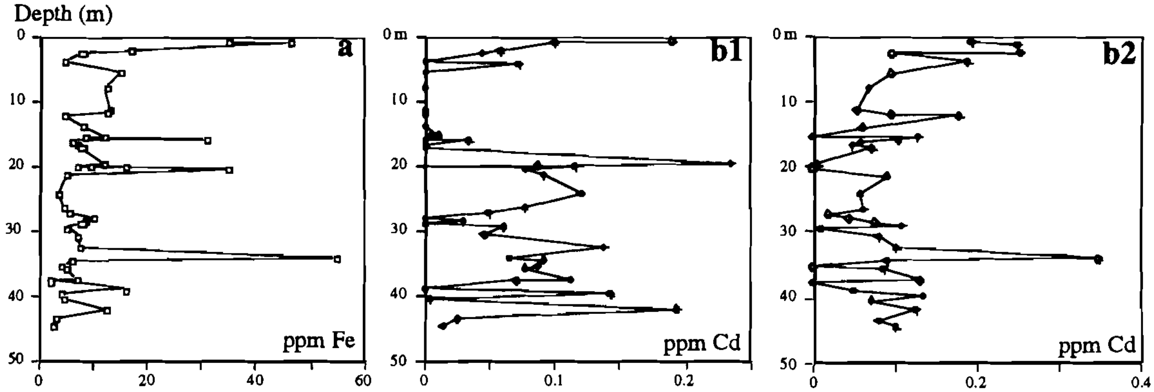


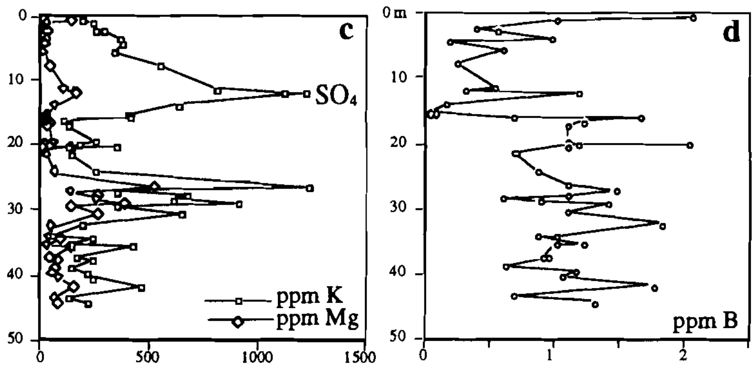


**Fig. 3.** Metal concentration profiles. **a** and **b2** have been obtained by extraction with N HCl, and **b1**, **c** and **d** using distilled water. In **c**, $SO_4$ corresponds to an increase in sulphates (thenardite, polyhalite).

The salt body outcropping in the open pits of Salinas Punta de Lobos (northern part of the salar) (Cabrera *et al.*, 1995) is about 45 m thick. Beneath it, fine clastic sediments of volcanic origin, bearing gypsum and halite cement, are present. In its lower 10m the salt body displays a thinly banded structure (*lower banded halite*, LBH). The bands or cycles (1 to 2 cm thick) are formed by chevron-like halite crystals, cm- to mm- in size. Cycles are separated by dissolution surfaces that smooth or truncate the chevron apex. Very few sulphate minerals (mainly glauberite, thenardite and polyhalite, µm-sized) and clays are present along these dissolution surfaces as well as interstitially between the halite crystals. Towards the upper part, the halite crystal aggregates evolve to coarse (reaching several cm in size), disoriented, and masive (*upper massive halite*, UMH), becoming more brownish due to the presence of interstitial terrigenous material. Euhedral thenardite crystals (cm in size) are common on levels 2 and 3 (Fig. 2). Thenardite crystals act as a diagenetic cement, replacing halite and displaying poikylitic growths and solid inclusions of glauberite, clay, and micrite. Polyhalite is the most abundant sulphate, always related with grain boundaries and dissolution surfaces. The transition between lower and upper halite units is made through a several-meter-thick interval displaying alternances of both lithofacies. Moreover, synsedimentary halite, another generation of very coarse grained (until 50 cm in size), masive, extremely pure halite, is present as pockets (reaching tens of meters in diameter). Large halite crystals infill the pockets following a geode-like arrangement. Some levels, bearing isolated thenardite crystals (until 5 cm in size) are present in the UMH. The entire salt body is affected by cracks. The lateral edges of the salt body are affected by dissolution and encrustment; the salt rock is in direct contact with the substrate rocks. No concentric mineral pattern is evident. Nevertheless, anhydrite levels (some meters thick) displaying selenite gypsum pseudomorphs (reaching some decimeters in size) are present on the SE and S margins. At the SE end of the salar there is an anhydrite level located at the top of the salt body which continues eastwards towards the Salar de Llamara. There is no physical continuity (only in sulphate lithofacies) between these two salars.

## GEOCHEMICAL DATA OF ROCK SALT

### Minor and trace elements

Twenty-six elements (Al, As, B, Ba, Be, Ca, Cd, Co, Cr, Cu, Fe, K, Li, Mg, Mn, Mo, Ni, P, Pb, S, Se, Si, Sr, Ti, V and Zn) have been determined in 50 salt rock samples scattered along a vertical section (Fig.2; Mina Loberas section) of the salt body. PCA performed on this analytical dataset reveales three well defined correlation factors. The first factor (involving Al, Fe, Mn, P, Si and Ti; Fig. 3a) is related to the particulate silicate fraction (eolian dust, volcanic ash, terrigenous material) always mixed in minor amounts with rock salt. The second factor (involving As, Cd, Co, Cr, Cu, Ni, Pb, Se, V and Zn; Fig. 3b) is strongly related to sulphide ore (leachate) inputs entering the salar through the hydrologic system. The third factor (involving B, Ca, K, Li, Mg and Sr) is mainly related to minor amounts of accessory saline minerals (glauberite, thenardite, polyhalite; Fig. 3c) and to the interstitial brines (Fig. 3d) present as fluid inclusions in the halite.

### Fluid inclusion composition

The LBH displays a number of primary (synsedimentary) fluid inclusions in its chevron-like halite crystals whereas the UMH only shows grain boundary fluid inclusions. Cryo-SEM-EDS analysis (Ayora *et al.*, 1994a) were performed on the primary fluid inclusions of the banded halite of the LBH and on a sample of a banded halite alternance located in level 4 (Table 1).

| Sample-m | Na | Mg | $SO_4$ | Cl | K | Sat. Ind. |
|---|---|---|---|---|---|---|
| 181-27,00m | 5.65 | 0.39 | 0.90 | 5.48 | 0.63 | -0.0279 |
| 188-27,90m | 5.71 | 0.40 | 0.89 | 5.41 | 0.62 | -0.0469 |
| 263-35,80m | 5.66 | 0.37 | 0.82 | 5.56 | 0.58 | -0.0282 |
| 287-37,70m | 5.62 | 0.33 | 0.83 | 5.60 | 0.59 | -0.0523 |
| 317-41,10m | 5.18 | 0.49 | 0.97 | 5.15 | 0.70 | -0.0301 |
| 340-44,50m | 5.21 | 0.50 | 0.76 | 5.83 | 0.77 | -0.0488 |

**Table 1.** Average contents of solutes (mol/kg $H_2O$) in fluid inclusions.

The brine chemical composition is very homogeneous. This implies that during the sedimentation of the Salar Grande halite, the parental brines reached a steady-state without significant changes in their solute content.

Brines are of the Cl-$SO_4$-Na-K type, very rich in $SO_4$ and depleted in Mg y Ca. The high concentration of $SO_4$ is explained by the kind of imputs entering the basin (recycled volcanic S) and by the extremely low Ca content in the brine. More Ca give rise to an increase of sulphate mineral (gypsum, anhydrite or glauberite) precipitation. When Ca is lacking, dissolved $SO_4$ increases by evaporation trending to saturation in thenardite. Nevertheless, halite saturation was reached before, lowering the Na concentration of the brines. K is also very abundant in the Salar Grande brines, being similar to that measured in halite samples from marine potash salts (Ayora *et al.* 1994b).

| Sample | Halite | Sylvite | Thenardite | Glauberite | Anhydrite |
|---|---|---|---|---|---|
| 181 | -0.07 | -0.68 | -0.11 | -0.16 | -0.64 |
| 188 | -0.07 | -0.69 | -0.10 | -0.18 | -0.67 |
| 263 | -0.07 | -0.70 | -0.13 | -0.19 | -0.67 |
| 287 | -0.07 | -0.70 | -0.13 | -0.18 | -0.64 |
| 317 | -0.16 | -0.67 | -0.18 | -0.27 | -0.68 |
| 340 | -0.06 | -0.54 | -0.22 | -0.26 | -0.64 |

**Table 2.** Mineral saturation index of brines.

The mineral saturation index data (Table 2) implies that parental brines trapped in the Salar Grande halite are in equilibrium with halite and thenardite. Sylvite subsaturation is due to the high Na concentration that had led previously to halite precipitation. Assuming a Ca concentration of 0.001 mol/kg $H_2O$ (under the detection limit of the *cryo-SEM-EDS* analytical method used), brines are close to saturation in glauberite and clearly subsaturated with respect to anhydrite.

## SEDIMENTOLOGICAL AND PALEOENVIRONMENTAL IMPLICATIONS

Halite lithofacies infilling the salar (LBH and UMH) implies the following paleohydrological evolution: (1) Early environments with cm-deep free brines showing banded halite with piramidal (*chevron*) texture. Dissolution surfaces indicate the ephemeral character of brines and the alternance of dessication and inundation stages. (2) A change to environments where brines are mostly in pore position, generating displacive halite (and thenardite) facies. This fact reveals a hydrological evolution where the amount of brine becomes gradually smaller. Halite is the only sedimentary product of precipitation. Thenardite, glauberite and polyhalite are early diagenetic precipitates developed in dissolution pockets and grain boundaries.

The type and distribution of facies, and the salar geometry, suggests that the salar underwent fracturation, brine losses, and surface erosion, the latter implying partial or total elimination of marginal and surficial facies. Nevertheless, the marginal facies preserved in S and SE edges are poorly developed. This, and the extreme purity of the halite body, implies evolved parental brines. Pore brines trapped as fluid inclusions show high potassium and sulphate contents, being saturated as regards halite and thenardite (and nearly saturated concerning glauberite). Ca-depletion was generated by precipitation of calcium sulphates. The waters coming from the Puna, moved towards the Central Depression which in turn acted as an endorreic system, making the Salar Grande basin the final container for the most evolved (Ca-depleted) brines. The Salar Grande basin was originally connected with the Central Depression at its SE edge. Their disconnection is probably related to recent movements of the Atacama Fault System. The absence of significant terrigenous levels indicates a dominant underground recharge.

The content and distribution of minor elements through the salt body reflects the inputs entering the salt lake: 1) Terrigenous inputs growing towards the upper part (Fig. 3a) indicating a progressive increase of interstitial processes; 2) Trapped brine content (as fluid inclusions in halite) higher in the lower part of the series (LBH, Fig. 3d), and sulphate minerals higher towards the upper part of the salt body (Fig. 3c) reflecting the halite facies distribution; 3) Trace metals present in rock salt in two forms: one, extractable with distilled water (Fig. 3b1), probably related to fluid inclusions, and another extractable with N HCl, binded to terrigenous inputs.

**Acknowledgments.** We are indebted to the Minera Punta de Lobos Company (Chile), for helping us with sampling and general field work. We also wish to thank Frances Luttikhuizen for her help with the English draft of this paper. Analytical work (ICP and *crio*-SEM-EDS determinations) were performed in the Scientific-Technical Surveys division of Barcelona University. This research was carried out thanks to the EC contract n: CI1*-CT94-0069 (DG 12 HSMU).

## REFERENCES

Ayora, C.; García Veigas, J. and Pueyo, J.J. 1994a. X-ray microanalysis of fluid inclusions and its importance to the geochemical modeling of evaporite basins. *Geochimica et Cosmochimica Acta*, 58, 43-55.

Ayora, C.; García Veigas, J. and Pueyo, J.J. 1994b. The chemical and hydrological evolution of an ancient potash-forming evaporite basin as constrained by mineral sequence, fluid inclusion composition, and numerical simulation. *Geochimica et Cosmochimica Acta*, 58, 3379-3394.

Cabrera, Ll.; Chong, G.; Jensen, A.; Pueyo, J.J.; Sáez, A. and Wilke, H.G. 1995. *Cenozoic and Quaternary lacustrine systems in northern Chile (Central Andes, Arc and Fore-Arc zones).* Recent and Ancient Lacustrine Systems in Convergent Margins. GLOPALS-IAS Meeting (Antofagasta 12-18th November 1995). Excursion Guidebook. 77 p.

Chong, G. 1984. Die Salare in Nordchile. Geologie, struktur und geochemie. *Geotek. Forsch.*, 67, 146p.

# THE ROLE OF ORGANIC MATTER IN HIGH TEMPERATURE HYDROTHERMAL REGIMES

Gaston GIULIANI[1, 2], Alain CHEILLETZ[2, 3], Christian FRANCE-LANORD[2] and Félix RUEDA[4]

(1) ORSTOM, 213 rue La Fayette, 75480 Paris cedex 10, France
(2) CRPG-CNRS, BP 20, 54520 Vandoeuvre-lès-Nancy, France,
(3) ENSG-INPL, BP 452, 54001 Vandoeuvre-lès-Nancy, France,
(4) MINERALCO S.A., calle 32, N°13-07, Apartado aéreo 17878, Bogotá, Colombia

**KEY WORDS:** organic matter, black shale, thermochemical sulfate reduction, pyrite, Colombia

## INTRODUCTION

The generation of petroleum in basins involves accumulation of organic matter (OM), its gradual burial, diagenesis breakdown and maturation via biodegradation or thermal cracking processes within a 75-150°C "oil window" temperature range. In hydrothermal regimes, as illustrated by active submarine rift basins (Simoneit, 1985), transformation of OM in sediments by high temperature fluids, up to 360°C, is an effective and more rapid process than in conventional basins. The study of such systems are of great interest to understand sulfate-hydrocarbon redox reactions specially for the thermochemical sulfate reduction (TSR), because the hydrothermal fluid discharge contains base-metal sulfides, sulfates, carbonates and petroleum. Moreover, the existence of a thermal gradient induced between ambient and supercritical waters, permit to define the minimum temperature at which TSR reaction began. Hydrothermal experiments have shown that TSR take place at temperatures as low as 175°C whereas geological evidences suggest lower minimum temperatures, 100-140°C, as illustrated by the formation of the Pine Point Mississippi Valley type deposit (Powell and Macqueen, 1984). This paper deals with characterization of OM associated with the Colombian emerald deposition and its key role in TSR through high temperature hydrothermal regimes.

## THE EXEMPLAR CASE OF COLOMBIAN EMERALD DEPOSITS

The Colombian emerald deposits are found within two narrow zones, located along the two major polyphased thrusted limits of the Eastern Cordillera (EC), corresponding to the original borders of an huge basin in Cretaceous time. The eastern zone consists of the mining districts of Gachalá, Chivor and Macanal and the western zone, of the districts of Coscuez, Muzo, La Palma-Yacopí. Both are contained in Early Cretaceous black shale (BS) series. Two distinct ages of formation of the emerald deposits have been obtained for the western and eastern emerald zones, respectively, 38-32 Ma for the Coscuez-Muzo mines (Cheilletz et al., 1994), and 65 Ma for the Chivor mine (Cheilletz et al., 1995). The deposits result from a two-stage cinematic process in which shortening tectonics affects the two borders of the EC, leading to decollement planes, thrusting, and thrust-fault related folds (Cheilletz and Giuliani, 1996). Stage 1 is characterized by decollement planes which focused the circulation of hydrothermal fluids inducing albitisation and calcitisation of the BS. This metasomatism leads to leaching of major (Si, Al, K, Ti, Mg, P), trace (Ba, Be, Cr, V, C, B, U) and REE-elements from the enclosing BS; this stage is accompanied by the development of a vein system filled by fibrous calcite and pyrite. Stage 2 is marked by the formation of breccias along thrust faults, and thrust related anticlines; it is characterized by extensional vein sets and hydraulic breccia development filled by muscovite, albite, rhomboedral calcite and dolomite, pyrite and finally by the precipitation in drusy cavities of fluorite, apatite, parisite, REE-bearing dolomite, emerald and quartz.

Microthermometric, Raman-probe and SEM analysis demonstrate the presence of $H_2O$-$NaCl$-$CaCl_2$-$KCl$-$CO_2$-$N_2$ rich-brines trapped into emerald (Giuliani et al., 1992; Cheilletz et al., 1994; Ottaway et al., 1994), carbonate and pyrite (Giuliani et al., 1995). The trapping temperatures of fibrous calcite from stage 1 and rhomboedric carbonates and emerald from stage 2, are estimated respectively, at 150-200°C and 300°C (Cheilletz et al., 1994; Giuliani et al., 1995). Oxygen and carbon isotope composition of quartz and carbonates in all the deposits indicates a basinal formation water origin for the mineralizing fluid (Giuliani et al., 1992), data confirmed by Ottaway et al. (1994) for the Muzo mines. The $\delta^{34}S$ values of $H_2S$ in solution in equilibrium with pyrite from emerald deposits (Giuliani et al., 1995) demonstrate the evaporitic origin for the mineralizing brines. Cation analysis of fluid inclusions by crush-leach technique (Banks et al., 1995) confirms that fluid in emerald, fluorite and quartz are derived from the dissolution of primary halite and are predominantly Na-Cl-Fe-Ca-K brines.

## CHARACTERIZATION OF SEDIMENTARY AND HYDROTHERMAL ORGANIC MATTER RELATED TO EARLY CRETACEOUS BLACK SHALES AND EMERALD MINERALIZATION

The EC of Colombia corresponds, in its central part, to a fold belt which thrusts, on the East, the Llanos basin and on the West, the Magdalena basin. The Cretaceous sediments were deposited in a two arm basin, Tablazo-Magdalena at the west, and Cocuy at the east, separated by the Santander high. These basins were deformed and inverted at Cenozoic times. Fabre (1987) provides important estimations on burial and geothermal history of the EC basin during Cretaceous and Tertiary times. He showed that the basin formed by extension on a strongly thinned lithosphere which provoked a major thermal event coupled with intrusion of mafic magmatism. Fabre and Delaloye (1983), dated these different basic rocks and showed that an Early Cretaceous thermal episode developed from 118 to 93 Ma, up to the Albian-Cenomanian boundary. The vitrinite reflectance data from different portions of the Cocuy paleobasin (Fabre, 1987) indicate increase of matury in sediments from Une (Albian; $0.5 < PR < 1$) to Macanal (Berriasian; $2.5 < PR < 4.5$) formations, as well as the presence of blackened pollens. Hébrard (1985, in Fabre 1987) evidences also the neoformation of pyrophyllite from detrital muscovite and quartz, and measured illite crystallinity up to 4.5. These data and the burial curves show that the basal section of the Cretaceous i.e., Macanal BS series, reached a temperature of 300°C (near the anchizone) until the Campanian. Rock-Eval realized on the Macanal (Cocuy basin) and Paja-Simiti BS (Barremian-Albian serie from Tablazo-Magdalena basin) which contain emerald mineralizations, confirm the overmaturity of OM ($6 <$ Hydrogen Index $< 61$; $1 <$ Oxygen Index $< 20$; $0.2 <$ TOC $< 1.1$ %). The carbon isotopic composition of OM of the Macanal BS ($-28.2 < \delta^{13}C < -21.7$ ‰; mean: -24 ‰) is different from the isotopic composition of Paja-Simiti BS ($-22.2 < \delta^{13}C < -18.4$ ‰; mean: -20.5 ‰). This difference evidences the variation of sedimentation between the two arms basins: continental input from Guyana shield with precipitation of humic OM within the Cocuy basin versus marine mudstone within the Tablazo-Magdalena basin.

Carbonaceous hydrothermal material is closely associated with emerald mineralization (Giuliani et al., 1993b; Cheilletz and Giuliani, 1996). Petrographic investigations show that this material precipitated during the two stages of vein opening and until emerald deposition. Solid hydrocarbon (bitume) exhibits massive form (up to 2 cm in diameter) and sometimes infilled fractures. It shows conchoidal fractures and both in hand specimen and under the SEM, can present numerous hollow spheres and small voids ranging from 10 microns to 1 mm in diameter. Daughter mineral phases were identified in some bubbles as calcite, dolomite, anhydrite, vanadium-iron oxides, vanadium-rich muscovite, barite and zinc oxide. Bitumen has a low sulfur content (0.2 to 1.2 %) and important trace concentrations (V up to 2000 ppm, Zn up to 740 ppm , Cr up to 87 ppm, U up to 37 ppm and Mo up to 60 ppm). X-ray diffractograms display a broad band between 10 and 18 degrees defining the amorphous character of the material. The first order Raman spectra of bitumen display a band located around 1590 $cm^{-1}$, which corresponds to C-C vibrations in the aromatic layers, and a second broad band at 1350 $cm^{-1}$ which is attributed to defects in the graphite structure. The area ratio S 1590 / S 1350 is about 0.7. These data indicate a low structural degree of structural ordering and the non-graphitic character for the solidified bitumen. The micro-transmission infrared microspectroscopy spectra show the lack of aliphatic and aromatic bands and the disappearance of oxygen species. These results added to Rock-Eval data (Hydrogen Index< 1; 19 < Oxygen Index< 61) confirm the important thermal cracking suffered by these bitumen. $\delta^{13}C$ values for bitumen range from -23.8 to -21.2 ‰ and are similar to thoses obtained for the OM in the BS. $\delta D$ values are comprised between -73.2 and -122 ‰ and the H/C ratios are around 0.1. These isotopic data suggest a genetic relationship between OM and hydrothermal bitumen, and indicate the complete consumption of organic hydrogen during degradation of OM.

## THE ROLE OF ORGANIC MATTER IN THE THERMOCHEMICAL SULFATE REDUCTION IN COLOMBIAN EMERALD DEPOSITS

Colombian emerald deposits have no magmatic connection and they can be considered as pyrite deposits hosted by carbonate veins, emerald being an accessory mineral. Sulfide-sulfur source is evaporitic but the chemical process responsible for the reduction of sulfate in sulfide is still in debate (Ottaway et al., 1994; Cheilletz and Giuliani, 1996). The presence of both OM in the enclosing BS and in the hydrothermal carbonate-pyrite veins opens to discussion of the possible role of OM in emerald deposit.
Four main conditions are necessary to establish that OM has played a key role on TSR (modified from Leventhal, 1990):

1- OM is now present in the ore body; it is the case in colombian deposits where hydrothermal bitumen are found,

2- OM was present when the different stages of the hydrothermal system developed and at the time of ore formation: in fact, hydrothermal bitumen precipitated during stages 1 and 2 and are found as daughter minerals within primary fluid inclusions hosted by emerald,

3- two types of OM are present: in our case, original, i.e., OM in the BS, and hydrothermal, i.e., bitume in the veins. The organic-matter-bearing BS enclosing the emerald mineralization has suffered a thermal degradation due to burial and thermal history of the EC basin during Cretaceous time. The fluids related to emerald formation at Cenozoic times remobilized this OM provoking changes, differences in chemical composition and precipitation of bitumen,

4- the chemical change in the altered OM is compatible with TSR:

4.1- sulfate reduction implies always oxidation of OM. Oxidation of OM contained in the BS and subsequent carbonates precipitation in equilibrium with $CO_2$ would result in the formation of low $\delta^{13}C$ carbonates. $\delta^{13}C$ of the carbonates will depend on their temperature of formation and the initial isotopic composition of OM. Calcite-graphite $^{13}C/^{12}C$ fractionation factors were calculated using the calibration of Bottinga (1969). The difference of 4.5‰ in $\delta^{13}C$ found between OM from Macanal and Paja -Simiti (?) BS, implies that the $\delta^{13}C$ of carbonates from stages 1 and 2 of the eastern emerald zone are lighter than those of the western one. In fact, there are two isotopic populations of carbonates. The higher $\delta^{13}C$ values correspond to Coscuez, Muzo, Yacopí deposits ($-9.3<\delta^{13}C< -0.4$‰). The more negative values are associated with the Chivor, Gachalá, Macanal mines ($-16.7<\delta^{13}C< -3.1$‰). In conclusion, it appears that carbonates crystallized in equilibrium with organic carbon at temperatures determined by microthermometry,

4.2- a definitive change is a loss of hydrogen characterized by a lower H/C ratio or more by an aromatic structure. Rock-Eval analyses on both sedimentary and hydrothermal OM, coupled with hydrogen-carbon isotope data, have shown that organic hydrogen was consumed during the reduction.

The four main conditions for TSR reaction are checked in the case of Colombian emerald mineralization: OM acted as reactant and product, the chemical changes producing a considerable loss of hydrogen as shown by the low H/C ratio (H/C: 0.1) and the oxidation of OM produced large quantities of $CO_2$ necessary to form $HCO_3^-$.

Many reactions have been proposed for TSR and Machel (1987) summarized them in a global net balance exothermic reaction: hydrocarbon + $SO_4^{--}$ --> altered hydrocarbon + bitumen + $HCO_3^-$ + $H_2S$ + $CO_2$ (?) + heat. Considering the different products found in the colombian hydrothermal samples and the measured changes in chemical composition of OM, the following reaction is proposed to explain the role of OM in TSR (Cheilletz and Giuliani, 1996): $Ra\ (CH_2O)_2 + SO_4^{--} \rightarrow Rb + 2HCO_3^- + H_2S$ where $CH_2O$ represents a carbohydrate and R(a,b) large organic molecules. $HCO_3^-$ and $H_2S$ produced by the reaction reacted with $Ca^{2+}$ and $Fe^{2+}$ carried by the hydrothermal fluids to induce the precipitation of calcite and pyrite i.e., $HCO_3^- + Ca^{2+} \rightarrow CaCO_3$ (calcite) + $H^+$ and $7H_2S + Fe^{2+} + SO_4^{--} \rightarrow 4FeS_2$ (pyrite) + $4H_2O + 4H^+$.

## CONCLUSIONS

The geochemical study of OM in the Colombian emerald deposits provided new informations and confirmed previous data on the degree of maturity of the Early Cretaceous BS of the EC and the burial history of the ore-filled area. It constraints also the possible role of OM on the mode of formation of emerald ore bodies. Bitumen appears to have been derived locally from the transformation of OM from sediments by high temperature hydrothermal fluids, up to 300°C. The question of genetic relationships between sulphides, OM and bitumen is solved. Sulfate-hydrocarbon redox reactions occurred at high temperature as described in active submarine rift basins, and isotopic evidences are suggestive of the effective role of OM in the formation of hydrogen sulfide necessary to produce sulfides (pyrite). The mechanism proposed involves the reaction between sulfate of evaporitic origin and OM, without the production of an intermediary elemental sulfur, to produce hydrogen sulfide. This redox reaction process has been already verified experimentally and invoked in dessiminated or stratiform base metals or Mississippi Valley type deposits.

## REFERENCES

Banks D.A., Yardley B.W.D., Giuliani G., Cheilletz A. and Rueda F. 1995. Chemistry and source of the high temperature brines in the Colombian emerald deposits. Mineral deposits, Pasava, Kribek & Zak (eds), Balkema, Rotterdam, 557-560.

Bottinga Y. 1969. Calculated fractionation factors for carbon and hydrogen isotope exchange in the system calcite-carbon dioxide-graphite-methane-hydrogen-water vapor. Geochim. Cosmochim. Acta, 33, 49-64.

Cheilletz A., Féraud G., Giuliani G. and Rodriguez C.T. 1994. Time-pressure-temperature constraints on the formation of Colombian emeralds: a laser-probe and fluid inclusion study. Econ. Geol. 89, 2,362-380

Cheilletz A., Giuliani G., Zimmermann J.L. and Ribeiro-Althoff A.M. 1995. Ages, geochemical signatures and origin of Brazilian and Colombian emerald deposits: a magmatic versus sedimentary model. Mineral deposits, Pasava, Kribek & Zak (eds), Balkema, Rotterdam, 569-572.

Cheilletz A. and Giuliani G. 1996. The genesis of Colombian emeralds: a restatement. Mineralium Deposita (in press).

Fabre A. 1987. Tectonique et génération d'hydrocarbures: un modèle de l'évolution de la Cordillère Orientale de Colombie et du bassin des Llanos pendant le Crétacé et le Tertiaire. Arch. Sc. Genève, 40, 2, 145-190.

Fabre A. and Delaloye M. 1983. Intrusiones básicas cretácicas en las sedimentitas de la parte central de la Cordillera Oriental. Geol. Norandina, 6, 19-29.

Giuliani G., Sheppard S.M.F., Cheilletz A. and Rodriguez, C.T. 1992. Fluid inclusions and $^{18}O/^{16}O$, $^{13}C/^{12}C$ isotope geochemistry contribution to the genesis of emerald deposits from the Oriental Cordillera of Colombia. C. R. Acad. Sci. Paris, 314, série II, 269-274.

Giuliani G., Cheilletz A., Arboleda C., Carrillo V., Rueda F. and Baker J. 1995. An evaporitic origin of the parent brines of Colombian emeralds: fluid inclusion and sulfur isotope evidence. Eur. Journal of Mineralogy 7, 151-165.

Leventhal, J.S. 1990. Organic matter and thermochemical sulfate reduction in the Viburnum trend, Southeast Missouri. Econ. Geol., 85, 622-632.

Machel H.G. 1987. Some aspects of diagenetic sulphate-hydrocarbon redox reactions. Geol. Soc. Special Pub. "Diagenesis of Sedimentary sequences", Marshall J.D. (eds), 36, 15-28.

Ottaway T.L., Wicks F.J., Bryndzia L.T., Kyser T.K. and Spooner E.T.C. 1994. Formation of the Muzo hydrothermal emerald deposit in Colombia. Nature, 369, 552-554.

Powell T.G. and Macqueen R.W. 1984. Precipitation of sulfide ores and organic matter: sulfate reactions at Pine Point, Canada. Science, 224, 63-66.

Simoneit B.R.T. 1985. Hydrothermal petroleum: genesis, migration and deposition in Guaymas basin, Can. J. Earth Sci., 22, 1919-1929.

# THE PUNTA DEL COBRE BELT, NORTHERN CHILE: INTRUSION-RELATED MID-CRETACEOUS Cu(-Fe) MINERALIZATION

Robert MARSCHIK and Lluís FONTBOTÉ

*Département de Minéralogie, Université de Genève, Rue des Maraîchers 13, 1211 Genève 4, Switzerland*

The Punta del Cobre belt is located about 15 km south of Copiapó, northern Chile. The belt comprises several Cu(-Fe) deposits in the Punta del Cobre (e.g., Carola, Resguardo, Santos, Socavón Rampa, and Trinidad mines) and southern Ladrillos districts (Mantos de Cobre mine), east of the Copiapó river, as well as the new La Candelaria deposit (Ryan et al., 1994) in the Ojancos Nuevo district west of the river (Fig. 1). The Cu(-Fe) deposits are hosted by the largely volcanic pre-upper Valanginian Punta del Cobre Formation, which is exposed in the core of the Tierra Amarilla anticline. The lower part of the Punta del Cobre Formation in the districts Punta del Cobre and Ladrillos, consists of altered calc-alkaline andesitic (Lavas Inferiores, Kpcli) and dacitic ("Albitófiro", Kpcfa) volcanic rocks (Fig. 1). Above a red, in the lower part volcaniclastic, breccia (Basal Breccia, Kpcsb) follows a mainly continental sedimentary sequence consisting essentially of siltstone, chert, and limestone (Trinidad Member, Kpcs). Basalts to basaltic andesites, in part with chemical affinities to mid-ocean ridge basalts, tuffs, and reworked tuffs form the upper part of the formation (Lavas Superiores, Kpcls). In the southern part of the study area the Punta del Cobre Formation is represented by the Quebrada Los Algarrobos Sequence (Kpcla), consisting of volcaniclastic rocks, basaltic andesites and andesites, and the Lavas Superiores (Marschik et al., 1994).

The Punta del Cobre Formation is overlain by Neocomian limestones of the Chañarcillo Group, which were deposited in the marine Andean backarc basin. Continental conditions established in middle Cretaceous as a result of regional uplift. Middle Cretaceous intrusive rocks of mainly dioritic, granodioritic, and quartz monzonitic composition, which form the batholith in the Copiapó area, were emplaced into the Neocomian rocks in the western part of the belt causing intense contact metamorphism (Tilling, 1963, 1976).

Contact metamorphism is expressed in the volcanic rocks of the Punta del Cobre Formation as parallel largely overlapping alteration zones (Fig. 2) that are characterized, from west to east, by the alteration mineral assemblages: (a) Ca-amphibole ± biotite ± sericite, (a) biotite ± chlorite ± sericite ± epidote (discontinuous zone), and (c) epidote-chlorite ± quartz, ± calcite. These three zones are superposed on pre-existing centers of alkali metasomatism, in which an early episode of sodium metasomatism was locally followed by potassic alteration. Mineralization is spatially associated with alkali metasomatism, in particular with potassic alteration (Marschik and Fontboté, 1994, in press).

Copper is mined in the Punta del Cobre belt from breccia bodies, veins, stockworks, and concordant lens-shaped bodies (mantos). The mineralization is characterized by a simple hypogene mineral assemblage of chalcopyrite, pyrite, magnetite, and hematite. Average Cu grades are between 1.1 and 2% and may reach more than 8% in veins. Massive magnetite occurs as veins and irregularly shaped bodies. In the Punta del Cobre and Ladrillos districts the mineralization is controlled by NNW to NW-trending structures.

Sulfur isotope ratios from chalcopyrite and pyrite show a narrow range in $\delta^{34}S$ values between -0.7 and +1.1 ‰ (Fig. 3). These data suggest that sulfur was leached from the underlying igneous rocks or contributed by magmatic fluids (R. Marschik, in press).

A $^{40}Ar/^{39}Ar$ incremental-heating experiment on hydrothermal biotite, interpreted to have formed synchronous with the Cu(-Fe) mineralization, yielded an inverse isochron age of 114.9±0.5 Ma (Marschik et al., 1996). This age is consistent with field evidence (Ryan et al., 1994) that suggest that mineralization predates batholith emplacement (K/Ar hornblende age 109.6±1.7 Ma, K/Ar biotite age 97.9 ±1.5 Ma, Farrar et al., 1970; ages converted following Dalrymple, 1979).

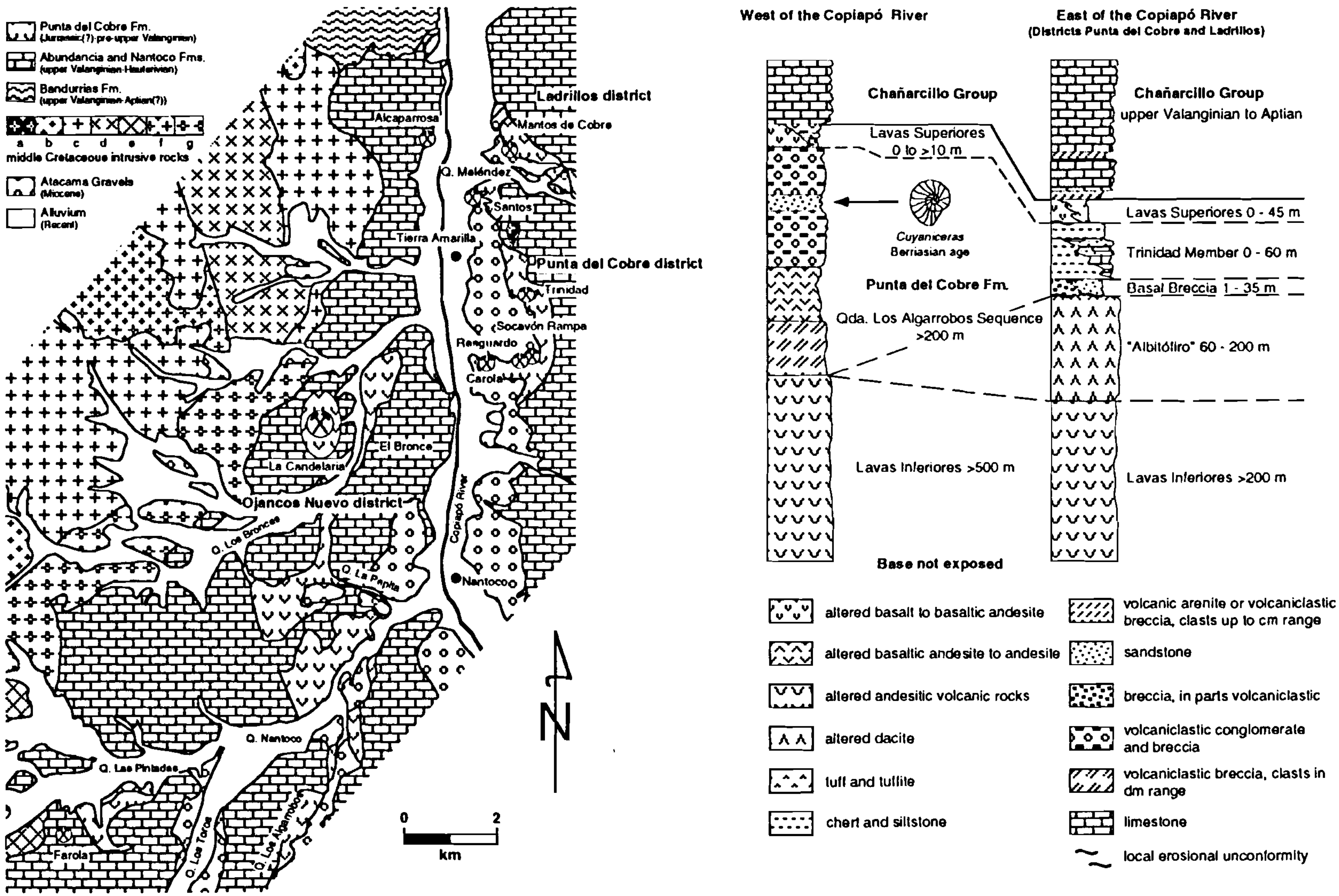


Figure 1. Geologic map of the main part of the Punta del Cobre belt (geology modified from Tilling, 1976; a) lamprophyre, b) meladiorite, c) diorite, d) leucodiorite, e) tonalite, f) quartz monzonite, g) albite granite). The Stratigraphy of the Punta del Cobre Formation east of the Copiapó river (Punta del Cobre and Ladrillos districts) and west of the river (Ojancos Nuevo district, Quebradas Nantoco, Los Algarrobos, and Los Toros) is summarized in two schematic sections.

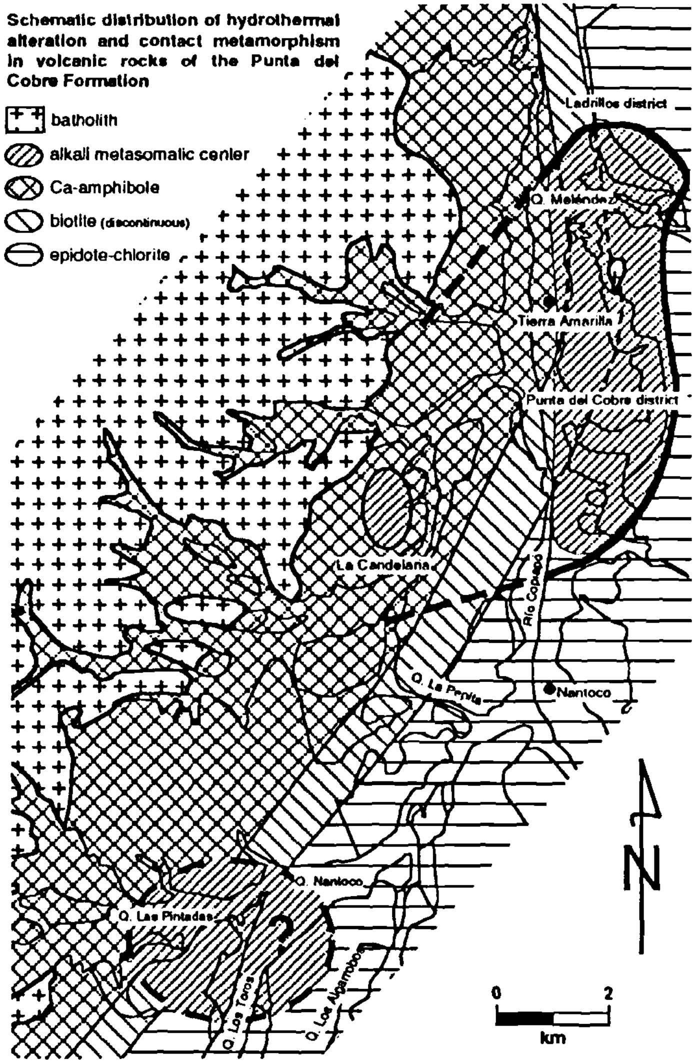


Figure 2. Limits of diagnostic minerals in the volcanic rocks of the Punta del Cobre Formation marked on the geologic map of Figure 1. Outlines of alkali metasomatic centers are also shown.

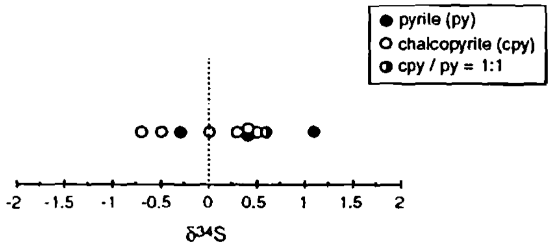


Figure 3. Sulfur isotope ratios of chalcopyrite an pyrite from the mines Santos and Socavón Rampa, Punta del Cobre district.

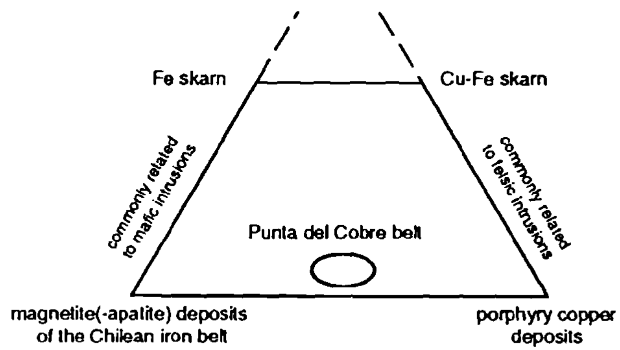


Figure 4. Schematic representation of the Punta del Cobre belt in comparison to other Andean intrusion-related deposit types.

Fluids in inclusions hosted by postore calcite have salinities between 29.2 and 33.6 wt.% $NaCl_{equiv.}$ and contain 12 to 24 wt.% NaCl and 13 to 23 wt.% $CaCl_2$. Assuming burial between 2 and 3 km in the mid-Cretaceous, the corrected formation temperatures for postore calcite lie between 122° and 174°C, and 149° and 203°C for hydrostatic and lithostatic pressure conditions, respectively (Marschik, in press).

The alteration pattern, geometry of the orebodies, ore formation temperatures of about 400° to 500°C (Hopf, 1990), and the age of potassic alteration point to a mineralization event associated with deep-seated magmatic intrusion(s) that predates emplacement of the middle Cretaceous batholith. The sulfur isotope compositions of chalcopyrite and pyrite and saline fluid inclusions of post-ore calcite may indicate that these intrusion(s) not only provided heat but also contributed with magmatic fluids. Not excluding that the Punta del Cobre belt could represent an external part of a system similar to those known from porphyry coppers, the large amounts of magnetite found in the deposits of the Punta del Cobre permits a comparison with the magnetite(-apatite) deposits of the "Chilean iron belt", which show similar mineralization temperatures and ages, and are hosted by Neocomian rocks in the vicinity of mid-Cretaceous intrusives. These magnetite(-apatite) deposits are frequently characterized by the presence of skarn parageneses. In a scheme considering porphyry copper deposits, magnetite(-apatite) deposits, and Fe and Cu-Fe skarns as endmembers, the Punta del Cobre district is interpreted to genetically occupy a transitional position between the "Chilean iron belt" and Andean porphyry copper deposits (Fig. 4; Marschik and Fontboté, in press).

## References


Dalrymple, G.B. 1979. Critical tables for conversion of K-Ar ages from old to new constants. *Geology*, 7, 558-560.

Farrar, E., Clark, A.H., Haynes, S.J., Quirt, G.S., Conn, and H. Zentilli, M. 1970. K-Ar evidence for the post-Paleozoic migration of granitic intrusion foci in the Andes of northern Chile. *Earth and Planetary Science Letters*, 10, 60-66.

Hopf, S. 1990. The Agustina Mine, a volcanic-hosted copper deposit in northern Chile. In Fontboté, L., Amstutz, G.C., Cardozo, M., Cedillo, E., and Frutos, J., eds., Stratabound ore deposits in the Andes. *Springer*, Berlin-Heidelberg, 421-434.

Marschik, R. Cretaceous Cu(-Fe) mineralization in the Punta del Cobre belt, northern Chile. *Terre et Environment*, Univ. of Geneva, in press.

Marschik, R., Fontboté, L., and Delaloye, M. 1994. Volcanic rocks of the Lower Cretaceous Punta del Cobre Formation: Petrology and implication for its paleotectonic setting. *Congreso Geológico Chileno*, 7th, Concepción, 1994, Actas, 2, 1110-1114.

Marschik, R., and Fontboté, L. 1994. Potassium and sodium alteration related to Cu-mineralization in the Punta del Cobre Formation, northern Chile. *Congreso Geológico Chileno*, 7th, Concepción, 1994, Actas, 2, 1591-1595.

Marschik, R., Singer, B.S., Munizaga, F. Tassinari, C., and Fontboté, L. 1996. Age of Cu(-Fe) mineralization and Cretaceous to Paleocene Thermal evolution of the Punta del Cobre district, northern Chile. *Brazilian Geological Congress*, 39th, Bahia, 1996.

Marschik, R. and Fontboté, L. Copper(-iron) mineralization and superposition of alteration events in the Punta del Cobre belt, northern Chile. *Economic Geology*, Special Publication No. 4, in press.

Ryan, P.J., Lawrence, A.I., Jenkins, R.A., Matthews, J.P., Zamora, J.C., and Marino, E. 1994. The Candelaria copper-gold deposit, Chile. *Congreso Geológico Chileno*, 7th, Concepción, 1994, Actas, 2, 1616-1617.

Tilling, R. 1963. Disequilibrium skarns of the Tierra Amarilla aureole, Atacama province, Chile. *Geological Society of America*, Special Paper 76 (abst.), 167.

Tilling, R. 1976. El Batholito Andino cerca de Copiapó, Provincia de Atacama. Geología y Petrología. *Revista Geológica de Chile*, 3, 1-24.

# METALLOGENIC BELTS IN THE CHILEAN PATAGONIA, BETWEEN 44° AND 48°S

Carlos PALACIOS M., Alfredo LAHSEN A., and Miguel PARADA R.

Department of Geology, Universidad de Chile. P.O. Box 13518, Correo 21, Santiago, CHILE, FAX 56-2-696-3050.

**KEY WORDS: Mineralization, Chile, Patagonia**

## INTRODUCTION

The purpose of this paper is 1) to describe the different types of mineralization present in the Chilean Patagonia between 44° and 48°S (Aysén region), and 2) to interpret, on a regional scale, its occurrence in metallogenic belts.

## GEOLOGY

The oldest rocks of the region have been grouped into the Metamorphic Basement extended along the western margin and the southern part of the region. They are low to medium grade metamorphic rocks, represented by schists, phyllites, quartzites and marbles of probably Upper Paleozoic age. This basement is unconformably overlayed by Upper Jurassic volcanoclastic rocks of rhyolitic to andesitic composition (Ibañez Formation). At the end of the Ibañez volcanic activity, started a back-arc marine transgressive-regressive cycle, corresponding to the Coyhaique Formation. This includes limestones, coquinas, black shales and sandstones of Lower Cretaceous age. The marine regression was accompained by the begining of the volcanism of the Divisadero Formation (Upper Cretaceous), represented by rhyolitic, dacitic, andesitic and minor basaltic rocks. These volcanic rocks underlie rhyolitic to basaltic rocks (Chile Chico Formation), that are products of a bimodal volcanism of Eocene age. In the Early Cenozoic, along the western side of the region, another volcanic arc was developped (Traiguén Formation), represented by silicic ash-flow tufs, sediments, and rhyolitic to basaltic lavas (Hervé et al., 1995). Along the eastern part of the region, the Chile Chico Formation underlie deposits of marine (Guadal Formation) and continental (Rio Frias Formation) Cenozoic basins. Most of the intrusive rocks are part of the North Patagonian Batholith, which is about 100 km wide Meso-Cenozoic composite plutonic belt that crosses the region from north to south. This huge batholith range in composition from granites to gabbros, and it's ages vary from Late Jurassic to Pliocene (Pankhurst and Hervé, 1994). The most important tectonic feature of the region is the dextral intra-arc strike-slip Liquiñe-Ofqui fault zone, at least active since the Early Cenozoic (Cembrano et al., 1996). Holocene volcanism and Early Cenozoic volcano-sedimentary deposits (Traiguen Formation) have a close causal relationships with this fault zone.

## MINERALIZATION

Mineralization in the last 170 Ma is generally restricted to three longitudinal metallogenic belts, in which hydrothermal activity was focused along the respective magmatic arcs: (Fig. 1).

1) **Upper Jurassic belt**, along which Au-Ag epithermal and Zn-Pb-Ag±Au mesothermal mineralization were formed.

2) **Lower Cretaceous belt**, which contains Au-Ag epithermal, Zn-Au skarn, and low grade porphyry copper mineralization, and

3) **Miocene belt**, which hosts Au epithermal and porphyry copper mineralization.

**The Upper Jurassic Belt.** Precious metal epithermal mineralization is hosted in felsic volcanic and subvolcanic rocks of the Ibañez formation. It is related to silicic and sericitic alteration and consists of stockworks and disemination of pyrite, arsenopyrite, native gold, electrum, and minor sphalerite, galena, and chalcopyrite. The ore bodies are stratiform horizons and funnel-shaped pipes. Grades vary from 0.2 to 4 ppm Au and 10 to 70 ppm Ag. Basic metals mesothermal mineralization consists of irregular bodies containing stockwork and dissemination of pyrite, arsenopyrite, sphalerite, Ag-bearing galena, and minor gold. Mineralization is hosted in felsic volcanic and subvolcanic rocks of the Ibañez formation, which present sericitic alteration. Ore grades vary from 2 to 8% Zn, 0.4 to 3% Pb, 10 to 100 ppm Ag, and 40 to 1,100 ppb Au. Field observations, structural interpretations and radiometric dating indicate that both type of mineralization occurred synchroneously with a magmatic and tectonic activity, in an Upper Jurassic (152-140 Ma) intra-arc pull-apart basin environment. Probably, both types of mineralization correspond to an hydrothermal system peripheral to porphyry copper (Palacios et al., 1996a; Parada et al., 1996).

**The Lower Cretaceous belt.** Precious metal epithermal mineralization is hosted in felsic volcanic rocks and domes of the Ibañez and Divisadero formations. Au-Ag mineralization occurs within sericitic and silicic alterations and consists of veins, hydrothermal breccias, stockwork and dissemination. Metallic assemblage is pyrite, silver sulphosalts, native gold, galena, and sphalerite. Ore grades vary from 0,3 to 15 ppm Au and 10 to 1,000 ppm Ag. Radiometric dating indicate that epithermal activity occurred between 99 and 113 Ma (Townley, 1996). Calc-silicate Au-Zn skarn mineralization is hosted in a fossiliferous limestone unit of the Coyhaique formation. Hydrothermal mineralization consists of sphalerite, native gold, electrum, hessite, scheelite, pyrrhotite, pyrite, arsenopyrite, galena, chalcopyrite, and maldonite. Geological information and radiometric data indicate that mineralization occurred between 100 and 108 Ma, related to felsic and dioritic intrusive magmatism (Palacios et al., 1996b). Low-grade porphyry copper mineralization consists of quartz dioritic stocks that intruded felsic tuffs of the Ibañez and Divisadero formations. Hydrothermal alteration corresponds to a potassic centre surrounded by phyllic and propilitic envelopes. Mineralization includes a weak stockwork with pyrite, chalcopirite,

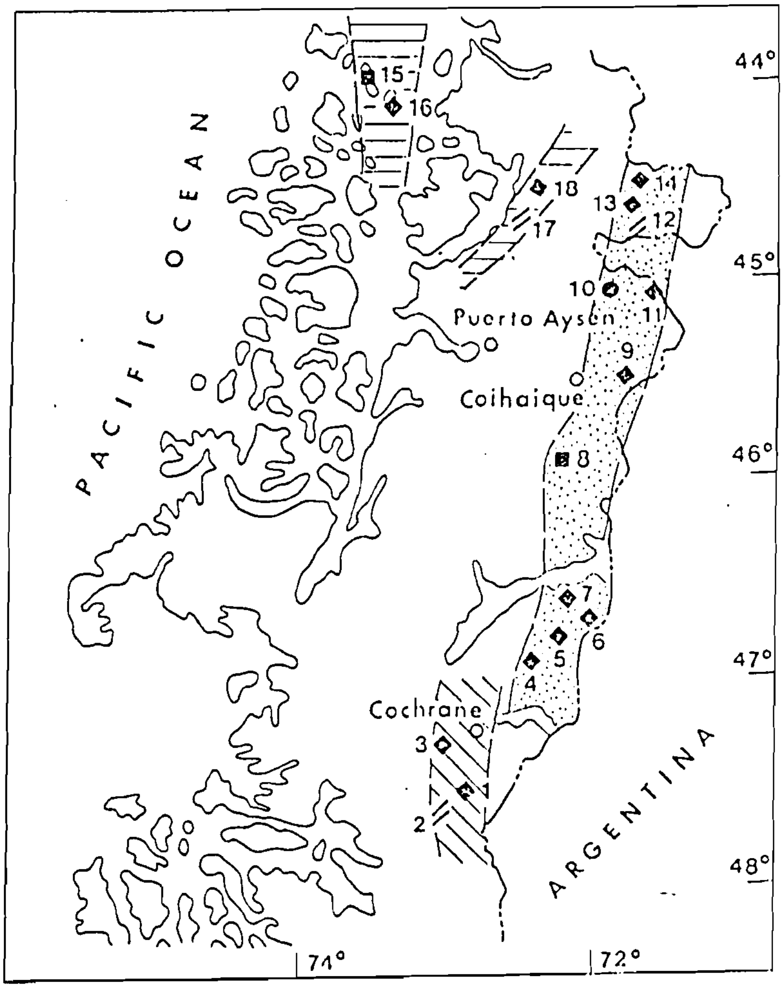


***Fig. 1: Metallogenic belts in the Chilean Patagonia.***
*Inclined dash: Upper Jurassic belt; Dotted zone: Lower Cretaceous belt; Horizontal dasch: Miocene belt; Diamand: epithermal mineralization; Parallel lines: veins (mainly epithermal); Circle: skarn mineralization; Square: porphyry copper mineralization.*
*1. El Faldeo prospect, 2. Lago Chacabuco prospect, 3. Lago Azul prospect, 4. Rio Furioso project, 5. Rio Amarillo prospect, 6. Rocoso prospect, 7. Fachinal mine, 8. Turbio prospect, 9. Castor-Pollux prospect, 10. El Toqui mine, 11. Katerfeld project, 12. Santa Teresa prospect, 13. Las Quemas prospect, 14. Cerro Agujas prospect, 15. Leucayec prospect, 16. Mulchey prospect, 17. El Queulat bajo prospect, 18. El Queulat alto prospect.*

molybdenite and magnetite. Ore-grades vary from 0,1 to 0,2% Cu and 200 to 750 ppm Mo (Candia et al., 1994).

**The Miocene belt.** Consists in two metallogenic lineaments (oriented NS and NE) that follow the strike of the major fault-zones of the Liquiñe-Ofqui structure. Au-rich epithermal mineralization consists of veins, and irregular lens hosted in Paleozoic filites and Miocene microdioritic stocks, or forms stockwork in felsic volcanics of the Traiguén formation. Mineralization contains pyrite, arsenopyrite, and gold related to silicic and/or sericitic alteration. Ore grades vary from 0,2 to 60 ppm Au. Field observations suggest that the epithermal mineralization is strongly related to the epizonal intrusion of microdioritic stocks, dated in 5 Ma. Low-grade porphyry copper mineralization corresponds to quartz dioritic stocks that intrude the volcanic rocks of the Traiguén formation. Recognized hydrothermal alteration includes a phyllic centre with propylitic envelop, and mineralization (mainly as stockwork) is pyrite and chalcopyrite, with minor bornite and molybdenite. Ore-grades range from 0,2 to 0,5% Cu and 50 to 100 ppm Mo. Both types of mineralization developed in a intra-arc pull-apart basin tectonic environment.

## REFERENCES

**Candia, W., Suchomel, B. Kakarieka, A., and Oates, C.** 1994. Turbio, un sistema tipo pórfido cuprífero en la Cordillera Castillo, Aysén. 7° Congr. Geol. Chile., Concepción, 2, 751-755.

**Cembrano, J., Hervé, F., and Lavenu, A.,** 1996. The Liquiñe-Ofqui fault zone: a long-lived intra-arc fault system in Southern Chile. Tectonophysic, Special Issue on Andean Geodynamics (in press).

**Hervé, F., Pankhurst, R.J., Drake, R. and Beck, M.** 1995. Pillow metabasalts in a mid tertiary extensional basin adjacent to the Liquiñe-Ofqui fault zone: The Isla Magdalena area, Aysen, Chile. Journal of South American Earth Sciences, 8, 1, 33-46.

**Palacios, C.M., Parada, M.A., and Lahsen, A.A.** 1996a. Upper Jurassic Au-Zn mineralization in El Faldeo district, Chilean Patagonia. Internal Report, 35 p.

**Palacios, C.M., Bertens, A.N., and Ruz, L.C.** 1996b. Polymetallic skarn mineralization at El Toqui, Aysen Province, Southern Chile. Zentralblatt für Geologie und Palaont. In press.

**Pankhurst, R.J. and Hervé F.,** 1994. Granitoid age distribution and emplacement control in the North Patagonian Batholith in Aysen (44°-47°S). 7° Congreso Geologico Chileno, Concepción, 2, 1409-1413.

**Parada, M.A., Palacios, C.M., and Lahsen, A.A.** 1996. Geology, geochronology and tectonic evolution of the El Faldeo Au-Zn district in the Chilean Patagonia. This volume.

**Townley, B.** 1996. Ore deposits, tectonic and metallogeny of the continental XI Region, Chile. PhD Thesis. Queen's Univ. At Kingston, Canada, 413 p.

# REMOBILIZATION OF ZN AND PB FROM THE PALEOZOIC BASEMENT A SOURCE OF MINERALIZATION AT EL FALDEO DISTRICT, CHILEAN PATAGONIA: GEOCHEMICAL AND ISOTOPIC EVIDENCES

**Carlos PALACIOS M., Alfredo LAHSEN A., Miguel PARADA R. and Susana MAGRI**

Department of Geology, Universidad de Chile. P.O. Box 13518, Correo 21, Santiago, Chile. FAX 56-2-696-3050

**KEY WORDS:** Zn - Pb Mineralization, Geochemistry, Isotope, Chilean Patagonia.

## INTRODUCTION

The El Faldeo district is located in the Patagonian precordillera of Aysen, Chile (72°20'W-47°27'S). The purpose of this paper is to discuss the source of the Zn and Pb mineralization using geochemical and isotopic evidences.

## GEOLOGY OF THE DISTRICT

The oldest rocks in the district are upper Paleozoic schists, phyllites, quartzites, shales, and marbles. These rocks are unconformably overlayed by a 200 m thick upper Jurassic sequence of felsic tuffs and lavas (Ibañez formation). The rocks are intruded by a dacitic intrusive-efusive complex which consists of brecciated stocks, sills and felsic tuffs. In turn, these rocks are intruded by tonalitic to dioritic stocks and dikes dated at 151 Ma (Palacios et al., 1996a). The rocks in the district are pervasively altered and the primary mineral components are obscured by alteration.

## MINERALIZATION AND HYDROTHERMAL ALTERATION

Hydrothermal alteration in the district is widespread affects entirely the Paleozoic and Jurassic rocks and covers approximately 12 $Km^2$. In the district, two types of mineralization have been recognized (Palacios et al., 1996b): Au-Ag epithermal and Zn-Pb mesothermal mineralization, constituting the last one the focus of our studies. Basic metals mineralization consists of irregular pipe-like bodies of 100 to 200 m in diameter containing stockwork and dissemination of pyrite, arsenopyrite, sphalerite, and Ag-bearing galena. Mineralization is hosted by Jurassic volcanic and intrusive rocks, which present sericitic alteration. A propylitic and silicic halo surround the mineralized bodies. Ore grades varies from 2 to 8% Zn, 0,4 to 3% Pb, and 10 to 100 ppm Ag. Although the mineralization in the Paleozoic rocks is restricted only to few veinlets, the ore and alteration mineralogy is similar to those exhibit by Jurassic rocks. Fluid inclusions data indicate ore deposition during boiling at homogenization temperature varying between 250° to 330°C, and salinities ranging between 4 and 23wt% NaCl equiv.

## GEOCHEMISTRY OF THE PALEOZOIC ROCKS

Table 1 show the statistic behaviour of Zn and Pb (analyzed by ICP) in 250 chip samples of Paleozoic rocks. In general the curves exhibit 2 break-points defining 3 different populations, which can be interpreted as negative, background,and positive anomalies respectively.

**TABLE 1.-** Statistic populations of Zn and Pb, defined using log-probabilities analysis

| Elements (ppm) | Negative anomaly | Background | Positive anomaly |
|---|---|---|---|
| Zn | < 30 | 30 - 140 | > 140 |
| Pb | < 25 | 25 - 130 | > 130 |

Samples of the background population are unaltered rocks, which were taken far from the district. They probably represent the normal concentration of Zn and Pb of the Paleozoic rocks. In contrast to the former, the samples that lie within the anomalous population were taken from altered rocks in the district. Samples of the negative anomaly correspond to unmineralized rocks that mainly present propylitic alteration. Mineralized samples with sericitic alteration form the positive anomaly population. Correlation coefficients of the elements considered in this analysis range between 0.72 and 0.89 in each population. These results suggest that Zn and Pb were leached from the Paleozoic rocks during propylitic alteration, and probably the elements were reconcentred in the sericitized and mineralized rocks.

## ISOTOPIC GEOCHEMISTRY

Sulfur isotope data from sphalerite separates exhibit $\delta^{34}S$ values between 1.0 to 2.8 per mil. The data support that the $H_2S$ in the hydrothermal fluid was derived from two sources: sulfate leached from the basement marine sediments and magmatic emanations (Ohmoto and Skinner, 1983; De Ronde and Blattner, 1988). Lead isotopic data from galena separates define a field above the orogenic growth curve in both uranogenic and thorogenic diagrams (Fig. 1). The position of this field could reflect a lower crust (Godwin et al., 1988) - upper crust mixing, indicating that the source of Pb had low U/Pb and Th/Pb ratios.

Isotopic data on Jurassic dioritic to tonalitic stocks evidence Sr87/Sr86 ratios of 0.706951 and 0.708203, and $\varepsilon$Nd of -2.9 and -3.7 suggesting an important crustal contribution (Parada et al., 1996).

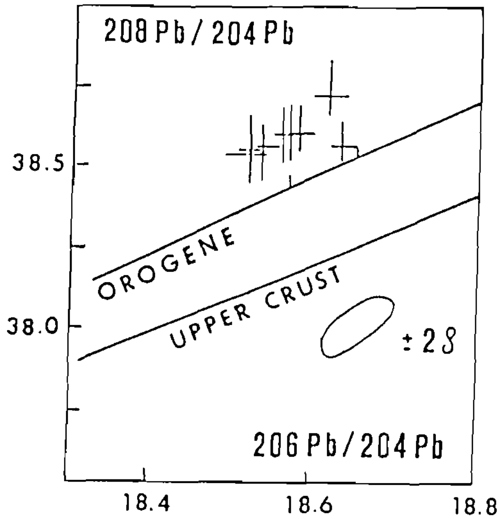


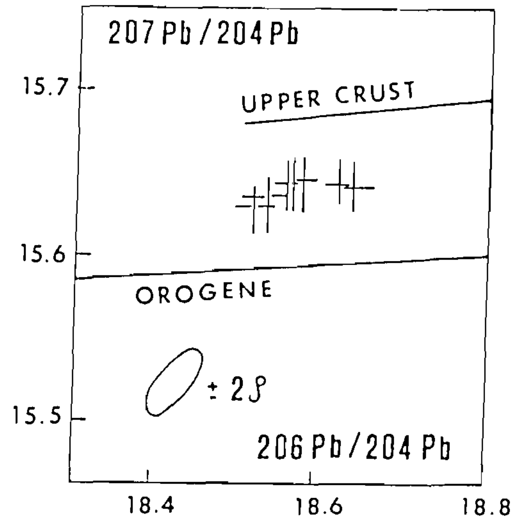


**Fig. 1.-** Uranogenic and thorogenic diagrams showing the lead isotopic data from galena separates.

## REFERENCES

**De Ronde, C.E.J., and Blattner, P.** 1988. Hydrothermal alteration, stable isotopes, and fluid inclusions of the Golden Cross epithermal gold-silver deposit, Waihi, New Zealand, Econ. Geol., 83, 859-917.

**Godwin, C.I. Gabites, J.E., and Andew, A.** 1988. Lead Table: A galena lead isotope data base for the Canadian cordillera. Mineral Resources Division. Geol. Survey of Canada, Paper 1988-4, 188 p.

**Ohmoto, H. and Skinner, B.J.** 1983. The Kuroko and related volcanogenic massive sulfide deposits. Introduction and summary of new findings. Econ. Geol. Monograph 5, 1-8.

**Palacios, C.M., Parada, M.A., and Lahsen, A**. 1996a. Upper Jurassic Au-Zn mineralization in El Faldeo district, Chilean Patagonia. Internal Report.

**Palacios, C.M., Lahsen, A.A., and Parada, M.A.** 1996b. Metallogenic belts in the Chilean Patagonia, between 44° and 48°S. Third International Symposium on Andean Geodynamics. This volume.

**Parada, M.A., Palacios, C.M. and Lahsen A.A.,** 1996. Geology, geochronology and tectonic evolution of the El Faldeo Au-Zn district in the Chilean Patagonia. Third International Symposium on Andean Geodynamics. This volume.

# GEOLOGY, GEOCHRONOLOGY AND TECTONIC EVOLUTION OF THE EL FALDEO Au-Zn DISTRICT IN THE CHILEAN PATAGONIA

Miguel A. PARADA, Carlos PALACIOS and Alfredo LAHSEN

Departamento de Geología, Universidad de Chile, Casilla 13518 correo 21, Santiago, Chile.

**KEY WORDS:** Patagonian Andes, tectonic, geochronology, Au-Zn mineralization.

## INTRODUCTION

The El Faldeo Au-Zn district is the southernmost Andean prospect, and is located in a Recent back-arc position, about 100 km east of the axis of the Patagonian Andes at 47°27'S - 72°20'W. Two segments of the Patagonian Andes have been recognized on the basis of structure and magmatic configuration (Ramos and Kay, 1992). The El Faldeo district is located in the southern segment, which differs from the northern one by the presence of extensive exposures of deep-seated Paleozoic metamorphic basement, a foreland fold and thrust belt, a gap in the Recent volcanic arc, Tertiary molasse deposits and Upper Cenozoic plateau basalts. The origin of the segmentation is attributed to the Miocene to Recent collision of the Chile ridge with the trench at about 46°30'S.

The discovery of the El Faldeo mineralization was recently made (Lahsen et al., 1994) as a result of a base and precious metal exploration project in the Chilean Patagonia. The mineralization is mainly hosted in dacitic and rhyolitic tuffs and subvolcanic porphyries (Palacios et al., 1996), and consists of early epithermal (140° - 170°C) gold mineralization and late Zn mineralization deposited at higher temperatures (250° - 330°C) and greater depth (op. cit.). This paper provides a case study of a metallic district in the modern Patagonian back-arc, where the integration of field, radiometric and geochemical data, led to the recognition of its tectono-magmatic evolution on a regional scale and its metallogenic implications.

## GEOLOGY OF THE DISTRICT

### Stratigraphy

The oldest rocks in the district are polymetamorphic and poyideformed schist, phyllites, quartzites, shales and marbles of the Paleozoic basement (Fig. 1). These rocks are unconformably overlain by an Upper Jurassic homoclinal sequence (N80°E - N80°W/20 - 30N) of sedimentary and volcanic beds, which represents the lowest 200 m of the Ibáñez formation. This sequence occupies two discrete depositional centers and consists from bottom to top of a 50 m thick basal sedimentary breccia and 150 m thick seccession of dacitic and rhyolitic tuffs, felsic lavas, hydrothermal eruption breccia and their sedimentary reworked equivalents. Two intrusive units are recognized in the district: Quebrada Colorada Granodiorite (QCG) and Cordón Esmeralda Tonalite (CET). The former unit is the more extensive and consists of epizonal granodioritic bodies intruding the Ibáñez formation as plutons, sills and dikes. Strong to moderate hydraulic brecciation is a striking feature of most of the QCG exposures. The CET is composed of hornblende-bearing tonalites and diorites, which form two plutons and some related sills and dikes. The CET plutons intrude the Paleozoic metamorphic basement, the Ibáñez formation and the QCG. Their shapes and orientations are clearly controlled by N-S and NW-SE faults.

### Petrography of the Ibáñez formation and associated intrusive units

The basal sedimentary breccias of the Ibáñez formation are polymictic, formed by abundant (> 80 vol.%) fragments of schist, quartzite and phyllite of the Paleozoic basement, in a clay matrix. The fragments are both poorly sorted, and rounded, and have sizes variable between 2 and 10cm. The upper sedimentary beds are composed of breccias formed mainly of reworked tuffs, hydrothermal breccias and silicified igneous rocks similar to those outcroping in the district. The fragments are moderately sorted, have centimetric to decimetric sizes and are included in a fine-grained to medium-grained clastic matrix (5-20%), which in places is cemented by barite. The igneous rocks of the district are, in most cases, pervasively silicified and locally argillized, and therefore, primary minerals and textures can be observed in only few remnants. The dacitic and rhyolitic tuffs exhibit variations in grain size from lapilli to ash. Clasts consist of felsic pumice, volcanic rocks and crystal fragments of quartz and feldspar. Rocks of the QCG contain plagioclase, quartz, uralitic amphiboles, biotite, sphene and apatite. The hydraulic fracturing and brecciation that affected the plutons and sills of this unit, gave rise to stockworks or breccias with abundant (> 90%) angular, randomly rotated, granodioritic fragments with a scarce matrix of powdered rock. The CET rocks show an equigranular intergrowth grading to a porphyric texture. The primary mineralogy is partially propylitized and consists of plagioclase, quartz, amphibole, biotite, K-feldspar, magnetite, apatite and zircon.

**Mineralization and hydrothermal alteration**

The mineralization and hydrothermal alteration of the El Faldeo district developed in four stages (Palacios, et al., 1996), and affected about 12 km2 of Upper Jurassic rocks. Propylitic replacement of primary paragenesis and disseminated mineralization of pyrite characterize the first stage. The second stage gave rise to silicic alteration and to dissemination and veinlets of pyrite, arsenopyrite and gold. Brecciation, stockwork and dissemination were associated with a quartz - sericite - calcite alteration and with pyrite, sphalerite, galena and gold mineralization. The last stage is an open-space filling event, in which quartz, calcite, barite, pyrite and chalcopyrite were deposited. The above mentioned structures of the mineralization and alteration associated with the first three stages, suggest a progressive rupture of the host rocks.

## U-Pb, $^{40}$Ar-$^{39}$Ar, K-Ar AND FISSION TRACK AGES

Four zircon fractions from a sample of the CET were prepared for conventional multigrain U-Pb geochronologic analysis. They have discordant U-Pb ages that lie in an array parallel to concordia (Fig. 2). Regressing the U-Pb data results in a chord which intersects concordia at 147 ± 10 Ma, and is interpreted to indicate a late Jurassic crystallization age for the sample. $^{40}$Ar-$^{39}$Ar biotite dating of two samples of the two CET plutons exhibit well-defined weighted mean plateau ages (Fig. 3) of 157.7 ± 1.5 and 158.9 ± 1.5 Ma. K-Ar whole rock dating of two pervasively sericitized samples gave ages of 140 ± 4 and 142 ± 5 Ma. These similar ages are indicative of rapid cooling of the magmatism - alteration - mineralization system at a shallow crustal level. Two apatite mineral separates from CET have been analyzed using the fission track dating technique. Fission tracks ages of the samples are 7 ± 4 and 14 ± 4 Ma.

## STRUCTURAL AND TECTONIC SETTING

The most important structures in the district are steeply dipping faults, which in general strike NW-SE, N-S and ENE-WSW (Fig. 1). The NW-SE faults are continuously traceable for about forty kilometers. Shear-sense indicators such as horizontal slickensides and grooves are locally observed, suggesting dextral strike movements. The N-S and the ENE-WSW faults are normal, and most of the dikes and veins were emplaced along them.

The presence of separate depositional centers in the Ibáñez formation, and its thickening and inclination towards the ENE boundary faults, indicate that these faults were active during sedimentation giving rise to a half graben array (Fig. 1). The fault-controlled distribution of the Ibáñez sequence, plutons, dikes and veins, suggests a coeval formation of tectonic basins and spaces for magma emplacement and mineralization. The post-basement units are bounded by linear NW-SE transform segments and N-S and ENE-WSW normal faults, as is expected to occur in a pull-apart basin model in which simultaneous strike-slip movements and extension subparallel to the strike of the transform takes place (Ben-Avraham and Zoback, 1992).

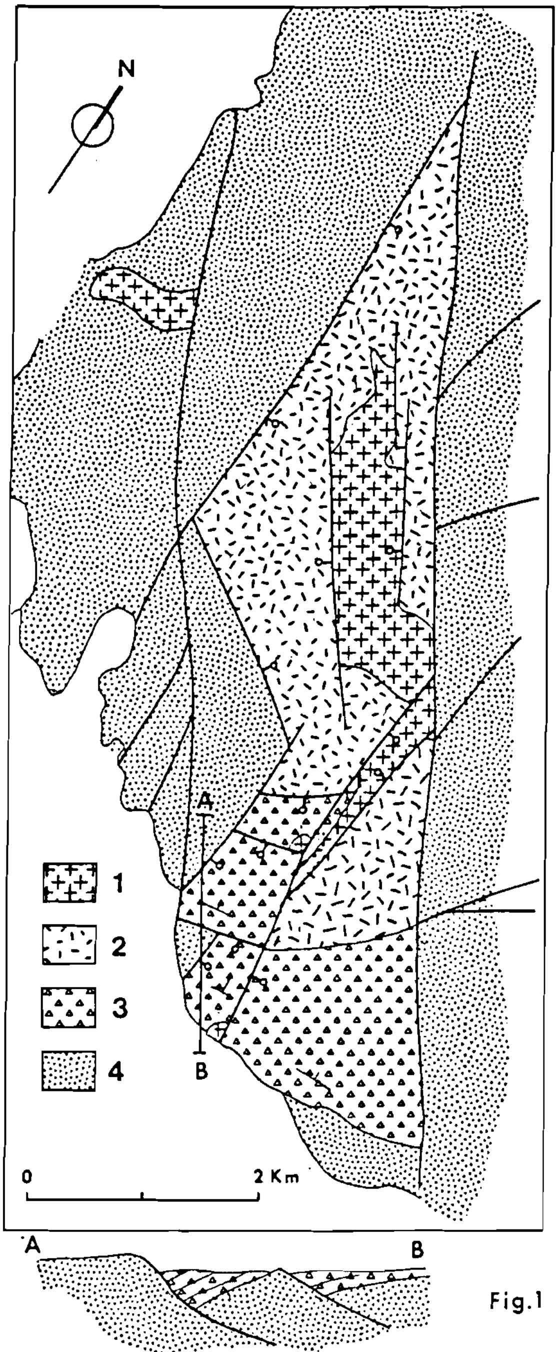


Fig.1

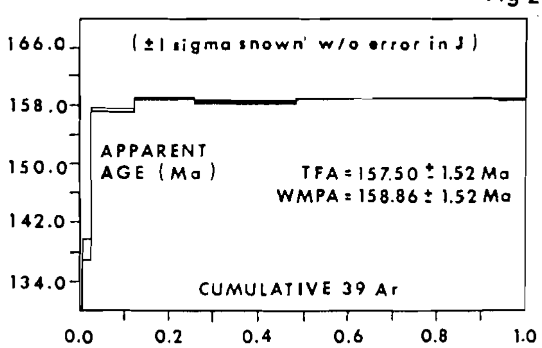


Fig.2

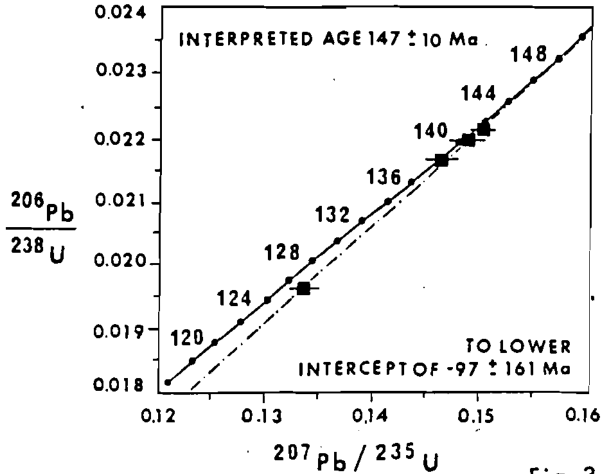


Fig. 3

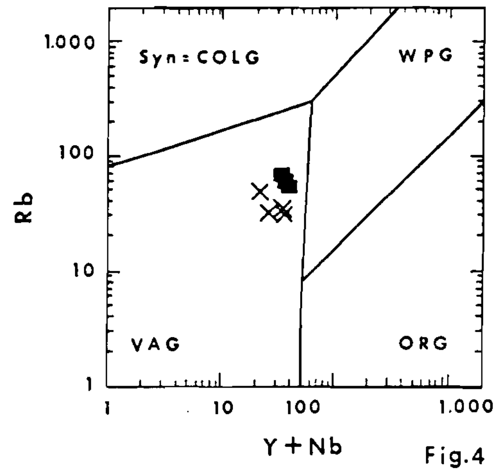


Fig.4

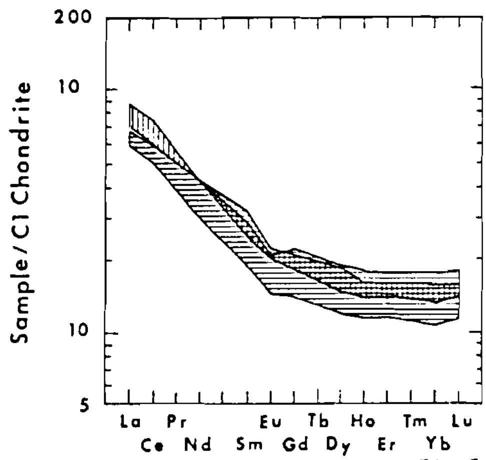


Fig.5

The greater exposure of igneous rocks than sedimentary rocks in the El Faldeo district, indicates that magma supply exceeded sedimentation rate. An effect of the subsidence - filling of the basins is the common presence of sills intruded by vertical dikes forming part of the same magmatic event. Such an intrusive relationship is an indication that sufficiently thick magmatic and sedimentary overburden was present to produce a change of the least principal stress from vertical to horizontal. It is worth noting that the magmatic pressure must exceed the least principal horizontal stress and the tensile strength of the rock cover in order to form discordant intrusions.

A few samples of the CET were geochemically and isotopically analyzed. They exhibit volcanic arc signatures (Fig. 4) and REE patterns similar to typical subduction-related Upper Cenozoic tonalites of the North Patagonian Batholith (Fig. 5). They have $Sr^{87}/Sr^{86}$ ratios of 0.706951 and 0.708203 and $\varepsilon$Nd of -2.9 and -3.7 suggesting an important crustal contribution in the formation of the CET.

## METALLOGENIC IMPLICATIONS

The integration of field, radiometric, geochemical and isotopic data, constrains the alteration - mineralization of the El Faldeo district to an Upper Jurassic extensional arc regime associated with dextral strike-slip and related subsiding pull-apart basin. The results highlight the close links between tectonism, magmatism and mineralization, in which the continental crust made a significant contribution to the origin of both the magmas and the mineralization. Subsidence - filling and coeval mineralization may explain the higher temperature and depth of the late mineralization stage as compared to the earlier one. Release of progressively higher volatile pressure would have been necessary to produce the increase in the degree of rupture of the rocks hosting the mineralization, from veinlets in the first stage, to hydraulic brecciation in the third stage.

The El Faldeo district was preserved at depth for an interval of about 140 m.y. after which the uplift and erosion caused by the Chile ridge - trench collision, brought it to the present position in Late Miocene time.

## REFERENCES

Ben-Avraham, Z. & Zoback, M.D. 1992. Transform-normal extension and asymmetric basins: An alternative to pull-apart models. Geology, 20, 423 - 426.

Lahsen, A., Palacios, C., Parada, M. A., Sánchez, G., Townley, B. & Villegas, J. 1994. Exploración Geoquímica Estratégica en la Regiôn de Aisén. Iternal Report, Departamento de Geología, Univ. de Chile, 367 p.

Palacios C., Parada, M. A. & Lahsen, A. (1996). Upper Jurassic Au-Zn mineralization in the El Faldeo district, Chilean Patagonia. Internal Report, Departamento de Geologia, Univ. de Chile, 33p.

Ramos, V. & Kay, S. 1992. Southern Patagonian plateau basalts and deformation: backarc testimony of ridge collisions.Tectonophysics, 205, 261 - 282.

## LEGEND OF FIGURES

Fig. 1. Geological sketch of the El Faldeo district. 1: Cerro Esmeralda Tonalites (CET). 2: Quebrada Colorada Granodiorites (QCG). 3: Ibáñez formation. 4: Paleozoic metamorphic basement.

Fig. 2. A portion of the concordia diagram showing the U-Pb isotopic data for a CET sample.

Fig. 3. Age spectrum measured on biotite from the same sample as figure 2.

Fig. 4. Rb vs. Y + Nb discriminant diagram for CET samples (crosses). Upper Cenozoic granitoids of the Northern Patagonian Batholith (squares) are also shown for comparison.

Fig. 5. Ranges of chondrite-normalized REE patterns of CET samples (horizontal hatch) and Upper Cenozoic granitoids of the Northern Patagonian Batholith (vertical hatch).

# ORIGIN OF SULFATE IN THE SALAR DE ATACAMA AND THE CORDILLERA DE LA SAL, INITIAL RESULTS OF AN ISOTOPIC STUDY

Baruch SPIRO(1) and Guillermo CHONG(2)

(1) NERC Isotope Geosciences Laboratory, Keyworth, Nottingham, NG12 5GG U.K.

(2) Departamento de Geosciencias, Universidad Catolica del Norte, Antofagasta, Chile.

KEY WORDS: Salar, evaporites, isotopes, sulfur, strontium

## INTRODUCTION

Salars occur in inland basins in the arid zones throughout South America from near-shore areas to the Altiplano. The origin of salts in the salars can be attributed to oceanic input as described for example for SW Australia (Chivas et al. 1991), or to a volcanic source. While the distribution of evaporites can be modified by subsequent dissolution-precipitation episodes, triggered by exposure of evaporitic deposits to weathering due to uplift. The Salar de Atacama in Northern Chile located about 200 Km from the Pacific coast at an altitude of 2300m with ridges of up to 3000m elevation in between, provides an excellent setting to adress the problem. Moreover the adjacent Cordillera de la Sal located to the west of the Salar contains a thick section of evaporites in the San Pedro Formation deposited in the Oligocene and deformed during the Miocene (Naranjo et al. 1994), provides a comparison to test wehether or not the same sources and processes were active at that time.

The present reconnaissance study uses the isotopic composition of sulfur and strontium as tracers for the origin of sulfate in the waters feeding the Salar de Atacama, the currently forming evaporitic deposits, and those exposed in the Cordillera de la Sal.

## RESULTS

Water samples were collected from springs and wells to the north and east of the Salar de Atacama and within the salar itself, locally with the associated evaporites. The variation in chemistry of the water (not further discussed here) bears evidence to the complexity of the hydrological system. Several evaporite samples were collected along a transect across the San Pedro Formation in the Cordillera de la Sal.

The isotopic composition of the water ($\delta^{18}O$ and $\delta D$) was determined in order to characterise the fluids associated with the transportation of the solutes of interest. The copositions range between -8.7, -64.1 and +5.9 and -1.7‰ for $\delta^{18}O$ and $\delta D$ respectively. The lower values fall on the Global Meteoric Water Line and the variations between samples are probably due mainly to differences between recharge areas. The higher values form an array which indicates evaporation under low humidity conditions.

The sulfur isotope results ($\delta^{34}$SCDT) of the dissolved sulfate are in the range 3.4 to 7.0‰ and show no relation to the concentrations of dissolved sulfate or chloride. These values are lower than those of sea water sulfate throughout the Phanerozoic (e.g. Claypool et al. 1980). The initial $\delta^{34}S$ of the dissolved sulfate seems to be determined by that of the SO2 emitted by volcanoes and subsequently modified by leaching of the volcanic rocks. The two values recorded from evaporites within the Salar (4.3 and 5.4‰) are within this range. The $\delta^{34}S$ of the Cordillera de la Sal sulfates have a range 3.0 to 5.4‰ i.e. in the lower part of the range of the present day dissolved sulphate.

Strontium isotope ratios ($^{87}Sr/^{86}Sr$) recorded from the water samples are in the range 0.70755 to 0.70980, which in general correspond with values recorded from the volcanic rocks in the adjacent volcanoes. The values recorded from the Cordillera de la Sal (0.70681 to 0.70799) are in part lower than those of dissolved sulfate and corresponds to the values measured in the nearby Codillera Domeyko (Pankhurst, unpublished). The lowest ratios are recorded in the water of the San Pedro de Atacama spring where the spring waters are flowing next to the exposed evaporites of the Cordillera de la Sal and at Reine near the southern end of the salar ($^{87}S/^{86}Sr$ of 0.70760) where the spring waters pass Cretaceous limestones with $^{87}Sr/^{86}Sr$ of 0.70775. All the values recorded are lower than the 0.70910 ratio of present day ocean water. These ratios seem to relate to the ratios of the bedrocks with which the solutions come in contact

## CONCLUSIONS

The waters draining into the Salar de Atacama have isotopic compositions ($\delta^{34}S$ and $^{87}Sr/^{86}Sr$) indicative of igneous origin of the respective solutes.

The evaporites of the San Pedro Formation in the Cordillera de la Sal have similar $\delta^{34}S$ and lower $^{87}Sr/^{86}Sr$ ratios, in line with change in bedrock which is or was in contact with the fluids.

The isotopic composition of species dissolved in waters currently draining into the Salar de Atacama, in evaporitic minerals precipitating from these waters or of evaporitic minerals deposited during the Oligocene, do not support the hypothesis that seawater is the main source of solutes for the Salar de Atacama nor did it contribute significantly to the Oligocene evaporites of the Cordillera de la Sal.

These results and conclusions have implications on the assessment of sources of salinity in arid zones.

REFERNCES

Chivas A.R. Andrew, A.S. Lyons W.B. Bird M.I. and Donnelly T.H. 1991. Isotopic constraints on the origin of salts in Australian Playas, 1. Sulphur. Paleogeogr. Paleoclimatol., Paleoecol., 84 309-332.

Claypool G.E. Holser W.T., Kaplan I.R. Sakai H. and Zak I. 1980. The age curves of sulfur and oxygen isotopes in marine sulfate and their mutual interpretation. Chem. Geol. 28 199-260.

Naranjo J.A. Remirez C.F. and Peskoff R.1994. Morphostratigraphic evolution of the northwestern margin of the Salar de Atacama basin (23°S-68°W). Revista Geologica de Chile 21 91-103.

# PARENTAL BRINE EVOLUTION IN THE CHILEAN NITRATE DEPOSITS (Pedro de Valdivia, II Región de Antofagasta). MINERALOGICAL AND PETROGRAPHIC DATA

Marta VEGA[1], G. CHONG[1] and Juan J. PUEYO[2].

[1] Departamento de Ciencias Geológicas. Universidad Católica del Norte. Avda.Angamos, 0610. Casilla 1280. Antofagasta.
[2] Facultat de Geología. Universitat de Barcelona. Zona Universitaria de Pedralbes. 08028 Barcelona .

**KEYWORDS:** nitrates, iodates, saline minerals, paragenesis, porosity, brine evolution.

## INTRODUCTION

The Chilean nitrate deposits have been formed by complex paragenesis of saline minerals (locally named *caliche*) that infill the porosity of rocks ranging in age from Paleozoic to Cenozoic. Minerals which are normally extremely rare - nitrates, nitrate-sulphates, iodates and iodate-sulphates - are common in the Chilean nitrates. Located in the Atacama Desert (North Chile; between 19°30' and 25°30' S latitude, and 69°30' and 70°30' W longitude), the deposits follow an irregular N-S swathe, a few km wide (reaching a maximum of several tens of km). The distribution of the deposits parallels the contact between the Coastal Range and the Central Depression.

The nitrate (and saline) ores can infill either cracks (joints, fractures) in the country rocks (volcanic, intrusive or sedimentary), porosity in breccias and conglomerates from alluvial fans and pediments, or porosity created by previous alteration processes. Ericksen (1981) divided the different styles of occurrence as *deposits in rock* and *sedimentary deposits*. Deposits in rock are characterized by

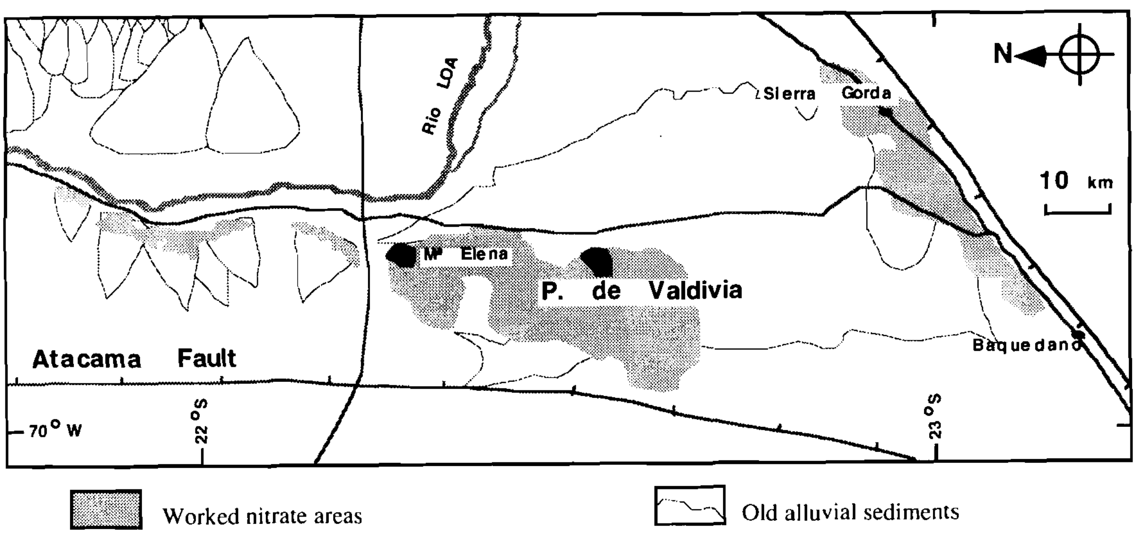


**Fig. 1.** Distribution of worked nitrate areas in the Pedro de Valdivia area. See the relationships between the nitrate deposits and tertiary alluvial sediments on the NW alluvial fans.

open fracture systems, and so can reach high local concentrations in sodium chloride and nitrate. Sedimentary deposits are characterized by narrow pore spaces, commonly millimetre-scale or smaller.

The Pedro de Valdivia deposit is located 160 km to the NNE of Antofagasta (22°45' S, 69°40' W), close to the centre of the area in which nitrate occur, in the Chilean Central Depression. It extends over a width of about 15km, and is elongated 40km in the N-S direction (Fig. 1). The altitude is 1500m on average, the topography being very uniform (±200m). The geological setting (Araya & Toro, 1983) is dominated by volcanic and intrusive rocks. The volcanic sequence is Jurassic (350m of andesitic flows -*La Negra Formation*), Cretaceous? (150m of acid piroclastic tuffs and breccias), Paleocene-Eocene (150m of tuffs and ignimbrites), Miocene (alluvial clastic and volcanoclastic rocks -bearing the nitrate-ore; Fig.1-) and finally (overlying in angular discordance the previous materials) Quaternary unconsolidated alluvium and colluvium. Intrusives are represented by mesozoic granites and monzodiorites, and cenozoic acid porphyries. The fault system has a dominant N-S trend, with subordinate trends to about N40E and E-W. Nitrate ores occur within the Miocene sediments (*caliche negro*) and are also present as disseminations (and infilling voids) in the sustrate rocks (*caliche blanco*) (Chong, 1991, 1994). The ore (running at less than 11% $NO_3$) can reach depths of 10m, more commonly being less than 3m deep.

## PETROGRAPHY AND PARAGENETIC RELATIONSHIPS

SEM, optical mineralogy and XRD have been used to identify the minerals (Table 1) in the Pedro de Valdivia deposit.

**Table 1**

| | | |
|---|---|---|
| *Chlorides:* | Halite | $NaCl$ |
| *Sulphates:* | Anhydrite | $CaSO_4$ |
| | Bloedite | $Na_2Mg(SO_4)_2.4H_2O$ |
| | Glauberite | $Na_2Ca(SO_4)_2$ |
| | Gypsum | $CaSO_4.2H_2O$ |
| | Löweite | $Na_{12}Mg_7(SO_4)_{13}.15H_2O$ |
| | Polyhalite | $Ca_2MgK_2(SO_4)_4.2H_2O$ |
| | Starkeyite | $MgSO_4.4H_2O$ |
| | Thenardite | $Na_2SO_4$ |
| *Carbonates:* | Calcite | $CaCO_3$ |
| *Nitrates:* | Nitratine | $NaNO_3$ |
| | Niter | $KNO_3$ |
| | Darapskite | $Na_3[NO_3SO_4].H_2O$ |
| | Humberstonite | $K_3Na_7Mg_2[(NO_3)_2(SO_4)_6].6H_2O$ |
| *Borates:* | Kaliborite | $KMg_2H[B_6O_8(OH)_5]_2.4H_2O$ |
| | Probertite | $NaCa[(B_5O_7)(OH)_4].3H_2O$ |
| *Iodates:* | Lautarite | $Ca(IO_3)_2$ |
| | Hectorfloresite | $Na_9[(IO_3)(SO_4)_4]$ |
| | Fuenzalidaite | $K_6(Na,K)_4Na_6Mg_{10}(SO_4)_{12}(IO_3)_{12}.12H_2O$ |
| *Chromates:* | Dietzeite | $Ca_2[(IO_3)_2CrO_4]$ |
| *Oxides:* | Hematites | $Fe_2O_3$ |
| *Silicates:* | Quartz, heulandite, laumontite. | |

The petrographic study shows that interstitial processes (Chong & Pueyo, 1992) are the main control on mineralisation in both kind of deposits (*sedimentary* and *in rock*). In the Pedro de Valdivia area these processes are principally controled by the composition of the volcanic host rock and the strongly saline solutions from which the ore minerals precipitate.

The precipitation sequence and arrangement of minerals is as follows:

a) Submillimetre-scale fissures in a silicate host mineral showing a first generation of halite in the walls and a central infilling of nitratine or, sometimes, mixtures of saline minerals (halite, nitratine, darapskite). Ocassionally, the first salt generation is euhedral to subhedral.

b) Residual porosity in the saline precipitate itself, forming geodes, where halite and nitratine coprecipitate. Geode cavities develop in a mass formed by the silicate matrix and saline minerals (halite, nitratine, humberstonite, darapskite). Halite and nitratine represent the last interstitial precipitates. Euhedral iodates (lautarite, hectorfloresite, and fuenzalidaite) and borates (probertite) coprecipitate in the residual porosity.

c) Subcentimetre-scale fissures in the host rock, infilled by a first generation of zeolite (commonly heulandite or laumontite), followed by another generation of coarse sparry calcite. This sequence can be recurrent, each couplet being separated by dissolution surfaces. Both minerals, zeolite and calcite, are present as mm-size cristals. A final zeolite generation is followed by sulphate mineral precipitation (anhydrite, glauberite). Moreover, the rock shows fissures between, around, and inside the grains, following exfoliation planes. These fissures, μm in size, are total or partially infilled by anhydrite, glauberite, halite or nitratine.

d) Porosity almost totally obliterated by saline materials, where the last generation is nitratine. Nitratine infills previous voids between halite, glauberite, and silicate matrix. Nitratine exhibits abundant inclusions and triple junction voids. A sequence of minerals (nitratine between halite grains, and niter, lautarite, dietzeite, hectorfloresite and fuenzalidaite within nitratine) which precipitate in these voids represent the last stages of evolution of the residual brine.

e) Submillimetre-scale fissures in the host rock, infilled by the sequence polyhalite (fibrous radiated), anhydrite, and nitratine. Other irregular porosities are infilled by euhedral, μm-size bloedite (or löweite) and, finally, nitratine.

Other frequently associated minerals are darapskite-nitratine (or -humberstonite) and löweite-bloedite. K-Mg minerals (fuenzalidaite-niter-polyhalite-(sylvite?)) frequently form an association with each other, and also with nitratine or nitratine-halite boundaries. Euhedral tabular kaliborite (μm-size) has been observed in cavities between humberstonite grains.

## BRINE EVOLUTION INFERENCES

A synthesis of the precipitation sequences, deduced from petrographic observation, is presented in Figure 2.

The general evolution of brines is as follows:

1) A first precipitation of Ca-bearing minerals (Ca-zeolites - calcite - anhydrite).

2) A group of Na-Ca and Na-Mg (-K) minerals (glauberite - bloedite - polyhalite), defining two main evolutionary trends: a) A Na-trend, represented by the series glauberite - darapskite - (halite - nitratine) - hectorfloresite; and b) A Na-Mg-K trend represented by the series bloedite - (polihalite) - humberstonite - (halite - nitratine) - fuenzalidaite.

The final minerals, which precipitate in the residual porosity, are nitrate-sulfates, iodate-sulfates, iodates, chromates and borates. Commonly these minerals precipitate in the last stages of brine evolution, when (or after) halite and nitratine coprecipitate. These minerals include elements that either are not compatible with previously precipitated minerals, or have not previously been consumed.

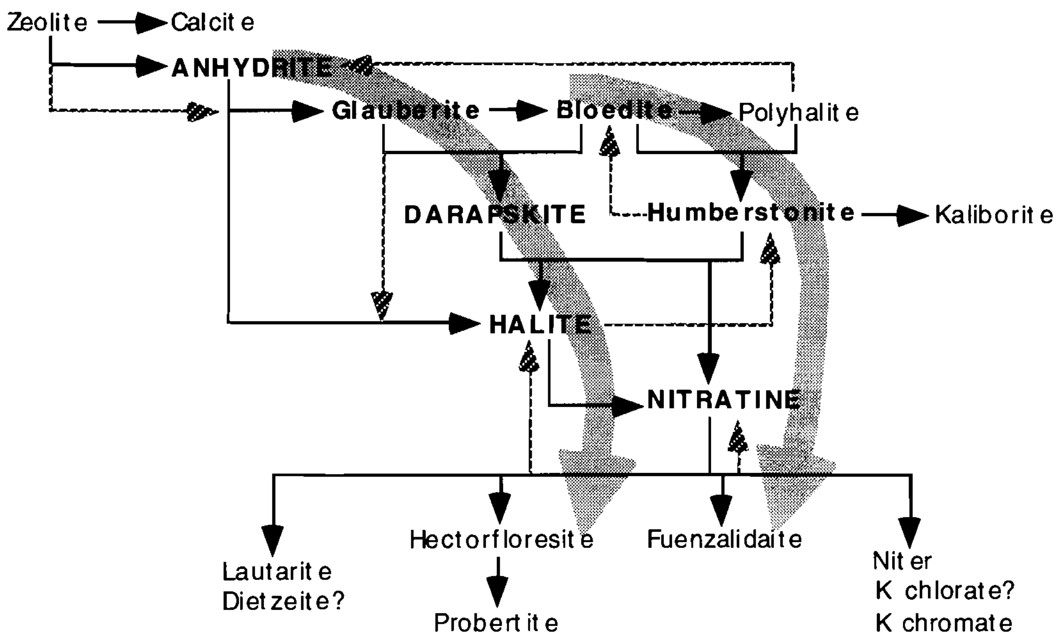


**Fig. 2.** Synthetic diagram of parental brine evolution in the Pedro de Valdivia deposit. The main paragenetic relationships are indicated in solid lines. The main general trends are marked by thick hatched arrows.

**Acknowledgments.** This work was enabled by EC contract n: CI1*-CT94-0069 (DG 12 HSMU). It was also supported by a grant of the Fundación Andes (Chile) (ref. C-12777/4; 2ª etapa 1995). Analytical work (SEM and XRD determinations) were performed in the Scientific-Technical Surveys division of Barcelona University.

## REFERENCES

Araya, H. and Toro, J.C. 1983. *Geología de los yacimientos de Pedro de Valdivia y María Elena. II Región, Chile.* Universidad del Norte, Depto. Ciencias Geológicas. Memoria de título inédita.

Chong, G. 1991. Geología de los Yacimientos de Nitratos de Chile. Antecedentes para establecer una teoría sobre su génesis. In: *Génesis de formaciones evaporíticas. Modelos andinos e ibéricos* (Pueyo, J.J., Ed.). Publicaciones de la Universidad de Barcelona: 377-415.

Chong, G. 1994. The nitrate deposits of Chile. In: Tectonics of the Southern central Andes. Structure and evolution of an active continental margin (K.J. Reutter, E. Scheuber & P.J. Wigger, Eds.). Springer, 303-316.

Chong, G. and Pueyo, J.J. 1992. Mineralización y tipos de yacimientos de nitratos y yodo. Norte de Chile. *Actas del VIII Congreso Latinoamericano de Geología* (Salamanca, 22-26 Junio 1992). Tomo 4, Petrología y Geoquímica: 173-178.

Ericksen, G.E. 1981. Geology and origin of the chilean nitrate deposits. *U.S. Geological Survey, Prof. Paper* 1188, 37 pp.

# PROCESSUS DE SURFACE / GEOMORPHOLOGIE
# SURFACE PROCESSES / GEOMORPHOLOGY
# PROCESOS DE SUPERFICIE / GEOMORFOLOGIA

# PALEOENVIRONMENT EVOLUTION IN THE BOLIVIAN ANDES DURING THE UPPER PLEISTOCENE

Jaime ARGOLLO (1) & Philippe MOURGUIART (2)

(1) Instituto de Investigaciones Geológicas, P.O. Box 12198, La Paz, Bolivia.
(2) Misión ORSTOM, P.O. Box 9214, La Paz, Bolivia.

**KEY WORDS**: (Andes, Bolivia, Paleoenvironment, Lacustrine, Glaciation).

## INTRODUCCION

The Bolivian Altiplano (3650-3900 masl), is situated en the heart of the Andes (66-71° long. West, 14-22° lat. South), between Eastern and Western branchs, which surpass the 6000 masl (figure 1)

Nowdays, the lacustrine extensions (Titicaca, Poopó, Coipasa and Uyuni) are the result of the pluviometric gradient, very stepped, from the Norhteast (Eastern Cordillere, Lake Titicaca basin) to the Southeast of the Altiplano (Western Cordillera, Uyuni salines basin); the yearly precipitation change from 800 mm to 200 mm, while the estimate evaporation would vary from near 1500 mm per year in the North to near 2000 mm at the South (Roche et al., 1992; Grsjean, 1994). These climatic gradients are consecuences of the latitude displacement of the Interpropical Convergence Zone.

## METHODS AND RESULTS

We had analized several kinds of registers, aiming to reconstruction the paleoenvironment scenarios; the registers were from big geomorphologic units of the Altiplano: the Titicaca lake, the southern basins and the chain valleys.

In the Titicaca lake, the sedimentological study of the TD1 sample of 5.4 meters long (figure 1), and the radiocarbonic date give us two kinds of information, related to the temperature and the high of the water level at the time when the sediment was settled. The lower part of the sample (540-200 cm) characterize lower lacustrine levels. The mean atmospheric temperature, rebuilt from the palinologic data, is 3.5°C to 4°C lower to the actual temperature; and has a period of deep freezing (-6°C) between 20 000 and 19 000 years BP. There is an important hiatus at 200 cm of the sediment, which correspond to near 18 000 to 15 000years BP. This hiatus is synonymous of a very hard drought. From 200 to 155 cm (15 000 to 18 000 years BP). Neither the palinologic data nor the lower sediment index permit us to be precise at mark the maximun level reached by the lake in that time, nor limit its radiometric age, which is around 13 180 ± 130 years BP. Aparently, this has happened simultaneously with the so called Tauca phase (Servant & Fontes, 1978). The temperatures are lower than today (-2°C). The existence of gypsum indicates the dryness of the Huiñaimarca lake at the end of this period (Wirrmann & Oliveira Almeida, 1987). from 155 to 10 cm, the paleodepths are rebuilt from a tranference function of ostracodes/bathymetry values (figure 2) Mourguiart et al., 1992). from 10 to 0 cm, the absense of ostracodes cannot allow to rebuilt quantitatively the evolution of the lake levels.

The deposits distribuited along the perimeters of the main basins in the South (Poopó, Coipasa and Uyuni) are completely different. They show essentially as carbonated sediments, clayly or limely. In the figure 3 appear the rates age/high. The ages were fixed by dating of organism and carbonated deposits (molluscs, vegetal bioherms and microcrystalline crust). The Tauca phase extended from 14 000 to 10 500 years BP. While during this humid phase, there were hydric balance with oscilations of great magnitude.

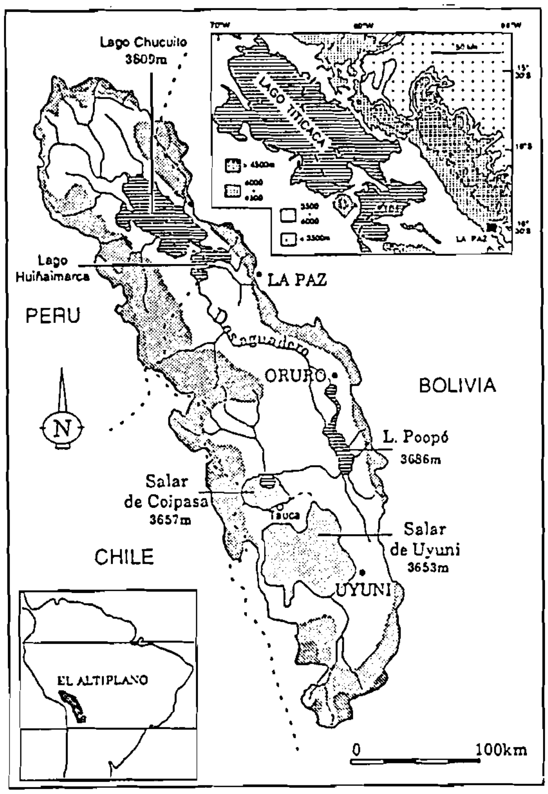


Figure 1: The Altiplano. Location of the cordilleras, lakes, and salines. The site of sampling TD1 is marked in the Huiñaimarca lake.

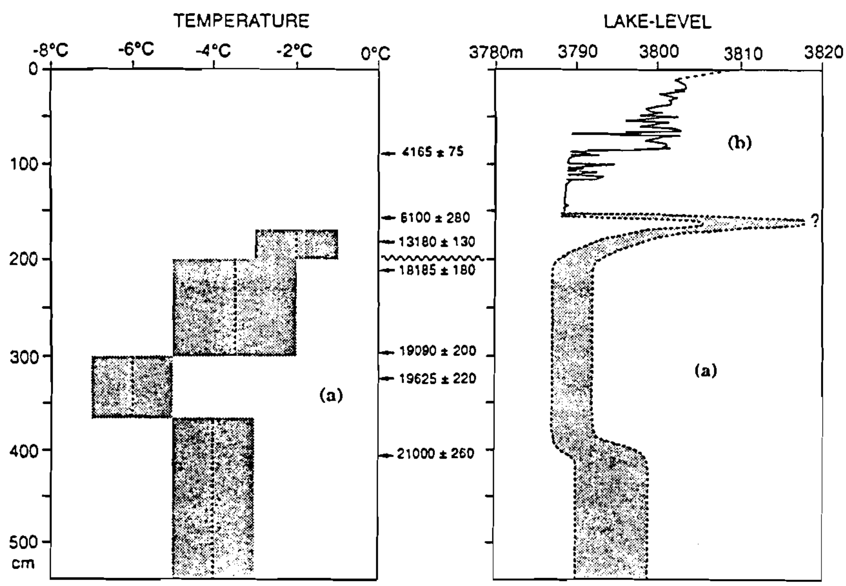


Figure 2. The reconstruction of the paleoclimatology and paleohydro'ogy of the Huiñaimarca lake (sonde TD1). The shadowed are the rebuilt from data analysis of the palinomorfes (Ybert, 1992). The continuos line in graph at right represents the results from the transference function ostracodes/water depth (Mourguiart et al., 1992).

The traces of forewent glaciations and diverse kind of flowings that happen in the time were identified by radiocarbon dating. We find five groups of moraines (figure 4). they are called: M1a, chronologically situated after 23 000 years BP; M1b, which is after 14 300 years BP and is considered as the last maximun glacier in the Bolivian Andes; M2, with unknow precise chronological position; M3, dated to be before 10 500 and 10 000 years BP, seems to be sinchronic with the Younger Dryas; M4, which correspond to the Little Ice Age, period of the centuries XVI to XIX ( Thompson et al., 1986).

## CONCLUSIONS

The paleoenvironment evolution of the Bolivian Altiplano from aproximately 30 000 years BP, is fairly complex. Anyway it can be described as folows:

-From 25 000 to 18 000 Years BP, progressive dryness of the Titicaca lake. It would correspond to the final phase of the Minchin lake. An advance of the M1a glacier around 19 000 years BP.
- From 18 000 to 14 500 years BP, there is no information neither at the North nor the South of the Altiplano. The climate phase was dry.
- From 14 500 to 10 500 years BP, is the lake Tauca phase, with an advance of the glaciers (moraines M1b, M2, M3).
- From 10 500 to 8000 years BP a new dryness of the Titicaca lake and a quick recease of the glaciers.
- From 8000 to 3900 years BP, a little improvement in the water balances of the Titicaca lake.
- From 3900 years BP to ? a notorious rise of the lake levels, but with dry phases, shorts but important.
- From ? to nowadays, the Little Ice Age (moraine M4) and the actual period are characterized by a complex evolution of the lakes and glaciers.

## REFERENCES

Bills, B.G., de Siva, S.L., Currey, D.R., Emenger, R.S., Lillquist, K.D., Donnellan, A. & Worden, B. 1994. Hydro-sostatic deflection and tectonic tilting in the central Andes: Initial results of a GPS survey of lake Minchin shorelines. Geophysical Research Letters, 21 (4), 293-296.

Mourguiart, Ph., Wirrmann, D., Fournier, M. & Servant, M. 1992.Reconstruction quantitative des niveaux du petit lac Titicaca au cours de l'Holocene. C.R. Acad. Sci. Paris, serie II, 315: 875-880.

Servant, M. Fournier, M., Argollo, J., Servant-Vildary, S., Sylvestre, F., Wirrmann, D. & Ybert, J.P. 1995. La derniere transition glaciaire/interglaciaire des Andes tropicales sud (Bolivia) d'après l'etude des variation des niveaux lacustres et de fluctuations glaciaires. C.R. Acad. Sci. Paris, serie IIa 320: 729-739.

Thompson, L.G., Mosley-Thompson, E.P., Dasgaard, W. & Grootes, P.M. 1986. The Little Ice Age as recorded in the stratigraphy of the Quelcaya ice cap. Science, 234, 361-364.

Wirrmann, D. & Oliveira Almeida, L.F. 1987. Low Holocene level 7700 to 3650 years ago of lake Titicaca (Bolivia). Palaeogeography, Palaeoclimatology, palaeoecology, 59, 315-323.

Ybert, J. P. 1992. Ancient lake environments as deduced from pollen analysis. in: lake Titicaca. A syntesis of Limnological Knowledge (C. Dejoux & A. Iltis eds.): 49-60, Monogr. Biol., 86, Kluwer Academic Publishers.

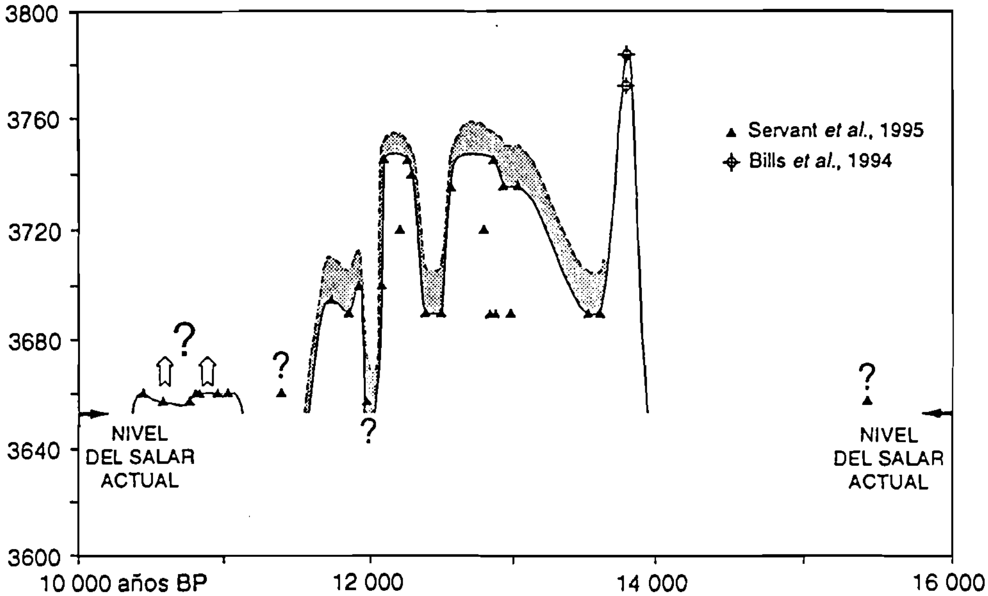


Figure 3. Projected dates from the salines zones versus the high of the sampling site. The wide line correspond to a minimum level of the lake; the two dating on the narrow line correspond to a shore line. The question marks point out isolated dates to be confirmed.

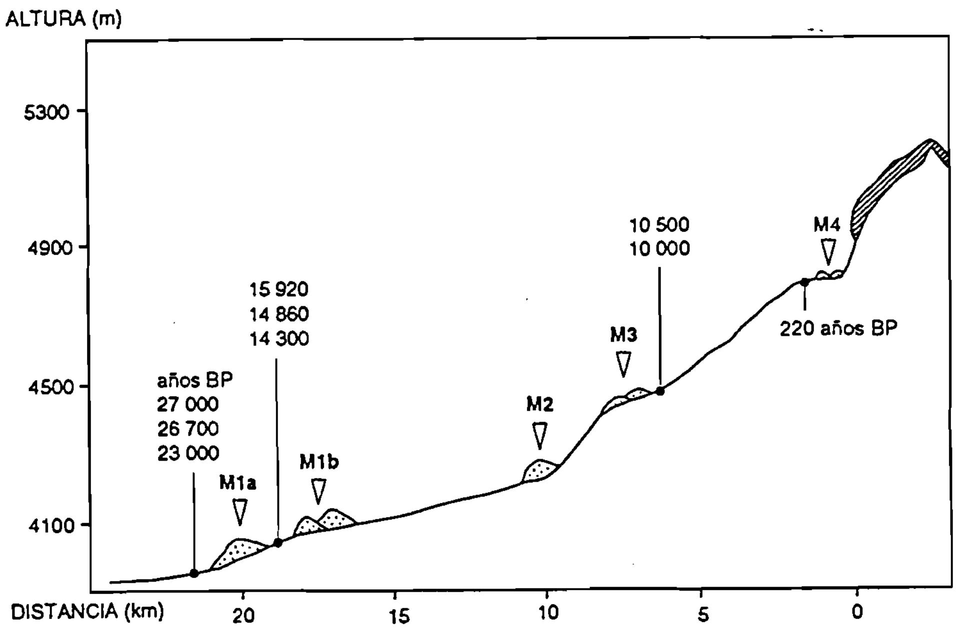


Figure 4. Draw showing the location of the moraines relative to the today's glacier front and the estimate age. The distances are given only in an indicative mode.

# TECTONIC AND CLIMATIC CONTROL OVER THE GEOMORPHOLOGICAL EVOLUTION OF THE CHILEAN MARGIN BETWEEN 36° AND 38° S

Umberto FRACASSI

Department of Geology, Royal Holloway, University of London, Egham, Surrey TW20 0EX, U.K.

**KEY WORDS:** airborne imagery, neotectonics, morphological controls, margin dynamics

## INTRODUCTION

The active margin of central Chile is a remarkable feature of the Pacific rim (Aguirre, 1985; Dalziel, 1986; Hervé et al., 1987, Mordojovich, 1974; see figure; Cicco, 1994). To develop an aerophotogrammetric approach of its geology, a study has been conducted to frame the subduction processes belonging to a margin with an alternate tectonic history and relatively shallow seismic foci (Barazangi, 1976) that drove to look for tangible evidences within the surface structures.

The investigation was aimed at the local morphologies observed using airborne imagery in the Gulf of Arauco. Also, from the detected features, the study has subsequently addressed those large- and medium-scale structures produced by the evolution of the margin (Aguirre, 1985; Hervé et al., 1987, Jordan et al., 1983).

Notably, this work has focused on the two-way link existing between the morphological evolution of a turbulent area such as the one herewith described and the relatively deeper phenomena close to the crust-atmosphere interface (Barazangi, 1976; Jordan et al., 1983). Such interaction may show up with a substantial influence on the landscape setting.

Morphotectonic maps arising from the study of the available aerial stereo-imagery are herewith presented, to display the five main geomorphological domains observed. The phenomena described are in most cases ongoing, when not in their infancy (Kaizuka et al., 1974).

## CONCLUSIONS

The morphotectonic evolution of the VIII Chilean region is heavily influenced by two basic factors. The tectonic framework, both past and present, is active and it actively shapes the drainage pattern. As opposing to this constraint, the wind action is such to condition distribution of continental sedimentation and river discharge (Thornburg, Kulm and Hussong, 1990).

The present tectonic setting displays a N-S fault system which generated the Arauco graben west of the Coastal Cordillera. Swarms of lineations and faults are bound NE-SW and displace the western rim of the N-S graben. The lithologies thus exposed govern the abrupt morphology of the foot wall in the grabens.

The activity of the wind, from SW towards NE, is witnessed by the vigourous erosion due to the Pacific wavesets, by extensive dune fields and by the control over the drainage pattern, especially in flat

Location Map

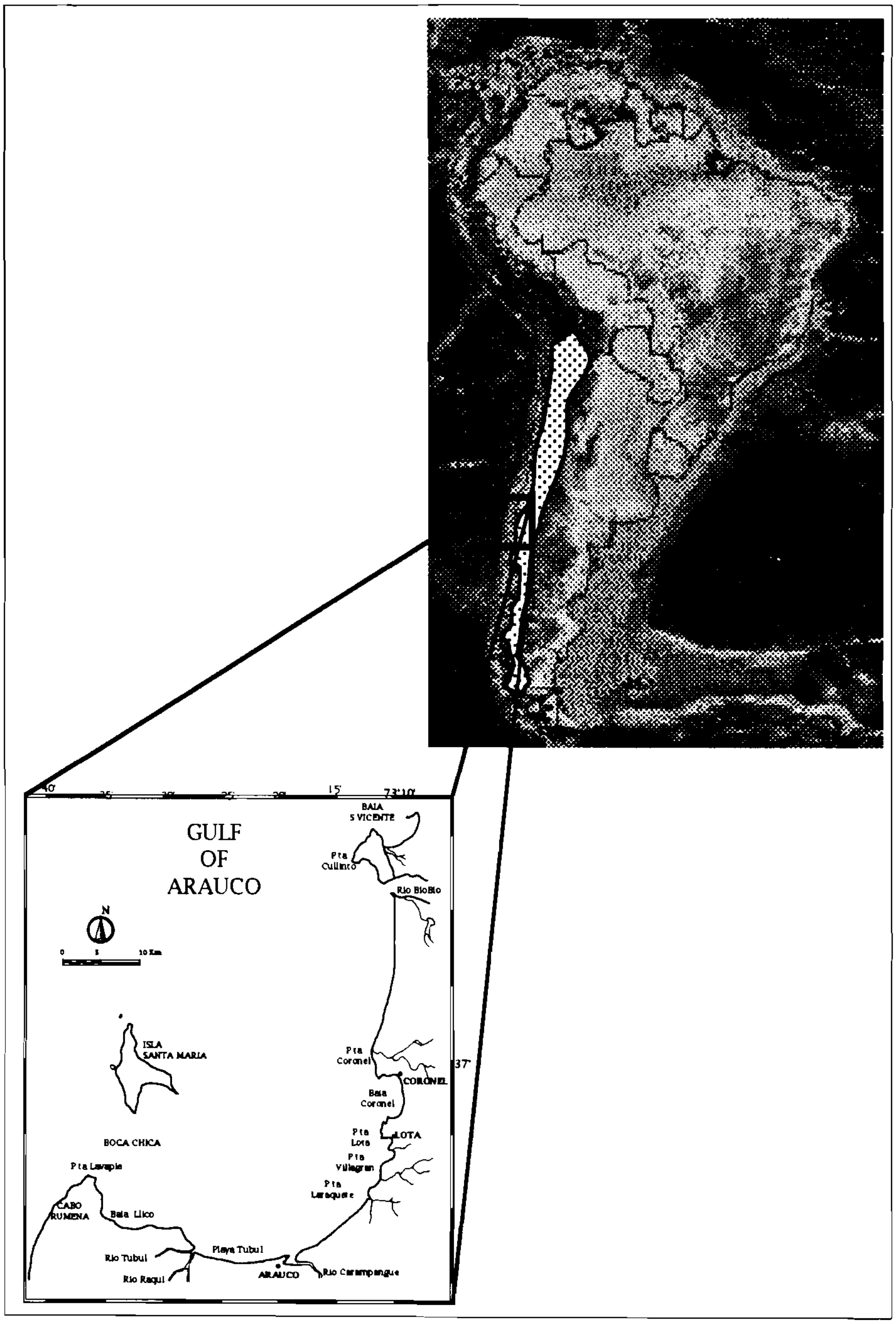

areas and nearby the shoreline. In several cases, rivers are forced by the tectonic pattern to flow shorebound, whereas the action of the wind pushes the streams landwards.

As a result of this steady interaction, a morphotectonic element is deemed to be caused. The system is composed by the N-S graben, the western promontory displaced by the NE-SW faults and the following pocket beach, open towards SW. Conversely, the displaced promontory is exposed to erosion; the pocket beaches get the reworked and redeposited material being transported northwards alongshore.

On a regional scale, the above system is envisaged to be repeated several times along the Chilean margin, from 20° to 40° S (Armijo and Thiele, 1990), and a remarkable example of such system is represented by the Gulf of Arauco (37° S).

## REFERENCES

Aguirre L., 1985, The Southern Andes, in: Nairn A.E.M., Stehli F.G. and Uyeda S. (eds.), The Ocean Basins and Margins, Plenum Press, pp. 265-360

Armijo R. and Thiele R., 1990, Active faulting in northern Chile: ramp stacking and lateral decoupling along a subduction plate boundary?, Earth and Pl. Sc. Lett., 98, pp. 40-61

Barazangi M. and Isacks B.L., 1976, Spatial distribution of earthquakes and subduction of the Nazca plate beneath South America, Geology, 4, 11, pp. 686-692

Cicco L.N., 1994, Caratteri ed evoluzione degli ambienti marini e costieri del margine continentale della VIII Regione Cilena, Ph. D. Thesis, Environmental and Marine Sciences Consortium amongst the Universities of Trieste, Genova and Urbino (Italy)

Dalziel I.W.D., 1986, Collision and Cordilleran orogenesis: an Andean perspective, in: Coward M.P. and Ries A.C. (eds.), Collision Tectonics, Geol. Soc. of London Spec. Publ. # 19, pp. 389-404

Hervé F., Godoy E., Parada M., Ramos V., Rapela C., Mpodozis C. and Davidson J., 1987, A general view on the Chilean-Argentine Andes, with emphasis on their early history, in: Monger J.W.H. and Franchetau J. (eds.), Circum-Pacific Orogenic Belts and Evolution of the Pacific Ocean Basin, Amer. Geoph. Union Geodyn. Series # 18, Intern. Lithosph. Prog. Publ. # 0132, pp. 97-113

Jordan T.E., Isacks B.L., Allmendinger R.W., Brewer, J.A., Ramos V.A. and Ando C.J., 1983, Andean tectonics related to geometry of subducted Nazca plate, Geol. Soc. of Amer. Bull., 94, 3, pp. 341-361

Kaizuka S., Matsuda T., Nogami M. and Yonekura N., 1973, Quaternary Tectonic and Recent Seismic Crustal Movements in the Arauco Peninsula and its Environs, Central Chile, Geogr. Rep. Tokyo Metrop. Univ., 8, pp. 1-38

Mordojovich K., C., 1974, Geology of a Part of the Pacific Margin of Chile, in: Burk C.A. and Drake C.L. (eds.), The Geology of Continental Margins, Springer-Verlag, pp. 591-598

Thornburg T.M., Kulm La V.D. and Hussong D.M., 1990, Submarine-fan development in the southern Chile Trench: A dynamic interplay of tectonics and sedimentation, Geol. Soc. of Amer. Bull., 102, 12, pp. 1658-1680

# LATE-GLACIAL AND HOLOCENE TEPHROSTRATIGRAPHY AND ENVIRONMENT AS RECORDED IN THE LAGUNA SALINAS, SOUTH PERU

Etienne JUVIGNE[(1)], Jean-Claude THOURET[(2)], Alain GOURGAUD[(3)], and Kurt GRAF[(4)]

(1) FNRS, Université de Liège, Dept. Géographie Physique, Start-Tilman B12, 4000 Liège, Belgium.
(2) ORSTOM (UR14)-Instituto Geofisico del Peru, La Molina, Lima 100, Peru.
(3) CRV-URA 10-CNRS, Dept. Géologie, Université Blaise Pascal, 5 rue Kessler, 63000 Clermont-Ferrand, France.
(4) Geographisches Institüt, Zürich Universität, 8057, Zürich, Switzerland.

KEY WORDS : Laguna Salinas, saline lake, tephrostratigraphy, Late Glacial, Holocene

The Laguna Salinas, an undrained basin in the Central Andean Volcanic Zone, lies at 4300 m in elevation on the Western Cordillera (16°22'S, 71°08'W, 4,300 m, Southern Peru: Fig. 1A,B). The Laguna is a saline playa, termed *salar*, which has acted and still acts as a sedimentary trap. The flat floor of the *salar* is occupied by a shallow saline lake 35 km$^2$ in area, in the western part of the basin 12 km across. The volcano-tectonic basin is open in upper Tertiary lava flows, overlain by volcaniclastic sediments Pleistocene in age. The Laguna Salinas is surrounded by high, extinct stratovolcanoes such as Pichu Pichu to the West and South, which have been heavily glaciated. Front moraines end at about 4500 m in elevation and glacial outwash has formed fans that are overlain by lacustrine and palustrine deposits towards the *salar*. Within 50 km distance from the basin, the Misti, Ubinas, and Huaynaputina stratovolcanoes have been active for the past five centuries (Fig. 1B).

Seven tephras are recorded in this area since the end of the Last Glacial, when glaciers melted away. Two groups of tephras were recognized, the first in two quarries to the West of the Laguna Salinas, the second in two cores drilled in the salar (section sites in Fig. 1C).

To the West, the pyroclastic sequence observed along the Arequipa-Puno road encompasses 4 tephras (from top to base, sections a and b, Fig. 1D): (1) the 10-cm-thick white ash fall T.H., dacitic in composition, from Huaynaputina volcano; (2) a 65-cm-thick, white coarse Plinian pumice-fall, T.P.1, andesitic in composition; (3) a 40-cm-thick pumice and lithic-rich tephra-fall, T.P.2, andesitic in composition; (4) a 135-cm-thick Plinian pumice-fall, T.P.3, dacitic in composition; (5) a 25-cm-thick yellowish lithic-rich pumice-fall, T.P.4, andesitic in composition. A few thin eolian deposits and poorly developped soils in ash are interbedded in these tephra-fall deposits, suggesting that the fallout occured repeatedly, precluding long-lasting episodes of quiescence in the area. Interestingly, this pyroclastic sequence is missing on the formerly glaciated high-plateau to the East and NE.

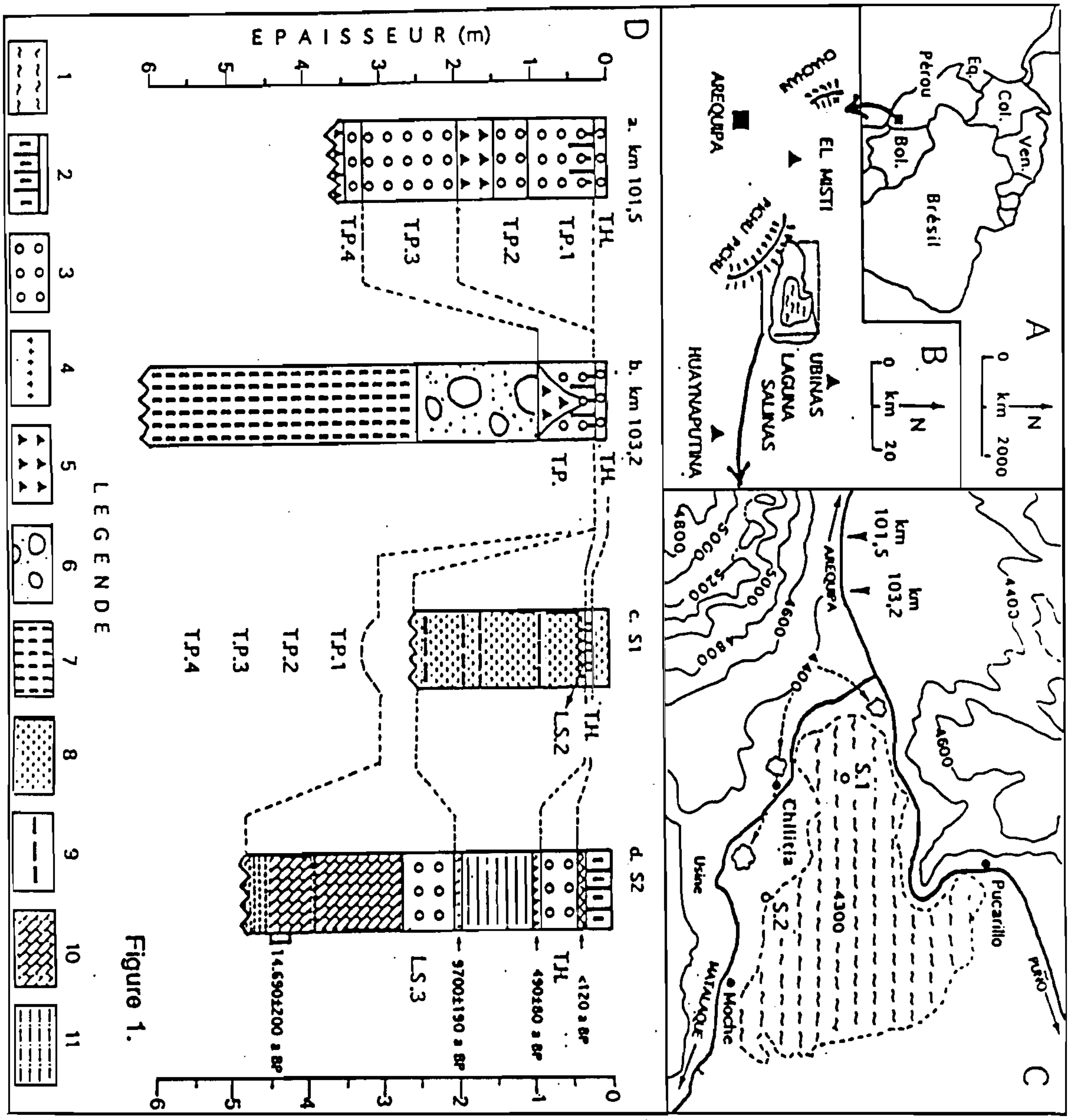


Location of Laguna Salinas (A and B) and coring sites (C). Description of studied sequences (D): a) road Arequipa-Puno, road-cut at km 101.5; b) road Arequipa-Puno, km 103.2, pit; c) S1, core taken with a "russian corer"; d) S2, core taken with a "russian corer". Abbreviations of tephra beds: T.H., Huaynaputina Tephra; LS.2, Laguna Salinas Tephra 2; LS.3, Laguna Salinas Tephra 3; T.P.1 to 4, pumiceous tephra beds 1 à 4, at km 101.5 (road Arequipa-Puno); T.P., pumiceous tephra at km 103.2 (road Arequipa-Puno).

Two cores were drilled in the southern part of the *salar*, the first in the upper lacustrine deposits (S1, Fig. 1C and section c, Fig. 1D) and the second in the palustrine deposits (S2, Fig. 1C and section d, Fig. 1D). The sequence of the second core S2 corresponds to the last 15,000 years, although the drilling was blocked by an unidentified coarse layer. The 4.7-m-thick S2 core includes 3 tephra-fall layers interspersed in thick peat or gyttja and salt: (1) the 50-cm-thick white ashfall TH from Huaynaputina, dacitic in composition (whose thickness has been exaggerated by runoff); (2) a black, scoriaceous, fine ash layer 5 mm thick, LS2 (section c, Fig. 1D), olivine-bearing andesitic in composition; (3) a 70-cm-thick pumice and ashfall deposit, dacitic in composition.Four $^{14}C$ datings (section d, Fig. 1D) and tephrostratigraphy in the Misti-Huaynaputina area allow us to correlate and rank the three tephras in a time frame. The dacitic TH tephra belongs to the A.D. 1600 Plinian fallout of Huaynaputina. The black scoriaceous, andesitic ashfall was delivered by El Misti at A.D. 1440-1480, based on the time span and rate of peat sedimentation between TH and LS2, and correlated to historical accounts. The third thick pumice fallout is slightly older than 9700 ± 190 yr B.P., i.e., at the transition between Late Glacial and lower Holocene.

Correlation with the pyroclastic sequence along the Puno road (Fig. 1D) shows that the coarse tephra-fall deposits T.P.1 to T.P.4, missing in the cores, are to be found below the radiocarbon dated peat layer at 14,690 ± 200 yr B.P., i.e., before the Late Glacial period. However, the tephras TP1, TP2, and TP3 are probably placed close to the end of the Last Glacial period when the glaciers melted away, while the tephra TP4 may be contemporaneous with that period. Conversely, the lowermost tephra ≥ 9700 yr B.P. old in the core is missing in the pyroclastic sequence to the West of the Laguna Salinas : it has been either eroded away or removed in eolian deposits and soils.

Polen analysis has been carried out on the second core at 200 to 400 cm in depth (section d, Fig. 1D). Based on $^{14}C$ datings, this part of the core corresponds to the Late Glacial. The polen record shows that the paleovegetation was uniform: steppe graminae (Poaceae), cushion plants (Caryophyllaceae) and shrub (Asteraceae) prevailed. Such a steppe vegetation point to arid to semi-arid climate in that area throughout the Late Glacial. Evaporation and drought increased or decreased according to temperature fluctuations, a fact that explains the observed changes in the polen record.

We distinguish two phases with distinct environments. The Salinas I phase (Late Glacial) is characterized by a *tolar* vegetation in the *puna* vegetation, i.e. dwarf trees (*Asteraceae*), *Polylepis*, and a few graminae which point to a cold and semi-arid climate (less dry than that prevailing today). The Salinas II phase (transition from Late Glacial to lower Holocene) reflects a drier environment including graminae from desert steppe (*Poaceae*), alike that of the dry altiplano today. The vegetation was poor and the climate very dry. The transition between Salinas I and II occurs close to 280 cm in depth and may represent the Late Glacial-Holocene boundary.

## Reference

Juvigné E., Thouret J.-C., Gilot E., Gourgaud A., Graf K., Leclercq L., Legros F. et Uribe M. 1996. Téphrostratigraphie et environnement tardiglaciaire enregistrés dans la Laguna Salinas, Pérou méridional. Soumis à *Géographie Physique et Quaternaire* (Canada).

Laguna Salinas
16°24'S/71°9'W, 4300 m
Kurt Graf

Figure 2.

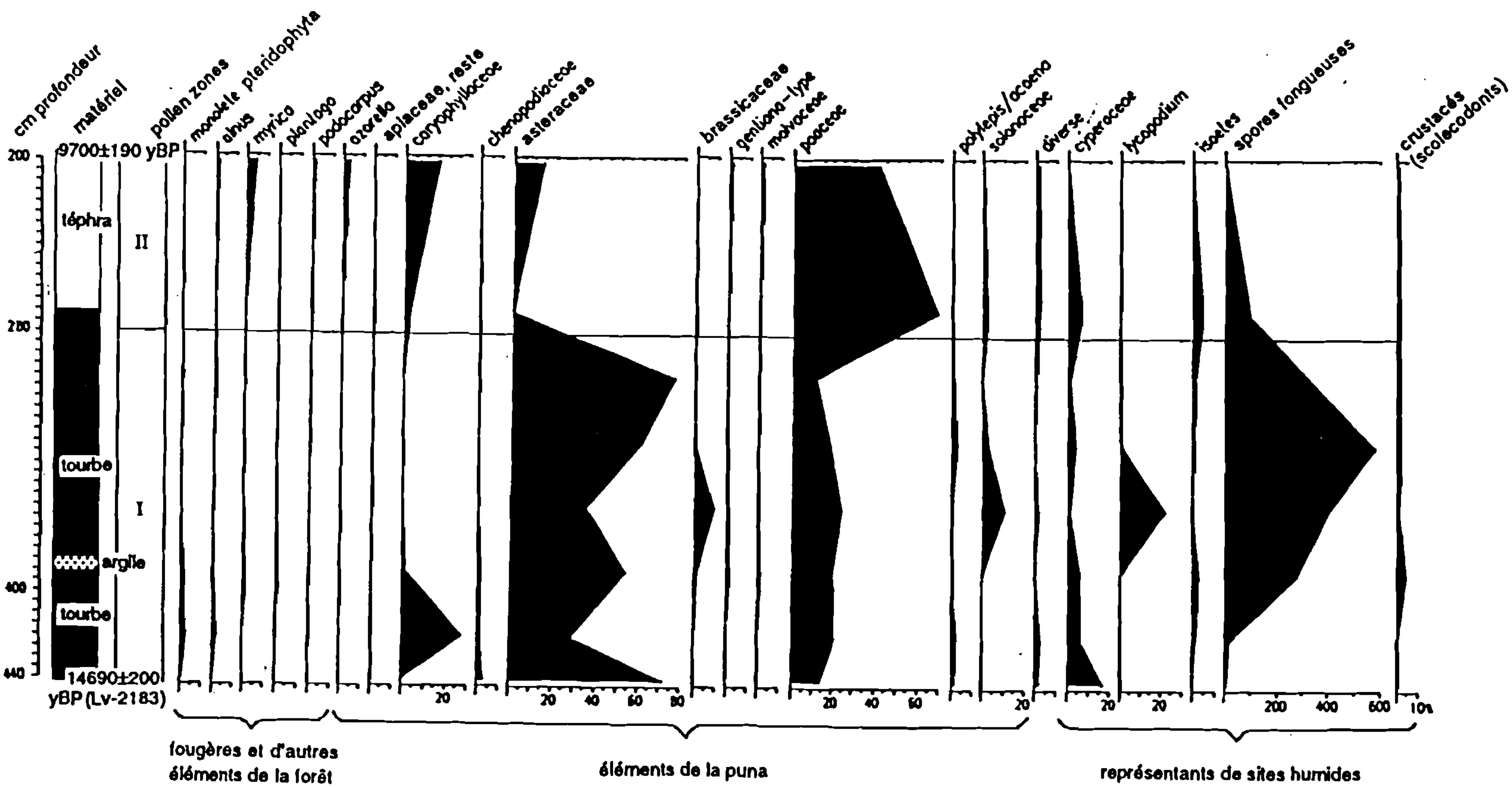


Pollen diagramme of the peat sequence 200 to 440 cm (depth) of core S2.

# ON THE USE OF REMOTE SENSING FOR THE MAPPING OF TWO TERTIARY VOLCANIC FORMATIONS OF THE SW OF CUENCA (WEST ANDES OF ECUADOR)

Gérard LAUBACHER [1] and Annick LEGELEY-PADOVANI [2]

(1) ORSTOM - ESPOL, Apartado Postal; 5963, Guayaquil, Ecuador
(2) ORSTOM, Lab. Géophysique, 32 avenue H. Varagnat, 93143 Bondy Cedex, France

**KEY WORDS** : automatic mapping, Landsat TM, Tertiary and Quaternary volcanic, SouthEcuador

## INTRODUCTION

Since Oligocene, the Andes of Ecuador are caracterized by an calcalcaline volcanic arc related to the subduction of the Pacific plate beneath the continental margin of the Andes. In southern Ecuador, emplacement chronology and modalities of this volcanism remain badly constrained. However, published radiometric data (Kennerley, 1980; Barberi et *al.*, 1988; Lavenu et *al.*, 1992) evidence several volcanic pulses, ranging from Oligocene to Early Pliocene. Large volcanic deposits, named Tarqui Formation, are considered of latest Pleistocene (Bristow & Hoffstetter, 1977). However, it seems that most of this outcrops are older, Pliocene to Pleistocene, and in some cases Miocene in age.

### 1 - Study area and methods of analysis

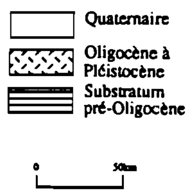


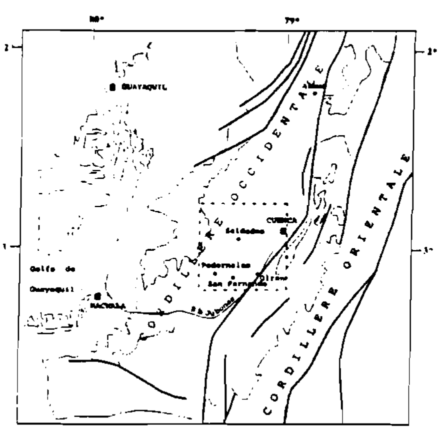


**Figure 1** : Situation of the study zone Quaternay, Oligocene to Miocene, Pre-Oligocene

The aim of the present work is to cartography volcanic deposits previously assigned to the Tarqui Formation (Baldock, 1982) from the southwestern Cordillera of Ecuador using satellitel data and field control (fig. 1).

We define as "Pedernales Formation", the oldest terms of this deposits that we consider to be of Pliocene to Pleistocene in age and, as "Quimsacocha volcanism" the younger terms made of overlying dacitic and andesitic lava-flows of a an eroded and poorly conserved volcanic crater.

The spacial data we used are extract from a Landsat TM scene of 7 bands adquiered the 02/03/1990 at 14hrs49mn05sec TU and we applied :

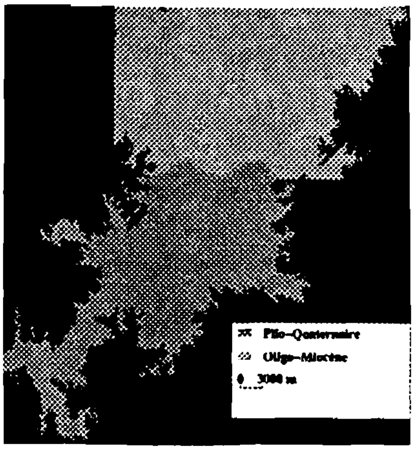


**Figure 2** : Mapping of the Oligo-miocene and Plio-Quaternay volcanisms

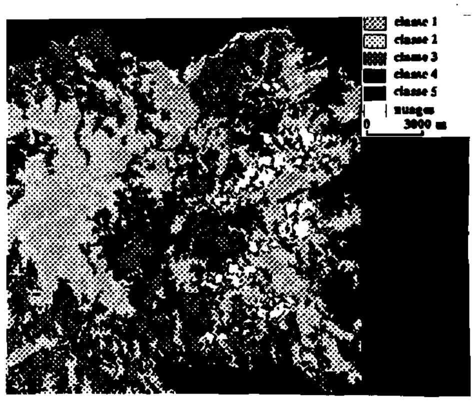


**Figure 4** : Image of unsupervised clustering classification

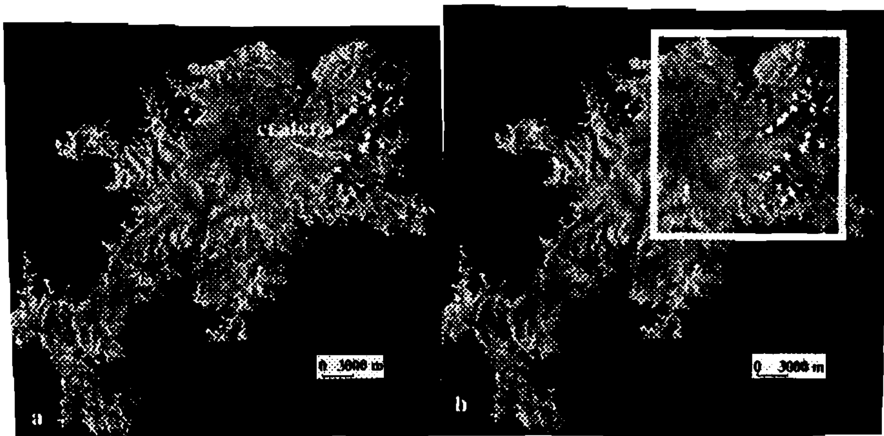


**Figure 3** : Images of frst main component obtained from channels 1 to 5 and 7. **a** - raw image; **b** - filtered image, the inner box shows the Quimsacocha volcano area

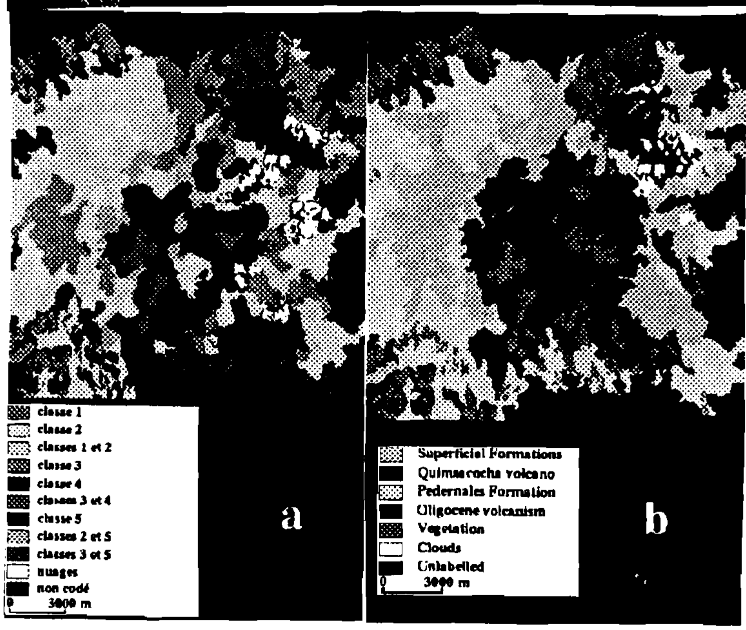


**Figure 5** : Mapping of Quimsacocha volcano. **a** - automatic mapping; **b** - interpreted mapping with field data

- classical methodes of image-processing : colored compositons, automatic unsupervised multispectral clustering classification (Diday, 1971) and automatic labelling of a binary image (Legeley et *al.*, 1995),
- Principal Components Analysis (PCA) that improves contrasts of the image so as of the geological structures and the main litological units (Vandemelbrouck et al., 1993),
- morphological transformations on binary images (Serra, 1982; Callot et *al.*, 1994) and greytone images (Crespo et *al.*, 1993; Serra, 1988).

**2 - The mapping of Plio-Quaternary volcanism**

The Plio-Quaternary volcanic deposits crop out largely in the southern part of the image but acces to the outcrops is not easy. The extension bounds of these deposits are relatively detectable except in the northeastern part where their limits with older volcanic outcrops of Oligo-Miocene age are unclear. In a first step, we tried to determine the bound between both volcanism by caracterizing first the recent volcanic deposits and then the older one. The result is shown on Fig.2.

**3 - The mapping of the "Quimsacocha volcanism"**

On the image of the first Principal Component calculated from all the bands (except Bd 6, thermal band), shows the center of the volcano in dark grey color (**fig. 3a**). The image was smoothed using an alternative filter whose aim is to realize a *closing* and *opening* by *geodesic reconstruction* (**fig. 3b**).

For the Plio-Quaternay volcanic deposits, the study was on the Quimsacocha volcanism. In order to automatically subdivide the image, we use the unsupervised multidimensional clustering classification; we limited at 6 the number of classes (**fig. 4**), the last one comprising clouds and shadows. Each class was individualy processed and then they were put together. This automatic cartography (Fig.5a) has been tested during a short field trip in the study zone. On the basis of the new field observations we modified the automatic cartography and improved it (Fig 5b).

## CONCLUSION

In the present study, Landsat TM imagery facilitated the indentification of two recent volcanic formations and the determination of the extension : the Pedernales Formation of probable Pliocene to Pleistocene age and the somewhat younger overlying Quimsacocha volcanism.

With "Mathematical Morphological processing" applied on satellital data we obtained an acceptable a cartographical document without manual intervention (Fig.5a) that was then improved by field data (Fig.5b). However, to the north, processing results were unsuffisant to separate clearly the Plio-Quaternary volcanic deposits from the Oligo-Miocene ones and the bounds were better defined using field data. The delimitation of the Quimsacocha volcanism was made difficult by the strong erosion suffered by the volcanic center on one hand and by the abondant superficiels deposits that soft differences between the Pedernales formation and the Quimsacocha volcanic cover on other hand. However, the crater of the Quimsacocha volcanoe was clearly located on the image : it's a large depression of approximately 5 km of diameter whose ground is plane. This morphology and structural observations on the crater are in agreement with a caldera structure Perez (1990).

## REFERENCES

BALDOCK J.W., 1982 - Geologia del Ecuador, Boletin de explicacion del Mapa. *Geológico de la Republica del Ecuador*. Direc. Gen. Geol. Minas, Quito, 70p.

BARBERI F., COLTELLI M., FERRARA G., INNOCENTI F., NAVARRO J.M. & SANTOCROCE R., 1988 - Plio-Quaternary Volcanism in Ecuador. *Geological Magazine*, **125**, (1), 1-14.

BRISTOW C.R. & HOFFSTETTER R., 1977 - *Lexique stratigraphique international.* Amérique Latine, 2ème édition, Equateur, CNRS, Paris.

CALLOT Y., MERING C. & SIMONIN A., 1994 - Image-analysis and cartography of sand hill massifs on high resolution images - application to the Great Western Erg (NW of Algerian Sahara). *International Journal of Remote Sensing*, **15**, (18), p. 3799-3822.

CRESPO J., SERRA J. & SCHAFFER R.W., 1993 - Image segmentation using connected filters, *in* : "Mathematical Morphologie and its applictions to signal Proceding", Barcemona, May 12-14, p. 52-57.

DIDAY E., 1971 - La méthode des Nuées Dynamiques. *Revue de Statistiques Appliquées*, **19**, p. 19-34.

EGUEZ A. & NOBLET C., 1988 - Nuevos datos sobre la estratigarfia de la cuenca de Cuenca (sur del Ecuaqor): implicaciones geológicas y geodnámicas. *Politécnica*, Monografia de Geologia 6, **XIII**, (3), 33-48, Quito.

KENNERLEY J.B., 1980 - Outline of the geology of Ecuador. *Overseas Geology and Mineral Ressources*, **55**, 17p.

LAVENU A., NOBLET C., BONHOMME M.G., EGUEZ A., DUGAS F. & VIVIER G., 1992 : New K-Ar age dates of Neogene and Quaternary volcanic rocks from the Ecuadorian Andes : implications for the relation-ship between sedimentation, volcanism and tectonics. *Journal of South American Earth Sciences*, **5**, (3/4), 309-320.

LEGELEY-PADOVANI A., MERING C., GUILLANDE R. & HUAMAN D., 1995 - Methode de cartographie des coulees de lave par traitement des images SPOT - L'exemple du Sabancaya (Perou). *Photo-interpretation*, **1**, p. 3-17 et 33-41.

NOBLET C., LAVENU A. & SCHNEIDER F., 1988 - Etude géodynamique d'un bassin intramontagneux tertiaire sur décrochements dans les Andes du sud de l'Equateur : l'example du bassin de Cuenca.. *Géodynamique*, **3** (1-2):117-138.

PEREZ OVIEDO H., 1990 - Sansahuin y Quimsacocha : centros de emision de la "Formación Tarqui". *Boletin Geológico Ecuatoriano*, v. 1 (1), 69-73.

SERRA J., 1982 - *Image Analysis and Mathematical Morphology*, Theorical Advances, vol. 2, (London - Academic Press), 422p.

SERRA J., 1988 - *Image Analysis and Mathematical Morphology*, vol. 2, (London - Academic Press), 628p.

VANDEMELBROUCK L., THOURET J.-C. et DEDIEU J.-P., 1993 - Reconnaissance par télédétection des produits éruptifs et des lahars autour de la calotte glaciaire du Nevado del Ruiz, Colombie. *Bulletin de la Societe Geologique de France*, **164**, p. 795-806.

# UPDATING ON THE GEOLOGICAL MAPPING OF THE SW ECUADORIAN SHORE, BETWEEN GUAYAQUIL AND THE SANTA ELENA PENINSULA, WITH A TM LANDSAT IMAGE

Edison NAVARRETE [1], Annick LEGELEY-PADOVANI [2] and Gérard LAUBACHER [1,2]

(1) ESPOL, Lab. de teledeteccion-FICT, Apartado Postal; 09-01-5863, Guayaquil, Ecuador
(2) ORSTOM, Lab. Géophysique, 32 avenue H. Varagnat, 93143 Bondy Cedex

**KEY WORDS** : Digital methodology, TM Landsat, , Geological Cartography.

---

## INTRODUCTION

The geological maps 1:100000 of the Ecuadorian shore were published in the 60's and 70's. A general geological map 1:1000000 of the Ecuador gave a first regional approach.

Recent works (80's - 90's) in Petroleum Geology has developed the geological knowledge of this part of the Ecuador. Then, a geological map updating seems necessary.

### 1. Study area description and Digital Methodology

This study is placed in an area between Guayaquil and the Santa Elena Peninsula known as the Progreso Bassin, that for many years has represented petroleum interest.

The original image used in this work is an extraction of a TM Landsat from 21 February 1990.

We used the following digital methodology:

- colour composite produced from the 3, 5, 4 TM Landsat channels;
- principal component analysis of the 3, 5, 4 TM Landsat channels;
- unsupervising classification by *Nuees dynamiques* of the first and the second principal components and application of the method of mathematical morphology to obtain an automatic map (figure 1);
- supervising classification by *Moyenne Euclidienne* of the colour composite of the 3, 5, 4 channels and application of the method of mathematical morphology to obtain another automatic map (figure 2).

### 2. Geological Cartography

The results of the geological interpretation of figures 1a and 2a after a field revision are in figures 1b and 2b respectively.

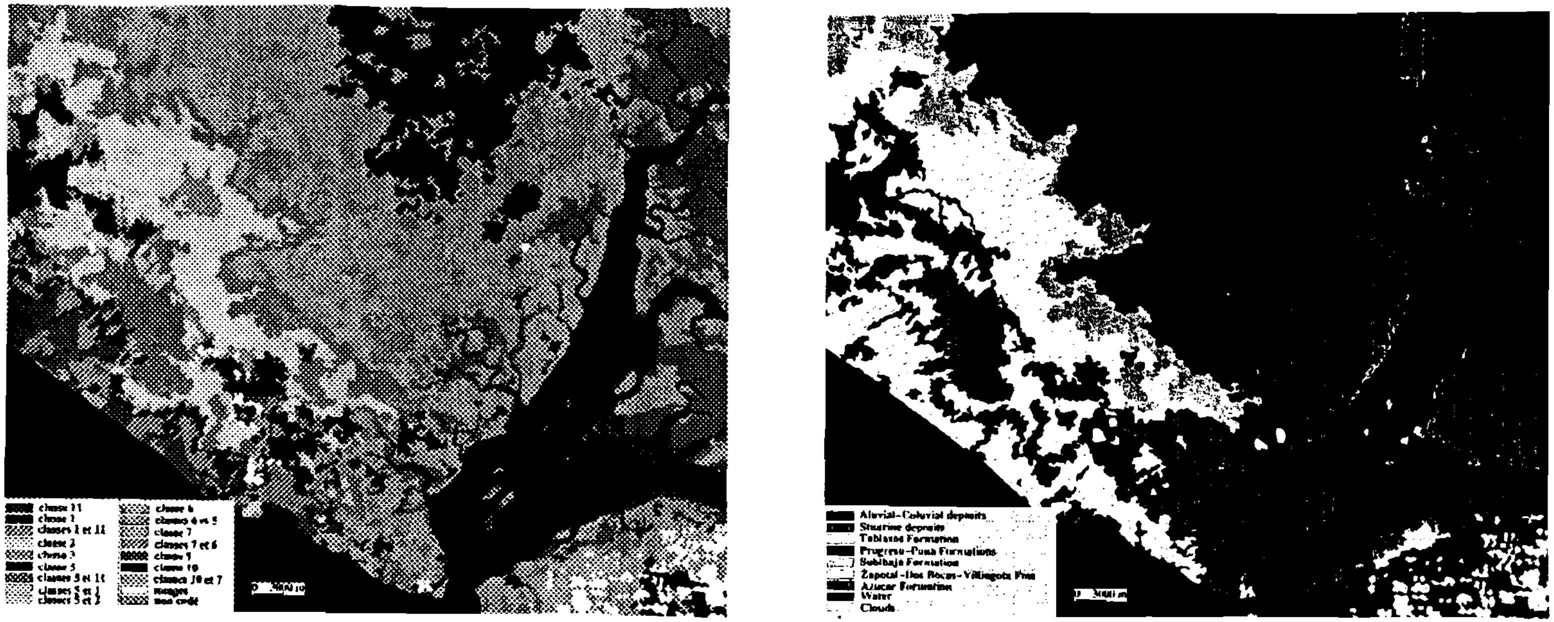


a b

**Figure 1** : Unsupervising classification by *Nuees Dynamiques* . **a** - automatic mapping; **b** - interpreted mapping with field data

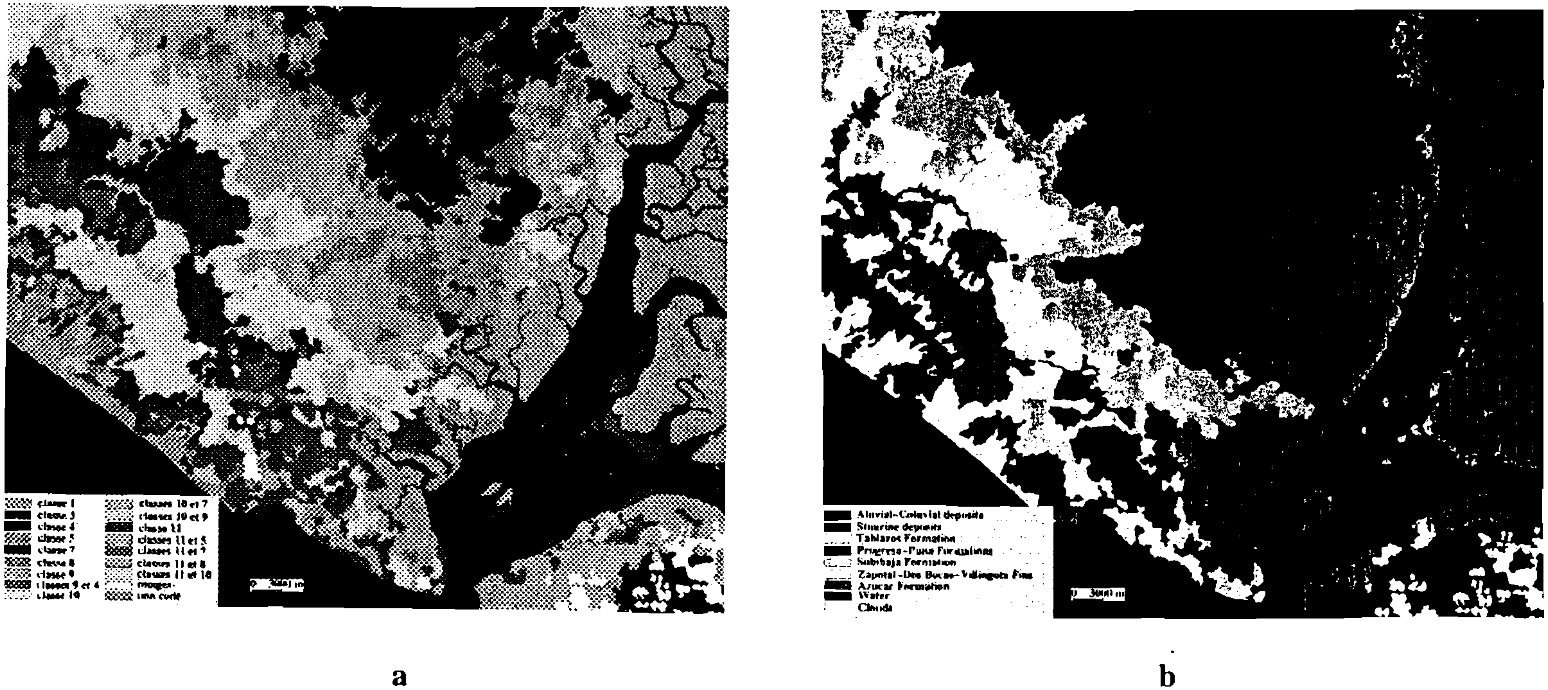


**Figure 2 :** Supervising classification by *Moyenne Euclidienne*. **a** - automatic mapping; **b** - interpreted mapping with field data

In general terms, in the two maps (figures 1b and 2b) we can distinguish the great stratigraphic sets of:

- Paleocene-Eocene: Azucar Formation;
- Miocene-Pliocene: Zapotal-Dos Bocas- Villingota Formations;
- Quaternary: Tablazos Formation, Alluvial-Colluvial deposits, estuarine deposits.

## CONCLUSIONS

The automatic processing of the TM Landsat image with the two classification methods gave similar results with little differences because of the treatment techniques.

We could make the great stratigraphic sets cartography, but we could not make the small units detailed mapping mainly because of the vegetation covering.

The cartography results are in concordance with the recent researches (Benitez, 1995) in the South Ecuadorian shore Lithostratigraphy and Geodynamic Evolution.

## REFERENCES

BENITEZ S., 1995 - Evolution géodynamique de la province côtière sud-équatorienne au Crétacé supérieur-tertiaire. Thèse de doctorat, Univ. J. Fourier-Grenoble 1, 221 p.

MAPA GEOLOGICO NACIONAL DE LA REPUBLICA DEL ECUADOR, 1982 - Escala 1:1 000 000, Ministerio de Recursos nationales y Energeticas, DGGM, Quito, Ecuador.

# ACTIVE TECTONIC CONTROL ON ALLUVIAL AND FLUVIAL DEPOSITS OF SAN JUAN RIVER. SAN JUAN, ARGENTINA.

**Lucía RUZYCKI (1) and Juan PAREDES (2)**

(1) Gabinete de Neotectónica y Dpto. de Geofisica, UNSJ, Cereceto y Meglioli, 5400 San Juan, Argentina
(2) Gabinete de Neotectónica y CONICET, UNSJ, Cereceto y Meglioli, 5400 San Juan, Argentina

**KEY WORDS**: Neotectonics * Cuaternary Alluvial and Fluvial Deposits * Precordillera * Andes Centrales

## INTRODUCTION

Tectonics is a first-degree control which influences the arquitectural features of a basin, the climate conditions of the areas producing sediments as well as the sediment receptive ones, the magnitude of the flows, the valley slopes, the type, zize and amount of sediment to be eroded and transported and, finally, the arquitectural characteristiscs of the deposits.

This study take place in the middle-west portion of the Argentine Republic (Fig.1) and involves the basin of lower de Los Patos river-San Juan river. It extends between 67°52' and 70°25' in western lenght and 30°16' and 32°25' in southern latitude. This basin has an extension of 32492 Km2 wiht a NW-SE oriented main axis of 294 Km and its principal heigts being the cerro Mercedario (6670 masl) and the Lagunas de Guanacache (515 masl). Its drainage system is part of the Desaguadero-Colorado fluvial system which empties its waters into the Atlantic Ocean whit the normal predictive flow in accordance with the other fluvial systems following the Horton laws and whit an alometric growth (Ruzycki, 1993). This drainage system covers the geological areas belonging to the Andes range, the Precordillera and the Pampeanas Range. The main trunk river (lower de Los patos river-San Juan river) is placed in the Barreal-Calingasta and Tulum valleys. It shows an antecedent section when it crosses the geological area of the Precordillera whit some minor sector of a subsequent type.

The basin and its fluvial system is situated in the Central Andes Range which is related to the flat subduction between the Nazca Plate and the South American plate.

This study takes into account the control of the cuaternary tectonic activity in the aluvial and fluvial deposits which are present along a fluvial section of 100 Km long. In this section, the San Juan river finds its way through the subprovinces of Western and Central Precordilleras inciceing its own deposits and the terminal portions of its tributaries fans.

## GEOLOGICAL CONTEXT

The active thin-skinned thrust and fold belt of the argentine Precordillera, whith eastward vergence, forms a N-S mountain chain , about 400 Km long and 80 Km wide, whith maximun of more than 4000 masl. It is composed of a thick sequence of early to late paleozoic sediments while mesozoic deposits are mainly preserved in basin structures along the western and eastern margins. Late terciary clastic sediments with volcanic intercalations and cuaternary deposits fill some intramountain basins.

The structural style of deformation is generally characterized by N-S striking imbricated faults with easternward vergence which are interpreted as plunging reverse faults on the west showing a tendency

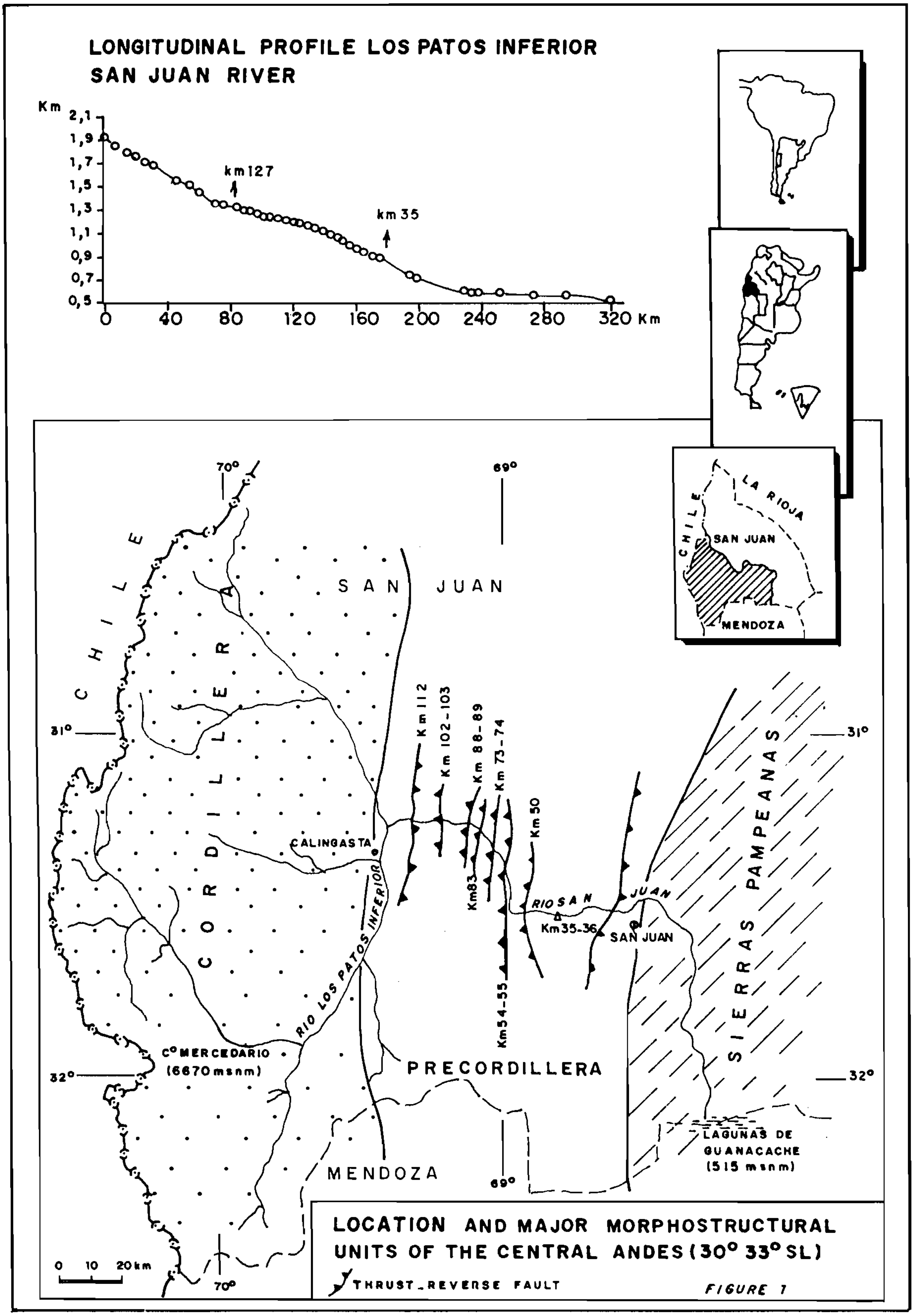
LONGITUDINAL PROFILE LOS PATOS INFERIOR
SAN JUAN RIVER
Km
2,1
1,9
1,7
1,5
1,3
1,1
0,9
0,7
0,5
km 127
km 35
0
40
80
120
160
200
240
280
320 Km
SAN JUAN
LA RIOJA
CHILE
MENDOZA
70°
69°
31°
32°
CHILE
CORDILLERA
SAN JUAN
Km 112
Km 102-103
Km 88-89
Km 73-74
Km 50
Km83
CALINGASTA
RIO LOS PATOS INFERIOR
RIO SAN JUAN
Km 35-36
SAN JUAN
Km54-55
SIERRAS PAMPEANAS
C° MERCEDARIO
(6670 msnm)
PRECORDILLERA
MENDOZA
LAGUNAS DE
GUANACACHE
(515 msnm)
0 10 20km
LOCATION AND MAJOR MORPHOSTRUCTURAL
UNITS OF THE CENTRAL ANDES (30° 33° SL)
THRUST_REVERSE FAULT
FIGURE 1

to become horizontal in depth.

This Central Andes segment has a distinctive tectonic platte setting. Earthquake locations shape a Wadatti-Benioff zone which gently deepens to the east forming a shallow subduction zone (Isacks, 1988). This flat subduction segment, between Nazca plate snd South American plate, is characterized by an eastern dip with a 5°-10° range at about 100 Km deep and it is flanked by steeper segments to the north and south whit an about 30° easter deepining (Jordan et al, 1983).

The present San Juan river valley is flanked by precuaternary (paleozoic and tertiary) and cuaternary rocks mainly represented by two principal facial associations: fluvial and aluvial (in aluvial-fluvial-lacustral sectors).

The first association is composed of the present deposits and several continuos and discontinous levels of constructional terraces made up of thick and thin debris belonging to the Andes Range and the Precordillera.

The second associations is represented by its incisive tributaries fans (at present active) grading the San Juan River. It is copmposed of two (or three) superimposed generations of tributaries fans and debris from the local Precordillera section.

These two associations are interdidigitalized in at least eight erosion-acumulation levels (Ruzycki, 1996; in rev.).

**LONGITUDINAL PROFILE**

Ruzycki (1993) considers that the present lower de Los Patos river-San Juan River (Fig. 1), with a wandering morphology in almost all of its antecedent section (Ruzycki, 1992, 1994), shows an upward conves longitudinal profile when crossing the Precordillera due to a complex tectonic, lithologic and hidrologic factors interrelation ship, being the tectonic one the most relevant.

Ruzycki (1996, in rev.) also states, correlates and provides the longitudinal profiles of seven main erosion-accumulation levels (0= actual river, 0I, I, II, III, IV, V) and three main sublevels (0I1, I1, II1) in the precordillera section of San Juan river between Km 127 and 35 of the Provincial Road N°20 linking San Juan city with the main town of the Calingasta Department.

In general, both the seven main leves and the trhee main sublevels are upwardly convexed and show some kind of parallelism with an almost steady heigh difference among them.

In particular, it can be seen that the convexity and the height difference between the levels and sublevels increase in some sections, that it is asymmetric and that there can also be some parallelism difference between the main levels and sublevels.

In the main leves 0 and 0I erosion whit minor accumulation intervals prevails.

The main levels I and II, with a relative heigh between 10 and 20 metres, are entirely erosive.

The main level III consist of an accumulation period that came to an end about 30000 years B.P. (Ruzycki and Paredes, 1996; in rev).

The main levels IV and V are erosive. They are characterized by carved surfaces in the paleozoic rocks with a thin aluvial-fluvial cover. These two last levels prevail only in some localized sections, mainly to the west of the Sassito river.

Out of the three main sublevels: II1, I1 and 0I1, only I1 and II1 are mainly erosive. They extend between Km 111-53 (from the west margin of the Tontal hill to the Sasso river mouth) and the Km 102-42 (from the Los Ratones river to near Quebrada Aspera river) and between Km 84-37 (from the north of La Fortuna river to a little to the north of the Qubrada Albarracín river), repectively.

Ruzycki (1996, in rev.) states that, in general, bouth the seven main levels and the main three main sublevels are upwardly convexed and show some kind of parallelism whit an approximate difference in heights among them. In particular, concludes that the convexity is asymmetric and that the height difference between the levels and sublevels increases in some sections. Also she points out that the main levels parallelism is practically constant whereas such parallelism is not constant either between the levels and sublevels or among the sublevels themselves.

## CONCLUSIONS

As the presence of a spatial periodicity between the main levels involving cyclical-episodic (climatic) events and also the presence of convex longitudinal profiles, interpreted as a consequence of an uprising, can be conclude that the main levels are a complex answer to climatic and tectonic events which have ocurred at a regional level during the mid-Pleistocene and Holocene periods. These periods brought about the geomorphological threshold excess external to the system.

The climatic processes would be mainly connected to glacial and interglacial periods that affected the superior basin catchment influencing the hydrologic fluctuations and the transported sedimentary load.

The tectonic processes are mainly the result of the Andes efforts to provoke an important shortening in the Precordillera estimated over the 50% (Von Gosen, 1992; Allmendinger, 1990).

Morever, it can be conclude that the main sublevels would be mainly linked to local tectonic processes provoking the local geomorphologic thresholds in the river stream. These influence not only the pattern of the different fluvial sections but also the deformations of the distinctive fluvial and aluvial levels existing in Precordillera.

This work was supported in part by CONICET, PIA No 0144/89 and by UNSJ (CICITCA) consenting to H. Bastías

## REFERENCES

Allmendinger R.W., D. Figueroa, D. Synder, J. Beer,C. Mpodozis and B. L. Isacks. 1990. Foreland shortening and crustal balancing in the Andes at 30°S Latitude. Tectonics 9, 789-809.

Isacks B. L. 1988. Uplift of the Central Andean plateau and bending of he Bolivian orocline. Journal Geophysical Research,93: 3211-3231.

Jordan T. E., B. L. Isacks, R. W. Allmendinger, J. Brewer, V. A. Ramos and C. Ando. 1983. Andean tectonics related to geometry of subducted plates. *Geological Society of America*, Bulletin 94: 341-361.

Ruzycki L. 1992. Diseño del Río San Juan entre Las Juntas y el Dique Punta Negra,San Juan,Argentina.IV Reun. Arg.de Sedimentologia,La Plata, Actas II, p151.-158.

Ruzycki L.1993. Características Morfométricas de la Cuenca de Drenaje del Río de los Patos inferior-Río San juan, Prov. de San Juan, Argentina. *XII Cong. Geol. Arg. y II Cong. de Expl.de Hidrocarburos, Mendoza, Argentina*,T6.

Ruzycki L. 1994. Variaciones en la Geometría del Curso del Río San Juan entre el Cerro Tambolar y el Río Uruguay, San Juan, Argentina. 3° Simp.Arg. de Teledetección, Prov. de Córdoba, Argentina.

Ruzycki L. 1995. Morfología y caracteristicas texturales de un rio conglomerádico errante (wandering gravel river) : rio de los Patos infrior - rio San Juan, provincia de San Juan, Argentina. IX Congreso *Latinoamericano de Geología, Venezuela*, Actas: en impresión.

Ruzycki L. 1996. Niveles de erosión-depositación en la quebrada del río San Juan através de las Precordilleras Occidental y Central y cambios climáticos en el Cuaternario, Prov. de San Juan, Argentina. *XIII Congreso Geológico Argentino y III Congreso de Exploración de Hidrocarburos*, in rev.

Ruzycki L. and Paredes. 1996. Active tectonic control on alluvial-lacustrine-fluvial deposits at Km 84 of San Juan river. San Juan, Argentina. *XIII Congreso Geológico Argentino y III Congreso de Exploración de Hidrocarburos*, in rev.

# ACTIVE TECTONIC DEFORMATION AND RESPONSE OF SAN JUAN RIVER CHANNEL PATTERN IN TULUM VALLEY. SAN JUAN, ARGENTINA.

**Lucía RUZYCKI (1) and Cristian WETTEN (2)**

(1) Gabinete de Neotectónica y Dpto. de Geofísica, UNSJ, Cereceto y Meglioli, 5400 San Juan, Argentina.
(2) C.R.A.S. y Dpto. de Geología, UNSJ, Cereceto y Meglioli, 5400 San Juan, Argentina.

**KEY WORDS**: Neotectonics* Fluvial Patterns * Tulum Valley * Pampean Ranges * Central Andes

## INTRODUCTION

The lower de Los Patos river-San Juan river basin (Lam. 1a) is placed in the middle-west of Argentina, in the Central Andes area, in relation to the flat subduction between the Nazca and South American plates (Isack, 1988). This basin is part of the Desaguadero-Colorado fluvial system flowing to the Atlantic Ocean. Its drainage system, in the geological areas of the Andes Range, Precordillera and Pampean Ranges, has a predictive normal pattern similar to the other fluvial systems, follows the Horton laws and shows an alometric growth (Ruzycki, 1993).

The lower de Los Patos-San Juan colector river is 320 Km long, grows in the Andes Range (1950 masl), flows to into the Lagunas de Guanacache (515 masl) and shows a double transversal - longitudinal desing in relations to the regional structures (Ruzycki, 1993), (Lam. 1a). Both longitudinal profile (Lam. 1b) and the design of its first order channel show the existence of intrinsic and extrinsic factors interfering with its environmental adjustement (Ruzycki, 1992-1993; Ruzycki and Paredes, 1996).

In general, the colector river changes in pattern from its origin to the mouth, presenting the form of the multichannel with a low sinuosity (braided) at the beginning, then with a meandering shape, after forming an aluvial fan, and finally, keeping straight (Ruzycki, 1992).

This study considers the control that neotectonics has over the river pattern morphology when crossing Tulum Valley.

Tulum Valley is an active broken-foreland basin placed in the pedemountain of the Oriental Precordillera (fault-thrust belt), mainly in the geological area of the Pampean Ranges and it is characterized by a series of crystalline basament blocks of Precambrian - Early Paleozoic Age. This basement was partially covered by a series of continental deposits consisting of the late Paleozoic Paganzo Group and terciary - cuaternary (Miocene to present) synorogenic deposits of alluvial and fluvial facies associated with the development of broken-foreland basin related to the broken-foreland Precordilllera and Pampean Ranges uplift (González Bonorino, 1950; Jordan et al, 1983). The main valley structure ("Tulum Fault") is composed of several high angle reverse faults, almost all with NNW-SSE strike, and normal faults almost with ENE-WSW strike, originating differencial uplifts in the basament blocks, turned according to their axis, and downfalls to the SSE (Zambrano and Suvires, 1978).

In ordre to know the precuaternary basament relief (mainly the Terciary) in the valley, a diagram block (Lam. 2) was drawn using drill data and geophisical methods (Vertical Electric Sounding) carried out by CRAS since 1965 till present.

In this valley, wiht a neotectonic activity (Zambrano and Suvires, 1987; Bastías et al, 1990), the river presents a topographic unlevelling of 200 metres with a mean gradient of 0.0016 m/m (Ruzycki,

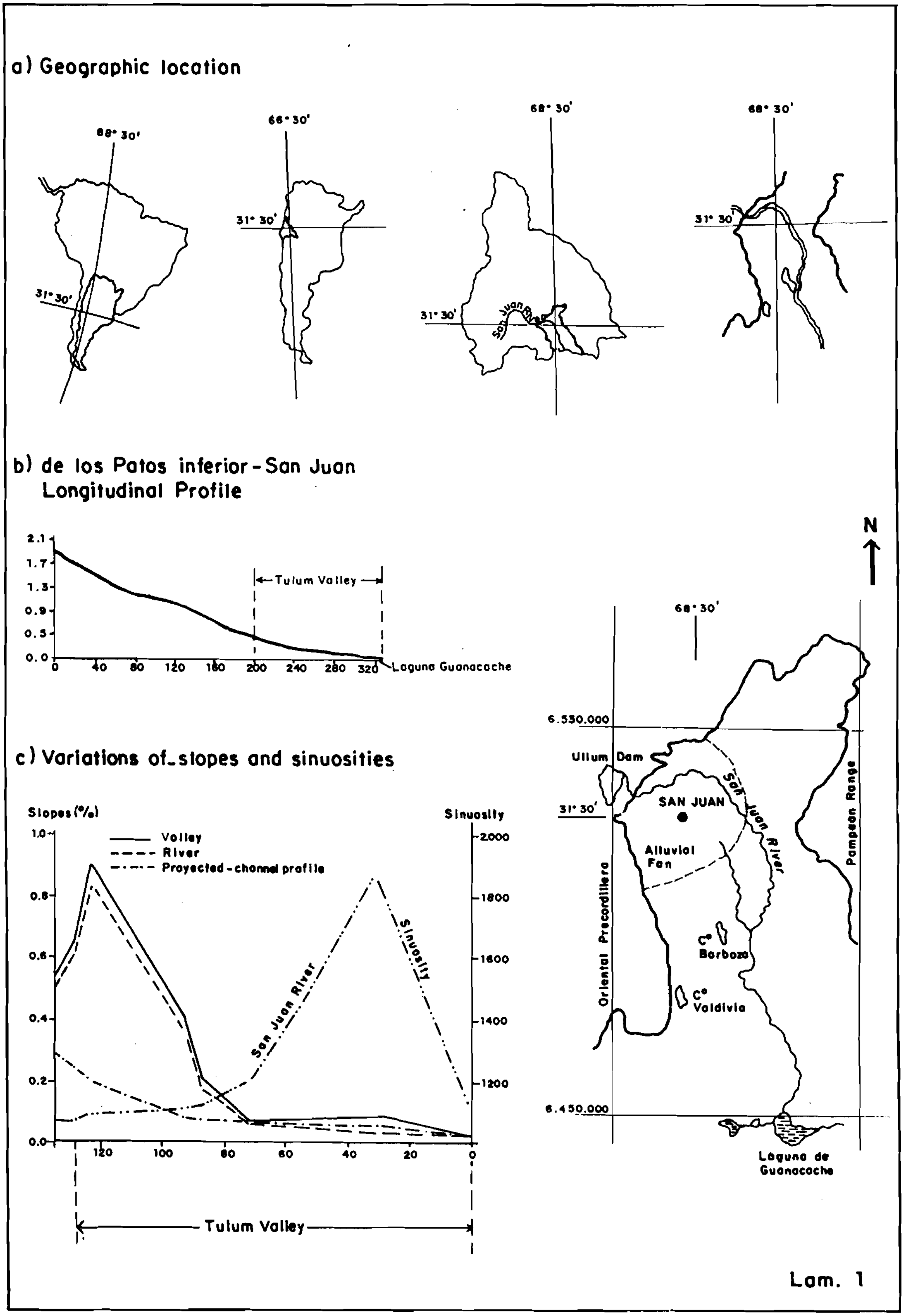
a) Geographic location
68° 30'
31° 30'
San Juan River
b) de los Patos inferior - San Juan
Longitudinal Profile
2.1
1.7
1.3
0.9
0.5
0.0
0
40
80
120
160
200
240
280
320
Tulum Valley
Laguna Guanacache
c) Variations of slopes and sinuosities
Slopes (%)
Sinuosity
Valley
River
Proyected - channel profile
1.0
0.8
0.6
0.4
0.2
0.0
2.000
1800
1600
1400
1200
120
100
80
60
40
20
0
San Juan River
Sinuosity
Tulum Valley
N
68° 30'
6.550.000
Ullum Dam
31° 30'
SAN JUAN
San Juan River
Alluvial Fan
Oriental Precordillera
Pampean Range
C° Barboza
C° Valdivia
6.450.000
Laguna de Guanacache

Lam. 1

1992) and a several of the flowing sections coincide with traces of satellite alignment or underground faults (Zambrano and Suvires, 1978).

**DISCUSION**

In general, Lam. 1c shows that both valley and river slopes are almost paralell and present two principal main slopes: one taking place in the fluvial plain of San Juan river (between the mouth to Km 70 the fluvial stream), and the other in the aluvial fan of San Juan river (between Km 70 and 129).

In particular it can be established that, in the fluvial sections (measured from the mouth) between Km 0 and 50 (fluvial plain) and Km 93 and 123 (apical and mid-superior sections of the aluvial fan) there is a loss of parallelims between the river and the valley slopes, being always the valley slope the steepest.

The approximate sinuosity (Lam. 1c) of the fluvial stream is 1.115 between the mouth and Km 30, 1.885 between Km 30 and 50, 1.515 between Km 50 and 70, 1.21 between Km 70 and 87, 1.115 between Km 93 and 123 and 1.095 between Km 123 and 129.

The channel pattern is a low sinuosity river with suspended-mixed load between the mouth and Km 30, a highly sinous meandering river whit mixed-suspended load between Km 30 and 50, a meandering river with mixed-suspended load and presence of bank erosion and flooding cutoff between Km 50 and 70, a low sinuosity river with bed load between Km 70 and 87, and a very low sinuosity river with bed load between Km 87 and 129.

**CONCLUSIONS**

Changes in channel morphology go with the evidences in the valley neotectonic activity:

**I-** Firstly, the neotectonic activity originate local steppings in the valley slope: **1-** an abrupt reduction between km 87 and 70 which shows the underground existence of reverse fault dippening to the East approximately at Km 87 and infering the underground existence of a normal fault with a lip falling down to the north approximately at Km 70, and **2-** an increase a) an abrupt slope between Km 129-123 as a consequence of the existence of a sinclinal approximately at Km 123, b) a moderate slope between Km 30-50 showing the underground existence of faults with a lip falling down to the South at Km 50 and at Km 30.

**II-** In the second place, the neotectonic activity originate a bigger sedimentary agrading in **1-** between Km 123-93 due to the sinclinal existence and in **2-**between Km 50 and the mouth due to the subsidencies originated by the underground faults at Km 50 and 30.

This work was supported by UNSJ (Res.194/94CS) and CRAS.

**REFERENCES**

Allmendinger R., D. Figueroa, D. Synder, J. Beer, C. Mpodozis and B. Isacks. 1990. Foreland shortening and crustal balancing in the Andes at 30°S Latitude. *Tectonics* 9, 789-809.

Bastías H., E. Uliarte ,J.Paredes, A. Sánches, J. Bastías, L. Ruzycki and P. Perucca. 1990. Neotectónica de la Provincia de San Juan. *XI Cong.Geol.Arg., San Juan*, Relatorio: 228-244.

González Bonorino F., 1950. Geologic cross- section of the Cordillera de Los Andes at about parallel 33°S (Argentina-Chile). *Geological Society of America*, Bulletin 61: 17-26

Isacks B.1988. Uplift of the Central Andean plateau and bending of he Bolivian orocline. *Journal Geophysical Research*, 93: 3211-3231.

Jordan T., B. Isacks, R. Allmendinger, J. Brewer, V. Ramos and C. Ando. 1983. Andean tectonics related to geometry of subducted plates. *Geological Society of America*, Bulletin 94: 341-361.

Ruzycki L. 1992. Diseño del Río San Juan entre Las Juntas y el Dique Punta Negra,San Juan,Argentina.*IV Reun. Arg.de Sedimentologia,La Plata*, Actas II, p151.-158.

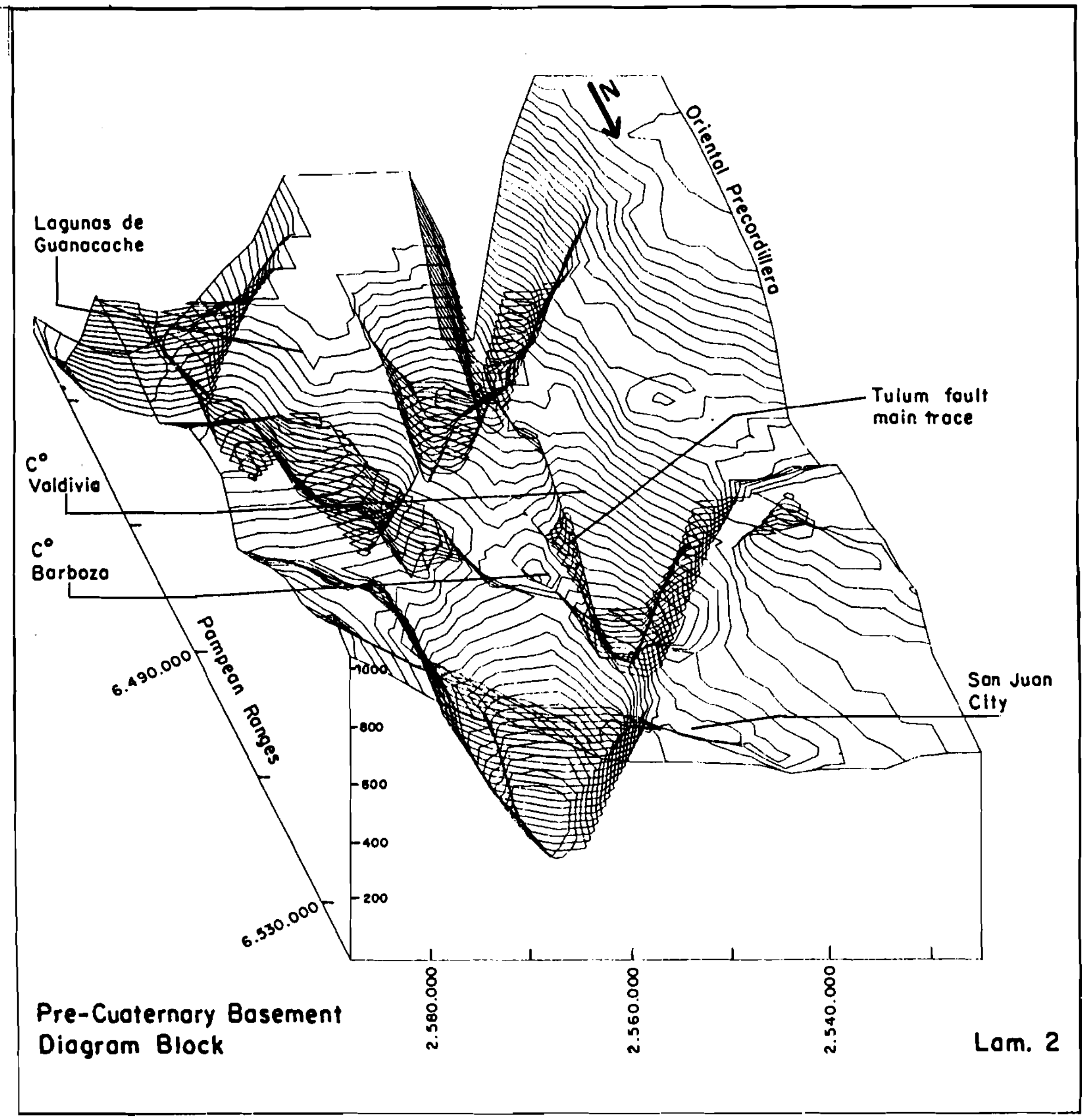


Ruzycki L.1993. Características Morfométricas de la Cuenca de Drenaje del Río de los Patos inferior-Río San Juan,San Juan,Argentina.*XII Cong. Geol. Arg. y II Cong. de Expl.de Hidroc.*, Mendoza, Argentina,T6.
Ruzycki L. and J. Paredes. 1996. Active tectonic control on alluvial and fluvial deposits of San Juan river. San Juan, Argentina.*Third International Symposium on Andean Geodynamics*. In press.
Zambrano J.J. and G.M. Suvires. 1987. La Estructura Superficial y Profunda en el Valle de Tulum, Prov. de San Juan, Argentina. *X Cong.Geol.Arg.*, TomoI, p.267-270.

# DISTRIBUTION AND EVOLUTION OF GEOMORPHIC PROCESS ZONES IN THE EASTERN CORDILLERA OF BOLIVIA

Elizabeth B. SAFRAN and Thomas DUNNE

Department of Geological Sciences
University of California
Santa Barbara, CA 93106
U. S. A.

KEY WORDS: morphology, erosion, landscape evolution, Eastern Cordillera

## INTRODUCTION

Large mountain ranges exhibit striking regional scale heterogeneities in landscape form and geomorphic process which affect the rate and style of morphologic evolution of the landscape, control the rate and locus of sediment removal from mountains, thereby feeding back into tectonic processes (Koons, 1990; Beaumont et al., 1992; Isacks, 1992; Small and Anderson, 1995), and dictate regionally appropriate forms of land use. A mechanistic understanding of how these hillslope and fluvial geomorphic process zones evolve is necessary for interpreting the morphologic variability of mountain ranges and for predicting how shifts in climatic or tectonic regime would affect the distribution and rate of erosion and sedimentation both within mountain landscapes and beyond the range front, where human populations are often concentrated.

In this study, we document and explain the evolution of major regional patterns of morphology and geomorphic process within a large mountain range: the Eastern Cordillera and Subandes of Bolivia (hereafter referred to collectively as the Eastern Cordillera). These patterns are dominantly controlled by the incision history of the channel network, since fluvial incision 1) creates relief, which strongly modulates the type and rate of geomorphic processes acting on hillslopes; and 2) governs channel gradients throughout the network, which influences the ability of rivers to transport the sediment supplied to them. Therefore, our approach to explaining geomorphic patterns involves quantifying the fluvial incision history of two major drainage basins (Beni and Pilcomayo) in the Eastern Cordillera during the latest phase of Andean deformation (approximately 10 mya) and linking hillslope and fluvial characteristics resulting from incision to specific types and rates of geomorphic processes.

## NATURE OF GEOMORPHIC VARIATION IN THE EASTERN CORDILLERA

In the Eastern Cordillera, downstream geomorphic variation is evident in basins that extend from the Altiplano to the foreland basin, such as the Beni and Pilcomayo basins. Systematic field surveys reveal that in the headwaters of the Beni, most streams are floored by bedrock and strewn with large cobbles and boulders, and deep-seated landslides >100,000 $m^3$ in volume are common in the steep, deeply dissected landscape. Further downstream, river channels are entrenched in narrow canyons alternating with reaches containing large gravel bars, broader valleys, and occasional patches of floodplain. High-relief hillslopes are scarred by numerous landslides several meters deep, tens of meters wide, and sometimes hundreds of meters long which remove the upper 1-3 m of colluvium and 1-3 m of weathered bedrock. In the Subandes, numerous reaches of trunk rivers lie in broad valleys and have permanent floodplains associated with them, relief is moderate, and many ridges exhibit shallow landsliding.

The Pilcomayo basin exhibits distinctly different downstream trends in geomorphic process and landscape morphology. Although landsliding occurs in some deeply incised valleys in the headwater region, extensive areas throughout the cordillera proper are characterized by extremely broad valleys and slightly rounded bedrock hillslopes with colluvium aprons dissected in some places by gullies. Satellite imagery illustrates these vast tracts of relatively subdued topography at high elevation, scored by a few deep canyons along which erosion is focused. Many streams in moderately dissected portions of the Pilcomayo basin occupy wide channels mantled by alluvium which appear to be actively widening. The western Subandean region of the basin is characterized by sharp ridges of moderate relief which support large, relatively shallow landslides of the kind described above, while in the easternmost Subandes, both landslides and gullies are rare.

Field observations and image interpretations of these landscapes were combined to produce a map, stored in a Geographic Information System, of regions dominated by particular geomorphic processes. Using Landsat TM and MSS imagery, SPOT imagery, SIR-C radar data, and aerial photographs, and guided by our field mapping, we delineated zones dominated by three major hillslope processes: 1) diffusive processes, such as soil creep and rock ravel; 2) shallow landsliding, primarily of colluvium and a thin layer of weathered bedrock; and 3) deep-seated landsliding with failure surfaces tens to hundreds of meters below the land surface. We also divided river reaches into three major regimes: 1) incisional, with little sediment deposition; 2) transitional, with some sediment deposition or alluvial mantle but no permanent floodplain; and 3) alluvial, with permanent floodplain.

Several types of morphometric analyses were performed on these landscapes to determine whether regional boundaries determined by eye on the basis of process are systematically reflected in form. For each geomorphic process zone, we calculated: a) fractal dimension, which has been shown by Outcalt et al. (1994) to be an effective discriminator of physiographic regions when applied to 30-arc-second digital elevation models of the United States; b) ruggedness number, which reflects degree of dissection of the topography; c) local relief (valley depth) and hillslope; and c) channel width to valley width ratio, which is strongly correlated with the presence of sediment in the valley bottom and therefore is a good predictor of fluvial regime. The topographic database used for these analyses consists of 1:50,000 topographic maps and swaths of digital topographic data derived from SIR-C and TOPSAR radar interferometry.

## QUANTIFYING FLUVIAL INCISION

To explain the modern distribution of geomorphic process zones, and to illustrate the evolution of these processes throughout a large mountain drainage basin, we utilized a simple one-dimensional model of fluvial incision into an uplifting landmass. The incision model is constrained by field data on rock mass quality, a significant control on incision rates, and by data on downstream variations in channel geometry and discharge. The uplift history of the Eastern Cordillera over the last 10 mya is derived from the geodynamic model of Masek et al. (1994) and is constrained by estimates of the timing and magnitude of shortening in different parts of the range (e.g., Allmendinger et al., 1983; Roeder, 1988; Hérail et al., 1990; and Kley and Reinhardt, 1994). Specifically, the incision model generates relief and dictates slope down the drainage network according to a widely cited hypothesis that the rate of fluvial incision, ε, is related to stream power, a measure of work done on the channel bed by the flow, and the rate of change of bed elevation (z) is therefore:

$$\frac{\partial z}{\partial t} = \varepsilon + U(x,t) \qquad (1)$$

where

$$\varepsilon = -K(x,t)A^m S^n \qquad (2)$$

Here, A is drainage area, S is slope, U is a temporally and spatially variable rate of uplift, m and n are exponents that vary among environments (Howard et al., 1994), and K(x,t) is a measure of rock mass quality.

The fluvial incision component of the model described above simply cuts vertically through topography according to equation (1). From this information we obtained an estimate of the pattern and maximum amount of exhumation that has occurred during the last 10 mya. This pattern will be checked against exhumation rates derived from fission-track analyses on igneous and metamorphic rocks collected in each basin which we are currently performing.

## GEOMORPHIC IMPLICATIONS OF INCISION

Based on the results of the fluvial incision model, a series of off-line calculations were made to determine: 1) the distribution of hillslopes currently at the limit of relief they can support; 2) hillslope-averaged rates of denudation required to convert hillslopes previously at the limits of their relief to their current shape and relief; and 3) temporal changes in the loci of incisional and depositional regimes.

The depth of canyons created by fluvial incision is limited by the strength of the rock mass into which the rivers incise. Topographically induced stresses in the rock mass eventually become great enough to produce extensive cracking at certain loci (Miller, 1993), and a portion of the canyon wall fails as a deep-seated, bedrock landslide. The morphologic conditions -- gradient, relief -- under which such failures will occur have been calculated simply with a Culmann wedge stability calculation (Spangler, 1951). This calculation also identifies the location of the failure plane and the post-failure geometery. Continued incision of the river causes renewed slope instability and migration of the break in gradient between the undissected plateau and the slope adjacent to the channel toward the midpoint between channels. When the entire hillslope has failed back to a stable angle and has reached its maximum length (approximately half the distance between channels), the rate of ridgecrest lowering becomes equal to or greater than the rate of fluvial incision. Since the model describes the spatial and temporal distribution of incision rates throughout the network, we calculated the time required to incise a canyon deep enough to produce a hillslope unstable to deep-seated bedrock failure, as well as the time required to produce subsequent failures and the time required to reach steady-state. Because we also know the hillslope morphology after each failure, we were able to calculate rates of hillslope lowering by bedrock failures.

Hillslope morphology is also altered through processes other than bedrock failures. We observe that the gradients of some hillslopes are lower than the angle at which hillslopes are just stable with respect to bedrock landsliding, which indicates that interfluve lowering has occurred faster than slope toe lowering for some portion of the hillslope's history. Because we have observed in the field that the resulting slopes are only very slightly convex and can be well-approximated by planes, the reduction of hillslope gradient by processes other than bedrock landsliding can be described with an erosion rate that decreases linearly from ridgecrest to channel and immediately adjacent to the channel is equal to the rate of fluvial incision. Because we have a model of fluvial incision rate through time, and because this model tells us when hillslopes reached their limits of relief, we can calculate the subsequent average interfluve lowering rate required to produce the current hillslope morphology. We will compare our calculated lowering rates to rates derived from field measurements. The average lowering rate of a hillslope or of all the hillslopes in a small basin can be determined by analysis of cosmogenic isotopic abundance in the colluvium at the base of the slope or in the alluvium at the mouth of the basin (Bierman and Steig, in press). We are currently conducting such analyses on sediment samples collected at a number of points throughout the Beni and Pilcomayo basins from places where deep-seated bedrock landsliding is not the dominant hillslope lowering process.

To identify the loci of the three types of fluvial regime, we focused only on the Beni basin and made three simple assumptions based on field observations: 1) where long-term transport capacity of a river, $T_c$, is greater than or equal to long-term sediment supply rate, $Q_s$, the fluvial regime is incisional, with valley width and channel width approximately equal; 2) where $T_c = Q_s$, the channel is in a transitional state, is mantled with patchy alluvium, and may be both widening its valley and incising; 3) where $T_c < Q_s$, the river becomes alluvial, with a permanent floodplain. To estimate long-term sediment transport capacity throughout the drainage network, we used a water balance and flow routing model to calculate the probability distribution of daily discharge at every point in the modern drainage network of the Eastern Cordillera, given an empirically defined precipitation pattern and a probability distribution of daily rainfall amounts that represents the climate. We then determined the quantity of sediment moved by each of these flows using Bagnold's (1980) sediment transport equations for gravel-bedded rivers. Finally, we calculated the total amount of sediment transported at each point in the drainage network and fit the results with a statistical model that is a function of local slope, drainage area, and upstream precipitation. To estimate sediment supply throughout the network, we assumed a steady-state landscape has persisted throughout the latest phase of uplift of the Eastern Cordillera, so the local sediment supply was assumed to equal the rate of fluvial incision times the drainage area. This allows us to illustrate generally how the loci of incision and deposition change as a channel network incises an uplifting mountain range.

## CONCLUSION

The distribution and evolution of geomorphically distinct regions in a large mountain range can be explained with a quantitative model of the history of fluvial incision into the range and several simple, related calculations. Geochronologic data are currently being analyzed which will allow more specific and quantitative tests of our landscape evolution model.

## REFERENCES


Allmendinger, R. W., V. A. Ramos, T. E. Jordan, M. Palma, and B. L. Isacks. 1983. Paleogeography and Andean structural geometry, north-west Argentina. Tectonics, 2, 1-16.

Bagnold, R. A. 1980. An empirical correlation of bedload transport rates in flumes and natural rivers. Proc. Roy. Soc. London, Ser. A, 372, 453-473.

Beaumont, C., P. Fullsack, and J. Hamilton. 1992. Erosional control of active compressional orogens. In: Thrust Tectonics, ed. K. McClay and A. Unwin, Chapman Hall, London, pp 1-18.

Bierman and Steig. Estimating rates of denudation using cosmogenic isotope abundances in sediment. Earth Surf. Proc. Land., in press.

Hérail, G., P. Baby, J. M. López, J. Oller, O. López, R. Salinas, T. Sempere, G. Beccar, and H. Toledo. 1990. Structure and kinematic evolution of Subandean thrust system of Bolivia. In: Proceedings, International Symposium on Andean Geodynamics, Grenoble, France, pp. 179-182.

Howard, A. D., W. E. Dietrich, and M. A. Seidl. 1994. Modeling fluvial erosion on regional to continental scales. J. Geophys. Res., 99, 13,971-13,986.

Isacks, B. L. 1992. 'Long-term' land surface processes: Erosion, tectonics, and climate history in mountain belts. In: TERRA-1: Understanding the Terrestrial Environment: The Role of Earth Observations from Space, ed. P. M. Mather, Taylor and Francis, London, pp. 21-36.

Kley, J. and M. Reinhardt. 1994. Geothermal and tectonic evolution of Eastern Cordillera and Subandean ranges of southern Bolivia. In: Tectonics of the Southern Central Andes, Springer-Verlag, Heidelberg, pp. 155-170.

Koons, P. O. 1990. Two-sided orogen: Collision and erosion from the sandbox to the Southern Alps, New Zealand. Geology, 18, 679-682.

Masek, J. G., B. L. Isacks, T. L. Gubbels, and E. J. Fielding. 1994. Erosion and tectonics at the margins of continental plateaus. J. Geophys. Res. 99, 13,941-13,956.

Miller, D. J. 1993. Topographically induced stress fields and patterns of bedrock fracturing. Ph. D. thesis, University of Washington, 286 pp.

Outcalt, S. I., K. M. Hinkel, and F. E. Nelson. 1994. Fractal physiography? Geomorphology, 11, 91-106.

Roeder, D. 1988. Andean-age structure of Eastern Cordillera (Province of La Paz, Bolivia). Tectonics, 1, 23-39.

Small, E. E. and R. S. Anderson. 1995. Geomorphically driven Late Cenozoic rock uplift in the Sierra Nevada, California. Science, 270, 277-280.

Spangler, M. G. 1951. Soil Engineering, International Textbook Co., Scranton, PA. 458 pp.

# Landscape Evolution in Northernmost Chile (18.5°-19.5°S): its Implication in the Tectonic, Sedimentary, and Magmatic History of the Central Andes

Dieter Uhlig [1], Hartmut Seyfried [1], Gerhard Wörner [2], Ingrid Kohler [1], Wolfgang Schröder [2]

1) Universität Stuttgart, Institut für Geologie, Herdweg 51, 70174 Stuttgart, Germany; email: dieter.uhlig@po.uni-stuttgar.de
2) Georg August-Universität Göttingen, Geochemisches Institut, Goldschmidtstr. 1, 37077 Göttingen

**Keywords**: Central Andes, landscape, tectonics, half-graben, landslides, ancient ground water

## Introduction

For about the past 20 Ma, the Western Andean Escarpment of the Altiplano in northernmost Chile (18°S) has had an extremely arid climate with intermittant periods of abundant (glacial?) water. In consequence, tectonic movements were only moderately compensated by erosion. However, the products of uplift, erosion and sedimentation are well documented. This results in an excellent geological record for the processes and timing of Andean uplift at the Western Escarpment near 18°S.
The landscape evolution of the Northern Central Andes between 17.5° and 19.5°S is characterized by :
(1) one of the driest deserts on earth with annual precipitation ranging from 2 to 330 mm depending on elevation (ABELE, 1984).
(2) one of the steepest gradients on earth from the subduction trench at > 7000 m.b.s.l. to > 5000 m a.s.l. of the Western Cordillera over a lateral distance of only 250 km. A Precordillera such as in the south does not exist. The Western Escarpment of the Andes rises to the Altiplano in a huge ramp, modified by one giant antithetically rotated block of 40km by 20km dimension.
(3) the lower parts of the Western Andean Escarpment and the Coastal Cordillera are dissected by several major valleys which all are up to 1200 m deep in the middle course (from N to S: Quebrada Lluta, Azapa, Vitor, Camarones, and Tiliviche). Such deep valleys are unusual for the Chilean Longitudinal Valley and Andean Front and result from enhanced precipitation and glaciers at high elevations (FISCHER 1991) in the geological past (and also today) depending on the influence of the subtropical high pressure zone.

## Abstract

The landscape evolution of the Western Andean Escarpment at 18° S can be described as an interplay between individual stages of uplift, erosion, sedimentation, and gravitative collaps at various scales. Prior to the Miocene episode of Andean uplift, during the Jurassic and Cretaceous the region was characterized by low elevations, terrestrial redbed sedimentation and volcanism. Apart from the earlier Cretaceous and Jurassic units (arc and back arcs), the Longitundinal Valley represents the oldest and most persistent geological structure. It has accumulated sediments since at least 25Ma and is still active in its central undissected part. Structurally, it represents a half-graben formed between the eastward-tilted Jurassic Coastal Cordillera and the initial western Andean slope. Huge volumes of Miocene alluvial fan sediments, up to 1000m thick, derived from Cretaceous and minor Jurassic igneous rocks formed the ramp-like Western Slope of the Andes in northernmost Chile. These alluvial fan deposits distally grade into fluvio-lacustrine sediments east of the dam-like Costal Cordillera. This first sedimentary episode is interpreted as a first major stage of Andean uplift and crustal thickening: increased topographic relief in

combination with still abundant water produced the thick pile of alluvial sediments (c. 25 Ma to 20 Ma). This episode ended with the deposition of ignimbrite sheets of up to 900 m in total thickness. The age of the youngest ignimbrite sheet is 19.3 ± 0.01 Ma (Ar/Ar sanidine step heating age, Walfort et al., 1995) which is in perfect agreement with age determinations of Naranjo & Paskoff (1985) for the same ignimbrites. Crustal melting after a period of thermal relaxation (several Ma) and, probably continued magmatic input from the mantle wedge were responsible for the formation of the ignimbrites at around 19Ma. Alluvial ramps overlain by ignimbrites are also known from regions further south (20° to 21°S). Here, however, the ignimbrites are younger (16 to 17 Ma; Baker & Keynes, 1977) and the tectonic style affecting the ignimbrites in Late Miocene times is dextral strike slip (in the W Salar de Huasco pull apart basin) rather than normal block faulting (see below).
During the following short episode of volcanic and tectonic quiescence a westward oriented dendritic drainage pattern eroded the ignimbrites. Mafic andesite volcanism (Ar/Ar amphibole total fusion age: 18,7 ± 0.8 Ma) shortly followed the erosional event. The typical dense and mostly aphyric andesites of the shield volcanoes are found as characteristic detritus of the conglomerates of the Formaci6n Diabolo. This deposit, however, was considered by Tobar et al. (1968) and Vogel & Vila (1980) to be Quaternary in age. In our interpretation the Formaci6n Diabolo must be at least of Late Miocene age.

A second episode of uplift resulted in westward steepening of the Miocene sediment and ignimbrite ramp, normal faulting and antithetic rotation of the Pampa de Oxaya block. As a result, the Pampa de Oxaya today is tilted to an east dipping position forming a new, upper, half-graben within the upper reaches of the Western Slope. Lacustrine, fluvial, and alluvial fan sediments filled up this new sedimentary basin. Furthermore, tilting partly reversed the drainage pattern of the Pampa de Oxaya leading to sedimentation within the upper courses of its valleys. The extensional style of this movement is clearly documented by graben structures which cut the valleys of the Pampa de Oxaya. The age of the second stage of uplift must be younger than the initial andesitic volcanism (c. 18 Ma) and older than the 8- 9Ma old mammal fossils found within the upper half-graben sediments (SALINAS et al. 1991). Our conclusions contradict those of Muñoz & Sepulveda (1992) and Munoz & Charrier (pers. comm.) who interpreted their observations in the region as compressional structures. Compressional structures in our working area are limited to the Bel6n metamorphic basement rocks and their Createaceous cover. Although we cannot entirely exclude compressional tectonic structures of Late Miocene age, the *general* tectonic, topographic and morphological regime indicates extension, uplift and normal faulting rather than compression.
The Early Miocene ignimbrites and the overlying low angle mafic andesite shield volcanoes are restricted to the region between 17°S and 19°S, coinciding with the distinct structural and evolutionary style of the Western Andean escarpment described here.
An important secondary effect of the uplift of the Pampa de Oxaya was the partial oversteepening of its western slope which resulted in a giant gravitational collapse. The "Lluta Collapse" is exposed on both sides of the Quebrada Lluta for 20 km to the E of Poconchile. It covers an area of about 600 $km^2$ and displaced a rock section over 800m thick. This displaced mass is characterized by large tilted blocks and an unregular topography which in some places rises up to 200 m over the undisturbed ignimbrite ramp. Compressional faults are abundant in its lower parts. The collapse forms an amphitheater shaped scar E of the Pampa Plazuela. In the basal detachment zone of the collapse structure soft sediment deformations imply landsliding above a (wet?) clayey sand layer. Further, diatomite deposits were formed in small basins within the Lluta-Collapse area. The formation of these pure diatomite lakes, lacking significant clastic input by rivers, must be explained by groundwater seeping into small basins within the collapse. The ponds formed in this way provided constant suitable conditions for the diatomites independent of the typical fluctuations of rivers in dry climates. The giant Lluta-collapse thus shows several features suggesting the presence and potential role of an extensive ancient groundwater body in the collapse process.
The age of the collapse is difficult to establish : It must be younger than the second stage of tectonic uplift (8 - 19 Ma) but older than the development of the Lluta valley (> 3 Ma). This time span also falls into the time of formation of the upper half graben sediments and the lacustrine sediments of the lauca Basin (Kött et al. 1995), again indicating the presence of water more abundantly than during the Holocene. This landscape was sealed by the 2.72 ± 0.01 Ma (Ar/Ar sanidine age, Walfort et al. 1995) Lauca-Perez Ignimbrite which forms an extensive outflow sheet in western Bolivia and the Western Andean Escarpment (Schröder & Wörner, this meeting).

The incision of the deep valleys Lluta, Azapa, Vitor, Camarones, and Tiliviche finally dissected the Coastal Cordillera, the Western Slope and the tilted Oxaya block. By passing the Coastal Cordillera these rivers now gave way to all sediments to be carried directly into the sea. The 2.7 Ma Lauca-Perez ignimbrite entering the valleys of Lluta, Cardones, and Azapa - at least partly - postdates this dissection. Remnants of Lauca-Perez ignimbrite within a fluvial terrace 10 m above the valley floor and 500 m below the valley shoulders in the lower parts of the Lluta valley are evidence that erosion significantly had dissected the Western Slope prior to the ignimbrite event. These deeply incised valleys control the further history of the landscape in the Arica area. They truncate the Miocene dendritic drainage pattern leaving hanging valleys up to nearly one thousand meters above the valley bottoms. The walls of the major valleys are mostly undissected and smooth, showing steep slopes often with angles > 45°. Landsat imagery presents beautiful evidence for frequent collapse of these steep valley walls along most of its middle and lower course where incision reached up to 1200 m. The valley walls are subdivided by younger collapses formed by rotational sliding of blocks up to 400m in thickness and its conspicuous smooth detachment planes. Such landsliding often dammed the rivers evidenced by up to several tens of meters of lacustrine sediments upstream. Oversteepening of the valley walls during incision has certainly been the dominant cause for landsliding with earthquakes possibly serving as the ultimate trigger. The role of water as a lubricating (or instrumental) agent in the collapse process is difficult to evaluate. The water of allochthone rivers could not reach the detachment zone of the landslides which initiated above the valley bottom. Episodic heavy rainfalls could have provided abundant water even within a desert. However, such running water neither caused erosion to connect the hanging valleys to the main valley floors nor erased the character of the ancient dendritic drainage pattern still preserved since the Early Miocene. Obviously, the quantity of rain water was not significant and therefore could hardly cause the failure along the detachment planes. The only other possibility to provide water may be by groundwater. Prior to the incision of the deep valleys, aquifers within the permeable conglomerates of the Lower Oxaya Formation may have been charged by glaciers on the Altiplano. Incision of the valleys and the subsequent draining of groundwater aquifers may have produced the conditions for gravitational sliding along the oversteepened valley walls. Complete drainage of the groundwater and reduced recharge since about 3 Ma finally stabilized the valley walls.

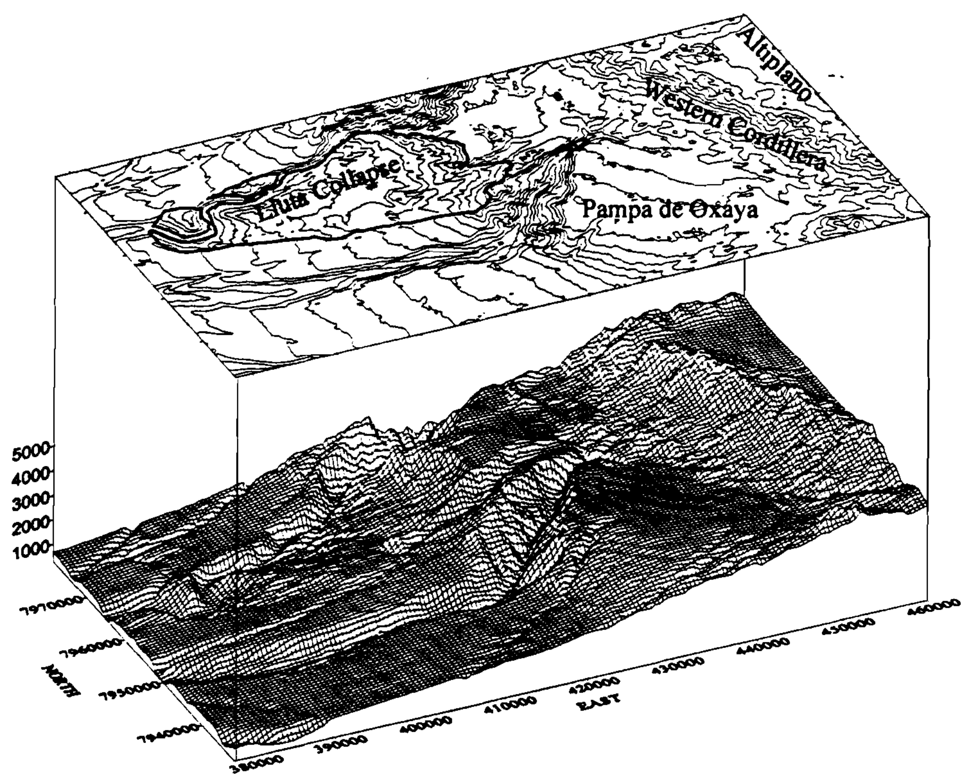


**Fig.: Digital Elevation Model (UTM-Coordinates) of the tilted Pampa de Oxaya Block and the Lluta Collapse along the Western Slope of the Andes E of Arica**

**Conclusions**

1)The landscape of the Andes between 17.5° and 19.5°S is the product of two main phases of uplift in the Early Miocene (c. 25 to 20 Ma) and Middle Miocene (c. 9 to 19 Ma), which both resulted in distinct episodes of erosion and sediment deposition.
2) Differential uplift and the formation of half-grabens were responsible for the present morphotectonic units: Coastal Cordillera, Western Slope, and Altiplano.
3) Since the Miocene the general tectonic style of the area has been uplift, normal faulting, and extension probably related to the frontal subduction of the Nazca Plate. This is in contrast to the southern Central Andes where subduction is oblique and tectonics are linked to strike slip processes.
4) The Formación Diabolo must be at least of Late Miocene age. The dissection of the Western Slope and the deposition of the Pliocene Lauca-Perez ignimbrite within these valleys clearly postdate this sedimentary sequence.
5) Oversteepening of the Western Slope resulted in a giant gravitational collapse covering an area of about 600 $km^2$. This "Lluta Collapse" predates the incission of the Lluta valley and is partly covered by the 2.7 Ma Lauca-Perez ignimbrite.
6) We presume an ancient extensive aquifer within the sediments of the Oxaya Formation. The Lluta Collapse and the landslides along the walls of the deep valleys could have been facilitated by water seeping onto the detachment planes. Furthermore, the pure diatomite deposits in the Lluta Collapse area probably arised from ancient lakes fed by groundwater.
7) Dissection of the Coastal Cordillera and subsequent headward erosion of deep valleys ceased sedimentation on the Western Slope. The steep walls of these valleys frequently collapsed and repeatedly dammed its rivers during incision.

**References**


Abele G. 1982. Geomorphologische und hygrische Höhenzonierung des Andenwestabfalls im peruanisch-chilenischen Grenzgebiet. *Erdkunde*, 36, 266-278.

Baker M.C.W., Keynes M. 1977. Geochronology of upper Tertiary volcanic activity in the Andes of North Chile. *Geologische Rundschau* ,66: 455-465.

Fischer K. 1991. Oberpliozäne - pleistozäne Talbildung auf der Westabdachung der mittleren Anden zwischen 18° und 27° südlicher Breite. *Bamberger Geographische Schriften*, 11, 69-80.

Kött A., Gaupp R., Wörner G. 1995. Miocene to Recent history of the Western Altiplano in northern Chile revealed by lacustrine sedimensts of the Lauca Basin (18°15'-18°40'S/69°30'-69°05'W). Geol Rundsch 84 :770-780.

Naranjo J.A., Paskoff R. 1985. Evolucion cenozoica del piedemonte Andino en la Pampa del Tamarugal, Norte de Chile (18°-21°S). *Actas, IV Congreso Geologico Chileno, Servicio Nacional de Geologia y Mineria*, Santiago de Chile, 149-165.

Salinas P., Villaroel C., Marshall L., Sepulveda P., Muñoz N. 1991 Typotheriopsis sp. (Notoungulata Mesotheriidae), mamifero del Mioceno Superior en las cercanias de Belen, Arica, Norte de Chile. *Congresso Geologico Chileno, Resumen Expandidos*, 314-317.

Seyfried H., Wörner G., Uhlig D., & Kohler I. 1995. Eine kleine Landschaftsgeschichte der Anden in Nordchile. *Wechselwirkungen - Jahrbuch 1994 der Universität Stuttgart* , 60-72.

Tobar A., Salas Y., & Kast R. F. 1968. Carta Geologica de Chile, Cuadrángulos Camarca y Azapa. *Santaiago de Chile: Instituto de Investigaciones Geológicas*.

Vogel S., & Vila T. 1980. Carta Geologica de Chile, Cuadrángulos Arica y Poconchile, *Santiago de Chile: Instituto de Investigationes Geológicas*.

Walfort B., Hammerschmidt K., Wörner G. 1995. New Ar/Ar ages from Tertiary volcanics in the North Chilean Andes (18 S) : Implication for tectonic and magmatic evolution. *EUG-meeting Strasburg, April 1995. Terra Abstracts, Terra Nova* 7, 354.

# GEODYNAMIQUE PRE-ANDINE
# PRE-ANDEAN GEODYNAMICS
# GEODINAMICA PRE-ANDINA

# EVENT STRATIGRAPHY AND ALLOSTRATIGRAPHIC SUBDIVISIONS FOR THE ORDOVICIAN SYSTEM OF THE ARGENTINE PRECORDILLERA, SOUTHWESTERN GONDWANA

Ricardo A. ASTINI [1]

[1] *CONICET & Cátedra de Estratigrafía y Geología Histórica, Universidad Nacional de Córdoba, Vélez Sársfield 299, C.C. 395, 5000 Córdoba, Argentina.*

**KEY WORDS:** allostratigraphy, event-stratigraphy, basin analysis, Ordovician, Precordillera, Argentina.

## INTRODUCTION

As in other regions of the world a rather abundant stratigraphic nomenclature has been used to name Lower Paleozoic units in the Argentine Precordillera (Furque & Cuerda, 1979; Baldis *et al.*, 1982). In several cases different names are used for the same stratigraphic interval (Astini, 1994, 1995) in different areas of the basin. An allostratigraphic approach (*cf.* Walker, 1990; Woodcock, 1990) where strong emphasis is given to the sedimentary breaks, allows simplification of the stratigraphic picture and greatly helps in basin analysis and event-stratigraphic studies. In this contribution an allostratigraphic division for the Ordovician of the eastern tectofacies (according to Astini, 1992) of the Argentine Precordillera is presented. This method allows differentiation of the main breaks in the sedimentary record by considering a chronostratigraphic framework for the basin and also addresses the problems and causes of the disrupted stratigraphic record. The method can be applied in the Precordillera because of the relatively good knowledge on its faunas and their resolution and the relative clarity of the regional context (Astini *et al.*, 1995).

## ALLOSTRATIGRAPHIC APPROACH FOR SEQUENCE STRATIGRAPHY AND BASIN ANALYSIS

Several tentative and partial sequence stratigraphic schemes have been published in recent years on the Lower Paleozoic of the Argentine Precordillera including those of the author. Nevertheless, a main discussion on weather the Vail (several authors in Wilgus *et al.*, 1988, Van Wagoner *et al.*, 1990) or the Galloway (1989) criteria fits better is still lacking. Much of this problem could be solved by considering the bounding unconformities and their nature. A good starting point is that of an Allostratigraphic approach. Although of limited predictive potential (Martinsen *et al.*, 1993) this may offer operational advantages over the other schemes and may be more useful than sequence stratigraphic models in basins with complicated tectonism and variable sources, where the relativity of sea level cannot be ignored.

The relative magnitude and extent of different unconformities in a given basin can be assessed by constructing the rock preservation curve (Astini, 1993). This technique is described in detail by Woodcock (1990) and allows understanding the basin fill. On the basis of eleven generalized

Woodcock (1990) and allows understanding the basin fill. On the basis of eleven generalized chronostratigraphic logs carried out in a south-north trend in the Ordovician System of the Precordillera a rock preservation curve was constructed (Fig. 1). Although some outcrop limitations affect the proved hierarchy of some of the gaps, showing them as of a more limited extent (local unconformities), by considering the intervening facies their local versus regional origin can be estimated. Such is the case of the two lower units (not everywhere exposed) which are entirely carbonate and represent members of an evolved passive margin succession (Astini *et al.*, in press) or the upper units, which, although of limited outcrop extent, have a distinctive glacial origin. In both cases a global (eustatic) character for their bounding unconformities can easily be accepted.

Although a detail analysis of the driving mechanisms behind the above defined sequence stratigraphy is beyond the scope of this paper, a tentative interpretation is possible on an event-stratigraphic level. For this purpose a smoothed version of the rock preservation curve was drawn (Fig. 2), which can be interpreted as a relative sea-level curve, considering that the unconformities are due to relative base level fluctuations. Taking in consideration the cases outlined in the previous paragraph, the relative extent of the unconformities point out the local versus worldwide origin. Short-life widespread unconformities as those located between the carbonate alloformations (A & B, base of La Silla and base of San Juan Afms, respectively) as well as those related with the Late Ordovician glaciation (F & G, base and top of Don Braulio Afm) are interpreted as eustatic. Tectonic or subsidence components are ruled out in A and B due to their position in relation to a mature passive margin evolutionary stage. F and G are related respectively with wax and wane stages of the Hirnantian glaciation that affected Gondwana. Longer-life interruptions in the sedimentary record (D & E) (Llandeilo and Caradoc draw-downs) are, at least in the Precordillera, related to main tectonic events like the accretion of Precordillera terrane to western Gondwana and the postcollisional relaxation period, although enlarging eustatic components cannot be ruled out. The longer span gap in C is locally expanded due to the diachronic effect given by the progress of a migrating foredeep during the approach of the Precordillera Terrane to western Gondwana in the Early-Mid Ordovician. This widely developed diachronous unconformity partially overlaps with global sea-level fluctuations.

## CONCLUSIONS

A rock preservation curve based on eleven generalized chronostratigraphic logs carried out in the Ordovician System of the Argentine Precordillera (western Argentina), serves as a basis to highlight continuous sedimentation episodes separated by local and/or area-wide unconformities. Several allostratigraphic units were recognized and served as a ground for an event-stratigraphic approach based on presence and absence of rock record. Finally, a relative sea-level curve was constructed reflecting the extent of the recognized unconformities. This approach greatly simplifies basin analysis focusing on event-stratigraphy as a major tool in revealing basin evolution and basin fill architecture. Minor extent unconformities are interpreted as due to local subsidence pulses, whereas major unconformities are due either to sea-level eustatic changes or to regional tectonic events. Short-life widespread unconformities as those located between the carbonate alloformations (La Silla and San Juan Afms) or those related with the Late Ordovician glaciation (Don Braulio Afm) are interpreted as eustatic. Longer life interruptions in the sedimentary record (Llandeilo and Caradoc draw-downs) are, at least in the Precordillera, related to main tectonic events like the accretion of Precordillera to western Gondwana and the postcollisional relaxation period. The longer span gap is locally expanded due to the diachronic effect of tectonism.

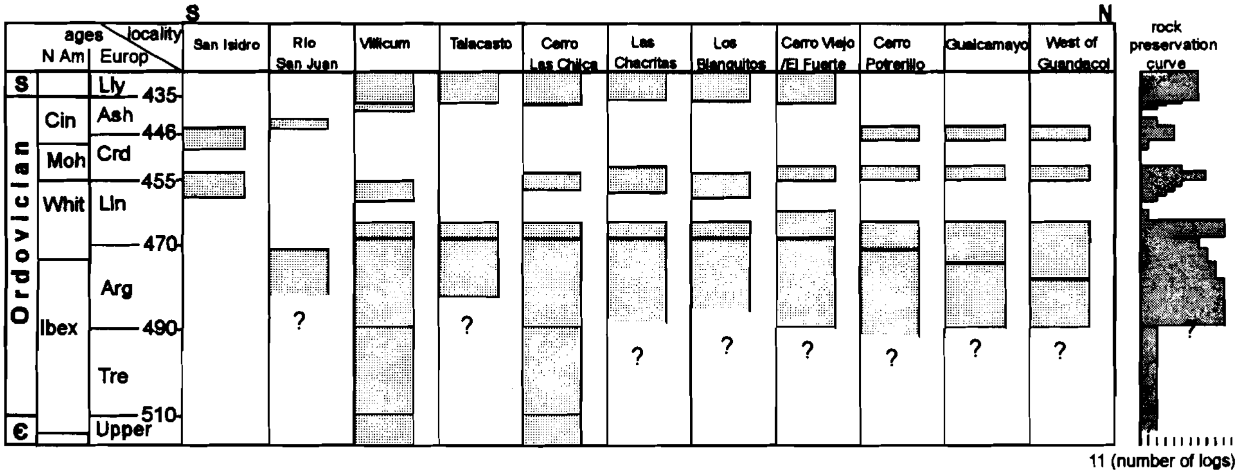


Fig. 1: Rock preservation curve constructed for the Ordovician System of the Argentine Precordillera based on eleven chronostratigraphic logs distributed in a south-north trend along the Precordilleran trhust belt.

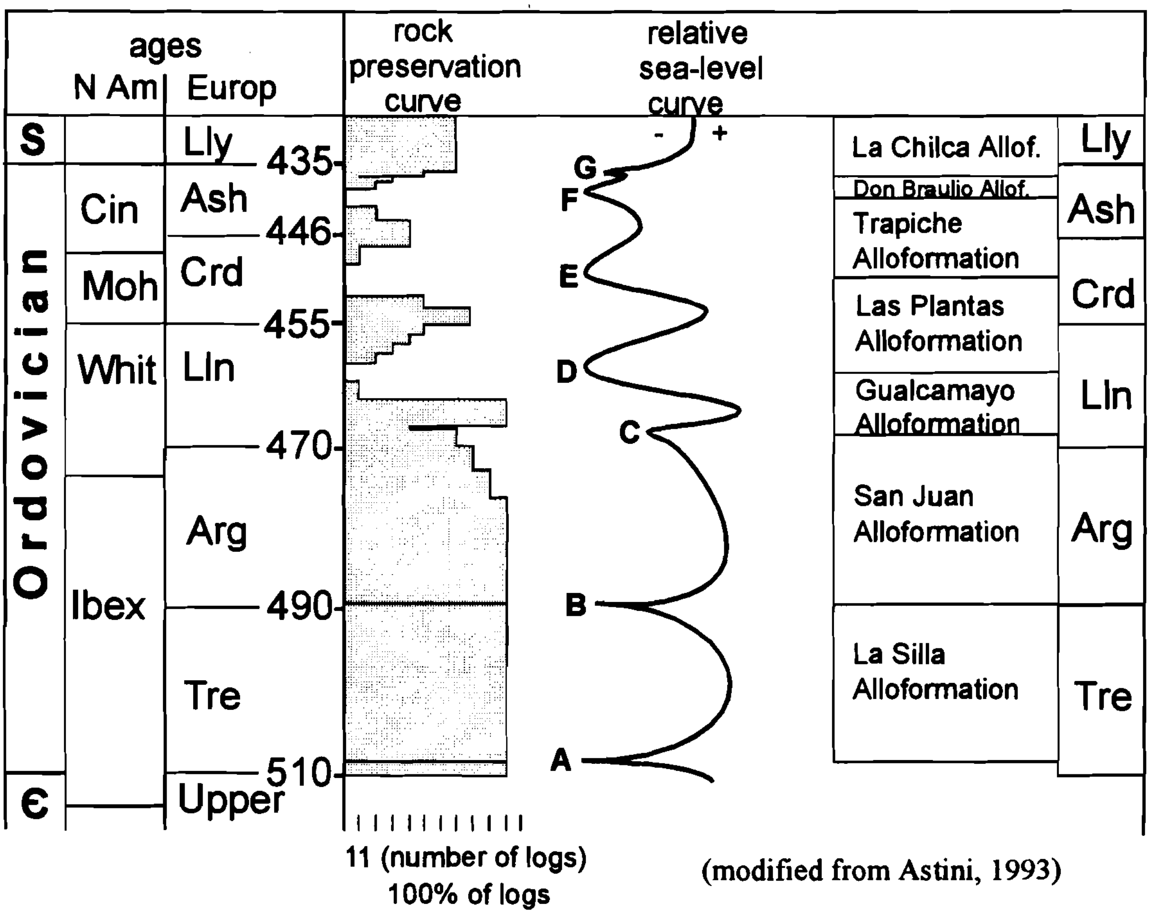


Fig. 2: Smoothed rock preservation curve and allostratigraphic division of the Ordovician of the Precordillera basin. For discussion on the curve see text.

**REFERENCES**

ASTINI, R.A., 1993. Secuencias deposicionales y niveles del mar en el Sistema Ordovícico de la Precordillera Argentina. *Bol. R. Soc. Esp. Hist. Nat. (Sec. Geol.)*, 88:113-126.

ASTINI, R.A., 1994. Paleoambientes y análisis secuencial de las unidades de pelitas negras (Aloformación Gualcamayo) que suprayacen a las sucesiones carbonáticas eo-ordovícicas en la Precordillera argentina. *Revista de la Asociación Geológica Argentina*, 49:71-84.

ASTINI, R.A., 1995. Sedimentología de la Formación Las Aguaditas (talud carbonático) e implicancias estratigráficas en la cuenca precordillerana oriental durante el Ordovícico. *Revista de la Asociación Geológica Argentina*. 50:143-164.

ASTINI, R.A.; J.L. BENEDETTO & N.E. VACCARI, 1995. The Early Paleozoic evolution of the Argentine Precordillera as a Laurentian rifted, drifted and collided terrane: A Geodynamic model. *Geol. Soc. Am. Bull.*, 107:253-273.

ASTINI, R.A.; V.A. RAMOS; J.L. BENEDETTO; E.N. VACCARI & F.L. CAÑAS, in press. La Precordillera: un terreno exótico a Gondwana. *XIII° Cong. Geol. Argentino y III° Cong. de Explor. Hidrocarb.*, Actas.

BALDIS, B.A.; M. BERESI; O. BORDONARO & A. VACA, 1982. Síntesis evolutiva de la Precordillera Argentina. Quinto Congreso Latinoamericano de Geología, 4:399-445. Buenos Aires.

FURQUE, G. & A. CUERDA, 1979. Precordillera de La Rioja, San Juan y Mendoza: Segundo Simposio de Geología Regional Argentina, Academia Nacional de Ciencias, 1:455-522. Córdoba.

GALLOWAY, W.E., 1989a. Genetic stratigraphic sequences in basin analysis I: Architecture and genesis of flooding-surface bounded depositional units. *AAPG Bull.*, 73:125-142.

MARTINSEN, O.J.; R.S. MARTINSEN & J.R. STEIDTMANN, 1993. Mesaverde Group (Upper Cretaceous), southeastern Wyoming: Allostratigraphy versus sequence stratigraphy in a tectonically active area. *AAPG Bull.*, 77:1351-1373.

VAN WAGONER, J.C.; R.M. MITCHUM; K.M. CAMPION & V.D. RAHMANIAN, 1990. *Siliciclastic sequence stratigraphy in well logs, cores and outcrops: concepts for high resolution of time and facies.* AAPG Methods in Exploration 7: 55 pgs.

WALKER, R.G., 1990. Facies modeling and sequence stratigraphy. *Jour Sed. Petrol.*, 60:777-786.

WILGUS, C.K; B.S. HASTINGS; C.G.St. KENDALL; H.W. POSAMENTIER; C.A. ROSS & J.C. VAN WAGONER (Eds.), 1988. *Sea-level changes: an integrated approach*, SEPM Spec. Publ., 42: 425 pgs.

WOODCOCK, N.H., 1990. Sequence stratigraphy of the Palaeozoic Welsh Basin. *J. Geol. Soc. London*, 157:537-547.

# PALEOENVIRONMENTAL FEATURES AND BASIN EVOLUTION OF A COMPLEX VOLCANIC ARC REGION IN THE PRE-ANDEAN WESTERN GONDWANA: THE FAMATINA BELT

Ricardo A. ASTINI[(1)] and Juan L. BENEDETTO[(2)]

[(1) (2)] *Cátedra de Estratigrafía y Geología Histórica, Fac. Cs. Ex., Fís. y Nat., Universidad Nacional de Córdoba, Av. Vélez Sársfield 299, CC 395, 5000 Córdoba, Argentina. CONICET*

**KEY WORDS:** Western Gondwana Pre-Andean margin, Early Ordovician, Famatina System, vulcano-sedimentary complex, island-arcs, Argentina.

## INTRODUCTION

The present day Famatina System, a north-south trending orogenic entity extended between the Sierras Pampeanas and the Precordillera in northwestern Argentina (Fig. 1a) was an active volcano-sedimentary setting during the Early-Middle Ordovician. Several studies carried out during the recent years (for a review see in Durand *et al.*, 1994) consider the Famatina belt as a complex magmatic arc typical of active margins (Toselli *et al.*, 1993; Sosa Gómez & Cisterna, 1994 and references therein) which may have extended to the north into the Faja Eruptiva of the Puna and to the south into the Pampeanas Ranges in what is known as the Sierra de Paganzo and probably the Sierra de Los Llanos. According to this the Famatina System has more than 800 km in length and is exposed to different levels of erosion in the south and north. Whereas in the south the host rocks are low, medium and high grade metamorphic rocks of Pampean affinities, in the north, the host is a complex marine vulcano-sedimentary association of Lower to Middle Ordovician Age. These substrate differences might be interpreted as a progressive evolution from Island-arc complexes in the north to a predominantly active margin setting within the south. Not until recently, the Island-arc hypothesis for at least part of the evolution of the Famatina System was suggested (Mannheim & Miller, 1992). Based on sedimentary features a back-arc setting was suggested for at least part of the Ordovician successions (Clemens, 1993; Benedetto & Astini, 1993). In a regional context, Benedetto & Astini (1993) and Astini *et al.* (1995) considered the Famatina as the volcanic arc related with the accretion of the Precordillera terrane to western Gondwana, which took place in the Middle-Late Ordovician. Recent paleomagnetic data presented by Conti *et al.*, (1995) as well as faunal studies (Benedetto & Sanchez, 1994, in press) allow considering the Famatina as a partly exotic island-arc complex with connections to the well known intra-Iapetus island-arcs within the Celtic province.

## NEW STUDIES

Recent surveys in the central region of the Famatina mountain belt located in western Argentina between the Precordillera and the Pampean Ranges allowed the recognition of a fairly continuous sedimentary history during the Arenig-Lower Llanvirn interval (Vaccari & Waisfeld, 1994; Albanesi & Vaccari, 1994; Toro & Brussa, 1995), which reflects the evolution of a rather complex tectonically controlled back-arc basin. Outcrops in the Cachiyuyo region include more than 2000 m of continuous section. Paleontological and sedimentological studies are still in progress but several informal members can be identified from bottom to top (Fig. 1b): a) silicified black shales with thin tuff partings, b) grey-bluish laminated shales, c) bioturbated grey sandy siltstones with calcareous fossiliferous nodules, and d) greenish-yellowish *Cruziana* rich sandstones and bioturbated siltstones with frequent coquina lenses comprise the Suri Formation, whereas e) lower red and purple silt-and sandstones, f) green volcanic breccias with tuffaceous fossiliferous siltstones and sandstones, and g) upper red and purple silt- and sandstones comprise the Los Molles Formation. Many of these members were formerly recognized as different units when studied scatterdly throughout the Famatina ranges. The succession in covered by an extensive mainly rhyolitic to intermediate volcanism of the Morado Formation correlated with the Las Planchadas Formation in the north (Mángano & Buatois, 1994). Active volcanism in the Famatina belt may have ceased after the collision of the Precordillera in the Middle-Late Ordovician, and may have been the source of the recently discovered K-bentonites in the Precordillera which occur in largely synchronous rocks.

This succession can be interpreted as the progressive filling of a back-arc basin with provenance from both foreland and arc derived sources (Fig. 1c). The first stage involved a rapidly subsiding trough reflecting the inception of initial thermal subsidence. This stage is characterized by starved-basin graptolitic black shales with minor marly hemipelagic beds. After a lag-period the succession shallowed upward indicating high sediment rates and decreasing accommodation space. Several stack-up shorefaces develop in a recurrent pattern dominated by storm-influenced environments and prograding volcanic-volcaniclastic wedges. Rapid facies associations shifts indicate a narrow shelf with predominantly high gradients, subjected to periodical base level drops, herein mostly related to local tectonic activity. Final stages of deposition, recorded in the Los Molles Fm, involved subaerial and marginal marine environments with prograding volcanic aprons and periodical emergence with short-life transgressions also driven by active tectonics (relative sea-level changes).

Throughout the Arenig and possibly culminating in the Early-Mid Llanvirn increasing volcanic activity took place. Silicified chonites and white-yellowish laminated and graded tuff horizons firstly appear in the *B. deflexus* Zone (Toro & Brussa, 1995). Increasing coarse volcaniclastics and volcanic breccias are common in the upper part of the Suri Fm., where they alternate with coarse shallow marine clastics and coquina layers. In most of the Los Molles Fm., they are interbedded with pink cross-bedded tidally influenced sandstones (herring-bone stratification) with abundant features of subaerial exposure and variegated shales with scarce fauna. Minor transgressive levels with abundant brachiopods (*Paralenorthis* and *Famatinorthis*, see Benedetto, 1994) seldom occur. The volcaniclastic beds yield trough and planar cross-beds. The coarsening and thickening upward trend reflects an increasing gradient typical of volcanic aprons and high gradient shelfal environments adjacent to volcanic or Island-arc complexes. As previously recognized (Mángano & Buatois, 1995), in the upper part of the succession, the low diversity faunal composition with unusually large individuals, the unstable paleocommunity structure and the low diversity *Cruziana* assemblage suggest the existence of extremely stressful environments.

Paleocurrents and sandstone composition indicate a double provenance. Most of the quartz-rich sandstones were derived from the east and are related to stable cratonal sources and subordinated recycled orogen. The volcanic source was located to the west and most of the paleocurrents measured in cross-beds show progradation toward the east-northeast. Most of the volcanic breccias and pyroclastics are derived from andesitic volcanism with minor felsic and basaltic components.

The available paleomagnetic data (Conti *et al.*, 1995), the faunal similarities to those of other island-arc complexes (Mángano y Buatois, 1992), and the predominance of Celtic mid-Iapetus brachiopods (Benedetto, 1994; Benedetto & Sanchez, in press) reveal a possible early stage island-arc setting. On the contrary, most of the features in the Arenig-Early Llanvirn suggest a back-arc environment. If a true island-arc complex developed in the early Famatinian history then it should have accreted to western Gondwana previous to the Precordillera terrane accretion in the Middle-Late Ordovician. Magmatic composition and isotopic relationships support an initial volcanic arc setting with no influence of continental crust contamination and a later collisional stage with acid peraluminous magmas generated by crustal anatexis intruding the Ordovician succession (Mannheim, 1993). Hence, it can be suggested that we should expect to find either two magmatic arcs in western Gondwana or, in the case of successively developed opposite dipping subduction, two superimposed or amalgamated magmatic arcs of slightly different ages in the context of the Famatina ranges (Fig. 1d).

## CONCLUSIONS

Available sedimentological data in the central region of the Famatina belt shows a fairly continuous sedimentary record with no evident breaks through the Arenig and possibly the Lower Llanvirn. The inception of frequent sandy layers and volcaniclastic debris in an open-marine starved-basin with black shales indicates the initial closure of the basin, which was originally considered as a back-arc trough with a twofold provenance, from a volcanic arc to the west and from a cratonal region to the present east. However, new paleomagnetic and faunal data suggest a probable early stage volcanic-arc setting as suggested from its magmatism, which still remains to be demonstrated on a sedimentological ground.

## REFERENCES

ALBANESI, G.L. & N.E. VACCARI, 1994. Conodontos del Arenigiano en la Formación Suri, Sistema del famatina, Argentina. *Rev. Española de Micropaleontología*, 26:125-146.

ASTINI, R.A., J.L. BENEDETTO y N.E. VACCARI, 1995a. The Early Paleozoic evolution of the Argentine Precordillera as a Laurentian rifted, drifted and collided terrane: A Geodynamic model. *Geological Society of America Bulletin*, 107:253-273.

BENEDETTO, J.L., 1994. Braquiópodos ordovícicos (Arenigiano) de la Formación Suri en la región del Río Chaschuil, Sistema de Famatina, Argentina. Ameghiniana, 31:221-238.

BENEDETTO, J.L. y R.A. ASTINI, 1993. A collisional model for the stratigraphic evolution of the Argentine Precordillera during the Early Paleozoic. *II ISAG 93* (Oxford), 501-504, París.

BENEDETTO, J.L. & T.M. SANCHEZ, 1994. Paleobiogeography of brachiopod and molluscan faunas along the South American margin during the Ordovician. *2nd Internat. Meeting du project IGCP 351 "Early Paleozoic evolution in NW Gondwana"* Abs:143-144. Rabat.

BENEDETTO, J.L. & SANCHEZ,T.M., en prensa a. Paleobiogeography of brachiopod and molluscan faunas along the South American margin during the Ordovician. *Correlación Geológica*. Tucumán.

CONTI, C.M.; A.E. RAPALINI; B. COIRA & M. KOUKHARSKY, 1995. Paleomagnetic evidence of an early Paleozoic accreted terrane in NW Argentina. Its implications in Gondwana-Laurentia interaction. IGCP 376, *Laurentian-Gondwanan connections before Pangea Field Conference*, Abs:11p. Jujuy.

CLEMENS, K., 1993. Sedimentología, proveniencia y desarrollo geotectónico del Sistema de Famatina en el noroeste de Argentina durante el Paleozoico Inferior. *XII° Cong. Geol. Argentino*. I:310-320.

DURAND, F.R.; A.J. TOSELLI; F.G. ACEÑOLAZA & J.R de TOSELLI, 1994. Evolución geológica del Sistema de Famatina durante el Precámbrico y Paleozoico. Fac. Cs. Nat. e Inst. Miguel Lillo, Universidad Nac. Tucumán, *Serie Monografía y Didáctica* 14:1-76.

MANGANO, M.G. & L.A. BUATOIS, 1992. Análisis genético de concentraciones fósiles n una secuencia volcaniclástica de plataforma, Formación Suri (Ordovícico del Sistema de Famatina). *Ameghiniana*: 29:135-151.

MANGANO, M.G. & L.A. BUATOIS, 1994. Estratigrafía y ambiente de sedimentación de la Formación Suri en los alrrededores del Río Chaschuil, Ordovícico del Sistema del Famatina, noroeste argentino. *Asoc. Arg. Sedimentología Revista*, 1:143-169.

MANGANO, M.G. & L.A. BUATOIS, 1995. Biotic response to volcanic and sedimentologic processes in a Gondwanic active plate margin basin: The Arenig-Llanvirn Suri Formation, Famatina Basin, Northwest Argentina. *In*: J.D. Cooper, M.L.Droser & S.C. Finney (Eds.), *Ordovician Odyssey*. SEPM Pacific Section, 77:229-232.

MANNHEIM, R., 1993. Génesis de las vulcanitas eopaleozoicas del Sistema del Famatina. noroeste de Argentina. *XII° Cong. Geol. Argentino*, 4:147-155.

MANNHEIM, R. & H. MILLER, 1992. Sistema de Famatina, NW Argentina: acreción de un arco volcánico en el margen occidental del Gonwana en el Paleozoico Inferior. *Publ. Mus. Extremadura*, 2:102-103.

SOSA GOMEZ, J. & C.E. CISTERNA, 1994. Sistema de Famatina: Arco magmático heterogéneo durante el Paleozoico Inferior. *Serie Correlación Geológica*. Resúmenes: 78-79. Tucumán.

TOSELLI, A.J.; J.R.DE TOSELLI; E. PELLITERO & J. SAAVEDRA, 1993. El arco magmático granítico del Paleozoico Inferior del Sistema de Famatina, Argentina. *XII° Cong. Geol. Argentino*, 4:7-15.

TORO, B.A. & E.D. BRUSSA, 1995. Graptolitos de la Formación Suri (Arenigiano) en la Sierra del Famatina, Argentina. Importancia bioestratigráfica y paleobiogeográfica. Reunión de Comunicaciones de la Asoc. Paleont. Arg., *Ameghiniana*, en prensa. Buenos Aires.

VACCARI, N.E. & B.G. Waisfeld, 1994. Nuevos trilobites de la Formación Suri (Ordovícico temprano) en la región de Chaschuil, Provincia de Catamarca. Implicancias bioestratigráficas. *Ameghiniana*, 31:73-86.

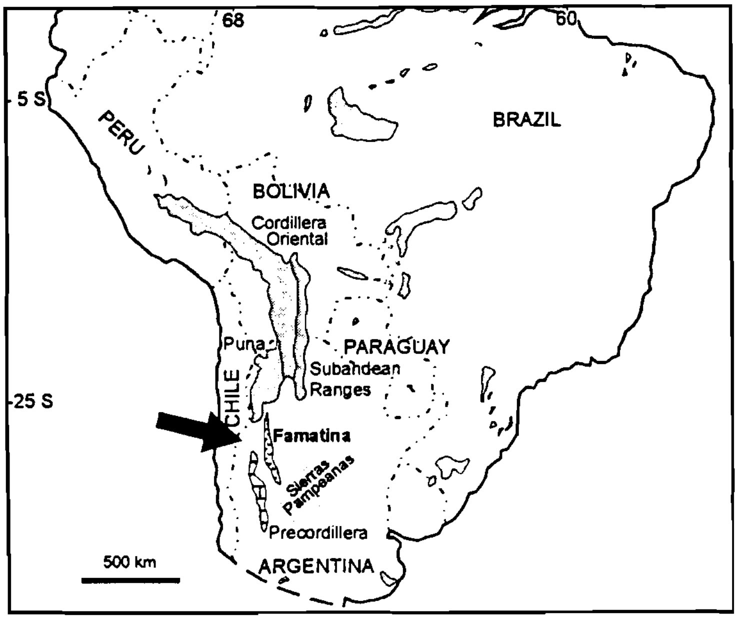


Fig. 1a: Location map of the Famatina System in the context

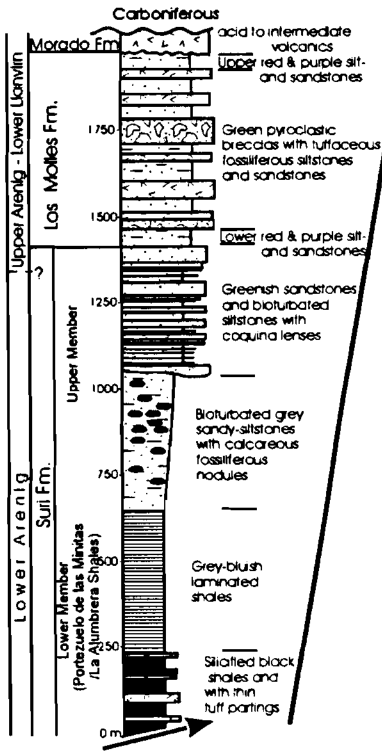


Fig. 1b: columnar log of the Lower Ordovician strata of the

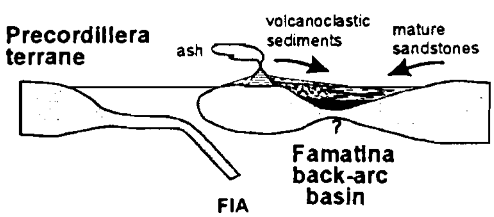


Fig. 1c: depositional model for the evolution of the Famatina basin fill with a twofold provenance from

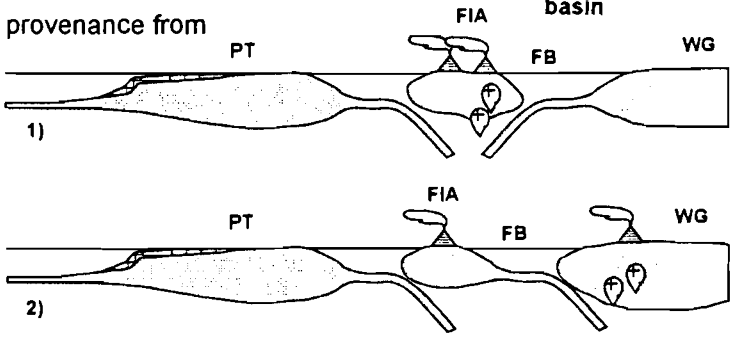


Fig 1d: Schematic diagrams of the two possible settings for the Famatina island-arc (FIA) hypothesis. PT:Precordillera terrane, WG: Western Gondwana, PB:represents the hypothetical Famatina basin depocenter. In 1) the two magmatic arcs are amalgamated in the same

# TECTONOSTRATIGRAPHIC DEVELOPMENT AND HISTORY OF AN ALLOCHTHONOUS TERRANE IN THE PREANDEAN GONDWANA MARGIN: THE ARGENTINE PRECORDILLERA

Ricardo A. ASTINI[(1)] and J.L. BENEDETTO[(2)]

[(1)(2)] *Cátedra de Estratigrafía y Geología Histórica, Fac. Cs. Ex., Fís. y Nat., Universidad Nacional de Córdoba, Av. Vélez Sársfield 299, CC 395, 5000 Córdoba, Argentina. CONICET*

**KEY WORDS:** Argentine Precordillera, exotic terrane, Lower Paleozoic, Pre-Andean Gondwana margin.

## INTRODUCTION

There seems to be a general consensus that the Argentine Precordillera represents a continental fragment that was rifted from the Ouachita embayment in Laurentia and subsequently accreted to Western Gondwana, present western South America (Astini *et al.*, 1995a). Its origin from the Ouachita embayment is documented by several lines of evidence, including similar ages and geochemistry of the basement rocks, similarities in the faunas and stratigraphy, and similar sizes of the Ouachita embayment and the Precordillera terrane (in the order of 800-1000 km length). Several new aspects on the rifting, drifting and docking of the exotic block, as well as on the postcollisional history of the Precordillera are considered in this contribution.

## TECTONOSTRATIGRAPHIC DEVELOPMENT

Three main evolutionary stages can be differentiated in the history of the Precordillera: a) passive margin, b) foreland basin I and c) foreland basin II.

The passive margin stage involves the complete carbonate bank which starts in the Lower Cambrian evolving from synrift to a mature stage platform. Rifting of the Precordillera from the Ouachita embayment is recorded in its stratigraphy, and the geometry of the three-dimensional rift system should have had critical implications in the later contractional histories of both margins. In the context of low-angle extension models for continental rifting (*e.g.* Lister *et al.*, 1986), Astini (1986) and Thomas & Astini (1986) have suggested that the western margin of the Precordillera is the conjugate of the Ouachita rift and its northern margin was defined originally by the Alabama-Oklahoma transform. The model suggests that the Ouachita rift margin is an upper-plate setting, whereas the Precordillera is considered to be the lower-plate margin, and hence, show complementary asymmetry. Thermal doming under the upper-plate Ouachita margin prevent development of synrift rocks, and as predicted by the model, retarded the passive margin sedimentation in almost 20 m.y. In contrast, "samples" of the initial rift stage were found in western Precordillera, and a thick carbonate bank overlying locally important graben-fills (red clastics and evaporites) developed since the late Early to early Middle Cambrian, as a result of a lower-plate configuration. The Early Cambrian graben-fill in the northern region of the Precordillera could represent an intracratonic graben developed in the Precordillera, similar to those of the Birmingham and Mississippi Valley grabens, orthogonally related to the Alabama-Oklahoma transform. The onset of the passive-margin stage is recorded in an upward transition to a thick carbonate bank deposit, that apparently was controlled by thermotectonic subsidence and eustatic sea-level fluctuations. The subsidence history of the Precordilleran platform was already closely compared to the Appalachian curve by Bond *et al.* (1984).

The foreland I stage (FI) starts with the inception of anoxic depocenters which reflects the progressive migration of a foredeep related with the incipient peripheral foreland developed during the transformation from a passive to an active margin. This stage includes the clastic Ordovician units which prograde westward as a clastic wedge over a complex paleogeography with predominance of tectonism over sea-level as the major accommodation control. Carbonate remnants persist into the Middle Ordovician in the Central Precordillera, where the peripheral forebulge was active. As a consequence of the collision, east-vergent deformation and metamorphism in the basement rocks to the east was developed. Associated magmatism in Pampeanas yields ages of ~465 m.y. (Ramos *et al.*, 1996).

The third stage comprises from the latest Ordovician and Early Silurian through the Devonian, time when the Lower Paleozoic dominantly marine Famatinian cycle gives place to the Upper Paleozoic Gondwanic cycle. This rocks are included in the second foreland stage (FII). This foreland basin was developed on top of the former passive margin of the Precordillera terrane and partly overlapped the first foreland as well. It developed as a response of contractional tectonics driven by the approach and collision of the Chilenia terrane to the present west. However, several relaxation episodes are present in between, shortly after each episode of shortening. Relaxation features include the generation of peripheral bulges, which cyclically affected the central Precordillera, generating erosive unconformities and local block faulting with associated clastic wedges. The FII was bounded by the west by an incipient thrust front yielding low-grade metamorphosed Ordovician rocks of the accretional prism and to the east by a thrust front affecting Grenville basement rocks (present day Pampeanas Occidentales Ranges), originated in the old reactivated suture between Precordillera and Gondwana. The eastern thrust front also affected the Eastern Precordillera (~400 m.y. according to Ramos *et al.*, 1996) and subsequently serve as the fundamental source of the Devonian clatic sediments which developed an oversupplied shelf-deltaic complex, opposite to the accommodation regime which predominate during the Silurian.

## PALEOGEOGRAPHY

None of the three stages mentioned before are present in the Western Gondwanic basins with these characteristics, what allows considering the Precordillera as an exotic terrane. Large lithological and faunal contrasts of the Cambrian and Lower Ordovician (passive margin stage) with the surrounding synchronous basins of Gondwana (Astini *et al.*, 1995a; Vaccari, 1995; Sánchez y Waisfeld, 1995), suggest that the Precordillera is an allochthonous terrane to Gondwana (*cf.* Ramos *et al.*, 1986; Astini, 1995; Astini *et al.*, 1995a, Benedetto *et al.*, 1995). By contrary, its strong faunal and stratigraphic similarities with successions in the southern cone of Laurentia point out to an unequivocal provenance from North America (Benedetto, 1993; Benedetto *et al.*, 1995, Astini *et al.*, 1995a y 1995b). Recent studies carried out on basement xenoliths in the Precordillera are summarized in Kay *et al.*, (1996) and conclude on basis of U-Pb zircon ages, whole rock Pb and Nd isotopic data that the affinities of the Precordilleran basement are as those of the North American Grenville basement, and particularly close to that outcropping in Texas. Furthermore, Tosdal (1996) and Kay *et al.*, (1996) suggest an origin as a rifted fragment from Laurentia pointing out the strong differences with other basements present in Western Gondwana. According to this, the Precordillera is considered as a terrane exotic to Gondwana that rifted from Laurentia in the Early-Middle Cambrian and collided with Western Gondwana in the Middle-Late Ordovician (Fig. 1). An intermediate history of drifting and gradual geographic isolation is necessary to explain the faunal differentiation and endemism noted by Benedetto *et al.* (1995). It also explains the gradual cooling that affected the Precordillera since Arenig. The lithological indicators of climatic shift from low-latitude Bahamian-type carbonates in the Cambrian-lowermost Ordovician to glacial tills in the Late Ordovician (Astini, 1995). Faunal links with Gondwana started in Llandeilo-Caradoc times. The conclusive effects of the Hirnantian glaciation together with the typical *Hirnantia* fauna are categorical in favor of its definite connection with Gondwana.

## CONCLUSIONS

An up-to-date synthesis of the geologic evolution of the Argentine Precordillera during the Lower Paleozoic considers it as an allochthonous terrane that rifted from the Ouachita embayment in North America and collided with Western Gondwana in the Mid-Late Ordovician. Its Grenville basement has similar geochemical characteristics than the Grenville belt of southeastern North America and its closest match is with that of the Texas Promontory. Its basement outcrops in the present Sierras Pampeanas Occidentales from the Sierra de Pie de Palo in San Juan down to the Ponon Trehué area in Mendoza.

Three main evolutionary stages can be defined in its history: a) a passive-margin stage, characterized by a common history with Laurentia including the asymmetric rifting and drifting stages, b) a first foreland basin stage, characterized by a clastic wedge prograding west, and deformation of the basement to the east due to the accretion of Precordillera to Gondwana (Ocloyic diastrophism), and c) a second foreland basin stage, which characterizes the postcollisional interval and ends with the accretion of the Chilenia terrane in Middle Paleozoic times (Precordilleran distrophism). From a paleobiogeographical viewpoint a pure Laurenitan stage (Cambrian-Tremadoc), a dominantly isolated - with major endemism- drift stage (Arenig-Llandeilo) and a dominantly Gondwanic stage (Caradoc-Ashgill) can be differentiated in the Cambrian-Ordovician history, where the Arenig and the Caradoc represent main turnover moments, hence transitional stages. The Silurian and Devonian faunas and environments of Precordillera are clearly Gondwanic and do not differ, as well as those of the late Ordovician, from those of surrounding South American basins.

On the basis of contrasted basements and passive-margin stage rocks and faunas the Argentine Precordillera in considered a unique exotic terrane which can be differentiated from the rest of the surrounding regions and Lower Paleozoic basins in western Gondwana.

## REFERENCES

ASTINI, R.A., 1995. Paleoclimates and paleogeographic paths of the Argentine Precordillera during the Ordovician: evidence from climatically sensitive lithofacies. *In*: Cooper, J.D., M.L. Droser & S.C. Finney (Eds.), *Ordovician Odyssey*. SEPM Pacific Section, Book 77:177-180.

ASTINI, R.A., 1996. The Argentine Precordillera-lower plate of the Ouachita conjugate-pair rift: a suitable explanation for their stratigraphic differences. *Geol. Soc. Am. South-Central Meeting, Abs. & Prog.* 28:15p., Austin.

ASTINI, R.A., J.L. BENEDETTO & N.E. VACCARI, 1995a. The Early Paleozoic evolution of the Argentine Precordillera as a Laurentian rifted, drifted and collided terrane: A Geodynamic model. *Geological Society of America Bulletin*, 107(3):253-273. Boulder.

ASTINI, R.A., VACCARI, N.E., THOMAS, W.A., RAYMOND, D.E. & OSBORNE, W.E., 1995b. Shared evolution of the Argentine Precordillerra and the Southern Appalachians during the Lower Cambrian. *Geological Society of America, Abstracts with Programs*, v27(6):A-458. New Orleans.

BENEDETTO, J.L., 1993. La hipótesis de la aloctonía de la Precordillera Argentina: un test estratigráfico y bioestratigráfico. *XII° Congreso Geológico Argentino*, v.3:375-384.

BENEDETTO, J.L. N.E. VACCARI; M.G.CARRERA & T.M. SÁNCHEZ, 1995. The evolution of faunal provincialism in the Argentine Precordillera during the Ordovician: new evidence and paleontological implications. *In*: Cooper, J.D., M.L. Droser & S.C. Finney (Eds.), *Ordovician Odyssey*. SEPM Pacific Section, Book 77:181-184.

BOND, G.C.; P.A. NICKELSON & M.A.KOMINZ, 1984. Breakup of a supercontinent between 625 Ma and 55 Ma: new evidence and implications for continental histories. *Earth and Planetary Science Letters*, 70: 325-345.

KAY, S.M.; S. ORRELL & J.M. ABRUZZI, 1996. Zircon and whole rock Nd-Pb isotopic evidence for a Grenville age and Laurentian origin for the basement of the Precordilleran terrane in Argentina. *Journal of Geology* (in press.).

LISTER, G.S; M.A. ETHRIDGE & P.A. SYMONDS, 1986. Detachment faulting and the evolution of passive continental margins. *Geology*, 14:246-250.

RAMOS, V.A; T.E. JORDAN; RW. ALLMENDINGER; C. MPODOZIS; S.M. KAY; J.M. CORTES & M.A. PALMA, 1986. Paleozoic terranes of the central Argentine Chilean Andes. *Tectonics*, 5:855-880.

RAMOS, V.A.; G.I. VUJOVICH & D. DALMEYER, 1996. Klippes y ventanas tectónicas de la Sierra de Pie de Palo: sus relaciones con la colisión de Precordillera. *XIII° Congreso Geológico Argentino*, Actas. Buenos Aires (este congreso).

SÁNCHEZ, T.M. & B.N.WAISFELD, 1995. Benthic assemblages in the northwestern of Gondwana: a test of the Ordovician evolutionary radiation model. *In*: Cooper, J.D., M.L. Droser & S.C. Finney (Eds.), *Ordovician Odyssey*. SEPM Pacific Section, Book 77:409-412.

THOMAS, W. & R.A. ASTINI, 1996. Asymmetric conjugate pair rift margins of the Ouachita rift and the Argentine Precordillera. *Geol. Soc. Am. South-Central Meeting*, Abs & Prog. 28:45p *Austin*.

TOSDAL, T.M., 1996. The Amazon-Laurentia connection as viewed from Middle Proterozoic rocks, western Bolivia and northern Chile. *Tectonics* (in press.).

VACCARI, N.E., 1995. Early Ordovician trilobite biogeography of Precordillera and Famatina, western Argentina: preliminary results. *In*: Cooper, J.D., M.L. Droser & S.C. Finney (Eds.), *Ordovician Odyssey*. SEPM Pacific Section, Book 77:193-196.

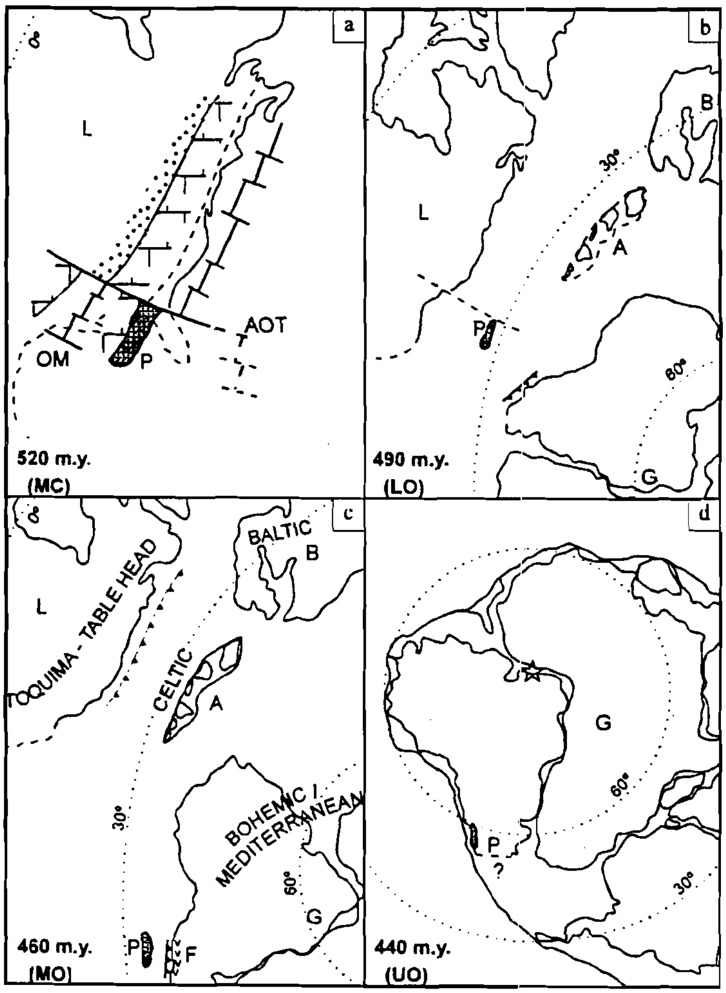


Fig. 1: Series of maps showing the paleogeographic evolution of the Precordillera terrane between the Middle Cambrian (MC) and the Upper Ordovician (UP) (modified from Astini et al., 1995). c) includes the Ordovician brachiopod biogeographic provinces. L:Laurentia, P:Precordillera, B:Baltica, A:Avalon, G:Gondwana, F:Famatina, OM:Ouachita mid-ocean ridge, AOT:Alabama-Oklahoma transform.

# NEW AGES (U-Pb,Rb-Sr,K-Ar) FROM SUPPOSED PRE-CAMBRIAN UNITS IN NORTHERN CHILE: SOME GEOTECTONIC IMPLICATIONS

Miguel A. BASEI[1], Reynaldo CHARRIER[2] and Francisco HERVE[2]

(1) Centro de Pesquisas Geocronológicas, Instituto de Geociências, Universidad de São Paulo, CEP 05508-900, Brasil.
(2) Departamento de Geología, Universidad de Chile, Casilla 13518, Correo 21, Santiago, Chile.

KEYWORDS: Andes, Chile, Altiplano, Early Paleozoic, Basement, Geochronology.

## INTRODUCTION

Since the first dating of Proterozoic rocks (1,000 Ma) on the westflank of the Altiplano in northernmost Chile (Pacci et al., 1980) other rock units at different localities have been surveyed in order to determine their possible Precambrian age. Mentions of the existence of Proterozoic ages or of ages near the Proterozoic-Phanerozoic boundary have been made by Damm et al. (1990) and Díaz et al. (1985).

The presence of rocks of that age supported the existence in the basement of the Andes of northern Chile of the Arequipa-Antofalla Craton Massif (Ramos, 1988), considered to be an allochtonous terrane of Laurentia provenance by Dalziel et al., (1994).

A dating program was carried out to ascertain the Proterozoic age of the Belén Metamorphic Complex (BMC), and the Mejillones Metamorphic Complex (MMC) (Fig. 1).

Samples were dated at the Centro de Pesquisas Geocronológicas of the Instituto de Geociências, Universidad de São Paulo, Brazil, by M.A.B.

## GEOLOGIC FRAMEWORK

The Belén Metamorphic Complex (BMC) forms a narrow strip along a high angle, west-vergent thrust system located on the western slope of the chilean Altiplano plateau between Chapiquiña and Tignamar (Muñoz and Charrier, in press) (Fig. 1). Along these faults the CMB is westwardly thrusted over late Tertiary deposits. Unconformably covering the BMC are Jurassic marine deposits, and Tertiary volcaniclastic and continental sedimentary deposits (Montecinos, 1963; Salas et al., 1966; Pacci et al., 1980; Muñoz et al., 1988; Muñoz, 1991; García, 1996). The BMC is mainly composed by foliated amphibolites and subordinately by quartz mica schists, gneissic schists, orthogneisses and serpentinites. It is intruded by a small gabbro stock and mafic, aplitic and felsic dikes.

The Mejillones Metamorphic Complex (MMC) consists of mica-schists, amphibolites, gneisses and migmatites (Baeza, 1984) intruded by mafic and granitic plutonic rocks (Fig. 1).

GEOCHRONOLOGIC IMPLICATIONS

In the Belén Metamorphic Complex (BMC) the following ages were obtained:

1. 544+/-22 Ma (Rb-Sr, whole rock isochron) in the quartz mica schists of Quebrada Saxamar (locality 3, Fig. 1).
2. 536 to 516 Ma (K-Ar on minerals) in the Quebrada Saxamar schists (locality 3, Fig. 1).
3. 507+/-48 (U-Pb zircon age) in the quebrada de Achacagua orthogneiss (locality 2, Fig. 1).
4. 475+/-31 Ma (U-Pb in zircon) on granitic veins at Quebrada Saxamar (locality 3, Fig. 1).
5. 417 to 365 Ma (K-Ar on minerals) for the Saitoco orthogneiss (locality 1, Fig. 1).

Ages in 1 and 2 are considered to be associated to the regional metamorphism of the BMC. The younger 516 Ma K-Ar age (see 2) could indicate uplift and cooling of the metamorphic complex.

Intrusive events (3 & 4), though largely concordant within errors, appear to be slightly younger than ages (1 & 2) in the metamorphic rocks.

Ages for the Saitoco orthogneiss, given in 5, are considered to be cooling ages of the intrusive body.

Model Nd-Sm ages of 1,746 and 1,543 Ma of the Quebrada Saxamar schists testify of a long previous crustal origin of its constituents.

In the Mejillones Metamorphic Complex (MMC) the Jorgino Formation, constituted by gneisses and amphibolites gave K-Ar ages of 147 and 162 Ma (biotite) and 159 Ma (hornblende). Crosscutting granite veins were dated at 144+/-1 Ma (U-Pb in zircons) and 152 and 143 Ma (K-Ar in muscovite).

CONCLUSIONS

The above results indicate that the main signature in the BMC are Pampean (middle Cambrian) plutonic and metamorphic events. Our data cast some doubt on the validity of the 1,000 Ma event previously determined in the BMC (Pacci et al., 1980), because there is no indication of it in the analysed samples, which were collected at the same localities as the previously dated 1,000 Ma dated rock suite.

The Jorgino gneisses and amphibole schists (MMC) bear the evidence of a Jurassic intrusive event that may have reset the K-Ar system of the metamorphic rocks, which might be older as previous Rb-Sr studies indicate. The BMC bears no evidence of Mesozoic events as the MMC which is located farther West, at the leading edge of South America.

---

Fig. 1. Location map of the studied region in South America. a. Morphostructural units of the central Andes of Northern Chile, Southern Perú, and Western Bolivia: CR. Coastal Range, CD. Central Depression, PC. Precordillera, PD. Preandean depression, A. Altiplano, EC: Eastern Cordillera, SS. Subandean Sierras. b. Geological sketch map of the western Altiplano between Chapiquiña and Tignamar with sample localities in the BMC (based on García, 1996): 1. BMC, 2. Livilcar Formation (Jurassic, marine), 3. Lupica Formation (Lower Miocene), 4. Joracane Formation (Middle Miocene, syntectonic conglomerates), 5. Porphyric intrusives (Middle Miocene), 6. Huaylas Formation (Upper Miocene, syntectonic conglomerates), 7. Plio-Pleistocene deposits, 8. Sample localities.

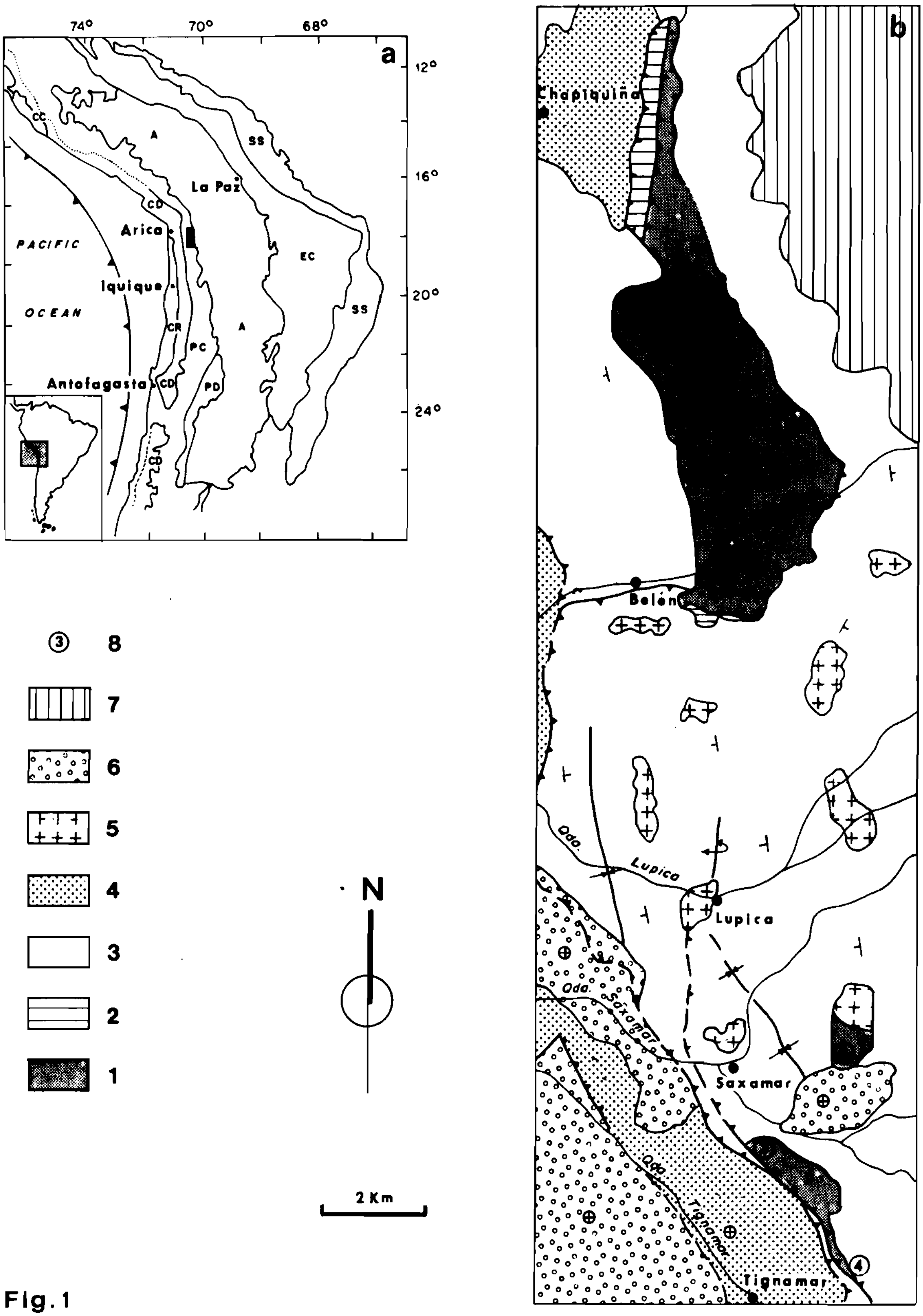
a
74°
70°
68°
12°
16°
20°
24°
CC
A
SS
La Paz
CD
Arica
PACIFIC
EC
Iquique
OCEAN
SS
CR
A
PC
Antofagasta
CD
PD
CD
b
Chapiquiña
Belén
Qda.
Lupica
Lupica
Qda.
Saxamar
Saxamar
Qda.
Tignamar
Tignamar
4
8
7
6
5
4
3
2
1
N
2 Km

Fig.1

## ACKNOWLEDGEMENTS

This study was funded by Grant N° 1224-91 of the Comisión Nacional de Investigación Científica y Tecnológica (CONICYT), Chile. This article is a contribution to IGCP Projects N° 345 "Andean Lithospheric Evolution" and N° 376 "Gondwana-Laurentia Connections".

## REFERENCES

DALZIEL, I.A.W., DALLA SALDA, L. and GAHAGAN, L., 1994. Paleozoic Laurentia-Gondwana interaction and the origin of the Appalachian-Andean mountain system. Geological Society of America Bulletin, Vol. 106, p. 243-252.

DAMM, W., PICHOWIAK, S., HARMON, R.S., TODT, W., KELLEY, S., OMARINI, R. AND NIEMEYER, H., 1990. Pre-Mesozoic evolution of the Central Andes; the basement revisited, in Mahlburg Kay, S., and Rapela, C.W., eds., Plutonism from Antactica to Alaska: Geological Society of America Special Paper N° 241, p. 101-126.

DIAZ, M., CORDANI, U.G., KAWASHHITA, K., BAEZA, L., VENEGAS, R., HERVÉ, F. AND MUNIZAGA, F., 1985. Preliminary radiometric ages from the Mejillones Peninsula, northern Chile. Comunicaciones, N° 35, p. 59-67.

GARCIA, M., 1996. Estratigrafía, estructura y evolución tectónica del borde occidental del Altiplano entre Zapahuira y Tignamar. Thesis, Departamento de Geología, Universidad de Chile, Santiago, 135 p.

MONTECINOS, F., 1963. Observaciones de geología en el Cuadrángulo de Campanani, Departamento de Arica, Provincia de Tarapacá. Thesis, Departamento de Geología, Universidad de Chile, Santiago, 109 p.

MUÑOZ, N., 1991. Marco geológico y estratigrafía de un sistema fluvio-lacustre, Paleogeno. Altiplano de Arica, Norte de Chile. Actas 6th. Congreso Geológico Chileno, Viña del Mar, p. 201-204.

MUÑOZ, N., ELGUETA, S. y HARAMBOUR, S., 1988. El Sistema Jurásico en el curso superior de la quebrada Azapa, I Región: Implicancias paleogeográficas. Actas 5th. Congreso Geológico Chileno, Santiago, Tomo 1, p. A403-A415.

MUÑOZ, N. and CHARRIER, R., in press. A west vergent fault system at the western border of the Altiplano in Northern Chile: implications for the uplift of the Altiplano-Puna plateau. Journal of South American Earth Sciences.

PACCI, D., HERVE, F., MUNIZAGA, F., KAWASHITA, K and CORDANI, V., 1980. Acerca de la edad Rb/Sr precámbrica de rocas de la Formación Esquistos de Belén, Departamento de Parinacota, Chile. Revista Geológica de Chile, N° 11, p. 43-50, Santiago.

RAMOS, V.A., 1988. Late Proterozoic - Early Paleozoic of South America-a collisional history. Episodes, Vol. 11, N° 3, p. 168-174.

SALAS, R., KAST, R., MONTECINOS, F. y SALAS, R., 1966. Geología y recursos minerales del Departamento de Arica, Provincia de Tarapacá. Instituto de Investigaciones Geológicas, Santiago, Bol. 21, 114 p.

# PREANDEAN GEOTECTONIC SETTINGS OF SOUTHWESTERN SOUTH AMERICA

Luis H. Dalla Salda [1] , Monica G. López de Luchi [2] , Carlos Cingolani [1] and Ricardo Varela [1]

(1) Centro de Investigaciones Geológicas. Calle 1 N° 644. 1900 La Plata. Argentina

(2) Centro de Investigaciones en Recursos Geológicos. J. Ramírez de Velasco 847. 1414 Buenos Aires Argentina

Key Words: Preandean-Tectonic setting-Occidentalia-Famatinian Belt

East of the Andean Cordillera, three major geotectonic units contributed to the pre Gondwanic crustal evolution of southwestern South America. From west to east they are: the Precambrian Occidentalia Terrane that crops out along both edges of the Andes as highly tectonized blocks, the Late Precambrian-Middle Palaeozoic Famatinian Orogenic Belt, which comprises the Pampean Ranges, the Puna and the North Patagonian Massif and the Precambrian westernmost Rio de la Plata-Brazil-Southern Africa cratonic area .Occidentalia and the Famatinian Orogenic Belt have been yuxtaposed as a result of Middle Ordovician (ca. 460 Ma) Laurentia-Gondwana collision (Dalla Salda et al, 1992 a,b). Several narrow discontinuos basic-ultrabasic belts dated as late Precambrian to Lower Paleozoic exist west of the more granitized Famatinian belt.

**Occidentalia** is composed by metamorphic and granitoid rocks (several radiometric ages indicate Grenville ages) trending nearly north-south mostly along the western side of the Famatinian Orogenic Belt, form northernmost Chile to Patagonia. It includes the Chilenia terrane (Ramos et al., 1986) and is partially covered by the Precordillera Cambrian to Tremadocian carbonate platform, recently accepted as a terrane of Laurentia provenance (Dalziel et al., 1996).Dalla Salda et al. (1992 a,b) and Dalziel et al.(1994) interpreted it as a relic of eastern Laurentia detatched after the Taconian collision during Iapetus closure.

The **Famatinian Orogenic Belt** is a complex metamorphic-igneous belt whose evolution covers the span from late Proterozoic to Devonian and includes two distinct metamorphic and plutonic cycles, Pampean and Famatinian in the Eastern Pampean Ranges.*Pampean Cycle* covers a span from Late Proterozoic (640 Ma) to Lower Cambriam (530-540 Ma) and it includes metamorphic and igneous rocks.In the Eastern Pampean Ranges, scattered outcrops of trondjhemitic to tonalitic granitoids and metaigneous rocks (metanorites) older than 520 Ma has been asigned to this cycle (Rapela et al., 1990). A low grade metamorphic event is associated. The ca. 550 Ma limit Pampean/Famatinian Cycle is very difficult to set. Tilcarica defórmational event, which affects the sin-rift sequences of the Puncoviscana Formation to the north of the Pampean Ranges, could be pointing out to the change in the geotectonic regime along the western margin of Gondwana. Since a rift separated Gondwana from Laurentia from Late Proterozoic (750Ma) on (Dalla Salda et al, 1992a, b), sometime between the rift-drift regime and the generation of the Famatinian active margin, a major change to a convergence regime would have happened. A continuous subduction regime installed along the western margin of Gondwana from the Cambrian;diacronous opening could explain magmatic arc signature coeval to passive margin affinities or more tholeithic compositions closer to the inferred spreading center.

*Famatinian Cycle* (520-360Ma) comprehends an extensive period of metamorphism and igneous activity with peaks of metamorphic and igneous activity.This cycle can be considered as equivalent to G2 granitoids (Rapela et al, 1990); D2 and D3 deformational domains (Dalla Salda,1987) are related to the Famatinian evolution. D2 involves NNW structures,it is essentially a ductile deformation associated to the higher metamorphic grade and migmatitization. Peak metamorphic temperatures seem to postdate D2 (due to tectonic uplift). D3 is a higher crustal level episode with an associated retrogradation. Three main groups of granitoids are distinguished on the basis of geochemical features and their relation to D2 and D3 deformational events:a pre-Taconic group,a Taconic group and a late Taconic (Acadian) group(Lopez de Luchi and Dalla Salda, 1995).

Pre-Taconic granitoid group(520-460 Ma) is represented by medium to small granitic plutons or polifacial batholiths with sligthly discordant to concordant contacts, moderately to highly strained. This magmatism like calc-alkaline, metaluminous to peraluminous and have and arc-like signature. If the Pre-taconic granitoids of the Famatina Arc are considered, an Andean type arc system parallels a coeval more mature arc inwards the eastern continent.Meanwhile in the Eastern Pampean Ranges, Pre-Taconian granitoids are intruded in metamorphic rocks, in the Famatina Arc, they are intruded in metasedimentites and metavulcanites. Volcanism associated to Lower Ordovician sedimentary basins, appears in north and central Famatina Arc and the Puna. Gabroids considered as roots of a magmatic arc emplaced in granulites appears in Sierra de Ancasti and Sierra de Fiambala. Famatinian Lower Ordovician granitoids are poorly defined in the Famatina. Continental arc signature corresponds to Taconian ages (460-440Ma); being so, a magmatic Famatinian arc would be coeval to collisional granitoids inward the continent. Subduction process could have continued locally during the collision because of the irregular shape of the continents (the Famatina and the Puna magmatic arcs).Resetting of older ages might be an alternative explanation at least for a part of the Famatina Arc since 460-440 Ma ages are mostly K/Ar mica ages in moderately deformed rocks or Rb/Sr whole rock ages in granitoids with different geochemical signature (i.e. in Paiman Ranges).

Taconic granitoid group (460-440 or 420 Ma) include syntectonic plutons concordant to regional structures or in a complex relation to the polyphasial deformation in the orogen. All of them share collisional signature. Trace element inter-element relations show a marked Rb enrichment(Lopez de Luchi

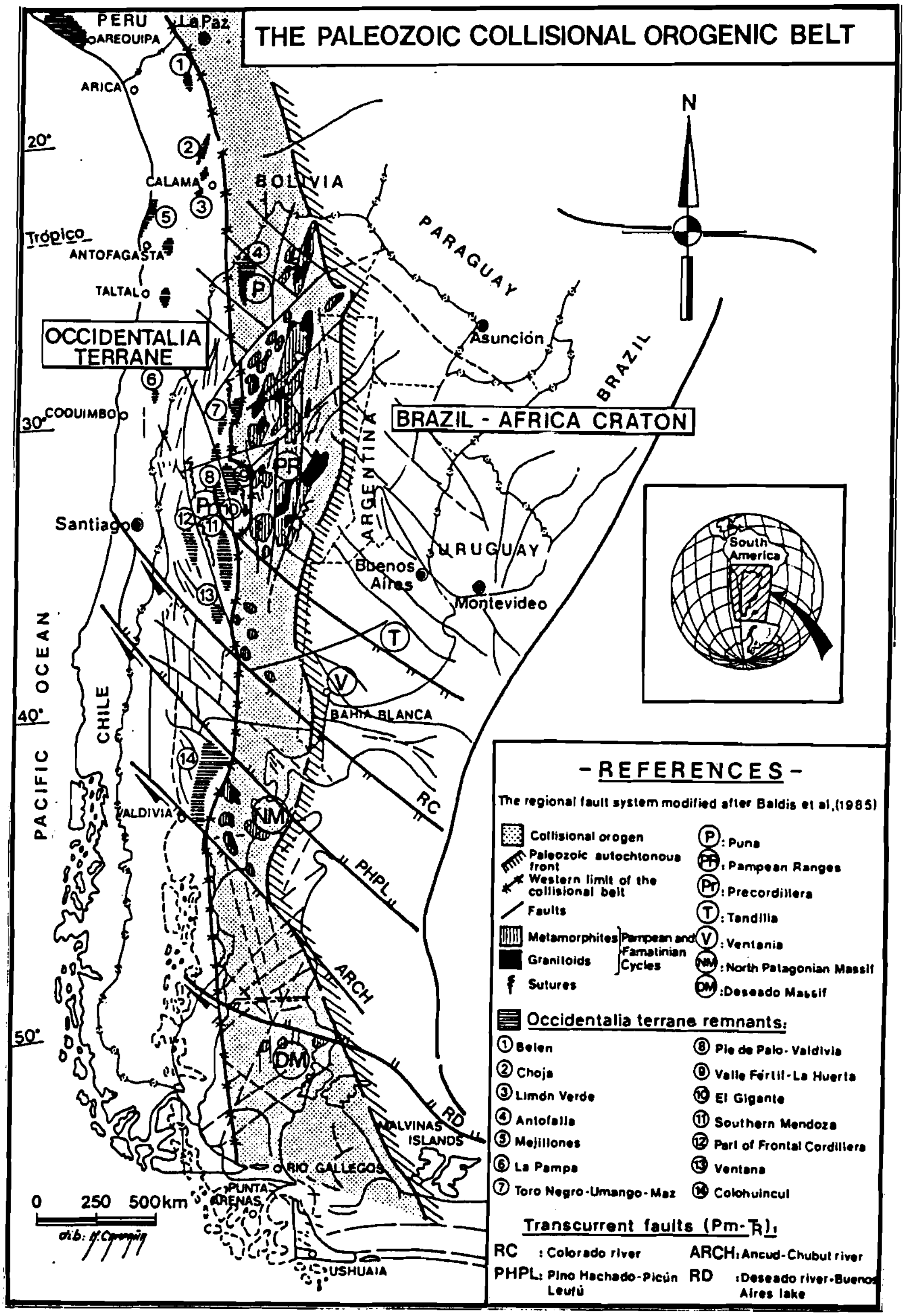


Southern South America Famatinian Orogenic Belt showing the main units referred to in text. Also shown is the Occidentalia Terrane with the Lower Paleozoic Precordillera belt .Continental megafractures (considered as Permo-Triassic), shifting the Famatinian Orogenic belt are represented.

and Dalla Salda, 1995).Taconic granitoids are associated to a granitic migmatitization unlike the tonalitic migmatitization of the Lower Ordovician rocks. Crustal thickening, overthrusting and ramp tectonics associated to continent-continent collision overlap different structural levels. Regional controlling structures of the Lower Ordovician plutons are NNW-SSE (except for San Luis Hills).

Late-Taconic granitoid group (440 to 420-360) is characterized by large batholiths like Achala, Capillitas, with a more syenogranitic composition, NNE fault controlled emplacement and contact aureoles or smaller ellipsoidal plutons (Batolito de Renca, Batolito de Las Chacras-Piedras Coloradas) that are predominantly monzogranites to syenogranites. The former are peraluminous to sligthly peralkaline crustal granites but share a collisional to within plate trace element signature. The latter are metaluminous to middle peraluminous, richer in MgO with a mixed mantle and crustal signature.During the Devonian, granitoid signature, metamorphism, structure and paleogeographic reconstructions allowed to interpret a dextral transpresive Laurentia-Gondwana collision (Dalziel et al.,1994). Granitoid plutons emplaced at an epizonal environment indicates post-Ordovician uplift.Peri-orogenic syn to postcollisional sedimentary basins formed as a consequence of this uplift.

As it has been already stated (Dalla Salda et al.,1996, GSA, Austin) if Occidentalia was part of eastern Laurentia, it is feasible to suggest that the Appalachians-Ouachitas-Marathon and Occidentalia-Precordillera-Famatina Orogenic Belt may fit in a single geotectonic setting .

## References


Dalziel, I.; Dalla Salda, L.H. and Gahagan, L.M., 1994. Paleozoic Laurentia-Gondwana interaction and the origin of the Appalachian-Andean mountain system. *Geol. Soc. Amer. Bull.*, 106, 243-252

Dalziel, I.; Dalla Salda, L.H and Cingolani, C. and Palmer. P. 1996.The Argentina Precordillera: A Laurentia Terrane? Penrose Conference Report, *GSA Today* , 16-18

Dalla Salda, L., 1987, Basement tectonics of the southern Pampean Ranges. *Tectonics*, 6, 3:249-266.

Dalla Salda, L.; Cingolani, C. and Varela, R. 1992a. Early Paleozoic orogenic belt of the Andes in South America: Result of Laurentia-Gondwana collision. *Geology*, 20, 616-620.

Dalla Salda, L., Dalziel, I. ,Cingolani, C. and Varela, R. 1992b. Did the Taconic Appalachians continue into South America? *Geology*, 20, 1059-1062.

Dalla Salda, L.; Cingolani, C.; Varela, R. and Lopez de Luchi, M.G., 1996. Taconian Laurentia-Gondwana Collision: Evidence from a Geological Fit. *Geological Society of America. 30th Annual Meeting, Abstracts with Programs,* N° 38742,10, Austin, Texas.

Lopez de Luchi, M.G. and Dalla Salda, L.H.,1995.Some Pampean Pretaconic and Famatinian Taconic Granites of Southwestern South America. In Brown, M and Piccoli, P M. (eds) The Origin of Granites and Related Rocks, Thrird Hutton Symposium. Abstracts. U.S. Geological SurveyCircular 1129, 91.

Ramos, V., Jordan,T., Allmendinger,R., Mpodozis, C, Kay, S., Cortés, J and Palma, M., 1986, Paleozoic terranes of the central Argentine-Chilean Andes. *Tectonics.*, 5, 855-880

Rapela, C.; Toselli, A.; Heaman, L. and Saavedra, J. 1990 , Granite plutonism of the Sierras Pampeanas; An inner cordilleran Paleozoic arc in the southern Andes.In Kay, S.M. and Rapela, C.W.(eds.): Plutonism from Antarctica to Alaska. *Geol. Soc. Am., Spec. Pap.*, 241, 77-90

# THE ATLANTIC OROGENIC BELT OF SOUTHERN BRAZIL: AN OROGEN OF ANDEAN TYPE OF NEOPROTEROZOIC AGE ?

Michel DEMANGE[(1)] and Romulo MACHADO[(2)]

(1) Ecole des Mines, 35 rue Saint-Honoré, 77 305 Fontainebleau, FRANCE
(2) Universidade de São Paulo, Instituto de Geociências, Caixa Postal 11 348, São Paulo, BRAZIL

KEY WORDS : Braziliano orogeny, transpressional orogen, Neoproterozoic, granite

## INTRODUCTION

The structure of the Brazilian shield is mostly due to the Brasiliano orogenic cycle, which occured between 1 and 0,5 Ga (Almeida et al., 1973; Brito Neves and Cordani, 1991). Several mobile belts formed during this cycle, surround cratonic areas that are made of earlier terranes and their stable cover. In the south-eastern Brazil, the Atlantic orogenic belt (Ferreira, 1972; Machado and Endo, 1993; Endo and Machado, 1993) streches for more than 2000 km from Uruguay to the Espírito Santo state in Brazil, on the edge of the São Francisco and Rio de la Plata cratons. The Luiz Alves intermediate craton divides the Atlantic belt into two domains: the Paraíba do Sul belt in the North and the Dom Feliciano belt in the South (fig.1).

This orogen shares several features with the Mesozoic-Cenozoic Cordilheras of the western Americas:

## 1- AN OROGEN BUILT ON A CONTINENTAL CRUST

The Atlantic orogenic belt is made of several longitudinal domains separated by major complex faults (fig.1 and 2). In every domain, both basement and cover series are recognized. The basement is made of Archean and Trans-Amazonian para- and orthogneisses. The cover series of Middle to Upper-Proterozoic age, are largely shelf sediments with minor interbeded volcanics. In the Alto Rio Grande domain these volcanics exhibit a geochemical zoning of active margin type (Campos Neto, 1991).

## 2- A TRANSPRESSIONAL OROGEN

The Atlantic orogenic belt exhibits a positive flower structure (Machado and Endo, 1993, fig.3): the northwestern units are thrusted on the São Francisco and Rio de la Plata cratons while the south-eastern units are thrusted south- eastwards. In the Dom Feliciano belt, the Pelotas batholith separates the domains of opposite vergences.

This pattern is due to a polyphase orogenic evolution where two main cycles are recognized:

1- the Brasiliano 1 cycle (850-750 Ma, Trompette, 1994), still poorly documented, produced the subduction of the "ophiolites" (described at the northwestern edge of the belt, Soares et al., 1990; Pedrosa-Soares et al., 1992; Röig and Schrank, 1992), the collision of the entire Atlantic belt terranes with the São Francisco and Rio de la Plata cratons and the emplacement of the G1 granites.

2- the Brasiliano 2 cycle (650-490 Ma) comprise a first transpressional stage of contemporaneous thrusting and dextral shear faulting which is responsible of the remarkable positive flower structure of the belt. G2 granites, usually metamorphosed into orthogneisses (dated between 630 and 570 Ma), emplaced during this first stage. Later stages produced gentle folding and sinistral reactivation of previous shear zones. G3 and G4 granites (570-490 Ma) are contemporanous or postdate these late events.

## 3- THE GRANITES: PETROLOGY, GEOCHEMISTRY AND REPARTITION IN SPACE AND TIME

The G2 and G3-G4 granites form complex batholiths and stocks, emplaced at various levels of the

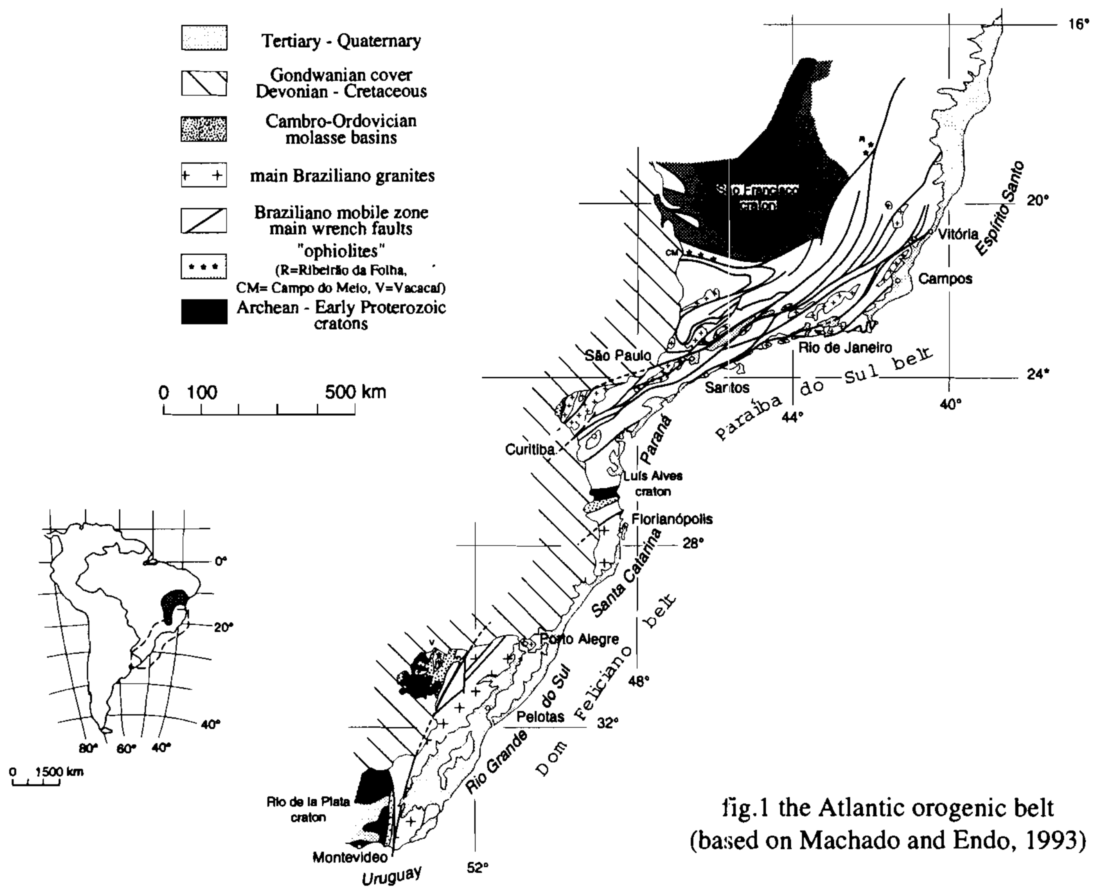

fig.1 the Atlantic orogenic belt (based on Machado and Endo, 1993)

crust from greenschist to the granulite facies, scattered through the whole belt with the exception of the more external units towards the cratons.

All these granites are complex intrusions that associate basic, intermediate and acidic rocks. These associations define magmatic series that present such variety that they cover almost the entire field of the granitoids (fig.4). These series share many common characteristics: same subalumineous character (the most differenciated members become slighly peralumineous), same iron-magnesium ratio that is comparable to the one of calcalkaline series, same sodium level. The variety of the rock types is due to the opposition between calcic and potassic series (confirmed by many other elements).

Repartition in space and times of these magmatic series is noteworthy: G2 granites exhibit a zonality through the belt with the most calcic series in internal position and the most potassic ones in external position toward the craton. The late G3-G4 series are potassic ones: in the Paraíba du Sul belt they are all in internal position superimposed on the domain of the early calcic series. The Pelotas batholith exhibit a weak zonation with less potassic series at the East (Pelotas suite) and more potassic series at the West (Encruzilhada suite) . The youngest intrusion are alcaline syenites. Brown (1982) considers such spatial and temporal disposition as characteristic of an active continental margin involving an old basement.

## CONCLUSION

The tectonic pattern in positive flower structure, the presence everywhere of an old basement, the type and distribution in space and time of the magmatism, is similar to the Andean cordilhera model (Soler, 1991; Smitz et al., 1993): the Atlantic belt of Southern Brazil is a remarkable example of an orogen of this type of Neoproterozoic age. Moreover, this belt exhibits a level of erosion that has not yet been reached in more recent orogens. It is thus a unique example of the deep-seated parts of an Andean type orogen.

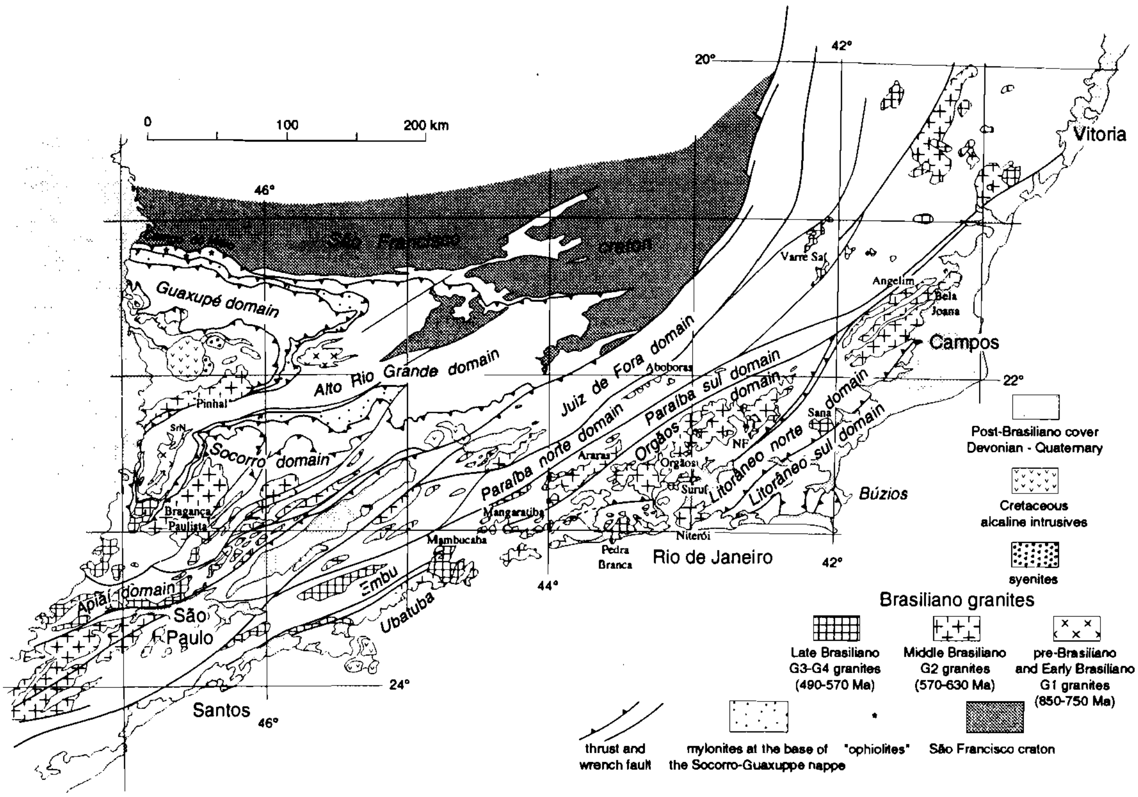


fig.2 map of the Paraíba do Sul belt
(based on the compilation by Demange and Machado, in press)

N S

G3-4 granites : high K

G2 granites : high K <----------------------------------> high Ca / low K

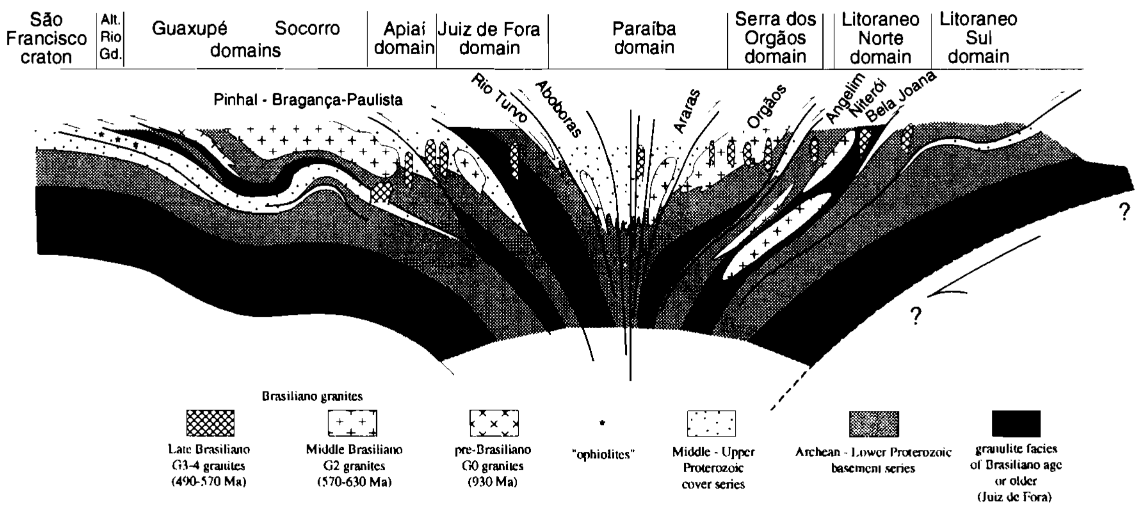


fig.3 schematic cross-section of the Paraíba do Sul belt

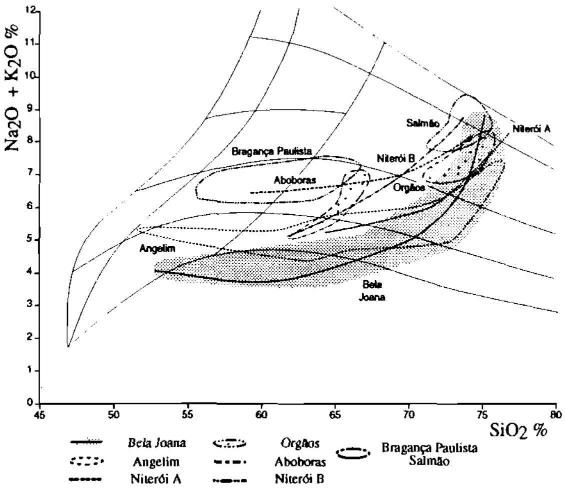


fig.4a Paraíba do Sul belt early G2 granites

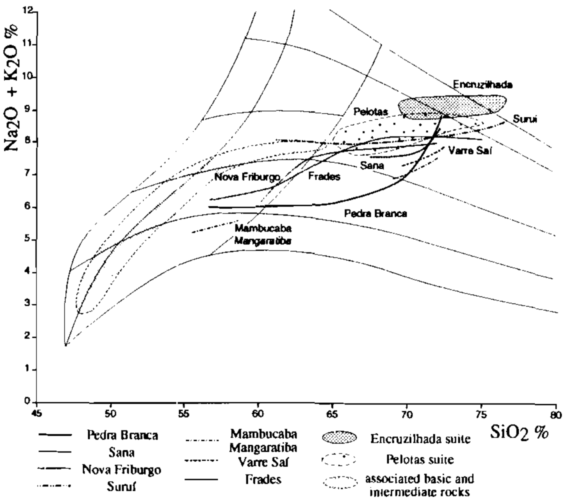


fig.4b Paraíba do Sul belt late G3-4 granites and Pelotas batholith

REFERENCES

Almeida, F.F.M., Amaral, G., Cordani, U.G. and Kawashita, K., 1973. The Precambrian evolution of the South American cratonic margins South of the Amazon river. In: Nairm, A.E.M. and Stehli, F.G., editors, Ocean basins and margins. V.1. Plenum Publ. Co, New York, 411-446

Brito Neves, B;B. and Cordani, U.G., 1991. Tectonic evolution of South America during late Proterozoic. Precambrian Res., 53, 23-40

Brown, G.C., 1982. Calcalkaline intrusive rocks: their diversity, evolution and relation to volcanic arcs. In Thorpe, R.S., editor, Andesites. John Willey and sons, New Yok, 437-461

Campos Neto, M.C., 1991. A porção ocidental da Faixa Alto Rio Grande - Ensaio de Evolução tectônica. PhD thesis, Inst. Geoc., Univ.São Paulo, 210 p. (unpublished)

Demange, M. and Machado, R. Neoproterozoic granites of the Paraíba do Sul belt (Rio de Janeiro state, Southern Brazil): Geology, petrography, geochemistry and tectonic implications. Precambrian Res., 53, (in press)

Endo, I. and Machado, R., 1993. O sistema de cisalhamento transatlântico: um modelo neotectônico transpressional para o neoproterozóico do Brasil Oriental. IV Simp. Nac. Estudos Tectônicos, Belo Horizonte, 12: 356-359

Ferreira, E.O., 1972. Explanatory note of the tectonic map of Brazil. Bol. Dep. Nac. Prod. Min., 1, Rio de Janeiro, 19 p.

Machado, R. and Endo, I., 1993. O cinturão de cisalhamento atlântico: um exemplo de tectônica transpressional neoproterozóica. IV Simp. Nac. Estudos Tectônicos, Belo Horizonte, 12: 191-198

Pedrosa-Soares, A.C., Noce, C.M., Vidal, P., Monteiro, R.L.B.P. and Salazar, E., 1992. Toward a new tectonic model for the Late-Proterozoic Araçuai (SE Brazil) - West Congolian (SW Africa) belt. J. S. Am. Earth Sci., 6 (1/2) 33-47

Röig, H.L. and Schrank, A., 1992. Caracterização da zona de sutura Jacuí-Conceição - limite norte do complexo de nappe do Guaxupé (MG). An. XXXVII Congr. Bras. Geol., Bol. Res. Exp., 1: 283-285.

Soares, P.C., Fiori, A.P. and Carvalho, S.G., 1990. Tectônica collisional oblíqua entre o bloco Paraná e a margen sul du Craton de São Francisco. An. XXXVI Congr. Bras. Geol., 6: 2723-2734.

Soler, P., 1991. Contribution à l'étude du magmatisme associé aux marges actives. Pétrographie, géochimie et géochimie isotopique du magmatisme crétacé à pliocène le long d'une transversale du Pérou central. PhD thesis, Univ. Paris VI, Paris, 846 p.

Schmitz, M., Giese, P. and Wieger, P., 1993. Crustal thickening in the Central Andes. Results from refraction and crustal balancing. II Symp. Intern. geodyn. Andine, Oxford (UK). ORSTOM, Paris, 33-36

Trompette, R., 1994. Geology of the Western Gondwana (2000 - 500 Ma): Pan-african - Brasiliano aggregation of South America and Africa. A.A. Balkema, Rotterdam, XII-350 p.

# ANATOMY OF THE PRECORDILLERA (ARGENTINA) DURING CAMBRO-ORDOVICIAN TIMES: IMPLICATIONS FOR THE LAURENTIA-GONDWANA TRANSFER OF THE CUYANIA TERRANE

Martin KELLER

Institut für Geologie und Mineralogie, Universität Erlangen, Schlossgarten 5, D-91054 Erlangen

KEY WORDS: Precordillera, sedimentary history, Cambro-Ordovician, Cuyania Terrane

## INTRODUCTION.

In recent discussions about the origin and provenance of the Argentine Precordillera, two basic models have been developed: 1) The Precordillera was part of Laurentia until Late Precambrian or Early Cambrian times, when it rifted away from Laurentia (Astini and others 1995) to form an indipendant microcontinent. During the Cambro-Ordovician, this microcontinent drifted across the Iapetus to finally collide with western Gondwana during the Middle Ordovician. 2) The Precordillera was integral part of Laurentia until the Middle/Upper Ordovician (Dalla Salda and others 1992, Dalziel and others 1994). The comparable history of the Appalachians and the Famatina System of South America are taken as evidence for a major continent-continent collision during Mid-Ordovician times.

Recently, the Precordillera was interpreted to be part of a much larger "Cuyania composite terrane" (Ramos 1995), which includes parts of the basement of the Sierras Pampeanas of western Argentina and several limestone outcrops in the provinces of Mendoza and La Pampa. The Cuyania terrane in turn is thought to represent part of the "Texas plateau" (Dalziel in press), a promontory of Laurentia and the crucial link between Laurentia and Gondwana to form the Mid-Ordovician supercontinent of "Artexia" (Dalziel in press).

In all models, the Ouachita Embayment along the southern margin of present-day North America is favoured as the almost unique candidate which might have accomodated the Cuyania Terrane until its separation from Laurentia.

In this paper, the Cambro-Ordovician sedimentary history of the Cuyania terrane is described and interpreted in order to discuss the Lower Paleozoic geotectonic history of the Precordillera.

## THE SEDIMENTS OF THE CUYANIA TERRANE

Basically, three different types of sedimentary successions can be distinguished during Cambro-Ordovician times: A "cratonal" setting, where carbonate platform rocks onlap crystalline basement during the Early Ordovician; a "miogeoclinal" setting showing a thick Lower Cambrian through early Middle Ordovician carbonate platform; and Ordovician slope and basin deposits.

A cratonal section is present near San Rafael (province of Mendoza), where about 80m of dolomites and limestones are exposed. These carbonates of Tremadocian through Mid-Arenigian age (Bordonaro and others in press) rest directly on crystalline basement yielding a Grenvillian age (Ramos pers. comm.). The succession starts with coarse dolomites of probable algal origin which upward grade into microbial laminites. Upsection, limestones with an abundant marine fauna are present. Most important is a reef-mound horizon which can be correlated to coeval strata in the Precordillera. The top of the preserved succession consists of nodular chert-bearing limestones.

The best documented sections of the miogeoclinal setting are the classical sections around San Juan. Continuous sections are present from late Middle Cambrian times onward. More than 500m of limestones with intercalations of siltstones were deposited towards the Middle/Upper Cambrian boundary (La Laja Fm.). The succession shows various 3rd and 4th order cycles and environments from the subtidal towards the lower intertidal. The Upper Cambrian mainly consists of dolostones. The Zonda Fm. (300m) is composed of mudstones and microbial laminites, the overlying La Flecha Fm. (400m-700m) of more than 100 small-scale peritidal shallowing-upward cycles. In the southwestern corner of the Precordillera (Cerro Pelado), these cycles are drowned and covered with deep-water limestones and marls during the uppermost Cambrian. Elsewhere, sedimentation continues during the Tremadocian with limestones (La Silla Fm.: 300m-400m) of a shallow-water environment. Dominant rocktypes are mudstones and wackestones with gastropods and nautiloids, together with peloidal and intraclast grainstones. Near the Tremadoc/Arenig boundary, there is a change towards sedimentation of limestones (San Juan Fm.: 300m-350m) with an abundant and diverse fauna indicating open marine conditions. In the northern part of the Precordillera, carbonate sedimentation stops during the Mid-Arenig, whereas further south this event occurs during the earliest Llanvirn. One important feature of the San Juan Fm. are reefs and reef mounds. Near the base of the formation, sponge-algal-receptaculitid mounds are present, which correlate to the mounds in the cratonal section. In the upper part of the San Juan Fm., stromatoporoid-dominated mounds developed with minor participation of sponges and algae.

During the Middle and Upper Ordovician, the former carbonate platform area accommodated several very different sedimentary successions. Locally, a carbonate slope environment (Las Aguaditas Fm.) developed above the San Juan Fm. and persisted until the Caradoc. Northeast of San Juan (Don Braulio section), a succession of siliciclastic rocks is present which starts with a prominent conglomerate unit (La Cantera Fm.) Upsection, mainly turbidites are developed and, after a hiatus, glaciomarine diamictites (Don Braulio Fm.) are found, attributed to the Ashgillian Gondwana glaciation. In the San Juan valley, a Caradocian pelagic carbonate platform rests on top of the deeply eroded San Juan Fm. West of Mendoza a 600m thick succession of shales with debris-flows and olistoliths is present (Empozada Fm.). To the west and to the east, carbonate platform rocks are present. The top of the succession shows shallow water calcareous sandstones which most probably are Ashgillian in age. In many places in the Precordillera, a chert-pebble conglomerate (latest Ordovician) seals these different successions.

Autochthonous slope and basin sediments older than Middle Ordovician have not yet been documented. A regional slope developed during latest Llanvirnian through Early Caradoc (?) times, where several 100m of shales and marlstones were deposited. They host a variety of mass flow deposits in which the entire spectrum of carbonate platform rocks is present. In addition, there are Middle and Upper Cambrian olistoliths consisting of deeper-water agnostid bearing limestones. These olistoliths may be as large as 300 thick and more than 1km long. In one section, they are associated with a boulder bed which consists of angular basement clasts up to 60cm across. Although the structural and age relations between the remaining slope and basin deposits are not always clear, the overall picture shows continental slope deposits along the western margin of the former carbonate platform. These sediments gradually pass into more distal turbitic successions and finally into basinal shales and siltstones. Rift-related pillow-basalts are intercalated into Caradocian graptolite shales.

## ANATOMY OF THE PRECORDILLERA DURING THE CAMBRIAN AND EARLY ORDOVICIAN

The Early Cambrian is only represented by some isolated outcrops. A redbed-evaporite succession is interpreted to be a rift-related graben fill, whereas the other occurrences are already attributed to a passive margin sequence. No paleocurrent data are available to interprete the provenance of the abundant siliciclastic rocks. During the Middle Cambrian, limestone-siltstone sequences are observed which closely resembling Depositional Grand Cycles. Depositional Grand Cycles are typically developed all around Laurentia at that time. During the Late Cambrian, mainly peritidal conditions prevailed on the platform, which led to the accumulation of almost 1000m of rocks. Middle and Upper Cambrian deep-water limestone olistoliths in the western slope facies are of local origin (Keller 1995) which implies that the carbonate platform passed into deeper water environments towards the west. This is also shown by the sudden drowning of platform rocks at Cerro Pelado, an event not observed on the remainder of the platform.

Both, grain size and abundance of the siliciclastic input onto the platform decreased during the Cambrian. An eastern or southeastern source area is most likely. There, the basement of the Cuyania terrane was exposed at that time. In the Lower Ordovician rocks no siliciclastics are found. This is explained by the ongoing onlap of the carbonates onto the basement which finally shut off sediment supply. The expansion of the carbonate platform is well documented in the cratonal section of San Rafael, where 80m are correlative to more than 400m in the Precordillera. Nevertheless, these 80m still show all major events present in the miogeoclinal setting.

Along the western margin of the platform, carbonate breccias and turbidites, in erosional contact with Middle Cambrian limestones, indicate the evolution of a local carbonate slope from the Cambro-Ordovician boundary on. In general, the Early Ordvician shows a relative rise in sea level, which culminates in the drowning of the platform during the Early Llanvirn. Until that time, more than 2100m of carbonates had accumulated around San Juan representing a thick passive margin succession (Baldis and others 1982).

If compared to coeval passive margin successions around Laurentia (e.g., Skehan 1988), the Precordillera platform is highly incomplete: Along its present-day eastern margin 2100m of miogeoclinal rocks are present and in a tectonically separated outcrop, 80m of a cratonal section are preserved. In the Appalachians, comparable sections are separated by about 600km. This distance results from slow but continuous transgression onto the craton. Even if regional differences are considered, timing and rate of onlap/transgression ought to be in the same order of magnitude.

Another clue to the dimensions of the carbonate platform are the Arenig reef mounds. Almost identical eco-systems are present along the southern margin of Laurentia where they are typical of a relatively narrow belt along the shelf edge (Alberstadt & Repetski 1989). Cratonward, a broad zone (several 100s of kilometers) of "continental interior shelf environments" is present. Except for the outcrops near San Rafael, this interior zone is not preserved in the Cuyania terrane. According to the present-day coordinates, this zone might have been developed to the east and in consequence might have been a thin cover of the basement of the Sierra Pie de Palo. Hence, there are several lines of evidence suggesting that the dimensions of the platform and, in consequence, of the Cuyania terrane must have been much larger and might have been in the order of 1000km in length and 600 to 800km in width.

## ANATOMY OF THE PRECORDILLERA DURING THE MIDDLE AND UPPER ORDOVICIAN

The main characteristics of the Precordillera during the Middle and Late Ordovician are the presence of highly varied sedimentary successions including a local carbonate slope, a pelagic carbonate platform, thick turbidite successions, and basinal shales with pillow basalts. An important feature is the development of a continental slope along steep escarpment faults which follow more or less the former carbonate platform margin. Along these faults, Middle and Upper Cambrian limestones and basement were exposed and gravitationally transported into the basin. Although collision between the Sierras Pampeanas and the eastern border of the Cuyania terrane is documented during the Middle Ordovician (Ramos 1988) no compressional structures of that age are present in the Precordillera. Instead, the highly varied sedimentary successions and the strongly varying thicknesses preserved underneath the pre-Silurian unconformity indicate an extensional regime responsable for the formation of horst and graben structures in the former platform area. Some of the grabens accomodated up to 600m of sediment (Empozada Fm.), whereas in a horst position, a pelagic carbonate platform developed during the Caradoc. Crustal extension culminated during the Llandeilo/Caradoc when huge amounts of pillow basalts extruded into the basin.

## CONCLUSIONS

During Cambrian and Early Ordovician times a passive continental margin developed on the Cuyania terrane. Comparisons with the Cambro-Ordovician margins of Laurentia show, that the original dimensions of the Precordilleran carbonate platform must have been much larger. The carbonates onlapped the Laurentian basement of the western Sierras Pampeanas during the Early Ordovician, hence the platform might have extended several 100 kms to the east or southeast. The Cuyania terrane was large enough, so that the effects of the collision at its eastern margin are hardly visible in the Precordillera.

During the Late Cambrian, the carbonate platform starts to disintegrate along its western margin (Cerro Pelado) where an isolated block was downfaulted and drowned. Similar events are observed in the Early Ordovician (slope facies, drowning at Guandacol) what is regarded as a precursor of the subsequent rifting. During the Middle and Upper Ordovician, sedimentation in the Precordillera was triggered by crustal extension. The formation of horst and graben structures accounts for the different sedimentary successions in the Precordillera. The relative movements of several 100m over a short time period together with the extrusion of basic magmas are interpreted as a result of rifting which marks the final separation of the Cuyania terrane from Laurentia. There are no indications that a major ocean was present prior to this time.
Hence, sedimentologic evidence supports the ideas of Dalla Salda and others (1992) and Dalziel and others (1994) about plate-tectonic constellations which place Laurentia and western Gondwana in close proximity.

## REFERENCES

Alberstadt, L. & Repetski, J.E. 1989. A Lower Ordovician Sponge/Algal facies in the Southern United States and its Counterparts elsewhere in North America. *Palaios*, 4, 225-242.

Astini, R.A.; Benedetto, J.L. & Vaccari, N.E. 1995. The early Paleozoic evolution of the Argentine Precordillera as a Laurentian rifted, drifted, and collided terrane: A geodynamic model. *Geological Society of America Bulletin*, 107, 253-273.

Baldis, B.A.; Beresi, M.; Bordonaro, O. & Vaca, A. 1982. Síntesis evolutiva de la Precordillera Argentina. *5. Congreso Latino-Americano de Geología Actas*, 4, 399-445.

Bordonaro, O.; Keller, M. & Lehnert, O. in press. El Ordovícico de Ponon Trehue en la Provincia de Mendoza (Argentina): redefiniciones estratigráficas. 13. Congreso Geológico Argentino.

Dalziel, I.W.D. in press. Terminal Proterozoic-Early Paleozoic Geography, Tectonics, and Environments. Invited review paper, *Geological Society of America Bulletin*.

Dalziel, I.W.D., Dalla Salda, L.H. & Gahagan. L.M. 1994. Paleozoic Laurentia-Gondwana interaction and the origin of the Appalachian-Andean mountain system. *Geological Society of America Bulletin*, 106, 243-252.

Keller, M. 1995. Continental slope deposits in the Argentine Precordillera: Sediments and geotectonic significance. *In*: Cooper, J.D.; Droser, M.L. & Finney, S.C. (eds.): *Ordovician Odyssey*, Pacific section SEPM 77, 211-215.

Ramos, V.A. 1988. Late Proterozoic - Early Paleozoic of South America: A Collisional History. *Episodes*, 11, 68-173.

Ramos, V.A. in press. Sudamérica: un mosaico de continentes y océanos. *Ciencias hoy*.

Skehan J.W. 1988. Evolution of the Iapetus Ocean and its borders in pre-Arenig times: a synthesis. *In*: Harris, A.L. & Fettes, D.J. (eds.): The Caledonian-Appalachian Orogen, *Geological Society Special Publication*, 38, 185-229.

# THE PALEOZOIC BASEMENT OF THE CENTRAL ANDES (18°-26°S) A METAMORPHIC VIEW.

F. Lucassen[1], H.G. Wilke[2], J. Viramonte[3], R. Becchio[3,1], G.Franz[1], A. Laber[1], K. Wemmer[4], P. Vroon[5]

(1)TU-Berlin, Petrologie-EB310, Straße des 17.Juni 135, 10623 Berlin, Germany
(2)U'Catolica del Norte, Dept. Geologia, Casilla 1280, Antofagasta, Chile
(3)U'Nacional de Salta-CONICET, Salta, Argentina
(4)Inst. f. Geologie u. Dynamik d. Lithosphäre, Goldschmidtstr.3, 37077 Göttingen, Germany
(5)RHBNC, Dept. of Geology, Egham, Surrey TW20 OEX, England

Keywords: Early Paleozoic metamorphism; P-T development; isotopic ages; N-Chile; NW-Argentina

## INTRODUCTION

Scarce outcrops of metamorphic rocks in the Central Andes (18°-26°S) occur in all mountain chains from the Coastal Cordillera in Chile to the Cordillera Oriental in Argentina (Fig.1). However, the present state of knowledge on the metamorphic conditions and on age relations of metamorphism and cooling did not allow a correlation of the scattered outcrops (summarized in Damm et al., 1990; Miller et al., 1994). Nevertheless, the occurrence of Pre-Mesozoic metamorphic rocks is very important for the different geotectonic interpretations of the Paleozoic Andean history that are mainly based on the sedimentary-faunistic record and the tectonic-magmatic evolution of the basins. The major lines of discussion are:

(1) The allochthonous terrane development of the Pacific Margin (23°-25°S; e.g. Ramos, 1988) started with the collision of the Arequipa-Antofalla craton in the Late Proterozoic (700-600 Ma, final collision at 570 Ma) and continued with a rifting-collision history of the Cambrian-Ordovician basins (540- 470 Ma) with a para-authochtonous Arequipa Massif (ensialic development, Damm et al., 1990). The last major event was the advent of the Chilenia terrane (440-360 Ma). A similar history for a section at ca 30°S was recently discussed by Astini et al. (1995).

(2) The ± continous subduction history of the Pacific margin started from a passive margin setting during the Mid-Ordovician. Since that time, subduction triggered the processes of magmatism, basin formation and tectonics (Coira et al., 1982). The collision of the Arequipa microplate was in the Late Ordovician.

(3) The Paleozoic Andes formed together with the North American Appalachians in a single orogeny during the collision of the Laurentia and Gondwana continents in the Ordovician (Dalziel et al., 1994).

(4) An intracratonic evolution of a Pre-Cambrian crystalline area that stabilized in Late Proterozoic-Early Cambrian was suggested for the Paleozoic by Hongn (1992) and Mon & Hongn (1991).

The collision of allochthonous terranes or the rifting and collision of para-allochthonous terranes should have a major impact on the crustal thickness and on the thermal regime in the crust, therefore on the physical conditions of metamorphism in the crust. The repeated process should lead to poly-deformation and poly-metamorphism or to belts of metamorphic rocks with different isotopic ages.

We present new data on the metamorphic conditions from all outcrops of high grade metamorphic rocks in N-Chile and from a selected area in NW-Argentina. Field relations (Fig. 1) in N-Chile (Lucassen et al., 1994) and in parts of the Hombre Muerto-Sierra de Quilmes in NW- Argentina (Becchio, Viramonte) were studied during several field trips. Based on the mineral chemistry we calculated P and T by various

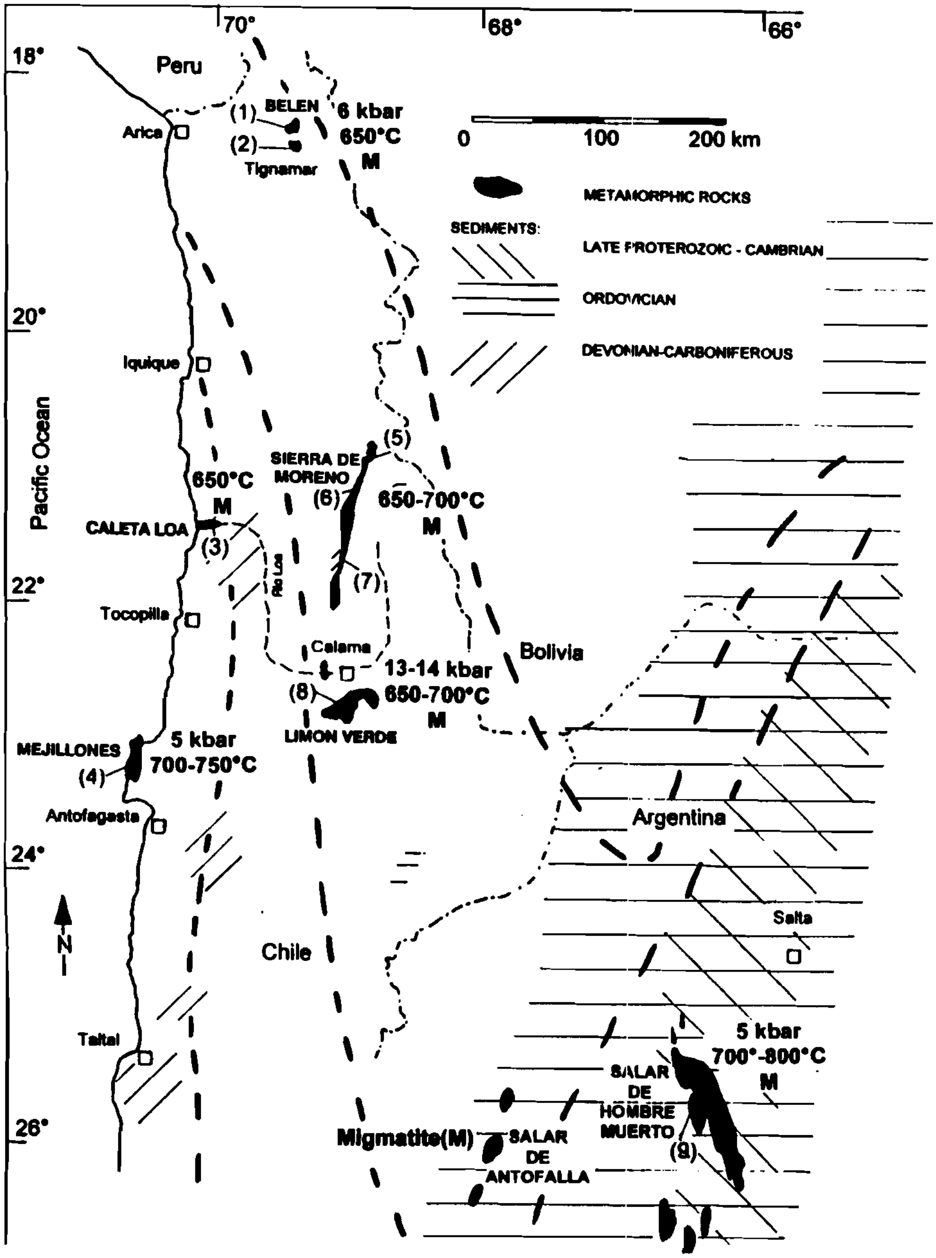


**Figure 1** Distribution of Paleozoic metamorphic basement and sediments (Bahlburg & Breitkreuz, 1991) in N-Chile and NW-Argentina. Peak-metamorphic conditions are shown for the different locations. Numbers in parentheses indicate the sample locations for age determinations (see text). Possible terranes (heavy dashed lines; Ramos, 1988) are from the Coast to the east at the latitude of Antofagasta: Mejillonia Displaced Terrane- Chilenia Terrane- Arequipa-Antofalla Craton-Pampean Terrane.

thermobarometers and multi-equilibria calculations (Berman, 1991). Along a W - E section, we determined ages on minerals in the Sm-Nd system and in the K-Ar system. Sm-Nd ages were determined at the isotope laboratory at the RHBNC, K-Ar ages at the laboratory at the Universität Göttingen and by Krueger Enterprise Inc., M.A., USA.

## METAMORPHIC CONDITIONS AND ISOTOPIC AGES

Ductile deformation causes one major foliation ($S_1$) N-S trend in all outcrops. $S_1$ is marked by the alignement of the peak-metamorphic mineral assemblages. A wider spaced foliation ($S_2$) is rare and was also formed close to peak-metamorphic conditions. Granoblastic fabrics are common in migmatite and in rocks transitional to granulite. $S_1$ in these rocks is frequently marked by compositional layering. We found no relics of the prograde development in metasedimentary rocks. Primary magmatic fabrics of the protolith are preserved in deformation-protected areas of some orthogneisses. Neither mineral relics nor fabric relics of older metamorphic and deformational events were found. Reaction textures between minerals are absent except retrograde reactions (sericitisation, chloritisation). The only prograde reaction texture found is the breakdown of muscovite into fibrous sillimanite (Hombre Muerto). Chemical zoning of minerals is absent or weak in most samples and restricted to small retrograde rims. A late brittle deformation is obvious in the kinking or disruption of grains and the formation of small quartz or calcite veins.

*Belen-Tignamar.* Temperature in the Belen paragneiss [biotite (bt)-garnet (grt)-kyanite (ky)-muscovite (ms)-plagioclase (pl)-quartz (qtz)] which occurs together with bt-hornblende (hbl) orthogneiss was 650°C at 6 kbar. The T at the given P agrees with the local occurrence of migmatite. Temperature of the Tignamar metapelite (bt-grt-ms-potassic feldspar (kfs)-staurolite (st)-pl) ca 15 km south of Belen was ~ 550°C at 5 kbar (PT from multi-equilibria, GASP barometry, gt-bt thermometry). Migmatites were not found in this area. Metabasites, which are garnet-free, are rare in both areas.

*Sierra de Moreno.* Gneiss or migmatite (bt-pl-qtz) are the most common rock types. Metabasite is rare and does generally not contain grt. Locally calcsilcate occurs. Mineral assemblages are not suitable for barometry. Calculated temperatures are 550°-650°C (grt-bt) and ~ 700°C (hbl-pl thermometry). This agrees with the occurrence of abundant migmatite.

*Caleta Loa.* Migmatite (bt-pl-qtz) is the dominant rock type. Grt-bt pairs yield temperatures between 600-750°C.

*Mejillones.* Gneiss (bt-pl-qtz±grt) with subordinate amphibolite (hbl-grt-pl±qtz) comprise the high grade rocks. Temperatures were around 700°C-750°C at ~ 5 kbar (PT from hbl-pl-grt thermobarometry, hbl-pl thermometry). Hbl-cpx equilibra were found in few samples, confirming the high T conditions.

*Limon Verde.* The metamorphic succession comprises mainly gneisses (bt-qtz-grt±pl) with small intercalations of amphibolite (hbl-grt-orthozoisite (zoi)±pl±qtz). Pressures are 13-14 kbar at 650-700°C. (PT from hbl-pl-grt thermobarometry; hbl-pl thermometry).

*Hombre Muerto - Sierra de Quilmes.* Main rock types are migmatic gneisses (bt-pl-kfs-qtz-ms±grt), cordierite (cd)-bearing in more aluminous whole rock compositions. Subordinate metabasites (hbl-cpx-pl± scapolite) and calcsilcate (calcite-cpx-grt-zoi-titanite (tit)-qtz) were found. Two samples (bt-grt-ms-pl-cd-qtz) from the Sierra de Quilmes yield T of ~ 700-800°C at 5 kbar for core compositions of the minerals with biotite I and ~ 470°C at 3 kbar for rim compositions with a secondarily formed biotite II that only occurs in contact with garnet (PT from multi-equilibria). The breakdown of muscovite is indicated by fibrous sillimanite in muscovite grains.

Locations of samples used for isotopic age determinations are labelled with numbers (Fig. 1). Sm- Nd mineral isochrons were determined at *Mejillones* (4): Amphibolite (hbl-pl-grt) 524±12 Ma, $Nd_i$=0.512332 ±13; *Sierra de Moreno (Qda. Choja)* (5): Calc-silicate (grt-zoi-cpx-tit) 512±18 Ma, $Nd_i$=0.511813±29; *Hombre Muerto (Argentina)* (9): Calc-silicate (grt-zoi-cpx-tit-wr) 508±3Ma, Ndi=0.511649±4; *Limon Verde* (8): amphibolite (hbl-zoi-grt-wr) 308±146, $Nd_i$=0.512349±179. The poorly defined Limon Verde age will be redone.

K-Ar ages on mineral separates were determined for the same locations and for additional samples from Belen-Tignamar, Caleta Loa and Sierra de Moreno. K-Ar ages on intrusions were made to evaluate the influence of Carboniferous to Permian intrusions on the isotope system of the metamorphic rocks. *Belen* (1) orthogneiss (hbl) 358±10Ma; *Tignamar* (2) orthogneiss (hbl) 389±11Ma; *Caleta Loa* (3) orthogneiss (bt) 170±3; *Mejillones* (4) amphibolite (hbl) 152±5Ma, gneiss (bt) 151±3Ma; *Sierra de Moreno* (5) amphibolite (hbl) 406±6Ma, migmatite (bt) 296±6Ma; (6) migmatite (hbl) 422±12Ma; (7) a sucession of samples from the contact with granite (bt) 300±8Ma, micaschist (bt) 284±6Ma, amphibolite (hbl) 327±9) Ma, amphibolite (hbl) 382±11Ma; *Limon Verde* (8) amphibolite (hbl) 235±6Ma; gneiss (bt) 234±5Ma; *Hombre Muerto* (9) migmatic gneiss (bt) 392±8Ma.

## DISCUSSION

High T, low P conditions of metamorphism in the high grade rocks of N-Chile (Belen-Tignamar, Caleta Loa, Mejillones, Sierra De Moreno) and of NW-Argentina (Hombre Muerto- Sierra de Quilmes) are very similar, indicating a high thermal gradient at mid-crustal levels (ca 15-20 km). Peak-metamorphism occurred at 500 Ma. A 500 Ma Rb-Sr age from metamorphic rocks is also known from Belen (Pacci et al., 1980 in Damm et al, 1990). K-Ar mineral ages indicate cooling of the metamorphic rocks to T below 500-300°C at around 400 Ma for Belen, Sierra de Moreno and Hombre Muerto. Similar ages were recently determined from the Salar de Antofalla basement (B. Kraemer, Berlin, pers. comun.) and are known for the whole area (Damm et al., 1990; Maksaev, 1990). Ages in the metamorphic rocks can be reset by Carboniferous intrusions, whereas K-Ar ages in the Coast Range (Mejillones, Caleta Loa) are reset to the cooling ages (140-170 Ma; Maksaev, 1990) of abundant Jurassic intrusions.

The exhumation close to the present erosion surface is indicated by erosional unconformities of Devonian(?)-Carboniferous to Permian (?) age and by the high-level intrusions of granites at ca. 300 Ma (Breitkreuz, 1986; Maksaev, 1990; our data). At Caleta Loa the metamorphic rocks are intruded by high-level granites with an age of 322 Ma (Maksaev, 1990), indicating, that these metamorphic rocks were already exhumed in the Carboniferous. Therefore, we suggest a similar metamorphic, cooling and exhumation history for Belen-Tignamar, Caleta Loa, Mejillones, Sierra de Moreno and the Hombre Muerto - Sierra de Quilmes area. The time between peak-metamorphism and cooling below 500-300°C is ca 100 Ma, pointing to a slow uplift and cooling or to a long residence of the rocks at the depth of their formation.

Metamorphic conditions in the Limon Verde rocks are different and reveal high P (corresponding to ~40 km depth) at a moderate geothermal gradient. In the given frame of Early Paleozoic metamorphic rocks and the belt of Devonian-Carboniferous sedimentary rocks (Fig.1) the meaning of this crustal unit is not yet clear. Age of metamorphism could be 300 Ma (Rb-Sr wr 300 Ma; Maksaev, 1990) or even younger (K-Ar ages of 235 Ma). Closely associated granites, which are separated from the metamorphic rocks by a fault, intruded at ~300 Ma, (Damm et al., 1990) into a high-level. The K-Ar ages (235 Ma) of the metamorphic rocks were not influenced by the granitoids.

Distribution, age and type of metamorphism does not support the ideas of continental growth by terrane accretion, regardless the mechanism, during the Late Proterozoic-Paleozoic for the area between 18°-26°S (Fig.1): No separate metamorphic belts with different ages developed, no relics of older metamorphic events (e.g. granulite metamorphism such as in the Peruvian Arequipa Massif at 1198-970 Ma, Wasteneys et al., 1993 in Dalziel et al., 1994) were found. With the closure of oceans and the accretion of terranes one would expect tectonic collision. Collision regimes (e.g. the Alpes) with crustal thickenning do not favour high T-low P metamorphism combined with slow exhumation. Interpretation of our data favours an event for the high grade metamorphism around 500 Ma with a high heat flow at mid-crustal level and without major crustal thickenning. The abundant intrusions in NW-Argentina with ages of 500-430 Ma (Rapela et al., 1990) that are also present in N-Chile (Damm et al., 1990) and the presence of orthogneisses and could be a hint to syntectonic magmatic activity.

## REFERENCES

***Astini, R.A. et al. 1995.*** GSA Bulletin, v. 107, p. 253-273. ***Bahlburg, H. & Breitkreuz 1991.*** Journal of South American Earth Sciences, v. 4, p. 171-188. ***Berman, R.G. 1991.*** Canadian Mineralogist, v. 29, p. 833-855. ***Breitkreuz, C. 1986.*** Geotektonische Forschungen, v. 70, Stuttgart, 88p. ***Coira, B. et al. 1982.*** Earth Science Reviews, v. 18, p. 303-332. ***Dalziel, I.W.D. et al. 1994.*** GSA Bulletin, v. 106, p.243-252. ***Damm, K.W. et al. 1990.*** Geological Society of America Special Paper 241, p. 101-126. ***Hongn, F. 1992.*** Unpublished PhD thesis, U'Nacional de Salta; Salta, Argentina. ***Lucassen, F. et al. 1994.*** 7° Congreso Geologico Chileno Concepcion 1994, Actas, Vol.I, p. 96 - 100. ***Maksaev, V., 1990.*** Unpublished PhD thesis, Dalhousie University Halifax, Nova Scotia, Canada, 1990. ***Miller, H. et al., 1994.*** Zentralblatt für Geologie und Paläontologie, Teil 1, p. 263-273. ***Mon, R. & Hongn F. 1991.*** Geologische Rundschau, v. 80, p.745-758. ***Ramos, V.A. 1988.*** Episodes, v. 11, p. 168-174. ***Rapela, C.W. et al. 1990.*** Geological Society of America Special Paper 241, p. 77-90.

# New petrological results on high-pressure, low-temperature metamorphism of the Upper Palaeozoic basement of Central Chile

Hans-J. MASSONNE[(1)], Francisco HERVÉ[(2)], Vlamir MUÑOZ[(2)] and Arne P. WILLNER[(1)]

(1) Institut für Mineralogie, Ruhr-Universität, D-44780 Bochum, F.R. Germany
(2) Departamento de Geologia, Universidad de Chile, Casilla 13518, Correo 21, Santiago de Chile, Chile

**KEY WORDS:** Blueschist, Greenschist, Amphibole, Phengite, Coastal Range, Central Chile

## INTRODUCTION

Similar to paired metamorphic belts, the metamorphic basement within the coastal ranges of Chile south of 34°S can roughly be divided into a Western Series of low grade metamorphic rocks locally containing high-pressure, low-temperature rocks (e.g. glaucophane schists) and an Eastern Series with intermediate to high grade rocks metamorphosed under low pressure conditions (Gonzalez Bonorino & Aguirre, 1971; Aguirre et al., 1972). In the Western Series metagreywackes and metapelites dominate. Subordinate are greenschists, which partly show relic pillow structures and MORB signature. Intercalated are lenses of serpentinite, massive Fe-Cu-Zn-sulphides and metacherts. The thick clastic sequences of the Western Series are probably of Silurian to Devonian sedimentary age. Metamorphic ages are not older than Carboniferous younging towards the South (Hervé, 1988). The low grade Western Series is interpreted as part of an accretionary prism (Hervé, 1988).

Because P-T data for the peak of metamorphism are very rare in the area and also related to some exceptional rocks (e.g. Collao et al., 1986), our aim was to study also the common metasediments for deciphering the P-T evolution. For that purpose, we concentrated strongly on the variable compositions of the minerals, mainly phengites and amphiboles, in the rocks. For the detailed petrological studies, we selected, so far, the following areas: (1) a region between Pichilemu and Constitucion, (2) an area around Mehuin N of Valdivia.

## PETROLOGICAL RESULTS

On the basis of numerous thin sections of various rock types a selection was made to investigate some rocks with the aid of the electron microprobe in detail. So far, we have studied several metapelites, greenschists, blueschists, meta-ironstones and quarzites.

Metapelites often contain the mineral assemblage chlorite, phengite, quartz and albite. Biotite can be occassionally present. Greenschists are also characterized by a common mineral assemblages: albite, chlorite, epidote, Ca-amphibole with minor phengite and quartz. Blueschists are very similar but contain Na-amphibole instead of Ca-amphibole and occasionally stilpnomelane. The latter mineral is abundant in meta-ironstones sometimes coexisting with garnet. Stilpnomelane, zussmanite, and quartz was also found in such rock types.

Blue amphiboles from Pichilemu are crossite or glaucophane sometimes surrounded by actinolites (Table 1), which typically occur in greenschists. Phengites from blueschists can contain Si contents around 7.0 per double formula unit, but rim compositions are clearly lower in Si and also show significant $Fe^{3+}$ (Table 1). The same compositional feature is also typical for metapelites.

First attempts were made to apply thermodynamic mineral data for the calculation of the metamorphic P-T conditions with the PTAX software package using the variable mineral compositions (cf. Massonne, 1995). Metamorphic temperatures were in the range 300° to 400°C. Maximum pressures were around 8 kbar. During the metamorphic evolution, a significant pressure decrease occurred.

**Table 1:** Representative analyses of minerals from a metapelite of the Mehuin area (sample CM9) and from blueschists from Pichilemu (samples MIL3404 and MIL3409). Structural formulae were calculated on the basis of (1) 42 Val. + Na + K + Ba/2 and a maximum of 4.1 octahedral cations for phengites and (2) 15 + A cations, O = 23 for amphiboles

| | **Metapelite** | | | **Metabasites** | | |
|---|---|---|---|---|---|---|
| | | **Phengites** | | | **Amphiboles** | |
| | **core** | **rim** | **core** | **rim** | **core** | **rim** |
| | 10666/64 | 10666/62 | 10078/96 | 10078/99 | 10112/10 | 10112/5 |
| Si | 6.981 | 6.541 | 6.982 | 6.782 | 7.950 | 7.710 |
| $Al^{[4]}$ | 1.019 | 1.459 | 1.018 | 0.218 | 0.050 | 0.290 |
| $Al^{[6]}$ | 2.930 | 2.869 | 2.717 | 2.534 | 1.350 | 0.049 |
| Cr | 0.013 | 0 | 0.004 | 0.004 | 0.002 | 0 |
| Ti | 0.018 | 0.020 | 0 | 0.003 | 0.006 | 0.005 |
| $Fe^{3+}$ | 0 | 0.351 | 0.097 | 0.473 | 0.678 | 0.382 |
| $Fe^{2+}$ | 0.452 | 0.172 | 0.423 | 0.114 | 1.155 | 1.623 |
| Mn | 0.009 | 0.013 | 0.006 | 0.006 | 0.018 | 0.039 |
| Mg | 0.600 | 0.675 | 0.853 | 0.965 | 1.792 | 2.902 |
| Ca | 0 | 0 | 0 | 0 | 0.065 | 1.721 |
| Na | 0.124 | 0.115 | 0.029 | 0.029 | 1.877 | 0.378 |
| K | 1.596 | 1.672 | 1.988 | 1.870 | 0.002 | 0.030 |
| F | 0.090 | 0.089 | 0 | 0 | 0 | 0 |

## CONCLUSIONS

Generalizing our new petrological results, the Palaeozoic metamorphic rocks of the Chilean Coastal Range had experienced very similar peak metamorphic conditions at high pressures and low temperatures. However, the rocks are strongly overprinted at greenschist facies conditions. High Si phengite compositions witness the high-pressure event even in clearly retrogressed metapelites. Relics of blue amphibole prove this in metabasites. Under these circumstances, the idea that the thick clastic sequence of the Western Series is part of an accretionary prism must strongly be considered.

## ACKNOWLEDGMENTS

The research project was financially supported by Billiton Minerals Chile and by the German Ministry of Research and Technology.

**REFERENCES**

Aguirre L., Herve F. and Godoy, E. 1972. Distribution of metamorphic facies in Chile: an outline. Krystallinikum, 9, 7-19.

Collao S., Kojima S. and Oyarzun R. 1986. Geotermobarometria en los sulfuros macizos de la franja metamórfica de esquistos verdes, Chile Cental-Sur. Rev.Geol. Chile, 28, 3-16.

Gonzalez Bonorino F. and Aguirre L. 1970. Metamorphism of the crystalline basement of Central chile. J.Petrol., 12, 149-175.

Herve F. 1988. Late Paleozoic subduction and accretion in Southern Chile. Episodes, 11, 183-188

Massonne, H.-J. 1995. III. Rhenohercynian Foldbelt, C. Metamorphic units (Northern phyllite zone), 4. Metamorphic evolution. - In: DALLMEYER R.D., FRANKE W. & WEBER K. (eds.): Pre-Permian geology of central and eastern Europe, 132-137. - Springer, Berlin.

# EARLY PALAEOZOIC GEOCHRONOLOGY AND OROGENIC EVENTS IN NW ARGENTINA

Hubert MILLER[(1)]

[(1)]Prof. Dr. Hubert Miller, Institut für Allgemeine und Angewandte Geologie der LMU, Luisenstr. 37, D-80333 München

Andes, Argentina, basement, granitoids, geochronology, deformation

## INTRODUCTION

For several years a lively discussion is in progress, whether the Early Palaeozoic orogenic events occurring at the South American active continental margin are due to the collision between Laurentia and Gondwana (e.g. DALZIEL et al. 1994) or not. Already published and new isotope data aim at a better understanding of the timing of intrusive, metamorphic and deformational events in NW Argentina. These age data are substantial for recognition of a potential Laurentia-Gondwana interaction during the Early Palaeozoic.

## AGES OF MAGMATISM AND METAMORPHISM

BACHMANN et al. (1986) described Rb-Sr thin slab ages of 554 Ma for gneisses from the Sierra de Ancasti and the Sierra de Aconquija (Catamarca, Tucumán). Similar K-Ar ages occur near Tucumán (ADAMS et al. 1989). These data document a strong late Vendian to Early Cambrian subduction of an accretionary wedge along the Gondwana/Pacific margin (WILLNER et al. 1987). The high velocity of burial and subsequent rising is further clearly proved by the very late Vendian to Early Cambrian age of some of the subducted sediments (DURAND & AZEÑOLAZA 1990, MILLER et al. 1994). At about 515 Ma sedimentation and metamorphism are followed by plutonism, which is acid in the north (BACHMANN et al. 1987) and basic in the south of the considered area (GRISSOM 1991; SCHALAMUK et al. 1983).

After this first stage of plutonism orogenic activity ceased and only reappeared at 480 Ma with wide-spread intrusions of granitic to trondhjemitic magmas (LORK et al. 1991, KNÜVER & MILLER 1982, RAPELA et al. 1992). This stage of magmatism is particularly important in the Sierra de Cachi (unpublished data by A. LORK). Magmatism and accompanying metamorphism continued till the end of the Ordovician and partly up to the Early Carboniferous. Hence, for NW Argentina the following Late Precambrian to Early Palaeozoic history is documented:

A Vendian to Early Cambrian passive continental margin (JEZEK & MILLER 1987) changed to an active one in the Middle Cambrian, when Laurentia probably was far off the margin of Gondwana (GRUNOW 1995).

Back-arc basins were filled up with volcanic and sedimentary rocks in the Early and Middle Ordovician, but a second phase of actual orogeny did not occur before the Middle and Late Ordovician (Famatina orogeny). The composition of magmas developed continuously from mantle source to strongly crustal contaminated (SCHÖN 1991, REISSINGER 1983, RAPELA et al. 1992).

Between 515 and 480 Ma magmatic, metamorphic and deformational events are remarkably scarce. However, in this time span magmas evolved within the crust becoming more acid and K-rich. Zircons which had formed in the first magmatic phase (volcanic events within the uppermost, Early Cambrian parts of the Puncoviscana Formation) are found in Middle Ordovician granitoids of the Sierra de Cachi (LORK et al. 1991). They can be deduced from the melting of Puncoviscana Formation volcano-sedimentary rocks within the Middle Ordovician magmas, but they can be simple relics of the Middle Cambrian magmas as well.

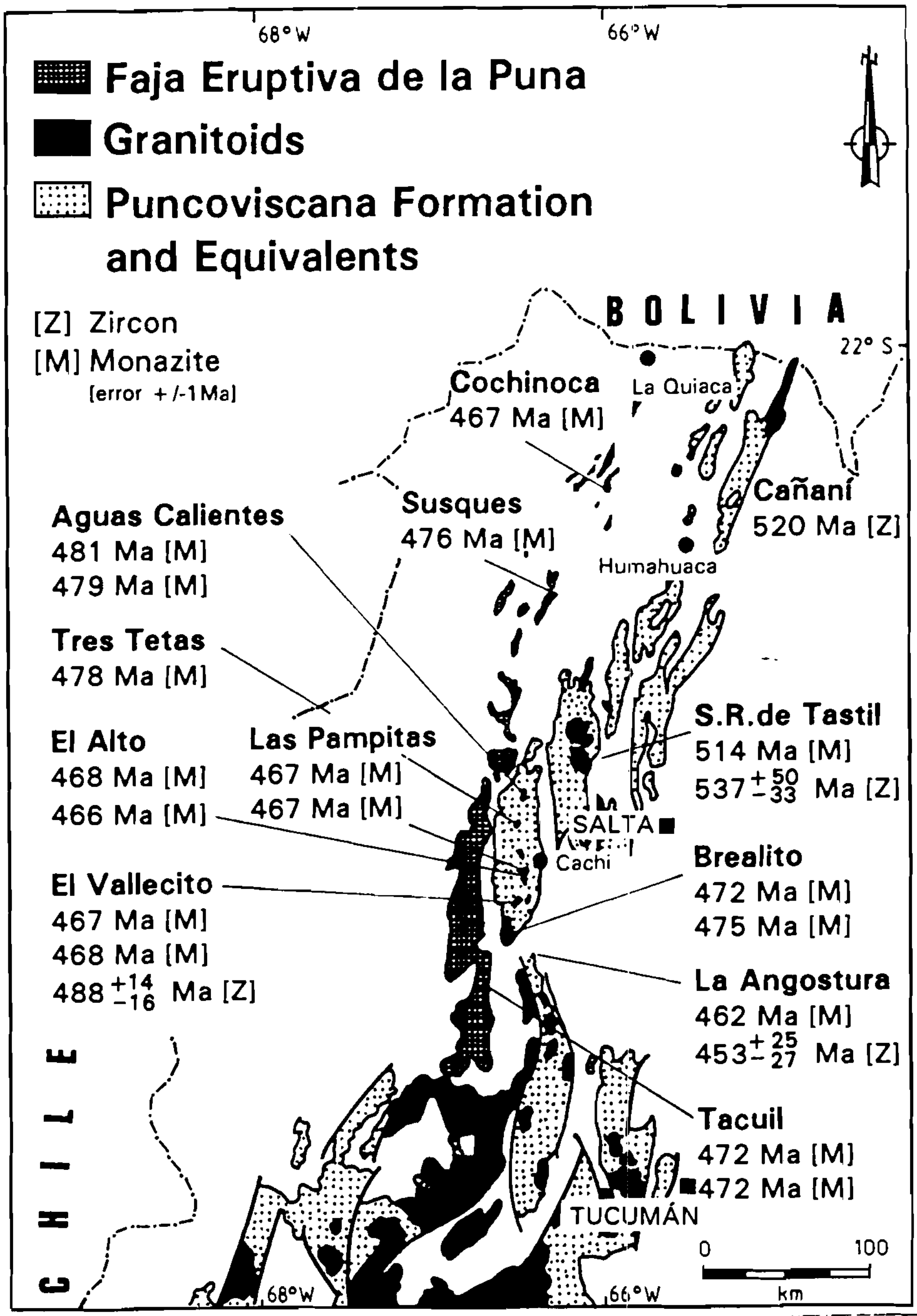


*Fig. 1. U-Pb ages of the Cordillera Oriental and Faja Eruptiva de la Puna; partly unpublished data by kind permission of A. Lork.*

CONCLUSIONS

Following isotope geochronology, the history of the NW Argentinian Gondwana margin in the Early Palaeozoic is mostly governed by a discontinuous ocean/continent subduction regime. An interruption of orogenic events occurred just at the time, when Gondwana may have been on the way to meet Laurentia (GRUNOW 1995). It is not clear, why during that time of very rapid moving together of both continents (several tens of m/a?) orogenic events in the Andean basement are lacking or at least unimportant. On the other hand they continued from the Middle Ordovician up to the Silurian, much time after the supposed collision of Laurentia with Gondwana had occurred (DALLA SALDA et al. 1992), and when Laurentia yet had moved away to find its Permian position. Hence, Laurentia may have indirectly influenced the history of the Andean basement, but not by an actual continent/continent collision.

This paper forms part of IGCP project 345, Andean Lithosperic Evolution. It was supported by Deutsche Forschungsgemeinschaft.

REFERENCES

Adams Ch., Miller H. & Toselli A.J. 1989. New K-Ar ages on the metamorphic history of the Puncoviscana Formation and equivalents, NW Argentina. *Zentralbl. Geol. Paläont. Teil I*, 1989, 987-997.

Bachmann G., Grauert B. & Miller H. 1986. Isotopic dating of polymetamorphic metasediments from NW-Argentina. *Zentralbl. Geol. Paläont. Teil I*, 1985, 1257-1268.

Bachmann G., Grauert B., Kramm U., Lork A. & Miller H. 1987. El magmatismo del Cámbrico Medio/Cámbrico Superior en el basamento del Noroeste Argentino: Investigaciones isotópicas y geocronológicas sobre los granitoides de los complejos intrusivos de Santa Rosa de Tastil y Cañaní. *10. Congr. Geol. Argent. Actas*, 4, 125-127.

Dalla Salda L., Cingolani C. & Varela R. 1992. Early Paleozoic orogenic belt of the Andes in southwestern South America: Result of Laurentia-Gondwana collision? *Geology*, 20, 617-620.

Dalziel I.W.D., Dalla Salda L.H. & Gahagan L.M. 1994. Paleozoic Laurentia-Gondwana interaction and the origin of the Appalachian-Andean mountain system. *Geol. Soc. Am. Bull.*, 106, 243-252.

Durand F.R. & Aceñolaza F.G. 1990. Caracteres biofaunísticos, paleoecológicos y paleogeográficos de la Formación Puncoviscana (Precámbrico superior - Cámbrico inferior) del Noroeste Argentino. *In: El ciclo Pampeano en el Noroeste Argentino, Serie Correlación Geológica*, 4, 71-112.

Grissom G.C. 1991. Empirical constraints on thermal processes in the deep crust of magmatic arcs: Sierra de Fiambalá, northwestern Argentina. *Unpubl. Ph.D. thesis*, Stanford University.

Grunow A.M. 1995. Implications for Gondwana of new Ordovician paleomagnetic data from igneous rocks in southern Victoria Land, East Antarctica. *J. Geophys. Res.*, 100, B7, 12.589-12.603.

Jezek P. & Miller H. 1987. Petrology and facies analysis of turbiditic sedimentary rocks of the Puncoviscana trough (Upper Precambrian - Lower Cambrian) in the basement of the NW Argentine Andes. *Gondwana Six, Geophys. Monogr.*, 40, 287-293.

Knüver M. & Miller H. 1982. Rb-Sr geochronology of the Sierra de Ancasti (Pampean Ranges, Argentina). *Actas V. Congr. latinoamer. Geol. Buenos Aires*, 3, 457-471.

Lork A., Grauert B., Kramm U. & Miller H. 1991. U-Pb investigations of monazite and polyphase zircon: Implications for age and petrogenesis of trondhjemites of the southern Cordillera Oriental, NW-Argentina. *6. Congr. Geol. Chil., resúm. expand.*, 398-402.

Miller H., Toselli, A.J., Rossi J. & Aceñolaza F.G. 1994. Regional and geochronological development of the metamorphic basement in Northwest Argentina. *Zentralbl. Geol. Paläont. Teil I*, 1993, 263-273.

Rapela C.W., Coira B., Toselli, A.J. & Saavedra J. 1992. El magmatismo del Paleozoico Inferior en el Sudoeste de Gondwana. *In: Paleozoico Inf. de Ibero-América, Gutiérrez Marco J.G. et al. ed.*, 22-68.

Reissinger M. 1983. Geología de la Sierra de Ancasti -6. Evolución geoquímica de las rocas plutónicas. *Münster. Forsch. Geol. Paläont.*, 59, 101-112.

Schalamuk I., Dalla Salda L., Angelelli V., Fernández R. & Etcheverry R. 1983. Geología de la Sierra de Ancasti -7. Rocas máficas y ultramáficas. Petrología y mineralización. *Münster. Forsch. Geol. Paläont.*, 59, 113-136.

Schön Ch. 1991. Magmenentwicklung und Intrusionsgeschichte im Südteil der Sierra de Cachi, NW-Argentinien. *Dr.rer.nat. Diss. LMU München*, 1-142.

Willner A.P., Lottner U.S. & Miller H. 1987. Early Paleozoic structural development in the NW Argentine basement of the Andes and its implication for geodynamic reconstructions. *Gondwana Six, Geophys. Monogr.*, 40, 229-239.

# "GONDWANA" MAGMATISM OF PATAGONIA: INNER CORDILLERAN CALC-ALKALINE BATHOLITHS AND BIMODAL VOLCANIC PROVINCES

Carlos W. Rapela(1), Robert J. Pankhurst(2), Eduardo J. Llambías (1), Carlos Labudía(3) & Analía Artabe(4)

(1) Centro de Investigaciones Geológicas, Universidad Nacional de La Plata, Calle 1 Nº 644, 1900 La Plata, Argentina.
(2) British Antarctic Survey c/o NERC Isotope Geosciences Laboratory, Kingsley Dunham Centre, Keyworth, Nottingham NG12 5GG, UK.
(3) Departamento de Geología, Universidad Nacional del Sur, San Juan 670, 8000 Bahía Blanca, Argentina.
(4) División Paleobotánica, Facultad de Ciencias Naturales y Museo, Universidad Nacional de La Plata, Paseo del Bosque s/n, 1900 La Plata, Argentina.

KEY WORDS: Patagonia, Magmatism, Gondwana, Batholiths, Rhyolite

## INTRODUCTION

The Permian to Jurassic silicic igneous provinces of southern South America are characteristic of the Gondwana supercontinental stage in this region. "Gondwana" magmatism exhibits distinctive composition, geological setting and spatial distribution compared with those typical of the Cretaceous to modern Andes. Whereas the large rhyolite provinces of Permian–Triassic and Middle Jurassic age have attracted much attention (e.g. Kay et al., 1989; Pankhurst & Rapela, 1995), the role of the intraplate batholiths has usually been overlooked. The precise timing and complete compositional characterization of both episodes are crucial to an understanding of the early stages that lead to "Andean type subduction" and the mechanisms that triggered the breakup of the supercontinent. New Rb-Sr geochronological and geochemical data are reported for three key localities of northern Patagonia that, together with results from previous studies, allow us to reach a broader view of the "Gondwana" magmatic episode and its possible tectonic scenario.

## INNER CORDILLERAN BATHOLITHS AND COEVAL VOLCANISM

Recent geochronological and geochemical studies have shown that a series of calc-alkaline batholiths and plutons was emplaced in central and south-eastern Patagonia during the interval from 220 to 200 Ma (Rapela et al., 1992; Rapela & Pankhurst, in press). This episode preceded the eruption of the widespread syn-extensional rhyolites and related rocks of the Patagonian Jurassic Volcanic Province (Fig.1) by some 10-30 Ma. The main subdivisions of this Late Triassic–Early Jurassic intrusive episode are: (a) the NNW-ESE Batholith of Central Patagonia, closely associated with the Gastre Fault System, (b) Subcordilleran plutonism between 40 and 44º S and (c) the monzonite suites of the Deseado Massif at 48º S. Permian intrusive rocks are restricted to north-central Patagonia, near the Chasicó area (Pankhurst et al., 1992).

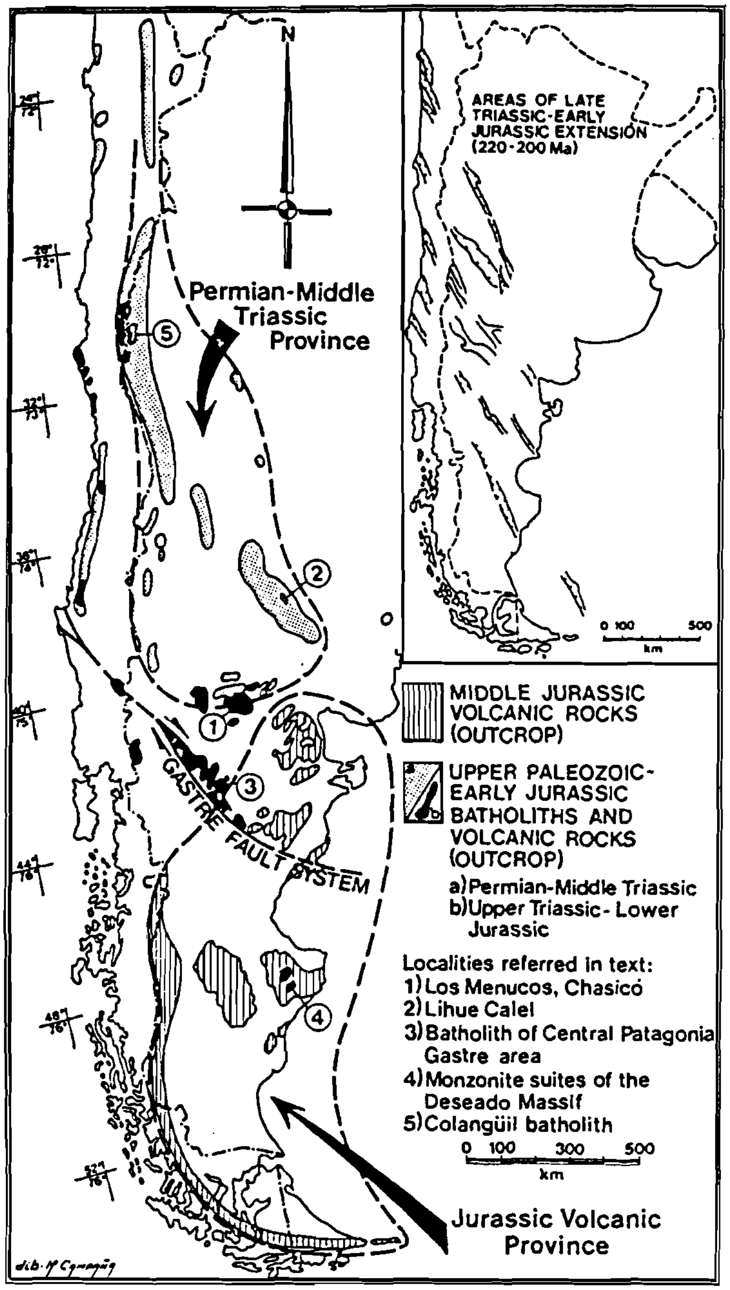


Figure 1: *Simplified geological map showing the distribution of Permian to Jurassic magmatic rocks in southern South America. Insert shows the regional distribution of the Triassic-Early Jurassic extensional basins (Uliana et al., 1989).*

A common characteristic of all these high-level or subvolcanic plutons is the predominance of an intermediate igneous facies ranging in composition from hornblende-biotite granodiorite to quartz-monzonite (typically 65–69% SiO2; Fig.2a). This facies shows a transition to abundant biotite granites (70-74% SiO2) and leucogranites (75-77% SiO2). Rocks with less than 65% SiO2 (diorite to quartz monzodiorite) have been found in the suites of the Deseado Massif, but they are restricted to a marginal facies and enclaves, which have been interpreted as cumulus-rich differentiates (Rapela & Pankhurst, in press). Geochemical data for the Batholith of Central Patagonia and Deseado suites display an arc-dominated signature, and the isotopic data (initial 87Sr/86Sr = 0.7048 to 0.7058 and εNdt = -0.3 to -3.1) are consistent with an origin in the mantle or depleted lower crust (Rapela et al., 1992; Rapela & Pankhurst, in press).

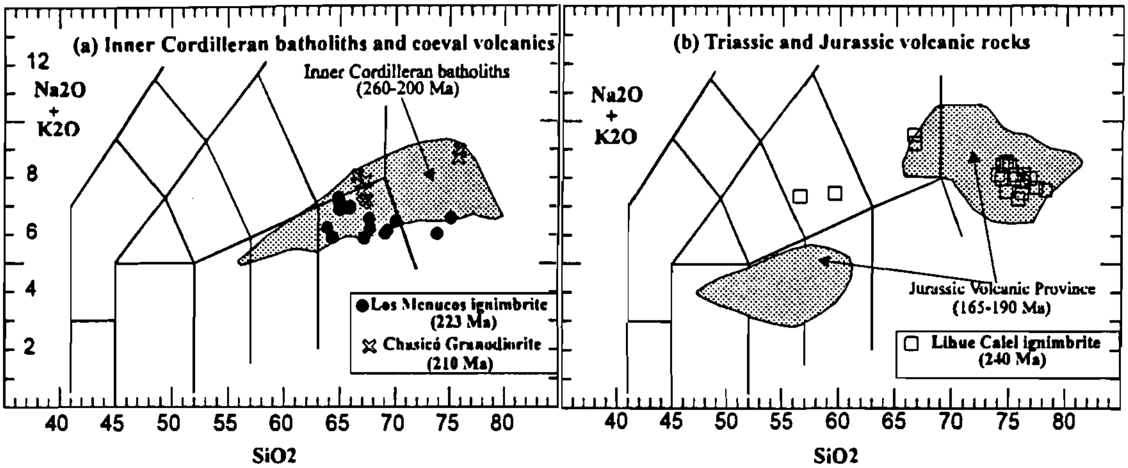


Figure 2: *Alkali-silica variation diagram of Permian to Jurassic magmatic rocks of Patagonia. (a) the field of plutonic rocks is from Rapela & Llambías, 1985; Rapela & Pankhurst 1996 and Rapela et al., 1992. (b) the field of the Jurassic Volcanic Province is from Pankhurst & Rapela, 1995. Note that the hornblende-bearing Late Triassic volcanic rocks of Los Menucos show a different compositional range to that of the silicic members of the Jurassic Volcanic Province.*

The hornblende-biotite dacite ignimbrites of Los Menucos in northern Patagonia (Figs 1, 2) are especially significant since related air-fall deposits carry a rich Dicroidium and other associated flora (Labudía et al., 1995). Fourteen ignimbrite samples define a perfect Rb-Sr whole-rock isochron (MSWD = 1.1), corresponding to an age of 222 ± 2 Ma and initial 87Sr/86Sr ratio of 0.7079 ± 0.0001. Hornblende-biotite granodiorites and consanguineous aplites of the Chasicó area 90 km north-west of Los Menucos (Fig. 1, 2a) give an isochron relationship (MSWD = 0.8) corresponding to an age of 210 ± 2 Ma and an initial 87Sr/86Sr ratio of 0.7058 ± 0.0001. These results indicate that equivalent intermediate-to-evolved calc-alkaline volcanism accompanied the intrusion of the early-emplaced suites of the Batholith of Central Patagonia in the Gastre area (220 ± 3 Ma, Rapela et al., 1992). The shallow emplacement of these granodioritic (dacitic) magmas seems to have occurred over a period of at least 20 Ma in northern Patagonia.

## VOLCANIC PROVINCES

The Jurassic volcanic rocks of eastern Patagonia are part of one of the largest known silicic igneous provinces (Fig. 1). Rb-Sr geochronology has indicated eruptive ages of 168-190 Ma and significant southward diachronism of activity (Pankhurst & Rapela, 1995). The whole province is dominated by high-K rhyolites, but less evolved rocks (47-62% SiO2) showing subalkaline major and trace element geochemistry are sometimes mappable as separate units or occur as a very minor phase within the rhyolite outcrops (Fig. 2b). At individual localities there is always a variable gap in SiO2 between the dominant rhyolites and the intermediate-basic volcanics, defining a bimodal assemblage (Fig. 2b). The majority of the rocks in the most intensively studied, northeastern, part of the province are isotopically uniform, with initial 87Sr/86Sr = 0.7067 ± 0.0003 and εNdt = -4 ± 2. It has been argued that this represents large-scale reworking of relatively unevolved Proterozoic lower crust.

New Rb-Sr isotope data on 13 samples for the Lihue Calel rhyolitic ignimbrites 250 km to the north of the Jurassic Province (Fig. 1) give a perfect fit to the isochron model (MSWD = 1.2), with an initial 87Sr/86Sr ratio of 0.7075 ± 0.0001and an age of 240 ± 2 Ma (Early Triassic). Like the Jurassic volcanic rocks this sequence is bimodal, but has a strongly alkaline signature (Fig. 2b). The more basic trachyandesite and trachydacite members plot on the same isochron as the dominant rhyolites, indicating a cogenetic origin. This observation also holds true for some of the andesites and rhyolites of the Jurassic suite (Pankhurst & Rapela, 1995).

The overall picture of Gondwana magmatism that is begining to emerge from these studies is one of repeated alternation between inner cordilleran calc-alkaline batholiths and bimodal volcanic rocks. The first of these cycles began north of Patagonia, at 28-38ºS, and is represented by calc-alkaline plutonic rocks of the Colangüil batholith (320-260 Ma; Llambías & Sato, 1995; see Fig. 1). This phase was followed by widespread eruption of rhyolites of the Choiyoi Province (Kay et al., 1989), with some coeval intermediate volcanic rocks and granites (s.s) (Llambías & Sato, 1995). The Lihue Calel ignimbrites are among the most easterly examples of this event. Calc-alkaline plutonism was then renewed in northern Patagonia (220-200 Ma), followed by the most widespread silicic volcanism in Jurassic times (190-165 Ma). The combined evidence of the plutonic and volcanic history thus reveals alternations that may reflect changes in the tectonic regime. It could be postulated, for example, that the plutonic episodes correspond to periods of oblique-slip subduction and that these alternated with periods of cessation or slowing of subduction during which magmatism was represented by extensive silicic volcanism.

## REFERENCES

Kay, S.M., Ramos V.A., Mpodozis, C. & Sruoga, P. 1989. Late Paleozoic to Jurassic silicic magmatism at the Gondwanaland margin: analogy to the Middle Proterozoic in North America? Geology, 17, 324-328.

Labudía, C.H., Llambías, E.J., Rapela, C.W. & Artabe, A. 1995. El Triásico de Los Menucos: procesos volcánicos y sedimentarios. Actas II Reunión del Triásico del Cono Sur, pp 17-21, Departamento de Geología, Universidad Nacional del Sur.

Llambías, E.J. & Sato, A.M. 1995. El batolito de Colangüil: transición entre orogénesis y anorogénesis. Revista Asociación Geológica Argentina, 50, 111-131.

Pankhurst, R.J. & Rapela, C.W. 1995. Production of Jurassic rhyolite by anatexis of the lower crust of Patagonia. Earth & Planetary Science Letters, 134, 23-36.

Pankhurst, R.J., Rapela, C.W., Caminos, R., Llambías, E. & Párica, C., 1992. A revised age for the granites of the central Somuncura Batholith, North Patagonian Massif. Journal of South American Earth Sciences, 5, 321-325.

Rapela, C.W. & Llambías, E.J., 1985. Evolución magmática y relaciones regionales de los complejos eruptivos de La Esperanza, provincia de Rio Negro. Revista Asociación Geológica Argentina, 40, 4-25.

Rapela, C.W & Pankhurst, R.J. 1996. Monzonite suites: the innermost Cordilleran plutonism of Patagonia. Transactions of the Royal Society of Edinburgh, Earth Sciences (in press).

Rapela, C.W., Pankhurst, R.J. & Harrison, S.M. 1991. Triassic "Gondwana" granites of the Gastre district, North Patagonian Massif. Transactions of the Royal Society of Edinburgh, Earth Sciences, 83, 291-304.

Uliana, M.A., Biddle, K.T., & Cerdan, J. 1989. Mesozoic extension and the formation of Argentine sedimentary basins. In Tankard, A.J. & Balkwill, H.R. (Eds) Extensional Tectonics and Stratigraphy of the North Atlantic Margins. America Association of Petroleum Geologists Memoir 46, 599-614.

# NATURE OF THE FRONTAL CORDILLERA METAMORPHIC ROCKS IN THE RIO DE LA TUNAS AREA, MENDOZA PROVINCE, ARGENTINA

María A. Ruviños(1) and Daniel A. Gregori(1-2)

(1) Departamento de Geología, Universidad Nacional del Sur, San Juan 670 8000 Bahía Blanca, Argentina
(2) Departamento de Geología, Universidad Nacional el Sur y CONICET, San Juan 670-8000 Bahía Blanca, Argentina

KEY WORDS: Basement, facies analysis, Frontal Cordillera, Argentina

## INTRODUCTION AND GEOLOGICAL SETTING

The Frontal Cordillera Basement (FCB) conforms a NNE-SSW elongated belt, 230 km long, running from the Rio Tunuyán in the south to the Precordillera in the north. Along this belt lithological differences can be appreciated. In the Precordillera area, most of the components of the basement are low grade metamorphic rocks such as calcareous schists, limestones, slates and phyllites. Scarce basic igneous rocks are interbedded in the metasedimentary sequence. The ultrabasic rocks are mostly represented in the northern area, (Cortaderas, Rivadavia and Mendocina Mines). In the Rio de Las Tunas area (Fig. 1) the basement rocks are represented by micaceous and quartz-feldspar schists, calcareous schists, limestones, metapelites, pillow lavas and igneous basic rocks. In the Rio Tunuyán area the basement rocks are mainly micaceous and quartz-feldspar rock, but not detailed work has been done. The FCB was considered by Ramos et at. (1986) as remains of the Chilenia terrane, that collided against the western border of the Gondwana during Devonian times. However only a few papers relative to the nature of the FCB rocks have been published (Caminos, 1965; Villar, 1969; Caminos et al., 1982; Villar and Donnari, 1989; Bjerg et al, 1990; Haller and Ramos, 1993; and Gregori and Bjerg, in press). Most of them are focused on the characteristics of the mafic and ultrabasic rocks but not on the metamorphic rocks. In this paper we present new lithological facies data and a brief description on the structure of the FCB rocks in the Rio de las Tunas, in order to obtain new information on the nature of these rocks.

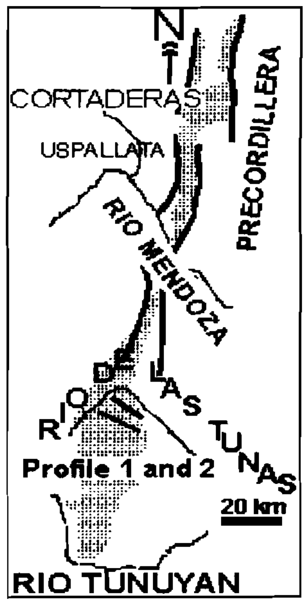


Figure 1. Map of localities.

## DESCRIPTION OF THE LITHOLOGICAL FACIES

Micaceous, calcareous and amphibole schists: This group encloses a set of metasedimentites, most of them rich in calcareous minerals, sometimes with nodular and horizontal layered segregation of quartz according with the schistosity. The micaceous schists contain muscovite and biotite in similar percentage. In the first profile (Fig. 2A), the amount of calcite increase and micas decrease gradually to the west, to turn into calcareous schists. In the calcareous schists the representative mineral is coarse grained calcite. Low quantities of tremolite occurs in thin lenses, interbedded with micaceous components. They usually conform fining upward sequences, foliated in the bottom grading to massive in upper layers. Small outcrops of amphibole schists, composed by segregation of quartz, feldspar and plagioclase alternating with layers of tremolite and epidote are interbedded in the other rocks

Metapelites: This group include fine grained lithologies, sometimes containing garnet. Most of them have high quantities of calcareous minerals giving these rocks a marly composition. Metapelites are deformed showing schistosity according with the regional foliation. They are interlayed with schists, forming the top of fining upward sequences.

Calcareous rocks. Calcareous rocks include limestones, mudstones and associated marbles. They are significant constituents of the FCB. Limestones are composed by coarse grained impure calcite. Usually, they are massive and interbedded with schists and pelitic rocks. These rocks are assembled as coarsening upward sequences showing disturbed structures, resembling calcareous bars. In the first profile (Fig. 2 a y b), they present low scale folding. In most cases the calcareous rocks conform extended bodies that changing to schists westwards. The mudstones occurs in the Rio de las Tunas profile (Fig. 2b) about 2 km. west of the cross section beginning. They show transitional contacts from limestones to mudstones, due to the increment of mud amount. A typical feature is the presence of stratification and banded structures. Folding in the order of 1-2 cm. is common. Silicified layers mainly restricted to the contact with metabasites are present in mudtones. Marble is a rare component in the basement. It is composed of white, coarse grained calcite enclosing big crystals of chlorite. This rock is interlayered with thin layers of calcareous and micaceous schists.

Metabasites and related rocks: Metamorphosed basic rocks and associated metasomatic rocks, as blackwall, are very voluminous in the FCB. The metabasites include four groups: pre-metamorphic dikes, syn metamorphic, post-metamorphic bodies and pillow lavas. Pre-metamorphic dikes have been mostly recognised in profile 1 (Fig. 2a). They are 1-2 m thick and intrude the sedimentary sequence. Porphiritic texture composed by hornblende, plagioclase and minor quantities of feldspar is typically displayed. Main metamorphic mineral is garnet and occurs as widespread coarse crystals. Abundant calcareous minerals replacing plagioclase conform a fine white matrix. The rocks are strongly affected by metamorphism and deformation. Syn and post metamorphic bodies were recognised in both profiles. Syn- metamorphic rocks are abundant in the 12 Hermanos Mine profile. They occur as dikes up to 60 m thick or sheet flows Dikes show porphiritic texture changing consecutively from coarse to fine grained attributed to dike in dike processes. Flow remains display alternating layers of brecciated and massive rock up to 3m thick beds. Foliation at the bottom of the beds and vesiculation at the top is clearly observed. Samples are composed by plagioclase and hornblende. According with the petrological and textural characteristics they are classified as amphibolites. Acidic segregation was found in transitional contact of 1 m thick within the syn metamorphic bodies. They are more abundant and better exposed in profile 2 (Fig 2 c) in up 5 m wide expositions whereas the acidic body itself reach thickness of 2-3 m. The rocks exhibit a coarse grained granular texture, mainly composed by quartz, plagioclase and biotite. The post-metamorphic bodies were recognised only in the first profile. They conform dark bodies up to 100 m diameter, intruding the calcareous schist and mudstones. These rocks are relatively undeformated and retain their original microgranular texture. Important outcrops of pillow lavas were identified at the studied area. They appear interbedded with calcareous and micaceous schist, as well as metapelites. These rocks have suffered alteration and deformation. Blackwall (40 m thick) and talc schists restricted to the contact between the pillow lavas and the schists are common. Lava bodies are altered to a talc and serpentine minerals. Individual pillow size ranges from 20 to 40 cm, but in some cases diameters up to 1 m were observed.

ARRANGEMENT OF LITHOLOGICAL FACIES AND STRUCTURAL CHARACTERISTICS

The FCB contains a variety of interlayered metasedimentary and metavolcanic rocks. Micaceous metasedimentary rocks are confined to the eastern area, grading into thick calcareous bodies westwards. Metasediments conforming fining upward and minor coarsening upward sequences are restricted to the eastern middle section. Limestones and marbles are predominant at the northwestern sides. (Fig. 2). Mudstones interlayered with metabasites are restricted to the west area. Metapelites are a

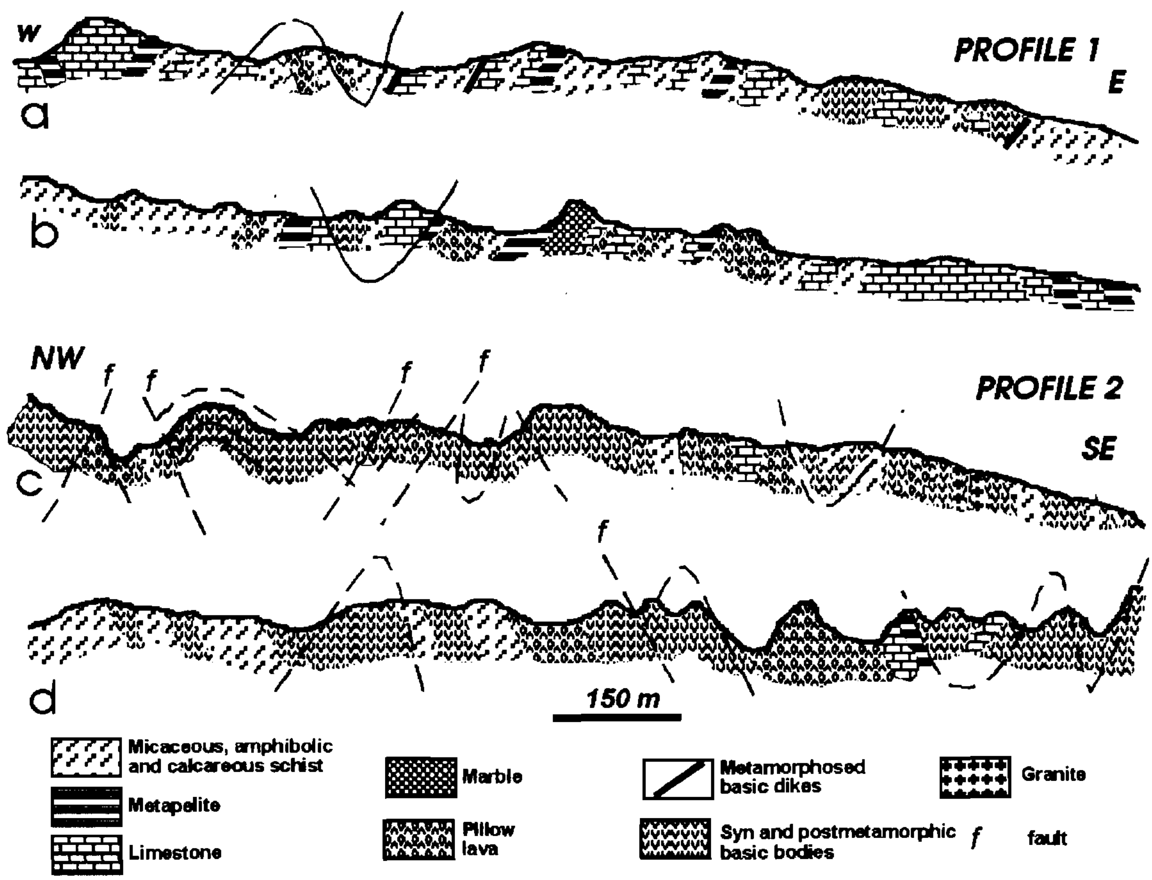


Figure 2. a-b: Rio de las Tunas profile. c-d: 12 Hermanos Mine profile.

rare element in this FCB section. They are interbedded with schists and metacarbonates forming the top of western sedimentary sequences. A remarkably large body of syn-metamorphic basic rocks predominates in the 12 Hermanos Mine profile represented by lava flows sequences. In the eastern side of the area the sheet flows are predominant. Similar textures and setting assemblages suggest the same volcanic origin for these rocks. conforming a typical volcanoclastic sequence. Pre and post metamorphic volcanic bodies are restricted to the northern area. Finally, pillow lavas are an important component in FCB, but specially predominant southwards. Localities in which well-preserved volcanic features were observed they form discontinuous layers with sharp conformable contact against the metasedimentary units. A brief structural analysis of the different components of this metamorphic belt section has been sketched. The FCB rocks have suffered a strong deformation represented by an important high scale folding (wavelength ~ 100 m) with minor low scale folds (wavelength ~ 10-20 cm) associated. In the second profile (Fig 2 d) metabasites exhibit overprint folding in two main directions: N 60°E and N 30° W. Folding features are interrupted by faulting representing a later deformational event.

## CONCLUSIONS

The clastic rocks of the FCB (calcareous and micaceous schists) were probably deposited in a marine platform environment, whereas the metapelites, lava flows and pillow lavas denote deeper environments. This assemblage represents an up to 3 km thick tectonic mélange. Similarities in the lithology and the emplacement features of the FCB components with California Klamath Mountains (Donato, 1989) suggest they are parts of an ophiolitic sequence. Villar & Donari (1989) described and interpreted an assemblage of mafic rocks to the south of 12 Hermanos Mine profile as belonging to an ophiolitic sequence. Also metavolcanic rocks with similar characteristics were recognised by Gregori & Bjerg (in press) in the Arroyo Metales, 20 km southwestwards. In the Precordillera, similar arrangements were found by Haller & Ramos (1993) and Davies et al (in press).

## REFERENCES

Bjerg, E.A., Gregori, D.A., Losada Calderón, A. y Labudía, C.H.. 1990. Las metamorfitas del faldeo oriental de la Cuchilla de Guarguaraz, Cordillera Frontal, Provincia de Mendoza. Revista de la Asociación Geológica Argentina, 45 (3-4), 234-245.

Caminos, R. 1965. Geología de la vertiente oriental del Cordón del Plata, Cordillera Frontal de Mendoza. Revista de la Asociación Geológica Argentina, 20 (3), 351-392

Caminos, R., Cingolani, C., Hervé, F and Linares, E. 1982. Geochronology of the pre-Andean metamorphism and magmatism in the Andean Cordillera between latitudes 30° and 36° S. Earth-Science Review, 18, 333-352.

Davis, S., Moores, E., Roeske, S, Kay, S, McClelland, W and Sneel, L. 1995. New data from the western margin of the Precordillera Terrane, Argentina: constrain scenarios for the Middle Paleozoic tectonics of western South America. IGCP Project 376 Meeting, Laurentian Gondwanan Connections before Pangea. Jujuy, Argentina (in press).

Donato, M.M.. 1989. Metamorphism of an ophiolitic tectonic mélange, northern California Klamath Mountains, USA. Journal Metamorphic Geology, 7, 515-528.

Gregori, D.A. and Bjerg, E.A. 1995. Eopaleozoic volcanism in the Frontal Cordillera: New evidences on the nature of the southern South American ophiolitic belt. (in press).

Haller, M y Ramos, V. 1993. Las ofiolitas y otras rocas afines. In: Geología y Recursos Naturales de Mendoza (edited by V.A. Ramos) pp 31-39. Relatorio del XII Congreso Geológico Argentino y II Congreso de Exploración de Hidrocarburos.

Ramos, V., Jordan, T., Allmendinger, R., Mpodozis, C., Kay, S., Cortés, J. and Palma, M. 1986. Paleozoic terranes of the central Argentine-Chilean Andes. Tectonics, 5 (6), 855-880.

Villar, L.M. 1969. El Complejo ultrabásico de Novillo Muerto, Cordillera Frontal, provincia de Mendoza, Argentina. Revista de la Asociación Geológica Argentina, 24 (3), 223-238.

Villar, L.M. y Donnari, E.I.. 1989. Geología y metalogénesis del Complejo Máfico-Ultramáfico de Los Gateados; Departamento Tupungato, Pcia. de Mendoza. Correlación Geológica, 3, pp 45-50.

# NEW EVIDENCE OF A WIDESPREAD PERMIAN REMAGNETIZING EVENT IN THE CENTRAL ANDEAN ZONE OF ARGENTINA

Silvia TRUCO and Augusto E. RAPALINI

Laboratorio de Paleomagnetismo Daniel Valencio, Depto de Ciencias Geológicas, FCEyN, Universidad de Buenos Aires, Ciudad Universitaria, Pabellón 2, 1428, Buenos Aires, Argentina.

**KEY WORDS**: Paleomagnetism, Permian, Ordovician, Remagnetization, Andes, Argentina

## INTRODUCTION

The pre-Andean tectonic evolution of the western continental margin of southern South America involves the possible accretion and displacement of mobile terranes during Late Proterozoic and Paleozoic times (e.g. Ramos, 1988). In particular, the Cambrian-Ordovician carbonate platform of the Argentine Precordillera, and its southward continuation in the San Rafael Block, has been proposed of being a Laurentian terrane that was accreted to Gondwana in the Early Paleozoic (e.g. Astini et al, 1995). However, up to date no paleomagnetic data has been obtained from rocks of that age from this region to test this proposal. Evidence of an important Permian remagnetizing event in Precordillera was firstly presented by Rapalini and Tarling (1993). This remagnetization has so far precluded from obtaining primary remanence directions from Cambrian-Ordovician limestones in this region. In order to constrain the paleogeographic evolution of this terrane in the Early Paleozoic a paleomagnetic study was carried out on the Middle Ordovician carbonatic rocks of the Ponón Trehué Fm. exposed in the San Rafael Block (western Argentina, Fig.2a). A complementary paleomagnetic study was also done on the Late Carboniferous clastic sediments of the El Imperial Formation, also exposed in the area. The results of this study show that both units carry an old characteristic magnetization that was acquired during the folding of the rocks in Early Permian times caused by the San Rafaelic tectonic event.

## RESULTS AND INTERPRETATION

Six and seven sampling sites (thirty eight and forty-four samples) were located on the Ponón Trehue and El imperial Formations respectively. The former was sampled on opposite limbs of a tight anticline, while the latter was sampled on two different sections separated around 5 km. One of these sections (sites PJ6 and PJ7) was overturned. Standard paleomagnetic demagnetization of all samples was done with either AF or thermal procedures. While the former was efficient only in four sites of the Ponón Trehué Fm., the latter was the most effective in isolating the magnetic components in all other sites. Figure 1 shows typical magnetic behaviour of samples from the Ponón Trehué Fm. (Fi.1a, 1b) and El Imperial Fm. (Fig.1c). In both cases most samples were carrier of two consistent magnetic components that were defined by principal component analyses (Kirshvink, 1980). One directed up and north (component A), coincident with the present dipole direction, was deleted in most cases at temperatures around 150 to 300° C (Fig.1b, 1c). This suggests a viscous and/or a chemical recent secondary magnetization. A second magnetic component (B) directed down and south was isolated between 300 and 550° C in the Ordovician limestones, suggesting magnetite as the main ferromagnetic carrier. A similar component was defined in the Carboniferous sandstones between 400 and 690° C, suggesting hematite as the carrier of the remanence. Mean sites direction were computed for component B (Table 1). Only mean site direction from PJ-3 was ruled out due to a high $\alpha 95$, all others showing very good within site consistency of directions ($\alpha 95<15°$). Application of stepwise structural correction and McFadden's (1990) fold test indicated that the remanence was acquired during deformation of the rocks. Maxima of Fisher's k parameter were attained for 21% (Ponón Trehue Fm.) and 38% (El Imperial Fm.) of structural corrections. In both cases the fold test was significant at a 99% confidence level.

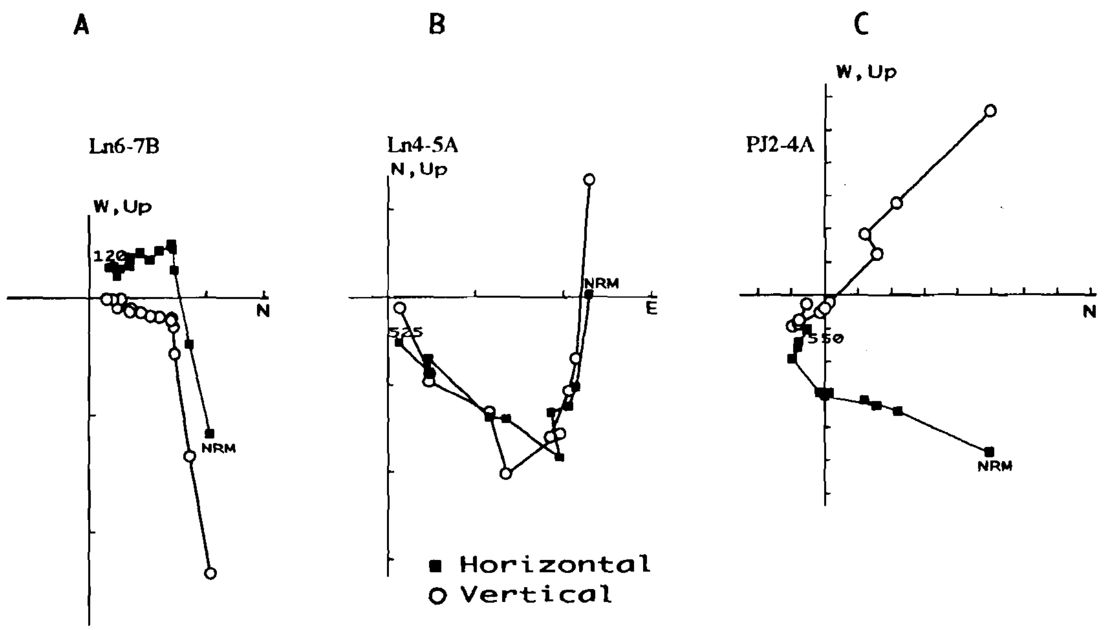


**Fig.1.** Representative magnetic behaviour of samples from the Ponón Trehué (A, B) and El Imperial (C) Formations

Two paleomagnetic poles were computed from the partially corrected mean remanence directions, PN: 25.0°E 53.4°S $\alpha95$: 8.8°, EI: 0.8°E 48.6°S $\alpha95$: 19.6° (Fig.2b). The position of these poles is close to other late Carboniferous and early Permian poles from South America. This is consistent with the Early Permian age of the San Rafaelic tectonic phase that affected the western margin of southern South America in the late Early Permian (280-272 Ma, LLambías & Sato, 1995). Late Permian volcanics in the study area are not affected by this deformation. It is remarkable the coincidence of PN and EI poles with other remagnetized poles from the Argentine Precordillera (e.g. the Hoyada Verde HV, the Alcaparrosa AL and the San Juan limestones SJ poles, see Fig.2). The latter were assigned to a remagnetizing event affecting the Central and Western Precordillera during Early Permian times and linked to the San Rafaelic tectonic phase. The new results suggests that the region affected by this remagnetizing event also comprises the San Rafaelic Block, several hundred km. south of Precordillera. Detailed rock magnetic studies of these units should shed light on the mechanisms of this regional remagnetizing events.

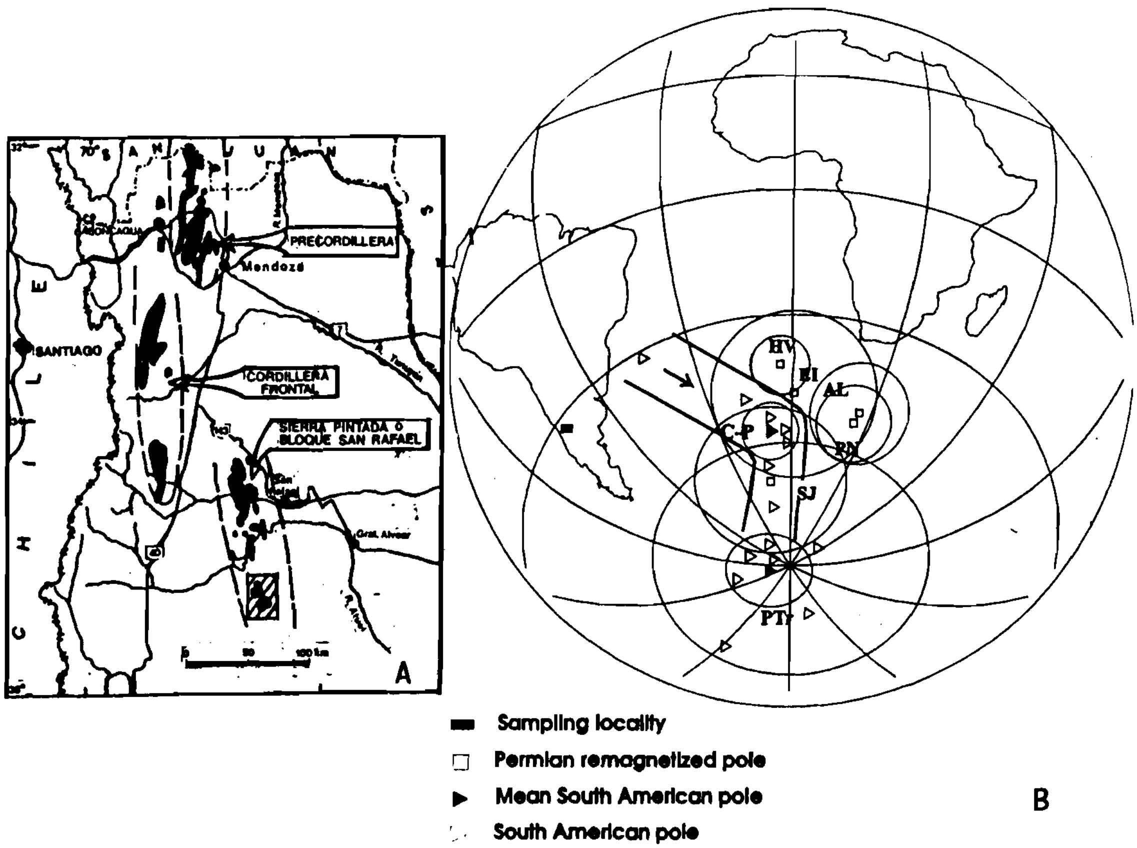


**Fig.2a.** Location map of the studied area (shaded rectangle). In black, outcrops of Early Paleozoic rocks (simplified from Cuerda et al, 1993). **2b.** Late Paleozoic apparent polar wander path for South America and distribution of remagnetized poles from Precordillera and San Rafael Block (squares). C-P and PTr: Late Carboniferous - Early Permian and Late Permian - Early Triassic mean poles for South America (Rapalini et al, 1993).

| FORMATION | SITE | N | REMANENCE (in situ) | | | | STRUCT. CORRECT. | | REM. (full corrected) | |
|---|---|---|---|---|---|---|---|---|---|---|
| | | | Dec. (°) | Inc. (°) | A95 (°) | K | Strike | Dip | Dec. (°) | Inc. (°) |
| Ponon Trehue F. | Ln-1 | 6 | 124.8 | 28.2 | 10.0 | 45.8 | 182 | 71 | 205.2 | 58.6 |
| | Ln-2 | 3 | 116.8 | 41.5 | 12.2 | 101.8 | 182 | 71 | 234.2 | 59.12 |
| | Ln-3 | 5 | 139.2 | 31.7 | 5.2 | 216.5 | 182 | 71 | 208.3 | 45.8 |
| | Ln-4 | 6 | 128.0 | 36.0 | 4.6 | 207.7 | 182 | 71 | 217.8 | 54.1 |
| | Ln-5 | 6 | 150.5 | 46.9 | 9.5 | 50.0 | 350 | 64 | 120.4 | 6.6 |
| | Ln-6 | 5 | 162.4 | 40.3 | 15.8 | 24.2 | 350 | 64 | 130.3 | 11.1 |
| Mean sites (in situ) | | 6 | 136.5 | 39.2 | 12.5 | 29.9 | | | | |
| Mean sites (100 % correct.) | | 6 | 174.6 | 49.6 | 40.4 | 3.7 | | | | |
| Mean sites (21 % correct.) | | 6 | 139.2 | 44.0 | 7.9 | 72 | | | | |
| El Imperial F. | Pj-1 | 5 | 114.8 | 34.1 | 14.0 | 30.7 | 155 | 81 | 191.6 | 37.9 |
| | Pj-2 | 5 | 118.7 | 26.3 | 8.0 | 91.6 | 155 | 81 | 181.1 | 59.1 |
| | Pj-3 | 3 | 127.7 | 28.6 | 30.4 | 17.5 | * | | | |
| | Pj-4 | 4 | 115.6 | 32.3 | 5.4 | 286.5 | 155 | 81 | 189.2 | 37.8 |
| | Pj-5 | 4 | 113.3 | 32.0 | 9.7 | 90.4 | 155 | 81 | 189.5 | 39.8 |
| | Pj-6 | 4 | 236.6 | 62.8 | 12.1 | 58.8 | 337 | 111 | 71.7 | 5.7 |
| | Pj-7 | 5 | 222.7 | 64.1 | 11.8 | 42.9 | 337 | 111 | 77.3 | 2.8 |
| Mean sites (in situ) | | 6 | 130.5 | 50.7 | 33.6 | 4.9 | | | | |
| Mean sites (100 % correct.) | | 6 | 150.5 | 41.2 | 54.7 | 2.5 | | | | |
| Mean sites (38 % correct.) | | 6 | 130.0 | 56.0 | 14.8 | 21.4 | | | | |

**Table 1.** Paleomagnetic data of the Ponón Trehué and El Imperial Formations.

## REFERENCES


Astini, R.A., Benedetto, J.L. & Vaccari, N.E. 1995. The early Paleozoic evolution of the Argentine Precordillera as a Laurentian rifted, drifted and collided terrane: a geodynamic model. *Geol. Soc. Amer. Bull.*, 107 (3), 253-273.

Cuerda A.J, Cingolani C & Bordonaro, O. 1993. Las secuencias sedimentarias eopaleozoicas. *XII Cong. Geol. Arg., Relatorio,* I (3) 21-30.

Kirshvink J.L. 1980. The least-squares line and plane and the analysis of palaeomagnetic data. *Geophys. J.R. astron. Soc.*, 62 699-718.

LLambías E.J. & Sato A.M. 1995. El batolito de Colangüil: transición entre orogénesis y anorogénesis. *Asoc. Geol. Arg. Rev.,* 50 (1-4), 111-131.

McFadden P.L. 1990. A new fold test for palaeomagnetic studies. *Geophys. J. Int.*, 103, 163-169.

Ramos V.A. 1988. Late Proterozoic - Early Paleozoic of South America - a collisional history. *Episodes*, 11, 3, 168-174.

Rapalini, A.E. Abdeldayem A.L. & Tarling D.H. 1993. Intracontinental movements in Western Gondwanaland: a palaeomagnetic test. *Tectonophysics*, 220, 127-139.

Rapalini A.E. & Tarling D.H. 1993. Multiple magnetizations in the Cambro-Ordovician carbonate platform of the Argentine Precordillera and their tectonic implications. *Tectonophysics*, 227, 49-62.

# GEODYNAMIQUE ANDINE

## ISAG 96

## Résumés

**Le nid de sismicité de Pisayambo (Equateur) : vers la naissance d'un volcan ?**
J. Aguilar, J.L. Chatelain, B. Guillier et H. Yepes

737 séismes enregistrés par le réseau local sont utilisés pour déterminer la géométrie du nid de sismicité de Pisayambo. Nous mettons en évidence qu'il est divisé en deux parties localisées l'une au-dessus de l'autre. A l'aide du paramètre E de la loi généralisée de Poisson, du paramèbre b et de la distribution temporelle des séismes, nous mettons en évidence la nature tectonique des séismes les plus superficiels, alors que les plus profonds sont d'origine volcanique, indiquant la possibilité d'un processus de naissance d'un volcan.

**Métamorphisme de bas degré dans les séquences volcaniques mésozoïques et cénozoïques de la Patagonie (43°-46° S), Chili**
L. Aguirre, J.A. Cortes, D. Morata et F. Hervé

Les séquences volcaniques de la Patagonie (43°-46° S), d'âge compris entre le Jurassique et le Néogène, ont subi un métamorphisme non déformatif de très bas à bas degré en faciès zéolite, prehnite-pumpellyite, prehnite-actinote et schistes verts. Le plus haut degré métamorphique correspond aux roches jurassiques tandis que les associations de plus faible degré caractérisent les laves du Néogène. Les associations schistes verts, particulières aux roches jurassiques, seraient en relation directe avec l'effet thermique des intrusions batholithiques d'âge c. 95 Ma.

**Stratigraphie, sédimentologie et évolution tectonique du bassin de Rio Cañete: chaînes côtières centrales du Pérou**
A.M. Aleman

Le bassin de Rio Cañete, dans les chaînes côtières centrales du Pérou, représente une séquence de front d'arc tardi-jurassique (Tithonique) à albienne, limitée par des failles, et formée par un processus d'étalement intra-arc avorté durant l'évolution précoce des Andes. La séquence, exposée dans la région de Lima, se compose de plus de 6000 m de sédiments volcanoclastiques, de coulées de lave, de boues calcaires, de pélites, de grès, et de quelques calcaires fossilifères et évaporites. La stratigraphie enregistre plusieurs épisodes de volcanisme et d'extension le long et à travers le bassin, et fournit de nouvelles données sur l'évolution et la croissance crustale des Andes centrales.

**La structure andine de la Cordillère orientale à partir de profils de sismique réflexion YPF retraités**
R.W. Allmendinger et T.R. Zapata

Pour la première fois, la structure profonde de la Cordillère orientale des Andes centrales de l'extrême nord argentin a a pu être imagée, grâce à des lignes de sismique réflection profonde obtenues par corrélation étendue de données Vibroseis standard fournies par YPF S.A. Une excellente réflectivité crustale autour de 13-15s permet d'imager un possible chevauchement au toit d'un duplex d'échelle crustale, ainsi que la rampe du mur du décollement subandin.

**Le séisme de Macas (Mw 6.8) du 3 octobre 1995 dans le Subandin équatorien**
A. Alvarado, M. Segovia, H. Yepes, B. Guillier, J. L. Chatelain, J. Egred, D. Villagomez, M. Ruiz, P. Samaniego et R. Santacruz

Le séisme de Macas, caractérisé par un mécanisme au foyer avec un plan nodal orienté N30E, s'est produit au niveau du bombement structural de Cutucú, sur la bordure occidentale de la zone subandine. Du 3 octobre au 31 décembre 1995, il a été enregistré environ 2100 répliques. Suite au séisme de 1987, le séisme de Macas met en valeur l'activité tectonique de la zone subandine.

**La faille de Liquiñe-Ofqui: résultats géophysiques dans la région de Puyuhuapi**
M. Araneda et M.S. Avendaño

Nous présentons des résultats gravimétriques dans le secteur de Puyuhuapi, le long d'un segment d'une mégastructure géologique où la faille de Luiquiñe-Ofqui n'affleure pas à la surface. Cette zone est une structure faillée d'une largeur moyenne de 1.5 km, qui se répète dans d'autres parties de la mégastructure.

**Gravimétrie dans le Sud des Andes centrales, 38°-40° S**
M. Araneda, M.S. Avendaño, S. Schmidt, M. Schmitz et H.J. Götze

Ce travail est la présentation de résultats préliminaires d'une étude faite à partir de données géophysiques entre les latitudes 38°-40° S. Cette étude consiste en un relevé gravimétrique composé de stations distantes de 200 mètres à 3 km. Le but est de déterminer les structures géologiques associées à des méga-failles dans une région de volcanisme récent, ainsi que la profondeur de la croûte et les structures mineures.

**Contraintes Tectoniques dans le Nord-Ouest de l'Argentine et leurs relations avec les principaux seismes superficiels**
M. Araujo et J.C Castano

Les principales sources sismogeniques dans le Nord-Ouest de l'Argentine sont ici étudiées. Ces séismes placent la région au deuxième rang quant à l'importance du risque sismique. Les tremblements de terre superficiels ont produit de nombreux dommages le long d'une zone orientée SSW-NNE. Ici, l'orientation de la contrainte horizontale maximale, produite par la collision de la plaque de Nazca et de l'Amérique du Sud a été modifiée par des contraintes locales. Une des raisons de cette modification pourrait être que les hautes Andes soient soumises à un processus d'extension transmis vers l'est dans la plaque Amérique du Sud.

**Stratigraphie séquentielle du bassin Mésozoïque de Domeyko, Nord Chili**
J. Ardill, S. Flint, I. Stanistreet et G. Chong

Le bassin de Domeyko du Nord Chili enregistre des dépôts marins carbonatés et siliciclastiques du Trias supérieur au Crétacé inférieur le long de la marge du Gondwana. Une analyse des variations relatives du niveau de la mer, avec des comparaisons à d'autres bassins marginaux sud-américains et de l'hémisphère nord permet une interprétation des contrôles dans le développement des séquences. Cinq baisses du niveau de la mer et 7 montées équivalentes dans le temps dans d'autres bassins des hémisphères nord et sud sont attribuées à un eustatisme global. Les baisses relatives du niveau de la mer du Bathonien inférieur, de l'Oxfordien supérieur, du Valanginien inférieur et du début du Cénomanien sont interprétés comme étant contrôlé tectoniquement par des événements à l'échelle continentale liés à la fragmentation du Gondwana.

**Tectonique transtensive du Jurassique à l'Éocène inférieur dans l'arc et l'arrière-arc de la région d'Atacama, Chili**
C. Arevalo et J. Grocott

Les résultats récents publiés sur des roches jeunes à l'est de l'arc Jurassique-Crétacé inférieur montrent l'existence d'événements dominés par de l'extension et des décrochements dans l'arrière-arc crétacé et dans l'arc d'âge Crétacé supérieur à Eocène inférieur. Ceci suggère que l'extension et/ou la transtension ont continué peut-être de façon intermittente, jusqu'à l'Eocène inférieur.

**Evolution du paléoenvironnement des Andes boliviennes au cours du Pléistocène supérieur**
J. Argollo et P. Mourguiart

Nous présentons une reconstruction climatique de l'Altiplano bolivien (Andes Centrales) basée sur des données géomorphologiques, sédimentologiques, et palynologiques, ainsi que sur l'analyse des faunes d'Ostracodes. Nous avons pu estimer la température et déterminer quantitativement les variations des niveaux lacustres depuis la fin du Pleistocène (30 000 ans BP).

**Stratigraphie et subdivisions allostratigraphiques de l'Ordovicien de la Précordillère argentine, Gondwana du sud-ouest**
R.A. Astini

Une approche allostratigraphique mettant l'accent sur les ruptures dans l'enregistrement sédimentaire a été entreprise dans les bassins ordoviciens de la Précordillère argentine. Les résultats contribuent à l'analyse des bassins et de leur stratigraphie événementielle, en permettant de discuter les ruptures dans l'enregistrement sédimentaire en termes d'histoire eustatique et tectonique du bassin.

**Paléoenvironnements et évolution des bassins sédimentaires dans une zone de complexe d'arc volcanique du Gondwana occidental préandin: la chaîne de Famatina**
R. Astini et J.L. Benedetto

Les données paléontologiques et les récentes données paléomagnétiques permettent de considérer la chaîne de Famatina, située entre la Précordillère et les Sierras Pampeanas, comme étant une portion d'un complexe d'arcs insulaires exotiques connecté à la province celtique d'arcs insulaires intra-Iapetus. Les données stratigraphiques disponibles montrent une sédimentation très continue depuis l'Arenig inférieur jusqu'au Llanvirn inférieur. L'analyse pétrographique et le mode d'empilement des unités génétiques indiquent un environnement de plateforme alimentée par un arc volcanique à l'ouest, et par un domaine cratonique à l'est, ce qui apparait typique des contextes de systèmes de dépôt de type arrière-arc.

**Evolution tectonostratigraphique d'un terrain allochtone dans la marge Gondwanienne préandine: la Précordillère argentine**
R. Astini et J.L. Benedetto

L'histoire tectonostratigraphique de la Précordillère est analysée depuis sa séparation de la Laurentia au Cambrien inférieur, jusqu'à sa collision avec le Gondwana occidental au cours de l'Ordovicien moyen à supérieur. Les données géométriques, stratigraphiques, ainsi que la composition des différentes unités conduisent à distinguer trois principaux stades: un stade marge passive, suivi de deux stades bassin d'avant pays. La Précordillère est considérée comme étant un véritable terrain exotique pendant l'histoire pré-andine de l'Amérique du sud.

**Roches ignées sodiques et épaississement crustal dans les Andes**
M.P. Atherton et N. Petford

Les roches ignées sodiques sont communes de l'Equateur au sud du Chili. Celles d'age tertiaire à quaternaire forment les volcans et les plutons au dessus de la croûte andine épaissie au Miocène. Avec les plus vieux plutons paléozoïques, ils sont considérés comme étant formés par fusion d'une croûte inférieure épaisse basaltique, et leur présence indique des périodes d'épaississement crustal.

**Le système de failles inverses de Guadalupe-Chuchure, bassin de Falcon, Vénézuela nord-occidental : exemple naturel et modélisation analogique d'une zone de transfert**

F.A. Audemard M. et S. Calassou

Le système de failles de Guadalupe-Mina de Coro-Chuchure s'étend sur une soixantaine de kilomètres en direction ENE-WSW au nord de l'état de Falcón (Vénézuéla nord-occidental). La trace de ce système présente deux virgations qui décalent le front de quelques kilomètres. Nous avons modélisé analogiquement la plus orientale des deux virgations au moyen de modèles en sable. Cette virgation s'avère être une zone de transfert dûe à la présence d'un rejet au niveau du socle, introduit par la faille normale de Los Médanos.

**Activite quaternaire d'un système chevauchant (Piémont Llanero, cordillère orientale de la Colombie): données géomorphologiques et géologiques issues de l'anticlinal de La Florida, entre les rivières Upia et Cusiana**

F. A. Audemard M. et K. Robertson

Situé dans le piémont de la cordillère orientale de la Colombie, l'anticlinal de la Florida, figurant également dans la bibliographie pétrolière sous le nom d'anticlinal de Cusiana, a été reconnu lors de l'exploration géophysique réalisée vers la fin des années 80. Nous présentons de nombreuses données géomorphologiques et géologiques de surface, permettant de démontrer, non seulement l'existence de cette structure, mais aussi son activité tectonique quaternaire.

**Séismicité et état de contrainte dans les Andes Centrales (région de l'Oroclinal bolivien)**

R. Ayala et G. Wittlinger

La séismicité des Andes Centrales est imagée en utilisant un modèle de vitesse en 3 dimensions. Cette séismicité montre une principale concentration de séismes crustaux localisée près du coude de l'oroclinal bolivien, et un amas de séismicité de profondeur intermédiaire au sud de la frontière Pérou-Bolivie. L'état de contrainte est caractérisé par une compression horizontale ENE dans l'avant-arc et dans la zone subandine, parallèle à la direction de convergence des plaques Nazca et Amérique du sud. Les hautes Andes occidentales montrent une extension horizontale N-S. La plaque Nazca est affectée par une contrainte extensive parallèle à la direction du plongement de la plaque.

**Géométrie de chevauchement néogène et équilibrage crustal dans les branches nord et sud de l'orocline bolivien (Andes centrales)**

P. Baby, P. Rochat, G. Hérail, G. Mascle et A. Paul

Deux coupes équilibrées d'échelle crustale ont été construites dans les branches nord et sud de l'orocline bolivien, à partir d'études régionales et de récentes données de géophysique nous renseignant sur la structure profonde de la chaîne. Le raccourcissement total augmente du nord vers le sud (191-231 km). Cette augmentation du raccourcissement coïncide avec une augmentation de l'épaisseur de la croûte et de la largeur de la chaîne. Les deux coupes équilibrées montrent que le raccourcissement néogène peut expliquer seulement une partie du surépaississement crustal connu sous la cordillère orientale de l'Altiplano.

**Evolution spatio-temporelle de l'activité hydrothermale dans un dôme volcanique, sur l'exemple des minéralisations de type épithermal du Cerro Bonete (Bolivie)**
L. Bailly et J.L. Leroy

La combinaison des études minéralogiques détaillées des altérations développées lors des circulations de fluides et celles des inclusions fluides associées permet de reconstituer l'évolution de ces systèmes hydrothermaux, en particulier leur température, les rapports eau-roche et les volumes percolés, de plus en plus limités avec le temps au drain principal.

**Pétrogénèse de l'arc magmatique équatorien sur une coupe à travers les Andes septentrionales: pétrologie, géochimie et observations isotopiques**
R Barragan Talenti et D.J. Geist

Comme dans la plupart des arcs, les laves des volcans équatoriens sont progressivement plus riches en potassium lorsque l'on s'éloigne de la fosse. Une assimilation crustale, bien que détectable avec les isotopes du strontium, ne modifie pas fortement les éléments traces et majeurs dans les magmas. C'est pourquoi, des différences fondamentales dans le régime de fusion de la source entraînent différents degrés de fusion partielle. Les magmas Atacazo (cordillère occidentale) montrent une large contribution de la plaque océanique et un fort taux fusion. Les magmas Sumaco (bassin oriental) montrent une faible contribution de la plaque océanique et un faible taux de fusion.

**Sur la prédiction du soulèvement côtier et de la subsidence dûes aux grands seismes au Chili**
S.E. Barrientos

Les changements d'élévation verticale qui ont été observées lors des trois grands tremblements de terre au Chili (1960, 1985 et 1995), sont utilisés pour déterminer l'extension de la zone sismogénique en profondeur. L'interpolation des axes de changement d'élévation nul observés pour ces trois grands séismes en fonction de leur distance à la fosse, et la comparaison à d'autres zones de subduction au Chili, permet d'obtenir des estimations des futurs changements d'élévation des lignes côtières.

**Sismicité intraplaque dans la région centrale du Chili**
S. Barrientos, E. Vera et T. Monfret

Plusieurs nids de sismicité superficielle intraplaque (0-20 km de profondeur), sans relation connue avec les failles en surface, sont détectés depuis déjà dix ans par les réseaux sismologiques, sur le flanc occidental des Andes dans la région centrale du Chili. La localisation de ces séismes est faite à partir d'un modèle de vitesses déduit d'un profil de réfraction sismique. Les mécanismes au foyer obtenus indiquent que cette région est soumise à un régime tectonique compressif principalement est-ouest.

**Nouveaux âges (U-Pb, Rb-Sr, K-Ar) d'unités réputées précambriennes (Chili du nord): quelques implications géotectoniques**
M.A. Basei, R. Charrier et F. Hervé

Nous avons obtenu des âges situés entre $544 \pm 22$ Ma et 365 Ma, pour le Complexe Métamorphique de Belén (CMB), et d'autres entre 167 et 142 Ma, pour celui de Mejillones (CMM). Pour le CMB, nous retenons un métamorphisme et un plutonisme cambrien supérieur et un refroidissement postérieur, remettant en cause l'âge précambrien précédemment obtenu. Au CMM, il y aurait eu un rechauffement d'âge jurassique.

**Bassins néogènes sur décrochements et le concept de "weak fault" pour les sutures de collision en Equateur et en Colombie**
R. Baudino

Les Andes d'Equateur et de Colombie se caractérisent par la présence de terrains allochtones accolés à la marge sud-américaine. L'étude géodynamique de bassins néogènes sur décrochements génétiquement liés aux sutures de collisions montre qu'ils ne peuvent être intepprétés selon le modèle classique des pull-apart. Par contre, le concept de "weak fault" peut être invoqué pour expliquer leur évolution.

**Etude des variations latérales d'amplitude des phases régionales à travers les Andes, le long d'un profil à 20°S**
D. Baumont et A. Paul

A partir de l'analyse des données sismologiques de l'expérience Lithoscope BOLIVIE/CHILI en 1994, nous étudions les variations latérales d'amplitude des phases régionales pour en déduire des caractéristiques de la structure crustale. Notamment, nous cherchons à préciser s'il existe effectivement une anomalie de propagation des ondes Lg perpendiculairement à la direction des unités géomorphologiques.

**Croûte anormale dans les Andes Centrales**
S. Beck, G. Zandt, S. Myers, T. Wallace, P. Silver, L. Drake et E. Minaya.

Un réseau large-bande passif déployé dans les Andes Centrales a enregistré de nombreux séismes régionaux. La modélisation des séismogrammes montre que la croûte de l'Altiplano est caractérisée par des vitesses P faibles, un rapport de Poisson de 0.25, et une épaisseur crustale de 65km. L'épaisseur crustale varie à travers l'orogène, de 70-74 km sous les cordillères Real et occidentale, à 43-47 km dans le sub-andin, et à 32-38 km sous la plaine du Chaco. Ces propriétés moyennes sont en accord avec un raccourcissement d'une lithosphère peu rigide entre deux lithosphères plus fortes.

**L'évolution du bassin d'Aysen (Chili): un bras de mer épicontinental d'âge crétacé inferieur à l'extrémité méridionale de l'Amérique du sud**
C. M. Bell, R. de la Cruz, M. Suarez et M. J. Townsend

Dans le Bassin d'Aysen, de direction N-S, plus de 1200 m de sédiments de plateforme se sont déposés au Crétacé inférieur, à partir d'une mer épicontinentale étroite, parallèle aux Andes méridionales. Le bassin s'est formé dans un contexte d'arrière-arc et par subsidence thermique, lors d'une période tectonique et volcanique plutôt calme. Vers le sud, il rejoignait le bassin de Magellan. La source des sédiments est à rechercher plus à l'est, dans le bassin continental de San Jorge.

**La trace active de la faille d' El Pilar (Vénézuela nord-oriental) : évidences néotectoniques et données paléosismologiques**
C. Beltran, A. Singer et J.A. Rodriguez

La trace active de la faille d' El Pilar, considérée comme un jalon de la limite sud des plaques caraïbe et sud-américaine, montre des évidences spectaculaires, et découvertes depuis peu en surface, d'un mouvement récent latéral dextre, observé également en tranchée, à l'est de Casanay. Cette tranchée a permis d'identifier

4 événements paléosismiques dont les âges C14 minimum sont les suivants : 7080 ± 1460 ; 5985 ± 735 ; 5595 ± 275 et 4805 ± 1050 BP.

**Evolution géodynamique en avant-arc du système de subduction équatorien**
S. Benitez

A l'aide d'observations stratigraphiques, sédimentologiques et structurales, appuyées par des données sismiques et sur puits, issues de l'industrie pétrolière, nous ré-évaluons l'histoire géodynamique de la Province Côtière en Equateur et en particulier la Péninsule de Santa Elena, ou se situe un des plus anciens champs de pétrole au monde.

**Caractéristiques sismotectoniques de la zone Wadati-Benioff dans la région des Andes**
J. Berrocal et C. Fernandes

La corrélation spatio-temporelle des séismes profonds sud-américains et sa corrélation apparente avec l'activité sismique dans la zone de Wadatti-Benioff suggère la continuité du slab en profondeur et latéralement dans la partie centrale de cette région. Ils suggèrent aussi que le slab est tordu vers le sud dans la région sud, et pratiquement pas dans la région Nord. Ce nouveau modèle de zone W-B sous la région Andine peut résoudre quelques unes des controverses existantes.

**Classification chimique des roches gabbro-dioritiques sur la base des teneurs en $TiO_2$, $SiO_2$, $FeO_{tot}$, MgO, $K_2O$, Y et Zr**
L. Biermanns

Comme des classifications des roches gabbro-dioritiques des Andes contribuent aussi à la compréhension de cette chaîne de montagne, on présente quelques diagrammes géochimiques qui permettent la classification des positions géotectoniques de ces roches, dont les âges varient du Précambrien au Cénozoïque. Les mêmes positions géotectoniques des roches andésitiques et basaltiques sont cependant souvent indiquées par des teneurs en éléments différentes de celles des roches gabbro-dioritiques.

**Un modèle structural pour le développement des minéralisations Fe-Cu dans le système de failles d'Atacama (25°00'S-27°15'S), nord Chili**
C.G. Bonson, J. Grocott et A.H. Rankin

Le système de failles d'Atacama, système de décrochements senestres de la cordillère côtière du nord Chili associé à la zone de subduction, est le siège deux styles de minéralisations hydrothermales Fe-Cu, qui peuvent être associées à différentes phases tectoniques au sein de l'arc magmatique crétacé. Les minéralisations riches en magnétite sont en général localisées le long de la zone de failles N-S et apparaissent être associées au développement de l'arrière-/intra-arc néocomien aux environs de 128-106 Ma. Plus tard, après 80Ma, le système d'Atacama se marque par la propagation de failles orientées NW-SE à travers l'avant-arc. Le long de ces failles, des brèches et des veines hydrothermales à spécularite sont présentes dans les zones d'ouverture.

**Failles de socle et inversion dans le nord du Bassin de Neuquén, Argentine**
J.L.M. Booth et M.P. Coward

Dans la partie Nord du Bassin de Neuquén (Argentine occidentale), des grabens d'âge mésozoïque inférieur ont subi une tectonique d'inversion. Des anticlinaux à axe N-S se sont formés par la remontée et le plissement d'unités de socle. Des failles inverses de haute angle sont relayées par des rétrochevauchements à travers une séquence de pélites noires d'âge syn-rift (Formation Los Molles). Il existe plusieurs niveaux de décollement (marnes et gyspses) aux propriétés mécaniques différentes.

**Mise en évidence de structures compressives sur les gisements d'émeraude de la Cordillère orientale de Colombie**
Y. Branquet, B. Laumonier, B. Lopes, A. Cheilletz, G. Giuliani et F. Rueda

Les gisements d'émeraude de Muzo et Coscuez localisés sur la bordure ouest de la Cordillère Orientale de Colombie, présentent une importante tectonique en chevauchement. Plusieurs phases compressives de vergences différentes développent ces chevauchements. Les datations radiométriques sur les phases fluides associées à ces événements compressifs fournissent à ces événements un âge limite Eocène-Oligocène.

**Structures en conductivité électrique dans le Nord du Chili**
H. Brasse, F. Echternacht, M. Eisel et S. Tauber

Des études électromagnétiques dans l'arc et l'avant-arc du Nord Chili indiquent des zones étendues de forte conductivité à des profondeur approximativement de 20 -60km sous l'arc volcanique de la Cordillère occidentale. La fusion partielle est discutée comme étant l'explication la plus probable de ces anomalies, particulièrement au regard des résultats de gravimétrie et de sismologie. Cependant, sur un profil près de la ville de Pica, la zone conductive est décalée vers l'avant-arc. Ceci est corrélé avec la lacune observée dans l'activité volcanique récente.

**Superposition de structures de différents styles, bassin de Maracaïbo, Venezuela**
E. Bueno R.

Le bassin de Maracaïbo, situé entre deux chaînes andines, présente des structures superposées de plusieurs styles, survenues au cours de son histoire géologique. Localisée dans une série de grabens, la sédimentation commence au Jurassique. Au Crétacé, les dépôts continuent dans un contexte de marge passive. A l'Eocène, la collision de la plaque caraïbe est responsable d'un raccourcissement NO-SE et d'une extension NE-SO, accumulées pendant plusieurs phases synsédimentaires.

**Réexamination du magmatisme cénozoïque d'arrière-arc dans le Sud du Pérou : conséquences sur l'évolution des Andes centrales durant les 50 derniers millions d'années**
G. Carlier, J.P. Lorand, M. Bonhomme et V. Carlotto

Dans le sud du Pérou, le magmatisme cénozoïque d'arrière-arc (de 40 Ma à actuel) montre différentes suites de nature calco-alcaline, shoshonitique et alcaline potassique (basanites, phonotéphrites et trachytes à leucite) à ultrapotassique (lamproïtes à phlogopite). L'âge, la position et la nature de ce magmatisme sont mis en relation avec les déplacements, pendant le Cénozoïque, de la Cordillère Occidentale sud-péruvienne le long de l'Altiplano et de la Cordillère Orientale. Il est suggéré que ces déplacements ont induit le chevauchement, vers le NE, de la Cordillère Orientale et de l'Altiplano sur le Bouclier Brésilien.

**Les couches rouges du Groupe San Jeronimo (Cuzco-Pérou) marqueurs de l'événement tectonique Inca 1**

V. Carlotto, G. Carlier, J. Cardenas, W. Gil et R. Chavez

Les couches rouges du Groupe San Jeronimo sont considérées de l'époque fini-Crétacé, et leur origine liée à la phase tectonique Péruvienne. Néanmoins, la succession stratigraphique, les observations de terrain, les corrélations et la datation radiométrique montrent que cette unité devrait être d'âge Eocène moyen à fini-Oligocène, et que la sédimentation serait liée la phase Inca 1, qui dans cette région est considérée comme un continuum tectonique compressif, associé à des failles décrochantes permettant la formation de bassins en pull-apart.

**Chevauchements et rétrochevauchements imbriqués sur le flanc nord-occidental des Andes de Merida entre Torondoy et Valera (Venezuela)**

J.T. Castrillo et Y. Hervouet

Ce travail, utilisant l'imagerie satellitaire (Landsat TM), des données de terrain, et la modélisation informatique des structures tectoniques, montre que le flanc nord-ouest des Andes de Mérida est constitué de chevauchements à pendage sud-est et de rétrochevauchements imbriqués à pendage nord-ouest fonctionnant du Miocène au Pleistocène. Les décollements dans la couverture se situent dans le Crétacé supérieur et le Néogène. Le chevauchement du socle sur le bassin de Maracaïbo atteint 35 km environ. Il se raccorde au chevauchement intracrustal responsable du soulèvement des Andes vénézueliennes.

**Nature et âge des déformations cénozoïque intra-arc du Chili méridional**

J. Cembrano,; E. Schermer, A. Lavenu, F. Hervé, S. Barrientos, B. McClelland et G. Arancibia

La géométrie et la cinématique des zones de cisaillement crustales pré-éocène (?) à pliocène, l'agencement régional des dikes basiques, la distribution spatiale des centres volcaniques holocènes, et les quelques séismes crustaux intra-arc, suggèrent que l'arc magmatique des Andes chiliennes du sud a subi des déformations transtensives à transpressives durant l'essentiel du Cénozoïque. La combinaison épisodique de décrochements et de déplacements verticaux , bien mise en évidence dans les zones fortement déformées et dans les failles fragiles affectant l'arc magmatique, pourrait refléter différents modes et différents degrés de partitionnement du vecteur de convergence entre les plaques Farallon (Nazca) et sud-amérique pendant le Cénozoïque

**Sismologie Sociale : Projet de Gestion du Risque Sismique à Quito (Equateur)**

J.L. Chatelain, B. Guillier, H. Yepes, J. Fernandez, J. Valverde, B. Tucher, M. Souris, G. Hoefer, F. Kaneko, T. Yamada, G. Bustamante et C. Villacis

Après avoir choisi des séismes pouvant affecter la ville, les intensités sismiques produites par ces événements ont été calculées afin d'estimer les dégâts aux bâtiments et aux réseaux. L'étude scientifique a été complétée par des entretiens avec les responsables des principaux services de la ville, afin de produire un récit des événements pendant et à diverses échelles de temps après un des séismes choisis. Enfin, une série de recommandations a été élaborée, devant permettre de réduire la vulnérabilité sismique de Quito.

**La structure du piémont andin dans la région de Chos Malal (bassin de Neuquen, Argentine)**
V. Chauveau, B. Nivière, P.R. Cobbold, E.A. Rossello, J.F. Ballard et H.T. Eichenseer

Dans la région de Chos Malal, le Bassin de Neuquén est affecté d'une déformation chevauchante d'age paléocène-éocène. La tectonique tégumentaire a fait intervenir au moins trois niveaux de décollement. Dans un domaine au nord, le socle est affecté de chevauchements profonds, réactivant des failles normales d'age jurassique. Quelques failles de transfert jurassiques, de direction NE, ont été reactivées sous forme de rampes latérales. La formation du Tromen, volcan quaternaire, a modifié le schéma structural.

**La limite Altiplano-Cordillère Orientale dans la région d'Urumbamba (Cuzco-Pérou)**
R. Chavez, W. Gil, V. Carlotto, J. Cardenas et E. Jaillard

La limite Altiplano-Cordillère Orientale dans la région d'Urumbamba (Cuzco-Pérou) est caractérisée par un haut structural contrôlé par une faille décrochante où la faille à vergence NE du domaine de l'Altiplano entre en contact avec la faille à vergence SW de la Cordillère. La structure actuelle montre que la déformation andine à d'abord affecté le domaine de l'Altiplano puis la bordure SW de la cordillère orientale, principalement au cours des phases tectoniques Inca et Quechua.

**Carte néotectonique de la zone de faille d'Atacama (Chili) d'après les images RSO ERS-1**
J. Chorowicz, J.C. Vicente, P. Chotin et C. Mering

Les images provenant du radar imageur à synthèse d'ouverture (RSO) du premier satellite européen de télédétection (ERS-1) couvrent chacune une région de 100x100 km, avec une résolution de 12,5 m. La morphologie est particulièrement bien exprimée sur ces images, ce qui en fait un outil idéal pour cartographier les failles récentes ou actives. Nous avons utilisé ces données pour séparer les failles relevant de la néotectonique des failles plus anciennes, dans la zone de faille d'Atacama au nord Chili. En effet, la région a été soumise à de nombreuses déformations depuis le Trias supérieur, avec une phase majeure de compression au Crétacé moyen. Les failles exprimées sur les images radar par des traits morphologiques nets sont actives depuis le Miocène supérieur et bordent des blocs basculés inclinés vers l'ouest.

**Résultats préliminaires de recherches géoscientifiques combinées à mer et à terre le long de la marge continentale du Chili du Nord**
Cinca study group (reporter : Christian Reichert)

En été 1995, quatre institutions de recherche allemandes (BGR, GFZ, FUB et GEOMAR) ont réalisé, en collaboration avec des instituts chiliens et espagnols, le projet CINCA (Etude de la croûte au large et à terre dans la zone des Andes Centrales. Les résultats obtenus par plusieurs méthodes géophysiques sont présentés, en particulier les données de la sismique réflexion et de la réfraction marine.

**La Déformation cénozoïque à travers l'Amérique du Sud : données à échelle continentale et modèles analogiques**
P.R. Cobbold, P. Szatmari, C. Lima et E.A. Rossello

Une synthèse de données géophysiques et géologiques permet de conclure que l'Amérique du Sud a subi des déformations cénozoïques d'intensité variable, maximale au niveau des Andes, mais n'épargant pas la marge atlantique et les régions centrales du continent. Les structures cénozoïques reprennent d'anciennes failles formées lors d'orogénèses paléozoïques ou alors précambriennes. La justification mécanique de ces phénomènes est fournie par des modèles analogiques.

**Héritage tectonique et styles structuraux dans les Andes de Mérida (Vénézuela occidental)**

B. Colletta, F. Roure, B. de Toni, D. Loureiro, H. passalacqua et Y. Gou

Contrairement aux Caraïbes et aux Andes centrales, les Andes de Mérida ne sont pas directement liées aux interactions entre le craton sud-américain et les zones d'arc ou les plaques océaniques voisines, mais elles résultent simplement de réajustements intraplaque mineurs entre la Cordillère orientale au sud et la marge transformante sud-caraïbe au nord. Différentes données, en particulier des profils de sismique réflexion et de gravimétrie, montrent le caractère transpressif des Andes vénézuéliennes, et soulignent que les structures héritées contrôlent les variation du style tectonique le long de la chaîne.

**Tomographie tridimensionnelle des ondes P autour d'Antofagasta, Nord Chili : distribution des contraintes le long de la partie la plus profonde de la plaque Nazca en subduction**

D. Comte, M. Pardo, T. Monfret, G. Asch, F. Graeber et A. Rudloff

La distribution de vitesses dans le modèle 3D indique l'existence d'une zone à faible vitesse entre 30 et 40 km de profondeur et la présence d'un prisme asténosphérique qui sépare le "slab" de la racine de la Cordillère des Andes. Des contraintes extensives et compressives s'observent simultanément autour de 100 et 200 km de profondeur.

**Evolution de la subsidence dans l'Oriente Nord-Péruvien (Bassin Marañon) depuis le Crétacé**

C. Contreras, E. Jaillard et M. Paz

La subsidence tectonique du Nord-Est du Pérou se produit en trois stades. Le premier (Crétacé moyene et supérieur) correspond à une subsidence faible apparemment contrôlée par les phases compressives albienne et sénonienne. Le deuxième (Paléogène) est intermédiaire. Le troisième (Néogène) traduit une forte subsidence liée à flexion de la plaque sud-américaine sous le poids de la chaîne andine en cours de surrection par épaississement crustal.

**Le Piemont des Andes patagoniennes à la latitude du Lago Viedma (49° 30' S) : Structure et cinématique**

I. Coutand, Y. Le Dez, M. Diraison, P.R. Cobbold, D. Gapais, E.A. Rossello et M. Miller

A 49° 30' S, le piémont des Andes Patagoniennes est constitué d'une ceinture plissée et chevauchée. A l'ouest, des failles inverses de haut angle font remonter en surface un socle anté-crétacé, dont l'intrusion granitique miocène du Monte Fitzroy. A l'est, la présence de plis de croissance dans les arénites du crétacé moyen et supérieur permet de conclure à un âge précoce pour le début de la déformation. D'autres structures témoignent de la présence de décrochements dextres parallèles à la chaîne. Nous attribuons cette cinématique à la collision oblique des plaques Nazca et Amérique du Sud.

**Inversion de bassins dans les Cordillères orientales**
M.P. Coward et A. Ries

Les bassins sub-andins fournissent d'excellents exemples de la géométrie et de la cinématique de l'inversion structurale de bassins. Les données sismiques permettrent en outre de réinterpréter différents basins sub-andins en termes d'inversion tectonique. Les implications concernent la tectonique andine à l'échelle crustale, et la modélisation de l'évolution des hydrocarbures.

**La haute Cordillère et son bassin d'avant-pays (32° s, Argentine)**
E. O. Cristallini et D.J. Perez

Dans la région de San Juan, nous avons étudié la structure cénozoïque de la Haute Cordillère et ses relations avec les dépôts du bassin d'avant-pays. L'étude des produits d'érosion au sein du bassin de Manantiales a permi de contraindre l'évolution de la ceinture plissée et chevauchée de La Ramada. Ce genre d'étude est un excellent moyen de dater le soulèvement de la Cordillère.

**Le contexte tectonique pré-andin du sud-ouest de l'Amérique du sud**
L.H. Dalla Salda, M.G. Lopez de Luchi, C. Cingolani et R. Varela

Au Paléozoïque Inférieur à Moyen, le S.O. de l'Amérique du Sud a subi un cycle orogénique complet, depuis un état d'avant-collision, passant par une collision continent-continent et se terminant par un soulèvement. La collision (depuis 460 Ma et jusqu'à 440 Ma, ou alors 420 Ma) est responsable de la chaîne orogénique famatinienne, dévéloppée à l'est de la cordillère mésozoïque andine. D'ouest en est, les unités tectoniques étaient trois: le terrain éxotique d'Occidentalia, la châîne famatinienne et le craton de La Plata-Brésil-Afrique.

**Modèles thermiques et gravimétriques de subduction d'une ride en expansion**
A.J. Daniel, P. Styles, N.J. Kusznir et R.E Murdie

Une ride est en train de subducter au niveau de la fosse Chili-Pérou à la latitude de 46°S. Les données de gravimétrie sont utilisées pour contraindre les modèles gravimétriques et thermiques d'une ride en subduction. Les modèles sont en accord avec les observations pour la partie de la ride non encore subduite mais la différence est forte pour la partie subduite entre 3 et 6 Ma ce qui indique que la partie sud de l'Amérique du sud n'est pas en équilibre isostatique.

**Prévision de la fin d'une lacune sismique: le grand séisme d'Antofagasta (nord Chili) du 30 juillet 1995**
B. Delouis, T. Monfret, L. Dorbath, M. Pardo, L. Rivera, D. Comte, H. Haessler, J.P. Caminade, L. Ponce, E. Kausel et A. Cisternas

Le séisme du 30 Juillet 1995 (Mw = 8.0) et sa séquence de répliques ont pu être étudiés grâce au réseau local installé antérieurement dans la région pour suivre l'évolution sismique de la lacune existant au nord-Chili depuis le séisme de 1877. Le processus de rupture de ce séisme du 30 Juillet 1995 est précisé grâce à une modélisation des ondes de volume et une étude fine de la distribution spacio-temporelle des répliques. Les conséquences de ce grand séisme sur la réactivation probable de la lacune du séisme de 1877, située juste au nord, sont évaluées.

**Régime de contrainte extensif dans la région côtière d'Antofagasta (nord Chili)**
B. Delouis, H. Philip et L. Dorbath

Une étude néotectonique sur les failles de la région côtière d'Antofagasta a été menée pour préciser la cinématique de leurs derniers rejeux. Les failles normales d'orientation proche de Nord-Sud dominent, mais des déplacements horizontaux sont observés localement. L'amplitude relative des déplacements horizontaux par rapport aux déplacements verticaux, et leur sens (dextre ou senestre) varient de manière cohérente en fonction de l'azimuth des failles. L'ensemble des observations de terrain indique que la zone côtière, avec le système de la faille d'Atacama dans la cordillère de la côte, est soumise à un régime de contraintes extensif, avec une direction d'extension E-O.

**La ceinture orogénique atlantique du Brésil méridional: un orogène de type andin d'âge néoprotérozoïque?**
M. Demange et R. Machado

La ceinture orogénique néoprotérozoïque atlantique du Sud du Brésil présente les caractères d'un orogène de type andin: orogène à double déversement en transpression construit entièrement sur croûte continentale, et organisation spatiale et temporelle des granites. Cette ceinture pourrait être un exemple des parties profondes d'un tel orogène.

**Géochimie des basaltes arrière-arc du début du tertiaire de la région d'Aysén, Chili du Sud (44-46° S): implications géodynamiques**
A. Demant, F. Hervé, R. J. Pankhurst et M. Suarez

Les basaltes début Tertiaire, de type tholéiites continentales, affleurant dans les régions de Balmaceda et Rio Cisnes ont des caractéristiques chimiques contrastées. Ceux de Rio Cisnes présentent, sur un diagramme multi-éléments, une anomalie négative en Ta et Nb, typique de basaltes provenant d'un manteau lithosphérique enrichi, alors que ceux de Balmaceda ont un tracé qui s'apparente à celui des OIB. Ceci n'est pas sans rappeler l'évolution observée dans la province du Basin and Range où, par suite de l'étirement progressif de la lithosphère, l'influence du manteau sous-continental décroît au profit du manteau asthénosphérique.

**Des basaltes sur l'Altiplano chilien, Andes Centrales du Sud**
B. Déruelle, O. A. Figueroa et S. Moorbath

Six basaltes ($SiO_2$<53 %) échantillonnés sur l'Altiplano chilien le long du linéament Calama-El Toro contiennent des phénocristaux de chromite. Ils sont plus riches en MgO, Ni, Cr et ont des rapports $^{87}Sr/^{86}Sr$ (ª0.706) plus élevés que les basaltes des Andes Méridionales. Leur genèse à partir d'un manteau lithosphérique est envisagée.

**Instabilité tectonique liée au développement du bassin paléozoïque de l'avant-pays des Andes Centrales boliviennes**
E. Diaz, R Limachi, V. Goitia, D. Sarmiento, O. Arispe et R. Montesinos

Le cycle Cordillerin de Bolivie (Silurien-Carbonifère inférieur) correspond au remplissage d'un bassin d'avant-pays adjacent à un système de chevauchements à l'ouest et au sud du bassin et lié à une subduction oblique à vergence est. L'empilement tectonique au front de déformation était une cause probable de la forte subsidence, de l'apport de sédiment et de l'instabilité tectonique qui ont facilité le transport des sédiments par courants gravitaires ainsi que le développement de reliefs entraînant des glaciations locales.

**Cinématique tertiaire des Andes australes et du bassin de Magellan (Patagonie)**
M. Diraison, P.R. Cobbold, D. Gapais et E.A. Rossello

De la Cordillère Patagonienne (de direction N-S), jusqu'à la Cordillère de Darwin ( de direction E-O), les Andes Australes forment un grand arc qui résulte des interactions entre les plaques Sud-américaine, Antarctique, Nazca et Scotia. Cette arc constitue à l'Ouest et au Sud la limite du Bassin de Magellan. D'après l'étude d'images satellitaires, nos observations de terrain, l'analyse cinématique de populations de failles et la modélisation analogique, la déformation dans les Andes Australes est caractérisée par un raccourcissement sub-orthogonal au front de la chaîne; par des décrochements (1) dextre le long de la Cordillère Patagonienne (2) sénestre le long de la Cordillère de Darwin; et par un étirement horizontal parallèle à la chaîne accommodé par un ensemble de grabens.

**Décrochevauchements dextres cénozoïques dans la région de Bariloche, Andes patagoniennes**
M. Diraison, P.R. Cobbold, E.A. Rossello et A.J. Amos

Dans le NW de la Patagonie, la Cordillère des Andes est formée de différentes unités morpho-structurales dont l'évolution résulte de la subduction de la plaque Nazca le long de la fosse du Chili. La Cordillère Principale et le domaine Sub-Andin entre 40 et 42°S sont orientés parallèlement à cette limite de plaques. L'étude d'un Modèle Numérique de Terrain et de sa surperposition avec des cartes géologiques, les données de terrain et l'analyse cinématique de populations de failles ont permis de mettre en évidence le caractère transpressif qui affecte cette région. Les chevauchements purs majeurs sont orientés NW-SE, ceux à forte composante décrochante dextre sont orientés N-S et leurs conjugués sénestres sont orientés E-W.

**Forme et continuité de la partie asismique de la plaque de Nazca dans le coude d'Arica par Tomographie télésismique**
C. Dorbath et le groupe Lithoscope Andes

Le long de la subduction Pérou-Chili, la subduction de la plaque de Nazca sous l'Amérique du Sud est bien soulignée par le plan de Wadati-Benioff. Dans les Andes Centrales, la sismicité définit une plaque modérément pentée jusqu'à une profondeur d'environ 325 km. L'observation de quelques séismes entre 550 et 650 km de profondeur après un silence sismique complet pose la question de la continuité de la plaque. Pour y répondre, nous avons effectué une tomographie télésismique du manteau à 20° S. L'image obtenue prouve clairement la continuité de la plaque subduite jusqu'au manteau inférieur, et nous permet de cartographier sa déformation dans le coude d'Arica.

**Néotectonique de la région côtière d'Equateur : un nouveau projet de recherche pluridisciplinaire**
J.F. Dumont, S. Benitez, L. Ortlieb, A. Lavenu, B. Guillier, A. Alvarado, C. Martinez, C. Jouannic, G. Toala, J. Vivanco et J.T. Poli

Le bloc côtier équatorien se trouve en position de ride et de bassin avant-arc entre la zone de subduction de la plaque Nazca à l'ouest et la Cordillère Andine à l'est. Un mouvement latéral vers le nord conduisant à l'ouverture du Golfe de Guayaquil se superpose aux déformations verticales. Diverses méthodes de néotectonique seront mises en jeu (télédétection, terrasses marines (plio)-quaternaires, microtectonique, morphologie fluviale et MNT) afin d'obtenir une vue synthétique de la géodynamique récente de ce bloc.

**Etude paléomagnétique sur le Nord du Chili : mise en évidence de rotations horaires dans les formations mésozoïques et tertiaires**

G. Dupont-Nivet, P. Roperch, P. Gautier, A. Chauvin, M. Gérard et G. Carlier

Un échantillonnage paléomagnétique détaillé (100 sites) de la marge nord-Chilienne entre 22 et 26°S montre des rotations horaires variables pouvant atteindre 60° localement. Ces rotations ne sont pas limitées à l'arc mésozoïque mais sont aussi enregistrées par les formations paléogènes. Notre étude montre l'importance des rotations dans les processus tectoniques au cours du Tertiaire.

**Le Licancabur, un volcan andésitique dans le Sud des Andes Centrales**

O. Figueroa et B. Deruelle

Le volcan Licancabur est un cône presque parfait, essentiellement constitué de coulées d'andésites à pnénocristaux de plagioclase (An 78-52), clionopyroxène, orthopyroxène (En 78) et Ti-magnétite, rarement d'olivine, Mg-hornblende et ilménite. Les laves du cône seraient issues du mélange entre, d'une part, les magmas ayant engendré les coulées anciennes et, d'autrre part, l'unique dacite reconnue.

**Magmatisme alcalin d'âge Oligocène supérieur-Miocène inférieur dans Altiplano Central de Bolivie**

M. Fornari, F. Espinoza, E. Baldellon et P. Soler

Les laves Oligocène supérieur à Miocène inférieur de la Formation Tambillo affleurent suivant une bande NNW-SSE de plus de 80 km le long de la bordure NE du Salar de Uyuni. Ces laves basaltiques à andésitiques, mises en place sous forme de sills, dykes et coulées sont d'affinité alcaline ; elles dérivent d'un magma produit par fusion à taux modéré de manteau de type lherzolite à grenat et d'une évolution plus superficielle par cristallisation fractionnée. Ces laves, ainsi que les affleurements de même nature identifiés en Bolivie, semblent dériver du manteau sous-continental en condition tectonique de transtension et posent le problème de leur signification dans le contexte de la subduction de la marge active occidentale.

**Contrôle tectonique et climatique sur l'évolution géomorphologique de la marge chilienne entre 36 et 38°S**

U. Fracassi

Le contexte tectonique le long de la côte chilienne entre 36° et 38° S est marqué par un système de failles N-S qui contrôle le graben d'Arauco. Les linéations et les failles sont orientées NE-SW et deplacent le bord ouest du graben. L'expression du vent dominant, dirigé du SW vers le NE, se voit dans les formes d'érosion et dans la géométrie du réseau de drainage.

**Le bord occidental de l'Altiplano de Belen (Chili du nord): un exemple d'évolution en avant-arc au Cénozoïque**

M. Garcia, G. Hérail et R. Charrier

Les dépôts cénozoiques les plus anciens ( avant 23 Ma et jusqu'à 18 Ma) reposent en discordance sur le Complexe Métamorphique de Belen d'âge Précambrien à Paléozoïque inférieur et sur des sédiments du Jurassique. Ils ont été mis en place en régime extensif, probablement dans un environnement de caldeira, puis ont été déformés en compression à partir de 18 Ma. Deux lames chevauchantes à vergence ouest se sont mises en place successivement. La plus ancienne, à l'est entre 18 Ma et 12 Ma, la plus récente à l'ouest après 11 Ma et avant 4 - 5 Ma.

**Minéralogie et géochimie des roches halitiques du Salar Grande (I Région de Tarapacá, Chile). Implications génétiques**
J. Garcia-Veigas, G. Chong et J.J. Pueyo

Le Salar Grande est le seul bassin évaporitique cénozoïque localisé dans la Cordillère Côtière au N du Chili. Il est placé dans une dépression tectonique de plus de 50 km de long et de direction N-S, qui est contrôlée par la faille d'Atacama. La dépression est remplie d'une roche halitique, très pure, dont l'épaisseur dépasse localement 100 mètres. La texture de la halite permet de distinguer deux unités: la halite litée inférieure, qui présente des cycles centimétriques avec des structures en chevron, et la halite massive supérieure, avec des cristaux plus grossiers, générés par un processus de croissance interstitielle. Un autre type de halite, avec des cristaux de grande taille (parfois métrique), remplit les cavités de dissolution de la halite plus ancienne. A partir des observations des textures halitiques, de la distribution des minéraux accessoires, de la distribution et des rapports des traces métalliques, et de la composition des saumures piégées dans les inclusions fluides, on peut reconstituer les détails de l'évolution sédimentaire et diagénétique du salar, et obtenir indirectement des informations paléogéographiques et paléoclimatiques.

**Le projet de recherche interdisciplinaire "Processus de déformation dans les Andes"**
P. Giese

Un groupe de recherche interdisciplinaire "Processus de déformation dans les Andes" a été constitué entre les instituts de géosciences de Berlin et Potsdam. Le segment des Andes centrales entre 20 et 25°S a été choisi parce que les processus de déformation y sont très bien développés.

**La nature de la sismicité intermédiaire dans les Andes Centrales**
P. Giese et G. Asch

La structure thermique d'une plaque en subduction révèle deux zones de gradient de températures. Tandis que la transformation basalte-éclogite se déroule dans la zone supérieure, la transformation de l'enstatite a lieu dans la zone inférieure. Ces deux processus sont associés à l'émission d'énergie sismique à une profondeur de 70 à 200 kilomètres.

**Un continuum tectonique au cours du Crétacé-Paléocène dans les Andes du bassin d'avant-pays Péruvien (Bassin du Maranon)**
W. Gil, P. Baby et M. Paz

Le bassin du Maranon, localisé dans le NE du Pérou, montre des inversions tectoniques de l'Aptien jusqu'au Paléocène. Il est possible de déterminer que ces inversions se distribuent de manière hétérogène dans tout le bassin. Une deuxième période d'inversions tectoniques apparaît à la fin du Tertiaire. Les interprétations montrent que durant le Crétacé-Paléocène la tectonique se manifeste de manière continue.

**Le rôle de la matière organique dans les systèmes hydrothermaux de haute température**
G. Giuliani, A. Cheilletz, C. France-Lanord et F. Rueda

L'étude des gisements d'émeraude de Colombie qui sont encaissés dans les schistes noirs riches en matière organique du Crétacé inférieur de la Cordillère orientale, nous a permis de préciser le rôle joué par la matière organique dans un système hydrothermal à haute températue (300° C). Elle permet le développement de réactions de thermoréduction de sulfates (TRS) qui provoquent la précipitation de pyrite, carbonate et bitume hydrothermaux.

**L'arc volcanique du Miocène moyen (Chili central): données sismiques et gravimétriques en faveur d'un épaississement tectonique**
E. Godoy, G. Yañez et E. Vera

Au Sud des 33° 45', l'arc volcanique du Miocène Moyen à Supérieur (Formation Farellones) est décollé à 2,5 km de profondeur sur sa base méso-cénozoïque. Sa limite occidentale correspond à une zone trianglulaire, entre chevauchement et rétrochevauchement.

**Résultats paléomagnétiques préliminaires sur le volcan pleistocène Villarica et la formation miocène de Farellones**
A. Goguitchaichvili, A. Chauvin, P. Roperch, M. Vergara et H. Moreno

Une étude paléomagnétique a été entreprise sur les coulées pleistocènes du volcan Villarica (21 sites) et sur la formation miocène de Farellones (31 sites). Sur la formation de Farellones deux renversements de polarité ont été enregistrés et les premiers résultats suggèrent une rotation horaire de 10 à 20° de la séquence depuis environ 17 Ma.

**Evolution géologique et pétrolière dans le Bloc Olleros, Système Santa Barbara, Salta, Argentine**
R. Gomez Omil et L.M. Albarino

Nous présentons l'évolution sédimentaire paléozoïque, crétacé et tertiaire, ainsi que l'histoire tectonique polyphasée, impliquant des chevauchements "thin-skinned et thick-skinned, du système de Santa Barbara dans la région de Salta. Le système pétrolier de cette région depuis le Crétacé supérieur jusqu'à l'actuel est également analysé.

**Contraintes chimiques sur le magmatisme mafique associé à une fenêtre asthénosphérique au Néogène dans le sud de la Patagonie**
M.A. Gorring, S.M. Kay et V.A. Ramos

Les larges coulées du plateau de Patagonie datant du Néogène (de 46,5° à 49,5°S) sont reliées à l'ouverture progressive de fenêtres asthénosphériques associées à des collisions de segments de la ride du Chili il y a 12 et 6 Ma. Les variations temporelles et spatiales en éléments traces, les volumes de magma extraits, et les rapports Sr-Nd-Pb sont cohérents avec un modèle dans lequel des taux de fusion variables sont produits par écoulement vers le haut à partir d'un manteau asthénosphérique de type OIB et à travers une fenêtre migrant vers le nord-est. Un manteau asthénosphérique anormalement chaud et (ou) ayant contenu des produits volatiles qui ont abaissé son point de fusion, permettrait d'expliquer les volumes de magmas, ainsi que les forts taux de fusion partielle.

**Champ de gravité et géoïde le long de la marge active sud-américaine (20° à 29°S)**
H.J. Götze, S. Schmidt, A. Kirchner, M. Kösters, M. Araneda et N.G. Lopez

De 1993 à 1995, le groupe international MIGRA constitué de participants du Chili, d'Argentine et d'Allemagne ont relevé environ 2000 nouvelles mesures gravimétriques le long d'un géotraverse des Andes couvrant le nord du Chili et le nord-ouest de l'Argentine entre 64°-71° ouest et 20°-29° sud. La base de données comprenant les coordonnées des stations, des grilles de données de 10x10 km de l'anomalie à l'air libre, de différents types d'anomalies de Bouguer ainsi que l'anomalie isostatique résiduelle sont ici représentés dans une carte du champ isostatique résiduel, avec une interprétation sommaire.

**Un modèle 3D des vitesses sismiques sous le Chili du Nord à partir de la tomographie de tremblements de terre locaux**
F.M. Graeber et G. Asch

Les durées de propagation d'ondes obtenues avec l'expérience sismologique PISCO'94 ont été inversées pour modéliser la structure 3D des vitesses de propagation dans la croûte et le manteau supérieur sous le Chili du Nord. La méthode est basée sur la technique "damped least squares". Dans le modèle calculé, deux des anomalies sismiques les plus importantes sont situées sous la Cordillère ouest et le long de la zone Wadati-Benioff.

**Mise en place des complexes plutoniques, déformation et partitionnement de la déformation dans la cordillère de la côte (25-27°S) Nord Chili**
J. Grocott et J. Wilson

Les mécanismes de mise en place des complexes plutoniques de la cordillère de la côte du Nord Chili sont réexaminées. La plupart des plutons se sont mis en place progressivement soit à la limite de zone de failles en extension ou transtensives, soit comme des lames avec des pressions de magma supérieures à la contrainte régionale perpendiculaire à la direction d'intrusion. L'anisotropie de susceptibilité magnétique du complexe plutonique Las Tazas du Crétacé inférieur montre cependant que certains plutons se sont localement mis en place en contexte transpressif.

**Microzonage et risque sismique à Quito, Equateur: résultats préliminaires**
P. Gueguen, J.L. Chatelain, B. Guillier, H. Yepes et J. Valverde

A la suite du projet de gestion du risque sismique à Quito, une opération de microzonage de la ville a été entreprise. A l'aide d'une station mobile, les microtremors sont enregistrés sur environ 400 sites. Sur chaque site, la fréquence de résonnance et l'amplitude potentielle relative sont obtenues en utilisant la technique de Nakamura. Nous présenterons des cartes isoamplitudes et isoperiodes. Celles-ci sont comparées avec le contenu spectral de séismes enregistrés à Quito afin d'évaluer l'aléa sismique de la ville. Finalement le risque sismique est évalué en croisant, à l'aide d'un SIG, ces données avec celles de la distribution du bâti.

**Expérience lithoscope dans le Nord de l'Equateur: résultats préliminaires**
B. Guillier, J.L. Chatelain, A. Alvarado, H. Yepes, G. Poupinet et J.F. Fels

La distribution spatiale de la sismicité obtenue à l'aide de 54 stations Lithoscope et 27 stations permanente révèle 3 lacunes de sismicité : une superficielle dans la plaque supérieure et deux à des profondeurs intermédiaires dans la plaque plongeante. L'étude plus détaillée de ces observations sera présentée, complétée par une cinquantaine de mécanismes au foyer.

**Conséquences de la subduction d'une dorsale active: sources magmatiques multiples dans la région de la Péninsule de Taitao (46-47°S, Point triple du Chili)**
C. Guivel, Y. Lagabrielle, J. Bourgois, R. Maury, H. Martin, N. Arnaud et J. Cotten

Pendant le Pliocène, la subduction de la ride du Chili sous la marge de l'Amérique du Sud s'accompagnait, dans la région de la Péninsule de Taitao, de la mise en place de suites intrusives et effusives. Parmi les produits magmatiques émis, on distingue quatre catégories liées à la subduction de la ride: (1) des laves provenant directement de la dorsale en subduction (MORB), (2) des MORB plus ou moins contaminés par la croûte continentale, (3) des plutons et laves intermédiaires à acides provenant de la fusion du coin de manteau (calco-alcalin), et (4) des plutons à "tendance adakitique" (contribution de la fusion de la croûte océanique subduite associée à celle du coin de manteau).

**Les zones de failles sismiquement actives à la bordure continentale des Andes centrales**
V. Hanus, J. Vanek et A. Spicak

Treize zones de failles sismiquement actives sont reconnues le long de la marge continentale sud-américaine entre 22°-35°S et 63°-72°W. On peut distinguer trois types de zones en fonction de leur orientation par rapport à la marge du Pérou-Chili: les zones parallèles à la fosse, les zones perpendiculaires à la fosse et les zones orientées à 45° de la direction de subduction. Leur fonction tectonique est discutée.

**Evolution Tectono-stratigraphique cénozoique de l'avant-pays andin du Nord Chili**
A.J. Hartley, G. May, S.J. Kape, P. Turner et G. Chong

La comparaison des séquences sédimentaires de la Cordillère de la Côte de la dépression Centrale, Précordillère et dépression pré-andine de l'avant-arc Chilien permet de contraindre l'évolution tectono-stratigraphique de cette région au Cénozoïque. Pendant cette période, la zone d'étude a connu des épisodes d'intense déformation compressive à transpressive, interrompus par des phases de subsidence contrôlées par des failles transtensives et générées par effondrement crustal.

**Structure de la Cordillère Andine d'Argentine entre 30°30' et 31°S**
N. Heredia, L.R. Rodriguez Fernandez et D. Ragona

Dans la Cordillère Andine d'Argentine, entre 30°30' et 31°S, deux groupes tectonostratigraphiques peuvent être définis: un socle paléozoïque avec une structure de type thin-skinned, et une couverture andine avec des structures d'extension inversées au cours d'événements compressifs tertiaires.

**Le batholite nord-patagonien (Aysen, Chili): âge et pressions de cristallisation d'après la teneur en Al des hornblendes**
F. Hervé, R. Pankhurst, A. Demant et E. Ramirez

Les pressions de cristallisation, obtenues d'après la teneur en aluminium des hronblendes, permettent d'établir des taux de soulèvement et d'érosion. Dans le batholithe nord-patagonien, ces taux sont nettement plus élevés (0.85 - 3.11 mm/an) pour les plutons miocènes de la partie centrale, où se trouvent les reliefs les plus hauts, qu'ils ne le sont pour les marges (0.08 - 0.17 mm/an). Le climat humide aurait permis des taux de soulèvement et d'érosion très importants. En revanche, les Andes du Chili central, plus hautes mais plus sèches, se sont érodées moins vite (0.15 - 0.26 mm/an).

**Sismicite holocène et activité de la faille de Quito (Equateur) : un enregistrement paléosismique dans des sédiments lacustres**
C. Hibsch, A. Alvarado, H. Yepes, M. Sébrier et V.H. Pérez

L'analyse des sédiments lacustres holocènes de Quito a permis de mettre en évidence plusieurs niveaux perturbés par des chocs sismiques. Une échelle d'attribution d'intensités sismiques est proposée d'après l'épaisseur du niveau déformé, en tenant compte d'exemples publiés, des courbes accélération/intensité et des 460 ans de sismicité historique. La paléosismicité ainsi définie complète l'enregistrement historique et met en évidence la possible présence d'un événement supérieur d'un degré d'intensité aux maximales historiques entre le 10ème et le 16ème siècle. Cet événement est corrélé avec des déformations sismotectoniques dans le bassin et désigne la faille de Quito comme la source probable du séisme.

**Déformation oligo-miocene et développement de bassins Piggyback dans la cordillère orientale du sud de la Bolivie**
B. Horton

Des dépôts alluviaux d'age Oligocène supérieur à Miocène du sud de la Bolivie enregistrent le développement et la propagation de plis et de failles dans une zone de chevauchements à vergence est. Les discordances dans les formations Tupiza et Oploca caractérisent cette déformation hors séquence.

**Traces de fission et stratigraphie néogène des bassins d'Equateur méridional: implications tectoniques**
D. Hungerbuehler, M. Steinmann, W. Winkler et D. Seward

Plusieurs bassins de la zone interandine de l'Equateur sont remplis par des sédiments volcanoclastiques, alluviaux et lacustres. Des datations par traces de fission sur zircon démontrent que la sédimentation dans les bassins s'est produite pendant des périodes relativement brèves au cours du Miocène moyen et supérieur. La majorité des formations sédimentaires a subi une déformation post-sédimentaire aux environs de 8 Ma, sous un régime compressif orienté est-ouest. Les faciès marins à saumâtre de la base de certains remplissages indiquent que ces bassins avoisinaient le niveau de la mer durant le Miocène moyen.

**CINCA 95: Sismologie passive sur et au large de la marge du Nord Chili**
S. Husen, G. Asch, M. Baumbach, C. Haberland, A. Rietbrook, A. Rudloff et K. Wylegalla

La sismicité naturelle a été observée au cours des mois d'août à octobre 1995 dans la région située au nord d'Antofagasta. Le réseau consiste de 35 stations à terre et de 9 OBS à prooximité de la côte. La sismicité qui a suivi grand tremblement de terre d'Antofagasta est extrêmement forte. Un catalogue contenant 4500 événements enregistrés sur CDROM et les temps de propagation seront utilisés pour une étude de tomographie locale détaillée.

**Les Andes d'Argentine-Chili: épaisseur crustale, isostasie, raccourcissement et détermination d'anomalies à partir d'études gravimétriques**
A. Introcaso, M.C. Pacino et F. Guspi

Nous présentons les résultats d'une étude de 14 sections E-W à travers les Andes d'Argentine et du Chili. Les anomalies gravimétriques, les modèles de croûte et les quantités de raccourcissement ont été établis pour chaque section. Une bonne corrélation est observée entre les anomalies de Bouguer et les masses; les racines calculées par inversion de ces anomalies correspondent à des racines isostatiques.

**Les couches rouges Crétacé terminal-Paléogène du Pérou, et les déformations andines précoces**
J. Jacay, E. Jaillard et R. Marocco

Dans les Andes du centre et du nord du Pérou, la sédimentation marine prend fin entre le Coniacien supérieur et le Campanien moyen, en raison de la tectonique compressive sénonienne qui affecte les régions côtières. Elle est suivie par le dépôt de couches rouges du Crétacé terminal, puis par une importante lacune qui indiquerait un soulèvement au cours du Paléocène. Des dépôts grossiers discordants témoignent de la phase tectonique compressive du Paléocène terminal-Eocène inférieur.

**Modèle sédimentaire pour le Bassin oriente d'Equateur au Crétacé**
E. Jaillard

La très faible énergie de dépôt des sédiments marins crétacés du bassin oriental équatorien s'explique par sa position d'arrière-arc distal, sa localisation sur le bord occidental d'un continent, sa très faible pente et la présence de barrières topographiques. Dans ce contexte, le climat équatorial chaud et humide a probablement induit une stratification thermo-haline du bassin, favorisant l'anoxie des dépôts. La très faible subsidence enregistrée par le bassin explique la nature des séquences sédimentaires, essentiellement contrôlées par la création d'espace disponible.

**Stratigraphie de la partie ouest du Bassin de Celica (Sud-Ouest Equateur)**
E. Jaillard, P. Bengtson, L. Bulot, A. Dhont, G. Laubacher et E. Robert

D'après de nouvelles données stratigraphiques, le "bassin de Celica" s'est formé vers la limite Albien moyen-supérieur, s'est rempli de turbidites jusqu'au Coniacien (?), puis a été déformé et a émergé au cours du Sénonien. Un nouveau bassin d'avant-arc, oblique et discordant sur le "bassin de Celica" s'est ensuite formé au Campanien (moyen?) et a fonctionné jusqu'au Maestrichtien ou Paléocène.

**Téphrostratigraphie et paléoenvironnement tardiglaciaire et holocène enregistrés dans la Laguna Salinas, Pérou méridional**
E. Juvigné, J.C. Thouret, A. Gourgaud et K. Graf

La Laguna Salinas (département d'Arequipa) est une dépression fermée d'origine volcano-tectonique, qui constitue un piège sédimentaire et un salar. Un sondage de reconnaissance a traversé les formations lacustro-palustres supérieures jusqu'à un niveau de matériau grossier non identifié. La séquence prélevée couvre les quinze derniers millénaires et regroupe sept téphras. La recherche pluridisciplinaire réalisée concerne la sédimentation, la corrélation et la géochimie des téphras, le diagramme de pollen, les diatomées, ainsi que 4 datations $C^{14}$.

**Basaltes mantelliques des Andes centrales et enrichissement du manteau au Néogène sous le plateau de la Puna**
S.M. Kay, C. Mpodozis et B. Coira

La comparaison des plus primitives des laves d'âges Oligocène et Pléistocène des Andes Centrales ($SiO2 <$ 53.5 %, $MgO > 9$ %, FeO/MgO Ÿ 0.8, $Cr > 500$ ppm, $Ni > 150$ ppm), indique que le manteau sous le plateau de la Puna a été enrichi par des processus de subduction depuis le début du récent cycle Andin, il y a 25 millions d'années. Les magmas du Pléistocène ont été mélangés avec des pôles de magma siliceux (Ÿ

20 %) au cours de leur rapide remontée à travers des zones de faille dans le sud de la zone volcanique centrale (CVZ), pour jaillir en surface à des altitudes atteignant ou dépassant 5 000 mètres.

**Structure de la précordillère argentine au Cambro-Ordovicien: arguments pour un transfert de Cuyania de la Laurentia vers le Gondwana**
M. Keller

Dans la Précordillère d'Argentine occidentale, la séquence carbonatée d'age cambrien inférieur à ordovicien inférieur est typique d'un marge passive, alors que les sédiments silicoclastiques d'age ordovicien moyen et supérieur sont d'épaisseur et de composition variables. Ces derniers ont été déposés dans un contexte tectonique d'extension qui évoque le début de leur séparation de la Laurentia.

**Composition et conditions PT du coin de manteau supérieur sous-andin: reconstruction à partir des xénolithes mantelliques des Andes du sud (50°S)**
R. Kilian

Les compositions chimiques des xénolithes mantelliques dérivés du "coin" de manteau supérieur sous les Andes du Sud (50°) ont été déterminées à l'aide de l'XRF et de l'ICP-MS. Les minéraux ont été analysés à la microsonde électronique et les résultats des calculs des conditions PT donnent: 0.7 à 2.1 GPa pour la pression et 900-140°C pour la température. Les harzburgites appauvries prédominent (20-25% de liquide extrait d´un manteau N-MORB) et ont été contaminées par des fluides de la plaque Antarctique subduite. Différents types d´infiltration auparavant appauvries produisent des lherzolites et des webstérites à olivine.

**Un modèle 3-D pour les Andes centrales basé sur l'interprétation sismique et gravimétrique**
A. Kirchner, H.J. Götze, K. Lessel et M. Schmitz

Nous présentons ici les résultats d'investigations gravimétriques et sismiques dans les Andes Centrales du sud (20°-28°S) effectuées durant les années 80 et le début des années 90. Les structures grossières de la croûte peuvent être déterminées de manière à couvrir les unités morphostructurales principales des Andes entre 21° et 25° sud. Les investigations gravimétriques et sismiques ont été centrées sur les structures de l'arc et de l'avant-arc afin de fournir une connaissance plus détaillée de la structure de la croûte dans cette région.

**Segmentation longitudinale du bassin d'avant-pays andin**
J. Kley, C.R. Monaldi et J.A. Salfity

La déformation d'avant-pays le long du front est des Andes est de trois types: plissements et chevauchements de type "thin-skinned", chevauchements de type "thick-skinned", et chevauchements d'avant-pays du type de celui des Sierras Pampeanas. A l'échelle de l'orogène, un contrôle du développement des différents styles structuraux par des discontinuités préexistantes, stratigraphiques ou structurales, est plus net qu'un lien direct avec la géométrie de la subduction de la plaque Nazca.

**Le champ de gravité de la transition continent-océan à l'Ouest de la marge continentale sud américaine**

M. Köster, J. Fritsch, S. Schmidt, H.J. Götze et M. Araneda C.

Dans le cadre du projet de recherche interdisciplinaire CINCA (Crustal Investigations Off- and Onshore Nazca/Central Andes), les levés gravimétriques du groupe international MIGRA avec des participants du Chili, d'Argentine et d'Allemagne ont été étendus à l'Océan Pacifique. En été 1995, MIGRA a pris part à l'essai offshore SO-104, entre 20°S et 24°S, du projet CINCA appartenant au navire de recherche allemand "Sonne". Les données gravimétriques offshore ont été connectées aux levés gravimétriques sur terre afin d'obtenir une représentation gravimétrique complète de la transition océan-continent.

**Coupe équilibrée régionale des Andes patagoniennes en Terre de Feu (Argentine et Chili)**

P.E. Kraemer

Nous avons construit une coupe équilibrée régionale des Andes patagoniennes par la méthode des plis sur rampe ("fault-bend folds"). Cette coupe permet de mieux relier les structures cénozoïques de la chaîne plissée au dôme métamorphique ("core complex") de la Cordillère de Darwin.

**Contraintes géochimiques sur la structure crustale à partir des roches volcaniques néogènes de la région du Salar d'Antofalla et de la Cordillère andine adjacente (24-26°S, 67-69°S)**

B. Kraemer, R. Wittenbrink, K. Hahne et H. Gerstenberger

Les données isotopiques Sr, Nd et Pb des roches volcaniques miocènes à récentes de la région du Salar d'Antofalla et de la Cordillère andine adjacente (sud Puna, NW Argentin) montrent une zonation entre ces deux régions. Ceci est attribué à des variations de composition du socle précambrien sous-jacent, et n'est pas dû à différents types de socles sous des terrains allochtones possiblement accrétés entre ces deux régions.

**Evolution géochimique des séries volcaniques jurassiques et triasiques du nord du Chili entre 20° et 26°30' de latitude sud**

W. Kramer et R. Ehrlichmann

Les séries volcaniques de la chaîne côtière, qui comprennent des reliques de l'arc magmatique jurassique et des témoins de grabens extensifs d'age triasique, ainsi que les volcanites de la précordillère, ont été caractérisées par les données géochimiques, en particulier les terres rares. Les séries se composent d'une part d'andésites basaltiques, de basaltes, de trachyandésites, de dacites et de rhyolites (ignimbrites) montrant une signature d'arc volcanique, et d'autre part de basaltes alcalins à olivine, d'affinité de type manteau asthénosphérique. La comparaison avec les résultats de l'analyse lithostratigraphique permet de corréler dans le temps les évolutions des tendances géochimiques au processus de subduction.

**L'arc jurassique-crétacé inférieur de la Cordillère de la côte près de Taltal (Chili): un assemblage de blocs crustaux**

D. Kurth, E. Schreuber et K.J. Reutter

Au sud de Taltal, la Cordillère de la Côte est séparée en deux blocs par le Système de Failles d'Atacama: à l'ouest, le bloc Cifuncho est composé de trois sous-blocs, limités par des failles, et constitués respectivement de sédiments paléozoïques, de sédiments triassiques à jurassiques, et de volcanites d'arc d'âge jurassique; à l'est, le bloc Pingo est constitué de roches paléozoïques surmontées par des volcanites du Crétacé inférieur. Cet assemblage de blocs est attribué à la subduction oblique.

**Déformation fragile dans la région d'Arc et d'anvant-Arc en régime transpressif dans le Crétacé inférieur, Cordillère côtière (26°-27° S) : réinterprétation microtectonique**

L. Lara, S. Gelcich, J. Carrasco et A. Diaz

L'inversion des données microtectoniques existant sur les failles mésoscopiques associées aux principaux linéaments du système de failles d'Atacama et de la région occidentale permet de définir deux domaines de déformation. Dans la région d'arc, cisaillement simple et cisaillement pur sont combinés, alors que dans la région d'avant-arc la déformation s'apparente à du cisallement pur associé a des rotations rigides. Cette géométrie, ainsi que la cinématique associée, permettent de décrire la déformation de ces domaines comme essentiellement liée à du cisaillement pur associé à la convergence oblique (> 20°) de la plaque Phoenix-Farallon réactivée avec l'ouverture de la dorsale de l'Atlantique, aux environs de 115 Ma à cette latitude.

**Apport de l'imagerie Landsat pour cartographier deux formations volcaniques tertiaires au SW de Cuenca (Andes occidentales d'Equateur)**

G. Laubacher et A. Legeley-Padovi

Dans la présente étude, l'utilisation de l'imagerie Landsat TM a permis d'individualiser et de délimiter l'extension de deux formations volcaniques récentes : la formation Pedernales d'âge Pliocène à Pleistocène probable et le volcanisme Quimsacocha qui surmonte la précédente formation et dont l'âge et quelque peu plus récent. Pour ce faire, nous avons utilisé les techniques de traitement d'images classiques : compositions colorées, classifications non dirigées, analyse en composantes principales. Les traitements de Morphologie Mathématique nous ont permis ici de produire, à partir des données physiques, une cartographie satisfaisante sans intervention manuelle que nous avons précisée à l'aide de données de terrain.

**Etat de contrainte néogène à quaternaire dans la dépression centrale et le long de la zone de faille Liquiñe-Ofqui (Chili central)**

A. Lavenu, J. Cembrano, F. Hervé, G. Arancibia, G. Vargas, I. Garrido, S. Barrientos et T. Monfret

L'étude néotectonique des Andes du Chili central (dépression centrale et zone de faille Liquiñe-Ofqui) montre un champ de contrainte avec $s_{Hmax}$ (s1) ± EW au Miocène supérieur-Pliocène (entre 10 et 3 Ma), sub-parallèle à la direction de convergence des plaques Nazca et Amérique du Sud. Le régime tectonique est transpressif à compressif. A partir de 3 Ma, $s_{Hmax}$ (s1) devient ±NS en régime tectonique transpressif à transtensif.

**Le volcanisme potassique néogène d'arrière-arc de l'Altiplano bolivien: une histoire pétrogénétique complexe**

P. Legros, P. Soler, A. Demant, C. Coulon et M. Fornari

Le volcanisme potassique néogène d'arrière-arc de l'Altiplano Bolivien, mis en place sur une croûte continentale surépaissie, présente des associations minéralogiques en déséquilibre et des xénolites de natures crustale et mantellique témoignant de l'intervention de processus complexes au cours de son histoire pétrogénétique : assimilation crustale au niveau de la croûte inférieure (confirmée par les données isotopiques) et mélange magmatique entre un pôle basique et un pôle plus acide dans des réservoirs crustaux peu profonds.

**Croûte profonde anormale sous les régions d'arc et d'avant-arc des Andes centrales (21°-23° S)**
K. Lessel, M. Schmitz et P. Giese

En continuation des projets précédents, le SFB 267 a réalisé des investigations de sismique de réfraction dans les régions d'avant-arc et d'arc en 1994 et 1995. La croûte continentale inférieure s'étend jusqu'à 45-50 km et le dessus de la plaque Nazca se trouve entre 70 et 80 km de profondeur. Entre la base de la croûte et la plaque plongeante, on observe une alternance de couches à grande et faible vitesse. Celles-ci impliquent une interprétation complexe de la croûte profonde.

**Les bassins transportés de la zone sub-andine (Bolivie): comparaison avec les résultats de modélisations numériques et analogiques**
P. Leturmy, J.L. Mugnier, P. Vinour, P. Baby et B. Colletta

Les bassins transportés de la zone sub-andine de Bolivie sont caractérisés par des phénomènes tectoniques, sédimentaires et érosifs qui agissent simultanément. Pour étudier l'interaction entre ces phénomènes et mieux comprendre l'évolution géodynamique de la zone sub-andine, des modélisations ont été réalisées. Des expériences analogiques impliquant la déformation de modèles en sable-silicone, et leur visualisation au scanner médical ont été effectués à l'IFP, tandis que des modèles cinématiques directs incorporant l'érosion ont été réalisés grâce à des procédures numériques. Il apparaît que les développements des bassins transportés du nord de la Bolivie et ceux du sud semblent sensiblement différents.

**Analyse, inversion et modélisation de sondages magnétotelluriques à travers la Cordillère orientale et le Chaco (NW Argentine)**
P. Lezaeta et M. Munoz

Les données obtenues par sondages magnétotelluriques effectués à travers la Cordillère orientale et le Chaco ont été analysées rigoureusement pour connaître les effets de la distorsion produite par des structures tridimensionnelles. L'inversion et la modélisation des données magnétotelluriques par plusieurs techniques conduit à un modèle bidimensionnel de distribution de la résistivité électrique . Le modèle obtenu est comparé aux données géophysiques régionales. On discute ce modèle en fonction des propriétés électriques des roches de la croûte et du manteau, et on fait quelques propositions sur les propriétés rhéologiques de la région.

**Socle métamorphique et stratigraphie de la couverture volcano-sédimentaires à 18°S: implications pour le style et l'histoire des déformations andines**
J. Lezaun, V. Heber, A. Beck, K. Hammerschmidt et G. Wörner

Une cartographie détaillée de la région de Belen-Chapuquina dans le nord du Chili améliore la connaissance de la stratigraphie et des relations tectoniques avec le socle de Belen, et apporte de nouvelles informations sur les roches permiennes marines de la couverture. Nous présentons de nouveaux arguments en faveur de chevauchements de grande échelle actifs jusqu'à l'Oligocène. Plus tard, les mouvements liés au récent soulèvement andin correspondent principalement à des failles normales.

**Le système de failles de Falla Oeste: enregistrement de sa signification régionale dans la mine à ciel ouvert de Chuquicamata, Nord Chili**
D. Lindsay, M. Zentilli et G. Ossandon

A l'intérieur du système de failles de Falla Oeste, on peut décrire plusieurs épisodes distincts de déformation. Les plus primitifs présentent des structures ductiles liées à la tectonique régionale et à la mise en place du complexe intrusif de Chuquicamata. La deuxième série de structures est formée dans la croûte superficielle cassante et est associée aux minéralisations hydrothermales à Chuquicamata. La dernière structure dans le système de failles est associée à la fissure ouest et découpe le complexe intrusif minéralisé.

**Le socle paléozoïque des Andes centrales (18°-26°S) - aspects métamorphiques**
F Lucassen, H.G. Wilke, J. Viramonte, R. Becchio, G. Franz, A. Laber, K. Wemmer et P. Vroon

Un métamorphisme de haut grade, haute température (600-750°C) et basse pression (environ 6 kb) est observé dans différents sites depuis le NW de l'Argentine jusqu'à la chaîne côtière du Nord Chili, avec des âges Sm-Nd de paroxisme métamorphique à 500 Ma. Les ages K-Ar sur minéraux indiquent un refroidissement des roches métamorphiques autour de 400 Ma. l'exhumation finale a eu lieu jusqu'au Carbonifère. Le degré de métamorphisme, la déformation et les relations d'âge montrent un événement métamorphique avec un fort flux de chaleur au niveau de la croûte moyenne. Ceci n'est pas en accord avec un développement de la marge continentale, à la fin du Protérozoique et au Paléozoïque, par un système multi-cycles "collision-ouverture de rifts".

**Formation de skarn sous le volcan Lascar, nord chili: arguments en faveur d'une l'extension occidentale de la Formation Yacoraite (Crétacé terminal) du nord-ouest argentin**
R. Marquillas et S.J. Matthews

L'étude détaillée, par diverses techniques géochimiques, des xénolites de skarn des produits d'éruption du volcan Lascar du Nord chilien a permis d'identifier l'encaissant comme étant les calcaires et les grès calaires de la Formation Yacoraite (Crétacé supérieur-Paléocène inférieur), qui fait partie du Groupe Salta (Crétacé-Eocène moyen) du Nord-Ouest argentin.

**La ceinture de Punta del Cobre (Chili du nord): une minéralisation cu (-fe) d'âge crétacé moyen liée au plutonisme**
R. Marschik et L. Fontbote

L'étude de la ceinture de Punta del Cobre montre que le modèle d'altération, la géométrie des corps minéralisés, les températures de formation du gisement d'environ 400° à 500° C, et l'âge de l'altération potassique indiquent une minéralisation associée à des intrusions magmatiques profondes.

**Modèles mécaniques de structuration crustale dûe à la convergence**
R.A. Mason et A. Ord

Une modélisation numérique préliminaire permet de contraindre la façon dont la déformation s'accumule sur les marges convergentes structurées. Nous décrivons quelques modèles mécaniques simples portant sur les relations entre tectonique et minéralisations pour les cas des Andes et de la Papouasie, et nous évaluons l'intérêt de la modélisation pour résoudre ce genre de problèmes.

**Tomographie par seismes locaux de la chaîne andine à 20°S**
F. Masson et C. Dorbath

Un réseau temporaire de 41 stations lithoscope a été maintenu pendant 6 mois au nord Chili et en Bolivie, coupant la chaîne andine dans son intégralité à 20°S. Au cours de cette campagne, nous avons enregistré un grand nombre de seismes associés à la subduction de la plaque de Nazca sous le réseau. L'inversion de leur temps d'arrivée le long du profil doit nous permettre d'obtenir simultanément la position précise des hypocentres et des modèles de vitesse en onde P et en onde S de la croûte et du manteau au dessus de la subduction.

**Le métamorphisme basse température du socle paléozoïque supérieur, Chili central: nouvelles données pétrologiques**
H.J. Massonne, F. Hervé, V. Muñoz et A. P. Willner

Dans la Cordillère de la Côte (Chili Central), la série occidentale est constituée de roches détritiques d'age paléozoïque qui ont subi des conditions métamorphiques maximales à haute pression et basse température. Cependant, elles sont rétromorphosées en faciès schistes verts. Des phengites à haut teneur en silice et des reliques d'amphiboles bleues témoignent de l'épisode haute pression. Ainsi, pour ces épais sédiments détritiques, les nouvelles données confortent l'hypothèse d'un métamorphisme au sein d'un prisme d'accrétion.

**Evolution sédimentaire et tectonique du Bassin de Calama (avant-arc du nord du Chili) de l'Oligocène à l'actuel**
G. May, A.J. Hartley et F.M. Stuart

Le bassin pré-andin de Calama, situé dans la région avant-arc du Nord du Chili (22° et 23° S) contient plus de 700 m de sédiments continentaux, regroupés en 5 séquences discordantes, d'âge oligocène à quaternaire. A partir d'âges $^{40}Ar/^{39}Ar$, nous avons cerné plusieurs phases de remontée et de déformation (Eocène Sup., Oligocène Inf. à Miocène Inf., Miocène Sup. et Pliocène Sup.). Ces périodes coincident avec les mouvements reconnus sur un sytème de failles bordant le bassin.

**Styles structuraux dans la Chaîne de Domeyko, nord Chili**
S. McElderry, G. Chong Diaz, D. Prior et S. Flint

La faille la plus à l'ouest du système de failles de la "West Fissure" se trouve le long d'un horizon évaporitique au niveau de sa terminaison nord, et le long d'une ignimbrite verticale au sud. La déformation dans les évaporites est diffuse. Dans les ignimbrites, il y a des surfaces striées ,et aussi un réseau de fissures sombres anastomosées. Nous avons entrepris l'analyse de ces fissures pour produire un modèle géométrique et cinématique de la déformation le long de la faille.Nous avons aussi analysé les différences de style de déformation dans les différentes lithologies.

**Détection des failles récentes et évaluation de leurs rejets verticaux sur les images Radar du satellite ERS1. L'exemple de la faille d'Atacama (nord Chili)**
C. Mering, J. Chorowicz, J.C. Vicente et C. Chalah

Les images Radar SAR du satellite SAR-ERS-1 contiennent des informations très pertinentes dans le domaine de la géomorphologie et de la tectonique récente. En effet, sur ces images, l'intensité du signal est directement influencée par la rugosité et les variations de la topographie. Les escarpements abrupts des failles récentes sont donc aisément reconnaissables sur les images. Les lignes de failles peuvent donc être extraites de l'image par traitement numérique. Par ailleurs, le lien existant entre la géométrie de la visée du radar et la topographie du relief étant connu, on évalue les hauteurs des escarpements déjà cartographiés le long de la ligne de faille par analyse numérique de l'image.

**Géochronologie du Paléozoïque inférieur et événements orogéniques dans le nord-ouest argentin**
H. Miller

Dans le socle du nord-ouest argentin, les âges du magmatisme et du métamorphisme indiquent une forte activité orogénique au cours du Vendien supérieur et du Cambrien inférieur à moyen, suivie 30 Ma plus tard par de nouveau événements d'âge Ordovicien supérieur. Ceci est comparé au régime supposé de déplacement des plaques à l'ouest du continent gondwanien.

**Interprétation des données historiques du séisme de Cumana (Vénézuela) de 1929**
A. Mocquet, C. Beltran, M. Lugo, J.A. Rodriguez et A. Singer

Le séisme de Cumana du 17 Janvier 1929 était associé à l'activité de la zone de failles de El Pilar, limite actuelle entre les plaques Caraïbes et Amérique du Sud dans la région nord-orientale du Venezuela. Les données macrosismiques montrent que la longueur de faille cassée durant ce séisme a dû être inférieure à 30 km. Celui-ci n'a donc pas contribué de manière significative à la libération des contraintes tectoniques dans cette région.

**Structure de la Cordillère Orientale dans le Nord-Ouest Argentin**
R. Mon

Le segment le plus méridional de la Cordillère orientale, situé entre 22° et 27° de lat. S, représente une ceinture de plis d'âge mio-pliocène avec une importante participation du socle précambrien. La couverture a été plissée avec le socle. Ces plis ont été cassés et charriés vers l'est par des chevauchements pliocènes-pleistocènes, plus jeunes que 1,5 Ma. Plus au sud que 24° de lat. S, la bordure occidentale est déversée vers l'Ouest et l'orientale vers l'Est. Ce segment montre des différences notables avec ceux-ci situés plus au nord dans le Pérou et la Bolivie.

**Fronts chevauchants de la vallée de Lerma (Salta, Argentine) synchrones du dépôt de la formation Piquete (Plio-Pléistocène)**
C.R. Monaldi, R.E. Gonzales et J.A. Salfity

Nous présentons une description synthétique de plusieurs fronts chevauchants ayant contrôlé les dépôts synorogéniques de la formation Piquete (d'age plio-pléistocene) dans une partie du bassin d'avant-pays néogène du N.O. argentin (vallées de Lerma et Metan).

**Atténuation des ondes coda avant et après l'événement sismique majeur d'Antofagasta du 30 juillet 1995**
T. Monfret

L'atténuation intrinsèque et l'atténuation "scattering" sont calculées pour des séismes qui se sont produits entre 1993 et 1996 à moins de 30 km de distance épicentrale de la station MEJ du réseau sismologique d'Antofagasta. Alors que l'atténuation intrinsèque ne montre aucune variation temporelle, l'atténuation "scattering" augmente à MEJ avant le tremblement de terre d'Antofagasta du 30 Juillet 1995 et regagne en 1996 son niveau de 1993.

**Les adakites d'Equateur: données préliminaires**

M. Monzier, J.P. Eissen, J. Cotten, M.L. Hall, C. Robin et P. Samaniego

Les premiers résultats du programme de volcanologie mené en Equateur par l'ORSTOM et l'Institut Géophysique de l'Ecole Polytechnique Nationale (Quito) montrent une forte proportion d'adakites parmi les roches échantillonnées sur les volcans quaternaires. Ces roches résultent de la fusion partielle d'une source basaltique. Les volcans concernés étant relativement éloignés de la fosse, il semble logique d'envisager une fusion en base de croûte plutôt qu'une fusion de la plaque plongeante lui-même.

**Caractéristiques chimiques des minéraux métamorphiques dans les laves basiques du Crétacé inferieur de la Cordillère côtière, Chili central**

D. Morata, M. Vergara, L. Aguirre, J. Cembrano et E. Puga

Dans la Cordillère Cotière du Chili central, les roches volcaniques du Crétacé inférieur, épaisses de 3 à 13 km, ont subi un métamorphisme de bas grade. Les coulées basiques se caractérisent par leurs paragénèses riches en chlorite, pumpellyite, épidote et felspath potassique (adulaire, riche en Ba). Ces minéraux montrent de fortes variations dans leurs compositions chimiques et ceci à plusieurs échelles d'observation, depuis celle de cristaux à l'intérieur d'amygdales. Cette hétérogénéité résulterait de fortes variations de la fugacité de l'oxygène durant l'évolution métamorphique du système.

**Potentiel pétrolier de l'Altiplano Bolivien**

I. Moretti et O. Aranibar

La partie est de l'Altiplano bolivien contient deux intervalles-roche mère: le Paléozoïque et le Crétacé supérieur. Le Paléozoïque est épais mais d'un potentiel moyen, le Crétacé (Fm Chaunaca et El Molino) est localement très riche mais peu épais. L'exploration y est rendu risquée par les différentes phases d'érosion qui ont pu faire disparaître ces roches mères et par le fait que certaines des structures sont très récentes, vraisemblablement post-migration des HC. A l'ouest de nombreuses inconnues demeurent du fait du manque d'affleurement et de calage sismique. Il est vraisemblable que le Paléozoïque moyen à supérieur soit absent et la richesse du Crétacé reste à prouver. L'existence localement d'autres séries riches en matière organique, Ordovicien ou Jurassique n'est pas à éliminer.

**Cartes de distribution de la densité du flux de chaleur terrestre en Amérique du sud**

M. Munoz et V.M. Hamza

Les cartes sont basées sur la compilation de 655 valeurs de flux de chaleur obtenues par des méthodes diverses. Dans ce travail, à chaque valeur de flux a été associée un indice de priorité. Les cartes ont été préparées automatiquement et par contourage manuel. Les mosaïques de variations de flux de chaleur obtenues lors de la fabrication de ces cartes sont discutées en relation avec les observations géophysiques sur le continent.

**Actualisation de la cartographie géologique de la côte SW équatorienne, entre Guayaquil et la Péninsule de Santa Elena, à l'aide d'imageries satellitaires**

E. Navarrette, A. Legeley-Padovani et G. Laubacher

Le traitement d'une image Landsat TM et d'une image SPOT XS par des méthodes classiques de classification, d'une part dirigée (moyenne euclidienne) et d'autre par non dirigée (Nuées Dynamiques à centres mobiles) ainsi que les techniques de Morphologie Mathématique ont permis de différencier et de cartographier les ensembles stratigraphiques principaux de cette partie côtière de l'Equateur. Les différents types de traitements ont donné des résultats similaires pour les grandes unités mais ils ont laissé quelques imprécisions. Celles-ci ont pu être bien identifiées sur le terrain. Ces résultats sont en accord avec les récents travaux de Benitez (1995) sur la lithostratigraphie et l'évolution géodynamique.

**Résultats structuraux préliminaires sur le batholite nord-patagonien (Chili, Aysen, 44°-45°30' S)**

A. Nédélec et A. Sanhueza

Le batholite nord-patagonien est caractérisé par la mise en place de granites alumineux récents en position axiale. Les structures de ces granites (foliations N-S fortement pentées vers l'Ouest; linéations de direction N à NE subhorizontales à moyennement plongeantes vers le SSW) et leurs microstructures (magmatiques ou déformées à l'état solide) sont compatibles avec une mise en place syntectonique guidée par le décrochement dextre de Liquine-Ofqui.

**Un modèle de coupes équilibrées pour l'évolution fini-cénozoique de l'arc et de l'arrière-arc sud-Bolivien.**

N. Okaya, S. Tawackoli et P. Giese

Les nouvelles données géologiques et géophysiques indiquent que l'arc et l'arrière-arc du sud de la Bolivie résultent de deux mécanismes d'épaississement. Le premier (27-5Ma) est du chevauchement par cisaillement simple crustal, avec épaississement de la croûte inférieure par cisaillement pur. Cette phase rend compte du raccourcissement entre l'Altiplano et la zone interandine, ainsi que de l'épaississement et du soulèvement dans l'Altiplano et la cordillère occidentale. La deuxième phase (0-5Ma) est de type subduction continentale et entraîne un raccourcissement dans la zone sub-andine, avec épaississement et soulèvement dans la cordillère orientale. Ce concept est étudié par un modèle de coupes équilibrées.

**Géochimie du volcan Huaynaputina, Pérou méridional**

R.A. Oliver, N. Vatin-Perignon, P. Goemans et F. Keller

Le volcan Huaynaputina, situé dans le Sud du Pérou, a fait sa dernière éruption en 1600. Ici, nous examinons la géochimie de cette dernière éruption ainsi que les laves antérieures. La géochimie de l'Huaynaputina ressemble à celle de la plupart des autres volcans du secteur, comme le Solimana et les volcans du nord du Chili. La géochimie, surtout les éléments trace et les données isotopiques, montre que le magma a subi une contamination crustale relativement importante.

**Pétrologie et mise en place des granitoïdes de la cordillère frontale, Province de Mendoza, Argentine occidentale (33-34°S)**

H.M. Orme, N. Petford, M.P. Atherton, D. Gregori, M.A. Ruvinos et S.G. Pugliese

Les intrusions de la cordillère frontale de Cacheuta et Guido dans l'ouest de l'Argentine sont des corps granitiques peu étudiés qui se trouvent dans un bassin sédimentaire et volcanique lié à un rift du Trias. La tectonique régionale suggère que la mise en place des granites a eu lieu au cours de mouvements décrochants senestre le long de linéaments principalement orientés N-S.

**Morphostratigraphie et déformations verticales quaternaires dans la péninsule de Mejillones, Nord Chili**

L. Ortlieb, J.L. Goy, C. Zazo, C. Hillaire-Marcel, B. Ghaleb, N. Guzman et R. Thiele

L'étude géologique, paléontologique et géochronologique des dépôts marins et littoraux plio-quaternaires de la péninsule de Mejillones (23°S) indique que le soulèvement de ce bloc crustal de la côte nord-chilienne n'a pas excédé les 200 mètres, comme le reste du secteur côtier Antofagasta-Iquique. L'attribution des exceptionnelles séries de cordons littoraux préservés dans la péninsule au Pléistocène moyen suggère que l'essentiel du soulèvement s'est produit lors des derniers 500 000 ans.

**Ceintures métallogéniques de la Patagonie chilienne entre 44° et 48°S**

C. Palacios M., A. Lahsen A. et M. Parada R.

La minéralisation est limité à trois ceintures métallogéniques, dans lesquelles l'activité hydrothermale est concentrée le long des arcs magmatiques correspondants. Au Jurassique supérieur, se forment des minéralisations épithermales Au-Ag et mésothermales Zn-Pb-Ag. Au cours du Crétacé inférieur, apparaissent des minéralisations Au-Ag épithermales, des skarns à Zn-Au, et des porphyres cuprifères. Au cours du Miocène, des minéralisations épithermales à or et des porphyres cuprifères se mettent en place.

**Remobilisation du Zn et du Pb du socle paléozoique comme source de minéralisation dans le district El Faldeo, Patagonie chilienne: arguments géochimiques et isotopiques**

C. M. Palacios, A. Lahsen A., M. Parada R. et S. Magri

La source des minéralisations à Zn-Pb est discutée à partir des données isotopiques et géochimiques. Les données de la géochimie indiquent un lessivage des roches paléozoïques au cours d'une altération propylitique et une reconcentration dans des roches minéralisées et séricitisées. Les données isotopiques S et Pb indiquent que le $H_2S$ et le plomb ont une source crustale. Les données isotopiques Sr et Nd sur roches intrusives liées à la minéralisation suggèrent une importante contribution crustale.

**Evolution magmatique de la partie orientale de la Patagonie chilienne (Région d'Aysen): contraintes géochronologiques et géochimiques**

M. A. Parada, A. Lahsen et C. Palacios

A partir de données radiométriques publiées et de 34 nouvelles datations, ainsi que de données géochimiques et isotopiques, cette étude contribue à la compréhension de l'évolution magmatique de la Patagonie chilienne. Les résultats confirment la zonation d'échelle régionale du batholite nord patagonien, mais montrent des variations géochronologiques et géochimiques à l'intérieur de zones particulières. Une corrélation est détectée entre le plutonisme et le volcanisme. Cependant, les produits de ces deux processus auraient une origine différente.

**Géologie, géochronologie et évolution tectonique du secteur Au-Zn El Faldeo dans la Patagonie Chilienne**

M.A. Parada, C. Palacios et A. Lahsen

La minéralisation à Au-Zn du secteur El Faldeo est contenue dans des tufs de la formation Ibanez et dans des porphyres subvolcaniques associés. Les observations de terrain, les âges radiométriques (U-Pb, Ar-Ar et K-Ar), et la distribution, contrôlée par failles, de la séquence Ibanez, des intrusions et des veines, suggèrent que l'espace pour mettre en place les magmas et les minéralisations dans l'arc Jurassique de la Patagonie chilienne est associé au développement de bassins extensifs.

**Sismotectonique et distribution des contraintes dans la région centrale du Chili, le long de la plaque Nazca en subduction (25°-40° S)**

M. Pardo, D. Comte, T. Monfret, E. Vera et N. Gonzalez

Les caractéristiques sismotectoniques de la région centrale du Chili sont analysées à partir de la distribution des hypocentres et des mécanismes au foyer des séismes locaux. Nous déterminons la géométrie de la paque Nazca en subduction, le champ de contraintes associé, et la forme du contact sismogénique inter-plaque.

**Etudes de sismique grand angle sur terre et en mer en Chili du nord au cours du projet Cinca 95**

R. Patzwahl, A. Schulze, P. Giese et J. Mechie

Du 31 juillet au 30 septembre 1995, deux études de sismique grand angle, sur terre et en mer ont eu lieu en Chili du nord, au cours du projet CINCA 95 (Crustal Investigations on- and off-shore Nazca/Central Andes). Ces études concernent les latitudes 19° et 26° sud et les longitudes 76° et 68° ouest. Nous montrons, selon l'état actuel de l'interprétation, les modèles 2D de structure de vitesse de la marge à l'ouest de la zone de subduction.

**Tomographie crustale des Andes Equatoriennes à partir de séismes locaux enregistrés lors de l'expérience Lithoscope 1995**

A. Paul, R. Bernal, B. Guillier, J.L. Chatelain et A. Alvarado

Nous présentons les résultats d'une inversion simultanée des localisations hypocentrales et de la structure 3D en vitesse d'ondes P sous les Andes Equatoriennes. Les données utilisées sont celles de l'expérience Lithoscope 1995 pendant laquelle 54 stations sismologiques courte-période ont été déployées sur 2 profils E-O et 3 profils N-S à travers la chaîne andine entre Quito et Robamba. Très peu de téléséismes ayant été enregistrés, nous utiliserons les séismes locaux bien localisés.

**L'arc magmatique plio-holocène entre 36° et 39°S: contrôles sur la géométrie du plan de Benioff**

A.E. Pesce

A partir des données géologiques, volcanologiques, pétrogénétiques, géophysiques et sismologiques, nous proposons un modèle théorique d'évolution de la plaque océanique en subduction entre 36° et 39° de latitude sud.

**Age et origine des basaltes des plateaux de Patagonie méridionale, Chili, Région de Chile Chico (46°45'S)**
N. Petford, M. Cheadle et B. Barreiro

De nouvelles données chimiques et radiométriques de la région de Chile Chico, à l'intérieur de l'actuelle lacune de volcanisme, sont présentées pour une coupe détaillée à travers une séquence inférieure de basaltes des plateaux constitués de tholéites à olivine et hyperstène normatif. Des âges $^{40}Ar/^{39}Ar$ de 51.7 ± 0.7 à 51.8 ± 0.9 impliquent une période d'éruption d'environ 0.1 Ma et confirment la similarité d'âge de ces roches avec les basaltes voisins d'Argentine. Les basaltes sont d'affinités OIB (Ba/La < 15, La/Nb < 1.6), avec des valeurs de Mg jusqu'à 67, des valeurs d'epsilon Nd allant de +6 à +2, et des rapports $^{87}SR/^{86}SR$ de 0.7030-0.7045. La corrélation entre La/Nb, TiO2, et la composition isotopique entre les séquences basaltiques inférieure et supérieure suggère un changement dans le temps de la région source, d'un manteau principalement asthénosphérique à un manteau lithosphérique.

**Age $^{40}Ar$-$^{39}Ar$ et reconnaissance paléomagnétique de roches ignées dans la région de Coyhaique, sud Chili (45°30'-47°S)**
N. Petford et P. Turner

Depuis l'Eocène, la Patagonie (sud-centrale) a connu plusieurs collisions de ride. Dans cette contribution, nous présentons les résultats d'une étude dont le but est de quantifier la réponse de la plaque continentale lors de la subduction d'une ride. Afin de mieux contraindre l'age de l'activité ignée et les possibles rotations tectoniques engendrées par les événements de subduction de ride, des datations $^{40}Ar$-$^{39}Ar$ et une étude paléomagnétique ont été entreprises sur des points clés au sud de Coyhaique, entre 45°30' et 47°S.

**Anisotropie des ondes S sous les Andes centrales à partir des expériences BANJO, SEDA et PISCO**
J. Polet, P. Silver, G. Zandt, S. Ruppert, R. Kind, G. Bock, G. Asch, S. Beck et T. Wallace

Nous avons analysé les données des stations portables des expériences BANJO, SEDA et PISCO afin de déterminer les paramètres de séparation des ondes S (direction de polarisation rapide F, retard dt) sous les réseaux. Les réseaux suivent une ligne EW à 20° à travers les Andes, et une ligne globalement NS de 16° à 26°. Le long de la ligne EW, F est le plus souvent orienté EW, alors qu'ailleurs il est le plus souvent parallèle à la zone de subduction. Nous en concluons que le signal principal vient de sous la plaque Nazca, ce qui indique un champ d'écoulement complexe avec une composante parallèle à la zone de subduction. Nous suggérons que le champ d'écoulement est relié à la structure des Andes à grande échelle.

**Une approche en conditions aux limites par une force dépendante de la vitesse de déformation pour la modélisation numérique de l'évolution d'un plateau - Application à la déformation andine**
R. Porth

Afin d'étudier l'effet des forces liées à la croissance d'un plateau, des conditions aux limites impliquant une force dépendante de la vitesse de déformation ont été appliquées à des modèles géométriques simples en 2D d'une lithosphère à différents stades de l'évolution d'un plateau. Le taux de raccourcissement diminue significativement lorsque l'altitude du plateau augmente, ce qui affecte non seulement la vitesse de déformation mais aussi le style de déformation à l'intérieur du modèle. Ceci montre l'importance de conditions aux limites impliquant une force dépendante de la vitesse de déformation pour les modèles numériques de l'évolution du plateau.

**Tomographie des Andes équatoriennes**
R. Prevot, J.L. Chatelain, B. Guillier et H. Yepes

Les temps d'arrivées d'ondes P et S de séismes locaux ainsi que des ondes P de téléséismes ont été utilisés pour définir les modèles de vitesses (1D et 3D) pour la croûte et le manteau supérieur, sous les Andes équatoriennes. Comme dans les Andes Centrales boliviennes, sous les cordillères, les vitesses sont plus rapides qu'au niveau de la partie centrale des Andes, Altiplano en Bolivie et dépression interandine en Equateur, le moho étant plus profond sous ces zones.

**Tectonique tertiaire du nord de la Patagonie: Évidence de vestiges de bassins chiliens.**
D. Prior, F. Ray et S. Flint

Les vestiges de bassins tertiaires dans le nord de la Patagonie fournissent un enregistrement de la tectonique de la marge. Le bassin molassique patagonien et la chaîne chevauchante d'avant-pays peuvent être liées à l'histoire de la subduction de la ride. Cependant, les informations chronologiques suggèrent que la sédimentation molassique et au moins une partie de la déformation ont commencé antérieurement. Il est possible que la formation initiale de la topographie et le bassin molassique résultent de la subduction d'une croûte plus jeune et plus légère lors de l'approche de la ride vers la marge.

**Evolution tectonique des Andes principales centrales au Paso Piuquenes (33° 30' s), Argentine et Chili**
V. A. Ramos, E. Godoy, V. Godoy et F. Pángaro

A la latitude 33° 30' S (Argentine et Chili), il y a une relation étroite entre le développement de la ceinture plissée et faillée d'Aconcague et l'évolution magmatique de la Cordillère Principale. Ainsi, le taux de raccoucissement calculé à partir de coupes équilibrées est compatible dans l'espace et le temps avec l'augmentation des rapports de terres rares, La/Yb et La/Sm, déterminés sur les roches volcaniques.

**Magmatisme gondwanien de Patagonie: batholithes calco-alcalins internes à la cordillère et provinces de volcanisme bimodal**
C.W. Rapela, R.J. Pankhurst, E.J. Llambias, C. Labudia et A. Artabe

Le magmatisme Gondwanien (Carbonifère supérieur à Jurassique) de l'Amérique du Sud Australe contient des alternances répétées entre des batholithes calco-alcalins internes à la cordillère et des provinces de volcanisme bimodal. Ceci peut refléter des changements dans le régime tectonique, avec des épisodes plutoniques correspondant aux périodes de forte obliquité de la subduction, les large provinces de volcanisme correspondant aux périodes d'arrêt ou de ralentissement de la subduction.

**Dynamique d'avant-arc et néotectonique de l'arc des Andes centrales, Nord du Chili**
C-D. Reuther et J. Adam

Les structures néotectoniques de surface entre la fosse du nord du Chili et la cordillère occidentale sont caractérisées par des failles normales parallèles à la fosse dans l'avant-arc côtier externe, et par des failles inverses à vergence ouest et est dans l'avant-arc interne, jusqu'au bord occidental de l'arc magmatique actif. plusieur structures en biseau ont été définies dans la croûte fragile de l'avant-arc. Des modèles de biseaux plastiques et à loi de friction aident à comprendre la dynamique de la croûte rigide contrôlant le soulèvement des blocs de socles de la chaîne côtière chilienne, avec simultanément de l'extension E-W dans l'avant-arc externe et de la compression E-W dans l'avant-arc interne.

**Pétrographie et géochimie des roches volcaniques océaniques et continentales d'âge crétacé moyen à paléocène du Sud-Ouest de l'Equateur**

C. Reynaud, H. Lapierre, E. Jaillard, S. Benitez, G. Berrones et G. Mascle

Le substratum d'origine océanique de la côte sud-équatorienne, d'âge crétacé moyen, présente des caractéristiques géochimiques de plateau océanique. Ceci expliquerait pourquoi il n'a pas été subducté et a supporté des arcs insulaires successifs au Crétacé supérieur et au Paléogène. Pendant la même période, la marge andine de l'extrême sud de l'Equateur est marquée par le fonctionnement discontinu d'arcs volcaniques continentaux.

**Les séquences du Crétacé-Paléogène et les premiers événements orogéniques andins dans le bassin de l'Oriente Equatorien**

M.V. Rivadeneira

Les séquences stratigraphiques du Crétacé-Paléogène du bassin de l'Oriente Équatorien sont influencées par des événements orogéniques andins très précoces. Faibles jusqu'au Santonien-Campanien et seulement mis en évidence par des érosions mineures, ces événéments sont mieux marqués dans les séquences Paléogène quand l'érosion s'accentue et qu'apparaissent les premiers dépôts molassiques qui mettent en évidence l'émersion des paleo-Andes à l'ouest du bassin. Les failles et les plis formés, ainsi que les sédiments déposés entre le Crétacé et le Paléogène, sont d'une importance critique pour la formation et l'accumulation du Pétrole dans le bassin.

**Dynamismes éruptifs contrastés associés à deux suites magmatiques distinctes (adakitique et andésitique) au volcan Mojanda, Equateur**

C. Robin, M. Jimenez, M. Hall, P. Escobar, M. Monzier, J. Cotten et J.P. Eissen

Deux centres volcaniques majeurs (Mojanda et Fuya Fuya), distants de seulement 4 km, constituent ce qui était considéré comme le Volcan Mojanda. Les développements et dynamismes éruptifs de ces deux appareils contemporains diffèrent. Le Mojanda s.s., formé par une suite d'andésites basiques et d'andésites, est essentiellement constitué de laves et de dépôts pyroclastiques résultant d'explosions phréatomagmatiques. Au Fuya-Fuya, les roches sont adakitiques ; l'activité, surtout explosive, est celle de coulées visqueuses et de dômes essentiellement dacitiques, dont les différentes phases de mise en place est intercalée à de nombreux événements pliniens dacitiques et rhyolitiques (coulées pyroclastiques, épaisses retombées de ponces).

**Genèse et cinématique de l'Altiplano en Bolivie du nord**

P. Rochat, P. Baby, G. Hérail, G. Mascle, O. Aranibar et B. Colletta

De l'Eocene à l'Oligocène Inférieur, l'Altiplano correspondait à un bassin rempli de sédiments en provenenance de l'Ouest. Jusqu'au Miocène, ce bassin se structurait en régime compressif, chevauché par la Cordillère Orientale. Au Pliocène Inférieur, une bonne partie de l'Altiplano a été érodée et recouverte de sédiments volcano-détritiques. En même temps, l'épaississement et la structuration en zone subandine ont conduit au soulèvement de toute la région.

**Magnétostratigraphie et rotation paléomagnétique de l'Altiplano bolivien nord-central**

P. Roperch, L. Aubry, G. Herail, M. Fornari et A. Chauvin

Une coupe magnétostratigraphique dans 2500 m de sédiments de la formation Totora au coeur du synclinal de Corque permet de déterminer un taux de sédimentation régulier et élevé de 970 m/Ma pour l'ensemble de la séquence entre 11.5 et 9 Ma. D'autre part, la rotation antihoraire de l'Altiplano central enregistrée par les formations Eocène-Oligocène est supérieure à 20°. Les résultats nombreux obtenus dans la formation Totora montrent que le bassin sédimentaire enregistre 12° de rotation depuis 9 Ma.

**Le volcanisme intra-plaque au sein des carbonates du Groupe Pucara (Triassique supérieur à Jurassique inférieur, Pérou central)**
S. Rosas, L. Fontboté et W. Morche

Au Pérou central, la série carbonatée du Groupe Pucará, d'age triassique à liassique, est intercalée avec des roches volcaniques, principalement des basaltes alcalins ou andésitiques. Leurs caractéristiques géochimiques témoignent d'une origine intgra-plaque. Le bassin de Pucará aurait pu se former dans un contexte de rift avorté sur la marge occidentale du craton brésilien.

**La structure en fleur de Valle Fertil et ses relations avec la Précordillère et les Sierras Pampeanas (30°-32° S, Argentine)**
E.A. Rossello, M.E. Mozetic, P.R. Cobbold, M. de Urreiztieta, D. Gapais et O. Lopez-Gamundi

Les structures andines ont une orientation sub-méridienne entre 27°S and 32°S. Cependant dans l'avant pays, à l'Est des chevauchements frontaux de la Précordillère, la faille de Desaguadero-Valle Fertil a une direction NO-SE. Elle constitue la limite orientale des Sierras Pampeanas. Les observations de surface et les données de sismique réflexion indiquent que cette faille a une structure en fleur et est caractérisée par un jeu transpressif senestre depuis le Néogène.

**Sismicité et paramètres focaux en Chili du Nord selon des observations par des réseaux sismologiques temporaires et locaux**
A.F. Rudloff et G. Asch

Cet article est un rapport sur deux réseaux sismologiques qui ont été opérationnels en Chili du nord pendant les années 1994 et 1995 (PISCO 1994 et CINCA 1995). Les études faisaient partie d'un projet du Centre Coopératif de Recherche SFB 267, ayant pour but d'expliquer le processus de déformation dans les Andes à l'aide des méthodes géophysiques et géologiques.

**Le séisme (Mw=8,1) d'Antofagasta (nord Chili) du 30/07/1995: premiers résultats à partir des données télésismiques et géodésiques**
J.C. Ruegg, R. Armijo, J. Campos, S. Barrientos et coll.

Le 30 juillet 1995, un très fort séisme (Mw=8,1) se produisait dans la région d'Antofagasta, au sud de la lacune sismique du nord Chili. Ce séisme a rompu une zone de 60x180 km de l'interface de subduction entre la plaque Nazca et la plaque Amérique du sud. Deux semaines après le séisme, nous avons remesuré avec GPS une partie du réseau géodésique mis en place antérieurement en 1992. Ici, nous présentons les déplacements géodésiques observés ainsi que les résultats de la modélisation du mécanisme focal obtenu à partir des données télésismiques, afin de préciser la position, la géométrie, et la dynamique de la rupture.

**Activité continue des séismes "Longue Période" du volcan Cotopaxi, Equateur**
M. Ruiz, J.L. Chatelain, B. Guillier et M. Segovia

Depuis 1991, l'activité sismique en événements LP du volcan Cotopaxi est continue. L'analyse de la distribution spatiale des séismes montre que ceux-ci sont situés à des profondeurs intermédiaires (8 à 18 km). De plus, la stabilité des paramètres tels que le contenu fréquenciel, la magnitude et la libération d'énergie montrent que l'activité LP est un comportement normal du Cotopaxi et non un signal pouvant servir de précurseur à une éruption, comme cela a été observé pour d'autres édifices.

**Nature des roches métamorphiques de la cordillère frontale dans la région du Rio de las Tuna, Province de Mendoza, Argentine**

M.A. Ruvinos et D.A. Gregori

Les roches métamorphiques du socle de la Cordillère frontale (calcaires et schistes micacés, métapélites, coulées et laves en coussins), qui peuvent atteindre jusqu'à 3km d'épaisseur, représentent probablement un mélange tectonique. Les similarités dans la lithologie et les mécanismes de mise en place des composantes du socle de la Cordillère frontale avec d'autres séquences de cette zone et de la précordillère suggèrent qu'elles appartiennent à une séquence ophiolitique.

**Contrôle de la tectonique active sur les dépôts alluviaux et fluviaux de la rivière San Juan, San Juan, Argentine.**

L. Ruzycki et J. Paredes

La construction et les corrélations de profils longitudinaux d'érosion-dépôt ont été effectuées pour les 7 principaux niveaux et les trois principaux niveaux intermédiaires de la rivière San Juan au niveau de la Précordillère, entre les km 127 et 35 de la route n°20 qui relie la ville de San Juan à la province de Calingasta. Les résultats montrent (1) que les niveaux principaux constituent une réponse complexe à des événements climatiques et tectoniques d'échelle régionale, intervenus au cours du pléistocène moyen et de l'holocène, et (2) que les principaux niveaux intermédiaires semblent être essentiellement liés à des processus tectoniques locaux, induisant des seuils morphologiques locaux dans le cours de la rivière. Ces seuils influencent non seulement la géométrie des différents profils, mais aussi les déformations des différents niveaux fluviaux et alluviaux existant dans la Précordillère.

**Effets de la tectonique active sur la géométrie des réseaux de chenaux de la rivière San Juan dans la vallée de Tulum, San Juan, Argentine**

L. Ruzycki et C. Wetten

Cette étude aborde le problème du contrôle néotectonique sur la morphologie de la rivière au passage de la vallée Tulum, qui correspond à la bordure active du bassin d'avant-pays au pied de la Précordillère orientale, principalement dans la province géologique des Sierras Pampéanas. A partir de la détermination et de la construction du profil longitudinal actuel et des changements dans la géométrie de canaux, il est établi que l'activité néotectonique entraîne la formation de ruptures de pente de la vallée, avec localement une plus grande agradation sédimentaire.

**Distribution et évolution des zones géomorphologiques dans la cordillère orientale de Bolivie.**

E.B. Safran et T. Dunne

Les chaînes de montagnes montrent de fortes hétérogénéités morphologiques régionales qui sont caractérisées par des processus géomorphologiques différents. Cette étude montre et explique la distribution et l'évolution de ces régions géomorphologiques distinctes dans une importante chaîne de montagne, la Cordillère orientale des Andes boliviennes. Le modèle quantitatif d'incision fluviale relie la morphologie des pentes et l'érosion fluviale.

**Les bassins post-Eocène des Andes Centrales d'Argentine**
J.A. Salfity, S.A. Gorustovich, R.E. Gonzalez, C.R. Monaldi, R.A. Marquillas, C.I. Galli et R.N. Alonso

Nous décrivons le contexte tectonique et la distribution régionale des bassins tertiaires developpés dans les Andes centrales argentines (22° - 36° latitude Sud) à l'époque post-incaïque (éocène précoce) et pré-diaguite (pliocène tardif - pléistocene précoce).

**Le volcan Cayambe (Equateur): tephrochronologie des derniers 5000 ans**
P. Samaniego, M. Monzier et C. Robin

Le volcan Cayambe se trouve dans la Cordillère orientale d'Equateur. Il a eu une très importante activité pyroclastique durant les 5000 dernières années, principalement durant deux périodes: la première entre 3900 et 1800 ans BP, la seconde entre environ 1000 ans BP et l'actuel. Les roches de la partie récente du Cayambe (Nevado Cayambe) présentent un net caractère adakitique, à la différence de celles de la partie ancienne (Vieux Cayambe).

**Extension tertiaire dans la basse vallée du Loa, Nord du Chili (21-22° S)**
P. Santanach, D. Serrat, A. Saez, L. Cabrera et G. Chong

Dans la région de la basse vallée du Loa, il y a eu deux étapes extensives pendant le Tertiaire. La Cordillera de la Costa est le résultat de la superposition des failles normales appartenant à ces deux phases. Sa limite avec la Vallée Longitudinale a été formée pendant la première phase (Oligocène (?)-Miocène) et son bord occidental, la falaise côtière, pendant la seconde (Miocène-Pliocène). L'activité tectonique extensive s'est donc déplacé de l'est vers l'ouest durant le Tertiaire.

**Les ignimbrites cénozoïques du nord Chili, de Bolivie occidentale et du sud Pérou: stratigraphie, extension géographique, corrélation et origine**
W. Schröder et G. Wörner

Les ignimbrites Miocène à Pliocène du Nord Chili fournissent des marqueurs stratigraphiques et des évidences pour de la fusion crustale à grande échelle en réponse à l'épaississement crustal. Des ignimbrites rhyolitiques d'age 20-19 Ma représentent un volume supérieur à 3000 Km3 et donc un court épisode de fusion crustale à cette époque. L'ignimbrite Lauca-Perez est un exemple inhabituel d'une ignimbrite (< 775 km3) qui s'est mise en place le long d'un trajet d'une altitude de 4500m jusqu'à la côte Pacifique. Les observations de terrain et les corrélations chimiques sont présentées pour ces ignimbrites et leur implication pour l'évolution andine à 18°S est discutée.

**Segmentation et vitesse de déplacement horizontal de la faille de El Tigre (Province de San Juan, Argentine)**
L. Siame, M. Sebrier, O. Bellier, D. Bourles, J.C. Castano, M. Aurojo, F. Yiou et G.M. Raisbeck

La géométrie et la segmentation de la faille de El Tigre ont été étudiés sur images SPOT. Cette zone de failles, qui borde la Précordillère argentine dans la vallée interandine de Calingasta-Iglesia, peut être caractérisée par trois segments majeurs qui totalisent une longueur de rupture en surface de 120 km. Une étude du risque sismique qui lui est associé et de sa vitesse de déplacement est également proposée.

**Couplage des plaques en profondeur, ou comment les Alpes ont contribué à la formation des Andes**
P.G. Silver et R.M. Russo

Le récent ralentissement du mouvement absolu de la plaque Afrique (Af) au cours des 30 derniers millions d'années, combiné au mouvement relatif plutôt uniforme entre Afrique et Amérique du sud (AS), impliquent que le déplacement de la plaque AS s'est accéléré durant cette même période. Nous proposons que le ralentissement soit dû à la collision avec l'Eurasie, et que l'accélération concommitente de l'AS soit dûe à l'existence d'un flux de masse constant de matériel mantellique vers le bassin atlantique. Ce couplage profond induit aussi un couplage des déformations des deux plaques, en l'occurrence les Alpes et la phase andine Quechua.

**Failles actives dans les Andes du Sud-Ouest vénézuélien et à la frontiere de la Colombie**
A. Singer et C. Beltrán

Vers son extrémité sud, le taux de déplacement de la faille de Boconó chute de façon significative. En effet, la vitesse pourrait passer en dessous de 1 mm/an, voir 0,5 mm/an, avant que la faille ne pénètre en territoire colombien. La ramification importante de la faille, son amortissement contre le système convergent de Bramón, et les modalités de sa connection cinématique avec les failles senestres du poinçon de Pamplona pourraient être à l'origine du fait signalé.

**Influence de la tectonique régionale sur la formation de caldeiras volcaniques miocène sur l'Altiplano-Puna, NW argentin: Le complexe de la caldeira Aguas Calientes**
C. Soriano, J. Maarti, I. Petrinovic et J. Viramonte

Une étude détaillée de la caldeira Aguas Calientes montre que la dynamique d'effondrement a été contrôlée par un réseau de décrochements régionaux et de failles inverses. Quelques unes de ces failles ont été réactivées en faille normale lors de courts événements d'effondrement de la caldeira et, après l'activité volcanique, ces failles ont été à nouveau actives en décrochement et en failles inverses.

**Paléogéographie mésozoïque de l'Amérique du sud Australe**
L.A. Spalleti et J. Franzese.

Huit cartes paléogéographique de Patagonie, entre la fin du Trias et la fin du Crétacé sont présentées en étapes de 15 à 30 Ma. Elles ont été compilées à partir d'une base de données paléogéographique incluant des informations stratigraphiques, structurales, sédimentaires, tectoniques et paléoenvironnementales.

**Distribution du flux de chaleur et implications pour la structure thermique de la croûte Andine**
M. Springer

A partir d'un nouveau jeu de données géothermiques et de la compilation des données existantes pour les Andes centrales, cette étude contribue à déterminer la distribution de la densité du flux de chaleur et, dans une deuxième étape, à modéliser le flux de chaleur en 2D sur une coupe E-W. Cette modélisation montre que le chauffage par friction le long du contact entre les deux plaques et la présence du coin asthénosphérique dans la région de l'arc ont un impact important sur les températures dans la plaque subduite et dans la plaque sus-jacente, mais contribuent de façon limitée au flux de chaleur en surface.

**L'origine des sulfates du Salar de Atacama et de la Cordillera de la Sal, résultats initiaux d'une étude isotopique**
B. Spiro et G. Chong

Les données isotopiques ($O^{34}S$ et $^{87}Sr/^{86}Sr$ des eaux des ruisseaux qui entrent dans le salar d'Atacama, ainsi que les eaux du salar lui même et le gypse associé, montrent que l'origine du sulfate est contrôlée par les émissions volcaniques, sans contributions significatives de sulfate maritime. Les données isotopiques de la Cordillera de la Sal, située au nord-ouest et ayant un âge Oligocène, indiquent que les sulfates ont la même origine.

**Evolution thermotectonique des Andes en équateur sud: étude de traces de fission**
M. Steinmann, D. Seward et D. Hungerbuehler

A partir de 14 échantillons de roches, prélevés dans le socle et dans des intrusions granitiques, 12 échantillons d'apatites et 11 de zircons ont pu être séparés. Les zircons sont d'âge crétacé à miocène; les apatites, d'âge paléocène à miocène. Pour les apatites, les traces confinées ont des longueurs moyennes de 13 à 14 mm et les distributions sont unimodales, évoquant une histoire simple d'exhumation tertiaire, à partir d'une profondeur de 3 à 4 km.

**Segmentation thermomécanique des Andes (15°-50° S): une approche par analyse flexurale**
A. Tassara et G. Yañez

L'analyse flexurale de 15 sections topo-gravimétriques a permis de caractériser la lithosphère andine d'un point de vue compositionnel, structural et thermomécanique. La relation entre les variations longitudinales de ces caractéristiques et la segmentation tectonique de l'orogène permet de spéculer sur les facteurs qui contrôlent la construction et l'évolution des Andes.

**La cordillère orientale du sud de la Bolivie: Une région clé dans l'histoire de la déformation et du soulèvement de l'arrière-arc andin**
S. Tawackoli, V. Jacobshagen, K. Wemmer et P. Andriessen

Les observations de terrain et les données de traces de fission dans les bassins tertiaires permettent de mieux comprendre l'évolution cénozoïque de la cordillère orientale du sud de la Bolivie. Après un soulèvement au début de l'Oligocène, les bassins néogène se sont formés vers 24-22 Ma, principalement par le fonctionnement de chevauchements a vergence ouest. Le développement structural a cependant été différent à l'intérieur des différents bassins.

**Paléomagnétisme, systèmes de failles décrochantes, et rotation crustale dans la région 25-27°S du nord Chili**
G. Taylor, D. Randall et J. Grocott

Les résultats paléomagnétiques entre 25-27°S dans le nord Chili montrent des rotations horaires qui diminuent de l'ouest vers l'est. la région est disséquée par 3 systèmes de failles orientés N-S, le système d'Atacama, le cisaillement de la vallée centrale et le système La Ternera-Domeyko. Nous pensons que la transpression sur ces systèmes de failles est principalement responsable des rotations observées.

**Le volcan Huaynaputina, Pérou méridional: site de l'éruption explosive majeure des Andes centrales au cours de l'histoire**
J.C. Thouret, A. Gourgaud et J.L. Le Pennec

L'éruption plinienne (VEI 6) du petit centre volcanique du Huaynaputina le 19 Février 1600 a mis en place une retombée ponceuse > 8500 $km^2$, des ignimbrites, des déferlantes et enfin des lahars. L'édifice pré-1600 a été détruit en grande partie, formant le cratère complexe, l'effondrement partiel de la paroi nord de la caldera d'avalanche pré-existante, et enfin trois cratères et tuf-cônes accolés. Deux processus de déclenchement sont suggérés par la petite quantité de magma basaltique dans la retombée et par plusieurs indices d'hydromagmatisme.

**Le strato-volcan El Misti, Pérou méridional: histoire éruptive et implications pour l'évaluation des menaces volcaniques**
J.C. Thouret, F. Legros, A. Gourgaud et M.L. Macedo

Environ 900 000 personnes vivent dans le bassin urbanisé d'Arequipa à 17 km du cratère du strato-volcan El Misti, qui comprend 2 édifices: un strato-cône récent (70 $km^3$) construit contre et sur un strato-volcan ancien, dont les avalanches de débris vers l'Ouest et le Sud attestent l'écroulement partiel. Depuis 40 000 ans B.P., des éruptions pliniennes dactiques et rhyolitiques ont alterné avec des périodes de croissance et destruction de dômes andésitiques. Les dépôts de l'ignimbrite de 1900 ans B.P. sont observés dans le périmètre d'Arequipa.

**Collisions mésozoïques et cénozoïques dans les Andes colombiennes**
J.F. Toussaint et J.J. Restrepo

De nouveaux résultats tectoniques, géochimiques et paléomagnétiques confirment que les Andes colombiennes sont formées d'une mosaique de blocs éxotiques (terranes), accrétés au Craton Amazonien. Un premier bloc océanique (Calima Terrane) a rejoint un bloc continental (Tahami Terrane) au Crétacé. Cet ensemble s'est ensuite accrété à l'autochtone à la fin du Crétacé. Au Miocène, le dernier collage d'un bloc océanique (Cuna Terrane) est responsable de l'orogénèse andine.

**La réaimantation régionale permienne dans l'Ouest de l'Argentine: données complémentaires**
S. Truco et A.E. Rapalini

Une étude paléomagnétique des formations Ponón Trehué (Ordovicien moyen) et El Imperial (Carbonifère supérieur), affleurant à travers le bloc de San Rafael, a mis en évidence une aimantation syntectonique acquise lors de l'évènement dit de San Rafael, d'age Permien inférieur. La région affectée par cet épisode de réaimantation serait donc plus vaste que ne le laissait entendre des études précédentes.

**L'évolution du paysage en Chili du nord (18.5°-19°.5S): son implication dans l'histoire tectonique, sédimentaire et magmatique des Andes centrales**
D. Uhlig, H. Seyfried, G. Wörner, I. Kohler et W. Schröder

Comme l'érosion ayant eu lieu depuis le Miocène est peu importante, il est possible de reconstruire les processus tectoniques, sédimentaires et magmatiques directement à partir du paysage. Pendant deux phases d'élévation des Andes centrales, des demi-fossés remplis de sédiments volumineux ont été formés. Il est possible de dater les étapes de l'évolution du paysage par les différentes couches d'ignimbrite.

**Restauration en plan des Sierras Pampeanas, limite méridionale de la Puna argentine**
M. de Urreiztieta, O. Bourgeois, D. Gapais, P.R. Cobbold, C. Le Corre, E.A. Rossello et D. Rouby

Dans le Nord-Ouest de l'Argentine (27°S), l'extrémité de la Puna est limitée au Sud par la zone transpressive dextre de Tucumán. A travers cette zone de transfert, les structures régionales d'âge néogène accommodent les variations latérales de la quantité de déformation continentale entre deux domaines crustaux. La Puna, au nord, est un secteur fortement raccourcit et épaissi, alors qu'au sud, les Sierras Pampeanas sont plus modérément déformées. Nous proposons une reconstruction de la bordure méridionale du haut-plateau andin et des Sierras Pampeanas obtenue par une méthode numérique de restauration en carte. Cette analyse numérique nous a permis d'estimer les champs de déplacements et de déformation finie associés à la tectonique andine dans cette région.

**Les terres rares et les éléments en trace du volcanisme néogène de la formation Farellones et du linéament WE Montenegro-Cerro Manquehue (Chili central)**
N. Vatin-Perignon, S. Rivano G., Mario Vergara M. et F. Keller

L'importante formation miocène Farellones, de l'arc volcanique NS du Chili central, se divise en un membre inférieur, rhyolitique et ignimbritique, et un membre supérieur, andesitique et lavique, associés à un linéament EW de necks basaltiques. Les caractéristiques géochimiques indiquent une identité de source entre l'arc andésitique NS et le linéament basaltique EW et une différence totale de ces volcanismes avec les ignimbrites.

**Evolution des saumures des gisements de nitrates du Chili (Pedro de Valdivia, région d'Antofagasta). Données minéralogiques et pétrographiques**
M. Vega, G. Chong et J.J. Pueyo

Les gisements de nitrate du Chili sont formés par des paragenèses complexes de minéraux salins qui remplissent la porosité de roches d'âge très variable (du Paléozoïque au Cénozoïque). Ces minéraux (nitrates, nitrate-sulfates, iodates, iodate-sulfates) sont très rares dans d'autres environnements. Les gisements sont situés dans le désert d'Atacama et suivent une frange irrégulière (N-S) au contact entre la Cordillère côtière et la dépression centrale. La saumure qui remplit la porosité intergranulaire (dans les sédiments terrigènes cénozoïques) ou de fracture (dans les roches du substratum) génère, par précipitation, des cortèges minéraux dont la composition dépend de l'activité des ions en solution. Deux lignes évolutives différentes ont été distinguées une évolution de type Na, donnant lieu à la succession glauberite-darapskite-halite-nitratine-hectorfloresite, et une évolution de type Na-Mg (-K), avec la succession bloedite-humberstonite-(halite-nitratine)-fuenzalidaite.

**Caractéristiques géochimiques du volcanisme oligo-miocène de la Précordillère de Talca et Linares (35° 20' - 35° 50' s), Chili**
M. Vergara, L. Lopez et I. Beccar

Dans cette région, les roches volcaniques possèdent une signature de Terres Rares à caractère tholéïtique, avec de faibles valeurs du rapport La/Yb. L'altération a donné lieu à des minéraux tels la wairakite et la laumontite. Leurs caractéristiques générales témoignent d'un magmatisme primitif ayant eu lieu dans une croûte très amincie, sous fort gradient thermique. Ces caractéristiques les différencient des autres roches volcaniques d'âge cénozoïque reconnues dans cette région des Andes.

**Mise en évidence par imagerie radar d'impacts successifs de la dorsale de Nazca avec la marge continentale du Pérou central-sud**
J.C. Vicente, C. Mering, D. Huaman et M. Cernicchiaro

Les traits néotectoniques du secteur de Marcona révélés par l'imagerie radar ERS-1 témoignent d'un chevauchement récent (Quaternaire ancien) vers l'ENE du Massif côtier du Huaricangana. Il s'accompagne de l'écaillage d'un bourrelet frontal (C° Los Pozos) et la déviation symétrique du réseau hydrographique. La compression, parallèle à la direction de convergence, est attribuée à l'impact de la Dorsale de Nazca avec la marge péruvienne. L'existence d'une structure comparable au niveau d'Ica traduirait un impact antérieur. Dans le cadre d'une convergence oblique ces impacts successifs résulteraient de la morphologie irrégulière et discontinue de la Dorsale.

**La transgression marine de l'Aptien-Albien supérieur dans le Bassin Oriente d'Equateur**
R. Villagómez, E. Jaillard, L. Bulot, M. Rivadeneira et R. Vera

La base des grès inférieurs transgressifs crétacés est d'âge Aptien supérieur (?) au Sud-Ouest, et Albien supérieur au Nord-Ouest de l'Oriente équatorien. De même, les argiles et calcaires marins sont d'âge Albien moyen basal à Albien supérieur basal du Sud-Ouest au Nord-Est du bassin. Cette disposition traduit la rétrogradation des faciès sédimentaires au cours de la grande transgression crétacé sur le bassin andin.

**Xénolites de croûte inférieure et de manteau dans le tuff Granitífera (Colombie du S-O): conséquences pour le magmatisme andin**
M. B.l. Weber, J. Tarney, R. Kent et P. D. Kempton

Le sud ouest de la Colombie est une région caractérisée par de grandes quantités de roches volcaniques alcalines. Les tuffs de la Toba Granatífera contiennent des inclusions provenant de la croûte inférieure et du manteau. Elles permettent de remonter, à travers des études en éléments traces et isotopiques, à la source des roches volcaniques et au rôle de la plaque subduite.

**Réactivation de failles dans le bloc Espinal, Colombie**
P.J. Wheeler, M.P. Coward et R. Gillcrist

Le Bloc Espinal est un excellent exemple des relations qui existent entre le système de rift mésozoique et la déformation andine qui a suivi, car les failles extensives ont été successivement réactivées en failles inverses depuis l'ouest vers l'est. Cette réactivation a eu lieu au Paléocène supérieur, à l'Eocène moyen et à la fin du Mio-Pliocène.

**Génèse de tonalites primitifs associée à un plateau océanique crétacé en voie d'accrétion: le batholithe d'Aruba et la formation des laves d'Aruba**
R.V. White, J. Tarney, G.Th. Klaver et A.V. Ruiz

Le batholithe crétacé à dominance tonalitique qui affleure sur l'île d'Aruba (Caraïbes) est caractérisé par (1) de faibles rapports $^{87}Sr/^{86}Sr$, témoins d'un manque de contamination par la croûte, et (2) des distributions en éléments traces rappelant celles des tonalites archéennes. Les données de terrain laissent penser que cette tonalite dérive de la fusion partielle survenue dans une zone de cisaillement en faciès amphibolite qui traverse la séquence de volcanites basiques (Formation Aruba Lavas). Cette zone de cisaillement aurait pu se former par imbrication du plateau, lors de sa collision avec une zone de subduction.

**Etude comparée des croûtes épaissies des Andes et du Tibet à l'aide de réseaux sismiques large-bande passifs**
G. Zandt, S.L. Beck, et T.J. Owens

Le déploiement d'un réseau sismique large-bande passif dans les Andes et au Tibet fournit un excellent échantillonnage des deux plus grands plateaux à la surface du globe. Les propriétés crustales moyennes des deux plateaux estimées à partir des deux expériences sismologiques sont significativement différentes. L'Altiplano est caractérisé par une croûte uniforme de 65 km d'épaisseur avec des faibles vitesses (P: 6.0 km/s) et un rapport de Poisson (RP) d'environ 0.25. Le Tibet montre des variations N-S systématiques de l'épaisseur crustale et du rapport de Poisson: 75km avec un RP de 0.25-0.27 au sud, 70km avec un RP de 0.27-0.28 aux latitudes centrales, et 55km avec un RP > 0.3 au nord. Alors que l'Altiplano apparaît être en équilibre isostatique, d'autres forces doivent agir pour maintenir le Tibet à son altitude uniforme.

**Evolution cénozoïque du bassin d'avant-pays andin entre 15°30' et 22° S**
D. Zubieta Rossetti, P. Baby et J.L. Mugnier

Les sédiments clastiques déposés dans le bassin d'avant-pays des Andes centrales au cours des derniers 27 Ma sont en relation directe avec le soulèvement de la Cordillère orientale et des chaînes sub-andines. La géométrie des sédiments accumulés dans le bassin est directement liée aux processus de déformation, érosion, transport et dépôt. Le style structural est lié à l'évolution géodynamique du front de la chaîne, et aux caractères structuraux et stratigraphiques pré-andins.

# INDEX DES AUTEURS
# AUTHOR INDEX
# INDICE DE LOS AUTORES

Achevé d'imprimer en septembre 1996 sur système Variquik
par l'imprimerie SAGIM à Courtry (77) - Tél. : 01-64 72 40 85
*Imprimé en France* - Dépôt légal : septembre 1996 - N° d'impression : 1825

ORSTOM éditions
213, rue La Fayette
F-75480 Paris Cedex 10
Diffusion
32, avenue Henri Varagnat
F-93143 Bondy Cedex
ISSN : 0767-2896
ISBN : 2-7099-1332-1

*Photographies de couverture :*

*Au centre, carte topographique de l'Amérique du Sud.*
*(Cliché : Global relief data CD Rom,*
*National Geophysical Data Center)*

*Dans le fond, paysage andin, province du Cotopaxi,*
*région du Quilotoa (Équateur).*
*Cliché : Michel Portais*